

**Dihapto-Coordination to a  $\pi$ -Basic Tungsten Fragment:  
Synthesis of Methylphenidate Derivatives and Functionalized  
Carbocycles**

**Megan Nell Ericson**  
Sycamore, Illinois

B.S., Chemistry, University of North Texas, 2017  
M.S., Chemistry, University of North Texas, 2019

A Dissertation Presented to the Graduate Faculty of the University of  
Virginia in Candidacy for the Degree of Doctor of Philosophy

Department of Chemistry

University of Virginia  
2025

## Abstract

**Chapter 1:** Small-molecule compounds dominate pharmaceuticals, yet much of chemical space remains unexplored. Expanding structural diversity, particularly through stereogenic centers and  $sp^3$  rich frameworks, enhances drug efficacy and protein selectivity. Dearomatization techniques, particularly tungsten-promoted dihapto-coordination, enables controlled synthesis of structurally complex cyclohexenes and tetrahydropyridines from readily available aromatic precursors like benzenes and pyridines. Expanding this methodology to pharmaceutical compounds, smaller carbocycles and larger carbocycles further broadens the scope. By leveraging organometallic dearomatization, this work advances the methodology for accessing complex and likely bioactive molecules, paving the way for new pharmaceutical compounds.

**Chapter 2:** Due to its efficacy as a cocaine agonist, methylphenidate (MPH) is of interest as a potential therapeutic for cocaine addiction. While numerous derivatives of MPH have been investigated for their potential medicinal value, the functionalization of the piperidine ring has not been explored. The pyridine borane ligand in [W]-pyBH<sub>3</sub> is dearomatized by the metal and can be elaborated to the analogous  $\eta^2$ -mesylpyridinium complex. Installing a methyl phenylacetate moiety at the C2' position via a Reformatsky reaction followed by a tandem protonation/nucleophilic addition sequence results in a library of erythro MPH analogues functionalized at the piperidyl C5' position. The functional group is added chemoselectively to C5', cis to the methyl phenylacetate. Repeating this procedure with an enantioenriched source of the tungsten reagent results in enantioenriched MPH derivatives. All identities of the newly reported compounds are supported by comprehensive 2D NMR and HRMS or crystallographic data. This work was conducted in conjunction with Jonathan Dabbs, who contributed to the methodology hydrogenations, and enantiopurity analysis.

**Chapter 3:** The tungsten fragment {Wtp(NO)(PMe<sub>3</sub>)} (Tp = trispyrazolylborate) is an effective dearomatization agent for benzene and its derivatives. The dihapto-coordination of this system to an arene disrupts its aromatic stability, thereby promoting facile electrophilic additions to the hydrocarbon. This preliminary study endeavors to extend this conceptual approach to other aromatic, non-aromatic, and anti-aromatic carbocycles. Dihapto-coordinated complexes of  $\eta^2$ -tropylium,  $\eta^2$ -cyclopentadienyl cation, and  $\eta^2$ -cyclooctatetraene have been synthesized and characterized using SC-XRD, DFT, CV, and <sup>1</sup>H, <sup>31</sup>P, and <sup>13</sup>C NMR (including COSY, NOESY, HSQC, HMBC). Their fluxional behavior and reactivity toward electrophilic/nucleophilic additions, such as protonation and methylation, are also demonstrated.

**Chapter 4:** A study on the functionalization of cyclopentane cores via dihapto-coordinate ligands, such as  $\eta^2$ -cyclopentadiene (CPD) and  $\eta^2$ -cyclopentadienyl cation, through electrophilic and nucleophilic additions was investigated. Selective deprotonation of  $\eta^2$ -cyclopentenyl cation for the isolation of a single isomer of  $\eta^2$ -CPD was explored but instead led to unintended products. Pursuit of this product through the use of enantiopure starting materials yielded tungsten-binuclear complexes. These  $\eta^2$ -cationic species had



regioselectivity toward nucleophiles and ultimately served as a route to chiral C(sp<sup>3</sup>)-C(sp<sup>3</sup>) coupling and single enantiomers of disubstituted cyclopentenenes. Coupling of carbocycles was achieved for cyclopentene-cyclopentene and cyclopentene-cyclohexene systems. Successful oxidation reactions led to the isolation of organic compounds.

**Chapter 5:** Eight-membered carbocycles, prevalent in bioactive natural products are often underrepresented in molecular libraries due to their tendency to form unexpected products, like bicyclic aromatic systems. Existing synthetic approaches typically emerge from total synthesis efforts leaving a gap in efficient methodologies for constructing highly functionalized and diverse cyclooctanes. The methodology developed here utilizes dihapto-coordinated cyclooctatetraene for the regioselective and stereoselective incorporation of nucleophiles and provides an approach to novel 3-monosubstituted cycloocta-1,4,6-trienes, 5,6-disubstituted cycloocta-1,3-dienes, and 3,4,8-trisubstituted cyclooctenes. This work lays the groundwork for further studies, potentially enhancing access to other isomers of functionalized cyclooctanes for applications in small molecule drug discovery.

**Chapter 6:** Preliminary investigations on the functionalization of seven-membered carbocycles through dihapto-coordination reveals the synthetic potential to transform  $\eta^2$ -cycloheptatriene (CHT) and  $\eta^2$ -tropylium into functionalized cycloheptanes through electrophilic and nucleophilic additions. Strategies such as catalytic oxidations and protonation-deprotonation were successful in the isolation of a single  $\eta^2$ -CHT isomer. Additionally, coordination of CHT to tungsten prevents pericyclic ring closures during Diels-Alder reactions, resulting in products where the seven-membered core is retained. The possibility of releasing products from the metal complex suggests the isolation of organic compounds with potential in drug discovery applications. Future work can focus on expanding scopes and further functionalizing the compounds synthesized in this study.

**Chapter 7:** Density Functional Theory (DFT) was utilized to provide key insights into the structural, thermodynamic, and kinetic properties of tungsten organometallic complexes. Calculations are done to compare the energetics of hyperdistorted dihapto-coordinated allylic conformations. Structures differ in ring shape, including *boat-like* and *chair-like* conformers and conformers where carbocation character is localized either *distal* or *proximal* to the phosphine ligand. Additionally, the influence of steric and electronic effects on the regioselectivity of addition reactions are explored. Thermodynamic preference for pyridine ring-opening reactions and anisole Diels-Alder reactions when bound to metal vs unbound are compared. Highly reactive intermediates are visualized providing insight on mechanistic pathways. Computational modeling significantly advanced the understanding of tungsten-mediated reactivity for a variety of experimental applications.

**Chapter 8:** This is a survey of the research described herein, comparing tungsten-mediated methods for the functionalized cyclohexanes, piperidines, cyclopentanes, cycloheptanes and cyclooctanes. Future directions are summarized.

## Copyright Information

Chapter 2 is a published work which is copyright by the American Chemical Society. This work is reproduced herein in accordance with Section II.1 of the American Chemical Society Journal Publishing Agreement. Jonathan Dabbs worked on method developments and hydrogenation reactions.

**Chapter 2:** Ericson, M. N.;<sup>#</sup> Dabbs, J. D.;<sup>#</sup> Wilde, J. H.; Lombardo, R. F.; Ashcraft, E. C.; Dickie, D. A.; Harman, W. D. The Tungsten-Promoted Synthesis of Piperidyl-Modified *erythro*- Methylphenidate Derivatives. *ACS Cent. Sci.* **2023**, 9 (9), 1775-1783.  
<sup>#</sup> joint first authorship

Chapter 3 is a full manuscript and will be submitted in whole promptly.

Chapter 4 is being transformed into a manuscript and may subsequently be published in whole or in part. Josh-Heman Ackah expanded on nucleophilic scopes and Alvin Meng worked on the scope of coupling reactions.

Chapter 5 is being expanded on and may subsequently be published in part. Josh Heman-Ackah worked on scope expansion.

Chapter 6 is being expanded on and subsequently may be published in part. Rachel Lombardo worked on addition reaction screening and Diels-Alder reactions.

Chapter 7 has compiled parts of published work. Some computational studies were performed alongside Karl Westendorff.

## Acknowledgements

Choosing an institution to pursue a doctoral degree is an intimidating but monumental decision in the career path of aspiring scientists. Admittedly, my choice to attend the University of Virginia in Charlottesville was influenced by my adoration for the Dave Matthews Band. Thank you, Dave, for being the impetus behind one of the best decisions I've made thus far. UVA and C'ville have provided me with invaluable lessons and opportunities to learn, grow and persevere. I want to express my deepest gratitude to those who have supported, guided and ultimately contributed to the success of my Ph.D. journey.

In a field notorious for fostering environments of unattainable expectations, harmful competition and a lack of support for women, I knew my experience would be shaped by my choice of lab. I was fortunate to find an advisor who defied these stereotypes and, in fact, actively cultivated an environment that encouraged collaboration, teamwork and the transformation of everyone's potential into individual achievements. With that said, thank you Dr. W. Dean Harman. I was lucky to join a lab overseen by such an intelligent, kind-hearted and passionate chemist and mentor.

Additionally, my experience in the lab was profoundly influenced by my colleagues. First, thank you Dr. Jonathan Dabbs. Your mentorship was essential to my growth as a scientist, particularly in building my confidence and creativity. I am thrilled to hear that you have chosen a path where you can use your natural talent as a mentor and contribute to the next generation of scientists. To my other colleagues, Dr. Spenser Simpson and Dr. Justin Weatherford-Pratt—I hope you know I was watching. As a young graduate student, I observed as you performed experiments, presented your data, defended your dissertations and moved on to meaningful careers. I learned from you, thank you.

Thank you to the current lab members, each of you has contributed to my experience in your own ways. To Daniel Siela—for reigniting my athletic passion. I learned one can be both a lab rat and a gym rat. Best gym buddy ever. To Jeremy Bloch—for engaging with my musical interest. “Can you guess what song I'm thinking about right now?” To Caleb Taylor—for the most unique conversations. I am especially grateful to have had someone to discuss every Taylor Swift song from The Tortured Poets Department when it was released. To Mason Ortiz—my grievance and political outlet. Your support truly made a difference. To Ben Livaudais—some of my loudest laughs came from the quote board. And last, but certainly not least, to Josh Heman-Ackah—I was lucky to have you as a mentee. Your commitment, curiosity, and respectful demeanor are inspiring. When you spend five years working on a research topic, it's hard to walk away knowing there are incredible discoveries below the surface. You have already assured me that you will do this work justice and make it your own.

In addition to my colleagues, I want to thank my incredible group of undergraduate students. My research would not be nearly as complete without your dedication. To Rachel Lombardo—you quickly transitioned from an undergrad mentee to a lab bestie. We made so many unforgettable memories together, and you were the perfect person to

ease my male-dominated doom. I had the best time watching you grow as a researcher and wish you all the best on your own Ph.D. journey. To Alvin Meng—wow! You can do it all: experimental design, computational modeling, technical support (PC and Mac!), and being a great friend. You are an unstoppable force, and I cannot wait to see where you go as a chemist. To Sofia Megert—I am so glad you joined the lab and brought your positive energy with you. Please remember me when you're the doctor performing my life-saving surgery.

I also owe a big thank you to the research staff at UVA. To Dr. Jeff Ellena—for being willing to help with NMR experiments. I could always count on your warm smile and hallways greetings. To Dr. Diane Dickie—I had so much fun learning crystallography from you, and your support has meant more to me than I can express. To Dr. Earl Ashcraft—for being a magician with broken vacuum pumps, glove box freezers and low-temperature probes.

My experience at UVA was fulfilling, and I was fortunate to be part of a supportive community. However, I never even considered pursuing a doctorate until a few of my undergraduate professors at the University of North Texas pulled me from the crowd and encouraged me to pursue research. Specifically, thank you to Dr. Sushama Dandekar for recognizing my potential early on and helping me build scientific confidence. And thank you to Mr. Zeitler, my high school chemistry teacher, for introducing me to my favorite subject.

Beyond my academic community, I could not have succeeded without my family. A huge thanks to my mom, who listened to far too many breakdowns and helped take my mind off work with countless concerts. Thanks to my dad because I couldn't have stayed in school this long without your support. A big thank you to my best bud, Lauren, for all the FaceTime calls and visits. Thanks to my grandma Nedra, who, despite knowing very little about chemistry, always found a way to ask the best questions about my research. Thanks to my Papa, who pushed me into advanced science in high school. I am beyond grateful. A special thank you to my partner, Marisa. You took a leap of faith moving to Virginia with me so I could pursue this degree, and in this process, I watched your own career take off. I couldn't be happier we chose to take this journey together. Lastly, I want to thank my Uncle Craig and Nanny for sparking my passion for learning. I was fortunate to spend my childhood surrounded by your love for teaching, which continually inspired me. Your dedication to my education fueled my motivation, and for that, I am forever appreciative. It is with great honor that I dedicate my thesis to my Nanny. I just know that if you were here, you'd be saying, "Look at the brain on Meggie!"

## Table of Contents

<b>Copyright Information .....</b>	<b>4</b>
<b>Acknowledgments .....</b>	<b>5</b>
<b>Table of Contents .....</b>	<b>7</b>
<b>List of Abbreviations .....</b>	<b>11</b>
<b>List of Figures .....</b>	<b>14</b>
<b>List of Tables .....</b>	<b>18</b>
<b>Chapter 1. Introduction.....</b>	<b>19</b>
<b>1.1 – Introduction.....</b>	<b>20</b>
1.1.1 – Small Molecule Compounds in Pharmaceuticals.....	20
1.1.2 – Stereogenic Properties of High-Quality Drug Candidates.....	20
<b>1.2 – Molecular Scaffolds with Pharmaceutical Relevance.....</b>	<b>21</b>
1.2.1 – Relevance and Synthesis of Piperidines.....	21
1.2.2 – Relevance and Synthesis of Carbocyclic Compounds.....	23
<b>1.3 – Organometallic Dearomatization through Dihapto-Coordination.....</b>	<b>25</b>
1.3.1 – Dearomatization Approaches.....	25
1.3.2 – Transition-Metal Mediated Dearomatization by Dihapto-Coordination.....	26
1.3.3 – Functionalization of Benzene, Benzene Derivatives and Pyridine by Dihapto-Coordination.....	28
<b>1.4 – Advancing Dearomatization Strategies for Functionalized Cycloalkenes and Medicinal Applications.....</b>	<b>32</b>
<b>References.....</b>	<b>34</b>
<b>Chapter 2. The Tungsten-Promoted Synthesis of Piperidyl-Modified <i>erythro</i>-Methylphenidate Derivatives.....</b>	<b>42</b>
<b>2.1 – Introduction.....</b>	<b>43</b>
<b>2.2 – Results and Discussion.....</b>	<b>46</b>
2.2.1 – Synthesis of Key DHP Complex.....	46
2.2.2 – Preparing a Library of THP Complexes.....	49
2.2.3 – Releasing the THP from the Metal.....	52
2.2.4 – Hydrogenation of the THP to Piperidine.....	52
2.2.5 – Enantioenriched THP's.....	54

<b>2.3 – Conclusions.....</b>	<b>56</b>
<b>References.....</b>	<b>58</b>
<b>Chapter 3. Dihapto-Coordinated Conjugated Carbocycles (<math>\eta^2\text{-C}_n\text{H}_n</math> n = 5-8): Blurring the line between aromatic and antiaromatic hydrocarbons.....</b>	<b>62</b>
<b>3.1 – Introduction.....</b>	<b>63</b>
<b>3.2 – Results and Discussion.....</b>	<b>64</b>
3.2.1 – Experimental.....	64
3.2.2 – Fluxional behavior.....	68
3.2.3 – Electrochemical Behavior.....	71
3.2.4 – Methylations.....	71
<b>3.3 – Conclusions.....</b>	<b>74</b>
<b>References.....</b>	<b>75</b>
<b>Chapter 4. The Unexpected Challenges and Successes of Functionalizing Five- Membered Carbocycles.....</b>	<b>87</b>
<b>4.1 – Introduction.....</b>	<b>88</b>
<b>4.2 – Results and Discussions.....</b>	<b>89</b>
4.2.1 – Mono-functionalized Cyclopentenes.....	89
4.2.2 – Disubstituted Cyclopentenes.....	91
4.2.3 – Binuclear Tungsten Species.....	93
4.2.4 – Oxidation Reactions.....	96
<b>4.3 – Future Studies.....</b>	<b>98</b>
<b>4.4 – Conclusions.....</b>	<b>99</b>
<b>References.....</b>	<b>101</b>
<b>Chapter 5. The Synthesis of Functionalized Eight-Membered Carbocycles: Trisubstituted Cyclooctenes.....</b>	<b>107</b>
<b>5.1 – Introduction.....</b>	<b>108</b>
5.1.1 – Synthetic Strategies to Eight-Membered Rings.....	108
5.1.2 – Organometallic Functionalization of Cyclooctatetraene.....	110
<b>5.2 – Results and Discussion.....</b>	<b>112</b>
5.2.1 – Dihapto-Coordination of Cyclooctatetraene.....	112
5.2.2 – First Protonation Reaction.....	113

5.2.3 – First Nucleophilic Addition Reactions.....	114
5.2.4 – Second Protonation Reactions.....	115
5.2.5 – Second Nucleophilic Additions.....	120
5.2.6 – Third Protonation and Third Nucleophilic Additions.....	121
5.2.7 – Organic Compounds.....	122
<b>5.3 – Future Studies.....</b>	<b>123</b>
5.3.1 – Kinetic $\eta^2$ – Cyclooctadienyl Cation.....	124
5.3.2 – Syn complexes and Alternative Isomerization Pathways.....	124
<b>5.4 – Conclusions.....</b>	<b>125</b>
<b>References.....</b>	<b>127</b>
<b>Chapter 6. Preliminary Studies on the Functionalization of Seven-Membered Carbocycles.....</b>	<b>136</b>
<b>6.1 – Introduction.....</b>	<b>137</b>
<b>6.2 – Results and Discussion.....</b>	<b>139</b>
6.2.1 – Isolation of $\eta^2$ -Cycloheptatriene Complexes.....	139
6.2.2 – Nucleophilic Addition Reactions.....	141
6.2.3 – Diels-Alder Reactions.....	142
<b>6.3 – Conclusions.....</b>	<b>144</b>
<b>References.....</b>	<b>146</b>
<b>Chapter 7. Summary on Supporting DFT Calculations for Energy and Conformational Comparisons.....</b>	<b>149</b>
<b>7.1 – Introduction.....</b>	<b>150</b>
<b>7.2 – Results and Discussion.....</b>	<b>152</b>
7.2.1 – Chair and Boat Conformations.....	152
7.2.2 – Tri-Substituted and Polycyclic Compounds.....	156
7.2.3 – Double Protonation Intermediates and Nitrosyl-Assisted Protonations.....	160
7.2.4 – Dihydropyridine Ring-Openings.....	164
7.2.6 – Diels-Alder and Retro-Diels-Alder Reactions.....	165
<b>7.3 – Conclusions.....</b>	<b>166</b>
<b>References.....</b>	<b>168</b>
<b>Chapter 8. Conclusions.....</b>	<b>170</b>

<b>8.1 – General Conclusions.....</b>	<b>171</b>
8.1.2 – Methylphenidate Derivatives.....	172
8.1.3 – Conjugated Carbocycles.....	172
8.1.4 – Five-Membered Rings.....	173
8.1.5 – Eight-Membered Rings.....	173
8.1.6 – Seven-Membered Rings.....	173
8.1.7 – Density Functional Theory.....	174
<b>8.2 – Future Developments.....</b>	<b>175</b>
<b>References.....</b>	<b>176</b>
<b>Appendix A: General Methods.....</b>	<b>179</b>
<b>Appendix B: Chapter 2 Data.....</b>	<b>182</b>
<b>Appendix C: Chapter 3 Data.....</b>	<b>266</b>
<b>Appendix D: Chapter 4 Data.....</b>	<b>390</b>
<b>Appendix E: Chapter 5 Data.....</b>	<b>492</b>
<b>Appendix F: Chapter 6 Data.....</b>	<b>783</b>
<b>Appendix G: Chapter 7 Data.....</b>	<b>841</b>



## List of Abbreviations

FDA – Food and Drug Administration

CC – Commercial Compounds

DC – Diverse Compounds

NP – Natural Products

Tp – Trispyrazolylborate

DMAP – 4-(dimethylamino)pyridine

CO – Carbonyl

NO – Nitrosyl

PMe<sub>3</sub> – Trimethylphosphine

1,3-DMB – 1,3-dimethoxybenzene

DPhAT – Diphenylammonium Triflate

EAS - Electrophilic Aromatic Substitution

HOTf – Triflic Acid

MPH – Methylphenidate

ADHD - Attention-Deficient Hyperactivity Disorder

SC-XRD - Single Crystal X-Ray Diffraction

DFT – Density Functional Theory

CV – Cyclic Voltammetry

NMR – Nuclear Magnetic Spectroscopy

COESY – Correlation Spectroscopy

NOESY – Nuclear Overhauser Effect Spectroscopy

HSQC – Heteronuclear Single Quantum Coherence

HMBC – Heteronuclear Multiple Bond Correlation

COT – Cyclooctatetraene

CHT – Cycloheptatriene

DAT – Dopamine Transporter

THP – Tetrahydropyridines

py – Pyridinium

PG – Protecting Group

Nu – Nucleophile

DHP – Dihydropyridine  
MBA – Methyl Bromoacetate  
MAPBA – Methyl  $\alpha$ -Phenyl Bromoacetate  
DME – Dimethoxy-ethane  
MeMgBr – Methyl Magnesium Bromide  
NaCNBH<sub>3</sub> – Sodium Cyano Borohydride  
LiCH(CO<sub>2</sub>Me)<sub>2</sub>/LiDiMM – Lithium Dimethyl Malonate  
NaCN – Sodium Cyanide  
(CN)<sub>2</sub>CH<sub>2</sub> – Malononitrile  
KOtBu – Potassium tert-Butoxide  
nBuLi – n-Butyl Lithium  
IR – Infrared Spectroscopy  
HRMS – High-Resolution Mass Spectroscopy  
DDQ – 2,3-Dichloro-5,6-dicyano-1,4-benzoquinone  
Ms - Mesyl  
Ts - Tosyl  
Ac - Acetyl  
DBTH – Dibenzoyl Tartaric acid  
TEA – Trimethylamine  
HPLC – High-Performance Liquid Chromatography  
EtOAc – Ethyl Acetate  
Cp – Cyclopentadienyl  
PBu<sub>3</sub> – Tributyl Phosphine  
IRC – Intrinsic Reaction Coordinate  
NHE – Normal Hydrogen Electrode  
BnMgCl – Benzyl Magnesium Chloride  
DCM - Dichloromethane  
C<sub>2</sub>H<sub>3</sub>MgBr – Vinyl Magnesium Bromide  
CAN – Ceric Ammonium Nitrate  
Ph<sub>3</sub>COTf – Tritylium Triflate  
NSAID – Non-Steroidal Anti-Inflammatory Drugs

CPD – Cyclopentadiene

DBU – 1,8-Diazabicyclo[5.4.0]undec-7-ene

NaBH<sub>4</sub> – Sodium Borohydride

NaBD<sub>4</sub> – Sodium Borodeuteride

FeCp\*<sub>2</sub> – Permethy Ferrocenium

DABCO – 1,4-diazabicyclo[2.2.2]octane

HOMO – Highest Occupied Molecular Orbital

CF<sub>3</sub> – Trifluoromethyl

DMSO – Dimethyl Sulfoxide

THF – Tetrahydrofuran

MMTP – 1-methoxy-2-methyl-1-(trimethylsiloxy)propene

DA – Diels-Alder

rDA – retro-Diels-Alder

Et<sub>2</sub>O – Diethyl Ether

MeCN – Acetonitrile

EtCN – Propionitrile

Na<sub>2</sub>SO<sub>4</sub> – Sodium Sulfate

Na<sub>2</sub>CO<sub>3</sub> – Sodium Carbonate

## List of Figures

### Chapter 1

<b>Figure 1.1.</b> Figures by Clemons et al. demonstrating that stereogenic complexity and protein binding specificity.....	21
<b>Figure 1.2.</b> Natural products and medicinal compounds that contain piperidine cores.....	22
<b>Figure 1.3.</b> Common synthetic approaches to piperidine cores.....	23
<b>Figure 1.4.</b> Natural products and medicinal compounds that contain substituted five-, seven- and eight-membered carbocyclic molecules.....	24
<b>Figure 1.5.</b> Common synthetic approaches to the dearomatization of benzene.....	25
<b>Figure 1.6.</b> Comparison of <i>hexahapto</i> - and <i>dihapto</i> -coordinate activation.....	27
<b>Figure 1.7.</b> Synthetic approach to 1,4-disubstituted cyclohexenes from benzene.....	29
<b>Figure 1.8.</b> Subtypes of functionalized cyclohexenes synthesized through tungsten-promoted dearomatization.....	30
<b>Figure 1.9.</b> Synthetic approach to 2,5-disubstituted tetrahydropyridine from pyridine.....	31

### Chapter 2

<b>Figure 2.1.</b> MPH diastereomers, previously reported analogues of MPH, and proposed dearomatization approach to C5'-substituted MPH analogs.....	43
<b>Figure 2.2.</b> Tungsten-promoted dearomatization of pyridines and its proposed application to MPH analogues.....	45
<b>Figure 2.3.</b> Synthesis of DHP precursor ( <i>erythro</i> -7D).....	47
<b>Figure 2.4.</b> Molecular structure determination of <i>erythro</i> -7D from SCXRD and DFT calculation.....	48
<b>Figure 2.5.</b> Synthesis of THP precursors to MPH derivatives.....	50
<b>Figure 2.6.</b> Molecular structure determination for $\eta^2$ -allyl complex 8P.....	51
<b>Figure 2.7.</b> Oxidative decomplexation of THP compounds.....	53

<b>Figure 2.8.</b> Hydrogenations of MPH and THP organics.....	54
--	----

<b>Figure 2.9.</b> Preparation of enantioenriched MPH analog.....	55
---	----

### Chapter 3

<b>Figure 3.1.</b> The elaboration of an $\eta^2$ -benzene into difunctionalized cyclohexenes and the potential parallel reactions.....	63
---	----

<b>Figure 3.2.</b> Synthetic details for the target compounds.....	66
--	----

<b>Figure 3.3.</b> Molecular structures for compounds $[\text{W}(\text{Tp})(\text{NO})(\text{PMe}_3)(\eta^2\text{-C}_n\text{H}_n)]^{m+}$ (where $m = 0$ for $n = 6$ or $8$ and $m = 1$ for $n = 5$ or $7$ ).....	67
--	----

<b>Figure 3.4.</b> Transition states for ring-walking of compounds.....	70
---	----

<b>Figure 3.5.</b> Exploratory methylation reactions to generate methylated polyene complexes.....	72
--	----

<b>Figure 3.6.</b> Conversion of COT to a trisubstituted cyclooctene complex.....	73
---	----

### Chapter 4

<b>Figure 4.1.</b> $\text{W}(\text{Tp})(\text{NO})(\text{PMe}_3)(\eta^2\text{-dicyclopentadiene})$ , $\text{W}(\text{Tp})(\text{NO})(\text{PMe}_3)(\eta^2\text{-cyclopentadiene})$ , and $\text{W}(\text{Tp})(\text{NO})(\text{PMe}_3)(\eta^2\text{-cyclopentenyl cation})$ .....	90
---	----

<b>Figure 4.2.</b> Scope of dihapto-coordinated mono-substituted cyclopentenenes.....	91
---	----

<b>Figure 4.3.</b> Scope of dihapto-coordinated mono-substituted cyclopentadienes.....	92
--	----

<b>Figure 4.4.</b> Synthetic approach to dihapto-coordinated di-substituted cyclopentene.....	93
---	----

<b>Figure 4.5.</b> Stereoisomers of binuclear coupled products.....	95
---	----

<b>Figure 4.6.</b> Dihapto-coordinated binuclear coupling allyl and nucleophilic scope.....	95
---	----

<b>Figure 4.7.</b> Selective deprotonation of dihapto-coordinated binuclear coupled allyl.....	96
--	----

<b>Figure 4.8.</b> Partially and fully oxidized binuclear species, the formation of a difunctionalized cyclopentene ring.....	97
---	----

<b>Figure 4.9.</b> Reaction of $\eta^2$ -cyclohexadiene with $\eta^2$ -cyclopentenyl cation.....	97
--	----

## Chapter 5

**Figure 5.1.** General strategies to form eight-membered carbocycles and the strategy pursued in this study for functionalized eight-membered rings.....109

**Figure 5.2.** Current organometallic approaches to the functionalized eight-membered rings.....111

**Figure 5.3.** SC-XRD comparisons of decomplexed cyclooctatetraene and dihapto-coordinated cyclooctatetraene.....112

**Figure 5.4.** The  $\eta^2$ -cyclooctatrienyl isomers and SC-XRD structure.....114

**Figure 5.5.** Nucleophile scope for the synthesis of 3-mono-substituted  $\eta^2$ -cycloocta-1,4,6-trienes.....115

**Figure 5.6.** SC-XRD for 3-mono-substituted  $\eta^2$ -cycloocta-1,4,6-trienes compounds....116

**Figure 5.7.** Protonation of mono-substituted  $\eta^2$ -trienes to forms initial  $\eta^2$ -cyclooctadienyl cations, *kinetic allyls* and final  $\eta^2$ -cyclooctadienyl cations, *thermodynamic allyls* with SC-XRD structures.....118

**Figure 5.8.** Proposed mechanism upon acid addition to 3-methyl-1,4,6-cyclooctatriene **15** into the  $\eta^2$  – cyclooctadienyl cation, **16T'** .....119

**Figure 5.9.** Scope and SC-XRD structures for dihapto-coordinated *cis*-5,6-disubstituted cycloocta-1,3-dienes.....120

**Figure 5.10.** Scope and SC-XRD structures for dihapto-coordinated cyclooctadienyl cations and trisubstituted cyclooctenes.....122

**Figure 5.11.** Scope of isolated organic compounds.....123

**Figure 5.12.** Possible products via *kinetic*  $\eta^2$  – cyclooctadienyl cations.....124

**Figure 5.13.** Complexes that have isomerized to place incorporated functional groups in a *syn* position.....125

**Figure 5.14.** The synthetic pathway to the synthesis of 3,4,8-trisubstituted cyclooctenes.....126

## Chapter 6

**Figure 6.1.** Pathways for the synthesis of natural products containing seven-membered carbocycles.....138

**Figure 6.2.** Pearson's work on organoiron approaches to functionalized seven-membered cores.....139

**Figure 6.3.** Coordination, protonation and deprotonation of dihapto-coordinated cycloheptatriene complexes.....141

**Figure 6.4.** Nucleophilic scope to the addition of the  $\eta^2$ -cycloheptentyl cation and the  $\eta^2$ -cycloheptatrienyl cation.....142

**Figure 6.5.** Diels-Alder scope for  $\eta^2$ -cycloheptatriene.....144

## Chapter 7

**Figure 7.1.** SC-XRD structure for [TpW(NO)(PMe<sub>3</sub>)( $\eta^2$ -C<sub>6</sub>H<sub>9</sub>)]OTf.....151

**Figure 7.2.** Reaction coordinate diagram for allyl cation isomerization.....151

**Figure 7.3.** The four conformations of  $\eta^2$  – cyclohexenyl cations and their energy comparisons.....153

**Figure 7.4.** Relative energy order of allyl conformations when substituted with a methyl, phenyl, and t-butyl groups.....154

**Figure 7.5.** Relative energy order of allyl conformations substituted with a fluoro, trifluoromethyl, and cyano groups.....155

**Figure 7.6.** Implicit solvent effects on conformational stability.....156

**Figure 7.7.** Energy comparison of the *proximal* and *distal* conformers.....157

**Figure 7.8.** Energetic comparisons of the  $\eta^2$ -allyl intermediates, their conformations and their products.....158

**Figure 7.9.** Mechanistic representation of the synthesis of fused and bridged tricyclic compounds and energetic comparisons.....159

**Figure 7.10.** Energy comparisons of ring closure and ring opened products for tethered nucleophiles.....159

**Figure 7.11.** Energy comparisons of isomers of ring-closure products with different substitution patterns.....160

**Figure 7.12.** The reaction pathway for the double protonation of  $\eta^2$  – benzene and the DFT optimized structure.....161

**Figure 7.13.** DFT optimized structure of  $[W(Tp)(NO)(PMe_3)(C_5H_6)]^{2+}$  .....161

**Figure 7.14.** The reaction sequence for the double protonation of  $\eta^2$  – anisole and the DFT optimized structure.....162

**Figure 7.15.** Comparison of first and second intramolecular protonations of benzene.....162

**Figure 7.16.** Proposed pathways to isolated alkene protonation, including nitrosyl-assisted stabilization and hydride shift.....163

**Figure 7.17.** Organic and organometallic DHP ring-opening.....164

**Figure 7.18.** Synclinal and antiperiplanar conformations.....165

**Figure 7.19.** Reaction scheme for organic and organometallic Diels-Alder and retro-Diels-Alder of  $\eta^2$ -anisole.....166

## List of Tables

**Table 2.1.** Experimental conditions in the synthesis of MPH tetrahydropyridines.... 51

**Table 5.1.** Frequency of cyclooctenes with different substitution patterns.....112



## **Chapter 1. Introduction**

## 1.1 Introduction

### 1.1.1 *Small Molecule Compounds in Pharmaceuticals*

Small-molecule compounds are fundamental to medicinal chemistry, accounting for 90% of all pharmaceutical drugs<sup>3</sup> and 69% of FDA-approved medicines in 2023.<sup>4</sup> These drugs are typically synthetic organic compounds with low molecular weights, designed to mimic, enhance, or inhibit natural biological processes, within the human body. They are generally administered through straightforward dosing regimens, after which they are absorbed in the gut, enter the bloodstream, and permeate cells to reach their biological targets. Small molecule drugs are meticulously designed and structurally optimized to selectively interact with specific intracellular targets.<sup>3</sup>

Molecular libraries—comprehensive databases containing millions of small molecule compounds—are essential tools for pharmaceutical drug discovery. They provide platforms for large-scale screening of organic compounds for potential biological activity. However, despite the vastness of molecular libraries, a significant portion of chemical space remains unexplored. Reymond et al. estimates that 0.1% of “druggable” compounds have been synthesized.<sup>3</sup>

The development of novel synthetic methods is crucial for accessing previously unattainable chemical compounds and advancing pharmaceutical drug discovery. Currently, molecular libraries are largely composed of structurally similar molecules due to the frequent reliance on well-established synthetic methods. This has resulted in libraries dominated by  $sp^2$ -rich compounds, leading to an overrepresentation of “flat” molecular structures.<sup>4</sup> In contrast, high-quality drug candidates tend to exhibit greater structural complexity, characterized by features such as increased polarity, molecular weight, rotatable bonds, hydrogen bond donors and acceptors, and the presence of stereogenic centers.<sup>5,6</sup> Thus, the development of innovative synthetic methods that enhance structural complexity is essential for driving progress in drug discovery.

### 1.1.2 *Stereogenic Properties of High-Quality Drug Candidates*

Natural products have long served as a source of inspiration for drug candidates due to their intricate chemical structures and remarkable ability to interact with biological systems for medicinal benefits. As illustrated by Clemons et al. in **Figure 1.1**, commercially produced chemical compounds (CC) exhibit the lowest stereochemical

diversity, whereas natural products (NP) display the highest. Additionally, commercial compounds are more likely to interact with six or more proteins, while natural products have the highest likelihood of binding selectively to a single protein.<sup>3</sup> This correlation between stereogenic centers and increased protein-binding specificity highlights the advantageous interactions between biological proteins and naturally occurring chemical compounds. In fact, studying the binding affinity between drugs and their target proteins is essential for understanding pharmacological mechanisms of action.<sup>4</sup> Synthetically diverse compounds (DC) which exhibit high stereochemical diversity, more closely resemble natural products, thereby increasing the likelihood of selective protein interactions and reducing off-target effects. To develop high-quality drug candidates, enhancing stereogenic character and sp<sup>3</sup>-rich frameworks in organic compounds represents a valuable structural modification.

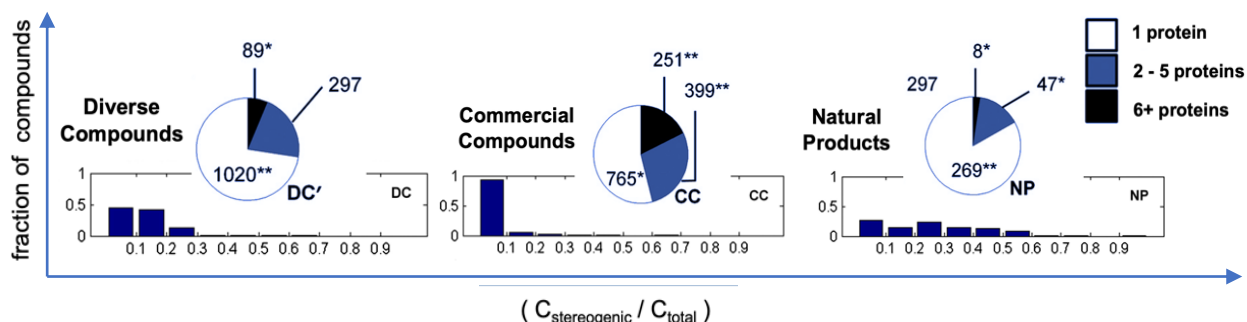


**Figure 1.2.** Figures by Clemons et al. demonstrating that stereogenic complexity increases from Commercial Compounds (CC) to Diverse Compounds (DC) to Natural Products (NP) and that affinity for a single protein also increases from CC to DC and NP being the most selective.<sup>3</sup>

## 1.2 Molecular Scaffolds with Pharmaceutical Relevance

### 1.2.1 Relevance and Synthesis of Piperidines

Certain molecular scaffolds frequently occur in nature and, due to their structural analogues often exhibiting significant therapeutic potential, they are referred to as *privileged scaffolds*. Examples include benzene-fused rings, nitrogen heterocycles, carbohydrates, and steroids.<sup>5</sup> Notably, nitrogen heterocycles are present in 59% of FDA-approved small-molecule drugs, with piperidine being the most prevalent N-heterocyclic motif.<sup>6, 7</sup> Piperidine derivatives appear in over twenty drugs classes and methodologies

for their synthesis continue to be actively explored.<sup>7, 8</sup> These drug classes include anticancer agents<sup>9, 10</sup>, antibiotics<sup>11</sup>, analgesics<sup>12, 13</sup>, antipsychotics<sup>14</sup>, antioxidants,<sup>15, 16</sup> treatments for Alzheimer's disease therapy<sup>17</sup>, among others. **Figure 1.2** highlights several pharmaceuticals containing piperidine cores, such as Crizotinib (chemotherapy)<sup>18</sup>, Icaridine (insect repellent)<sup>19</sup>, Risperidone (antipsychotic)<sup>20</sup>, Minoxidil (hair loss treatment)<sup>21</sup>, Nelfinavir (HIV treatment)<sup>22</sup>, Loratadine (antihistamine)<sup>23</sup>, and Methylphenidate (stimulant).<sup>24</sup>

The construction and functionalization of piperidine rings have been extensively studied and reviewed.<sup>7</sup> Three main synthetic strategies for functionalizing piperidine cores—dearomatization, intramolecular cyclizations and intermolecular cycloadditions—are summarized in **Figure 1.3**. Intermolecular cycloadditions are a widely utilized and involve the combination of two or more molecular components through transformations such as condensation, reductive amination, metathesis, aldol reactions, imino-Diels-Alder, aza-Diels-Alder, and other annulations like [5+1], [4+2] and [3+3] processes.<sup>25</sup> Additionally, intramolecular ring closures offer an alternative approach, typically involving the combination of a nitrogen source and an active site, such as alkenes, dienes or alkynes. While these methods provide access functionalized piperidines, they often require catalysts and oxidative or reductive conditions, posing challenges in regio- and stereoselectivity.

Finally, while pyridine functionalization has been widely explored<sup>26, 27</sup> its dearomative transformation into chiral piperidines remains historically challenging.

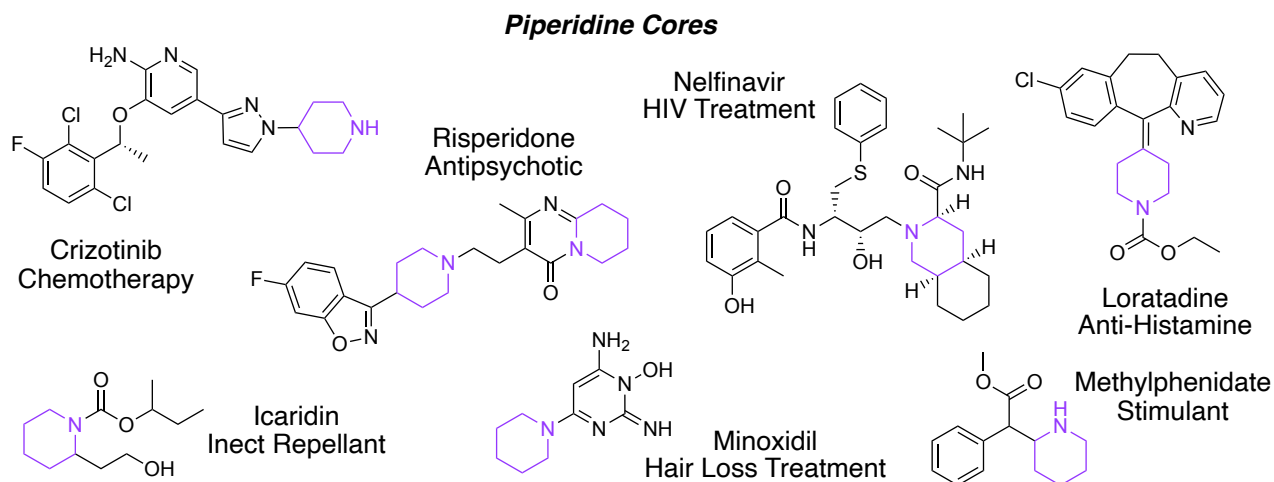


**Figure 1.2.** Natural products and medicinal compounds that contain piperidine cores.

However, this approach is particularly valuable due to pyridine's availability as an inexpensive chemical feedstock. The most common approach involves hydrogenation or reduction of functionalized pyridines, but this requires prefunctionalized substrates, harsh conditions and can be costly.<sup>7</sup> Although promising strategies have emerged for direct pyridine functionalization, methodologies that enable the introduction of multiple functionalities remain highly underdeveloped.<sup>28</sup>

### Piperidine Synthesis

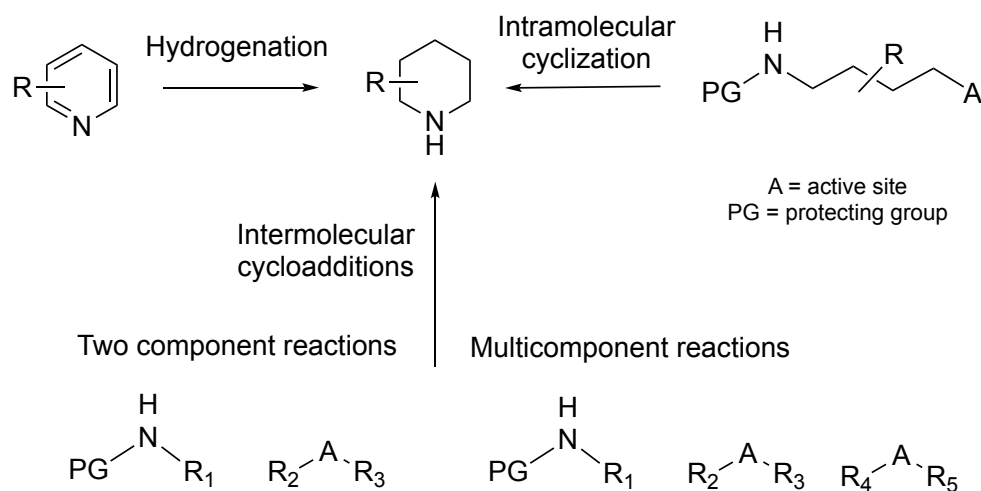


**Figure 1.3.** Common synthetic approaches to piperidine cores: Dearomatization, Intramolecular cyclization's and both two and multicomponent Intermolecular cycloadditions.<sup>5</sup>

#### 1.2.2 Relevance and Synthesis of Carbocyclic Compounds

In addition to six-membered heterocycles such as pyridine and piperidine, and carbocycles like benzene and cyclohexanes, five-, seven- and eight-membered carbocycles are prevalent in natural products and serve as important structural scaffolds in medicinal compounds.<sup>2, 29, 30</sup> Cyclopentanes, in particular, rank seventh among the most common ring systems found in natural products and considered *privileged scaffolds* in medicinal chemistry. Several therapeutic compounds contain substituted cyclopentanes, include Bimatoprost (glaucoma treatment)<sup>31</sup>, Ticagrelor (blood thinner)<sup>32</sup>, and Loxoprofen (NSAID)<sup>33</sup>. Likewise, medicinal compounds incorporating cycloheptane and cyclooctane cores include Rimegepant (migraine treatment)<sup>34</sup>, Amitriptyline (antidepressant)<sup>35</sup>, Paclitaxel (chemotherapy)<sup>36</sup>, Dezocine (analgesic)<sup>37</sup>, Retapamulin

(topical antibiotic)<sup>38</sup>, and other antibacterial agents. These examples are summarized in **Figure 1.4**.

Like piperidine, cyclopentane cores can be synthesized through various approaches; however, unlike piperidine, these methods are often tailored to specific targets rather than being broadly generalizable. While no universal strategy exists for cyclopentane synthesis, both inter- and intramolecular ring-closing reactions are commonly employed, facilitated by ionic mechanisms, metal-mediated radicals, pericyclic, and pseudo-pericyclic reactions. Additional cyclization strategies include reactions promoted by Grignard reagents, allyl and allenyl silanes, carbenes, Wittig and Horner-Wadsworth-Emmons reagents and Prins cyclizations. Moreover, ring expansion and contraction reactions provide alternative routes for cyclopentane synthesis. Baldwin's rules guide the favorability of these cyclization processes.<sup>39</sup> Despite the availability of these approaches, direct regio- and stereoselective functionalization of five-membered rings for the synthesis of chiral, substituted cyclopentanes remains a highly desirable goal.

Compared to cyclopentanes and piperidines, the synthetic availability of seven- and eight-membered carbocycles is even more limited. While inter- and intramolecular cyclizations and cycloadditions remain the primary methods for constructing cycloheptane and cyclooctane containing molecules, the formation of larger rings is inherently difficult due to entropic factors and non-bonding interactions in these cyclization transition states. These challenges frequently lead to the preferential formation of smaller

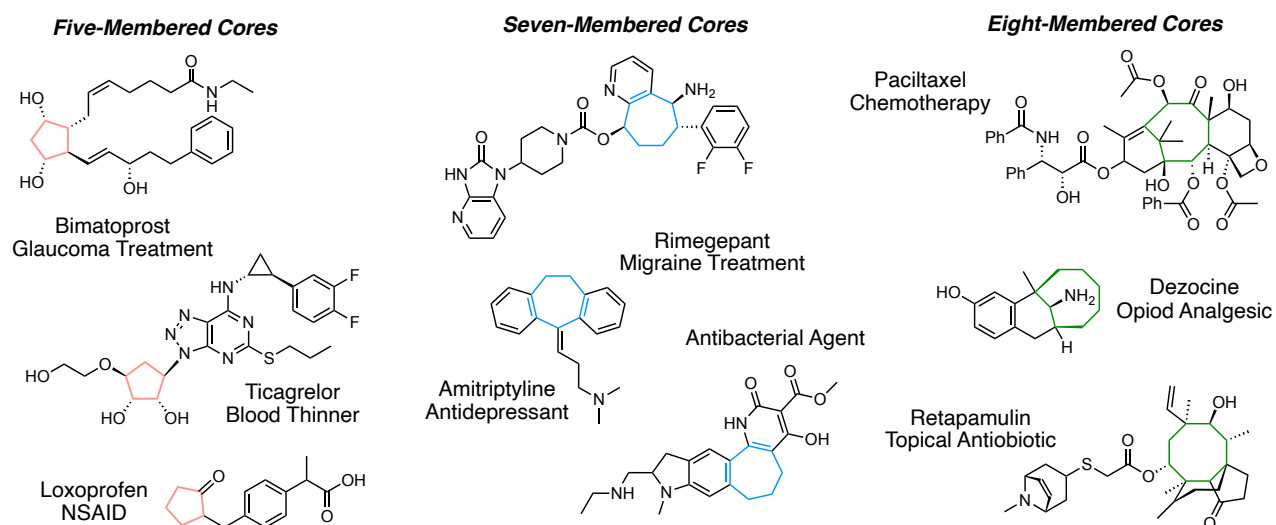


**Figure 1.4.** Natural products and medicinal compounds that contain substituted five-, seven- and eight-membered carbocyclic molecules.

bicyclic cores rather than the desired monocyclic products. Existing methodologies for cycloheptane synthesis include [2+2] and [5+2] cycloadditions, the Pauson-Khand and Friedel-Crafts reactions, ring-closing metathesis, rearrangements, and radical-mediated cyclizations.<sup>30</sup> Similarly, cyclooctane scaffolds can be synthesized using metal-mediated cyclizations, ring-closing metathesis, fragmentations, and transannular reactions including [4+2], [4+4], and [2+2] cycloadditions.<sup>2</sup>

While progress has been made in the synthesis of natural products containing larger carbocycles, the regio- and stereo-selective functionalization of electron-rich systems to generate highly substituted cycloheptane and cyclooctanes derivatives remains significantly underexplored. Continued development of innovative synthetic methodologies will be essential for expanding the chemical space of these valuable scaffolds and enhancing their utility in medicinal chemistry.

### 1.3 Organometallic Dearomatization through Dihapto-Coordination

#### 1.3.1 Dearomatization Approaches

Aromatic compounds constitute a vast and significant class of organic molecules. Their exceptional stability arises from their cyclic, planar structure and conjugated  $\pi$ -systems, which conform to Hückel's Rule. This stability is quantified by the stabilization

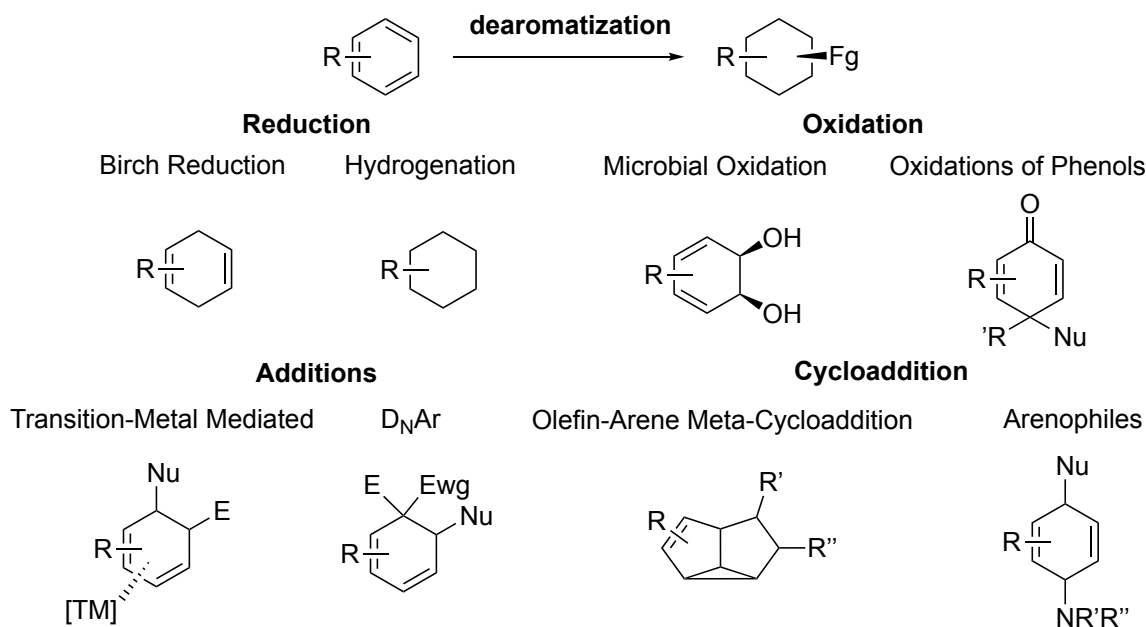


**Figure 1.5.** Common synthetic approaches to the dearomatization of benzene, its derivatives and the molecular outcome.

energy associated with delocalized electrons, and overcoming this energetic barrier is essential for facilitating aromatic reactivity. Despite their inherent stability, the structural simplicity, cost-effectiveness and widespread availability of aromatic compounds make them highly appealing as feedstock materials for the rapid synthesis of complex, high-value, and synthetically versatile compounds. One direct strategy for increasing molecular complexity is the conversion of  $sp^2$ -hybridized centers into  $sp^3$  centers.

Aromatic compounds can undergo chemical transformations such as nucleophilic aromatic substitutions and electrophilic aromatic substitutions including addition/elimination, nitration, halogenation, sulfonation, Friedel-Crafts acylation, and alkylation. However, these reactions often require activation via electron-donating and electron-withdrawing groups, and in most cases, aromaticity is restored in the final product. To initiate chemical reactivity in aromatic systems, transformations that disrupt the  $\pi$ -system—collectively referred to as dearomatization—are often necessary. Current dearomatization strategies include reductions, oxidations, additions, and cycloadditions. These approaches are summarized in **Figure 1.5**.<sup>40, 41</sup> In addition to these general methods, numerous specific examples have been documented in the literature.<sup>42-45</sup> While these dearomatization techniques are widely applicable to various types of arenes, additional methodologies have been developed for the dearomatization of heteroarenes. In particular, N-activation is the most commonly employed approach for pyridine dearomatization. Despite these advancements, major challenges remain in the dearomatization and functionalization of aromatic compounds, include functional group tolerance and achieving stereochemical control.

### 1.3.2 *Transition-Metal Mediated Dearomatization by Dihapto-Coordination*

The Harman laboratory at the University of Virginia has been investigating the dearomatization and organometallic activation of aromatic compounds to enhance their reactivity toward electrophiles, enabling the synthesis of highly functionalized compounds with cyclohexane cores.<sup>46-51</sup> Most transition-metal-mediated dearomatization strategies involve hexahapto-coordination to an electron-deficient metal center, which activates aromatic molecules by inducing electron flow from the arene to the metal, thereby promoting reactivity toward nucleophiles.<sup>41</sup>



In contrast, the Harman lab utilizes dihapto-coordination to an electron-rich metal center, activating aromatic compounds toward electrophiles. In this approach, dihapto-coordination ( $\eta^2$ -coordination) of an arene to a metal center disrupts the delocalization of the organic  $\pi$ -system through a critical  $\pi$ -backbonding interaction. Specifically, the metal donates electron density into an antibonding orbital of the  $\eta^2$ -arene, increasing the nucleophilic character of uncoordinated alkenes. **Figure 1.6** illustrates both *hexahapto*- and *dihapto*-coordination dearomatization techniques, emphasizing the key  $\pi$ -backbonding interaction responsible for aromatic activation in the dihapto-coordination approach.

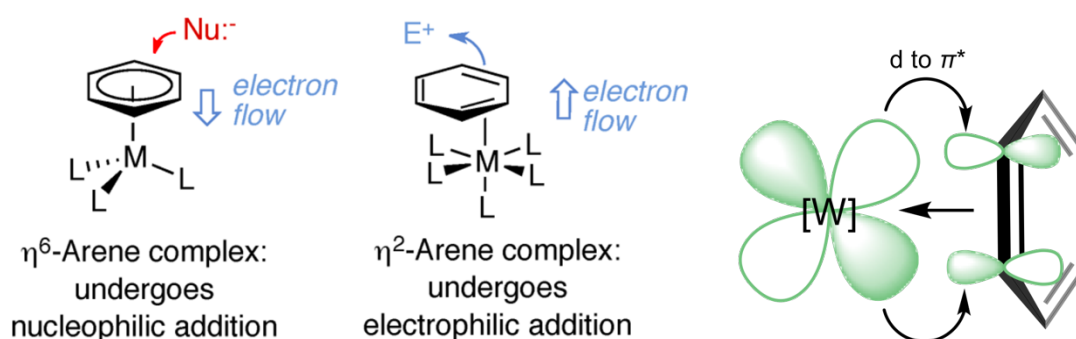


**Figure 1.6.** Comparison of *hexahapto*- and *dihapto*-coordinate activation and the  $\pi$ -backbonding interaction in the dearomatization of  $\eta^2$ -arenes.

The Harman Lab has developed several generations of dearomatization agents, including  $\{\text{Os}(\text{NH}_3)_5\}$ ,  $\{\text{Re}(\text{Tp})(\text{CO})(\text{MeIm})\}$ ,  $\{\text{Mo}(\text{Tp})(\text{NO})(\text{DMAP})\}$  and  $\{\text{W}(\text{Tp})(\text{NO})(\text{PMe}_3)\}$  where (Tp = trispyrazolylborate, DMAP = 4-(dimethylamino)pyridine, CO = carbonyl, NO = nitrosyl, and  $\text{PMe}_3$  = trimethylphosphine.)<sup>46</sup> The ligands in these systems are finely tuned to optimize the reduction potential of the complex; if the reductional potential is too high or too low, the complex cannot effectively bind arenes as dihapto-coordinated ligands. To date, these complexes have facilitated a wide range of organic transformations on dihapto-bound arenes, including electrophilic and nucleophilic additions, electrophilic aromatic substitutions, ring-closure reactions, and Diels-Alder cycloadditions. This methodology for binding and transforming ligands with  $\text{sp}^2$  character has been successfully applied to benzenes,<sup>47-56</sup> pyridines,<sup>57-64</sup> indolines,<sup>65-67</sup> pyrroles, ketones,<sup>68</sup> naphthalene,<sup>69, 70</sup> and more.<sup>71-74</sup>

Currently, the Harman Lab's preferred route to dearomatization involves reducing  $W(Tp)(NO)(PMe_3)(Br)$  to  $W(Tp)(NO)(PMe_3)(\eta^2\text{-arene})$ . This procedure can be scaled up to 40 grams and employs benzene or anisole as the arene of choice, both of which can be readily exchanged with various arenes and ligands via ligand substitution.

However, because the tungsten reagent is racemic ( $W_R$  and  $W_S$ ), selective transformations initially yield diastereomeric products. To address this, the lab has developed a procedure to isolate a single diastereomer of the metal complex. This approach involves coordinating 1,3-dimethoxybenzene (1,3-DMB) to the metal center, followed by protonation with a chiral salt, such as *L*- or *D*-dibenzoyltartaric acid, to selectively precipitate a single diastereomer. The resulting metal complex is then deprotonated, enabling the exchange of 1,3-DMB with the desired arene or alkene.<sup>75</sup> This method produces enantiopure organic compounds, which are essential for the discovery and development of high-quality pharmaceutical agents.

### 1.3.3 Functionalization of Benzene, Benzene Derivatives and Pyridine by Dihapto-Coordination

As mentioned above, benzene and its derivatives have been extensively explored via organometallic dearomatization to enhance their organic reactivity. In 2019, the direct functionalization of benzene through *dihapto*-coordination to tungsten was reported. When  $\eta^2$ -benzene (**1**) is exposed to an acid such as diphenylammonium triflate (DPhAT), protonation occurs forming a tungsten-stabilized carbocation and resulting in a hyperdistorted  $\eta^2$ -benzenium species (**2**). This cationic intermediate is isolable with a diastereomer ratio (d.r.) of 10:1 and exhibits high reactivity toward various nucleophiles.

The  $\eta^2$ -benzenium species adopts two distinct conformations with independent energy minima: the carbocation character can be stabilized either *distal* (**2D**) or *proximal* (**2P**) to the phosphine ligand. However, nucleophilic attack predominately occurs at the *distal* position, leading to a strong preference for monosubstituted  $\eta^2$ -cyclohexadiene, compound **3**, over the alternative regioisomer. Successful nucleophiles include protected enolates, methoxy groups, cyanide, phosphines, amines, and indole which proceeds through an electrophilic aromatic substitution (EAS) reaction. Additionally, stereoselectivity is observed, with nucleophiles favoring attack on the face *anti* to the bulky metal center.

Subsequent protonation of the dihapto-coordinated mono-substituted cyclohexadiene with triflic acid (HOTf) which again generates a tungsten-stabilized hyperdistorted  $\eta^2$ -allyl intermediate, existing in an equilibrium between *distal* (**4D**) and *proximal* (**4P**) conformations. As in the initial nucleophilic addition, the second nucleophilic attack exhibits stereoselectivity. Although regioselectivity varies depending on the nucleophile, the reaction generally favors the *proximal* conformation, due to steric effects, and produces 3,6-disubstituted cyclohexenes as the major product (**5**). Some second nucleophilic additions explored in this work include protected enolates, cyanide, amines, and Grignard reagents.

Finally, through an oxidation reaction, the organic compound can be liberated from the metal complex (**6**). This methodology is summarized in **Figure 1.7**.

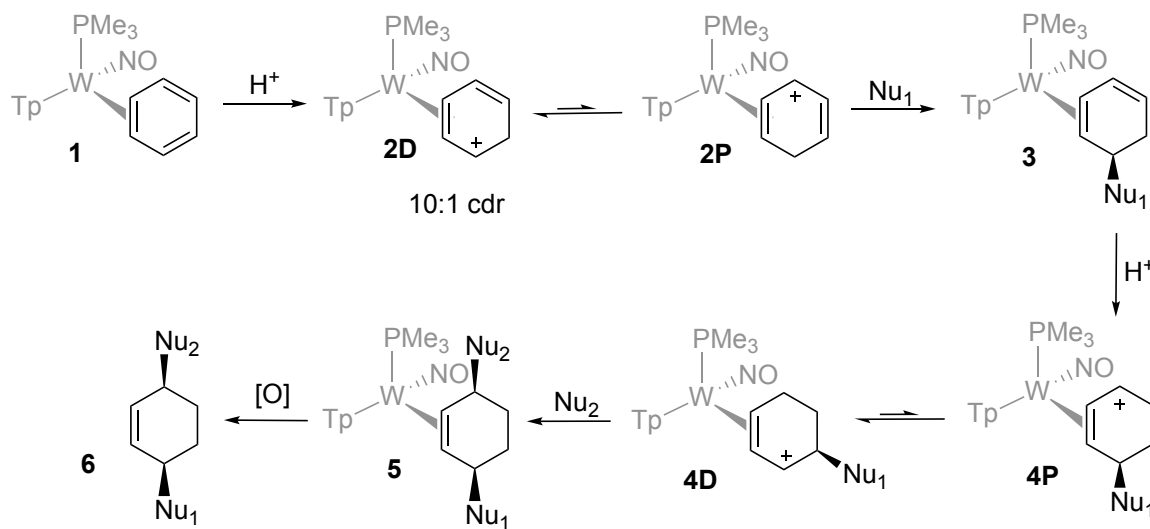


**Figure 1.7.** The synthetic approach to 1,4-disubstituted cyclohexene compounds using a tungsten-promoted approach to the dearomatization and functionalization of benzene.

The study of benzene dearomatization in the synthesis of 3,6-disubstituted cyclohexenes (**5a**) laid the foundation for several synthetic research directions in the Harman lab. These advancements include the *double protonation* of  $\eta^2$ -benzene, leading to a dicationic intermediate that enables Friedel-Crafts arylation without rearomatization, thereby expanding the nucleophilic scope to arenes (**5b**).<sup>48</sup> Additionally, the selective synthesis of both *trans*- and *cis*-3,6-disubstituted cyclohexenes was achieved through the *double protonation* of the  $\eta^2$ -anisole complex (**5c** and **5d**).<sup>49</sup> The incorporation of a third nucleophile was facilitated by coordinating benzene with a labile functional group, exemplified by the use of  $\eta^2$ -phenyl sulfone (**5e**).<sup>51</sup> When ester and amine groups are

introduced at neighboring positions, the resulting products can undergo lactam formation (**5f**).<sup>52</sup> Another study demonstrates the selective incorporation of deuterium from dihapto-coordinated benzene (**5g**).<sup>47</sup> Finally, ongoing research focuses on ring-closure reactions (**5h**). The various cyclohexene derivatives synthesized through organometallic dearomatization, and functionalization are illustrated in **Figure 1.8**.

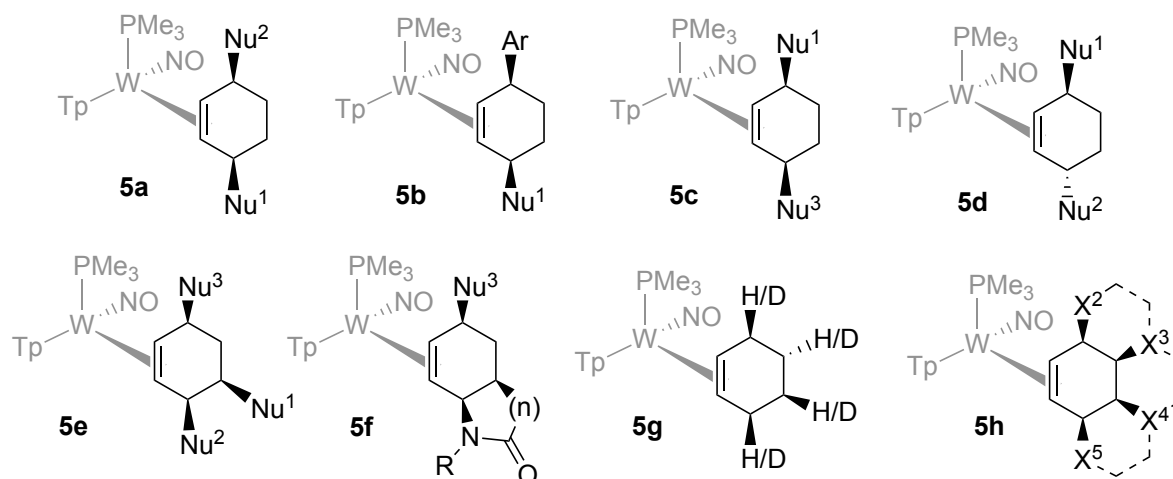


**Figure 1.8.** The different subtypes of functionalized cyclohexenes that have been synthesized through a tungsten-promoted dearomative organometallic approach.

The methodology described above was also applied to the dearomatization and functionalization of pyridine.<sup>61, 63, 64</sup> However, it was discovered that for pyridine to successfully participate in dihapto-coordination with the organometallic reagents developed in the Harman lab, its nitrogen lone pair must be blocked to prevent  $\kappa^1$ -coordination. The ligand exchange reaction between  $\eta^2$ -benzene (**1**) and pyridine are only effective when the ligand maintains an overall neutral charge; therefore, pyridine-borane is employed in the ligand exchange reaction. A key consideration in this exchange is the potential for tungsten to coordinate to different alkenes within the pyridine ring—a factor not encountered with benzene due to the equivalency of its three double bonds. Although three theoretical coordination diastereomers are possible, only C=C alkenes coordinate to the metal, resulting in the experimental observation of two diastereomers, with a c.d.r. of 3:1 (**6D:6P**).

Once  $\eta^2$ -pyridine-borane is synthesized, the borane is replaced with a proton to generate  $\eta^2$ -pyridinium, which also exhibits a 3:1 c.d.r. (**7**). At this stage, the N-H proton can be removed using a base and replaced with an electrophilic protecting group.

Successfully incorporated protecting groups includes methyl, acetyl, benzyl,  $\text{CH}_2\text{CH}_2\text{COMe}$ ,  $\text{CH}_2\text{CH}_2\text{CN}$ , tosyl and mesyl. This step further enriches the c.d.r., although the extent of enrichment varies depending on the protecting group. The driving force behind this enrichment is the metal's preference for the positive charge to reside at a more *distal* position. Initial functionalization studies were performed using acetyl-protected pyridinium, which exhibits a c.d.r. of 10:1 (**8**).

The  $\eta^2$ -acetylated pyridinium, being a charged species, undergoes resonance stabilization that activates the *distal* carbon (*ortho* to the nitrogen) for nucleophilic attack. A variety of nucleophiles, including hydrides, cyanide, nitronate, organozinc reagents, Grignard reagents, Barbier reactions, Reformatsky reactions, and indole through an EAS reactions were successful, yielding the corresponding products (**9**). Subsequent treatment with HOTf generates a hyperdistorted  $\eta^2$ -allyl species. As observed previously, charge stabilization favors the *distal* position (**10D**), while nucleophilic attack preferentially occurs at the *proximal* position (**10P**). This selectivity ultimately leads to the formation of 2,5-disubstituted tetrahydropyridines (**11**).

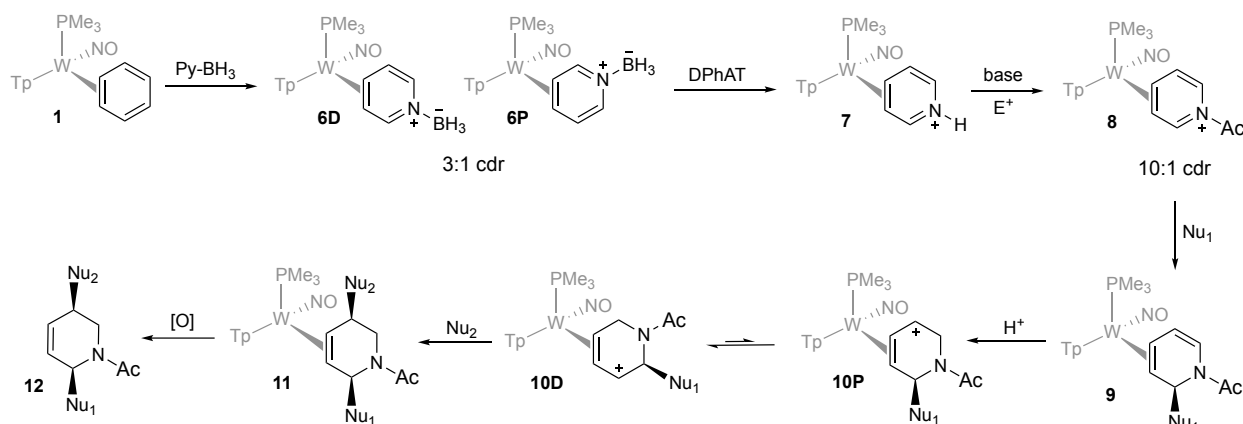


**Figure 1.9.** The synthetic approach to 2,5-disubstituted tetrahydropyridine using a tungsten-promoted approach to the dearomatization and selective functionalization of pyridine.

This substitution pattern is particularly significant because it enables functionalization at the C3/C5 (*meta*) positions of pyridine—an especially challenging feature, as most pyridine dearomatization methods predominately introduce functionality at C2 (*ortho*) and C4 (*para*) positions. Second nucleophilic additions include dimethyl malonate, cyanide, organozinc and amines. This approach was later extended to include

the incorporation of amine nucleophiles. Again, stereoselectivity is dictated by the metal bulk, and oxidation reactions are used to yield the final organic products (**12**). This methodology is summarized in **Figure 1.9**.

#### **1.4 Advancing Dearomatization Strategies for Functionalized Cycloalkenes and Medicinal Applications**

As discussed, developing reliable methods to transform of  $sp^2$  centers into  $sp^3$  centers is highly valuable in organic chemistry. This transformation is particularly significant in medicinal chemistry, where  $sp^3$ -rich and stereogenic centers play a crucial role in the selective interactions between small molecule drugs and biological targets. Dearomatization serves as a powerful strategy for converting highly unsaturated aromatic systems into chiral, saturated small molecules. Much of this work, utilizing organometallic dihapto-coordination, has focused on the dearomatization and selective functionalization of benzenes and pyridines to generate highly functionalized cyclohexanes and piperidines.

The organometallic dearomatization methodology described above has been extended to a pharmaceutical application. Specifically, in Chapter 2, tungsten-mediated pyridine dearomatization has been employed to synthesize a small molecular library of erythro-substituted methylphenidate (MPH) analogues. MPH is a pharmaceutical stimulant commonly used to treat of Attention-Deficient Hyperactivity Disorder (ADHD); however, it is associated with side effects such as insomnia, headaches, stomachaches, and anorexia.<sup>76, 77</sup> Developing synthetic approaches to novel MPH derivatives could enhance the drug's effectiveness and minimize adverse side effects. Increasing chiral functionality is a promising structural modification for improving medicinal properties. For the first time, methylphenidate derivatives with a diverse range of functional groups incorporated onto the piperidine ring have been synthesized using this strategy.

Building on the successful transformation of dihapto-coordination benzene ( $\eta^2$ -C<sub>6</sub>H<sub>6</sub>) into chiral disubstituted cyclohexenes, in Chapter 3, this approach has been extended to aromatic, non-aromatic and anti-aromatic conjugated carbocycles of varying ring size. Dihapto-coordinated complexes of  $\eta^2$ -tropylium,  $\eta^2$ -cyclopentadienyl cation, and  $\eta^2$ -cyclooctatetraene have been synthesized and characterized using single crystal X-ray diffraction (SC-XRD), density functional theory (DFT), cyclic voltammetry (CV), and

NMR spectroscopy ( $^1\text{H}$ ,  $^{31}\text{P}$ , and  $^{13}\text{C}$  NMR, including COSY, NOESY, HSQC, HMBC). Their fluxional behavior and reactivity toward electrophilic and nucleophilic additions, such as protonation and methylations, were explored. The ultimate goal of this study is to generate highly functionalized cycloalkenes across a range of ring sizes.

In Chapter 4, efforts to synthesize disubstituted cyclopentenes via nucleophilic and electrophilic addition reactions were explored but hindered by low regioselectivity. However, tungsten dimerization enabled  $\text{C}(\text{sp}^3)\text{-C}(\text{sp}^3)$  coupling of carbocycles, facilitating the selective incorporation of three stereocenters and yielding functionalized cyclopentene derivatives.

Methodology for the regio- and stereoselective synthesis of trisubstituted cyclooctenes was developed and presented in Chapter 5. Through the sequential electrophilic and nucleophilic additions to the dihapto-coordinated cyclooctatetraene (COT) complex, a small library of novel tri-substituted cyclooctenes was successfully generated, with structural validation through comparison with existing compound databases.

Chapter 6 focuses on preliminary studies on cycloheptene synthesis revealed challenges in regioselective nucleophilic addition. However, Diels-Alder cycloadditions on dihapto-coordinated cycloheptatriene (CHT) proceeded with highly selectivity, yielding products that retained the seven-membered core—a notable contrast to conventional organic Diels-Alder reactions, which often lead to ring rearrangement. A small library of these seven-membered products was established.

Density Functional Theory (DFT) calculations were extensively employed to investigate the energetics of tungsten-promoted transformations and summarized in Chapter 7. Across multiple experimental studies, DFT provided crucial insights by corroborating synthetic results, structurally characterizing elusive intermediates, and elucidating mechanistic pathways.

## References

- (1) Southey, M., W.Y., Bruvas, Michael. . Introduction of small molecule drug discovery and preclinical development *Front. Drug, Discov.* **2023**, 3.
- (2) Bai, Y.-R., Seng, Dong-Jie., Xu, Ying., Zhang, Yoa-Dong., Zhou, Wen-Juan., Jia, Yang-Yang., Song, Jian., He, Zhang-Xu., Liu, Hong-Min., Yuan, Shuo. A comprehensize review of small molecule drugs approved by the FDA in 2023: Advances and prospects. *Eur. J. Med. Chem.* **2024**, 276, 116706.
- (3) Welsch, M. E., Snyder, Scott A., Stockwell, B.R. Privledged Scaffolds for Library Design and Drug Discovery. . *Curr Opin Chem Biol* **2010.**, 14 (3), 347-361.
- (4) Vitaku, E., Smith, David T., Njardarson, Jon T. Analysis of the Structural Diversity, Substitution Patterns, and Frequency of Nitrogen Heterocycles among U.S. FDA Approved Pharmaceuticals. . *J. Med. Chem.* **2014**, 57, 10257 - 10274.
- (5) Frolov, N. A., Vereshchagin, Anatoly, N. Piperidine Derivatives: Recent Advances in Synthesis and Pharmacological Applications *Int J Mol Sci* **2023**, 24 (3), 2937.
- (6) Vardanyan, R. *Piperidine-based drug discovery*; Elvsevier, 2017.
- (7) McLornan, D. P., Pope, J.E., Gotlib, J., Harrison, C.N. Current and future status of JAK inhibitors. *Lancet* **2021**, 398, 803 - 816.
- (8) Goel, P., Alam, O., Naim, M.J., Nawaz, F., Iqbal, M., Alam, M.I. . Recent advancement of piperidine moiety in treatment of cancer-  
A review. *Eur. J. Med. Chem.* **2018**, 157, 480 - 502.
- (9) Ezelarab, H. A. A., Abbas, S.H., Hassan, H.A., Abuo-Rahma, G.E.-D.A. Recent updates of fluoroquinolones as antibacterial agents. *Arch. Der Pharm.* **2018**, 351, 1800141.
- (10) Martinelli, D., Bitetto, V., Tassorelli, C. Lasmiditan: An additional therapeutic option for the acute treatment of migraine. *Expert Rev. Neurother.* **2021**, 21, 491 - 502.
- (11) Ye, N., Qin, W., Tian, S., Xu, Q., Wold, E.A., Zhou, J., Zhen, X.-C. Small Molecules Selectively Targeting Sigma-1 Receptor for the Treatment of Neurological Diseases. *J. Med. Chem.* **2020**, 63, 15187 - 15217.
- (12) Rathore, A., Asati, V., Kashaw, K.S., Agarwal, S., Parwani, D., Bhattacharya, S., Mallick, C. . The Recent Development of Piperazine and Piperidine Derivatives as Antipsychotic Agents. *Mini-Rev. Med. Chem.* **2021**, 21, 362 - 379.



- (13) Mezeiova, E., Spilovska, K., Nepovimova, E., Gorecki, L., Soukup, O., Dolezal, R., Malinak, D., Janockova, J., Jun, D., Kuca, K., Profiling donepezil template into multipotent hybrids with antioxidant properties. *J. Enzym. Inhib. Med. Chem.* **2018**, 33, 583 - 606.
- (14) Rk, M., Begum, S., Begum, A., Koganti, B. Antioxidant potential of piperidine containing compounds—A short review. *Asian J. Pharm. Clin. Res.* **2018**, 11, 66.
- (15) Li, Q., He, S., Chen, Y., Feng, F., Qu, W., Sun, H. . Donepezil-based multi-functional cholinesterase inhibitors for treatment of Alzheimer's disease. *Eur. J. Med. Chem.* **2018**, 158, 463 - 477.
- (16) Blackhall, F., Cappuzzo, F. Crizotinib: from discovery to accelerated development to front-line treatment. *Ann Oncol.* **2016**, 29 (4), 1073.
- (17) Buchel, K., Bendin, Juliane., Gharbi, Amina., Rahlenbeck, Sibylle., Dautel, Hans. Repellent efficacy of DEET, Icaridin, and EBAAP against *Ixodes ricinus* and *Ixodes scapularis* nymphs (Acari, Ixodidae). *Ticks Tick Borne Dis* **2015**, 6 (4), 494 - 498.
- (18) Correll, C. U., Litman, Robert E., Filts, Yuriy., Llaudo, Jordi., Naber, Dieter., Torres, Ferran., Martinez, Javier. Efficacy and safety of once-monthly Risperidone ISM in schizophrenic patients with an acute exacerbation. *NPJ Schizophrenia* **2020**, 6 (37).
- (19) Suchonwanit, P., Thammarucha, Sasima., Leerunyakul, Kanchana. Minoxidil and its use in hair disorders: a review. *Drug Des Devel Ther* **2020**, 10 (14), 575.
- (20) Pai, V. B., Nahata, M.C. Nelfinavir mesylate: a protease inhibitor *Ann Pharmacother.* **1999**, 33 (3), 325 - 339.
- (21) Sidhu, G., Akhondi, Hossein. *Loratadine*; StatPearls, 2023.
- (22) Storebø, O. J., Storm, Maja Rosenberg Overby., Ribeiro, Johanne Pereira., Skoog, Maria., Groth, Camilla., Callesen, Henriette E., Schaug, Julie Perrine., Rasmussen, Pernille Darling., Huus, Christel-Mie L., Zwi, Morris., Kirubakaran, Richard., Simonsen, Erik., Gluud, Christian. Methylphenidate for children and adolescents with attention deficit hyperactivity disorder (ADHD). *Cochrane Database Syst Rev* **2023**, 3 (3).
- (23) Buffat, M. G. P. Synthesis of piperidines *Tetrahedron* **2004**, 60, 1701-1729.
- (24) Maity, S., Bera, Asish., Bhattacharjya, Ayantika., Maity, Pradip. C-H functionalization of pyridines. *Org. Biomol. Chem.* **2023**, 21, 5671.

- (25) Sindhe, H., Reddy, Malladi Mounika., Rajkumar, Karthikeyan., Kamble, Akshay., Singh, Amardeep., Kumar, Anand., Sharma, Satyasheel. Pyridine C(sp<sup>2</sup>)-H bond functionalization under transition-metal and rare earth metal catalysis *J. Org. Chem.* **2023**, *19*, 820 - 863.
- (26) Hu, M., Ding, Hao., DeSnoo, William., Tantillo, Dean J., Nairoukh, Zackaria. The Construction of Highly Substituted Piperidines via Dearomative Functionalization Reactions. *Angew Chem Int Ed* **2023**, *62*, e202315108.
- (27) Zhang, X., Xu, J. Five-Membered carbocycle construction in the synthesis of Daphniphyllum alkaloids: recent strategic methodological advances. *Org. Chem. Front.* **2022**, *9*, 6708.
- (28) Battiste, M. A., Pelphrey, P.M., Wright, D.L. The Cycloaddition Strategy for the Synthesis of Natural Products Containing Carbocyclic Seven-Membered Rings. *Chem. Eur. J.* **2006**, *12* (13), 3438-3447.
- (29) Hu, Y. J., Li, L.X., Han, J.C., Min, L., Li, C.C. Recent Advances in the Total Synthesis of Natural Products Containing Eight-Membered Carbocycles (2009-2019). *Chem. Rev.* **2020**, *120* (13), 5910-5953.
- (30) Curran, M. P. Bimatoprost: a review of its use in open-angle glaucoma and ocular hypertension *Drugs Aging.* **2009**, *26* (12), 1049 - 1071.
- (31) Dobesh, P. P., Oestreich, Julie H. Ticagrelor: pharmacokinetics, pharmacodynamics, chiral efficacy, and safety. *Pharmacotherapy.* **2014.**, *34* (10), 1077 - 1090.
- (32) Greig, S. L., Garnock-Jones, Karly P. Loxoprofen: A Review in Pain and Inflammation *Clin Drug Investig.* **2016**, *36* (9), 771 - 781.
- (33) Blair, H. A. Rimegepant: A Review in the Acute Treatment and Preventive Treatment of Migraine. *CNS Drugs* **2023**, *37* (3), 255 - 265.
- (34) Lawson, K. A Brief Review of the Pharmacology of Amitriptyline and Clinical Outcomes in Treating Fibromyalgia. *Biomedicine* **2017**, *5* (2), 24.
- (35) Sharifi-Rad, J., Quispe, Cristina., Patra, Jayanta Kumar., Singh, Yengkhom Disco., Panda, Manasa Kumar., Das, Gitishree., Adetunji, Charles Oluwaseun., Michael, Olugbenga Samuel., Sytar, Oksana., Polito, Letizia., Živković, Jelena., Cruz-Martins, Natália., Klimek-Szczykutowicz, Marta., Ekiert, Halina., Choudhary, Muhammad Iqbal.,

Ayatollahi, Seyed Abdulmajid., Tynybekov, Bekzat., Kobarfard, Farzad., Muntean, Ana Covilca., Grozea, Ioana., Daştan, Sevgi Durna., Butnariu, Monica., Szopa, Agnieszka., Calina, Daniela. . Paclitaxel: Application in Modern Oncology and Nanomedicine-Based Cancer Therapy. *Oxid Med Cell Longev* **2021**, 3687700.

(36) Childers, W. E., Abou-Gharbia, Magid A. "I'll Be Back": The Resurrection of Dezocine. *ACS Med. Chem. Lett.* **2021**, 12 (6), 961 - 968.

(37) Yang, L. P. H., Keam, Susan, J. Retapamulin: a review of its use in the management of impetigo and other uncomplicated superficial skin infections. . *Drugs* **2008**, 68 (8), 855 - 873.

(38) O'Malley, D. *Cyclopentane Synthesis*. 2005.  
[https://baranlab.org/images/grpmtgpdf/Omalley\\_Feb\\_05.pdf](https://baranlab.org/images/grpmtgpdf/Omalley_Feb_05.pdf) (accessed.

(39) Wertjes, W. C., Southgate, E.H., Sarlah, D. Recent advances in chemical dearomatization of non-activated arenes. . *Chem. Soc. Rev.* **2018**., 47, 7996.

(40) Huck, C. J., Sarlah, D. Shaping Molecular Landscapes: Recent Advances, Opportunities, and Challenges in Dearomatization. *Chem.* **2020**, 6, 1589-1603.

(41) Pape, A. R., Kaliappan, K.P., Kundig, E.P. Transition-Metal Mediated Dearomatization Reactions. *Chem. Rev.* **2000**, 100 (8).

(42) Rosillo, M., Dominguez, G., Perez-Castells, J. Chromium arene complexes in organic synthesis. *Chem. Soc. Rev.* **2007**, 37 (10), 1589-1604.

(43) Boyd, D. R., Bugg, T.D.H. Arene cis-dihydrodial formation: from biology to application. *Org. Biomol. Chem.* **2006**, 4 (2), 181-192.

(44) Ortiz, F. L., Iglesias, M.J. Fernandez, I., Andujar Sanchez, C.M., Gomez, G.R. Nucleophilic Dearomatization (DNAr) Reactions of Aromatic C<sub>6</sub>H-Systems. A Mature Paradigm in Organic Synthesis *Chem. Rev.* **2007**, 107 (5), 1580-1691.

(45) B.K. Liebov, W. D. H. Group 6 Dihapto-Coordinate Dearomatization Agents for Organic Synthesis. *Chem. Rev.* **2017**, 117, 13721-13755.

(46) J.A. Smith, K. B. W., R.E. Sonstrom, P. J. Kelleher, K.D. Welch, E.K. Pert, K.S. Westendorff, D.A. Dickie, X. Wang, B. H. Pate, W. D. Harman. Preparation of Cyclohexene Isotopologues and Stereoisomers from Benzene. *Nature* **2020**, 581, 288-293.

- (47) J.T. Weatherford-Pratt, J. A. S., J.M. Bloch, M.N. Ericson, J.T. Myers, K.S. Westendorff, D.A. Dickie, W.D. Harman. The Double-Protonation of Dihapto-Coordinated Benzene Complexes: An Enabling Strategy for Dearomatization Using Aromatic Nucleophiles. *Nature Comm* **2023**, *14*, 3145.
- (48) J.T. Weatherford-Pratt, J. M. B., J.A. Smith, M. N. Ericson, D.J. Siela, K. B. Wilson, M.H. Shingler, M.R. Ortiz, S. Fong, J.A. Laredo, I.U. Patel, M. McGraw, D. A. Dickie, W. D. Harman. Tungsten-anisole complex provides 3,6-substituted cyclohexenes for highly diversified chemical libraries. *Sci. Adv.* **2024**, *10* (7).
- (49) K.B. Wilson, J. A. S., H.S. Nedzbala, E. K. Pert, S.J. Dakermanji, D.A. Dickie, W.D. Harman Highly Functionalized Cyclohexenes Derived from Benzene: Sequential Tandem Addition Reactions Promoted by Tungsten *J. Org. Chem.* **2019**, *84* (10), 6094-6116.
- (50) S.R. Simpson, P. S., D.J. Siela, L.A. Diment, B.C. Song, K. S. Westendorff, M. N. Ericson, K. D. Welch, D. A. Dickie, W.D. Harman. Phenyl Sulfones: A Route to a Diverse Family of Trisubstituted Cyclohexenes from Three Independent Nucleophilic Additions. *J. Am. Chem. Soc.* **2022**, *144* (21), 9489-9499.
- (51) K.B. Wilson, H. S. N., S.R. Simpson, M. N. Ericson, K. S. Westendorff, M.D. Chordia, D.A. Dickie, W.D. Harman. Hydroamination of Dihapto-Coordinated Benzene and Diene Complexes of Tungsten: Fundamental Studies and the Synthesis of  $\gamma$ -Lycorane. *Chimica Acta* **2021**, *104* (10).
- (52) J.A. Smith, S. S., K.S. Westendorf, J. Weatherford-Pratt, J.T. Myers, J.H. Wilde, D.A. Dickie, W.D. Harman. Dihapto-Coordination of Electron-Deficient Arenes with Group 6 Dearomatization Agents. *Organometallics*. **2020**, *39* (13), 2493-2510.
- (53) J.A. Smith, K. B. W., R.E. Sonstrom, P. J. Kelleher, K.D. Welch, E.K. Pert, K.S. Westendorff, D.A. Dickie, X. Wang, B. H. Pate, W. D. Harman. Preparation of cyclohexene isotopologues and stereoisotopomers from benzene. *Nature* **2020**, *581*, 288-293.
- (54) K.B. Wilson, J. T. M., H.S. Nedzbala, L.A. Combee, M. Sabat, W.D. Harman. Sequential Tandem Additions to a Tungsten-Trifluorotoluene Complex: A Versatile Method for the Preparation of Highly Functionalized Trifluoromethylated Cyclohexenes. *J. Am. Chem. Soc.* **2017**, *139* (33), 11401-11412.

- (55) J.A. Pienkos, V. E. Z., D.A. Iovan, M.Li, D.P. Harrison, M. Sabat, R.J. Salomon, L. Strausberg, V.A. Teran, W.H. Myers, W.D. Harman. Friedel-Crafts ring-coupling reactions promoted by tungsten dearomatization agent. *Organometallics*. **2013**, 32, 691-703.
- (56) J.H. Wilde, J. T. M., D.A. Dickie, W.D. Harman. Molybdenum-Promoted Dearomatization of Pyridines. *Organometallics*. **2020**, 39 (8), 1288-1298.
- (57) J.A. Pienkos, A. T. K., B.L. McLeod, J.T. Myers, P.J. Shivatevich, V. Teran, M. Sabat, W.H. Myers, W.D. Harman. Double protonation of amino-substituted pyridine and pyrimidine tungsten complexes: Friedel-Crafts-like coupling to aromatic heterocycles. *Organometallics*. **2014**, 33, 5464-5469.
- (58) J.D. Dabbs, M. N. E., J.H. Wilde, R.F. Lombardo, E.C. Ashcraft, D.A. Dickie, W.D. Harman. The Tungsten-Promoted Synthesis of Piperidyl-Modified erythro-Methylphenidate Derivatives. *ACS Cent. Sci.* **2023**, 9 (9), 1775-1783.
- (59) D.P. Harrison, D. A. I., W. H. Myers, M. Sabat, S. Wang, V.E. Zottig, W.D. Harman. [4 + 2] Cyclocondensation reactions of tungsten-dihydropyridine complexes and the generation of tri- and tetrasubstituted piperidines. *J. Am. Chem. Soc.* **2011**, 133, 18378-18387.
- (60) D.P. Harrison, M. S., W.H. Myers, W.D. Harman. [145] Polarization of the pyridine ring: highly functionalized piperidines from tungsten-pyridine complex. *J. Am. Chem. Soc.* **2010**, 132, 17282-17295.
- (61) D.P. Harrison, G. W. K., V.M. Ramdeen, A.C. Nielander, S.J. Payne, M. Sabat, W.H. Myers, W.D. Harman. Tungsten-Promoted Pyridine Ring Scission: The Selective Formation of  $\eta^2$ -Cyanine and  $\eta^2$ -Merocyanine Complexes and Their Derivatives. *Organometallics*. **2010**, 29 (9), 1909-1915.
- (62) Harrison, D. P., Zottig, V.E., Kosturko, G.W., Welch, K.D., Sabat, M., Myers, W.H., Harman, W.D. Stereo- and Regioselective Nucleophilic Addition to Dihapto-Coordinated Pyridine Complexes *Organomet. Chem.* **2009**, 28, 5682-5690.
- (63) Wilde, J. H., Dickie, D.A., Harman, W.D. A Highly Divergent Synthesis of 3-Aminotetrahydropyridines. *J. Org. Chem.* **2020**, 85 (12), 8245 - 8252.
- (64) B.L. McLeod, J. A. P., K.B. Wilson, M. Sabat, W.H. Myers, W.D. Harman. Synthesis of Novel Hexahydroindoles from the Dearomatization of Indoline. *Organometallics*. **2016**, 35 (3), 370-387.

- (65) B.L. McLeod, J. A. P., J.T. Myers, M. Sabat, E.H. Myers, W.D. Harman. Stereoselective synthesis of trans-tetrahydroindolines promoted by a tungsten  $\pi$  base *Organometallics*. **2014**, 33, 6286-6289.
- (66) J.H. Wilde, D. A. D., W.D. Harman. Molybdenum-Promoted Synthesis of Isoquinuclidines with Bridgehead CF<sub>3</sub> Groups. *J. Am. Chem. Soc.* **2019**, 141 (47), 18890-18899.
- (67) E.C. Lis, D. A. D., Y. Lin, C.J. Mocella, M.A. Todd, W. Liu, M. Sabat, W.H. Myers, W.D. Harman The Uncommon Reactivity of Dihapto-Coordinated Nitrile, Ketone, and Alkene Ligands When Bound to a Powerful  $\pi$ -Base. *Organometallics*. **2006**, 25 (21), 5051-5058.
- (68) J.T. Myers, J. H. W., M. Sabat, D.A. Dickie, W.D. Harman. Michael-Michael Ring-Closure Reactions for a Dihapto-Coordinated Naphthalene Complex of Molybdenum. **2020**, 29 (8), 1404-1412.
- (69) L. Strausberg, M. L., D.P. Harrison, W.H. Myers, M. Sabat, W.D. Harman. Exploring the o-Quinodimethane Nature of Naphthalene: Cycloaddition Reactions with  $\eta^2$ -Coordinated Tungsten–Naphthalene Complexes. *Organometallics*. **2013**, 32, 915-925.
- (70) S.J. Dakermanji, K. S. W., E.K. Pert, K.B. Wilson, J.T. Myers, J.H. Wilde, D.A. Dickie, K.D. Welch, W.D. Harman. Spatial Recognition Within Terpenes; Redox and H-bond Promoted Linkage Isomerizations and the Selective Binding of Complex Alkenes. *Organometallics*. **2020**, 39 (10), 1961-1975.
- (71) J.A. Pienkos, A. T. K., B.K. Liebov, V. Teran, V.E. Zottig, M. Sabat, W.H. Myers, W.D. Harman. Tungsten-mediated selective ring opening of vinylcyclopropanes. *Organometallics*. **2014**, 33.
- (72) V.E. Zottig, M. A. T., A.C. Nielander, D.P. Harrison, M. Sabat, W.H. Myers, W.D. Harman. [144] Epoxidation, Cyclopropanation, and Electrophilic Addition Reactions at the meta Position of Phenol and meta-Cresol. *Organometallics*. **2010**, 29 (21), 4793-4803.
- (73) R.J. Salomon, M. A. T., M. Sabat, W.H. Myers, W.D. Harman. Single and Double Electrophilic Addition Reactions to the Aniline Ring Promoted by a Tungsten  $\pi$ -Base *Organometallics*. **2010**, 29 (4), 707-709.

- (74) A.W. Lankenau, D. A. I., J.A. Pienkos, R.J. Salomon, S. Wang, D.P. Harrison, W.H. Myers, W.D. Harman. Enantioenrichment of a Tungsten Dearomatization Agent Utilizing Chiral Acids. *J. Am. Chem. Soc.* **2015**, 137 (10), 3649-3655.
- (75) Morton, W. A., Stockton, Gwendolyn G. Methylphenidate Abuse and Psychiatric Side Effects. *Prim Care Companion J Clin Psychiatry* **2000**, 2 (5), 159 - 164.
- (76) Ribeiro, J. P., Arther, Emma Jasmine., Gluud, Christina., Simonsen, Erik., Storebo, Ole Jakob. Does Methylphenidate Work in Children and Adolescents with Attention Deficit Hyperactivity Disorder? *Ped Rep* **2021**, 13 (3), 434 - 443.

## **Chapter 2. The Tungsten-Promoted Synthesis of Piperidyl-Modified *erythro*-Methylphenidate Derivatives**



## 2.1 Introduction

The Center for Disease Control reported over 100,000 deaths in the United States due to overdoses in 2021, about a quarter of which were attributed to cocaine.<sup>1</sup> Small-molecule therapeutics have proven to be effective treatments for various drug addictions. Heroin addiction, for example, is a disorder most commonly treated with methadone, which prevents drug withdrawal symptoms while being less addictive than the original drug.<sup>2,3</sup> While pharmacotherapies exist for heroin and other opioids, effective

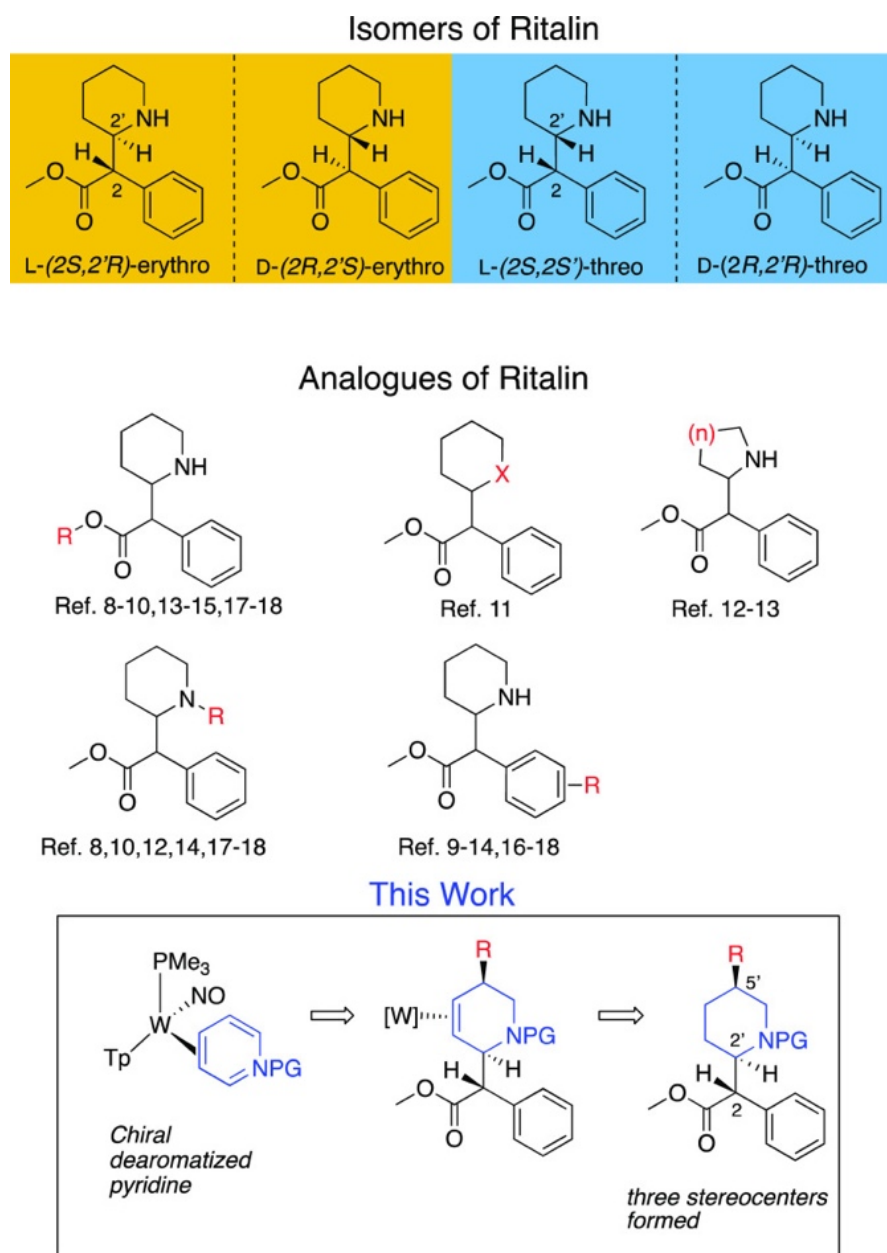


**Figure 2.1.** Two pairs of MPH diastereomers, previously reported analogues of MPH, and a proposed dearomatization approach to C5'- substituted MPH analogs.

therapeutics are lacking for cocaine addiction.<sup>4</sup> Methylphenidate (MPH), commercially known as Ritalin and prescribed extensively for treating attention deficit hyperactivity disorder (ADHD), behaves similarly to cocaine as a dopamine receptor agonist.<sup>5,6</sup> It is typically administered as a mixture of isomers, which consists of two diastereomers and their respective enantiomers (**Figure 2.1**). Numerous research groups have explored MPH analogues in hopes of identifying a compound that prevents cocaine from binding to the dopamine transporter (DAT) while allowing for the reuptake of dopamine.<sup>7</sup> Most of these studies confine the areas of structural diversity on the MPH scaffold to the ester, phenyl ring, piperidine nitrogen, or the heterocycle ring-size (**Figure 2.1**).<sup>8-18</sup> However, there appear to be no studies that incorporate functionality on the piperidine ring, largely owing to the lack of established general synthetic methods for such compounds. Herein we demonstrate an organometallic-based approach for synthesizing *erythro*-MPH analogues in which functionalized piperidyl variants are stereoselectively prepared from a chiral  $\eta^2$ -pyridine complex (**Figure 2.1**).

Previous work in our laboratory has demonstrated that highly functionalized tetrahydropyridines (THPs) can be synthesized stereoselectively from pyridine borane through its dihapto-coordination to  $\{\text{Wtp}(\text{NO})(\text{PMe}_3)\}$  (**Figure 2.2**; Tp = hydrotris-(pyrazolyl)borate).<sup>19,20</sup> The tungsten binds to C3 and C4 of the pyridine on either face of the ring, resulting in two “coordination diastereomers” (**1D**, **1P**). Their equilibrium ratio (cdr) is 3:1 favoring **1D**, with the nitrogen distal to the  $\text{PMe}_3$ . This complex can be converted to the pyridinium ( $\text{pyH}^+$ ) analogue via acetone and acid and then deprotonated in the presence of a protecting group (typically in the form of an anhydride), through which an array of protecting groups ( $\text{PG}^+$ ) can be added to the nitrogen (**2P**, **2D**; **Figure 2.2**). From this point, a range of different nucleophiles ( $\text{Nu}^{1-}$ ) can be added to C2 to generate dihydropyridine (DHP) complexes, which in turn can be protonated at C6' of the MPH core and then treated with a second nucleophile ( $\text{Nu}^{2-}$ ) at C5' to form THP complexes **3P** and **3D**. Oxidative decomplexation reveals *cis*-disubstituted THP products **4P** and **4D**. The two THP coordination diastereomers led to the same organic product under racemic conditions (**4P** = **4D**). However, if a single configuration of the tungsten complex was to be used, **4P** and **4D** would be enantiomers. Therefore, a high cdr of the pyridinium complex is essential if enantioenriched organic products are desired. Electron-withdrawing PGs have been shown to improve the cdr owing to a thermodynamic

preference of the complex to orient electron-deficient allylic carbons distal to the trimethylphosphine ligand.<sup>21</sup> They also render the C2 carbon more electrophilic, providing a broader range of possible nucleophiles. Our proposed strategy in preparing MPH derivatives was to install the methyl phenylacetate portion at C2 of a distal  $\eta^2$ -pyridine complex via a Reformatsky reaction, followed by elaboration of the resulting DHP to a *cis*-disubstituted THP or piperidine.

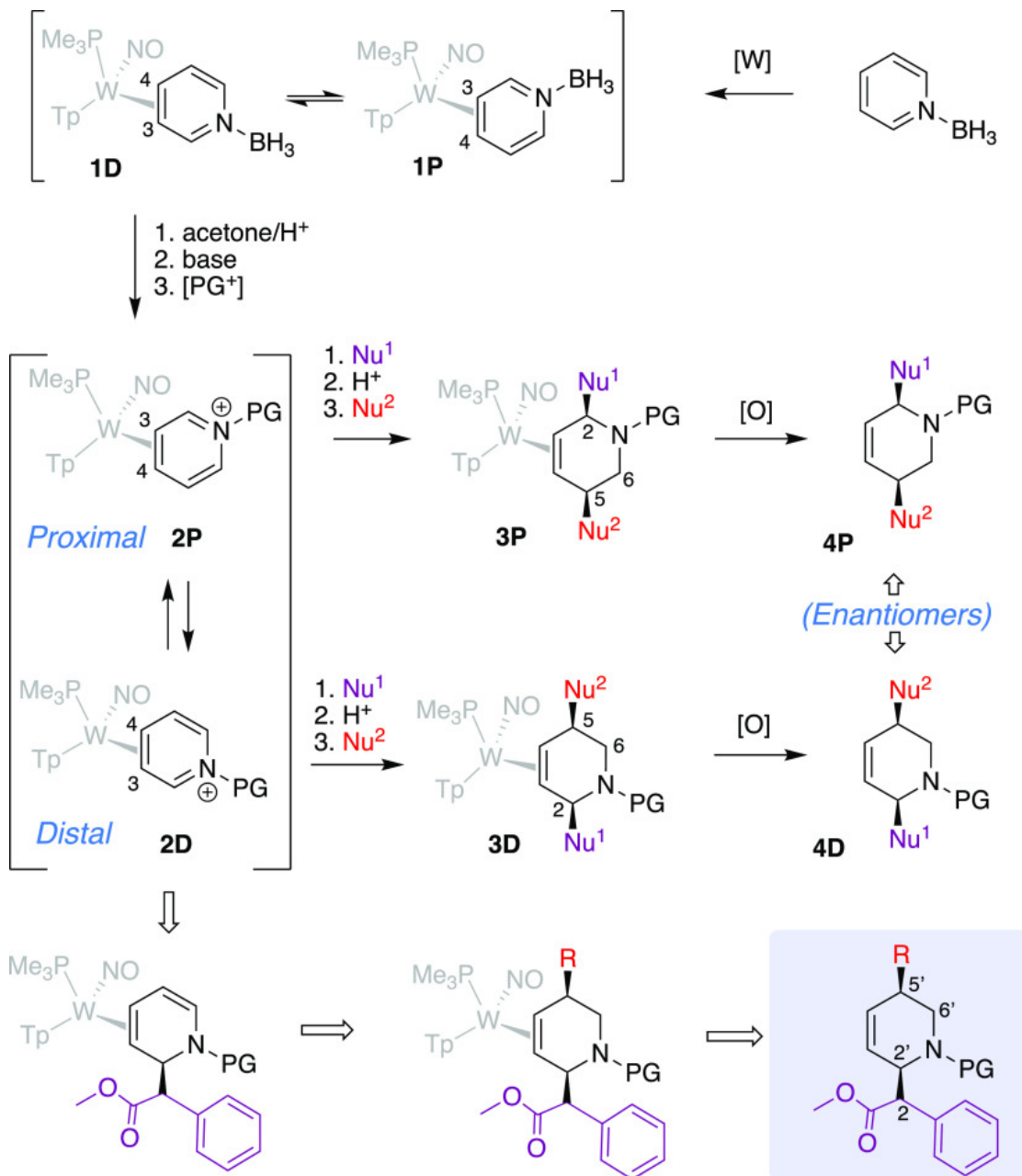


**Figure 2.2.** Tungsten-promoted dearomatization of pyridines and its proposed application to MPH analogues.

## 2.2 Results and Discussion

Previous studies exploring the tungsten-promoted dearomatization of pyridine utilized an acetyl protecting group (PG = Ac; **Figure 2.2**), where the corresponding pyridinium complex could be prepared in up to a 10:1 cdr mixture.<sup>22–24</sup> The *N*-acetyl-2-ethyl acetate-1,2-dihydropyridine complex **2D** was synthesized via a Reformatsky reaction between the corresponding pyridinium complex (**1**), methyl bromoacetate (MBA), and zinc.<sup>25</sup> Owing to the position of the metal, the addition cleanly occurs at C2, with no sign of competing C4 addition.<sup>26</sup> It was postulated that a similar strategy could be utilized to install the methyl phenylacetate moiety to the pyridinium core. However, the acetyl protecting group resulted in rotational isomers (~1:1) for all downstream complexes for this system due to hindered acetyl rotation,<sup>27</sup> and the Reformatsky reaction was not stereoselective (*erythro: threo* ratio: 1:1). Because comprehensive NMR analysis of these ~1:1:1:1 isomeric mixtures proved to be challenging, an alternative protecting group was sought. Given the broad use of sulfonamides in drug design,<sup>28</sup> we settled on a methanesulfonyl (mesyl or Ms) group to protect and activate the nitrogen. The reaction of mesyl anhydride in the presence of **1** and lutidine forms the new pyridinium complex **5**, and stirring the solution in an oil bath at 60 °C enriches the cdr from 3:1 to 10:1 as tracked by <sup>31</sup>P NMR. After the mixture was subjected to aqueous washes, coordination diastereomers **5D** and **5P** were precipitated in stirring diethyl ether. To our delight, triturating this powder mixture in ethyl acetate further enriched the cdr to >20:1 (**Figure 2.3**). Furthermore, any decomposition impurities are removed during this trituration, resulting in consistently clean and highly enriched material on a multigram scale.

### 2.2.1 Synthesis of Key DHP Complex

To ensure that the mesyl-substituted pyridinium complex (**5D**) behaved in a manner similar to the acetyl derivative,<sup>25</sup> a Reformatsky reaction with MBA was performed on **5D** resulting in the DHP complex **6D** (**Figure 2.3**). The structure was confirmed by 2D NMR analysis and single-crystal X-ray diffraction (SC-XRD). Under similar reaction conditions, **5D** smoothly undergoes a Reformatsky addition with methyl  $\alpha$ -phenyl bromoacetate (MAPBA) to produce a DHP complex (**7D**). Incorporation of the methyl phenyl ester moiety occurs exclusively *anti* to the metal at C2 of the pyridine ring. However, the product is formed as a 3:1 *erythro: threo* mixture of diastereomers. We

found that trituration in methanol followed by trituration in dimethoxy- ethane (DME) enriches the dr from 3:1 to >20:1. Whereas methanol trituration removes decomposition impurities, isomeric enrichment occurs during the DME trituration (Supporting Information). SC-XRD data were obtained for the *erythro* diastereomer (*erythro*-7D; **Figure 2.4**); however, to confirm the stereochemistry of the bulk material, NOE data were considered along with a DFT analysis. Calculations were performed using the M06 functional alongside a split basis set with LANL2DZ applied to tungsten and 6-31G(d,p) on all main group atoms for optimizations to the lowest energy conformations of the

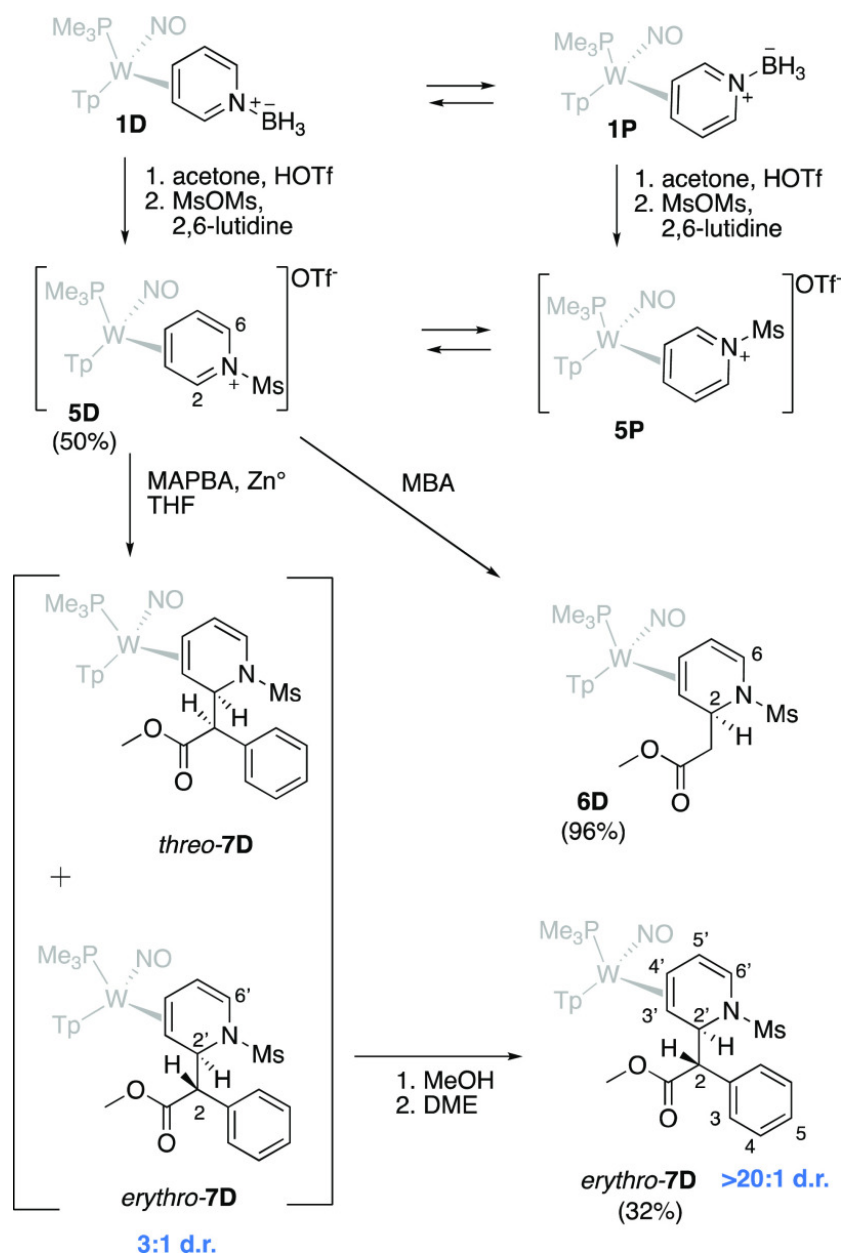


**Figure 2.3.** Synthesis of a key DHP precursor (*erythro*-7D) to piperidine analogs of MPH.

two diastereomers (Supporting Information). Hydrogen–hydrogen distances were determined and compared to experimental nuclear Overhauser effect spectroscopy (NOESY) data of a 3:1 dr sample, and several unique interactions were identified. The distance between H2 and H9 was 2.82 Å in the *erythro* diastereomer and 4.34 Å in the *threo* complex. Additionally, the distances between H7 and H4/H5 were 3.16 Å/3.51 Å in the *erythro* isomer and 4.10 Å/5.34 Å for *threo*. NOESY spatial interactions were present between H2'-H3, H2-H4', and H2-H5' in the major complex but absent in the minor complex (Supporting Information). Collectively, these observations support the hypothesis that the *erythro* diastereomer (*erythro*-**7D**) is the major complex, while the *threo* (*threo*-**7D**) diastereomer is the minor. The addition of the methyl phenyl ester moiety can be performed on a multigram scale (overall yield of 22% from **1D**; 2–3 g), resulting in a pure *erythro* methyl phenyl ester DHP complex (*erythro*-**7D**; dr > 20:1) without chromatography. We note that, while the *threo* isomer of MPH is most biologically active,<sup>5,6</sup> this is not necessarily the case for its derivatives,<sup>8–18</sup> so we continued our study with the high purity *erythro* isomer **7D**.

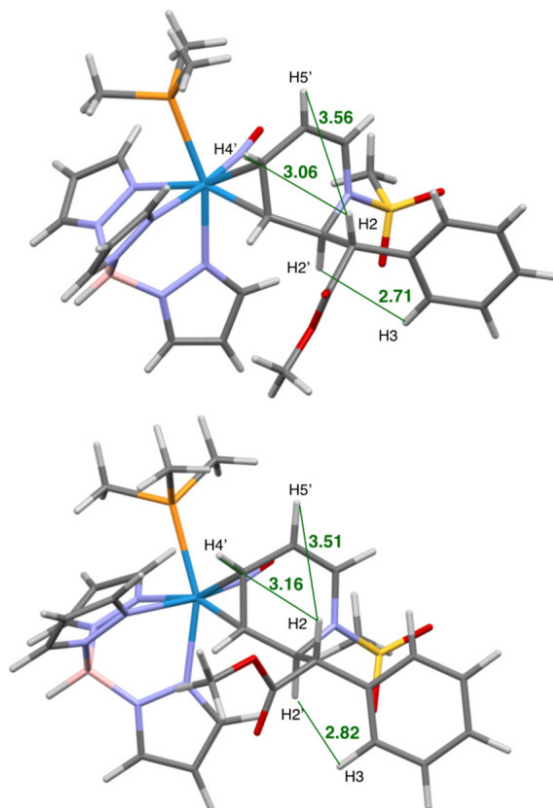


**Figure 2.4.** Molecular structure determination of *erythro*-**7D** from SCXRD (top) and DFT calculation (bottom).

### 2.2.2 Preparing a Library of THP Complexes

*Erythro-7D* could be protonated at C6' by triflic acid in propionitrile to form a single isomer of the allyl complex (**8P**, **Figure 2.5**). We note here that tungsten backbonding directs the proton to C6', rather than C5', the expected site of protonation for an organic enamide.<sup>22</sup> Precipitation was then induced by adding the solution to stirring ether to form a readily isolable powder. Previous studies have demonstrated how  $\pi$ -allyl complexes of {WTP(NO)(PMe<sub>3</sub>)} are hyperdistorted.<sup>21</sup> They are described herein as dihapto-coordinated with the central allylic carbon and one terminal carbon tightly bound to the tungsten and the other terminally bound carbon loosely coordinated (the carbenium-like carbon). DFT calculations indicate that for  $\eta^2$ -allyl complexes of {WTP(NO)(PMe<sub>3</sub>)}<sup>21</sup> there is a significant thermodynamic preference for placing the carbenium carbon distal to the trimethylphosphine ligand. Accordingly, NOESY shows a prominent interaction between the C6' methylene protons and trimethylphosphine ligand, indicating that **8P** is the thermodynamically favored allyl conformer. This is further supported by SC-XRD, which revealed that **8P** is the conformation present in the solid state (**Figure 2.6**). Yet nucleophilic attack is observed to occur at C5' (vide infra), indicating an allyl conformational shift to **8D** prior to nucleophilic addition.

With the goal of demonstrating modular diversity that would be amenable to forming combinatorial libraries, we explored the reactivity of allyl complex **8D** with various nucleophiles. *cis*-5-Substituted-2-(methyl phenylester)-1,2,5,6-tetrahydropyridine (THP) complexes (**Figure 2.5**) were formed in solution and then precipitated in stirring chilled hexanes or pentanes. The nucleophiles in **Table 2.1** were chosen to exemplify the broad compatibility of the metal complex with various classes of nucleophile and to demonstrate the potential of this methodology to directly access a wide range of functional groups. These nucleophiles, which include hydride, cyanide, enolates, Grignard reagents, amines, amides, imides, and thiols, can be added to isolated allyl complex **8D** or added in a one-pot reaction following the protonation of *erythro-7D*. Despite the preference of the carbenium to be distal to the PMe<sub>3</sub> (**8P**), all of these nucleophiles add to C5 exclusively via the minor conformer of the allyl species (**8D**). In all cases, there is a high stereochemical preference for the addition *anti* to the metal, as is indicated by SC-XRD and NOESY data (Supporting Information).

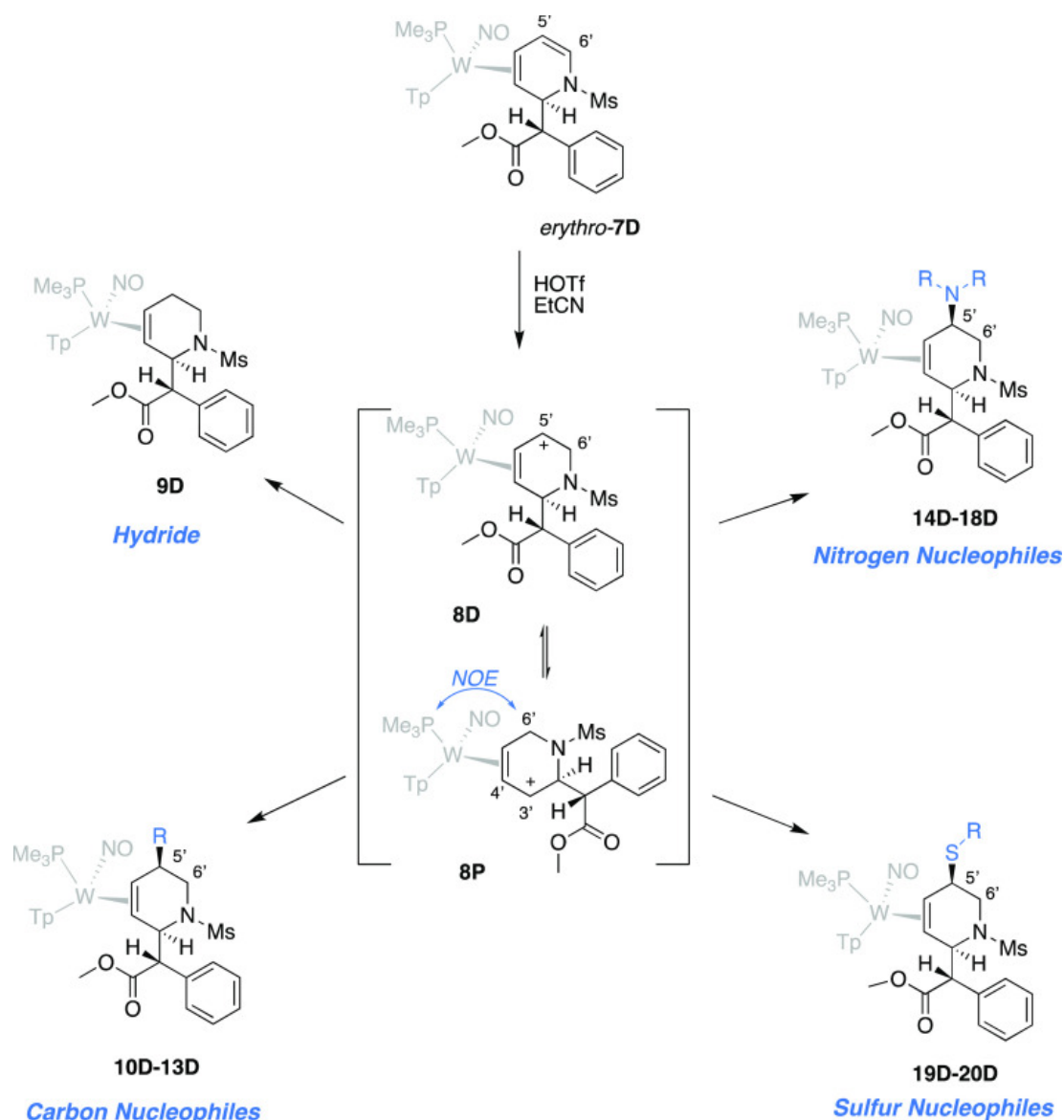


**Figure 2.5.** Synthesis of THP precursors to MPH derivatives.

While the parent THP complex (**9D**) was synthesized via the addition of sodium cyanoborohydride at  $-50\text{ }^{\circ}\text{C}$ , the addition of **8** to a lithium dimethyl malonate solution provided **10D**. Similarly, an allyl **8** solution was added to a cooled methanol solution ( $-50\text{ }^{\circ}\text{C}$ ) containing sodium cyanide to form **11D**. Malononitrile was also added successfully (**12D**) by combining cooled solutions of allyl **8** and deprotonated malononitrile. Grignard reagents are also compatible nucleophiles: Successful addition of  $\text{MeMgBr}$  occurs after reacting chilled reactants at  $-60\text{ }^{\circ}\text{C}$  for 60 h to form **13D**. Both aliphatic amines and amides can be incorporated, as well as N-heterocycles: Tryptamine addition (addition at primary amine) was achieved by combining it with potassium *tert*-butoxide and



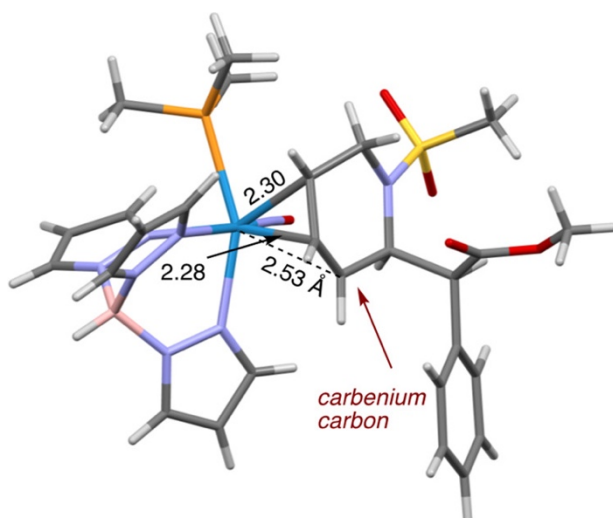


**Figure 2.6.** Molecular structure determination for  $\eta^2$ -allyl complex 8P showing carbenium carbon distal to the  $\text{PMe}_3$ .

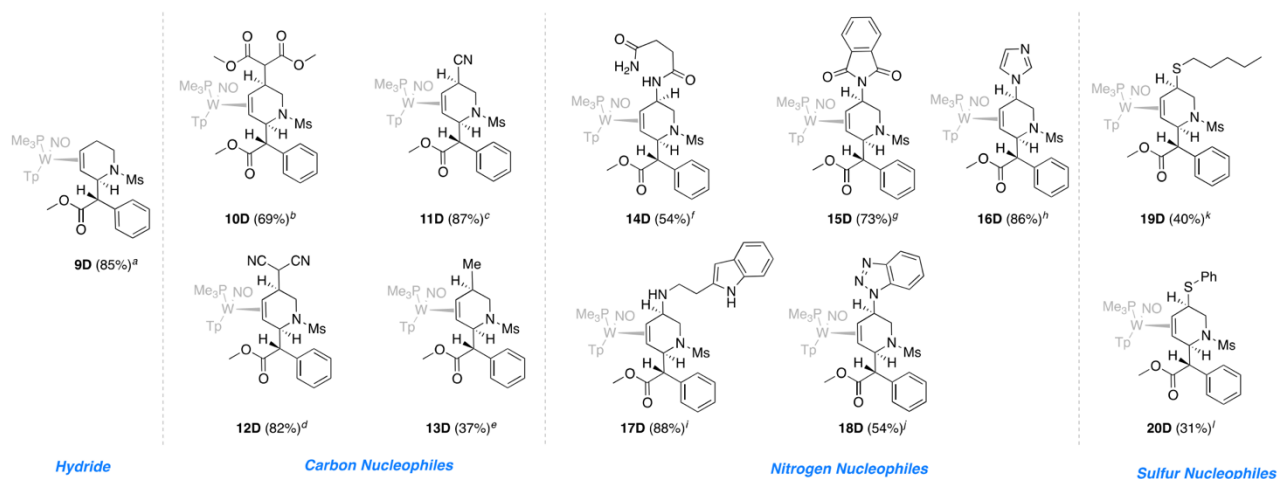


**Table 2.1.** <sup>a</sup>Step 1: **7D**, HOTf, 25°C; Step 2:  $\text{NaCNBH}_3$ , -50°C. <sup>b</sup>Step 1: **7D**, HOTf, 25°C; Step 2:  $\text{LiCH}(\text{CO}_2\text{Me})_2$ , -10°C. <sup>c</sup>Step 1: **7D**, HOTf, 25°C; Step 2:  $\text{NaCN}$ , -40°C. <sup>d</sup>Step 1: **7D**, HOTf, 25°C; Step 2:  $(\text{CN})_2\text{CH}_2$ ,  $\text{KOtBu}$ , 0°C. <sup>e</sup>**8**,  $\text{MeMgBr}$ , -60°C. <sup>f</sup>**8**, succinamide,  $\text{nBuLi}$ , -60°C. <sup>g</sup>Step 1: **7D**, HOTf, 25°C; Step 2: phthalimide,  $\text{KOtBu}$ , -60°C. <sup>h</sup>Step 1: **7D**, HOTf, 25°C; Step 2: imidazole,  $\text{KOtBu}$ , -30°C. <sup>i</sup>Step 1: **7D**, HOTf, 25°C; Step 2: tryptamine,  $\text{KOtBu}$ , -50°C. <sup>j</sup>Step 1: **7D**, HOTf, 25°C; Step 2: benzotriazole,  $\text{KOtBu}$ , -40°C. <sup>k</sup>Step 1: **7D**, HOTf, 25°C; Step 2: pentanethiol,  $\text{KOtBu}$ , -50°C. <sup>l</sup>Step 1: **7D**, HOTf, 25°C; Step 2: thiophenol,  $\text{KOtBu}$ , -40°C.

a solution of **8** to form **17D**. Similarly, **14D** was prepared by adding a solution of **8** to a solution of succinamide and base. Benzotriazole was treated with potassium *t*-butoxide and cooled before the addition of allyl complex **8**, to form **18D**. Phthalimide (**15D**) and imidazole (**16D**) followed a similar reaction course. Finally, thiol additions were accomplished using pentanethiol (**19D**) or thiophenol (**20D**) and base. Despite the

presence of strong acid and base in these reactions, the diastereomeric enrichment of these compounds is retained throughout the syntheses, resulting in THP complexes with diastereomeric ratios of >20:1. THP complexes are produced in yields ranging from 31 to 88% and were characterized by multiple spectroscopic techniques including  $^1\text{H}$  NMR,  $^{13}\text{C}$  NMR, 2D-NMR, and IR, as well as being characterized by SC-XRD, HRMS, and cyclic voltammetry.

### 2.2.3 Releasing the THP from the Metal

The functionalized THPs can be liberated by oxidation of the metal center. As an example, 9D undergoes chemical oxidation with four equivalents of DDQ in acetone, and subsequent chromatography results in purified THP organic (**21**). Incomplete oxidation was observed via  $^1\text{H}$  NMR when less than four equivalents were used. We attribute this to metal decomposition products undergoing multiple oxidation events, thus necessitating a greater amount of oxidant. Similarly, **22–25** were also oxidatively liberated via DDQ. All organics (**Figure 2.7**) were recovered through extraction or purified via chromatography. Similar procedures to those described above provided routes to both *N*-tosylated and *N*-acetylated variations of THP MPH derivatives (Supporting Information). As with the mesylated analogs, the Reformatsky reaction occurred with low stereoselectivity. Two examples of the parent methyl phenyl acetate THP (**21-Ac** and **21-Ts**) were prepared and are included in **Figure 2.7** for comparison.<sup>25,26</sup>

### 2.2.4 Hydrogenation of the THP to Piperidine

As a demonstration of the ability to generate the corresponding piperidines from THPs such as those reported in **Figure 2.7**, THP **21-Ms** was reduced to its saturated analogue (**26**) through hydrogenation. Using 5% Pd on activated carbon catalyst, the hydrogenation of **21-Ms** was carried out at 50 °C under 25 bar (~360 psi) of  $\text{H}_2$  (**Figure 2.8**). Complete conversion to the reduced form (**26**) occurred after 5 h. However, prematurely arresting the reaction revealed the presence of an intermediate (**21'**; Supporting Information). 2D NMR analysis indicated that this compound was likely a constitutional isomer of THP **21-Ms** in which the alkene has migrated to form the “enamide” **21'** (**Figure 2.8**). Similar

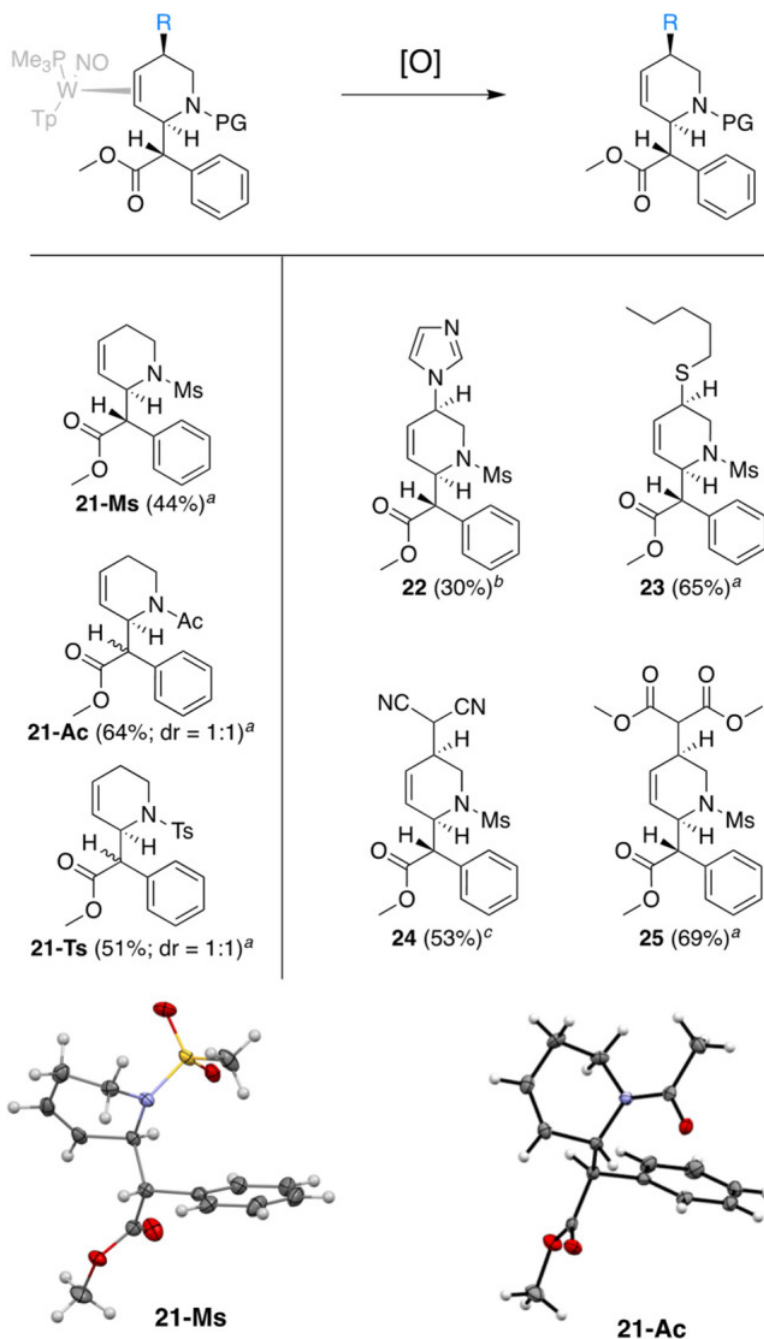


**Figure 2.7.** Oxidative decomplexation of THP compounds 21–25. <sup>a</sup>DDQ, 25 °C. <sup>b</sup>DDQ, HOTf, –40 °C. <sup>c</sup>CAN, 25 °C.

palladium-catalyzed isomerizations have been reported for other THPs and for a 3-pyrrolene, in which an enamide (2-pyrrolene) was formed.<sup>29–31</sup> As anticipated, further reduction of the mixture of **26** and **21'** resulted in complete conversion to the piperidine **26**. The structure of **26** was confirmed via SC-XRD. Compound **25** was also hydrogenated to **27** under identical conditions as confirmed by SC-XRD. Of note, Ellman et al. have

shown the value of 3,4-THPs as precursors to highly functionalized, oxygenated piperidines.<sup>32</sup> Several procedures have been published for removal of the mesyl group from secondary amines, but we have not explored this aspect in any detail.<sup>33–35</sup>

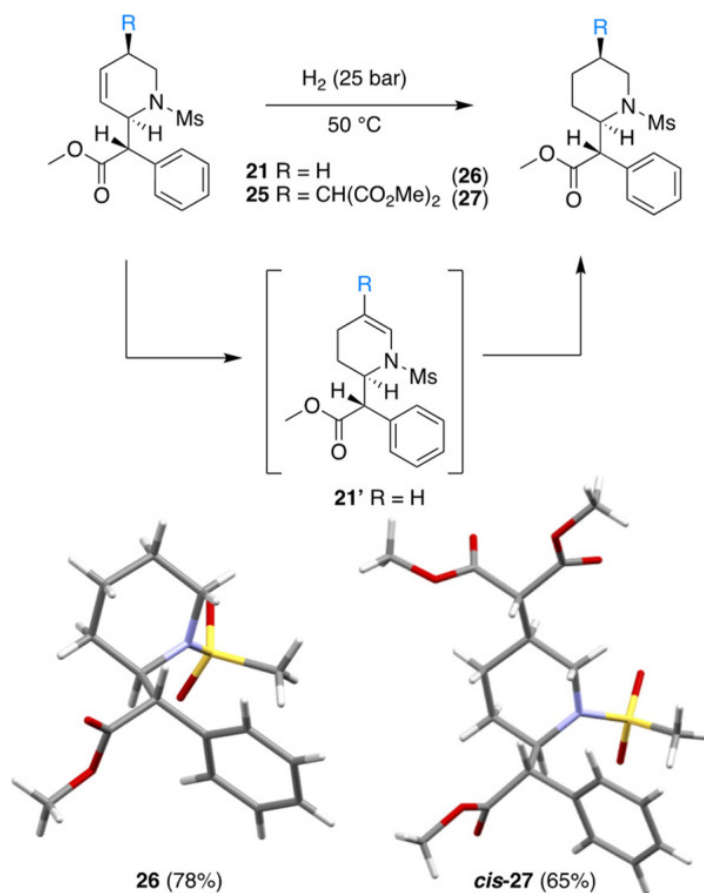


**Figure 2.8.** Hydrogenations of MPH and THP organics were performed to form the corresponding *erythro* MPH analogue. The presence of the *trans* isomer is attributed to an observed enamine intermediate formed from a Pd-promoted alkene isomerization.

### 2.2.5 Enantioenriched THP's

We next explored the possibility of using the methodology outlined above to obtain enantioenriched compounds. Previously, Lankenau et al. developed a general procedure for the resolution of WTP(NO)(PMe<sub>3</sub>)( $\eta^2$ -1,3-dimethoxybenzene) enantiomers,<sup>36</sup> and this process has since been modified and optimized.<sup>37</sup> The procedure resolves the *S* and *R* hands of the metal by protonating the corresponding racemic dimethoxybenzene complex with L-dibenzoyl tartaric acid (L-DBTH<sub>2</sub>) and then physically separating the resulting diastereomer salts based on their solubility differences. This robust approach allows for enriched samples of either hand on a gram scale, with ee's from 80 to 95+%, and the dimethoxybenzene ligand can be replaced with other

aromatic molecules (e.g., benzene, anisole) with complete retention of the metal stereocenter. Applying this technique to pyridines introduced several challenges. Synthesizing the pyridine borane **1** in an enantioenriched form required the deprotonation of  $[(R)\text{-WTP}(\text{NO})(\text{PMe}_3)(\eta^2\text{-dimethoxybenzenium})](\text{L-DBTH})$  (**29D**; dr  $\approx 10:1$ ) to generate an exchange-labile precursor (**28**; **Figure 2.9**). Deprotonation was conducted with basic alumina (owing to its ease of separation) in THF, and  $(R)\text{-WTP}(\text{NO})\text{-}(\text{PMe}_3)(\eta^2\text{-dimethoxybenzene})$  (**28**) was then precipitated with stirring hexanes. This compound was then combined with pyridine borane (30 equiv) and TEA (1.5 equiv) for 36 h. The workup

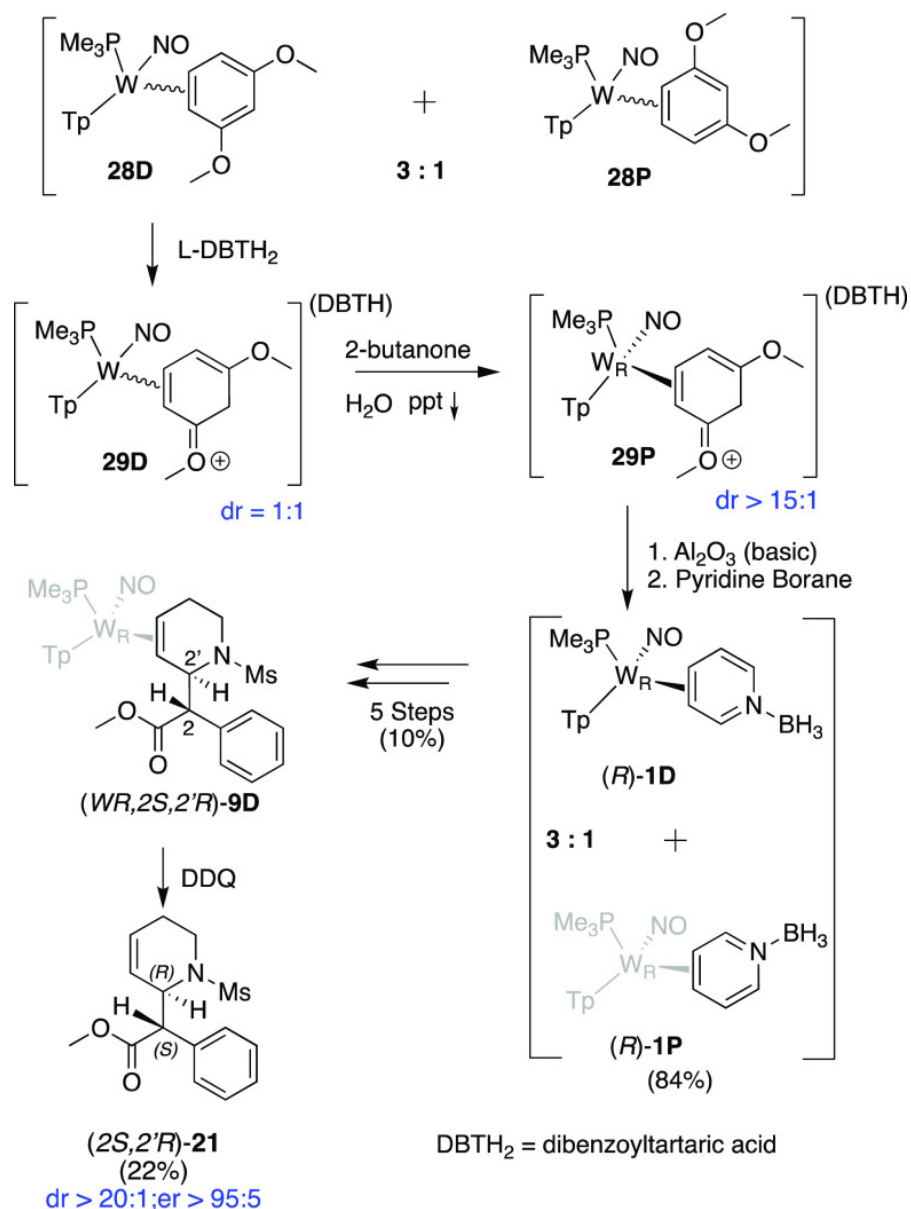


**Figure 2.9.** Preparation of enantioenriched MPH analog.

for this reaction was identical to the previously published version.<sup>19</sup> This enantioenriched (*R*)-**1** was then subjected to deprotection, mesylation, and Reformatsky addition (vide supra). However, the tandem methanol/DME triturations failed to clean and enrich the dr of (*WR,2S,2'R*)-**7D**, which, as in the racemic preparation, was present as a 3:1 mixture of isomers. This apparent difference in diastereomer solubilities was attributed to the enantioenriched **7D** crystallizing in a different space group than does racemic **7D**. The racemic material crystallizes from dimethoxyethane in the space group  $P\bar{1}$ , which, being centrosymmetric, requires both hands of the complex to be present in equal amounts. We found that purifying (*WR,2S,2'R*)-**7D** via a basic alumina column and tritulating the precipitated complex in ethanol improves the dr to >20:1. Clean (*WR,2S,2'R*)-**7D** was then protonated under conditions identical to the conditions used for the racemic mixture to form (*WR,2S,2'R*)-**8**. This compound was then converted to (*WR,2S,2'R*)-**9D** and the desired organic (*2S,2'R*)-**21** was then oxidatively liberated from the metal with DDQ. The ee of the free organic was determined by chiral HPLC to be >95:5 (Supporting Information). Notably, this compound has the configuration at C2' (*R*) that matches the desired D enantiomer of *threo*-MPH, and procedures have been developed by Novartis to convert (*2S,2'R*)-*erythro*-MPH to the desired (*2R,2'R*)-MPH (*D-threo*) in alkaline solution.<sup>38</sup> Of the numerous derivatives of MPH that have appeared in the academic and patent literature,<sup>8–18</sup> remarkably few have a substituent on a saturated piperidine ring.

Of those few examples that have been reported, most are prepared from piperidines or piperidones via the C–H activation and addition of the phenylacetate group adjacent to the ring nitrogen by a rhodium catalyst.<sup>39</sup> Although there do not appear to be examples of C5'-substituted MPH analogs prepared from this method, such an approach may be viable, but controlling stereochemistry would be challenging. It seems that the most general method for preparing such analogs would be from the hydrogenation of pyridine precursors. While hydrogenations of pyridines and pyridinium salts are well established<sup>40–42</sup> and have been used to prepare the parent MPH,<sup>43</sup> such an approach has not been applied to MPH analogs in which the piperidine was functionalized.

## 2.3 Conclusions

This study describes a methodology capable of accessing piperidine-functionalized *N*-mesyl *erythro* methylphenidate analogues with high degrees of regioselectivity, stereoselectivity, and functional group tolerance. A Reformatsky reaction involving a

{WTP(NO)(PMe<sub>3</sub>)} *N*-mesyl pyridinium complex and  $\alpha$ -phenylmethyl bromoacetate yields an *erythro* methylphenidate DHP complex, which is enriched to a dr of >20:1 through triturations. After the formation of an allyl complex, the successful incorporation of nucleophiles to form tetrahydropyridine complexes with high diastereoselectivity includes cyanide, malononitrile, dimethyl malonate, Grignard reagents, amines amides, imides, and thiols. This strategy provides access to a wide range of MPH analogues functionalized at the C5'-position on the piperidine ring that would be difficult to access via conventional methods. Furthermore, the ubiquity of the piperidine scaffold within small-molecule drugs underscores the potential utility of this system, which rapidly incorporates a broad range of functional groups and nucleophile types into piperidine cores. Efforts continue on developing a fully stereoselective Reformatsky reaction with an  $\eta^2$ -pyridinium system that would directly lead to the *threo* diastereomer family of C5-substituted MPHs, which, at least for the parent, is the most biologically potent.<sup>44</sup>

## References

- (1) U.S. Overdose Deaths In 2021 Increased Half as Much as in 2020 - But Are Still Up 15%. [https://www.cdc.gov/nchs/pressroom/nchs\\_press\\_releases/2022/202205.htm](https://www.cdc.gov/nchs/pressroom/nchs_press_releases/2022/202205.htm). Access date: 07/31/**2023**.
- (2) Ferri, M.; Minozzi, S.; Bo, A.; Amato, L. Slow-release oral morphine as maintenance therapy for opioid dependence. *Cochrane Database Syst. Rev.* 2013, **2013** (6), No. CD009879.
- (3) Whelan, P. J.; Remski, K. Buprenorphine vs methadone treatment: A review of evidence in both developed and developing worlds. *J. Neurosci Rural Practice* **2012**, 3 (1), 45–50.
- (4) Stotts, A. L.; Dodrill, C. L.; Kosten, T. R. Opioid dependence treatment: options in pharmacotherapy. *Expert Opin Pharmacother.* **2009**, 10 (11), 1727–1740.
- (5) Negus, S. S.; Henningfield, J. Agonist Medications for the Treatment of Cocaine Use Disorder. *Neuropsychopharmacology* **2015**, 40 (8), 1815–25.
- (6) Ritz, M. C.; Lamb, R. J.; Goldberg, S. R.; Kuhar, M. J. Cocaine receptors on dopamine transporters are related to self-administration of cocaine. *Science* **1987**, 237 (4819), 1219–23.
- (7) Deutsch, H. M.; Shi, Q.; Gruszecka-Kowalik, E.; Schweri, M. M. Synthesis and pharmacology of potential cocaine antagonists. 2. Structure-activity relationship studies of aromatic ring-substituted methylphenidate analogs. *J. Med. Chem.* **1996**, 39 (6), 1201–9.
- (8) Kim, D. I.; Deutsch, H. M.; Ye, X.; Schweri, M. M. Synthesis and pharmacology of site-specific cocaine abuse treatment agents: restricted rotation analogues of methylphenidate. *J. Med. Chem.* **2007**, 50 (11), 2718–31.
- (9) Froimowitz, M.; Gu, Y.; Dakin, L. A.; Kelley, C. J.; Parrish, D.; Deschamps, J. R. Vinylogous amide analogs of methylphenidate. *Bioorg. Med. Chem. Lett.* **2005**, 15 (12), 3044–7.
- (10) Froimowitz, M.; Gu, Y.; Dakin, L. A.; Nagafuji, P. M.; Kelley, C. J.; Parrish, D.; Deschamps, J. R.; Janowsky, A. Slow-onset, long- duration, alkyl analogues of methylphenidate with enhanced selectivity for the dopamine transporter. *J. Med. Chem.* **2007**, 50 (2), 219–32.
- (11) Davies, H. M.; Hopper, D. W.; Hansen, T.; Liu, Q.; Childers, S.R. Synthesis of methylphenidate analogues and their binding affinities at dopamine and serotonin



transport sites. *Bioorg. Med. Chem. Lett.* **2004**, 14 (7), 1799–802.

(12) Axten, J. M.; Krim, L.; Kung, H. F.; Winkler, J. D. A stereoselective synthesis of dl-threo-methylphenidate: Preparation and biological evaluation of novel analogues. *J. Org. Chem.* **1998**, 63 (26), 9628–9629.

(13) Meltzer, P. C.; Wang, P.; Blundell, P.; Madras, B. K. Synthesis and evaluation of dopamine and serotonin transporter inhibition by oxacyclic and carbacyclic analogues of methylphenidate. *J. Med. Chem.* **2003**, 46 (8), 1538–45.

(14) Schweri, M. M.; Deutsch, H. M.; Massey, A. T.; Holtzman, S. G. Biochemical and behavioral characterization of novel methylphenidate analogs. *J. Pharmacol Exp Ther* **2002**, 301 (2), 527–35.

(15) Casiraghi, A.; Longhena, F.; Straniero, V.; Faustini, G.; Newman, A. H.; Bellucci, A.; Valoti, E. Design and Synthesis of Fluorescent Methylphenidate Analogues for a FRET-Based Assay of Synapsin III Binding. *ChemMedChem.* **2020**, 15 (14), 1330–1337.

(16) Liu, W.; Babl, T.; Rother, A.; Reiser, O.; Davies, H. M. L. Functionalization of Piperidine Derivatives for the Site-Selective and Stereoselective Synthesis of Positional Analogues of Methylphenidate. *Chemistry* **2020**, 26 (19), 4236–4241.

(17) Wayment, H. K.; Deutsch, H.; Schweri, M. M.; Schenk, J. O. Effects of methylphenidate analogues on phenethylamine substrates for the striatal dopamine transporter: Potential as amphetamine antagonists? *J. Neurochem* **1999**, 72 (3), 1266–1274.

(18) Carroll, F. I.; Howell, L. L.; Kuhar, M. J. Pharmacotherapies for treatment of cocaine abuse: preclinical aspects. *J. Med. Chem.* **1999**, 42 (15), 2721–36.

(19) Harrison, D. P.; Welch, K. D.; Nielander, A. C.; Sabat, M.; Myers, W. H.; Harman, W. D. Efficient synthesis of an  $\eta^2$ -pyridine complex and a preliminary investigation of the bound heterocycle's reactivity. *J. Am. Chem. Soc.* **2008**, 130 (50), 16844–5.

(20) Welch, K. D.; Harrison, D. P.; Lis, E. C.; Liu, W. J.; Salomon, R. J.; Harman, W. D.; Myers, W. H. Large-scale syntheses of several synthons to the dearomatization agent {TpW(NO)(PMe<sub>3</sub>)} and convenient spectroscopic tools for product analysis. *Organometallics* **2007**, 26 (10), 2791–2794.

(21) Harrison, D. P.; Nielander, A. C.; Zottig, V. E.; Strausberg, L.; Salomon, R. J.; Trindle, C. O.; Sabat, M.; Gunnoe, T. B.; Iovan, D. A.; Myers, W. H.; Harman, W. D. Hyperdistorted Tungsten Allyl Complexes and Their Stereoselective Deprotonation to Form Dihapto-Coordinated Dienes. *Organometallics* **2011**, 30 (9),

2587–2597.

- (22) Harrison, D. P.; Sabat, M.; Myers, W. H.; Harman, W. D. Polarization of the pyridine ring: highly functionalized piperidines from tungsten-pyridine complex. *J. Am. Chem. Soc.* **2010**, *132* (48), 17282–95.
- (23) Harrison, D. P.; Kosturko, G. W.; Ramdeen, V. M.; Nielander, A. C.; Payne, S. J.; Sabat, M.; Myers, W. H.; Harman, W. D. Tungsten- Promoted Pyridine Ring Scission: The Selective Formation of  $\eta^2$ - Cyanine and  $\eta^2$ -Merocyanine Complexes and Their Derivatives. *Organometallics* **2010**, *29* (8), 1909–1915.
- (24) Kosturko, G. W.; Harrison, D. P.; Sabat, M.; Myers, W. H.; Harman, W. D. Selectfluor-mediated dialkoxylation of tungsten  $\eta^2$ - pyridinium complexes. *Organometallics* **2009**, *28* (2), 387–389.
- (25) Harrison, D. P.; Zottig, V. E.; Kosturko, G. W.; Welch, K. D.; Sabat, M.; Myers, W. H.; Harman, W. D. Stereo- and Regioselective Nucleophilic Addition to Dihapto-Coordinated Pyridine Complexes. *Organometallics* **2009**, *28* (19), 5682–5690.
- (26) Wilde, J. H. Synthetic Applications of Molybdenum and Tungsten Dearomatization Agents. Ph. D. Dissertation, University of Virginia, **2020**.
- (27) Wilde, J. H.; Dickie, D. A.; Harman, W. D. A Highly Divergent Synthesis of 3-Aminotetrahydropyridines. *J. Org. Chem.* **2020**, *85* (12), 8245–8252.
- (28) Zhao, C.; Rakesh, K. P.; Ravidar, L.; Fang, W. Y.; Qin, H.-L. Pharmaceutical and medicinal significance of sulfur (SVI)-Containing motifs for drug discovery: A critical review. *Eur. J. Med. Chem.* **2019**, *162*, 679–734.
- (29) Wanner, K.; Kärtner, A. Isomerization of N-Acyl-1,2,5,6- Tetrahydropyridines to N-Acyl-Enamines by Palladium on Carbon. *Heterocycles* **1987**, *26*, 917–919.
- (30) Kim, S. Y.; Kim, K. H.; Moon, H. R.; Kim, J. N. Synthesis of Tetrahydropyridines from Morita-Baylis-Hillman Acetates of  $\alpha,\beta$ - Unsaturated Aldehydes Via an Intramolecular 1,6-Conjugate Addition. *Bulletin of the Korean Chemical Society* **2016**, *37* (1), 95–98.
- (31) Sonesson, C.; Larhed, M.; Nyqvist, C.; Hallberg, A. Regiochemical Control and Suppression of Double Bond Isomerization in the Heck Arylation of 1-(Methoxycarbonyl)-2,5-dihydropyrrole. *J. Org. Chem.* **1996**, *61* (14), 4756–4763.
- (32) Chen, S.; Mercado, B. Q.; Bergman, R. G.; Ellman, J. A. Regio- and Diastereoselective Synthesis of Highly Substituted, Oxygenated Piperidines from Tetrahydropyridines. *J. Org. Chem.* **2015**, *80* (13), 6660–6668.

- (33) Naito, H.; Hata, T.; Urabe, H. Selective Deprotection of Selective Deprotection of Methanesulfonamides to Amines. *Org. Lett.* **2010**, *12* (6), 1228–1230.
- (34) Sabitha, G.; Reddy, B. V. S.; Abraham, S.; Yadav, J. S. Deprotection of sulfonamides using iodotrimethylsilane. *Tetrahedron Lett.* **1999**, *40* (8), 1569–1570.
- (35) Javorskis, T.; Orentas, E. Chemoselective Deprotection of Sulfonamides Under Acidic Conditions: Scope, Sulfonyl Group Migration, and Synthetic Applications. *J. Org. Chem.* **2017**, *82* (24), 13423–13439.
- (36) Lankenau, A. W.; Iovan, D. A.; Pienkos, J. A.; Salomon, R. J.; Wang, S.; Harrison, D. P.; Myers, W. H.; Harman, W. D. Enantioenrichment of a tungsten dearomatization agent utilizing chiral acids. *J. Am. Chem. Soc.* **2015**, *137* (10), 3649–55.
- (37) Wilson, K. B.; Smith, J. A.; Nedzbala, H. S.; Pert, E. K.; Dakermanji, S. J.; Dickie, D. A.; Harman, W. D. Highly Functionalized Cyclohexenes Derived from Benzene: Sequential Tandem Addition Reactions Promoted by Tungsten. *J. Org. Chem.* **2019**, *84* (10), 6094–6116.
- (38) Prashad, M. Approaches to the Preparation of Enantiomerically Pure (2R,2'R)-(+)-threo-Methylphenidate Hydrochloride. *Advanced Synthesis & Catalysis* **2001**, 343, 379–392.
- (39) Davies, H. M.; Venkataramani, C.; Hansen, T.; Hopper, D. W. New strategic reactions for organic synthesis: catalytic asymmetric C-H activation alpha to nitrogen as a surrogate for the Mannich reaction. *J. Am. Chem. Soc.* **2003**, *125* (21), 6462–8.
- (40) Chang, M.; Huang, Y.; Liu, S.; Chen, Y.; Krska, S. W.; Davies, I. W.; Zhang, X. Asymmetric hydrogenation of pyridinium salts with an iridium phosphole catalyst. *Angew. Chem., Int. Ed. Engl.* **2014**, *53* (47), 12761–4.
- (41) Huang, W. X.; Yu, C. B.; Ji, Y.; Liu, L. J.; Zhou, Y. G. Iridium- Catalyzed Asymmetric Hydrogenation of Heteroaromatics Bearing a Hydroxyl Group, 3-Hydroxypyridinium Salts. *ACS Catal.* **2016**, *6* (4), 2368–2371.
- (42) Wang, D. S.; Chen, Q. A.; Lu, S. M.; Zhou, Y. G. Asymmetric hydrogenation of heteroarenes and arenes. *Chem. Rev.* **2012**, *112* (4), 2557–90.
- (43) Patrick, K. S.; Kilts, C. D.; Breese, G. R. Synthesis and pharmacology of hydroxylated metabolites of methylphenidate. *J. Med. Chem.* **1981**, *24* (10), 1237–40.
- (44) Heal, D. J.; Pierce, D. M. Methylphenidate and its isomers: their role in the treatment of attention-deficit hyperactivity disorder using a transdermal delivery system. *CNS Drugs* **2006**, *20* (9), 713–38.

**Chapter 3:**  
**Dihapto-Coordinated Conjugated Carbocycles ( $\eta^2\text{-C}_n\text{H}_n$   $n = 5\text{-}8$ ):**  
**Blurring the line between aromatic and antiaromatic hydrocarbons**

### 3.1 Introduction

Over the past two decades, the  $\pi$ -base  $\{\text{WTp}(\text{NO})(\text{PMe}_3)\}$  has been shown to have the unusual ability to dearomatize benzenes through the coordination of two carbons ( $\eta^2$ ).<sup>78, 79</sup> Such binding renders the *uncoordinated* portion of the arene similar to a conjugated diene, both structurally and chemically. This feature has been used to actualize a wide variety of chemical transformations that are inaccessible by conventional organic methodologies. Through strong  $\pi$ -donation, the tungsten complex activates the benzene toward the addition of electrophiles and subsequently stabilizes the resulting arenium intermediates, thereby enabling the addition of nucleophiles. The resulting  $\eta^2$ -diene complexes can be treated sequentially with a second electrophile and nucleophile to provide 1,4-disubstituted cyclohexenes.<sup>80-82</sup> Owing to the steric bulk of the tungsten complex, electrophiles and nucleophiles stereoselectively add anti to the metal. Therefore, when an enantioenriched form of  $\{\text{WTp}(\text{NO})(\text{PMe}_3)\}$  is used,<sup>83</sup> organic compounds can be prepared in high

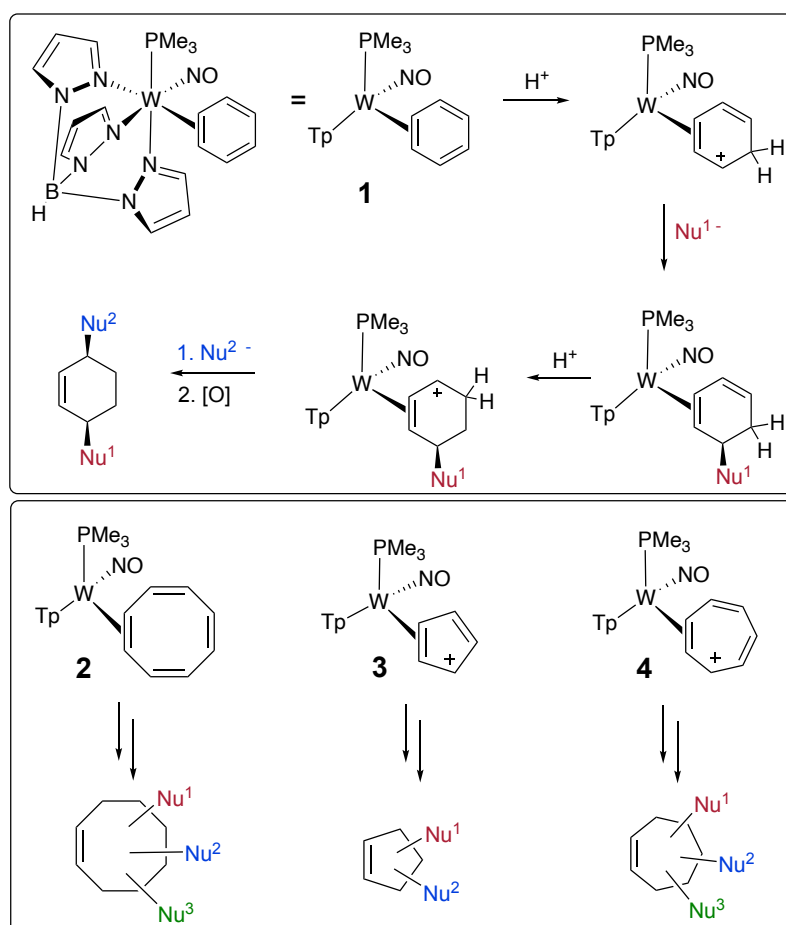


**Figure 3.1.** The elaboration of an  $\eta^2$ -C<sub>6</sub>H<sub>6</sub> complex (**1**) into difunctionalized cyclohexenes and the potential parallel reactions of  $\eta^2$ -C<sub>8</sub>H<sub>8</sub> (**2**),  $[\eta^2\text{-C}_5\text{H}_5]^+$  (**3**), and  $[\eta^2\text{-C}_7\text{H}_7]^+$  (**4**).

enantiomeric excess.<sup>80, 81</sup> We queried whether a similar process could be developed, starting from other aromatic, non-aromatic, and anti-aromatic hydrocarbons ( $[C_nH_n]^{m+}$ ), with an overall goal of generating additional ring sizes of highly functionalized cycloalkenes (**Figure 3.1**).

In contrast to maximally coordinated metal complexes of cyclic polyenes wherein the entire  $\pi$ -system of the ring is bound,  $\eta^2$ -coordination to cyclic polyenes that lack rotational symmetry may form multiple constitutional isomers, owing to the asymmetric nature of  $\{WTP(NO)(PMe_3)\}$ . The first milestone of our investigation and the primary subject of this report was to develop methods for the preparation of a family of complexes of the form  $[WTP(NO)(PMe_3)(\eta^2-C_nH_n)]^{m+}$ , where multiple isomers were not anticipated (where  $n = 6$  or  $8$  for  $m = 0$ , and where  $n = 5$  or  $7$  for  $m = 1$ ). A study of such a series of hydrocarbon complexes would be unparalleled and therefore could offer a new perspective on transition-metal polyalkene complexes. Hence, we endeavored to synthesize  $WTP(NO)(PMe_3)(\eta^2-C_8H_8)$  (**2**),  $[WTP(NO)(PMe_3)(\eta^2-C_5H_5)]^+$  (**3**), and  $[WTP(NO)(PMe_3)(\eta^2-C_7H_7)]^+$  (**4**), and compare their fundamental properties with those of  $WTP(NO)(PMe_3)(\eta^2-C_6H_6)$  (**1**).

## 3.2 Results and Discussion

### 3.2.1 Experimental

The dihapto-coordinate benzene complex **1** is conveniently prepared from  $W(CO)_6$  in a four-step procedure on a multi-gram scale. While this compound is a suitable precursor to other complexes of type  $WTP(NO)(PMe_3)(\eta^2-L)$ , we have found that the anisole derivative (**5**) is particularly convenient to synthesize on a large scale,<sup>84</sup> undergoes similar exchange reactions to **1**, and possesses greater thermal stability than the benzene analog (**1**; **Figure 3.2**). Therefore, **5** serves as a universal precursor to the desired hydrocarbon complexes. To synthesize the cyclooctatetraene (COT) complex **2**, a THF solution of **5** was heated with COT for 3 h at 50°C to drive the replacement of anisole by COT. This reaction mixture was loaded onto a silica column and eluted with ethyl acetate (EtOAc). The product COT complex **2** was precipitated from the solution through the addition of hexanes (yield = 70%). Crystals of **2** were grown from the hexanes filtrate, and its molecular structure was determined through single-crystal X-ray diffraction (SC-XRD; **Figure 3.3**). Organic cyclooctatetraene adopts a tub shape to avoid an anti-aromatic  $8\pi$ -electron system and to alleviate angular strain.<sup>85</sup> However, when reduced, organic  $COT^{2-}$  exhibits

*aromatic planarity*. COT has been shown to bind to transition metals as  $\eta^8$ -COT,  $\eta^4$ -COT, and  $\eta^2$ -COT, but most commonly maintains the tub conformation.<sup>86-89</sup> Similarly to COT<sup>2-</sup>, the  $\eta^2$ -COT ligand in **2** exhibits *semiaromatic planar* character.<sup>90, 91</sup> The tungsten causes lengthening in the C=C bonds (1.33 Å to 1.35 Å (mean)), and shortening of C-C bonds (1.47 Å to 1.44 Å (mean)), compared to free COT. These structural changes are consistent with the interpretation of **2** as a tungsten(II) complex of a semi-aromatic  $[\eta^2\text{-C}_8\text{H}_8]^{2-}$ . As seen in the tungsten system, semiaromatic planarity has been observed in crystal structures of  $(\text{Cp})_2\text{Ta}(n\text{-isopropyl})(\eta^2\text{-C}_8\text{H}_8)$ ,<sup>92</sup> (dippe or d**b**ppe)<sub>2</sub>Ni( $\eta^2$ -C<sub>8</sub>H<sub>8</sub>),<sup>93</sup> and CpMn(CO)<sub>2</sub>( $\eta^2$ -C<sub>8</sub>H<sub>8</sub>).<sup>94</sup>

To prepare the cationic dihapto-coordination complexes of  $[\text{C}_5\text{H}_5]^+$  and  $[\text{C}_7\text{H}_7]^+$ , we envisioned a hydride abstraction from the corresponding  $\eta^2$ -diene and  $\eta^2$ -triene complexes, analogous to that observed previously for WTp(NO)(PMe<sub>3</sub>)( $\eta^2$ -cyclopentene).<sup>95</sup> The  $\eta^2$ -allyl complex [WTp(NO)(PMe<sub>3</sub>)( $\eta^2$ -C<sub>5</sub>H<sub>7</sub>)]<sup>+</sup> can be prepared from WTp(NO)(PMe<sub>3</sub>)( $\eta^2$ -C<sub>5</sub>H<sub>8</sub>) and [CPh<sub>3</sub>]OTf. The cyclopentadiene complex **6** has been reported previously as a mixture of two coordination diastereomers.<sup>96</sup> Unexpectedly, the treatment of **6** with [CPh<sub>3</sub>]OTf results in the formation of an electrophilic addition product [WTp(NO)(PMe<sub>3</sub>)(Ph<sub>3</sub>C-C<sub>5</sub>H<sub>6</sub>)]<sup>+</sup>, which was not pursued. After screening several other potential alternative hydride abstractors (e.g., tris(pentafluorophenyl)borane, 1,4-benzoquinone, and naphthoquinone), we discovered that 2,3-dichloro-5,6-dicyano-1,4-benzoquinone (DDQ) could convert the diene mixture **6** to the desired cyclopentadienyl complex **3**. The molecular structure of **3** was determined through SC-XRD; crystals were grown from a dichloromethane solution at room temperature. The W-C bond lengths of the dihapto-coordinated carbons are 2.295(11) Å and 2.317(13) Å, while W-C distances of the unbound carbons are 2.946(13) Å, 3.065(14) Å, and 3.390(15) Å. Additionally, bond lengths within the carbon ring have some distortion, indicating that there is some preference for charge localization on the carbon 'distal' to the phosphine ligand,<sup>96</sup> but the lengthening of double bonds (1.35 Å) and shortening of single bonds (1.42 Å) is consistent with a resonance contributor of **3** where a semiaromatic  $[\text{C}_5\text{H}_5]^-$  ligand is dihapto-coordinated to W(II) (**Figure 3.3, 3**). Consistent with this notion, compound **3** is diamagnetic, an observation in contrast to the formally antiaromatic C<sub>5</sub>H<sub>5</sub><sup>+</sup> cation, which is computationally predicted to have a paramagnetic ground state.<sup>97</sup> Additionally, SC-XRD bond length data for the DDQ anion, the absence of an OH stretch in the IR data, and the absence of <sup>13</sup>C-NMR peaks for the anion indicate that

the DDQ anion is the paramagnetic radical  $\text{DDQ}^{\bullet-}$ . Presumably,  $\text{DDQH}^-$  produced in the purported hydride abstraction is completely consumed in the presence of excess DDQ to form  $\text{DDQ}^{\bullet-}$  and  $\text{DDQH}$ . The neutral  $\text{DDQH}$  is likely lost in the filtrate or deprotonated.<sup>98, 99</sup>

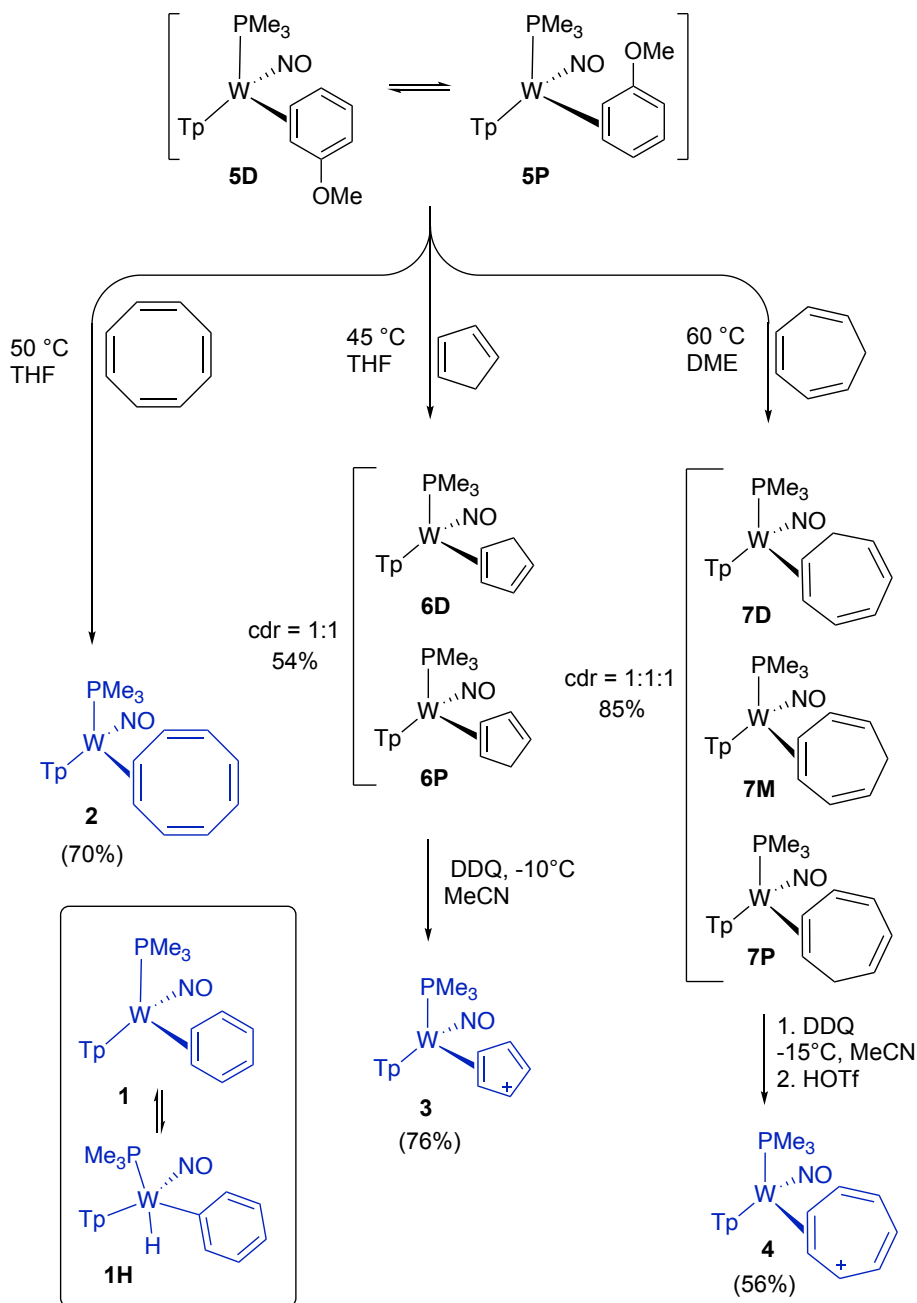


**Figure 3.2.** Synthetic details for the target compounds  $[\text{WTp}(\text{NO})(\text{PMe}_3)(\eta^2\text{-C}_n\text{H}_n)]^{m+}$  (where  $m = 0$  for  $n = 6$  or  $8$ , and  $m = 1$  for  $n = 5$  or  $7$ ). Inset: the analogous benzene complex **1** in equilibrium with its phenyl hydride isomer **1H**.

The cyclopentadienyl cation ( $\text{Cp}^+$ ) has been studied for its unique properties,<sup>100</sup> but as a ligand in organometallic complexes it is typically considered to be in its anionic, aromatic form ( $\text{Cp}^-$ ).<sup>101, 102</sup> Although usually bound as  $\eta^5\text{-Cp}$  and  $\eta^3\text{-Cp}$ ,  $\eta^1\text{-Cp}$



complexes have also been observed experimentally. But to our knowledge, **3** is the first well-characterized example of a monomeric  $\eta^2$ -cyclopentadienyl complex. The closest comparisons to this structure are either  $\eta^3$ -Cp<sup>103, 104</sup> and  $\eta^1$ -Cp complexes,<sup>104-107</sup> or  $\eta^3$ -indenyl complexes.<sup>104</sup> Rare examples of an  $\eta^2$ -Cp can be found in (Cp<sub>3</sub>Mn) clusters with K<sup>+</sup>, Mg<sup>2+</sup>, and Cs<sup>+</sup>,<sup>108, 109</sup> but these complexes have very weak Mn—C bonds ( $\sim 2.4$  Å), and virtually no distortion in the C-C bond distances ( $\pm 0.03$  Å).

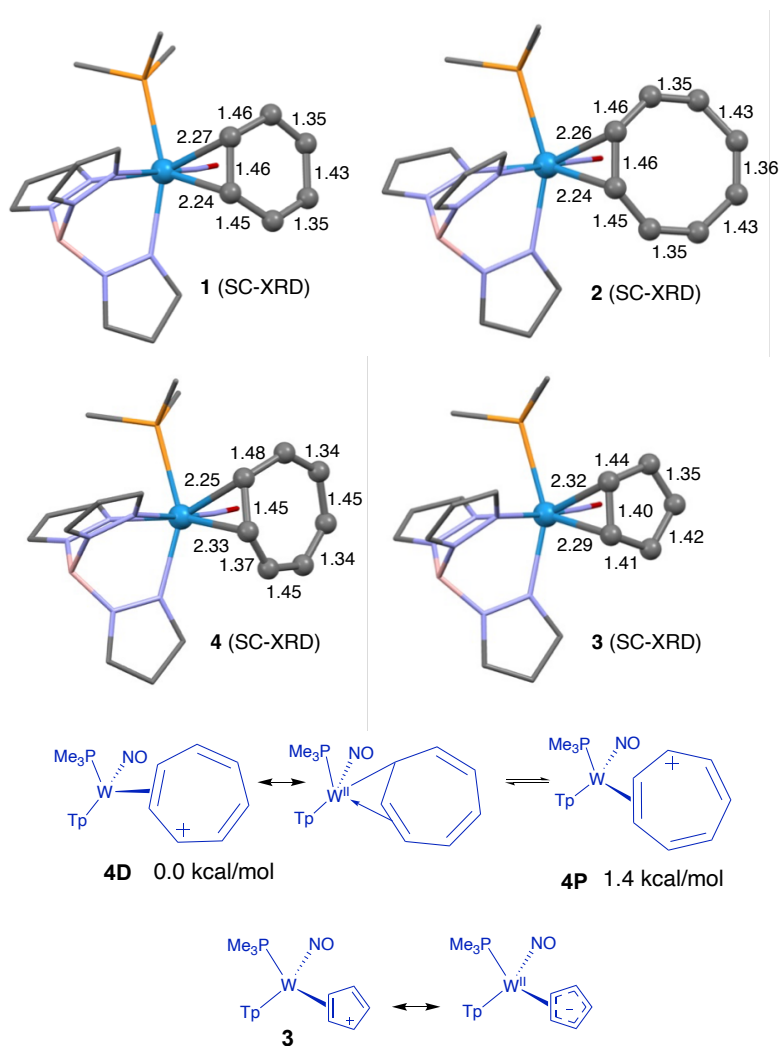


**Figure 3.3.** Molecular structures (all distances in Å) for compounds [WTP(NO)(PMe<sub>3</sub>)( $\eta^2$ -C<sub>n</sub>H<sub>n</sub>)]<sup>m+</sup> (where  $m = 0$  for  $n = 6$  or  $8$  and  $m = 1$  for  $n = 5$  or  $7$ ), and conformers and resonance contributors for **4**. For clarity, the crystal structures are displayed as sticks and ball-and-stick models. Thermal ellipsoid plots can be found in the SI.

Direct ligand exchange of tropylium salts for the anisole ligand of **5** were unsuccessful due to the oxidizing properties of this cation.<sup>110</sup> However, warming a DME solution of cycloheptatriene (CHT) and the anisole complex **5** for 1.5 h (60 °C) resulted in the synthesis of the corresponding CHT complex **7**, which was precipitated

from solution by addition of hexanes. NMR data indicate that **7** was isolated as a 1:1:1 mixture of three coordination diastereomers (**Figure 3.2**). Treating this isomeric mixture with DDQ in MeCN followed by an excess of trifluoromethanesulfonic acid (HOTf) resulted in hydride abstraction and anion metathesis, respectively, generating the targeted tropylium species **4**. Upon isolation of this species by precipitation in diethyl ether, crystals of **4** were grown from the filtrate and the molecular structure was determined by SC-XRD (**Figure 3.3**). The crystal structure shows that **4** is similar to  $\eta^2$ -coordinated allyl complexes,<sup>96</sup> with two short W-C bonds (2.327(2), 2.253(2) Å) and one much longer one (2.772(3) Å). Further, the uncoordinated portion of the  $\pi$  system is distinctly asymmetric, suggesting a  $\eta^1:\eta^2$ -resonance contributor (**Figure 3.3, 4D**).<sup>111</sup> Similar to the bond length changes observed in the  $\eta^2$ -benzene complex **1**, the tungsten fragment acts as a dearomatization agent in  $\eta^2$ -tropylium, diminishing the aromatic character of the ring. Whereas the organic tropylium cation has equivalent C-C bonds (1.35 Å),<sup>112, 113</sup> the unbound portion of the ring in compound **4** has alternating long and short C-C bonds (**Figure 3.3**). Additionally, the decrease in aromaticity can be seen through significant upfield-shift in the ring protons of **4** (*c.f.*, ~9.3 ppm).<sup>113</sup> Transition metal complexes of the cycloheptatrienyl cation are typically  $\eta^7$  or  $\eta^6$ ,<sup>114-116</sup> but occasionally have been reported as trihapto-coordinated ( $\eta^3$ ).<sup>117-119</sup> We are unaware of any reports of structurally characterized  $\eta^2$ -tropylium complexes.

### 3.2.2 Fluxional behavior

All four [WTP(NO)(PMe<sub>3</sub>)( $\eta^2$ -C<sub>n</sub>H<sub>n</sub>)]<sup>m+</sup> complexes exhibit fluxional behavior in their <sup>1</sup>H-NMR spectra. In the case of the neutral benzene (**1**) and COT (**2**) complexes, <sup>1</sup>H-NMR spectra are resolved at 25 °C, but elevating the temperature causes coalescence (**Figure 3.4**), with free energies of activation determined to be 16 ± 2 and 18 ± 2 kcal/mol, respectively. In contrast, the cationic complexes **3** and **4** show one doublet (*J*<sub>PH</sub> ~ 2 Hz) corresponding to all the ring protons, and although broadening occurred, the coalesced feature remained to the limit of our experiment (-90 °C), suggesting a very low activation barrier for ring-slipping. The  $\eta^2$ -benzene **1** was previously studied by Harman and Ess.<sup>120</sup> H-NMR data for **1** indicate that this species exists in equilibrium with its aryl hydride isomer (**1H**; **Figure 3.2**), and replacement of the PMe<sub>3</sub> ligand by PBu<sub>3</sub> changes the equilibrium ratio of **1**:**1H** from 10:1 to 1:2.5. For WTP(NO)(PBu<sub>3</sub>)( $\eta^2$ -benzene) the tungsten hydride was observed to undergo chemical exchange with all ring protons of dihapto-bound benzene, suggesting the aryl hydride

to be a possible participant in the ring-walk mechanism. A DFT study of **1** supported this notion but revealed a very flat potential energy surface near the transition state that includes a ring-slip transition state in which the benzene is fully rearomatized (**Figure 3.4**).

A tungsten hydride complex analogous to **1H** was not observed in the  $^1\text{H}$ -NMR spectrum of  $\text{WTP}(\text{NO})(\text{PMe}_3)(\eta^2\text{-COT})$  **2**, but we queried whether such a species was energetically accessible. Hence, DFT was used to further study the fluxional properties of the  $\eta^2$ -polyene complexes **2-4**. First, a small benchmarking study was performed (SI). Functionals and basis sets were chosen based on past studies,<sup>120</sup> but M06-2X alongside 6-31G(d,p) with the LANL2DZ effective core potential on W was found to best reproduce the crystallographic data for complexes **1-4** (**Figure 3.3**). The fluxional behavior of **2**, **3**, and **4** were modeled, essential intermediates and transition states were identified, and an intrinsic reaction coordinate (IRC) energy landscape was calculated for each system (SI). In the case of the  $\eta^2$ -COT complex **2**, a  $\eta^1$  transition state (**2 $^\ddagger$**  in **Figure 3.4**; +16.7 kcal/mol) could be identified as part of a ring-slip mechanism (**Figure 3.4**; SI), which, in contrast to the benzene analog **1**, was lower in energy than the corresponding hydride intermediates (+17.1 and +27.7 kcal/mol). From the calculated transition state **2 $^\ddagger$** , it was also determined that the COT ligand adopts a completely planar structure with C-C bond lengths around the ring approaching 1.4 Å (1.39-1.42Å)—a structure that is consistent with an aromatic COT dianion (**Figure 3.4**).

Similar to many  $[\text{WTP}(\text{NO})(\text{PMe}_3)(\eta^2\text{-allyl})]$  complexes,<sup>96</sup> the cycloheptatrienyl cation in **4** has two energetically independent conformational isomers where the charge is localized at the “proximal” (**4P**) and “distal” (**4D**) positions. We successfully minimized both conformations of  $\eta^2$ -tropylium, whose energy difference is 1.36 kcal/mol, favoring **4D** (**Figure 3.3**). In addition to a “carbene hydride” species (+17.4 kcal/mol; SI), two  $\eta^2$ -C-H complexes were identified (+13.0, +15.0 kcal/mol; SI), but all three structures were too high energy to be relevant to the ring-slip process. A two-step mechanism was identified, in which the distal conformer **4D** isomerizes to the proximal form **4P** through an “allyl shift” or “ring-slip” transition state (4.0 kcal/mol; **4 $^\ddagger$**  in **Figure 3.4**), wherein the  $\eta^2$ -bound carbons are moved by one position. In the second step of the mechanism, **4P** converts again to **4D** through a unique low-energy four-carbon charge transfer transition state (SI; 1.5 kcal/mol), *without changing which*

L	T <sub>c</sub> (°C)	ΔG <sup>‡</sup> (kcal/mol) <sup>a</sup>	ΔG <sup>‡</sup> <sub>calc</sub> (kcal/mol) <sup>b</sup>
[C <sub>5</sub> H <sub>5</sub> ] <sup>+</sup>	< -90	n/a	7.1
C <sub>6</sub> H <sub>6</sub>	35	16 ± 2 <sup>c</sup>	12.8
[C <sub>7</sub> H <sub>7</sub> ] <sup>+</sup>	< -90	n/a	4.0
C <sub>8</sub> H <sub>8</sub>	50	18 ± x	16.7

a. determined at the coalescence temperature

b. calculated for 25 °C.

c. determined for the PBU<sub>3</sub> analog

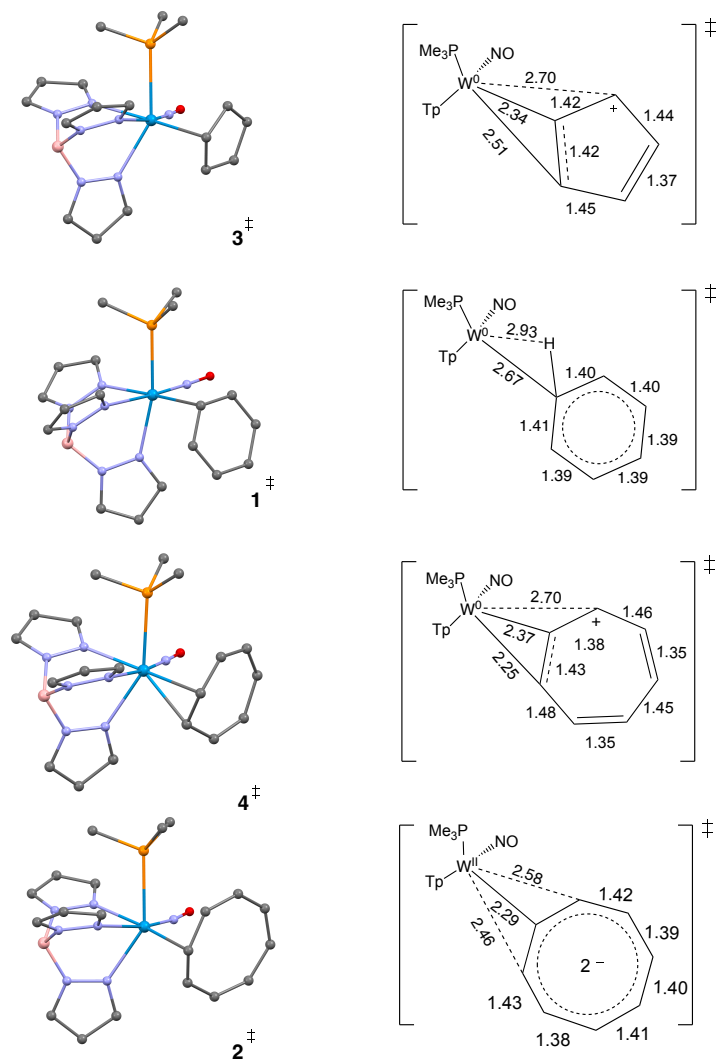


**Figure 3.4.** Transition states for ring-walking of compounds [WTP(NO)(PMe<sub>3</sub>)(η<sup>2</sup>-C<sub>n</sub>H<sub>n</sub>)]<sup>m+</sup> (where for m = 0 for n = 6 or 8 and m = 1 for n = 5 or 7). All distances in Å.

two carbons are η<sup>2</sup>-bound. As such, although this second transition state interconnects the same two species (**4D** and **4P**), the identities of the atoms have changed, and it is distinct from **4‡**. This transition state is also unique because the coordinated ring is mostly planar, with single bonds shortened and double bonds lengthened compared to the ground state (SI and **Figure 3.4**).

In contrast to the strongly asymmetric  $\eta^2$ -tropylium complex **4**, the crystal structure for the  $\eta^2$ -Cp analog **3** resembles a true dihapto-bound ligand with two short tungsten-carbon bonds, and much longer interactions to the adjacent carbons. A small amount of asymmetry is noted in the uncoordinated portion of the allyl, with one C-C bond having more double bond character than the other, yet separate “distal” and “proximal” conformations could not be computationally located. No carbene-hydride species were identified for **3**, but similar to **4**, two different  $\eta^2$ -C-H complexes were found at energies (+9.9, +12.6 kcal/mol; SI) too high to be integral to the ring-slip mechanism. Interestingly, the structure of **3**<sup>‡</sup> resembles a “proximal”  $\eta^2$ -allyl species, tightly binding two carbons while weakly interacting with the third (**Figure 3.4**).

### 3.2.3 Electrochemical behavior

Cyclic voltammetric data were collected for hydrocarbon complexes **1** – **4** in acetonitrile solution using tetrabutylammonium hexafluorophosphate as the electrolyte. The benzene complex **1** features an irreversible anodic wave at -0.13 V NHE at 100 mV/s, at a potential similar to, but lower than those typically observed for simple alkene complexes of {WTP(NO)(PMe<sub>3</sub>)} (*c.f.*, cyclopentene: 0.35 V, NHE).<sup>84</sup> Analogously, the  $\eta^2$ -COT complex **2** shows an anodic wave at 0.37 V (100 mV/s). In addition, however, this complex shows an apparent one-electron reduction with an  $E_{p,c}$  = -2.2 V (100 mV/s).

As expected, the cationic complexes **3** and **4** are far more resistant to oxidation than their neutral counterparts. The  $\eta^2$ -Cp complex **3** shows its first anodic wave at  $E_{p,a}$  = 1.26 V, but also features a cathodic wave at  $E_{p,c}$  = -0.43 V (100 mV/s). By contrast, the  $\eta^2$ -tropylium complex **4** shows no electrochemical activity between 1.2 V and -1.2 V (NHE). For comparison, typical  $\eta^2$ -allyl complexes of {WTP(NO)(PMe<sub>3</sub>)} show cathodic waves around -0.8 to -1.1 V at 100 mV/s (NHE).<sup>96</sup> Taken together, these data support the notion that the [C<sub>5</sub>H<sub>5</sub>]<sup>+</sup> complex **3** is far more prone to ligand reduction compared to typical  $\eta^2$ -allyl cation complexes of {WTP(NO)(PMe<sub>3</sub>)}, possibly leading to an aromatic [C<sub>5</sub>H<sub>5</sub>]<sup>-</sup>. Meanwhile, the tropylium analog **4**, which is already largely aromatic, is more resistant to such a reduction compared to analogous  $\eta^2$ -allyl cation complexes.

### 3.2.4 Methylations

The next phase of this study was to verify that species **2**, **3**, and **4** could be functionalized similarly to species **1**. Methylations were used to demonstrate this

synthetic potential. First, we needed to determine whether the reactivity of the  $\eta^2$ -COT species **2** was analogous to **1**, and whether it could be protonated to form cationic ligands suitable for reactions with nucleophiles. Indeed, the treatment of COT complex **2** with HOTf formed three isomers of the cyclooctatrienyl complex (**8**; See SI), enriched through equilibration from 3:3:1 to a ratio of 6:1:0. Preliminary experiments of combining **8** with the Grignard reagent MeMgBr indicate that a dominant triene isomer is formed (6:1) and one dominant triene isomer is isolated via acetonitrile precipitation (>20:1; **10**). A similar result was obtained for methylation of the benzene complex **1**. Secondly, we wanted to verify that the treatment of the cationic complexes **3** and **4** with nucleophiles could generate  $\eta^2$ -polyene complexes. Treatment of the  $\eta^2$ -tropylium complex **4** with NaBH<sub>4</sub> formed two coordination diastereomers of the CHT complex, **7D** and **7P**, in a 1:1 ratio. Notably, the constitutional isomer **7M** was not observed (see **Figure 3.2**). In a similar manner, the  $\eta^2$ -Cp complex **3** reacted with NaBH<sub>4</sub> to form **6D** and **6P** in a ratio of 2:1. This observation is significant, as the highly unstable anti-aromatic (Cp<sup>+</sup>) molecule has been stabilized by the tungsten, allowing it

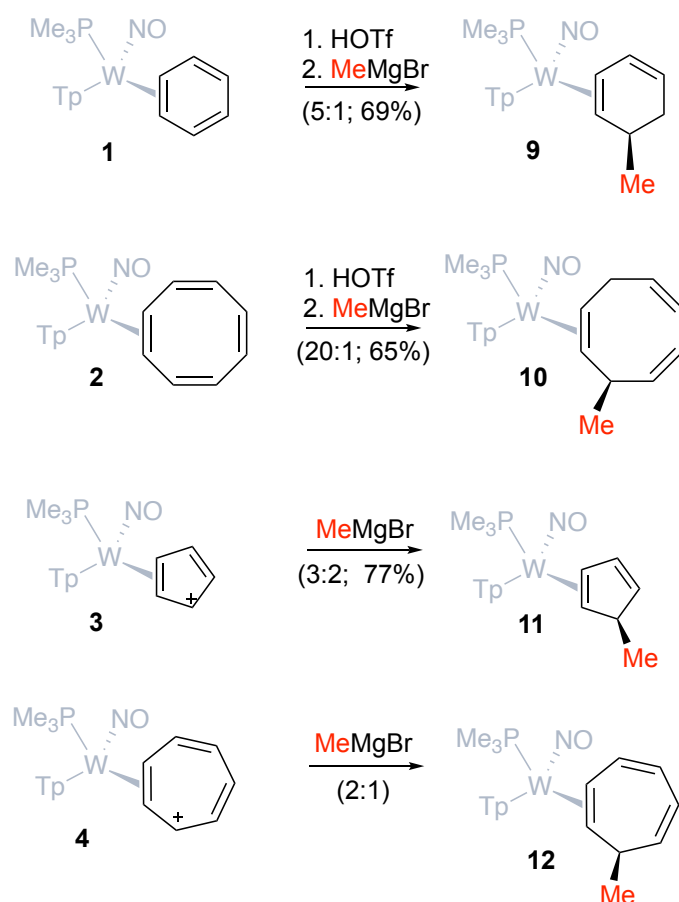


**Figure 3.5.** Exploratory methylation reactions with [WTp(NO)(PMe<sub>3</sub>)( $\eta^2$ -C<sub>n</sub>H<sub>n</sub>)]<sup>m+</sup> to generate methylated polyene complexes.

to undergo a nucleophilic addition with hydride.  $\{\text{Wtp}(\text{NO})(\text{PMe}_3)\}$  is an established dearomatization agent, but it apparently can also act as a “de-anti-aromatization agent.” Finally, we added a Grignard reagent ( $\text{MeMgBr}$ ) to the cationic complexes **3** and **4**. In both cases, the addition anti to the metal occurred smoothly, generating two methylated polyene complexes **11** and **12**, respectively. We note that while both complexes are generated in low diastereomeric excess, the free ligand for both diastereomers is identical. Of note, nucleophilic addition to  $\eta^5\text{-Cp}$  complexes is highly unusual,<sup>121</sup> although the analogous reaction with  $\eta^7\text{-C}_7\text{H}_7$  complexes is well established.<sup>122</sup>

Finally, to demonstrate proof of concept, we set out to elaborate the cyclooctatetraene complex **2** into a trisubstituted cyclooctene through the sequential addition of three independent nucleophiles. A full mechanistic investigation of such a process will be disclosed separately, but to demonstrate the synthetic potential of

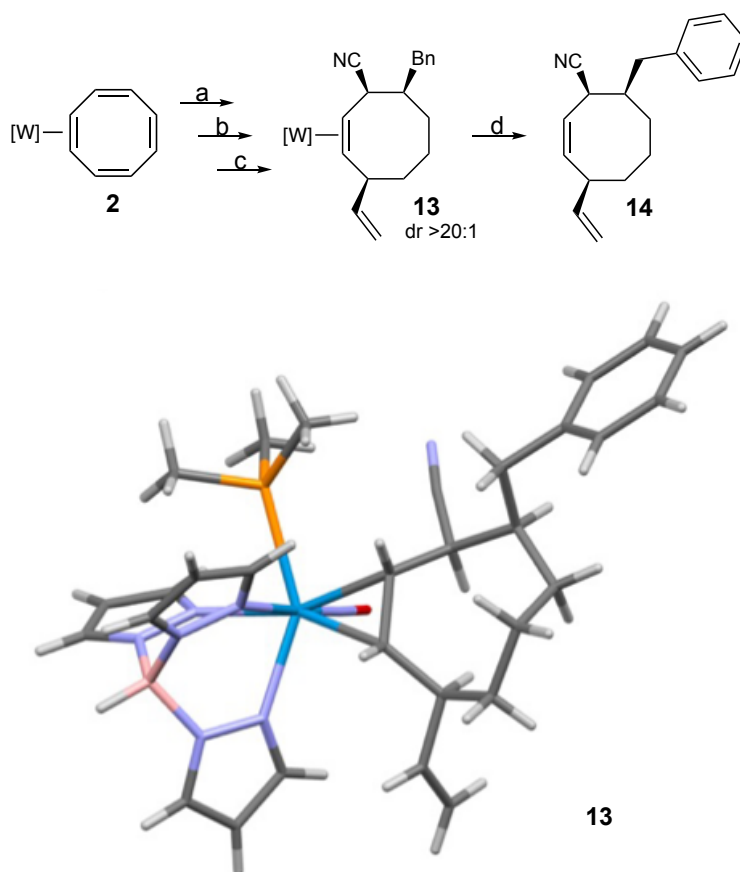


**Figure 3.6.** Conversion of COT complex **2** to a trisubstituted cyclooctene complex **13** and oxidative decomplexation of the cyclooctene ligand **14**. Structure of **13** was determined by SC-XRD. Reaction conditions:

a: 1.  $\text{HOTf}/\text{THF}$ ; 2.  $\text{BnMgCl}$ , (41%). b: 1.  $\text{HOTf}/\text{DCM}$ ; 2.  $\text{NaCN}$  (80%). c: 1.  $\text{HOTf}/\text{DCM}$ ; 2.  $\text{C}_2\text{H}_3\text{MgBr}$ , (80%). d:  $\text{CAN}$  (47%).

complexes **2** - **4**, we describe the following example: After treating the COT complex **2** with HOTf and equilibrating the resulting trienyl complexes (**8**; vide supra), we combined complex **8** with a benzyl Grignard reagent to form a substituted triene complex analogous to **10** (SI). This was followed by a second addition of proton and nucleophile, in this case NaCN, to generate a disubstituted diene complex (SI). A final protonation and addition of a vinyl Grignard reagent produced compound **13** as a single diastereomer of a 3,4,8-cyclooctene complex in which all three substituents were oriented anti to the metal (confirmed by SC-XRD; **Figure 3.6**). Finally oxidative decomplexation yielded the free organic **14**, a *cis*-trisubstituted 3,4,8-cyclooctene (dr and ir > 20:1). The overall yield of **14** from **2** was 12% over seven steps. Studies exploring the full scope of such nucleophilic addition sequences for **2** - **4** are currently underway.

### 3.3 Conclusions

With the ultimate goal of developing new methods for the functionalization of cyclic hydrocarbons, it is beneficial to understand the structural and electronic properties of these unique dihapto-coordinated conjugated carbocycles. Structural and electronic properties were studied with SC-XRD, DFT, CV, and NMR. Like the  $\eta^2$ -benzene complex **1**, the  $\eta^2$ -cyclooctatetraene complex **2** is fluxional at elevated temperatures. In contrast,  $\eta^2$ -Cp and  $\eta^2$ -tropylium complexes **3** and **4** are fluxional, but with coalescence occurring far below room temperature. The tungsten fragment used, {WTP(NO)(PMe<sub>3</sub>)}, has been successful in the dearomatization and functionalization of several types of aromatic compounds. In particular, WTP(NO)(PMe<sub>3</sub>)( $\eta^2$ -benzene) and its derivatives have been transformed into sophisticated organic molecules, and we plan to explore similar chemical pathways with the five- ( $\eta^2$ -Cp), seven- ( $\eta^2$ -tropylium), and eight- ( $\eta^2$ -COT) membered systems. Controlling the addition of nucleophiles and tungsten-alkene isomerizations of these systems will be an important next step in the development of new synthetic methodologies for the preparation of highly functionalized cyclopentanes, cycloheptanes and cyclooctanes based on dihapto-coordinated aromatic (and antiaromatic) hydrocarbons.



## References

- (1) Southey, M., W.Y., Bruvas, Michael. . Introduction of small molecule drug discovery and preclinical development *Front. Drug, Discov.* **2023**, 3.
- (2) Bai, Y.-R., Seng, Dong-Jie., Xu, Ying., Zhang, Yoa-Dong., Zhou, Wen-Juan., Jia, Yang-Yang., Song, Jian., He, Zhang-Xu., Liu, Hong-Min., Yuan, Shuo. A comprehensize review of small molecule drugs approved by the FDA in 2023: Advances and prospects. *Eur. J. Med. Chem.* **2024**, 276, 116706.
- (3) Welsch, M. E., Snyder, Scott A., Stockwell, B.R. Privledged Scaffolds for Library Design and Drug Discovery. . *Curr Opin Chem Biol* **2010.**, 14 (3), 347-361.
- (4) Vitaku, E., Smith, David T., Njardarson, Jon T. Analysis of the Structural Diversity, Substitution Patterns, and Frequency of Nitrogen Heterocycles among U.S. FDA Approved Pharmaceuticals. . *J. Med. Chem.* **2014**, 57, 10257 - 10274.
- (5) Frolov, N. A., Vereshchagin, Anatoly, N. Piperidine Derivatives: Recent Advances in Synthesis and Pharmacological Applications *Int J Mol Sci* **2023**, 24 (3), 2937.
- (6) Vardanyan, R. *Piperidine-based drug discovery*; Elvsevier, 2017.
- (7) McLornan, D. P., Pope, J.E., Gotlib, J., Harrison, C.N. Current and future status of JAK inhibitors. *Lancet* **2021**, 398, 803 - 816.
- (8) Goel, P., Alam, O., Naim, M.J., Nawaz, F., Iqbal, M., Alam, M.I. . Recent advancement of piperidine moiety in treatment of cancer-  
A review. *Eur. J. Med. Chem.* **2018**, 157, 480 - 502.
- (9) Ezelarab, H. A. A., Abbas, S.H., Hassan, H.A., Abuo-Rahma, G.E.-D.A. Recent updates of fluoroquinolones as antibacterial agents. *Arch. Der Pharm.* **2018**, 351, 1800141.
- (10) Martinelli, D., Bitetto, V., Tassorelli, C. Lasmiditan: An additional therapeutic option for the acute treatment of migraine. *Expert Rev. Neurother.* **2021**, 21, 491 - 502.
- (11) Ye, N., Qin, W., Tian, S., Xu, Q., Wold, E.A., Zhou, J., Zhen, X.-C. Small Molecules Selectively Targeting Sigma-1 Receptor for the Treatment of Neurological Diseases. *J. Med. Chem.* **2020**, 63, 15187 - 15217.
- (12) Rathore, A., Asati, V., Kashaw, K.S., Agarwal, S., Parwani, D., Bhattacharya, S., Mallick, C. . The Recent Development of Piperazine and Piperidine Derivatives as Antipsychotic Agents. *Mini-Rev. Med. Chem.* **2021**, 21, 362 - 379.
- (13) Mezeiova, E., Spilovska, K., Nepovimova, E., Gorecki, L., Soukup, O., Dolezal, R., Malinak, D., Janockova, J., Jun, D., Kuca, K.,. Profiling donepezil template into

multipotent hybrids with antioxidant properties. *J. Enzym. Inhib. Med. Chem.* **2018**, 33, 583 - 606.

(14) Rk, M., Begum, S., Begum, A., Koganti, B. Antioxidant potential of piperidine containing compounds—A short review. *Asian J. Pharm. Clin. Res.* **2018**, 11, 66.

(15) Li, Q., He, S., Chen, Y., Feng, F., Qu, W., Sun, H. . Donepezil-based multi-functional cholinesterase inhibitors for treatment of Alzheimer's disease. *Eur. J. Med. Chem.* **2018**, 158, 463 - 477.

(16) Blackhall, F., Cappuzzo, F. Crizotinib: from discovery to accelerated development to front-line treatment. *Ann Oncol.* **2016**, 29 (4), 1073.

(17) Buchel, K., Bendin, Juliane., Gharbi, Amina., Rahlenbeck, Sibylle., Dautel, Hans. Repellent efficacy of DEET, Icaridin, and EBAAP against *Ixodes ricinus* and *Ixodes scapularis* nymphs (Acari, Ixodidae). *Ticks Tick Borne Dis* **2015**, 6 (4), 494 - 498.

(18) Correll, C. U., Litman, Robert E., Filts, Yuriy., Llaudo, Jordi., Naber, Dieter., Torres, Ferran., Martinez, Javier. Efficacy and safety of once-monthly Risperidone ISM in schizophrenic patients with an acute exacerbation. *NPJ Schizophrenia* **2020**, 6 (37).

(19) Suchonwanit, P., Thammarucha, Sasima., Leerunyakul, Kanchana. Minoxidil and its use in hair disorders: a review. *Drug Des Devel Ther* **2020**, 10 (14), 575.

(20) Pai, V. B., Nahata, M.C. Nelfinavir mesylate: a protease inhibitor *Ann Pharmacother.* **1999**, 33 (3), 325 - 339.

(21) Sidhu, G., Akhondi, Hossein. *Loratadine*; StatPearls, 2023.

(22) Storebø, O. J., Storm, Maja Rosenberg Overby., Ribeiro, Johanne Pereira., Skoog, Maria., Groth, Camilla., Callesen, Henriette E., Schaug, Julie Perrine., Rasmussen, Pernille Darling., Huus, Christel-Mie L., Zwi, Morris., Kirubakaran, Richard., Simonsen, Erik., Gluud, Christian. Methylphenidate for children and adolescents with attention deficit hyperactivity disorder (ADHD). *Cochrane Database Syst Rev* **2023**, 3 (3).

(23) Buffat, M. G. P. Synthesis of piperidines *Tetrahedron* **2004**, 60, 1701-1729.

(24) Maity, S., Bera, Asish., Bhattacharjya, Ayantika., Maity, Pradip. C-H functionalization of pyridines. *Org. Biomol. Chem.* **2023**, 21, 5671.

(25) Sindhe, H., Reddy, Malladi Mounika., Rajkumar, Karthikeyan., Kamble, Akshay., Singh, Amardeep., Kumar, Anand., Sharma, Satyasheel. Pyridine C(sp<sup>2</sup>)-H bond functionalization under transition-metal and rare earth metal catalysis *J. Org. Chem.* **2023**, 19, 820 - 863.

- (26) Hu, M., Ding, Hao., DeSnoo, William., Tantillo, Dean J., Nairoukh, Zackaria. The Construction of Highly Substituted Piperidines via Dearomative Functionalization Reactions. *Angew Chem Int Ed* **2023**, 62, e202315108.
- (27) Zhang, X., Xu, J. Five-Membered carbocycle construction in the synthesis of Daphniphyllum alkaloids: recent strategic methodological advances. *Org. Chem. Front.* **2022**, 9, 6708.
- (28) Battiste, M. A., Pelphrey, P.M., Wright, D.L. The Cycloaddition Strategy for the Synthesis of Natural Products Containing Carbocyclic Seven-Membered Rings. *Chem. Eur. J.* **2006**, 12 (13), 3438-3447.
- (29) Hu, Y. J., Li, L.X., Han, J.C., Min, L., Li, C.C. Recent Advances in the Total Synthesis of Natural Products Containing Eight-Membered Carbocycles (2009-2019). *Chem. Rev.* **2020**, 120 (13), 5910-5953.
- (30) Curran, M. P. Bimatoprost: a review of its use in open-angle glaucoma and ocular hypertension *Drugs Aging.* **2009**, 26 (12), 1049 - 1071.
- (31) Dobesh, P. P., Oestreich, Julie H. Ticagrelor: pharmacokinetics, pharmacodynamics, chiral efficacy, and safety. *Pharmacotherapy.* **2014.**, 34 (10), 1077 - 1090.
- (32) Greig, S. L., Garnock-Jones, Karly P. Loxoprofen: A Review in Pain and Inflammation *Clin Drug Investig.* **2016**, 36 (9), 771 - 781.
- (33) Blair, H. A. Rimegepant: A Review in the Acute Treatment and Preventive Treatment of Migraine. *CNS Drugs* **2023**, 37 (3), 255 - 265.
- (34) Lawson, K. A Brief Review of the Pharmacology of Amitriptyline and Clinical Outcomes in Treating Fibromyalgia. *Biomedicine* **2017**, 5 (2), 24.
- (35) Sharifi-Rad, J., Quispe, Cristina., Patra, Jayanta Kumar., Singh, Yengkhom Disco., Panda, Manasa Kumar., Das, Gitishree., Adetunji, Charles Oluwaseun., Michael, Olugbenga Samuel., Sytar, Oksana., Polito, Letizia., Živković, Jelena., Cruz-Martins, Natália., Klimek-Szczykutowicz, Marta., Ekiert, Halina., Choudhary, Muhammad Iqbal., Ayatollahi, Seyed Abdulmajid., Tynybekov, Bekzat., Kobarfard, Farzad., Muntean, Ana Covilca., Grozea, Ioana., Daştan, Sevgi Durna., Butnariu, Monica., Szopa, Agnieszka., Calina, Daniela. . Paclitaxel: Application in Modern Oncology and Nanomedicine-Based Cancer Therapy. *Oxid Med Cell Longev* **2021**, 3687700.
- (36) Childers, W. E., Abou-Gharbia, Magid A. "I'll Be Back": The Resurrection of Dezocine. *ACS Med. Chem. Lett.* **2021**, 12 (6), 961 - 968.

- (37) Yang, L. P. H., Keam, Susan, J. Retapamulin: a review of its use in the management of impetigo and other uncomplicated superficial skin infections. . *Drugs* **2008**, 68 (8), 855 - 873.
- (38) O'Malley, D. *Cyclopentane Synthesis*. 2005. [https://baranlab.org/images/grpmtgpdf/Omalley\\_Feb\\_05.pdf](https://baranlab.org/images/grpmtgpdf/Omalley_Feb_05.pdf) (accessed).
- (39) Wertjes, W. C., Southgate, E.H., Sarlah, D. Recent advances in chemical dearomatization of non-activated arenes. . *Chem. Soc. Rev.* **2018**., 47, 7996.
- (40) Huck, C. J., Sarlah, D. Shaping Molecular Landscapes: Recent Advances, Opportunities, and Challenges in Dearomatization. *Chem.* **2020**, 6, 1589-1603.
- (41) Pape, A. R., Kaliappan, K.P., Kundig, E.P. Transition-Metal Mediated Dearomatization Reactions. *Chem. Rev.* **2000**, 100 (8).
- (42) Rosillo, M., Dominguez, G., Perez-Castells, J. Chromium arene complexes in organic synthesis. *Chem. Soc. Rev.* **2007**, 37 (10), 1589-1604.
- (43) Boyd, D. R., Bugg, T.D.H. Arene cis-dihydrodial formation: from biology to application. *Org. Biomol. Chem.* **2006**, 4 (2), 181-192.
- (44) Ortiz, F. L., Iglesias, M.J. Fernandez, I., Andujar Sanchez, C.M., Gomez, G.R. Nucleophilic Dearomatization (DNAr) Reactions of Aromatic C,H-Systems. A Mature Paradigm in Organic Synthesis *Chem. Rev.* **2007**, 107 (5), 1580-1691.
- (45) B.K. Liebov, W. D. H. Group 6 Dihapto-Coordinate Dearomatization Agents for Organic Synthesis. *Chem. Rev.* **2017**, 117, 13721-13755.
- (46) J.A. Smith, K. B. W., R.E. Sonstrom, P. J. Kelleher, K.D. Welch, E.K. Pert, K.S. Westendorff, D.A. Dickie, X. Wang, B. H. Pate, W. D. Harman. Preparation of Cyclohexene Isotopologues and Stereoisomers from Benzene. *Nature* **2020**, 581, 288-293.
- (47) J.T. Weatherford-Pratt, J. A. S., J.M. Bloch, M.N. Ericson, J.T. Myers, K.S. Westendorff, D.A. Dickie, W.D. Harman. The Double-Protonation of Dihapto-Coordinated Benzene Complexes: An Enabling Strategy for Dearomatization Using Aromatic Nucleophiles. . *Nature Comm* **2023**, 14, 3145.
- (48) J.T. Weatherford-Pratt, J. M. B., J.A. Smith, M. N. Ericson, D.J. Siela, K. B. Wilson, M.H. Shingler, M.R. Ortiz, S. Fong, J.A. Laredo, I.U. Patel, M. McGraw, D. A. Dickie, W. D. Harman. Tungsten-anisole complex provides 3,6-substituted cyclohexenes for highly diversified chemical libraries. *Sci. Adv.* **2024**, 10 (7).
- (49) K.B. Wilson, J. A. S., H.S. Nedzbala, E. K. Pert, S.J. Dakermanji, D.A. Dickie, W.D. Harman Highly Functionalized Cyclohexenes Derived from Benzene: Sequential

Tandem Addition Reactions Promoted by Tungsten *J. Org. Chem.* **2019**, *84* (10), 6094-6116.

(50) S.R. Simpson, P. S., D.J. Siela, L.A. Diment, B.C. Song, K. S. Westendorff, M. N. Ericson, K. D. Welch, D. A. Dickie, W.D. Harman. Phenyl Sulfones: A Route to a Diverse Family of Trisubstituted Cyclohexenes from Three Independent Nucleophilic Additions. *J. Am. Chem. Soc.* **2022**, *144* (21), 9489-9499.

(51) K.B. Wilson, H. S. N., S.R. Simpson, M. N. Ericson, K. S. Westendorff, M.D. Chordia, D.A. Dickie, W.D. Harman. Hydroamination of Dihapto-Coordinated Benzene and Diene Complexes of Tungsten: Fundamental Studies and the Synthesis of  $\gamma$ -Lycorane. *Chimica Acta* **2021**, *104* (10).

(52) J.A. Smith, S. S., K.S. Westendorf, J. Weatherford-Pratt, J.T. Myers, J.H. Wilde, D.A. Dickie, W.D. Harman. Dihapt-Coodination of Electron-Deficient Arenes with Gorup 6 Dearomatization Agents. *Organometallics*. **2020**, *39* (13), 2493-2510.

(53) J.A. Smith, K. B. W., R.E. Sonstrom, P. J. Kelleher, K.D. Welch, E.K. Pert, K.S. Westendorff, D.A. Dickie, X. Wang, B. H. Pate, W. D. Harman. Preparation of cyclohexene isotopologues and stereoisotopomers from benzene. *Nature* **2020**, *581*, 288-293.

(54) K.B. Wilson, J. T. M., H.S. Nedzbala, L.A.Combee, M. Sabat, W.D. Harman. Sequential Tandem Additions to a Tungsten-Trifluorotoluene Complex: A Versatile Method for the Preparation of Highly Functionalized Trifluoromethylated Cyclohexenens. *J. Am. Chem. Soc.* **2017**, *139* (33), 11401-11412.

(55) J.A. Pienkos, V. E. Z., D.A. Iovan, M.Li, D.P. Harrison, M. Sabat, R.J. Salomon, L. Strausberg, V.A. Teran, W.H. Myers, W.D. Harman. Friedel-crafts ring-coupling reactions promoted by tungsten dearomatization agent. *Organometallics*. **2013**, *32*, 691-703.

(56) J.H. Wilde, J. T. M., D.A. Dickie, W.D. Harman. Molybdenum-Promoted Dearomatization of Pyridines. *Organometallics*. **2020**, *39* (8), 1288-1298.

(57) J.A. Pienkos, A. T. K., B.L. McLeod, J.T. Myers, P.J. Shivokevich, V. Teran, M. Sabat, W.H. Myers, W.D. Harman. Double protonation of amino-substituted pyridine and pyrimidine tungsten complexes: friedel-crafts-like coupling to aromatic heterocycles. *Organometallics*. **2014**, *33*, 5464-5469.

(58) J.D. Dabbs, M. N. E., J.H. Wilde, R.F. Lombardo, E.C. Ashcraft, D.A. Dickie, W.D. Harman. The Tungsten-Promoted Synthesis of Piperidyl-Modified erythro-Methylphenidate Derivatives. *ACS Cent. Sci.* **2023**, *9* (9), 1775-1783.

- (59) D.P. Harrison, D. A. I., W. H. Myers, M. Sabat, S. Wang, V.E. Zottig, W.D. Harman. [4 + 2] Cyclocondensation reactions of tungsten-dihydropyridine complexes and the generation of tri- and tetrasubstituted piperidines. *J. Am. Chem. Soc.* **2011**, 133, 18378-18387.
- (60) D.P. Harrison, M. S., W.H. Myers, W.D. Harman. [145] Polarization of the pyridine ring: highly functionalized piperidines from tungsten-pyridine complex. *J. Am. Chem. Soc.* **2010**, 132, 17282-17295.
- (61) D.P. Harrison, G. W. K., V.M. Ramdeen, A.C. Nielander, S.J. Payne, M. Sabat, W.H. Myers, W.D. Harman. Tungsten-Promoted Pyridine Ring Scission: The Selective Formation of  $\eta^2$ -Cyanine and  $\eta^2$ -Merocyanine Complexes and Their Derivatives. *Organometallics*. **2010**, 29 (9), 1909-1915.
- (62) Harrison, D. P., Zottig, V.E., Kosturko, G.W., Welch, K.D., Sabat, M., Myers, W.H., Harman, W.D. Stereo- and Regioselective Nucleophilic Addition to Dihapto-Coordinated Pyridine Complexes *Organomet. Chem.* **2009**, 28, 5682-5690.
- (63) Wilde, J. H., Dickie, D.A., Harman, W.D. A Highly Divergent Synthesis of 3-Aminotetrahydropyridines. *J. Org. Chem.* **2020**, 85 (12), 8245 - 8252.
- (64) B.L. McLeod, J. A. P., K.B. Wilson, M. Sabat, W.H. Myers, W.D. Harman. Synthesis of Novel Hexahydroindoles from the Dearomatization of Indoline. *Organometallics*. **2016**, 35 (3), 370-387.
- (65) B.L. McLeod, J. A. P., J.T. Myers, M/ Sabat, E.H. Myers, W.D. Harman. Stereoselective synthesis of trans-tetrahydroindolines promoted by a tungsten  $\pi$  base *Organometallics*. **2014**, 33, 6286-6289.
- (66) J.H. Wilde, D. A. D., W.D. Harman. Molybdenum-Promoted Synthesis of Isoquinuclidines with Bridgehead CF<sub>3</sub> Groups. *J. Am. Chem. Soc.* **2019**, 141 (47), 18890-18899.
- (67) E.C. Lis, D. A. D., Y. Lin, C.J. Mocella, M.A. Todd, W. Liu, M. Sabat, W.H. Myers, W.D. Harman The Uncommon Reactivity of Dihapto-Coordinated Nitrile, Ketone, and Alkene Ligands When Bound to a Powerful  $\pi$ -Base. *Organometallics*. **2006**, 25 (21), 5051-5058.
- (68) J.T. Myers, J. H. W., M. Sabat, D.A. Dickie, W.D. Harman. Michael-Michael Ring-Closure Reactions for a Dihapto-Coodinated Naphthalene Complex of Molybdenum. **2020**, 29 (8), 1404-1412.
- (69) L. Strausberg, M. L., D.P. Harrison, W.H. Myers, M. Sabat, W.D. Harman. Exploring the o-Quinodimethane Nature of Naphthalene: Cycloaddition Reactions with

$\eta^2$ -Coordinated Tungsten–Naphthalene Complexes. *Organometallics*. **2013**, 32, 915-925.

(70) S.J. Dakermanji, K. S. W., E.K. Pert, K.B. Wilson, J.T. Myers, J.H. Wilde, D.A. Dickie, K.D. Welch, W.D. Harman. Spatial Recognition Within Terpenes; Redox and H-bond Promoted Linkage Isomerizations and the Selective Binding of Complex Alkenes. . *Organometallics*. **2020**, 39 (10), 1961-1975.

(71) J.A. Pienkos, A. T. K., B.K. Liebov, V. Teran, V.E. Zottig, M. Sabat, W.H. Myers, W.D. Harman. Tungsten-mediated selective ring opening of vinylcyclopropanes. *Organometallics*. **2014**, 33.

(72) V.E. Zottig, M. A. T., A.C. Nielander, D.P. Harrison, M. Sabat, W.H. Myers, W.D. Harman. [144] Epoxidation, Cyclopropanation, and Electrophilic Addition Reactions at the meta Position of Phenol and meta-Cresol. *Organometallics*. **2010**, 29 (21), 4793-4803.

(73) R.J. Salomon, M. A. T., M. Sabat, W.H. Myers, W.D. Harman. Single and Double Electrophilic Addition Reactions to the Aniline Ring Promoted by a Tungsten  $\pi$ -Base *Organometallics*. **2010**, 29 (4), 707-709.

(74) A.W. Lankenau, D. A. I., J.A. Pienkos, R.J. Salomon, S. Wang, D.P. Harrison, W.H. Myers, W.D. Harman. Enantioenrichment of a Tungsten Dearomatization Agent Utilizing Chiral Acids. *J. Am. Chem. Soc.* **2015**, 137 (10), 3649-3655.

(75) Morton, W. A., Stockton, Gwendolyn G. Methylphenidate Abuse and Psychiatric Side Effects. *Prim Care Companion J Clin Psychiatry* **2000**, 2 (5), 159 - 164.

(76) Ribeiro, J. P., Arther, Emma Jasmine., Gluud, Christina., Simonsen, Erik., Storebo, Ole Jakob. Does Methylphenidate Work in Children and Adolescents with Attention Deficit Hyperactivity Disorder? *Ped Rep* **2021**, 13 (3), 434 - 443.

(77) Keane, J. M.; Harman, W. D. A New Generation of  $\pi$ -Basic Dearomatization Agents. *Organomet.* **2005**, 24, 1786-1798.

(78) Liebov, B. K.; Harman, W. D. Group 6 Dihapto-Coordinate Dearomatization Agents for Organic Synthesis. *Chemical Reviews* **2017**, 117 (22), 13721-13755. DOI: 10.1021/acs.chemrev.7b00480.

(79) Wilson, K. B.; Smith, J. A.; Nedzbala, H. S.; Pert, E. K.; Dakermanji, S. J.; Dickie, D. A.; Harman, W. D. Highly Functionalized Cyclohexenes Derived from Benzene: Sequential Tandem Addition Reactions Promoted by Tungsten. *The Journal of Organic Chemistry* **2019**, 84 (10), 6094-6116. DOI: 10.1021/acs.joc.9b00279.

- (80) Wilson, K. B.; Myers, J. T.; Nedzbala, H. S.; Combee, L. A.; Sabat, M.; Harman, W. D. Sequential Tandem Addition to a Tungsten–Trifluorotoluene Complex: A Versatile Method for the Preparation of Highly Functionalized Trifluoromethylated Cyclohexenes. *Journal of the American Chemical Society* **2017**, *139* (33), 11401-11412. DOI: 10.1021/jacs.7b05118.
- (81) Simpson, S. R.; Siano, P.; Siela, D. J.; Diment, L. A.; Song, B. C.; Westendorff, K. S.; Ericson, M. N.; Welch, K. D.; Dickie, D. A.; Harman, W. D. Phenyl Sulfones: A Route to a Diverse Family of Trisubstituted Cyclohexenes from Three Independent Nucleophilic Additions. *Journal of the American Chemical Society* **2022**. DOI: 10.1021/jacs.2c03529.
- (82) Lankenau, A. W.; Iovan, D. A.; Pienkos, J. A.; Salomon, R. J.; Wang, S.; Harrison, D. P.; Myers, W. H.; Harman, W. D. Enantioenrichment of a Tungsten Dearomatization Agent Utilizing Chiral Acids. *Journal of the American Chemical Society* **2015**, *137* (10), 3649-3655. DOI: 10.1021/jacs.5b00490.
- (83) Welch, K. D.; Harrison, D. P.; Lis, E. C.; Liu, W.; Salomon, R. J.; Harman, W. D.; Myers, W. H. Large-Scale Syntheses of Several Synthons to the Dearomatization Agent {TpW(NO)(PMe<sub>3</sub>)} and Convenient Spectroscopic Tools for Product Analysis. *Organometallics* **2007**, *26* (10), 2791-2794. DOI: 10.1021/om070034g.
- (84) Eliel, E. L.; Wilen, S. H.; Mander, L. N. *Stereochemistry of Organic Compounds*; J. Wiley & Sons, Inc., 1994.
- (85) Dickens, B.; Lipscomb, W. N. Molecular and Valence Structures of Complexes of Cyclo-Octatetraene with Iron Tricarbonyl. *The Journal of Chemical Physics* **1962**, *37* (9), 2084-2093. DOI: 10.1063/1.1733429 (accessed 1/22/2025).
- (86) Benson, I. B.; Knox, S. A. R.; Stansfield, R. F. D.; Woodward, P.  $\eta^2$  Complexes of cyclic polyolefins: crystal structure of [Mn(CO)<sub>2</sub>( $\eta^2$ -C<sub>8</sub>H<sub>8</sub>)( $\eta$ -C<sub>5</sub>H<sub>5</sub>)]. *Journal of the Chemical Society, Dalton Transactions* **1981**, (1), 51-55, 10.1039/DT9810000051. DOI: 10.1039/DT9810000051.
- (87) Mak, T. C. W.; Ho, W. C.; Huang, N. Z. Metal  $\pi$ -complexes of cyclooctatetraenes: IV. Synthesis and crystal structure of benzocyclooctatetraenesilver(I) perchlorate: An example of arene and olefin ligands coordinated simultaneously to a silver(I) ion. *Journal of Organometallic Chemistry* **1983**, *251* (3), 413-421. DOI: [https://doi.org/10.1016/S0022-328X\(00\)98786-2](https://doi.org/10.1016/S0022-328X(00)98786-2).
- (88) Wang, H., Du, Q., Xie, Y., King, R.B., Schafer III, H.F. The hapticity of cyclooctatetraene in its first row mononuclear transition metal carbonyl complexes:



Several examples of octahapto coordination. *J. Organomet. Chem.* **2010**, 695 (2), 215-225.

(89) Hu, N.; Gong, L.; Jin, Z.; Chen, W. Crystal structure of cyclooctatetraenylpotassium,  $C_8H_8K_2 \cdot (OC_4H_8)_3$ . *Journal of Organometallic Chemistry* **1988**, 352 (1), 61-66. DOI: [https://doi.org/10.1016/0022-328X\(88\)83019-5](https://doi.org/10.1016/0022-328X(88)83019-5).

(90) A. Streitwieser, U. M.-W. Di- $\pi$ -cyclooctatetraenethorium. *Journal of the American Chemical Society. J. Am. Chem. Soc.* **1969**, 91.

(91) F. V. Bolhuis, A. H. K., J. H. Teuben. Synthesis, Properties and Crystal Structure of A Dicyclopentadienyl Tantalum Cyclooctatetraene Complex *J. Org. Chem.* **1981**, 206, 185-195.

(92) I. Bach, K. R. P., B. Proft, R. Goddard, C. Kopiske, C. Kruger, A. Rufinska, K. Seevogel. Novel Ni(0)-COT Complexes, Displaying Semiaromatic Planar COT Ligands with Alternating C-C and C=C Bonds. *J. Am. Chem. Soc.* **1997**, 119, 3773-3781.

(93) Benson, I. B., Knox, S.A.R., Standsfield, R.F.D., Woodward, P.  $\eta^2$ -Cyclooctatetraene: Crystal and Molecular Structure of  $[M(CO)_2(\eta^2-C_8H_8)(\eta^5-C_5H_5)]$ . *J.C.S. Chem. Comm.* **1977**., 404-405.

(94) Lis, E. C.; Delafuente, D. A.; Lin, Y.; Mocella, C. J.; Todd, M. A.; Liu, W.; Sabat, M.; Myers, W. H.; Harman, W. D. The Uncommon Reactivity of Dihapto-Coordinated Nitrile, Ketone, and Alkene Ligands When Bound to a Powerful  $\pi$ -Base. *Organometallics* **2006**, 25 (21), 5051-5058. DOI: 10.1021/om060434o.

(95) Harrison, D. P.; Nichols-Nieler, A. C.; Zottig, V. E.; Strausberg, L.; Salomon, R. J.; Trindle, C. O.; Sabat, M.; Gunnoe, T. B.; Iovan, D. A.; Myers, W. H.; et al. Hyperdistorted Tungsten Allyl Complexes and Their Stereoselective Deprotonation to Form Dihapto-Coordinated Dienes. *Organometallics* **2011**, 30 (9), 2587-2597. DOI: 10.1021/om200183m.

(96) Saunders, M.; Berger, R.; Jaffe, A.; McBride, J. M.; O'Neill, J.; Breslow, R.; Hoffmann, J. M.; Perchonock, C.; Wasserman, E.; et al. Unsubstituted cyclopentadienyl cation, a ground-state triplet. *Journal of the American Chemical Society* **1973**, 95 (9), 3017-3018. DOI: 10.1021/ja00790a049.

(97) Alsharif, M. A.; Raja, Q. A.; Majeed, N. A.; Jassas, R. S.; Alsimaree, A. A.; Sadiq, A.; Naeem, N.; Mughal, E. U.; Alsantali, R. I.; Moussa, Z.; et al. DDQ as a versatile and easily recyclable oxidant: a systematic review. *RSC Advances* **2021**, 11 (47), 29826-29858, 10.1039/D1RA04575J. DOI: 10.1039/D1RA04575J.

- (98) Huynh, M. T.; Anson, C.W.; Cavell, A.C.; Stahl, S.S.; Hammes-Schiffer, S. Quinone 1 e<sup>-</sup> and 2e<sup>-</sup>/2 H<sup>+</sup> Reduction Potentials: Identification and Analysis of Deviations from Systematic Scaling Relationships. *J. Am. Chem. Soc.* **2016**, *138*, 15903-15910.
- (99) Ranasinghe, S.; Martin, C. D.; Dutton, J. L. Cyclopentadienyl cations. *Chemical Science* **2025**, *16* (5), 2083-2088, 10.1039/D4SC07024K. DOI: 10.1039/D4SC07024K.
- (100) VanderWeide, A.; Prokopchuk, D.E. Cyclopentadienyl ring activation in organometallic chemistry and catalysis *Nat Rev Chem* **2023**, *7*, 561-572.
- (101) Evans, W. J. Tutorial on the Role of Cyclopentadienyl Ligands in the Discovery of Molecular Complexes of the Rare-Earth and Actinide Metals in New Oxidation States. *Organometallics*. **2016**, *35* (18), 3088-3100.
- (102) Huttner, G.; Brintzinger, H. H.; Bell, L. G.; Friedrich, P.; Bejenke, V.; Neugebauer, D. The structure of (C<sub>5</sub>H<sub>5</sub>W(CO)<sub>2</sub>) a compound containing a bent trihapto-cyclopentadienyl ligand. *Journal of Organometallic Chemistry* **1978**, *145* (3), 329-333. DOI: [https://doi.org/10.1016/S0022-328X\(00\)81301-7](https://doi.org/10.1016/S0022-328X(00)81301-7).
- (103) O'Connor, J. M.; Casey, C. P. Ring-slippage chemistry of transition metal cyclopentadienyl and indenyl complexes. *Chemical Reviews* **1987**, *87* (2), 307-318. DOI: 10.1021/cr00078a002.
- (104) Calderon, J.; Cotton, F. A.; Legzdins, P. Stereochemically nonrigid organometallic molecules. XXI. Crystal and molecular structures of tris (cyclopentadienyl) nitrosylmolybdenum. *Journal of the American Chemical Society* **1969**, *91* (10), 2528-2535.
- (105) Casey, C. P.; Jones, W. D. Conversion of an. eta. 5-cyclopentadienyl-metal complex to an. eta. 1-cyclopentadienyl-metal complex upon addition of trimethylphosphine. *Journal of the American Chemical Society* **1980**, *102* (19), 6154-6156.
- (106) Demir, S.; Mueller, T. J.; Ziller, J. W.; Evans, W. J. Tris(polyalkylcyclopentadienyl) Complexes: The Elusive [(η<sup>5</sup>-C<sub>5</sub>R<sub>5</sub>)<sub>2</sub>M(η<sup>1</sup>-C<sub>5</sub>R<sub>5</sub>)] Structure and Trihapto Cyclopentadienyl Coordination Involving a Methyl Substituent. *Angewandte Chemie International Edition* **2011**, *50* (2), 515-518. DOI: <https://doi.org/10.1002/anie.201005898> (accessed 2024/11/10).
- (107) Bond, A. D.; Layfield, R. A.; MacAllister, J. A.; McPartlin, M.; Rawson, J. M.; Wright, D. S. The first observation of the [Cp<sub>3</sub>Mn]<sup>-</sup> anion; structures of hexagonal [(η<sup>2</sup>-

Cp)<sub>3</sub>MnK·1.5thf] and ion-separated [(η<sup>2</sup>-Cp)<sub>3</sub>Mn]<sub>2</sub>[Mg(thf)<sub>6</sub>] ·2thf. *Chemical Communications* **2001**, (19), 1956-1957, 10.1039/B106366A. DOI: 10.1039/B106366A.

(108) Alvarez, C. S.; Bashall, A.; McInnes, E. J. L.; Layfield, R. A.; Mole, R. A.; McPartlin, M.; Rawson, J. M.; Wood, P. T.; Wright, D. S. Structural and Magnetic Studies of the Tris(cyclopentadienyl)manganese(II) “Paddle-Wheel” Anions [Cp<sub>3</sub>-(MeCp)Mn]<sup>-</sup> (n=0–3, MeCp=C<sub>5</sub>H<sub>4</sub>CH<sub>3</sub>, Cp=C<sub>5</sub>H<sub>5</sub>). *Chemistry – A European Journal* **2006**, 12 (11), 3053-3060. DOI: <https://doi.org/10.1002/chem.200501214>.

(109) Takeuchi, K. i.; Kurosaki, T.; Yokomichi, Y.; Kimura, Y.; Kubota, Y.; Fujimoto, H.; Okamoto, K. The one-electron reduction of carbonium ions. Part 14. Effect of successive introduction of methyl substituents on the reducibility of tropylium ion in chromium(II) ion and cathodic reductions. *Journal of the Chemical Society, Perkin Transactions 2* **1981**, (4), 670-674, 10.1039/P29810000670. DOI: 10.1039/P29810000670.

(110) Koby, R. F.; Doerr, A. M.; Rightmire, N. R.; Schley, N. D.; Long, B. K.; Hanusa, T. P. An η<sup>3</sup>-Bound Allyl Ligand on Magnesium in a Mechanochemically Generated Mg/K Allyl Complex. *Angewandte Chemie International Edition* **2020**, 59 (24), 9542-9548. DOI: <https://doi.org/10.1002/anie.201916410> (accessed 2024/11/25).

(111) Lamsa, M., Suorsa, T., Pursianinen, J., Huuskonen, J., Rissanen, K. Crystal Structure of an inclusion complex between dibenzo-24-crown-8 and tropylium tetrafluoroborate. *Chem. Commun.* **1996**, 1443.

(112) Zahra, F. T.; Saeed, A.; Mumtaz, K.; Albericio, F. Tropylium Ion, an Intriguing Moiety in Organic Chemistry. *Molecules* **2023**, 28 (10). DOI: 10.3390/molecules28104095 From NLM.

(113) Green, M. L. H.; Ng, D. K. P. Cycloheptatriene and -enyl Complexes of the Early Transition Metals. *Chemical Reviews* **1995**, 95 (2), 439-473. DOI: 10.1021/cr00034a006.

(114) Glöckner, A.; Tamm, M. The organometallic chemistry of cycloheptatrienyl zirconium complexes. *Chemical Society Reviews* **2013**, 42 (1), 128-142, 10.1039/C2CS35321K. DOI: 10.1039/C2CS35321K.

(115) Basse, R.; Vanicek, S.; Höfer, T.; Kopacka, H.; Wurst, K.; Müller, T.; Schwartz, H. A.; Olthof, S.; Casper, L. A.; Nau, M.; et al. Cationic Cycloheptatrienyl Cyclopentadienyl Manganese Sandwich Complexes: Tromancenum Explored with

High-Power LED Photosynthesis. *Organometallics* **2021**, 40 (15), 2736-2749. DOI: 10.1021/acs.organomet.1c00376 From NLM.

(116) Astley, S. T.; Takats, J.; Huffman, J. C.; Streib, W. E. Solid-state structure and fluxional solution behavior of the ambident organometallic nucleophiles ( $\eta^3$ -C<sub>7</sub>H<sub>7</sub>)M(CO)<sub>3</sub>- (M = ruthenium, osmium). *Organometallics* **1990**, 9 (1), 184-189. DOI: 10.1021/om00115a028.

(117) Beddoes, R. L.; Hussain, Z. I.; Roberts, A.; Barraclough, C. R.; Whiteley, M. W.  $\eta^7 \rightarrow \eta^3$  Hapticity interconversion in cycloheptatrienyl complexes of molybdenum and tungsten. Crystal structures of [Mo(NCS)(CO)<sub>2</sub>(C<sub>10</sub>H<sub>8</sub>N<sub>2</sub>)( $\eta^3$ -C<sub>7</sub>H<sub>7</sub>)] and [MoCl(CO)<sub>2</sub>(Ph<sub>2</sub>PCH<sub>2</sub>CH<sub>2</sub>PPh<sub>2</sub>)( $\eta^3$ -C<sub>7</sub>H<sub>6</sub>C<sub>6</sub>H<sub>4</sub>F-4)]. *Journal of the Chemical Society, Dalton Transactions* **1996**, (18), 3629-3637, 10.1039/DT9960003629. DOI: 10.1039/DT9960003629.

(118) Beddoes, R. L.; Hinchliffe, J. R.; Moorcroft, D.; Whiteley, M. W. Reactions of the cycloheptatrienyl complexes [MX(CO)<sub>2</sub>( $\eta$ -C<sub>7</sub>H<sub>7</sub>)] (M=Mo, X=Br; M=W, X=I) with CNBut: X-ray crystal structure of [Wl(CO)<sub>2</sub>(CNBut)<sub>2</sub>( $\eta^3$ -C<sub>7</sub>H<sub>7</sub>)]. *Journal of Organometallic Chemistry* **1998**, 560 (1), 265-272. DOI: [https://doi.org/10.1016/S0022-328X\(98\)00519-1](https://doi.org/10.1016/S0022-328X(98)00519-1).

(119) Smith, J. A., Scouten, A., Wilde, J.H., Westendorff, K.W., Dickie, D.A., Ess, D.H., Harman, W.D. Experiments and Direct Dynamics Simulations That Probe  $\eta^2$ -Arene/Aryl Hydride Equilibria of Tungsten Benzene Complexes. *J. Am. Chem. Soc.* **2020**, 142, 16437-16454.

(120) Pita-Milleiro, A.; Alférez, M. G.; Moreno, J. J.; Espada, M. F.; Maya, C.; Campos, J. Unveiling the Latent Reactivity of Cp\* Ligands (C<sub>5</sub>Me<sub>5</sub>-) toward Carbon Nucleophiles on an Iridium Complex. *Inorganic Chemistry* **2023**, 62 (15), 5961-5971. DOI: 10.1021/acs.inorgchem.2c04381.

(121) Pauson, P. L.; Todd, K. H. Cycloheptatriene and tropylium metal complexes. Part VIII. A study of directive effects in nucleophilic addition to substituted tricarbonyltropyliumchromiums. *Journal of the Chemical Society C: Organic* **1970**, (19), 2638-2641, 10.1039/J39700002638. DOI: 10.1039/J39700002638.

**Chapter 4.**  
**The Unexpected Challenges and Successes of Functionalizing**  
**Five-Membered Carbocycles.**

## 4.1 Introduction

Although synthetic chemists have developed numerous transformations for constructing molecular compounds, there remains a need for new synthetic methods.<sup>1</sup> Beyond enabling the synthesis of increasingly complex molecules, novel methodologies that improve selectivity or provide alternative routes to known compounds drive innovation in synthetic chemistry. In drug discovery, in particular, there is significant interest in synthetic approaches that yield  $sp^3$ -rich compounds, as existing methods—such as Suzuki–Miyaura and Buchwald–Hartwig couplings—have led to an overrepresentation of  $sp^2$ -hybridized structures.<sup>2–4</sup> Additionally, incorporating stereocenters and achieving stereochemical resolution are critical considerations in pharmaceutical development.<sup>5, 6</sup>

Cyclopentane cores are a common structural motif in both natural products and therapeutic drugs. Cyclopentanes rank as the seventh most common ring system in natural products, appearing in biologically active molecules such as prostaglandins, jatrophanes, and pactamycin.<sup>7</sup> Notable pharmaceutical compounds containing cyclopentane cores include Loxoprofen (NSAID), Bimatoprost (glaucoma treatment), and Ticagrelor (blood thinner).<sup>8–10</sup> Given the importance of five-membered carbocycles, efficient synthetic methods for cyclopentane construction remain a key focus in organic chemistry.<sup>11–13</sup> A major challenges in cyclopentane synthesis is the control of stereochemical outcomes. Strategies to address this challenge include selective rearrangements<sup>14–17</sup> and cycloadditions,<sup>18–30</sup> though methods that allow for the rapid construction of complex chiral five-membered carbocycles are still highly desirable. Expanding the molecular libraries of cyclopentane-based small molecules and screening for biological activity could significantly advance pharmaceutical development.<sup>31</sup>

Like five-membered carbocycles, six-membered carbocycles are widespread in both nature and medicinal chemistry. Harman and coworkers have demonstrated that dihapto-coordination of alkene-containing six-membered carbocycles—including benzenes—to the  $\pi$ -basic tungsten fragment,  $[W Tp(NO)(PMe_3)]$  ( $Tp$  = hydridotris(pyrazolyl)-borate,  $NO$  = nitrosyl, and  $PMe_3$  = trimethylphosphine) enables highly selective transformations, yielding complex cyclohexenes as single enantiomers.<sup>32–44</sup> This organometallic approach has also been applied to preparation of heteroaromatic systems such as pyrroles, furans and thiophene complexes.<sup>45–53</sup> Specifically, sequential electrophilic and nucleophilic additions to dihapto-coordinated

cyclopentadiene complexes of osmium(II), ruthenium(II), and rhenium(I) has been explored. While this methodology successfully produced regio- and diastereoselective disubstituted cyclopentenes, its scope was limited, and the metal systems employed did not allow for synthesis of single enantiomers.<sup>54</sup> To address these challenges and leverage the enrichment capabilities of the tungsten(0) system for isolating single enantiomers, this study investigates the expansion and limitations of cyclopentene functionalization using tungsten-based organometallic chemistry.

## 4.2 Results and Discussions

### 4.2.1 Mono-functionalized Cyclopentenes

Preliminary studies done on  $W(Tp)(NO)(PMe_3)(\eta^2\text{-cyclopentene})$  revealed that the addition of trityl triflate ( $Ph_3COTf$ ) led to hydride abstraction, forming the hyperdistorted  $\eta^2$ -allyl complex  $[W(Tp)(NO)(PMe_3)(\eta^2\text{-cyclopentenyl})]OTf$ .<sup>55</sup> Subsequently, it was discovered that coordination and protonation of  $W(Tp)(NO)(PMe_3)(\eta^2\text{-cyclopentadiene})$  with triflic acid ( $HOTf$ ) yielded the same hyperdistorted  $\eta^2$ -allyl. First, coordination of cyclopentadiene (CPD) involved the retro-Diels-Alder cracking of dicyclopentadiene to generate the cyclopentadiene monomer. Notably, if residual dicyclopentadiene remained in the sample, it could also coordinate to the metal complex CPD resulting in an additional five complexes. Column chromatography was used for their isolation. Two complexes were successfully isolated from the others using 45% EtOAc/55% hexanes on silica and characterized via 2D-NMR (**1D** and **1P**). Compounds **1D** and **1P** co-crystallized; their structures were confirmed through single-crystal x-ray diffraction (SC-XRD). The first challenge identified in this study was that incomplete isolation of cyclopentadiene monomer led to contamination of dihapto-coordination to the free alkenes of the CPD dimer.

When the cyclopentadiene monomer was cleanly isolated, it coordinated to tungsten in an approximately a 3:1 coordination diastereomeric ratio (c.d.r.), but precipitation from hexanes results in a c.d.r. closer to 1:1. (**2P:2D**). The structure of the major complex, **2P**, was confirmed through SC-XRD. Upon protonation of both complexes, a single isomer,  $[W(Tp)(NO)(PMe_3)(\eta^2\text{-cyclopentenyl})]OTf$ , was formed. This dihapto-coordinated allyl complex exhibited hyperdistorted character, and while both *distal* (**3D**) and *proximal* (**3P**) conformations are possible, the equilibrium favors

the *distal* conformation. These compounds and their crystal structures are summarized in **Figure 4.1**.

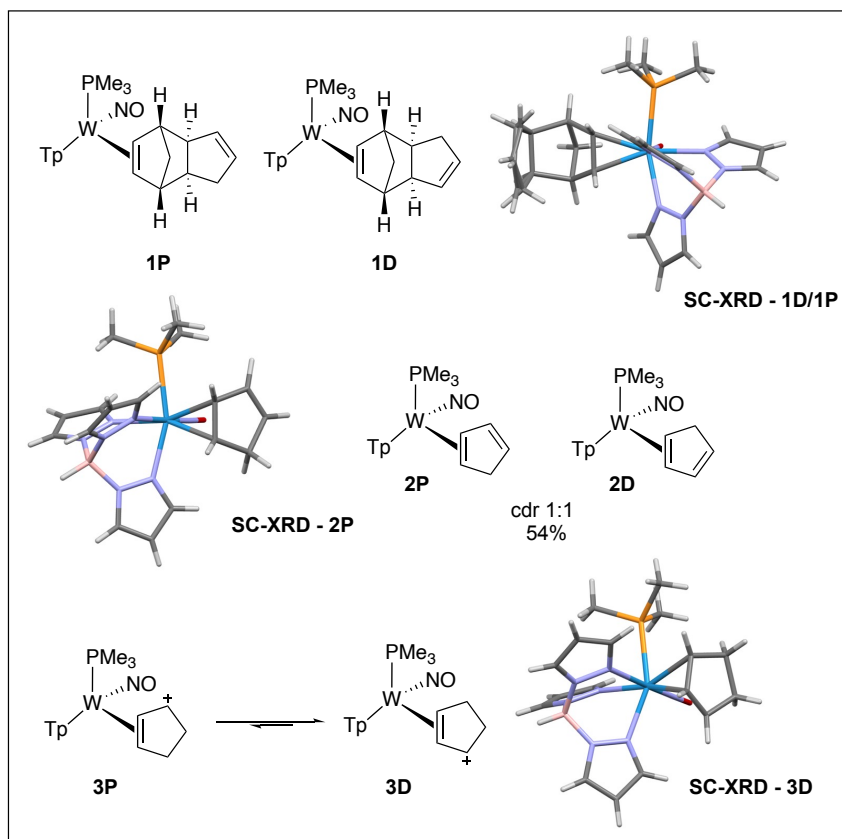


**Figure 4.1.** W(Tp)(NO)(PMe<sub>3</sub>)(η<sup>2</sup>-dicyclopentadiene), W(Tp)(NO)(PMe<sub>3</sub>)(η<sup>2</sup>-cyclopentadiene), and W(Tp)(NO)(PMe<sub>3</sub>)(η<sup>2</sup>-cyclopentenyl cation) and corresponding SC-XRD structures.

The electrophilic reactivity of η<sup>2</sup>-cyclopentenyl with a range of nucleophiles was investigated and demonstrated in **Figure 4.2**. The main goal was selectivity screening therefore yield recovery was not pursued. Nucleophiles such as cyano, *n*-butyl, dimethylmalonate, phenol, imidazole, 1,8-diazabicyclo[5.4.0] undec-7-ene (DBU), and deuterium (**4A – 4G**) were screened. Both the *distal* and *proximal* intermediates were capable of reacting with nucleophiles, and selectivity for each position was determined for individual nucleophiles, resulting in a range of diastereomer ratios (d.r.). Interestingly, more labile nucleophiles, such as imidazole and phenol, resulted in the lowest ratios, whereas less labile nucleophiles led to minimal side product formation. This observation is most likely due to a preferred kinetic position, yet similar thermodynamic preferences. Consistently, nucleophilic additions occurred exclusively *anti* to the metal bulk were observed. The successful functionalization of the η<sup>2</sup>-cyclopentene complex demonstrated the viability of this tungsten-based system for synthesizing single enantiomers of mono-substituted cyclopentenenes when starting



materials are enantiomerically enriched. However, the ultimate goal was to develop methodology for constructing more complex molecular architectures.

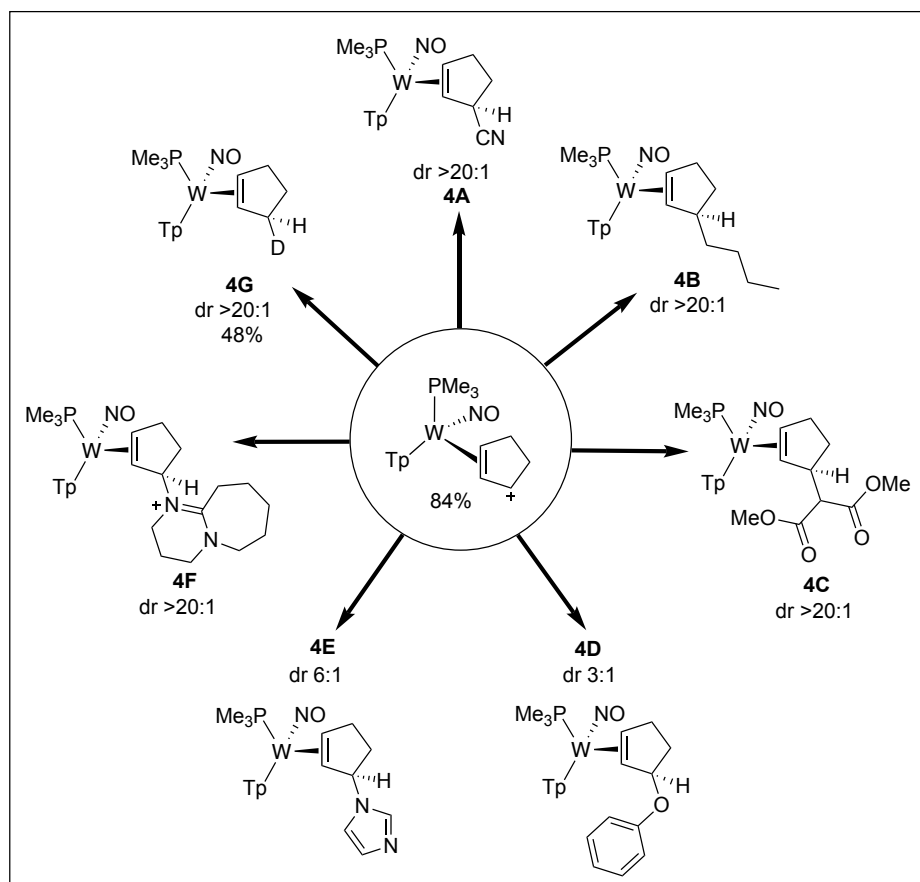


**Figure 4.2.** Scope of dihapto-coordinated mono-substituted cyclopentenenes.

#### 4.2.2 Disubstituted Cyclopentenenes

One of the initial attempts to selectively synthesize disubstituted cyclopentenenes involved using  $\text{Ph}_3\text{COTf}$  to abstract the hydride at the *proximal* position from a few of the dihapto-coordinated mono-substituted cyclopentenenes, thereby generating another  $\eta^2$ -allyl species. However, the targeted compounds were either resistant to the hydride abstraction reagent or abstraction occurred at an unintended site on the first nucleophile.

A subsequent approach utilized the recently developed  $\eta^2$ -cyclopentadienium cation (**5**) as a precursor for disubstituted cyclopentenenes. This complex was obtained via hydride abstraction from the  $\eta^2$ -cyclopentadiene complex. The synthesis of  $\text{W}(\text{Tp})(\text{NO})(\text{PMe}_3)(\eta^2\text{-cyclopentadienyl cation})$  was successfully achieved, and its reactivity toward nucleophiles like methyl Grignard, ( $\text{MeMgBr}$ ), sodium cyanide ( $\text{NaCN}$ ), lithium dimethylmalonate ( $\text{LiDiMM}$ ), sodium borohydride ( $\text{NaBH}_4$ ), and sodium borodeuteride ( $\text{NaBD}_4$ ) was screened for selectivity of addition to the distal

conformation over the proximal conformation, leading to the formation of  $\eta^2$ -mono-substituted cyclopentadienes (**6A – 6D**), and is shown in **Figure 4.3**. The scope was extended with the help of Josh Heman Ackah. Unfortunately, nucleophilic addition showed poor regioselectivity between the *distal* and *proximal* positions, producing diastereomers as products. Despite this, nucleophiles consistently added to the ring face *anti* to the metal bulk. Theoretically, oxidation of the metal center would release the mono-substituted cyclopentadiene ligand, yielding a single organic regioisomer. However, due to the lack of regioselectivity in the initial nucleophilic addition, the resulting organics produced would be collected as racemic material. A brief database search indicated no existing methodology for the straightforward incorporation of a nucleophile into a cyclopentadiene core.

The incorporation of a methyl group via a Grignard reagent resulted in a d.r. of 3:2, which improved to 2:1 after silica column chromatography using ether as an eluent. Despite the initial lack of regioselectivity, protonation and the subsequent incorporation of a second nucleophile were still investigated. Protonation of compound **6C** with HOTf yielded complexes **7A** and **7B** in a d.r. of 1.2:1. The mixture was then exposed to MeMgBr for the addition of a second methyl group. Complexes **7A** and **7B** exist as two hyperdistorted conformations: *distal* (**7A-D** and **7B-D**) and *proximal* (**7A-**

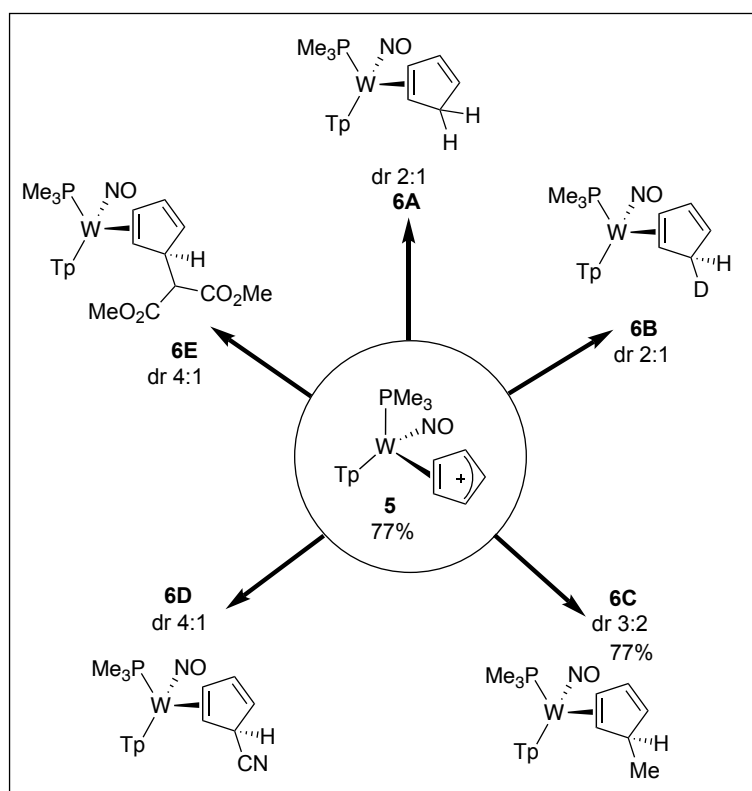


**Figure 4.3.** Scope of dihapto-coordinated mono-substituted cyclopentadienes.

**P** and **7B-P**). Methyl addition to **7A-P** or **7B-D** results in compound **8A**, whereas addition to **7A-D** yields compound **8B**. These three complexes were formed in a ratio of 1.5:1:0.2. Because of overlapping peaks in the proton NMR spectrum of this mixture, the characterization of the complexes was not pursued. Methyl was chosen as both the first and second nucleophile in the screening to simplify spectroscopic analysis since additions to **7A-P** and **7B-D** resulting in the same product. Using two different nucleophiles would have led to additional isomers. Although selectivity could potentially be improved by incorporating sterically bulky groups, the poor regioselectivity observed in both the first and second nucleophilic additions posed a major synthetic challenge. Consequently, this limitation prompted further exploration of alternate synthetic pathways. The methodology described above is summarized in **Figure 4.4**.

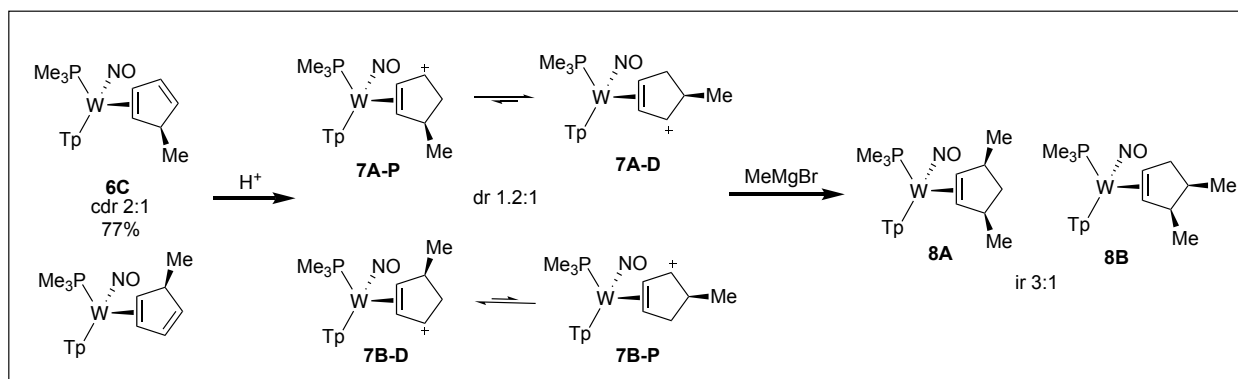


**Figure 4.4.** Synthetic approach to dihapto-coordinated di-substituted cyclopentene.

#### 4.2.3 Binuclear Tungsten Species.

Rather than the previously proposed scheme—where nucleophilic addition is followed by protonation and a second nucleophilic addition—a synthetic route involving the initial addition of a broader scope of electrophiles to [W]-CPD, followed by nucleophilic addition, could be imagined in the generation of stereoselective disubstituted cyclopentenes. Yet, the primary challenge in this approach is the ability to isolate a single diastereomer of the [W]-CPD complex. This ensures that upon introduction of the electrophile, a single  $\eta^2$ -allyl species is produced. Without prior enrichment to a single isomer, the resulting products would resemble complexes **7A** and **7B**. Preliminary evidence suggested that introducing free cyclopentadiene to a mixture of isolated [W]-CPD could increase the c.d.r. to 10:1, though this result lacked reproducibility.

A previous study on six-membered rings demonstrated that due to the hyperdistortion of [W]-cyclohexenyl cation, selective deprotonation with a base could enrich the coordination diastereomer ratio (c.d.r.) of [W]-cyclohexene from 1:1.1 to 10:1.<sup>38</sup> This methodology was explored for the analogous five-membered system. A screen of bases was conducted, revealing that while some bases added as nucleophiles, triethylamine (TEA) successfully enriched the c.d.r. of [W]-CPD to >20:1 when used in excess. However, upon isolation of the  $\eta^2$ -diene, the c.d.r. regressed to 4:1. Additionally, the choice of base, as well as the rate and equivalency of TEA introduction, led to complex impurity peaks in the <sup>1</sup>H-NMR spectra.

Further investigation revealed that adding 2,6-lutidine exclusively formed the “impurities” previously observed during deprotonation. 2D-NMR analysis suggested the formation of a tungsten dimer. Yet, due to the chirality of the metal complex, the coupling of racemic material produced two diastereomeric complexes along with their corresponding enantiomers: *mixed-hand* (**9D**) and *same-hand* (**10D**) coupling products, complicating proton assignments. To simplify spectroscopic analysis and isolate a single enantiomer, the same methodology was applied to an enriched metal starting material. It was confirmed that compound **3D** underwent partial deprotonation to **2D**, where the  $\eta^2$ -allyl then had the opportunity to act as an electrophile with the nucleophilic  $\eta^2$ -diene, yielding the *same-hand* product (**10D**). Interestingly, coupling occurred exclusively with the **3D** conformation, whereas the nucleophilic additions presented earlier in the study proceeded at both **3D** and **3P**, most likely due to sterics. Once again, stereoselectivity was achieved, with both chiral centers forming at the ring face opposite the metal bulk.

Unfortunately, due to the inability to isolate a single coordination diastereomer of [W]-CPD, the *mixed-hand* (**9D**) product remains inaccessible for isolation. While the formation of a tungsten dimer has been previously proposed as a side reaction between  $\eta^2$ -allyls and  $\eta^2$ -alkenes, this represents the first example of a cleanly synthesized and isolated binuclear coupled product. The four stereoisomers of racemic binuclear [W]-CPD species, and the reaction scheme for enriched coupling is shown in **Figure 4.5**. Further investigations on coupling products were completed with the help of Alvin Q. Meng.

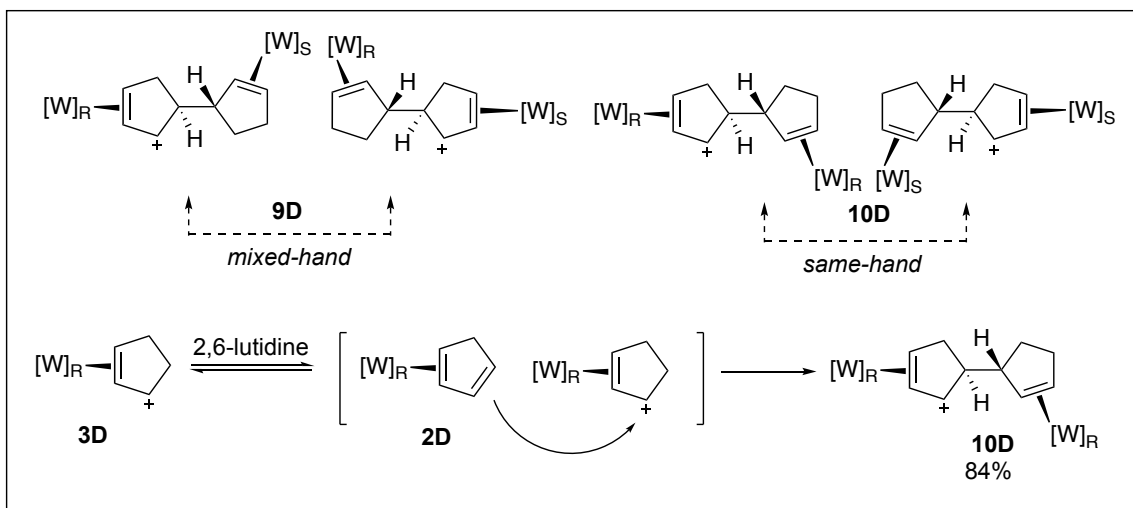


**Figure 4.5.** Stereoisomers of binuclear coupled products; dotted arrows link enantiomer pairs.

Since a binuclear dihapto-coordinated allyl had not been synthesized before, its reactivity toward nucleophiles was uncertain. However, its electrophilic behavior proved comparable to that of mononuclear species. As observed in spectroscopic data, the *distal* conformation (**10D**) is the most stable, but is still in equilibrium with its *proximal* conformation (**10P**). Interestingly, due to steric effects, **10P** was the preferred conformation for addition reactions, leading to the formation of second functionalized position of the cyclopentene core. Similar to the mononuclear species, these additions were largely regioselective and fully stereoselective. Although the study demonstrated these reactions using the  $[W]_S$  complex, the same methodology could be applied to  $[W]_R$  to obtain the other enantiomeric product. The allyl shift from **10D** to **10P** and the scope of nucleophilic additions are summarized in **Figure 4.6**.

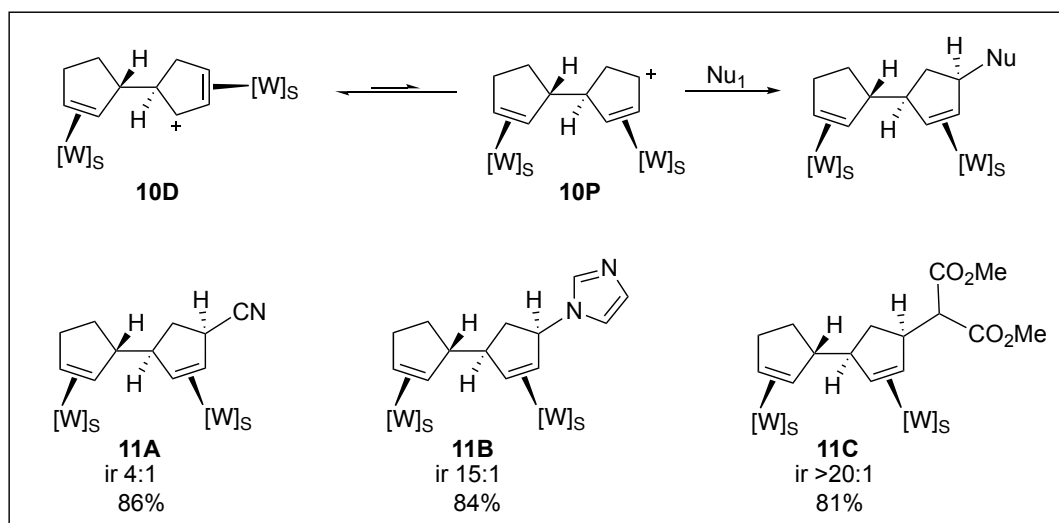


**Figure 4.6.** Equilibrium of dihapto-coordinated binuclear coupling allyl and nucleophilic

Given that the species was now binuclear, it was hypothesized that base addition might enable selective deprotonation, yielding a single substituted [W]-CPD. As with the mononuclear species, the addition of triethylamine selectively deprotonated the complex. However, unlike the mononuclear counterpart, deprotonation occurred exclusively from the proximal conformation (**10P**), and the d.r. was retained upon isolation—likely due to the inaccessibility of the neighboring hydrogen of the distal conformation. This species was confirmed through SC-XRD and is illustrated in **Figure 4.7**.

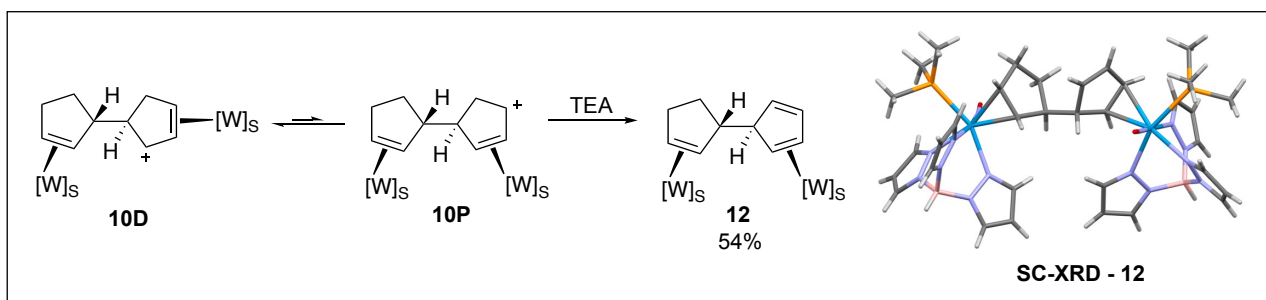


**Figure 4.7.** Selective deprotonation of dihapto-coordinated binuclear coupled allyl.

#### 4.2.4 Oxidation Reactions

The oxidation reaction for isolating the organic compound was investigated. Upon treatment of compound **11C** with two equivalents of 2,3-dichloro-5,6-dicyano-1,4-benzoquinone (DDQ), a mixture of two products was observed. It was determined that while one product was the fully organic species, the second species was a partially oxidized intermediate, **13**, as confirmed by SC-XRD. It is speculated that the first tungsten center to be released from the complex is the more sterically hindered one. Because excess DDQ led to a mixture of compounds **13** and **14**, alternative oxidizing agents were explored. The addition of six equivalents of ceric ammonium nitrate (CAN) successfully facilitated the complete oxidation of both tungsten centers in the binuclear species, leading to the clean removal and isolation of the organic difunctionalized cyclopentene, **14**. This methodology is summarized in **Figure 4.8**.

Lastly, it was investigated whether the analogous reaction mechanism could be applied to six-membered rings. As previously mentioned, the isolation of single coordination diastereomer of [W]-cyclohexadiene is achievable through consecutive protonation and deprotonation, owing to selective deprotonation from the *distal* conformation of the hyperdistorted  $\eta^2$ -cyclohexadienyl cation. Compound **15D** was obtained in a 17:1 ratio relative to its coordination diastereomer. The direct combination of **15D** with  $\eta^2$ -allyl **3D** resulted in a single product, whose <sup>1</sup>H-NMR

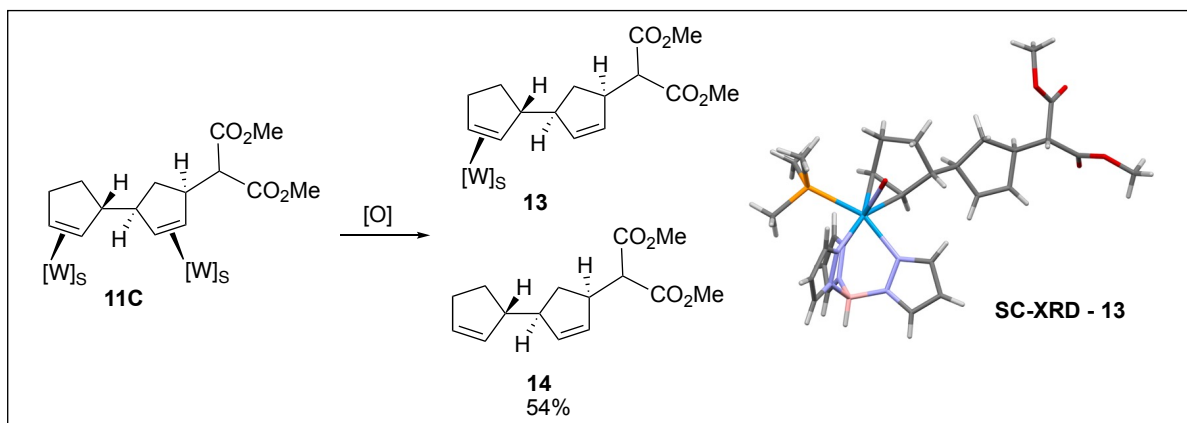


**Figure 4.8.** Partially and fully oxidized binuclear species, the formation of a difunctionalized cyclopentene ring.

spectrum was consistent with the coupled product **16D**. Treatment with a base (DBU) resulted in selective deprotonation of the *proximal* conformation (**16P**) yielding compound **17**. Additionally, treatment with sodium cyanide resulted in a selective addition to the *proximal* conformation (**16P**) yielding compound **18**, enabling further functionalization on the cyclohexene ring. This example provided a synthetic route for the *same-hand* coupling product. Notably, because [W]-cyclohexadiene can be isolated as a single coordination diastereomer, it could be exposed to the opposite metal enantiomer, facilitating a *mixed-hand* coupling reaction and allowing for the independent synthesis of all four enantiomers. These findings are summarized in **Figure 4.9**.

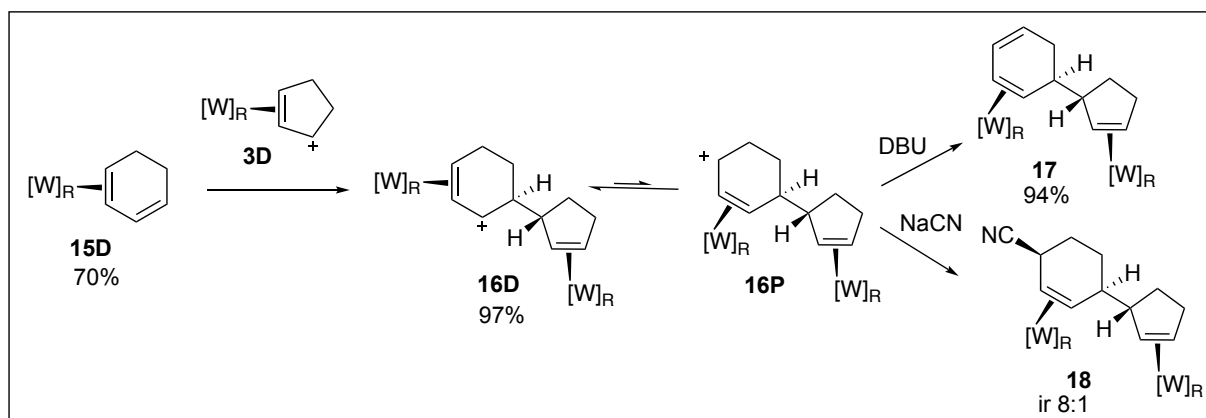


**Figure 4.9.** Reaction of  $\eta^2$ -cyclohexadiene with  $\eta^2$ -cyclopentenyl and  $\eta^2$ -cyclohexenyl cations.

Further exploration examined whether the [W]-cyclohexadiene and [W]-cyclohexadienyl cation coupling product could be generated. While evidence of coupling was observed, the starting materials remained the predominant species in solution. The relative integrations of the new species appeared dependent on the

solution concentration, suggesting a dynamic equilibrium between the binuclear and mononuclear species. This behavior contrasts with that of the  $\eta^2$ -cyclopentenyl cation, where coupling is instantaneous and irreversible, yielding a single, well-defined product. Overall, it was determined that the reactivity of the  $\eta^2$ -cyclopentenyl cation is the primary driving force for coupling reactions.

### 4.3 Future Studies

Several approaches were explored in an attempt to increase the selectivity of the  $\eta^2$ -cyclopentadienyl cation towards nucleophiles. These included employing a bulkier phosphine ligand, lowering reaction temperatures, and using catalytic amounts of an oxidant to alter the final ratio of substituted [W]-cyclopentadienes. However, none of these strategies yielded successful outcomes. If future efforts are directed toward the synthesis of functionalized cyclopentenes, they would likely be most effective in expanding the scope of coupled products.

One intriguing avenue for future research would be the incorporation of a fourth stereocenter on the ring. The greater the number of stereocenters that can be synthesized in a single enantiomer, the more complex and valuable the resulting molecules become. A key question is whether the  $\eta^2$ -cyclopentadienyl cation exhibits similar reactivity to the  $\eta^2$ -cyclopentenyl cation in coupling reactions. The increased steric bulk of the [W]-cyclopentadiene nucleophile could potentially enhance regioselectivity in these reactions. If successful in forming a binuclear species, the initially generated dihapto-coordinated allyl could react with a variety of nucleophiles while leaving an uncoordinated alkene. Subsequent acid treatment and exposure to a second nucleophile would further expand functionalization.

Additionally, given that selective deprotonation was achieved for the formation of compound **12**, this species should also allow for the selective incorporation of electrophiles. A potential electrophilic transformation could involve the introduction of a methoxy group via exposure to Selectfluor in methanol, forming an  $\eta^2$ -bound allyl intermediate reactive toward nucleophiles. Since the methoxy group is a labile group, it is also possible that it could dissociate, regenerating another  $\eta^2$ -bound allyl intermediate primed for nucleophilic attack—ultimately enabling selective functionalization of all three uncoordinated carbons of a single cyclopentene ring.

It was also demonstrated that a partially oxidized species, **13**, can be synthesized. If this species can be cleanly produced and isolated, it presents an



interesting opportunity: one alkene remains “protected” by tungsten while the other remains free to participate in a variety of organic transformations.

Lastly, another point of diversification for this methodology would be the introduction of nucleophiles to complex **16P** or the sequential addition of an electrophile followed by a nucleophile to compound **17**. Expanding the range of rings coupled to **3D** could also be valuable. For example, coupling with dihapto-coordinated pyridines, dihydropyridines, benzenes, cycloheptatrienes, cyclooctatetraene, and cyclooctadienes—complexes that have already been successfully synthesized in the lab—could broaden the applicability of this methodology.

#### 4.4 Conclusions

The investigation on the functionalization of cyclopentenes centered on the synthesis of dihapto-coordinated allylic cations, exploring their reactivity toward nucleophiles and their potentials for stereoselective synthesis. Initial efforts to generate disubstituted cyclopentenes were met with challenges. First, attempted hydride abstractions from mono-substituted [W]-cyclopentenes did not yield  $\eta^2$ -cyclopentenyl cations while nucleophilic additions to the  $\eta^2$ -cyclopentadienyl cation had low regioselectivity, yielding mixtures of diastereomers. While stereoselectivity was consistently observed—favoring addition anti to the bulky metal center—the lack of regioselectivity in both the first and second nucleophilic additions posed a significant synthetic challenge.

An alternative approach involved leveraging selective deprotonation strategies to enrich specific coordination diastereomers prior to functionalization. While successful for six-membered systems, initial attempts to apply this method to five-membered rings were met with setbacks due to equilibrium constraints. However, the unexpected formation of a tungsten-binuclear dihapto-coordinated allyl complex represented a breakthrough. This novel species not only provided insight into previously uncharacterized side reactions but also displayed reactivity comparable to mononuclear analogs, with regio- and stereoselective nucleophilic addition favoring the *proximal* conformation.

The successful oxidation of binuclear species further demonstrated that fully organic, difunctionalized cyclopentenes could be obtained. Notably, the choice of oxidant played a crucial role in reaction outcomes, with CAN proving more effective than DDQ in achieving clean and complete oxidation of both tungstens. Additionally, the isolation of a partially oxidized species provided a promising avenue for future

work, as it could serve as a selectively protected intermediate for further functionalization.

Despite challenges in regioselectivity, the methodologies developed here establish a foundation for further exploration of functionalized cyclopentenes. Future work could focus on improving selectivity through steric modifications of ligands and expanding the coupling reactions to include a broader range of substrates. The ability to introduce multiple stereocenters in a controlled manner opens new avenues for synthesizing complex chiral molecules.

## References

- (1) Reymond, J.-L., Awale, Mahendra. . Exploring Chemical Space for Drug Discovery Using the Chemical Universe Database. *ACS Chem Neurosci*. **2012.**, 3, 649 - 657.
- (2) Brown, D. G., Bostrom, Jonas. . Analysis of Past and Present Synthetic Methodologies on Medicinal Chemistry: Where Have All the New Reactions Gone? *J. Med. Chem*. **2015**, 59 (10), 4443 - 4458.
- (3) Lovering, F., Bikker, Jack., Humblet, Christine. Escape from Flatland: Increasing Saturation as an Approach to Improving Clinical Success. *J. Med. Chem*. **2009**, 52 (21), 6752 - 6756.
- (4) Clemons, P. A., Bodycombe, Nicole E., Carrinski, Hyman, A., Wilson, Anthony., Shamji, Alykhan, F., Wagner, Bridget K., Koehler, Angela N., Schreiber, Stuart L. . Small molecules of different origins have distinct distributions of structural complexity that correlate with protein-binding profiles. . *PNAS* **2010**, 107 (44), 18787-18792.
- (5) Scott, K. A., Ropek, Nathalie., Melillo, Bruno., Schreiber, Stuart L., Cravatt, Benjamin F., Vinogradova, Ekaterina V. Stereochemical diversity as a source of discovery in chemical biology. *Curr Res Chem Biol* **2022**, 2, 100028.
- (6) Islam, M. R., Mahdi, J.G., Bowen, I.D. Pharmacological importance of stereochemical resolution of enantiomeric drugs. *Drug Saf* **1997**, 17 (3), 149 - 165.
- (7) Chen, Y., Rosenkranz, Cara., Hirte, Steffen., Kirchmair, Johannes. Ring systems in natural products: structural diversity, physicochemical properties, and coverage by synthetic compounds. *Nat. Prod. Rep.* **2022**, 39 (8), 1544 - 1556.
- (8) Greig, S. L., Garnock-Jones, Karly P. Loxoprofen: A Review in Pain and Inflammation *Clin Drug Investig.* **2016**, 36 (9), 771 - 781.
- (9) Curran, M. P. Bimatoprost: a review of its use in open-angle glaucoma and ocular hypertension *Drugs Aging*. **2009**, 26 (12), 1049 - 1071.
- (10) Dobesh, P. P., Oestreich, Julie H. Ticagrelor: pharmacokinetics, pharmacodynamics, chiral efficacy, and safety. *Pharmacotherapy*. **2014.**, 34 (10), 1077 - 1090.
- (11) Hudlicky, T., Price, John D. Anionic Approaches to the Construction of Cyclopentanoids. *Chem Rev* **1989**, 89, 1467 - 1486.
- (12) Lautens, M., Klute, Wolfgang., Tam, William. Transition Metal-Mediated Cycloaddition Reactions. *Chem Rev* **1996**, 96, 49 - 92.
- (13) Heasley, B. Stereocontrolled Preparation of Fully Substituted Cyclopentanes: Relevance to Total Synthesis *Eur. J. Org. Chem.* **2009**, (10), 1460 - 1631.

- (14) Hudlicky, T., Reed, Josephine W. From discovery to application: 50 years of the vinylcyclopropane-cyclopentene rearrangement and its impact on the synthesis of natural products *Angew Chem Int Ed Engl* **2010**, 49 (29), 4864 - 4876.
- (15) Rubin, M., Rubina, Marina., Gevorgyan, Vladimir. Transition metal chemistry of cyclopropenes and cyclopropanes *Chem Rev* **2007**, 107 (7), 3117 - 31179.
- (16) Baldwin, J. E. Thermal Rearrangements of Vinylcyclopropanes to Cyclopentenenes. *Chem Rev* **2003**, 103 (4), 1197 - 1212.
- (17) Goldschmidt, Z., Crammer, B. Vinylcyclopropane rearrangements *Chem Soc Rev* **1988**, 17, 229 - 267.
- (18) Trost, B. M., Morris, Partrick J., Sprague, Simon J. Palladium-catalyzed diastereo- and enantioselective formal [3+2]-cycloadditions of substituted vinylcyclopropanes *J. Am. Chem. Soc.* **2012**, 134 (42), 17823 - 17831.
- (19) Nanteuil, F. d., Waser, Jerome. Catalytic [3+2] Annulation of Aminocyclopropanes for the Enantiospecific Synthesis of Cyclopentylamines. *Angew Chem Int Ed* **2011**, 50 (50), 12075 - 12079.
- (20) Liu, L., Montgomery, John. Dimerization of Cyclopropyl Ketones and Crossed Reactions of Cyclopropyl Ketones with Enones as an Entry to Five-Membered Rings. *J. Am. Chem. Soc.* **2006**, 128 (16), 5348 - 5349.
- (21) Trost, B. M., Lam, Tom M. Development of Diamidophosphite Ligands and Their Application to the Palladium-Catalyzed Vinyl-Substituted Trimethylenemethane Asymmetric [3+2] Cycloaddition. *J. Am. Chem. Soc.* **2012**, 134 (28), 11319 - 11321.
- (22) Trost, B. M., Silverman, Steven M., Stambuli, James P. Development of an Asymmetric Trimethylenemethane Cycloaddition Reaction: Application in the Enantioselective Synthesis of Highly Substituted Carbocycles. *J. Am. Chem. Soc.* **2012**, 133 (48), 19483 - 19497.
- (23) Fujiwara, Y., Fu, Gregory C. Application of a New Chiral Phoshepine to the Catalytic Asymmetric Synthesis of Highly Functionalized Cyclopentenenes That Bear An Array of Heteroatom-Substituted Quaternary Stereocenters. *J. Am. Chem. Soc.* **2011**, 133 (31), 12293 - 12297.
- (24) Zhu, G., Chen, Zhaogen., Jiang, Qiongzong., Xia, Dengming., Cao, Ping., Zhang, Xumu. Asymmetric [3+2] Cycloaddition of 2,3-Butadienoates with Electron-Deficient Olefins Catalyzed by Novel Chiral 2,5-Dialkyl-7-phenyl-7-phosphabicyclo[2.2.1]heptanes. *J. Am. Chem. Soc.* **1997**, 119 (16), 3836 - 3837.

- (25) Han, X., Wang, Youquing., Zhong, Fangrui., Lu, Yixin. Enantioselective [3+2] Cycloaddition of Allenes to Acrylates Catalyzed by Dipeptide-Derived Phosphines: Facile Creation of Functionalized Cyclopentenes Containing Quaternary Stereogenic Centers *J. Am. Chem. Soc.* **2011**, 133 (6), 1726 - 1729.
- (26) Sampath, M., Loh, Teck-Peng. Highly enantio-, regio-, and diastereoselective one-pot [2+3]-cycloaddition reaction via isomerization of 2-butynoates to allenates *Chem Sci* **2010**, 1 (6), 739 - 742.
- (27) Parr, B. T., Li, Zhanjie., Davies, Huw M.L. Asymmetric synthesis of highly functionalized cyclopentanes by a rhodium- and scandium-catalyzed five-step domino sequence *Chem Sci* **2011**, 2 (12), 2378 - 2382.
- (28) Cowen, B. J., Miller, Scott J. Enantioselective [3+2]-cycloaddition catalyzed by a protected, multifunctional phosphine-containing  $\alpha$ -amino acid *J. Am. Chem. Soc.* **2007**, 129 (36), 10988 - 10989.
- (29) Davies, H. M. L., Manning, James R. Catalytic C-H functionalization by metal carbenoid and nitrenoid insertion. *Nature* **2008**, 451, 417 - 424.
- (30) Parr, B. T., Davies, Huw M.L. Highly Stereoselective synthesis of cyclopentanes bearing four stereocenters by a rhodium carbene-initiated domino sequence *Nat Comm* **2014**, 5, 4455.
- (31) Heasley, B. Recent Developments in the Stereocontrolled Synthesis of Highly Substituted Cyclopentane Core Structures: From Drug Discovery Research to Natural Product Synthesis *Curr Org Chem* **2014**, 18 (6), 641 - 686.
- (32) Harman, W. D., Taube, Henry. The Selective Hydrogenation of Benzene to Cyclohexene on Pentaammineosmium(II). *J. Am. Chem. Soc.* **1988**, 110, 7906 - 7907.
- (33) Kopach, M. E., Hipple, William G., Harman, W. Dean. Phenol-Cyclohexadienone Equilibrium for  $\eta^2$ -Coordinated Arenes. *J. Am. Chem. Soc.* **1992**, 114, 1736 - 1740.
- (34) Kopach, M. E., Harman, W. Dean. Novel Michael Additions to Phenol Promoted by Osmium(II): Convenient Stereoselective Syntheses of 2,4- and 2,5-Cyclohexadienones. *J. Am. Chem. Soc.* **1994**, 116, 6581 - 6592.
- (35) Kopach, M. E., Kolis, Stanley P., Liu, Ronggang., Robertson, Jason W., Chordia, Mahendra D., Harman, W. Dean. Stereodirected Tandem Addition Reactions of  $\eta^2$ -Arenes: A Versatile Route to Functionalized Cyclohexenes. *J. Am. Chem. Soc.* **1998**, 120 (25), 6199 - 6204.

- (36) Chordiam Mahendra D., H. W. D. Asymmetric Dearomatization of  $\eta^2$ -Arene Complexes: Synthesis of Stereodefined Cyclohexenones and Cyclohexenes. *J. Am. Chem. Soc.* **2000**, *122*, 2725 - 2736.
- (37) Wilson, K. B., Myers, Jeffery T., Nedzbala, Hannah S., Combee, Logan A., Sabat, Michael., Harman, W. Dean. Sequential Tandem Addition to a Tungsten-Trifluorotoluene Complex: A Versatile Method for the Preparation of Highly Functionalized Trifluoromethylated Cyclohexenes. **2017**, *139*, 11401 - 11412.
- (38) D.P. Harrison, A. C. N., V. E. Zottig, L. Strausberg, R.J. Salomon, C.O. Trindle, M. Sabat, T.B. Gunnoe, D.A. Iovan, W.H. Myers, W.D. Harman. Hyperdistorted Tungsten Allyl Complexes and Their Stereoselective Deprotonation to Form Dihapto-Coordinated Dienes *Organometallics*. **2011**, *30* (9), 2587-2597.
- (39) K.B. Wilson, J. A. S., H.S. Nedzbala, E. K. Pert, S.J. Dakermanji, D.A. Dickie, W.D. Harman Highly Functionalized Cyclohexenes Derived from Benzene: Sequential Tandem Addition Reactions Promoted by Tungsten *J. Org. Chem.* **2019**, *84* (10), 6094-6116.
- (40) J.A. Smith, K. B. W., R.E. Sonstrom, P. J. Kelleher, K.D. Welch, E.K. Pert, K.S. Westendorff, D.A. Dickie, X. Wang, B. H. Pate, W. D. Harman. Preparation of Cyclohexene Isotopologues and Stereoisomers from Benzene. *Nature* **2020**, *581*, 288-293.
- (41) S.R. Simpson, P. S., D.J. Siela, L.A. Diment, B.C. Song, K. S. Westendorff, M. N. Ericson, K. D. Welch, D. A. Dickie, W.D. Harman. Phenyl Sulfones: A Route to a Diverse Family of Trisubstituted Cyclohexenes from Three Independent Nucleophilic Additions. *J. Am. Chem. Soc.* **2022**, *144* (21), 9489-9499.
- (42) J.T. Weatherford-Pratt, J. M. B., J.A. Smith, M. N. Ericson, D.J. Siela, K. B. Wilson, M.H. Shingler, M.R. Ortiz, S. Fong, J.A. Laredo, I.U. Patel, M. McGraw, D. A. Dickie, W. D. Harman. Tungsten-anisole complex provides 3,6-substituted cyclohexenes for highly diversified chemical libraries. *Sci. Adv.* **2024**, *10* (7).
- (43) A.W. Lankenau, D. A. I., J.A. Pienkos, R.J. Salomon, S. Wang, D.P. Harrison, W.H. Myers, W.D. Harman. Enantioenrichment of a Tungsten Dearomatization Agent Utilizing Chiral Acids. *J. Am. Chem. Soc.* **2015**, *137* (10), 3649-3655.
- (44) B.K. Liebov, W. D. H. Group 6 Dihapto-Coordinate Dearomatization Agents for Organic Synthesis. *Chem. Rev.* **2017**, *117*, 13721-13755.

- (45) Myers, W. H., Koontz, J.I., Harman, W.D. Tautomerizations, Protonations, and Electrophilic Additions of  $\eta^2$ -Coordinated Pyrroles *J. Am. Chem. Soc.* **1991**, *114* (14), 5684 - 5692.
- (46) Hodges, L. M., Gonzales, Javier., Koontz, Jason I., Myers, William H., Harman, W. Dean.  $\beta$ -Electrophilic Addition of Pentaammineosmium(II)  $\eta^2$ -Pyrrole Complexes *J. Org. Chem.* **1995**, *60*, 2125 - 2146.
- (47) Spera, M. L., Harman, W. D. Electrophilic Additions to  $\eta^2$ -Thiophene Complexes: Synthesis of Novel Thiophenium and Thiafulvenium Species *Organomet.* **1999**, *18*, 2988 - 2998.
- (48) Valahovic, M. T., Myers, William H., Harman, W. Dean Decrimination of Entiofaces and Stereoselective Electrophilic Addition Reactions for  $\eta^2$ -Pyrrole Complexes *Organomet.* **2002**, *21*, 4581 - 4589.
- (49) Friedman, L. A., Sabat, Michael., Harman, W. Dean Cycloaddition Reactions of Dihapto-Coordinated Furans *J. Am. Chem. Soc.* **2002**, *124*, 7395 - 7404.
- (50) Friedman, L. A., You, Fei., Sabat, Michael., Harman, W. Dean. Rhenium-Promoted Diastereo- and Enantioselective Cyclopentannulation Reactions: Furans as 1,3-Propene Dipoles *J. Am. Chem. Soc.* **2003**, *125*, 14980 - 14981.
- (51) Schiffler, M. A., Friedman, Lee A., Brooks, Benjamin, C., Sabat, Michael., Harman, W. Dean Stereoselective Aldehyde Addition to Rhenium-Coordinated Furans *Organomet.* **2003**, *22*, 4966 - 4972.
- (52) Welch, K. D., Smith, Philip L., Keller, Andrew P., Myers, William H., Sabat, Michael., Harman, W. Dean. Osmium(II)-, Rhenium(I)-, Tungsten(0)-Promoted Dipolar Cycloaddition Reactions with Pyrroles: Exploiting the Azomethine Ylide Character of this Heterocycle *Organomet.* **2006**, *25*, 5067 - 5075.
- (53) Welch, K. D., Harrison, Daniel P., Sabat, Michael., Hejazi, Emily Z., Parr, Brenden T., Fanelli, Matthew G., Gianfranceso, Nicole A., Nagra, Dalsher S., Myers, William H., Harman, W. Dean. Michael-Aldol Ring Closures with Dihapto-Coordinated Pyrrole Complexes and the Synthesis of Tetrahydroindole Cores *Organomet.* **2009**, *28*, 5960 - 5967.
- (54) Spera, M. L., Chin, R. Martin., Winemiller, Mark D., Lopez, Katherine W., Sabat, Michael., Harman, W. D. Sequential Electrophilic/Nucleophilic Additions for  $\eta^2$ -Cyclopentadiene Complexes of Osmium(II), Ruthenium (II), and Rhenium(I). *Organomet.* **1996**, *15*, 5447 - 5449.

(55) Lis, E. C., Delafuente, D.A., Lin, Y., Mocella, C.J., Todd, M.A., Liu, W., Sabat, M., Myers, W.H., Harman, W.D. The Uncommon Reactivity of Dihapto-Coordinated Nitrile, Ketone, and Alkene Ligands When Bound to a Powerful  $\pi$ -Base. . *Organometallics*. **2006**, 25 (21), 5051-5058.



**Chapter 5.**  
**The Synthesis of Functionalized Eight-Membered Carbocycles:**  
**Trisubstituted Cyclooctenes**

## 5.1 Introduction

As mentioned in Chapter 3, the ultimate objective of the dihapto-coordination of cyclooctatetraene is the synthesis of complex organic molecules, particularly highly functionalized eight-membered rings. Eight-membered rings are common structural motifs in a wide range of natural products, including terpenoid ring systems, sesquiterpenoids, diterpenoids, sesterterpenoids, lignans and pigments—many of which exhibit fascinating structural features and significant biological properties.<sup>1-3</sup> Moreover, eight-membered carbocycles are prominent in several pharmaceutical compounds, such as Paclitaxel (a chemotherapy agent),<sup>5</sup> Dezocine (an analgesic),<sup>6</sup> and Retapamulin (a topical antibiotic).<sup>7</sup> Despite their abundance in nature and growing presence in medicinal compounds, the synthesis of eight-membered carbocycles remains challenging due to ring strain, unfavorable entropic and enthalpic factors, and transannular interactions.<sup>1-3, 8</sup> While there is ongoing interest and progress in the synthesis of heterocyclic eight-membered cores,<sup>9-11</sup> this study specifically focuses on the functionalization of eight-membered carbocyclic cores, with an emphasis on carbon-carbon bond formation.

### 5.1.1 *Synthetic Strategies to Eight-Membered Rings*

Although synthetic methods used for both smaller and larger sized carbocycles have been applied to the synthesis of eight-membered rings, many of the reported strategies are specifically tailored to the total synthesis of natural products containing eight-membered cores. In fact, these approaches often rely on intramolecular bond-forming reactions, including cycloadditions, cyclizations, fragmentations, transannular reactions, ring-closing metathesis and transition metal-mediated carbocyclizations.

Cycloaddition reactions are among the most common strategies in the construction of eight-membered cores. These include [4+2] cycloadditions,<sup>12-20</sup> [4+4] cycloadditions,<sup>21-25</sup> [2+2] cycloadditions<sup>26, 27</sup> and others.<sup>28-38</sup> Cyclization methods have also played a crucial role in the synthesis of eight-membered rings in natural products, often proceeding through radical or organometallic intermediates. Although radical reactions are typically highly reactive and difficult to control, several examples have been reported in the formation of eight-membered natural products. Notable cyclization strategies include  $\text{SmI}_2$ -mediated reductive cyclizations,<sup>39-44</sup>  $\text{Mn(III)}$ -mediated oxidative cyclizations,<sup>45, 46</sup> McMurry coupling,<sup>47-51</sup> and various other transition metal-mediated carbocyclizations.<sup>52-61</sup> More recently, ring-closing

metathesis and transannular reactions have become widely used for eight-membered ring formation.<sup>62-70</sup> Additionally, fragmentations and transannular reactions, including bicyclic and tricyclic ring expansions, have provided access to cyclooctane structural cores.<sup>71-77</sup> While these reactions have been instrumental in natural product synthesis, they are often sensitive to substitution patterns and reaction conditions, limiting their scope and yield. **Figure 5.1A** summarizes previously reported synthetic strategies for constructing cyclooctane rings. Despite these advances, organic chemistry still lacks a direct and general methodology for the incorporating functional groups into a cyclooctane ring. The approach demonstrated in this study focuses on the direct functionalization of cyclooctatetraene, **Figure 5.1B**.

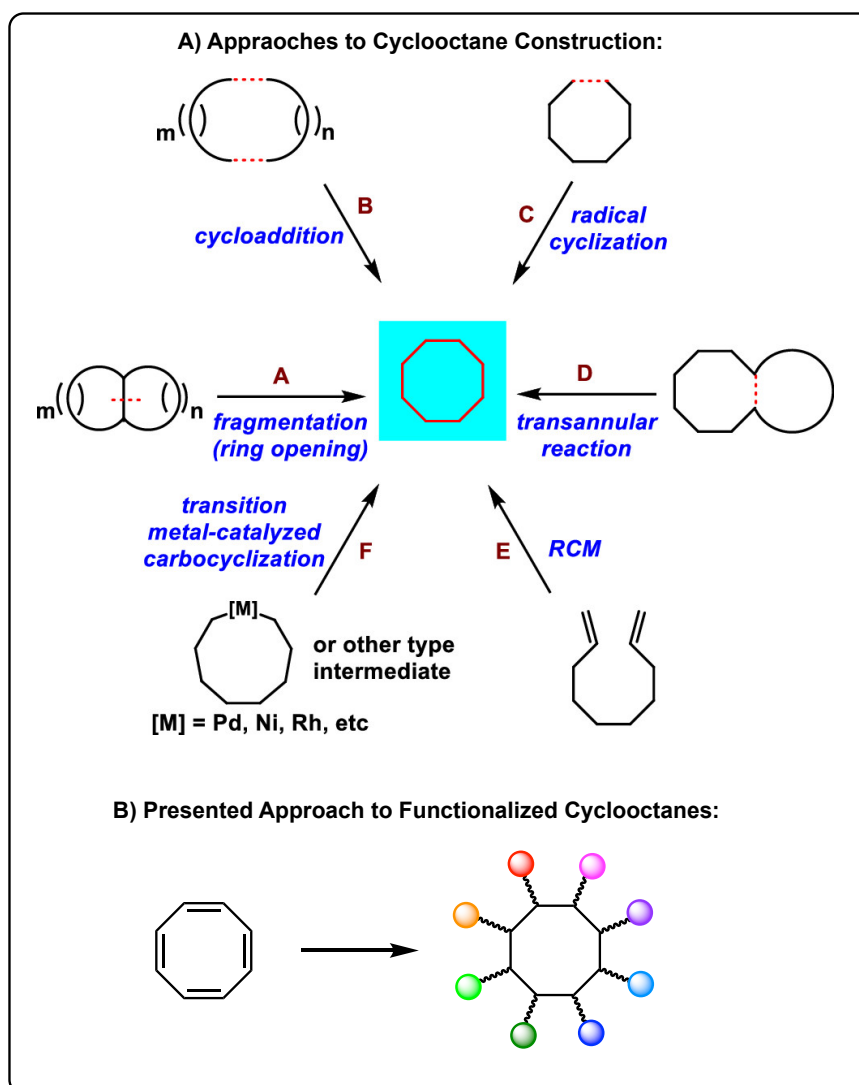


**Figure 5.1.** (A) General strategies to form eight-membered carbocycles, figure appended from review article.<sup>2</sup> (B) The strategy pursued in this study for functionalized eight-membered rings.

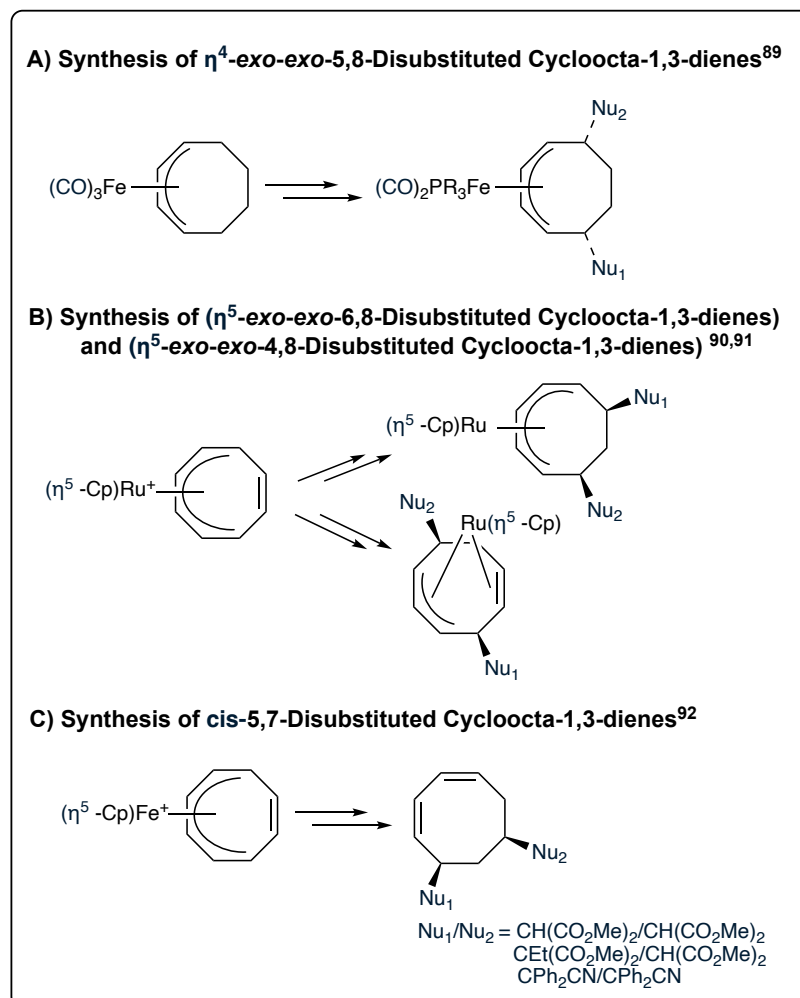
Diversity-oriented syntheses revolves around the idea that, rather than targeting a specific natural product, synthetic methodologies can be designed to generate a wide variety of small molecular complexes. This approach expands unexplored chemical space and provides molecular libraries for the discovery of biologically active compounds.<sup>78, 79</sup> Additionally, late-stage functionalization has revolutionized organic chemistry by enabling the incorporation of functional groups into established drugs, thereby rapidly diversifying screening libraries.<sup>80, 81</sup> These concepts in drug discovery are considered when designing synthetic methodologies for functionalized eight-membered cores.

#### 5.1.2 Organometallic Functionalization of Cyclooctatetraene

The direct functionalization of cyclooctatetraene (COT) is highly appealing to chemists; however, these reactions often yield unexpected products. Although COT possess eight  $\pi$  electrons, which is characteristic of an anti-aromatic species, it is non-aromatic due to its deviation from planarity, making it an isolable compound. Typically, COT undergoes rearrangement reactions to form aromatic ring systems.<sup>82-85</sup> When protonated, COT forms a homotropylium cation, which adopts a conformation that experiences aromatic stabilization and subsequently reacts with nucleophiles to generate bicyclic species.<sup>86</sup>

Despite its potential, organometallic methods for COT functionalization present significant synthetic challenges<sup>87, 88</sup> Initially, Pearson demonstrated that organoiron chemistry enables the transformation of cyclooctadiene into a disubstituted cyclooctadiene complex (**Figure 5.2A**).<sup>89</sup> Notably, Jürgen Heck expanded on this work, making significant progress in the selective transformation of cyclooctatetraene into substituted cyclooctadienes. Through hexahapto-coordination, COT is activated for iterative nucleophilic and electrophilic addition reactions. The transformation of  $[\text{Ru}(\text{Cp})(\eta^6\text{-COT})]^+$  into functionalized disubstituted cyclooctadienes was achieved, and regioisomers were obtained through haptomer rearrangement (**Figure 5.2B**).<sup>90, 91</sup> Finally,  $[\text{Fe}(\text{Cp})(\eta^6\text{-COT})]$  (Cp = cyclopentadienyl) was utilized for COT functionalization.<sup>92, 93</sup> This methodology enabled the synthesis and isolation of *cis*-5,7-disubstituted 1,3-cyclooctadienes (**Figure 5.2C**). However, its scope was limited to bulky nucleophiles, does not yield single enantiomers, and the synthetic pathway does

not facilitate the isolation of monosubstituted cyclooctatrienes or the selective incorporation of a third nucleophile to generate trisubstituted cyclooctenes.

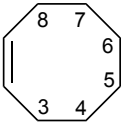


**Figure 5.2.** Current organometallic approaches to the functionalized eight-membered rings.

According to the SciFinder database, approximately 20,000 cyclooctenes have been reported, excluding polycyclic compounds. Of these, fewer than 6% contain more than one stereocenter in the ring, and those that do often exist as mixtures of diastereomers. Reported substitution patterns for trisubstituted cyclooctenes are summarized in **Table 5.1**. Methodology to directly transform cyclooctatetraene into saturated cyclooctenes have been explored.

The methodology presented herein employs the dihapto-coordination ( $\eta^2$ ) of COT to the fragment  $\{\text{W}(\text{Tp})(\text{PMe}_3)(\text{NO})\}$  ( $\text{Tp}$  = hydridotris(pyrazoyl)borate,  $\text{PMe}_3$  = trimethylphosphine, and  $\text{NO}$  = nitrosyl) to achieve the regioselective and stereoselective synthesis of organic monosubstituted, disubstituted and trisubstituted cyclooctene complexes. This strategy enables access to highly functionalized eight-

membered rings, which have historically been difficult to synthesize. To date, this appears to be the largest small-molecule library of functionalized C<sub>8</sub> rings. Scopes were expanded with the help of Josh Heman-Ackah.

	
Substitution	Number
3,4,5-	15
3,4,6-	0
3,4,7-	0
3,4,8-	2
4,5,6-	3
4,5,7-	0
4,5,8-	22
3,5,6-	0
3,5,7-	2
3,5,8-	7
Total Cyclooctenes: ~20,0000	

**Table 5.1.** Frequency of cyclooctenes with different substitution patterns.

## 5.2 Results and Discussion

### 5.2.1 *Dihapto-Coordination of Cyclooctatetraene*

The dihapto-coordination of aromatic compounds has been successfully employed for the dearomatization of arenes, enabling their transformation into structurally sophisticated small molecules. Many of these reactions focus on the formation of six-membered carbocyclic and heterocyclic cores.<sup>94-102</sup> The complex

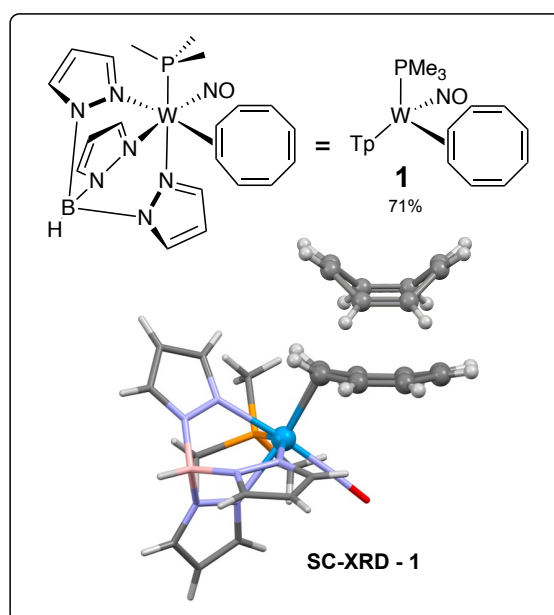


**Figure 5.3.** SC-XRD comparisons of decomplexed cyclooctatetraene<sup>4</sup> and dihapto-coordinated cyclooctatetraene.

[W(Tp)(NO)(PMe<sub>3</sub>)( $\eta^2$ -COT)] (**1**) was reported in Chapter 3. A distinctive feature of this complex is its *semiaromatic planarity*, whereas uncomplexed COT adopts a tub-shaped conformation to avoid anti-aromaticity, **Figure 5.3**. Additionally,  $\eta^2$ -coordination of COT leads to other noticeable geometric changes: the C=C bonds lengths increase from 1.33 Å to an average of 1.35 Å, while the C-C bonds lengths decrease from 1.47 Å to an average of 1.44 Å, compared to free COT, causing the ring to appear more aromatic when bound to the metal.

### 5.2.2 First Protonation Reaction

Dihapto-coordinated cyclooctatetraene undergoes protonation upon the addition of triflic acid (HOTf) in solution. Initially, complexes **2A**, **2B** and **2C** are observed in a 2A:2B:1C ratio. However, after a few hours in solution or a few days as a solid, the isomeric distribution thermodynamically shifts to a ratio of 6A:1B:0C. The major complex (**2A**) was confirmed through single-crystal x-ray crystallography (SC-XRD), **Figure 5.4**. The three  $\eta^2$ -cyclooctatrienyl cationic species are classified as diastereomers because they cannot interconvert solely through charge movement; instead, their interconversion requires tungsten-alkene isomerizations, such as a *ring-walk*, *ring-slip* and/or *face-flip* mechanism. Additionally, each isomer exists in two conformations.<sup>103</sup> The more stable conformation for each isomer localizes the charge *distal* to the phosphine ligand, where one W-C interaction is longer than the other two W-C bonds (**2A-D**, **2B-D**, and **2C-D**). The less stable conformations (**2A-P**, **2B-P**, and **2C-P**) localizes the charge *proximal* to the phosphine. Both conformations for each isomer were structurally optimized through density functional theory (DFT) using the M06 functional with the 6-31G(d,p) basis set on main group atoms and LANL2DZ on tungsten, and compared energetically, **Figure 5.4**. Theoretically, multiple possible mechanisms allow for interconversion between **2A-D**, **2B-D** and **2C-D**. For example, **2C-D** can convert to **2A-P**, and **2C-P** can convert to **2A-D** via a *face-flip* isomerization. Additionally, a *ring-walk* reaction of **2B-D**, shifting the dihapto-coordinate bond to the alkene *proximal* to the phosphine, produces a resonance structure of **2A-D**, while a *ring-slip* reaction of **2B-P** results in the formation of **2A-D**. Furthermore, **2C-D** can form via a *ring-walk* from a resonance structure of **2B-D**, and **2C-P** can form via a *ring-walk* from a resonance structure of **2B-P**.

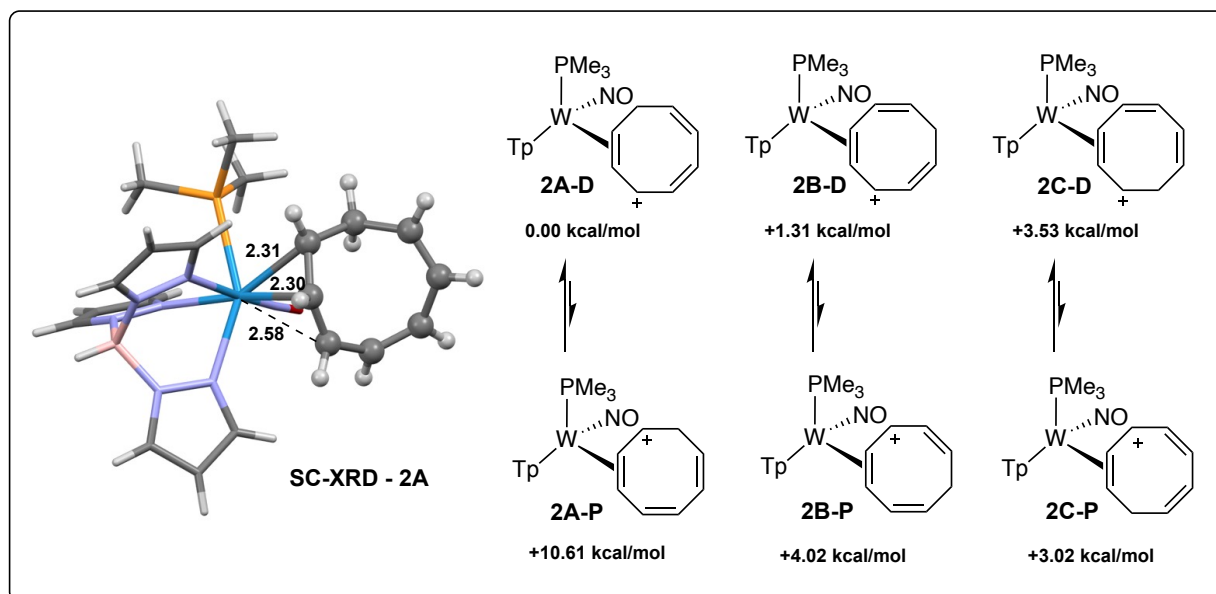


**Figure 5.4.** The three  $\eta^2$ -cyclooctatrienium isomers, the calculated energies of their *distal* (2A-D, 2B-D, 2C-D) and *proximal* (2A-P, 2B-P, 2C-P) conformations and the SC-XRD structure of the major isomer in the favored *distal* conformation.

### 5.2.3 First Nucleophilic Addition Reactions

The 6:1 isomer mixture of the  $\eta^2$ -cyclooctatrienyl cation, was then screened for its reactivity with nucleophiles. A wide range of nucleophiles were successfully added, including hydride (3), cyanide (4), an amine (5), an imidazole (6), an amide (7), a phosphine (8), enolates (9,10), thioacetate (11), and various Grignard reagents (12-15), **Figure 5.5**. Yields and isomeric ratios (ir) were recorded when available. The ir varied depending on the nucleophile and reaction conditions. For example, when cyanide is added as a nucleophile, the crude reaction mixture has an isomeric ratio of 10:1, the precipitate obtained via precipitation from chloroform/hexanes has a ratio of 15:1 and once collected via an acetonitrile solution, there is no observable minor product in the  $^1\text{H}$  NMR spectrum (>20:1). Due to steric effects, nucleophiles preferentially add to the face opposite the bulky metal center, yielding a single stereoisomer. Interestingly, the Green-Davies-Mingo's Rules state that nucleophilic additions to organotransition metal cations typically occur at a terminal position of a conjugated system.<sup>104</sup> Hence, the expected addition would result in a 1,3,5-triene. However, in this case, the nucleophile adds at a position that disrupts the conjugation within the  $\pi$ -system, resulting in a 1,4,6-triene. Many structures were confirmed with SC-XRD including compounds 3, 4, 7, 10, 12, 13, 14 and 15 were obtained, **Figure 5.6**. It was revealed that there is a *major* conformation of mono-substituted  $\eta^2$ -cyclooctatriene complexes. Most nucleophiles including cyanide (4), benzamide (7),



dimethylmalonate (**10**), allyl (**14**) and methyl (**15**) crystallized in a conformation where the nucleophile sits in a position *over* the ring and *anti* to metal bulk. On the other hand, nucleophiles such as benzyl (**13**) and phenyl (**12**) crystallized in a conformation where the nucleophile flips *away* from the ring and toward the metal bulk. Yet, all of these conformations have some rotation around the diene portion of the ring where interestingly, hydride (**3**) crystallized in a unique conformation where the uncoordinated diene resembles a fully *cis* conformation.

#### 5.2.4 Second Protonation Reactions

A >20:1 ratio of compound **15** dissolved in acetonitrile was protonated with triflic acid (HOTf). Initially, two compounds were observed via <sup>1</sup>H-NMR in a 10:1 ratio. Over six hours in solution or one week as a solid, the signal for the minor species **16T** grew, eventually replacing the signals for **16K** until the isomer ratio became >20:1. Analysis

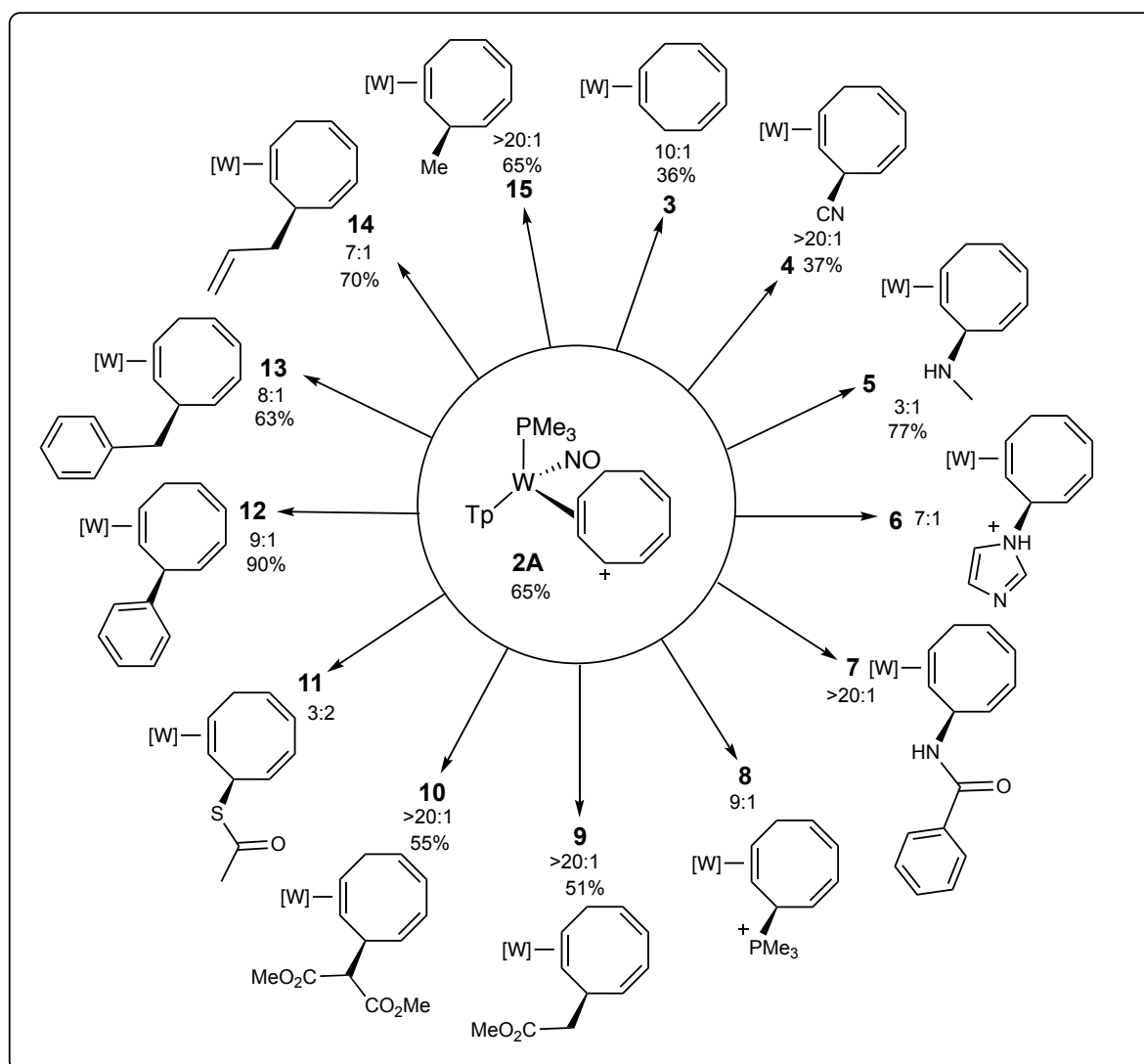


**Figure 5.5.** Nucleophile scope for the synthesis of 3-mono-substituted  $\eta^2$ -cycloocta-1,4,6-trienes.

of 2D-NMR data revealed that the initial major species (**16K**), referred to as the *kinetic allyl*, was structurally identified as an isomer of the final species (**16T**), the *thermodynamic allyl species*, according to **Figure 5.7**. Interestingly, as indicated by spectroscopic NMR data, the structure of **16T** represents a rare case where a *proximal* conformation appears to be more energetically favorable than its *distal* counterpart. Additionally, it is important note that **16K** and **16T** are isomers and not interconvertible through the movement of charge. The existence of *kinetic* and *thermodynamic allylic* species was also experimentally observed in the protonation of **9** (**17T**) and **11** (**18T**). The structures of compounds **17T'** and **19T'** were confirmed via SC-XRD, **Figure 5.7**. However, for the amide derivative **7** and the malonate derivative **10**, exposure to acid resulted in the detachment of the nucleophile from the ring, regenerating a solution of the  $\eta^2$ -cyclooctatrienyl cation (**2A** and **2B**) in a 6:1 diastereomer ratio.

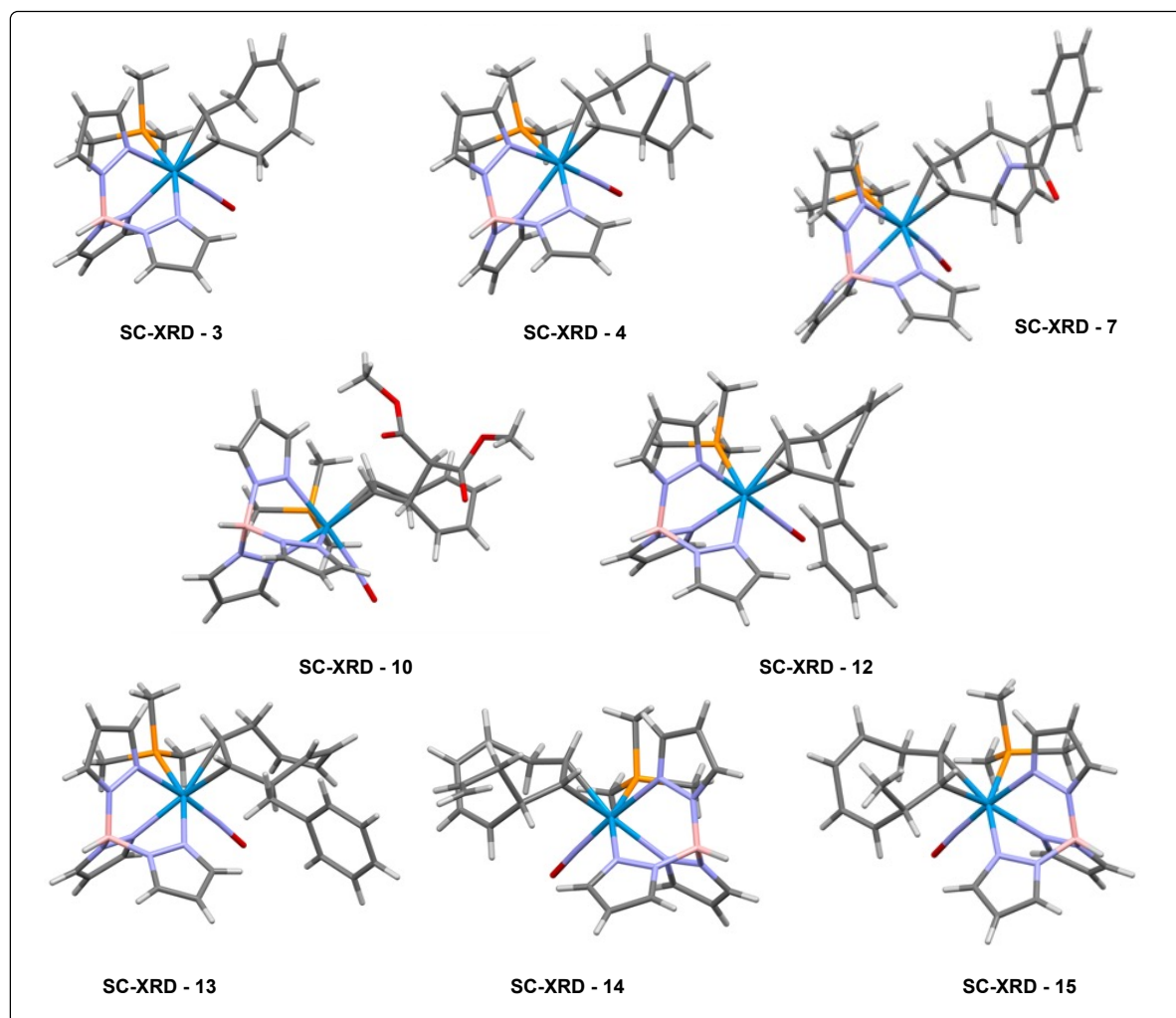


**Figure 5.6.** SC-XRD for 3-mono-substituted  $\eta^2$ -cycloocta-1,4,6-trienes compounds.

Uniquely, the protonation of compound **4** leads to the formation of the *kinetic* species **20K**, with no experimental evidence supporting the existence of the *thermodynamic* species **20T**. The structure for **20K** was confirmed via SC-XRD. It is hypothesized that the conversion of **20T** is unfavorable in cases where the first nucleophile is electron-withdrawing, and possibly that the proximal conformers of **16-19T** are stabilized through hyperconjugation with a neighboring electron-donating group or something native to the eight-membered ring conformation when an electron-withdrawing group is not next to the positive charge. These findings are summarized in **Figure 5.7**.

Possible mechanisms for the conversion of **15** into **16T'** are proposed, **Figure 5.8**, and by analogy **9** to **17T'**, **11** to **18T'**, and **12** to **19T'**. DFT analysis was used to compare the relative energies of reactants, proposed intermediates, and products. Again, calculations were performed using the M06 functional with a 6-31G(d,p) basis set applied to main group atoms and LANL2DZ on tungsten, additionally with acetonitrile SMD solvation applied. All energy values are respective to the lowest energy isomer, **16T'**. There are three possible intermediates for the direct protonation of compound **15**. Pathway A is the protonation of the nitrosyl ligand (**I**), while pathways B (**II**) and C (**III**) are alkene protonations and result in allyl intermediates where cations are not stabilized by the metal but stabilized by the nitrosyl ligand. All three intermediates are competitive species as their energies are within 3.0 kcal/mol. Interestingly, a species was found for compound **III** where the nitrosyl does not participate in stabilization, but it is 12.3 kcal/mol higher in energy and therefore not a competitive species.

Tungsten-alkene isomerizations are best understood to occur through *ring-walk*, *ring-slip*, and *ring-flip* mechanisms. Notably, the stereochemistry of the COT substituent (methyl) does not change from reactant to product hence a pathway involving a single *ring-flip* isomerization is not possible. Pathways for the isomerization of intermediates **II** and **III** into intermediate **16K** could not be conceptualized through the isomerizations approaches named but due to the complexity of tungsten-alkene isomerization mechanisms, could still be possible. On the other hand, the conversion of intermediate **I** into intermediate **IV** could be achieved through a *ring-walk* or *ring-slip* isomerization.

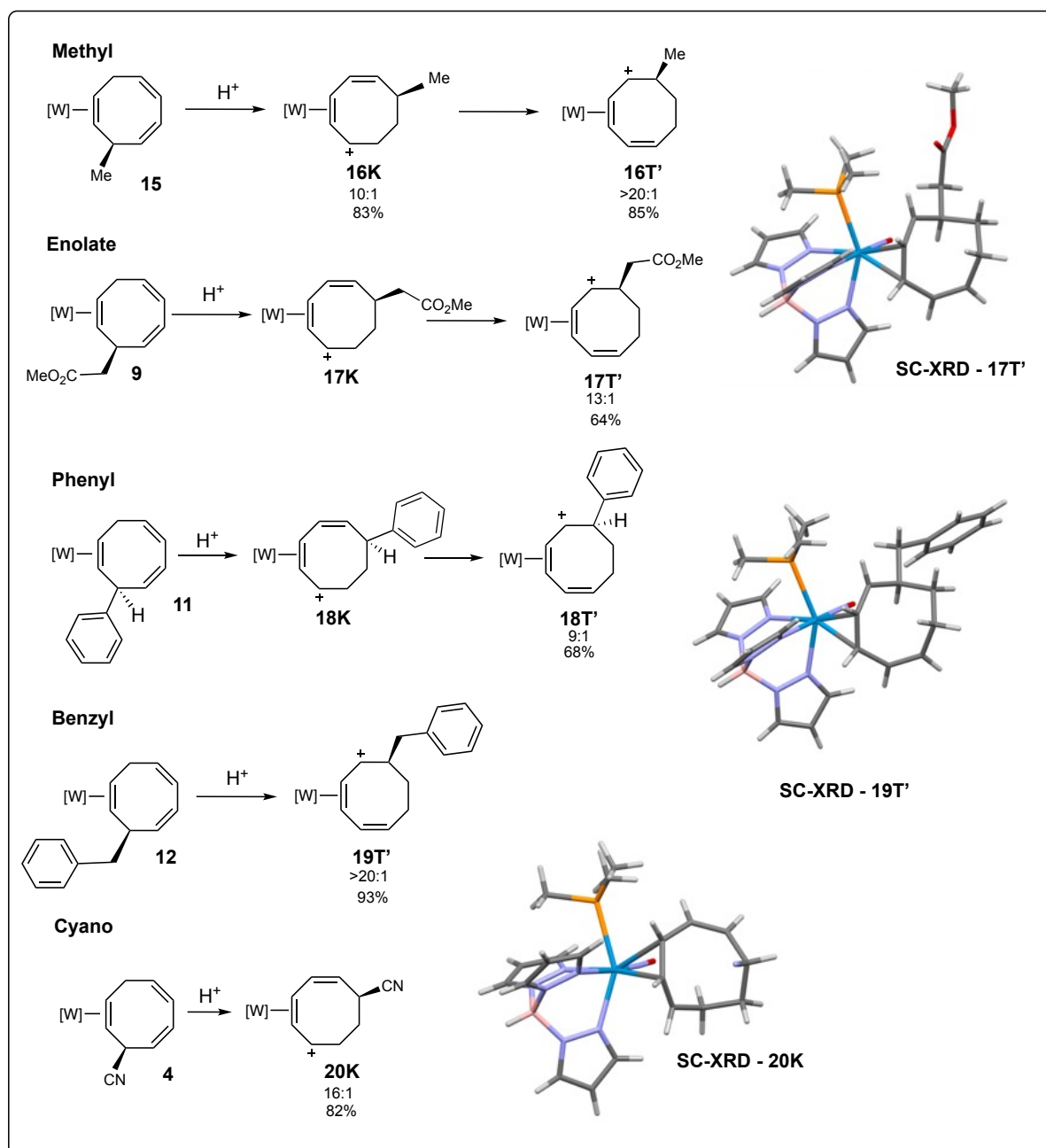


**Figure 5.7.** Protonation of mono-substituted  $\eta^2$ -trienes (**15**, **9**, **11**, **12**) forms initial  $\eta^2$ -cyclooctadienyl cations, *kinetic allyls* (**16K**, **17K**, **18K**) and final  $\eta^2$ -cyclooctadienyl cations, *thermodynamic allyls* (**16T'**, **17T'**, **18T'**, **19T'**). Protonation of compound **4** to **20K**. Obtained SC-XRD structures are included.

If intermediate **IV** were to exist, there are two alkenes that could pick up the nitrosyl proton. Pathway C results in a hyperdistorted allyl species (**V** and **VI**) and is thermodynamically favored, yet the structure of **IV** places the proton directly under the alkene that is not in conjugation with the metal. It is proposed that there is kinetic favorability for pathway D resulting in the formation of intermediate **VII**. An intermediate involving a nitrosyl stabilized cation was proposed for the protonation of  $\eta^2$ -1,4-

cyclohexadiene and in talked about further in Chapter 7. There is a thermodynamic drive ( $\Delta G = -14.2$  kcal/mol) or the formation of **16K** from **VII**, possible through a hydride shift. The transition state for the analogous six-membered system is also shown in Chapter 7 but transition states for the proposed mechanism above would be worthwhile.

It is understood that **16K** is in equilibrium with its *proximal* conformation (**16K'**), which has a resonance structure where the charge is not localized in a position stabilized by the metal. The resulting structure of a ring-slip isomerization to the adjacent alkene is **16T'**, confirmed to be uniquely lower in energy than its *distal* conformation (**16T**).

Additionally, upon exposure of **4** and **11** to acid, an intermediate species is initially observed in the  $^1\text{H}$  NMR spectrum but fully converts to **18K** and **20K** over time. However, due to its short-lived nature in solution, 2D-NMR experiments were unable to confirm its structure, but further investigation could confirm the identity of one of the proposed intermediates. Additionally, deuterium studies could be used to track the

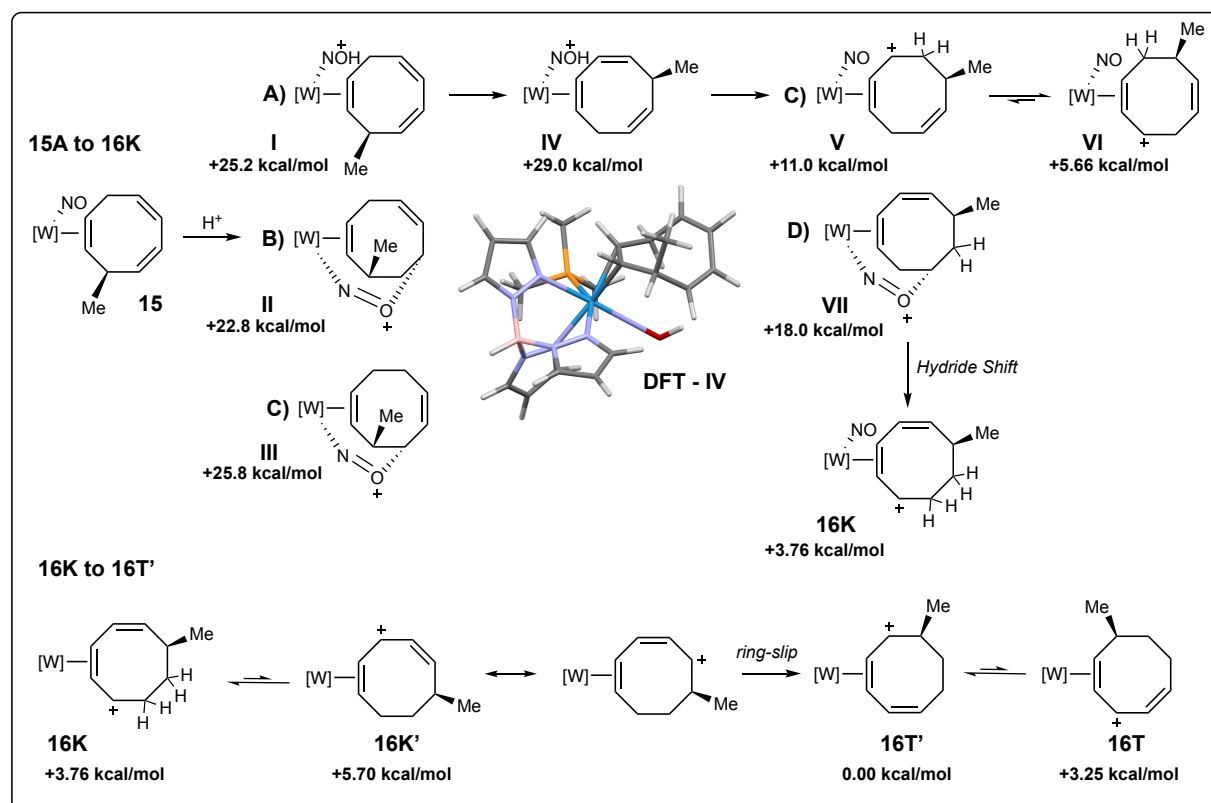


**Figure 5.8.** Proposed mechanism upon acid addition to 3-methyl-1,4,6-cyclooctatriene **15** into the  $\eta^2$  – cyclooctadienyl cation, **16T'**.

path of the proton and if delivered to the ring through the nitrosyl ligand, the deuterium should end up on the face syn to the metal.

### 5.2.5 Second Nucleophilic Additions

Given the fast isomerization of the *kinetic allyls*, and the ability to store the *thermodynamic allyls* for weeks at room temperature, the *thermodynamic allyls* were screened for second nucleophilic addition products. In a straightforward manner, nucleophiles most commonly attacked at the *proximal* cationic position. Stereoselectivity was again observed, with nucleophiles preferentially attacking from the face *anti* to the metal bulk. In the six-membered systems, where methodology typically yields 3,6-disubstituted cyclohexenes, it had been proposed that steric effects disfavor nucleophilic additions at neighboring positions. However, in the eight-membered system, steric hindrance appears to be less influential, most likely due to the large ring size, resulting in 5,6-disubstituted cycloocta-1,3-dienes as the major products. Although only confirmed for some examples, it is most likely the minor

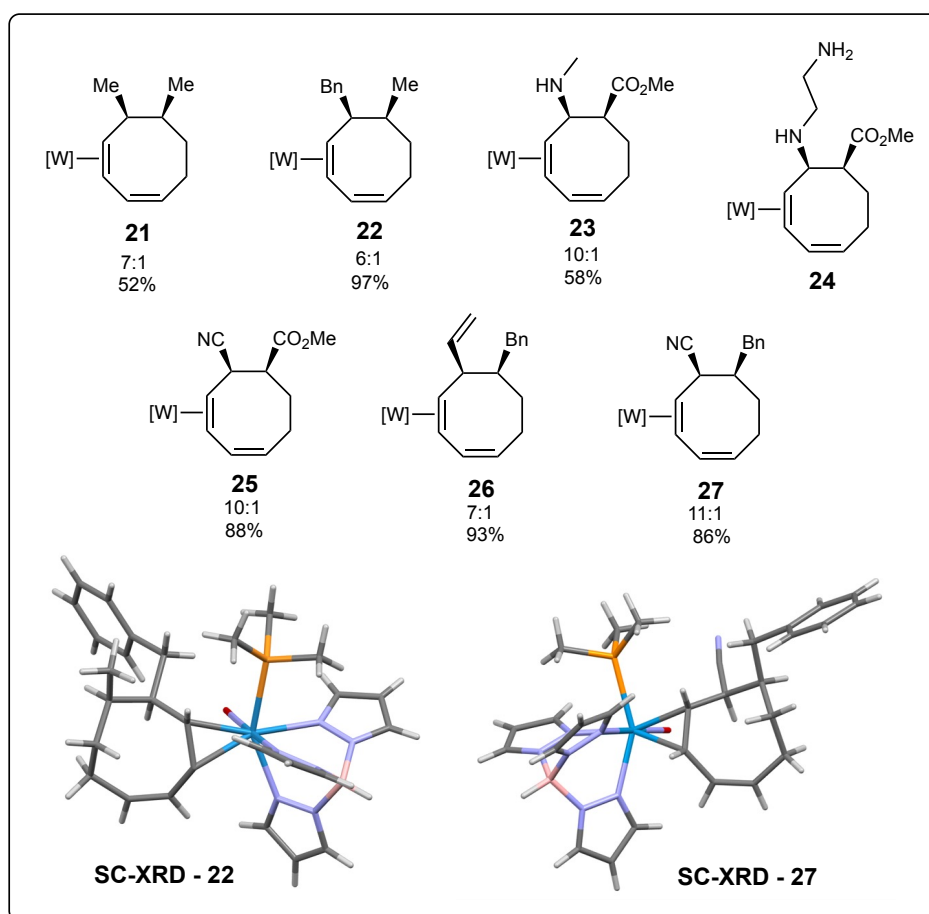


**Figure 5.9.** Scope and SC-XRD structures for dihapto-coordinated *cis*-5,6-disubstituted cycloocta-1,3-dienes.

products are coordination isomers where the attached ligand has either face-flipped, ring-walked, or both. This substitution pattern, along with the corresponding SC-XRD structures, is shown in **Figure 5.9**. Notably, this regioselectivity differs from that observed in the cyclooctadienes produced by Heck.<sup>90, 92</sup> Although steric effects do not initially pose a significant barrier to the second nucleophilic addition, in some cases, a tungsten-alkene isomerization is observed. It is proposed that this isomerization may be influenced by steric interactions between the nucleophile and the phosphine ligand, or that it occurs as a result of adopting a more stable conformation. However, further investigation is needed to confirm this. These observed isomerizations are discussed in detail later in this chapter.

### 5.2.6 Third Protonation and Third Nucleophilic Additions

The next step in our envisioned reaction sequence involves the protonation of the remaining uncoordinated alkene. Unlike the previous protonation, this alkene is in conjugation with the  $\eta^2$ -alkene, meaning that a straightforward protonation results in a hyperdistorted  $\eta^2$ -cyclooctenyl cation. Complexes **21**, **22**, **25**, and **27** were exposed to HOTf in acetonitrile, forming species **28**, **29**, **30** and **31**, respectively. The favorable conformation of  $\eta^2$ -cyclooctatrienyl cations is the *distal* one, whereas for  $\eta^2$ -cyclooctadienyl cations, the *proximal* conformation is preferred. In contrast to the  $\eta^2$ -cyclooctatrienyl and  $\eta^2$ -cyclooctadienyl cations, the  $\eta^2$ -cyclooctenyl cations, the energies of the *proximal* and *distal* conformations are nearly equal. Although these species are drawn as  $\eta^3$ -allyls, it is important to note that they remain hyperdistorted  $\eta^2$ -allyls. Evidence of this equilibrium is observed in NMR spectroscopic data, particularly through chemical shifts and 2D-NMR interactions. In most cases, the *proximal* conformation is slightly more stable, yet the third nucleophilic addition predominately adds to the *distal* conformation, presumably due to steric effects. This ultimately leads to major products where the tri-substituted cyclooctenes has substitutions at positions 3, 4 and 8. In some cases, a minor product is also observed, where the nucleophile attacks at the *proximal* position, resulting in a tri-substituted minor product with substitutions at positions 3, 4 and 5. As seen in previous nucleophilic additions, stereoselectivity is observed, as the syn face of the ring—oriented toward the metal bulk—is sterically hindered. The scope of  $\eta^2$ -cyclooctenyl cations,  $\eta^2$ -3,4,8-trisubstituted cyclooctenes, and their SC-XRD structures are summarized in **Figure 5.10**.

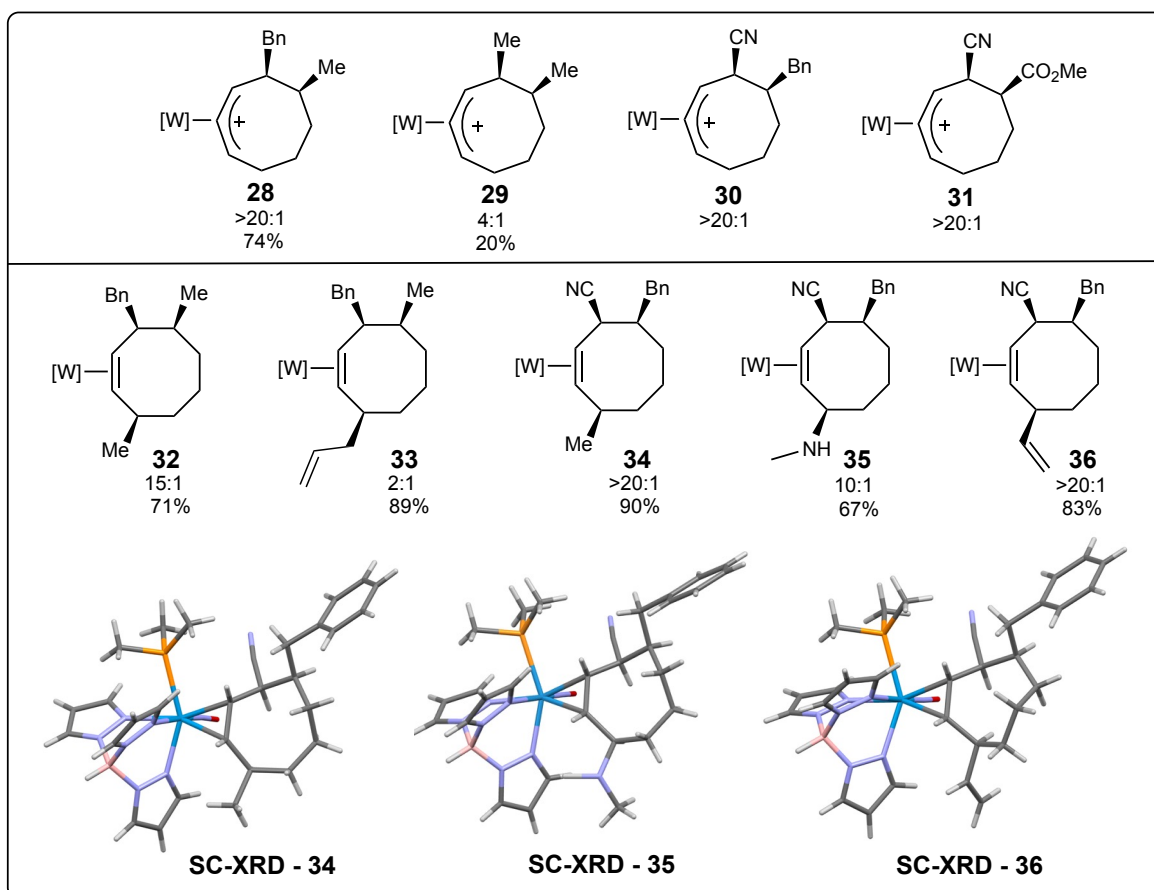


**Figure 5.10.** Scope and SC-XRD structures for dihapto-coordinated disubstituted cyclooctadienyl cations and dihapto-coordinated trisubstituted cyclooctenes.

### 5.2.7 Organic Compounds

Lastly, the ability to isolate trisubstituted cyclooctene as purely organic compounds has been explored. When tungsten is oxidized from W(0) to W(I), the  $\pi$ -backbonding essential to the dihapto-coordinated alkene weakens, leading to the release of the organic compound from the complex. Oxidation reactions can theoretically occur at three stages: 1) 3-substituted cyclooctatri-1,4,6-enes, 2) 5,6-disubstituted cyclooctadi-1,3-enes, and 3) 3,4,8-trisubstituted cyclooctenes. This suggests that any functionalized eight-membered ring of a neutral intermediate could be obtained as an organic compound. Several reagents have been investigated for oxidation reactions. It was observed that exposing certain  $\eta^2$ -cyclooctatriene complexes (e.g., **37**, **38** and **39**) to atmospheric  $O_2$  resulted in the release of the organic product. However,  $\eta^2$ -cyclooctadienes upon exposure to  $O_2$  in the atmosphere tends to induce an oxidative catalytic isomerization rather than full oxidation. Yet, the addition of cerium ammonium nitrate (CAN) yielded to release and collection of cyclooctadienes (**39**). Additionally, some tri-substituted cyclooctenes were released



upon exposure to O<sub>2</sub> in the atmosphere, while other required the addition of CAN to facilitate oxidation (**40**, **41** and **42**). The metal complex is usually synthesized in racemic form but is represented as the R-enantiomer throughout this study to illustrate stereoselectivity in product formation. However, the S-enantiomer can also be obtained, meaning that both enantiomers of all compounds can theoretically be isolated depending on the resolved metal complex used during synthesis. The scope of isolated organic compounds is summarized in **Figure 5.11**. When compared to Table 1, it is notable that only two structures with a 3,4,8-substitution pattern exist in the literature. This highlights how the methodology developed in this study fills a gap in the organic synthesis of cyclooctenes.

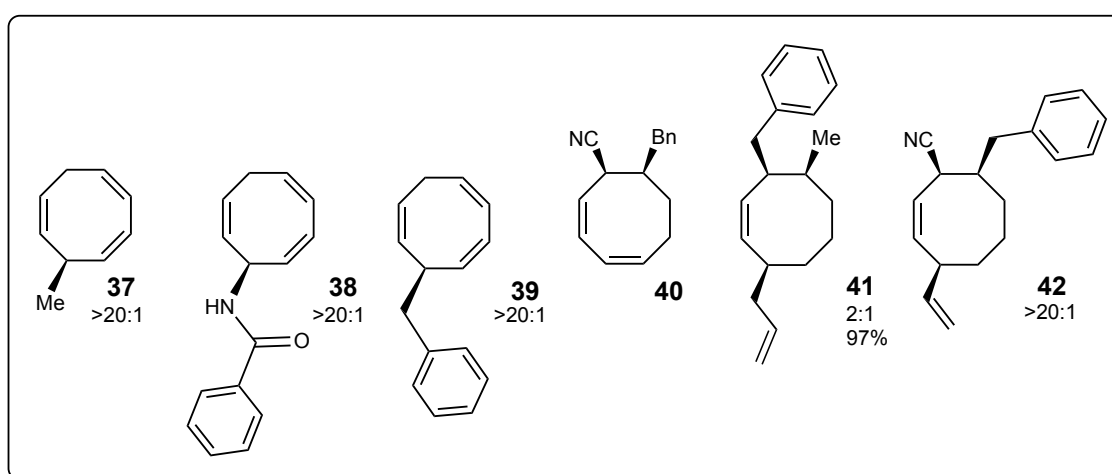


**Figure 5.11.** Scope of isolated organic compounds.

### 5.3 Future Studies

The methodology demonstrated above provides a synthetic route to 3,4,8-trisubstituted cyclooctenes; however, methodologies could also be developed for the synthesis of regioisomers and diastereomers. Following the functionalization of benzene in the synthesis of substituted cyclohexenes, significant research expanded upon the initial functionalization. These advances include: 1) incorporating additional functional groups via benzene complexation with labile groups, 2) expanding to aromatic nucleophiles through double protonation intermediates, 3) ring closure reactions to form bicyclic systems, and 4) selective deuterium incorporation. All of these methodologies could similarly be explored and adapted to the eight-membered system. Beyond these parallels, there are pathways unique to the eight-membered system that merit investigation.

### 5.3.1 Kinetic $\eta^2$ – Cyclooctadienyl Cation

The synthesis of 3,4,8-trisubstituted cyclooctenes relies on the isomerization of the *kinetic*  $\eta^2$  – cyclooctadienyl cation to the *thermodynamic*  $\eta^2$  – cyclooctadienyl cation. However, an alternative approach could utilize the *kinetic* species directly as the reactive electrophile. This could be achieved by either immediate nucleophilic addition before isomerization can occur or trapping the kinetic intermediate at low temperatures to prevent its rearrangement. To date, three *kinetic* cations have been isolated (**16K**, **17K** and **20K**), but two additional cations (**18K** and **19K**) are theoretically accessible. Ideally, nucleophiles would be either 3,4,7- trisubstituted cyclooctenes or 3,5,8 – trisubstituted cyclooctenes, depending on whether the third nucleophile adds to the *distal* or *proximal* position. Additionally, this methodology could generate a new class of cyclooctadienes, **Figure 5.12**.

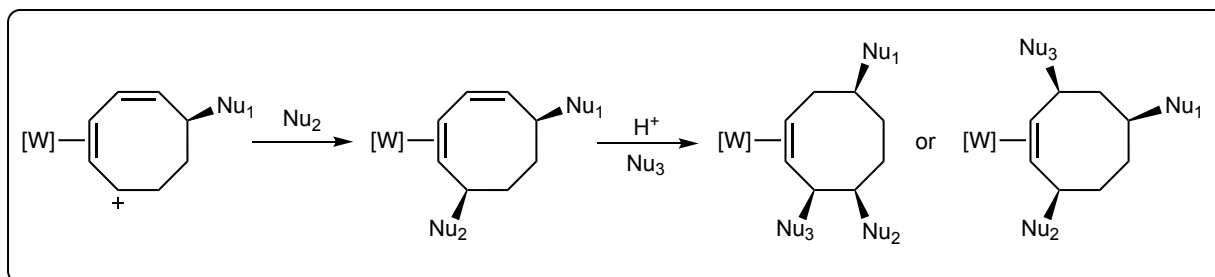


**Figure 5.12.** Possible products via *kinetic*  $\eta^2$  – cyclooctadienyl cations, *cis,cis*-3,4,7-trisubstituted cyclooctenes and *cis,cis*-3,5,8-trisubstituted cyclooctenes.

### 5.3.2 Syn complexes and Alternative Isomerization Pathways

Beyond the pathways described above, additional synthetic opportunities exist through alternative isomerization mechanisms. First, an isomerization of *cis*-5,6-disubstituted cycloocta-1,3-dienes to an alternative diastereomer was observed for compounds **21** and **22**, forming compounds **39** and **40**, respectively. Additionally, the protonation of compound **40** produced a spectroscopically unique  $\eta^2$  – cyclooctatrienyl cation (**28'**), which differs from the species obtained upon protonation of its initial isomer, compound **22**. Due to time constraints, compound **28'** wasn't characterized or pursued, but it likely represents a new class of trisubstituted cyclooctenes featuring *trans* stereochemistry, a notoriously difficult stereochemical pattern to achieve via this methodology. Although the isomerization of **22** into **40** occurred rapidly in solution, it is proposed that for compounds that do not naturally isomerize, the addition of a catalytic oxidant could facilitate this transformation. Additionally, when compound **15** was exposed to atmosphere O<sub>2</sub>, the organic complex became the major species in

solution, though crystallization yielded compound **41**. This suggests that oxidative catalytic isomerization could be intentionally pursued for other  $\eta^2$  – cyclooctatrienes shown in Figure 4. The protonation of this complex was not explored, but it likely produces a novel  $\eta^2$  – cyclooctadienyl cation. The *syn* complexes obtained to date, along with their SC-XRD structures are summarized in **Figure 5.13**.

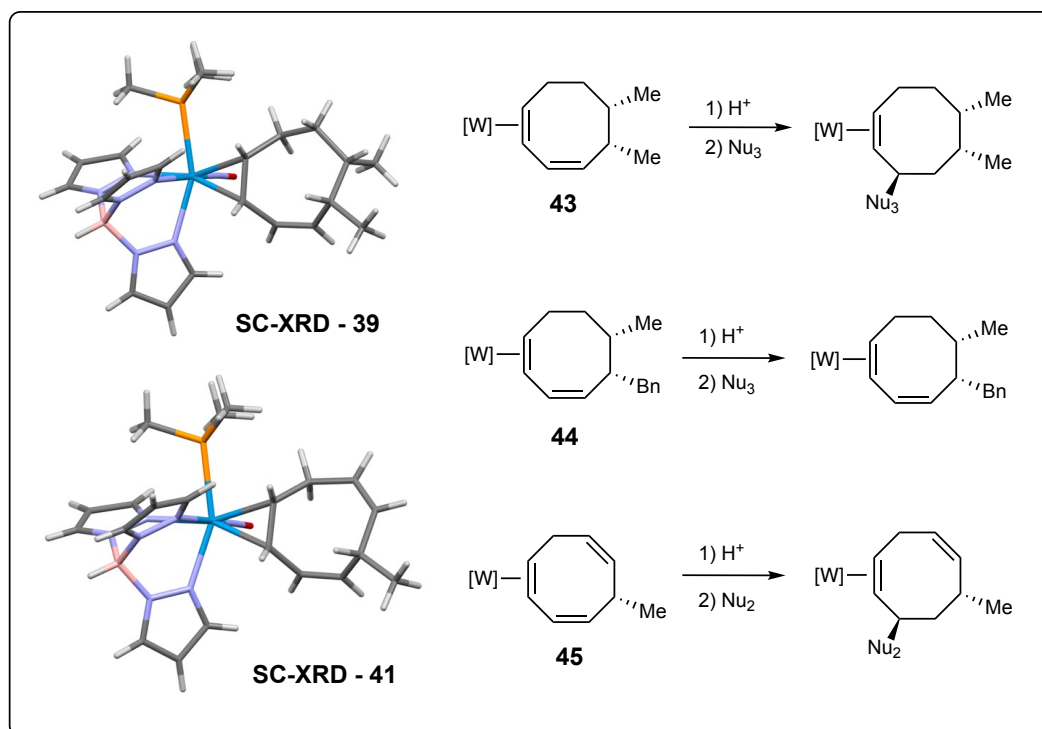


**Figure 5.13.** Dihapto-coordinated complexes that have isomerized to place incorporated functional groups in a *syn* position. SC-XRD structures are included.

## 5.4 Conclusions

The synthetic route to 3,4,8-trisubstituted cyclooctenes demonstrated in this study is summarized in **Figure 5.14**. Eight-membered carbocycles are commonly found in natural products with biological activity, yet small molecule eight-membered carbocycles are underrepresented in molecular libraries due to the inherent challenges in their synthesis. Their energetic preference for forming aromatic bicyclic systems makes their isolation particularly difficult. Most eight-membered carbocycles synthesized to date are part of total synthesis of a natural product, often constructed via cycloadditions, cyclizations, and ring-opening reactions, and ring-closure reactions, including metathesis and transannular reactions.

There remains a significant gap in the literature for methodologies efficiently generate eight-membered carbocycles, including 3-substituted cyclooctatrienes, 5,6-disubstituted cyclooctadienes and 3,4,8-trisubstituted cyclooctenes. The methodology

developed in this study provides a valuable synthetic approach to expand upon the limited examples found in literature, particularly by offering unique regiochemistry and the ability to isolate single stereoisomers. This work establishes a foundation for further exploration of eight-membered carbocycles, potentially broadening their accessibility for use in natural product synthesis and small-molecule drug discovery.

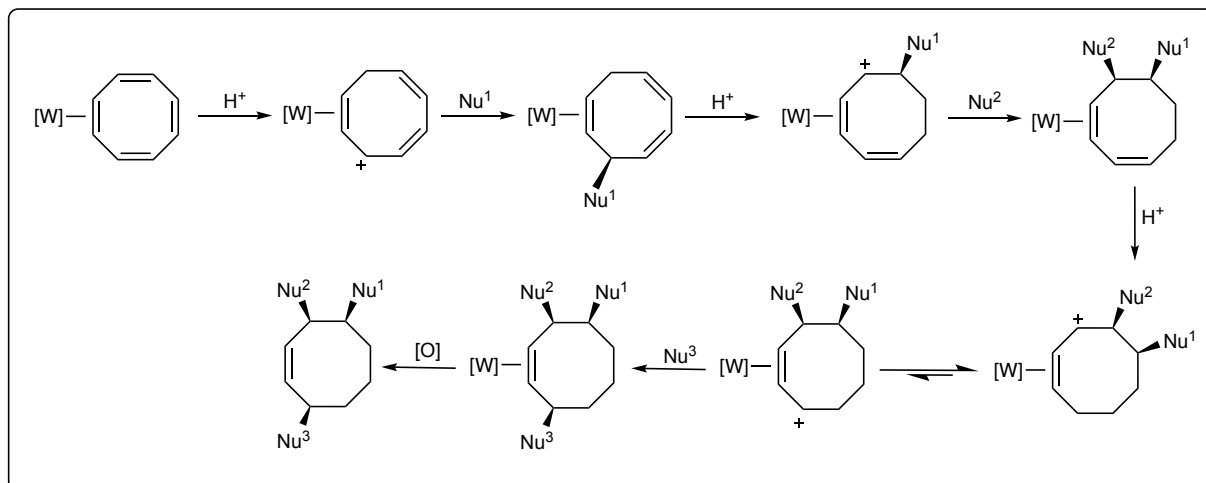


**Figure 5.14.** The synthetic pathway to the synthesis of 3,4,8-trisubstituted cyclooctenes developed in this study.

## References

- (1) Petasis, N. A., Patane, Michael A. The synthesis of carbocyclic eight-membered rings. . *Tetrahedron* **1992**, 48 (28), 5757 - 5821.
- (2) Hu, Y. J., Li, L.X., Han, J.C., Min, L., Li, C.C. Recent Advances in the Total Synthesis of Natural Products Containing Eight-Membered Carbocycles (2009-2019). *Chem. Rev.* **2020**, 120 (13), 5910-5953.
- (3) Mehta, G., Singh, Vishwakarma. Progress in the Construction of Cyclooctanoid Systems: New Approaches and Applications to Natural Product Syntheses. *Chem. Rev.* **1999**, 99, 881 - 930.
- (4) Claus, K. H., Kruger, C. Structure of cyclooctatetraene at 129K. *Acta Cryst.* **1988**, 44, 1632 - 1634.
- (5) Luck, H.-J., Roche, Henri. . Weekly paclitaxel: an effective and well-tolerates treatment in patients with advances breast cancer. . *Critical Reviews in Oncology/Hematology* **2002**., 44, 15 - 30.
- (6) Ye, R.-R., Jiang, Shuang., Xu, Xu., Lu, Yan., Wang, Yu-Jun., Liu, Jing-Gen. Dezocine as a potent analgesic: overview of its pharmacological characterization. . *Acta Phamacol Sin.* **2021**., 43 (7), 1646 - 1657.
- (7) Yang, L. P. H., Keam, Susan, J. Retapamulin: a review of its use in the management of impetigo and other uncomplicated superficial skin infections. . *Drugs* **2008**, 68 (8), 855 - 873.
- (8) Kirkland, T. A., Grubbs, Robert H. Effects of Olefin Substitution on the Ring-Closing Metathesis of Dienes. . *J. Org. Chem.* **1997**, 62, 7310 - 7318.
- (9) Kaur, N. *8-Membered Heterocycle Synthesis* Elsevier, 2023.
- (10) Li, J., Dong, Ziyang., Zhao, Changgui. Recent progress in the construction of eight-membered nitrogen-heterocycles. . *New J. Chem.* **2024**, 48, 4645 - 4669.
- (11) Yao, T., . Li, Jia., Jiang, Chengming., Zhao, Changgui. Recent advances for the catalytic asymmetric construction of medium-sized rings. *Chem Catalysis* **2022**, 2, 2929 - 2964.
- (12) Nicolaou, K. C., Snyder Scott A., Montagnon, Tamsyn., Vassilikogiannakis, Georgios. The Diels-Alder reaction in total synthesis *Angew Chem Int Ed Engl* **2002**, 41 (10), 1668 - 1698.
- (13) Takao, K.-i., Munakata, Ryosuke., Tadano, Kin-ichi. Recent Advances in the Natural Product Synthesis by Using Intramolecular Diels-Alder Reactions. *Chem. Rev.* **2005**, 105 (12), 4235 - 4807.

- (14) Juhl, M., Tanner, David. Recent applications of intramolecular Diels-Alder reactions to natural product synthesis. *Chem Soc Rev* **2009**, 38 (11), 2983 - 2992.
- (15) Heravi, M. M., Vavsari, Vaezah F. Recent applications of intramolecular Diels-Alder reaction in total synthesis of natural products. *RSV Adv* **2015**, 5 (63), 50890 - 50912.
- (16) Sakan, K., Smith, Douglas A., Babirad, Stefan A., Fronczek, Frank R., Houk, K.N. Stereoselectivities of Intramolecular Diels-Alder Reactions. Formation of the Taxane Skeleton. *J. Org. Chem.* **1991**, 56 (7), 2311.
- (17) Sakan, K., Craven, Bryan M. Synthetic Studies on the Taxane Diterpenes. Utility of the Intramolecular Diels-Alder Reaction for a Single-Step Stereocontrolled Synthesis of a Taxane Model System *J. Am. Chem. Soc.* **1983**, 105 (11), 3732.
- (18) Jackson, R. W., Higby, Richard G., Gilman, Jeffery W., Shea, Kenneth J. The chemistry of C-aromatic taxane derivatives atropisomer control of reaction stereochemistry. *Tetrahedron* **1992**, 48 (34), 7013 - 7032.
- (19) Alaimo, C., A., Coburn, Craig A., Danishefsky, Samuel J. Studies in the synthesis of baccatin III - steroid hybrid: A remarkably rapid intramolecular diels alder reaction *Tetrahedron Letters* **1994**, 35 (36), 6603 - 6606.
- (20) Winkler, J. D., Holland, Joanne M., Peters, David A. Synthesis of Cyclopropyl Taxane Analogs via Sequential Diels-Alder Reactions. *J. Org. Chem.* **1996**, 61 (26), 9074.
- (21) Wender, P. A., Correia, Carlos R.D. Intramolecular Photoinduced Diene-Diene Cycloadditions: A Selective Method for the Synthesis of Complex Eight-Membered Rings and Polyquinanes *J. Am. Chem. Soc.* **1987**, 108, 2523.
- (22) Wender, P. A., Ihle, Nathan C. Nickel-Catalyzed Intramolecular [4 + 4] Cycloadditions: A New Method for the Synthesis of Polycycles Containing Eight-Membered Rings *J. Am. Chem. Soc.* **1986**, 108, 4678 - 4679.
- (23) Seiburth, S., M., Joshi, Pramod, V. Intramolecular [4+4] Photocycloadditions: Substituent-Mediated Product Control *J. Org. Chem.* **1993**, 58, 1661 - 1663.
- (24) Seiburth, S. M., Lin, Chao-Hsiung. Intermolecularly selective [4+4] photocycloaddition of 2-pyridine mixtures *Tetrahedron Letters* **1996**, 37 (8), 1141 - 1144.
- (25) Kaupp, G., Mulzer, Johann., Waldmann, Herbert. *Organic Synthesis Highlights III; [4+4]-Cycloaddition Reactions in the Total Synthesis of Naturally Occuring Eight-Membered Ring Compounds* Wiley-VCH, 2008.

- (26) Phansavath, P., Aubert, Corinne., Malacria, Max. The [4+2], [2+2] strategy for the construction of the AB taxane ring system. *Tetrahedron Letters* **1998**, 39 (12), 1561 - 1564.
- (27) Winkler, J. D., Hey, John P., Hannon, Francis J., Williard, Paul G. Intramolecular Photocycloaddition on Dioxlenones: An Efficient Method for the Synthesis of Medium-Sized Rings *Heterocycles* **1987**, 25, 55.
- (28) Min, L., Lin, Xiaohong., Li, Chuang-Chuang. Asymmetric Total Synthesis of (-)-Vinigrol. *J. Am. Chem. Soc.* **2019**, 141 (40), 15773 - 15778.
- (29) Feldman, K. S., Come, Jon H., Freyer, Alan J., Kosmider, Ben J., Smith, Cynthia M. Synthesis of Eight-Membered Carbocycles via Intramolecular [6 $\pi$  + 2 $\pi$ ] Photocycloaddition of Alkenyltropone. *J. Am. Chem. Soc.* **1985**, 108.
- (30) Rigby, J. H., Henshilwood, James A. Transition Metal Template Controlled Cycloaddition Reactions. An Efficient Chromium(0)-Mediated [6 $\pi$  + 2 $\pi$ ] Cycloaddition. *J. Am. Chem. Soc.* **1991**, 113, 5122 - 5123.
- (31) Chaffee, K., Huo, Pei., Sheridan, John B., Barbieri, Anthony., Aistars, Arnis., Lalancette, Roger A., Ostrander, Robert L., Rheingold, Arnold L. Metal-Mediated [6 + 2] Cycloadditions of Alkynes to Cycloheptatriene and N-Carboethoxyazepine. *J. Am. Chem. Soc.* **1995**, 117, 1900 - 1907.
- (32) Rigby, J. H., Warshakoon, Namal C. A Convenient Synthesis of 1,2-Disubstituted Cyclooctatetraenes. *Tetrahedron Letters* **1997**, 38 (12), 2049 - 2052.
- (33) Mach, K., Antropiusova, Helena., Petrusova, Lidmila., Hanus, Vladimir., Turecek, Frantisek. [6+2] Cycloadditions Catalyzed by Titanium Complexes *Tetrahedron* **1984**, 40 (17), 3295 - 3302.
- (34) Cooper, J. C., Wong, Louis F., Venezky, David L., Margerum, Dale W. [2 $\pi$  + 6 $\pi$ ] Cycloaddition Reactions between Ligands Coordinated to an Iron Atom *J. Am. Chem. Soc.* **1974**, 96 (24), 7562 - 7564.
- (35) West, F. G., Hartke-Karger, Claudia., Koch, Daniel J., Kuehn, Cynthia E., Arif, A.M. Intramolecular [4+3]-Cycloadditions of Photochemically Generated Oxyallyl Zwitterion: A Route to Functionalized Cyclooctanoid Skeletons. *J. Org. Chem.* **1993**, 58, 6795 - 6803.
- (36) Harmata, M., Elomari, Saleh., Barnes, Charles L. Intramolecular 4 + 3 Cycloadditions. Cycloaddition Reactions of Cyclic Alkoxyallylic and Oxyallylic Cations *J. Am. Chem. Soc.* **1996**, 118, 2860 - 2871.

- (37) Harmata, M. Intramolecular Cycloaddition Reactions of Allylic Cations. *Tetrahedron* **1997**, 53 (18), 6235 - 6280.
- (38) Oh, J., Choi, Jong-Ryoo., Cha, Jin Kun. Synthetic Studies on Taxol. Assembly of the Bicyclo[5.3.1]undecane Moiety (AB Ring System) of Taxane Diterpenes. *J. Org. Chem.* **1992**, 57, 6664 - 6667.
- (39) Molander, G. A., Harris, Christina R. Sequencing Reactions with Samarium (II) Iodide *Chem Rev* **1996**, 96 (1), 307 - 338.
- (40) Edmonds, D. J., Johnston, Derek., Procter, David J., . Samarium(II)-Iodide-Mediated Cyclizations in Natural Product Synthesis. *Chem Rev* **2004**, 104 (7), 2271 - 3404.
- (41) Nicolaou, K. C., Ellery, Shelby P., Chen, Jason S. Samarium diiodide mediated reactions in total synthesis. *Angew Chem Int Ed Engl* **2009**, 48 (39), 7140 - 7165.
- (42) Szostak, M., Spain, Malcolm., Procter, David J. Recent advances in the chemoselective reduction of functional groups mediated by samarium(II) iodide: a single electron transfer approach. *Chem Rev* **2013**, 42 (23), 9155 - 9183.
- (43) Szostak, M., Fazakerley, Neal J., Parmar, Dixit., Procter, David J. Cross-Coupling Reactions Using Samarium (II) Iodide. *Chem Rev* **2014**, 114 (11), 5959 - 6039.
- (44) Molander, G. A., George, Kelly M., Monovich, Lauren G. Total Synthesis of (+)-Isoschizandrin Utilizing a Samarium (II) Iodide-Promoted 8-Endo-Ketyl-Olefin Cyclization. *J. Org. Chem.* **2003**, 68 (25), 9533 - 9540.
- (45) Snider, B. B., Merritt, John E. Formation of seven- and eight-membered rings by Mn(III)-based oxidative free-radical cyclization. *Tetrahedron* **1991**, 48 (41), 8663 - 8678.
- (46) Snider, B. B., Kiselgof, Eugenia, Y. Mn(III)-based oxidative free radical cyclizations of unsaturated 2-cyclohexenones and aldehydes *Tetrahedron* **1996**, 52 (17), 6073 - 6084.
- (47) McMurry, J. E. Carbonyl-Coupling Reactions Using Low-Valent Titanium *Chem Rev* **1989**, 89, 1513 - 1524.
- (48) McMurry, J. E., Rico, Joesph G. Synthesis of 1,2,-cycloalkanediols by intramolecular titanium-induced pinacol coupling. *Tetrahedron Letters* **1989**, 30 (10), 1169 - 1172.
- (49) Kende, A. S., Johnson, Stephen., Sanfilippo, Pauline., Hodges, John C., Jungheim, Louis N. Synthesis of Taxol Triene. *J. Am. Chem. Soc.* **1985**, 108, 3513.



- (50) Nicolaou, K. C., Yang, Z., Liu, J. J., Ueno, H., Nantermet, P. G., Guy, R. K., Claiborne, C. F., Renaud, J., Couladouros, E. A., Paulvannan, K., Sorensen, E. J. Total synthesis of taxol. *Nature* **1994**, 367, 630 - 634.
- (51) Imamura, Y., Yoshioka, Shun., Nagatomo, M., Inoue, Masayuki. Total Synthesis of 1-Hydroxytaxinine. *Angew Chem* **2019**, 131 (35), 12287 - 12291.
- (52) Kress, M. H., Ruel, Rejean., Miller, William H., Kishi, Yoshito. Synthetic Studies toward the taxane class of natural products *Tetrahedron Letters* **1993**, 34 (38), 5999 - 6002.
- (53) Kress, M. H., Ruel, Rejean., Miller, William H., Kishi, Yoshito. Investigations of the intramolecular Ni(II)/Cr(II)-mediated coupling reaction: Application to the taxane ring system *Tetrahedron Letters* **1993**, 34 (38), 6003 - 6006.
- (54) Muller, B., Ferezou, Jean-Pierre., Lallemand, Jean-Yves., Pancrazi, Ange., Prunet, Joelle., Prange, Thierry. "Abnormal" eight-membered ring formation through SN2' intramolecular Nozaki/Kishi reaction in a synthetic approach to a taxane precursor. *Tetrahedron Letters* **1998**, 39 (3-4), 279 - 282.
- (55) Wang, Z., Warder, Scott E., Perrier, Helene., Grimm, ERich L., Bernstein, Michael A. A Straightforward Approach to the Synthesis of the Tricyclic Core of Taxol *J. Org. Chem.* **1993**, 58, 2931 - 2932.
- (56) Masters, J. J., Link, J. T., Snyder, Lawrence B., Young, Wendy B., Danishefsky, Samuel J. A Total Synthesis of Taxol. *Angew Chem Int Ed Engl* **1995**, 34 (16), 1723 - 1726.
- (57) Kusama, H., Hara, Ryoma., Kawahara, Shigeru., Nishimori, Toshiyuki., Kashima, Hajime., Nakamura, Nobuhito., Morihira, Koichiro., Kuwajima, Isao. Enantioselective Total Synthesis of (-)Taxol. *J. Am. Chem. Soc.* **2000**, 122 (16), 3811 - 3820.
- (58) Shambayani, S., Crowe, William E., Schreiber, Stuart L. N-oxide promoted pauson-khand cyclizations at room temperature. *Tetrahedron Letters* **1990**, 31 (37), 5289 - 5292.
- (59) Watanabe, T., Oga, Kyohei., Matoba, Hiroaki., Nagatomo, Masanori., Inoue, Masayuki. Total Synthesis of Taxol Enabled by Intermolecular Radical Coupling and Pd-Catalyzed Cyclization. *J. Am. Chem. Soc.* **2023**, 145 (47), 25894 - 25902.
- (60) Ma, S., Negishi, Ei-ichi. Palladium-Catalyzed Cyclization of Omega-Haloallenes. A New General Route to Common, Medium and Large Ring Compounds via Cyclic Carbopalladation. *J. Am. Chem. Soc.* **1995**, 117 (23), 6345 - 6357.

- (61) Yu, X.-C., Zhang, Can-Can., Wang, Ling-Tao., Li Jiao-Zhe., Li, Ting., Wei, Wen-Ting. The synthesis of seven- and eight-membered rings by radical strategies. *Org. Chem. Front.* **2022**, 9, 4757 - 4781.
- (62) Miller, S. J., Kim, Soong-Hoon., Chen, Zhong-Ren., Grubbs, Robert H. Catalytic Ring-Closing Metathesis Diens: Application to the Synthesis of Eight-Membered Rings. *J. Am. Chem. Soc.* **1995**, 117, 2108 - 2109.
- (63) Tsuna, K., Noguchi, Naoyoshi., Nakada, Masahisa. Convergent Total Synthesis of (+)-Ophiobolin A. *Angew Chem Int Ed Engl* **2011**, 50, 9452 - 9455.
- (64) Hog, D. T., Huber, Florian M. E., Mayer, Peter., Trauner, Dirk. The Total Synthesis of (-)-Nitidasin. *Angew Chem Int Ed Engl* **2014**, 53 (32), 8513 - 8517.
- (65) Hog, D. T., Mayer, Peter., Trauner, Dirk. A Unified Approach to trans-Hydrindane Sesterterpenoids. *J. Org. Chem.* **2012**, 77 (13), 5838 - 5843.
- (66) Michaunt, A., Rodriguez, Jean. . Selective Construction of Carbocyclic Eight-Membered Rings by Ring-Closing Metathesis of Acyclic Precursors *Angew Chem Int Ed Engl* **2006**, 45 (35), 5740 - 5750.
- (67) Marsault, E., Toro, Andras., Nowark, Pawel., Deslongchamps, Pierre. The transannular Diels-Alder strategy: applications to total synthesis. *Tetrahedron* **2001**, 57 (20), 4243 - 4260.
- (68) Limanto, J., Snapper, Marc L. Sequetial Intramolecular Cyclobutadiene Cycloaddition, Ring-Opening Metathesis and Cope Rearrangement: Total Synthesis of (+)- and (-)-Asteriscanolide. *J. Am. Chem. Soc.* **2000**, 122 (33), 8071 - 8072.
- (69) Krafft, M. E., Cheung, Yiu-Yin., Juliano-Capucio, Carmelinda A. Synthesis of the First "Inside-Outside" Eight-Membered Ring via Ring-Closure Metathesis: A Total Synthesis of (±)-Asteriscanolide. *Synthesis* **2000**, 2000 (7), 1020 - 1026.
- (70) Tori, M., Mizutani, Reiko. Construction of Eight-Membered Carbocycles with Trisubstituted Double Bonds Using Ring Closing Metathesis Reaction. *Molecules*. **2010**, 15, 4242 - 4260.
- (71) Betkekar, V. V., Kaliappan, Krishna P. Strategic innovations for the synthesis of vinigrol. *Tetrahedron Letters* **2018**, 59 (26), 2485 - 2501.
- (72) Bajgrowicz, J. A., Petzilka, Martin. 3,3-dimethyl-7-methylenecycloocta-1,5-dione, a versatile building block for the preparation of substituted cyclooctadienones and  $\delta$ -valerolactones. *Tetrahedron* **1994**, 50 (25), 7461 - 7472.
- (73) Blechert, S., Jansen, Rolf., Velder, Janna. Synthesis of new taxoids. *Tetrahedron* **1994**, 50 (32), 9649 - 9656.

- (74) Brooker-Milburn, K. I., Cowell, Justin K., Harris, Laurence J. Model studies toward the total synthesis of asteriscanolide. *Tetrahedron Letters* **1994**, 35 (23), 3883 - 3886.
- (75) Ruder, S. M., Norwood, Bradley K. Cycloaddition of enamines with alkynylphosphonates. A route to functionalized medium sized rings *Tetrahedron Letters* **1994**, 35 (21), 3473 - 3476.
- (76) Holton, R. A. Synthesis of the Taxane Ring System. *J. Am. Chem. Soc.* **1984**, 106, 5731 - 5732.
- (77) Jansen, R., Velder, Janna., Blechert, Siegfried. Novel tandem reactions to taxane A,B-ring systems. *Tetrahedron* **1995**, 51 (33), 8997 - 9004.
- (78) Galloway, W. R. J. D., Isidro-Llobet, Albet., Spring, David R. . Diversity-oriented synthesis as a tool for the discovery of novel biologically active molecules *Nature Comm* **2010**, 1 (80).
- (79) Spring, D. R. Diversity-oriented synthesis; a challenge for synthetic chemists. *Org. Biomol. Chem.* **2003**, 1, 3867 - 3870.
- (80) Castellino, N. J., Montgomery, Andrew P., Danon, Jonathan J., Kassiou, Michael. . Late-stage Functionalization for Improving Drug-like Molecular Properties. *Chem Rev* **2023**, 123 (13), 8127 - 8153.
- (81) Guillemard, L., Kaplaneris, Nikolaos., Ackermann, Lutz., Johansson, Magnus J. Late-stage C-H functionalization offers new opportunities in drug discovery *Nat Rev Chem* **2021**, 5, 522 - 545.
- (82) Cantrell, T. S., Shechter, Harold. . Reactions of Cyclooctatetraene Dianion with Aldehydes and Ketones and the Chemistry of Its Products *J. Am. Chem. Soc.* **1967**, 89 (23), 5877 - 5884.
- (83) Saito, K., Omura, Yoichi., Maekawa, Etsuro. . Addition Reactions of Cyclooctatetraene with 1,3-diphenylisobenzofuran the benzene ring as dienophile in a [4+2] cycloaddition reaction *Tetrahedron Letters* **1984**, 25 (24), 2573 - 2576.
- (84) Kunichika, S. Cyclopolyolefins Derived from Acetylene. *Bulletin of the Institute for Chemical Research, Kyoto University.* **1953**, 31 (5), 323 - 335.
- (85) Fray, G. I., Saxton, R.G. *The Chemistry of Cyclo-Octatetraene and Its Derivatives* Cambridge University Press, 1978.
- (86) Keller, C. E., Pettit, R. The Protonation of Cyclooctatetraene *J. Am. Chem. Soc.* **1965**, 88 (3), 604 - 606.

- (87) Salzer, A. The Reactivity of Complexes Carbocycles. I. Nucleophilic Addition of Lewis Bases to Tropylium and Homotropylium Derivatives of Molybdenum and Tungsten Carbonyls. *Inorg Chem Acts* **1976**, 17, 221 - 224.
- (88) Faller, J. W., Chao, Kuo-Hua. Asymmetric Syntheses of (-)-Cycloocten-3-ol and (-)-3-Deuteriocyclooctene via Nucleophilic Attack on ( $\eta^3$ -Cyclooctenyl)molybdenum Complexes *Organomet.* **1984**, 3, 927 - 932.
- (89) Pearson, A. J., Balasubramanian, Srinivasan., Srinivasan, Kumar. Stereocontrolled functionalization of cyclooctadiene using organoiron chemistry. *Tetrahedron* **1993**, 49 (25), 5663 - 5672.
- (90) Heck, J., Lange, Gerhard., Reimelt, Oliver. Iterative Nucleophilic and Electrophilic Additions to Coordinated Cyclooctatetraene: An Efficient Route to cis-5,7-Disubstituted 1,3-cyclooctadienes. *Angew Chem Int Ed* **1998**, 37 (4), 520 - 522.
- (91) Lange, G., Reimelt, Oliver., Jessen, Lars., Heck, Jurgen. Regio- and Stereoselective Functionalization of cyclo-C8 Compounds by Iterative Nucleophilic and Electrophilic Addition to Coordinated Cyclooctatetraene. *Eur. J. Inorg. Chem.* **2000**, 1941 - 1952.
- (92) Riemelt, O., Heck, Jurgen. From Coordinated Cyclooctatetraene to cis-5,7-Disubstituted Cycloocta-1,3-diene by Iteratively Applied Nucleophilic and Electrophilic Addition. *Organomet.* **2003**, 22, 2097 - 2107.
- (93) Schorshusen, S., Heck, Jurgen. Metal-Mediated Transformations of Cyclooctatetraene to Novel Methylene-Bridged, Bicyclic Compounds. *Organomet.* **2007**, 26, 5386 - 5394.
- (94) B.K. Liebov, W. D. H. Group 6 Dihapto-Coordinate Dearomatization Agents for Organic Synthesis. *Chem. Rev.* **2017**, 117, 13721-13755.
- (95) J.A. Smith, K. B. W., R.E. Sonstrom, P. J. Kelleher, K.D. Welch, E.K. Pert, K.S. Westendorff, D.A. Dickie, X. Wang, B. H. Pate, W. D. Harman. Preparation of Cyclohexene Isotopologues and Stereoisomers from Benzene. *Nature* **2020**, 581, 288-293.
- (96) K.B. Wilson, H. S. N., S.R. Simpson, M. N. Ericson, K. S. Westendorff, M.D. Chordia, D.A. Dickie, W.D. Harman. Hydroamination of Dihapto-Coordinated Benzene and Diene Complexes of Tungsten: Fundamental Studies and the Synthesis of  $\gamma$ -Lycorane *Chimica Acta* **2021**, 104 (10).
- (97) K.B. Wilson, J. A. S., H.S. Nedzbala, E. K. Pert, S.J. Dakermanji, D.A. Dickie, W.D. Harman Highly Functionalized Cyclohexenes Derived from Benzene: Sequential

Tandem Addition Reactions Promoted by Tungsten *J. Org. Chem.* **2019**, *84* (10), 6094-6116.

(98) M.N. Ericson, J. D. D., J.H. Wilde, R.F. Lombardo, E.C. Ashcraft, D.A. Dickie, W.D. Harman. The Tungsten-Promoted Synthesis of Piperidyl-Modified erythro-Methylphenidate Derivates *ACS Cent. Sci.* **2023**, *9* (9), 1775-1783.

(99) S.R. Simpson, P. S., D.J. Siela, L.A. Diment, B.C. Song, K. S. Westendorff, M. N. Ericson, K. D. Welch, D. A. Dickie, W.D. Harman. Phenyl Sulfones: A Route to a Diverse Family of Trisubstituted Cyclohexenes from Three Independent Nucleophilic Additions. *J. Am. Chem. Soc.* **2022**, *144* (21), 9489-9499.

(100) J.H. Wilde, D. A. D., W.D. Harman. A Highly Divergent Synthesis of 3-Aminotetrahydropyridines. *J. Org. Chem.* **2020**, *85* (12), 8245-8252.

(101) J.T. Weatherford-Pratt, J. A. S., J.M. Bloch, M.N. Ericson, J.T. Myers, K.S. Westendorff, D.A. Dickie, W.D. Harman. The Double-Protonation of Dihapto-Coordinated Benzene Complexes: An Enabling Strategy for Dearomatization Using Aromatic Nucleophiles. *Nature Comm* **2023**, *14*, 3145.

(102) J.T. Weatherford-Pratt, J. M. B., J.A. Smith, M. N. Ericson, D.J. Siela, K. B. Wilson, M.H. Shingler, M.R. Ortiz, S. Fong, J.A. Laredo, I.U. Patel, M. McGraw, D. A. Dickie, W. D. Harman. Tungsten-anisole complex provides 3,6-substituted cyclohexenes for highly diversified chemical libraries. *Sci. Adv.* **2024**, *10* (7).

(103) D.P. Harrison, A. C. N., V. E. Zottig, L. Strausberg, R.J. Salomon, C.O. Trindle, M. Sabat, T.B. Gunnoe, D.A. Iovan, W.H. Myers, W.D. Harman. Hyperdistorted Tungsten Allyl Complexes and Their Stereoselective Deprotonation to Form Dihapto-Coordinated Dienes *Organometallics*. **2011**, *30* (9), 2587-2597.

(104) Davies, S. G., Green, Malcolm, L.H., Mingos, D. Michael P. Nucleophilic addition to organotransition metal cations containing unsaturated hydrocarbon ligands: A survey and interpretation. *Tetrahedron* **1978**, *34* (20), 3047 - 3077.

**Chapter 6.**  
**Preliminary Studies on the Functionalization of Seven-Membered Carbocycles.**

## 6.1 Introduction

A central theme of this thesis study is the development of methodologies for transforming  $sp^2$ -hybridized centers into  $sp^3$ -hybridized centers. This molecular transformation is crucial for constructing molecular complexity, particularly in the design of novel compounds for small-molecule drug discovery. Significant progress has been made in the functionalization of five- and eight-membered carbocycles through dihapto-coordination to tungsten. This study summarizes preliminary investigations and provides suggestions for future research on the synthesis of functionalized cycloheptene-containing compounds.

Seven-membered ring motifs are commonly found in a wide range of natural products, including alkaloids, terpenoids, and other bioactive compounds.<sup>1</sup> Additionally, pharmaceutical drugs have been designed based on naturally occurring seven-membered structural cores.<sup>2,3</sup> Notable examples of seven-membered heterocyclic medicinal compounds include Clozapine (antipsychotic), Diazepam (anxiolytic), Diltiazem (antihypertensive), Suvorexant (insomnia treatment), Rucaparib (anticancer agent), and Molibresib (antitumor activity).<sup>4-8</sup> Seven-membered carbocyclic compounds with medicinal applications include Colchicine (anti-inflammatory), Rimegepant (migraine treatment), Amitriptyline (antidepressant), Guanacastepene (antibiotic activity), and Bemcentinib (antitumor activity).<sup>9-11</sup> The ability seven-membered rings to adopt a broad conformational space provides medicinal chemists with a powerful tool for designing small molecules that adopt bioactive conformations.<sup>2,12-14</sup> In fact, replacing a six-membered ring with a seven-membered ring in the molecular structure of a Type II DNA Topoisomerase inhibitor significantly enhanced its antibacterial activity.<sup>15</sup>

Traditional methods for constructing seven-membered carbocycles are often challenging due to enthalpic and entropic factors, leading to limited synthetic approaches. However, significant progress has been made in the synthesis of natural products featuring seven-membered rings, such as tropones, tropolones, bridged azabicyclics, and benzocycloheptene motifs.<sup>16-18</sup> Many synthetic approaches to cycloheptane cores in natural products rely on cyclization methods,<sup>19</sup> including the Pauson-Khand reaction, [2+2] cycloadditions, Friedel-Craft reactions, Type II [5+2] cycloadditions, ring-closing metathesis, rearrangement reactions and radical-

mediated cyclizations. These methods, along with examples of natural products synthesized using these approaches, are summarized in **Figure 6.1**.

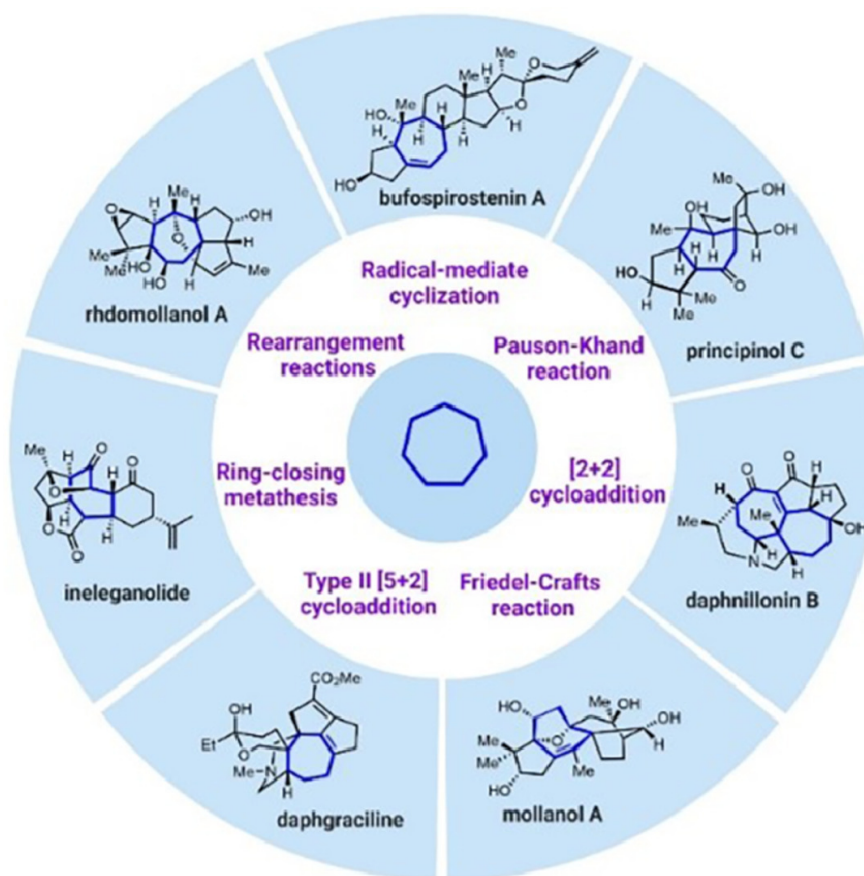


**Figure 6.1.** Pathways for the synthesis of natural products containing seven-membered carbocycles; figure appended from review article by Chen et al.<sup>1</sup>

Although cycloadditions have been essential for constructing natural products containing cycloheptanes, methodologies for the formation of functionalized cycloheptanes remain significantly underdeveloped. Organic transformations involving seven-membered rings often lead to unexpected products due to unfavorable entropic and enthalpic factors. The direct transformation of unsaturated seven-membered rings into chiral, functionalized cycloheptane cores could provide access to previously unobtainable seven-membered ring-containing compounds.

Iron-mediated transformations utilizing tetrahapto-coordinated cycloheptadienes and pentahapto-coordinated cycloheptadienyl cations have successfully yielded stereoselective heptitol derivatives and bridged bicyclic species. While these approaches effectively convert alkenes within seven-membered rings into functionalized cycloheptanes, their scope is surprisingly narrow, primarily limited to C-O bond formations. Pearsons's work is summarized in **Figure 6.2**.<sup>20-24</sup> Furthermore,



these methods have focused more on synthesizing natural products rather than rapidly diversifying complex cycloheptane scaffolds for drug discovery applications.

Tungsten-mediated transformations utilizing dihapto-coordination have been extensively studied for the functionalization of six-membered cores derived from unsaturated, often aromatic, ligands. This methodology has even been extended to the synthesis of functionalized piperidines from pyridine. More recently, tungsten-mediated approaches have shown promise in generating functionalized cyclopentane and cyclooctane cores. In this study, with the assistance of my undergraduate student mentee, Rachel F. Lombardo, we have preliminary extended this approach to the functionalization of cycloheptane cores using highly unsaturated species, specifically cycloheptatriene and tropylium

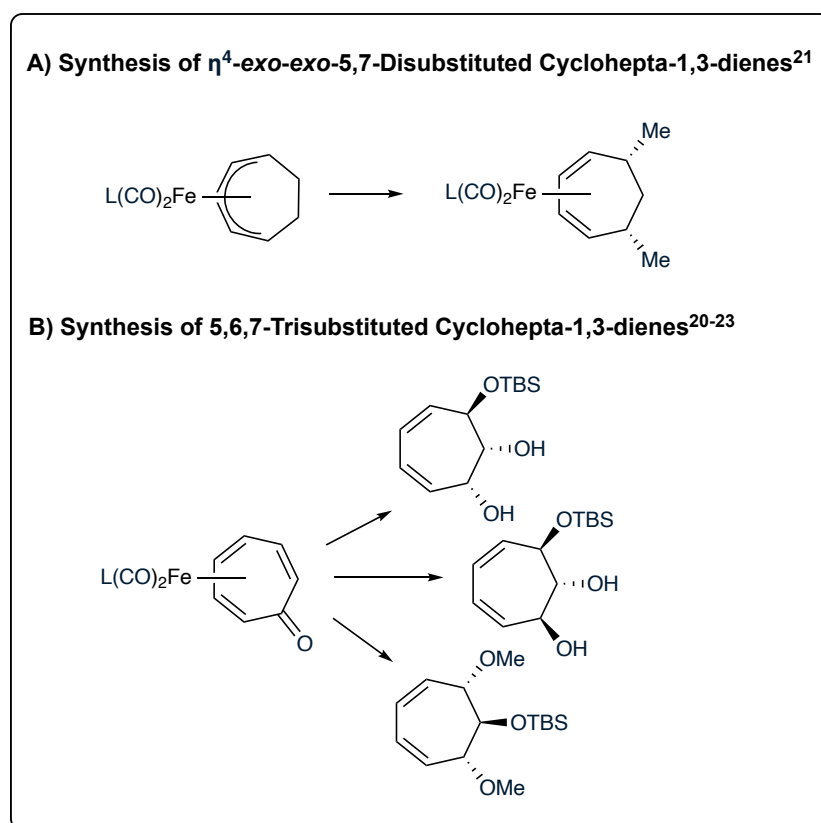


**Figure 6.2.** Pearson's work on organoiron approaches to functionalized seven-membered cores.<sup>20-23</sup>

## 6.2 Results and Discussion.

### 6.2.1 Isolation of $\eta^2$ -Cycloheptatriene Complexes

First introduced in Chapter 3, cycloheptatriene (CHT) was dihapto-coordinated to the tungsten fragment  $\{\text{Wtp}(\text{NO})(\text{PMe}_3)\}$  (Tp = trispyrazolylborate, NO = nitrosyl, and  $\text{PMe}_3$  = trimethylphosphine). 1,3,5-CHT coordinates to tungsten in a 1:1:1 ratio of

diastereomers. The initial challenge of this study was to isolate these diastereomers, not only for characterization purposes but also to further explore their reactivity.

Previous studies demonstrated that the addition of a catalytic amount of a mild oxidant could transiently oxidize the metal center, weakening its coordination to the organic ligand and promoting tungsten-alkene isomerization to a thermodynamically preferred complex through either face-flip or ring-slip mechanisms. Specifically, it was shown that treating a mono-substituted  $\eta^2$ -cyclohexene with 0.1 equivalents of permethyl ferrocenium bistriflimide ( $\text{FeCp}^*_2](\text{Tf}_2\text{N})$ ) resulted in complete conversion from the kinetically trapped isomer and the thermodynamically favored isomer.<sup>25</sup> When this methodology was applied to the 1:1:1 mixture of dihapto-coordinated CHT complexes, the diastereomeric ratio shifted to 7:2:1 for compounds **1A**, **1B**, and **1C**, respectively. Further experiments revealed that both ferrocenium ( $\text{FeCp}_2$ ) and permethyl ferrocenium ( $\text{FeCp}^*_2$ ) catalytically oxidized the linkage isomers. However, the presence of an organic side product indicated that these oxidants also facilitated the full release of the CHT ligand. Additional experiments confirmed that exposing a 1:1:1 mixture of these complexes to atmospheric  $\text{O}_2$  also led to an isomeric distribution of 7:2:1 without free CHT formation.

Another approach for isolating a single diastereomer involved protonation to generate a hyperdistorted  $\eta^2$ -allyl intermediate, followed by selective deprotonation. This strategy had been previously employed for the  $\eta^2$ -cyclohexadienyl cation, successfully yielding a single coordination diastereomer of  $\eta^2$ -cyclohexadiene.<sup>26</sup> To apply this methodology for the  $\eta^2$ -CHT complexes, a 1:1:1 mixture was treated with triflic acid ( $\text{HOTf}$ ), producing three initial species in a 3(**2A**):3(**2C**):1(**2B**) ratio. Similar to the allylic conversion of  $\eta^2$ -cyclooctatrienyl cations, allowing these  $\eta^2$ -cycloheptenyl cations to stir in solution for 24 hours or sit as a solid for a week resulted in a d.r. shift to 6(**2A**):1(**2B**):0(**2C**). Compound **2A** became the major species, compound **2B** became the minor species, and compound **2C** completely disappeared, likely due to conversion into the major species. Allylic species can interconvert spontaneously through processes such as *allyl shifts*, *ring-walks*, *face-flips* and *ring-slips*. Due to the thermodynamic enrichment of a single diastereomer, single-crystal X-ray diffraction (SC-XRD) was successfully obtained for compound **2A**.

The next step in this methodology was the selective deprotonation using a base. Several bases were screened for their ability to deprotonate the  $\eta^2$ -cycloheptenyl cation. While 1,8-diaza[5.4.0]bicycloundecene (DBU) and morpholine acted as nucleophiles instead of bases, diazabicyclo[2.2.2]octane (DABCO) was successful in deprotonation. However, the highest diastereomer ratio was obtained using triethylamine (TEA). Interestingly, the preferred isomer from the selective deprotonation was compound **1C**, the least thermodynamically favored product from the catalytic oxidation reaction. Since the *distal* conformation of the major species (**2A**) is not set up for an elimination reaction, it is proposed that deprotonation occurs at the adjacent position of the minor *proximal* conformation, **2A-P**. On the other hand, the minor complex (**2B**) can be deprotonated from its *distal* conformation. The selective deprotonation of these dihapto-coordinated allylic species led to the isolation of compound **1C** in a d.r. of >20:1. SC-XRD analysis was also successfully obtained for **2C**. The results described above are summarized in **Figure 6.3**.

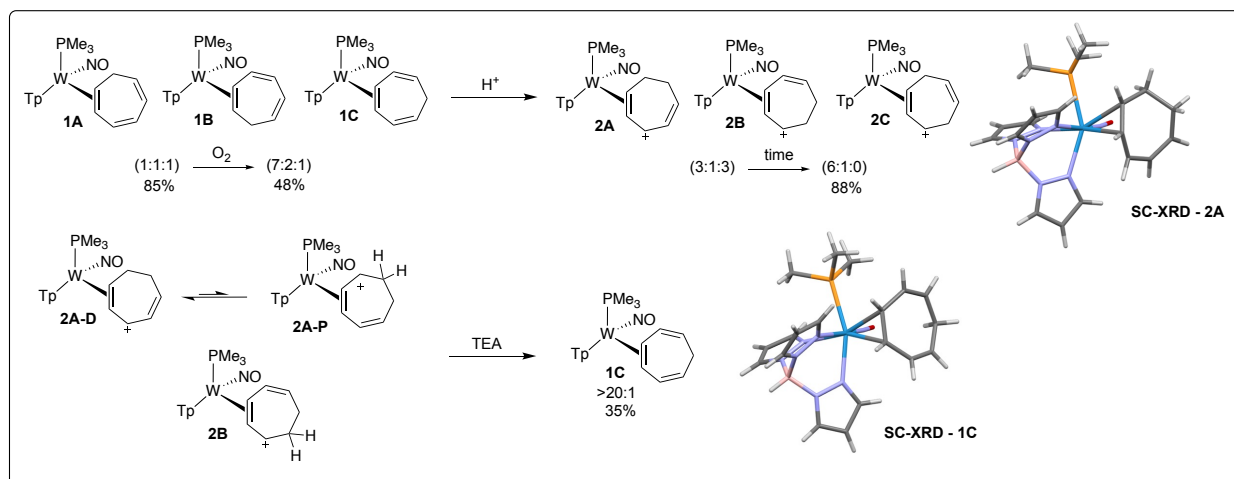


**Figure 6.3.** Coordination, protonation and deprotonation of dihapto-coordinated cycloheptatriene complexes.

### 6.2.2 Nucleophilic Addition Reactions

The next phase of this study involved screening the electrophilic reactivity and selectivity of the  $\eta^2$ -cycloheptadienyl cation. Compound **2A** had exhibited some reactivity with nucleophiles like DBU and morpholine, though with poor regioselectivity. Additionally, the  $\eta^2$ -allyl complex (6:1 cdr) reacted with nucleophiles such as sodium cyanide and imidazole; however, these reactions also proceeded with low regioselectivity, with nucleophiles adding to the both the *distal* and *proximal*

conformations. Due to these limitations, the resulting complexes were not isolated or further studied, and yields were not collected, **Figure 6.4**.

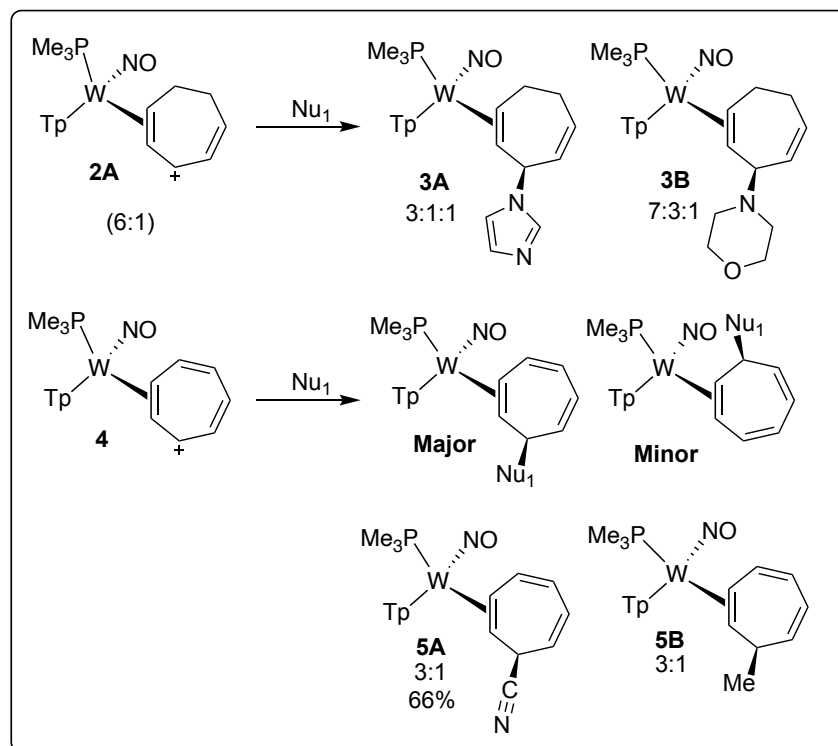


**Figure 6.4.** Nucleophilic scope to the addition of the  $\eta^2$ -cycloheptentyl cation and the  $\eta^2$ -cycloheptatrienyl cation.

Furthermore, it was demonstrated that treatment of dihapto-coordinated  $\eta^2$ -cycloheptatriene with 2,3-dichloro-5,6-dicyano-1,4-benzoquinone (DDQ) could abstract the remaining hydride from all three isomers, forming a single  $\eta^2$ -tropylium species. This complex was also tested for its reactivity as an electrophile with nucleophiles such as methyl Grignard and sodium cyanide. Again, the selectivity for addition at the *distal* versus *proximal* position was low. One factor to consider is that when multiple  $\eta^2$ -cycloheptatriene complexes were present upon initial coordination, their ratios could be altered either by catalytic addition with a mild oxidant or by protonation to form  $\eta^2$ -allylic cations. These methods were not applied to substituted  $\eta^2$ -cycloheptatriene complexes but should be explored in future studies. The initial scope of nucleophilic additions to both  $\eta^2$ -cycloheptentyl cation and  $\eta^2$ -cycloheptatrienyl cation is summarized in **Figure 6.4**.

### 6.2.3 Diels-Alder Reactions

During the hydride abstraction reaction of  $\eta^2$ -cycloheptatriene with DDQ, a side product was observed under certain conditions. By increasing the equivalents of DDQ

and lowering the temperature, this side product was successfully isolated and characterized as a Diels-Alder product. It is hypothesized that compound **1C** initially reacts as a diene in a Diels-Alder reaction with DDQ acting as the dienophile, leading to the formation of product **6A**. However, spectroscopic analysis of the isolated product suggested a different final structure. Due to DDQ's oxidative properties, a tungsten-alkene isomerization occurred, resulting in tungsten coordinating to the newly formed alkene, yielding compound **6B** (Figure 6.5). Interestingly, in the absence of metal coordination, cycloheptatriene typically undergoes Diels-Alder reactions via its pericyclic partner, norcaradiene, which is more reactive as a diene and predominantly yields bicyclic products.<sup>27</sup> The altered reactivity and highly selective reaction of dihapto-coordinated cycloheptatriene prompted an investigation into expanding the scope of this transformation with other dienophiles.

A 1:1:1 mixture of **1A**, **1B** and **1C** was treated with dienophiles such as maleic anhydride, maleimide, and methyl maleimide in diglyme at temperatures ranging from 75°C to 110°C over a period of two to six hours. Two products were consistently observed in ratios ranging from 5:1 to 8:1. Structural analysis revealed that the major product resulted from the endo addition to diene **1A**, while the minor product corresponded to the endo addition to diene **1B**. The structure of the minor product for compound **7C** was confirmed through SC-XRD. Other dienophiles including fumaronitrile, benzoquinone, and dimethyl malonate did not yield new products.

Despite being introduced in equal proportions, **1C** was found to be unreactive in the Diels-Alder reaction due to its non-conjugated diene system, leading either to its isomerization or decomposition in solution. Additionally, compound **1B** likely isomerizes to the major complex **1A**, as indicated by the consistent formation of a major product without significant loss in overall yield. Notably, through the monitoring of <sup>31</sup>P NMR, compound **1C** was the first species to disappear from the reaction mixture, while the ratio of **1A** to **1B** gradually shifted in favor of **1A** as the reaction progressed. The product selectivity is proposed to result from the electronic influence of the tungsten fragment, enhancing the reactivity of compound **1A** toward dienophiles. Furthermore, the thermal equilibrium of the system, which favors **1A**, contributes to its predominant formation. Given the precedent for protonation of non-conjugated alkenes in dihapto-coordinated systems to form hyperdistorted  $\eta^2$ -allyl intermediates, it would be valuable to explore the protonation and further functionalization of these products. It would also be interesting to study the reactivity of mono-substituted  $\eta^2$ -

cycloheptatriene synthesized via nucleophilic additions to  $\eta^2$ -tropylium; although the nucleophilic addition selectivity was low, there could be factors favoring the reactivity of one isomer over the other toward Diels-Alder reactions. A summary of the Diels-Alder chemistry explored with  $\eta^2$ -cycloheptatriene is summarized in **Figure 6.5**.

Finally, preliminary reactions were conducted to investigate the release of the newly formed product from the metal using oxidants. Copper (II) bromide, ceric ammonium nitrate (CAN), and DDQ were screened for their effectiveness in this transformation. Spectroscopic analysis revealed that the addition of CAN led to the formation of an organic species, but further characterization should be explored. Interestingly, when the major and minor products are released as organic compounds, they are enantiomers.

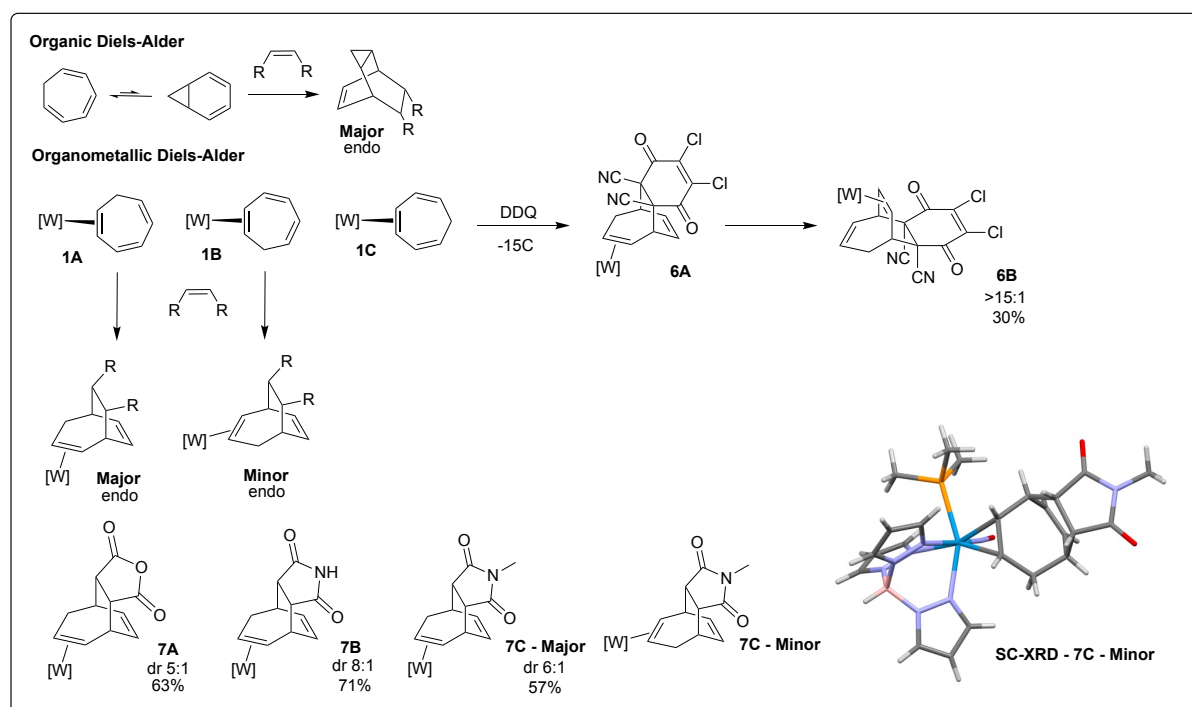


**Figure 6.5.** Diels-Alder scope for  $\eta^2$ -cycloheptatriene.

### 6.3 Conclusions

This preliminary study has explored the functionalization of cycloheptane rings through tungsten-mediated dihapto-coordination, providing new insights into the reactivity and synthetic potential of  $\eta^2$ -cycloheptatriene and  $\eta^2$ -tropylium. Traditional methods for constructing functionalized seven-membered carbocycles remain limited due to enthalpic and entropic challenges and highly rely on cyclizations. However, strategies investigated here—ranging from catalytic oxidation and selective protonation-deprotonation to nucleophilic additions and Diels-Alder reactions—have

demonstrated the versatility of dihapto-coordinated cycloheptatriene complexes as reactive intermediates. Although preliminary, and challenges in regioselectivity persist, the formation of functionalized cycloheptane derivatives highlights the ability to obtain molecules with unique structural motifs and the potential for development in drug discovery applications. Future work will focus on expanding reaction scopes, improving selectivity, and exploring new functionalization strategies to harness the full synthetic potential of these  $\eta^2$ -seven-membered carbocyclic systems.

## References

- (1) Chen, P., Liang, Lijuan., Xing, Zhimin., Jia, Zhenhua., Loh, Teck-Peng. Strategies for constructing seven-membered rings: Applications in Natural Product Synthesis *Chi Chem Lett* **2024**, 35, 109229
- (2) Ouvry, G. Recent applications of seven-membered rings in drug design. *Bioorg. Med. Chem.* **2022**, 57 (116650).
- (3) Stempel, E., Gaich, Tanja. Cyclohepta[b]indoles: A Privileged Structure Motif in Natural Products and Drug Design. *Acc. Chem. Res.* **2016**, 49, 2390 - 2402.
- (4) Yoo, M., Park, T Ae Hyun., Yoo, Miyouun., Kim, Yeongrin., Lee, Joo-Youn., Lee, Kyu Myung., Ryu, Seong Eon., Lee, Byung Il., Jung, Kwan-Young., Park, Chi Hoon. Synthesis and Structure-Activity Relationships of Aristoyagonine Derivatives as Brd4 Bromodomain Inhibitors with X-ray Co-Cystal Research *Molecules.* **2021**, 26 (6), 1689.
- (5) Saha, D., Jain, Garima., Sharma, Anuj. Benzothiazepines: chemistry of a priveleged scaffold. *RSC Adv* **2015**, 5 (86), 70619.
- (6) Roecker, A. J., Cox, Christopher D., Coleman, Paul J. Orexin Receptor Antagonists: New Therapeutic Agents for the Treatment of Insomina *J. Med. Chem.* **2015**, 59 (2), 504 - 530.
- (7) Cox, C. D., Breslin, Michael J., Whitman, David B., Schreier, John D., McGaughey, Georgia B., Bogusky, Michael J., Roecker, Anthony J., Mercer, Swati P., Bednar, Rodney A., Lemaire, Wei., Bruno, Joseph G., Reiss, Duane R., Harrell, C. Meacham., Murphy, Kathy L., Garson, Susan L., Doran, Scott M., Prueksaritanont, Thomayant., Anderson, Wayne B., Tang, Cuyue., Roller, Shane., Cabalu, Tamara., Cui, Donghui., Hartman, George D., Young, Steven D., Koblan, Ken S., Winrow, Christopher J., Renger, JOhn J., Coleman, Paul J. Discovery of the dual orexin receptor antagonist [(7R0-4-(5-chloro-1,3-benzoxazol-2-yl)-7-methyl-1,4-diazepan-1-yl)][5-methyl-2-(2H-1,2,3-triazol-2-yl)phenyl]methanone (MK-4305) for the treatment of insomnia *J. Med. Chem.* **2010**, 53 (14), 5320 - 5332.
- (8) Zhao, y., Yang, Chao-Yie., WAng, Shaomeng. The Making of I-BET762, a BET Bromodomain Inhibitor Now in Clinical Development *J. Med. Chem.* **2013**, 56 (19), 7498 - 7500.
- (9) Van Tamelen, E. E., Spencer, Thomas A., Allen, Duff S., Orvis, Roy L. The Total Synthesis of Cochicine. *J. Am. Chem. Soc.* **1959**, 81 (23), 6341 - 6342.



- (10) Holland, S. J., Pan, Alison., Franci, Christian., Hu, Yuanming., Chang, Betty., Li, Weiqun., Duan, Matt., Torneros, Allan., Yu, Jiaxin., Heckrodt, Thilo J., Zhang, Jing., Ding, Pingyu., Apatira, Ayodele., Chua, Joanne., Brandt, Ralf., Pine, Polly., Goff, Dane., Singh, Rajinder., Payan, Donald G., Hitoshi, Yasumichi. R428, a selective small molecule inhibitor of Axl kinase, blocks tumor spread and prolongs survival in models of metastatic breast cancer. *Cancer Res.* **2010**, 70 (4), 1544 - 1554.
- (11) Singh, M. P., Janso, J.E., Luckman, S.W., Brady, S.F., Clardy, J. Biological Activity of Guanacastepene, a Novel Diterpenoid Antibiotic *J. Antibiotics.* **2000**, 53 (3), 256 - 261.
- (12) Brameld, K. A., Kuhn, Bernd., Reuter, Deborah C., Stahl, Martin. Small Molecule Conformational Preferences Derived from Crystal Structure Data. A Medicinal Chemistry Focused Analysis *J. Chem. Info. Model.* **2008**, 48 (1), 1-24.
- (13) Zheng, Y., Tice, Colin M., Singh, Suresh B. Conformational control in structure-based drug design. *Bioorg. Med. Chem. Lett.* **2017**, 27 (13), 2825 - 2837.
- (14) Jarvis, A., Ouvry, Gilles. Essential Ingredients for rational drug design *Bioorg. Med. Chem. Lett.* **2019**, 29 (20), 126674.
- (15) Gerasyuto, A. I., Arnold, Michael A., Wang, Jiashi., Chen, Guangming., Zhang, Xiaoyan., Smith, Sean., Woll, Matthew G., Baird, John., Zhang, Nanjing., Almstead, Neil G., Narasimhan, Jana., Peddi, Srinivasa., Dumble, Melissa., Sheedy, Josephine., Weetall, Marla., Branstrom., Prasad, J.V.N., Karp, Gary M. Discovery and Optimization of Indolyl-Containing 4-Hydroxy-2-Pyridone Type II DNA Topoisomerase Inhibitors Active against Multidrug Resistant Gram-negative Bacteria *J. Med. Chem.* **2018**, 61 (10), 4456 - 4475.
- (16) Liu, N., Song, Wangze., Schienebeck, Casi M., Zhang, Min., Tang, Weiping. Synthesis of naturally occurring tropones and tropolones. *Tetrahedron* **2014**, 70, 9281 - 9305.
- (17) Shoemaker, A. H., Griffith, Daniel R. Synthetic Approaches to Non-Tropane, Bridged, Azapolycyclic Ring Systems Containing Seven-Membered Carbocycles. *Synthesis* **2020**, 53, 65 - 78.
- (18) Fan, J.-H., Hu, Ya-Jian., Li, Li-Xuan., Wang, Jing-Jing., Li, Shao-Ping., Zhao, Jing., Li, Chang-Chang. Recent Advances in total synthesis of natural products containing the benzocycloheptane motif *Nat. Prod. Rep.* **2021**, 38, 1821 - 1851.

- (19) Battiste, M. A., Pelphrey, P.M., Wright, D.L. The Cycloaddition Strategy for the Synthesis of Natural Products Containing Carbocyclic Seven-Membered Rings. *Chem. Eur. J.* **2006**, 12 (13), 3438-3447.
- (20) Pearson, A. J., Srinivasan, Kumar. . Stereocontrolled Functionalization of Cycloheptatrieneiron Complexes. Synthesis of Polyhydroxylated Cycloheptane Derivatives *J. Chem. Soc. Chem. Comm.* **1991**, (6), 392 - 394.
- (21) Pearson, A. J., Srinivasan, Kumar. Approaches to the Synthesis of Heptitol Derivatives via Iron-Mediated Stereocontrolled Functionalization of Cycloheptatrienone. *J. Org. Chem.* **1992**, 57 (14), 3965 - 3973.
- (22) Pearson, A. J., Kole, Sandra H., Chen, Bruce. Organoiron complexes in organic synthesis. Approach to stereochemically defined cycloheptadiene derivatives using organoiron chemistry. *J. Am. Chem. Soc.* **1983**, 105 (13), 4483 - 4484.
- (23) Pearson, A. J., Khan, Nazrul I. Stereo- and Regio-Controlled Functionalization of Cycloheptene Using Organomolybdenum. *Tetrahedron Letters* **1985**, 26 (11), 1407 - 1410.
- (24) Blankenfeldt, W., Liao, Jin-Wei., Lo, Li-Chin., Yeh, Ming-Chang P. Sequential Additions of Nucleophiles to Tricarbonyl( $\eta^4$ -cycloheptadienyl)iron Tetrafluoroborate. *Tetrahedron Letters* **1996**, 37 (41), 7361- 7364.
- (25) S. J. Dakermanji, Westendorff, Karl S. Pert, Emmit K., Wilson, Katy B., Myers, Jeffery T., Wilde, Justin H., Dickie, Diane A., Welch, Kevin D., Harman, W. Dean. Spatial Recognition Within Terpenes: Redox and H-bond Promoted Linkage Isomerizations and the Selective Binding of Complex Alkenes. *Organomet.* **2020** Vol. 39 Pages 1961 – 1975.
- (26) A. C. N. D.P. Harrison, V. E. Zottig, L. Strausberg, R.J. Salomon, C.O. Trindle, M. Sabat, T.B. Gunnoe, D.A. Iovan, W.H. Myers, W.D. Harman. Hyperdistorted Tungsten Allyl Complexes and Their Stereoselective Deprotonation to Form Dihapto-Coordinated Dienes. *Organometallics*. **2011** Vol. 30 Issue 9 Pages 2587-2597.
- (27) P.-P. Chen, Seeman, Jeffrey I., Houk, Kendall N. Rolf Huisgen's Classic Studies of the Cyclic Triene Diels-Alder Reactions Elaborated by Modern Computational Analysis. *Angew Chem Int Ed* **2020** Vol. 59 Issue 30 Pages 12506 - 12519

## **Chapter 7. Summary on Supporting DFT Calculations for Energy and Conformational Comparisons**

## 7.1 Introduction

The limited availability of new synthetic organic methodologies constrains drug discovery by restricting the synthetic approaches available for target molecule construction. This leads to molecular libraries dominated by achiral, aromatic compounds.<sup>1-3</sup> However, pharmaceutical success has been shown to increase with a higher fraction of  $sp^3$ -hybridized carbons, highlighting the need for organic reactions that enable the regiochemistry and stereochemistry of  $sp^3$  centers to expand chemical space.<sup>4,5</sup> Our research focuses on the activation of aromatic compounds through complexation with  $\pi$ -basic transition metals, such as  $\{\text{TpW}(\text{NO})(\text{PMe}_3)\}$  (Tp = hydridotris- (pyrazolyl)borate, NO = nitrosyl, and  $\text{PMe}_3$  = trimethylphosphine), a system under ongoing investigation for our group.<sup>6,7</sup>  $\eta^2$ -coordination to transition metals alters the reactivity of aromatic molecules by activating the uncoordinated diene, facilitating molecular transformations.<sup>8</sup> The unbound portion of the aromatic system becomes susceptible to electrophilic addition reactions, including protonation, which can subsequently lead to nucleophilic addition reactions.

Notably, tungsten allyl complexes formed through these reactions exhibit a structural distortion from an  $\eta^3$ - to an  $\eta^2$ -coordinated allylic carbocation.<sup>9</sup> Unlike  $\eta^3$ -coordinated metal allyl complexes, which display equidistant metal-carbon bond lengths, Density Functional Theory (DFT) and Single Crystal X-Ray Diffraction (SC-XRD) data of  $[\text{TpW}(\text{NO})(\text{PMe}_3)(\pi\text{-C}_6\text{H}_9)]\text{OTf}$  reveal an elongated W-C bond ( $\sim 2.6$  Å) at the allylic carbon vs shorter W-C bonds ( $\sim 2.3$  Å) at the dihapto-coordinated carbons, indicative of hyperdistortion, **Figure 7.1**. These hyperdistorted allyl complexes rapidly interconvert between two conformations, with the carbocationic center alternating between positions *distal* and *proximal* to the  $\text{PMe}_3$  ligand. The degree of orbital overlap between the  $\pi_{\text{nb}}$  and  $\pi^*$  orbital combination of the allyl and a major lobe of the tungsten  $d_{xy}$  orbital (HOMO) influences this distortion and dictates the preferred cationic conformation. Consequently, the regioselectivity of nucleophilic addition reactions can be influenced by the distortion, while stereoselectivity arises from steric interactions with the coordinated metal center. To further investigate these effects, transition state calculations were performed to model the interconversion of these allyl conformations, a process we have termed an *allyl shift*, **Figure 7.2**.

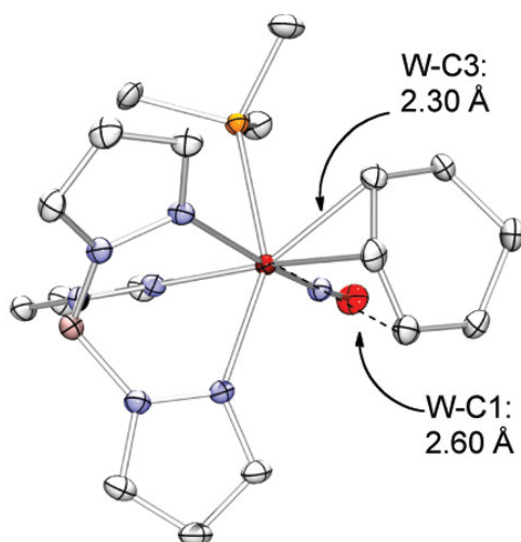


**Figure 7.1.** ORTEP diagram (30% probability) for allyl complex  $[\text{TpW}(\text{NO})(\text{PMe}_3)(\pi\text{-C}_6\text{H}_9)]\text{OTf}$ .<sup>9</sup>

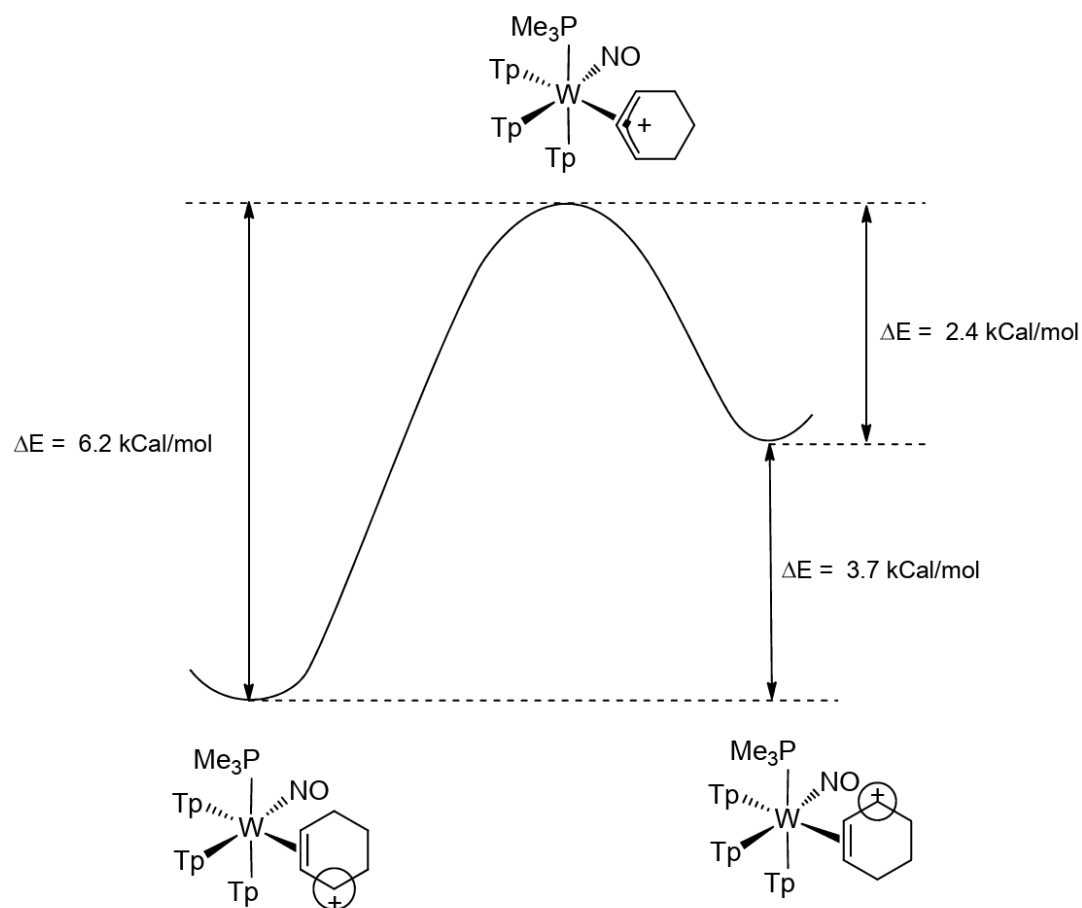


**Figure 7.2.** Reaction coordinate diagram for allyl cation isomerization in the complex  $[\text{TpW}(\text{NO})(\text{PMe}_3)(\pi\text{-C}_6\text{H}_9)]\text{OTf}$ .<sup>9</sup>

DFT is essential in computational chemistry because it allows scientists to bridge the gap between theory and experiments, making it an invaluable tool for modern synthetic chemists. Specifically, it serves as a powerful tool for understanding reaction mechanisms, optimizing molecular structures, and guiding experimental design. In this study, DFT calculations were employed to elucidate the structural and energetic properties of dihapto-coordinated complexes, providing insight on synthetic applications in the Harman Lab.

## 7.2 Results and Discussion

### 7.2.1 Chair and Boat Conformations

Alkene-containing six-membered rings adopt boat and half-chair conformations. When an  $\eta^2$ -coordinated cyclohexenium is bound to  $\{\text{TpW}(\text{NO})(\text{PMe}_3)\}$ , it is proposed that, beyond *distal* and *proximal* conformations, additional  $\eta^2$ -allyl conformations exist. It is suggested that both *distal* and *proximal* carbocations occur in “chair-like” and “boat-like” structures. In *distal* conformations, the positive charge is localized on C3, whereas in *proximal* structures, the charge is localized on C1. Bonds between tungsten and the carbocation are lengthened relative to those between tungsten and the  $\eta^2$  bound carbons.<sup>9</sup>

DFT was used to study the proposed conformations. The M06 functional is employed alongside a split basis set, where LANL2DZ pseudopotential is applied to tungsten, and 6-31G(d,p) is used for all other atoms. Thermodynamic energies are compared, and carbocation location is determined through W-C bond lengths and Mulliken charge analysis. The conformational equilibrium of allyl isomers is explored with variations of  $\pi$ -donor,  $\pi$ -accepting, and steric substituents at different positions of the cyclohexene ring. Solvent effects are also analyzed. Although these conformations present as a single structure in  $^1\text{H-NMR}$ , the observed chemical shift results from the averaging of the thermodynamic equilibrium of conformations.

In “boat-like” structures, C5 flips away from the metal center, whereas in “chair-like” structures, C5 flips toward the metal center. Consistent with previous predictions<sup>9</sup>, it was determined that the *distal boat* (0 kcal/mol) and *distal chair* (1.36 kcal/mol) conformations are the most thermodynamically stable, followed by the *proximal chair* (4.28 kcal/mol). The *proximal boat* isomer does not optimize in the gas phase, and instead converged to the *distal boat* conformation, **Figure 7.3**. To access the effects of electron-withdrawing, electron-donating, and sterically bulky substituents, different

groups were added to C4, C5 and C6. In some cases, conformations failed to converge or converged to a different conformation, which are noted in italics. Because nucleophilic addition reactions of tungsten-bound ligands occur stereoselectively, only complexes with substituents *trans* to the face of the metal were explored.

First, steric bulk is evaluated through the addition of methyl, phenyl and *tert*-butyl. It is determined that as steric bulk increases at C4, the *distal chair* conformation

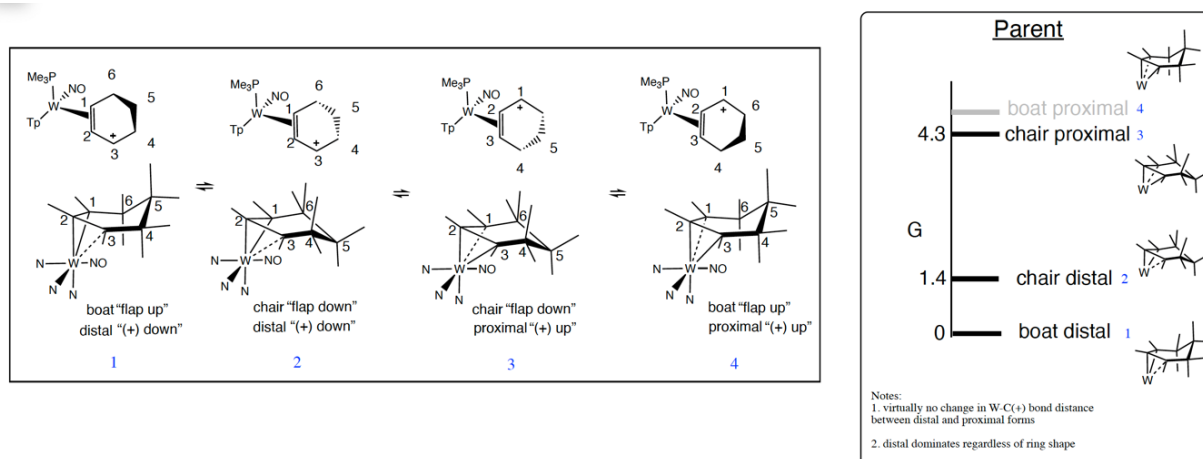


**Figure 7.3.** The four conformations of  $\eta^2$  – cyclohexenyl cations and their energy comparisons.<sup>10</sup>

becomes increasingly stable. Notably, when a methyl group is present at C4, the *proximal boat* conformation is more stabilized than the *proximal chair*, **Figure 7.4a**. The *distal chair* also gains stability with steric substituents at C5. Uniquely, when incorporated with a methyl, its energy is similar to that of the *distal boat*. However, as steric bulk increases at C5, the *distal boat* is destabilized due to 1,3-diaxial interactions. In the case of *t*-butyl substitution at C5, the *proximal chair* becomes lower in energy than the *distal boat*, **Figure 7.4b**. Similarly, when C6 is substituted with methyl or *t*-butyl, the *distal chair* is stabilized. Surprisingly, replacing C6 with a phenyl group destabilizes the *distal chair*, likely due to electronic effects. Additionally, the *distal boat* is significantly destabilized by steric interactions, while the *proximal boat* is stabilized when C6 contains a bulky *t*-butyl group, making it competitive with the *distal chair*, **Figure 7.4c**. In all cases, the *proximal chair* energy increases when a methyl is replaced with a phenyl but decreases when the phenyl is replaced with a *t*-butyl. Overall, it seems that distal to proximal ratios are relatively insensitive to steric effects.

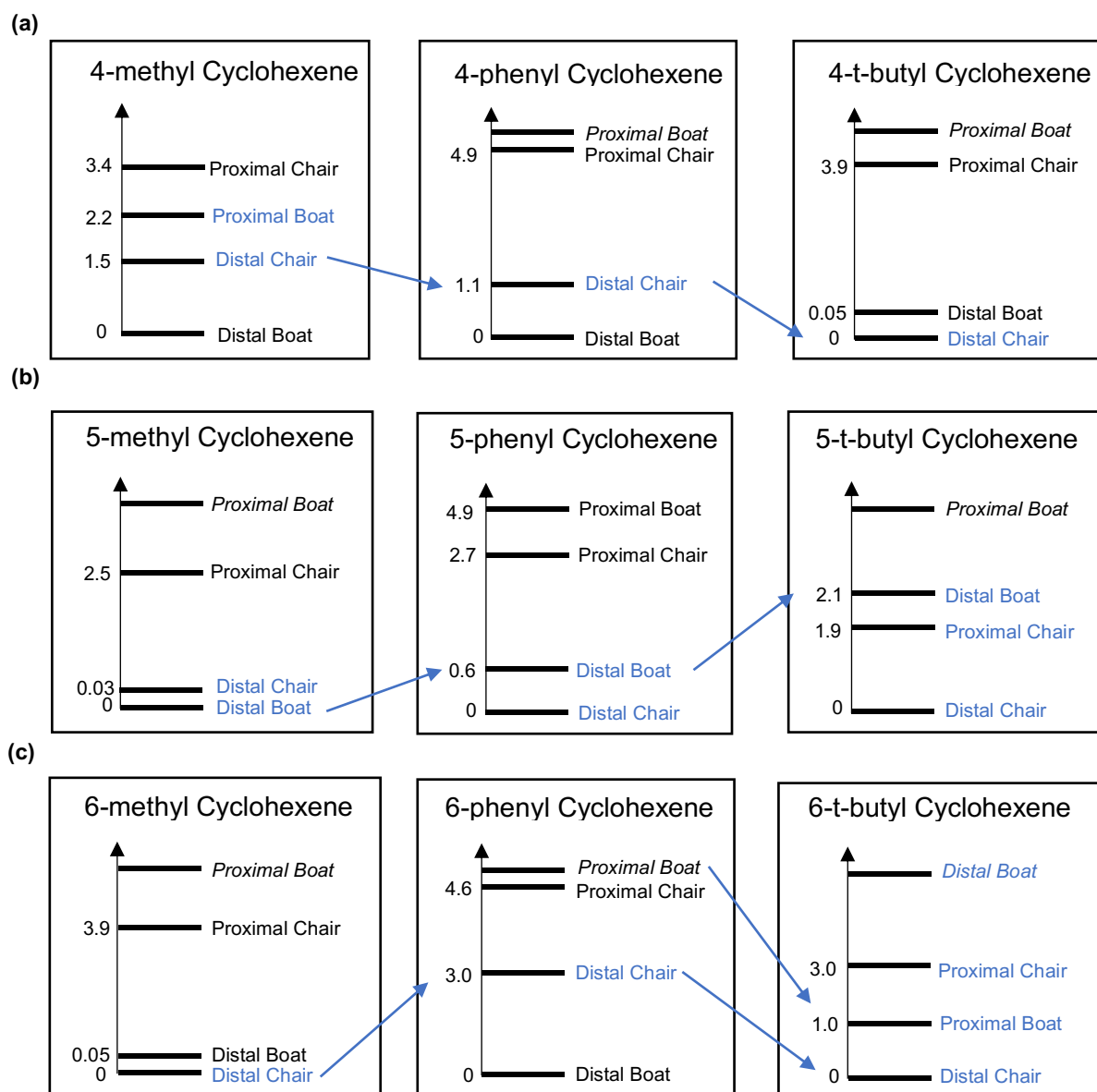


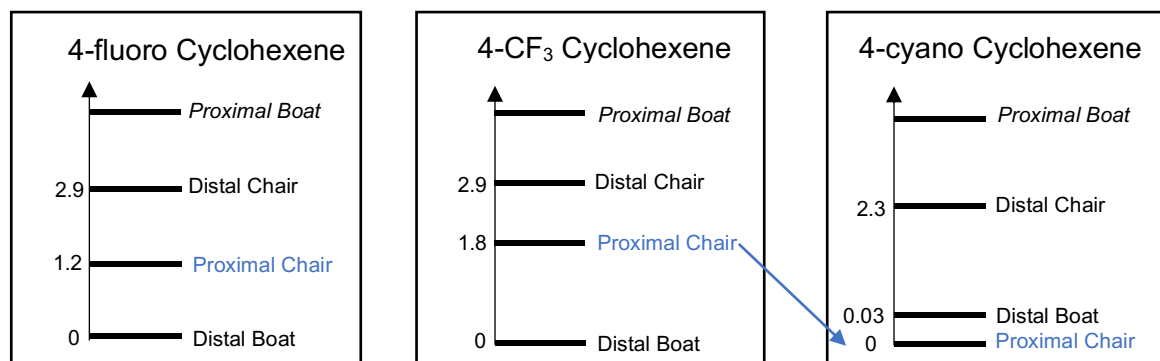
**Figure 7.4.** Relative energy order of allyl conformations when substituted with a methyl, phenyl, and t-butyl group. (a) at position C4 (b) at position C5 (c) at position C6. Italicized conformations did not optimize. Thermodynamic free energy calculations are reported in kcal/mol.

The conformational equilibrium of allyl isomers was further explored with electron-withdrawing groups such as cyano, fluoro, and trifluoromethyl, as well as an electron-donating methoxy group. Phenyl substitution is also reconsidered in the context of electron-donating effects. When electron-withdrawing groups were incorporated at C4, the *proximal chair* was stabilized and becoming the favored conformation when a cyano group is present. At C5, the presence of  $-CF_3$  stabilized both the *distal chair* and the *proximal chair*, **Figure 7.5**. Overall, the energy gap

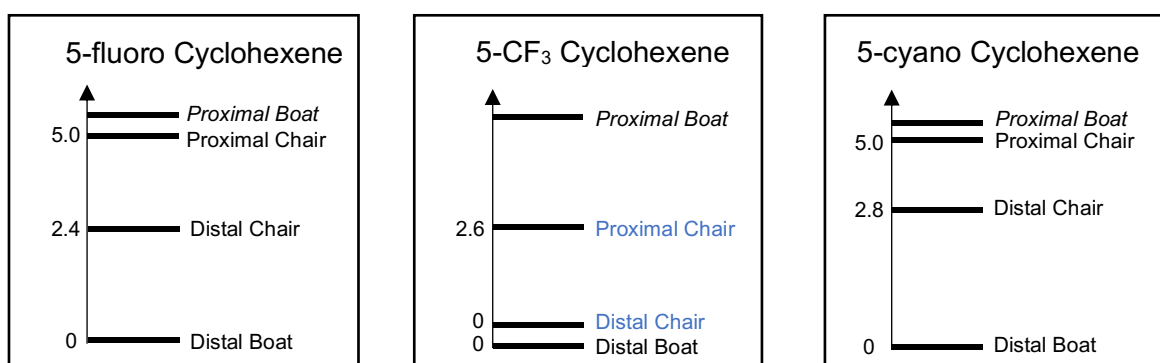


between distal and proximal forms is smallest when an EWG is incorporated at the C4 position.

(a)



(b)



(c)

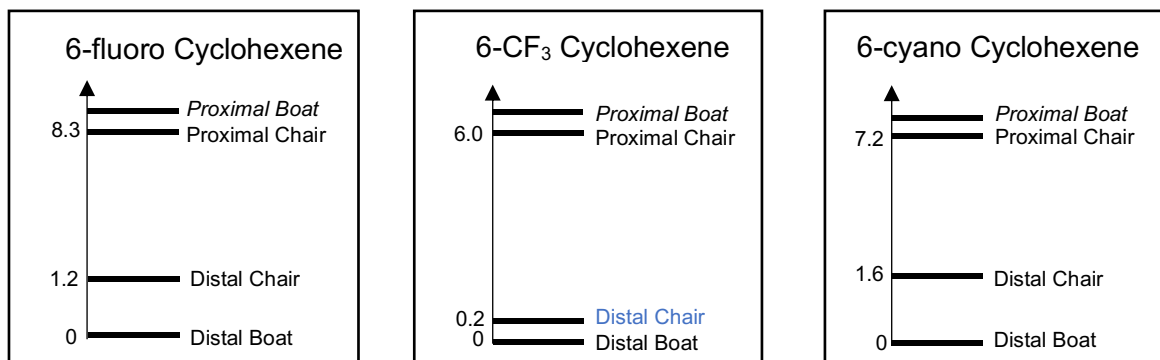


**Figure 7.5.** Relative energy order of allyl conformations substituted with a fluoro, trifluoromethyl, and cyano. (a) at position C4. (b) at position C5. (c) at position C6. Italicized conformations did not optimize. Thermodynamic free energy calculations are reported in kcal/mol.

To account for the influence of solvation, the unsubstituted cyclohexene system was examined using the SMD implicit solvation model, a model that incorporates dielectric constants as a key parameter. Although the proximal boat conformation did not optimize in the gas phase, it successfully converged upon inclusion of solvent effects. Overall, increasing solvent polarity, as defined by dielectric constants, stabilizes the *proximal chair* while destabilizing the *proximal boat*. Increasing polarity

from dichloromethane to acetone lowers the energy of the *distal chair* but further increasing the polarity with acetonitrile and dimethyl sulfoxide raises its energy, **Figure 7.6**. Interestingly, DMSO, the most cation-stabilizing solvent reduces the *distal-proximal* gap in the gas phase from 4.3 kcal/mol to 1.7 kcal/mol.

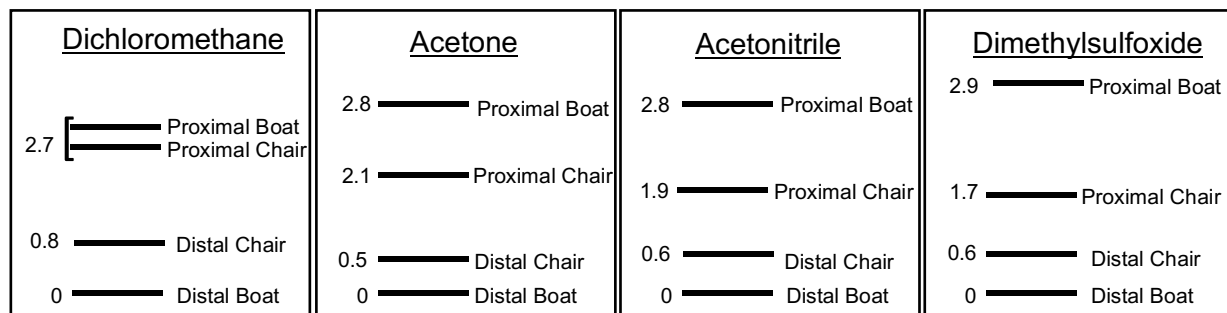


**Figure 7.6.** Implicit solvent effects on conformational stability of dihapto-coordinated cyclohexene allylic cations. Energies are reported in kcal/mol.

### 7.2.2 Tri-Substituted and Polycyclic Compounds

Energy comparisons of  $\eta^2$ -allyl conformations and  $\eta^2$ -cyclohexenes are performed to better understand the reactivity of synthetic reactions, including the hydroamination of dihapto-coordinated benzene and diene tungsten complexes.<sup>10</sup> Additionally, these energetic comparisons were used in the study of dihapto-coordinated phenyl sulfones and their route to trisubstituted cyclohexenes.<sup>11</sup>

When aryl sulfones are  $\eta^2$ -bound to  $\{W(Tp)(NO)(PMe_3)\}$ , two coordination diastereomers are produced (**1a** and **1b**). Upon protonation, these complexes yield two unique  $\eta^2$ -allyl species that are not interconvertible by a simple *allyl-shift* (**2a** and **2b**). At cold temperatures ( $-30^\circ\text{C}$ ), experiments show that isomers **2a** and **2b** both react with nucleophiles, resulting in a mixture of 1,3-diene diastereomers **3a** and **3b**. On the other hand, when experimental reactions are performed at  $0^\circ\text{C}$ , there is a strong preference for the formation of diastereomer **3b**. Computational optimizations of **2a** and **2b** and their energy comparisons corroborated experimental observations, showing that the *distal* conformation of **2b** was 3.0 kcal/mol more stable than the *proximal* conformation of **2a**. These synthetic pathways are shown in **Figure 7.7**.

When MMTP is incorporated as a first nucleophile at  $0^\circ\text{C}$ , the resulting structure is a class **3b** diastereomer. When compound **4** is exposed to acid then a second nucleophile, the addition occurs at the same *distal* position whether the incorporation of a hydride (**5A**) or dimethyl malonate (**7A**) is pursued. Again, in both cases, the sulfone ligand leaves resulting in a  $\eta^2$ -allyl species. Species **5E** and **5F** were optimized and energetically compared, showing that the *distal* conformation was more stable

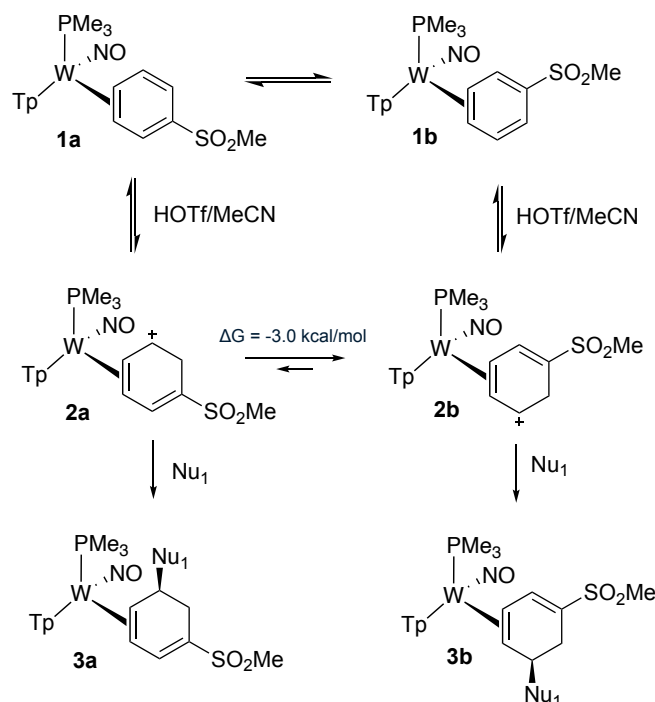


**Figure 7.7.** Energy comparison of the *proximal* conformer of isomer **2a** and the *distal* conformer of isomer **2b**.

than the *proximal* conformer by 1.7 kcal/mol. As expected, a second hydride incorporates at the *distal* position, resulting in compound **6**. Although **7B** and **7C** also show favorability for the *distal* conformer, a second DiMM incorporates at the *proximal* position resulting in complex **8**. **7B** is more stable than **7C** by 1.3 kcal/mol, steric interactions apparently inhibit the incorporation at the *distal* position. A rare case of tungsten epimerization was observed for the sterically encumbered complex **8**, which converted to **9**. Energetic comparisons confirmed that these two species were nearly equal in energy (0.6 kcal/mol), making the experimentally observed interconversion energetically feasible. **Figure 7.8** illustrates the synthetic pathway, energetic comparisons for **5E/5F**, **7B/7C**, and **8/9**.

Another study utilized  $\eta^2$ -aryl sulfones for the synthesis of heteropolycyclic compounds, where energetic comparisons of intermediates and products were employed to analyze competing mechanisms. First, *distal* (**ID**) and *proximal* (**IP**) conformations of dihapto-coordinated cyclohexenium substituted with methyl sulfone and a simple methyl group were compared. Results showed that conformer **ID** was 4.77 kcal/mol more stable than conformer **IP**, aligning with experimental findings that species **ID** was most likely to react with a nucleophilic amine. An additional allylic comparison was performed on the dihapto-coordinated lactam. Due to the electron-withdrawing nature of the amide, the *distal* conformer was found to be nearly equal in

energy to the *proximal* conformer (0.51 kcal/mol). This result was consistent with the synthetic finding that, although a tethered nucleophilic addition occurs at species **IIID**, an alternative tricyclic species is observed at low temperatures where the tethered nucleophile adds to **IIIP**, as shown in.

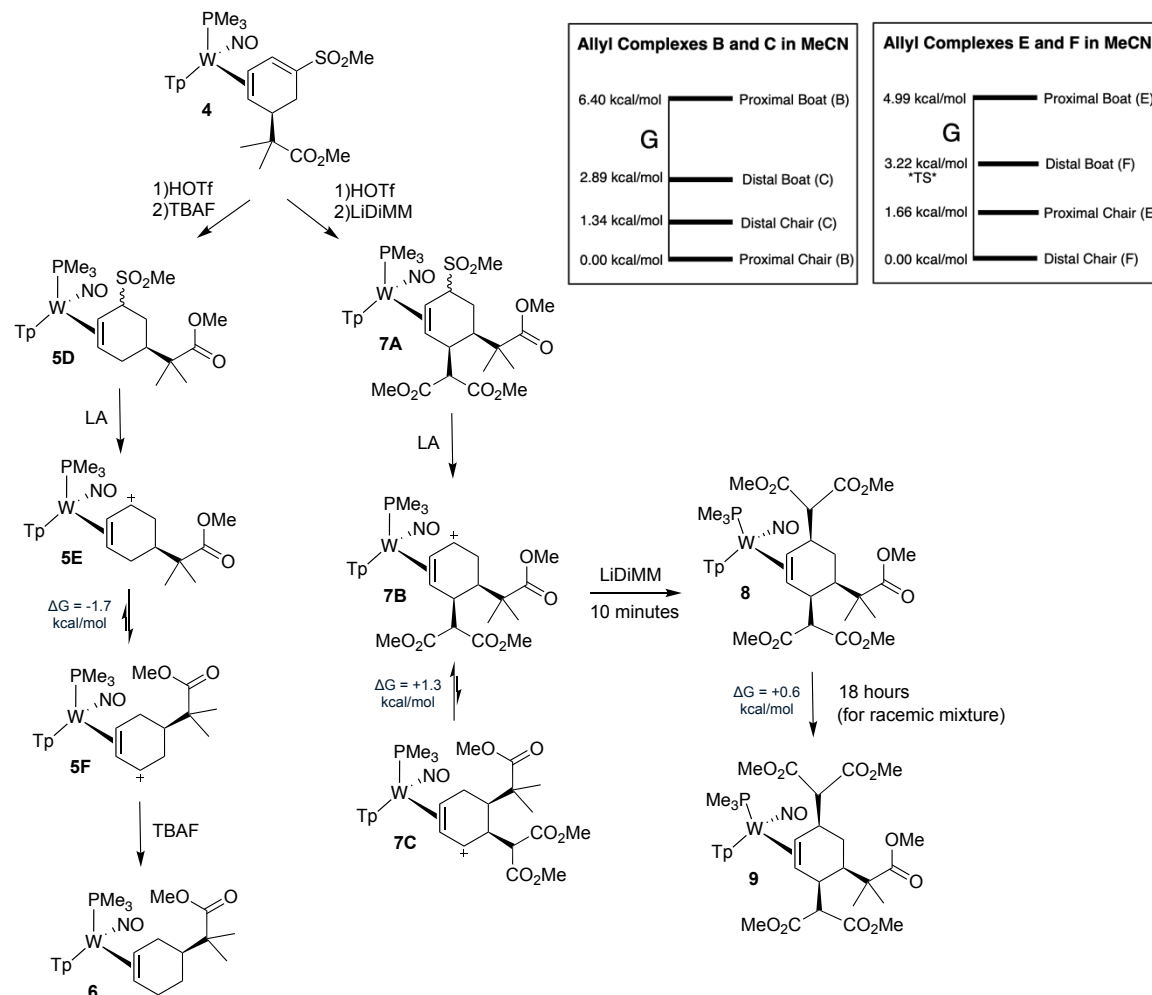


**Figure 7.8.** Double Nucleophilic Additions to  $\eta^2$ -1-Sulfonyl-1,3-diene Complexes (Racemic Mixture) and energetic comparisons of the  $\eta^2$ -allyl intermediates, their conformations and their products.

The theoretical addition products versus elimination products for a tethered addition were also analyzed energetically. It was observed the tethered addition at the *proximal* position resulted in a product (**VIII**) that was 11.85 kcal/mol higher in energy than the product formed by addition at the *distal* position (**VII**). Furthermore, the product where the nucleophile adds *syn* to the metal, rather than *anti*, was not energetically unfavorable (+0.66 kcal/mol, **VI**) yet it was not experimentally observed, suggesting the presence of a significant kinetic barrier. Lastly, two elimination products were examined; DFT calculations placed **IX** about 3 kcal/mol higher in energy than **V**,

with no indication of a purported dienamide isomer of type **V**, again implying kinetic factors are at play. A summary of this work is shown in **Figure 7.9**.

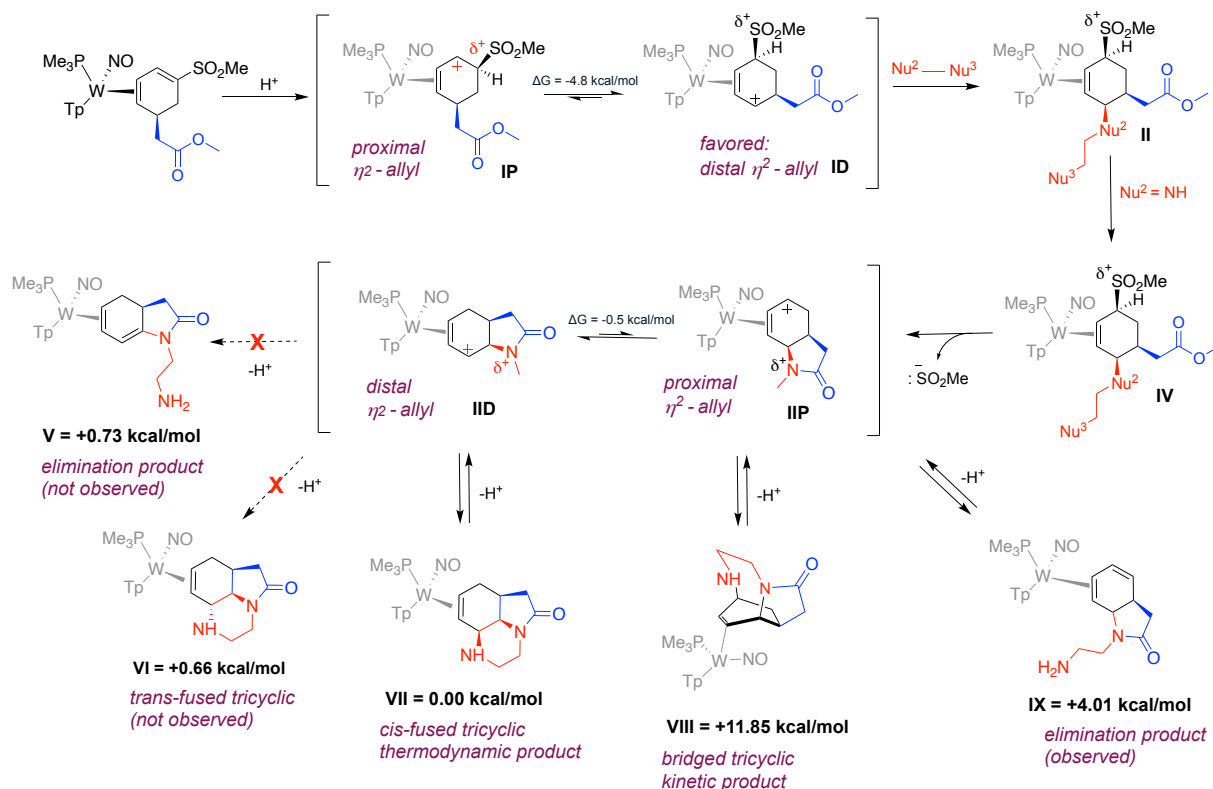


**Figure 7.9.** Mechanistic representation of the synthesis of fused and bridged tricyclic compounds and energetic comparisons.

Additional calculations were performed to gain further insight into the energy comparisons of different products, both observed and theoretical. Compounds **10** and **12** were synthesized under basic conditions whereas compounds **11** and **13** were synthesized under acidic conditions. Because both examples are observed experimentally yet they show different energetic preferences, it is likely that the driving force for ring opening is not thermodynamically driven, **Figures 7.10**.

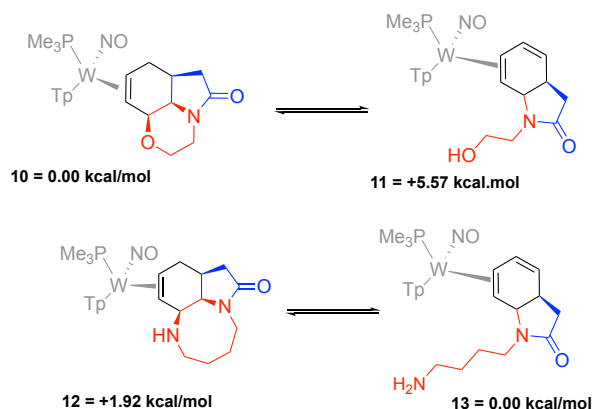


**Figure 7.10.** Energy comparisons ring closure and ring opened products for tethered nucleophiles.

In some cases, lactamization did not occur, but depending on which end of the tethered nucleophile adds first and to which allyl that addition occurs results in products with different substitution patterns. Compounds **14**, **15**, **18** and **19** are experimentally observed while compounds **16** and **17** are not. Interesting, all compounds are energetically accessible, hence the conclusion that factors other than product stability is controlling regiochemical outcomes, **Figure 7.11**.

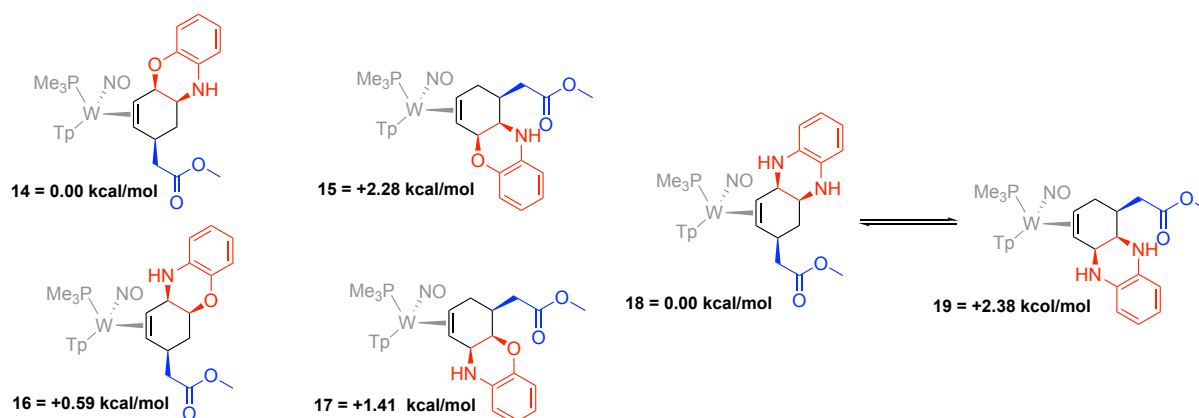


**Figure 7.11.** Energy comparisons of isomers of ring-closure products with different substitution patterns.

### 7.2.3 Double Protonation Intermediates and Nitrosyl-Assisted Protonations

“Double protonation” refers to the ability of the tungsten fragment  $\{W(Tp)(NO)(PMe_3)\}$  to stabilize  $\eta^2$ -ligands with dicationic character, synthesized via a mechanism in which two protons are added to the ligand. Several studies have explored applications of this property. First, the double protonation intermediate of benzene was successfully employed in the dearomatization and addition of aromatic nucleophiles, significantly expanding the scope of synthesized cyclohexenes via our organometallic approach.<sup>13</sup> However, isolating and characterizing this intermediate proved challenging, so DFT modeling was used to further analyze its structure, **Figure 7.12**. Structural analysis revealed that the doubly protonated benzene complex can be described as a highly distorted  $\eta^4$ -tungsten(II)-diene complex, with elongated bond lengths between tungsten and the terminal diene carbons (W-C1 and W-C4: 2.66, 2.79 Å; cf. W-C2 and W-C3: 2.30, 2.37 Å). These structural distortions resemble those observed in the  $\eta^2$ -allyl species described earlier. Additionally, a search of the Cambridge Structural Database failed to identify any similarly distorted  $\eta^4$ -diene structures, highlighting the unique structural properties of this intermediate.

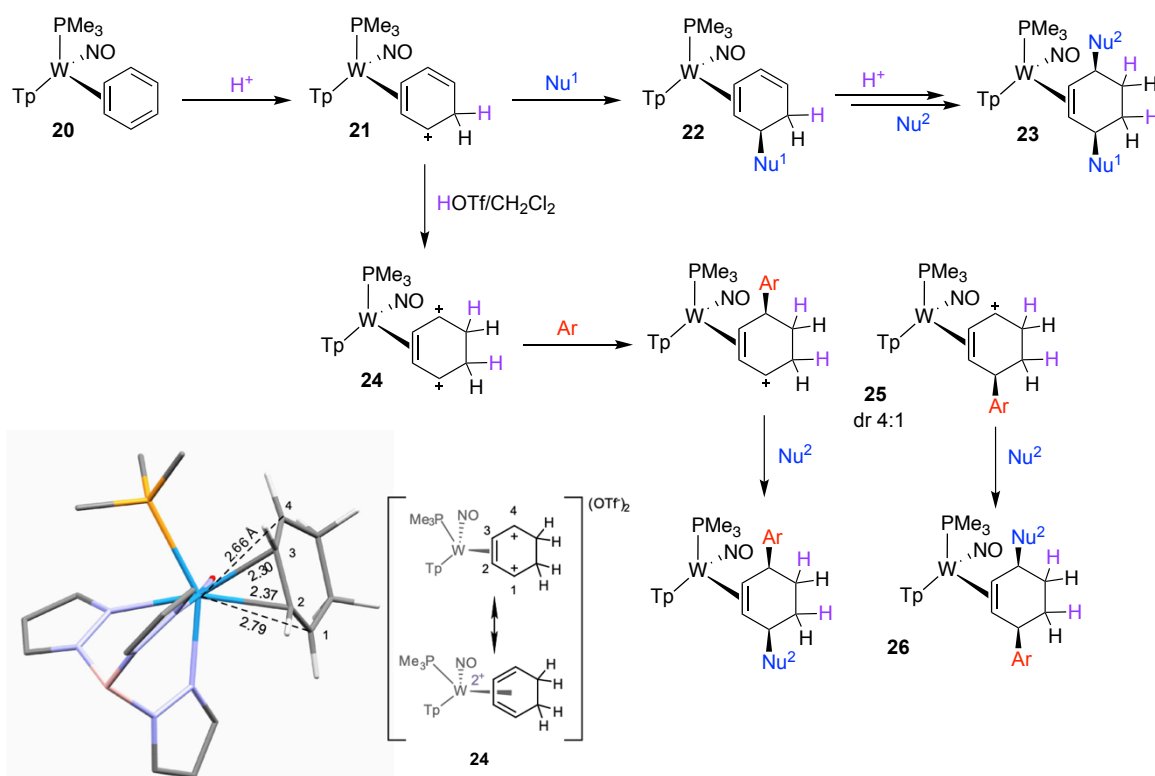


**Figure 7.12.** The reaction pathway for the double protonation of  $\eta^2$  – benzene and the DFT optimized structure of  $[W(Tp)(NO)(PMe_3)(C_6H_8)]^{2+}$

Although only preliminary experimental studies have been conducted on the analogous five-membered system, theoretical modeling of a distorted  $\eta^4$ –diene intermediate suggests the potential for synthetic success, **Figure 7.13**.

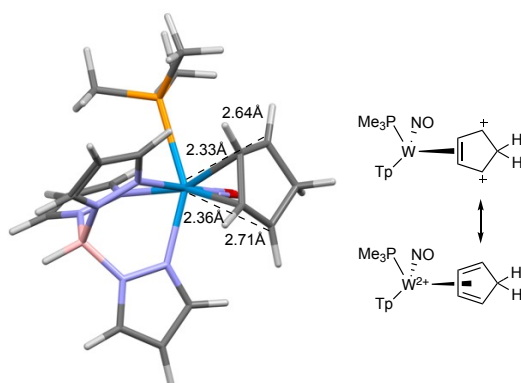


**Figure 7.13.** DFT optimized structure of  $[W(Tp)(NO)(PMe_3)(C_5H_6)]^{2+}$ , the theoretical result of the protonation of  $[W(Tp)(NO)(PMe_3)(C_5H_5)]^+$ .

Finally, a dicationic intermediate has been applied in the synthesis of a tungsten-anisole complex, expanding the scope and improving selectivity, diversifying the chemical library generated via the double protonation of benzene.<sup>14</sup> This intermediate was also modeled and is shown in **Figure 7.14**.

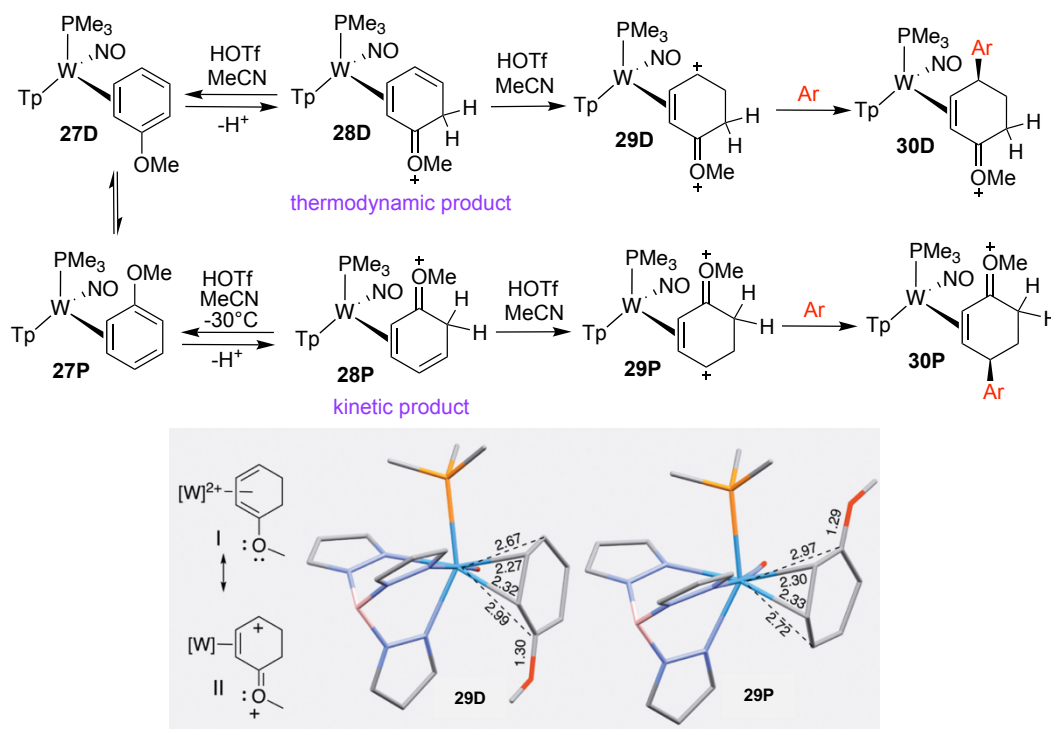


**Figure 7.14.** The reaction sequence for the double protonation of  $\eta^2$ -anisole and the DFT optimized structure of  $[\text{W}(\text{Tp})(\text{NO})(\text{PMe}_3)(\text{C}_7\text{H}_{10}\text{O})]^{2+}$ .

Beyond double protonation, another key concept in understanding benzene functionalization is the possibility of nitrosyl-assisted protonations. Deuterium studies confirmed that the first protonation of  $\eta^2$ -benzene occurs *syn* to the metal.<sup>15</sup> DFT calculations further demonstrated that a proton transfer from the NO ligand to the ring can occur, with a modest transition state energy of 8.2 kcal/mol and a free energy change of  $-8.8$  kcal/mol, **Figure 7.15**. Additional calculations suggest that an analogous NO-assisted second protonation is possible (TS = 6.1 kcal/mol,  $\Delta G = -13.9$  kcal/mol). However, deuterium studies on the double protonation of  $\eta^2$ -benzene unambiguously show a trans arrangement of the two ring protons, indicating that the second protonation occurs primarily through an intermolecular pathway, *anti* to the

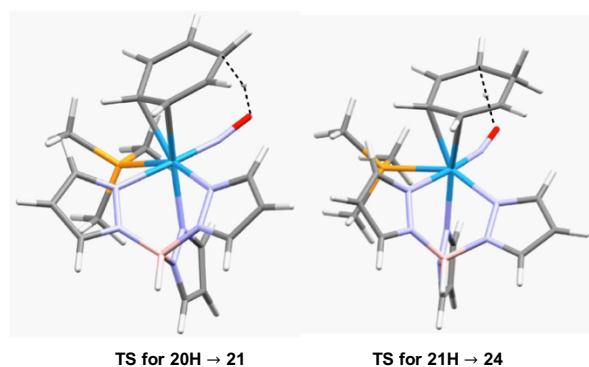


**Figure 7.15.** Comparison of first (left) and second (right) intramolecular protonations of benzene.



metal. Overall, nitrosyl-assisted protonations have been identified as an alternative mechanism to the protonation of  $\eta^2$ -ligands and should be considered when proposing reaction mechanisms.

Lastly, the protonation of  $\eta^2$ -cyclohexa-1,4-diene (**30**) leads to the formation of a tungsten-stabilized  $\eta^2$ -cyclohexenium complex (**34**). Whether protonation occurs intermolecularly or intramolecularly, there are two proposed intermediates. One species localizes the positive charge in a position that is not in conjugation with the dihapto-bond (**31**) and a nitrosyl-assisted cation (**32**). Computational studies were performed to optimize these intermediates. Although the nitrosyl-stabilized species was identified (**32**), no stable species with an “isolated” carbenium could be located. In fact, attempts to optimize this structure resulted in the nitrosyl-stabilized species. Either the mechanism is step-wise with a very low transition state energy between **31** and **32**, or the mechanism is concerted, directly incorporating a proton while forming intermediate **32**. Next, it was determined that there was a thermodynamic driving force of -13.6 kcal/mol for **32** to undergo a hydride shift to form the experimentally observed  $\eta^2$ -allyl (**34**). The transition state was located, revealing an accessible barrier of +11.1 kcal/mol. These calculations are summarized in **Figure 7.16**.

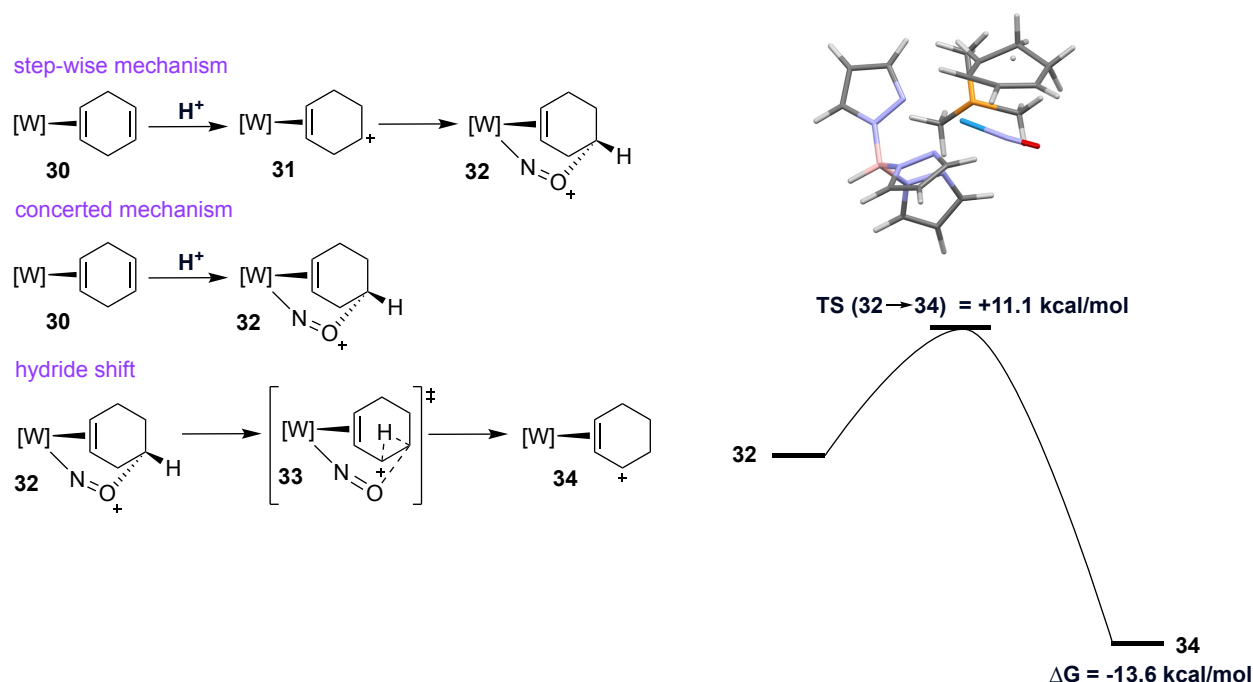


**Figure 7.16.** Proposed pathways to isolated alkene protonation, including nitrosyl-assisted stabilization and hydride shift.

#### 7.2.4 Dihydropyridine Ring-Openings

It was discovered that 6 $\pi$ -azaelectrocyclic dihydropyridine (DHP) ring-opening can be promoted via dihapto-coordination to a  $\pi$ -basic tungsten fragment. The driving force behind this reaction is hypothesized to be the generation of a 1-azatriene ligand, an excellent  $\pi$ -acceptor for the  $\pi$ -basic [W] fragment.<sup>16</sup> DFT calculations indicate that the organometallic ring-opening reaction has an overall free energy change is  $-2.8$  kcal/mol. Typically, the reverse reaction—the electrocyclic ring closure—occurs spontaneously,<sup>16</sup> unless the nitrogen bears a strong withdrawing group and a  $\pi$ -donating substituent at C2 of the DHP.<sup>17</sup> DFT calculations further indicate that the organic conversion of the dihydropyridine ligand is 0.7 kcal/mol more stable than the azatriene ligand, **Figure 7.17**.

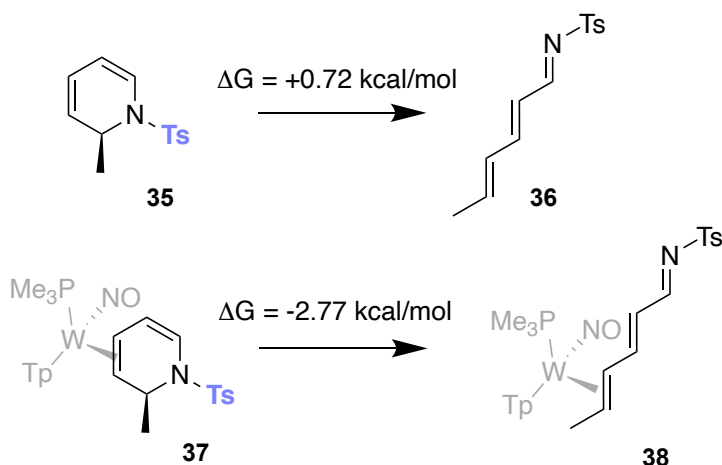


**Figure 7.17.** Organic and organometallic 6 $\pi$ -azaelectrocyclic dihydropyridine (DHP) ring-opening.

It was also noted that while the ester-substituted DHP readily undergoes ring-opening, the bulkier analogue remains stable, even after prolonged ( $\sim 3$  days) heating at elevated temperatures ( $\sim 80^\circ\text{C}$ ). A plausible explanation for this stability is steric interaction in the requisite antiperiplanar conformation between the geminal dimethyl moiety and the [W] fragment. Approximating the R group with a t-butyl group. DFT calculations find that the conformation leading to the transition state is 15.7 kcal/mol above the synclinal ground state, whereas for R = Me, the energetic cost is only 8.3 kcal/mol, **Figure 7.18**. This steric interaction was later confirmed in the crystal structure.

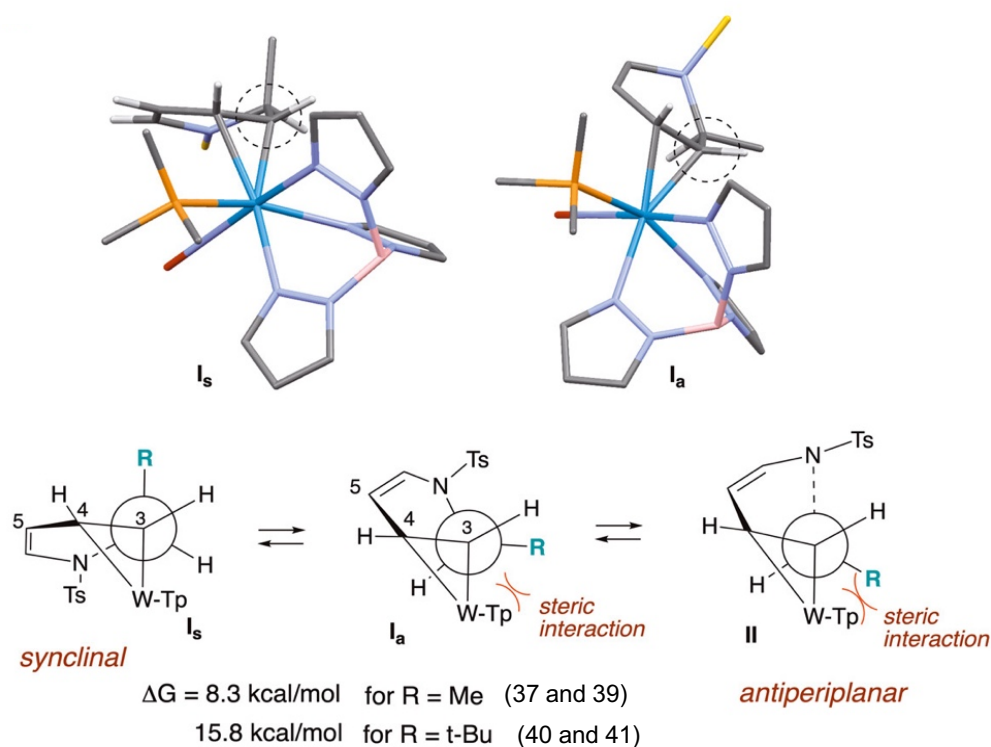


**Figure 7.18.** Synclinal and antiperiplanar conformations, and the energy change between these conformations substituted with sterically small and bulky R groups.

### 7.2.6 Diels-Alder and Retro-Diels Alder Reactions

DFT calculations were used to better understand the thermodynamics and kinetics of organic and organometallic Diels-Alder (DA) and retro-Diels-Alder (rDA) reactions of *barrelene* complexes. The reaction between decomplexed anisole (**42**) and ethyl 4,4,4-trifluoro-2-butynoate (**43**) was compared to the analogous reaction with  $\eta^2$ - anisole (**45**). The organic cycloaddition to form **44** ( $\Delta G = +3.6 \text{ kcal/mol}$ ) is thermodynamically unfavorable, consistent with the fact that this reaction does not occur experimentally. However, once bound to the  $\pi$ -basic tungsten fragment, the reaction of the  $\eta^2$ -anisole complex (**45**) with dienophile **43** to form compound **46** becomes thermodynamically favorable ( $\Delta G = -20.1 \text{ kcal/mol}$ ).

The rDA reaction for organic compound **44** has two theoretical pathways including the reversal of the Diels-Alder ( $\Delta G = -3.55 \text{ kcal/mol}$ ) and the formation of a trisubstituted benzene (**47**) and acetylene (**48**) ( $\Delta G = -5.54 \text{ kcal/mol}$ ). Although they are both favorable reactions, there is only a small preference for one reaction over the other and neither experimentally occur due to the inability to form the Diels-Alder product.

The rDA for organometallic compound **46** is also investigated. In this case, there are three possible modes of reactivity. The direct reversal for the

DA reaction, leading to the liberation of **43**, is theoretically unfavorable ( $\Delta G = +20.1$  kcal/mol). Additionally, a rDA reaction producing acetylene (**48**) and the corresponding metal complex (**49**) is also thermodynamically unfavorable ( $\Delta G = +15.5$  kcal/mol). However, a rDA pathway leading to the formation of W- $\eta^2$ -acetylene (**50**) is calculated to be thermodynamically favorable ( $\Delta G = -12.3$  kcal/mol) and is the only pathway observed experimentally.

Lastly, while the rDA of **51** to form W- $\eta^2$ -acetylene (**50**) and **52** is thermodynamically favorable ( $\Delta G = -5.05$  kcal/mol), the reaction is not observed experimentally. This finding may indicate that the kinetic barrier for the formation of **52** is higher than the kinetic barrier for the formation of **47**. All of these results are summarized in **Figure 7.19**.

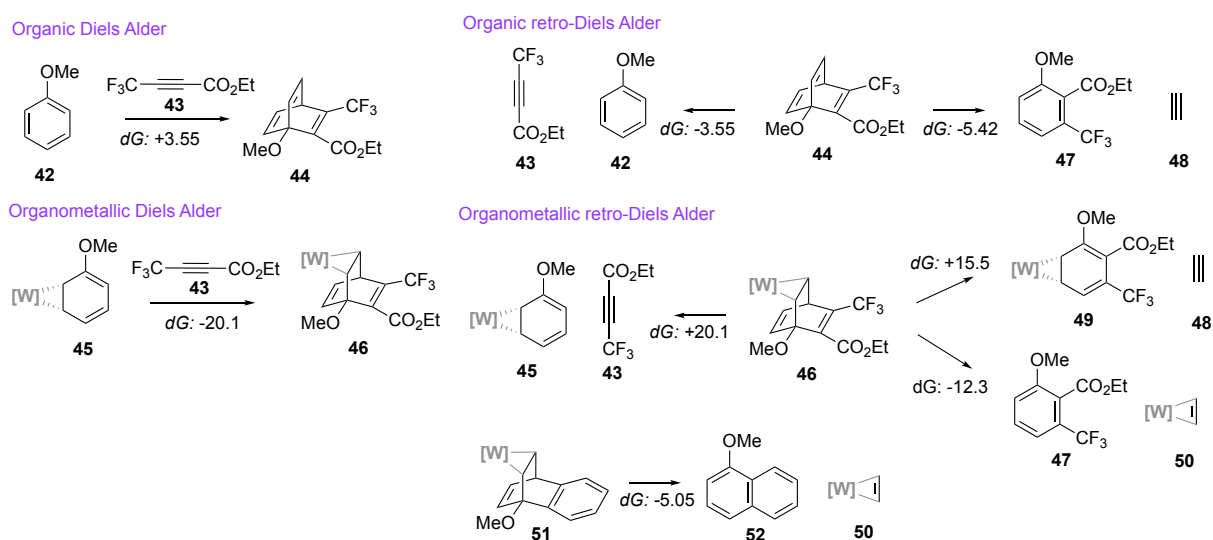


**Figure 7.19.** Reaction scheme for organic and organometallic Diels-Alder of anisole, and reaction scheme for retro-Diels-Alder reactions.

### 7.3 Conclusions

DFT calculations provided valuable insights into the structural, thermodynamic and kinetic properties of tungsten-stabilized  $\eta^2$ -ligands. The computational analysis confirmed the existence of distinct carbocation conformations in tungsten-bound cyclohexenium species, including *distal chair*, *distal boat*, *proximal chair* and *proximal boat*, highlighting the influence of steric and electronic effects on conformational stability. Solvent effects were also examined, demonstrating their role in stabilizing specific conformations. Additionally, these calculations were helpful in better understanding the hydroamination of dihapto-coordinated benzene and diene tungsten complexes.

DFT calculations showed that protonation of  $\eta^2$ -coordinated aryl sulfones produces distinct, non-interconvertible  $\eta^2$ -allyl species, influencing nucleophilic reactivity. Steric effects dictated conformational studies on dihapto-coordinated aryl sulfones clarified competing reaction pathways, confirming that substituent electronics impact conformer stability. Kinetic factors, rather than thermodynamic alone, were found to drive regioselectivity in nucleophilic additions and elimination reactions.

The study of double protonation mechanisms revealed the formation of highly distorted  $\eta^4$ -diene tungsten complexes, which exhibit unique electronic and structural characteristics. Additionally, nitrosyl-assisted protonation was identified as a viable alternative mechanism for stabilized  $\eta^2$ -ligand protonation.

The investigation into azaelectrocyclic ring-opening reactions demonstrated the dihapto-coordination to a  $\pi$ -basic tungsten center facilitates ring-opening by stabilizing the resulting 1-azatriene ligand. Steric effects were shown to play a crucial role in determining reaction feasibility, with bulkier substituents significantly increasing the energy barrier to ring-opening.

Lastly, DFT calculations were used to better understand the thermodynamic and kinetic factors governing organometallic Diels-Alder and retro-Diels-Alder reactions. The coordination of a  $\pi$ -basic tungsten fragment was found to favor DA reactivity while selectively promoting a rDA pathway leading to W- $\eta^2$ -acetylene formation. These findings enhance the understanding of tungsten-mediated reactivity and contribute to the broader field of organometallic chemistry.

## References

- (1) Lovering, F., Bikker, J., Humblet, C. Escape from flatland: increasing saturation as an approach to improving clinical success. *Med. Chem.* **2009**, *52*, 6752-6756.
- (2) Brown, D. G., Brostrom, J. Analysis of Past and Present Synthetic Methodologies on Medicinal Chemistry: Where Have All the New Reactions Gone? *Med. Chem.* **2016**, *59*, 4443-4458.
- (3) Reymond, J. L., Awale, M. . Exploring Chemical Space for Drug Discovery Using the Chemical Universe Database. *ACS Chem. Neurosci.* **2012**, *3*, 649-657.
- (4) Clemmons, P. A., Bodycombe, N. E., Carrinski, H.A., Wilson, A. Shamji, A.F., Wagner, B. K., Koehler, A.N., Schreiber, S.L. Small molecules of different origins have distinct distribution of structural complexity that correlate with protein-binding profiles. *PNAS.* **2010**, *107*, 18787-18792.
- (5) Blakemore, D. C., Castro, L., Churcher, I., Rees, D.C., Thomas, A.W., Wilson, D.M., Wood, A. Organic synthesis provides opportunities to transform drug discovery. *Nat. Chem.* **2018**, *10*, 383-394.
- (6) Meiere, S. H., Brooks, B.C., Gunnoe, T.B., Sabat, M., Harman, W.D. A Promising New Dearomatization Agent: Crystal Structure, Synthesis, and Exchange Reactions of the Versatile Complex  $\text{TpRe}(\text{CO})(1\text{-methylimidazole})(\eta^2\text{-benzene})$  (Tp = Hydridotris(pyrazolyl)borate). *Organometallics.* **2001**, *20*, 1038-1040.
- (7) Keane, J. M., Harman, W.D. A New Generation of  $\pi$ -Basic Dearomatization Agents. *Organometallics.* **2005**, *24*, 1786-1798.
- (8) Liebov, B. K., Harman, W.D. Group 6 Dihapto-Coordinate Dearomatization Agents for Organic Synthesis. *Chem. Rev.* **2017**, *117*, 13721-13755.
- (9) Harrison, D. P., Nichols-Nieler, A.C., Zottig, V.E., Strausberg, L., Salomon, R.J., Trindle, C.O., Sabat, M., Gunnoe, T.B., Iovan, D.A., Myers, W.H., Harman, W.D. Hyperdistorted Tungsten Allyl Complexes and Their Stereoselective Deprotonation to Form Dihapto-Coordinated Dienes. *Organometallics.* **2011**, *30*, 2587-2597.
- (10) Wilson, K. B., Smith, J.A., Nedzbala, H.S., Simpson, S.R., Ericson, M.N., Westendorf, K.S., Chordia, Mahendra D., Dickie, D.A., Harman, W.D. Hydroamination of Dihapto-coordinated Benzenes and Diene Complexes of Tungsten: Fundamental Studies on the Synthesis of  $\gamma$ -Lycorane. *Helvetica Chimica Acta.* **2021**, *104*, 10.
- (11) Simpson, S.R., Siano, P., Siela, D.J., Diment, L.A., Song, B.C., Westendorff, K.S., Ericson, M.N., Welch, K.D., Dickie, D.A., Harman, W.D. Phenyl Sulfones: A Route to

a Diverse Family of Trisubstituted Cyclohexenes from Three Independent Nucleophilic Additions. *JACS*. **2022**. 144(21), 9489 – 9499.

(12) Siano P., Diment, L.A., Siela D.J., Ericson M.N., McGraw M., Dickie D.A., Harman, W.D. An organometallic approach to the synthesis of heteropolycyclic compounds from benzenes. Manuscript is Submission.

(13) J.T. Weatherford-Pratt, J.A. Smith, J.M. Bloch, M.N. Ericson, J.T. Myers, K.S. Westendorff, D.A. Dickie, and W.D Harman. The Double-Protonation of Dihapto-Coordinated Benzene Complexes: An Enabling Strategy for Dearomatization Using Aromatic Nucleophiles. *Nature Communications*. **2023**. 14, 3145.

(14) J.A. Smith, J. T. Weatherford-Pratt, J.M. Bloch, M.N. Ericson, D.J. Siela, K.B. Wilson, M.H. Shingler, M.R. Ortiz, S. Fong, J. Laredo, I. Patel, M. McGraw, D.A. Dickie, W.D. Harman. Tungsten-anisole complex provides 3,6-cyclohexenes for highly diversified chemical libraries. *Sci. Adv*. **2024**. 10(7).

(15) Smith, Jacob A., Wilson, Katy B., Sonstrom, Reilly, E., Kelleher, Patrick J., Welch, Kevin D., Pert, Emmit K., Westendorff, Karl S., Dickie, Diane A., Wang, Xiapong., Pate, Brooks H., Harman, W. Dean. Preparation of Cyclohexene Isotopologues and Stereoisotopomers from Benzene. **2020**. *Nature*. 581(7808), 288 – 293.

(16) Vargas, D. F.; Larghi, E. L.; Kaufman, T. S. The  $6\pi$ -azaelectrocyclization of azatrienes. Synthetic applications in natural products, bioactive heterocycles, and related fields. *Nat. Prod. Rep*. **2019**, 36 (2), 354–401.

(17) Toscano, R. A.; Hernandez-Galindo, M. D. C.; Rosas, R.; Garcia-Mellado, O.; Rio Portilla, F. D.; Amabile-Cuevas, C.; Alvarez-Toledano, C. Nucleophilic Reactions on 1-Trifluoromethanesulfonylpyridinium Trifluoromethanesulfonate (Triflylpyridinium Triflate, TPT). Ring-Opening and “Unexpected” 1,4-Dihydropyridine Reaction Products. *Chem. Pharm. Bull*. **1997**, 45 (6), 957–961.

## **Chapter 8. Conclusions**



## 8.1 General Conclusions

Small-molecule compounds are a foundation to medicinal chemistry, comprising 90% of pharmaceutical drugs. These synthetic organic molecules are designed for precise interactions with biological targets, making them essential for drug development.<sup>1</sup> Molecular libraries enable large-scale screening of small molecules, yet they cover only a fraction of the vast chemical space.<sup>2</sup> Current libraries are dominated by  $sp^2$ -rich, structurally similar molecules due to conventional synthetic methods, limiting access to more complex, three-dimensional structures. Since high-quality drug candidates often feature increased polarity, stereogenic centers, and molecular diversity, advancing synthetic methodologies for the incorporation of chiral  $sp^3$  centers is critical for expanding chemical space and driving pharmaceutical innovation.<sup>3</sup>

Aromatic compounds are highly stable due to their conjugated  $\pi$ -systems, yet their structural simplicity, cost-effectiveness, and availability make them valuable feedstock for synthesizing complex molecules. Dearomatization, which disrupts aromaticity to introduce molecular complexity, includes reductions, oxidations, additions, and cycloadditions, but challenges remain in functional group tolerance and stereochemical control.<sup>4, 5</sup>

Research alongside W. Dean Harman has pioneered the dearomatization of aromatic compounds using dihapto-coordination to electron-rich metal centers, enhancing their reactivity toward electrophiles for the synthesis of complex small molecule compounds. This methodology has enabled a range of organic transformations, including electrophilic and nucleophilic additions, ring-closure reactions, and Diels-Alder cycloadditions, applied to various arenes such as benzenes and pyridines.<sup>6-22</sup> To improve selectivity, the lab has developed a procedure using chiral salts to isolate single diastereomers of tungsten complexes, allowing for the synthesis of enantiopure organic compounds essential for pharmaceutical development.<sup>23</sup>

The dearomative approach through the dihapto-coordination of arenes and heteroarenes to a tungsten fragment was successful in the selective synthesis of highly functionalized cyclohexanes and piperidines. The study provided herein expands this organometallic methodology to the synthesis of functionalized methylphenidate derivatives. Additionally, we explored whether this methodology can

be extended to other sized conjugated carbocycles for the synthesis of highly functionalized cyclopentanes, cycloheptanes and cyclooctanes.

### 8.1.2 Methylphenidate Derivatives

A study presenting the methodology for the synthesis of piperidine-functionalized N-mesyl erythro methylphenidate analogues with high regioselectivity, stereoselectively, and functional group tolerance is summarized in Chapter 2. The approach utilizes an aza-Reformatsky reaction between a [W]- $\eta^2$ -bound N-mesyl pyridinium complex and methyl  $\alpha$ -phenyl bromoacetate, yielding an erythro methylphenidate DHP complex, which is enriched to a d.r. of >20:1 through triturations. Subsequent allyl complex formation enables the incorporation of various nucleophiles—including cyanide, malononitrile, dimethylmalonate, Grignard reagents, amines, amides, imides, and thiols—resulting in tetrahydropyridine complexes with high diastereoselectivity. This strategy provides access to a diverse range of MPH analogues functionalized at the C5-position on the piperidine ring, a challenge for conventional methods. Given the prevalence of the piperidine scaffold in small-molecule drugs, this system offers a valuable approach for rapidly incorporating diverse functional groups and nucleophiles into piperidine cores.

### 8.1.3 Conjugated Carbocycles

To develop new methods for the functionalization of cyclic hydrocarbons, dihapto-coordinated conjugated carbocycles were synthesized and their structural and electronic properties were studied in Chapter 3. Their properties were investigated using single crystal X-ray diffraction (SC-XRD), density functional theory (DFT), cyclic voltammetry (CV), and nuclear magnetic resonance ( $^1\text{H}$ -NMR,  $^{13}\text{C}$ -NMR, and  $^{31}\text{P}$ -NMR). Similar to the  $\eta^2$ -benzene complex, the  $\eta^2$ -cyclooctatetraene complex exhibits fluxional behavior at elevated temperatures. Additionally,  $\eta^2$ -cyclopentadienyl cation and  $\eta^2$ -cycloheptatrienyl cation complexes are also fluxional, but their coalescence occurs well below room temperature. The tungsten fragment  $\{\text{W}(\text{Tp})(\text{NO})(\text{PMe}_3)\}$  has proven effective in the dearomatization and functionalization of various aromatic compounds. Notably,  $\text{WTP}(\text{NO})(\text{PMe}_3)(\eta^2\text{-benzene})$  and its derivatives have been successfully transformed into complex organic molecules, and we aim to explore similar transformations with five- ( $\eta^2$ -Cp), seven- ( $\eta^2$ -tropylium), and eight-membered ( $\eta^2$ -COT) systems. The development of novel synthetic methodologies for constructing

highly functionalized cyclopentanes, cycloheptanes, and cyclooctanes from dihapto-coordinated aromatic, non-aromatic and antiaromatic hydrocarbons.

#### 8.1.4 *Five-Membered Rings*

Chapter 4 demonstrates a study on the functionalization of cyclopentanes via dihapto-coordinate ligands and highlights the challenges in regioselectivity and strategies to overcome them. Initial nucleophilic additions to  $\eta^2$ -cyclopentenyl and  $\eta^2$ -cyclopentadienyl cations lacked regioselectivity, downstream leading to mixed isomeric products. Selective deprotonation was explored in the isolation of single  $\eta^2$ -cyclopentadiene diastereomer, instead unintended products were observed and isolated. Interestingly, this synthetic pathway led to the discovery of novel tungsten-binuclear complexes that did exhibit regio- and stereoselective nucleophilic additions. Ultimately, the chiral C(sp<sup>3</sup>)-C(sp<sup>3</sup>) coupling of cyclopentene-cyclopentene and cyclopentene-cyclohexene systems were accomplished. Successful oxidations of the binuclear species demonstrated the potential for generating fully organic, difunctionalized cyclopentenenes. Despite regioselectivity challenges initially encountered, these findings offer new synthetic opportunities for stereocontrolled complex chiral five-membered containing molecules.

#### 8.1.5 *Eight-Membered Rings*

A synthetic approach to 3,4,8-trisubstituted cyclooctenes is presented in Chapter 5, overcoming the challenges associated with methodology of eight-membered carbocycles. These structures, prevalent in bioactive natural products are often underrepresented in molecular libraries due to their tendency to form unexpected products, like bicyclic aromatic systems. Existing synthetic approaches typically emerge from total synthesis efforts and rely on cycloadditions and cyclizations, leaving a gap in efficient methodologies in constructing highly functionalized and diverse cyclooctanes. The methodology developed here provides a novel approach to trisubstituted cyclooctenes and the ability to isolate single stereoisomers, offering a valuable expansion to the limited synthetic strategies currently available. This work lays the groundwork for further studies, potentially enhancing access to functionalized cyclooctanes for applications in small molecule drug discovery.

#### 8.1.6 *Seven-Membered Rings*

Chapter 6 involves preliminary investigations on the functionalization of cycloheptane rings through tungsten-mediated dihapto-coordination reveals the

reactivity and synthetic potential of  $\eta^2$ -cycloheptatriene and  $\eta^2$ -tropylium complexes. Despite challenges in regioselectivity of nucleophilic additions to  $\eta^2$ -cycloheptadienyl and  $\eta^2$ -cycloheptatrienyl cations, strategies such as catalytic oxidation, protonation-deprotonation and Diels-Alder reactions were successful in the isolation of single isomers. The possibility of releasing products from the metal complex suggests potential in drug discovery applications. Future work can focus on isolating single diastereomers of mono-substituted cycloheptatriene complexes, expanding the dienophile scope of Diels-Alder reactions, and developing new functionalization strategies.

#### 8.1.7 *Density Functional Theory*

DFT calculations, compiled in Chapter 7, provided key insights into the structural, thermodynamic, and kinetic properties of tungsten  $\eta^2$ -ligands, revealing the influence of steric and electronic effects on the stability of organometallic complexes. Analysis confirmed distinct conformations in tungsten-stabilized cyclohexenium species and demonstrated solvent effects on stabilization. Protonation of  $\eta^2$ -coordinated aryl sulfones results in distinct, non-interconvertible  $\eta^2$ -allyl species, highlighting steric and electronic factors governing reactivity as an electrophile and regioselectivity of nucleophilic additions. Theoretical products for ring-closing reactions were energetically analyzed and compared to experimental results. Additionally, investigations into double protonation mechanisms uncovered highly distorted  $\eta^4$ -diene intermediates. Nitrosyl assistance in protonation and cation stabilization emerged as viable intermediates and alternative mechanistic pathways. Azaelectronic ring-opening reactions were shown to be facilitated by dihapto-coordination, though steric effects influenced feasibility. Furthermore, studies on organometallic Diels-Alder and retro-Diels-Alder reactions revealed that  $\pi$ -basic tungsten coordination enhances DA reactivity while selectively promoting rDA pathways to [W]-  $\eta^2$ -acetylene formation. These computational findings significantly advanced the understanding of tungsten-mediated reactivity.

### 8.3 Future Developments

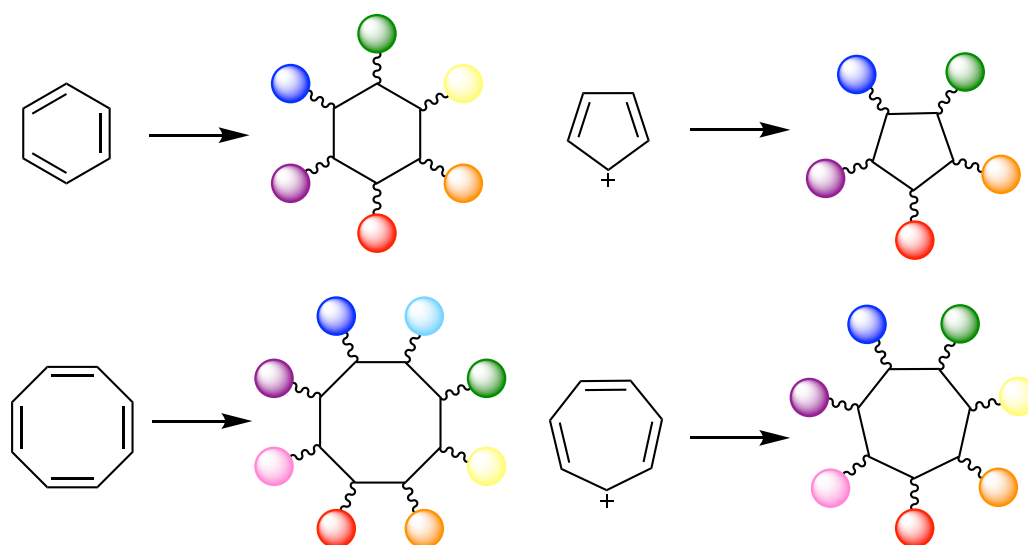


**Figure 8.1** Transformation of conjugated carbocycles into functionalized rings.

Much of the recent chemistry from the Harman lab has focused on transforming aromatic compounds into sophisticated small molecules, with a particular emphasis on the dearomatization and functionalization of benzenes and pyridines. This thesis demonstrates that the organometallic approach to functionalization utilizing dihapto-coordination can be extended to conjugated ring systems of varying sizes, includes anti-aromatic cyclopentadienyl cation, aromatic tropylium and non-aromatic cyclooctatetraene.

Significant progress has been made on the synthesis of functionalized five-, seven-, and eight-membered rings, though further developments in their functionalization could yield even more desirable products. Several avenues remain for advancing the synthesis of functionalized cyclopentenes. Because coordination diastereomer ratios were enriched for the deprotonated coupled products (compounds **4.12** and **4.17**), one such approach involves the incorporation of electrophiles, other than protons. Once electrophiles are introduced, the resulting products are allylic species, which can subsequently undergo nucleophilic additions. This pathway is particularly compelling when applied to compound **4.12**, as it opens the possibility of generating trisubstituted cyclopentenes, an increase in functionality to the disubstituted cyclopentenes demonstrated in this study. Similarly, applying this method to compound **4.17** offers a route to trisubstituted cyclohexenes. While trisubstituted cyclohexenes have already been synthesized via tungsten-based methodology

discussed in the thesis, this approach broadens the scope to include different functional group incorporations and access to other diastereomers.

Additionally, due to limited methodologies available for synthesizing seven- and eight- membered ring systems, further development of the approaches demonstrated in this thesis could make invaluable contributions to novel molecule development and drug discovery. In particular, advancing methodology for the regio- and stereoselective incorporation of nucleophiles into substituted cycloheptenes presents a promising avenue for exploration. Following protonation of [W]-cycloheptatriene and formation of the [W]-cycloheptadienyl cation (compound **6.2**), preliminary studies investigated the incorporation of a nucleophile; however, regioselectivity was found to be low. This issue should be further examined by varying nucleophile size, solvent conditions and temperatures to determine whether selectivity can be improved. It may also be worth exploring whether the catalytic addition of an oxidant affects product distribution. Furthermore, protonation of these products could be used to assess whether the formation of an allylic species initiates tungsten-mediated isomerization, funneling products into a single diastereomer, as observed in the eight-membered system.

Similarly, nucleophilic incorporation into the [W]-tropylium intermediate also showed low regioselectivity, though this may likewise be improved by adjusting nucleophilic size and reaction conditions. Diastereomeric outcomes may also be influenced by the catalytic use of an oxidant such as exposure to atmospheric oxygen or protonation, thereby offering an increase in tungsten-alkene isomerization pathways, compared to neutral systems. Importantly, both the [W]-CHT and [W]-tropylium systems allow for the incorporation of a second nucleophile, with the latter also permitting the addition of a third nucleophile. Hence, if regioselectivity can be effectively controlled through experimental conditions, these strategies could enable the synthesis of disubstituted and trisubstituted cycloheptenes.

An additional pathway worth exploring in the synthesis of substituted cycloheptenes involves the unique reactivity of [W]-CHT complex. It has been shown that a single coordination diastereomer of [W]-CHT (compound **6.1C**) can be isolated with a coordination diastereomeric ratio greater 20:1 via a protonation/deprotonation mechanism. Notably, this complex contains two alkenes in conjugation with the dihapto-coordinate bond, effectively “set-up” for further functionalization. This opens the possibility for sequential electrophilic and nucleophilic additions, potentially enabling the synthesis of tetrasubstituted and/or multicyclic cycloheptenes.

Additionally, exposing this species to an excess of strong acid could generate a dicationic intermediate capable of undergoing electrophilic aromatic substitution. If the arenes contains a tethered nucleophile, this transformation could provide an alternative route to constructing multicyclic core structures.

Lastly, the Diels-Alder chemistry of [W]-CHT should be expanded, as it represents a promising strategy for assessing unique cycloheptene scaffolds. Expanding the scope of compatible dienophiles, as well as investigating the protonation of the  $\eta^2$ -Diels-Alder adducts, could yield valuable insights. While the remaining alkene in these products is not conjugated with the dihapto-coordinate bond, there is precedent for “isolated” alkenes to still participate in the formation of hyperdistorted  $\eta^2$ -allylic species. This, in turn, would offer an additional site for functionalization within these already structurally distinctive compounds.

There are also numerous avenues to explore in the functionalization of cyclooctenes. First, nucleophilic scopes should be expanded in the synthesis of 3,4,8-trisubstituted cyclooctenes. Second, incorporating nucleophiles that contain a second, tethered nucleophile, could enable intramolecular cyclization pathways, facilitating the formation of multicyclic compounds. Several strategies for such transformations have been demonstrated on six-membered systems, including lactam formation, incorporation of labile ligands such as methoxy groups, and the use of dicationic intermediates, but have yet to be applied to the eight-membered system.

Another important focus is the formation of regio- and stereoisomers of trisubstituted cyclooctenes. As discussed in Chapter 5, one promising pathway involves the use of the *kinetic* [W]-cyclooctadienyl cations (e.g., compounds **5.16K** – **5.20K**) to incorporate a second nucleophile at a position that yields 5,8-cyclooctadienes. Subsequent protonation and introduction of a third nucleophile could result in either 3,6,8- or 3,4,7-trisubstituted cyclooctene. Additionally, some 5,6-cyclooctadienes were observed to undergo isomerization, leading to a different coordination diastereomer where the first two nucleophiles occupy positions syn to the metal bulk. Preliminary evidence suggests that this species can be protonated to form a unique [W]-cyclooctenyl cation, which may facilitate incorporation of a nucleophile to generate a cis-trans-3,5,6-trisubstituted cyclooctene. Achieving trans functionality through this approach is particularly noteworthy, as it is traditionally difficult but highly desirable. Finally, there are a few examples where dihapto-coordinated 5-monosubstituted cyclooctatrienes also undergo a tungsten-alkene isomerization,

positioning the first nucleophile syn to the metal. Pursuing the addition of second and third nucleophiles in this system could also lead to trisubstituted cyclooctenes with trans functionality, offering another compelling direction for future studies.

Lastly, it would be valuable to explore Diels-Alder reactions in eight-membered systems. Preliminary studies involving [W]-COT demonstrated that although Diels-Alder reactivity occurred, the resulting products mirrored those of organic pathway, forming pericyclic intermediates that ultimately yielded fused six- and four-membered ring systems and hence, losing the eight-membered core. Interestingly, the tungsten complex still promoted Diels-Alder reactivity under significantly milder conditions, requiring less heat and shorter reaction times. To preserve the eight-membered ring, several alternative pathways could be pursued. First, the Diels-Alder reactivity of [W]-5-monosubstituted cyclooctatrienes should be investigated. In these systems, the classical pericyclic intermediate is no longer accessible, creating an opportunity to retain the eight-membered core. This approach also enables initial functionalization of the ring prior to Diels-Alder cycloaddition. Another promising strategy involves exploring the reactivity of 5,6-cyclooctadienes, once they are liberated from the metal. These compounds contain a conjugated diene that could undergo a conventional Diels-Alder reaction, but again, would be incapable of forming pericyclic products that collapse the ring. This is synthetically appealing, especially if the dienes are pre-functionalized with two nucleophiles. If the substituents are sufficiently bulky, they may influence facial selectivity during the cycloadditions, enabling regioselective reactions and potentially preserving stereoselectivity, particularly when enantioenriched reagents are used with symmetrical dienophiles.

Finally, once synthetically unique compounds are achieved through this tungsten-mediated methodology, the organic products should be liberated and isolated. These novel structures could then be submitted for biological activity screening. Investigating their potential pharmaceutical applications would be a fascinating extension of this work and could provide meaningful contributions to drug discovery.



## References

- (1) Southey, M., W.Y., Bruvas, Michael. . Introduction of small molecule drug discovery and preclinical development *Front. Drug, Discov.* **2023**, 3.
- (2) Welsch, M. E., Snyder, Scott A., Stockwell, B.R. Privledged Scaffolds for Library Design and Drug Discovery. . *Curr Opin Chem Biol* **2010.**, 14 (3), 347-361.
- (3) Clemons, P. A., Bodycombe, Nicole E., Carrinski, Hyman, A., Wilson, Anthony., Shamji, Alykhan, F., Wagner, Bridget K., Koehler, Angela N., Schreiber, Stuart L. . Small molecules of difference origins have distinct distributions of structrual complexity that correlate with protein-binding profiles. . *PNAS* **2010**, 107 (44), 18787-18792.
- (4) Wertjes, W. C., Southgate, E.H., Sarlah, D. Recent advances in chemical dearomatization of non-activated arenes. . *Chem. Soc. Rev.* **2018.**, 47, 7996.
- (5) Huck, C. J., Sarlah, D. Shaping Molecular Landscapes: Recent Advances, Opportunities, and Challenges in Dearomatization. *Chem.* **2020**, 6, 1589-1603.
- (6) B.K. Liebov, W. D. H. Group 6 Dihapto-Coordinate Dearomatization Agents for Organic Synthesis. *Chem. Rev.* **2017**, 117, 13721-13755.
- (7) D.P. Harrison, D. A. I., W. H. Myers, M. Sabat, S. Wang, V.E. Zottig, W.D. Harman. [4 + 2] Cyclocondensation reactions of tungsten-dihydropyridine complexes and the generation of tri- and tetrasubstituted piperidines. *J. Am. Chem. Soc.* **2011**, 133, 18378-18387.
- (8) D.P. Harrison, M. S., W.H. Myers, W.D. Harman. [145] Polarization of the pyridine ring: highly functionalized piperidines from tungsten-pyridine complex. *J. Am. Chem. Soc.* **2010**, 132, 17282-17295.
- (9) Harrison, D. P., Zottig, V.E., Kosturko, G.W., Welch, K.D., Sabat, M., Myers, W.H., Harman, W.D. Stereo- and Regioselective Nucleophilic Addition to Dihapto-Coordinated Pyridine Complexes *Organomet. Chem.* **2009**, 28, 5682-5690.
- (10) J.A. Pienkos, A. T. K., B.L. McLeod, J.T. Myers, P.J. Shivokevich, V. Teran, M. Sabat, W.H. Myers, W.D. Harman. Double protonation of amino-substituted pyridine and pyrimidine tungsten complexes: friedel-crafts-like coupling to aromatic heterocycles. *Organometallics.* **2014**, 33, 5464-5469.
- (11) J.A. Pienkos, V. E. Z., D.A. Iovan, M.Li, D.P. Harrison, M. Sabat, R.J. Salomon, L. Strausberg, V.A. Teran, W.H. Myers, W.D. Harman. Friedel-crafts ring-coupling

- reactions promoted by tungsten dearomatization agent. *Organometallics*. **2013**, 32, 691-703.
- (12) J.A. Smith, K. B. W., R.E. Sonstrom, P. J. Kelleher, K.D. Welch, E.K. Pert, K.S. Westendorff, D.A. Dickie, X. Wang, B. H. Pate, W. D. Harman. Preparation of Cyclohexene Isotopologues and Stereoisomers from Benzene. *Nature* **2020**, 581, 288-293.
- (13) J.H. Wilde, J. T. M., D.A. Dickie, W.D. Harman. Molybdenum-Promoted Dearomatization of Pyridines. *Organometallics*. **2020**, 39 (8), 1288-1298.
- (14) J.T. Myers, J. H. W., M. Sabat, D.A. Dickie, W.D. Harman. Michael-Michael Ring-Closure Reactions for a Dihapto-Coordinated Naphthalene Complex of Molybdenum. **2020**, 29 (8), 1404-1412.
- (15) J.T. Weatherford-Pratt, J. A. S., J.M. Bloch, M.N. Ericson, J.T. Myers, K.S. Westendorff, D.A. Dickie, W.D. Harman. The Double-Protonation of Dihapto-Coordinated Benzene Complexes: An Enabling Strategy for Dearomatization Using Aromatic Nucleophiles. . *Nature Comm* **2023**, 14, 3145.
- (16) J.T. Weatherford-Pratt, J. M. B., J.A. Smith, M. N. Ericson, D.J. Siela, K. B. Wilson, M.H. Shingler, M.R. Ortiz, S. Fong, J.A. Laredo, I.U. Patel, M. McGraw, D. A. Dickie, W. D. Harman. Tungsten-anisole complex provides 3,6-substituted cyclohexenes for highly diversified chemical libraries. *Sci. Adv.* **2024**, 10 (7).
- (17) K.B. Wilson, H. S. N., S.R. Simpson, M. N. Ericson, K. S. Westendorff, M.D. Chordia, D.A. Dickie, W.D. Harman. Hydroamination of Dihapto-Coordinated Benzene and Diene Complexes of Tungsten: Fundamental Studies and the Synthesis of  $\gamma$ -Lycorane. . *Chimica Acta* **2021**, 104 (10).
- (18) K.B. Wilson, J. A. S., H.S. Nedzbala, E. K. Pert, S.J. Dakermanji, D.A. Dickie, W.D. Harman Highly Functionalized Cyclohexenes Derived from Benzene: Sequential Tandem Addition Reactions Promoted by Tungsten *J. Org. Chem.* **2019**, 84 (10), 6094-6116.
- (19) K.B. Wilson, J. T. M., H.S. Nedzbala, L.A. Combee, M. Sabat, W.D. Harman. Sequential Tandem Additions to a Tungsten-Trifluorotoluene Complex: A Versatile Method for the Preparation of Highly Functionalized Trifluoromethylated Cyclohexenes. *J. Am. Chem. Soc.* **2017**, 139 (33), 11401-11412.
- (20) S.R. Simpson, P. S., D.J. Siela, L.A. Diment, B.C. Song, K. S. Westendorff, M. N. Ericson, K. D. Welch, D. A. Dickie, W.D. Harman. Phenyl Sulfones: A Route to a

Diverse Family of Trisubstituted Cyclohexenes from Three Independent Nucleophilic Additions. . *J. Am. Chem. Soc.* **2022**, *144* (21), 9489-9499.

(21) V.E. Zottig, M. A. T., A.C. Nielander, D.P. Harrison, M. Sabat, W.H. Myers, W.D. Harman. [144] Epoxidation, Cyclopropanation, and Electrophilic Addition Reactions at the meta Position of Phenol and meta-Cresol. *Organometallics*. **2010**, *29* (21), 4793-4803.

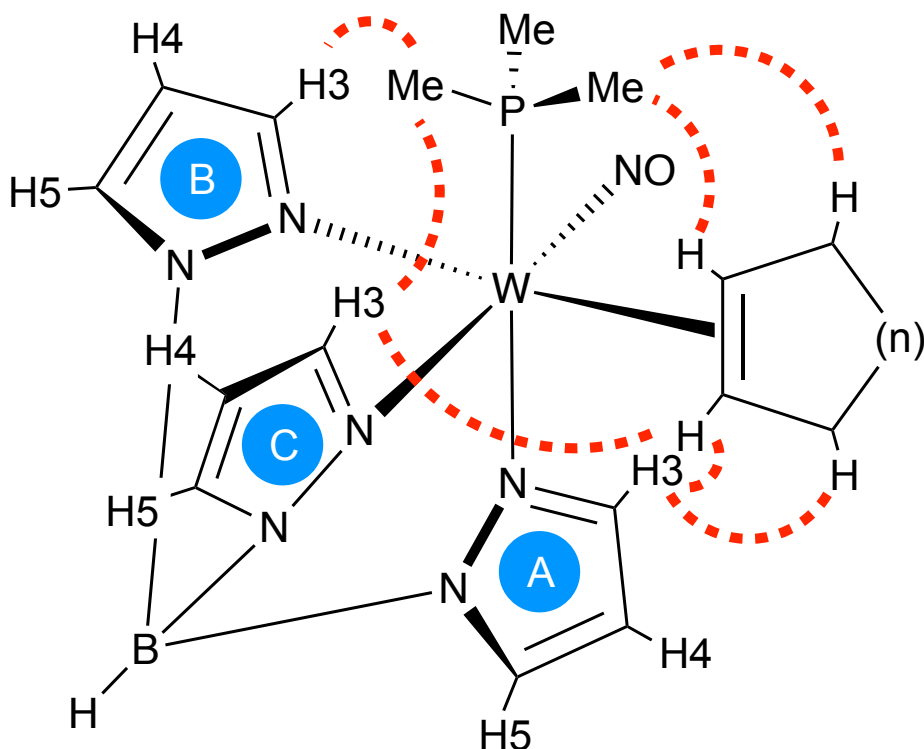
(22) Wilde, J. H., Dickie, D.A., Harman, W.D. A Highly Divergent Synthesis of 3-Aminotetrahydropyridines. *J. Org. Chem.* **2020**, *85* (12), 8245 - 8252.

(23) A.W. Lankenau, D. A. I., J.A. Pienkos, R.J. Salomon, S. Wang, D.P. Harrison, W.H. Myers, W.D. Harman. Enantioenrichment of a Tungsten Dearomatization Agent Utilizing Chiral Acids. *J. Am. Chem. Soc.* **2015**, *137* (10), 3649-3655.

## **Appendix A: General Methods**

## Experimental Methods:

Unless specified otherwise, all syntheses were conducted inside of a glovebox under an inert N<sub>2</sub> atmosphere. Unless otherwise specified, all cationic complexes are triflate salts. NMR spectra were obtained on a 400, 600 or 800 MHz spectrometer. Chemical shifts are referenced to tetramethylsilane (TMS) utilizing residual <sup>1</sup>H or <sup>13</sup>C signals of the deuterated solvents as internal standards. Chemical shifts are reported in ppm and coupling constants (*J*) are reported in hertz (Hz). Infrared Spectra (IR) were recorded on a spectrometer as a glaze on a diamond anvil ATR assembly, with peaks reported in cm<sup>-1</sup>. Electrochemical experiments were performed under a nitrogen atmosphere. Most cyclic voltammetry (CV) data were recorded at ambient temperature at 100 mV/s, unless otherwise noted, with a standard three-electrode cell from +1.25 V to -1.25 V with a platinum working electrode, *N,N*-dimethylacetamide (DMA) or acetonitrile solvent, and tetrabutylammonium hexafluorophosphate (TBAH) electrolyte (~1.0 M). All potentials are reported versus the normal hydrogen electrode (NHE) using cobaltocenium hexafluorophosphate (*E*<sub>1/2</sub> = -0.78 V, -1.75 V) or ferrocene (*E*<sub>1/2</sub> = 0.55 V) as an internal standard. The peak separation of all reversible couples was less than 100 mV. All synthetic reactions were performed in a glovebox under a dry nitrogen atmosphere unless otherwise noted. All solvents were purged with nitrogen prior to use. Deuterated solvents were used as received from Cambridge Isotopes. NMR assignments of all compounds were determined using 2D NMR methods, including NOESY, COSY, HMBC, H2BC and HSQC. When possible, pyrazole (Pz) protons of the (trispyrazolyl) borate (Tp) ligand were uniquely assigned (e.g., "PzB3") using two-dimensional NMR data (see Figure S1). If unambiguous assignments were not possible, Tp protons were labeled as "Pz3/5 or Pz4". All *J* values for Pz protons are 2 (±0.4) Hz. BH peaks (around 4-5 ppm) in the <sup>1</sup>H NMR spectra are not assigned due to their quadrupole broadening. High-resolution electrospray ionization mass 132 spectrometry (ESI-MS analyses were taken on an Agilent 6545B Q-TOF LC/MS using purine and hexakis(1H, 1H, 3H-tetrafluoropropoxy)phosphazine as internal standards. Samples were dissolved in MeCN and eluted with a MeCN/H<sub>2</sub>O solution containing 0.1% formic acid.



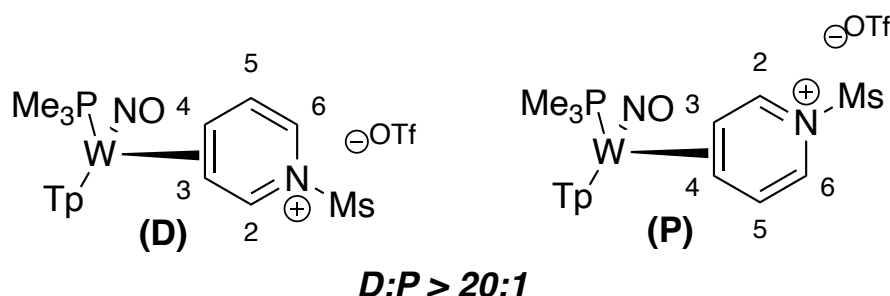
The red lines indicate observable NOE interactions between protons spectroscopically observed for most complexes.

### Computational Methods:

Ground-state structures were optimized at varying levels of theory including M06 and M06-2X using the 6-31G\*\* [LANL2DZ for W] basis set in Gaussian 16. Conformational analysis was performed by optimizing multiple conformations and determining the lowest energy conformation. Previous literature demonstrates that this functional and basis set choice accurately corroborates experimental results. Vibrational frequency analysis verified that optimized structures were minima, and optimized and rigid-rotor-harmonic-oscillator thermochemical chemical corrections were applied at 298 K and 1 atm utilizing Gaussian's default implementation.

## **Appendix B: Chapter 2 Data**

**Synthesis and characterization of  $\text{Wtp}(\text{NO})(\text{PMe}_3)(\eta^2\text{-(N-mesyl)pyridinium})$  (OTf) (**5D**)**



Methanesulfonic anhydride (5.87 g, 33.70 mmol),  $\text{Wtp}(\text{NO})(\text{PMe}_3)(\eta^2\text{-pyridinium})(\text{OTf})$  (9.87 g, 13.48 mmol), and EtCN (40 mL) were charged to a flame-dried 100 mL round-bottom flask with a 1-inch stir bar. Lutidine (3.69 g, 34.43 mmol) was added to initiate the reaction, and the flask was submerged in a pre-heated oil bath set to 55 °C. After stirring the solution for ~2 hours, the solution was diluted with 150 mL of DCM and added to a separatory funnel. This solution was washed 3x with 200 mL of saturated aqueous  $\text{NaHCO}_3$ . The organic layer was isolated and set aside. The combined aqueous layers were combined and back-extracted with 50 mL of DCM to prevent product loss. The organic layers were combined in a single flask and dried with anhydrous  $\text{MgSO}_4$ . This powder was then filtered off into a 60 mL coarse porosity fritted funnel and washed with DCM. The dried organic layers were then reduced *in vacuo* down to dryness. The residue in the flask was redissolved in minimal DCM (approximately 10 mL). The solution was then slowly added to 500 mL of stirring diethyl ether. An orange precipitate formed immediately and was allowed to stir for ~10 minutes to ensure total precipitation. This powder was collected on a 60 mL medium porosity frit and washed 2x with 30 mL of ether. This powder was dried in a desiccator under vacuum for ~30 minutes. The dried powder was gently added to a stirring solution of 150 mL of HPLC grade ethyl acetate and triturated overnight. The final orange precipitate was collected on the F frit, washed 2x with 30 mL of ethyl acetate and 2x with 30 mL of diethyl ether, and dried in the desiccator overnight under vacuum (5.5 g, 50% yield).

$^1\text{H}$  NMR ( $\text{CD}_2\text{Cl}_2$ ,  $\delta$ , 25 °C): (**D**): 9.14 (d,  $J$  = 5.9 Hz, 1H, H2), 7.97 (d,  $J$  = 2.1 Hz, 1H, PzB3), 7.96 (d,  $J$  = 2.3 Hz, 1H, PzC5), 7.93 (d,  $J$  = 2.4 Hz, 1H, PzB5), 7.90 (d,  $J$  = 2.1



Hz, 1H, PzA3), 7.76 (d,  $J = 2.4$  Hz, 1H, PzA5), 7.65 (d,  $J = 2.1$  Hz, 1H, PzC3), 6.64 (ddd,  $J = 1.8, 5.6, 7.8$  Hz, 1H, H5), 6.48 (t,  $J = 2.3$  Hz, 1H, PzC4), 6.45 (dd,  $J = 1.6, 7.8$  Hz, 1H, H6), 6.44 (t,  $J = 2.2$  Hz, 1H, PzB4), 6.39 (t,  $J = 2.3$  Hz, 1H, PzA4), 4.16 (dt,  $J = 6.2, 12.4$  Hz, 1H, H4), 3.61 (s, 3H, Ms), 3.08 (td,  $J = 1.8, 6.2$  Hz, 1H, H3), 1.26 (d,  $J_{PH} = 9.2$  Hz, 9H, PMe<sub>3</sub>). (**P**): 9.43 (d,  $J = 5.1$  Hz, 1H, H2), (2 other Pz3/5 signals buried) 7.93 (d,  $J = 2.3$  Hz, 1H, Pz3/5), 7.91 (d,  $J = 2.4$  Hz, 1H, Pz3/5), 7.78 (d,  $J = 2.4$  Hz, 1H, Pz3/5), 7.58 (d,  $J = 2.1$  Hz, 1H, Pz3/5), 6.81 (dd,  $J = 1.0, 6.7$  Hz, 1H, H5), 6.42 (t,  $J = 2.3$  Hz, 1H, Pz4), 6.41 (t,  $J = 2.3$  Hz, 1H, Pz4), 6.32 (t,  $J = 2.2$  Hz, 1H, Pz4), 6.31 (dd,  $J = 1.4, 7.3$  Hz, 1H, H6), 4.21 (q,  $J = 6.2$  Hz, 1H, H4), 3.71 (s, 3H, Ms), 2.86 (t,  $J = 6.7$  Hz, 1H, H3), 1.33 (d,  $J_{PH} = 8.80$  Hz, 9H, PMe<sub>3</sub>).

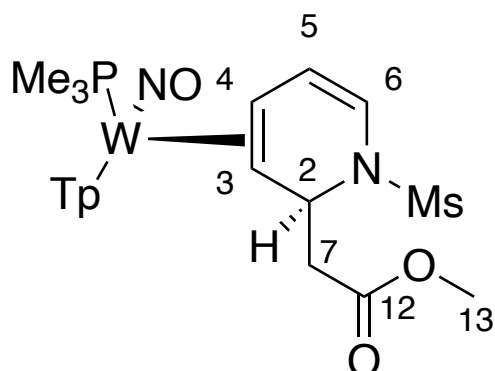
<sup>13</sup>C NMR (CD<sub>2</sub>Cl<sub>2</sub>,  $\delta$ , 25 °C): (**D**): 167.9 (C2), 146.8 (PzA3), 145.8 (d,  $J_{PC} = 2.0$  Hz, PzB3), 141.9 (PzC3), 138.9 (PzC5), 138.7 (PzB5), 137.8 (PzA5), 124.1 (d,  $J_{PC} = 3.0$  Hz, C5), 121.5 (q,  $J_{FC} = 320.5$  Hz, TfO<sup>-</sup>), 115.2 (C6), 108.4 (PzC4), 108.3 (PzB4), 108.0 (PzA4), 67.1 (d,  $J_{PC} = 13.9$  Hz, C4), 66.1 (C3), 44.2 (Ms), 13.2 (d,  $J_{PC} = 31.3$  Hz, 3C, PMe<sub>3</sub>). (**P**): 163.0 (C2), 144.7 (Pz3/5), 142.4 (Pz3/5), 141.1 (Pz3/5), 138.6 (Pz3/5), 138.1 (Pz3/5), 137.1 (Pz3/5), 127.3 (C5), 112.6 (C6), 108.1 (Pz4), 108.0 (Pz4), 106.9 (Pz4), 68.1 (C4), 65.1 (C3), 43.4 (Ms), 13.8 (d,  $J_{PC} = 30.3$  Hz, 3C, PMe<sub>3</sub>).

IR  $\nu(\text{NO}) = 1617 \text{ cm}^{-1}$ ,  $\nu(\text{BH}) = 2519 \text{ cm}^{-1}$ .

CV (DMA; 100 mV/s)  $E_{p,a} = +1.18 \text{ V}$  (NHE),  $E_{p,c} = -0.96 \text{ V}$  (NHE).

HRMS (ESI)  $m/z$ : [M]<sup>+</sup> Calcd for C<sub>18</sub>H<sub>27</sub>BN<sub>8</sub>O<sub>3</sub>PSW<sup>+</sup> 661.1261; Found 661.1261

**Synthesis and characterization of  $\text{WTP}(\text{NO})(\text{PMe}_3)(\eta^2\text{-(N-mesyl)-2-(methylacetate)-1,2-dihydropyridine})$  (**6D**)**



Methyl bromoacetate (107 mg, 0.70 mmol), (**5D**) (204 mg, 0.25 mmol), and THF (3.0 mL) were charged to a flame-dried 50 mL round-bottom flask with a 1-inch stir bar. Zinc powder (67 mg, 1.02 mmol) was added to initiate the reaction, and the heterogenous solution was stirred for 1 hour. The zinc was removed by filtering the solution through a celite plug set up in a 60 mL coarse porosity frit with 1 inch of celite, which was then washed with residual DCM to prevent loss of product. The solution was diluted with 150 mL of DCM and added to a separatory funnel. This solution was washed 3x with 200 mL of saturated aqueous  $\text{NaHCO}_3$ . The organic layer was isolated and set aside. The combined aqueous layers were combined and back-extracted with 50 mL of DCM to prevent product loss. The organic layers were combined in a single flask and dried with anhydrous  $\text{MgSO}_4$ . This powder was then filtered off into a 60 mL coarse porosity fritted funnel and washed with DCM. The dried organic layers were then reduced *in vacuo* to dryness. The residue in the flask was redissolved in minimal DCM (approximately 10 mL). The solution was then slowly added to 200 mL of stirring pentane. A tan precipitate formed immediately and was allowed to stir for ~10 minutes to ensure total precipitation. This powder was collected on a 60 mL medium porosity frit and washed 2x with 30 mL of pentane. This powder was dried in a desiccator under vacuum for ~30 minutes (178 mg, 96% yield).

$^1\text{H}$  NMR ( $\text{CD}_2\text{Cl}_2$ ,  $\delta$ , 25 °C): 8.12 (d,  $J$  = 1.9 Hz, 1H, PzA3), 8.08 (d,  $J$  = 1.9 Hz, 1H, PzB3), 7.78 (d,  $J$  = 2.3 Hz, 1H, PzB5), 7.75 (d,  $J$  = 2.3 Hz, 1H, PzC5), 7.69 (d,  $J$  = 2.3 Hz, 1H, PzA5), 7.28 (d,  $J$  = 2.1 Hz, 1H, PzC3), 6.36 (t,  $J$  = 2.2 Hz, 1H, PzB4), 6.32 (t,

$J = 2.3$  Hz, 1H, PzA4), 6.23 (t,  $J = 2.3$  Hz, 1H, PzC4), 5.86 (d,  $J = 7.8$  Hz, 1H, H6), 5.66 (ddd,  $J = 0.7, 5.1, 7.8$  Hz, 1H, H5), 5.06 (m, 1H, H2), 3.47 (s, 3H, H9), 3.19 (s, 3H, Ms), 3.09 (dd,  $J = 3.8, 14.7$  Hz, 1H, H7), 3.00 (dd,  $J = 9.0, 14.7$  Hz, 1H, H7'), 2.79 (ddd,  $J = 5.1, 10.6, 13.1$  Hz, 1H, H4), 1.55 (d,  $J = 10.6$  Hz, 1H, H3), 1.17 (d,  $J_{PH} = 8.5$  Hz, 9H, PMe<sub>3</sub>).

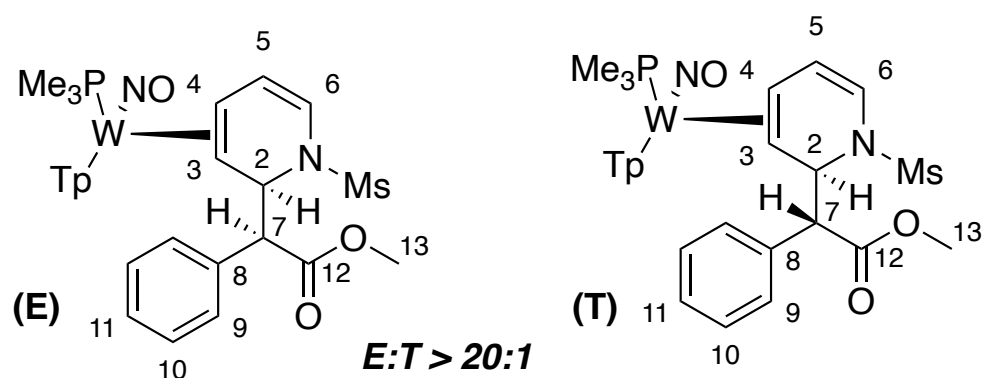
<sup>13</sup>C NMR (CD<sub>2</sub>Cl<sub>2</sub>,  $\delta$ , 25 °C): 172.5 (C8), 143.5 (PzA3), 143.3 (d,  $J_{PC} = 1.7$  Hz, PzB3), 140.7 (PzC3), 137.3 (PzC5), 136.6 (PzB5), 136.4 (PzA5), 115.3 (C6), 112.6 (d,  $J_{PC} = 3.0$  Hz, C5), 107.1 (PzB4), 106.6 (PzC4), 106.4 (PzA4), 62.2 (d,  $J_{PC} = 1.4$  Hz, C3), 53.2 (C2), 51.7 (C10), 44.9 (C7), 44.5 (d,  $J_{PC} = 10.5$  Hz, C4), 42.4 (Ms), 13.3 (d,  $J_{PC} = 28.6$  Hz, 3C, PMe<sub>3</sub>).

IR  $\nu(\text{NO}) = 1537$  cm<sup>-1</sup>,  $\nu(\text{BH}) = 2483$  cm<sup>-1</sup>,  $\nu(\text{C=O}) = 1725$  cm<sup>-1</sup>

CV (DMA; 50 mV/s)  $E_{p,a} = +0.53$  V (NHE)

SC-XRD data on S65.

### Synthesis and characterization of WTp(NO)(PMe<sub>3</sub>)( $\eta^2$ -(*N*-mesyl)-2-(methyl- $\alpha$ -phenylacetate)-1,2-dihydropyridine) (7D)



Methyl  $\alpha$ -phenylbromoacetate (1.69 g, 7.38 mmol), (**5D**) (1.75 g, 2.16 mmol), and THF (10 mL) were charged to a flame-dried 50 mL round-bottom flask with a 1-inch stir bar. Zinc powder (490 mg, 7.49 mmol) was added to initiate the reaction, and the heterogenous solution was stirred for 1 hour. The zinc was removed by filtering the solution through a celite plug set up in a 60 mL coarse porosity frit with 1 inch of celite,

which was then washed with residual DCM to prevent loss of product. The solution was diluted with 150 mL of DCM and added to a separatory funnel. This solution was washed 3x with 200 mL of saturated aqueous NaHCO<sub>3</sub>. The organic layer was isolated and set aside. The combined aqueous layers were combined and back-extracted with 50 mL of DCM to prevent product loss. The organic layers were combined in a single flask and dried with anhydrous MgSO<sub>4</sub>. This powder was then filtered off into a 60 mL coarse porosity fritted funnel and washed with DCM. The dried organic layers were then reduced *in vacuo* to dryness. The residue in the flask was redissolved in minimal DCM (approximately 10 mL). The solution was then slowly added to 200mL of stirring pentane. A tan precipitate formed immediately and was allowed to stir for ~10 minutes to ensure total precipitation. This powder was collected on a 60 mL medium porosity frit and washed 2x with 30 mL of pentane. This powder was dried in a desiccator under vacuum for ~30 minutes. The dried powder was gently added to a 4-dram vial containing a stir pea, filled with 15 mL of stirring MeOH, and triturated overnight. The tan precipitate was collected on a 15 mL fine porosity frit and washed 2x with 10 mL of MeOH. After drying in a desiccator for 2 hours, the highly pure tan precipitate was added to a 4-dram vial and stir pea filled with 15 mL of DME and triturated overnight. The highly enriched tan powder was collected on a 15 mL fine porosity frit and washed 1x with 10 mL of DME and 2x with 10 mL of diethyl ether. This powder was then dried in the desiccator (560 mg, 32% yield).

<sup>1</sup>H NMR (CD<sub>2</sub>Cl<sub>2</sub>, δ, 25 °C): (**E**): 8.15 (d, *J* = 1.8 Hz, 1H, PzA3), 8.10 (d, *J* = 1.9 Hz, 1H, PzB3), 7.78 (d, *J* = 2.4 Hz, 1H, PzB5), 7.75 (d, *J* = 2.3 Hz, 1H, PzC5), 7.67 (d, *J* = 2.4 Hz, 1H, PzA5), 7.41 (m, 2H, H9), 7.25 (m, 1H, PzC3), 7.24 (m, 2H, H10), 7.20 (m, 1H, H11), 6.35 (t, *J* = 2.2 Hz, 1H, PzB4), 6.29 (t, *J* = 2.2 Hz, 1H, PzA4), 6.23 (t, *J* = 2.2 Hz, 1H, PzC4), 5.78 (ddd, *J* = 0.7, 5.0, 7.7 Hz, 1H, H5), 5.72 (d, *J* = 7.7 Hz, 1H, H6), 5.22 (dd, *J* = 1.1, 8.3 Hz, 1H, H2), 4.34 (d, *J* = 8.3 Hz, 1H, H7), 3.42 (s, 3H, H13), 2.90 (ddd, *J* = 4.9, 10.7, 14.5 Hz, 1H, H4), 2.60 (s, 3H, Ms), 1.64 (dd, *J* = 1.1, 10.7 Hz, 1H, H3), 1.20 (d, *J*<sub>PH</sub> = 8.5 Hz, 9H, PMe<sub>3</sub>). (**T**): 8.14 (d, *J* = 1.8 Hz, 1H, Pz3/5), 8.05 (d, *J* = 1.9 Hz, 1H, Pz3/5), 7.77 (d, *J* = 2.4 Hz, 1H, Pz3/5), 7.73 (d, *J* = 2.2 Hz, 1H, Pz3/5), 7.68 (d, *J* = 2.3 Hz, 1H, Pz3/5), (H9, 10, and 11 are buried), 6.34 (t, *J* = 2.2 Hz, 1H, Pz4), 6.33 (t, *J* = 2.2 Hz, 1H, Pz4), 6.21 (t, *J* = 2.2 Hz, 1H, Pz4), 5.61 (d, *J* = 7.8 Hz, 1H, H6), 5.50 (dd, *J* = 0.9, 5.4 Hz, 1H, H2), 5.17 (dd, *J* = 4.9, 7.8 Hz, 1H, H5), 4.54

(d,  $J = 5.4$  Hz, 1H, H7), 3.44 (s, 3H, H13), 3.23 (s, 3H, Ms), 2.54 (ddd,  $J = 4.9, 10.7, 13.6$  Hz, 1H, H4), 1.42 (dd,  $J = 0.9, 10.7$  Hz, 1H, H3), 1.08 (d,  $J_{PH} = 8.5$  Hz, 9H, PMe<sub>3</sub>).

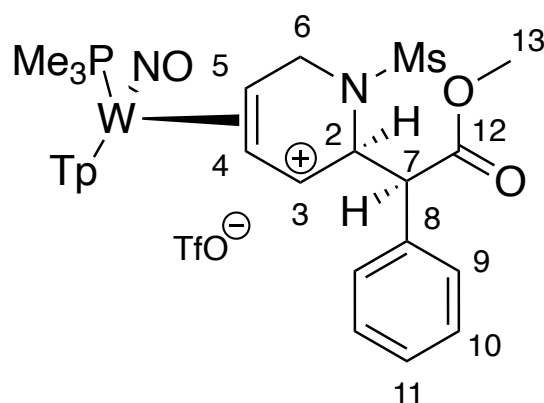
<sup>13</sup>C NMR (CD<sub>2</sub>Cl<sub>2</sub>,  $\delta$ , 25 °C): (**E**): 173.70 (C12), 144.17 (PzA3), 143.10 (d,  $J_{PC} = 1.6$  Hz, 1C, PzB3), 140.16 (PzC3), 137.83 (C8), 137.22 (PzC5), 136.61 (PzB5), 136.11 (PzA5), 130.29 (2C, C9), 128.51 (2C, C10), 127.90 (C11), 116.02 (C6), 114.92 (d,  $J_{PC} = 2.6$  Hz, 1C, C5), 107.01 (PzB4), 106.61 (PzC4), 106.40 (PzA4), 64.11 (d,  $J_{PC} = 1.6$  Hz, 1C, C3), 60.19 (C7), 59.36 (C2), 52.02 (C13), 44.57 (d,  $J_{PC} = 10.4$  Hz, 1C, C4), 42.15 (Ms), 13.25 (d,  $J_{PC} = 28.0$  Hz, 3C, PMe<sub>3</sub>). (**T**): 173.11 (C12), 143.65 (Pz3/5), 143.18 (d,  $J_{PC} = 2.2$  Hz, 1C, Pz3/5), 140.36 (Pz3/5), 137.26 (Pz3/5), 136.81 (Pz3/5), 136.41 (Pz3/5), (C8 obscured), 131.52 (2C, C9/C10), 127.73 (2C, C9/C10), 127.22 (C11), 115.94 (C6), 112.22 ((d,  $J_{PC} = 3.0$  Hz, 1C, C5), 107.07 (Pz4), 106.61 (Pz4), 106.26 (Pz4), 60.98 (C7), 58.25 (C2), 57.85 (d,  $J_{PC} = 1.4$  Hz, 1C, C3), 52.00 (C13), 46.16 (d,  $J_{PC} = 10.6$  Hz, 1C, C4), 42.37 (Ms), 13.10 (d,  $J_{PC} = 28.0$  Hz, 3C, PMe<sub>3</sub>).

IR:  $\nu(\text{NO}) = 1557 \text{ cm}^{-1}$ ,  $\nu(\text{BH}) = 2489 \text{ cm}^{-1}$ ,  $\nu(\text{CO}) = 1732 \text{ cm}^{-1}$ .

CV (DMA; 100 mV/s):  $E_{p,a} = +0.52 \text{ V}$  (NHE).

SC-XRD data on S66.

### Synthesis and characterization of WTp(NO)(PMe<sub>3</sub>)( $\eta^2$ -(*N*-mesyl)-2-(methyl- $\alpha$ -phenylacetate)-1,2,3,6-tetrahydropyridinium (OTf) (**8**)



**Erythro-7D** (97 mg, 0.12 mmol) was added to a 4-dram vial containing a stir pea and diluted with propionitrile (3 mL). To a separate 4-dram vial, propionitrile (1 mL) and TfOH (24 mg, 0.16 mmol) were added. The acid/propionitrile solution was slowly

added to the **erythro-7D**/propionitrile solution and stirred for 5 minutes. The reaction was then slowly added to 100 mL of stirring diethyl ether, which immediately formed a tan precipitate. This powder was triturated in the ether solution for 10 minutes and then collected on a 30 mL medium porosity frit. The collected powder was then washed 2x with 20 mL of diethyl ether and dried in a desiccator (104 mg, 90% yield).

$^1\text{H}$  NMR ( $\text{CD}_2\text{Cl}_2$ ,  $\delta$ , 25 °C): 8.31 (d,  $J$  = 2.2 Hz, 1H, PzB3), 8.14 (d,  $J$  = 2.3 Hz, 1H, PzC3), 7.90 (d,  $J$  = 2.3 Hz, 1H, PzC5), 7.81 (d,  $J$  = 2.3 Hz, 1H, PzB5), 7.60 (d,  $J$  = 2.4 Hz, 1H, PzA5), 7.54 (d,  $J$  = 7.4 Hz, 2H, H9), 7.46 (t,  $J$  = 7.4 Hz, 2H, H10), 7.42 (t,  $J$  = 7.4 Hz, 1H, H11), 6.86 (d,  $J$  = 2.2 Hz, 1H, PzA4), 6.58 (t,  $J$  = 2.3 Hz, 1H, PzC4), 6.47 (t,  $J$  = 2.4 Hz, 1H, PzB4), 5.98 (t,  $J$  = 2.4 Hz, 1H, PzA4), 5.89 (d,  $J$  = 7.9 Hz, 1H, H3), 5.46-5.48 (m, 1H, H2), 5.23 (t, 7.8 Hz, 1H, H4), 4.81 (dd,  $J$  = 2.3, 12.7 Hz, 1H, H6), 4.78 (d,  $J$  = 5.3 Hz, 1H, H7), 4.53-4.58 (m, 1H, H5), 4.12 (d,  $J$  = 12.7 Hz, 1H, H6'), 3.84 (s, 3H, H13), 2.95 (s, 3H, Ms), 1.27 (d,  $J_{\text{PH}}$  = 9.7 Hz, 9H,  $\text{PMe}_3$ ).

$^{13}\text{C}$  NMR ( $\text{CD}_2\text{Cl}_2$ ,  $\delta$ , 25 °C): 171.3 (C12), 146.4 (PzA3), 144.4 (d,  $J_{\text{PC}}$  = 2.2 Hz, PzB3), 142.7 (PzC3), 138.9 (PzC5), 138.7 (PzA5/B5), 138.6 (PzA5/B5), 134.6 (C8), 129.7 (2C, C10), 129.0 (2C, C9), 128.8 (C11), 121.4 (q,  $J_{\text{FC}}$  = 320.4 Hz,  $\text{TfO}^-$ ), 120.0 (C3), 109.1 (PzB4/C4), 108.9 (PzB4/C4), 107.3 (PzA4), 98.3 (d,  $J_{\text{PC}}$  = 3.0 Hz, C4), 65.3 (d,  $J_{\text{PC}}$  = 14.5 Hz, C5), 58.7 (C2), 55.9 (C7), 53.0 (C13), 42.9 (d,  $J_{\text{PC}}$  = 2.5 Hz, C6), 41.1 (Ms), 13.5 (d,  $J_{\text{PC}}$  = 33.0 Hz, 3C,  $\text{PMe}_3$ ).

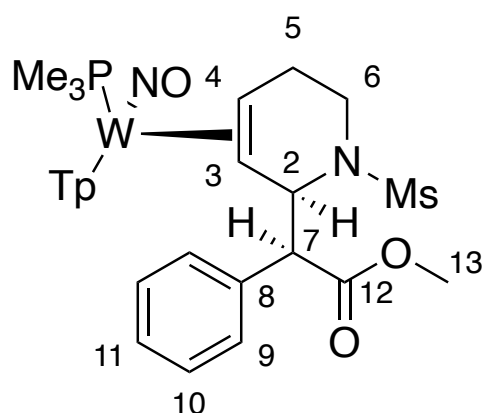
IR:  $\nu(\text{NO})$  = 1661  $\text{cm}^{-1}$ ,  $\nu(\text{BH})$  = 2511  $\text{cm}^{-1}$ ,  $\nu(\text{CO})$  = 1733  $\text{cm}^{-1}$ .

CV (MeCN; 100 mV/s):  $E_{\text{p,c}}$  = -0.74 V (NHE).

HRMS (ESI)  $m/z$ :  $[\text{M}]^+$  Calcd for  $\text{C}_{27}\text{H}_{37}\text{BN}_8\text{O}_5\text{PSW}^+$  811.1942; Found 811.1945

SC-XRD data on S67.

**Synthesis and characterization of  $\text{Wtp}(\text{NO})(\text{PMe}_3)(\eta^2\text{-(N-mesyl)-2-(methyl-}\alpha\text{-phenylacetate)-1,2,5,6\text{-tetrahydropyridine) (9D)}$**



Cyanoborohydride (136 mg, 2.16 mmol) and methanol (2.0 mL) were added to a screw-cap test tube and placed in a cold bath at  $-30\text{ }^{\circ}\text{C}$ . To another tube, **erythro-7D** (185 mg, 0.228 mmol) and propionitrile (3.0 mL) were added. Triflic acid (41 mg, 0.273 mmol) was then added to the **erythro-7D** solution, which was swirled until dissolution and then also added to the cold bath. Both tubes were chilled for approximately 15 minutes before the cyanoborohydride/methanol solution was added to the solution of **8**, which sat in the cold bath for 16 hours. This solution was diluted with 50 mL of DCM and was washed 3x with 50 mL of saturated aqueous  $\text{NaHCO}_3$ . The organic layer was isolated and set aside. The combined aqueous layers were combined and back-extracted with 50 mL of DCM to prevent product loss. The organic layers were combined in a single flask and dried with anhydrous  $\text{MgSO}_4$ . This powder was then filtered off into a 60 mL coarse porosity fritted funnel and washed with DCM. The dried organic layers were then reduced *in vacuo* down to dryness. The residue in the flask was redissolved in minimal DCM (approximately 10 mL). The solution was then slowly added to 100 mL of stirring pentane. A tan precipitate formed immediately and was allowed to stir for  $\sim 10$  minutes to ensure total precipitation. This powder was collected on a 15 mL fine porosity frit and washed 2x with 10 mL of pentane. This powder was dried in a desiccator under vacuum overnight (172 mg, 93% yield).

$^1\text{H}$  NMR ( $(\text{CD}_3)_2\text{CO}$ ,  $\delta$ ,  $25\text{ }^{\circ}\text{C}$ ): 8.27 (d,  $J = 1.8\text{ Hz}$ , 1H, PzA3), 8.10 (d,  $J = 1.8\text{ Hz}$ , 1H, PzB3), 7.92 (d,  $J = 2.3\text{ Hz}$ , 1H, PzC5), 7.91 (d,  $J = 2.4\text{ Hz}$ , 1H, PzB5), 7.78 (d,  $J = 2.3\text{ Hz}$ , 1H, PzA5), 7.43 (d,  $J = 2.0\text{ Hz}$ , 1H, PzC3), 7.35-7.38 (m, 2H, H9), 7.15-7.17 (m,

3H, H10/11), 6.38 (t,  $J = 2.2$  Hz, 1H, PzB4), 6.32 (t,  $J = 2.2$  Hz, 1H, PzC4), 6.26 (t,  $J = 2.2$  Hz, 1H, PzA4), 5.57 (dd,  $J = 1.5, 6.8$  Hz, 1H, H2), 4.13 (d,  $J = 6.8$  Hz, 1H, H7), 3.41 (dt,  $J = 4.3, 13.0$  Hz, H6'), 3.22 (s, 3H, H13), 2.98 (ddd,  $J = 3.8, 10.9, 14.6$  Hz, 1H, H6), 2.86-2.92 (m, 1H, H4), 2.64-2.70 (m, 1H, H5'), 2.58-2.62 (m, 1H, H5), 2.49 (s, 3H, Ms), 1.26 (d,  $J_{PH} = 8.4$  Hz, 9H, PMe<sub>3</sub>), 0.94 (d,  $J = 11.7$  Hz, 1H, H3).

<sup>13</sup>C NMR: ((CD<sub>3</sub>)<sub>2</sub>CO,  $\delta$ , 25 °C): 172.8 (C12), 144.0 (PzA3), 143.9 (d,  $J_{PC} = 1.5$  Hz, PzB3), 141.2 (PzC3), 138.1 (C8), 137.4 (PzB5/C5), 137.0 (PzB5/C5), 136.6 (PzA5), 130.8 (2C, C9), 128.6 (2C, C10), 127.9 (C11), 107.0 (PzB4), 106.9 (PzC4), 106.6 (PzA4), 63.3 (C7), 60.7 (C2), 53.8 (t,  $J_{WC} = 32.3$  Hz, C3), 51.4 (C13), 47.3 (d,  $J_{PC} = 12.5$  Hz, C4), 42.0 (C6), 40.5 (Ms), 28.8 (d,  $J_{PC} = 2.2$  Hz, C5), 13.5 (d,  $J_{PC} = 27.9$  Hz, 3C, PMe<sub>3</sub>).

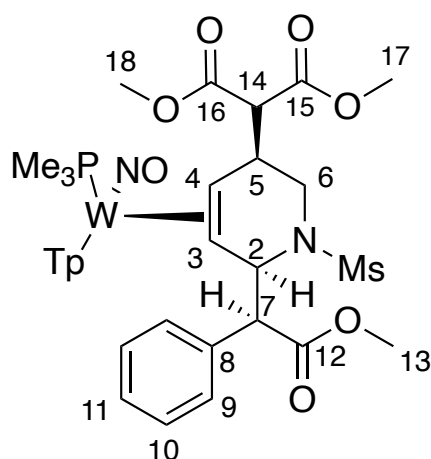
IR:  $\nu(\text{NO}) = 1538 \text{ cm}^{-1}$ ,  $\nu(\text{BH}) = 2486 \text{ cm}^{-1}$ ,  $\nu(\text{CO}) = 1729 \text{ cm}^{-1}$

CV (DMA; 100 mV/s):  $E_{p,a} = +0.44 \text{ V}$  (NHS)

HRMS (ESI)  $m/z$ : [M]<sup>+</sup> Calcd for C<sub>27</sub>H<sub>37</sub>BN<sub>8</sub>O<sub>5</sub>PSW<sup>+</sup> 811.1942; Found 811.1945

SC-XRD data on S68.

### Synthesis and characterization of WTp(NO)(PMe<sub>3</sub>)( $\eta^2$ -(*N*-mesyl)-5-dimethylpropanedioate-2-(methyl- $\alpha$ -phenylacetate)-1,2,5,6-tetrahydropyridine (10D)



**Erythro-7D** (200 mg, 0.247 mmol) was dissolved in 1 mL acetonitrile in a test tube with a stir pea. HOTf (38 mg, 0.253 mmol) was added to the test tube, and the mixture was stirred at room temperature for 5 minutes. The dark brown solution was cooled at



-10 °C for 15 minutes. Lithium dimethylmalonate (227 mg, 1.64 mmol) was dissolved in 1 ml acetonitrile in a test tube with a stir pea. The solution was then cooled to -10 °C for 15 minutes. The allyl solution was added to the lithium dimethylmalonate solution and reacted for 30 minutes at 0 °C. The solution was stirred at room temperature for an additional 30 minutes. The solution was diluted with DCM (10 mL), washed with H<sub>2</sub>O (3 x 5 mL), and the aqueous solution was back extracted with DCM (3 x 2 mL). The solution was dried with MgSO<sub>4</sub>, removed on a 15 mL medium porosity frit, washed with DCM (3 x 2 mL), and the resulting filtrate was evaporated to dryness. The product was dissolved in minimal DCM and added to a stirring solution of hexanes (75 mL), yielding a precipitate. This precipitate was isolated on a 15 mL fine porosity frit, washed with hexanes (10 mL), and desiccated to yield **10D** (160 mg, 69% yield).

<sup>1</sup>H NMR (CD<sub>2</sub>Cl<sub>2</sub>, δ, 25 °C): 8.42 (d, *J* = 1.0 Hz, 1H, PzA3), 8.08 (d, *J* = 1.8 Hz, 1H, PzB3), 7.77 (d, *J* = 2.2 Hz, 1H, PzC5), 7.76 (d, *J* = 2.5 Hz, 1H, PzB5), 7.70 (d, *J* = 2.3 Hz, 1H, PzA5), 7.42 (d, *J* = 7.2 Hz, 2H, H9), 7.30 (t, *J* = 7.3 Hz, 2H, H10), 7.25 (t, *J* = 7.3, 1H, H11), 7.07 (d, *J* = 2.0 Hz, 1H, PzC3), 6.34 (t, *J* = 2.5 Hz, 1H, PzA4), 6.31 (t, *J* = 2.2 Hz, 1H, PzB4), 6.26 (t, *J* = 2.2 Hz, 1H, PzC4), 5.54 (d, *J* = 9.4 Hz, 1H, H2), 4.13 (d, *J* = 9.6 Hz, 1H, H7), 3.95 (bs, 4H, H14/17/18), 3.77 (s, 3H, H17/18), 3.49 (m, 2H, H6/H5), 3.38 (m, 1H, H6), 2.97 (s, 3H, H13), 2.57 (ddd, *J* = 3.4, 13.7, 15.1 Hz, 1H, H4), 1.88 (s, 3H, Ms), 1.23 (d, *J*<sub>PH</sub> = 8.0 Hz, 9H, PMe<sub>3</sub>), 0.72 (d, *J* = 6.6 Hz, 1H, H3).

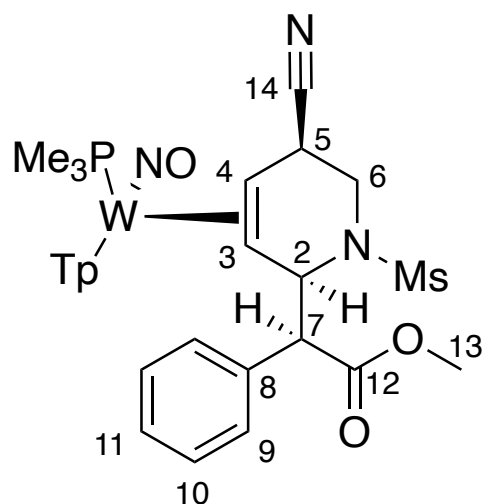
<sup>13</sup>C NMR (CD<sub>2</sub>Cl<sub>2</sub>, δ, 25 °C): 172.3 (C12), 169.5/169.3 (2C, C15/16), 144.6 (PzA3), 143.8 (PzB3), 140.4 (PzC3), 137.6 (C8), 137.1 (PzC5), 136.9 (PzB5), 136.5 (PzA5), 129.9 (2C, C9), 129.0 (2C, C10), 128.4 (C11), 106.4 (PzA4), 106.7 (PzB4), 106.6 (PzC4), 61.8 (C7), 58.7 (C2), 56.8 (C3), 56.3 (C14), 53.0/53.1 (2C, C17/18), 51.5 (C13), 46.6 (d, *J*<sub>PC</sub> = 12.0 Hz, C4), 40.4 (C6), 39.5 (C5), 37.1 (Ms), 14.5 (d, *J*<sub>PC</sub> = 27.6 Hz, 3C, PMe<sub>3</sub>).

IR: ν(NO) = 1543 cm<sup>-1</sup>, ν(CO) = 1728 cm<sup>-1</sup>

CV (DMA; 100 mV/s): *E*<sub>p,a</sub> = +0.61 V (NHE)

HRMS (APCI) *m/z*: [M]<sup>+</sup> Calcd for C<sub>32</sub>H<sub>46</sub>BN<sub>8</sub>O<sub>9</sub>PSW<sup>+</sup> 943.2365; Found 943.2368

**Synthesis and characterization of WTp(NO)(PMe<sub>3</sub>)( $\eta^2$ -(*N*-mesyl)-5-cyano-2-(methyl- $\alpha$ -phenylacetate)-1,2,5,6-tetrahydropyridine (11D)**



**Erythro-7D** (469 mg, 0.578 mmol) was dissolved in 3 mL propionitrile in a test tube with a stir pea. HOTf (375 mg, 2.50 mmol) was added to the test tube, and the mixture was allowed to stir at room temperature for 5 minutes. The dark brown solution was cooled at -40 °C for 15 minutes. Sodium cyanide (235 mg, 4.79 mmol) was dissolved in 3 mL methanol in a test tube with a stir pea. The solution was then cooled to -40 °C for 15 minutes. The allyl solution was added to the sodium cyanide solution and reacted for 12 hours at -40 °C. The solution was warmed to room temperature. The solution was diluted with DCM (10 mL), washed with Na<sub>2</sub>CO<sub>3</sub> (3 x 5 mL), and the aqueous solution was back extracted with DCM (3 x 2 mL). The solution was dried with MgSO<sub>4</sub>, removed on a 15 mL medium porosity frit, washed with DCM (3 x 2 mL), and the resulting filtrate was evaporated to dryness. The product was dissolved in minimal DCM and added to a stirring solution of hexanes (75 mL), yielding a precipitate. This precipitate was isolated on a 15 mL fine porosity frit, washed with hexanes (10 mL), and desiccated to yield **11D** (421 mg, 87% yield).

<sup>1</sup>H NMR (CD<sub>2</sub>Cl<sub>2</sub>,  $\delta$ , 25 °C): 8.44 (d, *J* = 1.3 Hz, 1H, PzB3), 8.05 (d, *J* = 1.7 Hz, 1H, PzA5), 7.77 (d, *J* = 2.2 Hz, 1H, PzA3), 7.76 (d, *J* = 2.2 Hz, 1H, PzC5), 7.72 (d, *J* = 2.6 Hz, 1H, PzB5), 7.41(d, *J* = 7.3 Hz, 2H, H9), 7.32 (t, *J* = 7.3 Hz, 2H, H10), 7.27 (t, *J* = 7.7 Hz, 1H, H11), 7.13 (d, *J* = 1.7 Hz, 1H, PzC3) 6.39 (t, *J* = 2.2 Hz, 1H, PzB4), 6.34 (t, *J* = 2.2 Hz, 1H, PzA4), 6.27 (t, *J* = 2.2 Hz, 1H, PzC4), 5.53 (dd, *J* = 1.4, 10.4 Hz,

<sup>1</sup>H, H2), 4.03 (d, *J* = 10.3 Hz, 1H, H7), 3.82 (ddd, *J* = 5.1, 5.8, 11.3 Hz, 1H, H5), 3.67 (dd, *J* = 4.8, 13.2 Hz, 1H, H6), 3.18 (dd, *J* = 11.3, 13.2 Hz, 1H, H6), 2.92 (ddd, *J* = 6.0, 11.4, 14.1 Hz, 1H, H4), 2.83 (s, 3H, H13), 1.73 (s, 3H, Ms), 1.30 (d, *J*<sub>PH</sub> = 8.0 Hz, 9H, PMe<sub>3</sub>), 0.46 (d, *J* = 11.9 Hz, 1H, H3).

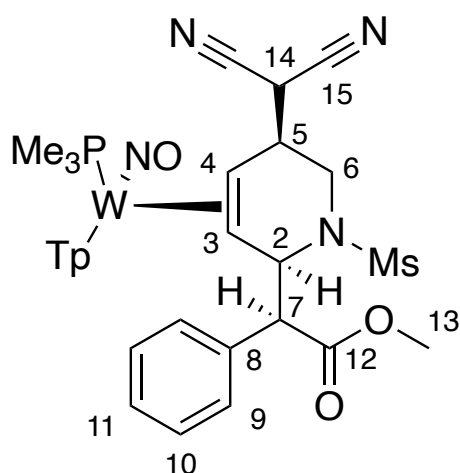
<sup>13</sup>C NMR (CD<sub>2</sub>Cl<sub>2</sub>, δ, 25 °C): 171.9 (C12), 144.7 (PzB3), 143.6 (PzA5), 140.0 (PzC3), 137.8 (C13), 136.9 (PzA3), 136.8 (PzC5), 136.4 (PzB5), 129.6 (2C, C9), 129.2 (2C, C10), 128.5 (C11), 123.6 (C14), 106.8 (PzA4), 106.6 (PzB4), 106.6 (PzC4), 61.9 (C7), 58.4 (C2), 52.9 (C3), 51.4 (13), 43.4 (d, *J*<sub>PC</sub> = 13.6 Hz, C4), 42.7 (C6), 40.7 (Ms), 29.6 (C5), 14.2 (d, *J*<sub>PC</sub> = 29.0 Hz, 3C, PMe<sub>3</sub>).

IR: ν(NO) = 1556 cm<sup>-1</sup>, ν(CO) = 1732 cm<sup>-1</sup>, ν(CN) = 2225 cm<sup>-1</sup>

CV (DMA; 100 mV/s): *E*<sub>p,a</sub> = +0.68 V (NHE)

HRMS (ESI) *m/z*: [M]<sup>+</sup> Calcd for C<sub>30</sub>H<sub>38</sub>BN<sub>9</sub>O<sub>5</sub>PSW<sup>+</sup> 838.2051; Found 838.2055

### Synthesis and characterization of WTp(NO)(PMe<sub>3</sub>)(η<sup>2</sup>-(*N*-mesyl)-5-dicyanomethyl-2-(methyl-α-phenylacetate)-1,2,5,6-tetrahydropyridine (12D)



**Erythro-7D** (200 mg, 0.247 mmol) was dissolved in ~0.5 mL propionitrile in a test tube with a stir pea. HOTf (44 mg, 0.293 mmol) was added to the test tube, and the mixture was allowed to stir at room temperature for 5 minutes. The dark brown solution was cooled to 0 °C for 15 minutes. Malononitrile (162 mg, 2.45 mmol) was dissolved in ~0.5mL THF in a test tube with a stir pea. tBuOK (20% wt., 692 mg, 1.23 mmol) was added. The solution was then cooled to 0 °C for 15 minutes. The allyl solution was

added to the deprotonated malononitrile solution and reacted for 4 hours at 0 °C. The solution was warmed to room temperature, diluted with DCM (10 mL), washed with Na<sub>2</sub>CO<sub>3</sub> (3 x 5 mL), and the aqueous solution was back extracted with DCM (3 x 2 mL). The solution was dried with Na<sub>2</sub>SO<sub>4</sub>, removed on a 15 mL medium porosity frit, washed with DCM (3 x 2 mL), and the resulting filtrate was evaporated to dryness. The product was dissolved in minimal DCM and added to a stirring solution of cold pentanes (75 mL), yielding a precipitate. This precipitate was isolated on a 15 mL fine porosity frit, washed with pentanes (5mL), and desiccated to yield **12D** (177 mg, 82% yield).

<sup>1</sup>H NMR (CD<sub>2</sub>Cl<sub>2</sub>, δ, 25 °C): 8.28 (bs, 1H, PzA3), 8.17 (d, *J* = 1.7 Hz, 1H, PzB3), 8.01 (d, *J* = 2.2 Hz, 1H, PzC5), 7.97 (d, *J* = 2.4 Hz, 1H, PzB5), 7.82 (d, *J* = 2.0 Hz, 1H, PzA5), 7.49 (d, *J* = 2.0, 1H, PzC3), 7.35 (d, *J* = 7.0 Hz, 1H, H9), 7.26 (t, *J* = 7.3 Hz, 1H, H11), 7.23 (t, *J* = 6.2 Hz, 2H, H10), 6.45 (t, *J* = 2.0 Hz, 1H, PzC4), 6.43 (t, *J* = 2.4 Hz, 1H, PzB4), 6.24 (t, *J* = 2.1 Hz, 1H, PzA4), 5.72 (bs, 1H, H2), 4.39 (bs, 1H, H7), 3.74 (dd, *J* = 3.2, 13.1 Hz, 1H, H6), 3.58 (dd, *J* = 4.4, 13.1 Hz, 1H, H6), 3.54 (s, 3H, H13), 3.44 (bs, 1H, H5), 3.32 (bs, 1H, H14), 2.91 (s, 3H, Ms), 2.63 (t, *J* = 11.3 Hz, 1H, H4), 1.38 (dd, *J* = 11.6 Hz, 1H, H3), 1.25 (d, *J*<sub>PH</sub> = 8.5 Hz, 9H, PMe<sub>3</sub>).

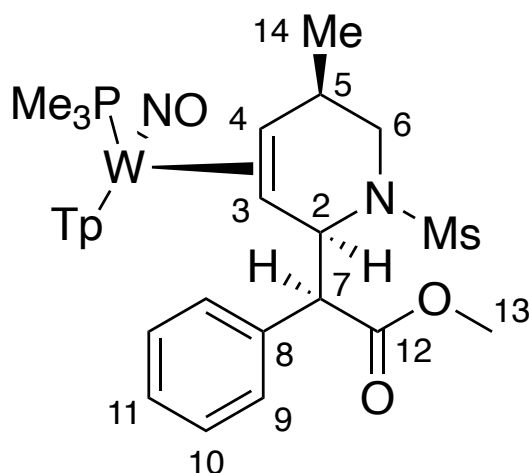
<sup>13</sup>C NMR (CD<sub>2</sub>Cl<sub>2</sub>, δ, 25 °C): 173.1 (C12), 144.3 (PzB3), 143.5 (PzA3), 141.6 (PzC3), 138.3 (PzC5), 137.6 (PzA5), 137.5 (PzB5), 137.0 (C8), 132.0 (2C, C9), 129.1 (2C, C10), 128.1 (C11), 114.2/113.1 (2C, C15), 107.6 (2C, PzC4/PzB4), 107.1 (PzA4), 63.3 (C7), 61.3 (C2), 52.5 (C3), 52.0 (C13), 50.0 (d, *J*<sub>PC</sub> = 12.7Hz, C4), 44.2 (C6), 41.3 (C5), 36.0 (Ms), 23.4 (C14), 13.3 (d, *J*<sub>PC</sub> = 28.4 Hz, 3C, PMe<sub>3</sub>).

IR: ν(NO) = 1538 cm<sup>-1</sup>, ν(CO) = 1725 cm<sup>-1</sup>, ν(CN) = 2221 cm<sup>-1</sup>

CV (MeCN; 100 mV/s): *E*<sub>p,a</sub> = +0.83 V (NHE)

HRMS (ESI) *m/z*: [M]<sup>+</sup> Calcd for C<sub>30</sub>H<sub>39</sub>BN<sub>10</sub>O<sub>5</sub>PSW<sup>+</sup> 877.2160; Found 877.2150.

**Synthesis and characterization of WTp(NO)(PMe<sub>3</sub>)( $\eta^2$ -(*N*-mesyl)-5-methyl-2-(methyl- $\alpha$ -phenylacetate)-1,2,5,6-tetrahydropyridine (13D)**



**8** (100 mg, 0.104 mmol) was dissolved in ~0.5 mL propionitrile in a test tube with a stir pea. The solution was cooled to -60 °C for 2 hours. MeMgBr (3M, 0.173 mL, 5.20 mmol) was added to 0.5 mL THF and chilled to -60 °C for 2 hours. The allyl solution was added to the Grignard solution and allowed to react for 60 hours. The solution was warmed to room temperature, diluted with DCM (10 mL), washed with Na<sub>2</sub>CO<sub>3</sub> (3 x 5 mL), and the aqueous solution was back extracted with DCM (3 x 2 mL). The solution was dried with Na<sub>2</sub>SO<sub>4</sub>, removed on a 15 mL medium porosity frit, washed with DCM (3 x 2 mL), and the resulting filtrate was evaporated to dryness. The product was dissolved in minimal DCM and added to a stirring solution of cold hexanes (75 mL), yielding a precipitate. This precipitate was isolated on a 15 mL fine porosity frit, washed with hexanes (5 mL), and desiccated to yield **13D** (32 mg, 37% yield).

<sup>1</sup>H NMR (CD<sub>3</sub>CN,  $\delta$ , 25 °C): 8.4 (bs, 1H, PzA3), 8.0 (d, *J* = 1.5 Hz, 1H, PzB3), 7.8 (d, *J* = 3.0 Hz, 1H, PzC5), 7.83 (d, *J* = 2.4 Hz, 1H, PzB5), 7.79 (d, *J* = 2.5 Hz, 1H, PzA5), 7.37 (d, *J* = 7.3 Hz, 2H, H9), 7.27 (t, *J* = 7.0 Hz, 2H, H10), 7.23 (t, *J* = 7.0 Hz, 1H, H11), 7.20 (d, *J* = 1.5 Hz, 1H, PzC3), 6.36 (t, *J* = 2.2 Hz, 1H, PzA4), 6.34 (t, *J* = 2.3 Hz, 1H, PzB4), 6.27 (t, *J* = 2.2 Hz, 1H, PzC4), 5.50 (dd, *J* = 1.4, 9.6 Hz, 1H, H2), 4.06 (d, *J* = 9.6 Hz, 1H, H7), 3.20 (dd, *J* = 4.9, 13.3 Hz, 1H, H6), 2.83 (s, 3H, H13), 2.68 (dd, *J* = 11.4, 13.1 Hz, 1H, H6), 2.67 (ddd, *J* = 4.4, 11.6, 15.6 Hz, 1H, H4), 1.97 (s, 3H, Ms),

1.26 (d,  $J = 6.7$  Hz, 3H, H14), 1.31 (m, 1H, H5), 1.25 (d,  $J_{PH} = 8.2$  Hz, 9H,  $\text{PMe}_3$ ), 1.18 (d,  $J = 8.6$  Hz, 1H, H3).

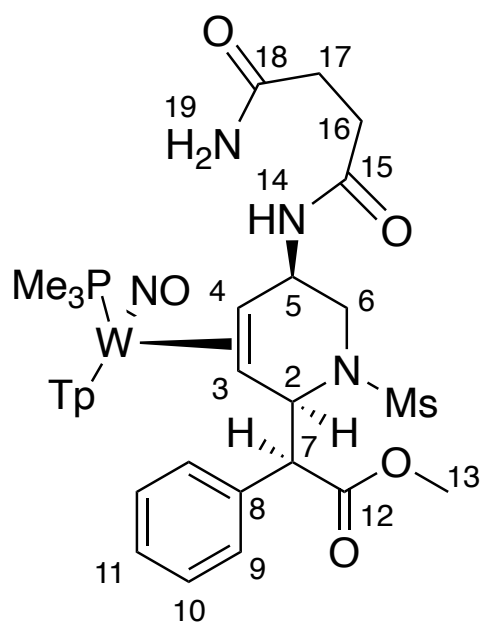
$^{13}\text{C}$  NMR ( $\text{CD}_3\text{CN}$ ,  $\delta$ , 25 °C): 173.1 (C12), 144.8 (PzA3), 144.4 (PzB3), 141.3 (PzC3), 138.7 (C8), 137.4 (PzC5), 137.3 (PzB5), 137.0 (PzA5), 130.4 (2C, C9), 129.3 (2C, C10), 128.6 (C11), 107.1 (PzC4), 107.0 (PzA4), 106.9 (PzB4), 62.6 (C7), 59.1 (C2), 57.3 (C3), 52.1 (d,  $J_{PC} = 10.7$  Hz, C4), 51.6 (C13), 47.8 (C6), 40.7 (Ms), 23.0 (C5), 22.0 (C14), 14.4 (d,  $J_{PC} = 30.0$  Hz, 3C,  $\text{PMe}_3$ ).

IR:  $\nu(\text{NO}) = 1537\text{ cm}^{-1}$ ,  $\nu(\text{CO}) = 1730\text{ cm}^{-1}$

CV (MeCN; 100 mV/s):  $E_{p,a} = +0.50\text{V}$  (NHE)

SC-XRD data on S69.

### Synthesis and characterization of $\text{WTP}(\text{NO})(\text{PMe}_3)(\eta^2\text{-(N-mesyl)-5-succinamide-2-(methyl-}\alpha\text{-phenylacetate)-1,2,5,6-tetrahydropyridine (14D)}$



**8** (150 mg, 0.156 mmol) was dissolved in ~1 mL THF in a test tube with a stir pea. The solution was cooled to -60 °C for 15 minutes. Succinamide (155 mg, 1.56 mmol) was dissolved in 1 mL THF in a test tube with a stir pea, *n*-butyl lithium (1.5 M, 0.2 mL, 0.30 mmol) was added and allowed to react for 10 minutes. The solution was then cooled to -60 °C for 15 minutes. The allyl solution was added to the deprotonated succinimide

solution and reacted for 60 hours at -60 °C. The solution was warmed to room temperature. The solution was diluted with DCM (10 mL), washed with Na<sub>2</sub>CO<sub>3</sub> (3 x 5 mL), and the aqueous solution was back extracted with DCM (3 x 2 mL). The solution was dried with Na<sub>2</sub>SO<sub>4</sub>, removed on a 15 mL medium porosity frit, washed with DCM (3 x 2 mL), and the resulting filtrate was evaporated to dryness. The product was dissolved in minimal DCM and added to a stirring solution of chilled hexanes (200 mL), yielding a precipitate. This precipitate was isolated on a 15 mL fine porosity frit, washed with hexanes (10 mL), and desiccated to yield **14D** (78 mg, 54% yield).

<sup>1</sup>H NMR (CD<sub>3</sub>CN, δ, 25 °C): 8.47 (bs, 1H, PzA3), 8.03 (d, *J* = 2.3 Hz, 1H, PzB3), 7.86 (d, *J* = 2.3 Hz, 1H, PzB5), 7.84 (d, *J* = 2.3 Hz, 1H, PzC5), 7.82 (d, *J* = 2.4 Hz, 1H, PzA5), 7.41 (d, *J* = 7.3 Hz, 2H, H9), 7.32 (t, *J* = 7.4 Hz, 2H, H10), 7.26 (t, *J* = 7.2 Hz, 1H, H11), 7.13 (d, *J* = 2.2 Hz, 1H, PzC3), 6.41 (t, *J* = 2.3 Hz, 1H, PzA4), 6.36 (t, *J* = 2.1 Hz, 1H, PzB4), 6.28 (t, *J* = 2.3 Hz, 1H, PzC4), 5.52 (d, *J* = 10.4 Hz, 1H, H2), 5.36 (m, 1H, H5), 4.42 (d, *J* = 10.3 Hz, 1H, H7), 3.53 (dd, *J* = 11.1, 12.9 Hz, 1H, H6), 3.41 (bs, 2H, H19), 3.28 (s, 1H, H14), 3.10 (dd, *J* = 6.5, 12.9 Hz, 1H, H6), 3.02 (ddd, *J* = 3.8, 12.0, 14.4 Hz, 1H, H4), 2.91 (s, 3H, 13), 2.77 (m, 4H, H16/H17), 1.85 (s, 3H, Ms), 1.05 (d, *J*<sub>PH</sub> = 8.3 Hz, 9H, PMe<sub>3</sub>), 0.58 (d, *J* = 12.1 Hz, 1H, H3). Minor Complex – DHP **erythro-7D**.

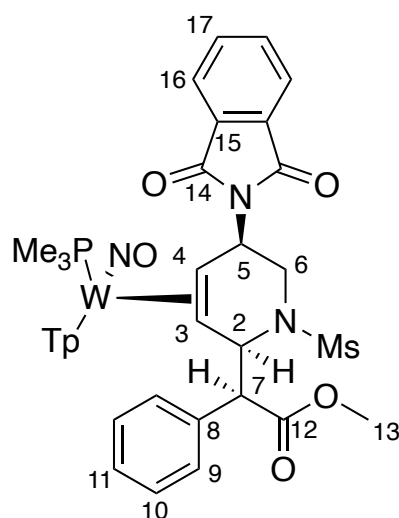
<sup>13</sup>C NMR (CD<sub>3</sub>CN, δ, 25 °C): 178.9 (2C, C15/C18), 173.2 (C12), 145.1 (PzA3), 143.5 (PzB3), 140.7 (PzC3), 138.7 (C8), 137.5 (2C, PzB5/C5), 137.3 (PzA5), 130.3 (2C, C9), 129.6 (2C, C10), 128.9 (C11), 107.5 (PzB4), 107.3 (PzA4), 107.0 (PzC4), 62.0 (C8), 58.7 (C2), 56.6 (C3), 51.7 (C13), 50.0 (C5), 45.6 (d, *J*<sub>PC</sub> = 12.0 Hz, C4), 40.6 (Ms), 40.1 (C6), 29.0. (2C, C16/C17), 14.0. (d, *J*<sub>PC</sub> = 30.8 Hz, 3C, PMe<sub>3</sub>).

IR: ν(NO) = 1553 cm<sup>-1</sup>, ν(Ester CO) = 1735 cm<sup>-1</sup>, ν(Amide CO) = 1695 cm<sup>-1</sup>

CV (MeCN; 100 mV/s): *E*<sub>p,a</sub> = +0.63V (NHE)

HRMS (ESI) *m/z*: [M]<sup>+</sup> Calcd for C<sub>31</sub>H<sub>43</sub>BN<sub>10</sub>O<sub>6</sub>PSW<sup>+</sup> due to H<sub>2</sub>O loss from McLafferty rearrangement of amide 909.2422; Found 909.2412.

**Synthesis and characterization of WTp(NO)(PMe<sub>3</sub>)( $\eta^2$ -(*N*-mesyl)-5-phthalimide-2-(methyl- $\alpha$ -phenylacetate)-1,2,5,6-tetrahydropyridine (15D)**



**Erythro-7D** (50 mg, 0.062 mmol) was dissolved in ~0.5 mL propionitrile in a test tube with a stir pea. HOTf (57 mg, 0.380 mmol) was added, and the mixture was allowed to stir at room temperature. The dark brown solution was cooled at -60 °C for 15 minutes. Phthalimide (46 mg, 0.312 mmol) was dissolved in 0.5 mL EtCN in a test tube with a stir pea, tBuOK/THF (20% wt., 70 mg, 0.125 mmol) was added and allowed to react for 10 minutes. The solution was then cooled to -60 °C for 15 minutes. The allyl solution was added to the deprotonated phthalimide solution and reacted for 12 hours at -60 °C. The solution was warmed to room temperature. The solution was diluted with DCM (10 mL), washed with Na<sub>2</sub>CO<sub>3</sub> (3 x 5 mL), and the aqueous solution was back extracted with DCM (3 x 2 mL). The solution was dried with Na<sub>2</sub>SO<sub>4</sub>, removed on a 15 mL medium porosity frit, washed with DCM (3 x 2 mL), and the resulting filtrate was evaporated to dryness. The product was dissolved in minimal DCM and added to a stirring solution of chilled hexanes (200 mL), yielding a precipitate. This precipitate was isolated on a 15 mL fine porosity frit, washed with hexanes (10mL), and desiccated to yield **15D** (42 mg, 73% yield).

<sup>1</sup>H NMR (CD<sub>3</sub>CN,  $\delta$ , 25 °C): 8.51 (bs, 1H, PzA3), 8.07 (d, *J* = 1.8 Hz, 1H, PzB3), 7.80-7.94 (m, 4H, H16/H17), 7.75 (d, *J* = 2.5 Hz, 1H, PzB5), 7.73 (d, *J* = 2.5, 3.1 Hz, 2H, PzC5/PzA5), 7.45 (d, *J* = 7.3 Hz, 2H, H9), 7.29 (t, *J* = 7.3 Hz, 2H, H10), 7.23 (t, *J* = 6.3 Hz, 1H, H11), 7.10 (d, *J* = 2.1 Hz, 1H, PzC3), 6.40 (t, *J* = 2.1 Hz, 1H, PzA4), 6.32



(t,  $J = 2.3$  Hz, 1H, PzB4), 6.20 (t,  $J = 2.3$  Hz, 1H, PzC4), 5.57 (d,  $J = 10.3$  Hz, 1H, H2), 5.55 (m, 1H, H5), 4.52 (d,  $J = 10.1$  Hz, 1H, H7), 3.58 (dd,  $J = 10.8, 12.7$  Hz, 1H, H6), 3.25 (dd,  $J = 6.7, 12.8$  Hz, 1H, H6), 3.11 (ddd,  $J = 3.8, 12.1, 14.3$  Hz, 1H, H4), 2.98 (s, 3H, H13), 1.92 (bs, 3H, Ms), 1.02 (d,  $J_{PH} = 8.4$  Hz, 9H, PMe<sub>3</sub>), 0.71 (d,  $J = 11.8$  Hz, 1H, H3). Minor Complex – DHP **erythro-7D**.

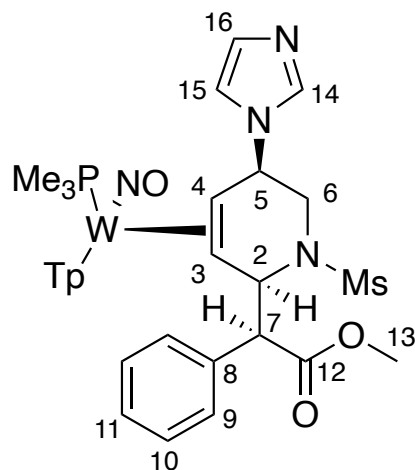
<sup>13</sup>C NMR (CD<sub>3</sub>CN,  $\delta$ , 25 °C): 172.7 (C12), 168.7 (2C, C14), 144.9 (PzA3A), 142.8 (PzB3), 139.8 (PzC3), 138.1 (C8), 136.6 (PzA5), 136.6 (PzC5), 136.3 (PzB5), 134.7 (2C, C16), 132.3 (2C, C15), 129.9 (2C, C9), 129.0 (2C, C10), 128.3 (C11), 123.7 (2C, C17), 106.8 (PzB4), 106.5 (PzC4), 106.5 (PzC4), 61.5 (C7), 58.4 (C2), 56.1 (C3), 51.5 (C13), 49.0 (C5), 45.7 (d,  $J_{PC} = 11.7$  Hz, C4), 40.8 (C6), 40.7 (Ms), 13.9 (d,  $J_{PC} = 28.6$  Hz, PMe<sub>3</sub>).

IR:  $\nu(\text{NO}) = 1557 \text{ cm}^{-1}$ ,  $\nu(\text{Ester CO}) = 1732 \text{ cm}^{-1}$ ,  $\nu(\text{Imide CO}) = 1705 \text{ cm}^{-1}$

CV (DMA; 100 mV/s):  $E_{p,a} = +0.58\text{V}$  (NHE)

HRMS (APCI)  $m/z$ :  $[M]^+$  Calcd for C<sub>35</sub>H<sub>43</sub>BN<sub>9</sub>O<sub>7</sub>PSW<sup>+</sup> 958.2262; Found 958.2270.

### Synthesis and characterization of WTp(NO)(PMe<sub>3</sub>)( $\eta^2$ -(*N*-mesyl)-5-imidazole-2-(methyl- $\alpha$ -phenylacetate)-1,2,5,6-tetrahydropyridine (16D)



**Erythro-7D** (250 mg, 0.308 mmol) was dissolved in 1 mL propionitrile in a test tube with a stir pea. HOTf (55.5 mg, 0.370 mmol) was added to form the allyl species, and the mixture was allowed to stir at room temperature. The dark brown solution was cooled at -30 °C for 15 minutes. Imidazole (210 mg, 3.08 mmol) was dissolved in 1.5 mL methanol in a test tube with a stir pea and cooled to -30 °C for 15 minutes. The

allyl solution was added to the imidazole solution and reacted for 12 hours at -30 °C. tBuOK/THF (20% wt, 346 mg, 0.617 mmol) was added at -30 °C and allowed to react for 10 minutes. The solution was warmed to room temperature. The solution was diluted with DCM (10 mL), washed with Na<sub>2</sub>CO<sub>3</sub> (3 x 5 mL), and the aqueous solution was back extracted with DCM (3 x 2 mL). The solution was dried with Na<sub>2</sub>SO<sub>4</sub>, removed on a 15 mL medium porosity frit, washed with DCM (3 x 2 mL), and the resulting filtrate was evaporated to dryness. The product was dissolved in minimal DCM and added to a stirring solution of hexanes (200 mL), yielding a precipitate. This precipitate was isolated on a 15 mL fine porosity frit, washed with hexanes (10 mL), and desiccated to yield **16D** (232 mg, 86% yield).

<sup>1</sup>H NMR (CD<sub>3</sub>CN, δ, 25 °C): 8.47 (bs, 1H, PzA3), 8.03 (d, *J* = 1.7 Hz, 1H, PzB3), 7.85 (bs, 1H, H14), 7.76 (d, *J* = 2.4 Hz, 1H, PzB5), 7.75 (d, *J* = 2.1 Hz, 1H, PzC5), 7.73 (d, *J* = 2.3 Hz, 1H, PzA5), 7.43 (bs, 1H, H15), 7.40 (d, *J* = 7.3 Hz, 2H, H9), 7.29 (t, *J* = 7.4 Hz, 2H, H10), 7.24 (t, *J* = 7.3 Hz, 1H, H11), 7.15 (bs, 1H, H16), 7.10 (d, *J* = 2.1 Hz, 1H, PzC3), 6.40 (d, *J* = 2.2 Hz, 1H, PzA4), 6.33 (t, *J* = 2.1 Hz, 1H, PzB4), 6.25 (t, *J* = 2.1 Hz, 1H, PzC4), 5.62 (dd, *J* = 1.7, 10.0 Hz, 1H, H2), 5.30 (m, 1H, H5), 4.14 (d, *J* = 10.0 Hz, 1H, H7), 3.47 (dd, *J* = 5.2, 13.1 Hz, 1H, H6), 3.05 (dd, *J* = 11.2, 13.1 Hz, 1H, H6), 2.94 (ddd, *J* = 4.6, 11.6, 14.0 Hz, 1H, H4), 2.88 (s, 3H, 13), 1.76 (s, 3H, Ms), 0.86 (d, *J*<sub>PH</sub> = 8.4 Hz, 9H, PMe<sub>3</sub>), 0.65 (d, *J* = 12.2 Hz, 1H, H3). Minor Complex – DHP **erythro-7D**.

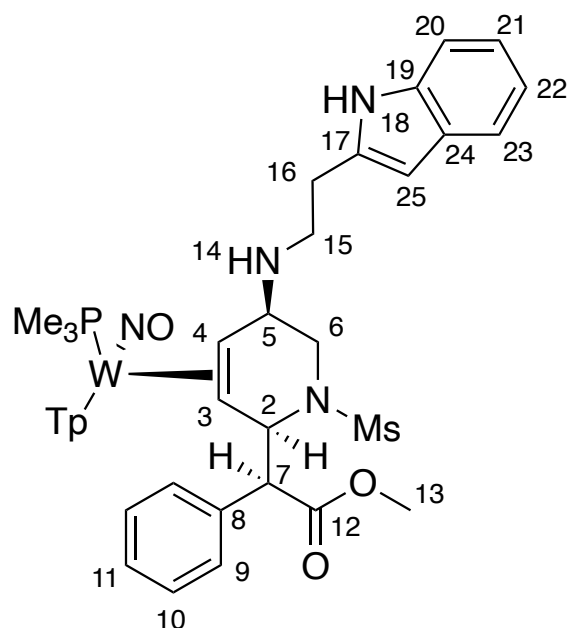
<sup>13</sup>C NMR (CD<sub>3</sub>CN, δ, 25 °C): 172.2 (C12), 144.8 (PzA3), 143.0 (PzB3), 139.7 (PzC3), 137.9 (C8), 137.1 (PzB5), 136.8 (C14), 136.7 (PzC5), 136.5 (PzA5), 130.2 (C16), 129.6 (2C, C9), 129.2 (2C, C10), 128.5 (C11), 118.2 (C15), 106.9 (PzB4), 106.6 (PzA4), 106.6 (PzC4), 62.0 (C7), 58.5 (C2), 56.2 (C5), 54.5 (C3), 51.5 (C13), 48.6 (d, *J*<sub>PC</sub> = 12.6 Hz, C4), 47.2 (C6), 40.7 (Ms), 13.6 (d, *J*<sub>PC</sub> = 28.4 Hz, 3C, PMe<sub>3</sub>).

IR: ν(NO) = 1563 cm<sup>-1</sup>, ν(Ester CO) = 1728 cm<sup>-1</sup>

CV (DMA; 100 mV/s): *E*<sub>p,a</sub> = +0.57V (NHE)

HRMS (APCI) *m/z*: [M]<sup>+</sup> Calcd for C<sub>30</sub>H<sub>41</sub>BN<sub>10</sub>O<sub>5</sub>PSW<sup>+</sup> 879.2317; Found 879.2318.

**Synthesis and characterization of WTp(NO)(PMe<sub>3</sub>)( $\eta^2$ -(*N*-mesyl)-5-tryptamine - 2-(methyl- $\alpha$ -phenylacetate)-1,2,5,6-tetrahydropyridine (17D)**



**Erythro-7D** (100 mg, 0.123 mmol) was dissolved in ~0.5 mL propionitrile in a test tube with a stir pea. HOTf (24 mg, 0.160 mmol) was added, and the mixture was allowed to stir at room temperature. The dark brown solution was cooled at -50 °C for 15 minutes. Tryptamine (85 mg, 0.531 mmol) was dissolved in 0.5 mL EtCN in a test tube with a stir pea, tBuOK/THF (20% wt., 114 mg, 0.203 mmol) was added and allowed to react for 10 minutes. The solution was then cooled to -50 °C for 15 minutes. The allyl solution was added to the deprotonated tryptamine solution and reacted for 12 hours at -40 °C. The solution was warmed to room temperature. The solution was diluted with DCM (10 mL), washed with Na<sub>2</sub>CO<sub>3</sub> (3 x 5 mL), and the aqueous solution was back extracted with DCM (3 x 2 mL). The solution was dried with MgSO<sub>4</sub>, removed on a 15 mL medium porosity frit, washed with DCM (3 x 2 mL), and the resulting filtrate was evaporated to dryness. The product was dissolved in minimal DCM and added to a stirring solution of chilled pentanes (200 mL), yielding a precipitate. This precipitate was isolated on a 15 mL fine porosity frit, washed with pentanes (10 mL), and desiccated to yield **17D** (103 mg, 88% yield).

<sup>1</sup>H NMR (CD<sub>2</sub>Cl<sub>2</sub>, δ, 25 °C): 8.52 (bs, 1H, H18), 8.38 (d, *J* = 1.5 Hz, 1H, PzA3), 8.01 (d, *J* = 1.9 Hz, 1H, PzB3), 7.73 (d, *J* = 2.3 Hz, 1H, PzB5), 7.71 (d, *J* = 2.2 Hz, 1H,

PzC5), 7.68 (d,  $J = 2.4$  Hz, 1H, PzA5), 7.64 (d,  $J = 7.8$  Hz, 1H, H23), 7.38 (d,  $J = 8.0$  Hz, 1H, H20), 7.36 (d,  $J = 7.2$  Hz, 2H, H9), 7.25 (t,  $J = 7.2$  Hz, 2H, H10), 7.21 (t,  $J = 7.2$  Hz, 1H, H11), 7.16 (t,  $J = 7.9$  Hz, 1H, H22), 7.11 (d,  $J = 7.2$  Hz, PzC3), 7.09 (t,  $J = 8.1$  Hz, 1H, H21), 7.07 (d,  $J = 2.2$  Hz, 1H, H25), 6.32 (t,  $J = 2.3$  Hz, 1H, PzA4), 6.28 (t,  $J = 2.0$  Hz, 1H, PzB4), 6.20 (t,  $J = 2.2$  Hz, 1H, PzC4), 5.50 (d,  $J = 9.4$  Hz, 1H, H2), 4.02 (d,  $J = 9.5$  Hz, 1H, H7), 3.56-3.83 (m, 1H, H5), 3.64 (dd,  $J = 4.8, 12.6$  Hz, 1H, H6), 3.27 (dt,  $J = 6.8, 13.8$ , 1H, H15), 3.00 (td,  $J = 6.47, 13.83$  Hz, 1H, H17), 2.98 (td,  $J = 6.87, 13.95$  Hz, 1H, H17), 2.88 (dt,  $J = 6.7, 10.9$  Hz, 1H, H15), 2.84 (s, 3H, H9), 2.47-2.42 (m, 2H, H6/H4), 1.92 (s, 3H, H7), 1.43 (bs, 1H, H14), 1.18 (d,  $J_{PH} = 8.7$  Hz, 9H, PMe<sub>3</sub>), 0.47 (d,  $J = 11.7$  Hz, 1H, H3).

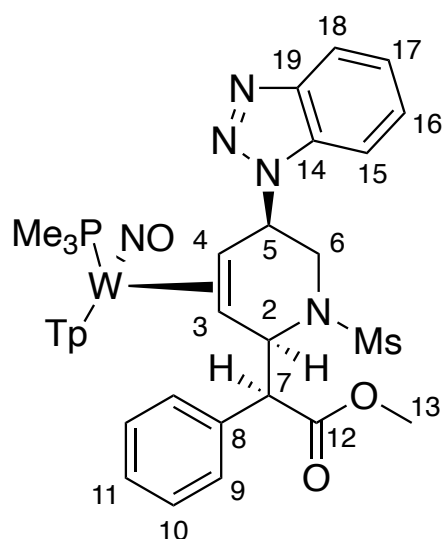
<sup>13</sup>C NMR (CD<sub>2</sub>Cl<sub>2</sub>,  $\delta$ , 25 °C): 172.5 (C12), 144.4 (PzA3), 143.6 (PzB3), 140.1 (PzC3), 138.0 (C8) 136.9 (C24), 136.5 (PzB5), 136.4 (PzC5), 136.0 (PzA5), 129.9 (2C, C9), 128.8 (2C, C10), 128.1 (C11), 128.1 (C19), 122.7 (C25), 122.0 (2C, C22), 119.3 (2C, C21), 119.2 (2C, C23), 111.6 (2C, C20), 114.4 (C17), 106.4 (PzB4), 106.3 (PzA4), 106.2 (PzC4), 62.2 (C7), 58.9 (C2), 56.5 (C5), 54.9 (C3), 51.8 (d,  $J_{PC} = 13.4$  Hz, C4), 51.2 (C13), 47.4 (C15), 46.0 (C6), 40.5 (Ms), 27.1 (C16), 14.2 (d,  $J_{PC} = 28.9$  Hz, 3C, PMe<sub>3</sub>).

IR:  $\nu(\text{NO}) = 1563 \text{ cm}^{-1}$ ,  $\nu(\text{Ester CO}) = 1725 \text{ cm}^{-1}$

CV (DMA; 100 mV/s):  $E_{p,a} = +0.59\text{V}$  (NHE)

HRMS (APCI)  $m/z$ :  $[\text{M}]^+$  Calcd for C<sub>37</sub>H<sub>49</sub>BN<sub>10</sub>O<sub>5</sub>PSW<sup>+</sup> 971.2943; Found 971.2922.

**Synthesis and characterization of WTp(NO)(PMe<sub>3</sub>)( $\eta^2$ -(*N*-mesyl)-5-benzotriazole-2-(methyl- $\alpha$ -phenylacetate)-1,2,5,6-tetrahydropyridine (18D)**



**Erythro-7D** (50 mg, 0.062 mmol) was dissolved in 1ml propionitrile in a test tube with a stir pea. HOTf/MeCN (0.6 M, 260 mg, 0.093mmol) was added, and the mixture was allowed to stir at room temperature. The dark brown solution was cooled at -40 °C for 15 minutes. Benzotriazole (40 mg, 0.311 mmol) was dissolved in 0.5 mL THF in a test tube with a stir pea, tBuOK/THF (20% wt, 104 mg, 0.185 mmol) as added and allowed to react for 10 minutes. The solution was then cooled to -40 °C for 15 minutes. The allyl solution was added to the deprotonated benzotriazole solution and reacted for 12 hours at -40 °C. The solution was warmed to room temperature. The solution was diluted with DCM (10 mL), washed with Na<sub>2</sub>CO<sub>3</sub> (3 x 5 mL), and the aqueous solution was back extracted with DCM (3 x 2mL). The solution was dried with MgSO<sub>4</sub>, removed on a 15 mL medium porosity frit, washed with DCM (3 x 2 mL), and the resulting filtrate was evaporated to dryness. The product was dissolved in minimal DCM and added to a stirring solution of hexanes (75 mL), yielding a precipitate. This precipitate was isolated on a 15 mL fine porosity frit, washed with hexanes (10 mL), and desiccated to yield **18D** (31 mg, 54% yield).

<sup>1</sup>H NMR (CD<sub>2</sub>Cl<sub>2</sub>, δ, 25 °C): 8.52 (bs, 1H, PzA3), 8.07 (d, *J* = 1.6 Hz, 1H, PzB3), 7.96 (d, 2H, H15/H18), 7.77 (d, *J* = 2.3 Hz, 1H, PzB5), 7.74-7.76 (m, 2H, PzA5/C5), 7.45 (m, 4H, H9/H16/H17), 7.31 (t, *J* = 7.6 Hz, 2H, H10), 7.25 (t, *J* = 7.3 Hz, 1H, H11), 7.15

(d,  $J = 1.8$  Hz, 1H, PzC3), 6.43 (t,  $J = 2.2$  Hz, 1H, PzA4), 6.33 (t,  $J = 2.2$  Hz, 1H, PzB4), 6.23 (t,  $J = 2.2$  Hz, 1H, PzC4), 6.09 (ddd,  $J = 4.5, 10.2, 15.4$  Hz, 1H, H5), 5.67 (d,  $J = 10.1$  Hz, 1H, H2), 4.23 (d,  $J = 10.1$  Hz, 1H, H7), 3.63 (dd,  $J = 5.1, 12.9$  Hz, 1H, H6), 3.56 (ddd,  $J = 4.7, 11.6, 14.6$  Hz, 1H, H4), 3.50 (dd,  $J = 11.0, 12.8$  Hz, 1H, H6), 2.90 (s, 3H, H13), 1.79 (s, 3H, Ms), 0.78 (d,  $J_{PH} = 8.3$  Hz, 9H, PMe<sub>3</sub>), 0.68 (d,  $J = 7.7$  Hz, 1H, H3).

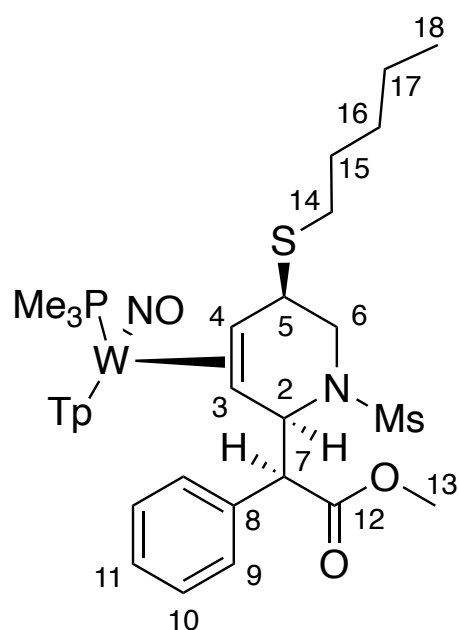
<sup>13</sup>C NMR (CD<sub>2</sub>Cl<sub>2</sub>,  $\delta$ , 25 °C): 172.1 (C12), 144.8 (4C, PzA3/C14/C19), 143.2 (PzB3), 140.1 (PzC3), 138.0 (C8), 136.7 (2C, PzA5/B5/C5), 136.4 (PzA5/B5/C5), 129.7 (2C, C9), 129.1 (2C, C10), 128.4 (C11), 126.7 (2C, C16/C17), 118.5 (2C, C15/C18), 106.8 (PzB4), 106.6 (PzA4), 106.5 (PzC4), 68.1, (C5), 65.6 (C7), 62.0 (C2), 58.9 (C3), 51.5 (C13), 47.8 (C4), 46.0 (C6), 40.7 (Ms), 13.5 (d,  $J_{PC} = 8.4$  Hz, 3C, PMe<sub>3</sub>).

IR:  $\nu(\text{NO}) = 1568 \text{ cm}^{-1}$ ,  $\nu(\text{Ester CO}) = 1731 \text{ cm}^{-1}$

CV (DMA; 100 mV/s):  $E_{p,a} = +0.67 \text{ V}$  (NHE)

HRMS (APCI)  $m/z$ : [M]<sup>+</sup> Calcd for C<sub>33</sub>H<sub>42</sub>BN<sub>11</sub>O<sub>5</sub>PSW<sup>+</sup> 930.2426; Found 930.2438.

### Synthesis and characterization of WTp(NO)(PMe<sub>3</sub>)( $\eta^2$ -(*N*-mesyl)-5-pentyl sulfide-2-(methyl- $\alpha$ -phenylacetate)-1,2,5,6-tetrahydropyridine (19D)



**Erythro-7D** (100 mg, 0.123 mmol) was dissolved in 1 mL propionitrile in a test tube with a stir pea. HOTf/MeCN (30 mg, 0.200 mmol) was added, and the mixture was allowed to stir at room temperature. The dark brown solution was cooled at -50 °C for 15 minutes. Pentanethiol (90 mg, 0.864 mmol) was dissolved in 0.5 mL THF in a test tube with a stir pea, tBuOK/THF (20% wt, 208 mg, 0.371 mmol) was added and allowed to react for 10 minutes. The solution was then cooled to -50 °C for 15 minutes. The allyl solution was added to the deprotonated pentanethiol solution and reacted for 12 hours at -50 °C. The solution was warmed to room temperature. The solution was diluted with DCM (10 mL), washed with Na<sub>2</sub>CO<sub>3</sub> (3 x 5 mL), and the aqueous solution was back extracted with DCM (3 x 2 mL). The solution was dried with Na<sub>2</sub>SO<sub>4</sub>, removed on a 15 mL medium porosity frit, washed with DCM (3 x 2 mL), and the resulting filtrate was evaporated to dryness. The product was dissolved in minimal DCM and added to a stirring solution of chilled stirring pentanes (75 mL), yielding a precipitate. This precipitate was isolated on a 15 mL fine porosity frit, washed with pentanes (10 mL), and desiccated to yield **19D** (44 mg, 40% yield).

<sup>1</sup>H NMR ((CD<sub>3</sub>)<sub>2</sub>CO, δ, 25 °C): 8.45 (bs, 1H, PzA3), 8.09 (d, *J* = 1.5 Hz, 1H, PzB3), 7.94 (d, *J* = 2.1 Hz, 1H, PzC5), 7.92 (d, *J* = 2.4 Hz, 1H, PzB5), 7.82 (d, *J* = 2.4 Hz, 1H, PzA5), 7.42 (d, *J* = 7.4 Hz, 2H, H9), 7.31 (d, *J* = 1.5 Hz, 1H, PzC3), 7.25 (t, *J* = 7.2 Hz, 2H, H10), 7.22 (t, *J* = 7.5 Hz, 1H, H11), 6.37 (t, *J* = 2.2 Hz, 1H, PzB4), 6.34 (m, 2H, PzC4/PzA4), 5.57 (dd, *J* = 1.7, 9.4 Hz, 1H, H2), 4.1 (d, *J* = 9.6 Hz, 1H, H7), 3.93 (ddd, *J* = 5.4, 10.3, 15.7 Hz, 1H, H5), 3.61 (dd, *J* = 4.9, 13.4 Hz, 1H, H6), 3.03 (dd, *J* = 10.9, 13.4 Hz, 1H, H6), 2.87 (s, 3H, H13), 2.72 (m, 3H, H4/H14), 2.00 (s, 3H, Ms), 1.74-1.64 (m, 2H, H15), 1.48-1.41 (m, 2H, H16/H17), 1.41-1.34 (m, 2H, H16/H17), 1.38 (d, *J*<sub>PH</sub> = 8.70 Hz, 9H, PMe<sub>3</sub>), 0.92 (t, *J* = 7.3 Hz, 3H, H18), 0.58 (d, *J* = 11.5 Hz, 1H, H3).

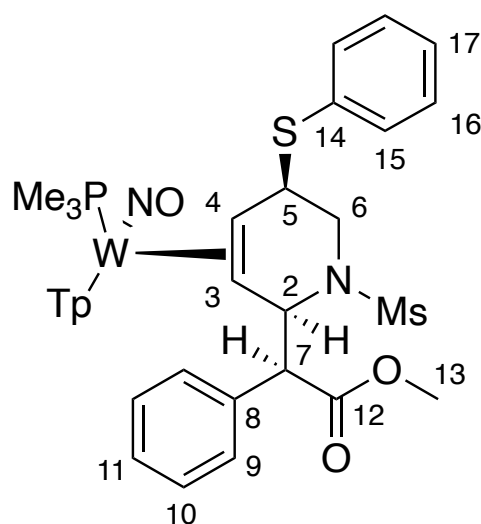
<sup>13</sup>C NMR ((CD<sub>3</sub>)<sub>2</sub>CO, δ, 25 °C): 172.6 (C12), 145.1 (PzA3), 144.3 (PzB3), 141.4 (PzC3), 138.9 (C8), 137.4 (PzC5), 137.3 (PzB5), 137.0 (PzA5), 130.6 (2C, C9), 129.3 (2C, C10), 128.5 (C11), 107.12/107.08 (PzC4/PzA4), 62.8 (C7), 59.1 (C2), 55.8 (C3), 51.4 (C13), 48.1 (d, *J*<sub>PC</sub> = 14.0 Hz, C4), 47.3 (C6), 43.9 (C5), 41.0 (Ms), 32.2/23.1 (2C, C16/C17), 31.7 (C14), 30.6 (C15), 14.4 (C18), 14.3 (d, *J*<sub>PC</sub> = 28.8 Hz, 3C, PMe<sub>3</sub>).

IR: ν(NO) = 1567 cm<sup>-1</sup>, ν(Ester CO) = 1732 cm<sup>-1</sup>

CV (DMA; 100 mV/s): *E*<sub>p,a</sub> = +0.54V (NHE)

HRMS (APCI)  $m/z$ :  $[M]^+$  Calcd for  $C_{32}H_{49}BN_8O_5PS_2W^+$  915.2602; Found 915.2581.  
SC-XRD data on S70.

**Synthesis and characterization of  $W Tp(NO)(PMe_3)(\eta^2-(N\text{-mesyl})\text{-}5\text{-benzyl sulfide-}2\text{-(methyl-}\alpha\text{-phenylacetate)-}1,2,5,6\text{-tetrahydropyridine (20D)}$**



**Erythro-7D** (100 mg, 0.123 mmol) was dissolved in 1 ml propionitrile in a test tube with a stir pea. HOTf/MeCN (30 mg, 0.200 mmol) was added, and the mixture was allowed to stir at room temperature. The dark brown solution was cooled at  $-40\text{ }^{\circ}\text{C}$  for 15 minutes. Benzenethiol (100 mg, 0.908 mmol) was dissolved in 0.5 mL THF in a test tube with a stir pea, tBuOK/THF (20% wt, 208 mg, 0.371 mmol) was added and allowed to react for 10 minutes. The solution was then cooled to  $-40\text{ }^{\circ}\text{C}$  for 15 minutes. The allyl solution was added to the deprotonated benzenethiol solution and reacted for 12 hours at  $-60\text{ }^{\circ}\text{C}$ . The solution was warmed to room temperature. The solution was diluted with DCM (10 mL), washed with  $Na_2CO_3$  (3 x 5 mL), and the aqueous solution was back extracted with DCM (3 x 2 mL). The solution was dried with  $MgSO_4$ , removed on a 15 mL medium porosity frit, washed with DCM (3 x 2 mL), and the resulting filtrate was evaporated to dryness. The product was dissolved in minimal DCM and added to a stirring solution of hexanes (75 mL), yielding a precipitate. This precipitate was isolated on a 15 mL fine porosity frit, washed with hexanes (10 mL), and desiccated to yield **20D** (34 mg, 31% yield).



$^1\text{H}$  NMR ( $(\text{CD}_3)_2\text{CO}$ ,  $\delta$ , 25  $^\circ\text{C}$ ): 8.53 (d,  $J$  = 1.5 Hz, 1H, PzA3), 8.10 (d,  $J$  = 2.2 Hz, 1H, PzB3), 7.97 (d,  $J$  = 2.2 Hz, 1H, PzC5), 7.94 (d,  $J$  = 2.2 Hz, 1H, PzB5), 7.85 (d,  $J$  = 2.8 Hz, 1H, PzA5), 7.48 (d,  $J$  = 8.7 Hz, 2H, H15), 7.44 (d,  $J$  = 7.7 Hz, 2H, H9), 7.37 (d,  $J$  = 2.2 Hz, 1H, PzC3), 7.32 (t,  $J$  = 7.7 Hz, 2H, H10), 7.26 (t,  $J$  = 7.7 Hz, 2H, H16), 7.23 (t,  $J$  = 7.2 Hz, 1H, H11), 7.19 (t,  $J$  = 7.0 Hz, 1H, H17), 6.38-6.37 (m, 2H, PzA4/PzB4), 6.36 (t,  $J$  = 2.2 Hz, 1H, PzC4), 5.60 (d,  $J$  = 9.8 Hz, 1H, H2), 4.60 (m,  $J$  = 4.5, 9.9 Hz, 1H, H5), 4.14 (d,  $J$  = 9.7 Hz, 1H, H7), 3.57 (dd,  $J$  = 4.7, 13.6 Hz, 1H, H6), 3.06 (dd,  $J$  = 10.8, 13.6 Hz, 1H, H6), 2.85 (s, 3H, H13), 2.77 (m, 1H, H4), 1.83 (s, 3H, Ms), 1.36 (d,  $J_{\text{PH}}$  = 8.5 Hz, 9H,  $\text{PMe}_3$ ), 0.59 (d,  $J$  = 10.9 Hz, 1H, H3).

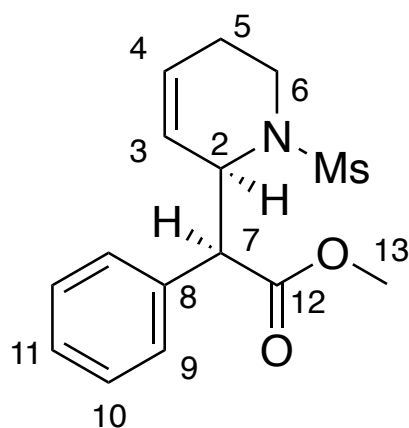
$^{13}\text{C}$  NMR ( $(\text{CD}_2\text{Cl}_2)$ ,  $\delta$ , 25  $^\circ\text{C}$ ): 172.2 (C12), 144.8 (PzA3), 143.7 (PzB3), 140.3 (PzC3), 138.1/136.4 (2C, C8/C14), 136.7 (PzC5), 136.7 (PzB5), 136.3 (PzA5), 129.0 (2C, C15), 129.7 (2C, C9), 129.6 (2C, C10), 128.9 (2C, C16), 128.3 (C11), 126.2 (C17), 106.5/106.4 (2C, PzA4/PzB4), 106.4 (PzC4), 62.0 (C7), 58.8 (C2), 55.6 (C3), 51.3 (C13), 46.5 (m, 2C, C4/C6), 43.60 (C5), 40.6 (Ms), 14.5 (d,  $J_{\text{PC}}$  = 30.8 Hz, 3C,  $\text{PMe}_3$ ).

IR:  $\nu(\text{NO})$  = 1559  $\text{cm}^{-1}$ ,  $\nu(\text{Ester CO})$  = 1732  $\text{cm}^{-1}$

CV (DMA; 100 mV/s):  $E_{\text{p,a}}$  = +0.59V (NHE)

HRMS (APCI)  $m/z$ :  $[\text{M}]^+$  Calcd for  $\text{C}_{33}\text{H}_{44}\text{BN}_8\text{O}_5\text{PS}_2\text{W}^+$  921.2132; Found 921.2136

### Synthesis and characterization of (*N*-mesyl)-2-(methyl- $\alpha$ -phenylacetate)-1,2,5,6-tetrahydropyridine (21-Ms)



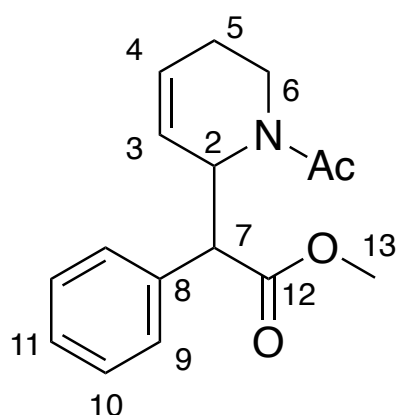
Acetone (3 mL), 2,3-dichloro-5,6-dicyano-1,4-benzoquinone (DDQ) (130 mg, 0.573 mmol), and **9D** (107 mg, 0.132 mmol) were added to a 4-dram vial containing a stir pea. The reaction was stirred in a fume hood for 4 hours. The solution was flushed through a 1 cm basic alumina plug set up in a 30 mL coarse porosity frit. This solution was diluted with 30 mL of DCM and was washed 3x with 50 mL of saturated aqueous NaHCO<sub>3</sub>. The organic layer was isolated and set aside. The combined aqueous layers were combined and back-extracted with 30 mL of DCM to prevent loss of product. The organic layers were combined in a single round-bottom flask to which 5 grams of basic alumina powder were added. The solution was then reduced off *in vacuo*, bringing the eluted organic into the basic alumina powder. This powder was then dry loaded onto an 8-gram Teledyne basic alumina column, upon which clean product was eluted off with 40% ethyl acetate in hexanes. The tubes containing organic were combined and reduced *in vacuo*, yielding a white residue (20 mg, 49% yield).

<sup>1</sup>H NMR ((CD<sub>3</sub>)<sub>2</sub>CO, δ, 25 °C): 7.45 (d, *J* = 7.2 Hz, 2H, H9), 7.36 (t, *J* = 7.8 Hz, 2H, H10), 7.31 (tt, *J* = 2.0, 7.4 Hz, 1H, H11), 5.95-5.98 (m, 1H, H4), 5.85-5.88 (m, 1H, H3), 4.90 (d, *J* = 10.7 Hz, 1H, H2), 3.89 (d, *J* = 10.7 Hz, 1H, H7), 3.68 (s, 3H, H13), 3.60 (ddd, *J* = 0.9, 6.5, 14.6 Hz, 1H, H6), 3.26 (ddd, *J* = 4.4, 11.9, 14.50 Hz, 1H, H6), 2.31-2.37 (m, 1H, H5), 2.06 (s, 3H, Ms), 2.00 (dt, *J* = 4.9 18.1 Hz, 1H, H5).

<sup>13</sup>C NMR ((CD<sub>3</sub>)<sub>2</sub>CO δ, 25 °C): 172.8 (C12), 137.6 (C8), 129.8 (2C, C9), 129.4 (2C, C10), 128.7 (C11), 128.5 (C4), 127.3 (C3), 56.5 (C7), 56.1 (C2), 52.5 (C13), 39.8 (Ms), 39.0 (C6), 24.7 (C5).

SC-XRD data on S71.

**Synthesis and characterization of (*N*-acetyl)-2-(methyl- $\alpha$ -phenylacetate)-1,2,5,6-tetrahydropyridine (**21-Ac**)**



**9D-Ac** (90 mg, 0.12 mmol) was dissolved in MeCN (3.0 mL) in a 4 dram vial containing a stir pea. Separately, DDQ (50 mg, 0.22 mmol) was dissolved in MeCN (1.0 mL). The DDQ solution was added to the solution of **9D-Ac**, and the resulting mixture was stirred for 5 min. The reaction mixture was then diluted with DCM (50 mL) and extracted with saturated aqueous NaHCO<sub>3</sub> (50 mL). The aqueous layer was back-extracted with DCM (15 mL), and the combined organic layers were dried with Na<sub>2</sub>SO<sub>4</sub>. The solids were filtered off on a 30 mL medium fritted funnel, and rinsed with DCM (10 mL). The filtrate was evaporated on a rotary evaporator. The residue was dissolved in DCM (2 mL) and added to stirring Et<sub>2</sub>O (100 mL). The precipitate was filtered off on a 30 mL medium porosity fritted funnel and rinsed with Et<sub>2</sub>O (10 mL). The filtrate was evaporated onto silica on a rotary evaporator. The desired product was purified by Combiflash flash chromatography using a 0-100% EtOAc in hexanes gradient 30 mL/min elution on a 12 g silica column. The desired product eluted at ~48% EtOAc. The fractions containing the product were combined and evaporated on a rotary evaporator. The residue was desiccated under high vacuum for 30 min to yield compound **21-Ac** as a colorless oil (22 mg, 66%).

*Erythro* isomer: A mixture of two rotamers **A**:**B** = 4:3. <sup>1</sup>H NMR (CDCl<sub>3</sub>,  $\delta$ , 25 °C): **A** 7.45-7.25 (m, 5H, H<sub>9</sub>-H<sub>11</sub>), 6.00 (m, 1H, H<sub>4</sub>), 5.88 (m, 1H, H<sub>3</sub>), 4.72 (dd, *J* = 13.1, 6.2 Hz, 1H, H<sub>6</sub>), 4.60 (m, 1H, H<sub>2</sub>), 3.87 (d, *J* = 10.4 Hz, 1H, H<sub>7</sub>), 3.76 (s, 3H, H<sub>13</sub>), 2.83 (m, 1H, H<sub>6'</sub>), 2.27 (m, 1H, H<sub>5</sub>), 2.04 (dt, *J* = 5.0, 18.1 Hz, 1H, H<sub>5'</sub>), 1.44 (s, 3H, *N*-Ac). **B** 7.45-7.25 (m, 5H, H<sub>9</sub>-H<sub>11</sub>), 5.88 (m, 1H, H<sub>4</sub>), 5.85 (m, 1H, H<sub>3</sub>), 5.60 (m,

1H, H2), 3.89 (d,  $J$  = 9.4 Hz, 1H, H7), 3.64 (dd,  $J$  = 13.9, 5.9 Hz, 1H, H6), 3.72 (s, 3H, H13), 3.22 (ddd,  $J$  = 4.2, 12.9, 13.9 Hz, 1H, H6'), 2.27 (m, 1H, H5), 1.96 (dt,  $J$  = 5.0, 18.3 Hz, 1H, H5'), 1.90 (s, 3H, *N*-Ac).

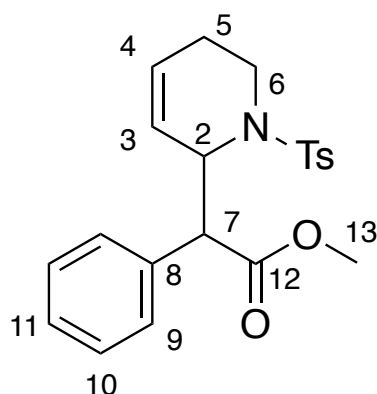
$^{13}\text{C}$  NMR ( $\text{CDCl}_3$ ,  $\delta$ ): **A** 172.0 (C12), 170.0 (*N*-Ac), 135.3 (C8), 129.1 (C9), 128.5 (C10), 127.8 (C11), 129.2 (C4), 126.2 (C3), 57.2 (C2), 55.3 (C7), 52.4 (C13), 34.8 (C6), 24.9 (C5), 20.9 (*N*-Ac). **B** 172.4 (C12), 169.1 (*N*-Ac), 134.8 (C8), 128.8 (C9), 128.4 (C10), 127.8 (C11), 126.6 (C3), 126.2 (C4), 55.3 (C7), 52.4 (C13), 51.6 (C2), 40.3 (C6), 24.5 (C5), 21.6 (*N*-Ac).

*Threo* isomer: A mixture of two rotamers **A**:**B** = 1:1.  $^1\text{H}$  NMR ( $\text{CDCl}_3$ ,  $\delta$ ): **A** 7.45-7.25 (m, 5H, H9-H11), 5.85 (m, 1H, H4), 5.27 (m, 1H, H3), 4.79 (m, 1H, H2), 4.66 (dd,  $J$  = 6.4, 13.5 Hz, 1H, H6), 3.94 (d,  $J$  = 10.2 Hz, 1H, H7), 3.69 (s, 3H, H13), 2.82 (m, 1H, H6'), 2.32 (s, 3H, *N*-Ac), 2.22 (m, 1H, H5), 2.08 (dt,  $J$  = 4.4, 17.2 Hz, 1H, H5'). **B** 7.45-7.25 (m, 5H, H9-H11), 5.85 (m, 1H, H4), 5.69 (m, 1H, H3), 5.54 (m, 1H, H2), 4.07 (d,  $J$  = 7.8 Hz, 1H, H7), 3.67 (s, 3H, H13), 3.54 (dd,  $J$  = 5.8, 13.8 Hz, 1H, H6), 2.63 (ddd,  $J$  = 3.9, 12.7, 14.1 Hz, 1H, H6'), 2.13 (s, 3H, *N*-Ac), 2.13 (m, 1H, H5), 1.90 (buried, 1H, H5').

$^{13}\text{C}$  NMR ( $\text{CDCl}_3$ ,  $\delta$ ): **A** 172.3 (C12), 170.6 (*N*-Ac), 135.3 (C8), 129.0 (C9), 128.6 (C4), 128.4 (C10), 128.3 (C11), 125.6 (C3), 57.3 (C2), 54.5 (C7), 52.3 (C13), 35.1 (C6), 24.6 (C5), 21.7 (*N*-Ac). **B** 172.5 (C12), 169.4 (*N*-Ac), 135.3 (C8), 129.9 (C9), 128.8 (C10), 128.4 (C11), 127.3 (C4), 126.2 (C3), 56.5 (C7), 52.3 (C2), 52.2 (C13), 40.5 (C6), 25.3 (C5), 22.1 (*N*-Ac).

ESI-MS: obs'd (%), calc'd (%), ppm, ( $\text{M}+\text{H}$ ) $^+$ : 274.1439 (100), 274.1438 (100), 0.4.  
SC-XRD data on S72.

## Synthesis and characterization of (*N*-tosyl)-2-(methyl- $\alpha$ -phenylacetate)-1,2,5,6-tetrahydropyridine (**21-Ts**)



**9D-Ts** (70 mg, 0.0788 mmol) was dissolved in MeCN (3.0 mL) in a 4 dram vial containing a stir pea. Separately, DDQ (40 mg, 0.176 mmol) was dissolved in MeCN (1.0 mL). The DDQ solution was added to the solution of **9D-Ts**, and the resulting mixture was stirred for 5 min. The reaction mixture was then diluted with DCM (50 mL) and extracted with saturated aqueous NaHCO<sub>3</sub> (50 mL). The aqueous layer was back-extracted with DCM (15 mL), and the combined organic layers were dried with Na<sub>2</sub>SO<sub>4</sub>. The solids were filtered off on a 30 mL medium fritted funnel, and rinsed with DCM (10 mL). The filtrate was evaporated on a rotary evaporator. The residue was dissolved in DCM (2 mL) and added to stirring Et<sub>2</sub>O (100 mL). The precipitate was filtered off on a 30 mL medium porosity fritted funnel and rinsed with Et<sub>2</sub>O (10 mL). The filtrate was evaporated onto silica on a rotary evaporator. The desired product was purified by Combiflash flash chromatography using a 0-100% EtOAc in hexanes gradient 30 mL/min elution on a 12 g silica column. The desired product eluted at ~48% EtOAc. The fractions containing the product were combined and evaporated on a rotary evaporator. The residue was desiccated under high vacuum for 30 min to yield compound **21-Ts** as a colorless oil which spontaneously crystallized (19 mg, 62%).

Two diastereomers **A**:**B**.

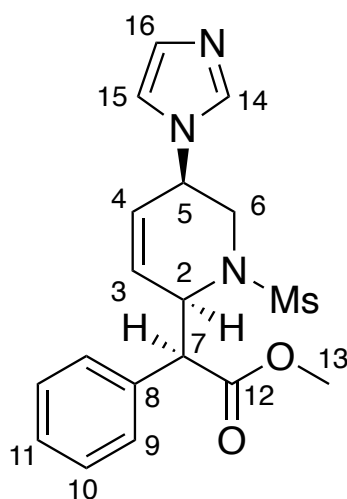
<sup>1</sup>H NMR (CDCl<sub>3</sub>,  $\delta$ , 25 °C): **A** 7.72 (d,  $J$  = 8.3 Hz, 2H, Ts), 7.36-7.28 (m, 5H, H<sub>9</sub>-H<sub>11</sub>), 7.25 (d,  $J$  = 8.3 Hz, 2H, Ts), 5.63 (m, 1H, H<sub>4</sub>), 5.54 (m, 1H, H<sub>3</sub>), 5.03 (m, 1H, H<sub>2</sub>), 4.00 (d,  $J$  = 8.2 Hz, 1H, H<sub>7</sub>), 3.68 (dd,  $J$  = 14.8, 6.4 Hz, 1H, H<sub>6</sub>), 3.66 (s, 3H, H<sub>13</sub>),

2.69 (dd,  $J = 14.8, 4.6$  Hz, 1H, H6'), 2.40 (s, 3H, Ts), 1.71 (m, 1H, H5), 1.58 (ddd,  $J = 18.0, 6.4, 4.6$  Hz, 1H, H5'). **B** 7.36-7.28 (m, 5H, H9-H11), 7.23 (d,  $J = 8.3$  Hz, 2H, Ts), 7.07 (d,  $J = 8.3$  Hz, 2H, Ts), 6.84 (m, 1H, H3), 5.79 (m, 1H, H4), 5.03 (m, 1H, H2), 3.80 (d,  $J = 9.8$  Hz, 1H, H7), 3.69 (s, 3H, H13), 3.54 (dd,  $J = 14.8, 6.4$  Hz, 1H, H6), 3.07 (ddd,  $J = 14.8, 12.0, 4.6$  Hz, 1H, H6'), 2.35 (s, 3H, Ts), 2.06 (m, 1H, H5), 1.80 (ddd,  $J = 18.0, 6.4, 4.6$  Hz, 1H, H5').

$^{13}\text{C}$  NMR ( $\text{CDCl}_3$ ,  $\delta$ ): **A** 171.9 (C12), 143.4 (Ts), 138.3 (Ts), 134.8 (C8), 129.7 (Ts), 129.7 (C09), 128.6 (C10), 128.0 (Ts), 127.2 (C11), 127.1 (C3), 125.0 (C4), 57.5 (C7), 55.3 (C2), 52.3 (C13), 38.8 (C6), 22.7 (C5), 21.6 (Ts). **B** 172.2 (C12), 143.1 (Ts), 137.4 (Ts), 135.6 (C8), 129.4 (C09), 129.0 (C10), 128.8 (Ts), 128.0 (Ts), 127.5 (C11), 127.3 (C4), 126.1 (C3), 56.7 (C7), 54.9 (C2), 52.4 (C13), 38.4 (C6), 22.9 (C5), 21.6 (Ts).

ESI-MS: obs'd (%), calc'd (%), ppm, (M+H) $^{+}$ : 386.1420 (100), 386.1421 (100), 0.2. (M+Na) $^{+}$ : 408.1242(100), 408.1240 (100), 0.5.

### Synthesis and characterization of (*N*-mesyl)-5-imidazole-2-(methyl- $\alpha$ -phenylacetate)-1,2,5,6-tetrahydropyridine (**22**)



**16D** (62 mg, 0.071 mmol) was dissolved in 2 mL propionitrile in a test tube with a stir pea. In a separate test tube, DDQ (16 mg, 0.070 mmol) was dissolved in 2 mL propionitrile, and HOTf (32 mg, 0.211 mmol) was added. Both test tubes were chilled

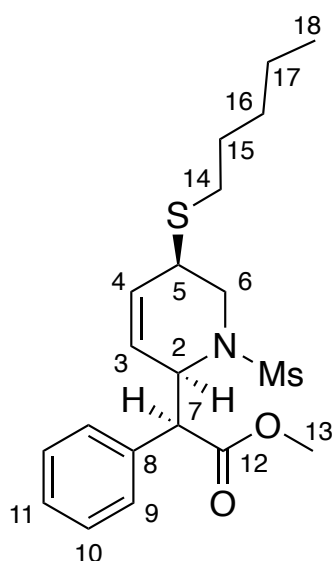
to -40 °C for 15 minutes. The DDQ/HOTf solution was added to the THP complex and allowed to stir for 1 minute. The solution was removed from the glove box and diluted with DCM (50 mL), and extracted with Na<sub>2</sub>CO<sub>3</sub> (2 x 20 mL). The aqueous solution was back extracted with DCM (3 x 6 mL). The organic solution was dried with Na<sub>2</sub>SO<sub>4</sub>, filtered on a 15mL medium porosity frit, and rinsed with 5 mL diethyl ether. The solvent was removed, dissolved in minimal DCM, and added to stirring hexanes. The precipitate was filtered off using a 15 mL medium porosity frit and washed with 15 mL diethyl ether. The filtrate was reduced, and **22** (8 mg, 30% yield) was isolated.

<sup>1</sup>H NMR ((CD<sub>3</sub>)<sub>2</sub>CO, δ, 25 °C): 7.70 (bs, 1H, H14), 7.48 (d, *J* = 7.5 Hz, 2H, H9), 7.39 (t, *J* = 7.2 Hz, 2H, H10), 7.34 (t, *J* = 7.6 Hz, 1H, H11), 7.20 (bs, 1H, H15), 6.98 (bs, 1H, H16), 6.2 (ddd, *J* = 2.5, 3.9, 6.4 Hz, 1H, H3), 6.01 (dd, *J* = 1.5, 10.5 Hz, 1H, H4), 5.1 (dd, *J* = 1.4, 10.4 Hz, 1H, H2), 5.05 (m, *J* = 2.1, 5.6, 8.1 Hz, 1H, H5), 4.17 (d, *J* = 10.6 Hz, 1H, H7), 3.88 (dd, *J* = 6.1, 14.2 Hz, 1H, H6), 3.72 (s, 3H, H13), 3.37 (dd, *J* = 10.5, 14.3 Hz, 1H, H6), 2.08 (s, 3H, Ms).

<sup>13</sup>C NMR ((CD<sub>3</sub>)<sub>2</sub>CO, δ, 25 °C): 172.9 (C12), 137.7 (C8), 137.4 (C14), 130.9 (C3), 130.0 (C16), 129.9 (2C, C9), 129.7 (2C, C10), 129.3 (C4), 129.0 (C11), 118.5 (C15), 56.0 (C2), 55.4 (C7), 52.8 (C13), 51.3 (C5), 45.2 (C6), 39.8 (Ms).

SC-XRD data on S73.

**Synthesis and characterization of (*N*-mesyl)-5-pentyl sulfide-2-(methyl- $\alpha$ -phenylacetate)-1,2,5,6-tetrahydropyridine (**23**)**



**19D** (88 mg, 0.096 mmol) was dissolved in 2 mL propionitrile in a test tube with a stir pea. In a separate test tube, DDQ (24 mg, 0.106 mmol) was dissolved in 2 mL propionitrile. The DDQ solution was added to the THP complex and allowed to stir for 10 minutes. The solution was removed from the glove box and packed onto a basic alumina column, **23** was collected after reducing the eluent from a 35% EtOAc/Hexanes solution (8 mg, 65% yield).

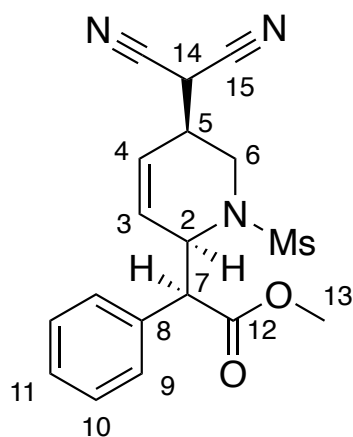
$^1\text{H}$  NMR (( $\text{CDCl}_3$ ),  $\delta$ , 25  $^\circ\text{C}$ ): 7.39 (d,  $J$  = 7.6 Hz, 2H, H9), 7.35 (t,  $J$  = 7.3 Hz, 2H, H10), 7.30 (t,  $J$  = 7.5 Hz, 1H, H11), 5.96 (ddd,  $J$  = 2.3, 4.1, 10.4 Hz, 1H, H3), 5.90 (ddd,  $J$  = 1.7, 3.3, 10.4 Hz, 1H, H4), 4.98 (dd,  $J$  = 1.9, 10.8 Hz, 1H, H2), 3.79 (dd,  $J$  = 6.0, 14.2 Hz, 1H, H6), 3.70 (s, 3H, H13), 3.69 (d,  $J$  = 10.8 Hz, 1H, H7), 3.54 (m, 1H, H5), 2.94 (dd,  $J$  = 11.3, 14.0 Hz, 1H, H6), 2.58 (dt,  $J$  = 2.9, 7.1 Hz, 2H, H14), 1.91 (s, 3H, Ms), 1.60 (q,  $J$  = 7.4, 14.8 Hz, 2H, H15), 1.36 (m, 2H, H16), 1.33 (m, 2H, H17), 0.90 (t,  $J$  = 7.51 Hz, 3H, H18).

$^{13}\text{C}$  NMR (( $\text{CDCl}_3$ ),  $\delta$ , 25  $^\circ\text{C}$ ): 171.77 (C14), 136.39 (C13), 130.53 (C4), 129.06 (C11), 128.86 (C10), 128.45 (C12), 128.12 (C3), 55.76 (C8), 55.44 (C2), 52.56 (C9), 45.07 (C6), 39.85 (C7), 38.70 (C5), 31.15 (C17), 30.66 (C15), 29.86 (C16), 22.38 (C18), 14.08 (C19).



HRMS (APCI)  $m/z$ :  $[M]^+$  Calcd for  $C_{20}H_{30}NO_4S_2^+$  412.1611; Found 412.1614.

**Synthesis and characterization of (*N*-mesyl)-5-malononitrile-2-(methyl- $\alpha$ -phenylacetate)-1,2,5,6-tetrahydropyridine (**24**)**



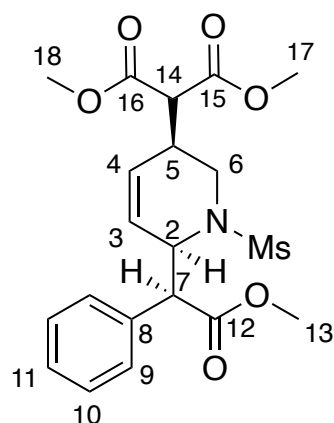
**12D** (134 mg, 0.153 mmol) was dissolved in 5 mL of acetone in a vial with a stir pea. Ammonium Cerium(IV) Nitrate (CAN) (345 mg, 0.629 mmol) was added to the solution and allowed to react for 4 hours. The solution was diluted with DCM (50 mL) and extracted with  $H_2O$  (3 x 300 mL). The aqueous solution was back extracted with DCM (3 x 6 mL). The organic solution was dried with  $Na_2SO_4$ , filtered, and rinsed with DCM. The solvent was removed and packed onto a basic alumina column rinsed with 40% EtOAc/Hexanes solution. **24** (30 mg, 53% yield) was isolated.

$^1H$  NMR ( $CDCl_3$ ,  $\delta$ , 25 °C): 7.46 (d,  $J$  = 8.03 Hz, 2H, H9), 7.40 (t,  $J$  = 7.42 Hz, 2H, H10), 7.35 (t,  $J$  = 7.42 Hz, 1H, H11), 6.29 (ddd,  $J$  = 2.34, 4.16, 6.38 Hz, 1H, H3), 5.98 (dd,  $J$  = 3.28, 10.41 Hz, 1H, H4), 5.03 (d,  $J$  = 10.82 Hz, 1H, H2), 4.79 (d,  $J$  = 5.14 Hz, 1H, H14), 3.93 (dd,  $J$  = 4.93, 13.08 Hz, 1H, H6), 3.87 (d,  $J$  = 10.72 Hz, 1H, H7), 3.70 (s, 3H, H13), 3.26 (bs, 1H, H5), 3.22 (dd,  $J$  = 11.00, 13.40 Hz, 1H, H6), 2.12 (s, 3H, Ms).

$^{13}C$  NMR ( $CDCl_3$ ,  $\delta$ , 25 °C): 172.6 (C12), 137.3 (C8), 132.7 (C3), 129.8 (4C, C9/C10), 129.1 (C11), 126.3 (C4), 113.0 (2C, C15), 56.4 (C7), 56.2 (C2), 52.8 (C13), 41.9 (C6), 40.0 (Ms), 35.8 (C5), 26.2 (C14).

HRMS (APCI)  $m/z$ :  $[M]^+$  Calcd for  $C_{18}H_{20}N_3O_4S^+$  374.1169; Found 374.1166.

**Synthesis and characterization of (*N*-mesyl)-5-dimethyl malonate-2-(methyl- $\alpha$ -phenylacetate)-1,2,5,6-tetrahydropyridine (**25**)**



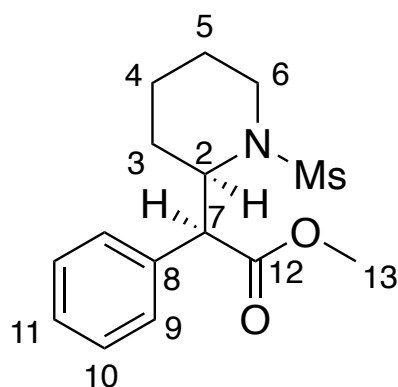
**10D** (62 mg, 0.066 mmol) was dissolved in 2ml of acetone in a vial with a stir pea. DDQ (38 mg, 0.167 mmol) was added to the solution and allowed to react for 3 hours. The solution was diluted with DCM (50ml) and extracted with  $H_2O$  (3 x 100 mL). The aqueous solution was back extracted with DCM (3 x 6 mL). The organic solution was dried with  $Na_2SO_4$ , filtered, and rinsed with DCM. The solvent was removed, redissolved in minimal DCM, and precipitated in hexanes. The precipitate was rinsed with ether, and the filtrate was reduced. **25** (20 mg, 69% yield) was isolated.

$^1H$  NMR ( $(CDCl_3)$ ,  $\delta$ , 25  $^{\circ}C$ ): 7.42 (d,  $J$  = 7.59 Hz, 2H, H9), 7.37 (t,  $J$  = 7.59 Hz, 2H, H10), 7.32 (t,  $J$  = 7.26 Hz, 1H, H11), 5.98 (ddd,  $J$  = 2.64, 4.12, 10.54 Hz, 1H, H3), 5.83 (dd,  $J$  = 1.45, 10.47 Hz, 1H, H4), 4.93 (d,  $J$  = 10.83, 1H, H2), 3.87 (d,  $J$  = 11.09, 1H, H7), 3.74-3.75 (m, 7H, H6/17/18), 3.68 (s, 3H, H13), 3.57 (d,  $J$  = 7.51 Hz, 1H, H14), 3.21 (dd,  $J$  = 11.07, 14.11 Hz, 1H, H6), 3.13 (m, 1H, H5), 2.06 (s, 3H, Ms).

$^{13}C$  NMR ( $(CDCl_3)$ ,  $\delta$ , 25  $^{\circ}C$ ): 172.80 (C12), 168.97/168.94 (2C, C15/16), 137.58 (C8), 129.80 (2C, C9), 129.65 (2C, C10), 129.55 (C11), 129.13 (C4), 128.93 (C3), 56.40 (C7), 56.08 (C2), 54.13 (C14), 52.99/52.97 (2C, C17/18), 52.68 (C13), 41.94 (C6), 39.92 (Ms), 34.63 (C5).

HRMS (APCI)  $m/z$ :  $[M]^+$  Calcd for  $C_{20}H_{26}NO_8S^+$  440.1374; Found 440.1380.

### Synthesis and characterization of *erythro*-(*N*-mesyl)-methylphenidate (26)



**21** (21 mg, 0.068 mmol) was dissolved in ethyl acetate (3 mL) and added to a 4-dram vial. This solution was then circulated through a ThalesNano H-Cube flow hydrogenator for 5 hours. The temperature was set to 50 °C, the  $H_2$  pressure to 25 bars, and the catalyst cartridge used contained 5%Pd on carbon. After circulation, the solution was collected and reduced to dryness (17 mg 78% yield).

$^1H$  NMR ( $(CD_3)_2CO$ ,  $\delta$ , 25 °C): 7.52 (d,  $J$  = 7.2, 2H, H9), 7.36 (tt,  $J$  = 1.3, 7.2 Hz, 2H, H10), 7.31 (tt,  $J$  = 1.3, 7.3 Hz, 1H, H11), 4.75 (dd,  $J$  = 5.1, 11.8 Hz, 1H, H2), 4.32 (d,  $J$  = 11.8 Hz, 1H, H7), 3.66 (s, 3H, H13), 3.47 (dd,  $J$  = 3.3, 14.2 Hz, 1H, H6), 3.11 (ddd,  $J$  = 2.8, 13.0, 14.2 Hz, 1H, H6), 1.91 (s, 3H, Ms), 1.81-1.88 (m, 1H, H4), 1.73-1.78 (m, 1H, H3), 1.70-1.73 (m, 1H, H3), 1.67-1.70 (m, 1H, H4), 1.61-1.65 (m, 1H, H5), 1.48-1.55 (m, 1H, H5).

$^{13}C$  NMR ( $(CD_3)_2CO$ ,  $\delta$ , 25 °C): 173.2 (C12), 138.0 (C8), 129.7 (C9), 129.5 (C10), 128.7 (C11), 56.2 (C2), 52.5 (C7), 51.4 (C13), 41.3 (C6), 39.7 (Ms), 29.0 (C3), 26.0 (C5), 19.5 (C4).

SC-XRD data on S74.

<sup>1</sup>H NMR (CD<sub>2</sub>Cl<sub>2</sub>), δ, 25 °C): 7.42 (d, *J* = 7.5 Hz, 2H, H9), 7.35 (t, *J* = 7.5 Hz, 2H, H10), 7.30 (t, *J* = 7.4 Hz, 1H, H11), 4.74 (dd, *J* = 5.0, 11.5 Hz, 1H, H2), 4.05 (d, *J* = 11.8 Hz, 1H, H7), 3.75 (s, 6H, H17/18), 3.66 (s, 3H, H13), 3.54 (dd, *J* = 3.5, 13.7 Hz, 1H, H6), 3.29 (d, *J* = 7.70 Hz, 1H, H14), 2.84 (dd, *J* = 11.8, 13.7 Hz, 1H, H6), 2.25-2.31 (m, 1H, H5), 1.92 (s, 3H, Ms), 1.84-1.90 (m, 1H, H3), 1.73-1.79 (m, 2H, H3/4), 1.67 (dq, *J* = 3.2, 12.8 Hz, 1H, H4).

SC-XRD data on S75.

## NMR Spectroscopy:

**Figure S1:**  $^1\text{H}$  NMR, 800 MHz,  $\text{CD}_2\text{Cl}_2$ , 25  $^\circ\text{C}$ , Compound **5**

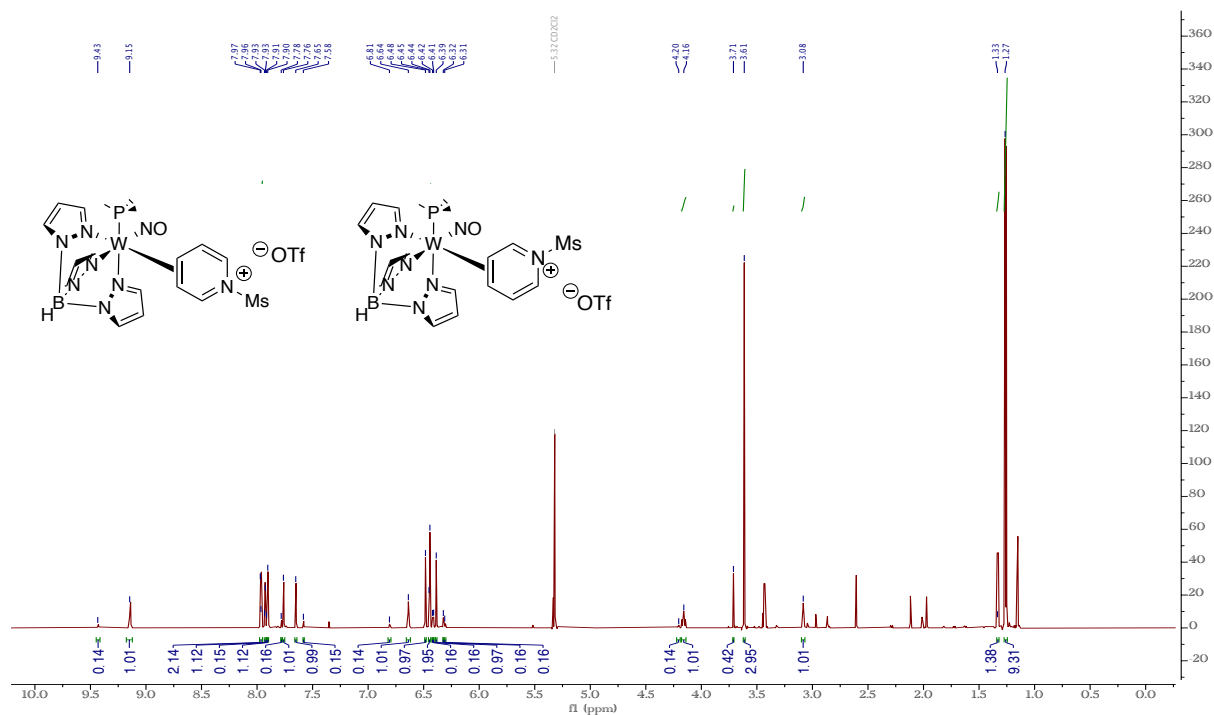


**Figure S2:**  $^1\text{H}$  NMR, 800 MHz,  $(\text{CD}_3)_2\text{CO}$ , 25  $^\circ\text{C}$ , Compound **5D**

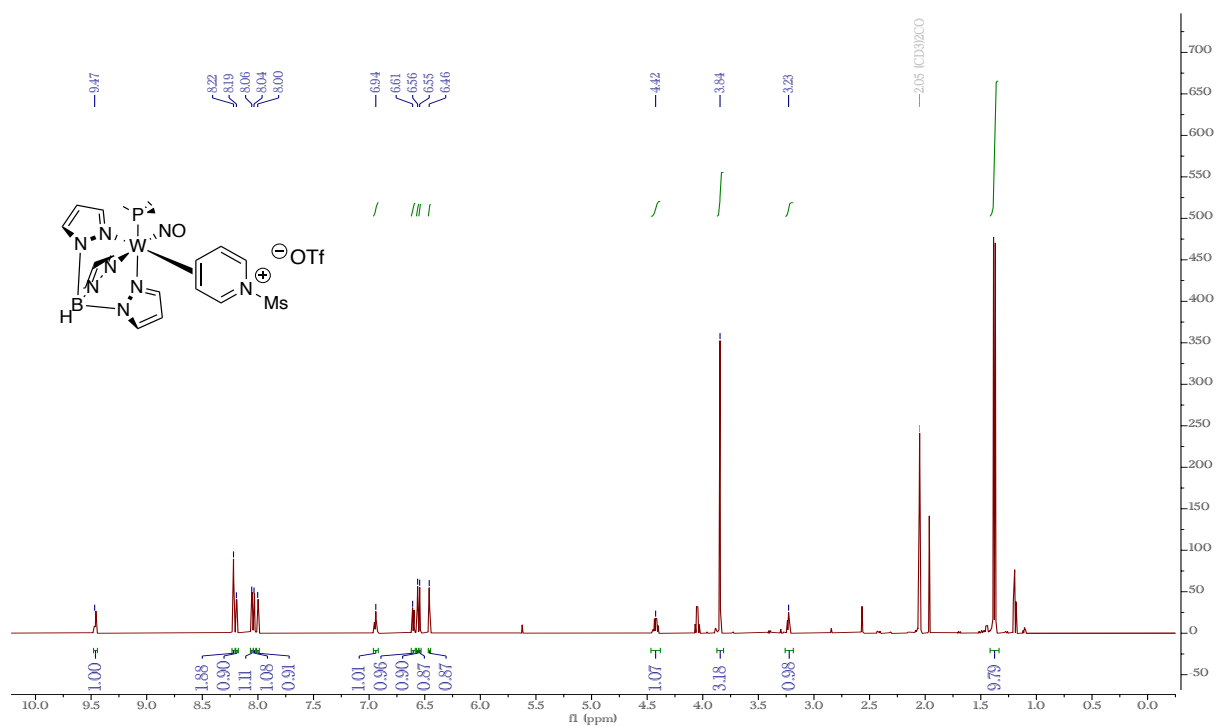


**Figure S3:**  $^{13}\text{C}$  NMR, 200 MHz,  $\text{CD}_2\text{Cl}_2$ , 25  $^\circ\text{C}$ , Compound **5**

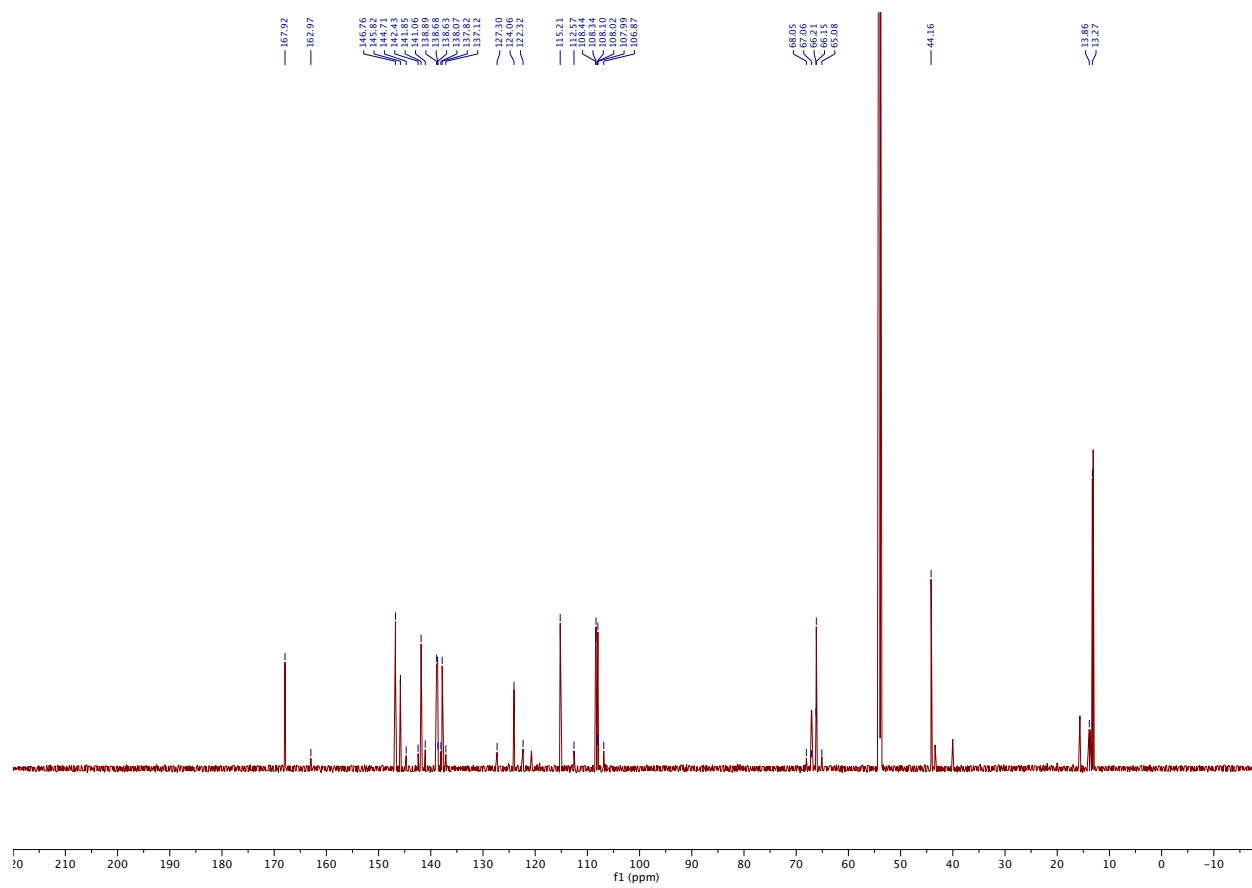


**Figure S4:**  $^1\text{H}$  NMR, 800 MHz,  $\text{CD}_2\text{Cl}_2$ , 25  $^\circ\text{C}$ , Compound **6D**

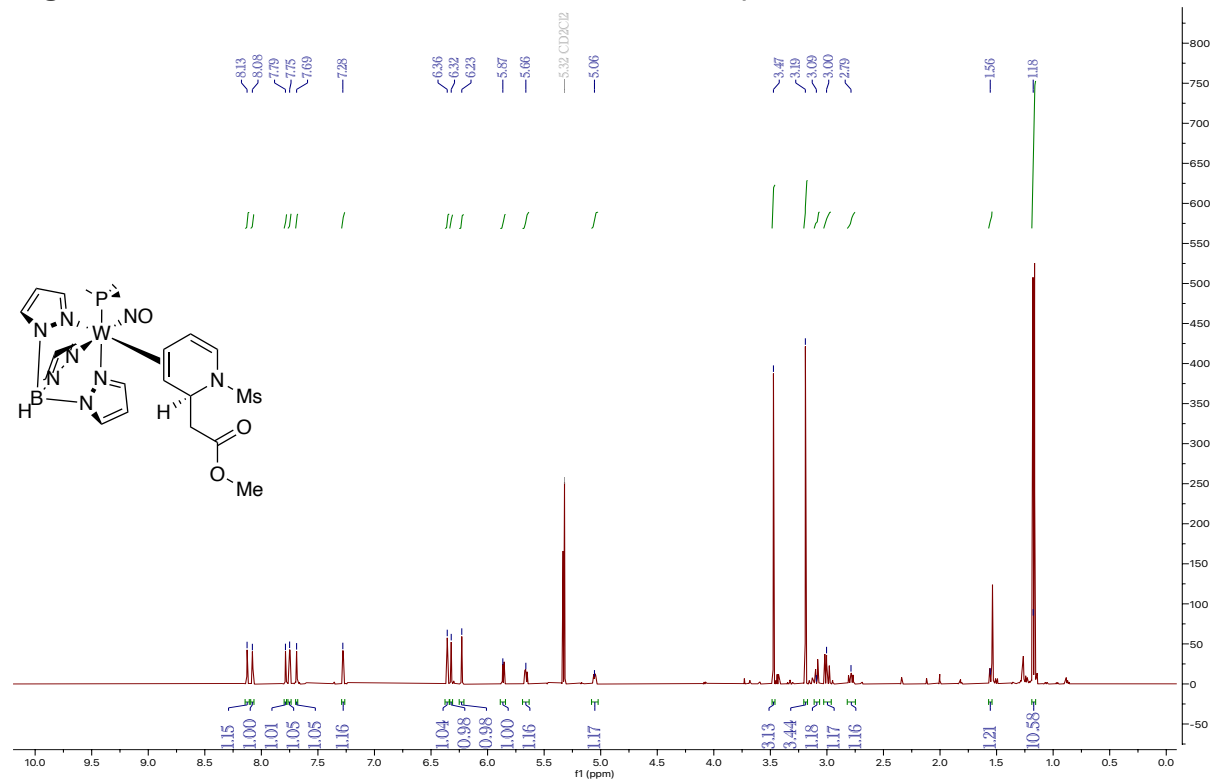


**Figure S5:**  $^{13}\text{C}$  NMR, 200 MHz,  $\text{CD}_2\text{Cl}_2$ , 25  $^\circ\text{C}$ , Compound **6D**

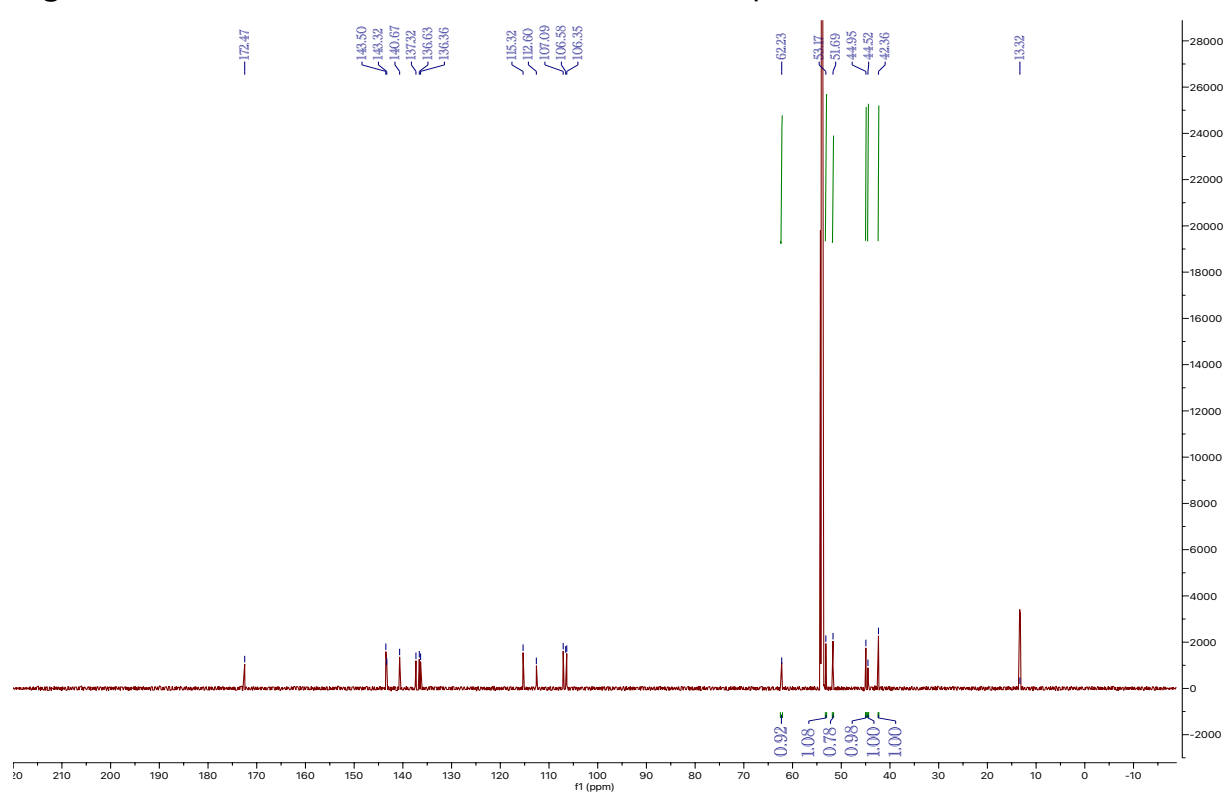


**Figure S6:**  $^1\text{H}$  NMR, 800 MHz,  $\text{CD}_2\text{Cl}_2$ , 25  $^\circ\text{C}$ , Compound **7D**

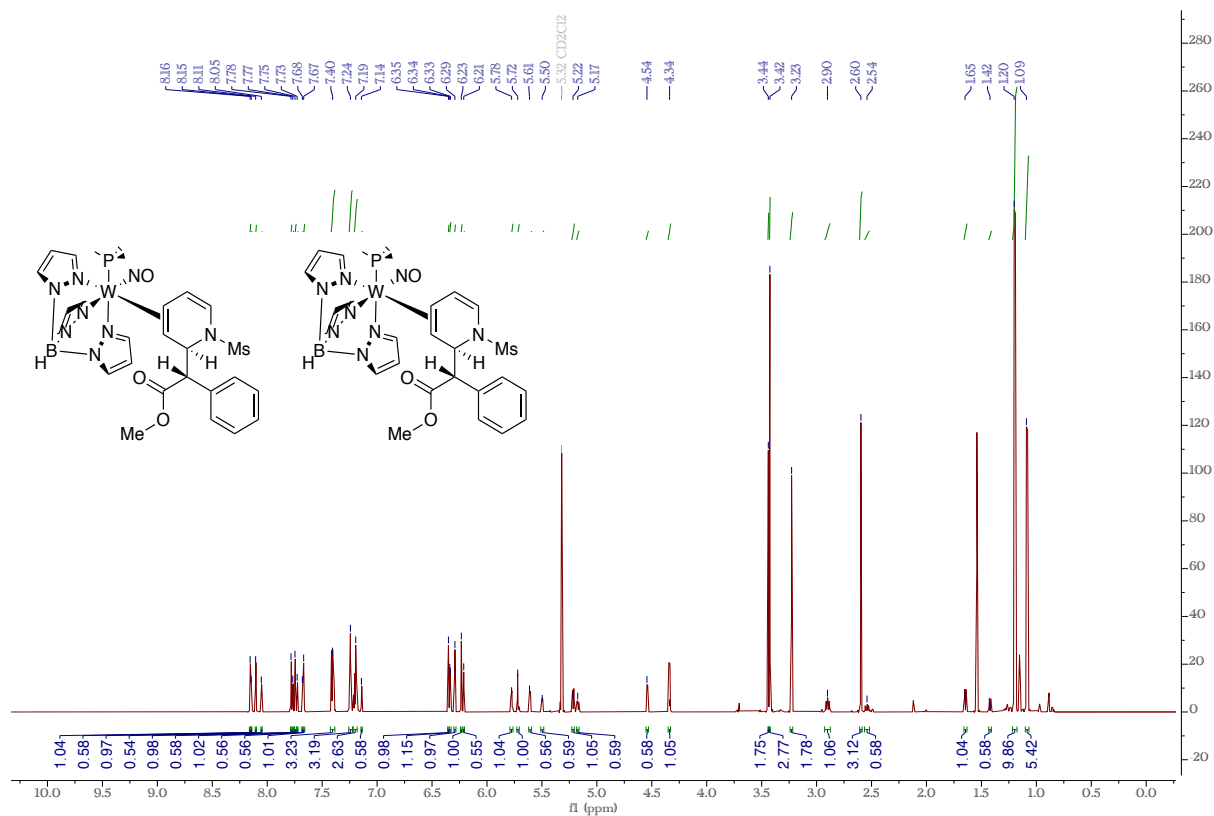


**Figure S7:**  $^{13}\text{C}$  NMR, 200 MHz,  $\text{CD}_2\text{Cl}_2$ , 25  $^\circ\text{C}$ , Compound **7D**

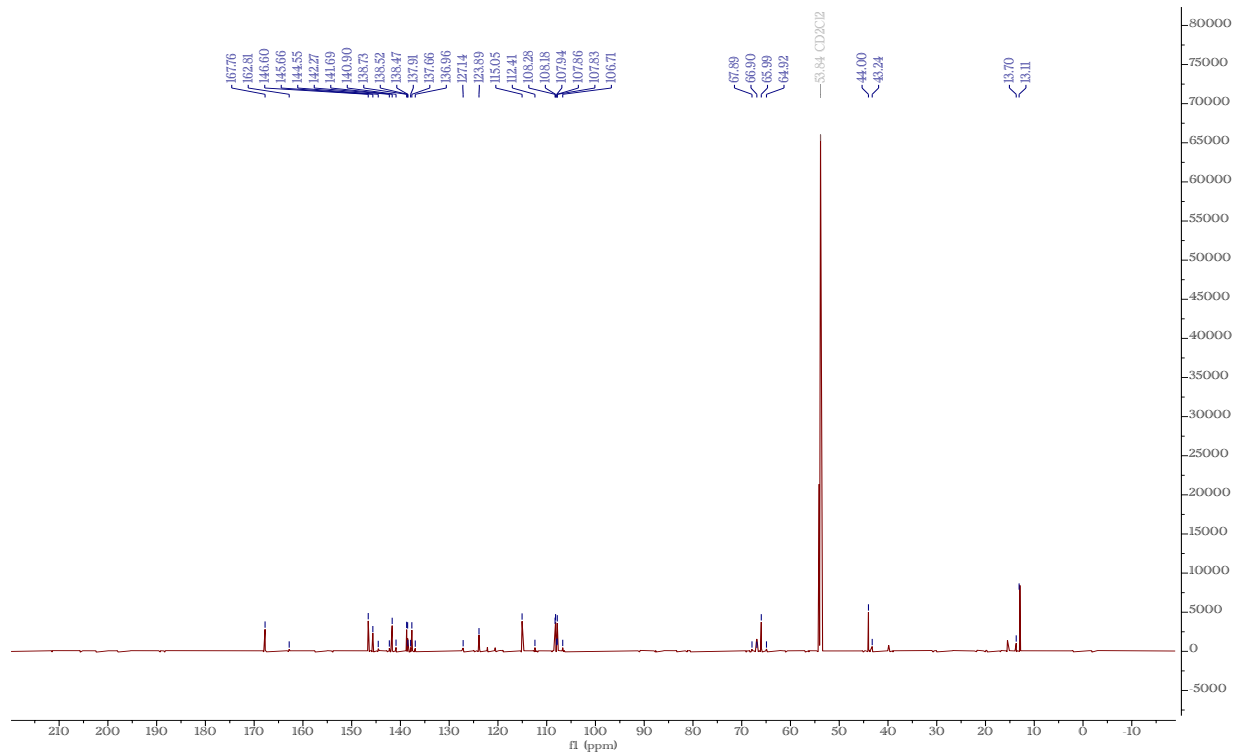




**Figure S8:**  $^1\text{H}$  NMR, 800 MHz,  $\text{CD}_2\text{Cl}_2$ , 25  $^\circ\text{C}$ , Highly Enriched Compound **erythro-7D**

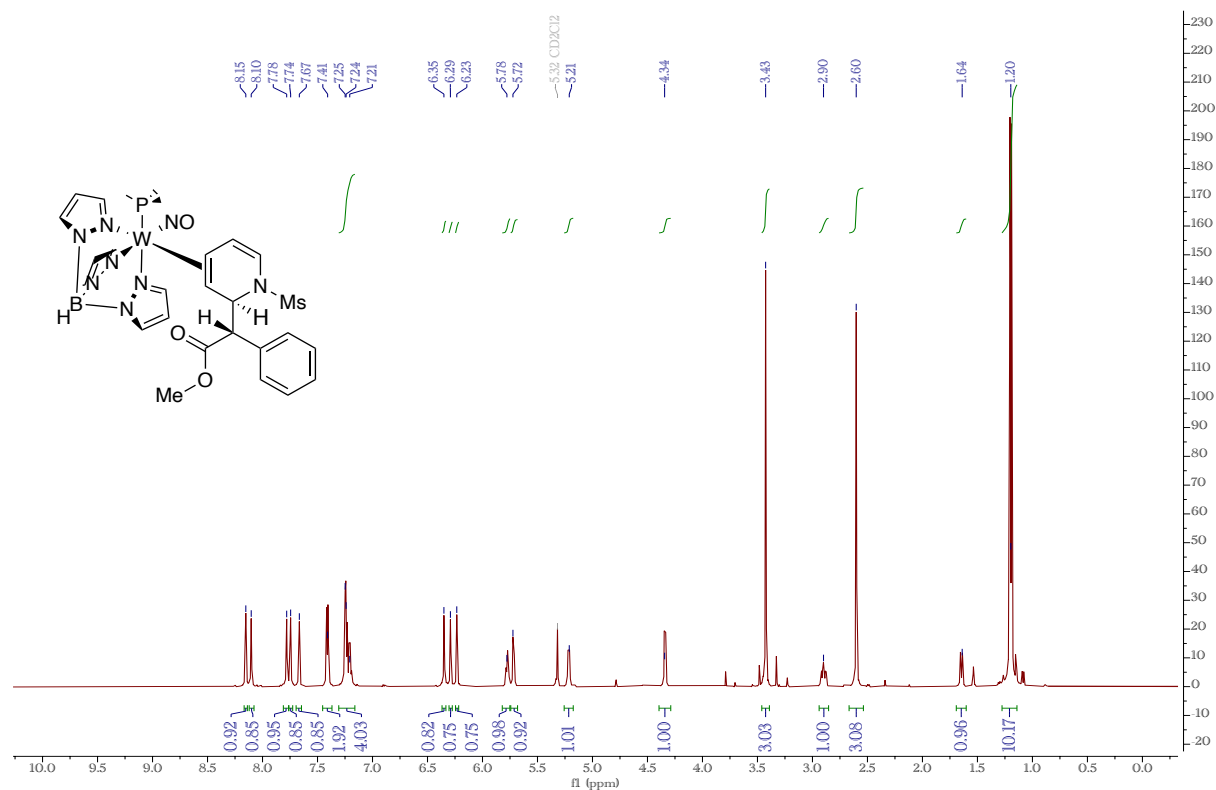


**Figure S9:**  $^{13}\text{C}$  NMR, 200 MHz,  $\text{CD}_2\text{Cl}_2$ , 25  $^\circ\text{C}$ , Compound **erythro-7D**

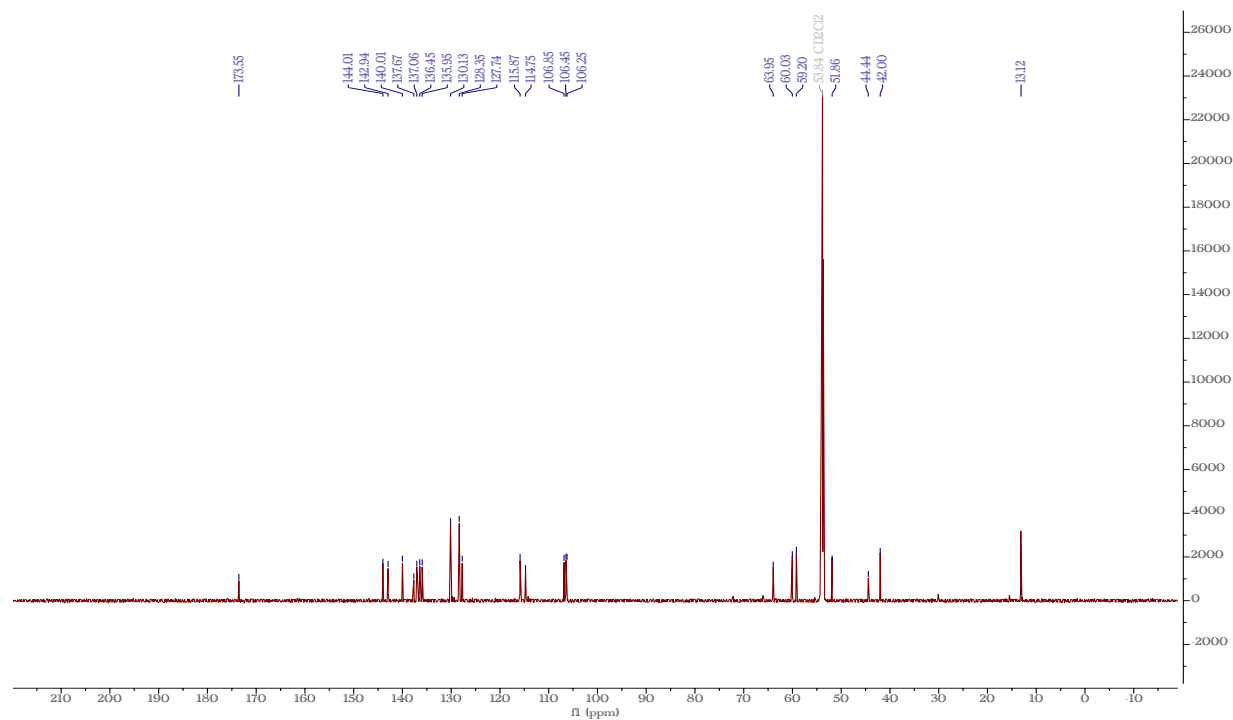


**Figure S10:**  $^1\text{H}$  NMR, 800 MHz,  $\text{CD}_2\text{Cl}_2$ , 25  $^\circ\text{C}$ , Compound **8**

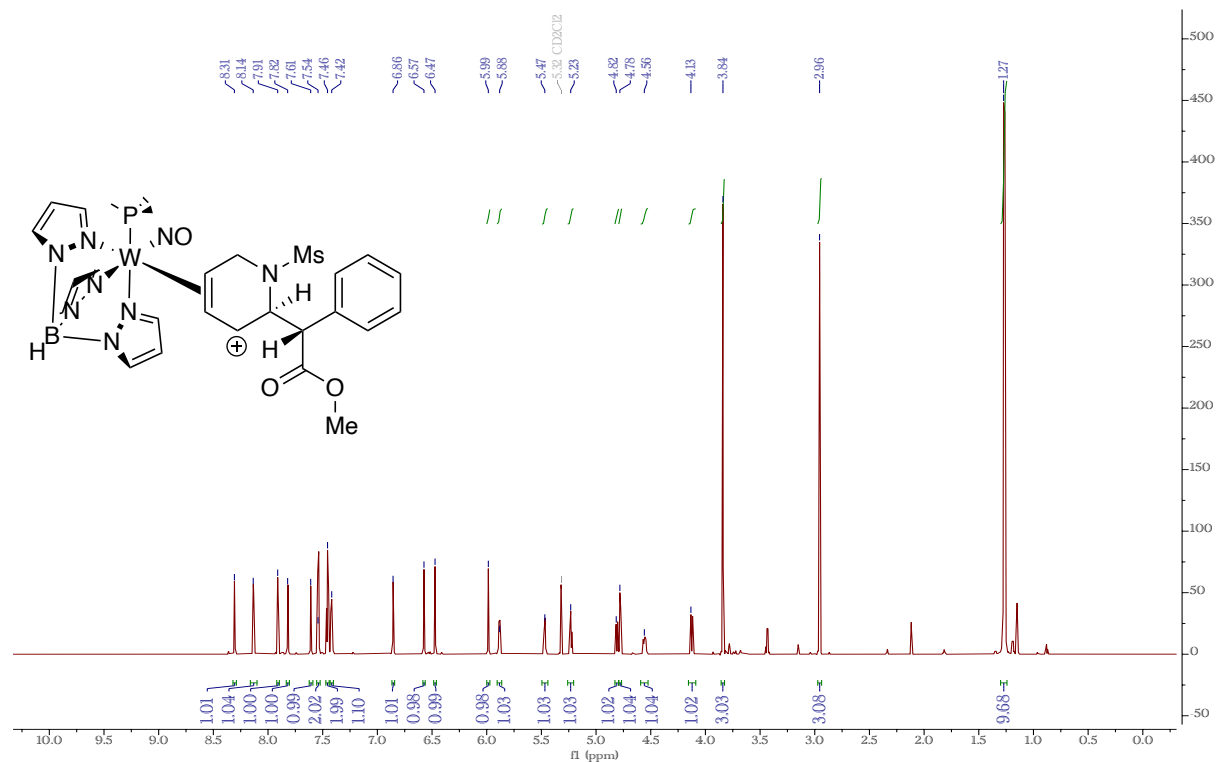


**Figure S11:**  $^{13}\text{C}$  NMR, 200 MHz,  $\text{CD}_2\text{Cl}_2$ , 25  $^\circ\text{C}$ , Compound **8**

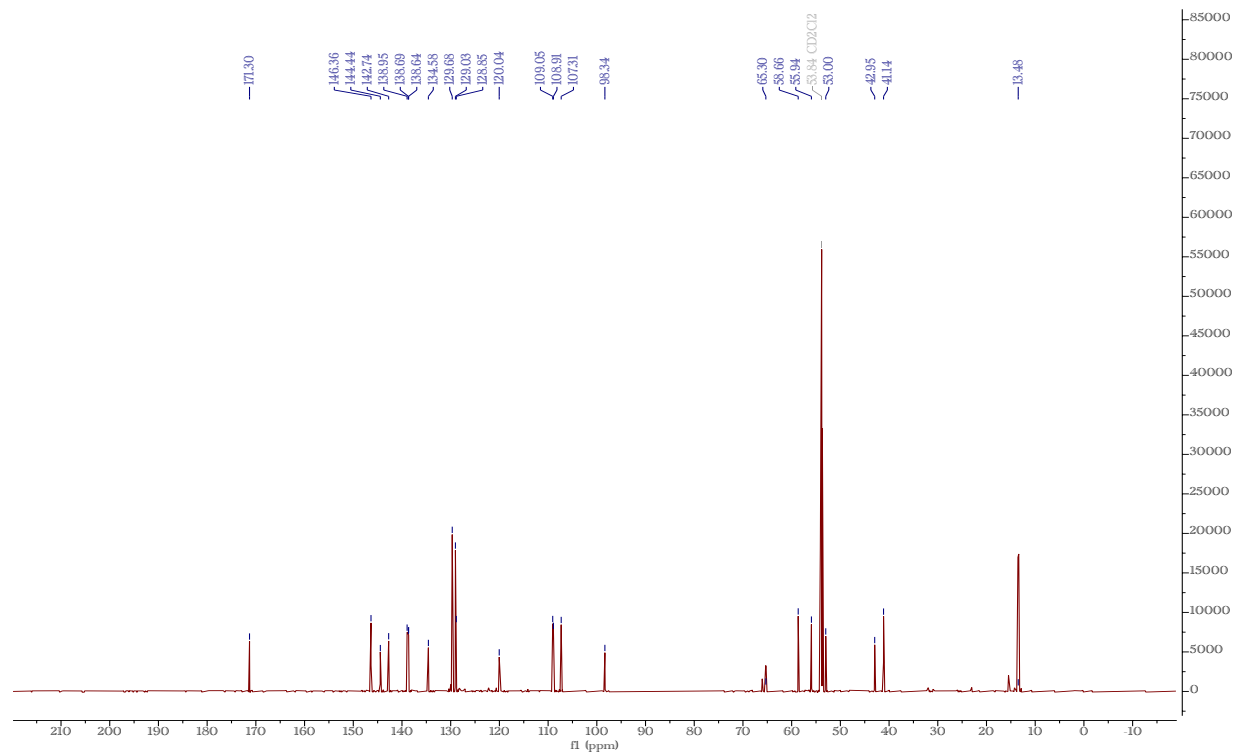


**Figure S12:**  $^1\text{H}$  NMR, 800 MHz,  $(\text{CD}_3)_2\text{CO}$ , 25  $^\circ\text{C}$ , Compound **9D**

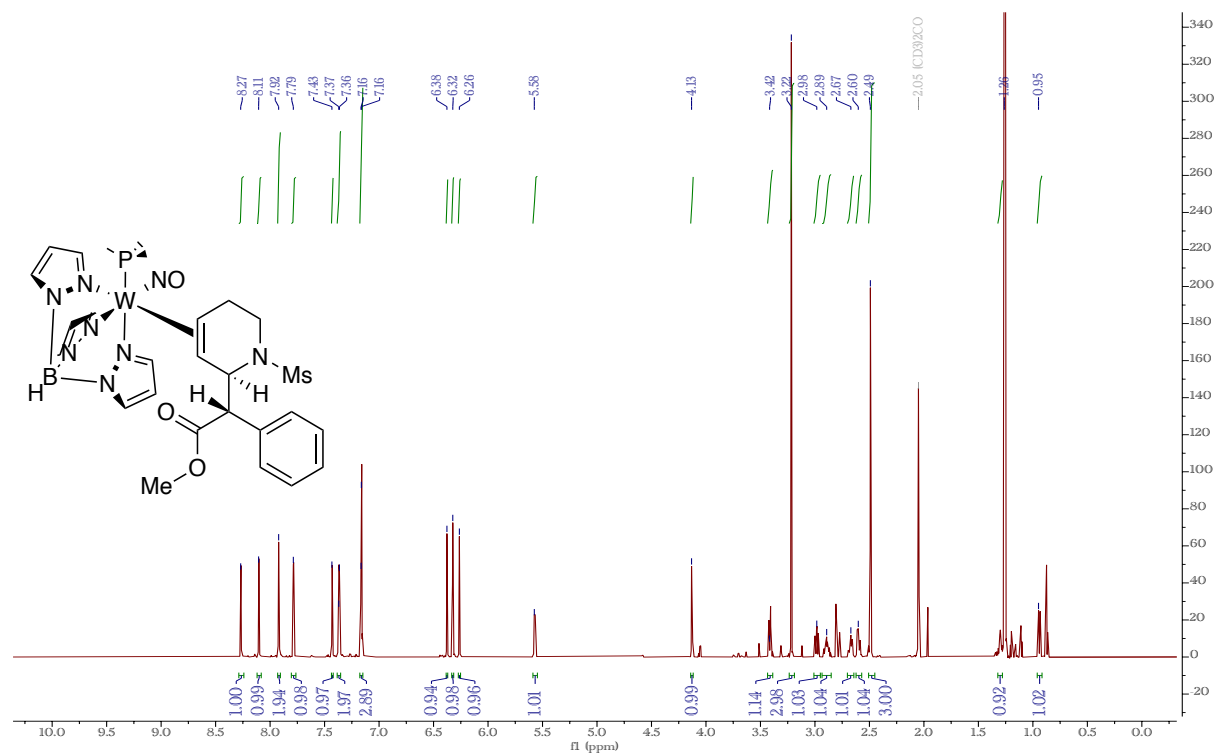


**Figure S13:**  $^{13}\text{C}$  NMR, 200 MHz,  $(\text{CD}_3)_2\text{CO}$ , 25  $^\circ\text{C}$ , Compound **9D**

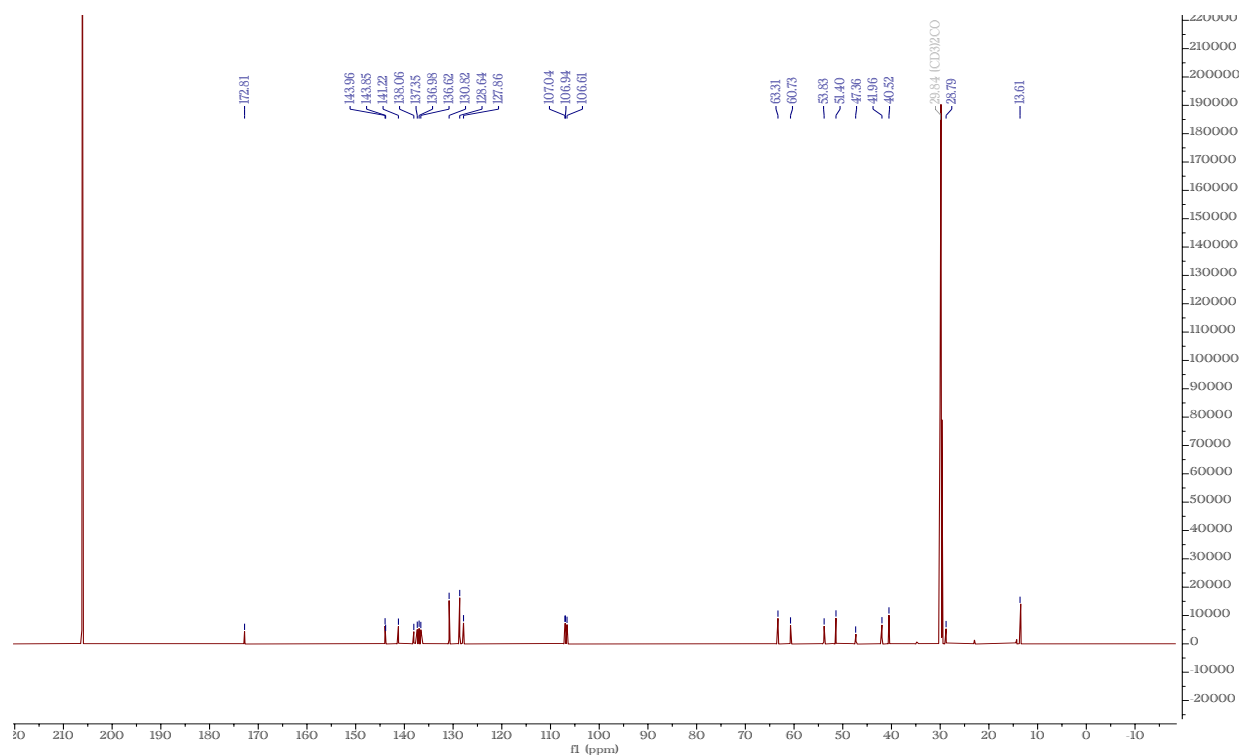


**Figure S14:**  $^1\text{H}$  NMR, 800 MHz,  $\text{CD}_2\text{Cl}_2$ , 25  $^\circ\text{C}$ , Compound **10D**

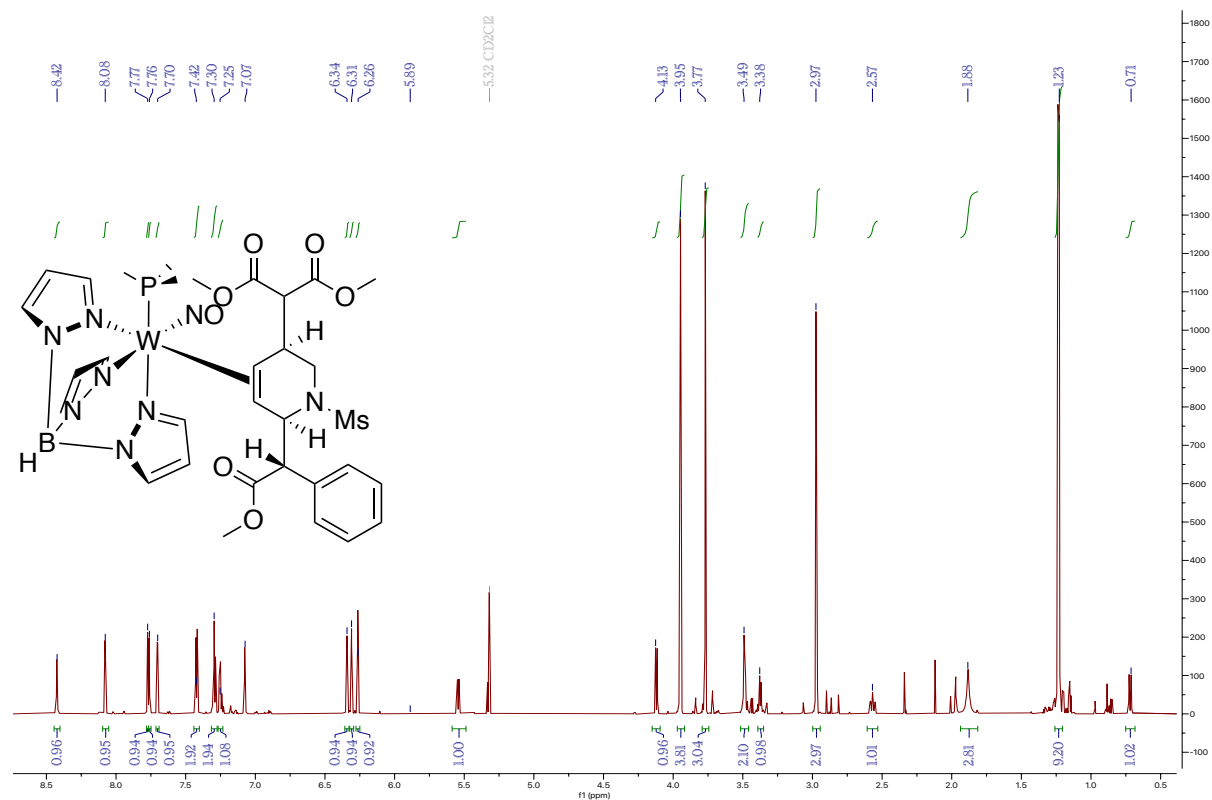


**Figure S15:**  $^{13}\text{C}$  NMR, 200 MHz,  $\text{CD}_2\text{Cl}_2$ , 25  $^\circ\text{C}$ , Compound **10D**

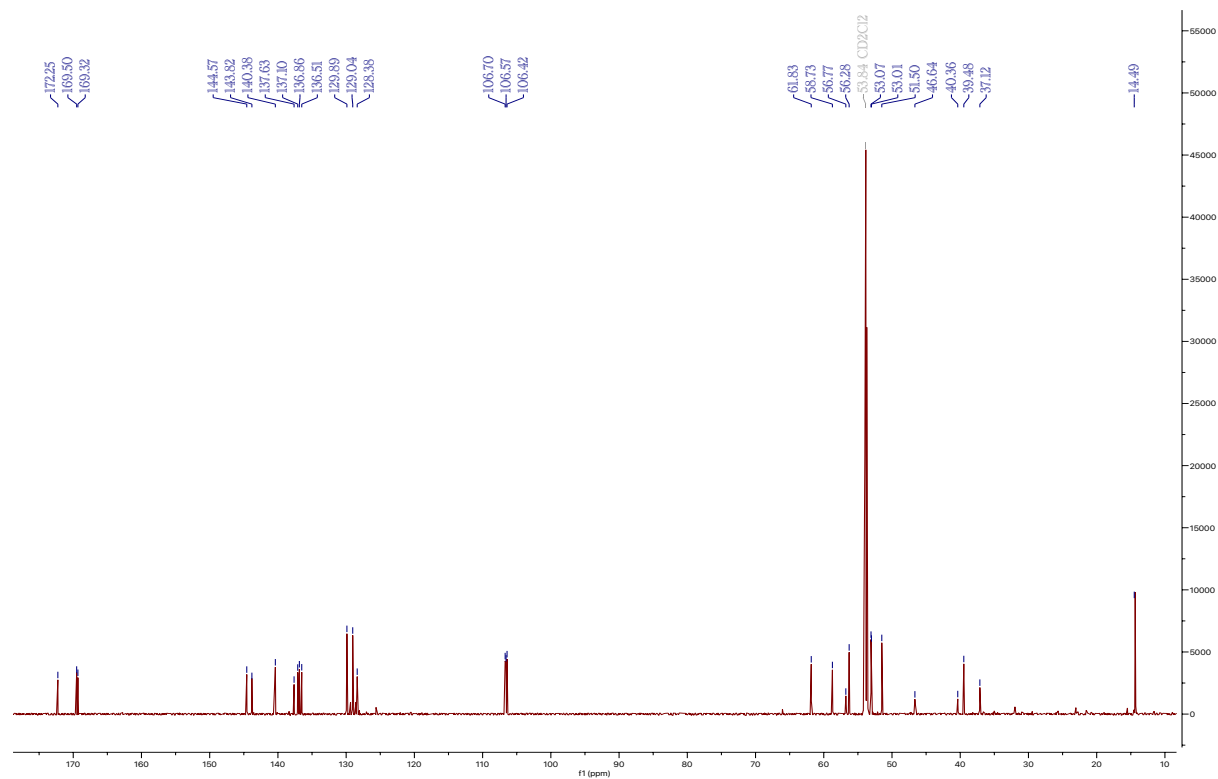


**Figure S16:**  $^1\text{H}$  NMR, 800 MHz,  $\text{CD}_2\text{Cl}_2$ , 25  $^\circ\text{C}$ , Compound **11D**

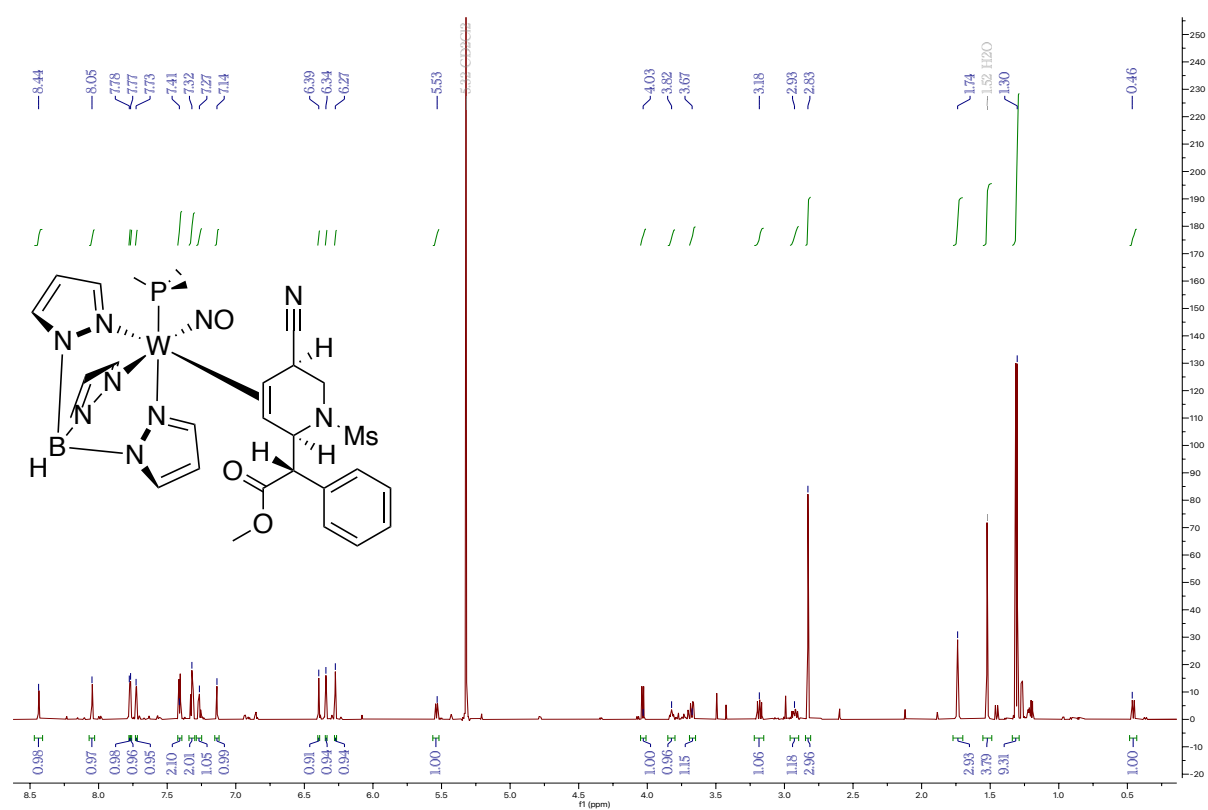


**Figure S17:**  $^{13}\text{C}$  NMR, 200 MHz,  $\text{CD}_2\text{Cl}_2$ , 25  $^\circ\text{C}$ , Compound **11D**

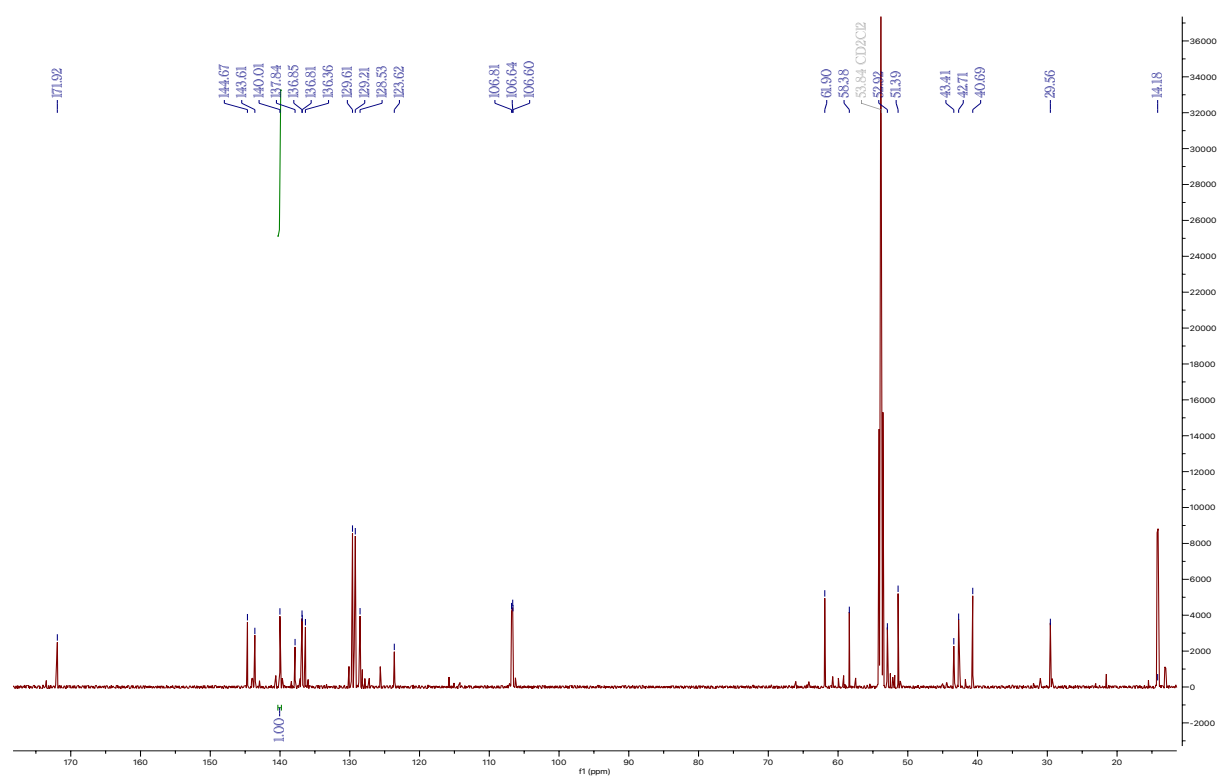


**Figure S18:**  $^1\text{H}$  NMR, 800 MHz,  $(\text{CD}_3)_2\text{CO}$ , 25  $^\circ\text{C}$ , Compound **12D**

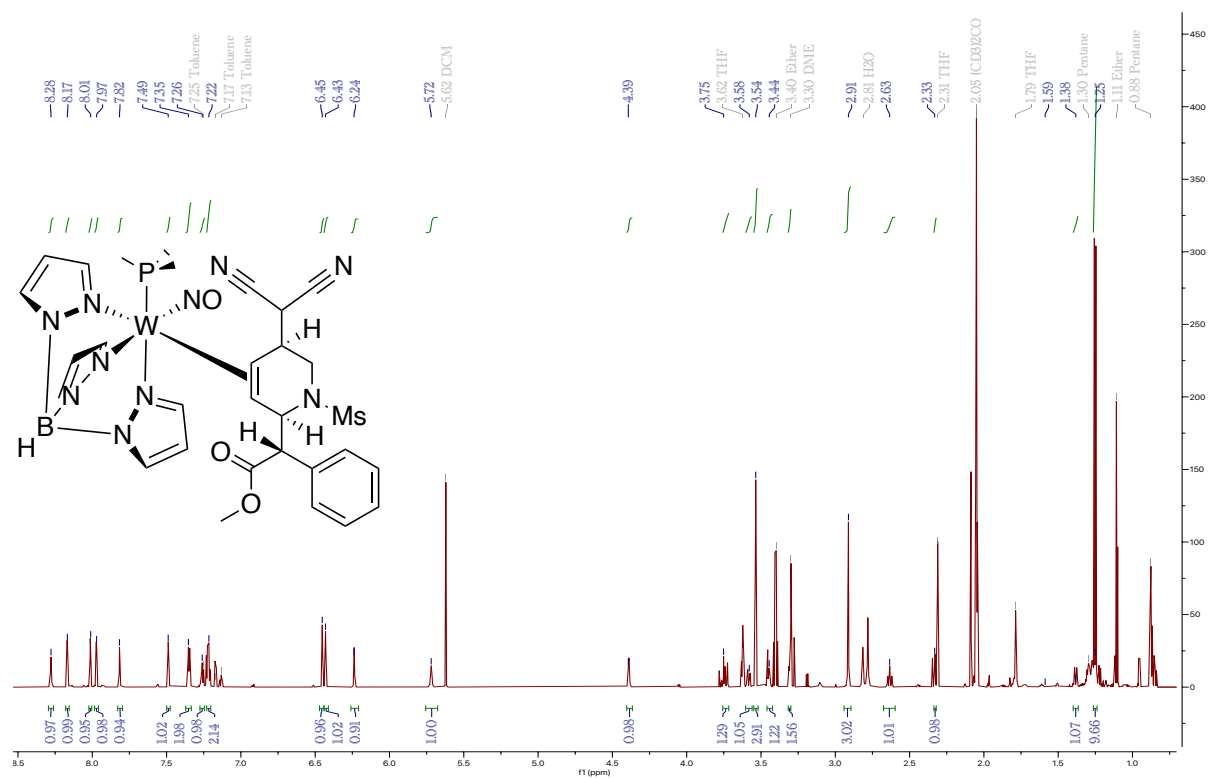


**Figure S19:**  $^{13}\text{C}$  NMR, 200 MHz,  $(\text{CD}_3)_2\text{CO}$ , 25  $^\circ\text{C}$ , Compound **12D**

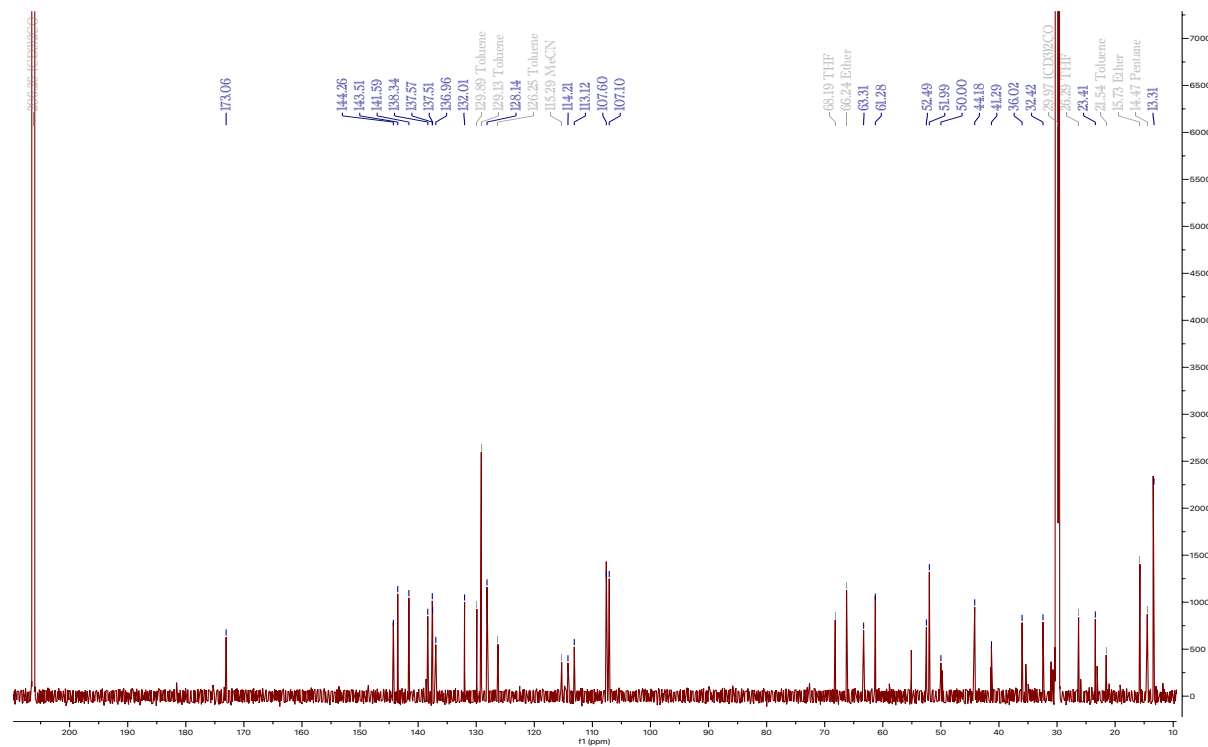


**Figure S20:**  $^1\text{H}$  NMR, 800 MHz,  $\text{CD}_3\text{CN}$ , 25  $^\circ\text{C}$ , Compound **13D**

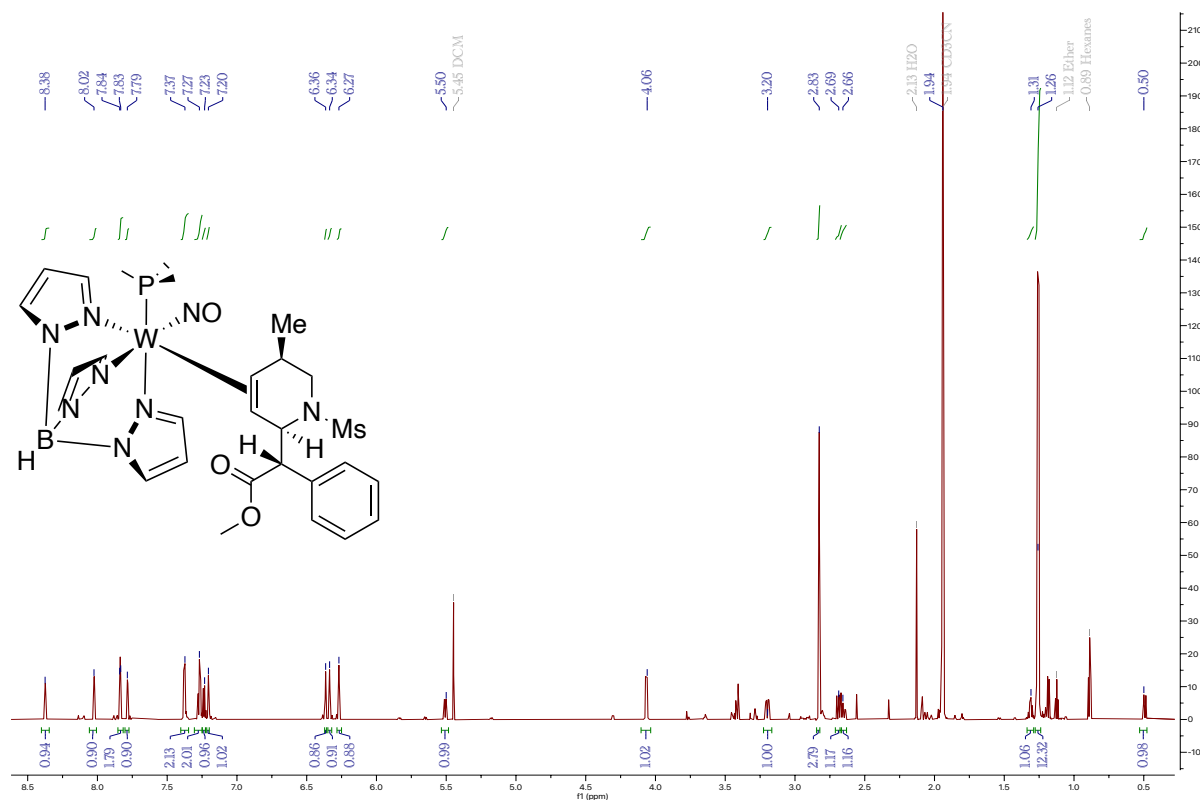


**Figure S21:**  $^{13}\text{C}$  NMR, 200 MHz,  $\text{CD}_3\text{CN}$ , 25  $^\circ\text{C}$ , Compound **13D**

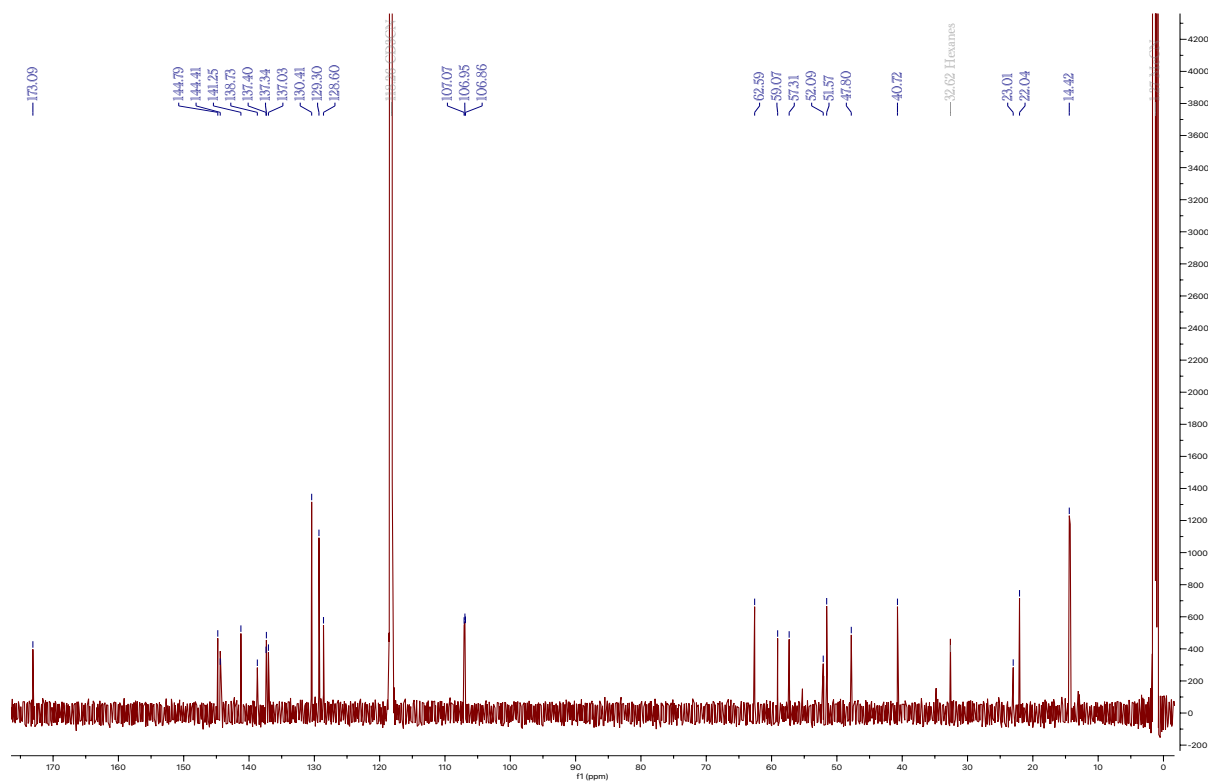


**Figure S22:**  $^1\text{H}$  NMR, 800 MHz,  $\text{CD}_3\text{CN}$ , 25  $^\circ\text{C}$ , Compound **14D**

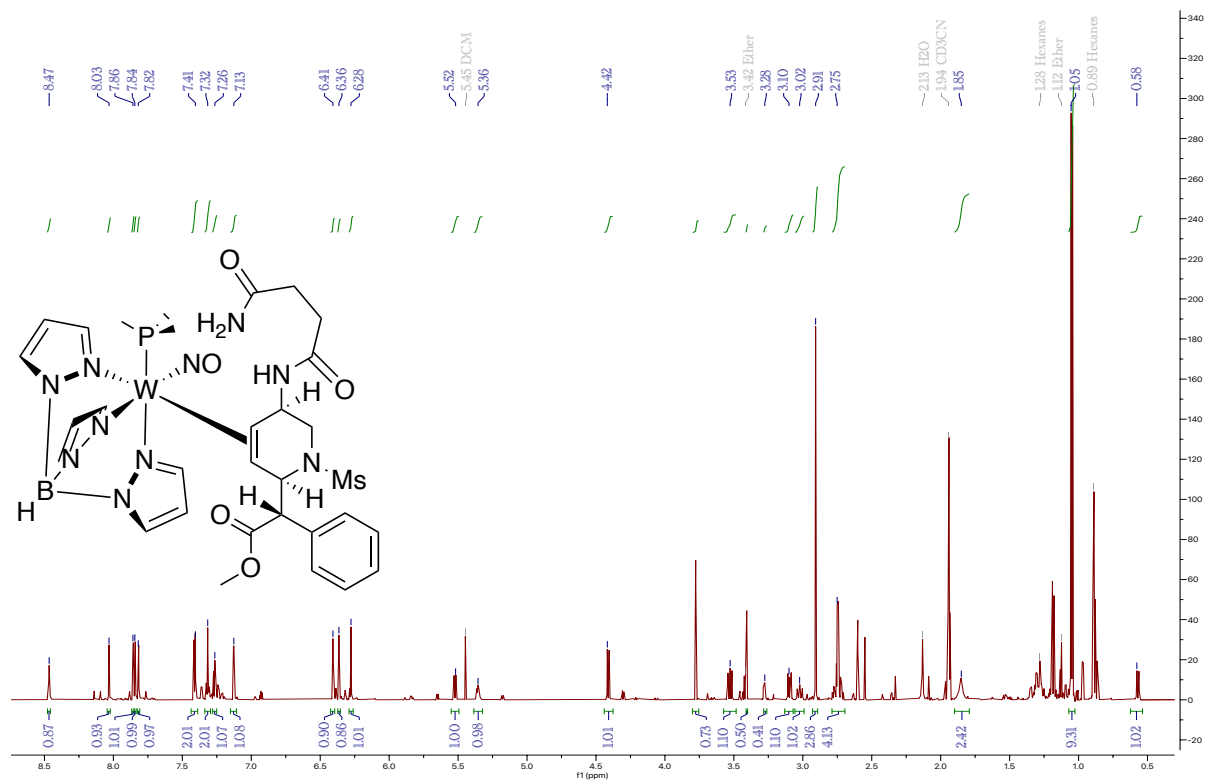


**Figure S23:**  $^{13}\text{C}$  NMR, 200 MHz,  $\text{CD}_3\text{CN}$ , 25  $^\circ\text{C}$ , Compound **14D**

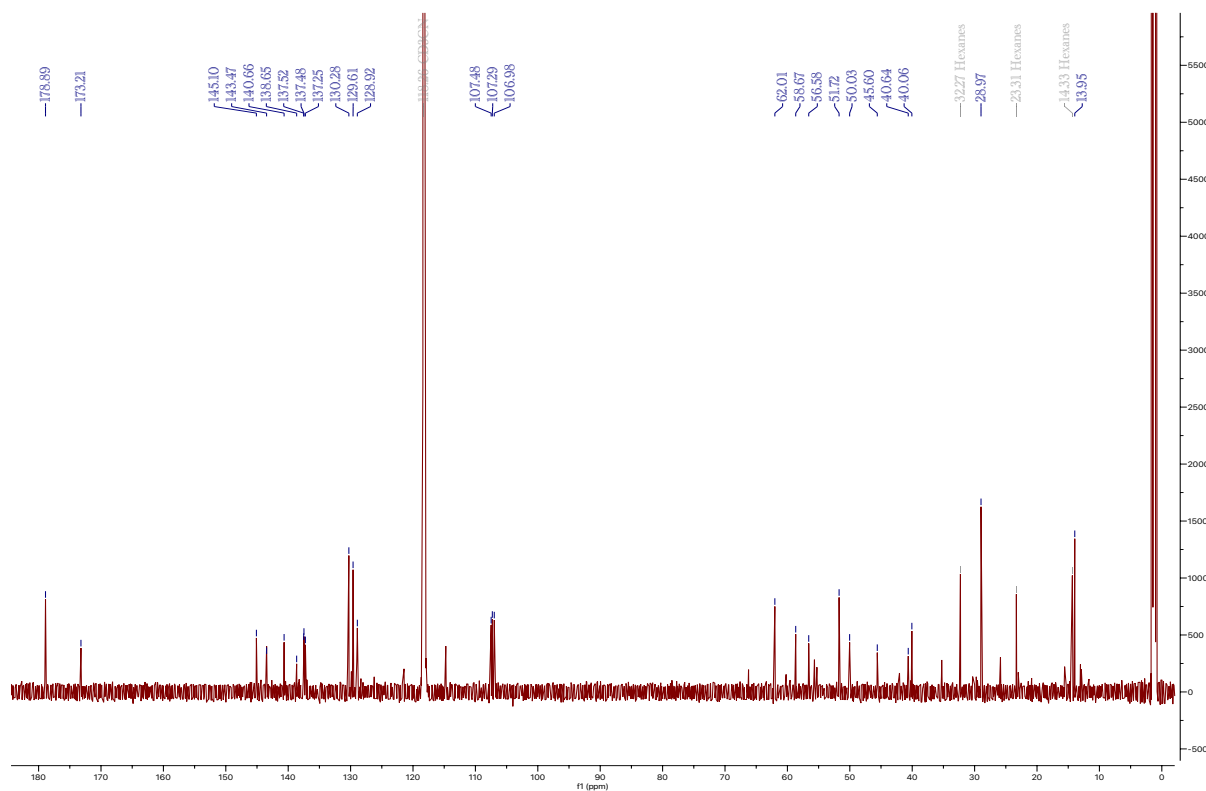




**Figure S24:**  $^1\text{H}$  NMR, 800 MHz,  $\text{CD}_2\text{Cl}_2$ , 25  $^\circ\text{C}$ , Compound **15D**

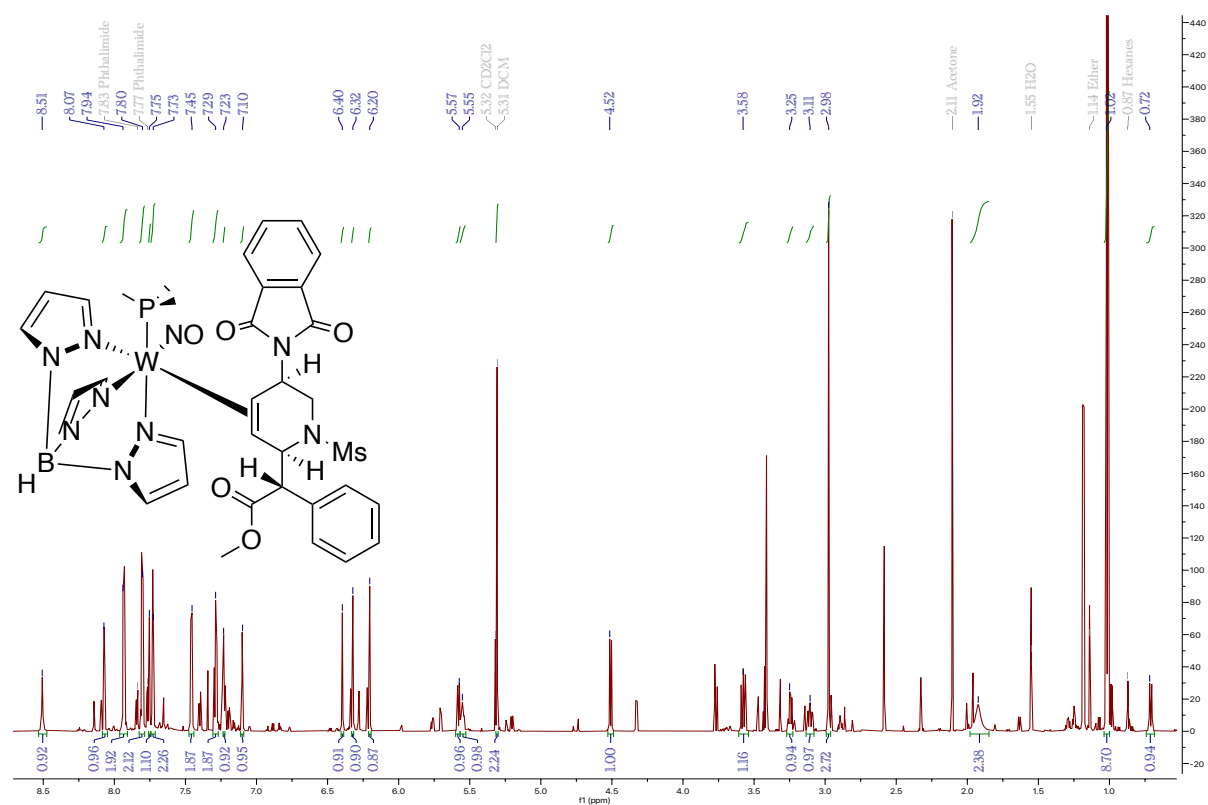


**Figure S25:**  $^{13}\text{C}$  NMR, 200 MHz,  $\text{CD}_2\text{Cl}_2$ , 25  $^\circ\text{C}$ , Compound **15D**

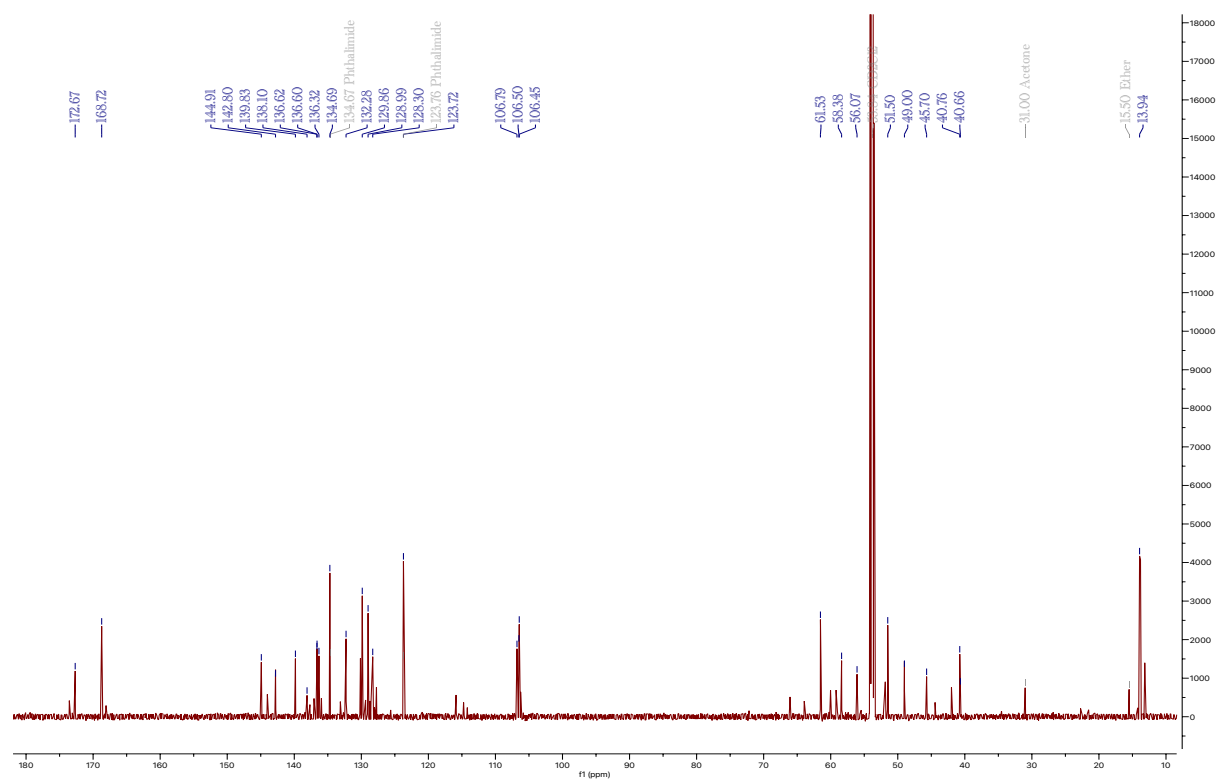


**Figure S26:**  $^1\text{H}$  NMR, 800 MHz,  $\text{CD}_2\text{Cl}_2$ , 25  $^\circ\text{C}$ , Compound **16D**

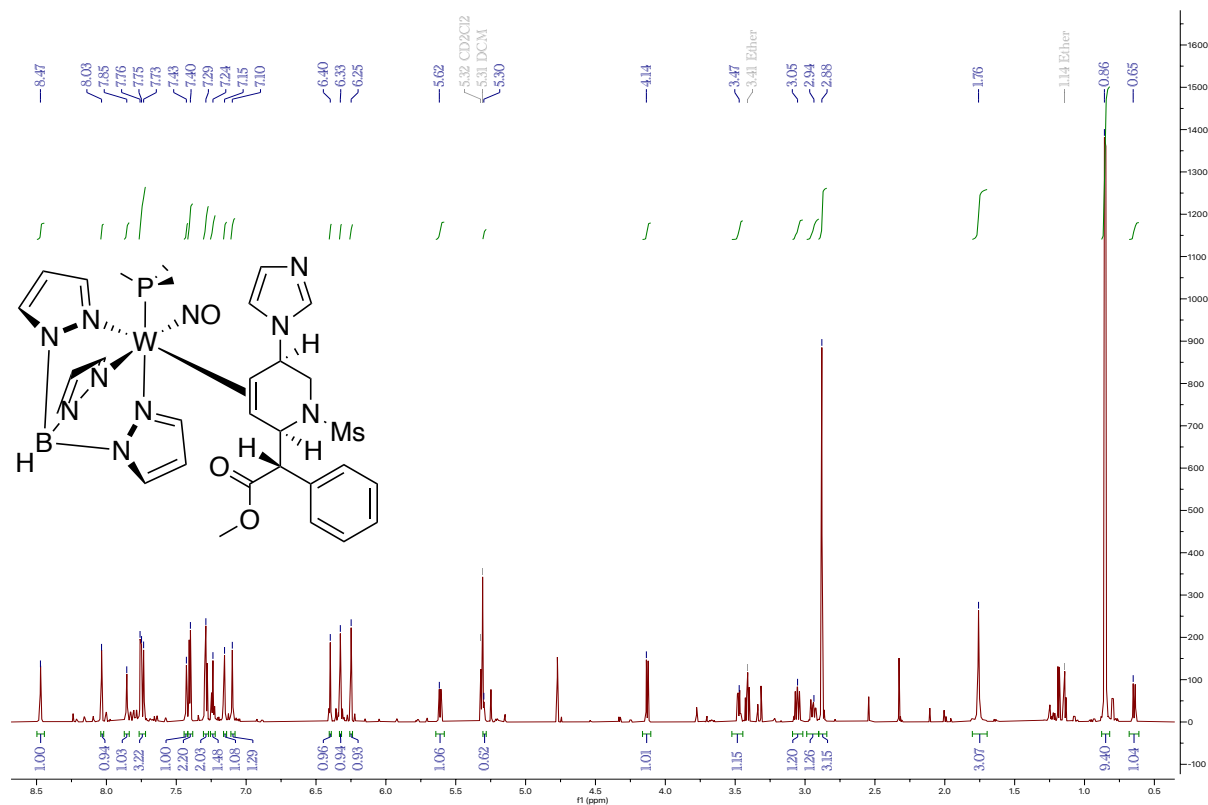


**Figure S27:**  $^{13}\text{C}$  NMR, 200 MHz,  $\text{CD}_2\text{Cl}_2$ , 25  $^\circ\text{C}$ , Compound **16D**

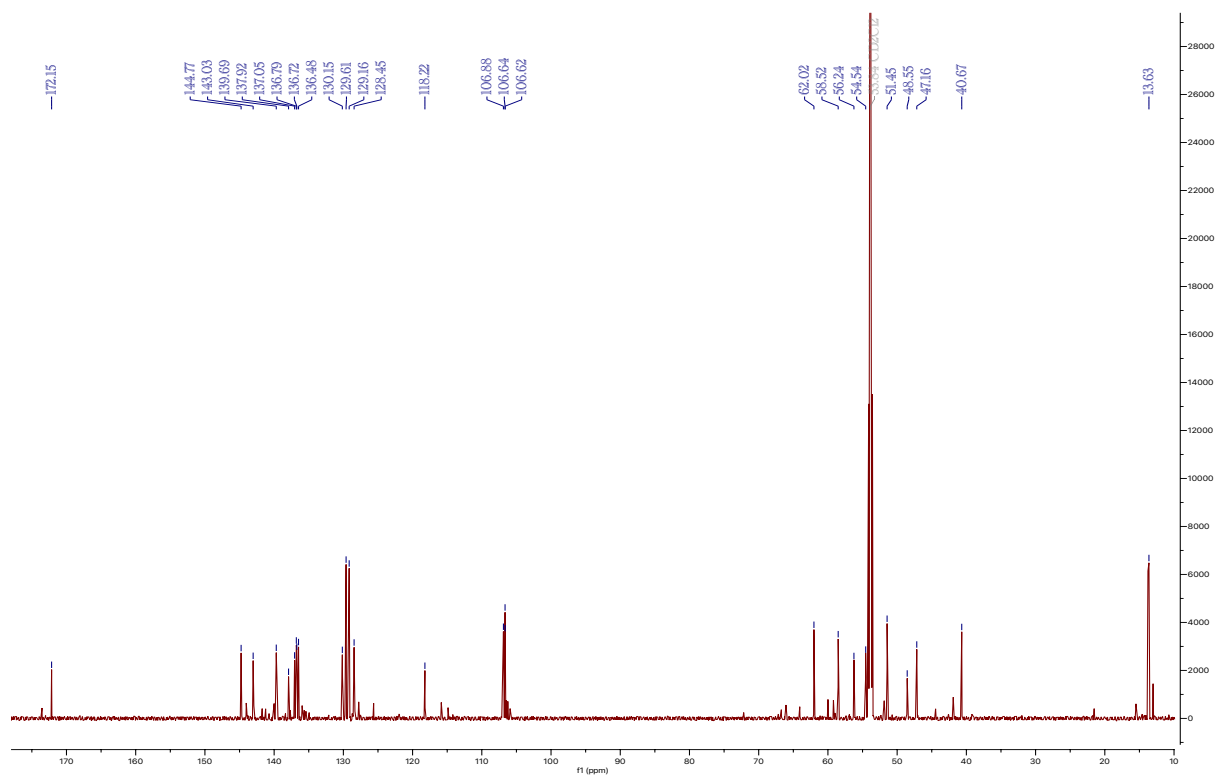


**Figure S28:**  $^1\text{H}$  NMR, 800 MHz,  $\text{CD}_2\text{Cl}_2$ , 25  $^\circ\text{C}$ , Compound **17D**

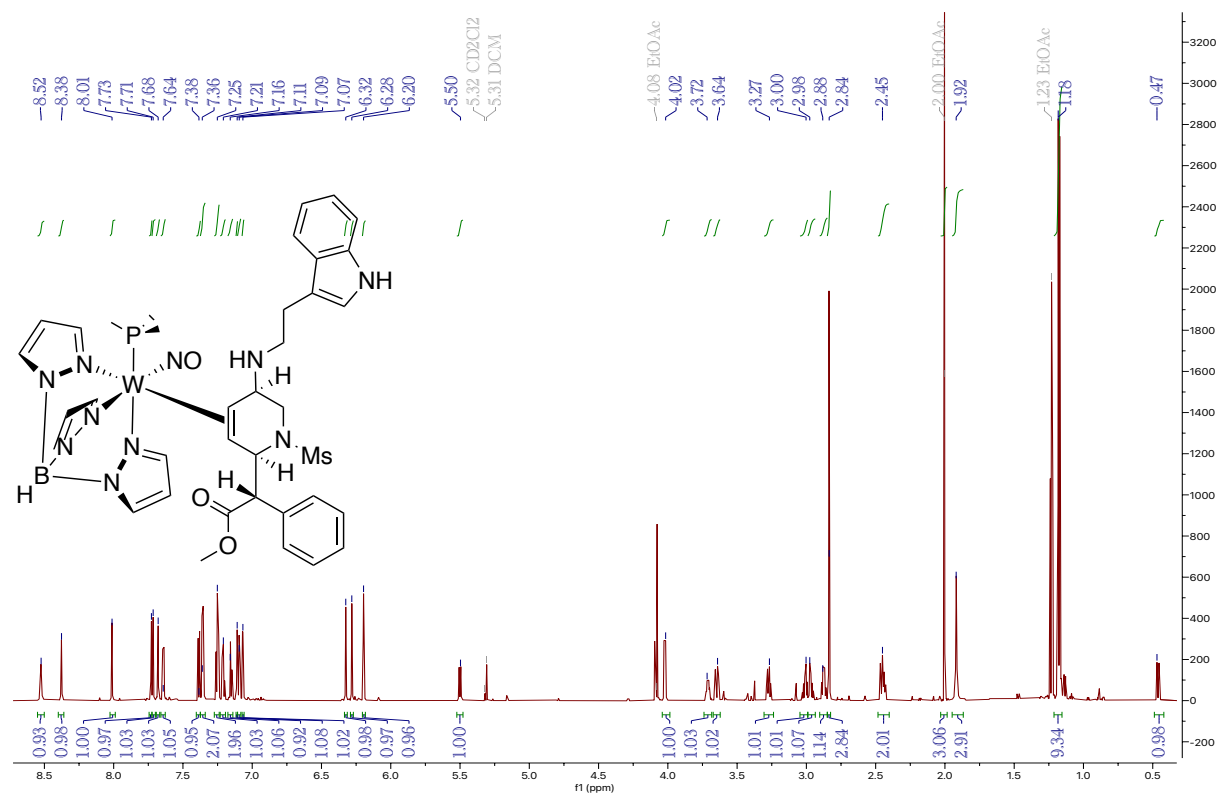


**Figure S29:**  $^{13}\text{C}$  NMR, 200 MHz,  $\text{CD}_2\text{Cl}_2$ , 25  $^\circ\text{C}$ , Compound **17D**

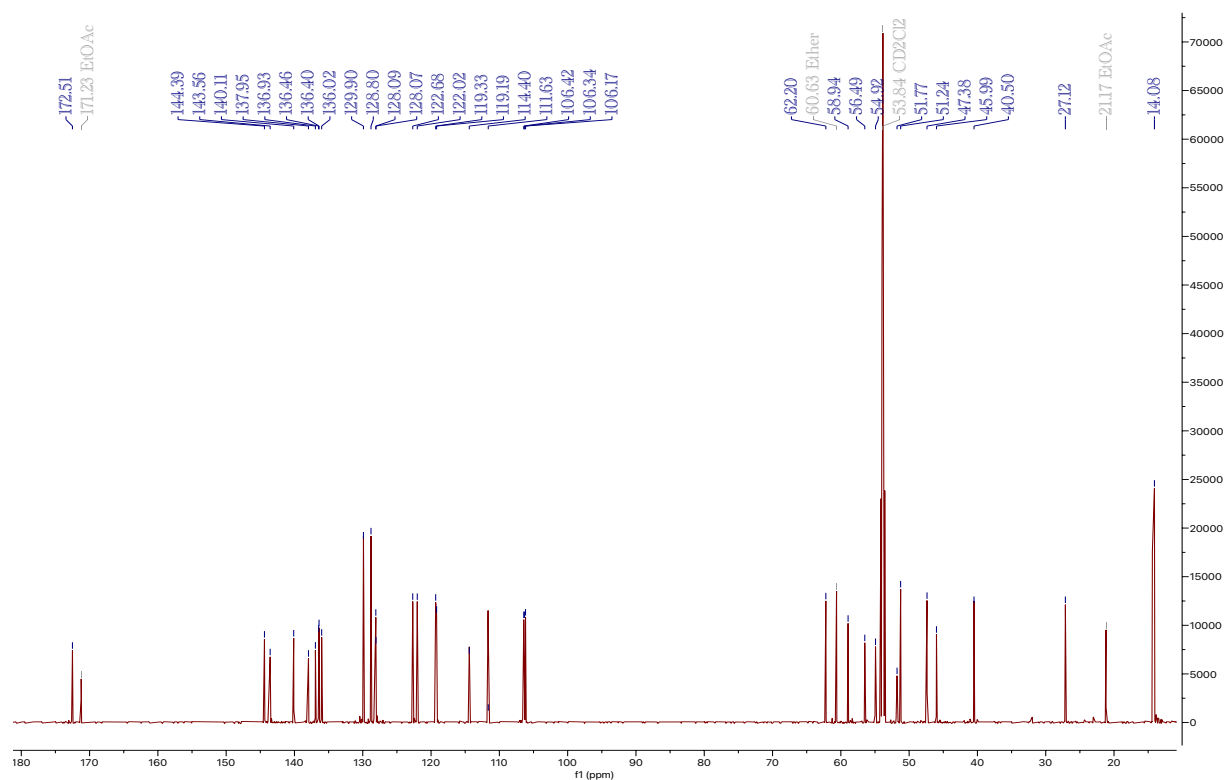


**Figure S30:**  $^1\text{H}$  NMR, 800 MHz,  $\text{CD}_2\text{Cl}_2$ , 25  $^\circ\text{C}$ , Compound **18D**

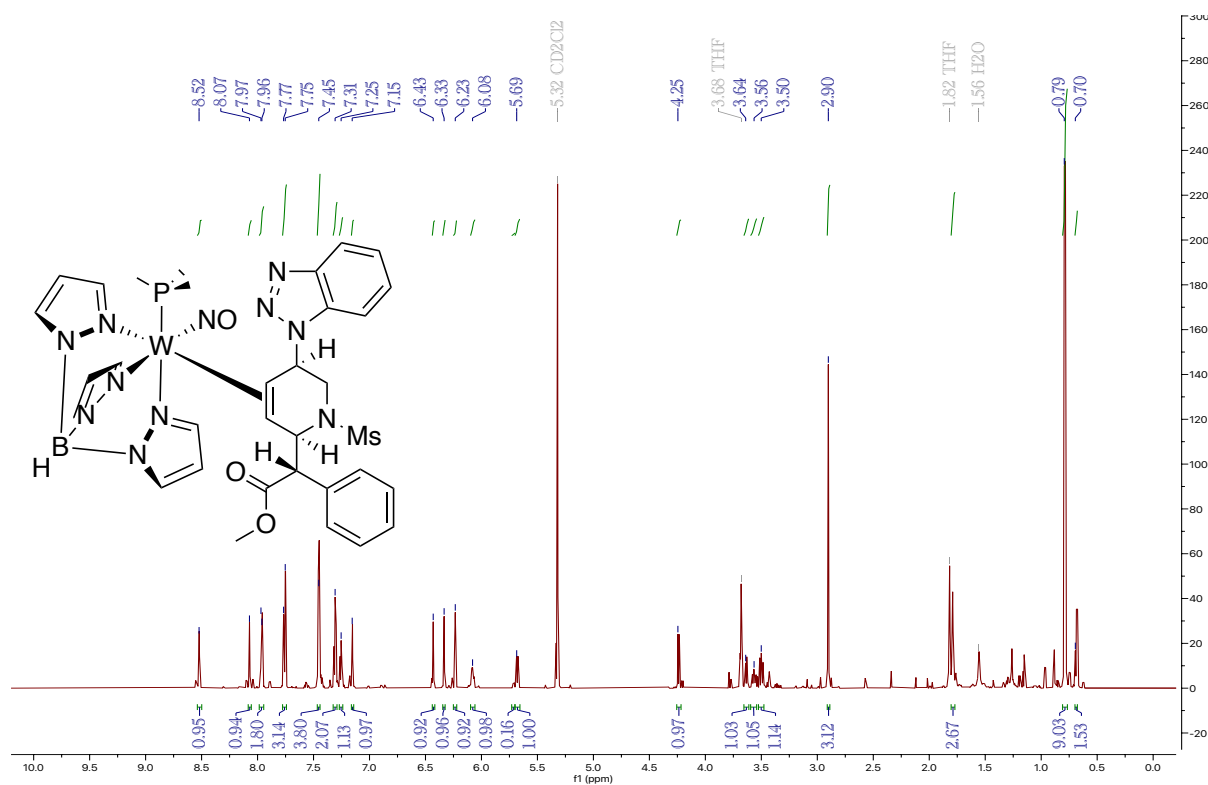


**Figure S31:**  $^{13}\text{C}$  NMR, 200 MHz,  $\text{CD}_2\text{Cl}_2$ , 25  $^\circ\text{C}$ , Compound **18D**

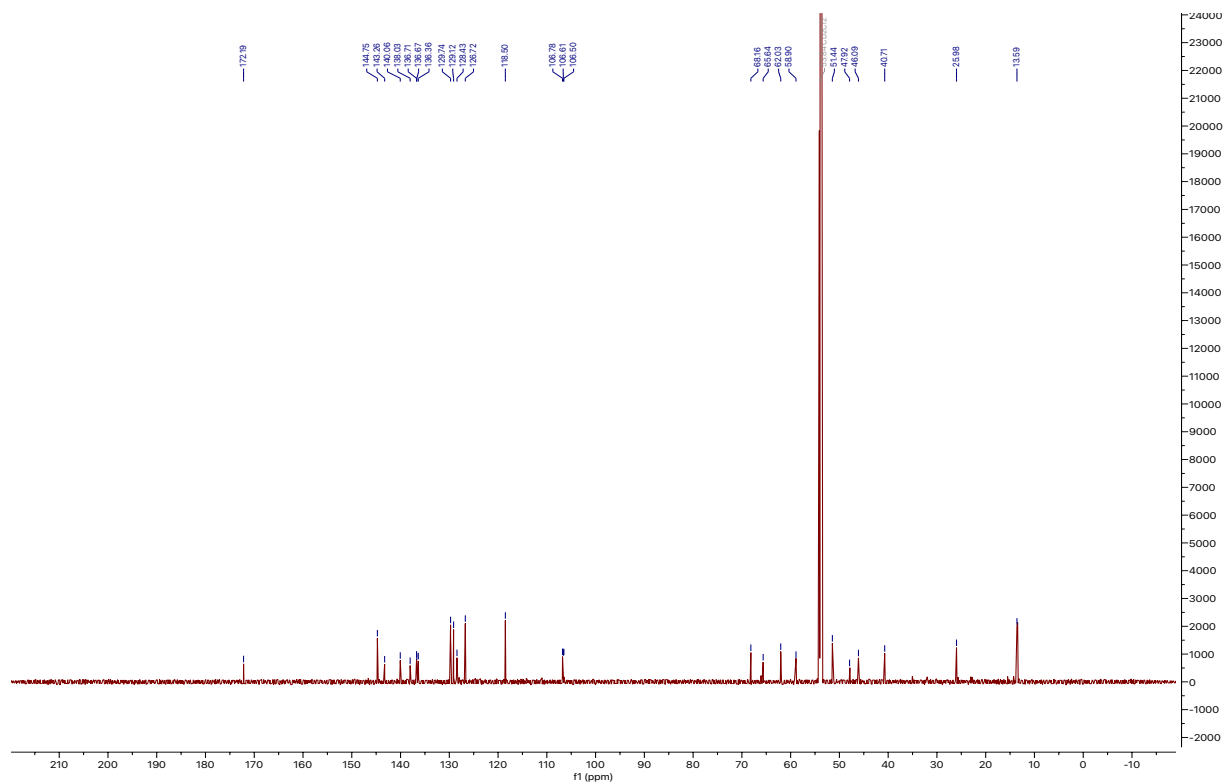


**Figure S32:**  $^1\text{H}$  NMR, 800 MHz,  $(\text{CD}_3)_2\text{CO}$ , 25  $^\circ\text{C}$ , Compound **19D**

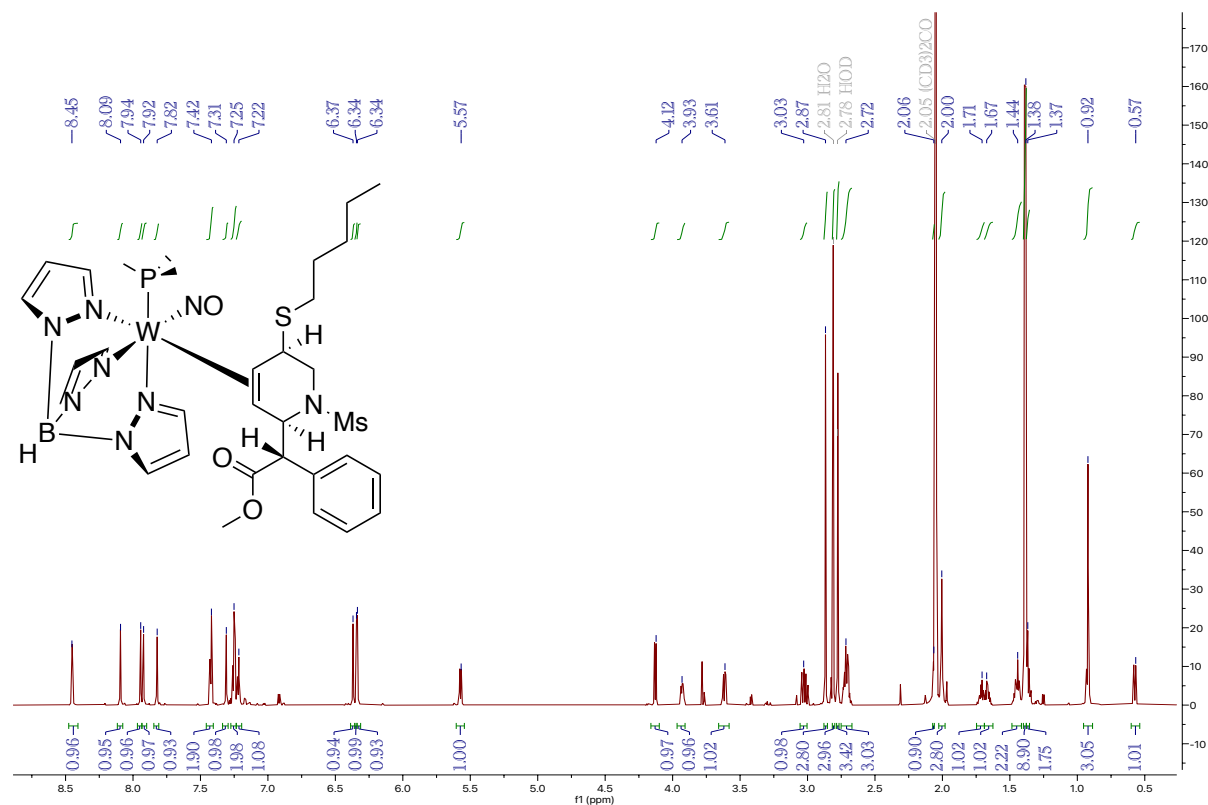


**Figure S33:**  $^{13}\text{C}$  NMR, 200 MHz,  $(\text{CD}_3)_2\text{CO}$ , 25  $^\circ\text{C}$ , Compound **19D**

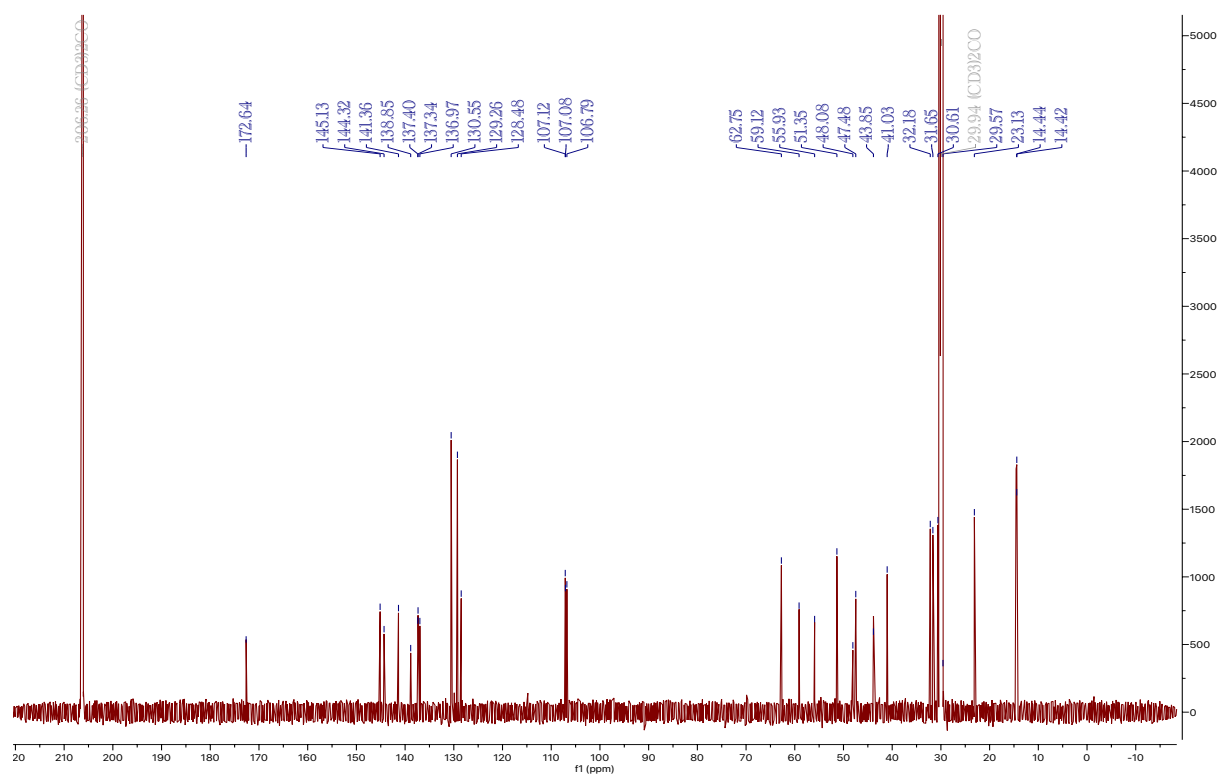


**Figure S34:**  $^1\text{H}$  NMR, 800 MHz,  $(\text{CD}_3)_2\text{CO}$ , 25 °C, Compound **20D**

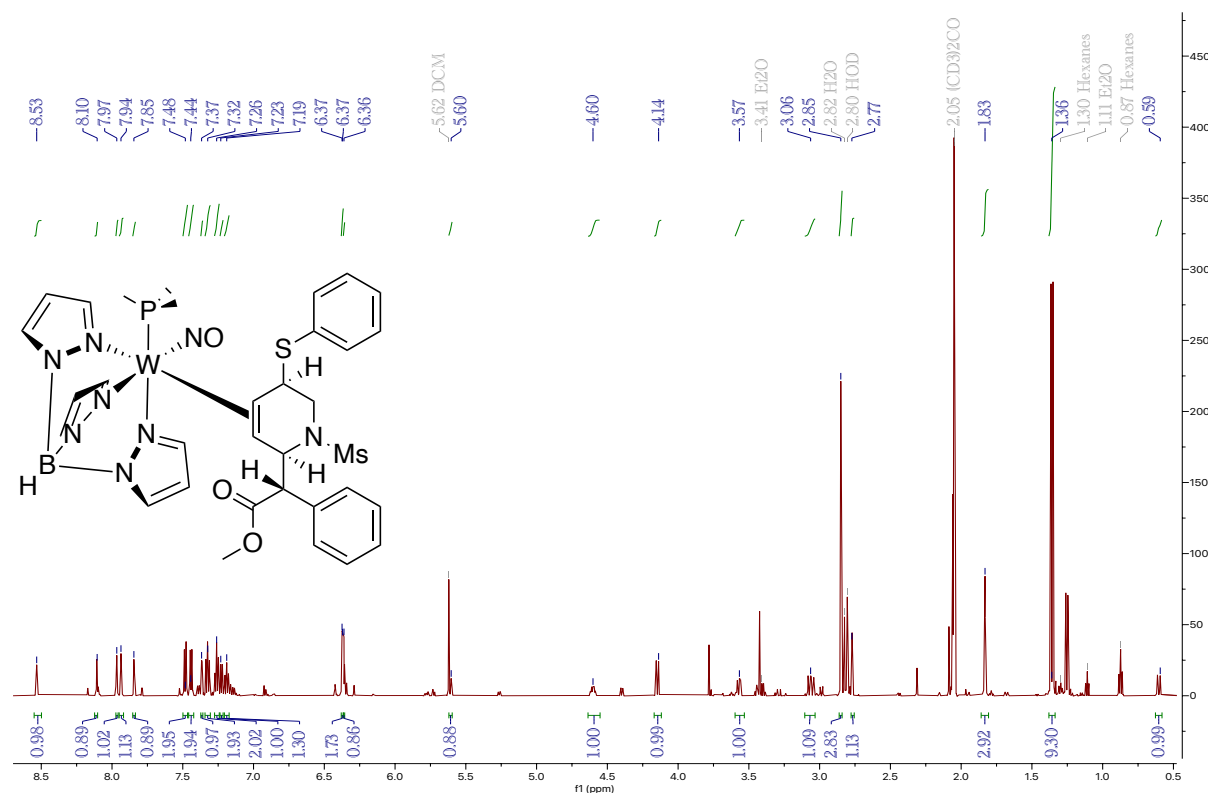


**Figure S35:**  $^{13}\text{C}$  NMR, 200 MHz,  $\text{CD}_2\text{Cl}_2$ , 25 °C, Compound **20D**

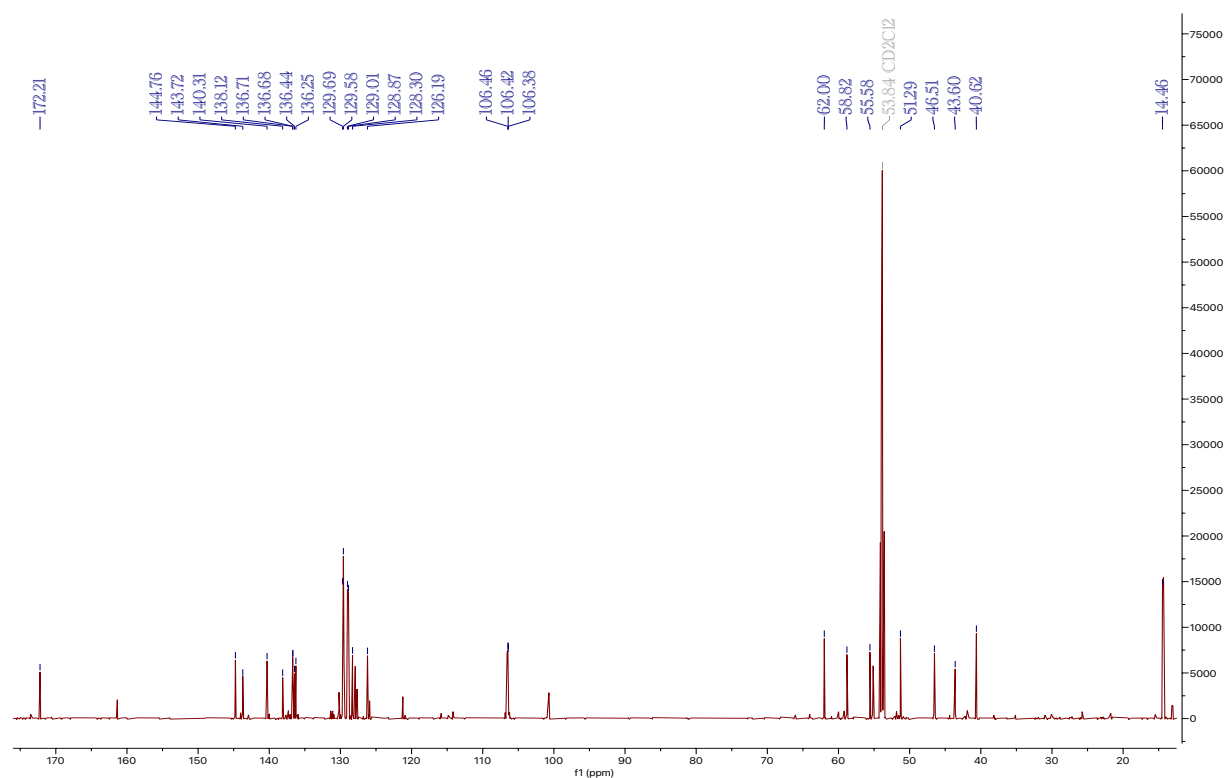


**Figure S36:**  $^1\text{H}$  NMR, 800 MHz,  $(\text{CD}_3)_2\text{CO}$ , 25 °C, Compound **21-Ms**

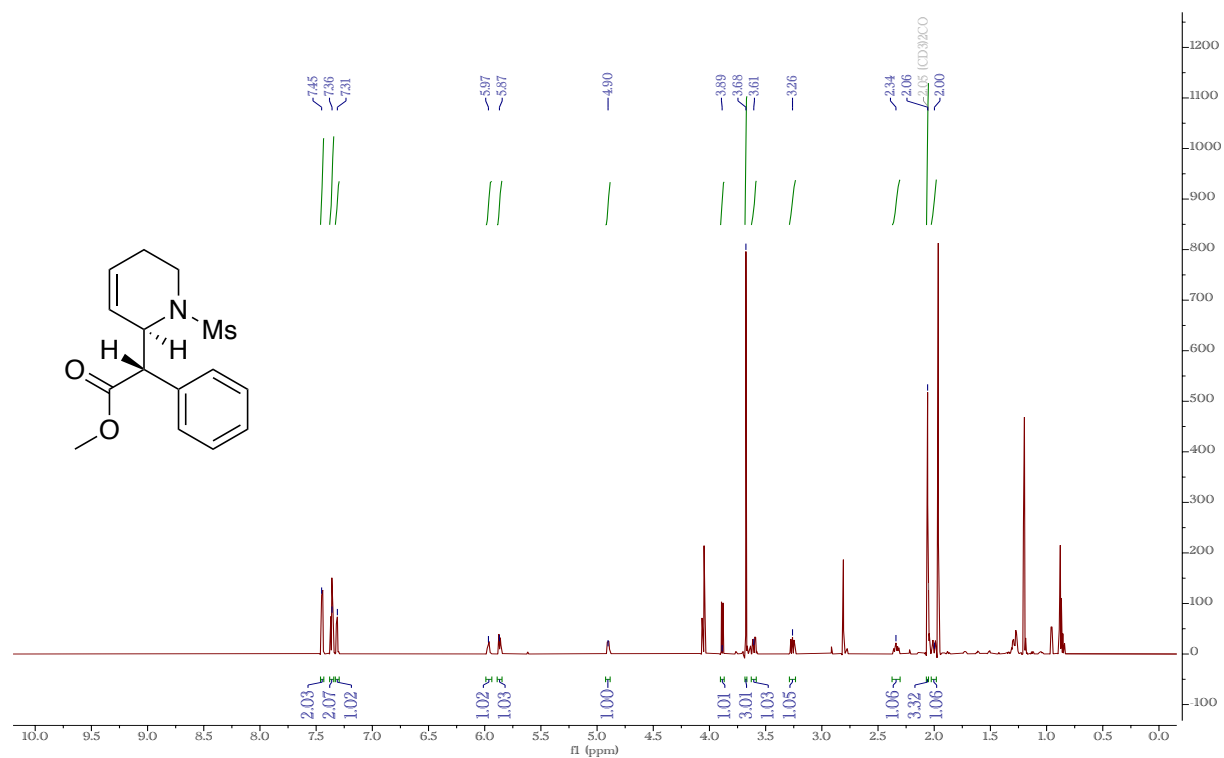


**Figure S37:**  $^{13}\text{C}$  NMR, 200 MHz,  $(\text{CD}_3)_2\text{CO}$ , 25 °C, Compound **21-Ms**

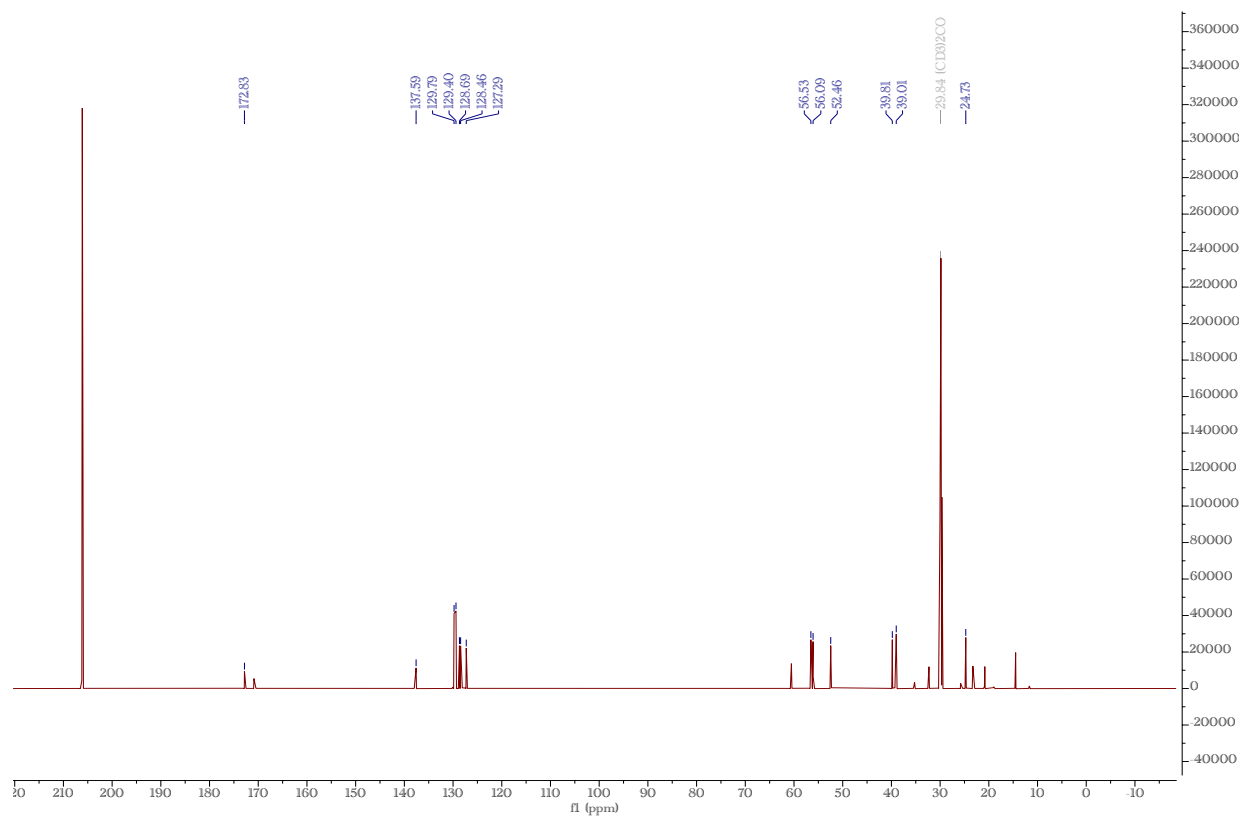


**Figure S38:**  $^1\text{H}$  NMR, 800 MHz,  $\text{CDCl}_3$ , 25  $^\circ\text{C}$ , Compound **21-Ac**

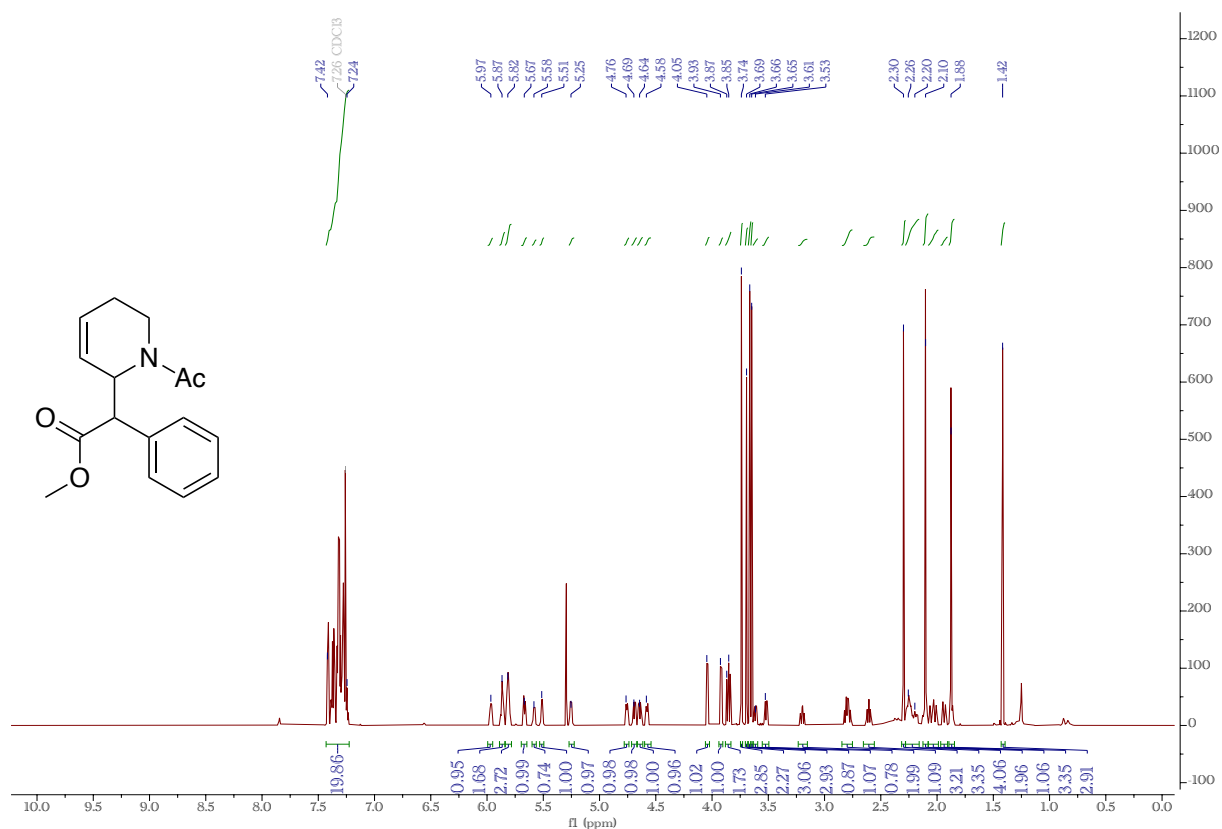


**Figure S39:**  $^{13}\text{C}$  NMR, 200 MHz,  $\text{CDCl}_3$ , 25  $^\circ\text{C}$ , Compound **21-Ac**

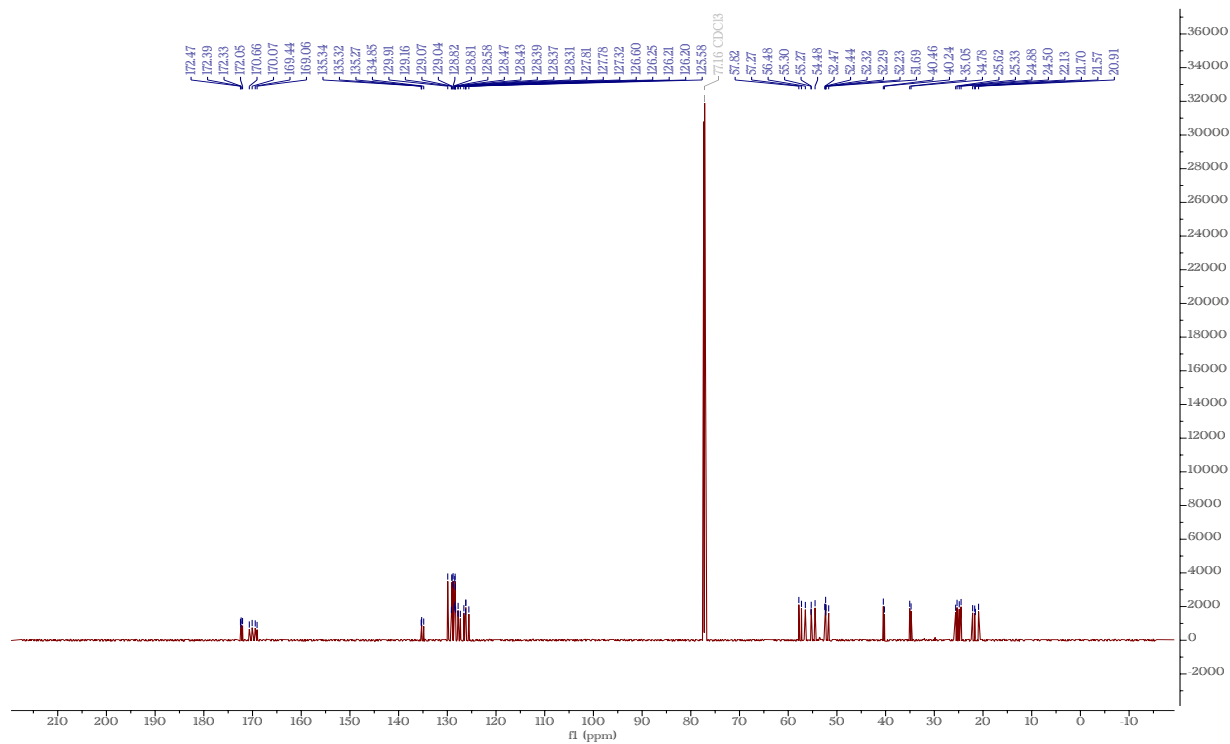




**Figure S40:**  $^1\text{H}$  NMR, 800 MHz,  $\text{CDCl}_3$ , 25  $^\circ\text{C}$ , Compound **21-Ts**

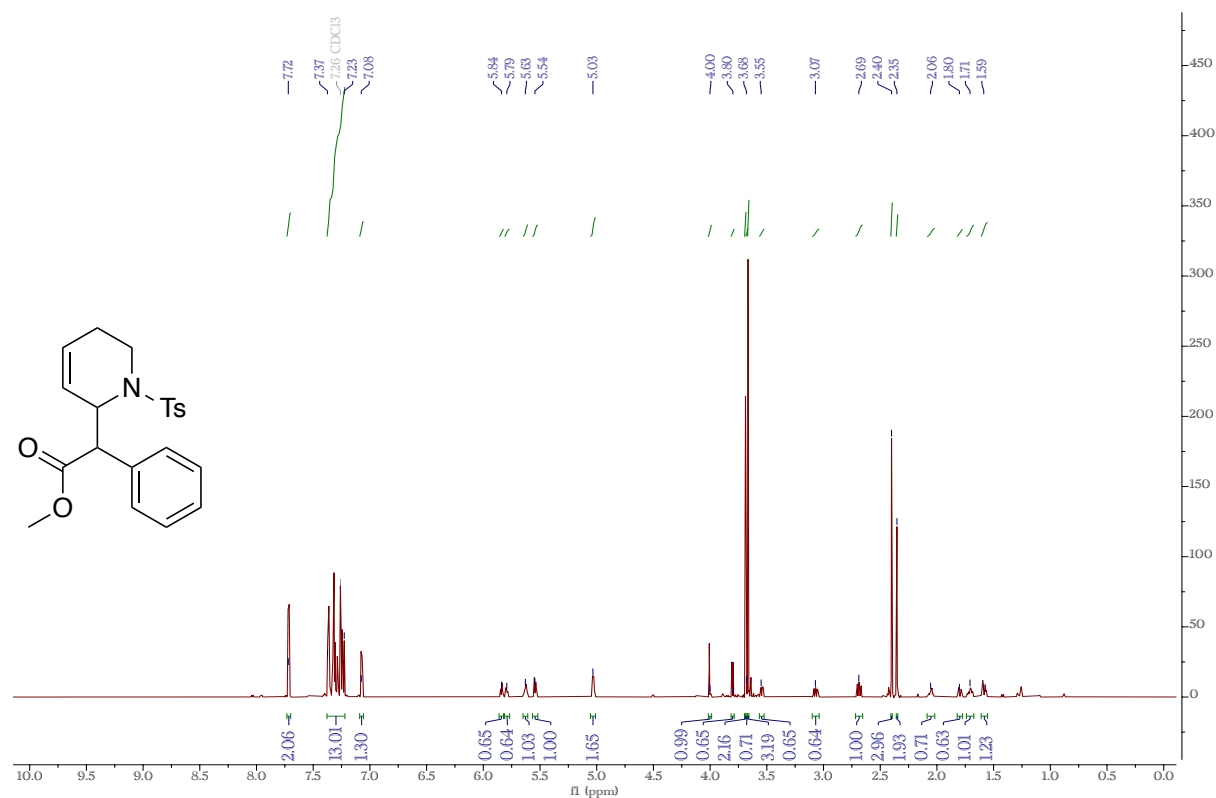


**Figure S41:**  $^{13}\text{C}$  NMR, 200 MHz,  $\text{CDCl}_3$ , 25  $^\circ\text{C}$ , Compound **21-Ts**

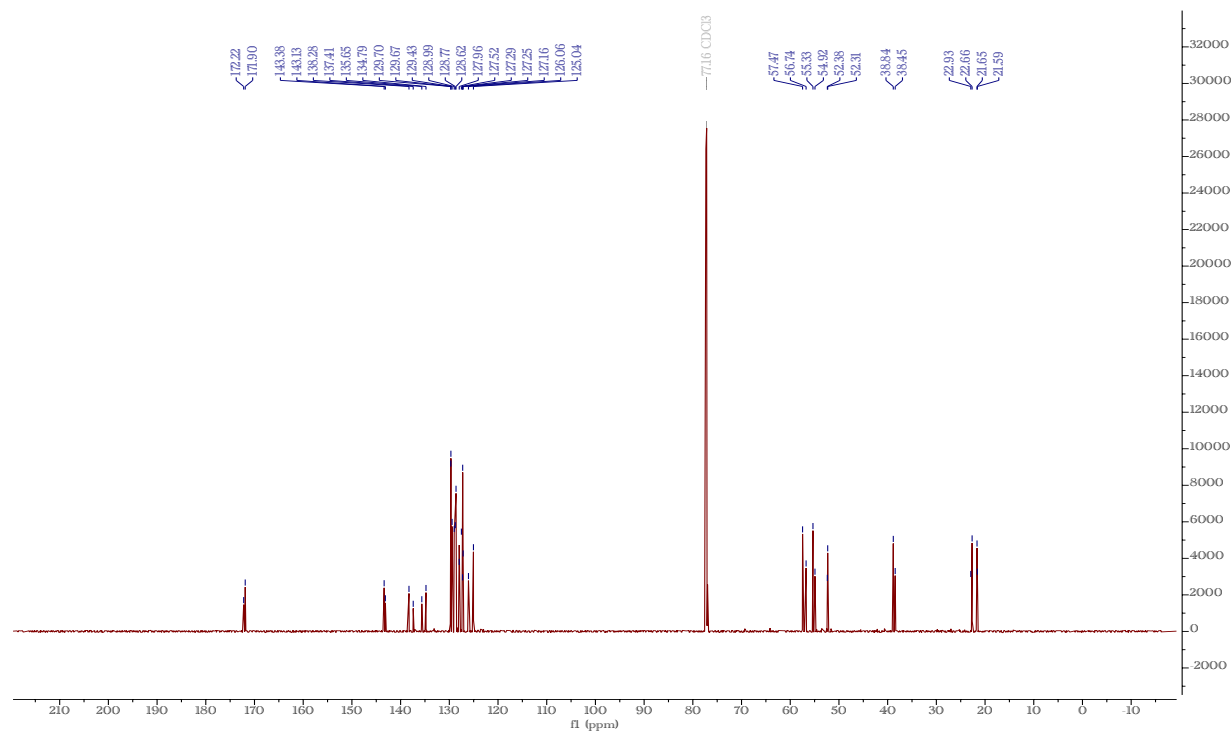


**Figure S42:**  $^1\text{H}$  NMR, 800 MHz,  $(\text{CD}_3)_2\text{CO}$ , 25  $^\circ\text{C}$ , Compound **22**

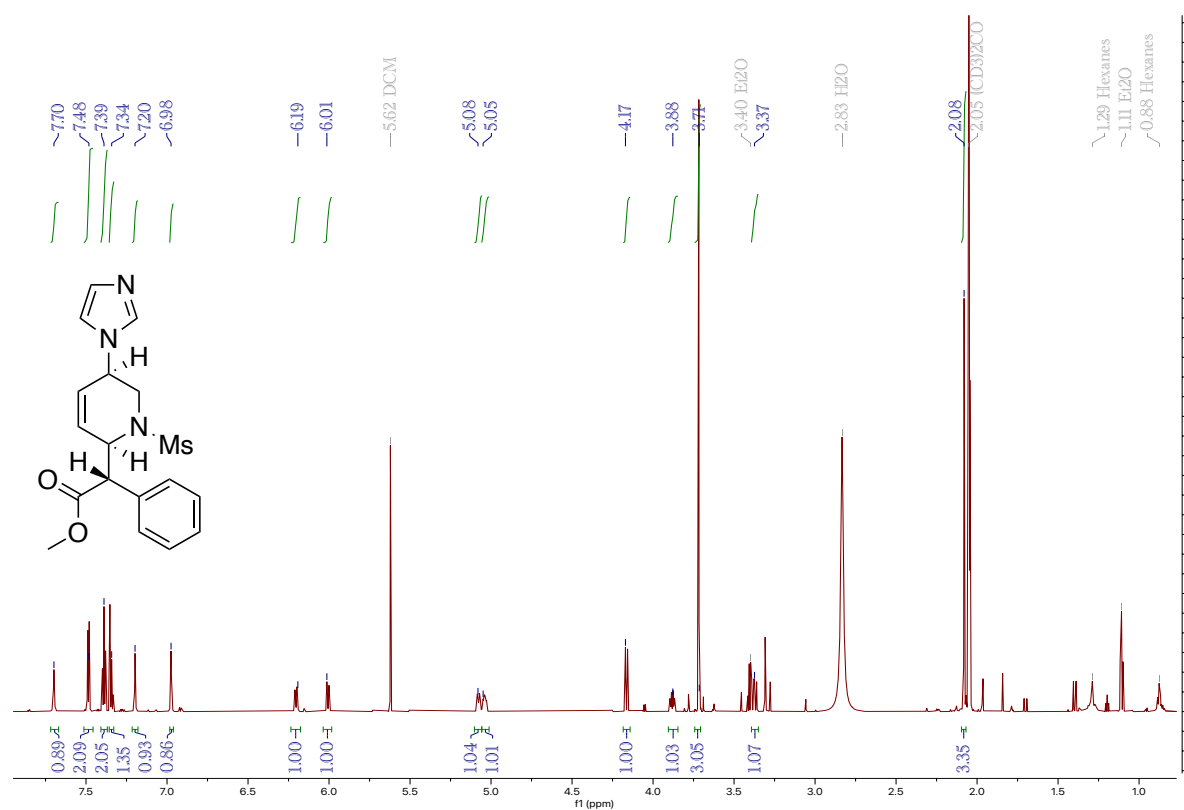


**Figure S43:**  $^{13}\text{C}$  NMR, 200 MHz,  $(\text{CD}_3)_2\text{CO}$ , 25  $^\circ\text{C}$ , Compound **22**

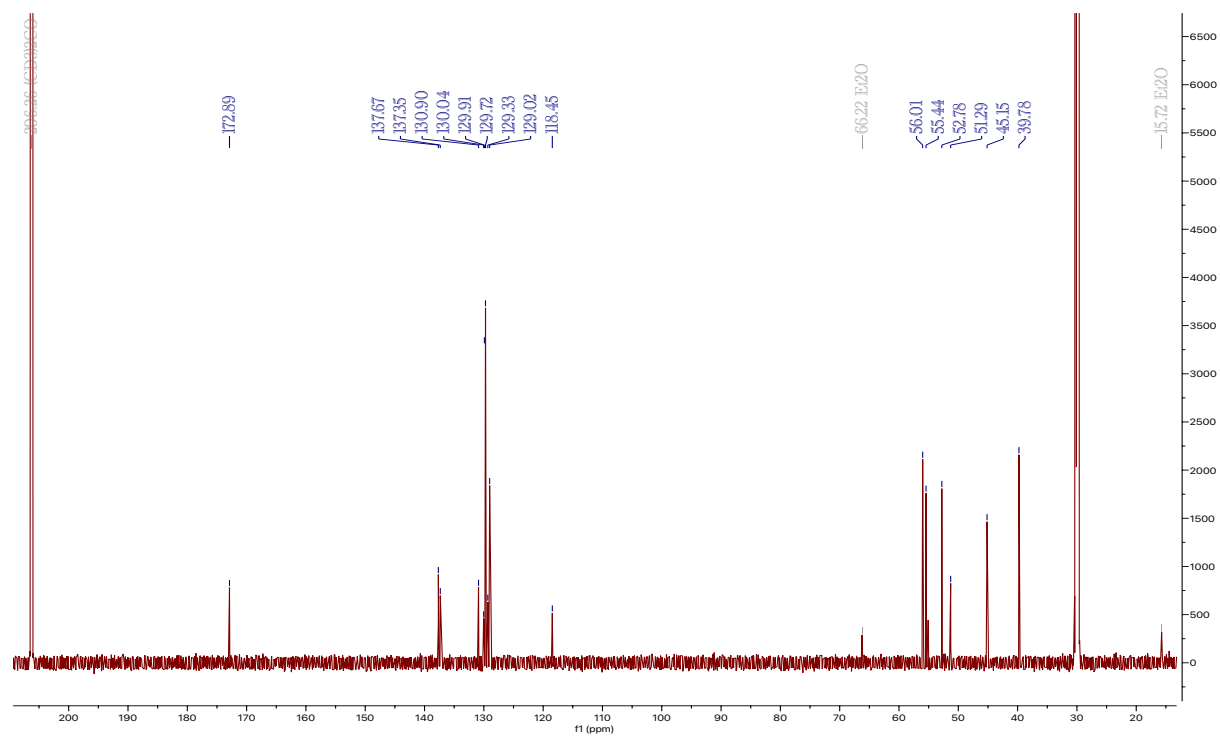


**Figure S44:**  $^1\text{H}$  NMR, 800 MHz,  $\text{CDCl}_3$ , 25  $^\circ\text{C}$ , Compound **23**

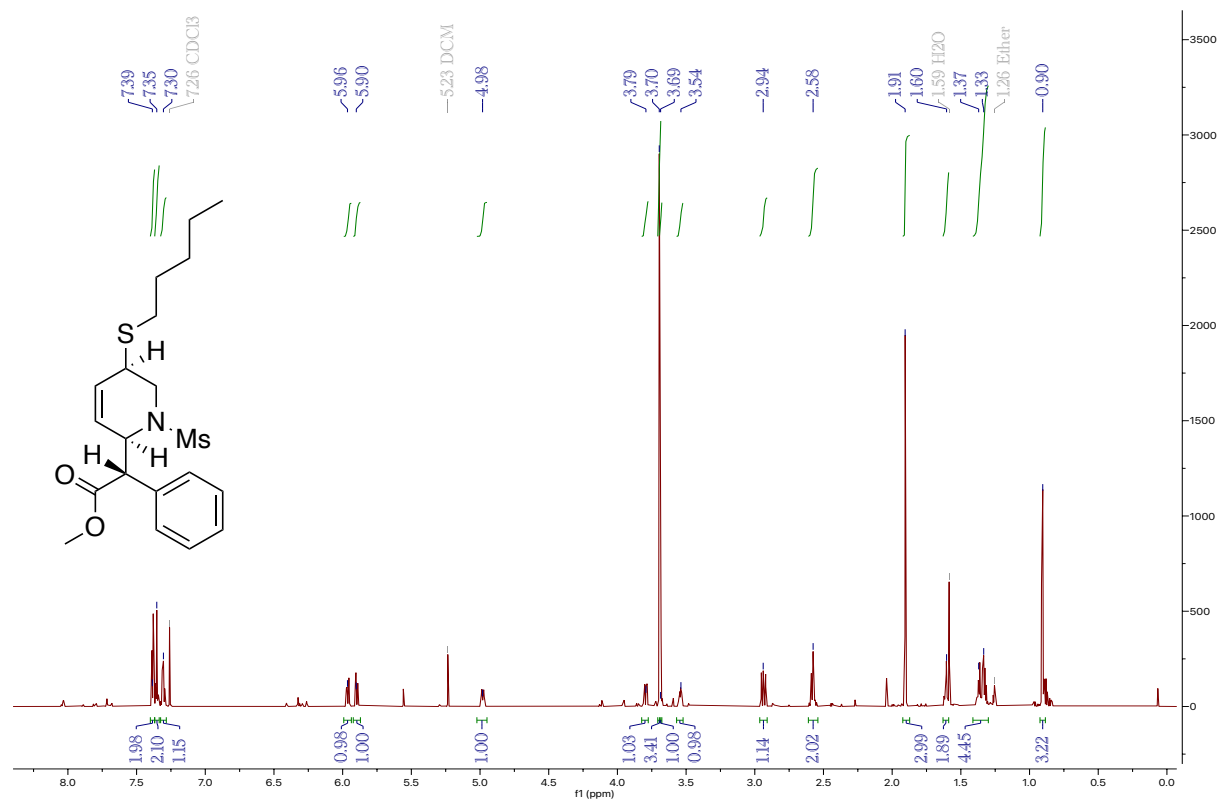


**Figure S45:**  $^{13}\text{C}$  NMR, 200 MHz,  $\text{CDCl}_3$ , 25  $^\circ\text{C}$ , Compound **23**

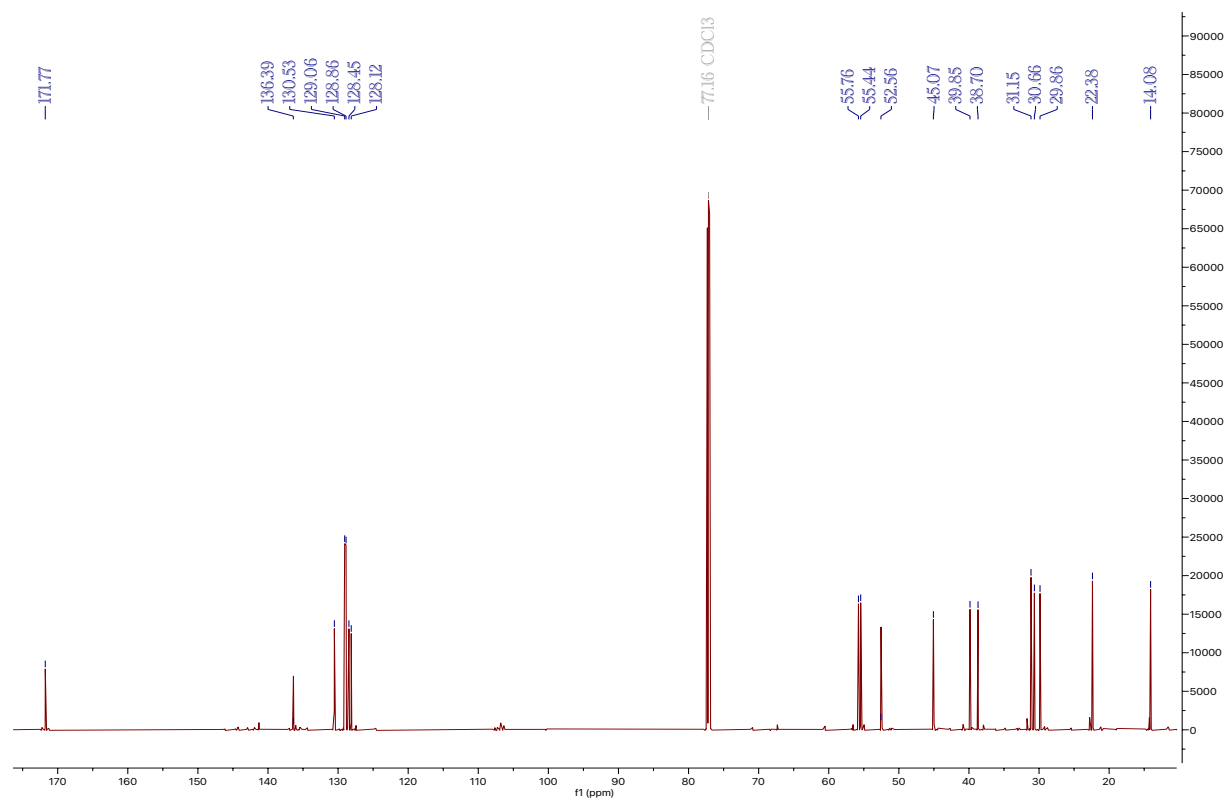


**Figure S46:**  $^1\text{H}$  NMR, 800 MHz,  $(\text{CD}_3)_2\text{CO}$ , 25  $^\circ\text{C}$ , Compound **24**

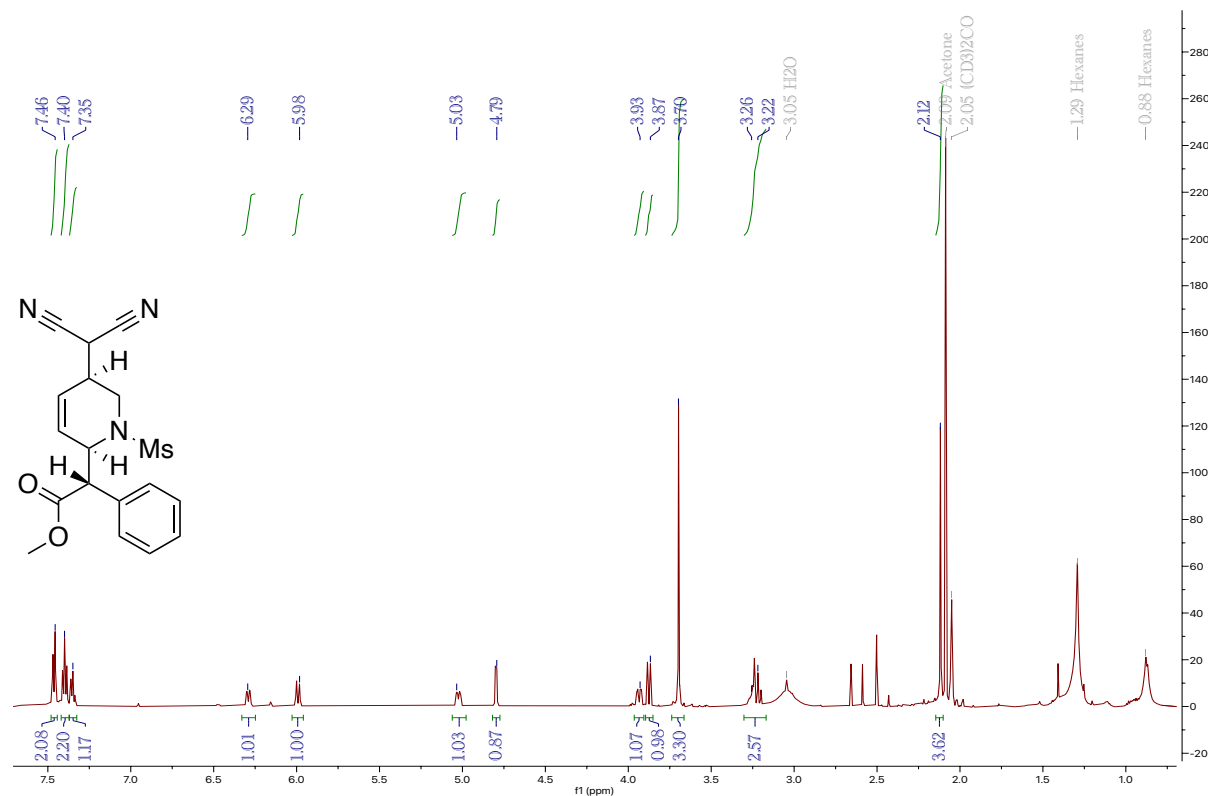


**Figure S47:**  $^{13}\text{C}$  NMR, 200 MHz,  $(\text{CD}_3)_2\text{CO}$ , 25  $^\circ\text{C}$ , Compound **24**

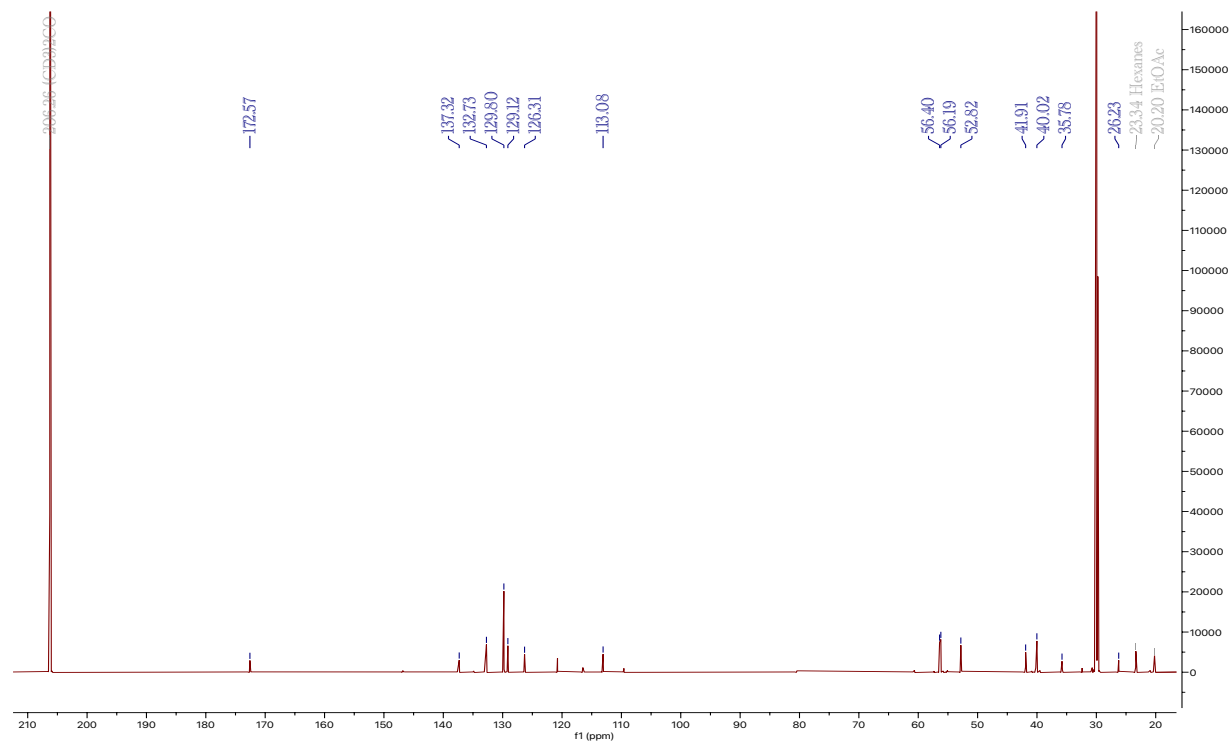


**Figure S48:**  $^1\text{H}$  NMR, 800 MHz,  $(\text{CD}_3)_2\text{CO}$ , 25  $^\circ\text{C}$ , Compound **25**

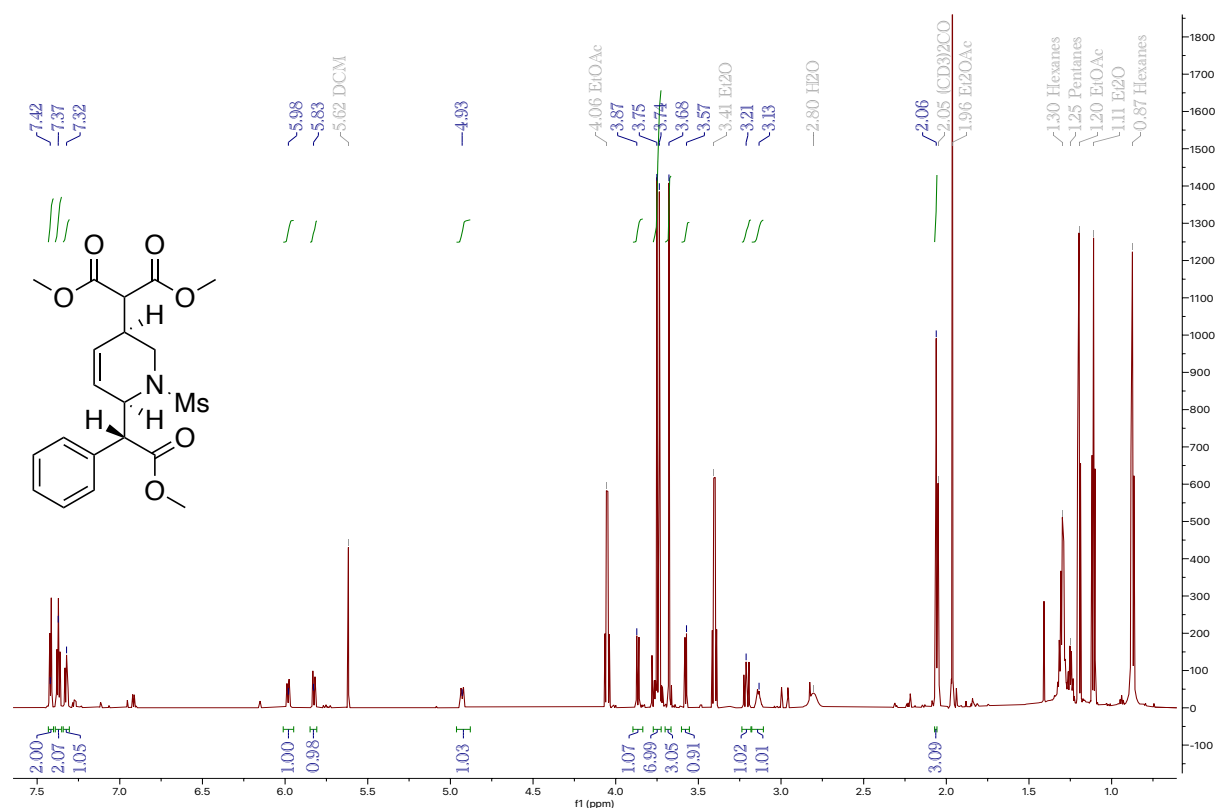


**Figure S49:**  $^{13}\text{C}$  NMR, 200 MHz,  $(\text{CD}_3)_2\text{CO}$ , 25  $^\circ\text{C}$ , Compound **25**

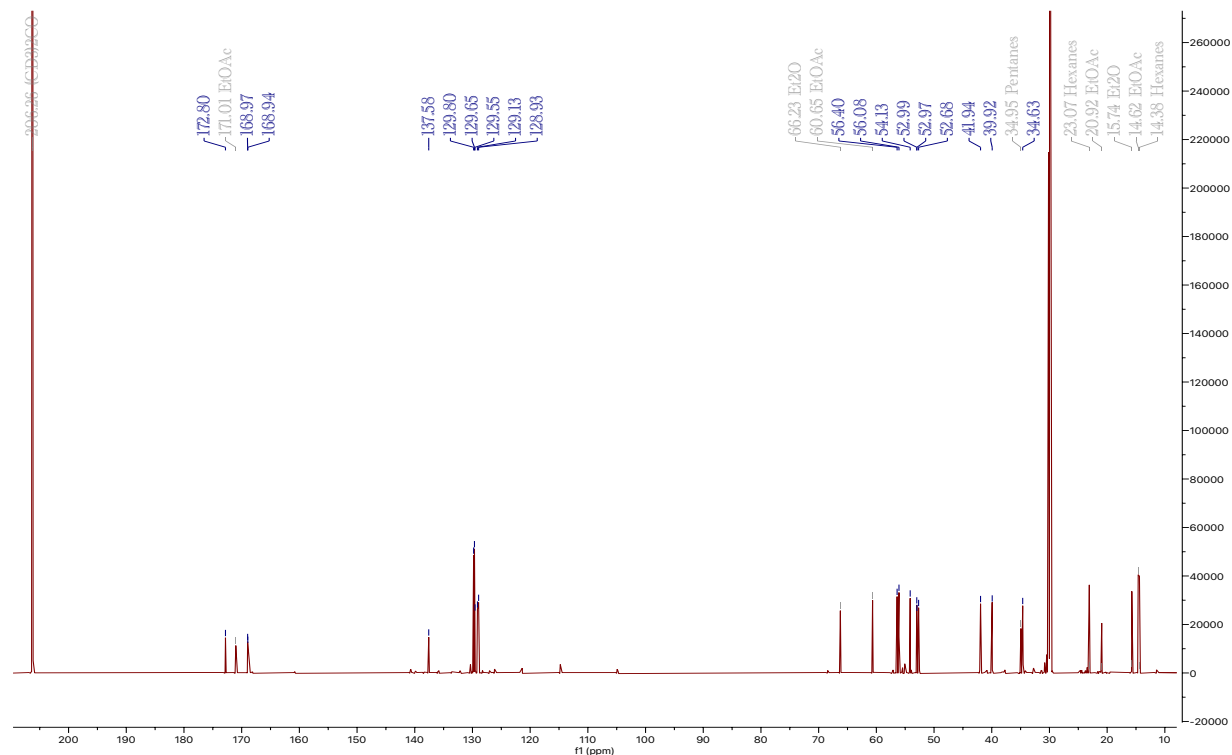


**Figure S50:**  $^1\text{H}$  NMR, 800 MHz,  $(\text{CD}_3)_2\text{CO}$ , 25  $^\circ\text{C}$ , Compound **26**

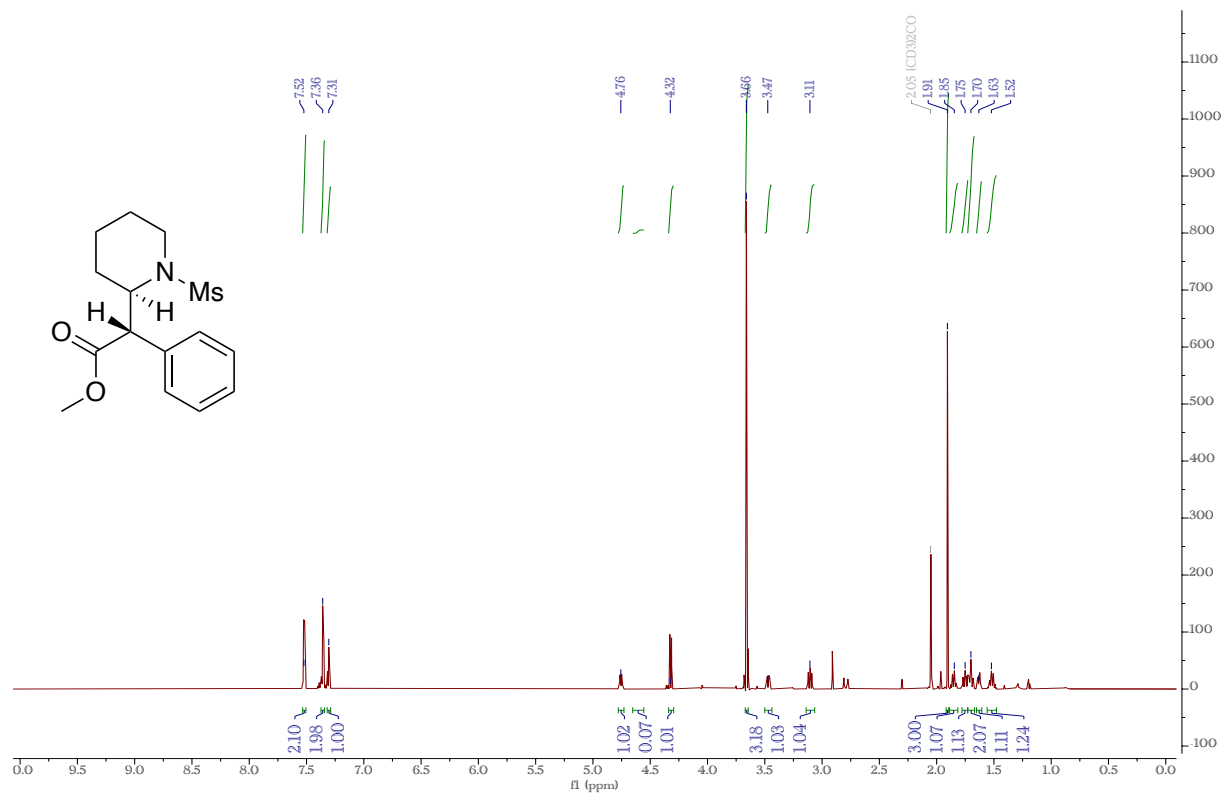


**Figure S51:**  $^{13}\text{C}$  NMR, 200 MHz,  $(\text{CD}_3)_2\text{CO}$ , 25  $^\circ\text{C}$ , Compound **26**

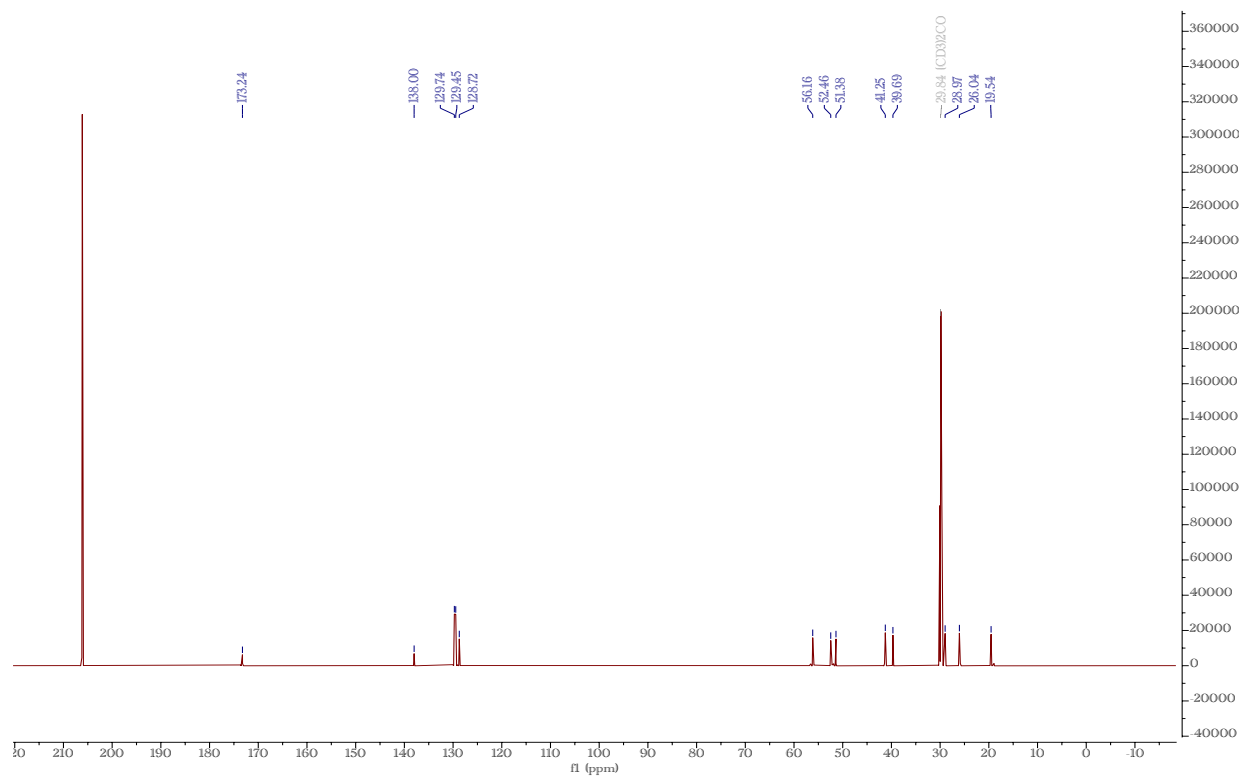


**Figure S52:**  $^1\text{H}$  NMR, 800 MHz,  $\text{CD}_2\text{Cl}_2$ , 25  $^\circ\text{C}$ , 3:1 ratio of Compound **26** to Compound **21'**.

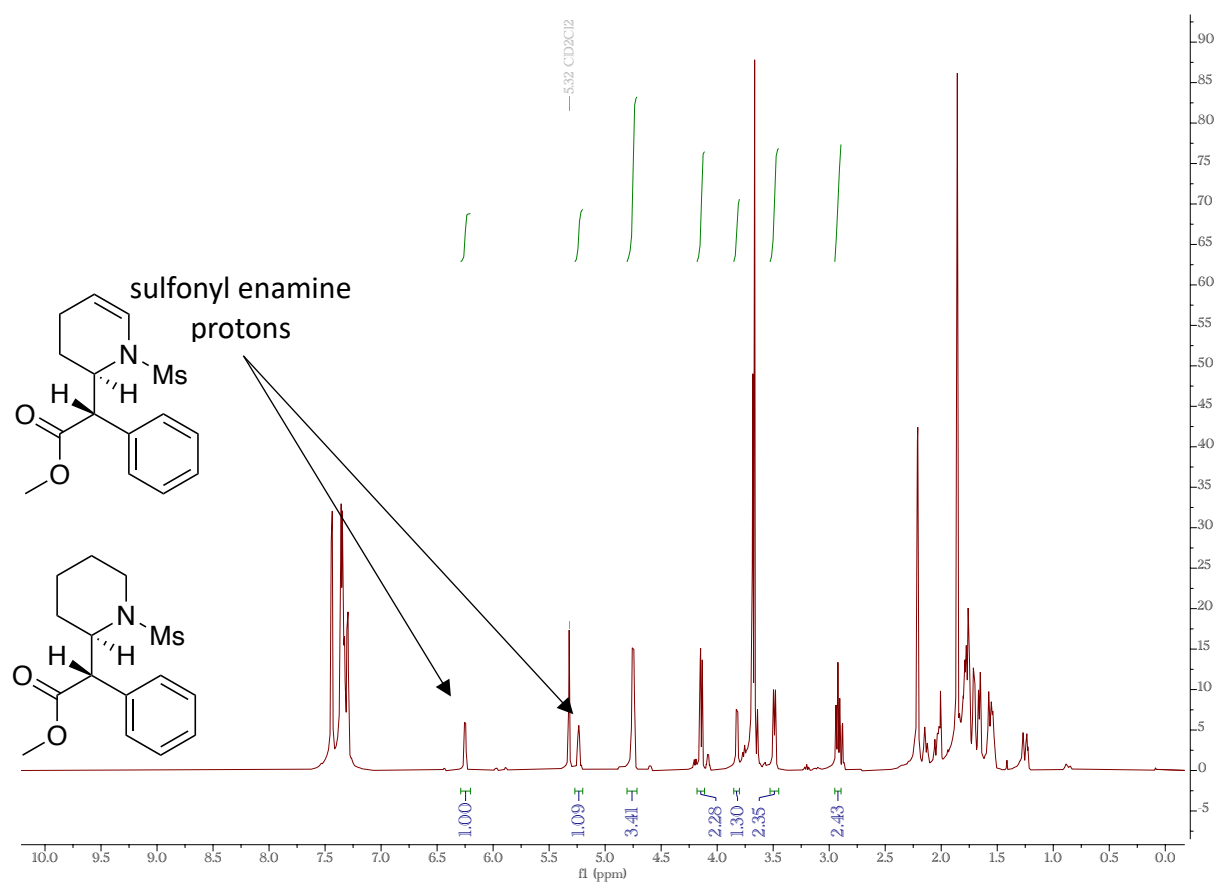


**Figure S53:**  $^1\text{H}$  NMR, 800 MHz,  $\text{CD}_2\text{Cl}_2$ , 25  $^\circ\text{C}$ , Compound **27**

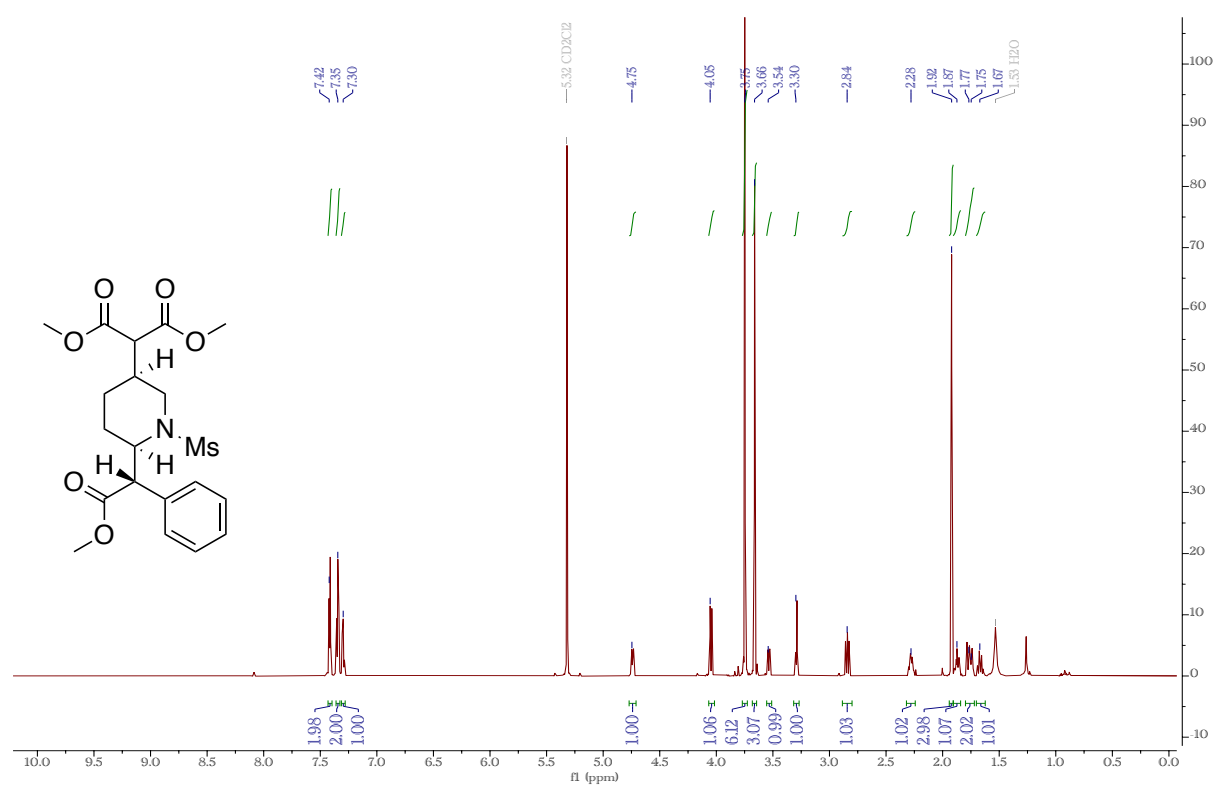
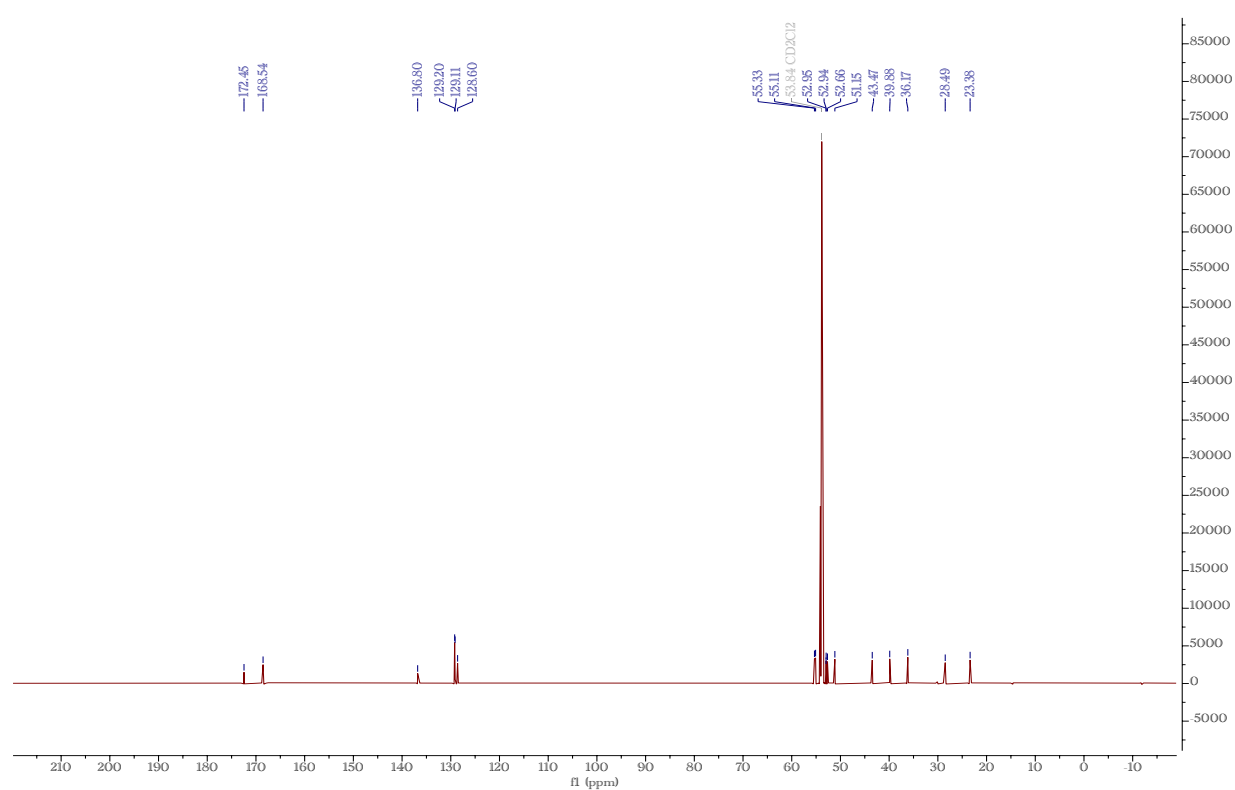


**Figure S54:**  $^{13}\text{C}$  NMR, 200 MHz,  $\text{CD}_2\text{Cl}_2$ , 25  $^\circ\text{C}$ , Compound **27**





### **Computational Methods and DFT Analysis for 7D.**

Ground-state structures were optimized at the M06 level of theory using the 6-31G\*\* [LANL2DZ for W] basis set in Gaussian 16. Conformational analysis was performed by optimizing multiple conformations and determining the lowest energy conformation. Previous literature demonstrates that this functional and basis set choice accurately corroborates experimental results. Vibrational frequency analysis verified that optimized structures were minima, and rigid-rotor-harmonic-oscillator thermochemical chemical corrections were applied at 298 K and 1 atm utilizing Gaussian's default implementation. Bond lengths were used to determine the likelihood of spatial interactions. 2D NMR analysis was performed on a 3 erythro : 1 threo sample using CD<sub>2</sub>Cl<sub>2</sub> as the solvent.

**Table S1: DFT Geometry Optimization, Energies and Coordinates for *erythro*-7D.**

Electronic Energy: -2695.646348 Hartree

Electronic Energy + Free Energy Correction: -2695.095613 Hartree

W	-1.277300	-0.358800	-0.127400
S	3.133200	-2.164600	0.838600
O	2.402400	3.114100	-1.759800
O	3.555700	-1.287700	1.921500
O	-0.812300	-3.271500	0.209300
O	2.635700	3.087700	0.473200
O	4.080800	-2.982800	0.095900
N	-0.871400	-2.065200	0.113500
N	2.298600	-1.207900	-0.256700
C	0.651400	0.573900	-0.489800
C	0.228400	0.027500	-1.762900
H	-0.113300	0.720500	-2.537900
C	0.987300	-1.135400	-2.253000
H	0.785800	-1.536700	-3.245700
C	2.041200	0.209100	-0.012300
H	2.184200	0.408700	1.055800
C	1.935100	-1.733100	-1.511100
H	2.494700	-2.608600	-1.830900
C	3.089800	1.073700	-0.787400
H	2.969000	0.837000	-1.852100
C	4.511300	0.775800	-0.376900
C	2.711200	2.518500	-0.592800
C	5.255800	-0.117200	-1.147900
H	4.811100	-0.543800	-2.047000
C	6.364900	0.939900	1.162800
H	6.794700	1.353000	2.072900
C	1.897900	-3.265800	1.488300
H	2.418700	-3.970700	2.141200
H	1.397000	-3.781400	0.666400
H	1.163100	-2.683100	2.049300
C	6.539700	-0.488000	-0.764800
H	7.099500	-1.198500	-1.368400
C	1.950200	4.457200	-1.636400
H	2.704700	5.082200	-1.149100
H	1.031500	4.500000	-1.039300
H	1.761700	4.810000	-2.651600
C	5.078400	1.302700	0.785800
H	4.498100	1.989300	1.397900
C	7.098100	0.042300	0.392200
H	8.101200	-0.247700	0.697200
H	0.457400	1.644000	-0.352400
P	-2.574400	-1.049400	-2.165200
C	-4.395800	-0.820100	-2.039600
H	-4.806900	-1.422700	-1.224600
H	-4.890100	-1.094100	-2.978900

H	-4.600100	0.234700	-1.816200
C	-2.286100	-0.253900	-3.796200
H	-2.493400	0.819800	-3.730900
H	-2.956700	-0.694700	-4.543000
H	-1.251100	-0.394100	-4.120500
C	-2.380700	-2.820400	-2.577300
H	-1.330300	-3.002500	-2.830300
H	-3.024800	-3.108200	-3.415800
H	-2.604500	-3.436000	-1.700600
N	-3.204800	-0.755100	0.932500
N	-2.171100	1.714000	-0.475400
N	-0.939400	0.492500	1.920100
N	-1.874400	1.292800	2.493200
N	-3.907700	0.208700	1.567100
N	-2.977800	2.273300	0.455700
C	0.055300	0.365800	2.801400
H	0.926200	-0.234800	2.562400
C	-1.459400	1.660900	3.722300
H	-2.079100	2.305500	4.332200
C	-3.850700	-1.908100	1.125800
H	-3.436100	-2.828200	0.727100
C	-2.071300	2.597500	-1.475200
H	-1.444100	2.377300	-2.332200
C	-0.226100	1.089400	3.963500
H	0.388400	1.184600	4.846400
C	-2.824300	3.740300	-1.198700
H	-2.940900	4.623800	-1.809200
B	-3.230700	1.577200	1.812100
C	-3.380200	3.488300	0.043100
H	-4.028200	4.087700	0.669400
C	-4.993200	-0.334700	2.150600
H	-5.667800	0.284500	2.727700
C	-5.006200	-1.692100	1.882200
H	-5.735700	-2.421500	2.202900
H	-3.921100	2.272800	2.509700

**Table S2: DFT Geometry Optimization, Energies and Coordinates for *threo*-7D.**

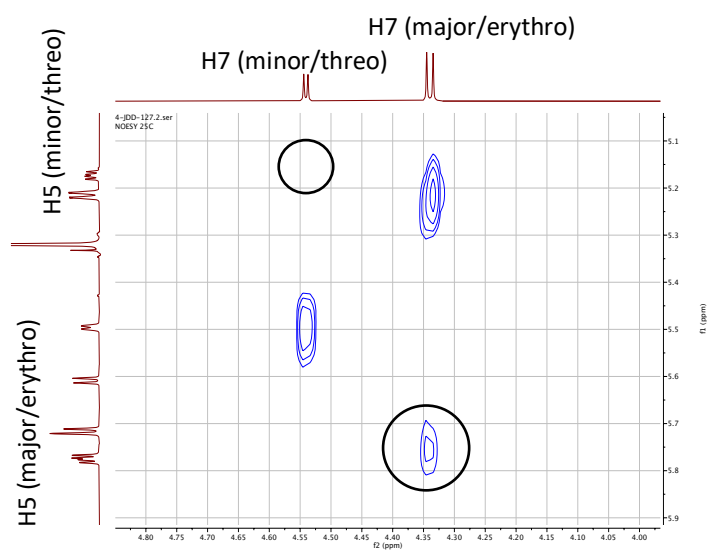
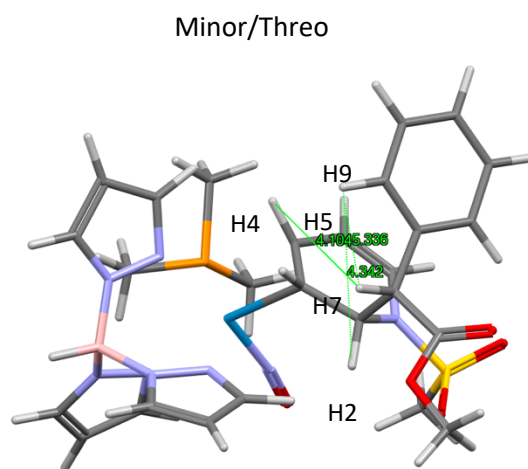
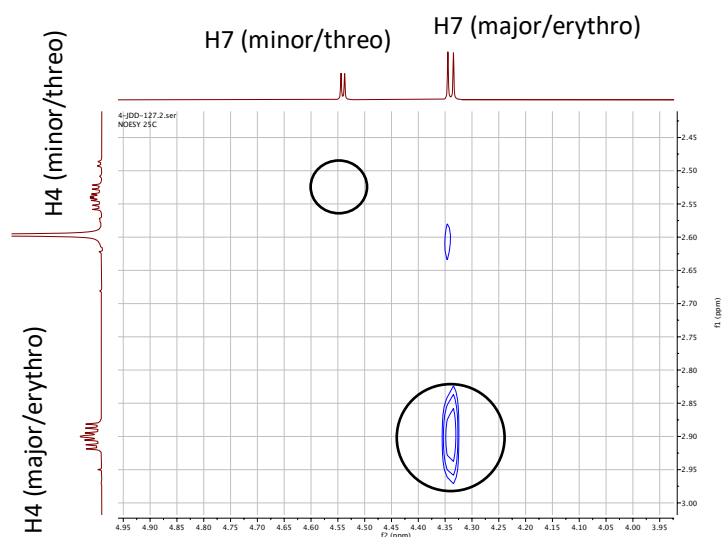
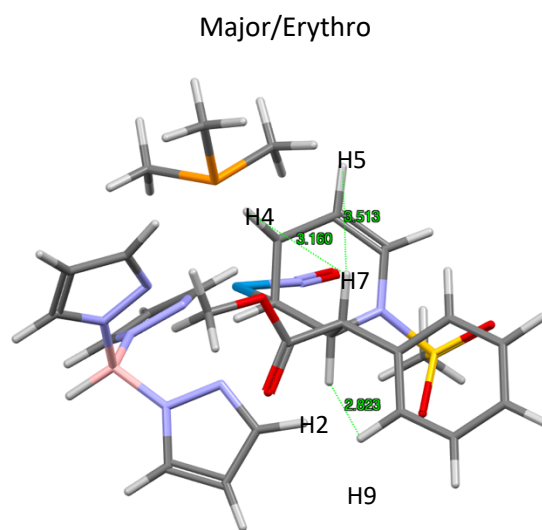
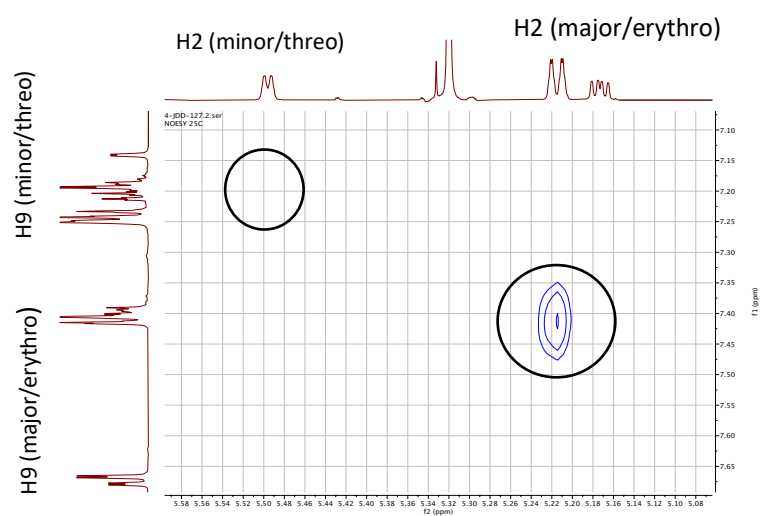
Electronic Energy: -2695.644006 Hartree

Electronic Energy + Free Energy Correction: -2695.092530 Hartree

O	-0.556500	0.328100	3.092900
N	-0.688300	0.185300	1.893500
W	-1.227500	-0.106900	0.235500
C	0.399200	-1.512200	-0.449400
C	0.721600	-0.130500	-0.720900
C	1.973600	0.501200	-0.126500
H	0.065600	-2.108100	-1.303900
H	0.575400	0.181700	-1.760500
H	1.767200	1.511900	0.242900
C	3.063300	0.647000	-1.246800
N	2.453000	-0.257900	1.039500
S	3.390000	0.477700	2.221800
O	4.606200	-0.303000	2.406400
O	3.450500	1.892200	1.875700
C	2.428500	0.305100	3.705100
H	2.231300	-0.756100	3.877400
H	3.035600	0.716100	4.515500
H	1.483500	0.839000	3.583900
C	3.636400	-0.676200	-1.674900
C	4.639400	-1.321400	-0.944200
C	3.100700	-1.321300	-2.791800
C	5.073400	-2.588000	-1.318300
H	5.079900	-0.831000	-0.080700
C	3.531900	-2.590200	-3.163100
H	2.328000	-0.820800	-3.376300
C	4.519600	-3.229800	-2.421600
H	5.853600	-3.077000	-0.738900
H	3.101200	-3.075100	-4.037000
H	4.863300	-4.221600	-2.708400
C	4.091400	1.697400	-0.875600
O	5.258200	1.524400	-0.629200
O	3.506500	2.912400	-0.885500
C	4.331900	3.968000	-0.401400
H	3.736200	4.879200	-0.479200
H	4.606000	3.774600	0.640100
H	5.242200	4.055400	-1.002500
H	2.515000	1.089200	-2.092700
C	1.258300	-2.251600	0.482500
C	2.234600	-1.640900	1.163000
H	1.167100	-3.332600	0.572800
H	2.938200	-2.167000	1.803900
N	-1.287600	1.962700	-0.709900
N	-2.422200	2.396000	-1.320700
N	-2.343800	-0.569900	-1.722000
N	-3.368300	0.221500	-2.121500
N	-3.204500	0.705500	0.898400

N	-4.126200	1.231000	0.063000
C	-2.223000	3.625800	-1.832200
C	-0.929000	4.017000	-1.552100
C	-0.386000	2.938800	-0.850300
C	-3.916900	-0.268100	-3.247000
C	-3.239900	-1.419900	-3.604300
C	-2.262700	-1.561400	-2.618300
C	-5.182700	1.670100	0.773200
C	-4.949100	1.415600	2.113100
C	-3.684200	0.821200	2.139800
B	-3.702800	1.538500	-1.386500
H	-4.577200	2.123700	-1.970400
H	-3.023700	4.128100	-2.359700
H	-0.443800	4.945400	-1.814800
H	0.614200	2.831700	-0.449900
H	-4.746200	0.246700	-3.714700
H	-3.419000	-2.056700	-4.458100
H	-1.499300	-2.323600	-2.520900
H	-6.016200	2.145100	0.271800
H	-5.593300	1.642700	2.950000
H	-3.081600	0.489700	2.979800
C	-3.952300	-2.389300	1.202300
H	-4.268300	-3.397000	1.496900
H	-4.303400	-1.667700	1.945400
H	-4.410700	-2.132800	0.238500
C	-1.499900	-2.764000	2.677100
H	-1.681700	-1.937000	3.372000
H	-1.969500	-3.682500	3.046600
H	-0.413300	-2.892100	2.609400
P	-2.122900	-2.307100	1.021400
C	-1.866800	-3.844700	0.048100
H	-2.266100	-4.701500	0.603400
H	-2.402200	-3.766800	-0.904400
H	-0.806100	-4.013600	-0.155400

**Figure S55: H-H Bond Lengths and NOESY Interactions.**



### Chiral HPLC Parameters:

Equipment: Agilent 1260 Infinity II Flexible Pump (G7104C), Agilent 1260 Vialsampler (G7129C), Agilent 1260 DAD HS (G7117C), Agilent 1260 RID (G7162A), Daicel IC-3 column, 3  $\mu$ m particle size, 4.6 mm x 250 mm

Method: 80/20 Mixed Hexanes (HPLC Grade)/Ethyl Acetate (HPLC Grade) isocratic, 1 ml/min for 35 minutes, 40 °C, 2.50  $\mu$ L injection volume

DAD: 254 nm, 265 nm with a bandwidth of 4 nm; Reference 390 nm with a bandwidth of 20 nm

**Figure S56: Chiral HPLC Spectrum for 3:1  $\pm$  *erythro*/*threo* 21-Ms**

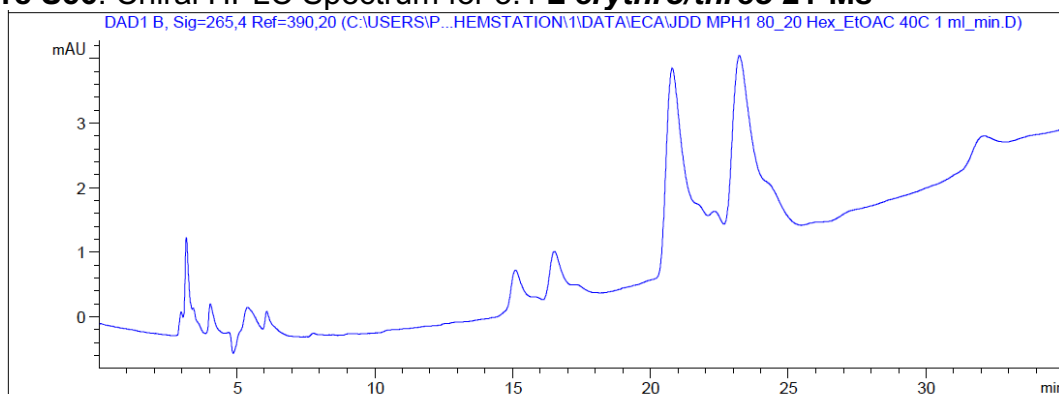


**Figure S57: Chiral HPLC Spectrum for  $\pm$  *erythro* 21-Ms**

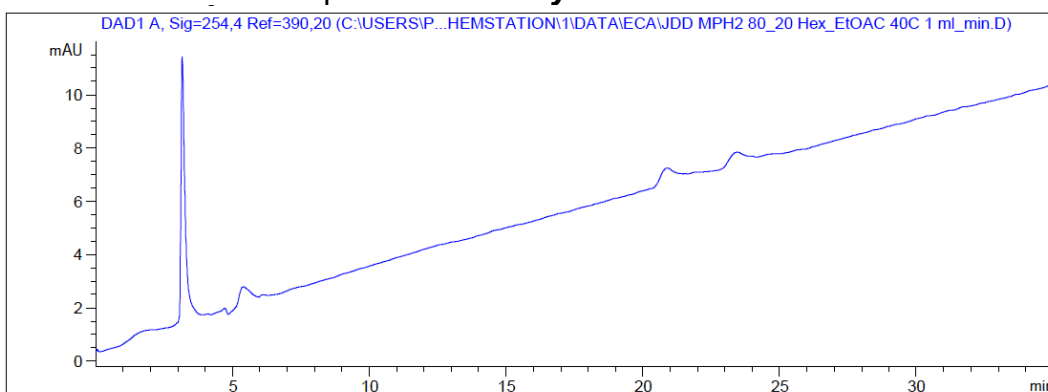
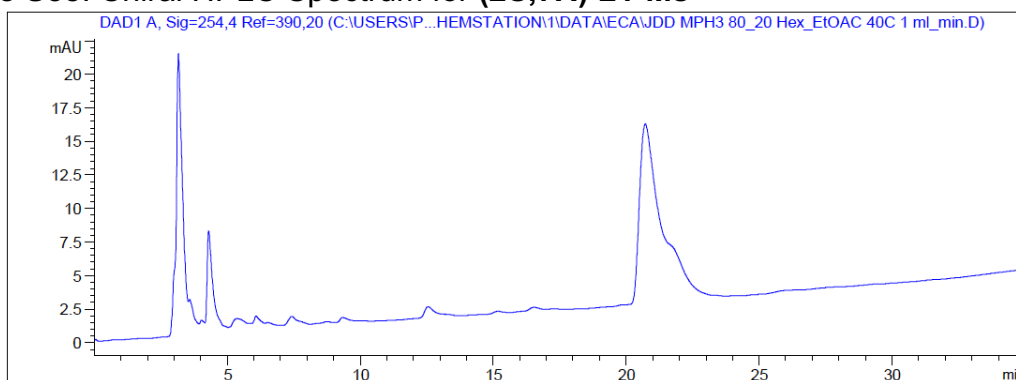


**Figure S58: Chiral HPLC Spectrum for (2*S*,7*R*)-21-Ms**



## Crystallography:

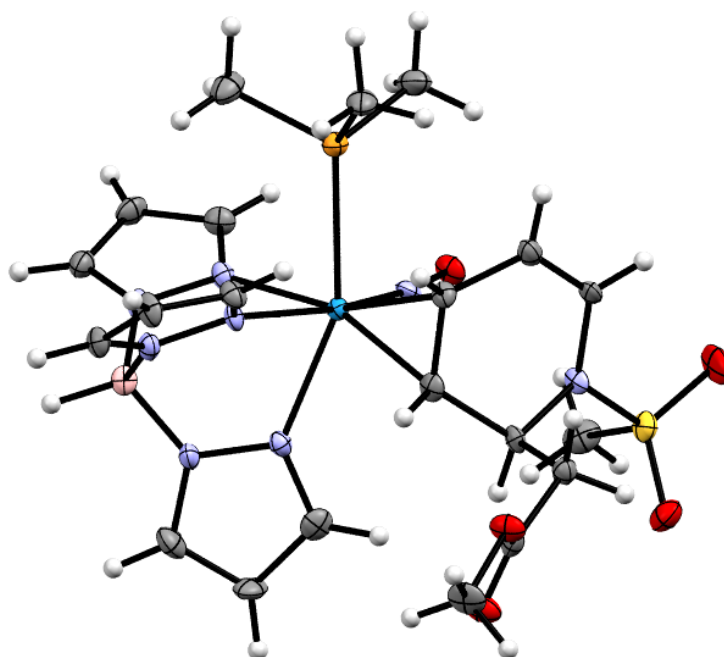


**Figure S59:** ORTEP/ellipsoid diagram of **6D**.

**Table S3:** SC-XRD data for **6D**.

CCDC 2256163	<b>Chemical Formula</b> <chem>C21H32BN8O5PSW</chem>	<b>FW (g/mol)</b> 734.22
T (K) 100(2)	$\lambda$ (Å) 0.71073	Crystal size (mm) 0.083 x 0.090 x 0.133
Crystal habit Yellow block	Crystal system Monoclinic	Space group P 2 <sub>1/n</sub>
a (Å) 11.4488(15)	b (Å) 20.387(3)	c (Å) 12.8800(18)
$\alpha$ (°) 90	$\beta$ (°) 104.213(2)	$\gamma$ (°) 2914.3(7)
V (Å <sup>3</sup> ) 2914.3(7)	Z 2	$\rho_{\text{calc}}$ (g/cm <sup>3</sup> ) 1.770
$\mu$ (mm <sup>-1</sup> ) 4.229	F(000) 1540	$\theta$ range (°) 1.91 to 28.29
Index ranges -15 ≤ h ≤ 15 -27 ≤ k ≤ 26 -17 ≤ l ≤ 17	Data/restraints/parameters 7221 / 0 / 385	Goodness-of-fit on F <sup>2</sup> 0.976
R <sub>1</sub> [I > 2σ(I)] 0.0361	wR <sub>2</sub> [all data] 0.0706	



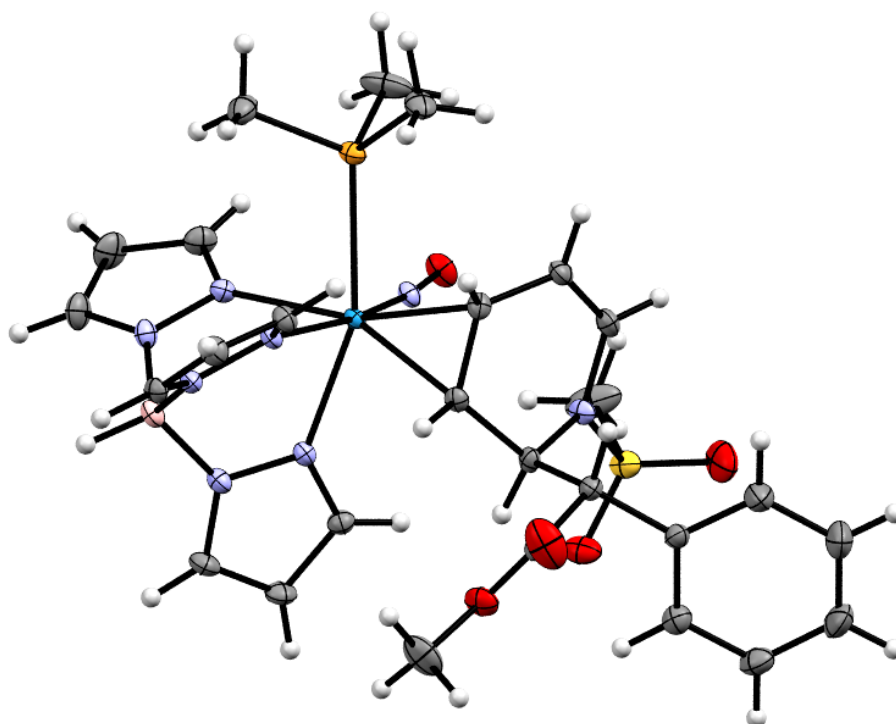


**Figure S60:** ORTEP/ellipsoid diagram of *erythro 7D*.

**Table S4:** SC-XRD data for **7D**.

CCDC 2256164	Chemical Formula $C_{27}H_{36}BN_8O_5PSW$	FW (g/mol) 810.33
T (K) 100(2)	$\lambda$ (Å) 0.71073	Crystal size (mm) 0.070 x 0.144 x 0.164
Crystal habit Colorless plate	Crystal system Triclinic	Space group P -1
a (Å) 9.8584(12)	b (Å) 12.0339(15)	c (Å) 14.6597(17)
$\alpha$ (°) 107.053(4)	$\beta$ (°) 95.521(4)	$\gamma$ (°) 103.067(4)
V (Å <sup>3</sup> ) 1594.8(3)	Z 2	$\rho_{calc}$ (g/cm <sup>3</sup> ) 1.687
$\mu$ (mm <sup>-1</sup> ) 3.787	F(000) 808	$\theta$ range (°) 1.48 to 30.57
Index ranges -14 $\leq h \leq$ 14 -17 $\leq k \leq$ 17 -20 $\leq l \leq$ 20	Data/restraints/parameters 9762 / 0 / 413	Goodness-of-fit on F <sup>2</sup> 1.025
R <sub>1</sub> [ $I > 2\sigma(I)$ ] 0.0221	wR <sub>2</sub> [all data] 0.0442	

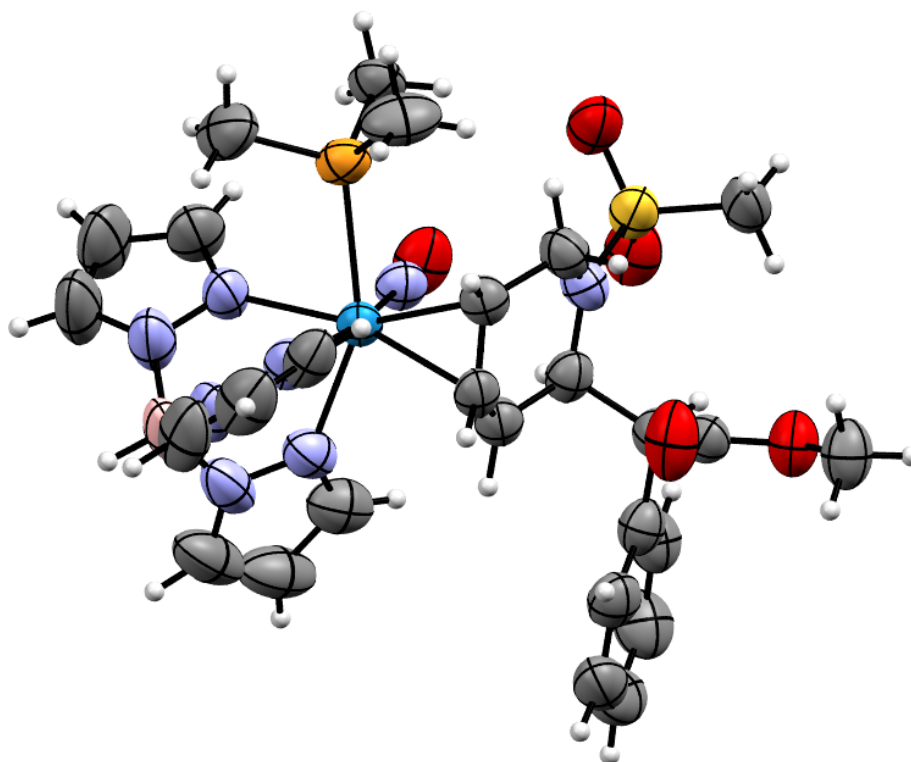


**Figure S61:** ORTEP/ellipsoid diagram of **8**.

**Table S5:** SC-XRD data for **8**.

CCDC 2256165	Chemical Formula $C_{28}H_{37}BF_3N_8O_8PS_2W$	FW (g/mol) 961.52
T (K) 200(2)	$\lambda$ (Å) 1.54178	Crystal size (mm) 0.057 x 0.081 x 0.092
Crystal habit Colorless plate-like	Crystal system monoclinic	Space group $P 2_1/c$
a (Å) 15.1929(6)	b (Å) 16.8559(7)	c (Å) 15.1263(6)
$\alpha$ (°) 90	$\beta$ (°) 106.0660(10)	$\gamma$ (°) 90
V (Å <sup>3</sup> ) 3722.4(3)	Z 4	$\rho_{calc}$ (g/cm <sup>3</sup> ) 1.716
$\mu$ (mm <sup>-1</sup> ) 7.851	F(000) 1914	$\theta$ range (°) 3.03 to 68.420
Index ranges -18 ≤ h ≤ 17 0 ≤ k ≤ 20 0 ≤ l ≤ 18	Data/restraints/parameters 6825 / 688 / 622	Goodness-of-fit on F <sup>2</sup> 1.061
R <sub>1</sub> [I > 2σ(I)] 0.0402	wR <sub>2</sub> [all data] 0.1196	

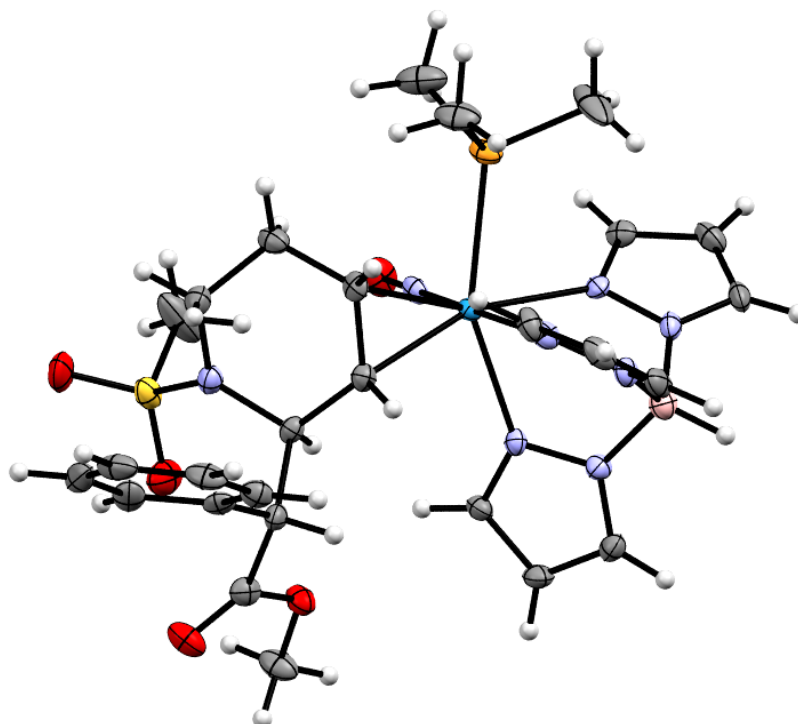


**Figure S62:** ORTEP/ellipsoid diagram of **9D**.

**Table S6:** SC-XRD data for **9D**.

CCDC 2256166	Chemical Formula $C_{27}H_{38}BN_8O_5PSW$	FW (g/mol) 812.34
T (K) 100(2)	$\lambda$ (Å) 0.71073	Crystal size (mm) 0.055 x 0.065 x 0.073
Crystal habit Colorless plate	Crystal system triclinic	Space group P -1
a (Å) 10.8643(5)	b (Å) 12.0141(6)	c (Å) 13.3520(7)
$\alpha$ (°) 92.992(2)	$\beta$ (°) 93.154(2)	$\gamma$ (°) 113.706(2)
V (Å <sup>3</sup> ) 1588.02(14)	Z 2	$\rho_{calc}$ (g/cm <sup>3</sup> ) 1.699
$\mu$ (mm <sup>-1</sup> ) 3.804	F(000) 812	$\theta$ range (°) 2.05 to 27.89
Index ranges -14 $\leq h \leq$ 12 -15 $\leq k \leq$ 15 -17 $\leq l \leq$ 17	Data/restraints/parameters 7570 / 0 / 413	Goodness-of-fit on F <sup>2</sup> 1.055
R <sub>1</sub> [ $I > 2\sigma(I)$ ] 0.0396	wR <sub>2</sub> [all data] 0.0792	

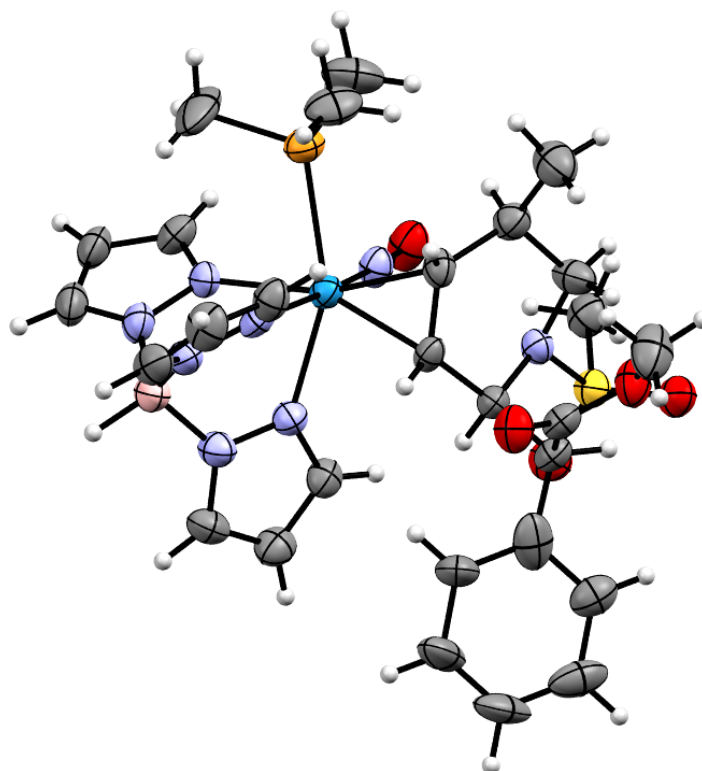


**Figure S63:** ORTEP/ellipsoid diagram of **13D**.

**Table S7:** SC-XRD data for **13D**.

CCDC 2256167	Chemical Formula $C_{28}H_{40}BN_8O_5PSW$	FW (g/mol) 826.37
T (K) 100(2)	$\lambda$ (Å) 1.54178	Crystal size (mm) 0.037 x 0.054 x 0.070
Crystal habit clear yellow needle	Crystal system triclinic	Space group P -1
a (Å) 8.6828(4)	b (Å) 12.4253(5)	c (Å) 16.5767(8)
$\alpha$ (°) 78.170(3)	$\beta$ (°) 77.152(4)	$\gamma$ (°) 71.616(4)
V (Å <sup>3</sup> ) 1636.96(14)	Z 2	$\rho_{calc}$ (g/cm <sup>3</sup> ) 1.677
$\mu$ (mm <sup>-1</sup> ) 8.020	F(000) 828	$\theta$ range (°) 2.76 to 67.72
Index ranges -10 ≤ h ≤ 10 -14 ≤ k ≤ 14 -19 ≤ l ≤ 19	Data/restraints/parameters 5819 / 162 / 454	Goodness-of-fit on F <sup>2</sup> 0.997
R <sub>1</sub> [I > 2σ(I)] 0.0457	wR <sub>2</sub> [all data] 0.1192	

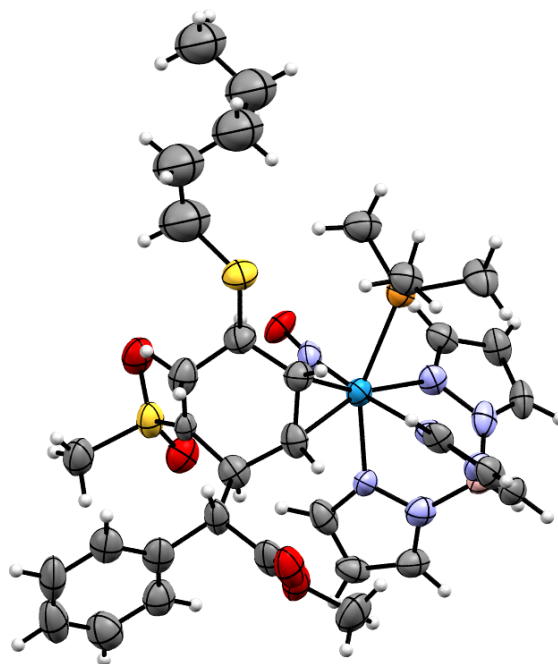


**Figure S64:** ORTEP/ellipsoid diagram of **19D**.

**Table S8:** SC-XRD data for **19D**.

CCDC 2256168	Chemical Formula $\text{C}_{32}\text{H}_{48}\text{BN}_8\text{O}_5\text{PS}_2\text{W}$	FW (g/mol) 914.53
T (K) 100(2)	$\lambda$ (Å) 0.71073	Crystal size (mm) 0.043 x 0.047 x 0.071
Crystal habit translucent colorless needle	Crystal system orthorhombic	Space group $P 2_12_12_1$
a (Å) 10.6315(5)	b (Å) 20.7318(12)	c (Å) 21.6035(12)
$\alpha$ (°) 90	$\beta$ (°) 90	$\gamma$ (°) 90
V (Å <sup>3</sup> ) 4761.6(4)	Z 4	$\rho_{\text{calc}}$ (g/cm <sup>3</sup> ) 1.273
$\mu$ (mm <sup>-1</sup> ) 2.586	F(000) 1844	$\theta$ range (°) 1.97 to 25.69
Index ranges -12 ≤ h ≤ 12 -25 ≤ k ≤ 25 -26 ≤ l ≤ 26	Data/restraints/parameters 9030 / 28 / 459	Goodness-of-fit on F <sup>2</sup> 1.058
R <sub>1</sub> [I > 2σ(I)] 0.0422	wR <sub>2</sub> [all data] 0.1021	

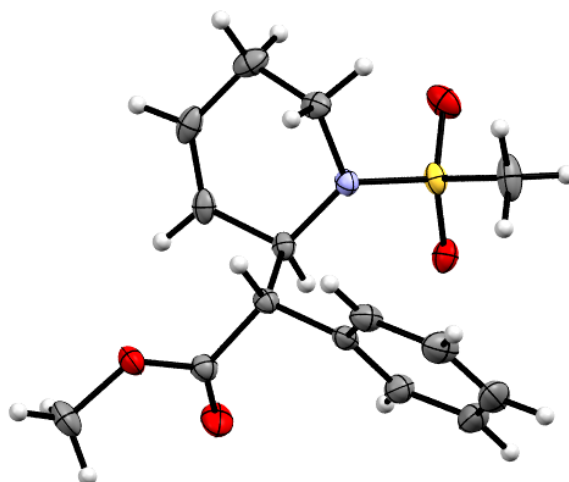


**Figure S65:** ORTEP/ellipsoid diagram of **21-Ms**.

**Table S9:** SC-XRD data for **21-Ms**.

CCDC 2256169	Chemical Formula $C_{15}H_{19}NO_4S$	FW (g/mol) 309.37
T (K) 100(2)	$\lambda$ (Å) 1.54178	Crystal size (mm) 0.100 x 0.222 x 0.438
Crystal habit Colorless plate	Crystal system monoclinic	Space group P 2 <sub>1</sub> /c
a (Å) 13.4105(4)	b (Å) 8.4916(3)	c (Å) 13.0180(4)
$\alpha$ (°) 90	$\beta$ (°) 94.6520(10)	$\gamma$ (°) 90
V (Å <sup>3</sup> ) 1477.56(8)	Z 4	$\rho_{\text{calc}}$ (g/cm <sup>3</sup> ) 1.391
$\mu$ (mm <sup>-1</sup> ) 2.090	F(000) 656	$\theta$ range (°) 3.31 to 72.31
Index ranges -16 ≤ h ≤ 16 -10 ≤ k ≤ 10 -16 ≤ l ≤ 16	Data/restraints/parameters 2912 / 0 / 192	Goodness-of-fit on F <sup>2</sup> 1.052
R <sub>1</sub> [I > 2σ(I)] 0.0297	wR <sub>2</sub> [all data] 0.0797	

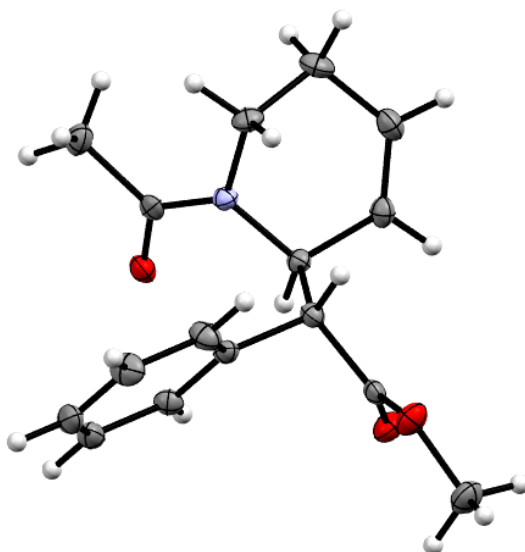


**Figure S66:** ORTEP/ellipsoid diagram of **21-Ac**.

**Table S10:** SC-XRD data for **21-Ac**.

CCDC 2260260	Chemical Formula $C_{16}H_{19}NO_3$	FW (g/mol) 273.32
T (K) 100(2)	$\lambda$ (Å) 1.54178	Crystal size (mm) 0.076 x 0.081 x 0.422
Crystal habit colorless rod	Crystal system monoclinic	Space group C 2/c
a (Å) 22.6503(8)	b (Å) 5.8701(2)	c (Å) 21.6027(8)
$\alpha$ (°) 90	$\beta$ (°) 96.692(3)	$\gamma$ (°) 90
V (Å <sup>3</sup> ) 2852.72(18)	Z 8	$\rho_{\text{calc}}$ (g/cm <sup>3</sup> ) 1.273
$\mu$ (mm <sup>-1</sup> ) 0.711	F(000) 1168	$\theta$ range (°) 3.93 to 68.30
Index ranges -27 ≤ h ≤ 27 -7 ≤ k ≤ 7 -23 ≤ l ≤ 26	Data/restraints/parameters 2596 / 0 / 183	Goodness-of-fit on F <sup>2</sup> 1.047
R <sub>1</sub> [I > 2σ(I)] 0.0382	wR <sub>2</sub> [all data] 0.1003	

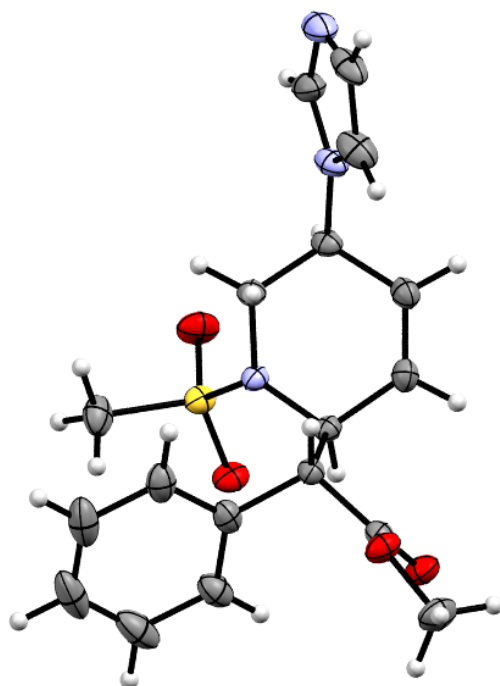


**Figure S67:** ORTEP/ellipsoid diagram of **22**.

**Table S11:** SC-XRD data for **22**.

CCDC 2256170	Chemical Formula $C_{18}H_{21}N_3O_4S$	FW (g/mol) 375.44
T (K) 100.0	$\lambda$ (Å) 0.71073	Crystal size (mm) 0.163 × 0.1 × 0.076
Crystal habit yellow plate	Crystal system monoclinic	Space group P2 <sub>1</sub> /c
a (Å) 10.9884(3)	b (Å) 13.2829(4)	c (Å) 12.9404(3)
$\alpha$ (°) 90	$\beta$ (°) 91.6820(10)	$\gamma$ (°) 90
V (Å <sup>3</sup> ) 1887.94(9)	Z 4	$\rho_{\text{calc}}$ (g/cm <sup>3</sup> ) 1.321
$\mu$ (mm <sup>-1</sup> ) 0.199	F(000) 792.0	$\theta$ range (°) 4.396 to 56.574
Index ranges -14 ≤ h ≤ 14 -17 ≤ k ≤ 17 -15 ≤ l ≤ 17	Data/restraints/parameters 4683 / 0 / 237	Goodness-of-fit on F <sup>2</sup> 1.050
R <sub>1</sub> [I > 2σ(I)] 0.0466	wR <sub>2</sub> [all data] 0.1331	



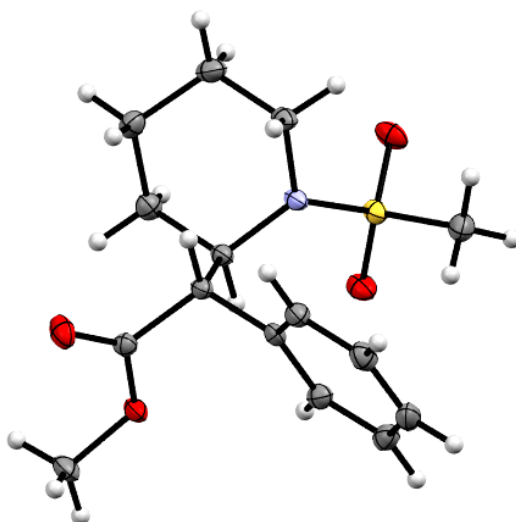


**Figure S68:** ORTEP/ellipsoid diagram of **26**.

**Table S12:** SC-XRD data for **26**.

CCDC 2256171	Chemical Formula $C_{15}H_{21}NO_4S$	FW (g/mol) 311.39
T (K) 100(2)	$\lambda$ (Å) 0.71073	Crystal size (mm) 0.096 x 0.155 x 0.261
Crystal habit colorless block	Crystal system triclinic	Space group P -1
a (Å) 8.7149(3)	b (Å) 9.2516(3)	c (Å) 10.3319(4)
$\alpha$ (°) 89.9360(10)	$\beta$ (°) 67.2660(10)	$\gamma$ (°) 80.0590(10)
V (Å <sup>3</sup> ) 754.80(5)	Z 2	$\rho_{calc}$ (g/cm <sup>3</sup> ) 1.370
$\mu$ (mm <sup>-1</sup> ) 0.230	F(000) 332	$\theta$ range (°) 2.14 to 29.59
Index ranges -12 ≤ h ≤ 12 -12 ≤ k ≤ 12 -14 ≤ l ≤ 14	Data/restraints/parameters 4232 / 0 / 192	Goodness-of-fit on F <sup>2</sup> 1.024
R <sub>1</sub> [I > 2σ(I)] 0.0326	wR <sub>2</sub> [all data] 0.0851	

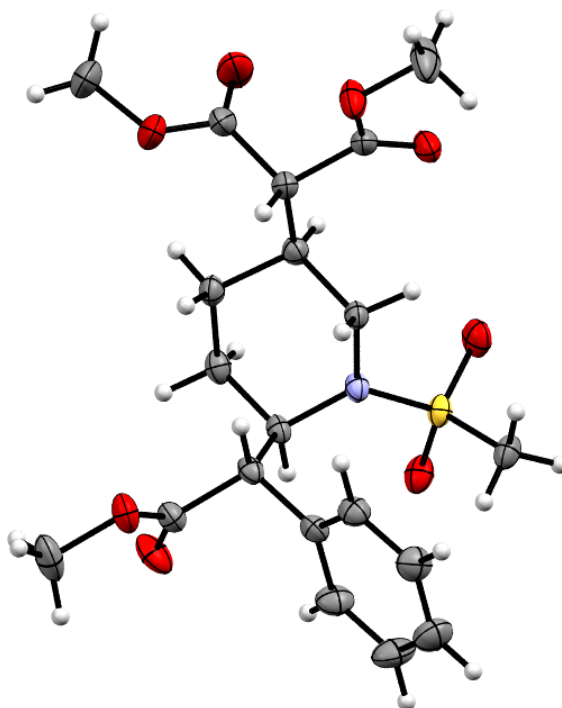


**Figure S69:** ORTEP/ellipsoid diagram of **27**.

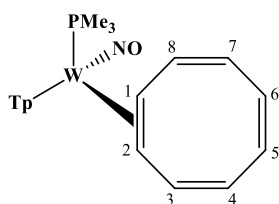
**Table S13:** SC-XRD data for **27**.

CCDC 2256172	Chemical Formula $C_{20}H_{27}NO_8S$	FW (g/mol) 441.48
T (K) 100(2)	$\lambda$ (Å) 1.54178	Crystal size (mm) 0.027 x 0.049 x 0.249
Crystal habit colorless needle	Crystal system monoclinic	Space group I a
a (Å) 13.1713(3)	b (Å) 8.4679(2)	c (Å) 19.5697(7)
$\alpha$ (°) 90	$\beta$ (°) 90.4740(10)	$\gamma$ (°) 90
V (Å <sup>3</sup> ) 2182.60(11)	Z 4	$\rho_{calc}$ (g/cm <sup>3</sup> ) 1.344
$\mu$ (mm <sup>-1</sup> ) 1.721	F(000) 936	$\theta$ range (°) 6.21 to 72.12
Index ranges -16 ≤ h ≤ 14 -10 ≤ k ≤ 10 -23 ≤ l ≤ 24	Data/restraints/parameters 4215 / 2 / 275	Goodness-of-fit on F <sup>2</sup> 1.035
R <sub>1</sub> [I > 2σ(I)] 0.0306	wR <sub>2</sub> [all data] 0.0812	

## **Appendix C: Chapter 3 Data**

**Experimental Procedures.** NMR spectra were obtained on 500, 600, or 800 MHz spectrometers. Chemical shifts are referenced to tetramethylsilane (TMS) utilizing residual  $^1\text{H}$  signals of the deuterated solvents as internal standards.  $\text{H}_2\text{O}$  MeCN- $\text{d}_3$  S47 Chemical Shifts are reported in ppm and coupling constants ( $J$ ) are reported in hertz (Hz). Infrared spectra (IR) were recorded as a solid on a spectrometer with an ATR crystal accessory, and peaks are reported in  $\text{cm}^{-1}$ . Electrochemical experiments were performed under a nitrogen atmosphere. Most cyclic voltammetric data were recorded at ambient temperature at 100 mV/ s, unless otherwise noted, with a standard three-electrode cell from +1.8 to  $-1.8$  V with a platinum working electrode, acetonitrile or N,N-dimethylacetamide (DMA) solvent, and tetrabutylammonium (TBAH) electrolyte ( $\sim 1.0$  M). All potentials are reported versus the normal hydrogen electrode (NHE) using cobaltocenium hexafluorophosphate ( $E_{1/2} = -0.78$  V,  $-1.75$  V) or ferrocene ( $E_{1/2} = 0.55$  V) as an internal standard. The peak separation of all reversible couples was less than 100 mV. All synthetic reactions were performed in a glovebox under a dry nitrogen atmosphere unless otherwise noted. All solvents were purged with nitrogen prior to use. Deuterated solvents were used as received from Cambridge Isotopes and were purged with nitrogen under an inert atmosphere. When possible, pyrazole protons of the tris(pyrazolyl)borate (Tp) ligand were uniquely assigned (e.g., "Tp3B") using two-dimensional NMR data (see Figure S1). If unambiguous assignments were not possible, Tp protons were labeled as "Tp3/5, Tp4, or Pz". All  $J$  values for Tp protons are  $2(\pm 0.4)$  Hz. BH peaks (around 4–5 ppm) in the  $^1\text{H}$  NMR spectra are not assigned due to their quadrupole broadening; However, confirmation of the BH group is provided by IR data (ca  $2500\text{ cm}^{-1}$ ). Compounds 1, 5, and 9 have been previously reported. Full characterization of compounds is provided in the SI. All cationic complexes have triflate as the counteranion unless explicitly noted otherwise.

## Characterization of Compounds.



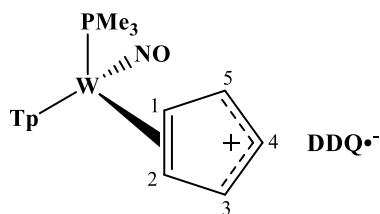
**Compound 2.** To a 50 mL round bottom flask were added a stir bar, **5** (3.00 g, 3.27 mmol), cyclooctatetraene (2.00 g, 19.2 mmol) and dried THF (6 mL). The round bottom flask was capped with a septum, and the reaction mixture was stirred for 3 hours at 55 °C in an oil bath. Afterwards, a silica column was set up with 60 mL of frit packed with 1 inch of silica over a 500 mL filter flask. The reaction mixture was flushed through with ethyl acetate (300 mL) and dark red decomposition product was caught on the silica. The black-orange filtrate was reduced in vacuo to dryness. The product was redissolved in minimal DCM and precipitated with hexanes (300 mL). The orange solid was collected on a 30 mL fine porosity fritted funnel and desiccated overnight to yield **2** (2.11 g, 70.8%).

**<sup>1</sup>H NMR (800 MHz, CD<sub>3</sub>CN, δ, 25 °C):** 8.34 (d, *J* = 1.90 Hz, 1H, Pz3A), 8.07 (d, *J* = 1.92 Hz, 1H, Pz3B), 7.86 (d, *J* = 2.17 Hz, 1H, Pz5C), 7.82 (d, *J* = 2.42 Hz, 1H, Pz5B), 7.73 (d, *J* = 2.42 Hz, 1H, Pz5A), 7.70 (d, *J* = 2.05 Hz, 1H, Pz3C), 6.42 (dd, *J* = 5.86, 13.05 Hz, 1H, H8), 6.37 (t, *J* = 2.27 Hz, 1H, Pz4B), 6.34 (t, *J* = 2.34 Hz, 1H, Pz4C), 6.33 (m, 1H, H3), 6.20 (t, *J* = 2.03 Hz, 1H, Pz4A), 5.41 (t, *J* = 3.40 Hz, 2H, H5/H6), 5.29 (d, *J* = 13.09 Hz, 1H, H4), 5.21 (d, *J* = 12.62 Hz, 1H, H7), 2.84-2.80 (m, 1H, H1), 1.66 (t, *J* = 7.71 Hz, 1H, H2), 1.13 (d, *J* = 8.58 Hz, 9H, PMe<sub>3</sub>).

**<sup>13</sup>C NMR (201 MHz, CD<sub>3</sub>CN, δ, 25 °C):** 146.0 (1C, Pz3A), 143.8 (1C, Pz3B), 141.8 (1C, Pz3C), 140.5 (1C, C3), 138.1 (1C, Pz5C), 137.6 (2C, Pz5A/Pz5B), 134.7 (d, *J*<sub>PC</sub> = 4.43 Hz, 1C, C8), 124.2 (2C, C5/C6), 120.1 (1C, C7), 118.8 (1C, C4), 107.8 (1C, Pz4B), 107.4 (1C, Pz4C), 106.3 (1C, Pz4A), 56.2 (d, *J*<sub>PC</sub> = 9.31 Hz, 1C, C1), 56.0 (1C, C2), 13.6 (d, *J*<sub>PC</sub> = 28.70 Hz, 3C, PMe<sub>3</sub>).

Composition of **2** confirmed by single crystal X-ray diffraction.

**CV** (MeCN, 100 mV/s): E<sub>p,a</sub> = +0.37 V, E<sub>p,c</sub> = -2.2V (NHE).



**Compound 3.** To a test tube were added **6** (129 mg, 0.227 mmol) and 3 mL MeCN. To a second test tube were added a stir pea, DDQ (129 mg, 0.569 mmol), and 2 mL MeCN. Both test tubes were chilled at  $-10^{\circ}\text{C}$  in a cold bath for 10 minutes. Next, the solution of **6** was quickly pipetted into the test tube containing DDQ as it remained cold. The dark red reaction mixture was stirred for 15 minutes at  $-10^{\circ}\text{C}$ . The reaction mixture was then poured into a 500 mL Erlenmeyer flask with  $\text{Et}_2\text{O}$  (300 mL). A purple precipitate was collected on a 15 mL porosity fritted funnel and desiccated under static vacuum to yield **3** as a salt with  $\text{DDQ}^{\bullet-}$  (148 mg, 82.1%).

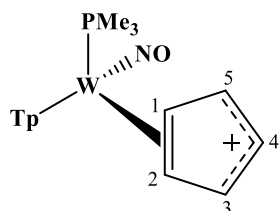
**$^1\text{H}$  NMR (800 MHz,  $\text{CD}_3\text{CN}$ ,  $\delta$ ,  $25^{\circ}\text{C}$ ):**  $\delta$  8.60 (d,  $J = 2.1$  Hz, 1H, Pz), 8.43 (d,  $J = 2.2$  Hz, 1H, Pz), 8.04 (d,  $J = 2.4$  Hz, 1H, Pz), 7.97 (d,  $J = 2.0$  Hz, Pz), 7.81 (d,  $J = 2.2$  Hz, 1H), 7.78 (d,  $J = 2.4$  Hz, 1H, Pz), 6.89 (d,  $J_{\text{PH}} = 2.4$  Hz, 5H, H1-5), 6.63-6.33 (t,  $J = 2.3$  Hz, 3H, Pz4A/Pz4B/Pz4C), 1.22 (d,  $J = 10.2$  Hz, 9H,  $\text{PMe}_3$ ).

**$^{13}\text{C}$  NMR (201 MHz,  $\text{CD}_3\text{CN}$ ,  $\delta$ ,  $25^{\circ}\text{C}$ ):** 148.0 (1C, Pz), 146.9 (1C, Pz), 144.7 (1C, Pz), 140.0 (1C, Pz), 139.7 (1C, Pz), 138.4 (1C, Pz), 129.2 (m, 5C, C1-C5), 110.6-108.3 (3C, Pz4A/Pz4B/Pz4C), 13.7 (d,  $J_{\text{PC}} = 33.2$  Hz, 3C,  $\text{PMe}_3$ ).

Composition of **3** confirmed by single crystal X-ray diffraction.

**APCI-HRMS** ( $m/z$ ):  $[\text{M}]^+$  calculated for 569.1450; found 569.1476.

CV (MeCN, 50 mV/s):  $E_{\text{p,a}} = +1.26$  V,  $E_{1/2} = +0.70$  and  $-0.09$  V,  $E_{\text{p,c}} = -0.431$  V (NHE).



**Compound 3A.** For this procedure, all glassware was flame-dried prior to use. To a 60 mL test tube with stir bar was added **6** (300 mg, 527  $\mu\text{mol}$ , 1 equiv.) and dry MeCN (4 mL). Separately, solutions of DDQ (269 mg, 1.19 mmol, 2.25 equiv.) in dry MeCN (3 mL), and butylated hydroxytoluene (290 mg, 1.32 mmol, 2.5 equiv.) and 2,6-

lutidinium triflate (143 mg, 556  $\mu\text{mol}$ , 1.05 equiv.) in dry MeCN (6 mL) were prepared in test tubes. All three solutions were chilled to  $-10\text{ }^{\circ}\text{C}$ . The DDQ solution was transferred to a 3 mL syringe and added *rapidly* to the solution of **6** under maximal stirring, which caused the yellow-brown solution to instantly darken to purple black. After 5 seconds the BHT/lutidinium mixture was added, accompanied by a subtle shift in tint to green/brown black over 30 seconds. The solution was then precipitated into stirring Et<sub>2</sub>O (275 mL,  $-30\text{ }^{\circ}\text{C}$ ), and the gray precipitate collected over a 30 mL fine-porosity fritted disk. Storage of the yellow-brown filtrate over 2 hours yielded numerous clusters of very small black needles suitable for single-crystal XRD analysis on the sidewall of the flask. The precipitate was rinsed through the fritted disk with dry MeCN (5 mL total) into a clean flask and re-precipitated into stirring Et<sub>2</sub>O (250 mL,  $-30\text{ }^{\circ}\text{C}$ ). The resulting precipitate was collected over a 30 mL fine-porosity fritted disk, rinsed with Et<sub>2</sub>O (50 mL) and pentane (25 mL), and desiccated under active vacuum to yield **3A** (275 mg, 73%) as a light gray, chunky powder.

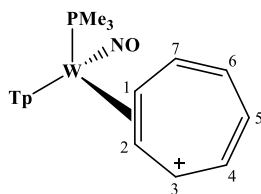
**<sup>1</sup>H NMR (600 MHz, CD<sub>3</sub>CN,  $\delta$ , 25  $^{\circ}\text{C}$ ):** 8.63 (d,  $J = 2.3\text{ Hz}$ , 1H, Pz), 8.43 (d,  $J = 2.3\text{ Hz}$ , 1H, Pz), 8.04 (d,  $J = 2.4\text{ Hz}$ , 1H, Pz), 7.97 (d,  $J = 2.5\text{ Hz}$ , 1H, Pz), 7.81 (d,  $J = 2.3\text{ Hz}$ , 1H, Pz), 7.78 (d,  $J = 2.5\text{ Hz}$ , 1H, Pz), 6.89 (d,  $J_{\text{PH}} = 2.3\text{ Hz}$ , 5H, H1-H5), 6.64 (t,  $J = 2.3\text{ Hz}$ , 1H, Pz), 6.55 (t,  $J = 2.3\text{ Hz}$ , 1H, Pz), 6.33 (t,  $J = 2.4\text{ Hz}$ , 1H, Pz), 1.23 (d,  $J_{\text{PH}} = 10.2\text{ Hz}$ , 9H, PMe<sub>3</sub>).

**<sup>13</sup>C NMR (201 MHz, CD<sub>3</sub>CN,  $\delta$ , 25  $^{\circ}\text{C}$ ):** 148.09 (Pz), 146.94 (Pz), 144.79 (Pz), 140.08 (Pz), 139.79 (d,  $J = 3.1\text{ Hz}$ , Pz), 138.41 (Pz), 129.03 (C1-C5), 122.17 (q,  $J_{\text{CF}} = 320.7\text{ Hz}$ , F<sub>3</sub>CSO<sub>3</sub>), 110.58 (Pz), 108.98 (Pz), 108.38 (d,  $J = 5.0\text{ Hz}$ , Pz), 13.72 (d,  $J_{\text{PC}} = 33.7\text{ Hz}$ , PMe<sub>3</sub>).

**IR (ATR, cm<sup>-1</sup>):**  $\nu(\text{BH})$  2513.90,  $\nu(\text{NO})$  1647.79,  $\nu(\text{F}_3\text{CS}-\text{O}_3)$  1260.46,  $\nu(\text{F}_3\text{CS}-\text{O}_3)$  1029.59,  $\delta(\text{F}_3-\text{CSO}_3)$  636.01.

**CV** (MeCN, 50 mV/s):  $E_{\text{p,c}} = -0.460\text{ V (NHE)}$ .

Composition of **3A** confirmed by single-crystal X-ray diffraction.



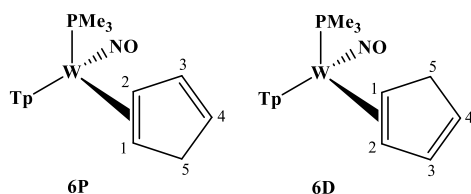
**Compound 4.** In a test tube charged with a stir bar, **7** (100 mg, 0.17 mmol) was dissolved in 2.0 mL MeCN and allowed to stir at RT. Another test tube containing 3,6-dichloro-1,2,4,5-tetrazine (51mg, 0.34 mmol) dissolved in 2 mL MeCN was chilled at -30 °C. After 10 minutes, the 3,6-dichloro-1,2,4,5-tetrazine solution was added to the complex. After 15 minutes hours, the reaction mixture was added to a stirring solution of diethyl ether (100 mL) and triflic acid (126 mg, 0.84 mmol). A dark grey solid was immediately precipitated in diethyl ether solution. The precipitate was collected on a fritted disk, washed with diethyl ether (50mL), then washed through the fritted disk with acetone into a clean filter flask. The acetone solution was added to stirring diethyl ether (100 mL), precipitating a light grey solid which was collected and dried desiccated under active vacuum. (90 mg, 0.12 mmol, 72% yield).

**<sup>1</sup>H NMR (800 MHz, CD<sub>3</sub>CN, δ, 25 °C):** 8.14 (d, *J* = 2.1 Hz), 8.09 (d, *J* = 2.3 Hz), 8.01 (d, *J* = 2.2 Hz), 7.87 (d, *J* = 2.2 Hz), 7.85 (d, *J* = 2.2 Hz), 7.74 (d, *J* = 2.2 Hz), 6.53 (t, *J* = 2.3 Hz), 6.45 (t, *J* = 2.3 Hz), 6.32 (t, *J* = 2.3 Hz) – Tp protons, 5.67 (d, *J*<sub>PH</sub> = 2.0 Hz, *J*<sub>WH</sub> = 20.0 Hz, 7H, H1-7) 1.21 (d, *J*<sub>PH</sub> = 9.6 Hz, 9H, PMe<sub>3</sub>).

**<sup>13</sup>C NMR (201 MHz, CD<sub>3</sub>CN, δ, 25 °C):** 146.6 (1C, PzB3), 145.2 (1C, PzA3), 142.6 (1C, PzC3), 139.4 (1C, PzB5), 139.1 (1C, PzA5), 139.7 (1C, PzC5), 123.3 (7C, C1-7), 108.6 (1C, PzC4), 108.9 (1C, PzB4), 107.6 (1C, PzA4), 12.9 (d, *J*<sub>PC</sub> = 32.0 Hz, 3C, PMe<sub>3</sub>).

**IR (ATR, cm<sup>-1</sup>):** ν(NO) = 1636 cm<sup>-1</sup>, DDQ anion ν(CN) = 2220 cm<sup>-1</sup>, triflate anion ν(CF<sub>3</sub>SO<sub>3</sub>) = 636 cm<sup>-1</sup>.

Composition of **4** confirmed by single crystal X-ray diffraction.



**Compounds 6P and 6D.** To a 50 mL round bottom flask were added a stir bar, **5** (2.00 g, 3.27 mmol), and 30 mL dried THF. The round bottom flask was sealed with a rubber



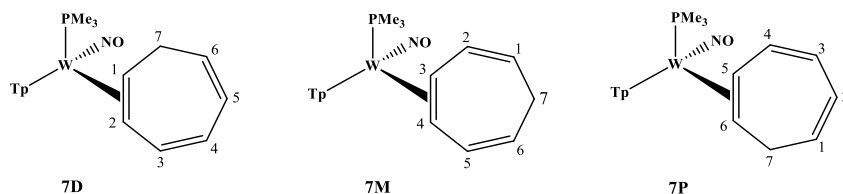
septum and heated at 45°C in an oil bath. To the stirring yellow solution, distilled cyclopentadiene monomer (2.81 mL, 2.27 g, 34.3 mmol) was syringed through the septum and into the flask. After stirring for 14 hours, the dark brown reaction mixture was poured into a 500 mL Erlenmeyer flask, and hexanes (350 mL) was added. A purple precipitate was filtered off in a 60 mL fine porosity fritted funnel over a 500 mL filter flask. The tan-colored filtrate was reduced in vacuo to ~100 mL, inducing precipitation. A whitish-tan solid was collected on a 15 mL fine porosity fritted funnel and desiccated under static vacuum to yield **6** (1.01 g, 54.2%) as a ~2:1 ratio of 6P to 6D.

**6P** (Major Isomer): <sup>1</sup>H NMR (800 MHz, CD<sub>3</sub>CN, δ, 25 °C): 8.37 (d, *J* = 2.0 Hz, 1H, Pz), 8.00 (d, *J* = 2.0 Hz, 1H, Pz), 7.87 (d, *J* = 2.4 Hz, 1H, Pz), 7.80 (d, *J* = 2.4 Hz, 1H, Pz), 7.76 (d, *J* = 2.4 Hz, 1H, Pz), 7.41 (d, *J* = 2.2 Hz, 1H, Pz), 6.38 (dd, *J* = 5.1, 2.2 Hz, 1H, H3), 6.36 (t, *J* = 2.2 Hz, 1H, Pz), 6.30 (t, *J* = 2.2 Hz, 1H, Pz), 6.22 (t, *J* = 2.2 Hz, 1H, Pz), 5.08 (dt, *J* = 4.9, 2.3 Hz, 1H, H4), 4.33 (ddq, *J* = 19.3, 6.1, 2.0 Hz, 1H, H5), 3.80 (dt, *J* = 19.4, 2.2 Hz, 1H, H5), 3.70 (ddt, *J* = 11.9, 7.4, 2.1 Hz, 1H, H2), 1.90 (td, *J* = 6.8, 2.9 Hz, 1H, H1), 1.25 (d, *J* = 8.4 Hz, 9H, PMe<sub>3</sub>).

<sup>13</sup>C NMR (201 MHz, CD<sub>3</sub>CN, δ, 25 °C): 144.0 (1C, Pz), 141.5 (1C, Pz), 140.7 (1C, Pz), 136.9 (d, *J*<sub>PC</sub> = 2.9 Hz, 1C, C3), 136.8 (1C, Pz), 136.0 (1C, Pz), 135.6 (1C, Pz), 121.5 (1C, C4), 106.4 (1C, Pz), 105.8 (1C, Pz), 105.7 (1C, Pz), 67.6 (d, *J*<sub>PC</sub> = 10.9 Hz, 1C, C2), 56.3 (1C, C1), 42.5 (1C, C5), 13.3 (d, *J*<sub>PC</sub> = 28.4 Hz, 3C, PMe<sub>3</sub>).

**6D** (Minor Isomer): <sup>1</sup>H NMR (800 MHz, CD<sub>3</sub>CN, δ, 25 °C): 8.16 (d, *J* = 2.0 Hz, 1H, Pz), 8.00 (d, *J* = 2.0 Hz, 1H, Pz), 7.88 (d, *J* = 2.4 Hz, 1H, Pz), 7.80 (d, *J* = 2.4 Hz, 1H, Pz), 7.74 (d, *J* = 2.4 Hz, 1H, Pz), 7.41 (d, *J* = 2.2 Hz, 1H, Pz), 6.57 (dq, *J* = 4.2, 2.0 Hz, 1H, H3), 6.37 (t, *J* = 2.2 Hz, 1H, Pz), 6.30 (t, *J* = 2.2 Hz, 1H, Pz), 6.22 (t, *J* = 2.2 Hz, 1H, Pz), 5.04 (dt, *J* = 4.9, 2.4 Hz, 1H, H4), 4.40 (ddt, *J* = 19.2, 6.8, 2.2 Hz, 1H, H5), 3.44 (m, 1H, H5), 3.40 (m, 1H, H1), 2.17 (dq, *J* = 7.5, 2.2 Hz, 1H, H2), 1.22 (d, *J* = 8.3 Hz, 9H, PMe<sub>3</sub>). <sup>13</sup>C NMR (201 MHz, CD<sub>3</sub>CN, δ, 25 °C): 144.1 (1C, Pz), 143.6 (1C, Pz), 141.2 (1C, Pz), 138.0 (1C, C3), 136.6 (1C, Pz), 136.2 (1C, Pz), 135.4 (1C, Pz), 121.2 (1C, C4), 106.5 (1C, Pz), 106.0 (1C, Pz), 105.9 (1C, Pz), 65.7 (1C, C2), 58.0 (d, *J*<sub>PC</sub> = 12.5 Hz, 1C, C1), 42.8 (d, *J*<sub>PC</sub> = 2.2 Hz, 1C, C5), 12.8 (d, *J*<sub>PC</sub> = 28.0 Hz, 3C, PMe<sub>3</sub>).

Composition of **6P** confirmed by single crystal X-ray diffraction.



**Compounds 7D, 7M, and 7P.** In an oven-dried round-bottom flask charged with a stir bar, **5** (2.5 g, 4.1 mmol) was combined with 1,3,5-cycloheptatriene (7.5 mL, 72.5 mmol) and 5 mL of DME. The round-bottom was capped with a septum and stirred in an oil bath at 60 °C for 1.5 h. A reaction precipitate was collected on a 30 mL fine porosity (F) frit. The remaining filtrate was precipitated in 1 L of chilled hexanes. The precipitate was filtered on a 60 mL F frit. The hexanes filtrate was evaporated in vacuo and the resulting precipitate was collected on a 30 mL F frit. The solids were desiccated (2.094 g, 3.51 mmol, 85% yield) as a 1:1:1 isomeric ratio of **7**.

IR (ATR, cm<sup>-1</sup>):  $\nu(\text{NO}) = 1561 \text{ cm}^{-1}$

CV (MeCN, 100 mV/s):  $E_{p,a} = +0.37 \text{ V (NHE)}$ .

APCI-HRMS (m/z):  $[\text{M}]^{+H}$  calculated for  $\text{C}_{19}\text{H}_{28}\text{BN}_7\text{OPW}^+$ , 596.1690 ; found 596.1673

**Isolation of 7D:** To a 4-dram vial charged with a stir bar, all isomers of **7** (100 mg, 0.17 mmol) dissolved in  $\text{CHCl}_3$  were left to stir outside of the glovebox for a full 24 h covered with an unscrewed cap to prevent evaporation. The reaction mixture was precipitated in hexanes. A brown precipitate was filtered, and the hexanes filtrate was reduced by 75%. The white solid **7D** formed from the filtrate was filtered over a 30 mL F frit and placed in the desiccator (48 mg, 0.08 mmol, 48% yield).

**<sup>1</sup>H NMR (800 MHz,  $\text{CDCl}_3$ ,  $\delta$ , 25 °C):** 8.31 (d,  $J = 1.4 \text{ Hz}$ , 1H, PzA3), 8.04 (d,  $J = 1.4 \text{ Hz}$ , 1H, PzB3), 7.70 (d,  $J = 2.4 \text{ Hz}$ , 1H, Pz5B), 7.69 (d,  $J = 1.7 \text{ Hz}$ , 1H, Pz5C), 7.64 (d,  $J = 2.4 \text{ Hz}$ , 1H, PzA5), 7.21 (d,  $J = 1.7 \text{ Hz}$ , 1H, PzC3), 6.28 (d,  $J = 2.2 \text{ Hz}$ , 1H, PzB4), 6.25 (d,  $J = 2.2 \text{ Hz}$ , 1H, PzA4), 6.15 (d,  $J = 2.2 \text{ Hz}$ , 1H, PzC4), 7.03 (dd,  $J = 11.0, 3.5 \text{ Hz}$ , 1H, H3), 6.21-6.18 (m, 1H, H5), 6.10-6.06 (m, 1H, H6), 5.76 (dd,  $J = 11.0, 5.4 \text{ Hz}$ , 1H, H4), 3.18-3.08 (m, 2H, H7), 2.83-2.77 (m, 1H, H1), 1.46-1.41 (m, 1H, H2), 1.26 (d,  $J_{\text{PH}} = 8.1 \text{ Hz}$ , 9H,  $\text{PMe}_3$ ).

**<sup>13</sup>C NMR (201 MHz,  $\text{CDCl}_3$ ,  $\delta$ , 25 °C):** 143.8 (PzA3), 143.5 (PzB3), 137.5-135.0 (2C, PzB5/PzC5), 136.2 (PzA5), 139.9 (PzC3), 107.7-105.0 (3C, PzB4/PzA4/PzC4), 141.90 (C3), 128.6 (C5), 128.70 (C6), 122.74 (C4), 34.0 (C7), 55.6 (C1), 55.0 (C2), 14.3 (d,  $J_{\text{PC}} = 27.3 \text{ Hz}$ , 3C,  $\text{PMe}_3$ ).

**<sup>31</sup>P NMR (500 MHz, DME,  $\delta$ , 25 °C):**  $J_{\text{WP}} = 144.8 \text{ Hz}$ .

Isolation of **7M**: After protonation of **7** with HOTf, the resultant WTP(NO)(PMe<sub>3</sub>)( $\eta^2$ -cycloheptadienyl) triflate salt, **7A**, (160 mg, 0.21 mmol) was dissolved in 3 mL CHCl<sub>3</sub> and allowed to stir at -15 °C. Another test tube containing triethylamine (TEA) (0.30 mL, 2.15 mmol) dissolved in 1 mL CHCl<sub>3</sub> was also chilled at -15 °C. After 10 minutes, the TEA test tube was added to the test tube containing the complex and the solution was allowed to stir for 15 minutes. Upon removal from the bath, the solution was diluted with 30 mL of CHCl<sub>3</sub> and extracted 5x with 30 mL of 1 M NaOH. The organic layer was dried with Na<sub>2</sub>SO<sub>4</sub>, filtered, and evaporated in vacuo until dryness. The dark brown material was redissolved in CHCl<sub>3</sub> and evaporated three times to remove excess TEA. The remaining material was dissolved in CHCl<sub>3</sub> and precipitated in 300 mL chilled hexanes. The black precipitate was collected on a 15 mL F frit and discarded. The hexanes filtrate was reduced by 150 mL. The white precipitate formed **7M** was filtered, dried in the desiccator, and collected on a 15 mL F frit (45 mg, 0.08 mmol 35%).

**<sup>1</sup>H NMR (800 MHz, CDCl<sub>3</sub>,  $\delta$ , 25 °C)**: 8.51 (d,  $J$  = 2.0 Hz, 1H, PzA3), 8.06 (d,  $J$  = 2.0 Hz, 1H, PzB3), 7.70 (d,  $J$  = 2.3 Hz, 1H, PzB5), 7.68 (d,  $J$  = 2.4 Hz, 1H, PzA5), 7.59 (d,  $J$  = 2.4 Hz, 1H, PzC5), 7.31 (d,  $J$  = 2.2 Hz, 1H, PzC3), 6.62-6.56 (m, 2H, H5/H6), 6.28 (t,  $J$  = 2.1 Hz, 1H, PzB4), 6.20 (t,  $J$  = 2.2 Hz, 1H, PzC4), 6.17 (t,  $J$  = 2.2 Hz, 1H, PzA4), 5.24 (dtd,  $J$  = 6.9, 4.0, 1.4 Hz, 1H, H1), 5.19 (dtd,  $J$  = 6.9, 4.0, 1.4 Hz, 1H, H2), 4.36 (dq,  $J$  = 20.9, 2.9 Hz, 1H, H7), 2.79 – 2.73 (m, 1H, H3), 2.72 (dt,  $J$  = 21.0, 6.9 Hz, 1H, H7), 1.53 – 1.44 (m, 1H, H4), 1.25 (d,  $J_{PH}$  = 8.3 Hz, 9H, PMe<sub>3</sub>).

**<sup>13</sup>C NMR (201 MHz, CDCl<sub>3</sub>,  $\delta$ , 25 °C)**: 143.6 (PzA3), 143.4 (PzB3), 137.5-135.0 (2C, PzB5/PzA5), 137.8 (PzC5), 140.3 (PzC3), 107.7-105.0 (3C, PzB4/PzA4/PzC4), 137.5/133.7 (C5/C6), 122.5 (C2), 123.4 (C3), 30.1 (C7), 55.6 (C3), 53.85 (C4), 13.8 (d,  $J_{PC}$  = 17.8 Hz, 3C, PMe<sub>3</sub>).

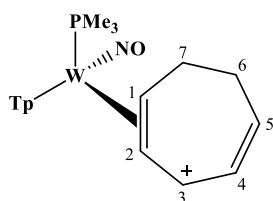
**<sup>31</sup>P NMR (500 MHz, DME,  $\delta$ , 25 °C)**:  $J_{WP}$  = 147.5 Hz.

Composition of **7M** confirmed by single crystal X-ray diffraction.

Attempts to isolate **7P** from its isomers were unsuccessful. **<sup>1</sup>H NMR (800 MHz, CDCl<sub>3</sub>,  $\delta$ , 25 °C)**: 8.15 (d,  $J$  = 2.0 Hz, 1H, PzA3), 8.06 (d,  $J$  = 1.7 Hz, 1H, PzB3), 7.70 (d,  $J$  = 1.7 Hz, 1H, Pz5B), 7.61 (d,  $J$  = 2.4 Hz, 1H, Pz5C), 7.59 (d,  $J$  = 2.4 Hz, 1H, PzA5), 7.23 (d,  $J$  = 2.0 Hz, 1H, PzC3), 6.28 (d,  $J$  = 2.2 Hz, 1H, PzB4), 6.22 (d,  $J$  = 2.2 Hz, 1H, PzA4), 6.17 (d,  $J$  = 2.2 Hz, 1H, PzC4), 6.86 (dd,  $J$  = 11.3, 4.5 Hz, 1H, H4), 6.10-6.05 (m, 1H, H2), 6.05-6.01 (m, 1H, H1), 5.61 (dd,  $J$  = 11.5, 5.6 Hz, 1H, H3), 3.54 (td,  $J$  =

14.5, 4.5, 1H, H7), 3.21-3.17 (m, 1H, H7), 2.80 (td,  $J = 21.0, 6.8$  Hz, 1H, H5), 1.87-1.83 (m, 1H, H6), 1.26 (d,  $J_{PH} = 8.1$  Hz, 9H,  $\text{PMe}_3$ ).

**$^{13}\text{C}$  NMR (201 MHz,  $\text{CDCl}_3$ ,  $\delta$ , 25 °C):** 142.8 (PzA3), 143.9 (PzB3), 137.5-135.0 (PzB5), 135.6, (PzC5) 135.4 (PzA5), 140.0 (PzC3), 106.6-105.0 (3C, PzB4/PzA4/PzC4), 140.3 (C4), 137.0 (C2), 135.4 (C1), 123.3 (C3), 32.1 (C7), 55.9 (C5), 67.4 (C6), 13.6 (d,  $J_{PC} = 17.6$ , Hz, 3C,  $\text{PMe}_3$ ).  **$^{31}\text{P}$  NMR (500 MHz, DME,  $\delta$ , 25 °C):**  $J_{WP} = 145.1$  Hz. CV (MeCN, 100 mV/s):  $E_{p,a} = +0.37$  V (NHE).

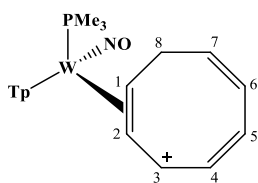


**Compound 7A.** To a 4-dram vial charged with a stir bar, compounds **7** (150 mg, 0.25 mmol) were dissolved in  $\text{CHCl}_3$ . HOTf diluted in MeCN was added (0.6 mM, 0.30 mmol) and the solution was allowed to stir at 25 °C for 24 h. The solution was pipetted into chilled hexanes. The precipitate obtained was dried in the desiccator and collected on a 30 mL F frit (164.4 g, 0.22 mmol, 87.5%).

**$^1\text{H}$  NMR (800 MHz,  $\text{CDCl}_3$ ,  $\delta$ , 25 °C):** 8.28 (d,  $J = 2.2$  Hz, 1H, PzB3), 8.19 (d,  $J = 2.4$  Hz, 1H, PzC3), 8.07 (d,  $J = 2.2$  Hz, 1H, PzA3), 7.86 (d,  $J = 2.4$  Hz, 1H, PzC5), 7.83 (d,  $J = 2.5$  Hz, 1H, PzB5), 7.70 (d,  $J = 2.5$  Hz, 1H, PzA5), 6.61 (t,  $J = 2.3$  Hz, 1H, PzC4), 6.54 (ddd,  $J = 10.5, 5.6, 2.6$  Hz, 1H, H4), 6.48 (t,  $J = 2.3$  Hz, 1H, PzB4), 6.36 (td,  $J = 9.5, 4.3$  Hz, 1H, H5), 6.31 (t,  $J = 2.3$  Hz, 1H, PzA4), 6.13 (dd,  $J = 6.5, 7.5$  Hz, 1H, H3), 5.24 (t,  $J = 9.0$  Hz, 1H, H2), 4.99 – 4.92 (m, 1H, H1), 3.17 (td,  $J = 10.9, 5.2$  Hz, 1H, H7), 3.02 (t,  $J = 13.3$  Hz, 1H, H7), 2.63 – 2.57 (m, 1H, H6), 2.37-2.32 (m, 1H, H6), 1.30 – 1.24 (m, 1H), 1.21 (d,  $J_{PC} = 9.3$  Hz, 9H,  $\text{PMe}_3$ ).

**$^{13}\text{C}$  NMR (201 MHz,  $\text{CDCl}_3$ ,  $\delta$ , 25 °C):** 145.0 (PzB3), 143.5 (PzC3), 146.9 (PzA3), 137.9-138.5 (3C PzC5/PzB5/PzA5), 109.3 (PzC4), 108.6 (PzB4), 107.4 (PzA4), 124.4 (C4), 138.4 (C5), 126.8 (C3), 109.5 (C2), 77.9 (C1), 36.8 (C7), 31.3 (C6). 14.1 (9C,  $J_{PH} = 32.2$  Hz,  $\text{PMe}_3$ ).

Composition of **7A** confirmed by single crystal X-ray diffraction.

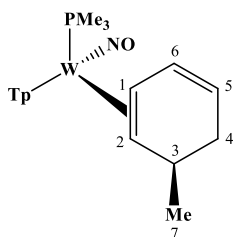


**Compound 8.** In a 25 mL Erlenmeyer flask charged with a stir bar, **2** (1.00 g, 1.65 mmol) was dissolved in 10 mL dried THF. Next, HOTf (294 mg, 1.96 mmol) was syringed into a test tube with 1 mL dried THF. The HOTf solution was pipetted into the stirring solution of **2** and was let stir for 15 minutes at R.T. as orange precipitate began to form. To further induce precipitation, the crude reaction mixture was chilled at -30°C for over 12 hours. Afterwards, the orange precipitate **8** was collected as a triflate salt on a 15 mL fine porosity fritted funnel, rinsed with dried THF, and dried in the desiccator (810 mg, 64.8%).

**<sup>1</sup>H NMR (800 MHz, CD<sub>3</sub>CN, **8**, 25 °C):** 8.33 (d, *J* = 2.02 Hz, 1H, Pz3B), 8.23 (d, *J* = 2.49 Hz, 1H, Pz5A), 8.00 (d, *J* = 2.46 Hz, 1H, Pz5B), 7.96 (d, *J* = 2.46 Hz, 1H, Pz5C), 7.85 (d, *J* = 1.88 Hz, 1H, Pz3C), 7.83 (d, *J* = 2.46 Hz, 1H, Pz3A), 6.88 (dd, *J* = 4.92, 11.64 Hz, 1H, H4), 6.52 (t, *J* = 2.35 Hz, 1H, Pz4C), 6.51 (t, *J* = 2.41 Hz, 1H, Pz4B), 6.49 (dd, *J* = 7.92, 10.45 Hz, 1H, H7), 6.36 (t, *J* = 2.45 Hz, 1H, Pz4A), 6.33 (dd, *J* = 4.68, 9.66 Hz, 1H, H3), 6.15 (dd, *J* = 3.97, 10.67 Hz, 1H, H6), 6.04 (dd, *J* = 3.85, 11.80 Hz, 1H, H5), 4.91 (t, *J* = 9.62 Hz 1H, H2), 4.40-4.35 (m, *J* = 8.41, 16.97, 24.16 Hz, 1H, H1), 3.60 (dt, *J* = 8.84, 13.07 Hz, 1H, H8), 2.48 (dt, *J* = 7.58, 14.09 Hz, 1H, H8), 1.16 (d, *J* = 9.88 Hz, 9H, PMe<sub>3</sub>). **<sup>13</sup>C NMR (201 MHz, CD<sub>3</sub>CN, **8**, 25 °C):** 148.0 (1C, Pz5A), 146.1 (1C, Pz3B), 144.3 (1C, C7), 143.5 (1C, Pz3C), 139.7-139.5 (3C, Pz5C/Pz5B/Pz3A), 133.3 (1C, C3), 131.7 (1C, C5), 130.2 (1C, C4), 129.5 (1C, C6), 109.6-108.9 (2C, Pz4C/Pz4B), 108.1 (1C, Pz4A), 106.5 (d, *J*<sub>PC</sub> = 13.28 Hz, 1C, C2), 73.5 (d, *J*<sub>PC</sub> = 11.96 Hz, 1C, C1), 30.7 (d, *J*<sub>PC</sub> = 3.73 Hz, 1C, C8), 13.3 (d, *J*<sub>PC</sub> = 33.1 Hz, 3C, PMe<sub>3</sub>).

Composition of **8** confirmed by single crystal X-ray diffraction.

**ESI-HRMS** (*m/z*): [M]<sup>+</sup> calculated for 608.1690; found 608.1697.

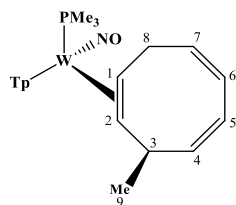


**Compound 9.** In an oven dried test tube charged with a stir pea, **1** (0.101 g, 0.17 mmol) was dissolved in 5 mL DCM. In another oven dried test tube charged with a stir pea, DPhAT (0.062 g, 0.19 mmol) was dissolved in DCM. Both test tubes were chilled to  $-30^{\circ}\text{C}$  for 20 minutes. The DPhAT solution was added to the solution of **1** and stirred for 30 minutes. The solution was precipitated into chilled ether and desiccated to yield resultant  $\text{WTP}(\text{NO})(\text{PMe}_3)(\eta^2\text{-cyclohexadienyl})$  triflate salt, **1A** (0.81mg, 0.11 mmol, 64%). In an oven dried test tube charged with a stir pea, **1A** (0.80 g, 0.11 mmol) was dissolved in 5 mL dried THF. At room temperature, with a syringe,  $\text{MeMgBr}$  (0.07mL, 0.21 mmol) was added to the solution. 1mL of  $\text{H}_2\text{O}$  was added to quench the reaction 10 minutes later. The solution was diluted with 10mL of DCM and extracted 3x with 10mL  $\text{H}_2\text{O}$ . The organic layer was collected, dried with  $\text{Na}_2\text{SO}_4$  and filtered over a 30mL fritted disc and rinsed with 5mL DCM. The remaining solution was reduced to dryness, redissolved in minimal DCM and precipitated into 100mL Hexanes. The precipitate was collected over a 15mL fritted disc and discarded. The remaining filtrate was reduced to dryness to yield yellow/white powder **9** in a 5 : 1 ratio (0.045 g, 69%).

**$^1\text{H}$  NMR (800 MHz,  $\text{CD}_2\text{Cl}_2$ ,  $\delta$ ,  $25^{\circ}\text{C}$ ):** 8.02 (bs, 2H, Pz3A/Pz3B), 7.74 (d,  $J = 2.45$  Hz, 1H, Pz5A or B), 7.72 (d,  $J = 2.21$  Hz, 1H, Pz5C), 7.67 (d,  $J = 2.45$  Hz, 1H, Pz5A or B), 7.32 (d,  $J = 2.10$  Hz, 1H, Pz3C), 6.42 (ddd,  $J = 2.97, 5.09, 8.63$  Hz, 1H, H6), 6.30 (t,  $J = 2.15$  Hz, 1H, Pz4A or B), 6.24 (t,  $J = 2.10$  Hz, 1H, Pz4A or B), 6.21 (t,  $J = 2.30$  Hz, 1H, Pz4C), 4.98 (ddd,  $J = 2.03, 6.30, 8.99$  Hz, 1H, H5), 2.86 (ddd,  $J = 4.94, 10.23, 14.09$  Hz, 1H, H1), 2.83 – 2.77 (m, 1H, H3), 2.77 – 2.67 (m, 1H, H4), 1.73 (dd,  $J = 6.46, 16.34$  Hz, 1H, H4), 1.25 (d,  $J = 8.44$  Hz, 9H,  $\text{PMe}_3$ ), 1.21 (d,  $J = 6.82$  Hz, 3H, H7), 1.09 (d,  $J = 10.32$  Hz, 1H, H2).

**$^{13}\text{C}$  NMR (201 MHz,  $\text{CD}_2\text{Cl}_2$ ,  $\delta$ ,  $25^{\circ}\text{C}$ ):** 143.4 (d,  $J_{\text{PC}} = 1.73$  Hz, 1C, Pz3A), 142.1 (1C, Pz3B), 140.7 (1C, Pz3C), 136.8 (1C, Pz5A or B), 136.2 (1C, Pz5C), 135.9 (1C, Pz5A or B), 130.9 (d,  $J_{\text{PC}} = 3.27$  Hz, 1C, C6), 117.4 (1C, C5), 106.5 - 105.9 (3C, Pz4A/Pz4B/Pz4C), 62.8 (1C, C2), 49.6 (d,  $J_{\text{PC}} = 9.61$  Hz, 1C, C1), 30.9 - 30.6 (2C, C3/C4), 26.7 (1C, C7), 14.1 (d,  $J_{\text{PC}} = 27.60$  Hz, 3C,  $\text{PMe}_3$ ).

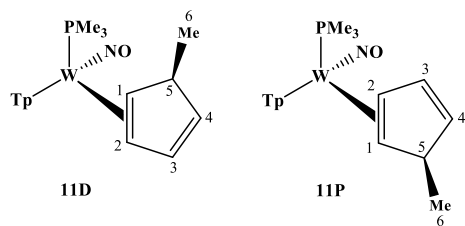
**ESI-HRMS** (m/z): [M+H]<sup>+</sup> calculated for 598.1847; found 598.1848.



**Compound 10.** In an oven dried test tube charged with a stir pea, **8** (0.591 g, 0.78 mmol) was dissolved in 50 mL dried THF. At room temperature, with a syringe, MeMgBr (1.12 mL, 1.68 mmol) was added to the solution. After 30 minutes of stirring, 2mL of H<sub>2</sub>O was added to quench the reaction. The solution was diluted with 100mL of CDCl<sub>3</sub> and extracted 3x with 100mL H<sub>2</sub>O. The organic layer was collected, dried with Na<sub>2</sub>SO<sub>4</sub> and filtered over a 60mL fritted disc and rinsed with 50mL CDCl<sub>3</sub>. The remaining solution was reduced to dryness, redissolved in minimal MeCN and precipitated into 300mL Et<sub>2</sub>O. The precipitate was collected over a 30mL fritted disc and discarded. The remaining ether filtrate was reduced to dryness to yield white powder **10** in a 20 : 1 ratio (0.326 g, 65%). **<sup>1</sup>H NMR (800 MHz, CD<sub>3</sub>CN, δ, 25 °C):** 7.97 (d, *J* = 2.12 Hz, 1H, Pz3A), 7.95 (d, *J* = 1.86 Hz, 1H, Pz3B), 7.82 (d, *J* = 2.18 Hz, 1H, Pz5C), 7.81 (d, *J* = 2.14 Hz, 1H, Pz5B), 7.78 (d, *J* = 2.63 Hz, 1H, Pz5A), 7.32 (d, *J* = 2.06 Hz, 1H, Pz3C), 6.31 (t, *J* = 2.33 Hz, 1H, Pz4B), 6.27 (t, *J* = 2.01 Hz, 1H, Pz4A), 6.26 (t, *J* = 2.12 Hz, 1H, Pz4C), 6.05 (dd, *J* = 3.06, 10.36 Hz, 1H, H6), 5.87 (q, *J* = 7.71 Hz, 1H, H7), 5.81 (dd, *J* = 7.71, 11.00 Hz, 1H, H5), 5.79 (dd, *J* = 2.97, 10.92 Hz, 1H, H4), 3.64 – 3.59 (m, 1H, H3), 2.78 – 2.70 (m, 1H, H1), 1.17 (d, *J* = 8.26 Hz, 9H, PMe<sub>3</sub>), 1.05 (d, *J* = 6.97 Hz, 3H, H9), 0.73 (dd, *J* = 4.18, 11.54 Hz, 1H, H2).

**<sup>13</sup>C NMR (201 MHz, CD<sub>3</sub>CN, δ, 25 °C):** 144.1 (1C, Pz3B), 144.0 (1C, Pz3A), 141.7 (1C, Pz3C), 140.9 (1C, C4), 137.6 – 137.5 (2C, Pz5A/P5C), 137.0 (2C, Pz5B/C7), 129.3 (1C, C6), 126.3 (1C, C5), 107.2 – 106.8 (3C, Pz4B/Pz4A/Pz4C), 62.4 (1C, C2), 53.8 (d, *J*<sub>PC</sub> = 11.62 Hz, 1C, C1), 37.8 (1C, C3), 34.1 (d, *J*<sub>PC</sub> = 2.70 Hz, 1C, C8), 27.3 (1C, C9), 13.26 (d, *J*<sub>PC</sub> = 27.43 Hz 1C, PMe<sub>3</sub>).

Composition of **10** has been confirmed by single crystal X-ray diffraction.



**Compounds 11D and 11P.** In an oven dried test tube charged with a stir pea, **5** (0.104 g, 0.18 mmol) was dissolved in 5 mL dried THF. In another oven dried test tube charged with a stir pea, DDQ (0.042 g, 0.19 mmol) was dissolved in 2 mL dried THF. Both test tubes were chilled to  $-15^{\circ}\text{C}$  for 15 minutes. The solution of DDQ was transferred into the test tube containing compound **5**. To the chilled solution (0.20 mL, 0.28 mmol) MeMgCl was added via syringe and was stirred at  $-15^{\circ}\text{C}$  for 30 minutes. The crude reaction mixture was then diluted with DCM and extracted 3x with 10 mL  $\text{H}_2\text{O}$ . The reaction was then dried with  $\text{Na}_2\text{SO}_4$  and filtered to remove drying agent. Afterwards the reaction was reduced to dryness in vacuo in a 125 mL filter flask. The remaining product on the flask was redissolved in minimal DCM, precipitated into 50mL hexanes and filtered over a 15mL fritted disc. The precipitate was discarded. The hexanes filtrate was reduced to dryness and weighed. The white solid **11D and 11P** was collected in a 3 : 2 ratio (0.082 g, 77%). **11D**:  $^1\text{H}$  NMR (800 MHz,  $\text{CD}_3\text{CN}$ ,  $\delta$ ,  $25^{\circ}\text{C}$ ): 8.14 (d,  $J = 2.0$  Hz, 1H, Pz), 8.01 (d,  $J = 2.0$  Hz, 1H, Pz), 7.87 (d,  $J = 2.4$  Hz, 1H, Pz), 7.80 (d,  $J = 2.3$  Hz, 1H, Pz), 7.73 (d,  $J = 2.3$  Hz, 1H, Pz), 7.45 (d,  $J = 2.2$  Hz, 1H), 6.47 (dt,  $J = 5.1, 1.9$  Hz, 1H, H3), 6.37 (t,  $J = 2.3$  Hz, 1H, Pz), 6.29 (t,  $J = 2.2$  Hz, 1H, Pz), 6.23 (t,  $J = 2.2$  Hz, 1H, Pz), 5.01 (dd,  $J = 5.1, 2.4$  Hz, 1H, H4), 3.54 (m, 1H, H5), 3.09 (dd,  $J = 13.4, 7.2$  Hz, 1H, H1), 2.08 (m, 1H, H2), 1.29 (d,  $J = 7.1$  Hz, 3H, H6), 1.22 (d,  $J = 8.3$  Hz, 9H,  $\text{PMe}_3$ ).

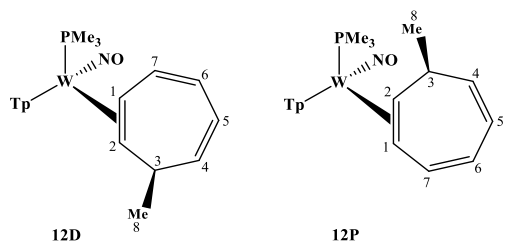
$^{13}\text{C}$  NMR (201 MHz,  $\text{CD}_3\text{CN}$ ,  $\delta$ ,  $25^{\circ}\text{C}$ ): 145.0 (1C, Pz), 144.6 (1C, Pz), 142.2 (1C, Pz), 137.7 (1C, Pz), 137.6 (1C, Pz), 137.2 (1C, C3), 136.3 (1C, Pz), 128.3 (1C, H4), 107.4 (1C, Pz), 107.0 (1C, Pz), 106.8 (1C, Pz), 68.4 (d,  $J = 12.4$  Hz, 1C, C1), 64.8 (1C, C2), 50.1 (1C, C5), 25.9 (1C, C6), 13.5 (d,  $J = 27.9$  Hz, 3C,  $\text{PMe}_3$ ).

**11P**:  $^1\text{H}$  NMR (800 MHz,  $\text{CD}_3\text{CN}$ ,  $\delta$ ,  $25^{\circ}\text{C}$ ): 8.34 (d,  $J = 2.0$  Hz, 1H, Pz), 8.01 (d,  $J = 2.0$  Hz, 1H, Pz), 7.87 (d,  $J = 2.4$  Hz, 1H, Pz), 7.80 (d,  $J = 2.3$  Hz, 1H, Pz), 7.76 (d,  $J = 2.3$  Hz, 1H, Pz), 7.40 (d,  $J = 2.2$  Hz, 1H, Pz), 6.37 (t,  $J = 2.3$  Hz, 1H, Pz), 6.30 (m, 2H, H3 & Pz), 6.22 (t,  $J = 2.2$  Hz, 1H, Pz), 5.05 (dd,  $J = 5.1, 2.4$  Hz, 1H, H4), 3.90 (dddd,  $J = 9.1, 7.1, 5.5, 1.9$  Hz, 1H, H5), 3.60 (ddt,  $J = 12.4, 7.2, 2.0$  Hz, 1H, H2), 1.61 (dd,  $J = 7.2, 2.8$  Hz, 1H, H1), 1.24 (d,  $J = 8.4$  Hz, 9H,  $\text{PMe}_3$ ), 1.15 (d,  $J = 7.2$  Hz, 3H, H6).



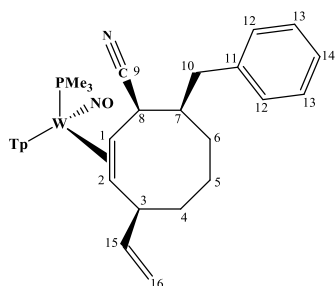
**$^{13}\text{C}$  NMR (201 MHz,  $\text{CD}_3\text{CN}$ ,  $\delta$ , 25 °C):** 145.0 (1C, Pz), 142.4 (1C, Pz), 141.4 (1C, Pz), 137.2 (1C, Pz), 137.0 (1C, Pz), 136.5 (1C, Pz), 136.3 (d,  $J_{\text{PC}} = 2.4$  Hz, 1C, C3), 128.9 (1C, C4), 107.3 (1C, Pz), 106.7 (1C, Pz), 106.7 (1C, Pz), 67.2 (1C, C1), 66.5 (d,  $J_{\text{PC}} = 10.8$  Hz, 1C, C2), 50.5 (1C, C5), 26.7 (1C, C6), 14.2 (d,  $J_{\text{PC}} = 28.6$  Hz, 3C,  $\text{PMe}_3$ ).

**APCI-HRMS (m/z):**  $[\text{M}+\text{H}]^+$  calculated for 584.1690; found 584.1690.



**Compound 12** – data in chapter 6.

**APCI-HRMS (m/z):**  $[\text{M}+\text{H}]^+$  calculated for  $\text{C}_{20}\text{H}_{30}\text{BN}_7\text{OPW}^+$ , 610.1846; found 610.1840



**Compound 13.** In an oven dried test tube charged with a stir pea, **8** (0.40 g, 0.53 mmol) was dissolved in 5 mL dried THF. To this solution,  $\text{BnMgCl}$  (0.80 mL, 0.79 mmol) was added via syringe and the reaction stirred for 30 minutes. The crude reaction mixture was then diluted with DCM and extracted 3x with 10 mL  $\text{H}_2\text{O}$ . The reaction was then dried with  $\text{Na}_2\text{SO}_4$  and filtered to remove drying agent. Afterwards, the reaction was reduced to dryness in vacuo in a 125 mL filter flask. The remaining product on the flask was redissolved in minimal DCM, precipitated into 50 mL hexanes and filtered over a 15 mL fritted disc. The precipitate was discarded. The hexanes filtrate was reduced to dryness and weighed. The white solid, a benzyl-substituted cyclooctatriene complex analogous to **10**, was collected (233 mg, 63.1%). Next, the resulting triene complex (286 mg, 0.41 mmol) was dissolved in 3 mL DCM, protonated with HOTf (70.4 mg, 0.47 mmol), and left to stir for 12 hours. Afterwards, 125 mL hexanes was added, precipitating out a whitish tan solid. The precipitated dieny

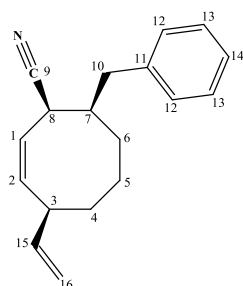
complex was collected as a triflate salt on a 15 mL fine porosity fritted funnel (314 mg, 93%). Then, in a test tube charged with a stir pea, the dienyl complex (300 mg, 0.35 mmol) was dissolved in 5 mL MeCN. To this solution, NaCN (173 mg, 3.53 mmol) was added with a few drops of DMSO. This reaction mixture was stirred for 12 hours. The crude reaction mixture was then diluted with DCM and extracted 3x with 10 mL H<sub>2</sub>O. The reaction was then dried with Na<sub>2</sub>SO<sub>4</sub> and filtered to remove drying agent. Afterwards the reaction was reduced to dryness and weighed in vacuo in a 125 mL filter flask. The resulting white solid, a disubstituted diene complex, was collected (220 mg, 85.7%). Following this, the diene complex (193 mg, 0.27 mmol) was dissolved in 3 mL DCM, protonated with HOTf (44 mg, 0.29 mmol), and stirred for 5 minutes. Afterwards, 150 mL hexanes was added, precipitating out a white solid. The precipitated allyl complex was collected as a triflate salt on a 15 mL porosity fritted funnel (224 mg, 96%). Next, in a test tube charged with a stir pea, the allyl complex (125 mg, 0.14 mmol) was dissolved in 5 mL dried THF. To the stirring solution, C<sub>2</sub>H<sub>3</sub>MgBr (3.06 mL, 0.42 mmol) was added via syringe. After reacting for 30 minutes, the crude reaction mixture was then diluted with DCM and extracted 3x with 10 mL H<sub>2</sub>O. The reaction was then dried with Na<sub>2</sub>SO<sub>4</sub> and filtered to remove drying agent. Afterwards the reaction was reduced to dryness in vacuo in a 125 mL filter flask. The remaining product on the flask was redissolved in minimal DCM, precipitated into 50mL hexanes and filtered over a 15mL fritted disc. The precipitate was discarded. The hexanes filtrate was reduced to dryness and weighed. The resulting white solid, the trisubstituted cyclooctene complex **13**, was collected (89 mg, 83%).

**<sup>1</sup>H NMR (600 MHz, CD<sub>2</sub>Cl<sub>2</sub>, δ, 25 °C):** 7.93 (d, *J* = 2.1 Hz, 1H, Pz), 7.82 (d, *J* = 2.0 Hz, 1H, Pz), 7.80 (d, *J* = 2.2 Hz, 1H, Pz), 7.70 (d, *J* = 2.4 Hz, 1H, Pz), 7.64 (d, *J* = 2.4 Hz, 1H, Pz), 7.33 – 7.28 (m, 4H, H12 & H13), 7.27 (d, *J* = 2.2 Hz, 1H, Pz), 7.20 (t, *J* = 6.1, 1H, H14), 6.32 (t, *J* = 2.2 Hz, 1H, Pz), 6.26 (t, *J* = 2.2 Hz, 1H, Pz), 6.08 (t, *J* = 2.2 Hz, 1H, Pz), 5.29 (m, 1H, H15), 4.22 (d, *J* = 17.5 Hz, 1H, H16), 4.17 (m, 1H, H16), 3.74 (m, 1H, H8), 3.37 (m, 1H, H10), 2.98 (m, 2H, H1 & H3), 2.75 (appt, *J* = 12.2 Hz, 1H, H10), 2.34 (m, 1H, H7), 1.94 (m, 1H, H5), 1.85 (m, 1H, H4), 1.65 – 1.52 (m, 2H, H6), 1.25 (m, 1H, H5), 1.13 (d, *J* = 8.1 Hz, 10H, PMe<sub>3</sub> & H4), 0.93 (appt, *J* = 10.3 Hz, 1H, H2).

**<sup>13</sup>C NMR (201 MHz, CD<sub>2</sub>Cl<sub>2</sub>, δ, 25 °C):** 148.1 (1C, C15), 146.5 (1C, Pz), 143.1 (1C, Pz), 141.5 (1C, C11), 139.9 (1C, Pz), 137.3 (1C, Pz), 136.7 (1C, Pz), 136.5 (1C, Pz), 129.8 (2C, C12 or C13), 128.6 (2C, C12 or C13), 127.7, (1C, C9), 126.3 (1C, C14),

109.2 (1C, C16), 106.8 (1C, Pz), 106.5 (1C, Pz), 106.0 (1C, Pz), 65.5 (1C, C2), 47.4 (1C, C7), 45.9 (1C, C4), 44.2 (1C, C1), 40.1 (1C, C8), 39.4 (1C, C10), 29.9 (1C, C6), 29.5 (1C, C3), 24.2 (d,  $J = 23.8$  Hz, 1C, C5), 14.2 (d,  $J = 27.2$  Hz, 3C, PMe<sub>3</sub>).

Composition of **13** confirmed by single crystal X-ray diffraction.



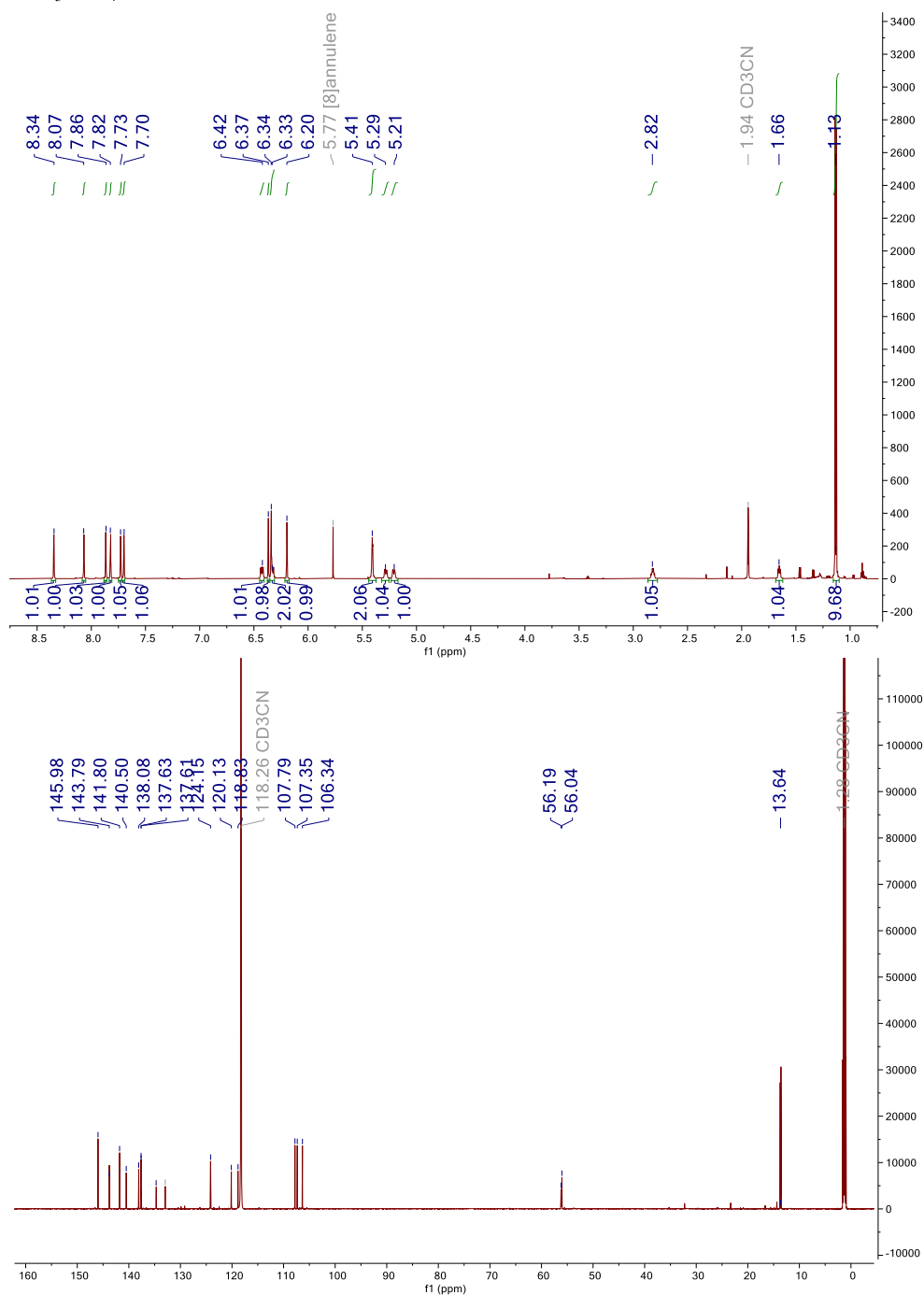
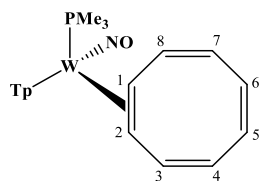
**Compound 14.** In an oven dried test tube charged with a stir pea, **13** (38 mg, 0.050 mmol) was dissolved in 1 mL acetone. In a separate test tube, cerium (IV) ammonium nitrate (33 mg, 0.060 mmol) was dissolved in 1 mL acetone. The solution of cerium (IV) ammonium nitrate was pipetted into the solution of **13**, and the reaction was stirred for 5 minutes. The crude reaction mixture was then diluted with DCM and extracted 3x with 10 mL H<sub>2</sub>O. The reaction was then dried with Na<sub>2</sub>SO<sub>4</sub> and filtered to remove drying agent. Afterwards the reaction was reduced to dryness in vacuo in a 125 mL filter flask. Minimal DCM was used to redissolve the product, and 50 mL hexanes was used to precipitate out an orange solid. The solid was discarded on a fritted funnel, and the clear filtrate was transferred into a round-bottom flask and rotovapped to dryness. The resulting white solid **14** was redissolved in MeCN and transferred into a vial, which was reduced to dryness and weighed (6.0 mg, 47%).

**<sup>1</sup>H NMR (800 MHz, CD<sub>3</sub>CN,  $\delta$ , 25 °C):** 7.29 (t,  $J = 7.7$  Hz, 2H, H13), 7.21 (m, 1H, H14), 7.20 (m, 2H, H12), 5.87 (ddd,  $J = 17.3, 10.3, 6.9$  Hz, 1H, H15), 5.73 (m, 1H, H2), 5.60 (t,  $J = 9.9$  Hz, 1H, H1), 5.07 (dd,  $J = 17.3, 1.4$  Hz, 1H, H16), 4.99 (m, 1H, H16), 4.03 (m, 1H, H8), 3.12 (m, 1H, H3), 3.05 (dt,  $J = 13.5, 3.0$  Hz, 1H, H10), 2.51 (t,  $J = 12.6$  Hz, 1H, H10), 2.34 (dp,  $J = 12.7, 4.4$  Hz, 1H, H7), 1.66 (m, 2H, H4 & H5), 1.47 (ddd,  $J = 20.3, 9.9, 4.9$  Hz, 1H, H6), 1.37 – 1.19 (m, 3H, H4, H5, & H6).

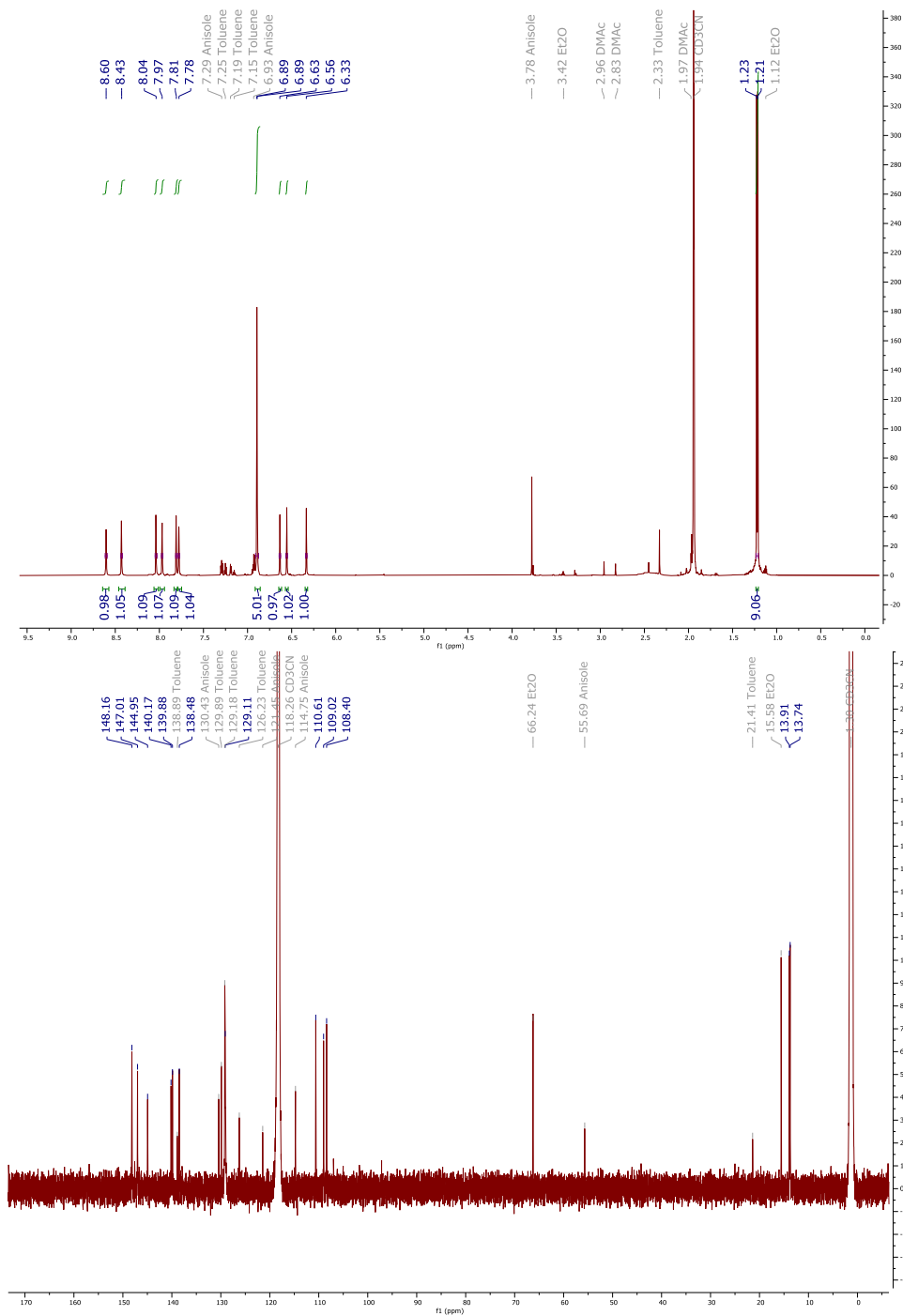
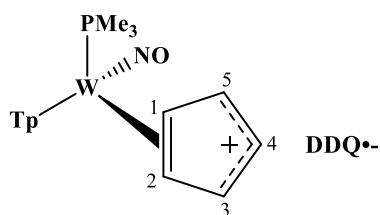
**<sup>13</sup>C NMR (201 MHz, CD<sub>3</sub>CN,  $\delta$ , 25 °C):** 143.13 (1C, C15), 141.10 (1C, C11), 138.08 (1C, C2), 130.01 (2C, C12), 129.32 (2C, C13), 127.11 (1C, C14), 122.53 (1C, C1), 114.23 (1C, C16), 104.97 (1C, C9), 45.64 (1C, C7), 41.96 (1C, C3), 37.44 (2C, C4 & C5), 37.06 (1C, C10), 34.22 (1C, C8), 29.55 (1C, C6).

**APCI-HRMS (m/z):** [M+H]<sup>+</sup> calculated for 252.1747; found 252.1733.

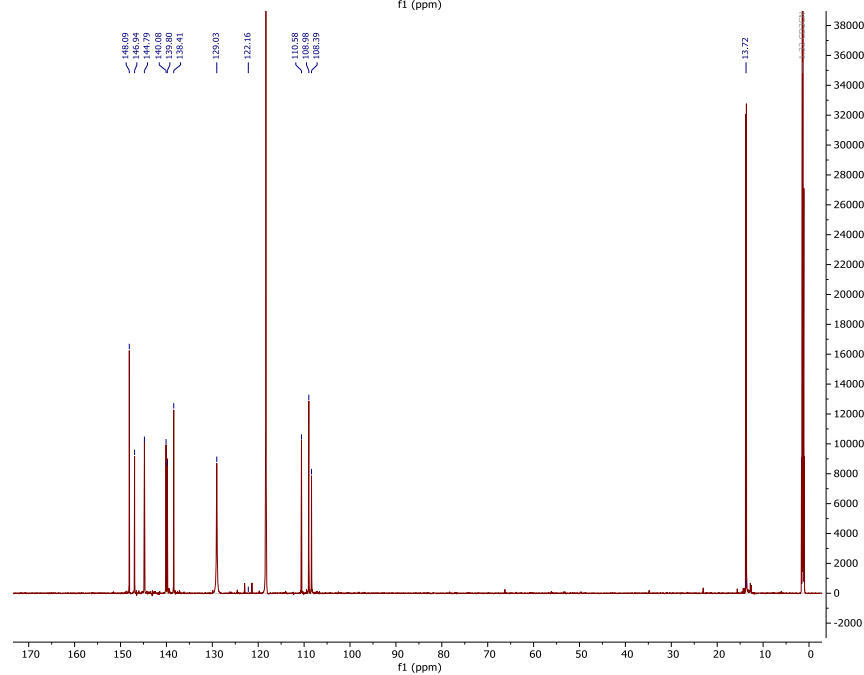
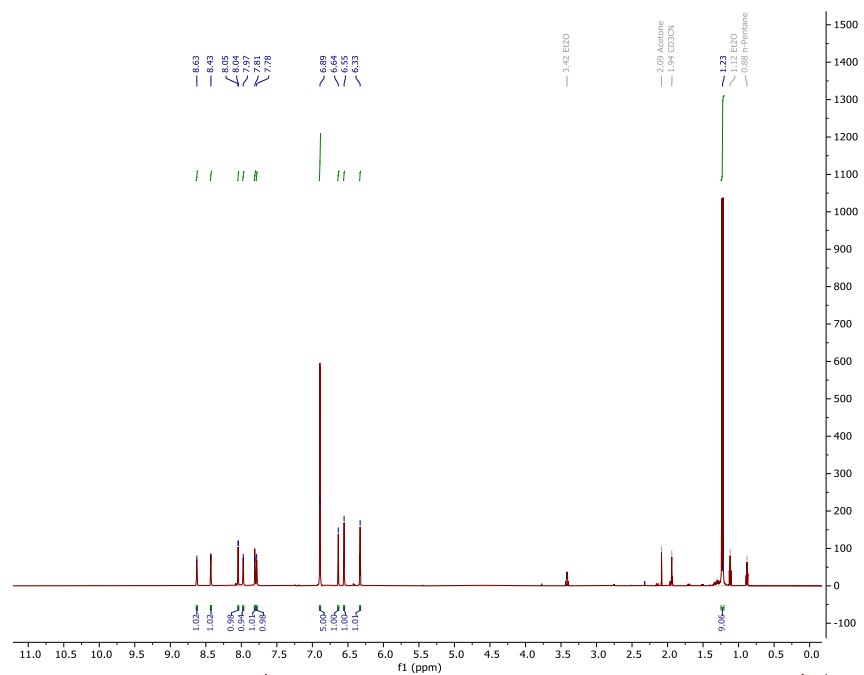
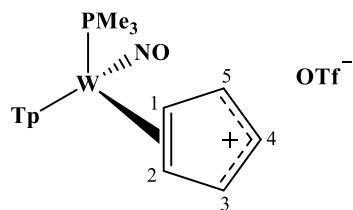
# <sup>1</sup>H-NMR (CD<sub>3</sub>CN) and <sup>13</sup>C-NMR (CD<sub>3</sub>CN) of Compound 2



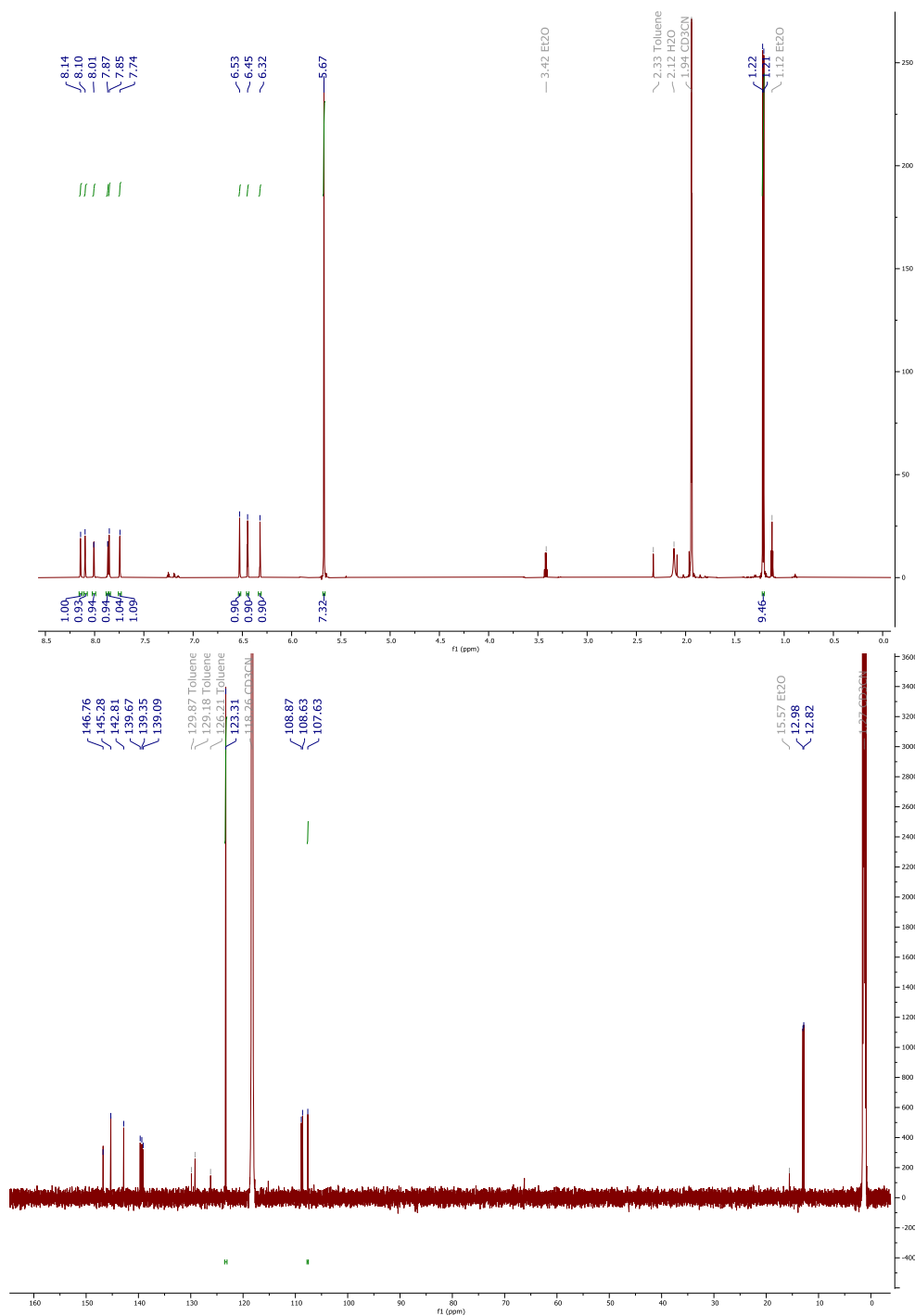
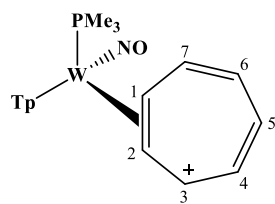
# <sup>1</sup>H-NMR (CD<sub>3</sub>CN) and <sup>13</sup>C-NMR (CD<sub>3</sub>CN) of Compound 3



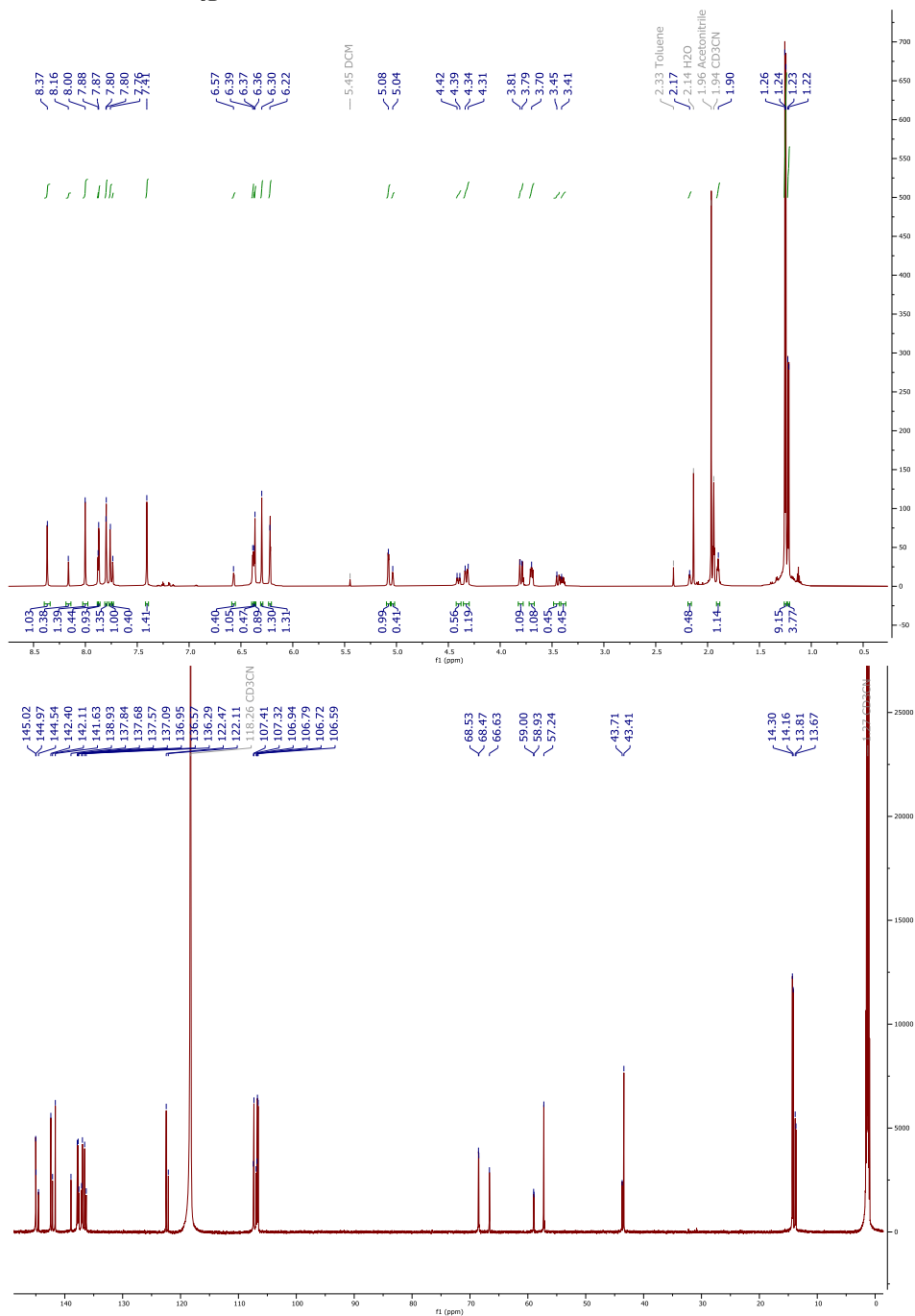
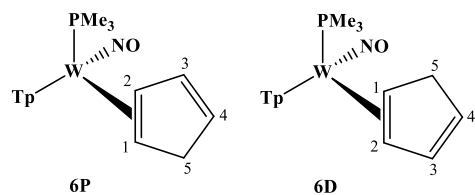
# <sup>1</sup>H-NMR (CD<sub>3</sub>CN) and <sup>13</sup>C-NMR (CD<sub>3</sub>CN) of Compound 3A



# <sup>1</sup>H-NMR (CD<sub>3</sub>CN) and <sup>13</sup>C-NMR (CD<sub>3</sub>CN) of Compound 4

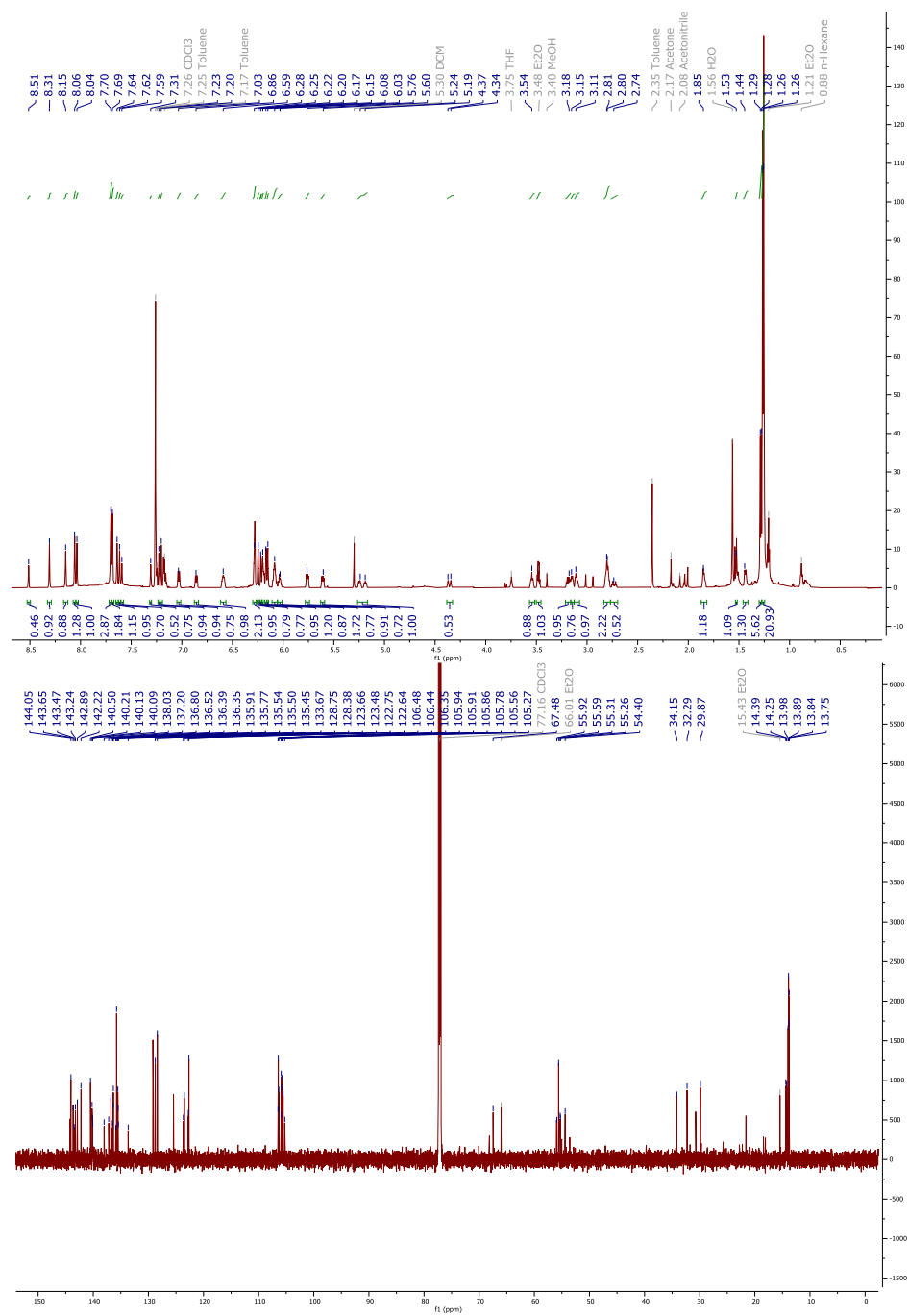
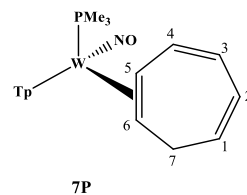
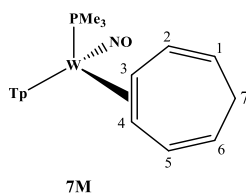
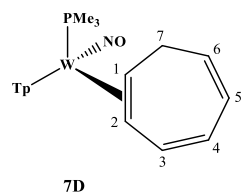


# <sup>1</sup>H-NMR (CD<sub>3</sub>CN) and <sup>13</sup>C-NMR (CD<sub>3</sub>CN) of Compounds 6D & 6P

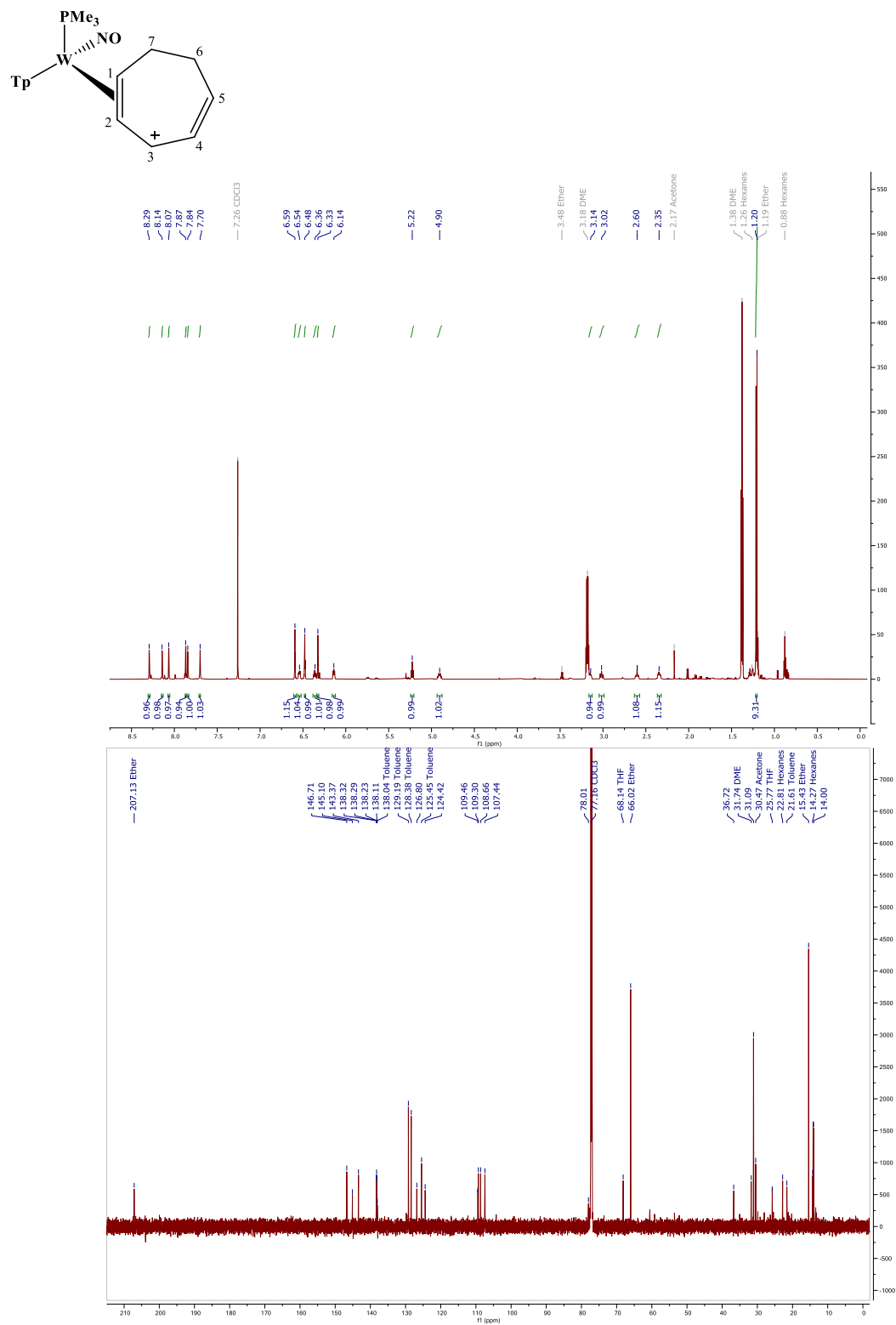




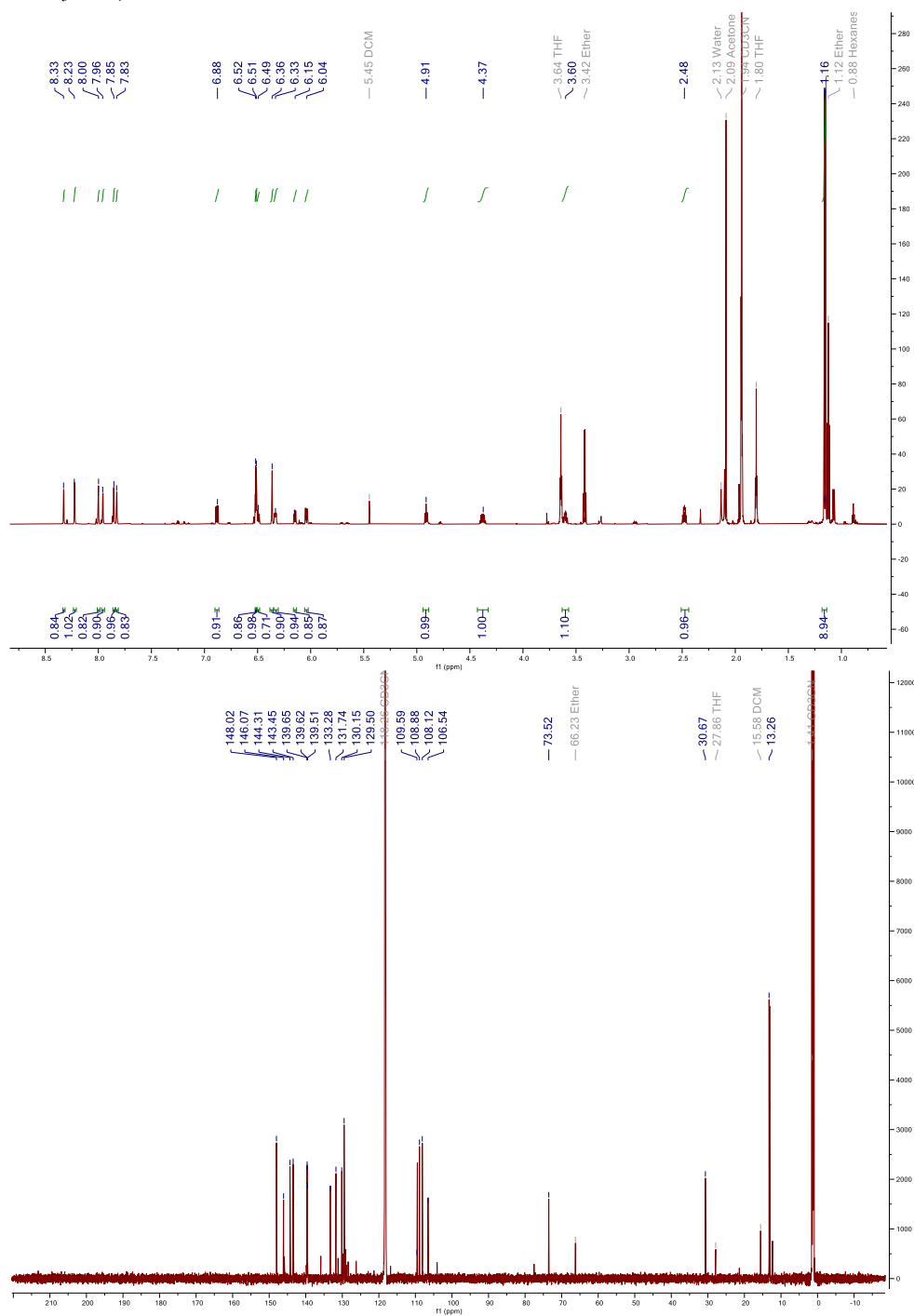
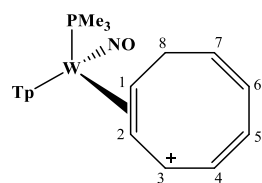
# <sup>1</sup>H-NMR (CDCl<sub>3</sub>) and <sup>13</sup>C-NMR (CDCl<sub>3</sub>) of Compounds 7D, 7M, & 7P



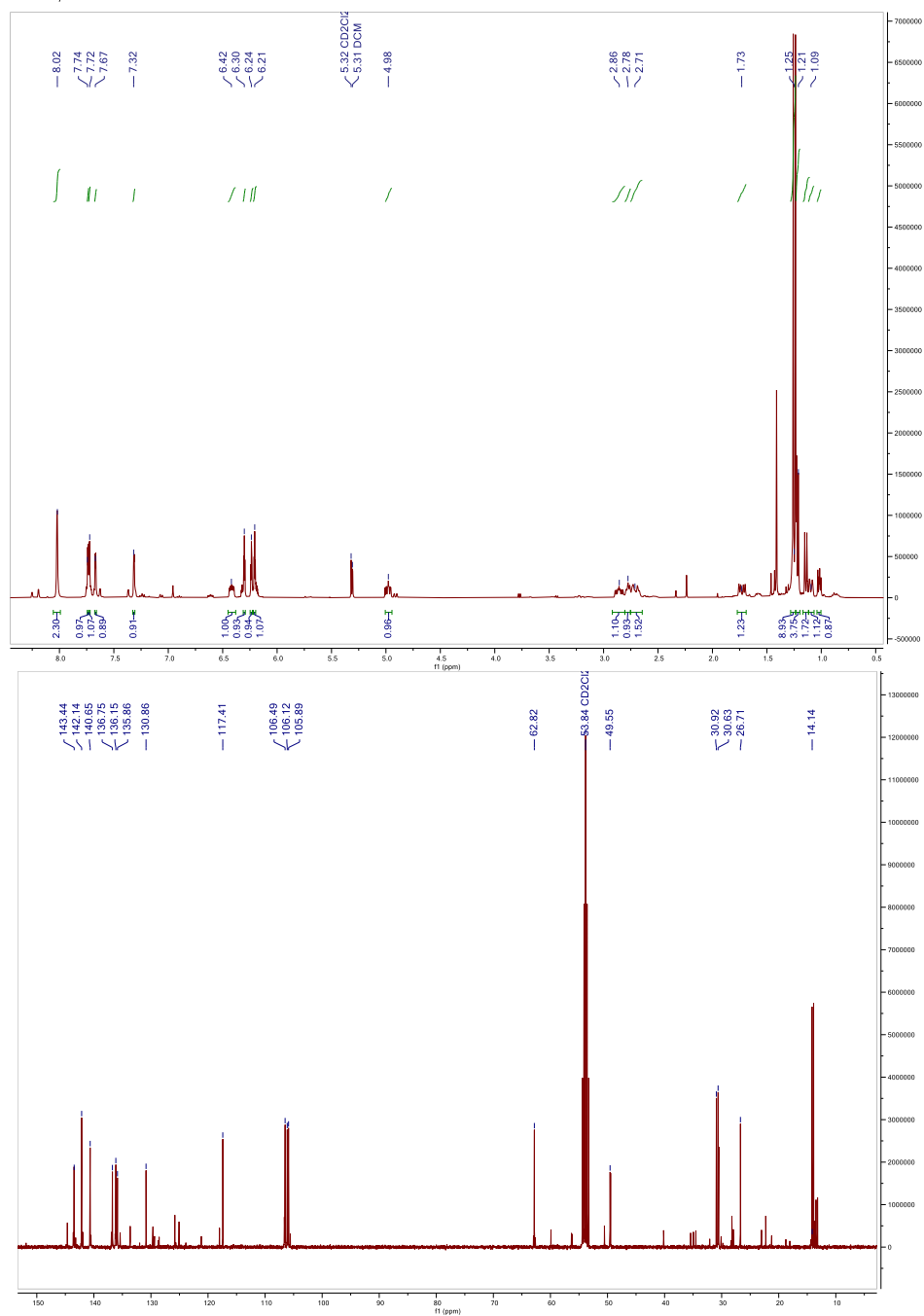
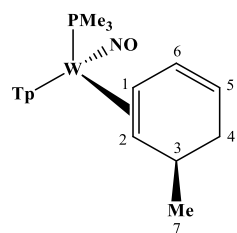
# <sup>1</sup>H-NMR (CDCl<sub>3</sub>) and <sup>13</sup>C-NMR (CDCl<sub>3</sub>) of Compound 7A



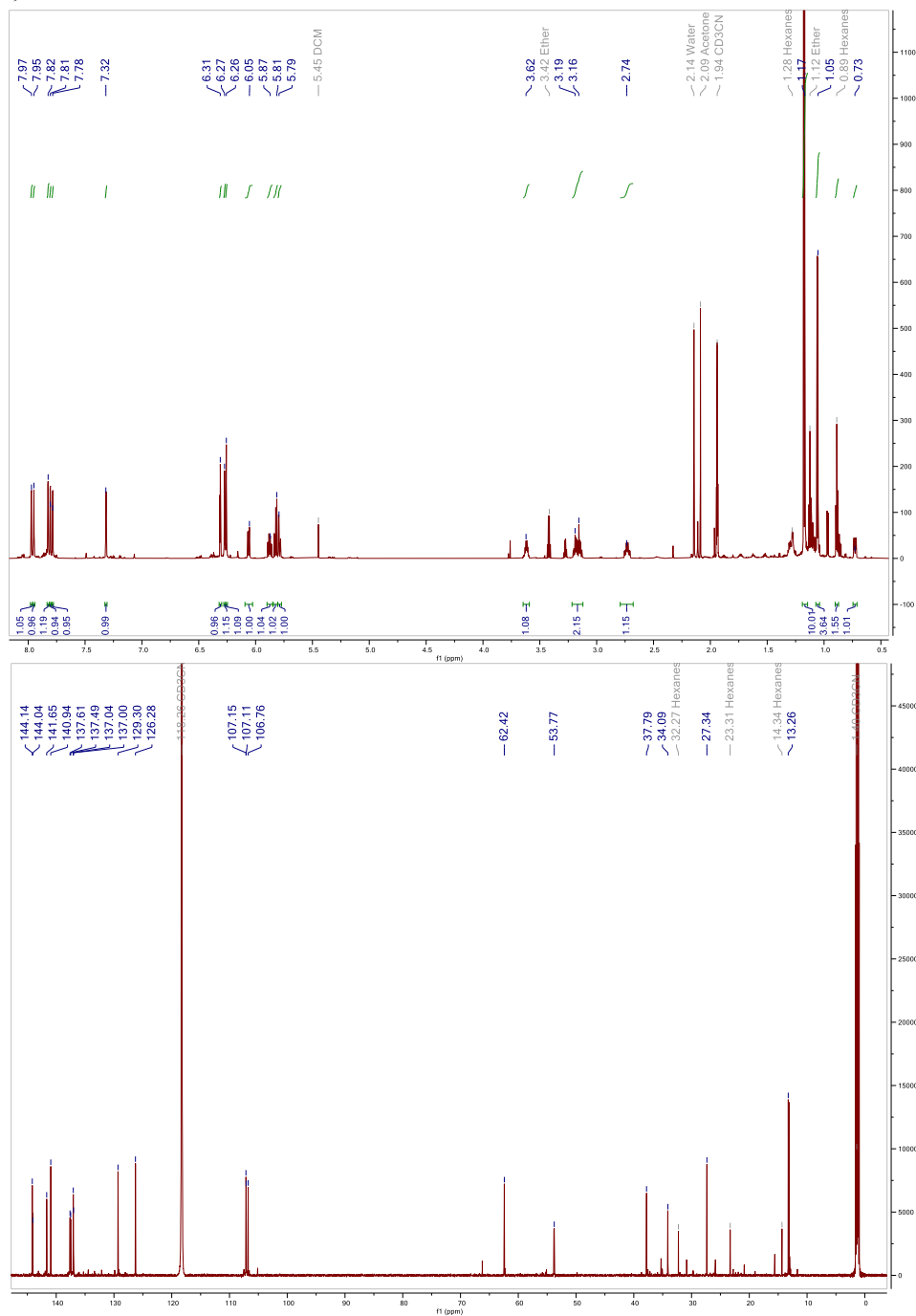
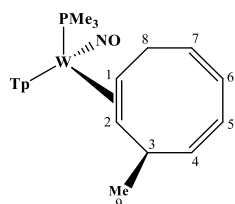
# <sup>1</sup>H-NMR (CD<sub>3</sub>CN) and <sup>13</sup>C-NMR (CD<sub>3</sub>CN) of Compound 8



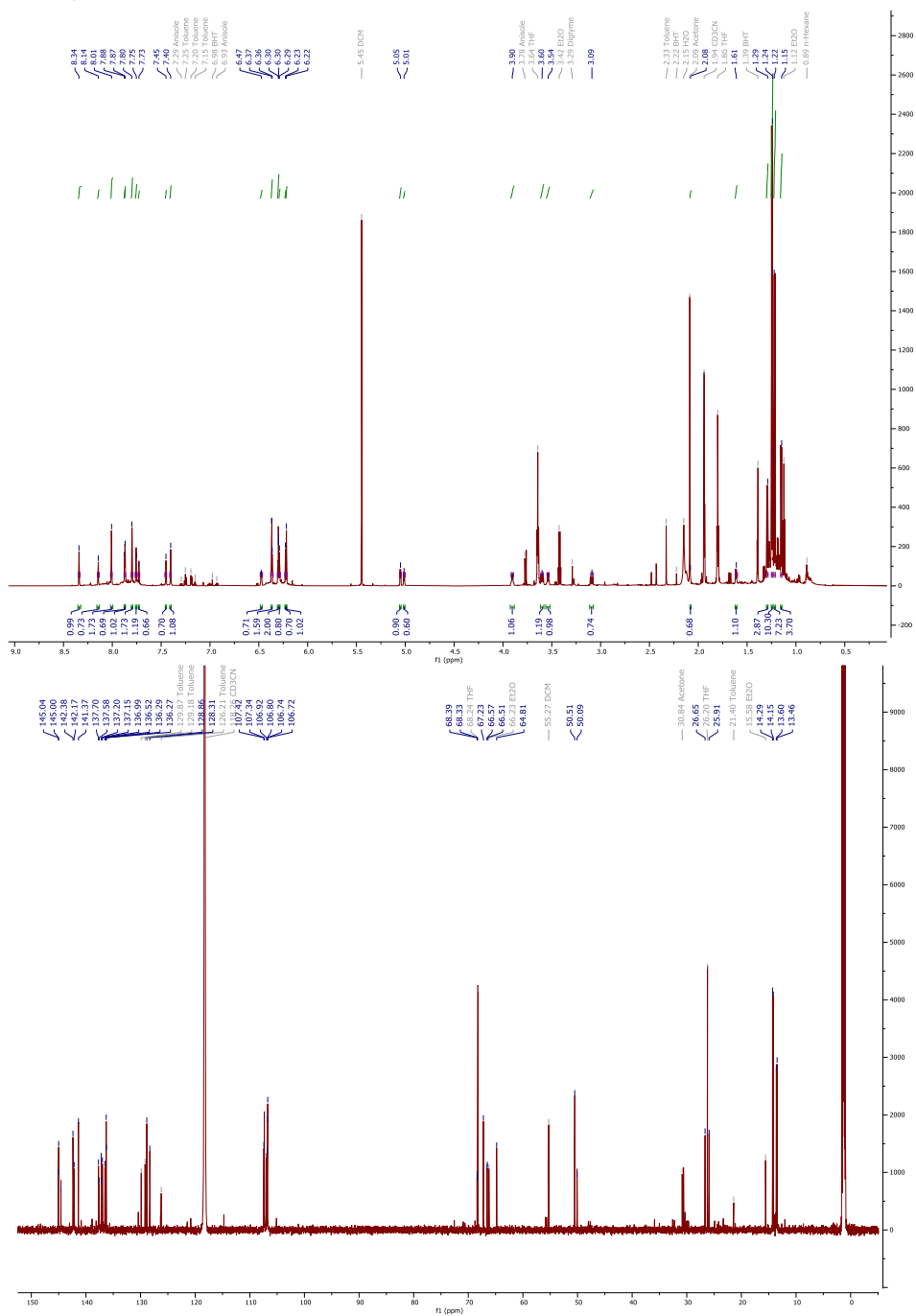
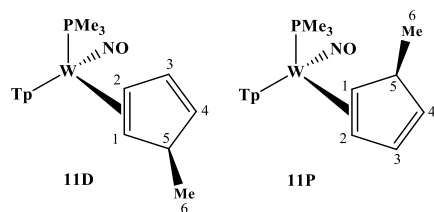
# <sup>1</sup>H-NMR (CD<sub>3</sub>CN) and <sup>13</sup>C-NMR (CD<sub>3</sub>CN) of Compound 9



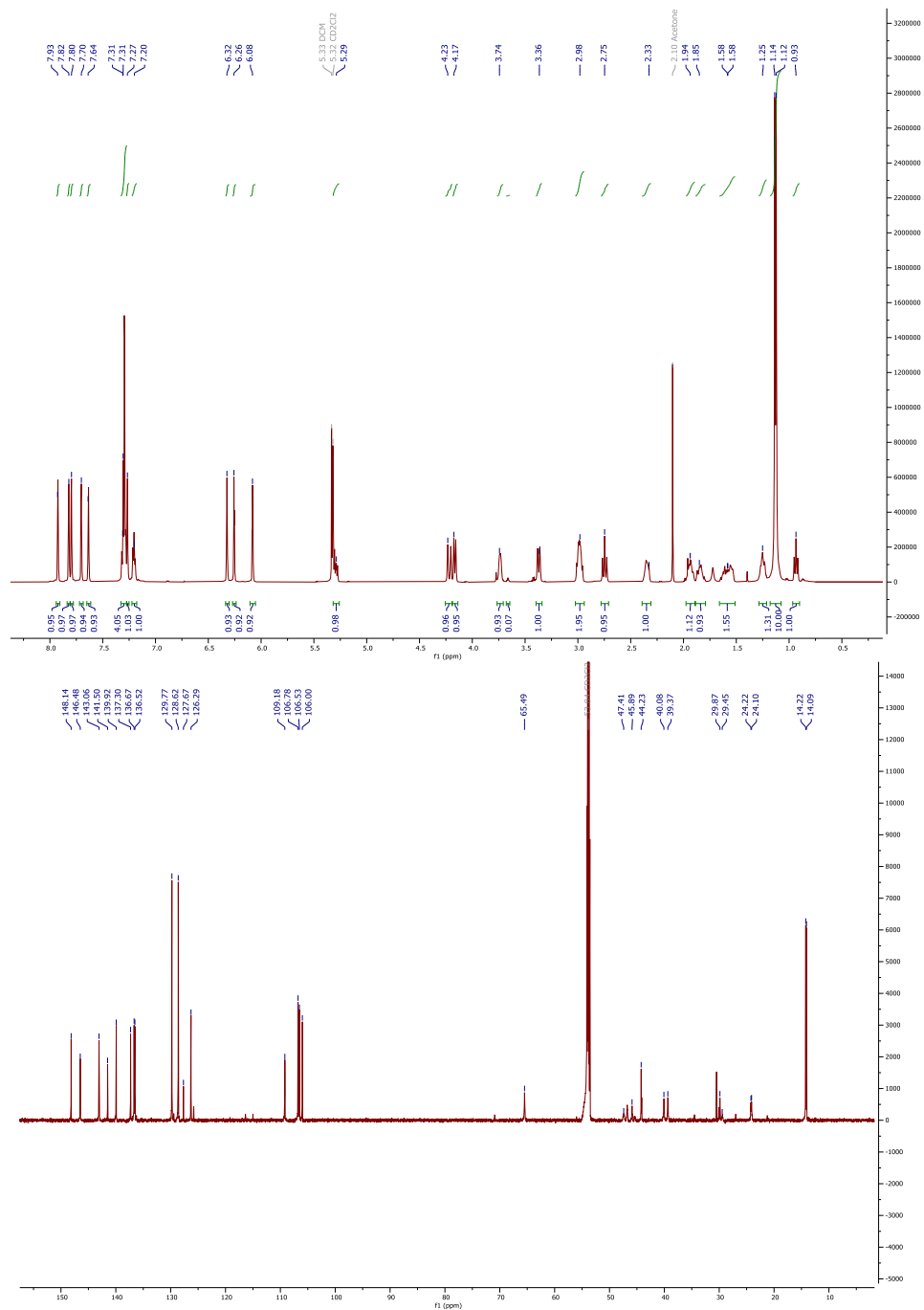
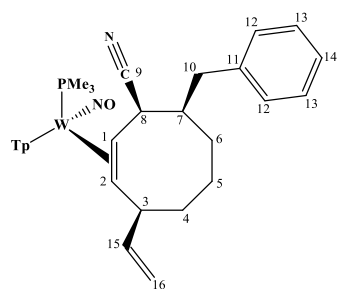
# <sup>1</sup>H-NMR (CD<sub>3</sub>CN) and <sup>13</sup>C-NMR (CD<sub>3</sub>CN) of Compound 10



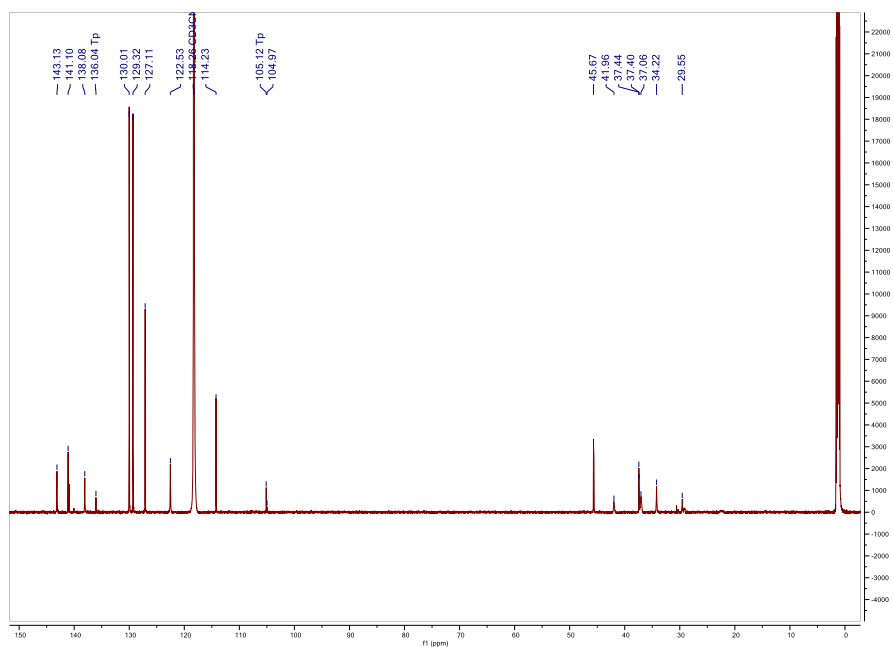
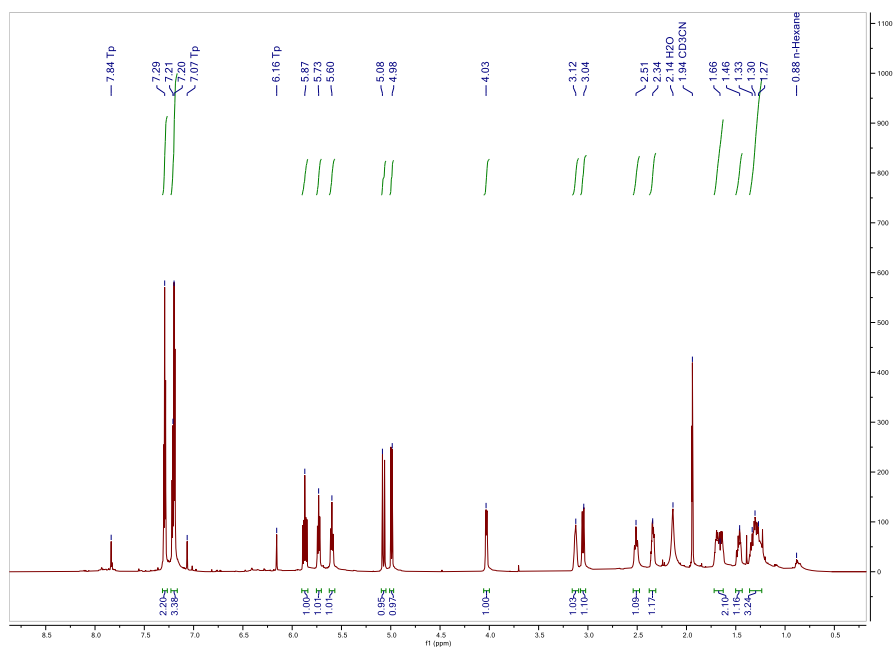
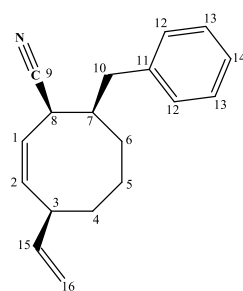
# <sup>1</sup>H-NMR (CD<sub>3</sub>CN) and <sup>13</sup>C-NMR (CD<sub>3</sub>CN) of Compound 11



# <sup>1</sup>H-NMR (CD<sub>3</sub>CN) and <sup>13</sup>C-NMR (CD<sub>3</sub>CN) of Compound 13



# <sup>1</sup>H-NMR (CD<sub>3</sub>CN) and <sup>13</sup>C-NMR (CD<sub>3</sub>CN) of Compound 14





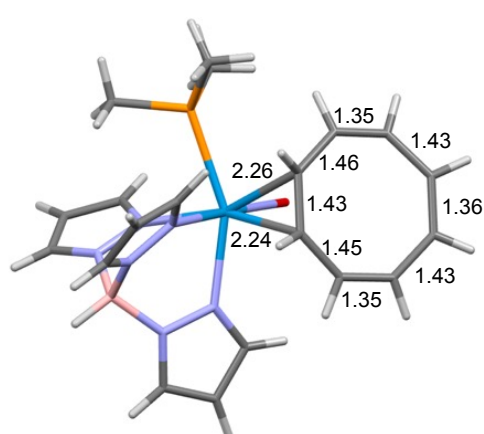
## DFT Analysis.

Previous literature demonstrates that an M06 functional and 6-31G\*\* [LANL2DZ for W] basis set choice accurately corroborates experimental results.<sup>1</sup> A small benchmarking study was performed and expanded to the  $\eta^2$ -tropylium system and compared to SC-XRD bond lengths. Ground-state structures were then optimized at the M062X level of theory using the 6-31G\*\* [LANL2DZ for W] basis set in Gaussian 16. Solvent effects of acetonitrile were modeled using SMD. Gaussian's default criteria were used for optimization, vibrational frequency analysis verified that structures were minima and thermal free energy corrections were applied. IRC calculations were used to confirm transition state studies.

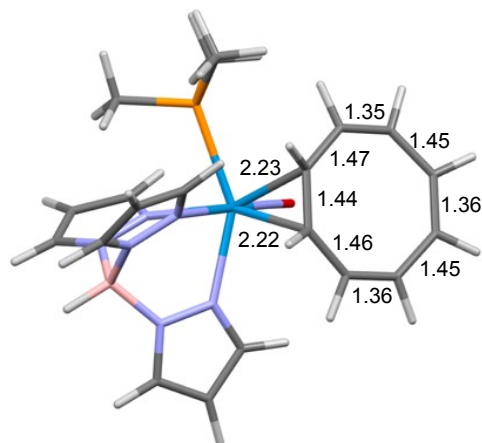
Benchmarking of Functionals and Basis Sets of  $\eta^2$ -tropylium with SC-XRD data.

Functional	Basis Set	Calculated 'Distal' Conformer (W-C3/W-C8)	XRD Bond Lengths (W-C3/W-C8)
M06	6-31G(d,p) & LANL2DZ on W	2.98/3.20	2.77/3.25
M06	CEP-31G	3.17/3.12	2.77/3.25
M062X	CEP-31G	2.98/3.29	2.77/3.25
<b>M062X</b>	<b>6-31G(d,p) &amp; LANL2DZ on W</b>	<b>2.80/3.22</b>	<b>2.77/3.25</b>
B3LYP	CEP-31G	3.25/3.18	2.77/3.25
B3LYP	6-31G(d,p) & LANL2DZ on W	3.09/3.22	2.77/3.25

Comparison of DFT using M062X/6-31G(d,p) & LANL2DZ on W and SC-XRD data of Compound 2.

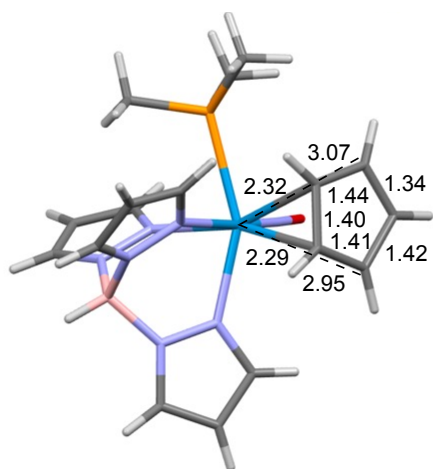


**Bond Lengths via SC-XRD.**

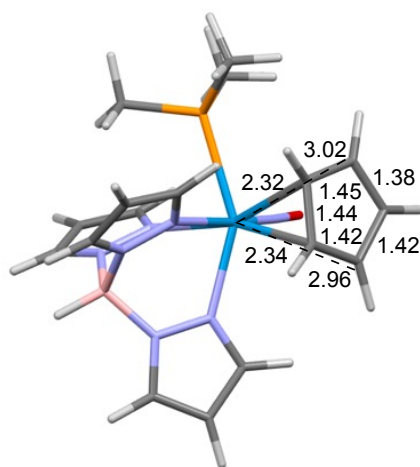


**Bond Lengths via DFT.**

Comparison of DFT using M062X/6-31G(d,p) & LANL2DZ on W and SC-XRD data of Compound 3.

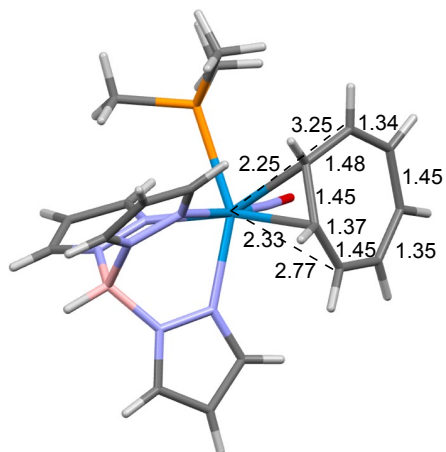


**Bond Lengths via SC-XRD.**

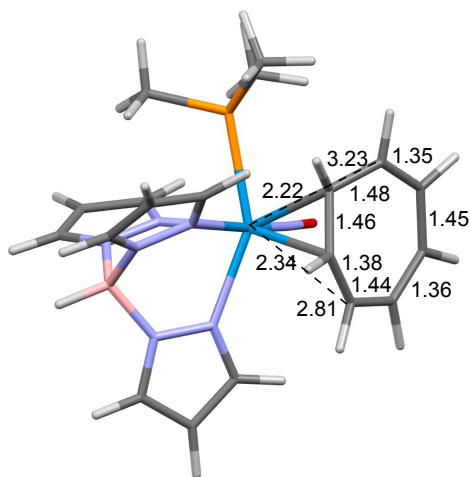


**Bond Lengths via DFT.**

Comparison of DFT using M062X/6-31G(d,p) & LANL2DZ on W and SC-XRD data of Compound 4.

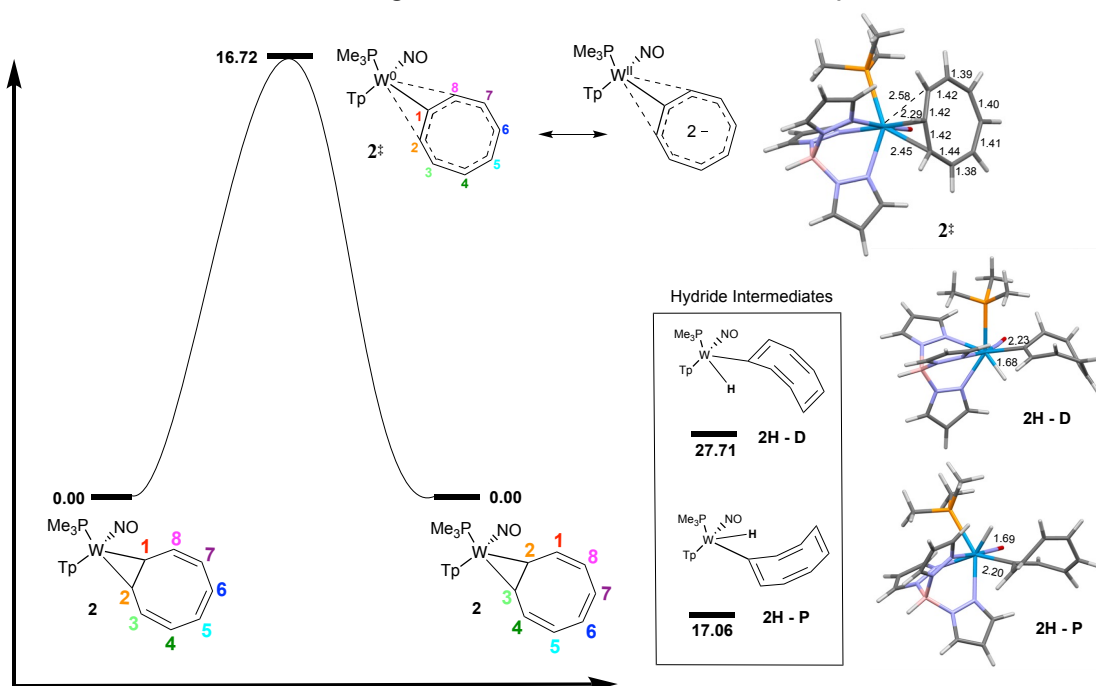


**Bond Lengths via SC-XRD.**



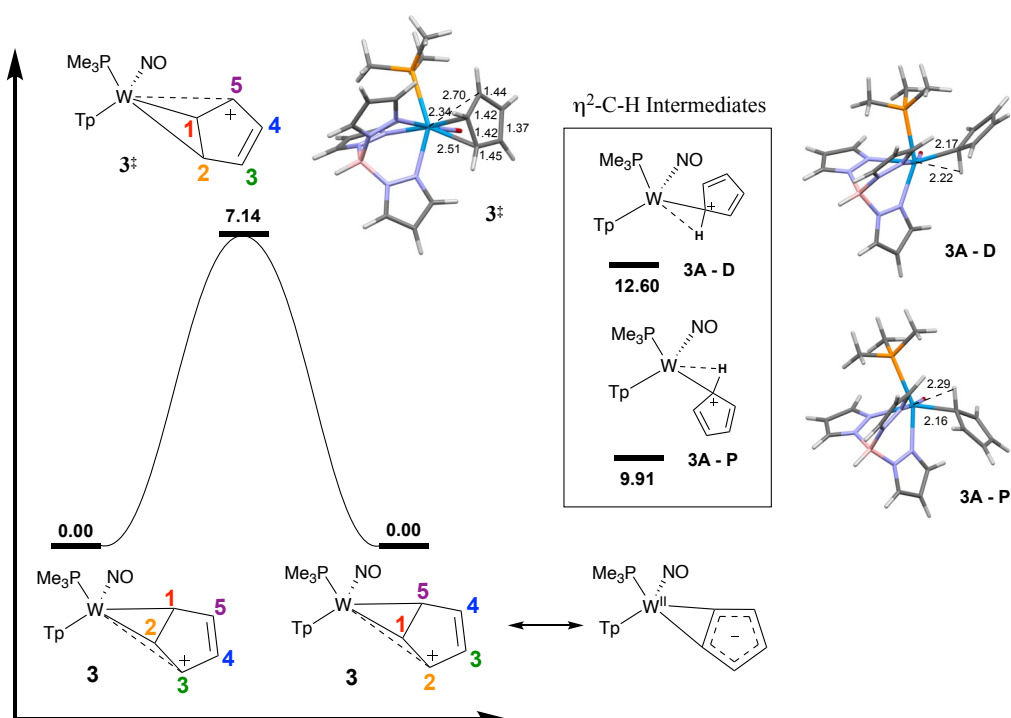
**Bond Lengths via DFT.**

## Reaction Mechanism of tungsten-alkene isomerization for $\eta^2$ -COT.

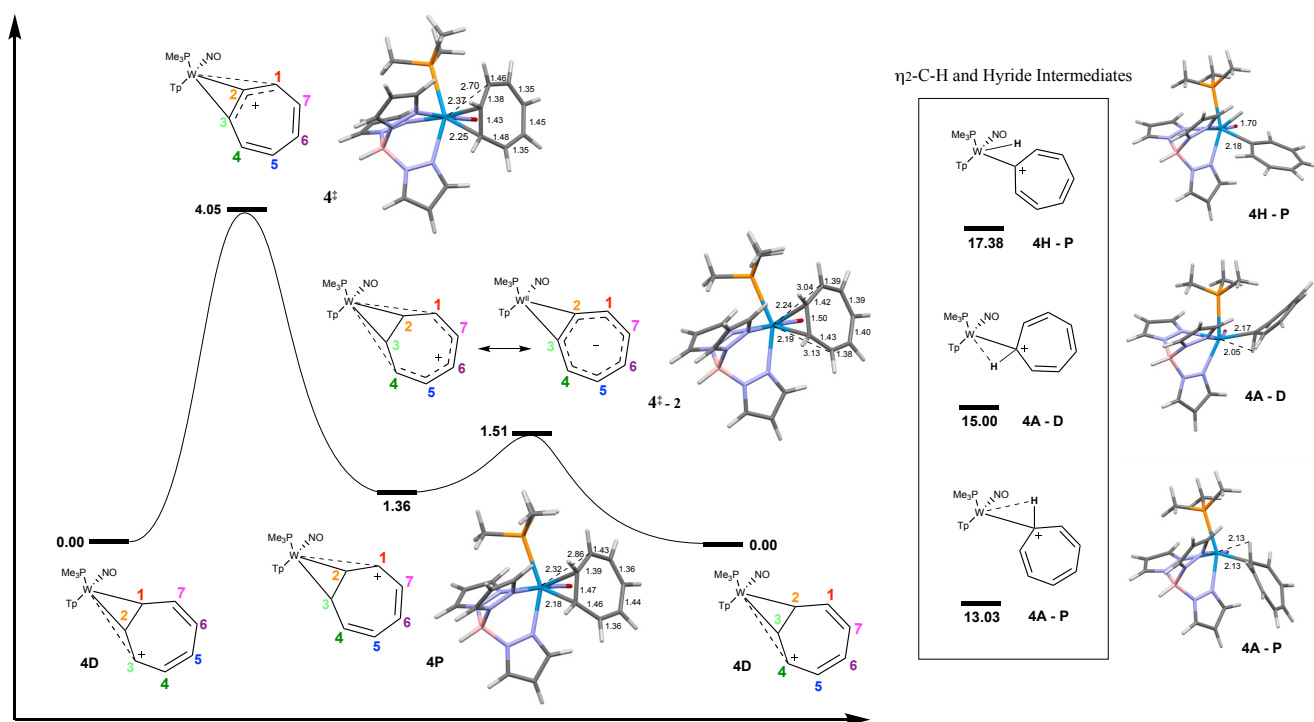


\*Mechanistic studies were performed with the conformation resembling the SC-XRD structure, although a lower energy minimum was identified in solution through DFT analysis, named compound **2B**.

## Reaction Mechanism of tungsten-alkene isomerization for $\eta^2$ -Cp.



## Reaction Mechanism of tungsten-alkene isomerization for $\eta^2$ -Tropylum.



Energy values of optimized minima and transition state structures.

Structure	Electronic Energy (Hartree)	Relative Free Energy (kcal/mol)
<b>2</b>	-1669.909974	0.00
<b>2<sup>‡</sup></b>	-1669.883334	+16.72
<b>2H - D</b>	-1669.867919	+27.71
<b>2H - P</b>	-1669.882783	+17.06
<b>2B</b>	-1669.912079	-1.32
<b>3</b>	-1553.774705	0.00
<b>3<sup>‡</sup></b>	-1553.763299	+7.16
<b>3A - D</b>	-1553.754627	+12.60
<b>3A - P</b>	-1553.758907	+9.91
<b>4D</b>	-1631.116013	0.00
<b>4P</b>	-1631.113800	+1.36
<b>4<sup>‡</sup></b>	-1631.109536	+4.05
<b>4<sup>‡</sup> - 2</b>	-1631.113580	+1.51
<b>4H - P</b>	-1631.088290	+17.38
<b>4A - D</b>	-1631.092080	+15.00
<b>4A - P</b>	-1631.095218	+13.03

**Compound 2** Electronic Energy: -1669.909974 Hartree

W	-0.269900	0.000800	-0.080800
O	-1.904000	0.345800	-2.519700
N	-1.267800	0.196200	-1.506100
P	0.038500	-2.533100	-0.175300
C	-0.497600	-3.574800	1.235600
H	-1.562100	-3.473500	1.449000
H	-0.280900	-4.620300	0.998100
H	0.071400	-3.292100	2.124900
C	-0.698000	-3.361700	-1.627900
H	-0.286500	-2.922100	-2.540000
H	-0.480400	-4.433300	-1.611300
H	-1.780000	-3.205200	-1.621500
C	1.808900	-3.012500	-0.243900
H	2.340900	-2.536000	0.585900
H	1.893300	-4.098600	-0.146700
H	2.264500	-2.700600	-1.185500
N	1.209400	-0.227000	1.679300
N	2.474400	0.228400	1.574600
N	2.802500	0.189700	-0.934100
N	1.578600	-0.170300	-1.363100
N	1.969500	2.245600	0.155500
N	0.651900	2.071300	-0.097000
C	1.106500	-0.806300	2.880100
H	0.170300	-1.240900	3.202800
C	2.325200	-0.731700	3.562600
H	2.556600	-1.105400	4.547800
C	3.166500	-0.059800	2.690400
H	4.200600	0.239000	2.784300
C	1.710400	-0.621200	-2.612700
H	0.841500	-0.963600	-3.159000
C	3.054400	-0.566200	-3.001300
H	3.483600	-0.860900	-3.946200
C	3.710100	-0.032900	-1.902100
H	4.749400	0.218100	-1.745000
C	0.168800	3.255300	-0.481000
H	-0.874700	3.353800	-0.744500
C	1.181000	4.221700	-0.464500
H	1.100200	5.268500	-0.712500
C	2.309300	3.530200	-0.058800
H	3.329800	3.854000	0.087400
B	2.930300	1.044100	0.351700
H	4.054900	1.421400	0.497200
C	-1.986300	-0.593300	1.217200
H	-1.625400	-1.216500	2.036900
C	-1.708500	0.805400	1.408200
H	-1.097300	0.980000	2.296800
C	-2.397100	2.036000	1.028900
H	-1.787400	2.905300	1.273600

C	-3.593400	2.359900	0.481300
H	-3.744700	3.432100	0.365400
C	-4.750500	1.598000	0.054700
H	-5.600000	2.244800	-0.161600
C	-5.006600	0.284100	-0.161100
H	-6.018600	0.094500	-0.516900
C	-4.235500	-0.942400	-0.073200
H	-4.757700	-1.779300	-0.535000
C	-3.048600	-1.287900	0.477100
H	-2.827900	-2.348500	0.360800

**Compound 2<sup>‡</sup>** Electronic Energy: -1669.883334 Hartree

W	-0.315900	0.161400	0.070800
O	-1.936800	0.601300	-2.340600
N	-1.356100	0.471100	-1.303600
P	-0.412900	-2.387800	-0.335900
C	-1.023000	-3.610400	0.886600
H	-2.101900	-3.524800	1.023200
H	-0.795000	-4.609400	0.504400
H	-0.519500	-3.475200	1.847000
C	-1.385100	-2.807600	-1.822300
H	-0.953500	-2.330700	-2.704400
H	-1.397700	-3.891300	-1.967400
H	-2.406200	-2.441400	-1.684200
C	1.257400	-3.081400	-0.654000
H	1.904000	-2.869100	0.204300
H	1.173600	-4.164800	-0.775800
H	1.703100	-2.657600	-1.555300
N	1.295600	-0.516800	1.579700
N	2.608000	-0.344500	1.336800
N	2.608700	-0.125600	-1.178600
N	1.291100	-0.166500	-1.455000
N	2.354900	1.887600	0.208900
N	1.010300	2.003300	0.100700
C	1.197900	-1.302000	2.658100
H	0.225200	-1.582400	3.041200
C	2.472000	-1.644000	3.122700
H	2.724900	-2.255400	3.974800
C	3.340000	-1.007700	2.248100
H	4.419500	-0.973100	2.212600
C	1.163600	-0.423600	-2.760600
H	0.180500	-0.477200	-3.209000
C	2.426700	-0.573800	-3.341200
H	2.659500	-0.790100	-4.372100
C	3.315500	-0.362500	-2.297200
H	4.395800	-0.346800	-2.273300
C	0.742300	3.306300	-0.023700
H	-0.279800	3.638000	-0.128400
C	1.923900	4.051700	0.009400

H	2.032400	5.122500	-0.062600
C	2.923500	3.104700	0.156300
H	3.997300	3.205600	0.222500
B	3.073400	0.516600	0.151900
H	4.259900	0.653500	0.166500
C	-1.687800	0.426500	1.887000
H	-1.016500	0.252200	2.723700
C	-1.633900	1.752500	1.378900
H	-0.893800	2.343000	1.916600
C	-2.540700	2.573600	0.629300
H	-2.235800	3.617400	0.598900
C	-3.727700	2.310600	-0.025900
H	-4.168800	3.213800	-0.451100
C	-4.516200	1.169800	-0.290500
H	-5.414900	1.409900	-0.856600
C	-4.374900	-0.202800	-0.062400
H	-5.183200	-0.777400	-0.518800
C	-3.478300	-1.023800	0.618500
H	-3.708000	-2.085900	0.556200
C	-2.329400	-0.750200	1.406600
H	-1.985800	-1.615400	1.968100

**Compound 2H – D** Electronic Energy: -1669.867919 Hartree

W	-0.049300	0.278800	-0.386200
O	-0.607000	0.299500	-3.283600
N	-0.417800	0.327100	-2.093300
H	-0.920600	1.683200	-0.101400
P	-0.413400	-2.312600	-0.140200
C	-1.782100	-2.958400	0.891200
H	-2.748900	-2.641500	0.495000
H	-1.732400	-4.051000	0.894400
H	-1.683000	-2.591500	1.915100
C	-0.627300	-3.244700	-1.704000
H	0.261900	-3.133100	-2.327500
H	-0.773200	-4.305900	-1.482300
H	-1.491900	-2.870000	-2.256900
C	1.042000	-3.139200	0.612800
H	1.262300	-2.694200	1.587400
H	0.825000	-4.203200	0.745100
H	1.914100	-3.030800	-0.036700
N	0.755300	-0.035600	1.795200
N	2.073500	0.101300	2.055500
N	3.102800	-0.418600	-0.178500
N	1.994200	-0.570300	-0.924000
N	2.562600	1.927700	0.395200
N	1.375000	2.021700	-0.240500
C	0.200200	-0.541700	2.902800
H	-0.858700	-0.750400	2.934000
C	1.167600	-0.733400	3.893800

H	1.026700	-1.117200	4.892200
C	2.347800	-0.308300	3.305900
H	3.358800	-0.263900	3.684800
C	2.345100	-1.237500	-2.026600
H	1.607700	-1.444900	-2.790400
C	3.709700	-1.546200	-1.984900
H	4.290800	-2.080900	-2.720000
C	4.152300	-0.992300	-0.792800
H	5.136200	-0.952000	-0.347700
C	1.257200	3.280600	-0.669600
H	0.366900	3.587600	-1.200300
C	2.390100	4.019300	-0.314500
H	2.593600	5.058900	-0.518600
C	3.191600	3.115800	0.364300
H	4.161600	3.229700	0.826700
B	3.071400	0.592300	0.989500
H	4.159000	0.728300	1.466200
C	-2.191300	0.099600	0.210200
C	-2.695900	0.384800	1.423800
H	-2.027100	0.771700	2.195400
C	-4.087700	0.186900	1.890900
H	-4.210600	-0.445200	2.772800
C	-5.178100	0.801400	1.413900
H	-6.128500	0.643200	1.923900
C	-5.204700	1.757600	0.293800
H	-5.733000	2.692700	0.479900
C	-4.724600	1.540900	-0.939900
H	-4.889800	2.311900	-1.692600
C	-4.116100	0.289000	-1.421100
H	-4.549300	-0.110500	-2.338900
C	-3.069900	-0.363200	-0.889700
H	-2.743300	-1.256800	-1.424000

**Compound 2H - P** Electronic Energy: -1669.882783 Hartree

W	0.031300	-0.364100	-0.469300
O	-0.208800	-1.359300	-3.245600
N	-0.109700	-0.945700	-2.116700
H	-0.961200	-1.563100	0.192600
P	1.260200	-2.441400	0.307000
C	0.355800	-3.596800	1.394500
H	-0.532700	-3.959300	0.871800
H	0.998400	-4.441900	1.657300
H	0.045300	-3.083500	2.307200
C	1.814600	-3.543400	-1.040600
H	2.507500	-3.021400	-1.703100
H	2.310200	-4.424600	-0.623500
H	0.940700	-3.856500	-1.618400
C	2.774800	-2.093900	1.277100
H	2.514700	-1.460100	2.130900



H	3.202600	-3.032100	1.642000
H	3.513300	-1.576400	0.660100
N	0.348900	0.286700	1.703300
N	1.188200	1.290600	2.025800
N	2.762000	1.235700	0.052300
N	2.196800	0.285200	-0.716200
N	0.771100	2.707700	-0.008900
N	-0.033000	1.900900	-0.735600
C	-0.108700	-0.223000	2.850500
H	-0.821700	-1.036000	2.834300
C	0.447800	0.457900	3.938400
H	0.273900	0.284300	4.988800
C	1.266800	1.417000	3.361700
H	1.892600	2.179500	3.803000
C	3.131600	-0.142500	-1.568500
H	2.892300	-0.903300	-2.298700
C	4.335700	0.532600	-1.338800
H	5.273400	0.410600	-1.858100
C	4.047400	1.408200	-0.303200
H	4.656900	2.149100	0.194000
C	-0.792000	2.687800	-1.500600
H	-1.529700	2.248900	-2.157700
C	-0.478000	4.031700	-1.271700
H	-0.914800	4.902200	-1.735600
C	0.523100	3.993800	-0.314400
H	1.078400	4.785000	0.168600
B	1.864600	2.139500	0.931500
H	2.503400	3.023000	1.421500
C	-2.116400	0.113800	-0.370800
C	-2.960200	-0.115000	-1.394700
H	-2.568600	-0.592200	-2.296700
C	-4.388400	0.257300	-1.486400
H	-4.683100	0.797100	-2.388200
C	-5.366900	-0.111900	-0.647000
H	-6.392800	0.149500	-0.907800
C	-5.215200	-0.931400	0.568600
H	-5.900900	-1.774500	0.655900
C	-4.393800	-0.681000	1.598900
H	-4.456600	-1.332800	2.470700
C	-3.497800	0.483100	1.717900
H	-3.598900	1.060700	2.637700
C	-2.552900	0.848500	0.839700
H	-1.949200	1.723600	1.092500

**Compound 2B** Electronic Energy-1669.912079 Hartree

W	-0.282100	0.040000	-0.020200
O	-1.796900	0.190100	-2.545400
N	-1.274900	0.198100	-1.452800
P	-0.458900	-2.478300	-0.101500

C	-1.057300	-3.429200	1.343900
H	-2.082000	-3.149200	1.591500
H	-1.025600	-4.496200	1.105300
H	-0.413700	-3.241300	2.206900
C	-1.539300	-3.067600	-1.451100
H	-1.219400	-2.621500	-2.396200
H	-1.513100	-4.158100	-1.527600
H	-2.561600	-2.736900	-1.243800
C	1.147100	-3.316500	-0.397300
H	1.866300	-2.977500	0.355800
H	1.020800	-4.399500	-0.312600
H	1.536300	-3.076500	-1.388300
N	1.323400	-0.373500	1.604300
N	2.614400	-0.043200	1.392600
N	2.725900	-0.118400	-1.125300
N	1.437300	-0.373300	-1.414100
N	2.219900	2.022600	0.017200
N	0.873400	1.998500	-0.092400
C	1.271200	-0.971500	2.799400
H	0.329600	-1.323000	3.197500
C	2.546500	-1.034000	3.370300
H	2.825700	-1.453800	4.324000
C	3.370000	-0.427400	2.435800
H	4.433600	-0.236500	2.439100
C	1.392300	-0.840700	-2.663500
H	0.438600	-1.095500	-3.108400
C	2.686500	-0.907000	-3.194600
H	2.984700	-1.246200	-4.174400
C	3.501300	-0.426000	-2.180900
H	4.569400	-0.267500	-2.139300
C	0.473500	3.258200	-0.274700
H	-0.579700	3.477700	-0.382100
C	1.576300	4.120900	-0.280600
H	1.578300	5.192600	-0.404500
C	2.665900	3.287500	-0.091500
H	3.723700	3.499300	-0.028500
B	3.055100	0.722400	0.129200
H	4.223000	0.973500	0.179500
C	-4.198000	-0.379400	0.298600
H	-5.089600	-1.007100	0.288800
C	-3.246100	-0.756900	1.173300
H	-3.526300	-1.622600	1.774200
C	-1.884800	-0.270400	1.494500
H	-1.482700	-0.850800	2.324100
C	-1.439500	1.110900	1.508300
H	-0.710100	1.279800	2.303200
C	-2.243700	2.336100	1.315000
H	-1.932800	3.136900	1.987500
C	-3.230900	2.688700	0.469200
H	-3.575000	3.719400	0.556400

C	-3.839800	1.956800	-0.642700
H	-4.042700	2.574300	-1.518300
C	-4.226700	0.674800	-0.719500
H	-4.702500	0.370400	-1.651400

**Compound 3** Electronic Energy: -1553.774705 Hartree

O	-1.782400	-1.327200	2.517700
N	-1.224000	-0.987700	1.529900
W	-0.417700	-0.413800	0.081600
N	1.469700	-1.553300	0.184800
N	2.661700	-0.967800	-0.061000
N	0.678500	0.545200	-1.688500
N	1.967700	0.922800	-1.546200
N	0.893600	0.816100	1.354700
N	2.118700	1.217400	0.955900
C	3.640700	-1.880000	0.042100
C	3.072200	-3.104700	0.361000
C	1.703700	-2.845200	0.444800
C	2.393600	1.553600	-2.652200
C	1.346600	1.597000	-3.558700
C	0.295100	0.948700	-2.907100
C	2.706300	1.915300	1.940200
C	1.833800	1.981100	3.018100
C	0.713400	1.259900	2.605700
B	2.771600	0.562500	-0.286800
H	3.910200	0.900100	-0.397000
H	4.670400	-1.591400	-0.113000
H	3.576500	-4.045700	0.515000
H	0.883800	-3.510600	0.675500
H	3.409000	1.917700	-2.715300
H	1.345800	2.025900	-4.548400
H	-0.703500	0.756400	-3.270500
H	3.708400	2.298800	1.811700
H	1.993300	2.468800	3.966900
H	-0.203000	1.038800	3.135800
C	-0.498900	3.244700	0.098900
H	-1.077900	4.167300	0.003400
H	0.092100	3.284500	1.016100
H	0.169800	3.147200	-0.762100
C	-2.704900	2.058900	1.593700
H	-2.113800	1.986100	2.507900
H	-3.182900	3.041300	1.549100
H	-3.471600	1.279100	1.600900
P	-1.650500	1.827800	0.126100
C	-2.776200	2.214600	-1.256300
H	-3.176500	3.219600	-1.095500
H	-2.231100	2.193600	-2.202500
H	-3.601700	1.500800	-1.289900
C	-3.209300	-1.314200	-0.632000

C	-2.089200	-0.893300	-1.449200
C	-1.166500	-1.991500	-1.471500
C	-1.700500	-2.988800	-0.615200
C	-2.979100	-2.591600	-0.152600
H	-2.173500	-0.135500	-2.215900
H	-0.335900	-2.122300	-2.155600
H	-3.594600	-3.137400	0.549600
H	-4.067500	-0.689900	-0.404800
H	-1.200600	-3.917900	-0.362600

**Compound 3<sup>‡</sup>** Electronic Energy: -1553.763299 Hartree

W	-0.427300	0.430500	0.000800
O	-1.681600	1.524500	-2.409000
N	-1.171200	1.113400	-1.426200
P	-1.706300	-1.787800	-0.315800
C	-0.551300	-3.202600	-0.394500
H	-1.137000	-4.122500	-0.472400
H	0.106000	-3.122600	-1.262000
H	0.050600	-3.235300	0.518700
C	-2.667500	-1.844800	-1.862000
H	-2.012600	-1.738600	-2.728500
H	-3.193800	-2.801400	-1.924200
H	-3.393400	-1.026900	-1.855300
C	-2.922300	-2.337800	0.933100
H	-3.110800	-3.403200	0.772600
H	-2.551300	-2.186000	1.948000
H	-3.858700	-1.793600	0.797700
B	2.766500	-0.611600	0.300200
H	3.903100	-0.963400	0.382200
N	1.491900	1.549300	-0.040900
N	2.667600	0.933700	0.214900
N	0.649200	-0.781800	1.644300
N	1.946400	-1.119500	1.494500
N	0.893300	-0.682600	-1.364700
N	2.117600	-1.126600	-1.010600
C	1.756100	2.841200	-0.265400
H	0.952100	3.529500	-0.487000
C	3.127500	3.072100	-0.148800
H	3.651500	4.007300	-0.267600
C	3.665900	1.829600	0.151200
H	4.687000	1.517100	0.316100
C	0.209700	-1.419900	2.737000
H	-0.813600	-1.308700	3.067000
C	1.236000	-2.181100	3.300500
H	1.193500	-2.797900	4.184400
C	2.325500	-1.957100	2.473100
H	3.339900	-2.327300	2.512100
C	0.723300	-0.970700	-2.662800
H	-0.187500	-0.687100	-3.171800

C	1.847400	-1.634700	-3.152100
H	2.013700	-2.002700	-4.152200
C	2.713000	-1.697900	-2.068500
H	3.715600	-2.091400	-1.980400
C	-1.581200	1.316700	1.837700
H	-1.157200	0.802500	2.688500
C	-1.083300	2.503200	1.247000
H	-0.211800	3.044200	1.591700
C	-2.136300	3.042900	0.405400
H	-2.067700	3.971500	-0.148600
C	-3.165000	2.137700	0.360800
H	-4.061600	2.203200	-0.242000
C	-2.789900	1.001800	1.170400
H	-3.427100	0.161700	1.408600

**Compound 3A – D** Electronic Energy: -1553.754627 Hartree

W	0.034200	0.121400	0.596400
O	-0.338400	2.577000	2.175200
N	-0.204400	1.538400	1.602400
C	-5.176000	-0.436300	0.494200
H	-6.192300	-0.069700	0.375400
C	-4.861800	-1.602300	-0.110900
H	-5.646200	-2.101300	-0.674000
C	-3.599500	-2.314300	-0.039400
H	-3.631200	-3.331700	-0.423200
C	-2.402900	-1.909400	0.438700
H	-1.614700	-2.660300	0.426100
C	-4.319100	0.378000	1.337600
H	-4.832800	1.179800	1.863000
C	-2.988700	0.299700	1.558100
H	-2.582000	1.031100	2.254600
C	-1.967800	-0.605900	0.985400
P	-1.216100	1.279000	-1.285900
C	-0.202600	1.544900	-2.783300
H	-0.852400	1.905500	-3.585400
H	0.586100	2.276400	-2.602800
C	-2.711300	0.494900	-1.976100
H	-2.484500	-0.486800	-2.393800
H	-3.474700	0.399000	-1.204600
C	-1.834600	2.920300	-0.791300
H	-2.345400	3.388300	-1.637200
H	-2.541300	2.790100	0.033900
H	-3.086300	1.142600	-2.774000
H	0.249200	0.594200	-3.083400
H	-1.016400	3.561600	-0.459500
N	0.511600	-1.420000	-1.070200
N	1.793300	-1.598500	-1.461300
N	2.752400	0.649400	-0.932400
N	1.670500	1.241800	-0.387200

N	2.897400	-1.164900	0.755700
N	1.848600	-0.765800	1.506600
C	-0.244600	-2.130000	-1.918700
H	-1.317500	-2.160200	-1.801900
C	0.553100	-2.770200	-2.868900
H	0.235100	-3.413700	-3.674000
C	1.846400	-2.400400	-2.536400
H	2.797900	-2.649600	-2.984000
C	3.127300	2.833000	-0.987800
H	3.583200	3.796500	-1.153300
C	3.644300	1.583700	-1.298800
H	4.586700	1.292800	-1.740500
C	2.118800	-1.085400	2.777700
H	1.406700	-0.852300	3.557600
C	3.367700	-1.704200	2.854900
H	3.870100	-2.074200	3.734700
C	3.826100	-1.726800	1.545100
H	4.749200	-2.095000	1.120700
B	2.957200	-0.874700	-0.766500
H	4.005900	-1.217100	-1.221800
C	1.890400	2.562200	-0.400800
H	1.156600	3.242800	0.008700
H	-1.259400	-0.853800	1.852200

**Compound 3A – P** Electronic Energy: -1553.758907 Hartree

W	0.050800	-0.591500	-0.201000
O	0.232800	-2.112600	-2.714200
N	0.140400	-1.516500	-1.695600
C	-2.543400	-1.177100	1.519600
H	-2.314700	-0.495200	2.329600
C	-2.316000	-2.679200	-0.263200
H	-1.874300	-3.318200	-1.019400
C	-1.536600	-1.801500	0.634100
H	-0.663900	-2.294800	1.153900
C	-3.775100	-1.545800	1.092100
C	-3.634500	-2.484400	-0.021400
H	-4.721800	-1.205400	1.496200
H	-4.461200	-2.934500	-0.559400
P	2.489800	-1.182600	0.382200
C	3.440500	0.250100	0.981400
H	4.442400	-0.076700	1.273500
H	3.518600	0.999100	0.188700
C	2.582500	-2.424700	1.715300
H	2.112700	-2.040300	2.622300
H	2.066900	-3.334000	1.396500
C	3.467000	-1.916900	-0.966400
H	4.456700	-2.187800	-0.588400
H	2.955500	-2.813300	-1.326700
H	3.632200	-2.654200	1.919900

H	2.930400	0.687700	1.843800
H	3.578100	-1.209800	-1.790200
N	0.070100	0.665900	1.676600
N	-0.133700	1.996700	1.641500
N	0.778700	2.426100	-0.655800
N	0.997600	1.170400	-1.101100
N	-1.636400	2.036200	-0.370800
N	-1.598200	0.743900	-0.764600
C	0.265000	0.330900	2.957200
H	0.434800	-0.702100	3.228900
C	0.188300	1.466900	3.766400
H	0.300000	1.526100	4.837600
C	-0.067000	2.505200	2.882000
H	-0.206300	3.564100	3.046700
C	2.285000	2.572700	-2.276700
H	2.994300	2.961200	-2.990300
C	1.536900	3.287000	-1.348200
H	1.483400	4.346600	-1.142800
C	-2.716400	0.497200	-1.453700
H	-2.896100	-0.490700	-1.854800
C	-3.503400	1.649800	-1.502600
H	-4.461300	1.775600	-1.982400
C	-2.773500	2.601800	-0.806700
H	-2.976000	3.642800	-0.598800
B	-0.410000	2.702000	0.301800
H	-0.580400	3.872100	0.456700
C	1.899300	1.246700	-2.091500
H	2.211800	0.352200	-2.612800

**Compound 4D** Electronic Energy: -1631.116013 Hartree

W	-0.367000	0.164300	-0.017500
O	-2.113700	0.831200	-2.293400
N	-1.397000	0.588200	-1.376700
P	-0.739500	-2.339500	-0.327700
C	0.825000	-3.263000	-0.554100
H	0.605600	-4.334000	-0.561600
H	1.317600	-2.992100	-1.489100
C	-1.519200	-3.328900	0.997600
H	-0.954000	-3.227500	1.927200
H	-2.553300	-3.024000	1.163100
C	-1.766600	-2.729100	-1.783300
H	-1.899600	-3.810800	-1.870200
H	-2.741200	-2.247400	-1.661400
H	-1.506000	-4.377200	0.686800
H	1.492700	-3.038900	0.284300
H	-1.293600	-2.347400	-2.690400
N	1.052100	-0.555400	1.631600
N	2.385900	-0.428900	1.471000
N	2.552800	-0.379700	-1.046900

N	1.252600	-0.395200	-1.403100
N	2.352500	1.742700	0.198600
N	1.026200	1.931100	0.005200
C	0.864500	-1.204100	2.787800
H	-0.132700	-1.418400	3.145900
C	2.092600	-1.504900	3.381300
H	2.268300	-2.017000	4.314300
C	3.034200	-0.988800	2.505200
H	4.113900	-0.973600	2.545200
C	2.483300	-0.939400	-3.191200
H	2.769500	-1.220400	-4.192600
C	3.314400	-0.698900	-2.106700
H	4.391200	-0.714100	-2.017500
C	0.850200	3.229800	-0.259600
H	-0.137600	3.617000	-0.468600
C	2.074600	3.900800	-0.223500
H	2.257800	4.951000	-0.387500
C	3.001100	2.912000	0.065900
H	4.074700	2.953200	0.180500
B	2.975500	0.323200	0.268800
H	4.164400	0.386200	0.350900
C	1.194500	-0.720300	-2.699500
H	0.239500	-0.785200	-3.203200
C	-1.576900	1.041500	1.782900
H	-0.906300	1.065000	2.638300
C	-1.826000	2.248500	1.162900
H	-1.229200	3.077500	1.539000
C	-2.848700	2.632300	0.220100
H	-2.791500	3.660100	-0.125500
C	-3.887900	1.876200	-0.209700
H	-4.611000	2.368200	-0.855600
C	-2.068100	-0.262900	1.341600
H	-1.863100	-1.034200	2.078500
C	-3.432600	-0.393700	0.790700
H	-3.894300	-1.364900	0.963200
C	-4.193200	0.500000	0.120300
H	-5.168800	0.153900	-0.209500

**Compound 4P** Electronic Energy: -1631.113800 Hartree

W	-0.392900	0.041300	-0.046400
O	-2.046600	0.698700	-2.394000
N	-1.404400	0.407100	-1.434700
C	-1.488300	1.166700	1.468500
H	-0.795000	1.377900	2.281600
C	-2.350000	2.313900	1.176000
H	-2.030100	3.243600	1.643700
C	-3.471600	2.389500	0.415700
H	-3.924700	3.370600	0.307800
C	-4.149500	1.318700	-0.262000



H	-4.965600	1.626600	-0.911900
C	-2.052100	-0.187700	1.565100
H	-1.722000	-0.846600	2.362700
C	-3.046100	-0.690400	0.734600
H	-3.255600	-1.752500	0.853900
C	-3.949600	-0.024700	-0.151500
H	-4.591800	-0.677000	-0.734700
P	-0.455200	-2.525800	-0.172200
C	1.210600	-3.236900	-0.435100
H	1.159900	-4.321000	-0.300500
H	1.577500	-3.016500	-1.438800
C	-0.984100	-3.472700	1.302900
H	-0.245400	-3.339400	2.096600
H	-1.964900	-3.168100	1.671000
C	-1.475900	-3.189700	-1.529700
H	-1.386100	-4.278400	-1.578000
H	-2.520700	-2.914700	-1.359800
H	-1.020700	-4.532300	1.033500
H	1.900500	-2.812800	0.301400
H	-1.144900	-2.752000	-2.475100
N	1.145200	-0.370900	1.619900
N	2.437000	-0.012500	1.453700
N	2.607700	-0.058900	-1.058800
N	1.327200	-0.307600	-1.391900
N	2.051300	2.054700	0.080600
N	0.717600	1.984200	-0.111900
C	1.065900	-0.968900	2.815700
H	0.122300	-1.342700	3.186800
C	2.320300	-1.003200	3.428800
H	2.575000	-1.417300	4.391800
C	3.162500	-0.379400	2.522300
H	4.221000	-0.165900	2.561800
C	2.627700	-0.827800	-3.136800
H	2.955000	-1.158900	-4.109900
C	3.411500	-0.358300	-2.092500
H	4.478100	-0.202100	-2.016300
C	0.289200	3.218000	-0.386800
H	-0.758200	3.397500	-0.587600
C	1.363600	4.113500	-0.362800
H	1.341300	5.177200	-0.540700
C	2.464100	3.326400	-0.065400
H	3.509800	3.574700	0.046600
B	2.905900	0.770000	0.214000
H	4.067700	1.032000	0.293600
C	1.319900	-0.764700	-2.648900
H	0.386200	-1.035000	-3.125000

**Compound 4<sup>‡</sup>** Electronic Energy: -1631.109536 Hartree

W	0.374600	0.175300	-0.013100
O	2.059300	0.881500	2.294000
N	1.385400	0.613500	1.354700
P	0.792900	-2.366500	0.319900
C	1.712000	-2.740100	1.851400
H	1.181300	-2.357300	2.724600
H	1.837800	-3.821800	1.951500
H	2.694300	-2.262400	1.795100
C	-0.810600	-3.238100	0.487700
H	-0.617800	-4.310000	0.585600
H	-1.358300	-2.892300	1.366100
H	-1.413800	-3.062500	-0.408900
C	1.648400	-3.434500	-0.898700
H	1.306200	-3.229700	-1.915300
H	2.728300	-3.284300	-0.837300
H	1.428600	-4.476500	-0.649900
B	-2.990900	0.343500	-0.249100
H	-4.180700	0.402000	-0.320100
N	-2.410700	-0.425000	-1.448200
N	-1.079100	-0.564500	-1.621100
N	-2.545600	-0.350700	1.063500
N	-1.239900	-0.334200	1.397400
N	-2.363300	1.755700	-0.185100
N	-1.038100	1.925100	0.013300
C	-0.912800	-1.339000	-2.702400
H	0.076800	-1.610300	-3.042000
C	-2.150500	-1.699500	-3.238100
H	-2.343600	-2.307000	-4.108200
C	-3.076400	-1.092900	-2.403200
H	-4.156900	-1.086000	-2.421500
C	-1.153400	-0.652600	2.694400
H	-0.190900	-0.682100	3.186200
C	-2.427900	-0.903900	3.206800
H	-2.690600	-1.189300	4.213300
C	-3.282200	-0.686700	2.134900
H	-4.359500	-0.731000	2.062700
C	-0.834500	3.227200	0.227600
H	0.162900	3.599300	0.416100
C	-2.046800	3.920400	0.162800
H	-2.210500	4.978800	0.291400
C	-2.991300	2.941500	-0.098600
H	-4.062900	2.999000	-0.224200
C	1.377400	1.690000	-1.341900
H	0.635100	2.168800	-1.975500
C	2.333500	2.649600	-0.744300
H	2.062200	3.694200	-0.884000
C	3.492500	2.412700	-0.096700
H	4.040000	3.282400	0.256100

C	4.116100	1.131700	0.193900
H	4.988300	1.177300	0.841300
C	3.767200	-0.090700	-0.263700
H	4.359900	-0.942600	0.057900
C	2.720600	-0.408600	-1.223900
H	2.811600	-1.390100	-1.676900
C	1.825700	0.431500	-1.863500
H	1.334500	0.045600	-2.750500

**Compound 4<sup>‡</sup> - 2** Electronic Energy: -1631.113580 Hartree

W	-0.377300	0.075000	-0.044300
O	-2.157900	0.786900	-2.287900
N	-1.432300	0.477800	-1.388200
C	-1.484900	1.140500	1.521700
H	-0.822600	1.284300	2.373000
C	-2.197900	2.319100	1.153200
H	-1.785600	3.234700	1.576200
C	-3.290700	2.502300	0.329100
H	-3.575900	3.530000	0.128500
C	-4.115900	1.511200	-0.226500
H	-4.937200	1.883800	-0.835200
C	-2.033600	-0.246800	1.431000
H	-1.763100	-0.913500	2.245100
C	-3.232700	-0.601900	0.765900
H	-3.532100	-1.640000	0.907200
C	-4.100800	0.131400	-0.036000
H	-4.900700	-0.429500	-0.507900
P	-0.552200	-2.472000	-0.212900
C	1.077500	-3.271300	-0.455500
H	0.959600	-4.355900	-0.383400
H	1.498600	-3.019800	-1.430200
C	-1.177700	-3.438700	1.210500
H	-1.173200	-4.497100	0.934600
H	-0.515300	-3.297000	2.067600
C	-1.578400	-3.042700	-1.609100
H	-1.587000	-4.134900	-1.660300
H	-2.598800	-2.672600	-1.473000
H	-2.192500	-3.152800	1.490400
H	1.760400	-2.929600	0.329100
H	-1.178500	-2.635600	-2.541100
N	1.131500	-0.427300	1.623900
N	2.440800	-0.142100	1.459300
N	2.611200	-0.169700	-1.057400
N	1.321900	-0.349600	-1.402700
N	2.165100	1.960300	0.109500
N	0.827700	1.974100	-0.077500
C	1.017200	-1.029700	2.813700
H	0.052000	-1.350300	3.180000
C	2.268300	-1.141800	3.425800

H	2.499200	-1.578400	4.384800
C	3.144900	-0.559500	2.524400
H	4.213900	-0.406800	2.565200
C	2.608000	-0.893700	-3.151900
H	2.924900	-1.217900	-4.130700
C	3.406600	-0.485100	-2.093800
H	4.478800	-0.381100	-2.008900
C	0.480000	3.234400	-0.346700
H	-0.552700	3.483400	-0.549800
C	1.608300	4.060600	-0.323500
H	1.652600	5.124400	-0.497000
C	2.657300	3.203800	-0.033400
H	3.716900	3.385200	0.075900
B	2.947600	0.627500	0.227000
H	4.121900	0.827700	0.308600
C	1.301300	-0.778100	-2.668900
H	0.358500	-0.989300	-3.156500

**Compound 4H – P** Electronic Energy: -1631.088290 Hartree

W	0.011600	-0.472600	-0.324500
O	-0.262800	-2.038900	-2.818800
N	-0.149200	-1.378600	-1.822700
C	-5.204900	0.145200	0.840800
H	-6.115200	0.533200	1.288500
C	-5.347400	-0.909500	-0.038600
H	-6.359300	-1.263600	-0.214000
C	-4.332100	-1.580300	-0.736700
H	-4.674700	-2.379300	-1.389800
C	-2.958200	-1.396700	-0.708300
H	-2.415100	-2.097100	-1.339800
C	-4.015900	0.793500	1.205600
H	-4.140700	1.629000	1.890200
C	-2.707200	0.543200	0.820100
H	-1.992100	1.244200	1.246100
C	-2.150100	-0.458100	-0.016900
P	1.577500	-2.216800	0.627500
C	3.072600	-1.502500	1.402400
H	3.667700	-2.303000	1.851100
H	3.674800	-0.976400	0.658400
C	0.931800	-3.310800	1.937500
H	0.616100	-2.715800	2.797300
H	0.072800	-3.865200	1.551700
C	2.198400	-3.406800	-0.608500
H	2.846300	-4.142000	-0.123100
H	1.345300	-3.916100	-1.064900
H	1.711200	-4.011100	2.250300
H	2.768000	-0.797100	2.181500
H	2.760000	-2.890100	-1.388800
N	0.338700	0.583300	1.659400

N	0.959100	1.777800	1.730000
N	2.391600	1.642000	-0.340700
N	1.992900	0.466000	-0.866700
N	0.146100	2.685900	-0.468700
N	-0.515100	1.618300	-0.966400
C	0.053600	0.214400	2.913300
H	-0.467000	-0.715800	3.097700
C	0.502400	1.184800	3.813700
H	0.420500	1.179600	4.889300
C	1.072200	2.163200	3.011900
H	1.544900	3.102600	3.260500
C	4.003100	0.984100	-1.711600
H	4.918800	0.940700	-2.280100
C	3.595400	1.978200	-0.835000
H	4.067500	2.904100	-0.539100
C	-1.464100	2.084700	-1.782700
H	-2.127500	1.396600	-2.289900
C	-1.420800	3.481100	-1.820100
H	-2.051600	4.148500	-2.386100
C	-0.378600	3.817300	-0.969500
H	0.030400	4.777400	-0.689400
B	1.388300	2.517800	0.447000
H	1.865700	3.579800	0.712600
C	2.952100	0.061900	-1.704700
H	2.837200	-0.861700	-2.255300
H	-0.726600	-1.641000	0.658900

**Compound 4A – D** Electronic Energy: -1631.092080 Hartree

W	0.034200	0.121400	0.596400
O	-0.338400	2.577000	2.175200
N	-0.204400	1.538400	1.602400
C	-5.176000	-0.436300	0.494200
H	-6.192300	-0.069700	0.375400
C	-4.861800	-1.602300	-0.110900
H	-5.646200	-2.101300	-0.674000
C	-3.599500	-2.314300	-0.039400
H	-3.631200	-3.331700	-0.423200
C	-2.402900	-1.909400	0.438700
H	-1.614700	-2.660300	0.426100
C	-4.319100	0.378000	1.337600
H	-4.832800	1.179800	1.863000
C	-2.988700	0.299700	1.558100
H	-2.582000	1.031100	2.254600
C	-1.967800	-0.605900	0.985400
P	-1.216100	1.279000	-1.285900
C	-0.202600	1.544900	-2.783300
H	-0.852400	1.905500	-3.585400
H	0.586100	2.276400	-2.602800
C	-2.711300	0.494900	-1.976100

H	-2.484500	-0.486800	-2.393800
H	-3.474700	0.399000	-1.204600
C	-1.834600	2.920300	-0.791300
H	-2.345400	3.388300	-1.637200
H	-2.541300	2.790100	0.033900
H	-3.086300	1.142600	-2.774000
H	0.249200	0.594200	-3.083400
H	-1.016400	3.561600	-0.459500
N	0.511600	-1.420000	-1.070200
N	1.793300	-1.598500	-1.461300
N	2.752400	0.649400	-0.932400
N	1.670500	1.241800	-0.387200
N	2.897400	-1.164900	0.755700
N	1.848600	-0.765800	1.506600
C	-0.244600	-2.130000	-1.918700
H	-1.317500	-2.160200	-1.801900
C	0.553100	-2.770200	-2.868900
H	0.235100	-3.413700	-3.674000
C	1.846400	-2.400400	-2.536400
H	2.797900	-2.649600	-2.984000
C	3.127300	2.833000	-0.987800
H	3.583200	3.796500	-1.153300
C	3.644300	1.583700	-1.298800
H	4.586700	1.292800	-1.740500
C	2.118800	-1.085400	2.777700
H	1.406700	-0.852300	3.557600
C	3.367700	-1.704200	2.854900
H	3.870100	-2.074200	3.734700
C	3.826100	-1.726800	1.545100
H	4.749200	-2.095000	1.120700
B	2.957200	-0.874700	-0.766500
H	4.005900	-1.217100	-1.221800
C	1.890400	2.562200	-0.400800
H	1.156600	3.242800	0.008700
H	-1.259400	-0.853800	1.852200

**Compound 4A – P** Electronic Energy: -1631.095218 Hartree

W	0.137600	-0.575000	-0.144800
O	0.043700	-2.139100	-2.637900
N	0.041000	-1.544700	-1.606900
C	-4.714700	-0.249800	0.740400
H	-5.572300	0.405800	0.870000
C	-4.784700	-1.181300	-0.234900
H	-5.693600	-1.217400	-0.830100
C	-3.790400	-2.189900	-0.553900
H	-4.137300	-2.980300	-1.215600
C	-2.497700	-2.270400	-0.170500
H	-1.940800	-3.129900	-0.539700
C	-3.643300	-0.071500	1.703900

H	-3.903400	0.544900	2.561700
C	-2.383800	-0.558500	1.692300
H	-1.771400	-0.309300	2.555100
C	-1.688400	-1.333000	0.640400
P	2.410400	-1.635200	0.501500
C	3.668100	-0.369800	0.882500
H	4.596700	-0.862000	1.185500
H	3.855000	0.247000	-0.000500
C	2.384900	-2.714100	1.973700
H	2.078500	-2.140600	2.851000
H	1.675900	-3.529800	1.811500
C	3.155000	-2.688600	-0.785500
H	4.105100	-3.092200	-0.424400
H	2.471200	-3.510800	-1.011500
H	3.383600	-3.127000	2.142500
H	3.308300	0.265900	1.696300
H	3.331500	-2.110200	-1.694500
N	0.497500	0.837800	1.611200
N	0.588500	2.171200	1.450000
N	1.457100	2.188000	-0.899300
N	1.386000	0.878700	-1.213400
N	-0.971100	2.362600	-0.509500
N	-1.238700	1.062800	-0.762000
C	0.720100	0.582900	2.906200
H	0.687400	-0.434600	3.273200
C	0.958800	1.773900	3.596100
H	1.166200	1.901500	4.647000
C	0.865800	2.760000	2.624100
H	0.976800	3.833100	2.684300
C	2.907200	1.844100	-2.540300
H	3.661000	1.995200	-3.296900
C	2.361900	2.792000	-1.683600
H	2.546600	3.852300	-1.586400
C	-2.410100	1.011200	-1.397900
H	-2.819000	0.056000	-1.696600
C	-2.923500	2.301900	-1.556900
H	-3.849900	2.591700	-2.027400
C	-1.970900	3.127500	-0.980400
H	-1.927000	4.202200	-0.877000
B	0.401100	2.799300	0.056900
H	0.495300	3.987900	0.104100
C	2.249200	0.658000	-2.214200
H	2.343700	-0.330800	-2.642100
H	-0.861900	-1.953900	1.132800

(1) Smith, J. A., Scouten, A., Wilde, J.H., Westendorff, K.W., Dickie, D.A., Ess, D.H., Harman, W.D. Experiments and Direct Dynamics Simulations That Probe  $\eta^2$ -Arene/Aryl Hydride Equilibria of Tungsten Benzene Complexes. *J. Am. Chem. Soc.* **2020**, *142*, 16437-16454.

## Crystallography.

### Crystal Structure Report for Harman\_2\_JKH\_151\_X2

A translucent pale yellow, plate-like specimen of  $C_{19}H_{28}BN_8OPW$ , approximate dimensions 0.029 mm x 0.084 mm x 0.089 mm, was coated with Paratone oil and mounted on a MiTeGen MicroLoop. The X-ray intensity data were measured on a Bruker D8 Venture Photon III Kappa four-circle diffractometer system equipped with an Incoatec I $\mu$ S 3.0 micro-focus sealed X-ray tube (Mo  $K\alpha$ ,  $\lambda = 0.71073$  Å) and a HELIOS double bounce multilayer mirror monochromator.

The total exposure time was 8.76 hours. The frames were integrated with the Bruker SAINT software package<sup>1</sup> using a narrow-frame algorithm. The integration of the data using a monoclinic unit cell yielded a total of 63074 reflections to a maximum  $\theta$  angle of 28.38° (0.75 Å resolution), of which 6185 were independent (average redundancy 10.198, completeness = 99.2%,  $R_{int} = 8.87\%$ ,  $R_{sig} = 4.77\%$ ) and 4646 (75.12%) were greater than  $2\sigma(F^2)$ . The final cell constants of  $a = 15.6977(6)$  Å,  $b = 12.3111(5)$  Å,  $c = 25.7548(15)$  Å,  $\beta = 92.2234(12)^\circ$ , volume = 4973.5(4) Å<sup>3</sup>, are based upon the refinement of the XYZ-centroids of 9910 reflections above  $20\sigma(I)$  with  $5.203^\circ < 2\theta < 55.31^\circ$ . Data were corrected for absorption effects using the Multi-Scan method (SADABS).<sup>2</sup> The ratio of minimum to maximum apparent transmission was 0.858. The calculated minimum and maximum transmission coefficients (based on crystal size) are 0.6780 and 0.8750.

The structure was solved and refined using the Bruker SHELXTL Software Package<sup>3</sup> within APEX5<sup>1</sup> and OLEX2,<sup>4</sup> using the space group  $I 2/a$ , with  $Z = 8$  for the formula unit,  $C_{19}H_{28}BN_8OPW$ . Non-hydrogen atoms were refined anisotropically. The B-H hydrogen atoms and those on the Cp ligand were located in the electron density map

---

<sup>1</sup> Bruker (2012). *Saint*; *SADABS*; *APEX5*. Bruker AXS Inc., Madison, Wisconsin, USA.

<sup>2</sup> Krause, L., Herbst-Irmer, R., Sheldrick, G. M., Stalke, D. "Comparison of silver and molybdenum microfocus X-ray sources for single-crystal structure determination" *J. Appl. Cryst.* (2015) 48, 3-10. doi:10.1107/S1600576714022985

<sup>3</sup> Sheldrick, G. M. (2015). *Acta Cryst.* A71, 3-8.

<sup>4</sup> Dolomanov, O. V.; Bourhis, L. J.; Gildea, R. J.; Howard, J. A. K.; Puschmann, H. *J. Appl. Cryst.* (2009). **42**, 339-341.



and refined isotropically. All other hydrogen atoms were placed in geometrically calculated positions with  $U_{iso} = 1.2U_{equiv}$  of the parent atom ( $U_{iso} = 1.5U_{equiv}$  for methyl). The acetonitrile solvent molecules were refined at 50% occupancy due to the symmetry of the position. The final anisotropic full-matrix least-squares refinement on  $F^2$  with 340 variables converged at  $R1 = 3.27\%$ , for the observed data and  $wR2 = 7.89\%$  for all data. The goodness-of-fit was 1.038. The largest peak in the final difference electron density synthesis was  $1.395 \text{ e}^-/\text{\AA}^3$  and the largest hole was  $-0.816 \text{ e}^-/\text{\AA}^3$  with an RMS deviation of  $0.151 \text{ e}^-/\text{\AA}^3$ . On the basis of the final model, the calculated density was  $1.630 \text{ g/cm}^3$  and  $F(000)$ , 2400  $e^-$ .

<b>Table 1. Sample and crystal data for Harman_2_JKH_151_X2.</b>		
<b>Identification code</b>	Harman_2_JKH_151_X2	
<b>Chemical formula</b>	$C_{19}H_{28}BN_8OPW$	
<b>Formula weight</b>	610.12 g/mol	
<b>Temperature</b>	100(2) K	
<b>Wavelength</b>	0.71073 Å	
<b>Crystal size</b>	0.029 x 0.084 x 0.089 mm	
<b>Crystal habit</b>	translucent pale yellow plate	
<b>Crystal system</b>	monoclinic	
<b>Space group</b>	I 2/a	
<b>Unit cell dimensions</b>	$a = 15.6977(6) \text{ Å}$	$\alpha = 90^\circ$
	$b = 12.3111(5) \text{ Å}$	$\beta = 92.2234(12)^\circ$
	$c = 25.7548(15) \text{ Å}$	$\gamma = 90^\circ$
<b>Volume</b>	$4973.5(4) \text{ Å}^3$	
<b>Z</b>	8	
<b>Density (calculated)</b>	$1.630 \text{ g/cm}^3$	
<b>Absorption coefficient</b>	$4.736 \text{ mm}^{-1}$	
<b>F(000)</b>	2400	

<b>Table 2. Data collection and structure refinement for Harman_2_JKH_151_X2.</b>	
<b>Diffractometer</b>	Bruker D8 Venture Photon III Kappa four-circle diffractometer
<b>Radiation source</b>	Incoatec I $\mu$ S 3.0 micro-focus sealed X-ray tube (Mo $K\alpha$ , $\lambda = 0.71073 \text{ Å}$ )
<b>Theta range for data collection</b>	$2.10$ to $28.38^\circ$
<b>Index ranges</b>	$-20 \leq h \leq 18$ , $-16 \leq k \leq 16$ , $-34 \leq l \leq 34$
<b>Reflections collected</b>	63074

<b>Independent reflections</b>	6185 [R(int) = 0.0887]	
<b>Coverage of independent reflections</b>	99.2%	
<b>Absorption correction</b>	Multi-Scan	
<b>Max. and min. transmission</b>	0.8750 and 0.6780	
<b>Structure solution technique</b>	direct methods	
<b>Structure solution program</b>	SHELXT 2018/2 (Sheldrick, 2018)	
<b>Refinement method</b>	Full-matrix least-squares on F <sup>2</sup>	
<b>Refinement program</b>	SHELXL-2019/1 (Sheldrick, 2019)	
<b>Function minimized</b>	$\sum w(F_o^2 - F_c^2)^2$	
<b>Data / restraints / parameters</b>	6185 / 1 / 340	
<b>Goodness-of-fit on F<sup>2</sup></b>	1.038	
<b><math>\Delta/\sigma_{\max}</math></b>	0.001	
<b>Final R indices</b>	4646 data; $I > 2\sigma(I)$	R1 = 0.0327, wR2 = 0.0710
	all data	R1 = 0.0556, wR2 = 0.0789
<b>Weighting scheme</b>	$w = 1/[\sigma^2(F_o^2) + (0.0396P)^2 + 2.5395P]$ where $P = (F_o^2 + 2F_c^2)/3$	
<b>Largest diff. peak and hole</b>	1.395 and -0.816 eÅ <sup>-3</sup>	
<b>R.M.S. deviation from mean</b>	0.151 eÅ <sup>-3</sup>	

**Table 3. Atomic coordinates and equivalent isotropic atomic displacement parameters (Å<sup>2</sup>) for Harman\_2\_JKH\_151\_X2.**

U(eq) is defined as one third of the trace of the orthogonalized U<sub>ij</sub> tensor.

	<b>x/a</b>	<b>y/b</b>	<b>z/c</b>	<b>U(eq)</b>
W1	0.05880(2)	0.11319(2)	0.13846(2)	0.02018(6)
P1	0.17873(7)	0.00375(10)	0.10542(5)	0.0263(3)
O1	0.1542(2)	0.3195(3)	0.11940(15)	0.0443(10)
N1	0.9426(2)	0.1198(3)	0.23570(15)	0.0248(8)
N2	0.9611(2)	0.1740(3)	0.19145(14)	0.0208(8)

	x/a	y/b	z/c	U(eq)
N3	0.9964(2)	0.9538(3)	0.15763(15)	0.0221(8)
N4	0.9751(2)	0.9312(3)	0.20703(15)	0.0243(8)
N5	0.1240(2)	0.0923(3)	0.21538(15)	0.0239(8)
N6	0.0858(2)	0.0425(3)	0.25599(15)	0.0236(8)
N7	0.1137(2)	0.2358(3)	0.12738(15)	0.0271(9)
C1	0.9108(3)	0.2608(4)	0.18904(19)	0.0241(10)
C2	0.8586(3)	0.2635(4)	0.23152(19)	0.0280(10)
C3	0.8806(3)	0.1728(4)	0.26025(19)	0.0272(10)
C4	0.9745(3)	0.8665(3)	0.1290(2)	0.0276(10)
C5	0.9389(3)	0.7870(4)	0.1603(2)	0.0331(11)
C6	0.9404(3)	0.8312(4)	0.2093(2)	0.0285(10)
C7	0.1407(3)	0.0416(4)	0.2978(2)	0.0294(11)
C8	0.2148(3)	0.0913(4)	0.2848(2)	0.0302(11)
C9	0.2022(3)	0.1224(4)	0.2331(2)	0.0291(10)
C10	0.2326(4)	0.9156(5)	0.1528(2)	0.0493(16)
C11	0.1631(3)	0.9073(4)	0.0524(2)	0.0378(13)
C12	0.2632(3)	0.0882(4)	0.0814(2)	0.0390(13)
C13	0.0175(3)	0.0872(4)	0.05563(19)	0.0277(11)
C14	0.0557(3)	0.1610(4)	0.01615(19)	0.0308(11)
C15	0.0182(3)	0.2575(5)	0.0165(2)	0.0377(12)
C16	0.9489(3)	0.2621(4)	0.0552(2)	0.0351(12)
C17	0.9548(3)	0.1501(4)	0.08089(19)	0.0276(10)
B1	0.9903(3)	0.0136(4)	0.2514(2)	0.0265(11)
N9	0.2474(10)	0.6172(10)	0.1057(5)	0.082(4)
C20	0.0936(7)	0.5539(9)	0.0826(5)	0.045(3)
C21	0.1780(10)	0.5881(9)	0.0952(5)	0.052(3)
N8	0.3719(9)	0.4564(11)	0.0698(5)	0.074(4)
C18	0.250(2)	0.3883(13)	0.9985(18)	0.121(8)
C19	0.3152(10)	0.4266(14)	0.0427(6)	0.071(4)

<b>Table 4. Bond lengths (Å) for Harman_2_JKH_151_X2.</b>			
W1-N7	1.767(4)	W1-N5	2.209(4)
W1-C17	2.210(5)	W1-N2	2.221(3)
W1-C13	2.229(5)	W1-N3	2.257(4)
W1-P1	2.4916(12)	P1-C12	1.812(5)
P1-C10	1.818(6)	P1-C11	1.819(5)
O1-N7	1.232(5)	N1-C3	1.350(5)
N1-N2	1.362(5)	N1-B1	1.551(6)
N2-C1	1.329(5)	N3-C4	1.340(6)
N3-N4	1.356(5)	N4-C6	1.348(6)
N4-B1	1.540(7)	N5-C9	1.345(6)
N5-N6	1.370(5)	N6-C7	1.352(6)

N6-B1	1.541(6)	C1-C2	1.393(6)
C1-H1	0.950000	C2-C3	1.376(7)
C2-H2	0.950000	C3-H3	0.950000
C4-C5	1.398(7)	C4-H4	0.950000
C5-C6	1.374(7)	C5-H5	0.950000
C6-H6	0.950000	C7-C8	1.367(7)
C7-H7	0.950000	C8-C9	1.391(7)
C8-H8	0.950000	C9-H9	0.950000
C10-H10A	0.980000	C10-H10B	0.980000
C10-H10C	0.980000	C11-H11A	0.980000
C11-H11B	0.980000	C11-H11C	0.980000
C12-H12A	0.980000	C12-H12B	0.980000
C12-H12C	0.980000	C13-C17	1.429(7)
C13-C14	1.505(7)	C13-H13	0.98(5)
C14-C15	1.326(7)	C14-H14	1.06(5)
C15-C16	1.505(7)	C15-H15	1.04(5)
C16-C17	1.530(7)	C16-H16A	1.10(4)
C16-H16B	1.11(4)	C17-H17	1.01(6)
B1-H1A	1.18(4)	N9-C21	1.169(18)
C20-C21	1.416(18)	C20-H20A	0.980000
C20-H20B	0.980000	C20-H20C	0.980000
N8-C19	1.170(18)	C18-C19	1.57(5)
C18-H18A	0.980000	C18-H18B	0.980000
C18-H18C	0.980000		

**Table 5. Bond angles (°) for Harman\_2\_JKH\_151\_X2.**

N7-W1-N5	91.87(16)	N7-W1-C17	93.91(18)
N5-W1-C17	158.45(16)	N7-W1-N2	99.43(15)
N5-W1-N2	78.16(13)	C17-W1-N2	80.41(16)
N7-W1-C13	95.38(18)	N5-W1-C13	161.64(16)
C17-W1-C13	37.56(17)	N2-W1-C13	117.03(15)
N7-W1-N3	175.51(15)	N5-W1-N3	83.81(13)
C17-W1-N3	90.56(16)	N2-W1-N3	80.94(13)
C13-W1-N3	88.39(16)	N7-W1-P1	91.56(13)
N5-W1-P1	85.03(10)	C17-W1-P1	115.50(13)
N2-W1-P1	160.14(10)	C13-W1-P1	77.94(12)
N3-W1-P1	86.84(9)	C12-P1-C10	104.1(3)
C12-P1-C11	101.4(3)	C10-P1-C11	99.2(3)
C12-P1-W1	112.24(18)	C10-P1-W1	115.57(18)
C11-P1-W1	121.84(17)	C3-N1-N2	109.6(4)
C3-N1-B1	129.4(4)	N2-N1-B1	121.0(3)
C1-N2-N1	106.7(3)	C1-N2-W1	131.7(3)
N1-N2-W1	121.6(3)	C4-N3-N4	106.6(4)

C4-N3-W1	132.9(3)	N4-N3-W1	120.5(3)
C6-N4-N3	109.9(4)	C6-N4-B1	128.4(4)
N3-N4-B1	121.6(4)	C9-N5-N6	106.5(4)
C9-N5-W1	131.1(3)	N6-N5-W1	122.4(3)
C7-N6-N5	109.1(4)	C7-N6-B1	130.3(4)
N5-N6-B1	119.8(4)	O1-N7-W1	178.0(4)
N2-C1-C2	110.4(4)	N2-C1-H1	124.800000
C2-C1-H1	124.800000	C3-C2-C1	105.0(4)
C3-C2-H2	127.500000	C1-C2-H2	127.500000
N1-C3-C2	108.2(4)	N1-C3-H3	125.900000
C2-C3-H3	125.900000	N3-C4-C5	110.1(5)
N3-C4-H4	124.900000	C5-C4-H4	124.900000
C6-C5-C4	105.0(4)	C6-C5-H5	127.500000
C4-C5-H5	127.500000	N4-C6-C5	108.4(4)
N4-C6-H6	125.800000	C5-C6-H6	125.800000
N6-C7-C8	108.9(5)	N6-C7-H7	125.600000
C8-C7-H7	125.600000	C7-C8-C9	105.5(4)
C7-C8-H8	127.300000	C9-C8-H8	127.300000
N5-C9-C8	110.1(4)	N5-C9-H9	125.000000
C8-C9-H9	125.000000	P1-C10-H10A	109.500000
P1-C10-H10B	109.500000	H10A-C10-H10B	109.500000
P1-C10-H10C	109.500000	H10A-C10-H10C	109.500000
H10B-C10-H10C	109.500000	P1-C11-H11A	109.500000
P1-C11-H11B	109.500000	H11A-C11-H11B	109.500000
P1-C11-H11C	109.500000	H11A-C11-H11C	109.500000
H11B-C11-H11C	109.500000	P1-C12-H12A	109.500000
P1-C12-H12B	109.500000	H12A-C12-H12B	109.500000
P1-C12-H12C	109.500000	H12A-C12-H12C	109.500000
H12B-C12-H12C	109.500000	C17-C13-C14	106.3(4)
C17-C13-W1	70.5(3)	C14-C13-W1	116.8(3)
C17-C13-H13	124.(3)	C14-C13-H13	113.(3)
W1-C13-H13	120.(3)	C15-C14-C13	110.4(4)
C15-C14-H14	127.(3)	C13-C14-H14	122.(3)
C14-C15-C16	111.7(5)	C14-C15-H15	124.(3)
C16-C15-H15	124.(3)	C15-C16-C17	102.7(4)
C15-C16-H16A	113.(3)	C17-C16-H16A	116.(3)
C15-C16-H16B	108.(3)	C17-C16-H16B	111.(3)
H16A-C16-H16B	105.(4)	C13-C17-C16	108.8(4)
C13-C17-W1	71.9(3)	C16-C17-W1	120.4(3)
C13-C17-H17	116.(3)	C16-C17-H17	120.(3)
W1-C17-H17	110.(4)	N4-B1-N6	109.4(4)

N4-B1-N1	107.6(4)	N6-B1-N1	106.5(4)
N4-B1-H1A	112.(2)	N6-B1-H1A	113.(2)
N1-B1-H1A	108.(2)	C21-C20-H20A	109.500000
C21-C20-H20B	109.500000	H20A-C20-H20B	109.500000
C21-C20-H20C	109.500000	H20A-C20-H20C	109.500000
H20B-C20-H20C	109.500000	N9-C21-C20	179.4(16)
C19-C18-H18A	109.500000	C19-C18-H18B	109.500000
H18A-C18-H18B	109.500000	C19-C18-H18C	109.500000
H18A-C18-H18C	109.500000	H18B-C18-H18C	109.500000
N8-C19-C18	170.1(18)		

**Table 6. Torsion angles (°) for Harman\_2\_JKH\_151\_X2.**

C3-N1-N2-C1	0.5(5)	B1-N1-N2-C1	-179.5(4)
C3-N1-N2-W1	-179.1(3)	B1-N1-N2-W1	0.9(5)
C4-N3-N4-C6	0.0(4)	W1-N3-N4-C6	-178.8(3)
C4-N3-N4-B1	-179.6(4)	W1-N3-N4-B1	1.6(5)
C9-N5-N6-C7	-0.6(5)	W1-N5-N6-C7	-180.0(3)
C9-N5-N6-B1	170.6(4)	W1-N5-N6-B1	-8.7(5)
N1-N2-C1-C2	-0.5(5)	W1-N2-C1-C2	179.0(3)
N2-C1-C2-C3	0.3(5)	N2-N1-C3-C2	-0.2(5)
B1-N1-C3-C2	179.7(4)	C1-C2-C3-N1	-0.1(5)
N4-N3-C4-C5	0.0(5)	W1-N3-C4-C5	178.5(3)
N3-C4-C5-C6	0.1(5)	N3-N4-C6-C5	0.1(5)
B1-N4-C6-C5	179.6(4)	C4-C5-C6-N4	-0.1(5)
N5-N6-C7-C8	0.4(5)	B1-N6-C7-C8	-169.6(4)
N6-C7-C8-C9	0.0(5)	N6-N5-C9-C8	0.6(5)
W1-N5-C9-C8	179.9(3)	C7-C8-C9-N5	-0.4(5)
C17-C13-C14-C15	-1.6(6)	W1-C13-C14-C15	-77.6(5)
C13-C14-C15-C16	-1.1(6)	C14-C15-C16-C17	3.1(6)
C14-C13-C17-C16	3.5(5)	W1-C13-C17-C16	116.8(4)
C14-C13-C17-W1	-113.3(3)	C15-C16-C17-C13	-4.0(5)
C15-C16-C17-W1	75.7(5)	C6-N4-B1-N6	122.3(4)
N3-N4-B1-N6	-58.2(5)	C6-N4-B1-N1	-122.4(4)
N3-N4-B1-N1	57.0(5)	C7-N6-B1-N4	-128.3(5)
N5-N6-B1-N4	62.5(5)	C7-N6-B1-N1	115.7(5)
N5-N6-B1-N1	-53.4(5)	C3-N1-B1-N4	121.1(5)

N2-N1-B1-N4	-58.9(5)	C3-N1-B1-N6	-121.7(5)
N2-N1-B1-N6	58.2(5)		

**Table 7. Anisotropic atomic displacement parameters (Å<sup>2</sup>) for Harman\_2\_JKH\_151\_X2.**

The anisotropic atomic displacement factor exponent takes the form:  $-2\pi^2 [h^2 a^{*2} U_{11} + \dots + 2 h k a^* b^* U_{12}]$

	<b>U<sub>11</sub></b>	<b>U<sub>22</sub></b>	<b>U<sub>33</sub></b>	<b>U<sub>23</sub></b>	<b>U<sub>13</sub></b>	<b>U<sub>12</sub></b>
W1	0.01424(8)	0.02216(10)	0.02411(10)	-0.00077(8)	0.00040(6)	-0.00067(7)
P1	0.0194(5)	0.0336(7)	0.0262(7)	0.0037(5)	0.0045(5)	0.0054(5)
O1	0.043(2)	0.046(2)	0.044(2)	0.0060(18)	-0.0068(17)	-0.0190(18)
N1	0.0190(17)	0.030(2)	0.025(2)	0.0006(17)	0.0041(14)	-0.0015(15)
N2	0.0180(16)	0.0196(19)	0.025(2)	-0.0017(15)	0.0020(14)	-0.0011(14)
N3	0.0163(17)	0.0205(19)	0.030(2)	0.0006(16)	0.0003(15)	0.0029(14)
N4	0.0177(17)	0.0267(19)	0.028(2)	0.0027(17)	-0.0005(15)	-0.0001(15)
N5	0.0171(17)	0.027(2)	0.027(2)	-0.0029(16)	-0.0004(15)	-0.0018(14)
N6	0.0259(19)	0.022(2)	0.023(2)	-0.0015(16)	-0.0001(15)	0.0029(15)
N7	0.0187(17)	0.035(2)	0.028(2)	0.0037(18)	-0.0016(15)	-0.0055(16)
C1	0.019(2)	0.023(2)	0.030(3)	0.0003(19)	-0.0040(18)	0.0005(17)
C2	0.019(2)	0.028(2)	0.037(3)	-0.007(2)	0.0023(19)	0.0012(18)
C3	0.023(2)	0.032(3)	0.028(3)	-0.002(2)	0.0057(18)	-0.0045(19)
C4	0.020(2)	0.024(3)	0.038(3)	-0.002(2)	-0.0019(19)	-0.0005(17)
C5	0.031(2)	0.023(2)	0.044(3)	0.003(2)	-0.006(2)	-0.002(2)
C6	0.019(2)	0.028(3)	0.038(3)	0.005(2)	-0.0028(19)	-0.0026(19)
C7	0.037(3)	0.023(2)	0.028(3)	-0.008(2)	-0.006(2)	0.003(2)
C8	0.025(2)	0.030(3)	0.035(3)	-0.006(2)	-0.011(2)	0.0012(19)
C9	0.019(2)	0.034(3)	0.034(3)	-0.003(2)	-0.0020(18)	0.0006(19)
C10	0.047(3)	0.059(4)	0.043(4)	0.004(3)	0.012(3)	0.027(3)
C11	0.033(3)	0.036(3)	0.044(3)	-0.007(2)	0.008(2)	0.004(2)
C12	0.025(2)	0.048(3)	0.045(3)	0.001(3)	0.009(2)	-0.003(2)
C13	0.025(2)	0.030(3)	0.027(3)	-0.002(2)	-0.0062(19)	0.0004(19)
C14	0.026(2)	0.041(3)	0.025(3)	0.001(2)	0.0011(19)	-0.001(2)
C15	0.037(3)	0.043(3)	0.032(3)	0.006(2)	-0.002(2)	-0.007(2)
C16	0.032(3)	0.036(3)	0.036(3)	0.001(2)	-0.004(2)	0.011(2)

	<b>U<sub>11</sub></b>	<b>U<sub>22</sub></b>	<b>U<sub>33</sub></b>	<b>U<sub>23</sub></b>	<b>U<sub>13</sub></b>	<b>U<sub>12</sub></b>
C17	0.023(2)	0.032(3)	0.028(3)	0.002(2)	-0.0029(19)	-0.001(2)
B1	0.024(2)	0.031(3)	0.025(3)	-0.001(2)	0.004(2)	0.000(2)
N9	0.095(10)	0.078(9)	0.071(9)	0.021(7)	-0.024(8)	-0.032(8)
C20	0.041(6)	0.040(6)	0.053(8)	0.019(6)	-0.009(5)	0.008(5)
C21	0.077(9)	0.034(7)	0.046(8)	0.003(5)	0.015(7)	0.002(6)
N8	0.092(9)	0.082(9)	0.049(8)	-0.009(7)	0.011(7)	-0.017(8)
C18	0.059(8)	0.122(13)	0.18(2)	0.113(19)	-0.021(10)	-0.039(15)
C19	0.068(10)	0.090(11)	0.056(10)	-0.019(9)	0.017(8)	0.002(9)

**Table 8. Hydrogen atomic coordinates and isotropic atomic displacement parameters (Å<sup>2</sup>) for Harman\_2\_JKH\_151\_X2.**

	<b>x/a</b>	<b>y/b</b>	<b>z/c</b>	<b>U(eq)</b>
H1	-0.0895	0.3136	0.1621	0.029000
H2	-0.1832	0.3164	0.2390	0.034000
H3	-0.1436	0.1513	0.2919	0.033000
H4	-0.0179	-0.1404	0.0927	0.033000
H5	-0.0818	-0.2825	0.1499	0.040000
H6	-0.0797	-0.2028	0.2395	0.034000
H7	0.1296	0.0114	0.3308	0.035000
H8	0.2644	0.1023	0.3065	0.036000
H9	0.2428	0.1595	0.2133	0.035000
H10A	0.2662	-0.0402	0.1778	0.074000
H10B	0.2705	-0.1341	0.1350	0.074000
H10C	0.1902	-0.1264	0.1713	0.074000
H11A	0.1245	-0.1506	0.0630	0.057000
H11B	0.2181	-0.1243	0.0439	0.057000
H11C	0.1382	-0.0552	0.0219	0.057000
H12A	0.2408	0.1322	0.0522	0.059000
H12B	0.3096	0.0421	0.0698	0.059000
H12C	0.2848	0.1362	0.1093	0.059000
H13	0.008(3)	0.014(4)	0.0424(18)	0.023(12)
H14	0.110(3)	0.138(4)	-0.005(2)	0.032(14)
H15	0.038(3)	0.324(4)	-0.005(2)	0.043(15)
H16A	-0.046(3)	0.332(4)	0.0814(19)	0.047(16)
H16B	-0.113(3)	0.273(4)	0.033(2)	0.051(16)
H17	-0.099(4)	0.111(5)	0.090(3)	0.061(19)
H1A	-0.037(3)	-0.018(3)	0.2906(18)	0.021(11)
H20A	0.0752	0.5835	0.0486	0.068000
H20B	0.0555	0.5801	0.1091	0.068000
H20C	0.0916	0.4744	0.0813	0.068000



	x/a	y/b	z/c	U(eq)
H18A	0.2798	0.3437	-0.0266	0.182000
H18B	0.2250	0.4518	-0.0191	0.182000
H18C	0.2048	0.3453	0.0138	0.182000

## Structure Report for mo\_harman\_nb2\_rjs\_triene\_0m

A yellow, needle-shaped crystal of mo\_harman\_nb2\_rjs\_triene\_0m was coated with Paratone oil and mounted on a MiTeGen micromount. crystallized from chloroform. Data were collected at 100.00 K on a Bruker D8 VENTURE dual wavelength Mo/Cu Kappa four-circle diffractometer with a PHOTON III detector. The diffractometer was equipped with an Oxford Cryostream 800Plus low temperature device and used Mo  $K_\alpha$  radiation ( $\lambda = 0.71073\text{\AA}$ ) from an Incoatec Ims 3.0 microfocus sealed X-ray tube with a HELIOS double bounce multilayer mirror as monochromator.

Data collection and processing were done within the Bruker APEX5 software suite.<sup>[1]</sup> All data were integrated with SAINT 8.40B using a narrow-frame algorithm and a Multi-Scan absorption correction using was applied.<sup>[2]</sup> Using Olex2 as a graphical interface,<sup>[3]</sup> the structure was solved by dual methods with XT and refined by full-matrix least-squares methods against  $F^2$  using XL.<sup>[4,5]</sup> All non-hydrogen atoms were refined with anisotropic displacement parameters. All C-bound hydrogen atoms were refined with isotropic displacement parameters. Some of their coordinates were refined freely and some on calculated positions using a riding model with their  $U_{\text{iso}}$  values constrained to 1.5 times the  $U_{\text{eq}}$  of their pivot atoms for terminal  $\text{sp}^3$  carbon atoms and 1.2 times for all other carbon atoms.

This report and the CIF file were generated using FinalCif.<sup>[6]</sup>

Table 1. Crystal data and structure refinement for mo\_harman\_nb2\_rjs\_triene\_0m

CCDC number	
Empirical formula	$\text{C}_{20}\text{H}_{27}\text{BCl}_3\text{N}_7\text{OPW}$
Formula weight	713.46
Temperature [K]	100.00
Crystal system	monoclinic
Space group (number)	$P2_1/n$ (14)
$a$ [ $\text{\AA}$ ]	10.3682(7)

<i>b</i> [Å]	12.4816(9)
<i>c</i> [Å]	20.3456(17)
$\alpha$ [°]	90
$\beta$ [°]	90.196(3)
$\gamma$ [°]	90
Volume [Å <sup>3</sup> ]	2632.9(3)
<i>Z</i>	4
$\rho_{\text{calc}}$ [gcm <sup>-3</sup> ]	1.800
$\mu$ [mm <sup>-1</sup> ]	4.781
<i>F</i> (000)	1396
Crystal size [mm <sup>3</sup> ]	0.066×0.12×0.125
Crystal colour	yellow
Crystal shape	needle
Radiation	Mo <i>K</i> <sub>α</sub> ( $\lambda$ =0.71073 Å)
2 $\theta$ range [°]	4.42 to 55.00 (0.77 Å)
Index ranges	−13 ≤ <i>h</i> ≤ 13 −16 ≤ <i>k</i> ≤ 13 −23 ≤ <i>l</i> ≤ 26
Reflections collected	34497
Independent reflections	6027 <i>R</i> <sub>int</sub> = 0.1138 <i>R</i> <sub>sigma</sub> = 0.0823
Completeness to $\theta$ = 25.242°	99.9
Data / Restraints / Parameters	6027 / 0 / 317
Goodness-of-fit on <i>F</i> <sup>2</sup>	1.017
Final <i>R</i> indexes [ $\geq 2\sigma(I)$ ]	<i>R</i> <sub>1</sub> = 0.0443 <i>wR</i> <sub>2</sub> = 0.0882
Final <i>R</i> indexes [all data]	<i>R</i> <sub>1</sub> = 0.0786 <i>wR</i> <sub>2</sub> = 0.1008
Largest peak/hole [eÅ <sup>-3</sup> ]	1.39/−1.50

Table 2. Atomic coordinates and Ueq [Å<sup>2</sup>] for mo\_harman\_nb2\_rjs\_triene\_0m

Atom	x	y	z	U <sub>eq</sub>
W1	0.55955(2)	0.62395(2)	0.66731(2)	0.01663(9)
P3	0.59923(17)	0.43968(15)	0.71011(9)	0.0211(4)
O1	0.8346(4)	0.6701(4)	0.7013(3)	0.0321(13)
N1	0.3474(5)	0.5854(5)	0.6610(3)	0.0207(13)
N2	0.2601(5)	0.6459(4)	0.6951(3)	0.0198(13)
N3	0.5151(5)	0.6621(4)	0.7706(3)	0.0201(13)
N4	0.3986(5)	0.7019(4)	0.7897(3)	0.0205(12)
N5	0.4883(5)	0.7913(5)	0.6625(3)	0.0213(13)
N6	0.3781(5)	0.8219(5)	0.6949(3)	0.0210(13)
N7	0.7228(5)	0.6528(4)	0.6837(3)	0.0222(13)
C1	0.2781(7)	0.5118(6)	0.6271(4)	0.0263(16)
H1	0.313687	0.458362	0.599331	0.032
C2	0.1480(6)	0.5259(6)	0.6387(4)	0.0262(17)
H2	0.078879	0.485238	0.620802	0.031
C3	0.1391(7)	0.6108(6)	0.6816(4)	0.0284(17)
H3	0.061524	0.639824	0.698809	0.034
C4	0.5896(7)	0.6623(6)	0.8248(4)	0.0259(16)
H4	0.676831	0.638994	0.826072	0.031
C5	0.5223(7)	0.7010(6)	0.8788(4)	0.0295(17)
H5	0.552248	0.708123	0.922748	0.035
C6	0.4053(8)	0.7261(6)	0.8548(4)	0.0307(18)
H6	0.337059	0.756401	0.879660	0.037
C7	0.5413(7)	0.8814(6)	0.6406(3)	0.0264(15)
H7	0.619164	0.884655	0.616181	0.032
C8	0.4676(7)	0.9706(6)	0.6579(4)	0.0299(18)
H8	0.484594	1.043710	0.648191	0.036
C9	0.3662(7)	0.9297(6)	0.6918(4)	0.0285(17)
H9	0.297896	0.970325	0.710335	0.034
C10	0.5905(7)	0.5335(6)	0.5732(4)	0.0258(16)
H10	0.520(7)	0.481(6)	0.569(3)	0.031
C11	0.5586(7)	0.6438(6)	0.5589(4)	0.0258(17)
H11	0.466(7)	0.649(6)	0.549(4)	0.03(2)
C12	0.6437(8)	0.7213(6)	0.5258(4)	0.0332(19)
H12	0.600516	0.781486	0.507528	0.040
C13	0.7692(8)	0.7212(7)	0.5174(4)	0.043(2)
H13	0.802633	0.781946	0.495036	0.051
C14	0.8656(8)	0.6411(8)	0.5374(5)	0.047(2)
H14A	0.899527	0.662738	0.580970	0.056
H14B	0.938301	0.645627	0.506075	0.056
C15	0.8272(7)	0.5272(7)	0.5420(4)	0.035(2)
H15	0.894455	0.477271	0.533840	0.042

C16	0.7150(7)	0.4845(6)	0.5554(4)	0.0294(17)
H16	0.713574	0.408436	0.553407	0.035
C17	0.5360(7)	0.4105(6)	0.7924(4)	0.0294(18)
H17A	0.579510	0.456141	0.824840	0.044
H17B	0.551596	0.335086	0.803127	0.044
H17C	0.443052	0.424864	0.793247	0.044
C18	0.7695(7)	0.4120(6)	0.7193(4)	0.0309(18)
H18A	0.809389	0.406877	0.675838	0.046
H18B	0.781063	0.344098	0.742835	0.046
H18C	0.810437	0.469949	0.744320	0.046
C19	0.5413(7)	0.3226(6)	0.6659(4)	0.0311(18)
H19A	0.447109	0.325602	0.662295	0.047
H19B	0.566576	0.257599	0.689708	0.047
H19C	0.579049	0.321371	0.621788	0.047
B1	0.3030(8)	0.7398(7)	0.7377(4)	0.0257(19)
H1A	0.226895	0.774824	0.758805	0.031
Cl1	0.1907(3)	0.7616(2)	0.54650(12)	0.0571(7)
Cl2	0.3327(3)	0.8906(3)	0.45552(13)	0.0730(9)
Cl3	0.1572(4)	0.9867(3)	0.54678(19)	0.1049(13)
C20	0.2668(9)	0.8848(7)	0.5337(4)	0.045(2)

$U_{eq}$  is defined as 1/3 of the trace of the orthogonalized  $U_{ij}$  tensor.

Table 3. Anisotropic displacement parameters ( $\text{\AA}^2$ ) for mo\_harman\_nb2\_rjs\_triene\_0m. The anisotropic displacement factor exponent takes the form:  $-2\pi^2[h^2(a^*)^2U_{11} + k^2(b^*)^2U_{22} + \dots + 2hka^*b^*U_{12}]$

Atom	$U_{11}$	$U_{22}$	$U_{33}$	$U_{23}$	$U_{13}$	$U_{12}$
W1	0.01419(13)	0.01989(14)	0.01581(14)	-0.00168(14)	0.00036(9)	0.00156(13)
P3	0.0174(8)	0.0212(9)	0.0248(10)	-0.0003(8)	0.0000(7)	0.0018(7)
O1	0.016(2)	0.033(3)	0.048(4)	-0.009(3)	-0.007(2)	-0.002(2)
N1	0.015(3)	0.024(3)	0.023(3)	0.003(3)	0.002(2)	0.006(2)
N2	0.014(3)	0.025(3)	0.020(3)	0.003(2)	0.002(2)	0.003(2)
N3	0.019(3)	0.022(3)	0.020(3)	-0.005(2)	0.000(2)	0.002(2)
N4	0.020(3)	0.021(3)	0.021(3)	-0.002(3)	0.001(2)	0.002(2)
N5	0.023(3)	0.024(3)	0.017(3)	0.001(3)	0.001(2)	0.004(3)
N6	0.020(3)	0.024(3)	0.019(3)	0.000(3)	-0.002(2)	0.007(3)
N7	0.029(3)	0.018(3)	0.020(3)	-0.007(2)	-0.001(3)	0.000(2)
C1	0.024(4)	0.025(4)	0.030(4)	-0.001(3)	-0.001(3)	-0.003(3)
C2	0.019(3)	0.032(4)	0.028(4)	0.010(3)	-0.010(3)	-0.009(3)
C3	0.025(4)	0.032(4)	0.029(4)	0.012(4)	0.003(3)	0.003(3)
C4	0.027(4)	0.023(4)	0.028(4)	0.000(3)	-0.005(3)	-0.006(3)
C5	0.041(5)	0.033(4)	0.015(4)	0.001(3)	0.000(3)	-0.001(4)
C6	0.040(5)	0.031(4)	0.021(4)	-0.003(3)	0.009(3)	0.009(4)

C7	0.032(4)	0.022(4)	0.025(4)	−0.003(4)	0.006(3)	−0.001(4)
C8	0.030(4)	0.022(4)	0.038(5)	0.000(3)	0.001(4)	−0.006(3)
C9	0.030(4)	0.027(4)	0.029(4)	−0.004(4)	−0.005(3)	0.008(3)
C10	0.024(4)	0.032(4)	0.022(4)	−0.007(3)	0.001(3)	−0.003(3)
C11	0.021(3)	0.035(5)	0.022(4)	0.000(3)	0.002(3)	0.007(3)
C12	0.054(5)	0.027(4)	0.019(4)	−0.004(3)	0.001(4)	0.005(4)
C13	0.045(5)	0.042(5)	0.042(5)	0.011(4)	0.018(4)	−0.011(4)
C14	0.028(4)	0.061(7)	0.052(6)	−0.005(5)	0.014(4)	−0.004(4)
C15	0.025(4)	0.043(5)	0.038(5)	−0.009(4)	0.004(4)	0.006(4)
C16	0.035(4)	0.029(4)	0.025(4)	0.000(3)	0.004(3)	0.002(3)
C17	0.027(4)	0.029(4)	0.032(5)	0.002(3)	0.001(3)	−0.002(3)
C18	0.023(4)	0.027(4)	0.043(5)	0.008(4)	−0.005(3)	0.006(3)
C19	0.029(4)	0.024(4)	0.041(5)	−0.004(4)	0.001(4)	−0.004(3)
B1	0.027(4)	0.026(4)	0.024(5)	−0.006(4)	0.005(4)	0.003(4)
Cl1	0.0689(17)	0.0533(15)	0.0488(15)	0.0159(12)	−0.0201(13)	−0.0162(13)
Cl2	0.0610(16)	0.117(3)	0.0411(15)	0.0104(16)	0.0104(12)	−0.0151(17)
Cl3	0.132(3)	0.064(2)	0.120(3)	0.010(2)	0.028(2)	0.050(2)
C20	0.054(5)	0.037(5)	0.044(5)	−0.006(4)	0.005(4)	−0.005(5)

Table 4. Bond lengths and angles for mo\_harman\_nb2\_rjs\_triene\_0m

Atom–Atom	Length [Å]
W1–P3	2.4931(18)
W1–N1	2.255(5)
W1–N3	2.205(6)
W1–N5	2.217(6)
W1–N7	1.761(6)
W1–C10	2.247(7)
W1–C11	2.220(7)
P3–C17	1.837(7)
P3–C18	1.808(7)
P3–C19	1.817(7)
O1–N7	1.231(7)
N1–N2	1.369(7)
N1–C1	1.354(9)
N2–C3	1.356(9)
N2–B1	1.524(10)
N3–N4	1.365(7)
N3–C4	1.344(9)
N4–C6	1.359(9)
N4–B1	1.523(10)
N5–N6	1.375(7)
N5–C7	1.330(9)
N6–C9	1.353(9)
N6–B1	1.555(10)
C1–H1	0.9500
C1–C2	1.381(9)

C2–H2	0.9500
C2–C3	1.376(10)
C3–H3	0.9500
C4–H4	0.9500
C4–C5	1.390(10)
C5–H5	0.9500
C5–C6	1.343(10)
C6–H6	0.9500
C7–H7	0.9500
C7–C8	1.397(10)
C8–H8	0.9500
C8–C9	1.359(10)
C9–H9	0.9500
C10–H10	0.98(7)
C10–C11	1.445(10)
C10–C16	1.475(10)
C11–H11	0.98(7)
C11–C12	1.473(11)
C12–H12	0.9500
C12–C13	1.312(11)
C13–H13	0.9500
C13–C14	1.471(12)
C14–H14A	0.9900
C14–H14B	0.9900
C14–C15	1.479(12)
C15–H15	0.9500

C15–C16	1.310(10)
C16–H16	0.9500
C17–H17A	0.9800
C17–H17B	0.9800
C17–H17C	0.9800
C18–H18A	0.9800
C18–H18B	0.9800
C18–H18C	0.9800
C19–H19A	0.9800
C19–H19B	0.9800
C19–H19C	0.9800
B1–H1A	1.0000
Cl1–C20	1.748(9)
Cl2–C20	1.734(9)
Cl3–C20	1.727(9)
<b>Atom–Atom– Atom</b>	<b>Angle [°]</b>
N1–W1–P3	89.00(15)
N3–W1–P3	84.31(15)
N3–W1–N1	83.9(2)
N3–W1–N5	76.6(2)
N3–W1–C10	162.1(3)
N3–W1–C11	157.3(2)
N5–W1–P3	159.86(15)
N5–W1–N1	82.8(2)
N5–W1–C10	119.0(2)
N5–W1–C11	81.4(2)
N7–W1–P3	87.98(19)
N7–W1–N1	172.3(2)
N7–W1–N3	88.8(2)
N7–W1–N5	97.8(2)
N7–W1–C10	97.1(3)
N7–W1–C11	99.6(3)
C10–W1–P3	79.1(2)
C10–W1–N1	89.2(2)
C11–W1–P3	116.8(2)
C11–W1–N1	88.1(2)
C11–W1–C10	37.7(3)
C17–P3–W1	116.2(3)
C18–P3–W1	111.9(3)
C18–P3–C17	102.7(4)
C18–P3–C19	102.6(4)
C19–P3–W1	121.0(3)
C19–P3–C17	100.0(4)
N2–N1–W1	120.0(4)
C1–N1–W1	133.6(5)
C1–N1–N2	106.4(5)

N1–N2–B1	121.4(5)
C3–N2–N1	109.4(6)
C3–N2–B1	129.2(6)
N4–N3–W1	122.6(4)
C4–N3–W1	131.4(5)
C4–N3–N4	105.8(6)
N3–N4–B1	119.3(6)
C6–N4–N3	108.4(6)
C6–N4–B1	129.7(6)
N6–N5–W1	121.2(4)
C7–N5–W1	132.4(5)
C7–N5–N6	105.7(5)
N5–N6–B1	120.2(6)
C9–N6–N5	109.3(6)
C9–N6–B1	129.4(6)
O1–N7–W1	173.9(5)
N1–C1–H1	125.0
N1–C1–C2	110.1(7)
C2–C1–H1	125.0
C1–C2–H2	127.0
C3–C2–C1	105.9(6)
C3–C2–H2	127.0
N2–C3–C2	108.2(6)
N2–C3–H3	125.9
C2–C3–H3	125.9
N3–C4–H4	124.4
N3–C4–C5	111.1(7)
C5–C4–H4	124.4
C4–C5–H5	127.8
C6–C5–C4	104.4(7)
C6–C5–H5	127.8
N4–C6–H6	124.9
C5–C6–N4	110.2(7)
C5–C6–H6	124.9
N5–C7–H7	124.4
N5–C7–C8	111.3(6)
C8–C7–H7	124.4
C7–C8–H8	127.7
C9–C8–C7	104.7(7)
C9–C8–H8	127.7
N6–C9–C8	109.1(7)
N6–C9–H9	125.5
C8–C9–H9	125.5
W1–C10–H10	108(4)
C11–C10–W1	70.1(4)
C11–C10–H10	116(4)
C11–C10–C16	123.1(7)
C16–C10–W1	123.0(5)

C16–C10–H10	111(4)
W1–C11–H11	102(4)
C10–C11–W1	72.2(4)
C10–C11–H11	109(4)
C10–C11–C12	125.4(7)
C12–C11–W1	121.8(5)
C12–C11–H11	117(4)
C11–C12–H12	114.5
C13–C12–C11	130.9(8)
C13–C12–H12	114.5
C12–C13–H13	115.2
C12–C13–C14	129.6(8)
C14–C13–H13	115.2
C13–C14–H14A	107.5
C13–C14–H14B	107.5
C13–C14–C15	119.2(7)
H14A–C14– H14B	107.0
C15–C14–H14A	107.5
C15–C14–H14B	107.5
C14–C15–H15	114.9
C16–C15–C14	130.1(8)
C16–C15–H15	114.9
C10–C16–H16	114.3
C15–C16–C10	131.4(8)
C15–C16–H16	114.3
P3–C17–H17A	109.5
P3–C17–H17B	109.5
P3–C17–H17C	109.5
H17A–C17– H17B	109.5

H17A–C17– H17C	109.5
H17B–C17– H17C	109.5
P3–C18–H18A	109.5
P3–C18–H18B	109.5
P3–C18–H18C	109.5
H18A–C18– H18B	109.5
H18A–C18– H18C	109.5
H18B–C18– H18C	109.5
P3–C19–H19A	109.5
P3–C19–H19B	109.5
P3–C19–H19C	109.5
H19A–C19– H19B	109.5
H19A–C19– H19C	109.5
H19B–C19– H19C	109.5
N2–B1–N6	109.4(6)
N2–B1–H1A	110.5
N4–B1–N2	110.2(6)
N4–B1–N6	105.6(6)
N4–B1–H1A	110.5
N6–B1–H1A	110.5
Cl2–C20–Cl1	110.7(5)
Cl3–C20–Cl1	109.1(5)
Cl3–C20–Cl2	111.9(5)

Table 5. Torsion angles for mo\_harman\_nb2\_rjs\_triene\_0m

Atom–Atom– Atom–Atom	Torsion Angle [°]
W1–N1–N2–C3	177.4(4)
W1–N1–N2–B1	−0.1(8)
W1–N1–C1–C2	−177.1(5)
W1–N3–N4–C6	−174.5(5)
W1–N3–N4–B1	−10.9(8)
W1–N3–C4–C5	174.8(5)
W1–N5–N6–C9	171.4(5)
W1–N5–N6–B1	2.1(8)
W1–N5–C7–C8	−169.9(5)
W1–C10–C11–C12	116.7(7)

W1-C10-C16-C15	-65.9(11)
W1-C11-C12-C13	70.4(11)
N1-N2-C3-C2	0.5(8)
N1-N2-B1-N4	-57.6(8)
N1-N2-B1-N6	58.1(8)
N1-C1-C2-C3	-0.3(8)
N2-N1-C1-C2	0.6(8)
N3-N4-C6-C5	-1.3(8)
N3-N4-B1-N2	64.4(8)
N3-N4-B1-N6	-53.7(8)
N3-C4-C5-C6	-1.2(9)
N4-N3-C4-C5	0.4(8)
N5-N6-C9-C8	-0.2(8)
N5-N6-B1-N2	-59.6(8)
N5-N6-B1-N4	58.9(8)
N5-C7-C8-C9	-0.1(9)
N6-N5-C7-C8	0.0(8)
C1-N1-N2-C3	-0.6(7)
C1-N1-N2-B1	-178.2(6)
C1-C2-C3-N2	-0.1(8)
C3-N2-B1-N4	125.4(7)
C3-N2-B1-N6	-119.0(7)
C4-N3-N4-C6	0.5(7)
C4-N3-N4-B1	164.1(6)
C4-C5-C6-N4	1.5(9)
C6-N4-B1-N2	-136.0(7)
C6-N4-B1-N6	106.0(8)
C7-N5-N6-C9	0.1(8)
C7-N5-N6-B1	-169.2(6)
C7-C8-C9-N6	0.1(9)
C9-N6-B1-N2	133.4(7)
C9-N6-B1-N4	-108.0(8)
C10-C11-C12-C13	-19.5(14)
C11-C10-C16-C15	20.6(13)
C11-C12-C13-C14	1.5(16)
C12-C13-C14-C15	29.5(15)
C13-C14-C15-C16	-29.2(14)
C14-C15-C16-C10	-2.8(16)
C16-C10-C11-W1	-117.1(7)
C16-C10-C11-C12	-0.4(12)
B1-N2-C3-C2	177.8(7)
B1-N4-C6-C5	-162.6(7)
B1-N6-C9-C8	167.9(7)



## Structure Report for mo\_harman\_mne\_octatetraene\_1\_0

A red, plate-shaped crystal of mo\_harman\_mne\_octatetraene\_1\_0 was coated with Paratone oil and mounted on a MiTeGen micromount. crystallized from hexanes filtrate. Data were collected at 100.00 K on a Bruker D8 VENTURE dual wavelength Mo/Cu Kappa four-circle diffractometer with a PHOTON III detector. The diffractometer was equipped with an Oxford Cryostream 800Plus low temperature device and used Mo  $K_\alpha$  radiation ( $\lambda = 0.71073\text{\AA}$ ) from an Incoatec  $\lambda/\text{ms}$  3.0 microfocus sealed X-ray tube with a HELIOS double bounce multilayer mirror as monochromator.

Data collection and processing were done within the Bruker APEX5 software suite.<sup>[1]</sup> All data were integrated with SAINT 8.40B using a narrow-frame algorithm and a Multi-Scan absorption correction using was applied.<sup>[2]</sup> Using Olex2 as a graphical interface,<sup>[3]</sup> the structure was solved by dual methods with SHELXT 2018/2 and refined by full-matrix least-squares methods against  $F^2$  using SHELXL 2018/3.<sup>[4,5]</sup> All non-hydrogen atoms were refined with anisotropic displacement parameters. All hydrogen atoms were refined with isotropic displacement parameters. Some of their coordinates were refined freely and some on calculated positions using a riding model with their  $U_{\text{iso}}$  values constrained to 1.5 times the  $U_{\text{eq}}$  of their pivot atoms for terminal  $\text{sp}^3$  carbon atoms and 1.2 times for all other carbon atoms.

This report and the CIF file were generated using FinalCif.<sup>[6]</sup>

Table 1. Crystal data and structure refinement for mo\_harman\_mne\_octatetraene\_1\_0

CCDC number	
Empirical formula	$\text{C}_{20}\text{H}_{27}\text{BN}_7\text{OPW}$
Formula weight	607.11
Temperature [K]	100.00
Crystal system	monoclinic
Space group (number)	$P2_1/c$ (14)
$a$ [ $\text{\AA}$ ]	12.2214(5)
$b$ [ $\text{\AA}$ ]	10.1317(4)
$c$ [ $\text{\AA}$ ]	19.2532(6)
$\alpha$ [ $^\circ$ ]	90
$\beta$ [ $^\circ$ ]	105.3930(10)
$\gamma$ [ $^\circ$ ]	90
Volume [ $\text{\AA}^3$ ]	2298.48(15)
$Z$	4

$\rho_{\text{calc}}$ [gcm <sup>-3</sup> ]	1.754
$\mu$ [mm <sup>-1</sup> ]	5.122
$F(000)$	1192
Crystal size [mm <sup>3</sup> ]	0.048×0.076×0.124
Crystal colour	red
Crystal shape	plate
Radiation	Mo $K_{\alpha}$ ( $\lambda=0.71073$ Å)
2 $\theta$ range [°]	4.58 to 55.08 (0.77 Å)
Index ranges	-15 ≤ h ≤ 15 -13 ≤ k ≤ 13 -25 ≤ l ≤ 23
Reflections collected	67248
Independent reflections	5292 $R_{\text{int}} = 0.0595$ $R_{\text{sigma}} = 0.0238$
Completeness to $\theta = 25.242^{\circ}$	99.9
Data / Restraints / Parameters	5292 / 0 / 295
Goodness-of-fit on $F^2$	1.099
Final $R$ indexes [ $\geq 2\sigma(I)$ ]	$R_1 = 0.0231$ $wR_2 = 0.0482$
Final $R$ indexes [all data]	$R_1 = 0.0278$ $wR_2 = 0.0498$
Largest peak/hole [eÅ <sup>-3</sup> ]	0.86/-1.50

Table 2. Atomic coordinates and Ueq [Å<sup>2</sup>] for mo\_harman\_mne\_octatetraene\_1\_0

Atom	x	y	z	U <sub>eq</sub>
W1	0.24683(2)	0.63750(2)	0.32292(2)	0.01100(4)
P1	0.26841(7)	0.87903(8)	0.29640(4)	0.01500(16)
O1	0.0496(2)	0.5909(3)	0.19500(13)	0.0306(6)
N1	0.3818(2)	0.6742(3)	0.42522(13)	0.0145(5)
N2	0.3601(2)	0.6558(3)	0.49064(13)	0.0152(5)
N3	0.1312(2)	0.7243(3)	0.38139(13)	0.0146(5)
N4	0.1545(2)	0.7192(3)	0.45491(14)	0.0155(5)
N5	0.2033(2)	0.4707(3)	0.38485(13)	0.0146(5)
N6	0.2064(2)	0.4843(3)	0.45608(13)	0.0147(5)
N7	0.1321(2)	0.6090(3)	0.24581(14)	0.0166(5)
C1	0.4918(3)	0.7065(3)	0.43900(17)	0.0179(6)
H1	0.530434	0.724882	0.403276	0.021
C2	0.5417(3)	0.7093(3)	0.51286(17)	0.0203(7)
H2	0.618306	0.729197	0.536930	0.024
C3	0.4554(3)	0.6769(3)	0.54339(17)	0.0186(7)
H3	0.462119	0.670394	0.593573	0.022
C4	0.0365(3)	0.7967(3)	0.35886(19)	0.0202(7)
H4	-0.000023	0.816088	0.309922	0.024
C5	-0.0006(3)	0.8392(3)	0.4176(2)	0.0240(7)
H5	-0.064919	0.892555	0.416737	0.029
C6	0.0757(3)	0.7874(3)	0.47682(19)	0.0214(7)
H6	0.073202	0.798128	0.525389	0.026
C7	0.1504(3)	0.3563(3)	0.36307(17)	0.0177(6)
H7	0.135712	0.322009	0.315555	0.021
C8	0.1201(3)	0.2945(3)	0.41996(18)	0.0205(7)
H8	0.082920	0.211998	0.419326	0.025

C9	0.1557(3)	0.3795(3)	0.47712(17) )	0.0181(6)
H9	0.146032	0.366286	0.523990	0.022
C10	0.3789(3)	0.6195(3)	0.26045(17) )	0.0154(6)
H10	0.440(3)	0.672(3)	0.2836(18)	0.015(9)
C11	0.3736(3)	0.4984(3)	0.29745(16) )	0.0154(6)
H11	0.426(3)	0.497(3)	0.3433(19)	0.016(9)
C12	0.3351(3)	0.3666(3)	0.27390(18) )	0.0203(7)
H12	0.330673	0.312003	0.313164	0.024
C13	0.3038(3)	0.3012(3)	0.21056(19) )	0.0220(7)
H13	0.281971	0.212620	0.215915	0.026
C14	0.2959(3)	0.3350(3)	0.13718(18) )	0.0215(7)
H14	0.287217	0.259972	0.106631	0.026
C15	0.2982(3)	0.4502(4)	0.10130(18) )	0.0235(7)
H15	0.292254	0.437194	0.051570	0.028
C16	0.3074(3)	0.5866(4)	0.12142(17) )	0.0223(7)
H16	0.285675	0.643663	0.080914	0.027
C17	0.3395(3)	0.6535(3)	0.18401(18) )	0.0213(7)
H17	0.335457	0.746253	0.176657	0.026
C18	0.4029(3)	0.9412(3)	0.28584(19) )	0.0218(7)
H18A	0.421214	0.896381	0.245236	0.033
H18B	0.462970	0.924198	0.330000	0.033
H18C	0.396788	1.036363	0.276606	0.033
C19	0.2529(3)	0.9897(4)	0.3679(2)	0.0318(9)
H19A	0.303503	0.961129	0.413904	0.048
H19B	0.174153	0.987705	0.370973	0.048
H19C	0.272700	1.079811	0.357206	0.048
C20	0.1625(3)	0.9377(4)	0.2172(2)	0.0300(9)
H20A	0.086821	0.929363	0.225033	0.045
H20B	0.166348	0.884813	0.175262	0.045
H20C	0.177360	1.030477	0.208547	0.045
B1	0.2422(3)	0.6162(3)	0.49569(19) )	0.0156(7)
H1A	0.246(3)	0.607(4)	0.5525(19)	0.021(9)

$U_{eq}$  is defined as 1/3 of the trace of the orthogonalized  $U_{ij}$  tensor.

Table 3. Anisotropic displacement parameters ( $\text{\AA}^2$ ) for mo\_harman\_mne\_octatetraene\_1\_0. The anisotropic displacement factor exponent takes the form:  $-2\pi^2[h^2(a^*)^2U_{11} + k^2(b^*)^2U_{22} + \dots + 2hka^*b^*U_{12}]$

Atom	$U_{11}$	$U_{22}$	$U_{33}$	$U_{23}$	$U_{13}$	$U_{12}$
W1	0.01149(6)	0.01027(6)	0.01120(6)	0.00163(4)	0.00295(4)	0.00011(5)
P1	0.0133(4)	0.0108(4)	0.0208(4)	0.0017(3)	0.0044(3)	-0.0003(3)
O1	0.0283(14)	0.0298(14)	0.0241(13)	-0.0021(11)	-0.0099(11)	-0.0083(11)
N1	0.0145(13)	0.0161(13)	0.0134(12)	0.0013(10)	0.0045(10)	-0.0007(10)
N2	0.0155(13)	0.0177(14)	0.0130(12)	0.0004(10)	0.0050(10)	0.0021(10)
N3	0.0114(13)	0.0165(13)	0.0156(12)	0.0002(10)	0.0032(10)	0.0004(10)
N4	0.0141(13)	0.0170(13)	0.0169(13)	0.0007(10)	0.0067(10)	-0.0007(10)
N5	0.0145(13)	0.0159(13)	0.0136(12)	0.0022(10)	0.0042(10)	0.0007(10)
N6	0.0134(13)	0.0179(14)	0.0132(12)	0.0040(10)	0.0039(10)	0.0004(10)
N7	0.0201(14)	0.0124(13)	0.0157(12)	0.0011(10)	0.0022(11)	-0.0009(10)
C1	0.0122(15)	0.0212(17)	0.0203(15)	0.0018(13)	0.0043(12)	0.0021(12)
C2	0.0117(15)	0.0247(18)	0.0213(16)	-0.0013(13)	-0.0013(12)	0.0009(13)
C3	0.0179(16)	0.0200(16)	0.0155(15)	0.0010(12)	0.0003(12)	0.0038(13)
C4	0.0106(15)	0.0214(17)	0.0278(17)	0.0045(14)	0.0040(13)	0.0015(13)
C5	0.0142(16)	0.0233(18)	0.037(2)	0.0044(15)	0.0113(14)	0.0056(13)
C6	0.0185(17)	0.0232(18)	0.0267(17)	-0.0009(14)	0.0135(14)	0.0005(13)
C7	0.0163(15)	0.0150(15)	0.0209(15)	0.0006(12)	0.0032(12)	0.0004(13)
C8	0.0190(17)	0.0159(16)	0.0293(18)	0.0030(13)	0.0110(14)	-0.0011(13)
C9	0.0171(15)	0.0172(16)	0.0215(16)	0.0075(12)	0.0077(12)	0.0021(12)
C10	0.0178(15)	0.0117(15)	0.0187(15)	-0.0008(12)	0.0081(12)	0.0012(12)
C11	0.0198(16)	0.0145(15)	0.0129(14)	-0.0002(12)	0.0061(12)	0.0009(12)
C12	0.0225(17)	0.0141(15)	0.0261(17)	0.0057(13)	0.0094(13)	0.0035(13)
C13	0.0149(16)	0.0170(16)	0.0336(19)	0.0006(14)	0.0056(14)	0.0011(13)
C14	0.0127(15)	0.0241(18)	0.0267(17)	-0.0096(14)	0.0033(13)	-0.0018(13)
C15	0.0155(16)	0.037(2)	0.0168(15)	-0.0066(14)	0.0027(13)	-0.0022(14)
C16	0.0224(17)	0.0299(18)	0.0154(15)	0.0051(14)	0.0064(13)	0.0027(15)
C17	0.0299(18)	0.0149(16)	0.0235(16)	0.0041(13)	0.0148(14)	0.0060(14)
C18	0.0201(17)	0.0156(16)	0.0298(18)	0.0042(13)	0.0072(14)	-0.0022(13)
C19	0.035(2)	0.0202(18)	0.046(2)	-0.0157(16)	0.0222(18)	-0.0070(16)
C20	0.0228(19)	0.0219(19)	0.039(2)	0.0158(16)	-0.0026(16)	-0.0022(14)

B1	0.0182(17)	0.0159(18)	0.0141(16)	0.0014(13)	0.0064(13)	0.0026(14)
----	------------	------------	------------	------------	------------	------------

Table 4. Bond lengths and angles for mo\_harman\_mne\_octatetraene\_1\_0

Atom–Atom	Length [Å]		
W1–P1	2.5279(8)	C12–H12	0.9500
W1–N1	2.239(3)	C12–C13	1.351(5)
W1–N3	2.209(3)	C13–H13	0.9500
W1–N5	2.213(3)	C13–C14	1.432(5)
W1–N7	1.774(3)	C14–H14	0.9500
W1–C10	2.262(3)	C14–C15	1.360(5)
W1–C11	2.243(3)	C15–H15	0.9500
P1–C18	1.821(3)	C15–C16	1.432(5)
P1–C19	1.824(4)	C16–H16	0.9500
P1–C20	1.818(3)	C16–C17	1.347(5)
O1–N7	1.218(3)	C17–H17	0.9500
N1–N2	1.367(3)	C18–H18A	0.9800
N1–C1	1.341(4)	C18–H18B	0.9800
N2–C3	1.344(4)	C18–H18C	0.9800
N2–B1	1.523(4)	C19–H19A	0.9800
N3–N4	1.369(3)	C19–H19B	0.9800
N3–C4	1.341(4)	C19–H19C	0.9800
N4–C6	1.341(4)	C20–H20A	0.9800
N4–B1	1.552(4)	C20–H20B	0.9800
N5–N6	1.369(3)	C20–H20C	0.9800
N5–C7	1.339(4)	B1–H1A	1.09(4)
N6–C9	1.346(4)		
N6–B1	1.543(4)	<b>Atom–Atom–</b>	<b>Angle [°]</b>
C1–H1	0.9500	N1–W1–P1	85.70(7)
C1–C2	1.391(4)	N1–W1–C10	91.04(11)
C2–H2	0.9500	N1–W1–C11	84.63(10)
C2–C3	1.376(5)	N3–W1–P1	80.36(7)
C3–H3	0.9500	N3–W1–N1	84.67(9)
C4–H4	0.9500	N3–W1–N5	75.64(9)
C4–C5	1.393(5)	N3–W1–C10	161.12(10)
C5–H5	0.9500	N3–W1–C11	159.04(10)
C5–C6	1.372(5)	N5–W1–P1	154.29(7)
C6–H6	0.9500	N5–W1–N1	83.06(9)
C7–H7	0.9500	N5–W1–C10	122.16(10)
C7–C8	1.395(4)	N5–W1–C11	85.21(10)
C8–H8	0.9500	N7–W1–P1	95.18(8)
C8–C9	1.373(5)	N7–W1–N1	175.59(11)
C9–H9	0.9500	N7–W1–N3	91.21(11)
C10–H10	0.93(4)	N7–W1–N5	94.41(11)
C10–C11	1.429(4)	N7–W1–C10	93.37(12)
C10–C17	1.463(4)	N7–W1–C11	98.79(12)
C11–H11	0.95(4)	C10–W1–P1	80.99(8)
C11–C12	1.447(4)	C11–W1–P1	116.69(8)

C11-W1-C10	36.98(11)
C18-P1-W1	120.19(11)
C18-P1-C19	98.59(17)
C19-P1-W1	113.92(13)
C20-P1-W1	113.37(12)
C20-P1-C18	104.82(17)
C20-P1-C19	103.8(2)
N2-N1-W1	120.67(19)
C1-N1-W1	132.9(2)
C1-N1-N2	106.3(2)
N1-N2-B1	120.9(2)
C3-N2-N1	109.5(3)
C3-N2-B1	129.7(3)
N4-N3-W1	121.74(19)
C4-N3-W1	131.8(2)
C4-N3-N4	106.3(3)
N3-N4-B1	118.4(2)
C6-N4-N3	109.6(3)
C6-N4-B1	130.1(3)
N6-N5-W1	121.07(19)
C7-N5-W1	131.1(2)
C7-N5-N6	106.5(2)
N5-N6-B1	120.8(2)
C9-N6-N5	109.2(3)
C9-N6-B1	128.9(3)
O1-N7-W1	176.6(3)
N1-C1-H1	124.7
N1-C1-C2	110.6(3)
C2-C1-H1	124.7
C1-C2-H2	127.6
C3-C2-C1	104.8(3)
C3-C2-H2	127.6
N2-C3-C2	108.9(3)
N2-C3-H3	125.6
C2-C3-H3	125.6
N3-C4-H4	124.9
N3-C4-C5	110.2(3)
C5-C4-H4	124.9
C4-C5-H5	127.5
C6-C5-C4	105.1(3)
C6-C5-H5	127.5
N4-C6-C5	108.8(3)
N4-C6-H6	125.6
C5-C6-H6	125.6
N5-C7-H7	124.8
N5-C7-C8	110.4(3)
C8-C7-H7	124.8
C7-C8-H8	127.6

C9-C8-C7	104.7(3)
C9-C8-H8	127.6
N6-C9-C8	109.1(3)
N6-C9-H9	125.5
C8-C9-H9	125.5
W1-C10-H10	107(2)
C11-C10-W1	70.78(17)
C11-C10-H10	113(2)
C11-C10-C17	131.1(3)
C17-C10-W1	115.1(2)
C17-C10-H10	111(2)
W1-C11-H11	98(2)
C10-C11-W1	72.23(18)
C10-C11-H11	111(2)
C10-C11-C12	133.6(3)
C12-C11-W1	117.5(2)
C12-C11-H11	111(2)
C11-C12-H12	111.7
C13-C12-C11	136.5(3)
C13-C12-H12	111.7
C12-C13-H13	112.7
C12-C13-C14	134.6(3)
C14-C13-H13	112.7
C13-C14-H14	112.7
C15-C14-C13	134.5(3)
C15-C14-H14	112.7
C14-C15-H15	112.7
C14-C15-C16	134.6(3)
C16-C15-H15	112.7
C15-C16-H16	112.3
C17-C16-C15	135.3(3)
C17-C16-H16	112.3
C10-C17-H17	111.9
C16-C17-C10	136.2(3)
C16-C17-H17	111.9
P1-C18-H18A	109.5
P1-C18-H18B	109.5
P1-C18-H18C	109.5
H18A-C18-H18B	109.5
H18A-C18-H18C	109.5
H18B-C18-H18C	109.5
P1-C19-H19A	109.5
P1-C19-H19B	109.5
P1-C19-H19C	109.5

H19A–C19– H19B	109.5
H19A–C19– H19C	109.5
H19B–C19– H19C	109.5
P1–C20–H20A	109.5
P1–C20–H20B	109.5
P1–C20–H20C	109.5
H20A–C20– H20B	109.5

H20A–C20– H20C	109.5
H20B–C20– H20C	109.5
N2–B1–N4	109.2(3)
N2–B1–N6	110.2(3)
N2–B1–H1A	107(2)
N4–B1–H1A	114.2(19)
N6–B1–N4	105.4(2)
N6–B1–H1A	111(2)

Table 5. Torsion angles for mo\_harman\_mne\_octatetraene\_1\_0

Atom–Atom– Atom–Atom	Torsion Angle [°]
W1–N1–N2–C3	176.6(2)
W1–N1–N2–B1	–2.9(4)
W1–N1–C1–C2	–175.9(2)
W1–N3–N4–C6	175.3(2)
W1–N3–N4–B1	–18.6(3)
W1–N3–C4–C5	–174.3(2)
W1–N5–N6–C9	168.0(2)
W1–N5–N6–B1	–0.9(4)
W1–N5–C7–C8	–167.1(2)
W1–C10–C11–C12	111.4(4)
W1–C10–C17–C16	–102.0(4)
W1–C11–C12–C13	101.7(4)
N1–N2–C3–C2	–0.1(4)
N1–N2–B1–N4	–56.4(4)
N1–N2–B1–N6	58.9(3)
N1–C1–C2–C3	0.0(4)
N2–N1–C1–C2	0.0(4)
N3–N4–C6–C5	–0.3(4)
N3–N4–B1–N2	69.5(3)
N3–N4–B1–N6	–48.9(3)
N3–C4–C5–C6	–0.8(4)
N4–N3–C4–C5	0.6(4)
N5–N6–C9–C8	0.9(4)
N5–N6–B1–N2	–57.0(3)
N5–N6–B1–N4	60.6(3)
N5–C7–C8–C9	1.1(4)
N6–N5–C7–C8	–0.6(3)

C1–N1–N2–C3	0.1(3)
C1–N1–N2–B1	–179.3(3)
C1–C2–C3–N2	0.1(4)
C3–N2–B1–N4	124.3(3)
C3–N2–B1–N6	–120.4(3)
C4–N3–N4–C6	–0.2(3)
C4–N3–N4–B1	165.8(3)
C4–C5–C6–N4	0.6(4)
C6–N4–B1–N2	–127.8(3)
C6–N4–B1–N6	113.8(3)
C7–N5–N6–C9	–0.2(3)
C7–N5–N6–B1	–169.1(3)
C7–C8–C9–N6	–1.2(4)
C9–N6–B1–N2	136.5(3)
C9–N6–B1–N4	–105.9(3)
C10–C11–C12–C13	10.5(7)
C11–C10–C17–C16	–16.2(7)
C11–C12–C13–C14	0.7(7)
C12–C13–C14–C15	–13.5(7)
C13–C14–C15–C16	–1.3(7)
C14–C15–C16–C17	16.1(7)
C15–C16–C17–C10	–0.6(7)
C17–C10–C11–W1	–107.0(4)
C17–C10–C11–C12	4.4(6)
B1–N2–C3–C2	179.2(3)
B1–N4–C6–C5	–164.2(3)
B1–N6–C9–C8	168.6(3)



## Structure Report for cu\_harman\_3\_jkh\_291\_x2\_0m

A yellow, needle-shaped crystal of cu\_harman\_3\_jkh\_291\_x2\_0m was coated with Paratone oil and mounted on a MiTeGen micromount. Data were collected at 100.00 K on a Bruker D8 VENTURE dual wavelength Mo/Cu Kappa four-circle diffractometer with a PHOTON III detector. The diffractometer was equipped with an Oxford Cryostream 800Plus low temperature device and used Cu  $K_\alpha$  radiation ( $\lambda = 1.54178\text{\AA}$ ) from an Incoatec I $\mu$ s 3.0 microfocus sealed X-ray tube with a HELIOS EF double bounce multilayer mirror as monochromator.

Data collection and processing were done within the Bruker APEX5 software suite.<sup>[1]</sup> All data were integrated with SAINT V8.40B using a narrow-frame algorithm and a Multi-Scan absorption correction using SADABS 2016/2 was applied.<sup>[2]</sup> Using Olex2 as a graphical interface,<sup>[3]</sup> the structure was solved by dual methods with SHELXT and refined by full-matrix least-squares methods against  $F^2$  using SHELXL.<sup>[4,5]</sup> All non-hydrogen atoms were refined with anisotropic displacement parameters. All C-bound hydrogen atoms were refined isotropic on calculated positions using a riding model with their  $U_{\text{iso}}$  values constrained to 1.5 times the  $U_{\text{eq}}$  of their pivot atoms for terminal  $\text{sp}^3$  carbon atoms and 1.2 times for all other carbon atoms. Disordered moieties were refined using bond lengths restraints and displacement parameter restraints.

This report and the CIF file were generated using FinalCif.<sup>[6]</sup>

### Refinement details for cu\_harman\_3\_jkh\_291\_x2\_0m

The relative occupancy of the disordered atoms was freely refined. Constraints and restraints were used as needed on the anisotropic displacement parameters and/or bond lengths of the disordered atoms.

Table 1. Crystal data and structure refinement for cu\_harman\_3\_jkh\_291\_x2\_0m

CCDC number	
Empirical formula	C <sub>26</sub> H <sub>26</sub> BCl <sub>4</sub> N <sub>9</sub> O <sub>3</sub> PW
Formula weight	879.99
Temperature [K]	100.00
Crystal system	monoclinic
Space group (number)	<i>P</i> 2 <sub>1</sub> / <i>c</i> (14)
<i>a</i> [Å]	9.5771(3)
<i>b</i> [Å]	25.8938(9)
<i>c</i> [Å]	13.4294(3)
$\alpha$ [°]	90
$\beta$ [°]	107.546(2)
$\gamma$ [°]	90
Volume [Å <sup>3</sup> ]	3175.38(17)
<i>Z</i>	4
$\rho_{\text{calc}}$ [gcm <sup>-3</sup> ]	1.841
$\mu$ [mm <sup>-1</sup> ]	10.708
<i>F</i> (000)	1724
Crystal size [mm <sup>3</sup> ]	0.018×0.027×0.127
Crystal colour	yellow
Crystal shape	needle
Radiation	Cu <i>K</i> $\alpha$ ( $\lambda$ =1.54178 Å)
2 $\theta$ range [°]	7.70 to 133.22 (0.84 Å)
Index ranges	−11 ≤ <i>h</i> ≤ 11 −29 ≤ <i>k</i> ≤ 30 −15 ≤ <i>l</i> ≤ 15
Reflections collected	25375
Independent reflections	5606 <i>R</i> <sub>int</sub> = 0.1649 <i>R</i> <sub>sigma</sub> = 0.1155
Completeness to $\theta$ = 66.612°	99.9
Data / Restraints / Parameters	5606 / 20 / 425
Goodness-of-fit on <i>F</i> <sup>2</sup>	1.046
Final <i>R</i> indexes [ $\geq 2\sigma(I)$ ]	<i>R</i> <sub>1</sub> = 0.0624 <i>wR</i> <sub>2</sub> = 0.1326
Final <i>R</i> indexes [all data]	<i>R</i> <sub>1</sub> = 0.1120 <i>wR</i> <sub>2</sub> = 0.1550
Largest peak/hole [eÅ <sup>-3</sup> ]	1.28/−0.76

Table 2. Atomic coordinates and Ueq [Å<sup>2</sup>] for cu\_harman\_3\_jkh\_291\_x2\_0m

Atom	x	y	z	U <sub>eq</sub>
W1	0.69439(6)	0.66631(2)	0.50049(4)	0.04236(17)
P1	0.5760(3)	0.70861(13)	0.3245(2)	0.0476(7)
O1	0.4411(9)	0.6959(4)	0.5733(6)	0.061(2)
N1	0.8812(10)	0.6556(4)	0.4383(7)	0.048(2)
N2	1.0146(11)	0.6795(4)	0.4860(7)	0.055(3)
N3	0.7693(11)	0.7459(3)	0.5316(6)	0.044(2)
N4	0.9176(11)	0.7570(4)	0.5580(6)	0.047(2)
N5	0.8626(9)	0.6592(4)	0.6505(6)	0.042(2)
N6	0.9959(10)	0.6804(4)	0.6677(7)	0.047(2)
N7	0.5430(12)	0.6828(4)	0.5450(7)	0.052(3)
C1	0.9041(12)	0.6320(4)	0.3546(9)	0.047(3)
H1	0.832950	0.611559	0.305888	0.056
C2	1.0420(16)	0.6411(6)	0.3487(11)	0.069(4)
H2	1.083539	0.628908	0.297208	0.083
C3	1.1074(13)	0.6716(6)	0.4332(9)	0.067(4)
H3	1.204286	0.684892	0.450607	0.080
C4	0.7005(16)	0.7900(5)	0.5320(8)	0.052(3)
H4	0.597576	0.793583	0.517395	0.062
C5	0.7986(17)	0.8299(5)	0.5565(9)	0.058(3)
H5	0.777552	0.865411	0.562186	0.069
C6	0.9318(16)	0.8083(5)	0.5710(9)	0.062(4)
H6	1.021772	0.826691	0.587818	0.074
C7	0.8591(13)	0.6357(4)	0.7414(8)	0.046(3)
H7	0.778318	0.617359	0.751010	0.055
C8	0.9917(15)	0.6432(5)	0.8161(9)	0.056(3)
H8	1.019320	0.631756	0.886612	0.067
C9	1.0768(13)	0.6707(5)	0.7676(9)	0.053(3)
H9	1.175378	0.681105	0.799104	0.063
C10	0.6855(16)	0.5778(4)	0.5028(10)	0.055(3)
H10	0.789105	0.574303	0.523948	0.066
C11	0.5945(16)	0.5936(5)	0.4048(10)	0.059(3)
H11	0.626433	0.604800	0.347903	0.071
C12	0.4450(15)	0.5901(5)	0.4052(11)	0.061(3)
H12	0.361163	0.598073	0.348193	0.073
C13	0.4441(17)	0.5736(5)	0.4996(10)	0.067(4)
H13	0.359352	0.566853	0.520353	0.081
C14	0.5910(15)	0.5680(5)	0.5633(10)	0.056(3)
H14	0.621057	0.559135	0.635249	0.068
C15	0.5187(13)	0.6678(6)	0.2086(8)	0.059(3)
H15A	0.474100	0.689259	0.147078	0.089

H15B	0.447196	0.642378	0.216759	0.089
H15C	0.604187	0.649841	0.199537	0.089
C16	0.4074(13)	0.7419(5)	0.3162(9)	0.054(3)
H16A	0.422943	0.765443	0.375656	0.081
H16B	0.331664	0.716639	0.317390	0.081
H16C	0.375926	0.761645	0.250984	0.081
C17	0.6958(14)	0.7546(5)	0.2927(8)	0.055(3)
H17A	0.645946	0.770662	0.225213	0.083
H17B	0.784512	0.737037	0.288465	0.083
H17C	0.722574	0.781292	0.346881	0.083
B1	1.0290(18)	0.7140(6)	0.5807(11)	0.057(4)
H1A	1.130232	0.728505	0.606556	0.068
Cl1	0.4851(4)	0.62270(11 )	-0.2043(2)	0.0569(8)
Cl2	0.4912(4)	0.50288(12 )	-0.2434(2)	0.0604(8)
O2	0.3653(9)	0.6484(3)	-0.0347(5)	0.0489(19)
O3	0.3655(12)	0.4426(3)	-0.1092(7)	0.070(3)
N8	0.1901(11)	0.6011(4)	0.1396(7)	0.052(2)
N9	0.1675(16)	0.4496(5)	0.0730(9)	0.077(4)
C18	0.3022(15)	0.5647(5)	0.0026(9)	0.052(3)
C19	0.3659(13)	0.6014(4)	-0.0512(8)	0.045(3)
C20	0.4245(13)	0.5798(4)	-0.1295(8)	0.044(3)
C21	0.4251(16)	0.5281(5)	-0.1489(9)	0.057(3)
C22	0.3644(17)	0.4892(5)	-0.0904(10 )	0.061(4)
C23	0.3000(13)	0.5096(4)	-0.0138(9)	0.043(3)
C24	0.2377(15)	0.5839(5)	0.0799(9)	0.053(3)
C25	0.2270(17)	0.4766(5)	0.0348(9)	0.061(4)
Cl3	-0.1076(7)	0.4378(2)	0.3873(5)	0.051(2)
Cl4	0.0178(9)	0.4987(3)	0.2556(5)	0.069(3)
C26	-0.077(4)	0.5001(8)	0.348(2)	0.087(11)
H26A	-0.172105	0.517703	0.317679	0.104
H26B	-0.019927	0.520141	0.409491	0.104
Cl4A	0.129(3)	0.5111(10)	0.319(2)	0.243(9)
C26A	-0.056(5)	0.494(3)	0.271(4)	0.243(9)
H26C	-0.072523	0.471720	0.208354	0.291
H26D	-0.117639	0.525101	0.251413	0.291
Cl3A	-0.100(3)	0.4602(12)	0.370(3)	0.243(9)

$U_{eq}$  is defined as 1/3 of the trace of the orthogonalized  $U_{ij}$  tensor.

Table 3. Anisotropic displacement parameters ( $\text{\AA}^2$ ) for cu\_harman\_3\_jkh\_291\_x2\_0m. The anisotropic displacement factor exponent takes the form:  $-2\pi^2[ h^2(a^*)^2U_{11} + k^2(b^*)^2U_{22} + \dots + 2hka^*b^*U_{12} ]$

Atom	$U_{11}$	$U_{22}$	$U_{33}$	$U_{23}$	$U_{13}$	$U_{12}$
W1	0.0485(3)	0.0472(3)	0.0337(2)	-0.0019(3)	0.01596(19)	-0.0008(3)
P1	0.0513(17)	0.0592(19)	0.0318(13)	-0.0004(13)	0.0118(13)	-0.0036(14)
O1	0.052(5)	0.082(6)	0.058(5)	-0.005(5)	0.030(4)	0.008(5)
N1	0.041(5)	0.061(7)	0.046(5)	0.012(5)	0.020(4)	0.010(5)
N2	0.044(5)	0.088(8)	0.037(5)	0.009(5)	0.019(4)	-0.002(5)
N3	0.069(6)	0.041(6)	0.026(4)	-0.004(4)	0.023(4)	-0.006(5)
N4	0.053(6)	0.054(6)	0.029(4)	0.002(4)	0.007(4)	-0.012(5)
N5	0.039(5)	0.048(6)	0.043(5)	0.005(4)	0.016(4)	0.005(4)
N6	0.036(5)	0.069(7)	0.034(5)	0.000(4)	0.007(4)	-0.001(4)
N7	0.067(7)	0.046(6)	0.043(5)	-0.009(4)	0.018(5)	-0.008(5)
C1	0.042(6)	0.050(7)	0.051(6)	-0.003(5)	0.018(5)	0.012(5)
C2	0.060(8)	0.097(11)	0.061(8)	0.009(8)	0.033(7)	0.000(8)
C3	0.040(6)	0.112(12)	0.047(7)	0.015(8)	0.010(5)	-0.001(8)
C4	0.087(9)	0.044(7)	0.028(5)	0.006(5)	0.024(6)	-0.001(7)
C5	0.101(11)	0.032(6)	0.043(6)	-0.001(6)	0.027(7)	-0.008(8)
C6	0.072(9)	0.066(9)	0.046(7)	0.006(6)	0.017(7)	-0.027(8)
C7	0.051(7)	0.053(7)	0.040(6)	0.003(5)	0.022(5)	0.004(6)
C8	0.072(9)	0.058(8)	0.039(6)	0.003(5)	0.021(6)	-0.005(7)
C9	0.045(6)	0.062(8)	0.048(6)	0.007(6)	0.008(5)	-0.003(6)
C10	0.068(8)	0.042(7)	0.061(7)	-0.004(6)	0.030(6)	-0.006(7)
C11	0.084(10)	0.051(8)	0.054(7)	-0.003(6)	0.036(7)	-0.017(7)
C12	0.059(8)	0.069(9)	0.067(8)	-0.007(7)	0.037(7)	-0.013(7)
C13	0.078(10)	0.070(9)	0.063(8)	-0.019(7)	0.035(8)	-0.022(8)
C14	0.070(9)	0.046(7)	0.055(7)	-0.001(6)	0.024(7)	-0.002(6)
C15	0.044(6)	0.086(10)	0.045(6)	-0.013(7)	0.009(5)	-0.022(7)
C16	0.054(7)	0.063(8)	0.043(6)	0.005(6)	0.012(6)	0.001(6)
C17	0.066(8)	0.072(9)	0.029(5)	0.006(5)	0.018(5)	0.002(7)
B1	0.064(9)	0.061(10)	0.049(8)	0.016(7)	0.024(7)	-0.011(8)
Cl1	0.083(2)	0.0479(17)	0.0496(15)	-0.0001(13)	0.0342(16)	-0.0036(15)
Cl2	0.090(2)	0.0485(18)	0.0545(16)	-0.0057(14)	0.0402(17)	-0.0011(16)
O2	0.062(5)	0.046(5)	0.036(4)	-0.001(3)	0.011(4)	0.003(4)
O3	0.110(8)	0.035(5)	0.077(6)	-0.005(4)	0.046(6)	-0.003(5)
N8	0.057(6)	0.054(6)	0.049(6)	0.006(5)	0.019(5)	0.013(5)
N9	0.114(11)	0.064(8)	0.071(8)	0.002(6)	0.056(8)	-0.008(7)
C18	0.054(7)	0.064(8)	0.042(6)	-0.004(6)	0.020(5)	0.006(7)
C19	0.049(7)	0.044(7)	0.039(6)	-0.004(5)	0.009(5)	0.001(5)
C20	0.055(7)	0.043(7)	0.034(5)	-0.001(5)	0.013(5)	0.002(5)
C21	0.083(10)	0.052(8)	0.046(7)	0.008(6)	0.035(7)	0.012(7)
C22	0.086(10)	0.056(9)	0.051(7)	-0.004(6)	0.034(7)	-0.011(7)

C23	0.046(6)	0.041(6)	0.051(6)	-0.014(5)	0.028(5)	-0.006(5)
C24	0.071(8)	0.055(8)	0.040(6)	0.003(5)	0.027(6)	0.009(6)
C25	0.088(10)	0.056(8)	0.045(7)	-0.007(6)	0.030(7)	-0.008(7)
Cl3	0.048(3)	0.058(4)	0.049(3)	0.003(2)	0.015(3)	0.014(3)
Cl4	0.078(5)	0.073(5)	0.062(4)	0.001(3)	0.029(3)	0.002(4)
C26	0.15(3)	0.052(16)	0.10(2)	0.030(15)	0.09(2)	0.040(17)
Cl4A	0.191(17)	0.23(2)	0.30(2)	0.012(16)	0.062(17)	0.014(15)
C26A	0.191(17)	0.23(2)	0.30(2)	0.012(16)	0.062(17)	0.014(15)
Cl3A	0.191(17)	0.23(2)	0.30(2)	0.012(16)	0.062(17)	0.014(15)

Table 4. Bond lengths and angles for cu\_harman\_3\_jkh\_291\_x2\_0m

Atom-Atom	Length [Å]		
W1-P1	2.540(3)	C8-H8	0.9500
W1-N1	2.208(8)	C8-C9	1.385(16)
W1-N3	2.181(9)	C9-H9	0.9500
W1-N5	2.175(9)	C10-H10	0.9500
W1-N7	1.779(10)	C10-C11	1.403(18)
W1-C10	2.295(11)	C10-C14	1.409(16)
W1-C11	2.317(13)	C11-H11	0.9500
P1-C15	1.824(12)	C11-C12	1.436(18)
P1-C16	1.803(12)	C12-H12	0.9500
P1-C17	1.794(12)	C12-C13	1.341(17)
O1-N7	1.198(12)	C13-H13	0.9500
N1-N2	1.391(14)	C13-C14	1.42(2)
N1-C1	1.354(13)	C14-H14	0.9500
N2-C3	1.310(14)	C15-H15A	0.9800
N2-B1	1.526(17)	C15-H15B	0.9800
N3-N4	1.387(13)	C15-H15C	0.9800
N3-C4	1.319(15)	C16-H16A	0.9800
N4-C6	1.341(16)	C16-H16B	0.9800
N4-B1	1.509(18)	C16-H16C	0.9800
N5-N6	1.344(12)	C17-H17A	0.9800
N5-C7	1.372(13)	C17-H17B	0.9800
N6-C9	1.356(14)	C17-H17C	0.9800
N6-B1	1.563(15)	B1-H1A	1.0000
C1-H1	0.9500	Cl1-C20	1.712(11)
C1-C2	1.368(17)	Cl2-C21	1.709(11)
C2-H2	0.9500	O2-C19	1.239(13)
C2-C3	1.37(2)	O3-C22	1.234(15)
C3-H3	0.9500	N8-C24	1.127(13)
C4-H4	0.9500	N9-C25	1.120(16)
C4-C5	1.367(18)	C18-C19	1.435(16)
C5-H5	0.9500	C18-C23	1.443(16)
C5-C6	1.351(19)	C18-C24	1.447(15)
C6-H6	0.9500	C19-C20	1.446(15)
C7-H7	0.9500	C20-C21	1.363(16)
C7-C8	1.374(17)	C21-C22	1.499(16)
		C22-C23	1.448(15)

C23–C25	1.385(16)
Cl3–C26	1.749(17)
Cl4–C26	1.743(16)
C26–H26A	0.9900
C26–H26B	0.9900
Cl4A–C26A	1.75(2)
C26A–H26C	0.9900
C26A–H26D	0.9900
C26A–Cl3A	1.75(2)
<b>Atom–Atom–Atom</b>	<b>Angle [°]</b>
N1–W1–P1	83.6(2)
N1–W1–C10	85.2(4)
N1–W1–C11	86.2(4)
N3–W1–P1	78.4(2)
N3–W1–N1	86.2(4)
N3–W1–C10	162.3(5)
N3–W1–C11	158.6(4)
N5–W1–P1	153.7(2)
N5–W1–N1	83.2(3)
N5–W1–N3	78.1(3)
N5–W1–C10	85.6(4)
N5–W1–C11	120.8(4)
N7–W1–P1	91.6(3)
N7–W1–N1	173.0(4)
N7–W1–N3	87.9(4)
N7–W1–N5	99.2(4)
N7–W1–C10	101.4(4)
N7–W1–C11	98.0(4)
C10–W1–P1	115.8(3)
C10–W1–C11	35.4(5)
C11–W1–P1	80.8(3)
C15–P1–W1	118.6(5)
C16–P1–W1	113.8(4)
C16–P1–C15	101.0(6)
C17–P1–W1	111.7(4)
C17–P1–C15	103.3(5)
C17–P1–C16	107.1(6)
N2–N1–W1	120.4(7)
C1–N1–W1	136.3(8)
C1–N1–N2	103.1(8)
N1–N2–B1	118.9(9)
C3–N2–N1	111.1(10)
C3–N2–B1	129.6(11)
N4–N3–W1	119.8(7)
C4–N3–W1	133.1(9)
C4–N3–N4	107.1(10)

N3–N4–B1	120.3(10)
C6–N4–N3	107.1(10)
C6–N4–B1	131.9(12)
N6–N5–W1	121.6(6)
N6–N5–C7	107.8(9)
C7–N5–W1	130.6(7)
N5–N6–C9	108.9(9)
N5–N6–B1	119.7(9)
C9–N6–B1	131.2(10)
O1–N7–W1	177.3(9)
N1–C1–H1	124.1
N1–C1–C2	111.8(12)
C2–C1–H1	124.1
C1–C2–H2	127.4
C1–C2–C3	105.1(11)
C3–C2–H2	127.4
N2–C3–C2	108.8(12)
N2–C3–H3	125.6
C2–C3–H3	125.6
N3–C4–H4	124.9
N3–C4–C5	110.3(13)
C5–C4–H4	124.9
C4–C5–H5	127.1
C6–C5–C4	105.8(12)
C6–C5–H5	127.1
N4–C6–C5	109.7(12)
N4–C6–H6	125.2
C5–C6–H6	125.2
N5–C7–H7	125.6
N5–C7–C8	108.8(10)
C8–C7–H7	125.6
C7–C8–H8	127.1
C7–C8–C9	105.9(10)
C9–C8–H8	127.1
N6–C9–C8	108.6(11)
N6–C9–H9	125.7
C8–C9–H9	125.7
W1–C10–H10	93.4
C11–C10–W1	73.1(7)
C11–C10–H10	127.2
C11–C10–C14	105.5(12)
C14–C10–W1	102.7(8)
C14–C10–H10	127.2
W1–C11–H11	91.1
C10–C11–W1	71.5(7)
C10–C11–H11	125.8
C10–C11–C12	108.5(11)
C12–C11–W1	107.2(8)

C12–C11–H11	125.8
C11–C12–H12	125.8
C13–C12–C11	108.3(14)
C13–C12–H12	125.8
C12–C13–H13	125.8
C12–C13–C14	108.3(12)
C14–C13–H13	125.8
C10–C14–C13	109.2(12)
C10–C14–H14	125.4
C13–C14–H14	125.4
P1–C15–H15A	109.5
P1–C15–H15B	109.5
P1–C15–H15C	109.5
H15A–C15– H15B	109.5
H15A–C15– H15C	109.5
H15B–C15– H15C	109.5
P1–C16–H16A	109.5
P1–C16–H16B	109.5
P1–C16–H16C	109.5
H16A–C16– H16B	109.5
H16A–C16– H16C	109.5
H16B–C16– H16C	109.5
P1–C17–H17A	109.5
P1–C17–H17B	109.5
P1–C17–H17C	109.5
H17A–C17– H17B	109.5
H17A–C17– H17C	109.5
H17B–C17– H17C	109.5
N2–B1–N6	108.1(10)
N2–B1–H1A	110.1
N4–B1–N2	112.5(11)
N4–B1–N6	105.8(10)
N4–B1–H1A	110.1

N6–B1–H1A	110.1
C19–C18–C23	124.5(10)
C19–C18–C24	118.1(11)
C23–C18–C24	117.4(10)
O2–C19–C18	122.4(10)
O2–C19–C20	122.2(10)
C18–C19–C20	115.3(10)
C19–C20–Cl1	116.8(9)
C21–C20–Cl1	120.2(8)
C21–C20–C19	122.9(10)
C20–C21–Cl2	122.7(9)
C20–C21–C22	122.3(10)
C22–C21–Cl2	114.9(9)
O3–C22–C21	121.4(11)
O3–C22–C23	122.2(11)
C23–C22–C21	116.3(11)
C18–C23–C22	118.6(10)
C25–C23–C18	121.6(10)
C25–C23–C22	119.6(10)
N8–C24–C18	176.7(14)
N9–C25–C23	179.1(15)
Cl3–C26–H26A	109.3
Cl3–C26–H26B	109.3
Cl4–C26–Cl3	111.5(13)
Cl4–C26–H26A	109.3
Cl4–C26–H26B	109.3
H26A–C26– H26B	108.0
Cl4A–C26A– H26C	110.2
Cl4A–C26A– H26D	110.2
Cl4A–C26A– Cl3A	107(3)
H26C–C26A– H26D	108.5
Cl3A–C26A– H26C	110.2
Cl3A–C26A– H26D	110.2

Table 5. Torsion angles for cu\_harman\_3\_jkh\_291\_x2\_0m

Atom–Atom– Atom–Atom	Torsion Angle [°]
W1–N1–N2–C3	–175.2(9)

W1–N1–N2–B1	–1.0(13)
W1–N1–C1–C2	174.7(9)
W1–N3–N4–C6	179.1(7)



W1-N3-N4-B1	-9.0(11)
W1-N3-C4-C5	-179.8(7)
W1-N5-N6-C9	179.0(8)
W1-N5-N6-B1	3.8(13)
W1-N5-C7-C8	-177.9(8)
W1-C10-C11-C12	-102.5(10)
W1-C10-C14-C13	80.7(11)
W1-C11-C12-C13	-74.7(12)
N1-N2-C3-C2	-1.3(16)
N1-N2-B1-N4	-56.7(13)
N1-N2-B1-N6	59.7(14)
N1-C1-C2-C3	0.3(16)
N2-N1-C1-C2	-1.0(13)
N3-N4-C6-C5	1.5(12)
N3-N4-B1-N2	63.5(12)
N3-N4-B1-N6	-54.3(13)
N3-C4-C5-C6	0.2(12)
N4-N3-C4-C5	0.7(11)
N5-N6-C9-C8	-1.0(14)
N5-N6-B1-N2	-62.7(14)
N5-N6-B1-N4	58.0(14)
N5-C7-C8-C9	-1.3(14)
N6-N5-C7-C8	0.8(13)
C1-N1-N2-C3	1.4(13)
C1-N1-N2-B1	175.6(10)
C1-C2-C3-N2	0.6(17)
C3-N2-B1-N4	116.3(15)
C3-N2-B1-N6	-127.3(14)
C4-N3-N4-C6	-1.4(10)
C4-N3-N4-B1	170.5(9)
C4-C5-C6-N4	-1.1(13)
C6-N4-B1-N2	-126.8(13)
C6-N4-B1-N6	115.4(12)
C7-N5-N6-C9	0.1(12)
C7-N5-N6-B1	-175.0(10)
C7-C8-C9-N6	1.4(14)
C9-N6-B1-N2	123.4(13)
C9-N6-B1-N4	-115.9(14)
C10-C11-C12-C13	1.0(15)
C11-C10-C14-C13	5.0(14)
C11-C12-C13-C14	2.2(16)
C12-C13-C14-C10	-4.6(16)
C14-C10-C11-W1	98.8(9)
C14-C10-C11-C12	-3.7(14)
B1-N2-C3-C2	-174.7(13)
B1-N4-C6-C5	-169.1(11)
B1-N6-C9-C8	173.4(12)
CI1-C20-C21-CI2	2.6(17)

CI1-C20-C21-C22	-176.0(11)
CI2-C21-C22-O3	1(2)
CI2-C21-C22-C23	-176.6(10)
O2-C19-C20-CI1	-3.4(16)
O2-C19-C20-C21	-179.6(12)
O3-C22-C23-C18	-179.4(14)
O3-C22-C23-C25	-5(2)
C18-C19-C20-CI1	173.7(9)
C18-C19-C20-C21	-2.5(18)
C19-C18-C23-C22	-1(2)
C19-C18-C23-C25	-175.0(13)
C19-C20-C21-CI2	178.7(10)
C19-C20-C21-C22	0(2)
C20-C21-C22-O3	179.8(14)
C20-C21-C22-C23	2(2)
C21-C22-C23-C18	-1.6(19)
C21-C22-C23-C25	172.7(13)
C23-C18-C19-O2	180.0(12)
C23-C18-C19-C20	2.8(18)
C24-C18-C19-O2	-1.1(19)
C24-C18-C19-C20	-178.3(11)
C24-C18-C23-C22	-179.7(12)
C24-C18-C23-C25	6.1(19)

## Structure Report for mo\_harman\_rfl\_3\_137\_0m

A orange, needle-shaped crystal of mo\_harman\_rfl\_3\_137\_0m was coated with Paratone oil and mounted on a MiTeGen micromount. evaporation of Et<sub>2</sub>O/HOTf solution. Data were collected at 100(2) K on a Bruker D8 VENTURE dual wavelength Mo/Cu Kappa four-circle diffractometer with a PHOTON III detector. The diffractometer was equipped with an Oxford Cryostream 800Plus low temperature device and used Mo  $K_{\alpha}$  radiation ( $\lambda = 0.71073\text{\AA}$ ) from an Incoatec \ms 3.0 microfocus sealed X-ray tube with a HELIOS double bounce multilayer mirror as monochromator.

Data collection and processing were done within the Bruker APEX5 software suite.<sup>[1]</sup> All data were integrated with SAINT 8.40B using a narrow-frame algorithm and a Multi-Scan absorption correction using was applied.<sup>[2]</sup> Using [Unknown program in \_computing\_structure\_refinement] as a graphical interface,<sup>[3]</sup> the structure was solved by direct methods with SHELXT and refined by full-matrix least-squares methods against  $F^2$  using SHELXL-2019/2.<sup>[4,5]</sup> All non-hydrogen atoms were refined with anisotropic displacement parameters. All hydrogen atoms were refined with isotropic displacement parameters. Some of their coordinates were refined freely and some on calculated positions using a riding model with their  $U_{\text{iso}}$  values constrained to 1.5 times the  $U_{\text{eq}}$  of their pivot atoms for terminal sp<sup>3</sup> carbon atoms and 1.2 times for all other carbon atoms.

This report and the CIF file were generated using FinalCif.<sup>[6]</sup>

Table 1. Crystal data and structure refinement for mo\_harman\_rfl\_3\_137\_0m

CCDC number	
Empirical formula	C <sub>20</sub> H <sub>26</sub> BF <sub>3</sub> N <sub>7</sub> O <sub>4</sub> PSW
Formula weight	743.17
Temperature [K]	100(2)
Crystal system	monoclinic
Space group (number)	$P2_1/n$ (14)
$a$ [Å]	14.6316(6)
$b$ [Å]	10.9406(3)
$c$ [Å]	18.1297(7)
$\alpha$ [°]	90
$\beta$ [°]	113.3850(10)

$\gamma$ [°]	90
Volume [Å <sup>3</sup> ]	2663.79(17)
<i>Z</i>	4
$\rho_{\text{calc}}$ [gcm <sup>-3</sup> ]	1.853
$\mu$ [mm <sup>-1</sup> ]	4.537
<i>F</i> (000)	1456
Crystal size [mm <sup>3</sup> ]	0.128×0.235×0.478
Crystal colour	orange
Crystal shape	needle
Radiation	Mo <i>K</i> <sub>α</sub> ( $\lambda$ =0.71073 Å)
2 $\theta$ range [°]	4.46 to 59.18 (0.72 Å)
Index ranges	−20 ≤ <i>h</i> ≤ 20 −15 ≤ <i>k</i> ≤ 11 −25 ≤ <i>l</i> ≤ 25
Reflections collected	47564
Independent reflections	7467 <i>R</i> <sub>int</sub> = 0.0453 <i>R</i> <sub>sigma</sub> = 0.0281
Completeness to $\theta$ = 25.242°	99.9
Data / Restraints / Parameters	7467 / 0 / 358
Goodness-of-fit on <i>F</i> <sup>2</sup>	1.051
Final <i>R</i> indexes [ <i>I</i> ≥ 2 $\sigma$ ( <i>I</i> )]	<i>R</i> <sub>1</sub> = 0.0213 <i>wR</i> <sub>2</sub> = 0.0505
Final <i>R</i> indexes [all data]	<i>R</i> <sub>1</sub> = 0.0243 <i>wR</i> <sub>2</sub> = 0.0520
Largest peak/hole [eÅ <sup>-3</sup> ]	0.94/−1.03

Table 2. Atomic coordinates and Ueq [Å<sup>2</sup>] for mo\_harman\_rfl\_3\_137\_0m

Atom	x	y	z	U <sub>eq</sub>
W1	0.32810(2)	0.38029(2)	0.66498(2)	0.01666(3)
P1	0.49566(4)	0.37625(5)	0.65455(3)	0.01961(11) )
O1	0.40278(12 )	0.21112(14 )	0.80558(9)	0.0232(3)
N1	0.28785(14 )	0.50161(18 )	0.55713(11 )	0.0216(4)
N2	0.22715(13 )	0.45740(17 )	0.48332(11 )	0.0206(4)
N3	0.31109(13 )	0.22804(17 )	0.58452(11 )	0.0190(3)
N4	0.24643(13 )	0.23088(17 )	0.50562(11 )	0.0193(3)
N5	0.16615(13 )	0.34432(18 )	0.61379(11 )	0.0208(3)
N6	0.11575(13 )	0.34159(17 )	0.53208(11 )	0.0204(3)
N7	0.36945(13 )	0.27796(16 )	0.74809(11 )	0.0187(3)
C1	0.31287(17 )	0.61541(19 )	0.54481(14 )	0.0227(4)
H1	0.355035	0.668187	0.585812	0.027
C2	0.26840(18 )	0.6455(2)	0.46346(14 )	0.0260(5)
H2	0.273805	0.720181	0.438737	0.031
C3	0.21479(16 )	0.5428(2)	0.42685(14 )	0.0233(4)
H3	0.175646	0.533998	0.370995	0.028
C4	0.35260(17 )	0.11641(18 )	0.59880(14 )	0.0206(4)
H4	0.399991	0.088949	0.649177	0.025
C5	0.31584(17 )	0.0470(2)	0.52881(14 )	0.0232(4)
H5	0.333441	−0.034461	0.521736	0.028
C6	0.24830(17 )	0.1219(2)	0.47185(14 )	0.0227(4)
H6	0.209453	0.100043	0.417646	0.027
C7	0.09781(17 )	0.3234(2)	0.64493(14 )	0.0236(4)
H7	0.111778	0.319081	0.700704	0.028
C8	0.00431(17 )	0.3091(2)	0.58388(15 )	0.0256(5)
H8	−0.056719	0.294184	0.589244	0.031

C9	0.01890(16) )	0.3213(2)	0.51373(14) )	0.0233(4)
H9	-0.031499	0.316213	0.460941	0.028
C10	0.40933(17) )	0.5403(2)	0.74104(14) )	0.0223(4)
H10	0.430(2)	0.593(3)	0.7122(18)	0.027(7)
C11	0.30527(18) )	0.5574(2)	0.72669(14) )	0.0230(4)
H11	0.268(2)	0.609(2)	0.6863(18)	0.026(7)
C12	0.25414(18) )	0.4982(2)	0.76502(14) )	0.0237(4)
H12	0.183750	0.499723	0.737342	0.028
C13	0.29017(18) )	0.4338(2)	0.84099(14) )	0.0257(5)
H13	0.241466	0.393098	0.854384	0.031
C14	0.38509(19) )	0.4252(2)	0.89477(14) )	0.0266(5)
H14	0.394676	0.384883	0.943715	0.032
C15	0.47425(18) )	0.4694(2)	0.88750(14) )	0.0268(5)
H15	0.533849	0.462774	0.934537	0.032
C16	0.48419(18) )	0.5186(2)	0.82325(14) )	0.0252(5)
H16	0.549922	0.543496	0.832072	0.030
C17	0.56593(18) )	0.5165(2)	0.66354(15) )	0.0263(5)
H17A	0.585000	0.550228	0.717702	0.039
H17B	0.524719	0.576009	0.623855	0.039
H17C	0.625960	0.498959	0.653920	0.039
C18	0.48622(19) )	0.3242(3)	0.55617(15) )	0.0308(5)
H18A	0.466082	0.238096	0.548915	0.046
H18B	0.551005	0.333039	0.552628	0.046
H18C	0.436505	0.373445	0.514133	0.046
C19	0.58498(17) )	0.2753(2)	0.72664(15) )	0.0281(5)
H19A	0.598880	0.304150	0.781216	0.042
H19B	0.646791	0.274775	0.717708	0.042
H19C	0.557596	0.192343	0.719989	0.042
B1	0.17129(18) )	0.3366(2)	0.47534(14) )	0.0207(4)
H1A	0.1204(18)	0.320(2)	0.4140(14)	0.014(6)
S1	0.53750(4)	0.86466(5)	0.71881(3)	0.02094(10) )
F1	0.62437(14) )	0.79320(15) )	0.62435(11) )	0.0438(4)

F2	0.56012(13) )	0.97355(17) )	0.59813(10) )	0.0436(4)
F3	0.69626(12) )	0.94434(16) )	0.70059(11) )	0.0429(4)
O2	0.44378(13) )	0.81910(17) )	0.66112(11) )	0.0310(4)
O3	0.53153(13) )	0.98319(15) )	0.75149(10) )	0.0271(3)
O4	0.59792(13) )	0.77586(15) )	0.77608(10) )	0.0282(4)
C20	0.60786(19) )	0.8951(2)	0.65712(16) )	0.0281(5)

$U_{eq}$  is defined as 1/3 of the trace of the orthogonalized  $U_{ij}$  tensor.

Table 3. Anisotropic displacement parameters ( $\text{\AA}^2$ ) for mo\_harman\_rfl\_3\_137\_0m.

The anisotropic displacement factor exponent takes the form:

$$-2\pi^2 [h^2(a^*)^2 U_{11} + k^2(b^*)^2 U_{22} + \dots + 2hka^*b^* U_{12}]$$

Atom	$U_{11}$	$U_{22}$	$U_{33}$	$U_{23}$	$U_{13}$	$U_{12}$
W1	0.01646(5)	0.01816(5)	0.01478(5)	-0.00011(3)	0.00558(3)	0.00005(3)
P1	0.0182(2)	0.0213(3)	0.0190(3)	-0.00067(19)	0.0070(2)	-0.00186(19)
O1	0.0260(8)	0.0226(8)	0.0188(7)	0.0035(6)	0.0064(6)	0.0007(6)
N1	0.0195(9)	0.0254(9)	0.0179(9)	0.0012(7)	0.0054(7)	0.0008(7)
N2	0.0181(8)	0.0253(9)	0.0165(8)	0.0006(7)	0.0048(7)	-0.0002(7)
N3	0.0169(8)	0.0232(9)	0.0155(8)	-0.0006(7)	0.0051(7)	0.0000(7)
N4	0.0182(8)	0.0237(9)	0.0151(8)	-0.0017(7)	0.0056(7)	-0.0012(7)
N5	0.0186(8)	0.0269(9)	0.0174(8)	-0.0011(7)	0.0078(7)	-0.0005(7)
N6	0.0186(8)	0.0241(9)	0.0171(8)	-0.0006(7)	0.0055(7)	-0.0001(7)
N7	0.0197(8)	0.0187(8)	0.0182(8)	-0.0014(7)	0.0081(7)	-0.0009(6)
C1	0.0217(10)	0.0222(11)	0.0228(11)	0.0032(8)	0.0074(9)	0.0003(8)
C2	0.0246(11)	0.0276(11)	0.0257(11)	0.0086(9)	0.0098(9)	0.0024(9)
C3	0.0188(10)	0.0294(11)	0.0207(10)	0.0050(9)	0.0067(8)	0.0023(8)
C4	0.0219(10)	0.0204(10)	0.0211(10)	0.0008(8)	0.0103(8)	-0.0014(7)
C5	0.0258(11)	0.0230(10)	0.0226(11)	-0.0029(8)	0.0115(9)	-0.0017(8)
C6	0.0234(11)	0.0276(12)	0.0178(10)	-0.0030(8)	0.0090(8)	-0.0033(8)
C7	0.0227(11)	0.0269(11)	0.0245(11)	-0.0005(9)	0.0129(9)	-0.0001(8)
C8	0.0190(10)	0.0285(11)	0.0314(12)	-0.0004(9)	0.0123(9)	-0.0016(8)
C9	0.0173(10)	0.0253(11)	0.0253(11)	-0.0027(8)	0.0064(8)	-0.0005(8)
C10	0.0253(11)	0.0172(9)	0.0240(11)	-0.0001(8)	0.0094(9)	-0.0005(8)
C11	0.0284(11)	0.0186(10)	0.0189(10)	-0.0020(8)	0.0060(9)	0.0056(8)
C12	0.0245(11)	0.0213(10)	0.0236(10)	-0.0045(8)	0.0077(9)	0.0030(8)
C13	0.0329(12)	0.0241(11)	0.0245(11)	-0.0009(9)	0.0160(10)	0.0042(9)
C14	0.0381(13)	0.0240(11)	0.0185(10)	-0.0008(9)	0.0121(10)	0.0061(10)
C15	0.0276(12)	0.0262(11)	0.0210(11)	-0.0052(9)	0.0038(9)	0.0037(9)
C16	0.0244(11)	0.0222(11)	0.0265(11)	-0.0058(9)	0.0075(9)	-0.0003(8)
C17	0.0233(11)	0.0241(11)	0.0314(12)	0.0012(9)	0.0107(10)	-0.0037(8)

C18	0.0291(12)	0.0403(14)	0.0282(12)	−0.0076(10)	0.0170(10)	−0.0087(10)
C19	0.0193(10)	0.0259(11)	0.0339(13)	0.0045(10)	0.0051(10)	0.0016(8)
B1	0.0187(11)	0.0253(12)	0.0165(10)	−0.0005(9)	0.0052(9)	−0.0001(9)
S1	0.0241(3)	0.0206(2)	0.0183(2)	−0.00068(19)	0.0086(2)	−0.00129(19)
F1	0.0623(11)	0.0389(9)	0.0473(10)	−0.0070(7)	0.0398(9)	−0.0017(8)
F2	0.0457(10)	0.0539(11)	0.0386(9)	0.0209(8)	0.0245(8)	0.0084(8)
F3	0.0258(8)	0.0457(10)	0.0575(11)	−0.0001(8)	0.0169(8)	−0.0075(7)
O2	0.0263(9)	0.0330(9)	0.0309(9)	−0.0037(7)	0.0083(7)	−0.0093(7)
O3	0.0336(9)	0.0235(8)	0.0217(8)	−0.0019(6)	0.0084(7)	0.0039(7)
O4	0.0373(10)	0.0231(8)	0.0227(8)	0.0019(6)	0.0104(7)	0.0051(7)
C20	0.0284(12)	0.0292(12)	0.0303(12)	0.0021(9)	0.0154(10)	−0.0014(9)

Table 4. Bond lengths and angles for mo\_harman\_rfl\_3\_137\_0m

Atom–Atom	Length [Å]		
W1–N7	1.7792(18)	C5–H5	0.9500
W1–N3	2.1626(18)	C6–H6	0.9500
W1–N5	2.2103(18)	C7–C8	1.385(3)
W1–N1	2.2401(19)	C7–H7	0.9500
W1–C10	2.253(2)	C8–C9	1.377(3)
W1–C11	2.327(2)	C8–H8	0.9500
W1–P1	2.5331(6)	C9–H9	0.9500
P1–C19	1.811(2)	C10–C11	1.451(3)
P1–C17	1.818(2)	C10–C16	1.477(3)
P1–C18	1.825(2)	C10–H10	0.90(3)
O1–N7	1.206(2)	C11–C12	1.369(3)
N1–C1	1.341(3)	C11–H11	0.92(3)
N1–N2	1.368(3)	C12–C13	1.447(3)
N2–C3	1.344(3)	C12–H12	0.9500
N2–B1	1.531(3)	C13–C14	1.347(3)
N3–C4	1.343(3)	C13–H13	0.9500
N3–N4	1.367(2)	C14–C15	1.446(4)
N4–C6	1.346(3)	C14–H14	0.9500
N4–B1	1.539(3)	C15–C16	1.343(3)
N5–C7	1.349(3)	C15–H15	0.9500
N5–N6	1.368(2)	C16–H16	0.9500
N6–C9	1.339(3)	C17–H17A	0.9800
N6–B1	1.545(3)	C17–H17B	0.9800
C1–C2	1.395(3)	C17–H17C	0.9800
C1–H1	0.9500	C18–H18A	0.9800
C2–C3	1.380(3)	C18–H18B	0.9800
C2–H2	0.9500	C18–H18C	0.9800
C3–H3	0.9500	C19–H19A	0.9800
C4–C5	1.391(3)	C19–H19B	0.9800
C4–H4	0.9500	C19–H19C	0.9800
C5–C6	1.380(3)	B1–H1A	1.08(2)
		S1–O4	1.4404(17)

S1–O3	1.4427(17)
S1–O2	1.4438(18)
S1–C20	1.826(3)
F1–C20	1.330(3)
F2–C20	1.332(3)
F3–C20	1.332(3)
<b>Atom–Atom– Atom</b>	<b>Angle [°]</b>
N7–W1–N3	89.77(7)
N7–W1–N5	101.02(8)
N3–W1–N5	76.26(7)
N7–W1–N1	174.39(7)
N3–W1–N1	86.99(7)
N5–W1–N1	82.67(7)
N7–W1–C10	92.93(8)
N3–W1–C10	154.52(8)
N5–W1–C10	127.77(8)
N1–W1–C10	88.05(8)
N7–W1–C11	100.50(8)
N3–W1–C11	164.96(8)
N5–W1–C11	90.89(8)
N1–W1–C11	83.58(7)
C10–W1–C11	36.90(8)
N7–W1–P1	92.20(6)
N3–W1–P1	77.98(5)
N5–W1–P1	150.88(5)
N1–W1–P1	82.65(5)
C10–W1–P1	76.60(6)
C11–W1–P1	112.23(6)
C19–P1–C17	103.27(11)
C19–P1–C18	105.54(13)
C17–P1–C18	99.90(12)
C19–P1–W1	113.54(8)
C17–P1–W1	120.55(8)
C18–P1–W1	112.24(8)
C1–N1–N2	106.24(18)
C1–N1–W1	134.49(16)
N2–N1–W1	119.22(14)
C3–N2–N1	109.75(19)
C3–N2–B1	128.55(19)
N1–N2–B1	120.87(17)
C4–N3–N4	107.14(18)
C4–N3–W1	130.42(15)
N4–N3–W1	122.34(13)
C6–N4–N3	108.99(18)
C6–N4–B1	130.11(19)
N3–N4–B1	119.36(17)

C7–N5–N6	106.20(18)
C7–N5–W1	134.74(15)
N6–N5–W1	119.06(13)
C9–N6–N5	109.58(18)
C9–N6–B1	127.82(19)
N5–N6–B1	121.46(17)
O1–N7–W1	176.35(16)
N1–C1–C2	110.6(2)
N1–C1–H1	124.7
C2–C1–H1	124.7
C3–C2–C1	104.7(2)
C3–C2–H2	127.6
C1–C2–H2	127.6
N2–C3–C2	108.7(2)
N2–C3–H3	125.6
C2–C3–H3	125.6
N3–C4–C5	109.8(2)
N3–C4–H4	125.1
C5–C4–H4	125.1
C6–C5–C4	105.1(2)
C6–C5–H5	127.4
C4–C5–H5	127.4
N4–C6–C5	108.9(2)
N4–C6–H6	125.6
C5–C6–H6	125.6
N5–C7–C8	110.2(2)
N5–C7–H7	124.9
C8–C7–H7	124.9
C9–C8–C7	105.1(2)
C9–C8–H8	127.4
C7–C8–H8	127.4
N6–C9–C8	108.9(2)
N6–C9–H9	125.6
C8–C9–H9	125.6
C11–C10–C16	120.4(2)
C11–C10–W1	74.30(13)
C16–C10–W1	119.52(15)
C11–C10–H10	112.1(19)
C16–C10–H10	113.9(19)
W1–C10–H10	110.8(19)
C12–C11–C10	126.4(2)
C12–C11–W1	93.57(14)
C10–C11–W1	68.80(12)
C12–C11–H11	115.0(19)
C10–C11–H11	118.5(19)
W1–C11–H11	106.5(18)
C11–C12–C13	130.3(2)
C11–C12–H12	114.8



C13–C12–H12	114.8
C14–C13–C12	127.2(2)
C14–C13–H13	116.4
C12–C13–H13	116.4
C13–C14–C15	128.3(2)
C13–C14–H14	115.9
C15–C14–H14	115.9
C16–C15–C14	128.7(2)
C16–C15–H15	115.6
C14–C15–H15	115.6
C15–C16–C10	130.4(2)
C15–C16–H16	114.8
C10–C16–H16	114.8
P1–C17–H17A	109.5
P1–C17–H17B	109.5
H17A–C17–H17B	109.5
P1–C17–H17C	109.5
H17A–C17–H17C	109.5
H17B–C17–H17C	109.5
P1–C18–H18A	109.5
P1–C18–H18B	109.5
H18A–C18–H18B	109.5
P1–C18–H18C	109.5
H18A–C18–H18C	109.5
H18B–C18–H18C	109.5

P1–C19–H19A	109.5
P1–C19–H19B	109.5
H19A–C19–H19B	109.5
P1–C19–H19C	109.5
H19A–C19–H19C	109.5
H19B–C19–H19C	109.5
N2–B1–N4	109.65(18)
N2–B1–N6	107.98(18)
N4–B1–N6	106.22(18)
N2–B1–H1A	111.5(13)
N4–B1–H1A	110.2(13)
N6–B1–H1A	111.2(13)
O4–S1–O3	115.48(10)
O4–S1–O2	115.09(11)
O3–S1–O2	114.39(11)
O4–S1–C20	103.33(11)
O3–S1–C20	103.21(11)
O2–S1–C20	102.91(11)
F1–C20–F3	107.3(2)
F1–C20–F2	108.2(2)
F3–C20–F2	106.9(2)
F1–C20–S1	111.56(17)
F3–C20–S1	111.24(18)
F2–C20–S1	111.44(17)

Table 5. Torsion angles for mo\_harman\_rfl\_3\_137\_0m

Atom–Atom–Atom–Atom	Torsion Angle [°]
C1–N1–N2–C3	−0.3(2)
W1–N1–N2–C3	−178.14(14)
C1–N1–N2–B1	−170.74(19)
W1–N1–N2–B1	11.4(3)
C4–N3–N4–C6	0.0(2)
W1–N3–N4–C6	−176.93(14)
C4–N3–N4–B1	167.23(18)
W1–N3–N4–B1	−9.7(2)
C7–N5–N6–C9	0.9(2)
W1–N5–N6–C9	−178.62(14)
C7–N5–N6–B1	−167.83(19)
W1–N5–N6–B1	12.7(3)

N2–N1–C1–C2	0.3(3)
W1–N1–C1–C2	177.60(16)
N1–C1–C2–C3	−0.1(3)
N1–N2–C3–C2	0.2(3)
B1–N2–C3–C2	169.7(2)
C1–C2–C3–N2	−0.1(3)
N4–N3–C4–C5	0.8(2)
W1–N3–C4–C5	177.36(15)
N3–C4–C5–C6	−1.2(2)
N3–N4–C6–C5	−0.8(2)
B1–N4–C6–C5	−166.2(2)
C4–C5–C6–N4	1.2(2)
N6–N5–C7–C8	−0.8(3)
W1–N5–C7–C8	178.54(17)

N5-C7-C8-C9	0.5(3)
N5-N6-C9-C8	-0.6(3)
B1-N6-C9-C8	167.2(2)
C7-C8-C9-N6	0.1(3)
C16-C10-C11-C12	-37.1(3)
W1-C10-C11-C12	78.3(2)
C16-C10-C11-W1	-115.4(2)
C10-C11-C12-C13	19.6(4)
W1-C11-C12-C13	85.8(2)
C11-C12-C13-C14	5.1(4)
C12-C13-C14-C15	-5.2(4)
C13-C14-C15-C16	-6.9(4)
C14-C15-C16-C10	-1.4(4)
C11-C10-C16-C15	26.5(4)
W1-C10-C16-C15	-61.9(3)
C3-N2-B1-N4	127.2(2)
N1-N2-B1-N4	-64.3(2)
C3-N2-B1-N6	-117.4(2)
N1-N2-B1-N6	51.0(3)
C6-N4-B1-N2	-132.4(2)
N3-N4-B1-N2	63.5(2)
C6-N4-B1-N6	111.2(2)
N3-N4-B1-N6	-52.9(2)
C9-N6-B1-N2	126.8(2)
N5-N6-B1-N2	-66.7(2)
C9-N6-B1-N4	-115.7(2)
N5-N6-B1-N4	50.8(3)
O4-S1-C20-F1	56.7(2)
O3-S1-C20-F1	177.37(18)
O2-S1-C20-F1	-63.4(2)
O4-S1-C20-F3	-63.05(19)
O3-S1-C20-F3	57.59(19)
O2-S1-C20-F3	176.86(17)
O4-S1-C20-F2	177.76(18)
O3-S1-C20-F2	-61.6(2)
O2-S1-C20-F2	57.7(2)

## Structure Report for mo\_harman\_mne\_nb3\_303b\_0m

A yellow, plate-shaped crystal of mo\_harman\_mne\_nb3\_303b\_0m was coated with Paratone oil and mounted on a MiTeGen micromount. crystallized from acetonitrile. Data were collected at 100(2) K on a Bruker D8 VENTURE dual wavelength Mo/Cu Kappa four-circle diffractometer with a PHOTON III detector. The diffractometer was equipped with an Oxford Cryostream 800Plus low temperature device and used Mo  $K_\alpha$  radiation ( $\lambda = 0.71073\text{\AA}$ ) from an Incoatec lms 3.0 microfocus sealed X-ray tube with a HELIOS double bounce multilayer mirror as monochromator.

Data collection and processing were done within the Bruker APEX5 software suite.<sup>[1]</sup> All data were integrated with SAINT 8.40B using a narrow-frame algorithm and a Multi-Scan absorption correction using was applied.<sup>[2]</sup> Using [Unknown program in \_computing\_structure\_refinement] as a graphical interface,<sup>[3]</sup> the structure was solved by direct methods with SHELXT and refined by full-matrix least-squares methods against  $F^2$  using SHELXL-2019/2.<sup>[4,5]</sup> All non-hydrogen atoms were refined with anisotropic displacement parameters. All C-bound hydrogen atoms were refined isotropic on calculated positions using a riding model with their  $U_{\text{iso}}$  values constrained to 1.5 times the  $U_{\text{eq}}$  of their pivot atoms for terminal  $\text{sp}^3$  carbon atoms and 1.2 times for all other carbon atoms. This report and the CIF file were generated using FinalCif.<sup>[6]</sup>

Table 1. Crystal data and structure refinement for mo\_harman\_mne\_nb3\_303b\_0m

CCDC number	
Empirical formula	$\text{C}_{21}\text{H}_{28}\text{BF}_3\text{N}_7\text{O}_4\text{PSW}$
Formula weight	757.19
Temperature [K]	100(2)
Crystal system	triclinic
Space group (number)	$P\bar{1}$ (2)
$a$ [ $\text{\AA}$ ]	9.5771(5)
$b$ [ $\text{\AA}$ ]	10.7462(5)
$c$ [ $\text{\AA}$ ]	13.8016(7)
$\alpha$ [ $^\circ$ ]	93.960(2)
$\beta$ [ $^\circ$ ]	109.386(2)
$\gamma$ [ $^\circ$ ]	91.001(2)

Volume [Å <sup>3</sup> ]	1335.46(12)
Z	2
$\rho_{\text{calc}}$ [gcm <sup>-3</sup> ]	1.883
$\mu$ [mm <sup>-1</sup> ]	4.527
<i>F</i> (000)	744
Crystal size [mm <sup>3</sup> ]	0.050×0.069×0.089
Crystal colour	yellow
Crystal shape	plate
Radiation	Mo <i>K</i> <sub>α</sub> ( $\lambda$ =0.71073 Å)
2 $\theta$ range [°]	3.80 to 56.56 (0.75 Å)
Index ranges	-12 ≤ <i>h</i> ≤ 12 -14 ≤ <i>k</i> ≤ 14 -18 ≤ <i>l</i> ≤ 14
Reflections collected	36468
Independent reflections	6614 <i>R</i> <sub>int</sub> = 0.0378 <i>R</i> <sub>sigma</sub> = 0.0298
Completeness to $\theta$ = 25.242°	99.7
Data / Restraints / Parameters	6614 / 0 / 355
Goodness-of-fit on <i>F</i> <sup>2</sup>	1.046
Final <i>R</i> indexes [ <i>I</i> ≥ 2 $\sigma$ ( <i>I</i> )]	<i>R</i> <sub>1</sub> = 0.0223 <i>wR</i> <sub>2</sub> = 0.0511
Final <i>R</i> indexes [all data]	<i>R</i> <sub>1</sub> = 0.0259 <i>wR</i> <sub>2</sub> = 0.0528
Largest peak/hole [eÅ <sup>-3</sup> ]	1.40/-0.53

Table 2. Atomic coordinates and  $U_{eq}$  [Å<sup>2</sup>] for mo\_harman\_mne\_nb3\_303b\_0m

Atom	x	y	z	$U_{eq}$
W1	0.51225(2)	0.26271(2)	0.82841(2)	0.01341(4)
P1	0.31686(7)	0.26396(6)	0.65066(6)	0.01549(14)
O1	0.3462(3)	0.4525(2)	0.90808(18)	0.0279(5)
N1	0.6222(2)	0.1291(2)	0.74868(19)	0.0162(5)
N2	0.7484(2)	0.1650(2)	0.73046(19)	0.0180(5)
N3	0.5963(2)	0.4103(2)	0.76103(19)	0.0169(5)
N4	0.7193(3)	0.3988(2)	0.73235(19)	0.0178(5)
N5	0.7443(2)	0.2975(2)	0.93350(19)	0.0157(4)
N6	0.8559(2)	0.3038(2)	0.89165(19)	0.0170(5)
N7	0.4163(3)	0.3767(2)	0.87928(19)	0.0187(5)
C1	0.5924(3)	0.0092(3)	0.7110(2)	0.0218(6)
H1	0.509728	-0.040001	0.712214	0.026
C2	0.6991(3)	-0.0327(3)	0.6702(3)	0.0256(6)
H2	0.704211	-0.113495	0.639298	0.031
C3	0.7952(3)	0.0679(3)	0.6844(2)	0.0224(6)
H3	0.881374	0.069004	0.664751	0.027
C4	0.5475(3)	0.5251(2)	0.7410(2)	0.0192(6)
H4	0.463129	0.558266	0.753365	0.023
C5	0.6392(3)	0.5878(3)	0.6993(2)	0.0231(6)
H5	0.630035	0.670237	0.677682	0.028
C6	0.7468(3)	0.5052(3)	0.6957(2)	0.0217(6)
H6	0.826774	0.521209	0.671355	0.026
C7	0.8073(3)	0.3266(3)	1.0347(2)	0.0190(6)
H7	0.755652	0.330691	1.082868	0.023
C8	0.9586(3)	0.3499(3)	1.0598(2)	0.0240(6)
H8	1.028862	0.371015	1.126240	0.029
C9	0.9849(3)	0.3359(3)	0.9678(2)	0.0209(6)
H9	1.078537	0.346914	0.959112	0.025
C10	0.3453(3)	0.1010(2)	0.8188(2)	0.0180(5)
H10	0.332906	0.036756	0.760323	0.022
C11	0.4743(3)	0.0884(2)	0.9057(2)	0.0183(5)
H11	0.536496	0.015326	0.902909	0.022
C12	0.5157(3)	0.1659(3)	0.9953(2)	0.0193(6)

H12	0.618474	0.151721	1.041471	0.023
C13	0.4270(3)	0.2302(3)	1.0508(2)	0.0211(6)
H13	0.462817	0.311336	1.082036	0.025
C14	0.3015(3)	0.1877(3)	1.0622(2)	0.0237(6)
H14	0.269800	0.234191	1.111614	0.028
C15	0.2069(3)	0.0782(3)	1.0081(3)	0.0239(6)
H15	0.176049	0.022184	1.048088	0.029
C16	0.1618(3)	0.0524(3)	0.9065(3)	0.0232(6)
H16	0.102713	-0.021649	0.877827	0.028
C17	0.2004(3)	0.1357(3)	0.8350(2)	0.0198(6)
H17A	0.209254	0.223467	0.864048	0.024
H17B	0.119492	0.128946	0.767671	0.024
C18	0.2180(3)	0.1213(3)	0.5808(2)	0.0212(6)
H18A	0.289306	0.061229	0.571763	0.032
H18B	0.150845	0.140530	0.513195	0.032
H18C	0.160629	0.085495	0.619974	0.032
C19	0.3897(3)	0.3145(3)	0.5530(2)	0.0244(6)
H19A	0.441212	0.396389	0.576007	0.037
H19B	0.307940	0.320536	0.488273	0.037
H19C	0.459301	0.253835	0.541994	0.037
C20	0.1730(3)	0.3717(3)	0.6490(2)	0.0204(6)
H20A	0.107966	0.337030	0.683230	0.031
H20B	0.114794	0.384882	0.577569	0.031
H20C	0.218230	0.451643	0.685439	0.031
B1	0.8251(3)	0.2934(3)	0.7753(3)	0.0187(6)
H1A	0.919139	0.303876	0.759713	0.022
S1	0.87116(8)	0.25477(7)	0.33332(6)	0.02197(15)
F1	0.8749(2)	0.2109(2)	0.51954(17)	0.0416(5)
F2	0.6576(2)	0.20130(19)	0.40635(17)	0.0367(5)
F3	0.7695(3)	0.37918(19)	0.46524(18)	0.0404(5)
O2	0.8938(3)	0.1235(2)	0.3189(2)	0.0370(6)
O3	1.0056(3)	0.3310(2)	0.3770(2)	0.0333(5)
O4	0.7578(3)	0.3065(3)	0.25116(19)	0.0373(6)
C21	0.7899(3)	0.2623(3)	0.4357(3)	0.0246(6)

$U_{eq}$  is defined as 1/3 of the trace of the orthogonalized  $U_{ij}$  tensor.

Table 3. Anisotropic displacement parameters ( $\text{\AA}^2$ ) for mo\_harman\_mne\_nb3\_303b\_0m.

The anisotropic displacement factor exponent takes the form:

$$-2\pi^2[ h^2(a^*)^2U_{11} + k^2(b^*)^2U_{22} + \dots + 2hka^*b^*U_{12} ]$$

Atom	$U_{11}$	$U_{22}$	$U_{33}$	$U_{23}$	$U_{13}$	$U_{12}$
W1	0.01579(6)	0.01307(5)	0.01132(6)	0.00207(4)	0.00425(4)	0.00056(3)
P1	0.0177(3)	0.0161(3)	0.0121(3)	0.0020(2)	0.0040(3)	-0.0008(2)

O1	0.0373(12)	0.0249(11)	0.0253(13)	0.0018(9)	0.0149(10)	0.0145(9)
N1	0.0169(10)	0.0165(10)	0.0150(12)	0.0005(9)	0.0053(9)	−0.0012(8)
N2	0.0175(11)	0.0209(11)	0.0156(12)	0.0011(9)	0.0058(9)	−0.0011(9)
N3	0.0186(11)	0.0168(11)	0.0139(12)	0.0014(9)	0.0037(9)	−0.0015(8)
N4	0.0193(11)	0.0186(11)	0.0155(12)	0.0014(9)	0.0059(9)	−0.0032(9)
N5	0.0164(10)	0.0163(10)	0.0144(12)	0.0018(9)	0.0051(9)	0.0017(8)
N6	0.0173(10)	0.0172(11)	0.0169(13)	0.0007(9)	0.0065(9)	−0.0002(8)
N7	0.0229(11)	0.0181(11)	0.0143(12)	0.0042(9)	0.0047(9)	0.0009(9)
C1	0.0267(14)	0.0181(13)	0.0221(16)	−0.0010(11)	0.0108(12)	−0.0019(11)
C2	0.0328(16)	0.0218(14)	0.0261(17)	−0.0047(12)	0.0166(13)	0.0003(12)
C3	0.0247(14)	0.0250(14)	0.0202(16)	−0.0013(12)	0.0117(12)	0.0011(11)
C4	0.0259(14)	0.0168(12)	0.0123(14)	0.0011(10)	0.0031(11)	−0.0008(10)
C5	0.0336(16)	0.0170(13)	0.0176(15)	0.0027(11)	0.0070(12)	−0.0049(11)
C6	0.0263(14)	0.0218(13)	0.0170(15)	0.0030(11)	0.0074(11)	−0.0070(11)
C7	0.0226(13)	0.0181(12)	0.0153(14)	0.0003(10)	0.0049(11)	0.0050(10)
C8	0.0229(14)	0.0241(14)	0.0196(16)	−0.0021(12)	0.0008(11)	0.0019(11)
C9	0.0170(12)	0.0184(13)	0.0232(16)	−0.0001(11)	0.0015(11)	0.0005(10)
C10	0.0204(13)	0.0163(12)	0.0196(15)	0.0051(10)	0.0088(11)	0.0013(10)
C11	0.0211(13)	0.0160(12)	0.0216(15)	0.0074(10)	0.0112(11)	0.0016(10)
C12	0.0207(13)	0.0209(13)	0.0191(15)	0.0097(11)	0.0083(11)	0.0043(10)
C13	0.0279(14)	0.0214(13)	0.0135(14)	0.0038(11)	0.0055(11)	0.0046(11)
C14	0.0273(14)	0.0278(15)	0.0172(15)	0.0066(12)	0.0074(12)	0.0106(12)
C15	0.0209(13)	0.0276(15)	0.0284(17)	0.0111(12)	0.0132(12)	0.0070(11)
C16	0.0207(13)	0.0235(14)	0.0277(17)	0.0056(12)	0.0105(12)	0.0028(11)
C17	0.0170(12)	0.0223(13)	0.0193(15)	0.0021(11)	0.0048(11)	0.0028(10)
C18	0.0221(13)	0.0200(13)	0.0172(15)	−0.0017(11)	0.0019(11)	−0.0026(10)
C19	0.0286(15)	0.0298(15)	0.0148(15)	0.0021(12)	0.0074(12)	−0.0060(12)
C20	0.0198(13)	0.0200(13)	0.0203(15)	0.0036(11)	0.0048(11)	0.0019(10)
B1	0.0193(14)	0.0199(14)	0.0161(16)	0.0005(12)	0.0055(12)	−0.0032(11)
S1	0.0266(3)	0.0209(3)	0.0168(4)	0.0027(3)	0.0050(3)	−0.0023(3)
F1	0.0359(11)	0.0619(14)	0.0264(12)	0.0229(10)	0.0063(9)	−0.0019(10)
F2	0.0273(10)	0.0433(11)	0.0388(13)	−0.0050(9)	0.0122(9)	−0.0121(8)
F3	0.0628(14)	0.0290(10)	0.0364(13)	−0.0049(9)	0.0277(11)	−0.0054(9)
O2	0.0461(14)	0.0233(11)	0.0468(17)	−0.0011(11)	0.0234(12)	−0.0017(10)
O3	0.0353(12)	0.0357(13)	0.0294(14)	0.0008(10)	0.0125(10)	−0.0129(10)

O4	0.0402(14)	0.0528(16)	0.0171(13)	0.0090(11)	0.0056(10)	0.0100(11)
C21	0.0268(15)	0.0236(14)	0.0202(16)	0.0030(12)	0.0039(12)	−0.0052(11)

Table 4. Bond lengths and angles for mo\_harman\_mne\_nb3\_303b\_0m

Atom–Atom	Length [Å]		
W1–N7	1.785(2)	C10–H10	1.0000
W1–N3	2.165(2)	C11–C12	1.380(4)
W1–N5	2.222(2)	C11–H11	1.0000
W1–N1	2.233(2)	C12–C13	1.471(4)
W1–C11	2.300(3)	C12–H12	1.0000
W1–C10	2.307(3)	C13–C14	1.340(4)
W1–P1	2.5452(7)	C13–H13	0.9500
W1–C12	2.583(3)	C14–C15	1.469(4)
P1–C20	1.811(3)	C14–H14	0.9500
P1–C19	1.820(3)	C15–C16	1.330(5)
P1–C18	1.820(3)	C15–H15	0.9500
O1–N7	1.193(3)	C16–C17	1.504(4)
N1–C1	1.344(3)	C16–H16	0.9500
N1–N2	1.368(3)	C17–H17A	0.9900
N2–C3	1.345(4)	C17–H17B	0.9900
N2–B1	1.540(4)	C18–H18A	0.9800
N3–C4	1.340(4)	C18–H18B	0.9800
N3–N4	1.366(3)	C18–H18C	0.9800
N4–C6	1.338(4)	C19–H19A	0.9800
N4–B1	1.548(4)	C19–H19B	0.9800
N5–C7	1.337(4)	C19–H19C	0.9800
N5–N6	1.376(3)	C20–H20A	0.9800
N6–C9	1.350(4)	C20–H20B	0.9800
N6–B1	1.528(4)	C20–H20C	0.9800
C1–C2	1.388(4)	B1–H1A	1.0000
C1–H1	0.9500	S1–O4	1.436(2)
C2–C3	1.368(4)	S1–O3	1.439(2)
C2–H2	0.9500	S1–O2	1.442(2)
C3–H3	0.9500	S1–C21	1.823(3)
C4–C5	1.388(4)	F1–C21	1.337(4)
C4–H4	0.9500	F2–C21	1.339(3)
C5–C6	1.383(4)	F3–C21	1.331(4)
C5–H5	0.9500		
C6–H6	0.9500	<b>Atom–Atom–</b>	<b>Angle [°]</b>
C7–C8	1.387(4)	<b>Atom</b>	
C7–H7	0.9500	N7–W1–N3	88.67(10)
C8–C9	1.373(5)	N7–W1–N5	101.98(9)
C8–H8	0.9500	N3–W1–N5	76.41(9)
C9–H9	0.9500	N7–W1–N1	173.87(10)
C10–C11	1.423(4)	N3–W1–N1	87.25(9)
C10–C17	1.526(4)	N5–W1–N1	81.51(8)
		N7–W1–C11	101.57(11)



N3-W1-C11	167.20(9)
N5-W1-C11	93.81(9)
N1-W1-C11	83.10(9)
N7-W1-C10	94.43(10)
N3-W1-C10	151.94(10)
N5-W1-C10	129.65(9)
N1-W1-C10	87.04(9)
C11-W1-C10	35.99(10)
N7-W1-P1	90.65(8)
N3-W1-P1	77.47(6)
N5-W1-P1	150.59(7)
N1-W1-P1	83.99(6)
C11-W1-P1	109.71(7)
C10-W1-P1	74.62(8)
N7-W1-C12	79.43(10)
N3-W1-C12	146.77(9)
N5-W1-C12	75.94(9)
N1-W1-C12	106.42(9)
C11-W1-C12	32.16(10)
C10-W1-C12	60.74(10)
P1-W1-C12	132.98(7)
C20-P1-C19	104.16(15)
C20-P1-C18	104.75(13)
C19-P1-C18	98.21(14)
C20-P1-W1	112.28(10)
C19-P1-W1	113.55(10)
C18-P1-W1	121.74(10)
C1-N1-N2	106.0(2)
C1-N1-W1	133.5(2)
N2-N1-W1	120.54(16)
C3-N2-N1	109.4(2)
C3-N2-B1	130.1(2)
N1-N2-B1	119.9(2)
C4-N3-N4	107.2(2)
C4-N3-W1	130.2(2)
N4-N3-W1	122.59(17)
C6-N4-N3	109.4(2)
C6-N4-B1	129.3(2)
N3-N4-B1	118.2(2)
C7-N5-N6	106.5(2)
C7-N5-W1	134.4(2)
N6-N5-W1	118.79(18)
C9-N6-N5	108.9(2)
C9-N6-B1	128.3(3)
N5-N6-B1	122.3(2)
O1-N7-W1	176.4(2)
N1-C1-C2	110.7(3)
N1-C1-H1	124.7

C2-C1-H1	124.7
C3-C2-C1	104.8(3)
C3-C2-H2	127.6
C1-C2-H2	127.6
N2-C3-C2	109.2(3)
N2-C3-H3	125.4
C2-C3-H3	125.4
N3-C4-C5	109.5(3)
N3-C4-H4	125.3
C5-C4-H4	125.3
C6-C5-C4	105.5(3)
C6-C5-H5	127.2
C4-C5-H5	127.2
N4-C6-C5	108.4(3)
N4-C6-H6	125.8
C5-C6-H6	125.8
N5-C7-C8	110.6(3)
N5-C7-H7	124.7
C8-C7-H7	124.7
C9-C8-C7	105.2(3)
C9-C8-H8	127.4
C7-C8-H8	127.4
N6-C9-C8	108.9(3)
N6-C9-H9	125.6
C8-C9-H9	125.6
C11-C10-C17	119.7(3)
C11-C10-W1	71.74(15)
C17-C10-W1	117.02(18)
C11-C10-H10	114.0
C17-C10-H10	114.0
W1-C10-H10	114.0
C12-C11-C10	124.8(3)
C12-C11-W1	85.30(17)
C10-C11-W1	72.27(16)
C12-C11-H11	117.6
C10-C11-H11	117.6
W1-C11-H11	117.6
C11-C12-C13	131.3(3)
C11-C12-W1	62.54(16)
C13-C12-W1	114.66(19)
C11-C12-H12	112.4
C13-C12-H12	112.4
W1-C12-H12	112.4
C14-C13-C12	127.5(3)
C14-C13-H13	116.3
C12-C13-H13	116.3
C13-C14-C15	128.2(3)
C13-C14-H14	115.9

C15–C14–H14	115.9
C16–C15–C14	124.1(3)
C16–C15–H15	118.0
C14–C15–H15	118.0
C15–C16–C17	122.8(3)
C15–C16–H16	118.6
C17–C16–H16	118.6
C16–C17–C10	111.8(2)
C16–C17–H17A	109.3
C10–C17–H17A	109.3
C16–C17–H17B	109.3
C10–C17–H17B	109.3
H17A–C17– H17B	107.9
P1–C18–H18A	109.5
P1–C18–H18B	109.5
H18A–C18– H18B	109.5
P1–C18–H18C	109.5
H18A–C18– H18C	109.5
H18B–C18– H18C	109.5
P1–C19–H19A	109.5
P1–C19–H19B	109.5
H19A–C19– H19B	109.5
P1–C19–H19C	109.5
H19A–C19– H19C	109.5

H19B–C19– H19C	109.5
P1–C20–H20A	109.5
P1–C20–H20B	109.5
H20A–C20– H20B	109.5
P1–C20–H20C	109.5
H20A–C20– H20C	109.5
H20B–C20– H20C	109.5
N6–B1–N2	108.5(2)
N6–B1–N4	106.0(2)
N2–B1–N4	110.2(2)
N6–B1–H1A	110.7
N2–B1–H1A	110.7
N4–B1–H1A	110.7
O4–S1–O3	115.21(16)
O4–S1–O2	116.24(16)
O3–S1–O2	114.37(15)
O4–S1–C21	101.78(15)
O3–S1–C21	103.34(14)
O2–S1–C21	103.15(15)
F3–C21–F1	107.0(3)
F3–C21–F2	106.8(3)
F1–C21–F2	106.5(3)
F3–C21–S1	112.3(2)
F1–C21–S1	112.0(2)
F2–C21–S1	111.9(2)

Table 5. Torsion angles for mo\_harman\_mne\_nb3\_303b\_0m

Atom–Atom– Atom–Atom	Torsion Angle [°]
C1–N1–N2–C3	−1.1(3)
W1–N1–N2–C3	178.36(19)
C1–N1–N2–B1	−172.8(3)
W1–N1–N2–B1	6.7(3)
C4–N3–N4–C6	0.4(3)
W1–N3–N4–C6	−178.49(19)
C4–N3–N4–B1	162.2(2)
W1–N3–N4–B1	−16.8(3)
C7–N5–N6–C9	0.3(3)
W1–N5–N6–C9	174.87(17)
C7–N5–N6–B1	−171.8(2)
W1–N5–N6–B1	2.7(3)
N2–N1–C1–C2	0.9(4)

W1–N1–C1–C2	−178.5(2)
N1–C1–C2–C3	−0.3(4)
N1–N2–C3–C2	0.9(4)
B1–N2–C3–C2	171.5(3)
C1–C2–C3–N2	−0.4(4)
N4–N3–C4–C5	0.0(3)
W1–N3–C4–C5	178.77(19)
N3–C4–C5–C6	−0.3(3)
N3–N4–C6–C5	−0.7(3)
B1–N4–C6–C5	−159.8(3)
C4–C5–C6–N4	0.6(3)
N6–N5–C7–C8	−0.9(3)
W1–N5–C7–C8	−174.2(2)
N5–C7–C8–C9	1.1(3)

N5–N6–C9–C8	0.4(3)
B1–N6–C9–C8	171.9(3)
C7–C8–C9–N6	–0.9(3)
C17–C10–C11–C12	–40.3(4)
W1–C10–C11–C12	70.9(3)
C17–C10–C11–W1	–111.3(2)
C10–C11–C12–C13	35.2(5)
W1–C11–C12–C13	99.8(3)
C10–C11–C12–W1	–64.6(3)
C11–C12–C13–C14	37.0(5)
W1–C12–C13–C14	111.2(3)
C12–C13–C14–C15	–12.2(5)
C13–C14–C15–C16	–47.8(5)
C14–C15–C16–C17	–1.6(4)
C15–C16–C17–C10	89.5(3)
C11–C10–C17–C16	–51.0(3)
W1–C10–C17–C16	–134.5(2)
C9–N6–B1–N2	128.6(3)
N5–N6–B1–N2	–60.9(3)
C9–N6–B1–N4	–113.1(3)
N5–N6–B1–N4	57.4(3)
C3–N2–B1–N6	–115.3(3)
N1–N2–B1–N6	54.4(3)
C3–N2–B1–N4	129.1(3)
N1–N2–B1–N4	–61.2(3)
C6–N4–B1–N6	108.0(3)
N3–N4–B1–N6	–49.6(3)
C6–N4–B1–N2	–134.8(3)
N3–N4–B1–N2	67.6(3)
O4–S1–C21–F3	–63.4(2)
O3–S1–C21–F3	56.4(2)
O2–S1–C21–F3	175.8(2)
O4–S1–C21–F1	176.2(2)
O3–S1–C21–F1	–64.0(2)
O2–S1–C21–F1	55.4(2)
O4–S1–C21–F2	56.8(2)
O3–S1–C21–F2	176.6(2)
O2–S1–C21–F2	–64.0(2)

## Structure Report for mo\_harman\_mne\_5\_029\_0m

A yellow, block-shaped crystal of mo\_harman\_mne\_5\_029\_0m was coated with Paratone oil and mounted on a MiTeGen micromount. Data were collected at 100(2) K on a Bruker D8 VENTURE dual wavelength Mo/Cu Kappa four-circle diffractometer with a PHOTON III detector. The diffractometer was equipped with an Oxford Cryostream 800Plus low temperature device and used Mo  $K_\alpha$  radiation ( $\lambda = 0.71073\text{\AA}$ ) from an Incoatec Ims 3.0 microfocus sealed X-ray tube with a HELIOS double bounce multilayer mirror as monochromator.

Data collection and processing were done within the Bruker APEX5 software suite.<sup>[1]</sup> All data were integrated with SAINT 8.40B using a narrow-frame algorithm and a Multi-Scan absorption correction using was applied.<sup>[2]</sup> Using [Unknown program in \_computing\_structure\_refinement] as a graphical interface,<sup>[3]</sup> the structure was solved by direct methods with SHELXT 2018/2 and refined by full-matrix least-squares methods against  $F^2$  using SHELXL-2019/2.<sup>[4,5]</sup> All non-hydrogen atoms were refined with anisotropic displacement parameters. All hydrogen atoms were refined with isotropic displacement parameters. The B-H hydrogen atom was located in the electron diffraction map and refined isotropically. All other hydrogen atoms were placed in calculated positions using a riding model with their  $U_{\text{iso}}$  values constrained to 1.5 times the  $U_{\text{eq}}$  of their pivot atoms for terminal  $\text{sp}^3$  carbon atoms and 1.2 times for all other carbon atoms.

This report and the CIF file were generated using FinalCif.<sup>[6]</sup>

Table 1. Crystal data and structure refinement for mo\_harman\_mne\_5\_029\_0m

CCDC number	
Empirical formula	$\text{C}_{22}\text{H}_{32}\text{BCl}_3\text{N}_7\text{OPW}$
Formula weight	742.52
Temperature [K]	100(2)
Crystal system	monoclinic
Space group (number)	$P2_1/c$ (14)
$a$ [ $\text{\AA}$ ]	11.6338(9)
$b$ [ $\text{\AA}$ ]	14.6139(10)
$c$ [ $\text{\AA}$ ]	16.7964(12)

$\alpha$ [°]	90
$\beta$ [°]	92.492(2)
$\gamma$ [°]	90
Volume [Å <sup>3</sup> ]	2852.9(4)
Z	4
$\rho_{\text{calc}}$ [gcm <sup>-3</sup> ]	1.729
$\mu$ [mm <sup>-1</sup> ]	4.416
$F(000)$	1464
Crystal size [mm <sup>3</sup> ]	0.043×0.054×0.072
Crystal colour	yellow
Crystal shape	block
Radiation	Mo $K_{\alpha}$ ( $\lambda=0.71073$ Å)
2 $\theta$ range [°]	3.50 to 46.52 (0.90 Å)
Index ranges	$-12 \leq h \leq 12$ $-16 \leq k \leq 16$ $-17 \leq l \leq 18$
Reflections collected	21647
Independent reflections	4096 $R_{\text{int}} = 0.1635$ $R_{\text{sigma}} = 0.1280$
Completeness to $\theta = 23.260^\circ$	99.9
Data / Restraints / Parameters	4096 / 0 / 332
Goodness-of-fit on $F^2$	1.003
Final $R$ indexes [ $I \geq 2\sigma(I)$ ]	$R_1 = 0.0608$ $wR_2 = 0.1309$
Final $R$ indexes [all data]	$R_1 = 0.1265$ $wR_2 = 0.1587$
Largest peak/hole [eÅ <sup>-3</sup> ]	1.60/−1.57

Table 2. Atomic coordinates and  $U_{eq}$  [ $\text{\AA}^2$ ] for mo\_harman\_mne\_5\_029\_0m

Atom	x	y	z	$U_{eq}$
W1	0.60940(6)	0.77086(4)	0.34090(3)	0.0325(2)
P1	0.6864(4)	0.9054(3)	0.2695(3)	0.0458(12)
O1	0.7208(9)	0.8162(8)	0.4992(6)	0.052(3)
N1	0.5079(11)	0.7412(7)	0.2267(6)	0.035(3)
N2	0.3901(11)	0.7446(7)	0.2257(7)	0.035(3)
N3	0.4706(12)	0.8683(8)	0.3654(7)	0.040(3)
N4	0.3605(11)	0.8555(8)	0.3373(7)	0.035(3)
N5	0.4748(11)	0.6856(8)	0.3916(6)	0.033(3)
N6	0.3619(12)	0.6921(8)	0.3653(7)	0.039(3)
N7	0.6782(10)	0.7964(7)	0.4322(7)	0.035(3)
C1	0.5372(15)	0.7174(10)	0.1541(9)	0.045(4)
H1	0.614029	0.711191	0.137919	0.054
C2	0.4416(17)	0.7033(10)	0.1063(9)	0.049(5)
H2	0.439259	0.684404	0.052104	0.058
C3	0.3528(16)	0.7209(10)	0.1499(9)	0.048(5)
H3	0.274483	0.717737	0.131516	0.058
C4	0.4690(15)	0.9462(10)	0.4081(8)	0.041(4)
H4	0.534553	0.972430	0.434994	0.050
C5	0.3598(14)	0.9828(10)	0.4079(8)	0.039(4)
H5	0.335833	1.036942	0.433671	0.046
C6	0.2943(13)	0.9243(10)	0.3627(9)	0.036(4)
H6	0.214086	0.930785	0.350877	0.044
C7	0.4762(15)	0.6343(10)	0.4573(9)	0.041(4)
H7	0.543296	0.618380	0.488587	0.050
C8	0.3637(17)	0.6073(10)	0.4734(10)	0.051(5)
H8	0.339786	0.570728	0.516460	0.061
C9	0.2967(16)	0.6448(11)	0.4140(11)	0.055(5)
H9	0.215568	0.638321	0.408007	0.066
C10	0.7674(14)	0.7088(10)	0.2891(9)	0.043(4)
H10	0.768131	0.711670	0.229634	0.052
C11	0.6934(13)	0.6367(10)	0.3198(8)	0.036(4)
H11	0.651994	0.606509	0.273404	0.043
C12	0.7234(16)	0.5639(10)	0.3818(8)	0.045(4)
H12	0.648318	0.544638	0.403244	0.055
C13	0.7959(19)	0.5888(12)	0.4514(11)	0.062(5)
H13	0.755823	0.603221	0.497882	0.075
C14	0.910(2)	0.5944(13)	0.4593(12)	0.071(6)
H14	0.945731	0.600189	0.511110	0.085
C15	0.9827(17)	0.5919(12)	0.3897(14)	0.075(6)
H15	1.038178	0.544506	0.386805	0.090
C16	0.9743(15)	0.6539(12)	0.3293(13)	0.069(6)
H16	1.023794	0.649955	0.285922	0.083

C17	0.8846(14)	0.7299(11)	0.3319(9)	0.051(4)
H17A	0.916764	0.785594	0.307835	0.061
H17B	0.871174	0.743924	0.388443	0.061
C18	0.7710(16)	0.4781(11)	0.3416(10)	0.060(5)
H18A	0.726780	0.466355	0.291598	0.091
H18B	0.764448	0.425395	0.377163	0.091
H18C	0.852011	0.487860	0.330275	0.091
C19	0.7689(15)	0.8897(10)	0.1819(10)	0.056(5)
H19A	0.842169	0.859884	0.196971	0.084
H19B	0.783930	0.949337	0.157848	0.084
H19C	0.725530	0.851248	0.143387	0.084
C20	0.7753(16)	0.9799(11)	0.3308(12)	0.076(6)
H20A	0.730649	1.003744	0.374448	0.115
H20B	0.801985	1.030973	0.298622	0.115
H20C	0.841778	0.945746	0.352934	0.115
C21	0.5755(16)	0.9810(11)	0.2287(11)	0.067(6)
H21A	0.525542	0.947214	0.190506	0.101
H21B	0.611344	1.032305	0.201565	0.101
H21C	0.529750	1.004307	0.271885	0.101
B1	0.3244(18)	0.7631(13)	0.3020(11)	0.044(5)
H1A	0.234(13)	0.759(9)	0.300(8)	0.053
Cl1	1.0850(6)	0.8373(6)	0.4912(4)	0.134(3)
Cl2	1.0300(6)	0.7400(5)	0.6282(4)	0.117(2)
Cl3	0.9365(7)	0.9146(6)	0.6080(6)	0.170(4)
C22	0.9793(17)	0.8227(13)	0.5601(17)	0.112(10)
H22	0.910194	0.796434	0.530837	0.134

$U_{eq}$  is defined as 1/3 of the trace of the orthogonalized  $U_{ij}$  tensor.

Table 3. Anisotropic displacement parameters ( $\text{\AA}^2$ ) for mo\_harman\_mne\_5\_029\_0m. The anisotropic displacement factor exponent takes the form:

$$-2\pi^2 [h^2(a^*)^2 U_{11} + k^2(b^*)^2 U_{22} + \dots + 2hka^*b^* U_{12}]$$

Atom	$U_{11}$	$U_{22}$	$U_{33}$	$U_{23}$	$U_{13}$	$U_{12}$
W1	0.0416(4)	0.0261(3)	0.0300(3)	0.0017(3)	0.0035(3)	-0.0004(4)
P1	0.051(3)	0.032(2)	0.055(3)	0.013(2)	0.014(2)	0.000(2)
O1	0.041(7)	0.069(8)	0.047(7)	-0.008(6)	-0.007(6)	0.005(6)
N1	0.048(9)	0.030(8)	0.027(7)	0.008(6)	0.012(6)	0.014(6)
N2	0.042(9)	0.033(8)	0.031(7)	0.002(5)	0.006(6)	0.008(6)
N3	0.059(10)	0.032(7)	0.027(7)	0.000(6)	-0.016(7)	-0.021(7)
N4	0.042(9)	0.032(8)	0.031(7)	0.006(6)	-0.004(7)	-0.002(7)
N5	0.055(10)	0.017(6)	0.026(7)	0.001(6)	0.007(6)	0.004(6)
N6	0.039(9)	0.037(8)	0.042(8)	0.001(6)	-0.001(7)	-0.005(7)
N7	0.043(8)	0.025(7)	0.038(8)	0.002(6)	0.001(6)	0.003(6)
C1	0.048(11)	0.035(10)	0.050(10)	-0.009(8)	-0.011(9)	-0.001(9)
C2	0.082(14)	0.031(10)	0.033(9)	-0.005(7)	0.010(10)	0.003(9)
C3	0.066(13)	0.044(10)	0.033(9)	-0.003(8)	-0.024(9)	-0.005(10)
C4	0.063(13)	0.027(9)	0.034(9)	-0.010(7)	-0.001(8)	0.001(9)

C5	0.052(12)	0.044(10)	0.021(8)	0.000(7)	0.018(8)	0.014(9)
C6	0.027(10)	0.040(10)	0.043(10)	−0.017(8)	0.004(8)	0.001(8)
C7	0.048(12)	0.033(9)	0.044(10)	−0.008(8)	0.006(9)	−0.003(8)
C8	0.081(15)	0.034(10)	0.038(10)	0.024(8)	0.012(10)	−0.003(10)
C9	0.053(13)	0.033(10)	0.080(14)	−0.024(10)	0.030(11)	−0.014(9)
C10	0.053(11)	0.041(11)	0.036(9)	0.007(8)	0.000(8)	−0.007(9)
C11	0.050(11)	0.037(9)	0.020(8)	0.005(7)	0.000(7)	0.024(8)
C12	0.071(13)	0.045(10)	0.020(8)	0.007(7)	0.004(8)	0.014(9)
C13	0.075(16)	0.061(13)	0.052(12)	0.001(10)	0.019(11)	0.003(11)
C14	0.084(18)	0.074(14)	0.055(13)	0.001(11)	0.015(12)	0.012(13)
C15	0.063(15)	0.040(11)	0.119(19)	−0.011(12)	−0.014(14)	0.010(10)
C16	0.042(12)	0.059(13)	0.107(17)	0.022(12)	0.007(11)	0.023(10)
C17	0.064(12)	0.046(10)	0.044(10)	0.010(9)	0.001(9)	−0.016(11)
C18	0.066(14)	0.057(12)	0.058(12)	0.000(10)	0.002(10)	0.020(10)
C19	0.065(13)	0.040(10)	0.063(12)	0.034(9)	0.006(10)	0.003(9)
C20	0.065(15)	0.047(12)	0.118(18)	0.008(11)	0.020(13)	−0.039(10)
C21	0.074(15)	0.050(11)	0.082(14)	0.033(10)	0.047(11)	0.015(10)
B1	0.045(12)	0.039(11)	0.046(11)	−0.016(10)	−0.013(10)	0.005(11)
Cl1	0.092(5)	0.222(9)	0.090(5)	0.016(5)	0.018(4)	−0.040(5)
Cl2	0.093(5)	0.161(6)	0.096(4)	0.028(4)	−0.013(4)	−0.030(5)
Cl3	0.099(6)	0.165(8)	0.241(10)	−0.103(7)	−0.046(6)	0.023(5)
C22	0.040(14)	0.034(12)	0.26(3)	0.006(16)	−0.021(17)	0.001(10)

Table 4. Bond lengths and angles for mo\_harman\_mne\_5\_029\_0m

Atom–Atom	Length [Å]	N6–B1	1.54(2)
W1–N7	1.739(12)	C1–C2	1.36(2)
W1–N5	2.201(12)	C1–H1	0.9500
W1–N3	2.205(14)	C2–C3	1.32(2)
W1–C11	2.226(13)	C2–H2	0.9500
W1–N1	2.251(12)	C3–H3	0.9500
W1–C10	2.257(16)	C4–C5	1.38(2)
W1–P1	2.489(4)	C4–H4	0.9500
P1–C20	1.797(18)	C5–C6	1.355(19)
P1–C19	1.806(16)	C5–H5	0.9500
P1–C21	1.810(17)	C6–H6	0.9500
O1–N7	1.245(14)	C7–C8	1.41(2)
N1–C1	1.326(18)	C7–H7	0.9500
N1–N2	1.370(16)	C8–C9	1.35(2)
N2–C3	1.372(17)	C8–H8	0.9500
N2–B1	1.54(2)	C9–H9	0.9500
N3–C4	1.346(17)	C10–C11	1.468(19)
N3–N4	1.358(16)	C10–C17	1.54(2)
N4–C6	1.348(17)	C10–H10	1.0000
N4–B1	1.53(2)	C11–C12	1.520(18)
N5–C7	1.335(17)	C11–H11	1.0000
N5–N6	1.371(16)	C12–C13	1.46(2)
N6–C9	1.332(19)	C12–C18	1.54(2)



C12–H12	1.0000
C13–C14	1.33(3)
C13–H13	0.9500
C14–C15	1.47(3)
C14–H14	0.9500
C15–C16	1.36(2)
C15–H15	0.9500
C16–C17	1.53(2)
C16–H16	0.9500
C17–H17A	0.9900
C17–H17B	0.9900
C18–H18A	0.9800
C18–H18B	0.9800
C18–H18C	0.9800
C19–H19A	0.9800
C19–H19B	0.9800
C19–H19C	0.9800
C20–H20A	0.9800
C20–H20B	0.9800
C20–H20C	0.9800
C21–H21A	0.9800
C21–H21B	0.9800
C21–H21C	0.9800
B1–H1A	1.05(14)
Cl1–C22	1.74(3)
Cl2–C22	1.75(2)
Cl3–C22	1.65(2)
C22–H22	1.0000
<b>Atom–Atom– Atom</b>	<b>Angle [°]</b>
N7–W1–N5	95.1(5)
N7–W1–N3	90.6(5)
N5–W1–N3	75.8(4)
N7–W1–C11	98.1(5)
N5–W1–C11	83.5(5)
N3–W1–C11	158.2(5)
N7–W1–N1	175.7(5)
N5–W1–N1	82.2(4)
N3–W1–N1	85.5(4)
C11–W1–N1	84.9(5)
N7–W1–C10	94.3(5)
N5–W1–C10	121.8(5)
N3–W1–C10	161.1(5)
C11–W1–C10	38.2(5)
N1–W1–C10	90.0(5)
N7–W1–P1	95.4(4)
N5–W1–P1	155.5(3)

N3–W1–P1	82.0(3)
C11–W1–P1	116.7(4)
N1–W1–P1	85.9(3)
C10–W1–P1	79.4(4)
C20–P1–C19	103.3(9)
C20–P1–C21	103.3(9)
C19–P1–C21	99.5(8)
C20–P1–W1	114.4(6)
C19–P1–W1	120.5(5)
C21–P1–W1	113.5(6)
C1–N1–N2	107.2(12)
C1–N1–W1	133.4(11)
N2–N1–W1	119.4(8)
N1–N2–C3	106.2(12)
N1–N2–B1	121.8(12)
C3–N2–B1	131.8(14)
C4–N3–N4	105.5(13)
C4–N3–W1	132.3(11)
N4–N3–W1	122.2(9)
C6–N4–N3	109.3(12)
C6–N4–B1	129.2(14)
N3–N4–B1	119.8(12)
C7–N5–N6	106.4(12)
C7–N5–W1	130.9(11)
N6–N5–W1	121.6(9)
C9–N6–N5	109.2(13)
C9–N6–B1	128.6(16)
N5–N6–B1	120.5(13)
O1–N7–W1	176.0(11)
N1–C1–C2	110.3(15)
N1–C1–H1	124.9
C2–C1–H1	124.9
C3–C2–C1	106.4(14)
C3–C2–H2	126.8
C1–C2–H2	126.8
C2–C3–N2	109.9(15)
C2–C3–H3	125.0
N2–C3–H3	125.0
N3–C4–C5	111.1(15)
N3–C4–H4	124.4
C5–C4–H4	124.4
C6–C5–C4	104.7(14)
C6–C5–H5	127.7
C4–C5–H5	127.7
N4–C6–C5	109.4(14)
N4–C6–H6	125.3
C5–C6–H6	125.3
N5–C7–C8	109.8(15)

N5-C7-H7	125.1
C8-C7-H7	125.1
C9-C8-C7	104.8(15)
C9-C8-H8	127.6
C7-C8-H8	127.6
N6-C9-C8	109.8(16)
N6-C9-H9	125.1
C8-C9-H9	125.1
C11-C10-C17	119.9(13)
C11-C10-W1	69.7(8)
C17-C10-W1	117.2(10)
C11-C10-H10	114.3
C17-C10-H10	114.3
W1-C10-H10	114.3
C10-C11-C12	128.5(14)
C10-C11-W1	72.1(8)
C12-C11-W1	126.7(9)
C10-C11-H11	108.3
C12-C11-H11	108.3
W1-C11-H11	108.3
C13-C12-C11	118.9(14)
C13-C12-C18	110.5(14)
C11-C12-C18	110.2(12)
C13-C12-H12	105.4
C11-C12-H12	105.4
C18-C12-H12	105.4
C14-C13-C12	129.4(18)
C14-C13-H13	115.3
C12-C13-H13	115.3
C13-C14-C15	121(2)
C13-C14-H14	119.3
C15-C14-H14	119.3
C16-C15-C14	123.4(18)
C16-C15-H15	118.3
C14-C15-H15	118.3
C15-C16-C17	119.3(18)
C15-C16-H16	120.3
C17-C16-H16	120.3
C16-C17-C10	115.6(14)
C16-C17-H17A	108.4
C10-C17-H17A	108.4
C16-C17-H17B	108.4
C10-C17-H17B	108.4
H17A-C17-H17B	107.4
C12-C18-H18A	109.5
C12-C18-H18B	109.5

H18A-C18-H18B	109.5
C12-C18-H18C	109.5
H18A-C18-H18C	109.5
H18B-C18-H18C	109.5
P1-C19-H19A	109.5
P1-C19-H19B	109.5
H19A-C19-H19B	109.5
P1-C19-H19C	109.5
H19A-C19-H19C	109.5
H19B-C19-H19C	109.5
P1-C20-H20A	109.5
P1-C20-H20B	109.5
H20A-C20-H20B	109.5
P1-C20-H20C	109.5
H20A-C20-H20C	109.5
H20B-C20-H20C	109.5
P1-C21-H21A	109.5
P1-C21-H21B	109.5
H21A-C21-H21B	109.5
P1-C21-H21C	109.5
H21A-C21-H21C	109.5
H21B-C21-H21C	109.5
N4-B1-N6	105.3(12)
N4-B1-N2	109.9(15)
N6-B1-N2	108.7(13)
N4-B1-H1A	109(8)
N6-B1-H1A	104(8)
N2-B1-H1A	119(8)
Cl3-C22-Cl1	117.4(12)
Cl3-C22-Cl2	110.0(17)
Cl1-C22-Cl2	107.0(11)
Cl3-C22-H22	107.3
Cl1-C22-H22	107.3
Cl2-C22-H22	107.3

Table 5. Torsion angles for mo\_harman\_mne\_5\_029\_0m

Atom–Atom– Atom–Atom	Torsion Angle [°]		
C1–N1–N2–C3	0.6(15)	W1–C10–C17–C16	147.3(12)
W1–N1–N2–C3	–178.2(8)	C6–N4–B1–N6	–110.9(16)
C1–N1–N2–B1	175.4(13)	N3–N4–B1–N6	52.3(18)
W1–N1–N2–B1	–3.4(16)	C6–N4–B1–N2	132.2(15)
C4–N3–N4–C6	0.0(15)	N3–N4–B1–N2	–64.6(17)
W1–N3–N4–C6	178.7(9)	C9–N6–B1–N4	106.2(18)
C4–N3–N4–B1	–166.2(13)	N5–N6–B1–N4	–57.9(18)
W1–N3–N4–B1	12.5(17)	C9–N6–B1–N2	–136.2(16)
C7–N5–N6–C9	–0.6(15)	N5–N6–B1–N2	59.8(17)
W1–N5–N6–C9	–169.9(9)	N1–N2–B1–N4	59.1(17)
C7–N5–N6–B1	166.3(12)	C3–N2–B1–N4	–127.6(16)
W1–N5–N6–B1	–3.1(17)	N1–N2–B1–N6	–55.6(18)
N2–N1–C1–C2	–1.3(16)	C3–N2–B1–N6	117.7(16)
W1–N1–C1–C2	177.2(9)		
N1–C1–C2–C3	1.6(18)		
C1–C2–C3–N2	–1.2(18)		
N1–N2–C3–C2	0.4(17)		
B1–N2–C3–C2	–173.7(15)		
N4–N3–C4–C5	0.2(16)		
W1–N3–C4–C5	–178.3(9)		
N3–C4–C5–C6	–0.3(17)		
N3–N4–C6–C5	–0.2(16)		
B1–N4–C6–C5	164.4(14)		
C4–C5–C6–N4	0.3(17)		
N6–N5–C7–C8	0.2(16)		
W1–N5–C7–C8	168.2(10)		
N5–C7–C8–C9	0.2(18)		
N5–N6–C9–C8	0.7(17)		
B1–N6–C9–C8	–164.8(14)		
C7–C8–C9–N6	–0.6(18)		
C17–C10–C11–C12	–12(2)		
W1–C10–C11–C12	–123.0(14)		
C17–C10–C11–W1	110.5(13)		
C10–C11–C12–C13	40(2)		
W1–C11–C12–C13	–56(2)		
C10–C11–C12–C18	–89.1(19)		
W1–C11–C12–C18	175.1(12)		
C11–C12–C13–C14	–83(2)		
C18–C12–C13–C14	46(3)		
C12–C13–C14–C15	12(3)		
C13–C14–C15–C16	60(3)		
C14–C15–C16–C17	–1(3)		
C15–C16–C17–C10	–93(2)		
C11–C10–C17–C16	66.2(19)		

## Structure Report for 4-jkh-013-x2

A colourless, needle-shaped crystal of 4-jkh-013-x2 was coated with Paratone oil and mounted on a MiTeGen micromount. Data were collected at 100.00 K on a Bruker D8 VENTURE dual wavelength Mo/Cu Kappa four-circle diffractometer with a PHOTON III detector. The diffractometer was equipped with an Oxford Cryostream 800 low temperature device and used Mo  $K_\alpha$  radiation ( $\lambda = 0.71073\text{\AA}$ ) from an Incoatec Ims 3.0 microfocus sealed X-ray tube with a HELIOS double bounce multilayer mirror as monochromator.

Data collection and processing were done within the Bruker APEX5 software suite.<sup>[1]</sup> All data were integrated with SAINT 8.40B using a narrow-frame algorithm and a Multi-Scan absorption correction using SADABS 2016/2 was applied.<sup>[2]</sup> Using Olex2 as a graphical interface,<sup>[3]</sup> the structure was solved by dual methods with SHELXT and refined by full-matrix least-squares methods against  $F^2$  using SHELXL.<sup>[4,5]</sup> All non-hydrogen atoms were refined with anisotropic displacement parameters. The B-H hydrogen atom as well as H10 and H11 were located in the electron density map and refined isotropically. All other hydrogen atoms were refined with isotropic displacement parameters using a riding model with their  $U_{\text{iso}}$  values constrained to 1.5 times the  $U_{\text{eq}}$  of their pivot atoms for terminal  $\text{sp}^3$  carbon atoms and 1.2 times for all other carbon atoms.

This report and the CIF file were generated using FinalCif.<sup>[6]</sup>

Table 1. Crystal data and structure refinement for 4-jkh-013-x2

CCDC number	
Empirical formula	$\text{C}_{30}\text{H}_{40}\text{BN}_8\text{OPW}$
Formula weight	754.33
Temperature [K]	100.00
Crystal system	monoclinic
Space group (number)	$P2_1/c$ (14)
$a$ [Å]	16.8919(6)
$b$ [Å]	18.6996(6)
$c$ [Å]	10.1419(4)
$\alpha$ [°]	90

$\beta$ [°]	97.0400(10)
$\gamma$ [°]	90
Volume [Å <sup>3</sup> ]	3179.4(2)
Z	4
$\rho_{\text{calc}}$ [gcm <sup>-3</sup> ]	1.576
$\mu$ [mm <sup>-1</sup> ]	3.721
<i>F</i> (000)	1512
Crystal size [mm <sup>3</sup> ]	0.059×0.081×0.151
Crystal colour	colourless
Crystal shape	needle
Radiation	Mo <i>K</i> <sub>α</sub> ( $\lambda$ =0.71073 Å)
2 $\theta$ range [°]	4.60 to 61.19 (0.70 Å)
Index ranges	-24 ≤ <i>h</i> ≤ 24 -20 ≤ <i>k</i> ≤ 26 -14 ≤ <i>l</i> ≤ 14
Reflections collected	71130
Independent reflections	9765 <i>R</i> <sub>int</sub> = 0.0909 <i>R</i> <sub>sigma</sub> = 0.0619
Completeness to $\theta$ = 25.242°	99.9
Data / Restraints / Parameters	9765 / 0 / 400
Goodness-of-fit on <i>F</i> <sup>2</sup>	1.005
Final <i>R</i> indexes [ <i>I</i> ≥ 2 $\sigma$ ( <i>I</i> )]	<i>R</i> <sub>1</sub> = 0.0367 <i>wR</i> <sub>2</sub> = 0.0724
Final <i>R</i> indexes [all data]	<i>R</i> <sub>1</sub> = 0.0627 <i>wR</i> <sub>2</sub> = 0.0813
Largest peak/hole [eÅ <sup>-3</sup> ]	1.14/-1.24

Table 2. Atomic coordinates and  $U_{eq}$  [ $\text{\AA}^2$ ] for 4-jkh-013-x2

Atom	x	y	z	$U_{eq}$
W1	0.30076(2)	0.49324(2)	0.67598(2)	0.01542(4)
P1	0.15734(6)	0.45050(5)	0.65278(10)	0.0197(2)
O1	0.31978(19)	0.47732(17)	0.3885(3)	0.0340(7)
N1	0.28015(18)	0.49815(14)	0.8891(3)	0.0171(6)
N2	0.31465(19)	0.45012(15)	0.9786(3)	0.0192(6)
N3	0.31271(19)	0.37635(16)	0.7074(3)	0.0191(7)
N4	0.3400(2)	0.34776(16)	0.8290(3)	0.0227(7)
N5	0.42603(19)	0.47367(16)	0.7596(3)	0.0197(6)
N6	0.4437(2)	0.43828(16)	0.8790(3)	0.0226(7)
N7	0.31343(19)	0.48493(16)	0.5062(3)	0.0206(6)
N8	0.1179(2)	0.55345(18)	0.3481(3)	0.0267(7)
C1	0.2300(2)	0.53664(19)	0.9545(4)	0.0193(7)
H1	0.197983	0.575004	0.916804	0.023
C2	0.2313(2)	0.5128(2)	1.0838(4)	0.0247(8)
H2	0.201402	0.530611	1.150097	0.030
C3	0.2854(3)	0.4578(2)	1.0950(4)	0.0248(9)
H3	0.299841	0.429797	1.172405	0.030
C4	0.2997(3)	0.3215(2)	0.6229(4)	0.0269(9)
H4	0.281010	0.325743	0.531011	0.032
C5	0.3175(3)	0.2574(2)	0.6890(5)	0.0373(12)
H5	0.312530	0.210388	0.653249	0.045
C6	0.3439(3)	0.2769(2)	0.8182(4)	0.0328(10)
H6	0.361911	0.244882	0.888250	0.039
C7	0.4938(2)	0.4760(2)	0.7056(4)	0.0248(8)
H7	0.499275	0.497000	0.621930	0.030
C8	0.5557(3)	0.4438(2)	0.7876(5)	0.0297(9)
H8	0.609821	0.438967	0.772314	0.036
C9	0.5216(2)	0.4206(2)	0.8944(4)	0.0272(9)
H9	0.548530	0.395809	0.968464	0.033
C10	0.2455(2)	0.60012(18)	0.6444(4)	0.0186(7)

H10	0.206(2)	0.611(2)	0.707(4)	0.022
C11	0.3285(2)	0.60820(19)	0.7019(4)	0.0195(8)
H11	0.335(2)	0.615(2)	0.792(4)	0.023
C12	0.3857(2)	0.65699(19)	0.6392(4)	0.0241(8)
H12	0.370891	0.655936	0.540641	0.029
C13	0.3766(3)	0.7349(2)	0.6874(4)	0.0293(9)
H13A	0.397254	0.737253	0.783017	0.035
H13B	0.410665	0.766220	0.639387	0.035
C14	0.2912(3)	0.7651(2)	0.6689(4)	0.0318(10)
H14A	0.258040	0.737124	0.724403	0.038
H14B	0.292470	0.815131	0.700892	0.038
C15	0.2523(3)	0.7633(2)	0.5258(4)	0.0308(10)
H15A	0.294949	0.757544	0.467800	0.037
H15B	0.226976	0.810359	0.504939	0.037
C16	0.1895(2)	0.70521(19)	0.4886(4)	0.0220(8)
H16	0.171818	0.711772	0.391555	0.026
C17	0.2224(2)	0.62739(18)	0.5034(4)	0.0200(8)
H17	0.272339	0.626765	0.459670	0.024
C18	0.1135(2)	0.7142(2)	0.5577(4)	0.0255(9)
H18A	0.081798	0.669555	0.547205	0.031
H18B	0.129049	0.722129	0.653848	0.031
C19	0.0625(2)	0.77588(19)	0.5014(4)	0.0230(8)
C20	0.0637(3)	0.8416(2)	0.5648(4)	0.0271(9)
H20	0.097306	0.848458	0.645958	0.033
C21	0.0164(3)	0.8975(2)	0.5111(5)	0.0321(11)
H21	0.018304	0.942280	0.555775	0.039
C22	-0.0329(3)	0.8893(2)	0.3950(5)	0.0354(11)
H22	-0.065305	0.927783	0.358962	0.042
C23	-0.0349(3)	0.8242(3)	0.3308(5)	0.0385(11)
H23	-0.069364	0.817863	0.250327	0.046
C24	0.0128(3)	0.7679(2)	0.3822(4)	0.0309(9)
H24	0.011577	0.723732	0.335779	0.037
C25	0.1639(2)	0.58286(19)	0.4195(4)	0.0212(8)
C26	0.4722(2)	0.6377(2)	0.6684(5)	0.0270(9)
H26	0.491713	0.623996	0.756673	0.032
C27	0.5228(3)	0.6385(2)	0.5796(6)	0.0377(12)
C28	0.0761(2)	0.5125(2)	0.6704(4)	0.0268(8)
H28A	0.088548	0.540196	0.752369	0.040
H28B	0.026624	0.485637	0.674140	0.040
H28C	0.069426	0.545093	0.594134	0.040

C29	0.1203(3)	0.4008(2)	0.5024(4)	0.0272(9)
H29A	0.128952	0.429065	0.423982	0.041
H29B	0.063155	0.391520	0.501531	0.041
H29C	0.148972	0.355334	0.501027	0.041
C30	0.1411(2)	0.3852(2)	0.7806(4)	0.0260(9)
H30A	0.175241	0.343462	0.772745	0.039
H30B	0.085027	0.370268	0.769099	0.039
H30C	0.154170	0.406847	0.868580	0.039
B1	0.3779(3)	0.3984(2)	0.9404(5)	0.0224(9)
H1A	0.408(2)	0.368(2)	1.030(4)	0.024(11)
H27A	0.502(2)	0.647(2)	0.487(4)	0.027(13)
H27B	0.577(3)	0.624(3)	0.597(5)	0.052(16)

$U_{eq}$  is defined as 1/3 of the trace of the orthogonalized  $U_{ij}$  tensor.

Table 3. Anisotropic displacement parameters ( $\text{\AA}^2$ ) for 4-jkh-013-x2. The anisotropic displacement factor exponent takes the form:

$$-2\pi^2[h^2(a^*)^2U_{11} + k^2(b^*)^2U_{22} + \dots + 2hka^*b^*U_{12}]$$

Atom	$U_{11}$	$U_{22}$	$U_{33}$	$U_{23}$	$U_{13}$	$U_{12}$
W1	0.01754(7)	0.01763(7)	0.01119(7)	0.00019(6)	0.00214(5)	0.00078(6)
P1	0.0198(5)	0.0225(5)	0.0167(5)	−0.0002(4)	0.0021(4)	−0.0018(4)
O1	0.0373(18)	0.0544(18)	0.0105(14)	−0.0033(13)	0.0036(13)	0.0084(15)
N1	0.0191(15)	0.0187(14)	0.0133(14)	−0.0014(11)	0.0015(11)	0.0004(12)
N2	0.0231(17)	0.0211(15)	0.0135(16)	0.0017(11)	0.0028(13)	0.0007(12)
N3	0.0191(17)	0.0237(15)	0.0142(16)	−0.0003(11)	0.0010(13)	0.0002(12)
N4	0.0286(19)	0.0213(15)	0.0195(17)	0.0042(12)	0.0073(14)	0.0040(13)
N5	0.0198(16)	0.0226(15)	0.0163(16)	0.0005(12)	0.0009(13)	0.0033(12)
N6	0.0238(18)	0.0265(16)	0.0165(17)	0.0014(12)	−0.0021(14)	0.0028(13)
N7	0.0211(16)	0.0263(16)	0.0147(15)	0.0013(12)	0.0039(12)	0.0039(13)
N8	0.0274(19)	0.0339(18)	0.0189(18)	0.0006(14)	0.0026(15)	0.0012(15)
C1	0.022(2)	0.0184(16)	0.0177(19)	0.0002(13)	0.0035(15)	0.0006(14)
C2	0.029(2)	0.0270(19)	0.0189(19)	−0.0049(15)	0.0076(16)	−0.0037(16)
C3	0.036(2)	0.0262(19)	0.0126(18)	0.0001(14)	0.0054(17)	−0.0038(16)
C4	0.036(3)	0.027(2)	0.019(2)	−0.0047(15)	0.0066(18)	0.0032(17)
C5	0.062(4)	0.0182(18)	0.032(3)	−0.0042(17)	0.009(2)	0.0043(19)
C6	0.047(3)	0.0223(19)	0.030(2)	0.0059(17)	0.011(2)	0.0064(18)
C7	0.022(2)	0.0252(19)	0.029(2)	−0.0040(16)	0.0079(17)	0.0006(15)
C8	0.020(2)	0.030(2)	0.039(3)	−0.0038(18)	0.0032(19)	0.0032(16)



C9	0.019(2)	0.033(2)	0.028(2)	−0.0007(17)	−0.0037(17)	0.0070(16)
C10	0.022(2)	0.0188(16)	0.0157(19)	0.0016(13)	0.0050(15)	0.0006(14)
C11	0.022(2)	0.0195(17)	0.0173(19)	−0.0002(14)	0.0025(16)	0.0003(14)
C12	0.025(2)	0.0227(18)	0.024(2)	0.0002(15)	0.0007(17)	−0.0075(15)
C13	0.030(2)	0.0224(19)	0.035(3)	−0.0008(17)	0.003(2)	−0.0035(16)
C14	0.040(3)	0.027(2)	0.030(2)	−0.0019(17)	0.009(2)	−0.0018(18)
C15	0.039(3)	0.0228(19)	0.031(2)	0.0053(17)	0.007(2)	0.0039(17)
C16	0.022(2)	0.0229(18)	0.021(2)	0.0060(14)	0.0029(16)	0.0038(15)
C17	0.022(2)	0.0225(17)	0.0161(19)	0.0011(14)	0.0029(15)	−0.0004(14)
C18	0.029(2)	0.0265(19)	0.021(2)	0.0056(15)	0.0045(17)	0.0024(16)
C19	0.022(2)	0.0236(18)	0.024(2)	0.0050(15)	0.0054(17)	0.0001(15)
C20	0.036(3)	0.0251(19)	0.021(2)	−0.0003(15)	0.0057(18)	0.0019(17)
C21	0.040(3)	0.0208(19)	0.038(3)	0.0038(17)	0.017(2)	0.0049(17)
C22	0.027(2)	0.036(2)	0.045(3)	0.019(2)	0.011(2)	0.0101(18)
C23	0.035(3)	0.052(3)	0.027(3)	0.012(2)	−0.006(2)	0.003(2)
C24	0.033(3)	0.031(2)	0.028(2)	−0.0003(17)	−0.0004(19)	−0.0010(18)
C25	0.028(2)	0.0228(18)	0.0137(18)	0.0057(14)	0.0066(16)	0.0070(15)
C26	0.024(2)	0.0210(18)	0.035(3)	−0.0004(16)	−0.0006(18)	−0.0021(15)
C27	0.028(3)	0.033(2)	0.053(4)	0.001(2)	0.012(2)	−0.0019(19)
C28	0.023(2)	0.034(2)	0.024(2)	−0.0008(16)	0.0043(16)	0.0037(17)
C29	0.029(2)	0.030(2)	0.021(2)	−0.0038(16)	−0.0054(17)	−0.0020(17)
C30	0.026(2)	0.028(2)	0.024(2)	0.0014(16)	0.0046(17)	−0.0064(16)
B1	0.023(2)	0.024(2)	0.019(2)	0.0044(16)	0.0004(18)	0.0022(17)

Table 4. Bond lengths and angles for 4-jkh-013-x2

Atom–Atom	Length [Å]		
W1–P1	2.5345(10)	P1–C29	1.829(4)
W1–N1	2.233(3)	P1–C30	1.826(4)
W1–N3	2.215(3)	O1–N7	1.220(4)
W1–N5	2.211(3)	N1–N2	1.356(4)
W1–N7	1.768(3)	N1–C1	1.346(4)
W1–C10	2.213(4)	N2–C3	1.342(5)
W1–C11	2.209(4)	N2–B1	1.526(5)
P1–C28	1.822(4)	N3–N4	1.371(4)
		N3–C4	1.338(5)

N4–C6	1.332(5)
N4–B1	1.551(6)
N5–N6	1.381(4)
N5–C7	1.329(5)
N6–C9	1.347(5)
N6–B1	1.532(5)
N8–C25	1.136(5)
C1–H1	0.9500
C1–C2	1.382(5)
C2–H2	0.9500
C2–C3	1.371(6)
C3–H3	0.9500
C4–H4	0.9500
C4–C5	1.388(6)
C5–H5	0.9500
C5–C6	1.380(6)
C6–H6	0.9500
C7–H7	0.9500
C7–C8	1.391(6)
C8–H8	0.9500
C8–C9	1.358(6)
C9–H9	0.9500
C10–H10	0.99(4)
C10–C11	1.459(6)
C10–C17	1.524(5)
C11–H11	0.91(4)
C11–C12	1.524(5)
C12–H12	1.0000
C12–C13	1.550(5)
C12–C26	1.499(6)
C13–H13A	0.9900
C13–H13B	0.9900
C13–C14	1.540(6)
C14–H14A	0.9900
C14–H14B	0.9900
C14–C15	1.519(6)
C15–H15A	0.9900
C15–H15B	0.9900
C15–C16	1.533(6)
C16–H16	1.0000
C16–C17	1.558(5)
C16–C18	1.545(5)
C17–H17	1.0000
C17–C25	1.479(5)
C18–H18A	0.9900
C18–H18B	0.9900
C18–C19	1.509(5)
C19–C20	1.386(5)

C19–C24	1.393(6)
C20–H20	0.9500
C20–C21	1.386(6)
C21–H21	0.9500
C21–C22	1.365(6)
C22–H22	0.9500
C22–C23	1.378(7)
C23–H23	0.9500
C23–C24	1.388(6)
C24–H24	0.9500
C26–H26	0.9500
C26–C27	1.315(6)
C27–H27A	0.97(4)
C27–H27B	0.95(5)
C28–H28A	0.9800
C28–H28B	0.9800
C28–H28C	0.9800
C29–H29A	0.9800
C29–H29B	0.9800
C29–H29C	0.9800
C30–H30A	0.9800
C30–H30B	0.9800
C30–H30C	0.9800
B1–H1A	1.13(4)
<b>Atom–Atom– Atom</b>	<b>Angle [°]</b>
N1–W1–P1	80.92(8)
N3–W1–P1	76.78(8)
N3–W1–N1	85.61(11)
N5–W1–P1	147.38(8)
N5–W1–N1	83.75(11)
N5–W1–N3	73.46(11)
N5–W1–C10	124.89(13)
N7–W1–P1	96.33(11)
N7–W1–N1	176.66(12)
N7–W1–N3	91.93(12)
N7–W1–N5	97.73(13)
N7–W1–C10	92.15(14)
N7–W1–C11	98.76(14)
C10–W1–P1	83.67(10)
C10–W1–N1	89.43(12)
C10–W1–N3	160.36(13)
C11–W1–P1	120.28(10)
C11–W1–N1	84.30(12)
C11–W1–N3	158.30(14)
C11–W1–N5	86.36(13)
C11–W1–C10	38.53(14)

C28-P1-W1	120.87(14)
C28-P1-C29	102.72(19)
C28-P1-C30	100.09(19)
C29-P1-W1	117.57(14)
C30-P1-W1	111.74(14)
C30-P1-C29	100.76(19)
N2-N1-W1	121.0(2)
C1-N1-W1	132.9(2)
C1-N1-N2	105.6(3)
N1-N2-B1	120.4(3)
C3-N2-N1	110.1(3)
C3-N2-B1	129.5(3)
N4-N3-W1	121.9(2)
C4-N3-W1	131.3(3)
C4-N3-N4	106.7(3)
N3-N4-B1	118.7(3)
C6-N4-N3	109.2(3)
C6-N4-B1	130.4(4)
N6-N5-W1	120.6(2)
C7-N5-W1	132.0(3)
C7-N5-N6	105.8(3)
N5-N6-B1	120.0(3)
C9-N6-N5	108.8(3)
C9-N6-B1	125.5(3)
O1-N7-W1	177.5(3)
N1-C1-H1	124.6
N1-C1-C2	110.9(3)
C2-C1-H1	124.6
C1-C2-H2	127.6
C3-C2-C1	104.7(3)
C3-C2-H2	127.6
N2-C3-C2	108.7(3)
N2-C3-H3	125.7
C2-C3-H3	125.7
N3-C4-H4	124.9
N3-C4-C5	110.1(4)
C5-C4-H4	124.9
C4-C5-H5	127.6
C6-C5-C4	104.8(4)
C6-C5-H5	127.6
N4-C6-C5	109.1(4)
N4-C6-H6	125.4
C5-C6-H6	125.4
N5-C7-H7	124.4
N5-C7-C8	111.2(4)
C8-C7-H7	124.4
C7-C8-H8	127.7
C9-C8-C7	104.7(4)

C9-C8-H8	127.7
N6-C9-C8	109.5(4)
N6-C9-H9	125.3
C8-C9-H9	125.3
W1-C10-H10	113(2)
C11-C10-W1	70.6(2)
C11-C10-H10	114(2)
C11-C10-C17	117.6(3)
C17-C10-W1	119.6(2)
C17-C10-H10	115(2)
W1-C11-H11	105(2)
C10-C11-W1	70.9(2)
C10-C11-H11	114(3)
C10-C11-C12	121.5(3)
C12-C11-W1	132.0(3)
C12-C11-H11	109(3)
C11-C12-H12	108.2
C11-C12-C13	109.8(3)
C13-C12-H12	108.2
C26-C12-C11	115.2(3)
C26-C12-H12	108.2
C26-C12-C13	107.2(3)
C12-C13-H13A	108.4
C12-C13-H13B	108.4
H13A-C13-H13B	107.4
C14-C13-C12	115.7(3)
C14-C13-H13A	108.4
C14-C13-H13B	108.4
C13-C14-H14A	108.9
C13-C14-H14B	108.9
H14A-C14-H14B	107.7
C15-C14-C13	113.4(4)
C15-C14-H14A	108.9
C15-C14-H14B	108.9
C14-C15-H15A	108.0
C14-C15-H15B	108.0
C14-C15-C16	117.1(3)
H15A-C15-H15B	107.3
C16-C15-H15A	108.0
C16-C15-H15B	108.0
C15-C16-H16	105.6
C15-C16-C17	114.2(3)
C15-C16-C18	113.6(3)
C17-C16-H16	105.6
C18-C16-H16	105.6

C18–C16–C17	111.4(3)
C10–C17–C16	116.8(3)
C10–C17–H17	106.2
C16–C17–H17	106.2
C25–C17–C10	115.3(3)
C25–C17–C16	105.4(3)
C25–C17–H17	106.2
C16–C18–H18A	109.1
C16–C18–H18B	109.1
H18A–C18–H18B	107.9
C19–C18–C16	112.3(3)
C19–C18–H18A	109.1
C19–C18–H18B	109.1
C20–C19–C18	121.9(4)
C20–C19–C24	118.0(4)
C24–C19–C18	120.1(4)
C19–C20–H20	119.6
C21–C20–C19	120.8(4)
C21–C20–H20	119.6
C20–C21–H21	119.5
C22–C21–C20	121.0(4)
C22–C21–H21	119.5
C21–C22–H22	120.5
C21–C22–C23	119.0(4)
C23–C22–H22	120.5
C22–C23–H23	119.6
C22–C23–C24	120.8(4)
C24–C23–H23	119.6
C19–C24–H24	119.8
C23–C24–C19	120.3(4)
C23–C24–H24	119.8
N8–C25–C17	174.3(4)
C12–C26–H26	118.0
C27–C26–C12	124.1(5)
C27–C26–H26	118.0
C26–C27–H27A	118(3)
C26–C27–H27B	124(3)

H27A–C27–H27B	117(4)
P1–C28–H28A	109.5
P1–C28–H28B	109.5
P1–C28–H28C	109.5
H28A–C28–H28B	109.5
H28A–C28–H28C	109.5
H28B–C28–H28C	109.5
P1–C29–H29A	109.5
P1–C29–H29B	109.5
P1–C29–H29C	109.5
H29A–C29–H29B	109.5
H29A–C29–H29C	109.5
H29B–C29–H29C	109.5
P1–C30–H30A	109.5
P1–C30–H30B	109.5
P1–C30–H30C	109.5
H30A–C30–H30B	109.5
H30A–C30–H30C	109.5
H30B–C30–H30C	109.5
N2–B1–N4	109.4(3)
N2–B1–N6	111.1(3)
N2–B1–H1A	112(2)
N4–B1–H1A	112(2)
N6–B1–N4	104.9(3)
N6–B1–H1A	107(2)

Table 5. Torsion angles for 4-jkh-013-x2

Atom–Atom–Atom–Atom	Torsion Angle [°]
W1–N1–N2–C3	–171.9(2)
W1–N1–N2–B1	9.0(4)
W1–N1–C1–C2	170.9(3)
W1–N3–N4–C6	–177.7(3)
W1–N3–N4–B1	–11.4(4)

W1–N3–C4–C5	178.5(3)
W1–N5–N6–C9	167.7(2)
W1–N5–N6–B1	13.0(4)
W1–N5–C7–C8	–166.1(3)
W1–C10–C11–C12	128.2(3)
W1–C10–C17–C16	–175.7(2)
W1–C10–C17–C25	59.8(4)

W1-C11-C12-C13	176.2(3)
W1-C11-C12-C26	-62.7(5)
N1-N2-C3-C2	-1.0(4)
N1-N2-B1-N4	-64.0(4)
N1-N2-B1-N6	51.3(5)
N1-C1-C2-C3	0.4(4)
N2-N1-C1-C2	-1.0(4)
N3-N4-C6-C5	-1.3(5)
N3-N4-B1-N2	65.2(4)
N3-N4-B1-N6	-54.0(4)
N3-C4-C5-C6	-1.4(5)
N4-N3-C4-C5	0.7(5)
N5-N6-C9-C8	0.1(4)
N5-N6-B1-N2	-64.8(4)
N5-N6-B1-N4	53.3(4)
N5-C7-C8-C9	0.8(5)
N6-N5-C7-C8	-0.7(4)
C1-N1-N2-C3	1.2(4)
C1-N1-N2-B1	-177.9(3)
C1-C2-C3-N2	0.4(4)
C3-N2-B1-N4	117.1(4)
C3-N2-B1-N6	-127.6(4)
C4-N3-N4-C6	0.4(4)
C4-N3-N4-B1	166.7(3)
C4-C5-C6-N4	1.6(5)
C6-N4-B1-N2	-131.8(4)
C6-N4-B1-N6	108.9(4)
C7-N5-N6-C9	0.4(4)
C7-N5-N6-B1	-154.4(3)
C7-C8-C9-N6	-0.5(5)
C9-N6-B1-N2	144.9(4)
C9-N6-B1-N4	-97.0(4)
C10-C11-C12-C13	84.3(4)
C10-C11-C12-C26	-154.7(4)
C11-C10-C17-C16	-93.4(4)
C11-C10-C17-C25	142.1(3)
C11-C12-C13-C14	-53.1(5)
C11-C12-C26-C27	137.5(4)
C12-C13-C14-C15	-57.3(5)
C13-C12-C26-C27	-100.0(5)
C13-C14-C15-C16	104.1(4)
C14-C15-C16-C17	-63.2(5)
C14-C15-C16-C18	65.9(5)
C15-C16-C17-C10	70.8(4)
C15-C16-C17-C25	-159.8(3)
C15-C16-C18-C19	72.5(4)
C16-C18-C19-C20	-100.3(4)
C16-C18-C19-C24	79.2(5)

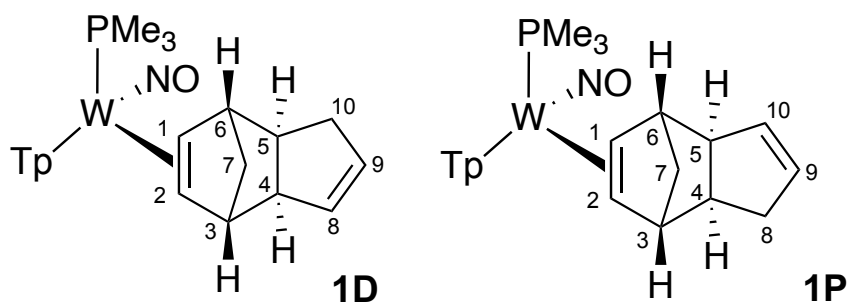
C17-C10-C11-W1	-114.0(3)
C17-C10-C11-C12	14.2(5)
C17-C16-C18-C19	-156.9(3)
C18-C16-C17-C10	-59.5(4)
C18-C16-C17-C25	69.9(4)
C18-C19-C20-C21	179.9(4)
C18-C19-C24-C23	179.3(4)
C19-C20-C21-C22	0.4(7)
C20-C19-C24-C23	-1.2(6)
C20-C21-C22-C23	-0.3(7)
C21-C22-C23-C24	-0.6(7)
C22-C23-C24-C19	1.3(7)
C24-C19-C20-C21	0.4(6)
C26-C12-C13-C14	-178.9(4)
B1-N2-C3-C2	178.0(4)
B1-N4-C6-C5	-165.4(4)
B1-N6-C9-C8	153.1(4)

## Bibliography

- [1] APEX5, *SAINT*, 8.40B, Bruker AXS Inc., Madison, Wisconsin, USA.
- [2] Krause, L.; Herbst-Irmer, R.; Sheldrick, G. M.; Stalke, D. Comparison of silver and molybdenum microfocus X-ray sources for single-crystal structure determination., *J. Appl. Cryst.* **2015**, 48, 3–10, doi:10.1107/S1600576714022985.
- [3] Dolomanov, O. V.; Bourhis, L. J.; Gildea, R. J.; Howard, J. A. K.; Puschmann, H. OLEX2: a complete structure solution, refinement and analysis program., *J. Appl. Cryst.* **2009**, 42, 339-341, doi:10.1107/S0021889808042726.
- [4] Sheldrick, G. M. SHELXT - integrated space-group and crystal-structure determination, *Acta Cryst.* **2015**, A71, 3–8, doi:10.1107/S2053273314026370.
- [5] Sheldrick, G. M. Crystal structure refinement with SHELXL., *Acta Cryst.* **2015**, C71, 3–8, doi:10.1107/S2053229614024218.
- [6] Kratzert, D., *FinalCif*, V144, <https://dkratzert.de/finalcif.html>.

## **Appendix D: Chapter 4 Data**

## Synthesis and characterization of [W(Tp)(NO)(PMe<sub>3</sub>)( $\eta^2$ - dicyclopentadiene)] (1)



In a 50 mL round bottom flask, [W]-anisole (2 g, 3.27 mmol) was added, followed by a 5:1 ratio of cyclopentadiene to dicyclopentadiene (5mL, 6.21 mmol) and 0.5 mL of DME. The reaction was heated to 50°C for 16 hours. The reaction mixture was added to a silica plug in the box and a tan band was eluted with 50 mL of ether. The ether filtrate was reduced to minimal solvent, 200 mL of hexanes were added, and the mixture was reduced to ~50 mL initiating precipitation. 450 mg of precipitate was collected over a 30 mL F fritted disc. The solid compound was loaded onto the Combi Flash and compounds 1D and 1P were eluted with 45% EtOAc/55% Hexanes.

**<sup>1</sup>H NMR (800 MHz, CDCl<sub>3</sub>,  $\delta$ , 25 °C) – 1D:** 8.14, 7.69, 7.62, 7.54, 7.23 (d, J = 2.05; 2.05; 2.22; 2.22 Hz, 6H, Tp protons), 6.28, 6.17, 6.11 (t, J = 2.47; 2.13; 2.13 Hz, 3H, Tp protons), 5.53, 5.46 (m, J = 1.71, 5.63; 2.13, 5.29, 2H, H8/H9), 3.41, 2.82 (m, 1H, H4/H5), 2.90 (d, J = 3.23 Hz, 1H, H3), 2.68 (d, J = 3.75 Hz, 1H, H6), 2.45 (m, 2H, H1/H10), 2.26 (dd, J = 2.20, 9.70 Hz, 1H, H10), 1.76 (d, J = 9.57 Hz, 1H, H7), 1.34 (d, 8.16 Hz, 9H, PMe<sub>3</sub>), 1.09 (dd, J = 2.93, 8.02 Hz, 1H, H2), 0.89 (d, J = 9.14 Hz, 1H, H7).

**<sup>1</sup>H NMR (800 MHz, CDCl<sub>3</sub>,  $\delta$ , 25 °C) – 1P:** 8.15, 8.14, 7.69, 7.63, 7.52, 7.19 (d, J = 2.35, 2.54, 2.28, 2.18, 1.85 Hz, 6H, Tp protons), 6.28, 6.16, 6.10 (t, J = 2.29, 2.18, 2.29 Hz, 3H, Tp protons), 5.68, 5.56 (dd, J = 2.09, 5.84; 2.09, 5.84 Hz, 2H, H9/H10), 3.41 (m, 1H, H4), 2.82 (m, 2H, H3/H6), 2.77 (bs, 1H, H5), 2.17 (m, J = 7.84, 14.26; 2.66 Hz, 2H, H1/H8), 2.07 (dd, J = 3.13, 9.72 Hz, 1H, H8), 1.73 (d, J = 9.72 Hz, 1H, H7), 1.35 (m, J = 3.12 Hz, 1H, H2), 1.32 (d, J = 8.20 Hz, 9H, PMe<sub>3</sub>), 0.89 (d, J = 9.41 Hz, 1H, H7).

**<sup>13</sup>C NMR (201 MHz, CDCl<sub>3</sub>,  $\delta$ , 25 °C) – 1D:** 144.6, 143.6, 140.4, 136.3, 135.3, 134.3 (7C, Tp carbons, C8 or C9), 130.2 (1C, C8 or C9), 106.1, 105.7, 105.4 (3C, Tp carbons), 62.2 (1C, C2), 58.4 (1C, C4), 57.3 (d, J = 8.94, 1C, C1), 49.3 (1C, C6), 48.2

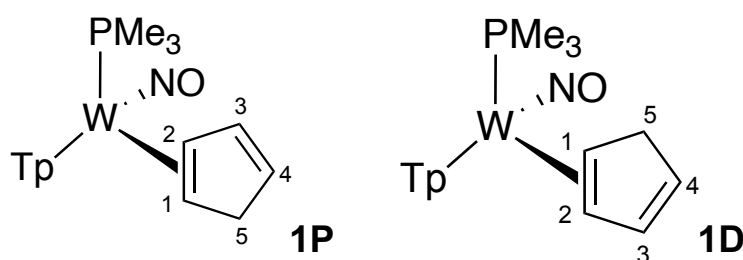


(1C, C5), 47.0 (1C, C3), 38.4 (1C, C7), 32.8 (1C, C10), 14.6 (d,  $J = 12.48$  Hz, 3C,  $\text{PMe}_3$ ).

**$^{13}\text{C}$  NMR (201 MHz,  $\text{CDCl}_3$ ,  $\delta$ , 25 °C) – 1P:** 144.5, 143.5, 140.7, 136.3, 135.3, 134.3 (6C, Tp carbons) 133.0, 131.7 (2C, C9/C10), 106.1, 105.7, 105.4 (3C, Tp carbons), 63.1 (d,  $J = 13.75$  Hz, C1), 58.2 (1C, C2), 48.2 (1C, C5), 45.6, 45.5 (2C, C3/C6), 38.5 (1C, C7), 32.8 (1C, C8), 14.5 (d,  $J = 12.93$  Hz, 3C,  $\text{PMe}_3$ ).

Composition of **1D/1P** has been confirmed by single crystal X-ray diffraction.

### Synthesis and characterization of $[\text{W}(\text{Tp})(\text{NO})(\text{PMe}_3)(\eta^2\text{-cyclopentadiene})]$ (**2**)



To a 50 mL round bottom flask were added a stir bar, **5** (2.00 g, 3.27 mmol), and 30 mL dried THF. The round bottom flask was sealed with a rubber septum and heated at 45°C in an oil bath. To the stirring yellow solution, distilled cyclopentadiene monomer (2.81 mL, 2.27 g, 34.3 mmol) was syringed through the septum and into the flask. After stirring for 14 hours, the dark brown reaction mixture was poured into a 500 mL Erlenmeyer flask, and hexanes (350 mL) was added. A purple precipitate was filtered off in a 60 mL fine porosity fritted funnel over a 500 mL filter flask. The tan-colored filtrate was reduced in vacuo to ~100 mL, inducing precipitation. A whitish-tan solid was collected on a 15 mL fine porosity fritted funnel and desiccated under static vacuum to yield **6** (1.01 g, 54.2%) as a ~2:1 ratio of 6P to 6D

**$^1\text{H}$  NMR (800 MHz,  $\text{CD}_3\text{CN}$ ,  $\delta$ , 25 °C) – 1P:** 8.37 (d,  $J = 2.0$  Hz, 1H, Pz), 8.00 (d,  $J = 2.0$  Hz, 1H, Pz), 7.87 (d,  $J = 2.4$  Hz, 1H, Pz), 7.80 (d,  $J = 2.4$  Hz, 1H, Pz), 7.76 (d,  $J = 2.4$  Hz, 1H, Pz), 7.41 (d,  $J = 2.2$  Hz, 1H, Pz), 6.38 (dd,  $J = 5.1, 2.2$  Hz, 1H, H3), 6.36 (t,  $J = 2.2$  Hz, 1H, Pz), 6.30 (t,  $J = 2.2$  Hz, 1H, Pz), 6.22 (t,  $J = 2.2$  Hz, 1H, Pz), 5.08 (dt,  $J = 4.9, 2.3$  Hz, 1H, H4), 4.33 (ddq,  $J = 19.3, 6.1, 2.0$  Hz, 1H, H5), 3.80 (dt,  $J = 19.4, 2.2$  Hz, 1H, H5), 3.70 (ddt,  $J = 11.9, 7.4, 2.1$  Hz, 1H, H2), 1.90 (td,  $J = 6.8, 2.9$  Hz, 1H, H1), 1.25 (d,  $J = 8.4$  Hz, 9H,  $\text{PMe}_3$ ).

**$^{13}\text{C}$  NMR (201 MHz,  $\text{CD}_3\text{CN}$ ,  $\delta$ , 25 °C) - 1P:** 144.0 (1C, Pz), 141.5 (1C, Pz), 140.7 (1C, Pz), 136.9 (d,  $J_{\text{PC}} = 2.9$  Hz, 1C, C3), 136.8 (1C, Pz), 136.0 (1C, Pz), 135.6 (1C,

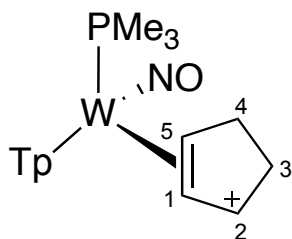
Pz), 121.5 (1C, C4), 106.4 (1C, Pz), 105.8 (1C, Pz), 105.7 (1C, Pz), 67.6 (d,  $J_{PC}$  = 10.9 Hz, 1C, C2), 56.3 (1C, C1), 42.5 (1C, C5), 13.3 (d,  $J_{PC}$  = 28.4 Hz, 3C, PMe<sub>3</sub>).

**<sup>1</sup>H NMR (800 MHz, CD<sub>3</sub>CN, δ, 25 °C) – 1D:** 8.16 (d,  $J$  = 2.0 Hz, 1H, Pz), 8.00 (d,  $J$  = 2.0 Hz, 1H, Pz), 7.88 (d,  $J$  = 2.4 Hz, 1H, Pz), 7.80 (d,  $J$  = 2.4 Hz, 1H, Pz), 7.74 (d,  $J$  = 2.4 Hz, 1H, Pz), 7.41 (d,  $J$  = 2.2 Hz, 1H, Pz), 6.57 (dq,  $J$  = 4.2, 2.0 Hz, 1H, H3), 6.37 (t,  $J$  = 2.2 Hz, 1H, Pz), 6.30 (t,  $J$  = 2.2 Hz, 1H, Pz), 6.22 (t,  $J$  = 2.2 Hz, 1H, Pz), 5.04 (dt,  $J$  = 4.9, 2.4 Hz, 1H, H4), 4.40 (ddt,  $J$  = 19.2, 6.8, 2.2 Hz, 1H, H5), 3.44 (m, 1H, H5), 3.40 (m, 1H, H1), 2.17 (dq,  $J$  = 7.5, 2.2 Hz, 1H, H2), 1.22 (d,  $J$  = 8.3 Hz, 9H, PMe<sub>3</sub>).

**<sup>13</sup>C NMR (201 MHz, CD<sub>3</sub>CN, δ, 25 °C) -1D:** 144.1 (1C, Pz), 143.6 (1C, Pz), 141.2 (1C, Pz), 138.0 (1C, C3), 136.6 (1C, Pz), 136.2 (1C, Pz), 135.4 (1C, Pz), 121.2 (1C, C4), 106.5 (1C, Pz), 106.0 (1C, Pz), 105.9 (1C, Pz), 65.7 (1C, C2), 58.0 (d,  $J_{PC}$  = 12.5 Hz, 1C, C1), 42.8 (d,  $J_{PC}$  = 2.2 Hz, 1C, C5), 12.8 (d,  $J_{PC}$  = 28.0 Hz, 3C, PMe<sub>3</sub>).

Composition of **2P** confirmed by single crystal X-ray diffraction.

### Synthesis and characterization of [W(Tp)(NO)(PMe<sub>3</sub>)(η<sup>2</sup>-cyclopentenyl cation)]OTf (**3**)



In a typical preparation, [W]-CPD **5** (300 mg, 0.527 mmol) was dissolved in MeCN (10 mL) and chilled to –20 °C, yielding a light brown solution. Separately, a solution of HOTf (95 mg, 0.633 mmol) in MeCN (1 mL) was prepared and chilled to –20 °C. The HOTf solution was added to [W]-CPD under strong stirring. After 5 minutes of stirring, the reaction mixture was added dropwise to stirring, chilled Et<sub>2</sub>O (–30 °C, 250 mL) to yield a pale yellow, wispy precipitate. The precipitate was collected by filtration over a fine porosity fritted funnel and desiccated to yield of an off-white powder( 320 mg, 0.445 mmol, 84%)

Previously characterized in Acetone-d<sup>6</sup>.

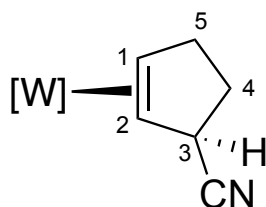
**$^1\text{H}$  NMR (800 MHz, Acetone- $\text{d}_6$ ,  $\delta$ , 25 °C):** 8.59, 8.38, 8.34, 8.19, 8.17, 7.96, (bs, 6H, Tp protons), 7.47 (bt, 1H, H2), 6.64, 6.63, 6.40 (bt, 3H, Tp protons), 4.86 (t,  $J = 3.6$ , 3.6 Hz, 1H, H1), 4.59 (dt,  $J = 15.6$ , 4.9, 4.9 Hz, 1H, H5), 3.84 (m, 1H, H4), 3.24 (m, 2H, H3, H3'), 2.47 (dd,  $J = 13.8$ , 5.6 Hz, 1H, H4'), 1.35 (d,  $J = 9.8$  Hz, 9H,  $\text{PMe}_3$ ).

**$^{13}\text{C}$  NMR (201 MHz, Acetone- $\text{d}_6$ ,  $\delta$ , 25 °C):** 150.8 (1C, C2), 148.6, 146.6, 144.2, 139.4, 139.3, 139.3 (6C, Tp carbons), 109.5, 109.0, 108.1 (3C, Tp carbons), 99.0 (d,  $J = 2.7$  Hz, 1C, C1), 74.1 (d,  $J = 14.2$  Hz, 1C, C5), 33.1 (C3), 32.0 (d,  $J = 3.2$  Hz, 1C, C4), 12.8 (d,  $J = 32.7$  Hz, 3C,  $\text{PMe}_3$ ).

**$^1\text{H}$  NMR (800 MHz,  $\text{CD}_3\text{CN}$ ,  $\delta$ , 25 °C):** 8.40, 8.04, 8.02, 7.99, 7.96, 7.78 (d,  $J = 2.70$ , 2.27, 2.27, 2.27, 2.33 Hz, 6H, Tp protons), 7.20 (m, 1H, H2), 6.52 (t,  $J = 2.01$  ; 2.28 Hz, 3H, Tp protons), 4.66 (t,  $J = 3.31$  Hz, 1H, H1), 4.31 (td,  $J = 4.34$ , 15.56 Hz, 1H, H5), 3.78 (ddd,  $J = 4.25$ , 9.08, 14.05 Hz, 1H, H4), 3.24 (dd,  $J = 9.66$ , 18.74, 1H, H3), 3.15 (d,  $J = 19.43$  Hz, 1H, H3), 2.38 (dd,  $J = 7.26$ , 13.79 Hz, 1H, H4), 1.19 (d,  $J = 9.56$  Hz, 9H,  $\text{PMe}_3$ ).

Composition of **3** confirmed by single crystal X-ray diffraction.

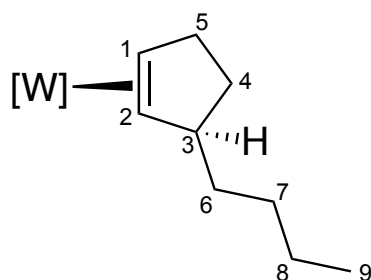
### Synthesis and characterization of $[\text{W}(\text{Tp})(\text{NO})(\text{PMe}_3)(\eta^2\text{-3-cyano-cyclopentene})]\text{OTf}$ (**4A**)



At an NMR scale, compound **3** was dissolved in 1 mL of d-MeCN. NaCN was added to the reaction, followed by a couple drops of d-DMSO.

**$^1\text{H}$  NMR (800 MHz,  $\text{CD}_3\text{CN}$ ,  $\delta$ , 25 °C):** 8.10, 8.03, 7.91, 7.84, 7.78, 7.49 (d,  $J = 1.66$ ; 1.80; 2.48; 2.24; 2.24 Hz, 6H, Tp protons), 6.38, 6.30, 6.24 (t,  $J = 2.32$ , 2.23, 2.23 Hz, 3H, Tp protons), [3.38 (d,  $J = 8.21$ , 1H); 3.66 (m, 1H); 3.03 (m,  $J = 6.90$ , 1H); 2.55 (dd,  $J = 6.57$ , 12.48 Hz, 1H); 2.18 (m,  $J = 8.21$ , 10.83, 13.10, 16.06, 21.13 Hz, 1H); 1.75 (dd,  $J = 9.60$ , 13.10 Hz, 1H); 1.54 (dd,  $J = 2.79$ , 8.73 Hz, 1H) H1 – H5]

### Synthesis and characterization of $[W(Tp)(NO)(PMe_3)(\eta^2\text{-3-n-butyl-cyclopentene})]$

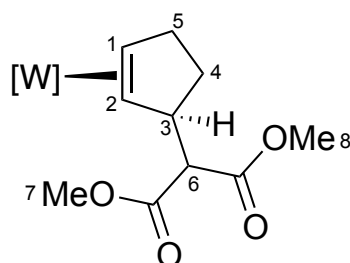


**(4B)**

In a 10 mL test tube, compound **3** (6.8 mg, 0.009 mmol) was dissolved in 1 mL of dried THF and cooled to 0°C for 15 minutes. In a separate 10 mL test tube, *n*BuLi (0.25 M) (0.038 mL, 0.009 mmol) was added, followed by 1 mL of dried THF and chilled to 0°C for 10 minutes. The basic solution was added to the [W] complex and stirred for 30 minutes. The reaction mixture was added to 50 mL of hexanes, the precipitate was collected over a 15 mL F fritted disc and discarded. The hexanes filtrate was reduced to dryness to yield compound **4B**.

**$^1H$  NMR (800 MHz,  $CD_3CN$ ,  $\delta$ , 25 °C):** 8.25, 8.05, 7.86, 7.79, 7.74, 7.43 (d,  $J$  = 1.55 ; 2.02 ; 2.50 ; 2.02 ; 1.55 Hz, 6H, Tp protons), 6.38, 6.27, 6.22 (t,  $J$  = 1.83, 2.40, 2.40 Hz, 3H, Tp protons), 3.57 (m, 1H, H5), 3.00 (ddd,  $J$  = 5.75, 7.94, 13.24 Hz, 1H, H1), 2.97 (dt, 6.73, 6.96 Hz, 1H, H3), 2.44 (dd,  $J$  = 8.86, 12.26 Hz, 1H, H5), 1.99 (m,  $J$  = 9.38 Hz, 1H, H4), 1.47 (dd,  $J$  = 2.65, 7.94 Hz, 1H, H2), 1.31 – 1.17 (m, 6H, H6 – H8), 1.19 (d,  $J$  = 8.40 Hz, 9H,  $PMe_3$ ), 0.87 (t,  $J$  = 7.10 Hz, 3H, H9).

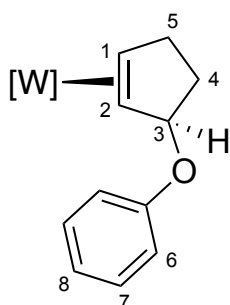
### Synthesis and characterization of $[W(Tp)(NO)(PMe_3)(\eta^2\text{-3-dimethylmalonate-cyclopentene})]$ (**4C**)



At an NMR scale, compound **3** was dissolved in 1 mL of *d*-MeCN. LiDiMM was added to the reaction.

**<sup>1</sup>H NMR (800 MHz, CD<sub>3</sub>CN, δ, 25 °C):** 8.29, 8.08, 7.87, 7.80, 7.74, 7.42 (d, J = 2.14, 2.14, 2.31, 2.85, 2.31, 2.31 Hz, 6H, Tp protons), 6.40, 6.30, 6.23 (t, J = 2.21, 2.21, 1.77 Hz, 3H, Tp protons), 3.69, 3.48 (s, 6H, H7/H8), 3.62 (dd, J = 7.81, 10.79 Hz, 1H) ; 3.58 (m, 1H) ; 3.35 (d, J = 10.27 Hz, 1H) ; 2.98 (ddd, J = 5.65, 7.70, 13.25 Hz, 1H) ; 2.44 (dd, J = 8.22, 12.94 Hz, 1H) ; 2.10 (m, J = 7.70, 10.68, 13.25, 15.51, 18.90 Hz, 1H) ; 1.27 (m, 2H) – H1 – H5.

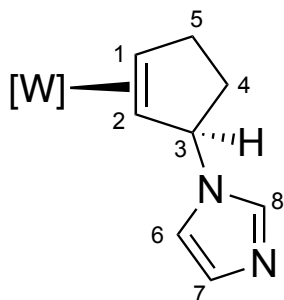
### Synthesis and characterization of [W(Tp)(NO)(PMe<sub>3</sub>)(η<sup>2</sup>-3-phenol-cyclopentene)] (4D)



In a 10 mL test tube compound **3** (10 mg, 0.014 mmol) is dissolved in 5 mL MeCN and chilled to -30°C for 15 minutes. In another 10 mL test tube, phenol (7 mg, 0.075 mmol) is dissolved in 1 mL of MeCN, followed by tBuOK (20% wt) (16 mg, 0.029 mmol) and chilled to -30°C for 15 minutes. The solution of nucleophile was added to the [W] solution at -30°C and stirred for 5 minutes. The solution is diluted with 10 mL of dichloromethane, extracted 3X with 10 mL of H<sub>2</sub>O. The organic solution is dried with Na<sub>2</sub>SO<sub>4</sub> and filtered over a 30 mL M fritted disc. The filtrate is reduced to dryness to yield compound **4D**.

**<sup>1</sup>H NMR (800 MHz, CD<sub>3</sub>CN, δ, 25 °C):** 8.24, 8.10, 7.83, 7.77, 7.72, 7.41 (d, J = 1.45, 1.81, 2.72, 1.90, 2.27, 2.27 Hz, 6H, Tp protons), 7.31 (t, J = 7.52, 1H, H8), 7.17 (t, J = 8.70 Hz, 2H, H7), 6.90 (d, J = 8.34 Hz, 2H, H6), 6.39, 6.31, 6.22 (t, J = 2.33, 2.33, 2.33 Hz, 3H, Tp protons), 5.48 (d, J = 4.88 Hz, 1H, H3), 3.83 (m, 1H) ; 3.21 (ddd, J = 5.85, 7.89, 13.74 Hz, 1H) ; 2.54 (dd, J = 8.18, 11.18 Hz, 1H) ; 2.38 (m, J = 5.23, 9.31, 14.16, 18.65 Hz, 1H) ; 2.12 (m, 1H) ; 1.91 (m, J = 7.08, 14.16 Hz, 1H) ; 1.73 (d, J = 8.09 Hz, 1H) - H1/H1/H4/H5, 1.24 (d, J = 8.13 Hz, 9H, PMe<sub>3</sub>).

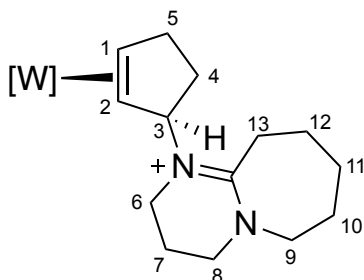
### Synthesis and characterization of $[W(Tp)(NO)(PMe_3)(\eta^2\text{-3-imidazole-cyclopentene})]$ (**4E**)



In a 20 mL test tube, compound **3** (10 mg, 0.014 mmol) was dissolved in 5 mL MeCN. The test tube was chilled to  $-30^{\circ}\text{C}$  for 15 minutes. To another 10 mL test tube, imidazole (5 mg, 0.074 mmol) was dissolved in 1 mL of MeOH and chilled to  $-30^{\circ}\text{C}$  for 15 minutes. The nucleophile solution was added to [W] and stirred for 12 hours. To the reaction mixture, t-BuOK (20% wt) (16 mg, 0.029 mmol) was added at  $-30^{\circ}\text{C}$  and stirred for 5 minutes. The reaction mixture was removed from the cold bath and warmed to room temp and reduced to dryness to yield compound **4E**.

**$^1\text{H}$  NMR (800 MHz,  $\text{CD}_3\text{CN}$ ,  $\delta$ ,  $25^{\circ}\text{C}$ ):** 8.25, 8.11, 7.89, 7.80, 7.74, 7.50 (d,  $J = 1.61$ , 1.92, 2.54, 2.31, 2.23, 2.31 Hz, 6H, Tp protons), 7.66, 6.99, 6.87 (bs, 3H, H6 – H8), 6.41, 6.29, 6.24 (t,  $J = 2.23$ , 2.19, 2.32 Hz, 3H, Tp protons), 5.48 (d,  $J = 6.64$  Hz, 1H, H3), 3.80 (m, 1H) ; 3.30 (ddd,  $J = 5.76$ , 8.15, 14.05 Hz, 1H) ; 2.58 (dd,  $J = 8.85$ , 12.39, 1H) ; 2.51 (m,  $J = 6.77$ , 10.23, 13.84, 17.01, 20.29 Hz, 1H) ; 1.59 (dd,  $J = 8.29$ , 12.79 Hz, 1H) ; 1.52 (dd,  $J = 2.16$ , 6.84 Hz, 1H) – H1/H2/H4/H5), 1.21 (d,  $J = 8.29$  Hz, 9H,  $\text{PMe}_3$ ).

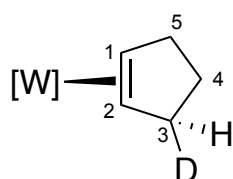
### Synthesis and characterization of $[W(Tp)(NO)(PMe_3)(\eta^2\text{-3-(1,8-Diazabicyclo[5.4.0]undec-7-ene)-cyclopentene})]$ (**4F**)



At an NMR scale, compound **3** was dissolved in 1 mL of d-MeCN. Excess DBU was added to the reaction dropwise.

**<sup>1</sup>H NMR (800 MHz, CD<sub>3</sub>CN, δ, 25 °C):** 8.08, 8.06, 7.88, 7.84, 7.78, 7.49 (d, J = 1.89, 1.89, 2.25, 2.25, 2.25, 1.89 Hz, 6H, Tp protons), 6.39, 6.30, 6.27 (t, J = 2.25, 2.25, 1.89 Hz, 3H, Tp protons), 5.45 (d, J = 7.21 Hz, 1H, H<sub>3</sub>), 3.83 (m, J = 4.76, 12.23 Hz, 1H), 3.68 (m, 1H), 3.65 (dd, J = 9.51, 15.18 Hz, 1H), 3.44 (m, 2H), 3.35 (m, 4H), 3.27 (m, 3H), 3.04 (m, 1H), 2.86 (dd, J = 10.42, 16.08 Hz, 1H), 2.58 (dd, J = 9.51, 12.23 Hz, 1H), 2.46 (m, J = 8.61, 17.90, 23.56 Hz, 1H), 2.00 (m, 1H), 1.90 (m, 2H), 1.78 (m, 2H), 1.24 (d, J = 7.70 Hz, 1H), - H<sub>1</sub>/H<sub>2</sub>/H<sub>4</sub> – H<sub>13</sub>), 1.18 (d, J = 8.61 Hz, 9H, PMe<sub>3</sub>).

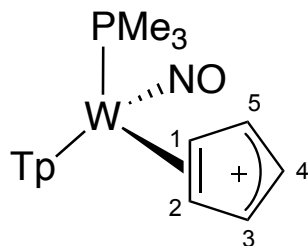
### Synthesis and characterization of [W(Tp)(NO)(PMe<sub>3</sub>)(η<sup>2</sup>-3-deutero-cyclopentene)] (4G)



In a 20 mL test tube, compound 3 (98 mg, 0.136 mmol) was dissolved in 5mL THF and chilled to -60°C for 15 minutes. To a 10 mL test tube, NaBD<sub>4</sub> (57 mg, 1.36 mmol) was dissolved in 2 mL THF and chilled to -60°C for 15 minutes. The deuterium solution was added to [W] and stirred for 1 hour. The solution was diluted with 15 mL dichloromethane and extracted 3X with 10 mL H<sub>2</sub>O. The organic solution was dried with Na<sub>2</sub>SO<sub>4</sub>, filtered over a 30mL M fritted disc and reduced to minimal DCM. The DCM solution was moved to a tared vial and reduced to dryness to yield compound **4G** (37 mg, 0.065 mmol, 48%).

**<sup>1</sup>H NMR (800 MHz, CD<sub>2</sub>Cl<sub>2</sub>, δ, 25 °C):** 7.97, 7.81, 7.62, 7.57, 7.48, 7.24 (d, J = 1.78, 2.20, 2.20, 2.20, 2.20 Hz, 6H, Tp protons), 6.10, 5.98, 5.95 (t, J = 2.20, 2.20, 2.20 Hz, 3H, Tp protons), 3.13 (m, 1H, H<sub>5</sub>), 2.73 (ddd, J = 6.54, 9.03, 13.08 Hz, 1H, H<sub>1</sub>), 2.48 (d, J = 7.79 Hz, 1H, H<sub>3</sub>), 2.22 (dd, J = 9.03, 10.59 Hz, 1H, H<sub>4</sub>), 1.61 (m, J = 9.34, 20.56 Hz, 1H, H<sub>2</sub>), 1.31 (dd, J = 3.74, 6.54 Hz, H<sub>5</sub>), 1.17 (ddd, J = 9.03, 11.84 Hz, 1H, H<sub>4</sub>).

### Synthesis and characterization of [W(Tp)(NO)(PMe<sub>3</sub>)( $\eta^2$ -cyclopentadienyl cation)]DDQ Anion (**5**)



To a test tube were added **6** (250 mg, 0.439 mmol) and 3 mL MeCN. To a second test tube were added a stir pea, DDQ (110 mg, 0.485 mmol), and 2 mL MeCN. Both test tubes were chilled at -10°C in a cold bath for 10 minutes. Next, the solution of **6** was quickly pipetted into the test tube containing DDQ as it remained cold. The dark red reaction mixture was stirred for 15 minutes at -10°C. The reaction mixture was then poured into a 500 mL Erlenmeyer flask with Et<sub>2</sub>O (300 mL). A purple precipitate was collected on a 15 mL porosity fritted funnel and desiccated under static vacuum to yield **3** (267 mg, 76.5%).

**<sup>1</sup>H NMR (800 MHz, CD<sub>3</sub>CN,  $\delta$ , 25 °C):**  $\delta$  8.60 (d,  $J$  = 2.1 Hz, 1H, Pz), 8.43 (d,  $J$  = 2.2 Hz, 1H, Pz), 8.04 (d,  $J$  = 2.4 Hz, 1H, Pz), 7.97 (d,  $J$  = 2.0 Hz, Pz), 7.81 (d,  $J$  = 2.2 Hz, 1H), 7.78 (d,  $J$  = 2.4 Hz, 1H, Pz), 6.89 (d,  $J_{PH}$  = 2.4 Hz, 5H, H1-5), 6.63-6.33 (t,  $J$  = 2.3 Hz, 3H, Pz4A/Pz4B/Pz4C), 1.22 (d,  $J$  = 10.2 Hz, 9H, PMe<sub>3</sub>).

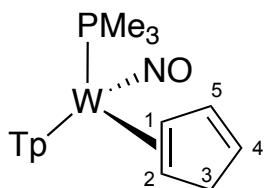
**<sup>13</sup>C NMR (201 MHz, CD<sub>3</sub>CN,  $\delta$ , 25 °C):** 148.0 (1C, Pz), 146.9 (1C, Pz), 144.7 (1C, Pz), 140.0 (1C, Pz), 139.7 (1C, Pz), 138.4 (1C, Pz), 129.2 (m, 5C, C1-C5), 110.6-108.3 (3C, Pz4A/Pz4B/Pz4C), 13.7 (d,  $J_{PC}$  = 33.2 Hz, 3C, PMe<sub>3</sub>).

Composition of **3** confirmed by single crystal X-ray diffraction.

**APCI-HRMS (m/z):** [M]<sup>+</sup> calculated for 569.1450; found 569.1476.

**CV** (MeCN, 50 mV/s): E<sub>p,a</sub> = +1.26 V, E<sub>1/2</sub> = +0.70 and -0.09V, E<sub>p,c</sub> = -0.431 V (NHE).

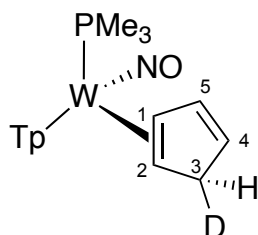
### Synthesis and characterization of [W(Tp)(NO)(PMe<sub>3</sub>)( $\eta^2$ -cyclopentadiene)] (**6A**)





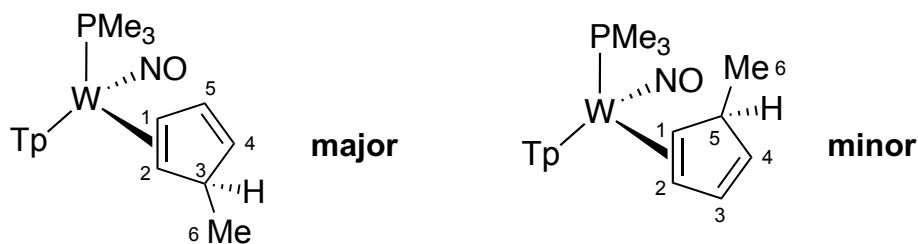
To an oven dried test tube, compound **5** (10 mg, 0.013 mmol) was dissolved in 1 mL dried THF. In a separate test tube, NaBH<sub>4</sub> (4.8 mg, 0.127 mmol) was dissolved in 1 mL dried THF. Both solutions were chilled at -30°C for 15 minutes. The cyclopentadienyl cationic complex solution was pipetted into the NaBH<sub>4</sub> solution and stirred at -30°C for 1 hr. The solution was diluted with 10 mL DCM and extracted 3X with 10 mL of water. The organic layer was dried over anhydrous Na<sub>2</sub>SO<sub>4</sub> and concentrated in vacuo. The film was dissolved in minimal MeCN and precipitated out in ~30 mL Et<sub>2</sub>O. The precipitate was collected on a 15 mL fine frit. Compound previously characterized.

### Synthesis and characterization of [W(Tp)(NO)(PMe<sub>3</sub>)( $\eta^2$ -5-deutero-cyclopentadiene)] (**6B**)



To an oven dried test tube, compound **5** (5.5 mg, 0.007 mmol) was dissolved in 1 mL dried THF. In a separate test tube, NaBD<sub>4</sub> (3.3 mg, 0.079 mmol) was dissolved in 1 mL dried THF. Both solutions were chilled at -15°C for 15 minutes. The cyclopentadienyl cationic complex solution was pipetted into the NaBD<sub>4</sub> solution and stirred at -15°C for 1 hr. The solution as diluted with 10 mL of DCM and extracted 3X with 10 mL of water. The organic layer was dried over anhydrous Na<sub>2</sub>SO<sub>4</sub> and concentrated in vacuo. The film was dissolved in minimal acetone and precipitated out in ~30 mL Et<sub>2</sub>O. The precipitated solid was collected on a 15 mL fine frit. Compound previously characterized with loss of H<sub>3</sub> proton.

## Synthesis and characterization of $[W(Tp)(NO)(PMe_3)(\eta^2\text{-5-methyl-cyclopentadiene})]$ (**6C**)



In an oven dried test tube charged with a stir pea, **5** (0.104 g, 0.18 mmol) was dissolved in 5 mL dried THF. In another oven dried test tube charged with a stir pea, DDQ (0.042 g, 0.19 mmol) was dissolved in 2 mL dried THF. Both test tubes were chilled to  $-15^{\circ}\text{C}$  for 15 minutes. The solution of DDQ was transferred into the test tube containing compound **5**. To the chilled solution (0.20 mL, 0.28 mmol) MeMgCl was added via syringe and was stirred at  $-15^{\circ}\text{C}$  for 30 minutes. The crude reaction mixture was then diluted with DCM and extracted 3x with 10 mL  $\text{H}_2\text{O}$ . The reaction was then dried with  $\text{Na}_2\text{SO}_4$  and filtered to remove drying agent. Afterwards the reaction was reduced to dryness in vacuo in a 125 mL filter flask. The remaining product on the flask was redissolved in minimal DCM, precipitated into 50mL hexanes and filtered over a 15mL fritted disc. The precipitate was discarded. The hexanes filtrate was reduced to dryness and weighed. The white solid **5C** was collected in a 3 : 2 ratio (0.082 g, 77%).

**$^1\text{H}$  NMR (800 MHz,  $\text{CD}_3\text{CN}$ ,  $\delta$ ,  $25^{\circ}\text{C}$ ) – 5C (major):** 8.14 (d,  $J = 2.0$  Hz, 1H, Pz), 8.01 (d,  $J = 2.0$  Hz, 1H, Pz), 7.87 (d,  $J = 2.4$  Hz, 1H, Pz), 7.80 (d,  $J = 2.3$  Hz, 1H, Pz), 7.73 (d,  $J = 2.3$  Hz, 1H, Pz), 7.45 (d,  $J = 2.2$  Hz, 1H), 6.47 (dt,  $J = 5.1, 1.9$  Hz, 1H, H3), 6.37 (t,  $J = 2.3$  Hz, 1H, Pz), 6.29 (t,  $J = 2.2$  Hz, 1H, Pz), 6.23 (t,  $J = 2.2$  Hz, 1H, Pz), 5.01 (dd,  $J = 5.1, 2.4$  Hz, 1H, H4), 3.54 (m, 1H, H5), 3.09 (dd,  $J = 13.4, 7.2$  Hz, 1H, H1), 2.08 (m, 1H, H2), 1.29 (d,  $J = 7.1$  Hz, 3H, H6), 1.22 (d,  $J = 8.3$  Hz, 9H,  $\text{PMe}_3$ ).

**$^{13}\text{C}$  NMR (201 MHz,  $\text{CD}_3\text{CN}$ ,  $\delta$ ,  $25^{\circ}\text{C}$ ) – 5C (major):** 145.0 (1C, Pz), 144.6 (1C, Pz), 142.2 (1C, Pz), 137.7 (1C, Pz), 137.6 (1C, Pz), 137.2 (1C, C3), 136.3 (1C, Pz), 128.3 (1C, H4), 107.4 (1C, Pz), 107.0 (1C, Pz), 106.8 (1C, Pz), 68.4 (d,  $J = 12.4$  Hz, 1C, C1), 64.8 (1C, C2), 50.1 (1C, C5), 25.9 (1C, C6), 13.5 (d,  $J = 27.9$  Hz, 3C,  $\text{PMe}_3$ ).

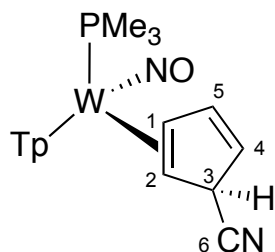
**$^1\text{H}$  NMR (800 MHz,  $\text{CD}_3\text{CN}$ ,  $\delta$ ,  $25^{\circ}\text{C}$ ) – 5C (minor):** 8.34 (d,  $J = 2.0$  Hz, 1H, Pz), 8.01 (d,  $J = 2.0$  Hz, 1H, Pz), 7.87 (d,  $J = 2.4$  Hz, 1H, Pz), 7.80 (d,  $J = 2.3$  Hz, 1H, Pz), 7.76 (d,  $J = 2.3$  Hz, 1H, Pz), 7.40 (d,  $J = 2.2$  Hz, 1H, Pz), 6.37 (t,  $J = 2.3$  Hz, 1H, Pz), 6.30 (m, 2H, H3 & Pz), 6.22 (t,  $J = 2.2$  Hz, 1H, Pz), 5.05 (dd,  $J = 5.1, 2.4$  Hz, 1H, H4), 3.90

(dddd,  $J = 9.1, 7.1, 5.5, 1.9$  Hz, 1H, H5), 3.60 (ddt,  $J = 12.4, 7.2, 2.0$  Hz, 1H, H2), 1.61 (dd,  $J = 7.2, 2.8$  Hz, 1H, H1), 1.24 (d,  $J = 8.4$  Hz, 9H,  $\text{PMe}_3$ ), 1.15 (d,  $J = 7.2$  Hz, 3H, H6).

**$^{13}\text{C}$  NMR (201 MHz,  $\text{CD}_3\text{CN}$ ,  $\delta$ , 25 °C) – 5C (minor):** 145.0 (1C, Pz), 142.4 (1C, Pz), 141.4 (1C, Pz), 137.2 (1C, Pz), 137.0 (1C, Pz), 136.5 (1C, Pz), 136.3 (d,  $J_{\text{PC}} = 2.4$  Hz, 1C, C3), 128.9 (1C, C4), 107.3 (1C, Pz), 106.7 (1C, Pz), 106.7 (1C, Pz), 67.2 (1C, C1), 66.5 (d,  $J_{\text{PC}} = 10.8$  Hz, 1C, C2), 50.5 (1C, C5), 26.7 (1C, C6), 14.2 (d,  $J_{\text{PC}} = 28.6$  Hz, 3C,  $\text{PMe}_3$ ).

APCI-HRMS ( $m/z$ ):  $[\text{M}+\text{H}]^+$  calculated for 584.1690; found 584.1690.

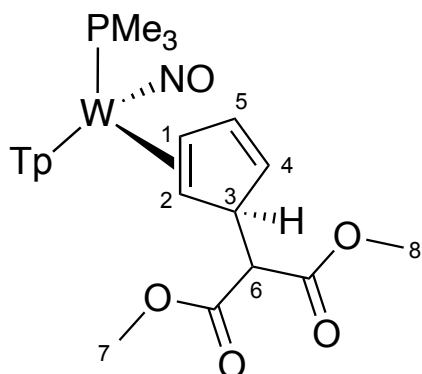
### Synthesis and characterization of $[\text{W}(\text{Tp})(\text{NO})(\text{PMe}_3)(\eta^2\text{-5-cyano-cyclopentadiene cation})]\text{DDQ Anion (6D)}$



To an oven dried test tube, compound **5** (10 mg, 0.044 mmol) was dissolved in 2 mL of EtCN. In another test tube, NaCN (3 mg, 0.061 mmol) was dissolved in 1 mL methanol and 1 mL EtCN. Both solutions were chilled at  $-60^\circ\text{C}$  for 15 minutes. The NaCN solution was pipetted into the  $[\text{W}]$  solution and stirred at  $-60^\circ\text{C}$  for 2 hours. The solution was diluted with 10mL of dichloromethane, extracted 3X with 10mL of water. The organic layer was dried over anhydrous  $\text{Na}_2\text{SO}_4$  and concentrated in vacuo. The film was dissolved in minimal DCM and precipitated into 40 mL Hexanes. The precipitated solid was collected on a 15 mL fine frit.

**$^1\text{H}$  NMR (800 MHz,  $\text{CD}_3\text{CN}$ ,  $\delta$ , 25 °C):** 8.27, 8.05, 7.93, 7.86, 7.82, 7.57 (d,  $J = 1.68, 2.00, 2.00, 2.00, 2.32$  Hz, 6H, Tp protons), 6.63 (m, 1H, H5), 6.42, 6.38, 6.29 (t,  $J = 2.06, 2.14, 2.35$  Hz, 3H, Tp protons), 5.02 (dd,  $J = 2.44, 4.88$  Hz, H4), 4.69 (bs, 1H), 3.61 (m, 1H), 1.94 (dd,  $J = 2.44, 7.78$  Hz, 1H) – H1 – H3, 1.25 (d,  $J = 8.25$  Hz, 9H,  $\text{PMe}_3$ ).

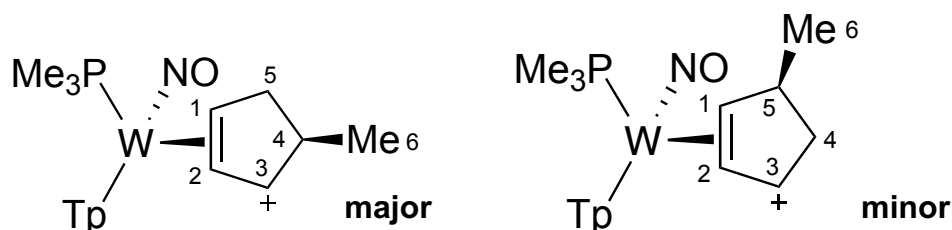
## Synthesis and characterization of $[W(Tp)(NO)(PMe_3)(\eta^2\text{-5-DiMM-cyclopentadiene cation})]DDQ$ Anion (**6E**)



To an oven dried test tube, compound **5** (50 mg, 0.063 mmol) was dissolved in 2 mL dried THF. In a separate test tube, LiDiMM (17.5 mg, 0.133 mmol) was dissolved in 1 mL dried THF. Both solutions were chilled at  $-60^{\circ}\text{C}$  for 30 minutes. The lithium dimethyl malonate solution was pipetted into the [W] complex solution and stirred for 1.5 hours at  $-60^{\circ}\text{C}$ . The solution was diluted with 10 mL dichloromethane and extracted 3X with 10 mL of water. The organic layer was dried over anhydrous  $\text{Na}_2\text{SO}_4$  and concentrated in vacuo. The film was dissolved in minimal MeCN and precipitated out in  $\sim 50$  mL  $\text{Et}_2\text{O}$ . The precipitated solid was collected on a 15 mL fine frit.

**$^1\text{H}$  NMR (800 MHz,  $\text{CD}_3\text{CN}$ ,  $\delta$ ,  $25^{\circ}\text{C}$ ):** 8.26, 8.05, 7.81, 7.78, 7.70, 7.41 (bs, 6H, Tp protons), 6.42 (d, 1H, H5), 6.38, 6.27, 6.22 (bs, 3H, Tp protons), 4.95 (bs, 1H, H4), 4.25 (d, 1H), 1.60 (d, 1H) – H1 – H3, 3.52 (s, 3H), 3.38 (s, 3H) – H6/H7, 1.20 (d, 9H,  $\text{PMe}_3$ ).

## Synthesis and characterization of $[W(Tp)(NO)(PMe_3)(\eta^2\text{-4-methyl-cyclopentenyl cation})]OTf$ (**7A/7B**)



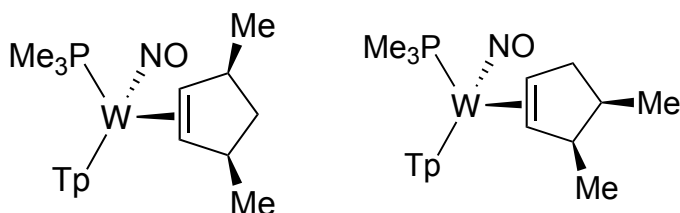
In a 10 mL test tube, compound **6C** (82 mg, 0.141 mmol) was dissolved in MeCN. In another 10 mL test tube, HOTf (21 mg, 0.140 mmol) was added, followed by 1 mL of MeCN. The acid solution was added to the [W] solution and then precipitated in 200

mL of ether. The precipitated was discarded and the ether filtrate was reduced to yield compounds **7A** and **7B**.

**$^1\text{H}$  NMR (800 MHz,  $\text{CD}_3\text{CN}$ ,  $\delta$ , 25 °C) – 7A :** 8.40, 7.99, 7.95, 7.78, 7.29 (d,  $J$  = 1.65, 1.96, 1.67 Hz, 6H, Tp protons), 6.90 (bs, 1H, H3), 6.52, 6.32 (t,  $J$  = 2.06 Hz, 3H, Tp protons), 4.66 (t,  $J$  = 4.12 Hz, H2), 4.30 (d,  $J$  = 15.52 Hz, H1), 3.40 (m,  $J$  = 6.19, 16.48 Hz, 1H), 3.22 (td,  $J$  = 3.73, 13.95), 2.71 (d,  $J$  = 19.14 Hz, 1H) – speculated as H4/H5, 1.30 (d,  $J$  = 7.00 Hz, 3H, H6), 1.18 (d,  $J$  = 9.67 Hz, 9H,  $\text{PMe}_3$ ).

**$^1\text{H}$  NMR (800 MHz,  $\text{CD}_3\text{CN}$ ,  $\delta$ , 25 °C) – 7B :** 8.10, 8.06, 8.02, 7.99, 7.95, 7.78 (d,  $J$  = 1.97, 2.13, 1.97 Hz, 6H, Tp protons), 7.12 (bs, 1H, H3), 6.52, 6.31 (t,  $J$  = 2.61 Hz, 3H, Tp protons), 4.63 (t,  $J$  = 3.22 Hz, 1H, H2), 4.13 (d,  $J$  = 16.12 Hz, 1H, H1), 3.36 (m, 1H), 3.29 (m, 1H), 2.61 (m, 1H) – speculated as H4/H5, 1.17 (d,  $J$  = 10.13 Hz, 9H,  $\text{PMe}_3$ ), 2.78 (d,  $J$  = 6.45 Hz, 3H, H6).

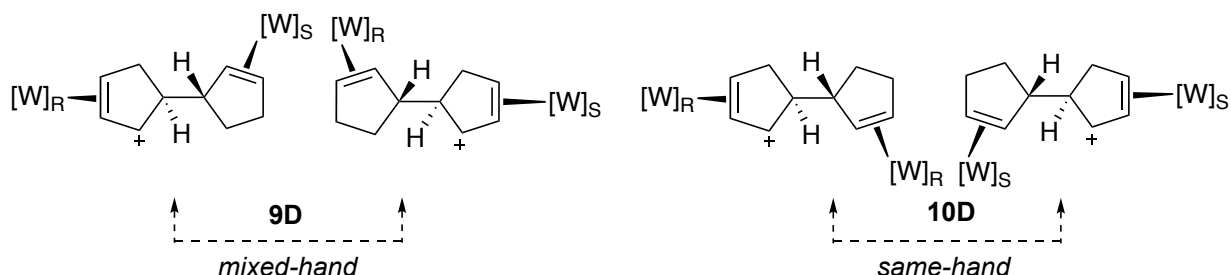
**Synthesis and characterization of  $[\text{W}(\text{Tp})(\text{NO})(\text{PMe}_3)(\eta^2\text{-3,5-dimethyl-cyclopentene})]$  (8A) and  $[\text{W}(\text{Tp})(\text{NO})(\text{PMe}_3)(\eta^2\text{-3,4-dimethyl-cyclopentene})]$  (8B)**



In a 10 mL test tube, compound **7** (75 mg, 0.102 mmol) was dissolved in 2mL THF.  $\text{MeMgBr}$  (1.5M) (0.07 mL, 0.105 mmol) was added and stirred for 15 minutes. The solution was diluted with 10mL of DCM, extracted 3X with 10 mL of water. The organic solution was dried with  $\text{Na}_2\text{SO}_4$  and reduced to minimal solvent and loaded onto a silica plug. 30mL of hexanes was run through the plug and discarded. 30 mL of  $\text{Et}_2\text{O}$  of ether was run through the plug and reduced to dryness to yield compounds **8A** and **8B**.

**$^1\text{H}$  NMR (800 MHz,  $\text{CD}_3\text{CN}$ ,  $\delta$ , 25 °C) :** protons were not assigned due to complicated spectrum from overlapping peaks.

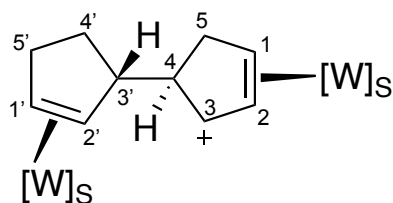
**Synthesis and characterization of  $\text{Wtp}(\text{NO})(\text{PMe}_3)_2((\mu\text{-}1,2,1',2'\text{-}\eta)\text{-}4\text{-(cyclopent-1'-en-3'-yl)cyclopent-1-en-3-ylidm}) \text{OTf (9/10)}$**



To a 10 mL test tube, a racemic metal mixture of compound **3** was dissolved in MeCN. 2,6-lutidine was added in excess to the reaction mixture at room temperature. The solution was stirred for 5 minutes then precipitated in ether. The solid was collected over a fine porosity fritted funnel and desiccated to yield a mixture of compounds **9** and **10**.

**$^1\text{H-NMR}$  (800 MHz,  $\text{CD}_3\text{CN}$ , 25 °C):** Due to mixed-hand and same-hand coupling products both present in the sample, proton peaks could not be assigned.

**Synthesis and characterization of  $\text{Wtp}(\text{NO})(\text{PMe}_3)_2((\mu\text{-}1,2,1',2'\text{-}\eta)\text{-}4\text{-(cyclopent-1'-en-3'-yl)cyclopent-1-en-3-ylidm}) \text{OTf (10)}$**



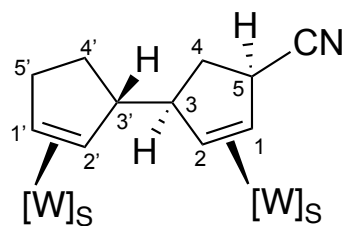
To a 10 mL test tube, an enantioenriched compound **3** (320 mg, 0.445 mmol) was dissolved in EtCN (5 mL) and chilled to  $-60\text{ }^\circ\text{C}$ . Separately, a solution of 2,6-lutidine (714 mg, 6.67 mmol) in EtCN (2 mL) was prepared and chilled to  $-60\text{ }^\circ\text{C}$ . The lutidine solution was added to [W] under strong stirring, and the reaction mixture was allowed to warm to room temperature over 45 minutes. The mixture was then added dropwise to 125 mL stirring  $\text{Et}_2\text{O}$ , chilled to  $-30\text{ }^\circ\text{C}$ , yielding a yellow precipitate. The precipitate was collected by filtration over a fine porosity fritted funnel and desiccated to yield compound **10** (240 mg, 0.374 mmol, 84%).

**$^1\text{H-NMR}$  (800 MHz,  $\text{CD}_3\text{CN}$ , 25 °C):**  $\delta$  8.38 (d,  $J = 2.3\text{ Hz}$ , 1H, Pz), 8.30 (d,  $J = 2.0\text{ Hz}$ , 1H, Pz), 8.07 (d,  $J = 2.1\text{ Hz}$ , 1H, Pz), 7.99 – 7.98 (m, 2H, Pz), 7.98 (d,  $J = 2.4\text{ Hz}$ ,

1H, Pz), 7.94 (d, J = 2.5 Hz, 1H, Pz), 7.88 (d, J = 2.3 Hz, 1H, Pz), 7.82 (d, J = 2.4 Hz, 1H, Pz), 7.76 – 7.74 (m, 2H, Pz), 7.47 (d, J = 2.2 Hz, 1H, Pz), 6.95 – 6.91 (m, 1H, H3), 6.51 (t, J = 2.4 Hz, 1H, Pz), 6.50 (t, J = 2.3 Hz, 1H, Pz), 6.40 (t, J = 2.2 Hz, 1H, Pz), 6.26 – 6.24 (m, 3H, Pz), 4.73 (t, J = 3.7 Hz, 1H, H2), 4.34 (d, J = 15.6 Hz, 1H, H1), 3.68 – 3.63 (m, 1H, H5'), 3.55 (dt, J = 14.1, 4.1 Hz, 1H, H5), 3.45 – 3.42 (m, 1H, H4), 3.32 – 3.27 (m, 1H, H3'), 3.13 (dt, J = 13.6, 7.4 Hz, 1H, H1'), 2.63 – 2.59 (m, 1H, H5'), 2.56 (dd, J = 14.3, 6.9 Hz, 1H, H5), 1.71 – 1.68 (m, 1H, H2'), 1.57 (dd, J = 13.1, 9.2 Hz, 1H, H4'), 1.19 (d, J = 8.3 Hz, 9H, PMe3B), 1.16 (d, J = 9.7 Hz, 9H, PMe3A), 1.14 (d, J = 9.8 Hz, 1H, H4'). **<sup>13</sup>C-NMR (201 MHz, CD<sub>3</sub>CN, 25 °C):** δ 152.81 (C3), 148.24, 146.26, 144.19, 143.78, 143.27, 142.50, 139.33, 139.18, 137.86, 137.07, 136.85, 109.36, 108.78, 107.98, 107.55, 106.89, 99.01 (C2), 75.66 (d, J = 12.2 Hz, C1), 63.25 (C2'), 62.89 (d, J = 11.4 Hz, C1'), 57.82 (C3'), 55.09 (C3), 37.72 (C5), 37.32 (C5'), 29.05 (C4'), 13.61 (d, J = 28.3 Hz, PMe3B), 12.83 (d, J = 32.8 Hz, PMe3A).

**HRMS-ACPI:** (m/z) calcd for C<sub>34</sub>H<sub>51</sub>B<sub>2</sub>N<sub>14</sub>O<sub>2</sub>P<sub>2</sub>W<sub>2</sub> 1139.2994, found 1139.2997.

### Synthesis and characterization of [{WTP(NO)(PMe<sub>3</sub>)<sub>2</sub>}(μ-1,2,1',2'-η)-3-(cyclopent-1'-en-3'-yl)-5-cyanocyclopentene] (11A)



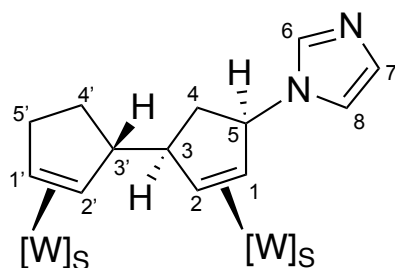
In a test tube, an enriched sample of compound **10** (100 mg, 0.077 mmol) was dissolved in DCM (2 mL). Separately, NaCN (19 mg, 0.388 mmol) was dissolved in a mixture of MeOH and DMSO (1:3, 5 mL total). Both solutions were chilled to –35 °C. The NaCN solution was added to the [W] mixture under strong stirring, and the mixture was allowed to warm to room temperature over 20 minutes. The solution was diluted to 10 mL, extracted 3× with 0.5 M NaHCO<sub>3</sub>, back-extracted 2×, dried with anhydrous Na<sub>2</sub>SO<sub>4</sub>, and evaporated in vacuo to 2 mL. The solution was added dropwise to stirring, chilled hexanes (–30 °C, 75 mL) to give an off-white precipitate, which was filtered over a fine porosity fritted funnel and desiccated to yield 78 mg (86%) of an off-white solid, with a c.d.r. of 4:1.

**<sup>1</sup>H-NMR (800 MHz, CD<sub>3</sub>Cl, 25 °C):** 8.47, 8.35, 8.07, 8.06, 7.85, 7.83, 7.69, 7.66, 7.58, 7.75, 7.47, 7.41 (d, J = 1.86, 2.16, 1.49, 1.86, 2.46, 2.16, 2.46, 2.16, 2.46, 2.76, 2.16,

1.86 Hz, 12H, Tp protons), 6.39, 6.38, 6.25, 6.21, 6.15, 6.13 (t,  $J = 2.21, 2.21, 2.21, 2.00, 2.21, 2.21$  Hz, 6H, Tp protons), 3.78 (m, 1H), 3.59 (d,  $J = 9.49$  Hz, 1H), 3.20 (m,  $J = 7.76, 7.62$  Hz 1H), 3.13 (m, 3H), 2.54 (dd,  $J = 8.91, 11.79$  Hz, 1H), 2.46 (m,  $J = 8.34$  Hz, 1H), 2.10 (m, 1H), 1.68 (dd,  $J = 2.44, 8.34$  Hz, 1H), 1.54 (m,  $J = 3.02$  Hz, 1H), 1.28 (m, 2H) – H1 – H5/H1' – H5'.

**HRMS-ACPI:** ( $m/z$ ) calcd for  $C_{35}H_{51}B_2N_{15}O_2P_2W_2$  1165.3030, found 1165.3028.

**Synthesis and characterization of  $\{W Tp(NO)(PMe_3)\}_2((\mu-1,2,1',2'-\eta)-3-(cyclopent-1'-en-3'-yl)-5-(imidazol-1-yl)cyclopentene)$  (11B)**



In a test tube, an enantioenriched sample of compound **10** (100 mg, 0.077 mmol) was dissolved in DCM (2 mL). Separately, imidazole (44.3 mg, 0.651 mmol) and KOtBu (20% in THF, 228 mg, 0.407 mmol) were dissolved in a mixture of THF and DMSO (1 mL each). Both solutions were chilled to  $-35$  °C. The imidazole solution was allowed to warm until melted before being added to the [W] complex under strong stirring, and the mixture was allowed to warm to room temperature over 20 minutes. The solution was diluted to 10 mL, extracted 3× with 1 M  $Na_2CO_3$ , back-extracted 2X, dried with anhydrous  $Na_2SO_4$ , and evaporated in vacuo to 2 mL. The solution was added dropwise to stirring, chilled hexanes ( $-30$  °C, 75 mL) to give an off-white precipitate, which was filtered over a fine porosity fritted funnel and desiccated to yield 88 mg (89%) of an off-white solid, with a c.d.r. of 15:1.

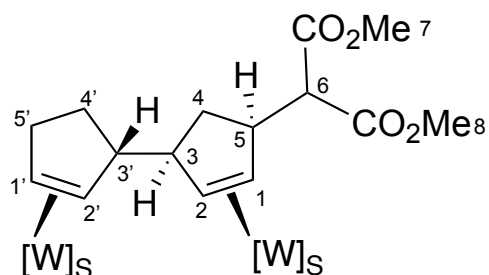
**$^1H$  NMR (800 MHz,  $CD_3CN$ , 25 °C):**  $\delta$  8.43 (d,  $J = 2.1$  Hz, 1H, Pz), 8.32 (d,  $J = 2.0$  Hz, 1H, Pz), 8.08 (d,  $J = 2.1$  Hz, 1H, Pz), 8.04 (d,  $J = 2.0$  Hz, 1H, Pz), 7.99 (s, 1H, H6), 7.86 (d,  $J = 2.3$  Hz, 1H, Pz), 7.82 (d,  $J = 2.4$  Hz, 1H, Pz), 7.70 (d,  $J = 2.3$  Hz, 1H, Pz), 7.67 (d,  $J = 2.3$  Hz, 1H, Pz), 7.62 (d,  $J = 2.4$  Hz, 1H, Pz), 7.60 (d,  $J = 2.4$  Hz, 1H, Pz), 7.50 (t,  $J = 1.2$  Hz, 1H, H8), 7.46 (d,  $J = 2.2$  Hz, 1H, Pz), 7.42 (d,  $J = 2.1$  Hz, 1H, Pz), 7.06 (t,  $J = 1.1$  Hz, 1H, H7), 6.41 (t,  $J = 2.2$  Hz, 1H, Pz), 6.36 (t,  $J = 2.2$  Hz, 1H, Pz), 6.30 (t,  $J = 2.2$  Hz, 1H, Pz), 6.28 (t,  $J = 2.2$  Hz, 1H, Pz), 6.15 (t,  $J = 2.2$  Hz, 1H, Pz), 6.14 (t,  $J = 2.2$  Hz, 1H, Pz), 5.30 (d,  $J = 7.8$  Hz, 1H, H5), 3.70 (dddd,  $J = 12.6, 10.9,$



8.7, 5.7 Hz, 1H, H5'), 3.25 (dd, J = 10.9, 9.8 Hz, 1H, H3), 3.12 (ddd, J = 13.5, 8.0, 5.6 Hz, 1H, H1'), 3.10 (dd, J = 11.9, 7.9 Hz, 1H, H1), 2.78 (dt, J = 14.3, 8.3 Hz, 1H, H4), 2.74 (ddd, J = 11.8, 7.4, 1.7 Hz, 1H, H3'), 2.47 – 2.43 (dd, J = 12.4, 8.7 Hz, H5'), 1.90 – 1.85 (m, 1H, H4'), 1.85 (dd, J = 7.9, 2.8 Hz, 1H, H2), 1.66 (d, J = 14.4 Hz, 1H, H4), 1.53 (dd, J = 8.2, 2.7 Hz, 1H, H2'), 1.34 (dd, J = 12.6, 8.6 Hz, 1H, H4'), 1.18 (d, J = 8.4 Hz, 9H, PMe3B), 1.08 (d, J = 8.4 Hz, 9H, PMe3A).

**<sup>13</sup>C NMR (201 MHz, CD<sub>3</sub>CN, 25 °C):** δ 144.15, 144.04, 143.72, 143.42, 142.60, 142.51, 138.18, 137.83, 137.21, 136.89 (C6), 136.86, 136.77, 129.49 (C7), 119.02 (C8), 107.74, 107.41, 106.92, 106.62, 106.60, 106.31, 69.34 (d, J = 3.6 Hz, C5), 66.30 (C2'), 65.11 (C2), 64.05 (d, J = 11.1 Hz, C1), 62.30 (d, J = 11.5 Hz, C1'), 60.87 (C3'), 59.50 (C3), 42.04 (C4), 35.93 (d, J = 2.1 Hz, C5'), 28.97 (C5), 13.64 (d, J = 28.3 Hz, PMe3B), 13.24 (d, J = 28.5 Hz, PMe3A).

**Synthesis and characterization of {Wtp(NO)(PMe<sub>3</sub>)}<sub>2</sub>((μ-1,2,1',2'-η)-3-(cyclopent-1'-en-3'-yl)-5-(1,3-dimethoxy-1,3-dioxopropan-2-yl)cyclopentene) - (11C)**



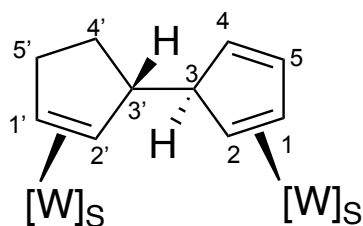
In separate test tubes, an enantioenriched sample of compound **10** (100 mg, 0.077 mmol) and LidiMM (54 mg, 0.391 mmol) were dissolved in DCM (2 mL each) and chilled to –40 °C. The LidiMM solution was added to **7** under strong stirring, and the mixture was allowed to warm to room temperature over 20 minutes. The solution was diluted to 10 mL, extracted 3× with 0.5 M NaHCO<sub>3</sub>, back-extracted 2×, dried with anhydrous Na<sub>2</sub>SO<sub>4</sub>, and evaporated in vacuo to 2 mL. The solution was added dropwise to stirring, chilled hexanes (–30 °C, 75 mL) to give an off-white precipitate, which was filtered over a fine porosity fritted funnel and desiccated to yield 80 mg (81%) of an off-white solid, with a c.d.r. of >20:1.

**<sup>1</sup>H-NMR (800 MHz, CD<sub>3</sub>CN, 25 °C):** δ 8.44 (d, J = 2.1 Hz, 1H, Pz), 8.41 (d, J = 2.1 Hz, 1H, Pz), 8.08 (dd, J = 2.0, 0.7 Hz, 1H, Pz), 8.07 (dd, J = 2.0, 0.6 Hz, 1H, Pz), 7.84 – 7.82 (m, 2H, Pz), 7.68 (d, J = 2.3 Hz, 1H, Pz), 7.66 (d, J = 2.3 Hz, 1H, Pz), 7.59 (dt,

$J = 2.4, 0.6 \text{ Hz}$ , 1H, Pz), 7.54 (dt,  $J = 2.4, 0.7 \text{ Hz}$ , 1H, Pz), 7.41 (d,  $J = 2.2 \text{ Hz}$ , 1H, Pz), 7.22 (d,  $J = 2.1 \text{ Hz}$ , 1H, Pz), 6.38 (t,  $J = 2.2 \text{ Hz}$ , 1H, Pz), 6.37 (t,  $J = 2.2 \text{ Hz}$ , 1H, Pz), 6.19 (t,  $J = 2.2 \text{ Hz}$ , 1H, Pz), 6.16 (t,  $J = 2.2 \text{ Hz}$ , 1H, Pz), 6.16 (t,  $J = 2.2 \text{ Hz}$ , 1H, Pz), 6.14 (t,  $J = 2.2 \text{ Hz}$ , 1H, Pz), 3.85 (s, 3H, H8), 3.83 (d,  $J = 10.5 \text{ Hz}$ , 1H, H6), 3.74 (s, 3H, H10), 3.75 – 3.71 (m, 1H, H5'), 3.43 (dd,  $J = 10.3, 7.8 \text{ Hz}$ , 1H, H5), 3.11 (ddd,  $J = 13.4, 8.2, 5.6 \text{ Hz}$ , 1H, H1'), 3.08 (dd,  $J = 12.0, 8.5 \text{ Hz}$ , 1H, H3'), 3.03 (dd,  $J = 11.9, 7.4 \text{ Hz}$ , 1H, H3), 2.67 (dd,  $J = 11.0, 7.9 \text{ Hz}$ , 1H, H1), 2.50 (dd,  $J = 12.5, 8.7 \text{ Hz}$ , 1H, H5'), 2.36 (dt,  $J = 13.9, 8.1 \text{ Hz}$ , 1H, H4), 2.05 (dddd,  $J = 12.5, 10.7, 8.7, 7.9 \text{ Hz}$ , 1H, H4'), 1.68 (dd,  $J = 8.0, 2.8 \text{ Hz}$ , 1H, H2), 1.57 (dd,  $J = 8.0, 2.8 \text{ Hz}$ , 1H, H2'), 1.47 (dd,  $J = 12.8, 8.8 \text{ Hz}$ , 1H, H4'), 1.37 (d,  $J = 14.0 \text{ Hz}$ , 1H, H4), 1.18 (d, JPH = 8.4 Hz, 9H, PMe3B), 1.11 (d, JPH = 8.4 Hz, 9H, PMe3A).  **$^{13}\text{C-NMR}$  (201 MHz,  $\text{CD}_3\text{CN}$ , 25 °C):**  $\delta$  171.13 (C7), 170.81 (C9), 144.34 (d,  $J = 2.0 \text{ Hz}$ ), 144.01 (d,  $J = 2.1 \text{ Hz}$ ), 143.81, 143.52, 142.53, 142.14, 138.16, 137.84, 137.08, 136.83, 136.72, 136.70, 107.54, 107.45, 106.86, 106.59, 106.35, 106.23, 66.42 (C2'), 65.24 (C2), 64.81 (C6), 64.15 (d, JPC = 11.3 Hz, C1), 62.71 (d, JPC = 11.6 Hz, C1'), 61.65 (C3), 59.54 (C3'), 53.05 (C8), 52.90 (C10), 50.54 (d, JPC = 2.3 Hz, C5), 36.28 (d, JPC = 2.7 Hz, C5'), 35.11 (C4), 29.09 (C4'), 13.6 (d, JPC = 27.9 Hz, PMe3B), 13.5 (d, JPC = 27.5 Hz, PMe3A).

**HRMS-ACPI:** (m/z) calcd for  $\text{C}_{39}\text{H}_{58}\text{B}_2\text{N}_{14}\text{O}_6\text{P}_2\text{W}_2$  1270.3344, found 1270.3322.

### Synthesis and characterization of $\{\text{Wtp}(\text{NO})(\text{PMe}_3)\}_2((\mu\text{-}1,2,1',2'\text{-}\eta)\text{-}3\text{-}(\text{cyclopent-1'-en-3'-yl})\text{cyclopenta-1,4-diene})$ (**12**)



In separate test tubes, compound **10** (50 mg, 0.041 mmol) and  $\text{NEt}_3$  (20.6 mg, 0.203 mmol) were dissolved in DCM (2 mL each) and chilled to  $-60^\circ\text{C}$ . The  $\text{NEt}_3$  solution was added to **7** under strong stirring, and the mixture was allowed to warm to room temperature. The solution was extracted 2× with 0.5 M  $\text{NaHCO}_3$ , dried with anhydrous  $\text{Na}_2\text{SO}_4$ , add dropwise to stirring hexanes (50 mL), and evaporated in vacuo to 10 mL. The resulting precipitate was collected by filtration over a fine porosity fritted funnel and desiccated to yield 25 mg (54%) of an off-white powder.

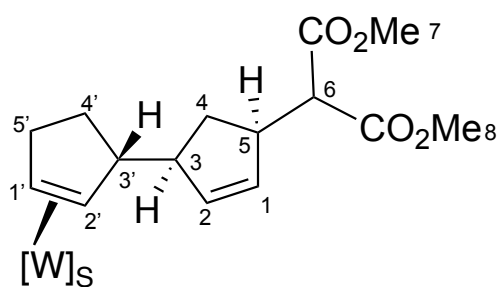
**<sup>1</sup>H NMR (800 MHz, CD<sub>3</sub>CN, 25 °C):** δ 8.46 (d, J = 2.1 Hz, 1H, Pz), 8.24 (d, J = 2.1 Hz, 1H, Pz), 8.05 (d, J = 2.0 Hz, 1H, Pz), 7.99 (d, J = 2.0 Hz, 1H, Pz), 7.82 (m, 2H, Pz), 7.69

(d, J = 2.3 Hz, 1H, Pz), 7.68 (d, J = 2.3 Hz, 1H, Pz), 7.58 (m, 2H, Pz), 7.46 (d, J = 2.1 Hz, 1H, Pz), 7.36 (d, J = 2.1 Hz, 1H, Pz), 6.38 (d, J = 5.4 Hz, 1H, H<sub>5</sub>), 6.36 (t, J = 2.2 Hz, 1H, Pz), 6.35 (t, J = 2.2 Hz, 1H, Pz), 6.24 (t, J = 2.2 Hz, 1H, Pz), 6.18 (t, J = 2.2 Hz, 1H, Pz), 6.15 (t, J = 2.2 Hz, 1H, Pz), 6.13 (t, J = 2.2 Hz, 1H, Pz), 5.30 (dd, J = 5.4, 2.1 Hz, 1H, H<sub>4</sub>), 3.80 – 3.78 (m, 1H, H<sub>3</sub>), 3.78 – 3.76 (m, 1H, H<sub>5'</sub>), 3.68 (ddt, J = 12.3, 7.2, 1.9 Hz, 1H, H<sub>1</sub>), 3.18 (ddd, J = 13.4, 8.1, 5.5 Hz, 1H, H<sub>1'</sub>), 2.71 (dd, J = 9.9, 8.0 Hz, 1H, H<sub>3'</sub>), 2.54 (dd, J = 12.4, 8.8 Hz, 1H, H<sub>5'</sub>), 2.08 – 2.02 (m, 1H, H<sub>4'</sub>), 1.78 (dd, J = 7.3, 2.7 Hz, 1H, H<sub>2</sub>), 1.69 (dd, J = 8.0, 2.8 Hz, 1H, H<sub>2'</sub>), 1.65 (dd, J = 12.5, 8.7 Hz, 1H, H<sub>4'</sub>), 1.22 (d, J = 8.4 Hz, 9H, PMe<sub>3</sub>A), 1.19 (d, J = 8.3 Hz, 9H, PMe<sub>3</sub>B).

**<sup>13</sup>C NMR (201MHz, CD<sub>3</sub>CN, 25 °C):** δ 144.99, 144.02, 143.55, 142.61, 142.32, 141.98, 137.86, 137.81, 136.91, 136.82 (C<sub>5</sub>), 136.63, 136.46, 127.73 (C<sub>4</sub>), 107.40, 106.66, 106.60, 106.45, 106.31, 66.77 (d, J = 10.8 Hz, C<sub>1</sub>), 65.54 (C<sub>2'</sub>), 63.40 (C<sub>2'</sub>), 62.71 (d, J = 11.4 Hz, C<sub>1'</sub>), 61.16 (C<sub>3'</sub>), 37.04 (d, J = 2.7 Hz, C<sub>5'</sub>), 28.81 (C<sub>4'</sub>), 14.17 (d, J = 28.2 Hz, PMe<sub>3</sub>A), 13.71 (d, J = 28.4 Hz, PMe<sub>3</sub>B).

Composition of compound **12** confirmed via SC-XRD.

### Synthesis and characterization of WTp(NO)(PMe<sub>3</sub>)(3-[5-(1,3-dimethoxy-1,3-dioxopropan-2-yl)cyclopent-1-en-3-yl]cyclopentene)- (**13**)



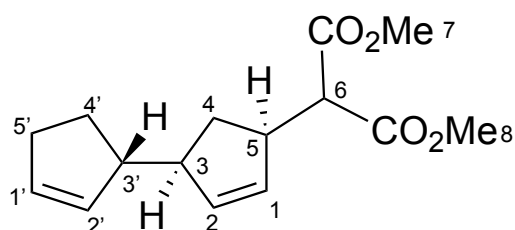
In separate test tubes an enantioenriched sample of compound **10** (100 mg, 0.078 mmol) and DDQ (37.5 mg, 0.165 mmol) were dissolved in MeCN (2 mL each) and chilled to –35 °C. The DDQ solution was added to the [W] complex under strong stirring, and the solution rapidly blackened. Stirring was continued for 10 minutes before the test tube was removed from the glovebox. The solution was diluted with sat. NaHCO<sub>3</sub> (40 mL) and extracted 3× with DCM. The combined organic layers were evaporated to dryness, dissolved in minimal DCM, and precipitated into stirring

hexanes (100 mL). The resulting dark precipitate was removed by filtration over a fine porosity fritted funnel, which was then thoroughly rinsed with Et<sub>2</sub>O (100 mL). The combined organics were evaporated to dryness to yield 34 mg of a light brown oil containing 10S, 11S, and various side products. Dissolution of the material in minimal DCM followed by slow evaporation overnight.

**<sup>1</sup>H NMR (800 MHz, CD<sub>3</sub>CN, 25 °C):** Proton peaks not assigned because of overlapping peaks between compounds **13** and **14** and decomposition products.

Composition of compound **13** confirmed via SC-XRD.

**Synthesis and characterization of dimethyl 2-((1S,1'S,3R)-[1,1'-bi(cyclopentane)]-2',4-dien-3-yl)malonate (**14**)**



In separate test tubes, compound **11C** (180 mg, 0.142 mmol) and CAN (466 mg, 0.850 mmol) were dissolved in MeCN (2 mL each) and chilled to -35 °C. The CAN suspension was added to the [W] solution under strong stirring, and the solution rapidly darkened to brown. Stirring was continued for 10 minutes before the test tube was removed from the glovebox. The solution was diluted with DCM (40 mL) and extracted 3× with H<sub>2</sub>O, which caused a white precipitate to form. The organic layer was dried with anhydrous Na<sub>2</sub>SO<sub>4</sub>, evaporated to dryness, dissolved in minimal DCM, and precipitated into stirring hexanes (150 mL). The resulting yellow precipitate was removed by filtration over a fine porosity fritted funnel, which was then thoroughly rinsed with Et<sub>2</sub>O (100 mL), and the combined organics were evaporated to dryness to yield 88 mg of a yellow-brown oil. 65 mg of this oil was dissolved in DCM (1 mL) and loaded onto a silica preparatory TLC plate. The plate was developed with a 92:8 hexanes:EtOAc mixture, and the product band, once identified by staining one edge with KMnO<sub>4</sub>, was scraped off the plate and loaded into a Pasteur pipette plugged with cotton. The silica was eluted with DCM (10 mL) and evaporated to dryness to yield 15 mg (54%) of a colorless oil with a pungent, mint-like odor.

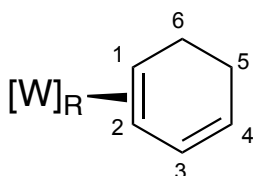
**<sup>1</sup>H NMR (800 MHz, CDCl<sub>3</sub>, 25 °C):** δ 5.77 (dt, J = 5.7, 2.2 Hz, 1H, H<sub>2</sub>), 5.76 (dq, J = 6.5, 2.2 Hz, 1H, H<sub>1'</sub>), 5.70 (dq, J = 6.2, 2.2 Hz, 1H, H<sub>5</sub>), 5.66 (dt, J = 5.8, 2.1 Hz, 1H,

H1), 3.74 (d,  $J = 1.4$  Hz, 6H, H8), 3.36 – 3.31 (m, 1H, H5), 3.29 (d,  $J = 9.6$  Hz, 1H, H6), 2.68 – 2.64 (m, 1H, H3), 2.64 – 2.59 (m, 1H, H3'), 2.37 – 2.29 (m, 1H, H5'), 2.31 – 2.23 (m, 1H, H5'), 2.26 (dt,  $J = 13.2, 8.0$  Hz, 1H, H4), 1.97 (dddd,  $J = 13.1, 9.1, 8.4, 4.9$  Hz, 1H, H4'), 1.47 (dddd,  $J = 13.0, 9.3, 6.4, 5.9$  Hz, 1H, H4'), 1.17 (dt,  $J = 13.2, 7.9$  Hz, 1H, H4).

**$^{13}\text{C}$  NMR (201 MHz,  $\text{CDCl}_3$ , 25 °C):**  $\delta$  169.18 (C7), 136.13 (C2), 133.44 (C2'), 131.81 (C1), 131.53 (C1'), 57.43 (C6), 52.46 (d,  $J = 6.0$  Hz, C8), 51.05 (C3'), 51.02 (C3), 45.24 (C5), 33.28 (C4), 32.19 (C5'), 27.73 (C4').

**HRMS-ACPI:** (m/z) calcd for  $\text{C}_{15}\text{H}_{20}\text{O}_4$  264.1362, found 264.1357.

### Synthesis and characterization of $[\text{W}(\text{Tp})(\text{NO})(\text{PMe}_3)(\eta^2\text{-cyclohexa-1,3-diene})]$ (15)

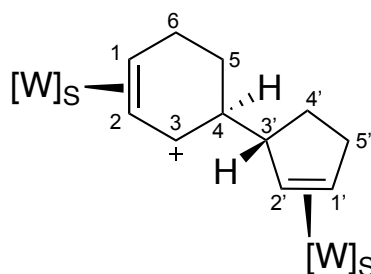


In a typical preparation,  $[\text{W}]$ -cyclohexenylium 12 (200 mg, 0.273 mmol, 1 equiv.; synthesis previously published) was dissolved in DCM (5 mL) and chilled to  $-15$  °C. Separately, a solution of DBU (206 mg, 1.35 mmol, 5 equiv.) in DCM (1 mL) was prepared and chilled to  $-15$  °C. The DBU solution was added to 12, and the reaction was allowed to stir for 1 min. The solution was then extracted 3 $\times$  with 1 M  $\text{Na}_2\text{CO}_3$ , and back-extracted 2 $\times$ . The combined organic layers were reduced to dryness in vacuo, and redissolved into THF (2 mL). The yellow solution was added dropwise to stirring, chilled hexanes ( $-30$  °C, 150 mL), and the volume was reduced in vacuo to 20 mL to induce the formation of a white precipitate, which was collected by filtration over a fine porosity fritted filter. Typical yield 70%. Slow evaporation of the remaining hexanes filtrate yielded large needles suitable for SC-XRD analysis.

**$^1\text{H}$  NMR (800 MHz,  $\text{CDCl}_3$ , 25 °C):** Compound previously characterized: 8.25 (d,  $J = 2.0$ , 1H, PzA3(d)), 8.08 (m, 1H, PzB3(p+d)), 8.05 (d,  $J = 2.0$ , 1H, PzA3(p)), 7.70 (d,  $J = 2.0$ , 1H, PzB5(p)), 7.68 (d,  $J = 2.0$ , 1H, PzB5(d)), 7.61 (d,  $J = 2.0$ , 1H, PzA5(p)), 7.57 (d,  $J = 2.0$ , 1H, PzA5(d)), 7.34 (d,  $J = 2.0$ , 1H, PzC3(d)), 7.28 (d,  $J = 2.0$ , 1H, PzC3(p)), 6.29 (t,  $J = 2.0$ , 1H, PzB4(d)), 6.27 (t,  $J = 2.0$ , 1H, PzB4(p)), 6.21 (t,  $J = 2.0$ , 1H, PzA4(p)), 6.18 (t,  $J = 2.0$ , 1H, PzA4(d)), 6.17/6.16 (t,  $J = 2.0$ , 1H, PzC4(p+d)), 1.28 (d,  $J = 8.3$ , 9H,  $\text{PMe}_3$ (p)), 1.27 (d,  $J = 8.2$ , 9H,  $\text{PMe}_3$ (d)), Distal Diene (d-Major isomer):

6.68 (ddd,  $J = 9.0, 5.6, 2.9$ , 1H, H3), 5.23 (ddd,  $J = 9.0, 6.6, 2.0$ , 1H, H4), 3.65 (m, 1H, H6), 2.66 (m, 1H, H1/H6'), 2.45 (m, 1H, H5), 1.94 (m, 1H, H5'), 1.68 (m, 1H, H2),  
 **$^{13}\text{C}$  NMR (201 MHz,  $\text{CDCl}_3$ , 25 °C):** Compound previously characterized: 144.5 (PzA3(d)), 143.4/143.3 (PzB3(p,d)), 142.1 (PzA3(p)), 140.2/140.1 (PzC3(p,d)), 136.4 (Tp5), 136.2 (Tp5), 135.6 (2 Tp5's), 135.2 (Tp5), 134.8 (Tp5), 106.3 (Tp4), 106.1 (Tp4), 105.7 (Tp4), 105.5 (3 Tp4's), 14.0 (d,  $J_{\text{PC}} = 27.8$ ,  $\text{PMe}_3(\text{p})$ ), 13.4 (d,  $J_{\text{PC}} = 27.8$ ,  $\text{PMe}_3(\text{d})$ ), Distal Diene: 133.4 (C3), 120.8 (C4), 56.6 (d,  $J_{\text{PC}} = 11.9$ , C1), 50.8 (C2), 23.5 (C5), 21.6 (C6),

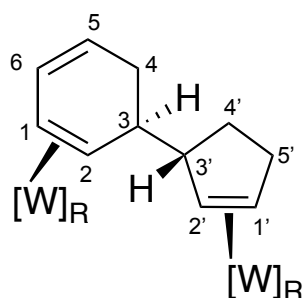
**Synthesis and characterization of  $\{\text{WTP}(\text{NO})(\text{PMe}_3)\}_2((\mu\text{-}1,2,1',2'\text{-}\eta\text{-}4\text{-}(\text{cyclopent-1'-en-3'-yl})\text{cyclohex-1-en-3-ylid})\text{OTf}$  (**16**)**



In separate test tubes, compound **15** (15 mg, 0.026 mmol) and compound **3** (16.8 mg, 0.023 mmol) were dissolved in DCM (1 mL) and chilled to 0 °C. The solution of **3** was added to **15** under strong stirring. The solution was stirred for 2 minutes then added dropwise to a stirring mixture of  $\text{Et}_2\text{O}$  (75 mL). The resulting precipitate was collected by filtration over a fine porosity fritted funnel and desiccated to yield 29 mg (97%) of a light-yellow powder.

**$^1\text{H}$  NMR (800 MHz,  $\text{CDCl}_3$ , 25 °C):** 8.30, 8.26, 8.10, 8.07, 7.95, 7.86, 7.83, 7.73, 7.69, 7.65, 7.59, 7.33 (d,  $J = 1.84, 1.11, 1.48, 1.94, 1.94, 1.94, 2.31, 2.21, 1.94, 1.84, 2.31, 1.48$  Hz, 12H, Tp protons), 6.59, 6.45, 6.33, 6.20, 6.19, 6.16 (t,  $J = 2.21, 2.21, 2.04, 2.04, 2.04, 2.04$ , 6H, Tp protons), 6.51 (d,  $J = 7.63$  Hz, 1H, H3), 5.05 (t,  $J = 6.96$  Hz, 1H), 4.43 (m,  $J = 6.96, 14.59$  Hz, 1H) – H1/H2. 3.63 (m, 1H), 3.59 (m,  $J = 5.70, 13.73$  Hz, 1H), 3.56 (m, 1H), 3.24 (dd,  $J = 10.59, 14.81$  Hz, 1H), 3.16 (m,  $J = 7.28, 14.81$  Hz, 1H), 3.08 (m,  $J = 6.52, 13.48$  Hz, 1H), 2.70 (t,  $J = 10.38$  Hz, 1H), 2.42 (t/dd,  $J = 7.78/3.35, 9.11$  Hz, 2H), 1.80 (m,  $J = 5.44, 11.90$  Hz, 1H), 1.75 (dd,  $J = 1.77, 8.29$  Hz, 1H), 1.71 (dd,  $J = 9.56, 13.48$  Hz, 1H) – H4 – H6/ H1' – H5'. 1.24 (d,  $J = 9.87$  Hz, 9H,  $\text{PMe}_3$ ), 1.22 (d,  $J = 7.78$  Hz, 9H,  $\text{PMe}_3$ ).

**Synthesis and characterization of  $\{Wtp(NO)(PMe_3)\}_2((\mu-1,2,1',2'-\eta)-3-(\text{cyclopent-1'-en-3'-yl})\text{cyclohexa-1,5-diene})$  (**17**)**

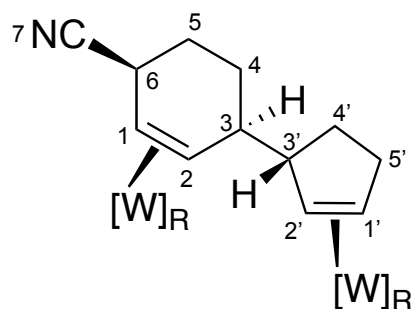


In separate test tubes, compound **16** (45 mg, 0.035 mmol) and DBU (26.3 mg, 0.173 mmol) were dissolved in DME (4 mL, 1 mL, resp.) and chilled to 0 °C. The DBU solution was added to **16** under strong stirring, which lightened in color from yellow to off-white. The solution was reduced in vacuo to 2 mL and added dropwise to a stirring mixture of hexanes/Et<sub>2</sub>O (1:1, 40 mL). The resulting precipitate was collected by filtration over a fine porosity fritted funnel and desiccated to yield 37 mg (94%) of an off-white powder.

**<sup>1</sup>H NMR (800 MHz, CDCl<sub>3</sub>, 25 °C):** δ 8.29 (d, *J* = 2.0 Hz, 1H, Pz), 8.15 (d, *J* = 2.0 Hz, 1H, Pz), 8.08 (m, 2H, Pz), 7.69 (d, *J* = 2.4 Hz, 1H, Pz), 7.68 (d, *J* = 2.1 Hz, 1H, Pz), 7.67 (d, *J* = 2.3 Hz, 1H, Pz), 7.64 (d, *J* = 2.2 Hz, 1H, Pz), 7.61 (d, *J* = 2.4 Hz, 1H, Pz), 7.56 (d, *J* = 2.4 Hz, 1H, Pz), 7.39 (d, *J* = 2.1 Hz, 1H, Pz), 7.33 (d, *J* = 2.2 Hz, 1H, Pz), 6.42 (ddd, *J* = 9.9, 4.8, 2.8 Hz, 1H, H<sub>6</sub>), 6.28 (t, *J* = 2.2 Hz, 1H, Pz), 6.25 (t, *J* = 2.2 Hz, 1H, Pz), 6.17 (t, *J* = 2.2 Hz, 1H, Pz), 6.14 (t, *J* = 2.2 Hz, 1H, Pz), 6.13 (t, *J* = 2.2 Hz, 1H, Pz), 6.10 (t, *J* = 2.2 Hz, 1H, Pz), 5.26 (ddd, *J* = 9.2, 6.3, 2.2 Hz, 1H, H<sub>5</sub>), 3.65 – 3.58 (m, 1H, H<sub>5'</sub>), 3.46 – 3.44 (m, 1H, H<sub>3</sub>), 3.17 (ddd, *J* = 13.3, 8.0, 5.7 Hz, 1H, H<sub>1'</sub>), 3.08 – 3.04 (m, 1H, H<sub>3'</sub>), 3.00 – 2.95 (m, 1H, H<sub>1</sub>), 2.60 (dd, *J* = 17.5, 8.9 Hz, 1H, H<sub>4</sub>), 2.52 – 2.48 (m, 1H, H<sub>5'</sub>), 2.46 (dd, *J* = 17.3, 6.2 Hz, 1H, H<sub>4</sub>), 2.21 – 2.17 (m, 1H, H<sub>4'</sub>), 1.91 – 1.84 (m, 1H, H<sub>4'</sub>), 1.79 – 1.75 (m, 1H, H<sub>2'</sub>), 1.43 (d, *J* = 10.2 Hz, 1H, H<sub>2</sub>), 1.27 (d, *J* = 8.2 Hz, 9H, PMe<sub>3</sub>A), 1.23 (d, *J* = 8.0 Hz, 9H, PMe<sub>3</sub>B).

**<sup>13</sup>C NMR (201 MHz, CDCl<sub>3</sub>, 25 °C):** δ 143.39, 143.12, 142.92, 141.67, 140.98, 140.69, 136.32, 136.17, 135.51, 135.48, 135.26, 134.90, 130.31 (C<sub>6</sub>), 120.45 (C<sub>5</sub>), 106.28, 106.13, 105.77, 105.45, 105.32, 105.19, 64.33 (C<sub>1'</sub>), 61.82 (C<sub>3</sub>), 60.07 (C<sub>2</sub>), 51.77 (C<sub>4</sub>), 44.40 (C<sub>3'</sub>), 37.81 (C<sub>4'</sub>), 25.92 (C<sub>5'</sub>), 23.96 (C<sub>1</sub>), 23.71 (C<sub>2'</sub>), 14.17 (d, *J* = 14.0 Hz, PMe<sub>3</sub>B), 14.04 (d, *J* = 13.9 Hz, PMe<sub>3</sub>A).

**Synthesis and characterization of {Wtp(NO)(PMe<sub>3</sub>)}<sub>2</sub>((μ-1,2,1',2'-η)-3-(cyclopent-1'-en-3'-yl)-6-(cyanocyclohexene) - (18)**



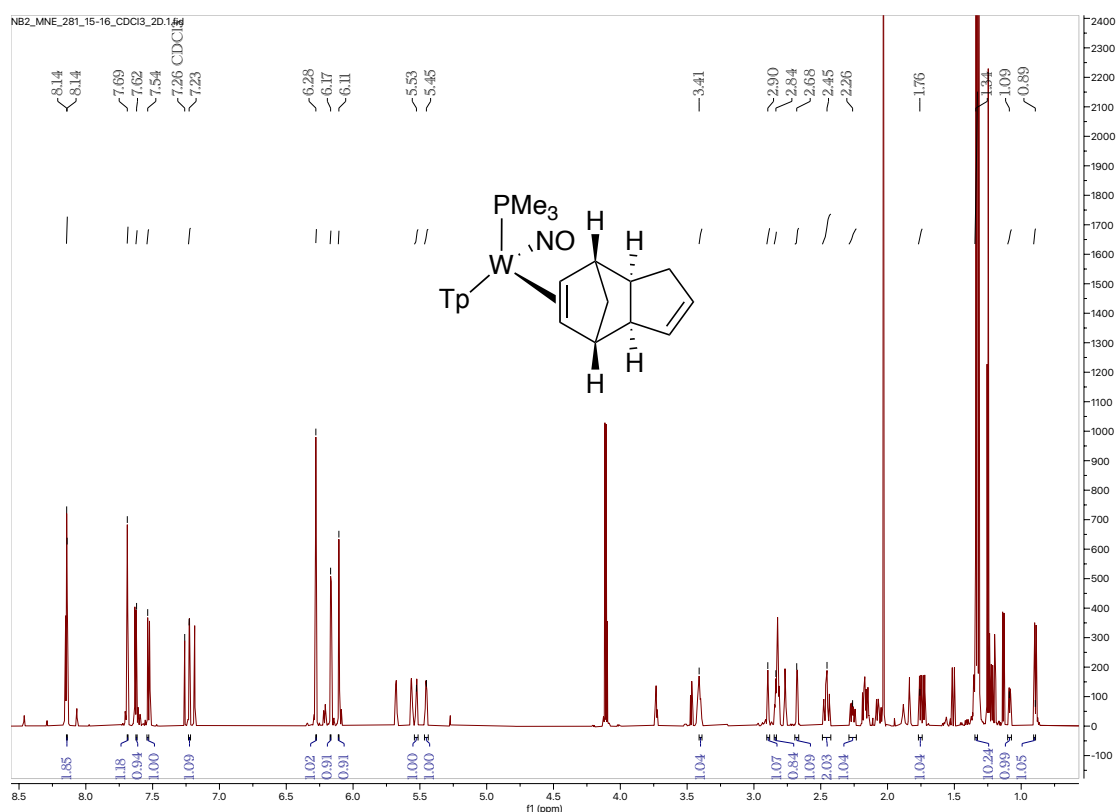
In a test tube compound **16** (22 mg, 0.017 mmol) was dissolved in 1 mL MeCN followed by 2 drops of MeOH. NaCN (4 mg, 0.082 mmol) was added to reaction and stirred for 5 minutes. The reaction was filtered over a fritted disc, then precipitated into stirring hexanes.

**<sup>1</sup>H-NMR (800 MHz, CD<sub>3</sub>Cl, 25 °C):** δ 8.49, 8.13, 8.01, 7.70, 7.68, 7.65, 7.61, 7.52, 7.41, 7.13 (d, J = 1.98, 1.92, 1.92, 2.25, 2.18, 2.51, 1.92, 2.51, 2.18, 1.92, 2.25, 12H, Tp protons), 6.30, 6.26, 6.23, 6.21, 6.14, 5.85 (t, J = 2.16, 2.23, 2.16, 2.16, 2.23, 2.16 Hz, 6H, Tp protons), 3.81 (m, 1H), 3.76 (m, J = 4.55, 11.07, 16.61 Hz, 1H), 3.12 (ddd, J = 5.54, 7.50, 14.15 Hz, 1H), 3.03 (m, J = 8.12, 14.64 Hz, 1H), 2.94 (m, 1H), 2.91 (m, J = 6.03 Hz, 1H), 2.36 (m, J = 8.96 Hz, 1H), 2.06 (m, 1H), 1.97 (m, J = 2.09, 12.05 Hz, 1H), 1.87 (m, J = 7.63, 2H), 1.68 (m, J = 8.00, 13.65, 20.66 Hz, 1H), 1.60 (m, J = 5.04, 12.55 Hz, 2H), 1.30 (m, 1H), 1.25 (m, 1H) – H1 – H6, H1' – H5'. 1.27 (d, J = 8.00, 9H, PMe<sub>3</sub>), 1.20 (d, 9H, PMe<sub>3</sub>).

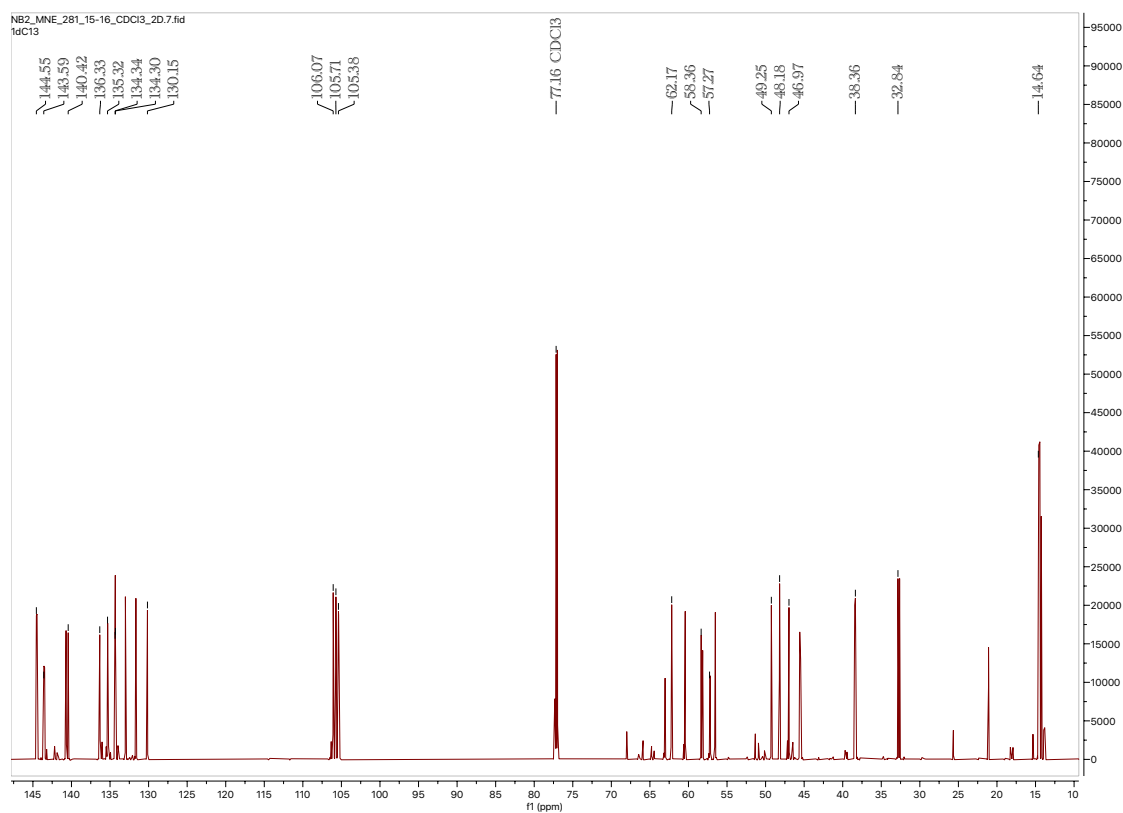
**<sup>13</sup>C NMR (201 MHz, CDCl<sub>3</sub>, 25 °C):** δ 144.8, 143.0, 142.9, 142.6, 139.8, 136.2, 135.9, 135.5, 135.3, 134.8 (12C, Tp carbons), 125.3 (1C, C7), 106.2, 106.0, 105.9, 100.4 (6C, Tp carbons), 62.3, 61.1 (d, J = 11.47 Hz), 58.3, 51.5, 50.8, 47.1 (d, J = 10.44 Hz), 35.3, 34.4, 28.5, 27.7, 26.9 (11C, C1 – C6, C1' – C5'). 14.28 (d, J = 27.66 Hz, 3C, PMe<sub>3</sub>), 13.73 (d, J = 27.54 Hz, 3C, PMe<sub>3</sub>).



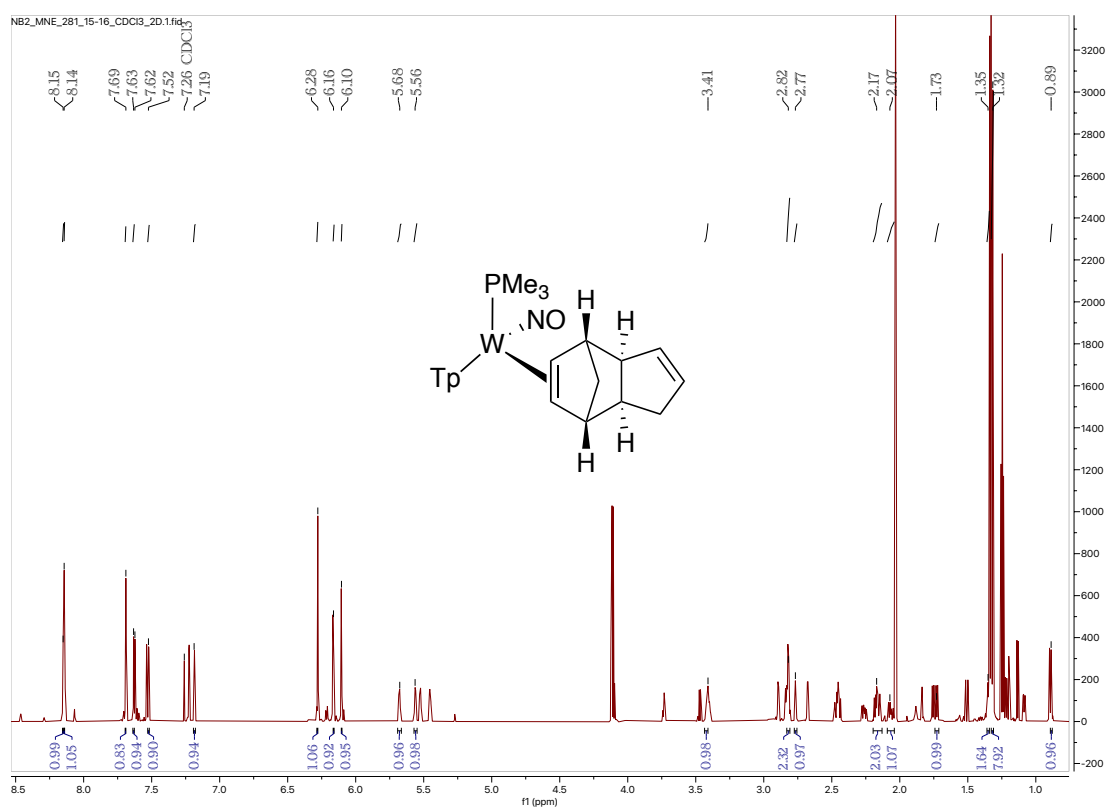
<sup>1</sup>H NMR (800 MHz, CDCl<sub>3</sub>, δ, 25 °C) of Compound **1D**



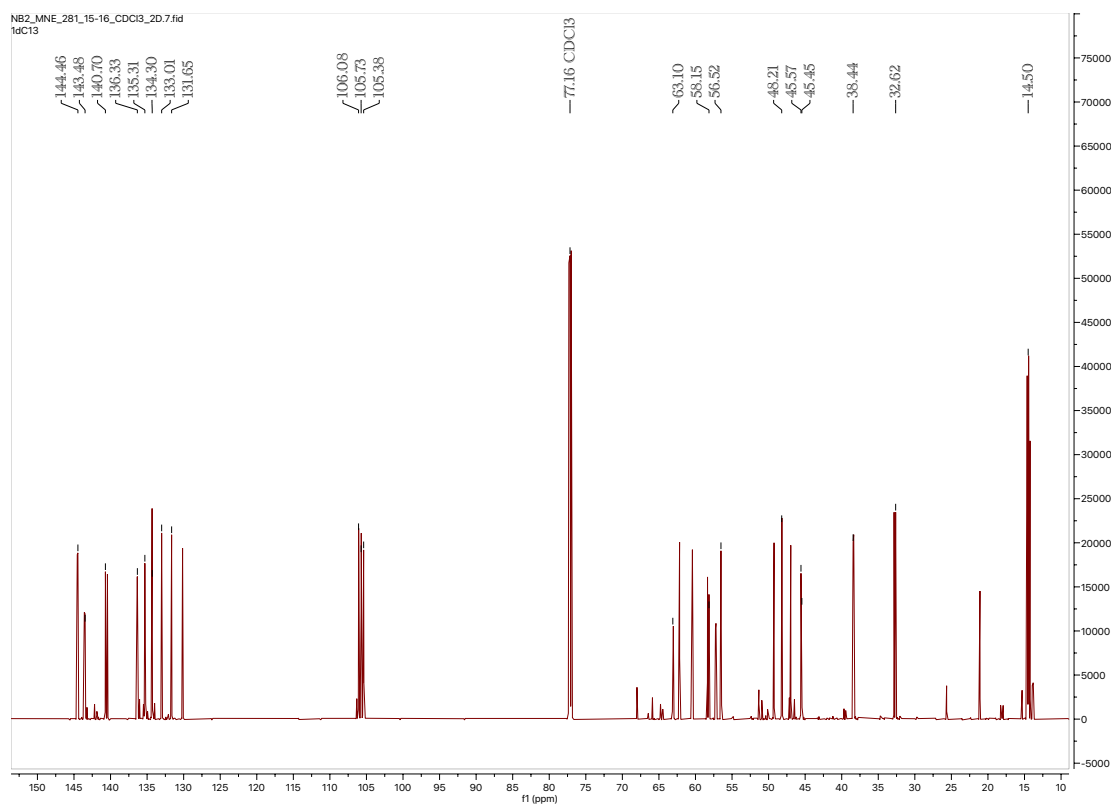
<sup>13</sup>C NMR (201 MHz, CDCl<sub>3</sub>, δ, 25 °C) of Compound **1D**



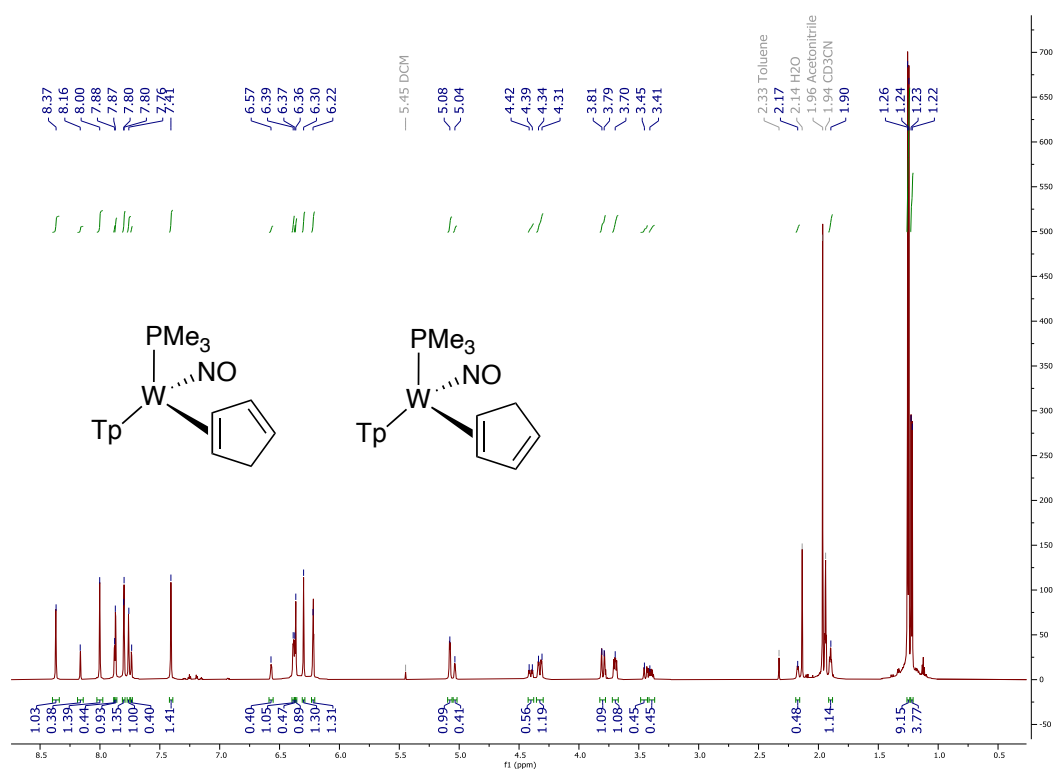
<sup>1</sup>H NMR (800 MHz, CDCl<sub>3</sub>, δ, 25 °C) of Compound **1P**



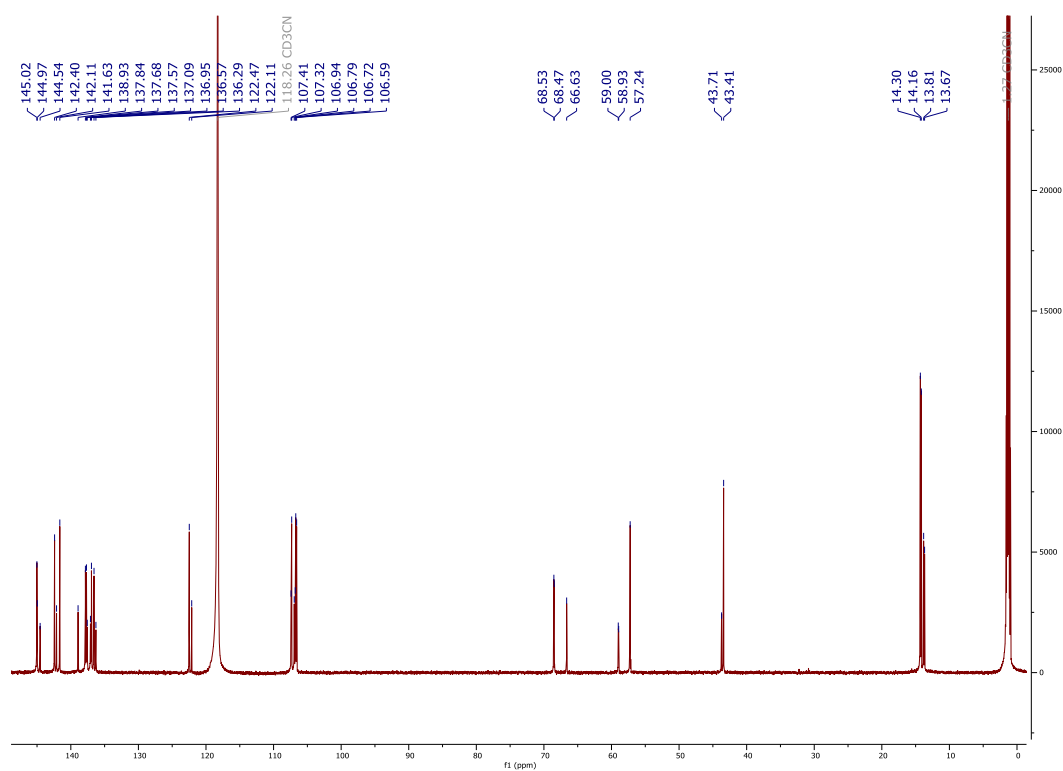
<sup>13</sup>C NMR (201 MHz, CDCl<sub>3</sub>, δ, 25 °C) of Compound **1P**



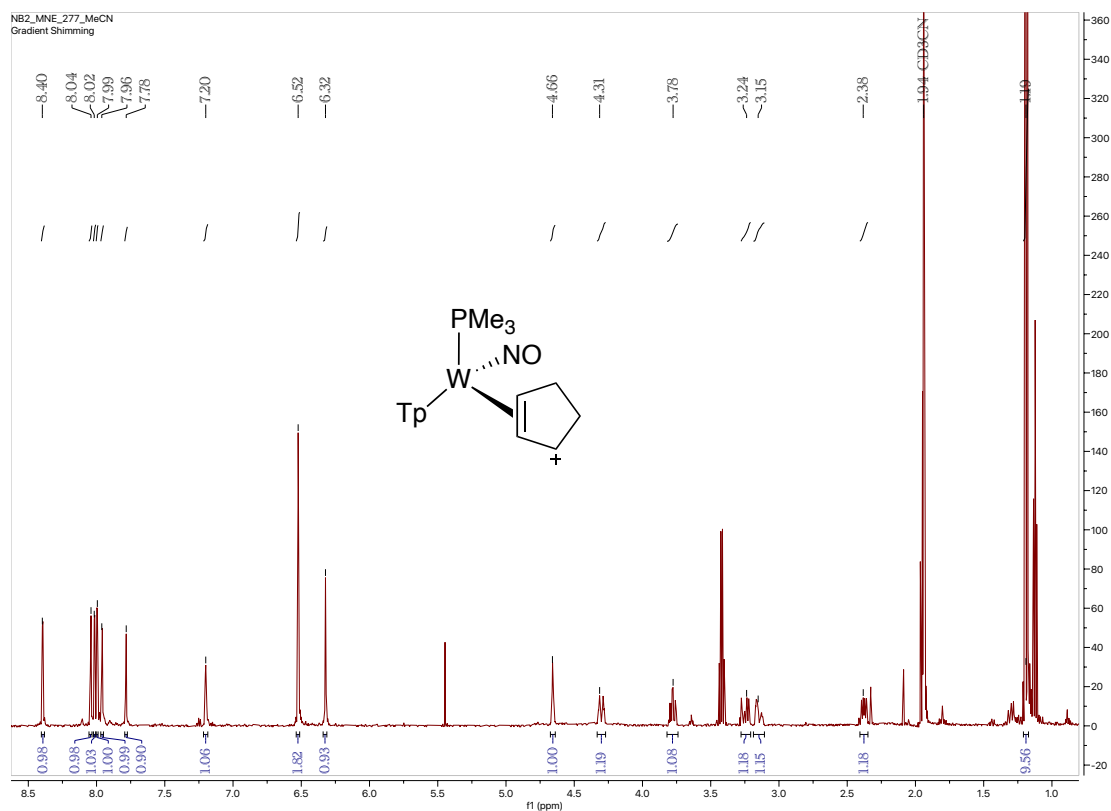
<sup>1</sup>H NMR (800 MHz, CD<sub>2</sub>CN, δ, 25 °C) of Compound **2P/2D**



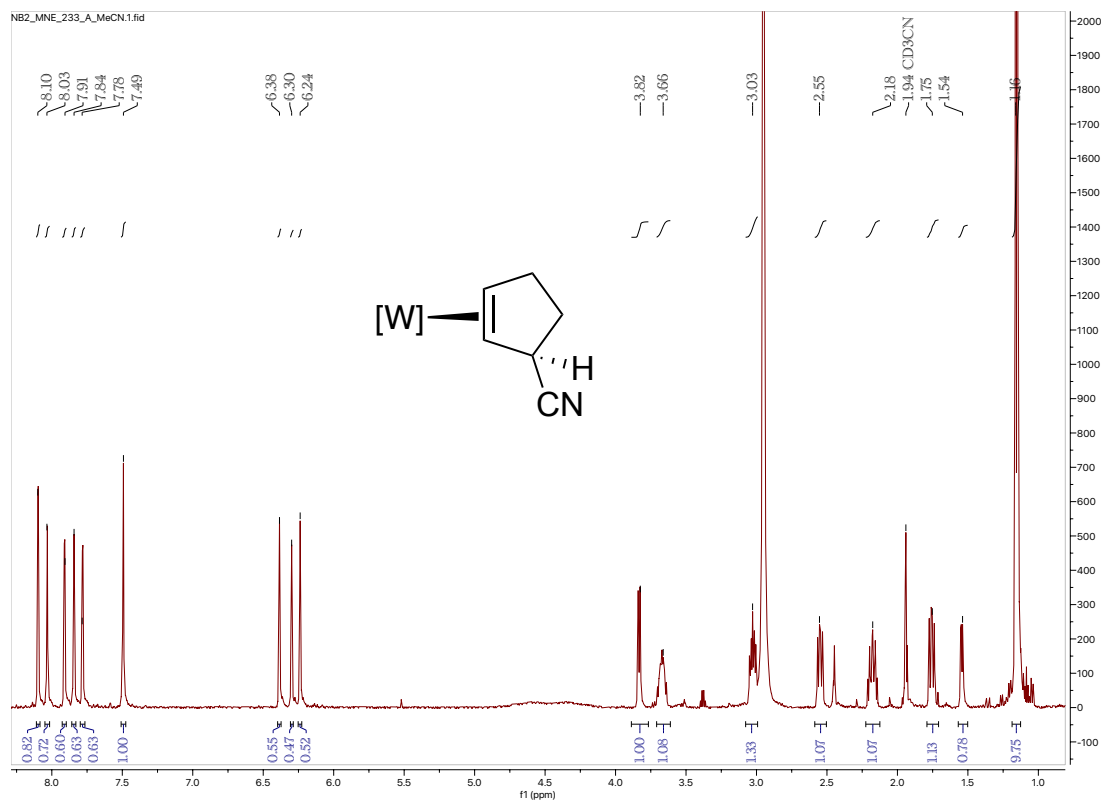
<sup>13</sup>C NMR (201 MHz, CD<sub>2</sub>CN, δ, 25 °C) of Compound **2P/2D**



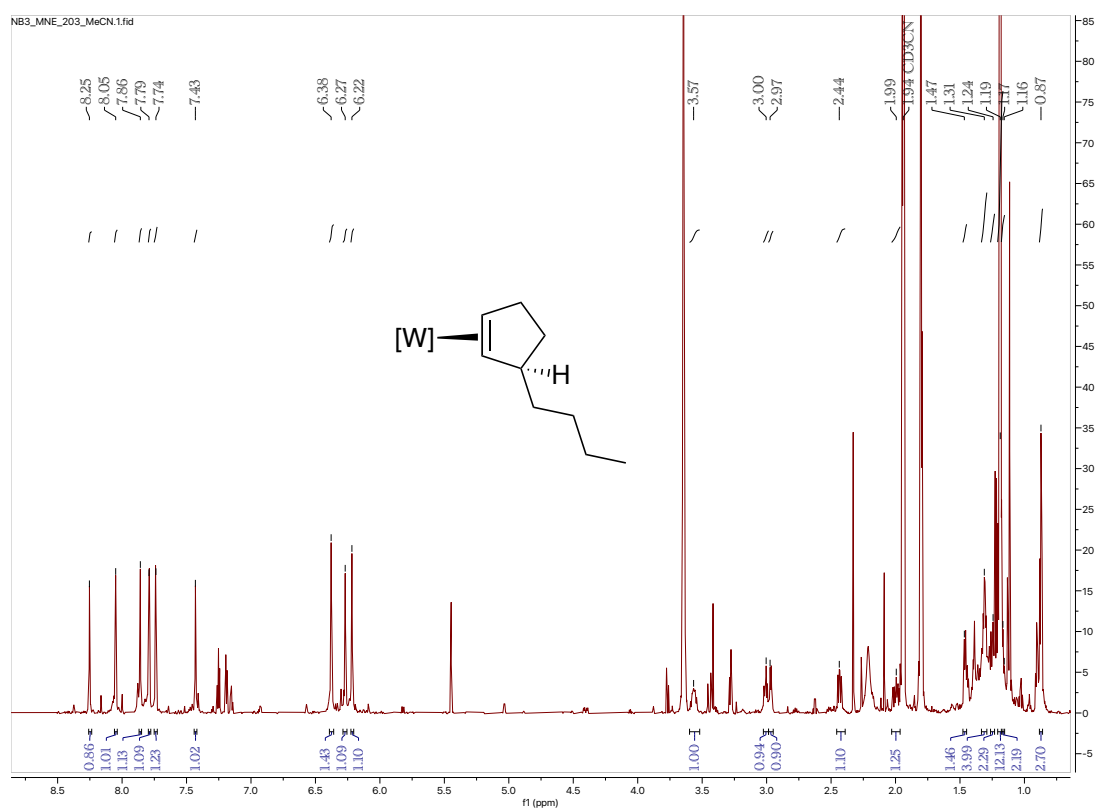
# <sup>1</sup>H NMR (800 MHz, CD<sub>2</sub>CN, δ, 25 °C) of Compound **3**



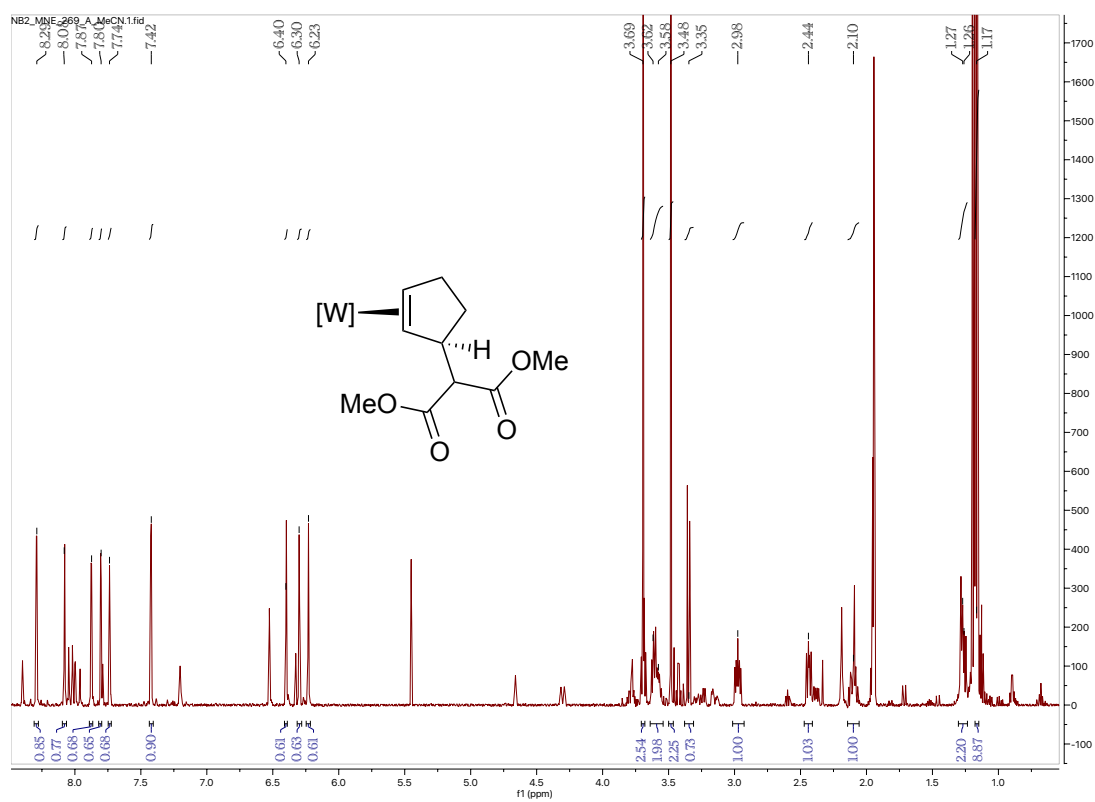
# <sup>1</sup>H NMR (800 MHz, CD<sub>2</sub>CN, δ, 25 °C) of Compound **4A**



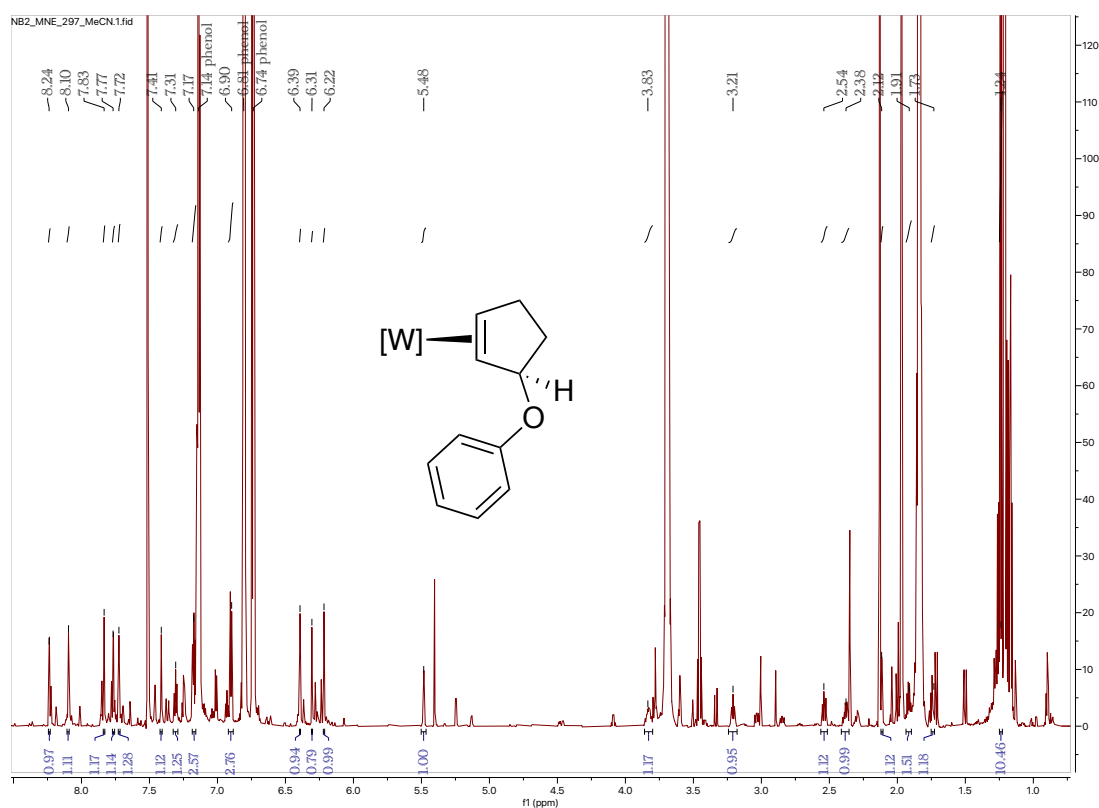
<sup>1</sup>H NMR (800 MHz, CD<sub>2</sub>CN, δ, 25 °C) of Compound **4B**



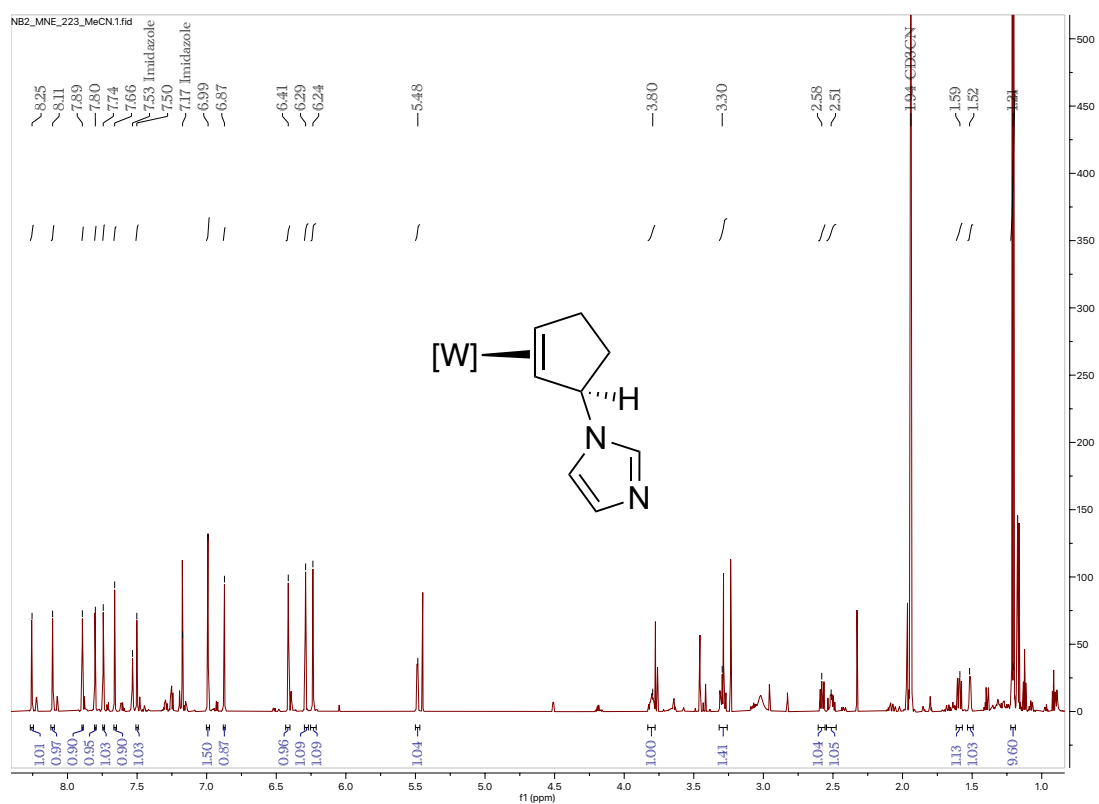
<sup>1</sup>H NMR (800 MHz, CD<sub>2</sub>CN, δ, 25 °C) of Compound **4C**



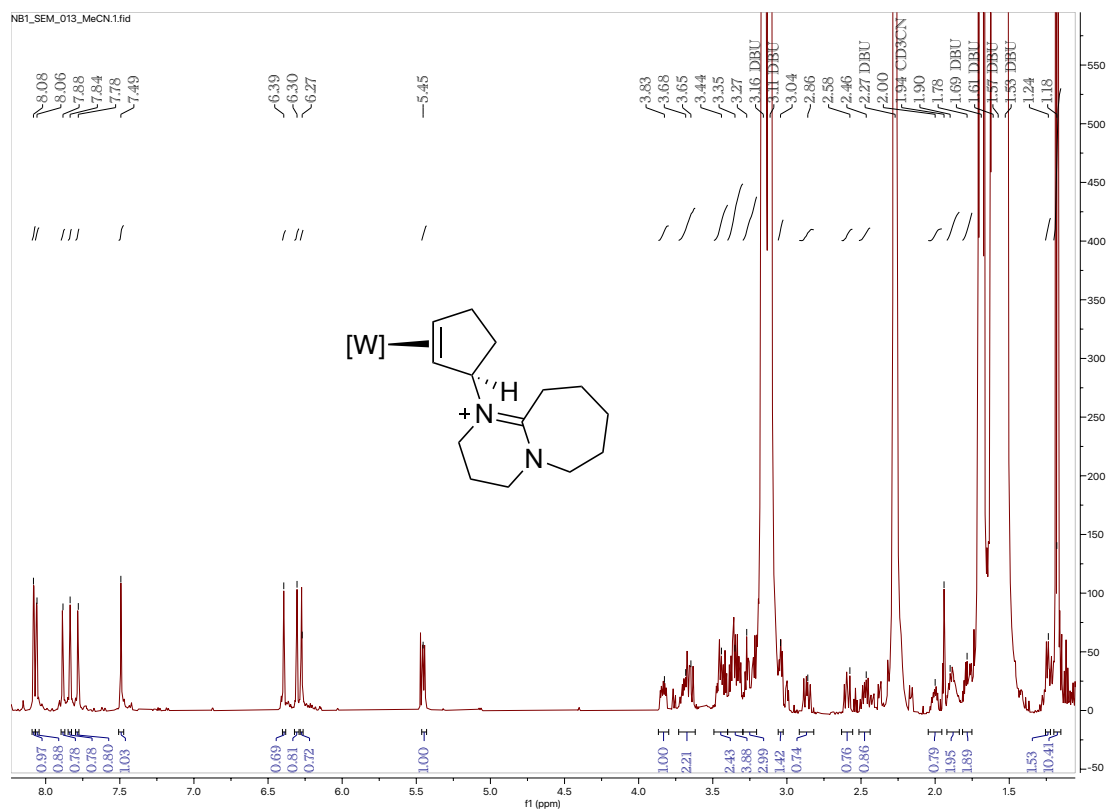
<sup>1</sup>H NMR (800 MHz, CD<sub>2</sub>CN, δ, 25 °C) of Compound **4D**



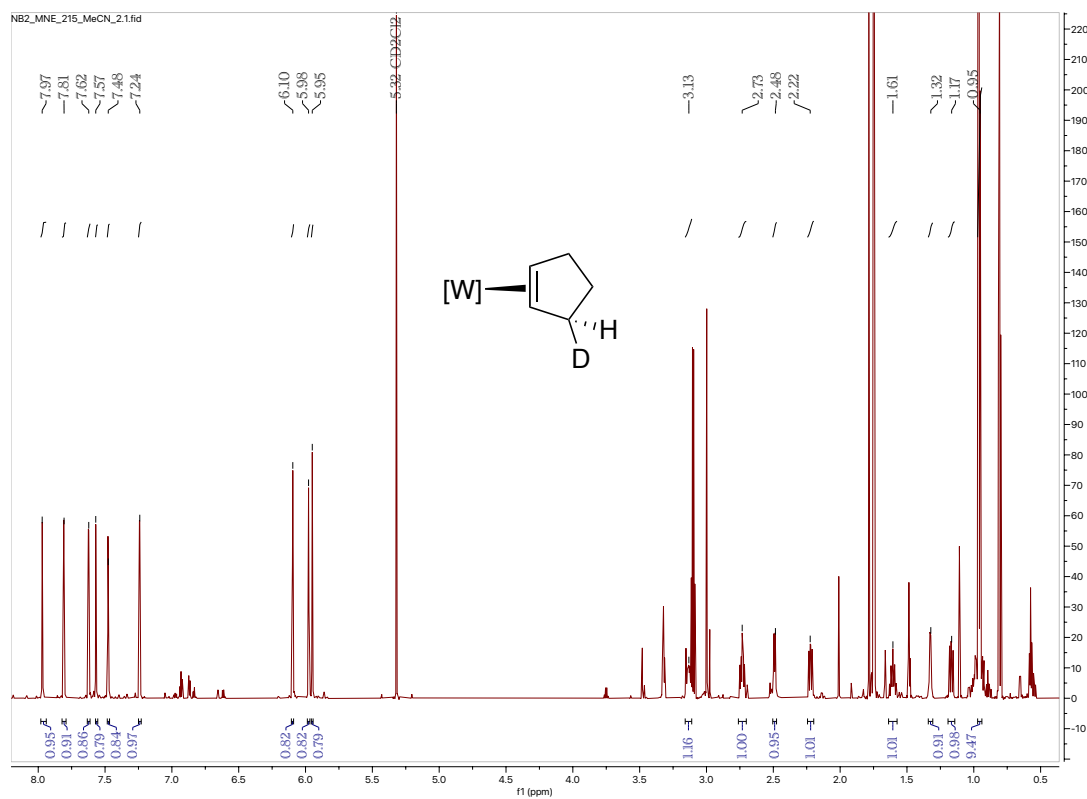
<sup>1</sup>H NMR (800 MHz, CD<sub>2</sub>CN, δ, 25 °C) of Compound **4E**



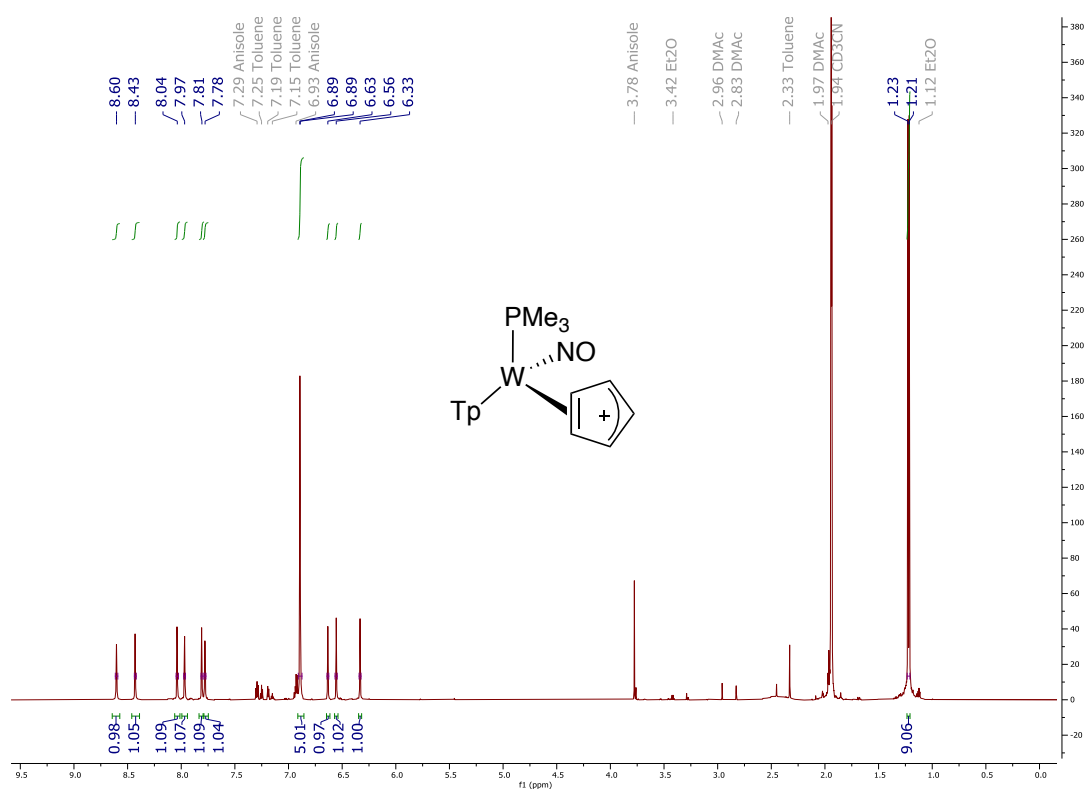
<sup>1</sup>H NMR (800 MHz, CD<sub>2</sub>CN, δ, 25 °C) of Compound **4F**



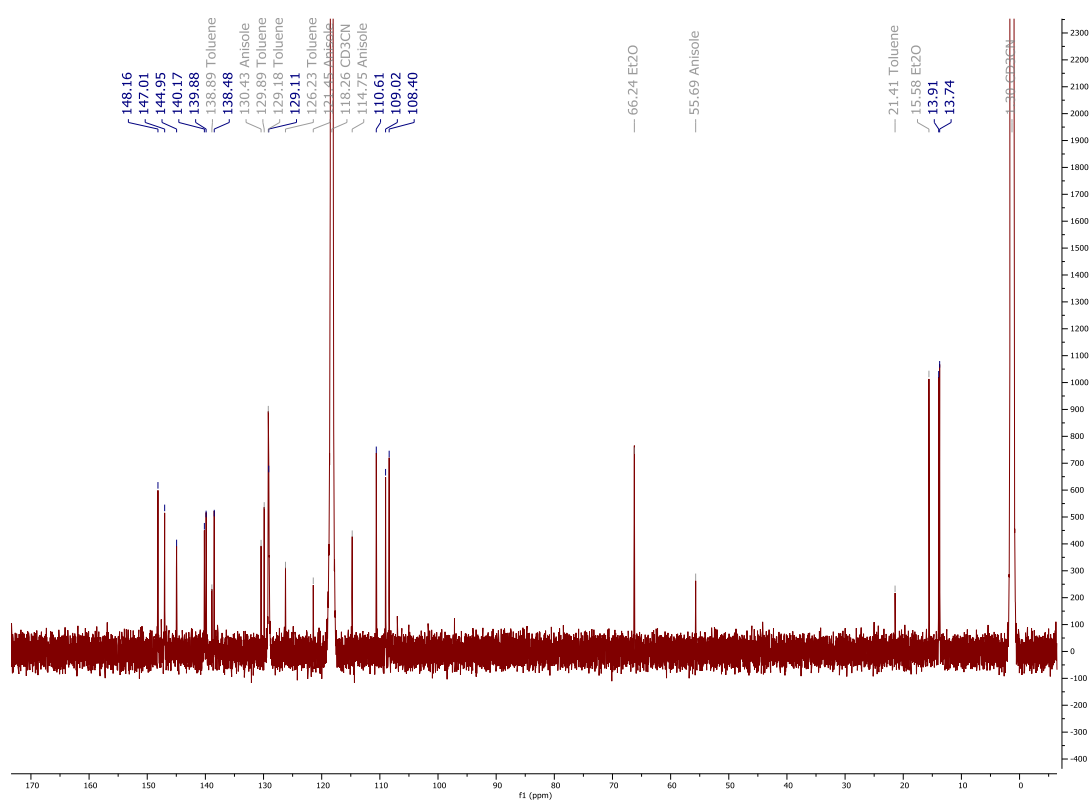
<sup>1</sup>H NMR (800 MHz, CD<sub>2</sub>CN, δ, 25 °C) of Compound **4G**



<sup>1</sup>H NMR (800 MHz, CD<sub>2</sub>CN, δ, 25 °C) of Compound **5**

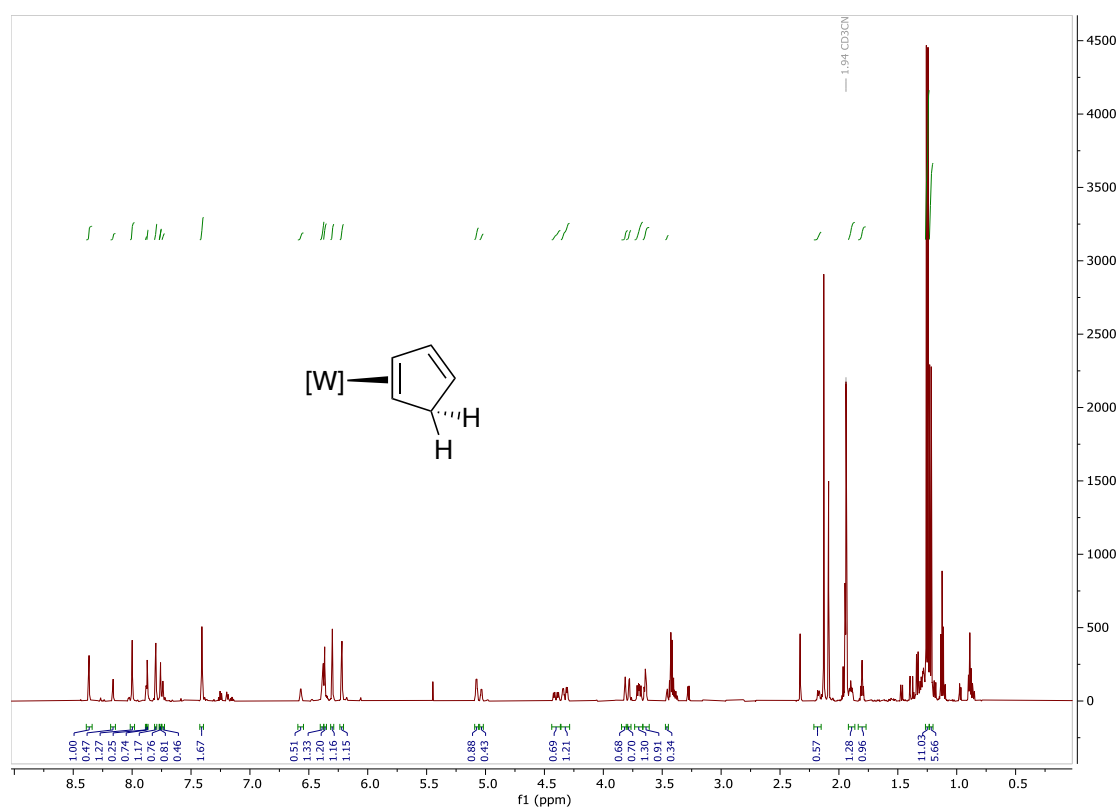


<sup>13</sup>C NMR (201 MHz, CD<sub>2</sub>CN, δ, 25 °C) of Compound **5**

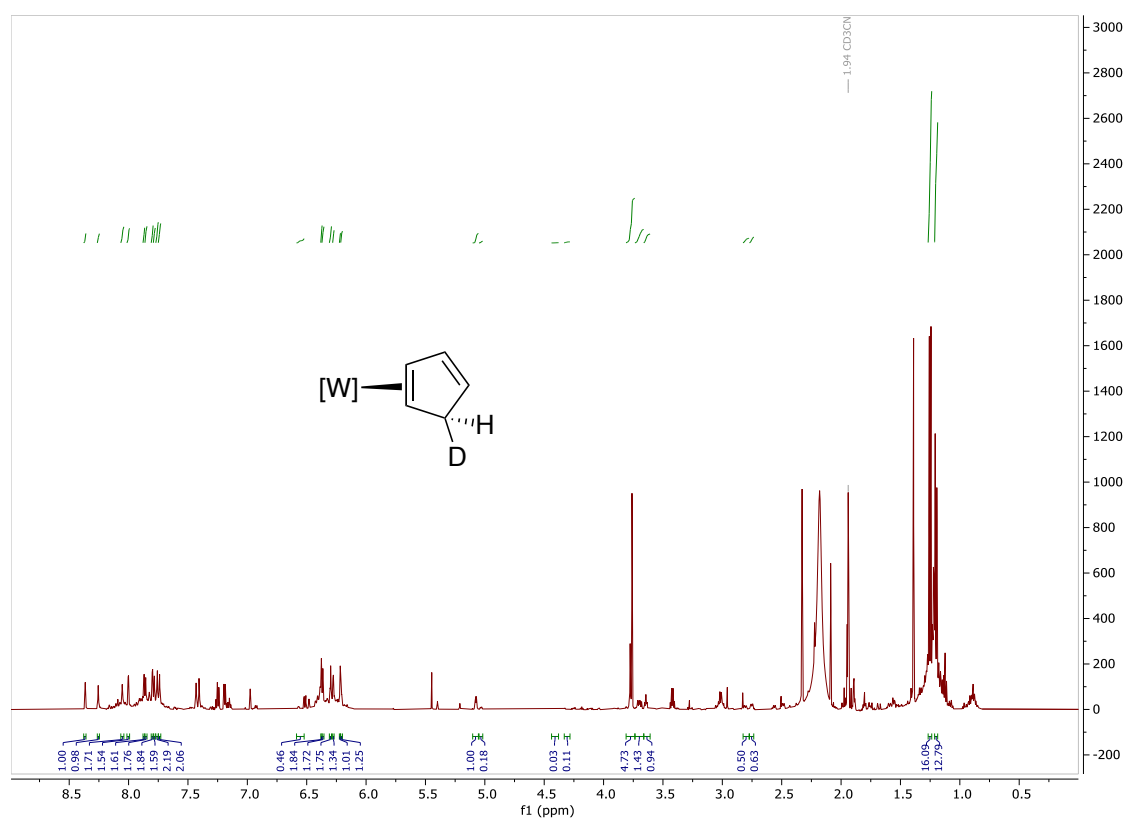




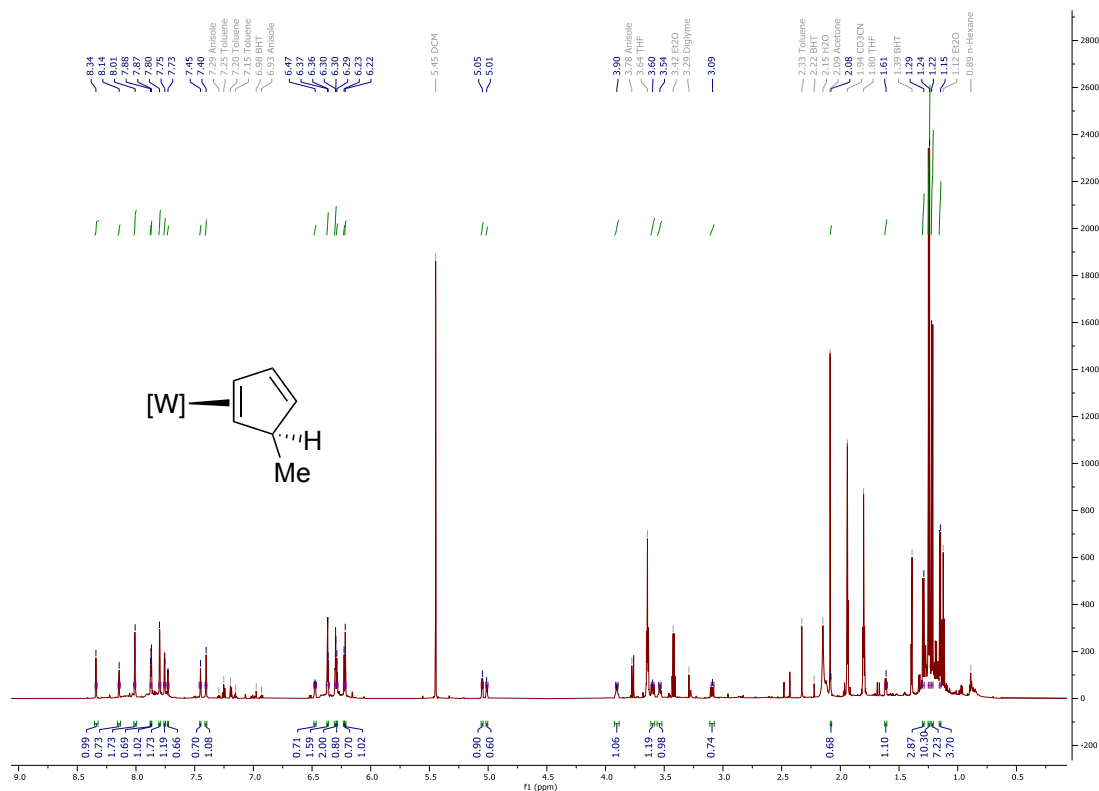
$^1\text{H}$  NMR (800 MHz,  $\text{CD}_2\text{CN}$ ,  $\delta$ , 25 °C) of Compound **6A**



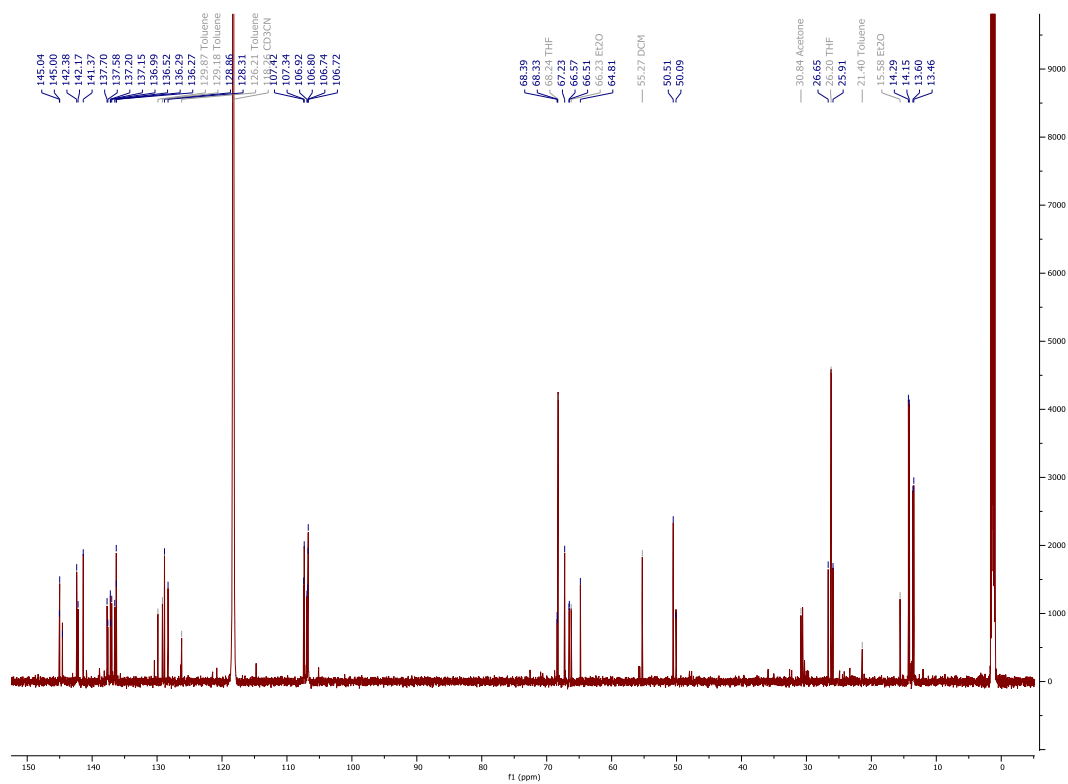
$^1\text{H}$  NMR (800 MHz,  $\text{CD}_2\text{CN}$ ,  $\delta$ , 25 °C) of Compound **6B**



<sup>1</sup>H NMR (800 MHz, CD<sub>2</sub>CN, δ, 25 °C) of Compound **6C**



<sup>13</sup>C NMR (201 MHz, CD<sub>2</sub>CN, δ, 25 °C) of Compound **6C**



Chemical structure: C#N[C@H](C=C)C=C (Note: The structure shown is a simplified representation of the molecule, which is (E)-1-((E)-3-cyano-4-iodopent-1-en-1-yl)-4-iodobut-1-ene).

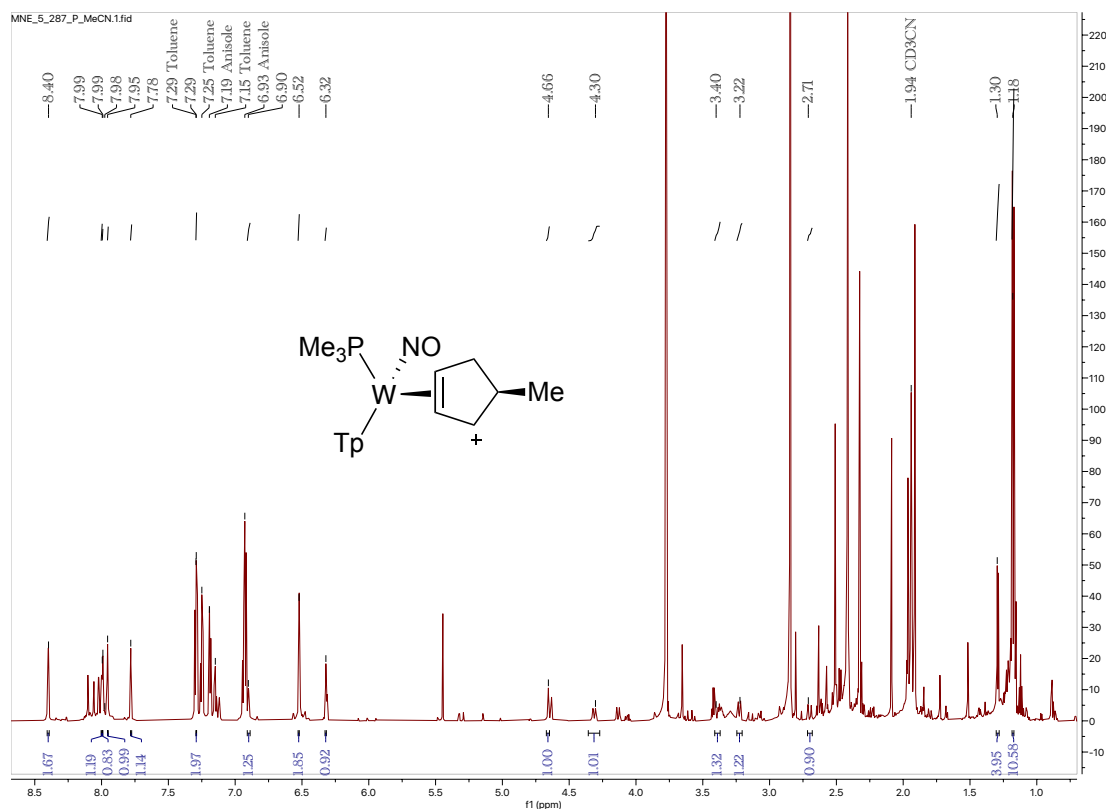
<sup>1</sup>H NMR spectrum (MeCN-d<sub>4</sub>) showing peaks from 0.5 to 8.5 ppm. Integration values are provided below the baseline.

Chemical structure: COC(=O)C([C@H]1C=CC(=O)O1)C(=O)OC

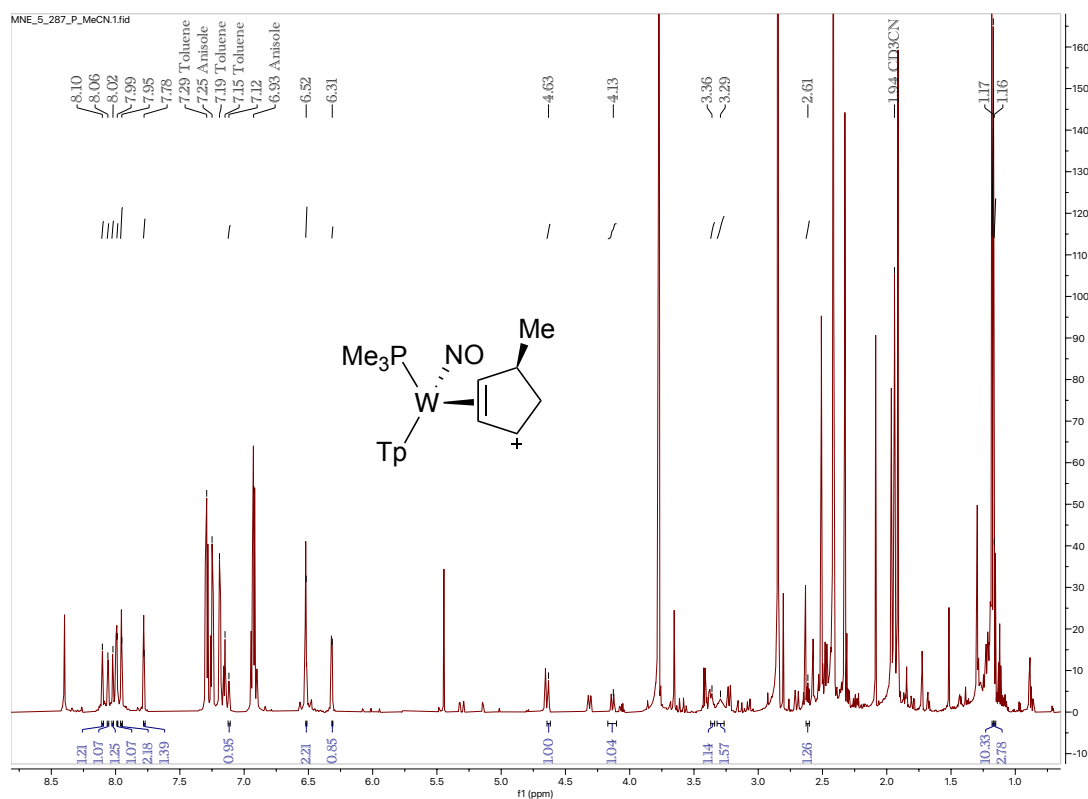
<sup>1</sup>H NMR spectrum (CDCl<sub>3</sub>) showing peaks from 0 to 9 ppm. Integration values are provided below the baseline.

Chemical Shift (ppm)	Integration
8.5 - 8.2	1.07
8.2 - 8.0	0.17
8.0 - 7.8	0.58
7.8 - 7.6	1.35
7.6 - 7.4	1.05
7.4 - 7.2	1.76
7.2 - 7.0	1.80
7.0 - 6.8	1.33
6.8 - 6.6	0.48
6.6 - 6.4	0.13
6.4 - 6.2	1.07
6.2 - 6.0	0.21
6.0 - 5.8	1.24
5.8 - 5.6	1.18
5.6 - 5.4	0.99
5.4 - 5.2	0.42
5.2 - 5.0	1.24
5.0 - 4.8	0.97
4.8 - 4.6	0.20
4.6 - 4.4	0.99
4.4 - 4.2	0.17
4.2 - 4.0	0.97
4.0 - 3.8	1.60
3.8 - 3.6	3.00
3.6 - 3.4	3.33
3.4 - 3.2	1.23
3.2 - 3.0	1.10
3.0 - 2.8	10.30
2.8 - 2.6	3.69

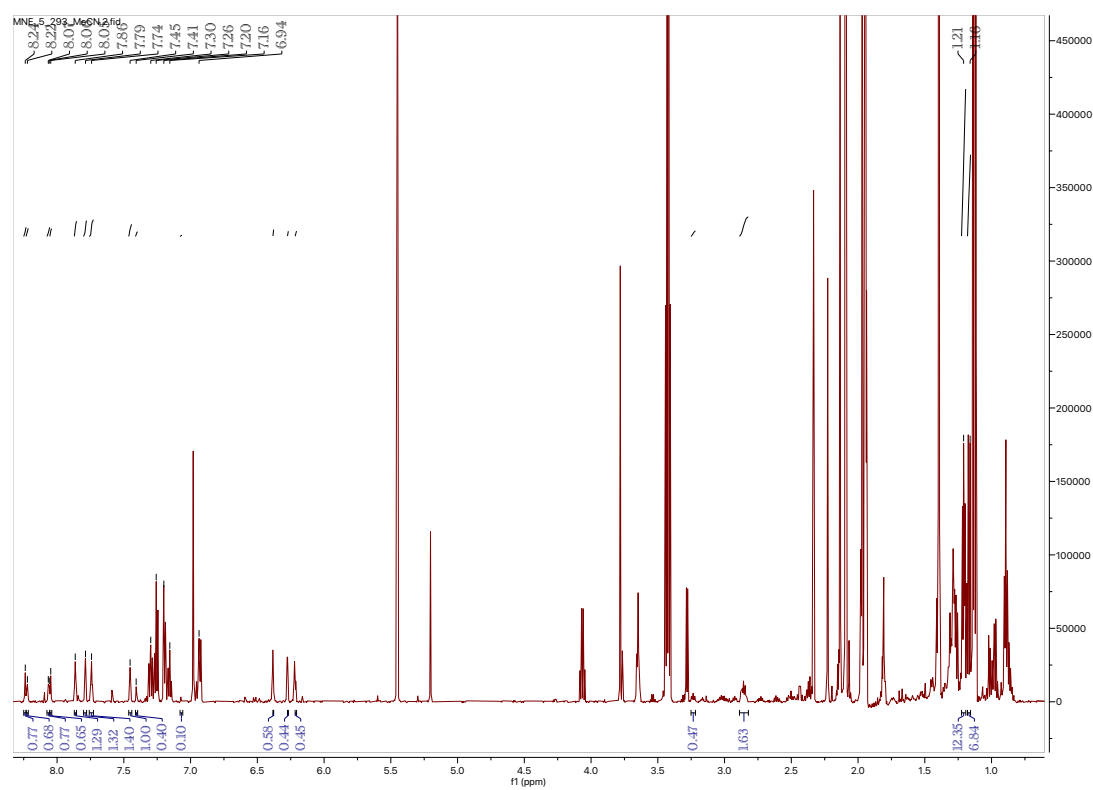
<sup>1</sup>H NMR (800 MHz, CD<sub>2</sub>CN, δ, 25 °C) of Compound **7A**



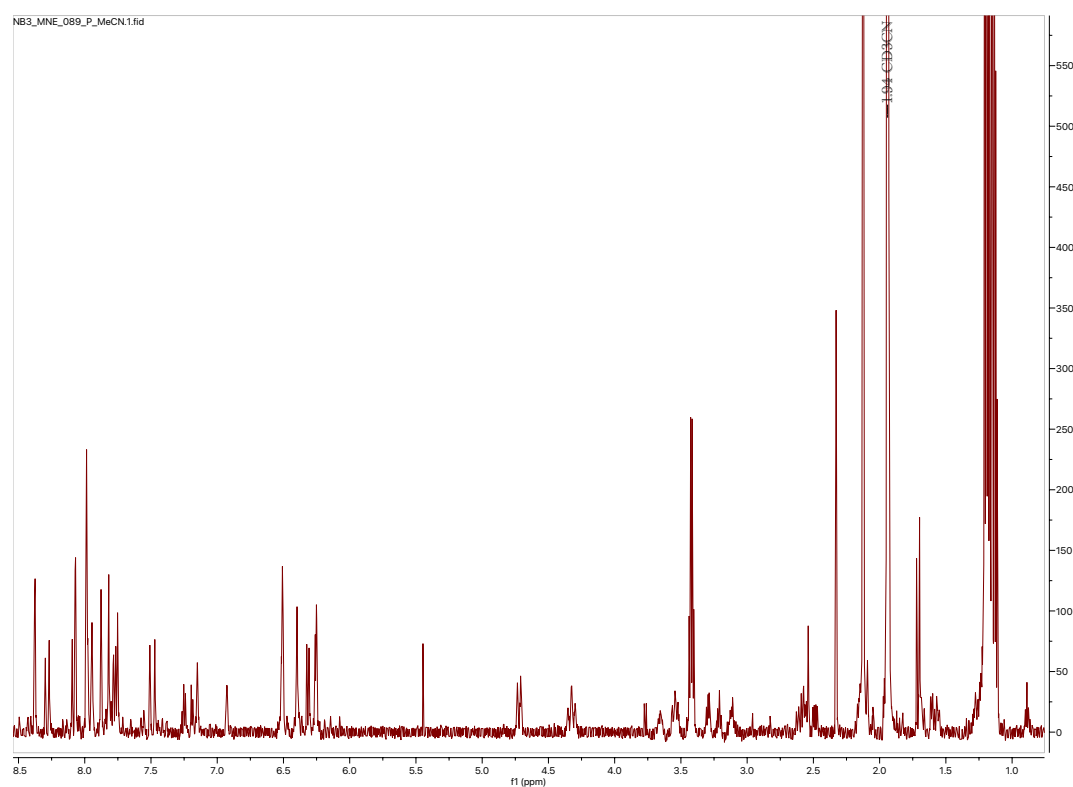
<sup>1</sup>H NMR (800 MHz, CD<sub>2</sub>CN, δ, 25 °C) of Compound **7B**



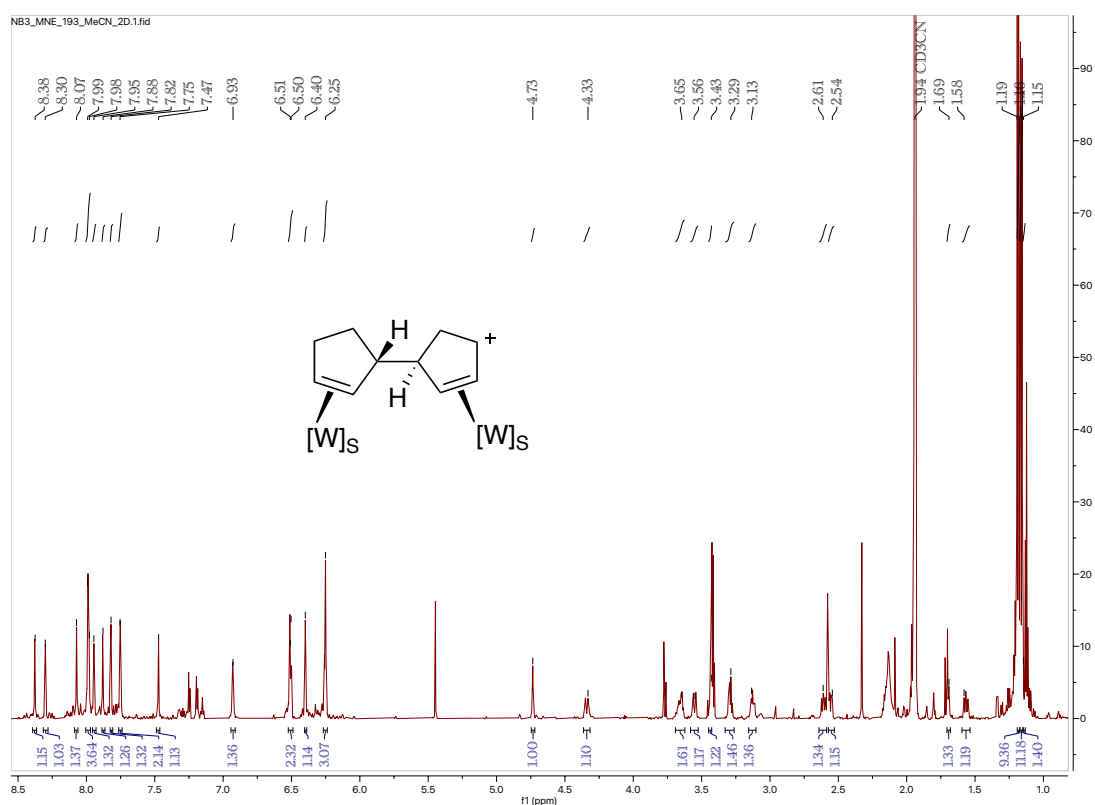
<sup>1</sup>H NMR (800 MHz, CD<sub>2</sub>CN, δ, 25 °C) of Compounds **8A/8B**



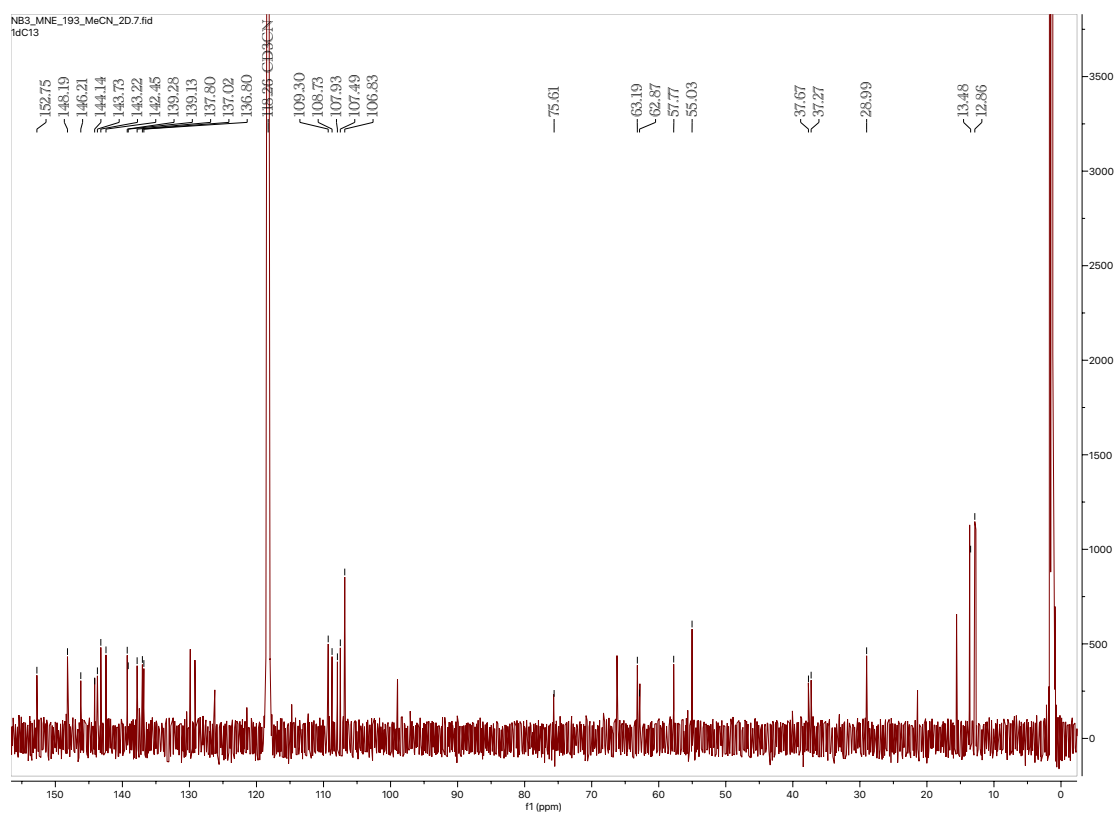
<sup>1</sup>H NMR (800 MHz, CD<sub>2</sub>CN, δ, 25 °C) of Compounds **9/10**



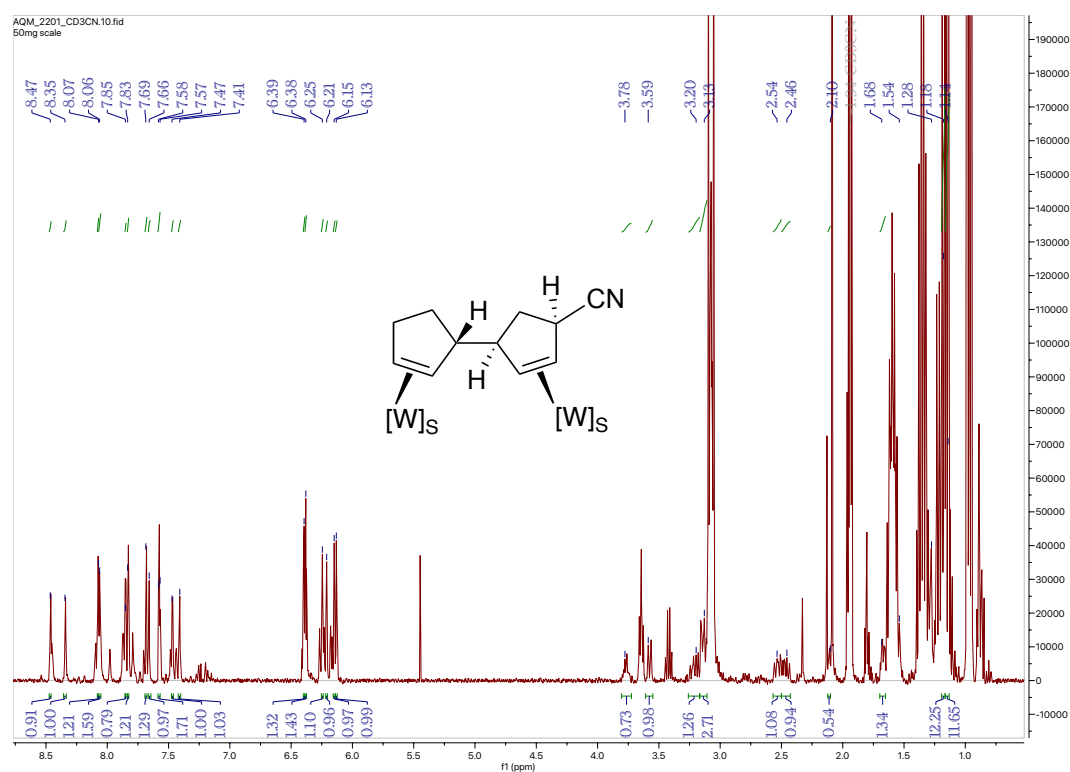
<sup>1</sup>H NMR (800 MHz, CD<sub>2</sub>CN, δ, 25 °C) of Compound **10**



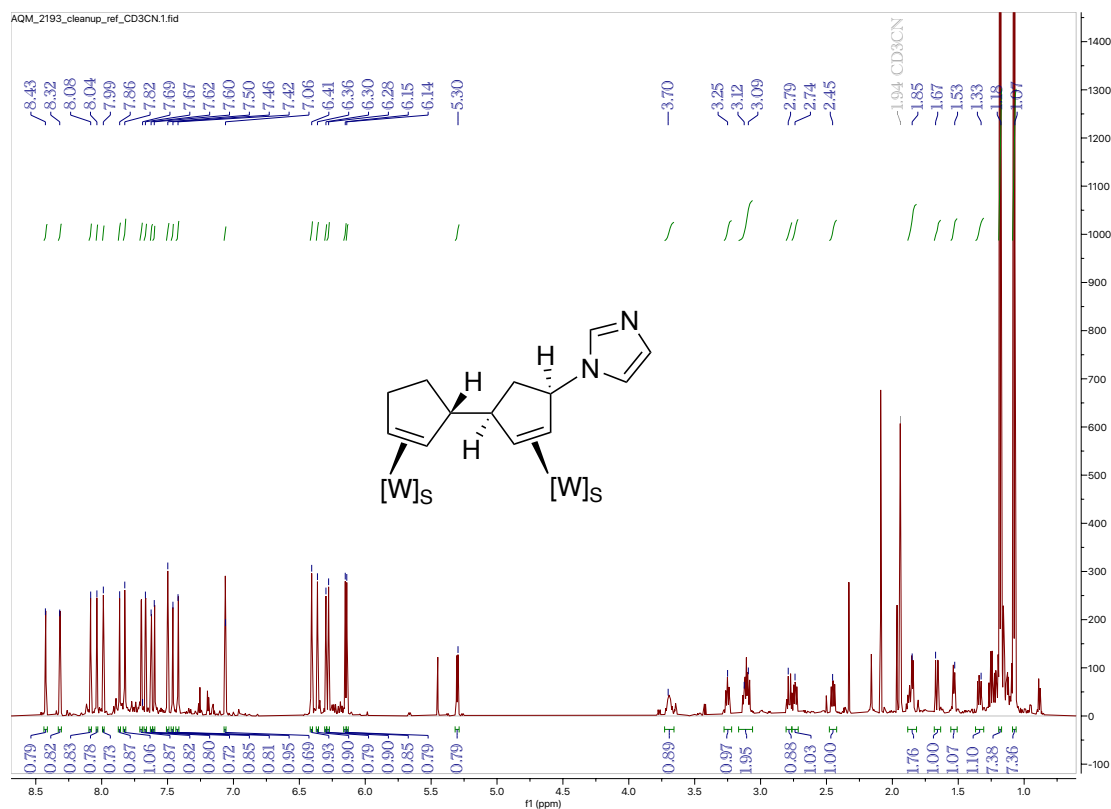
<sup>13</sup>C NMR (201 MHz, CD<sub>2</sub>CN, δ, 25 °C) of Compound **10**



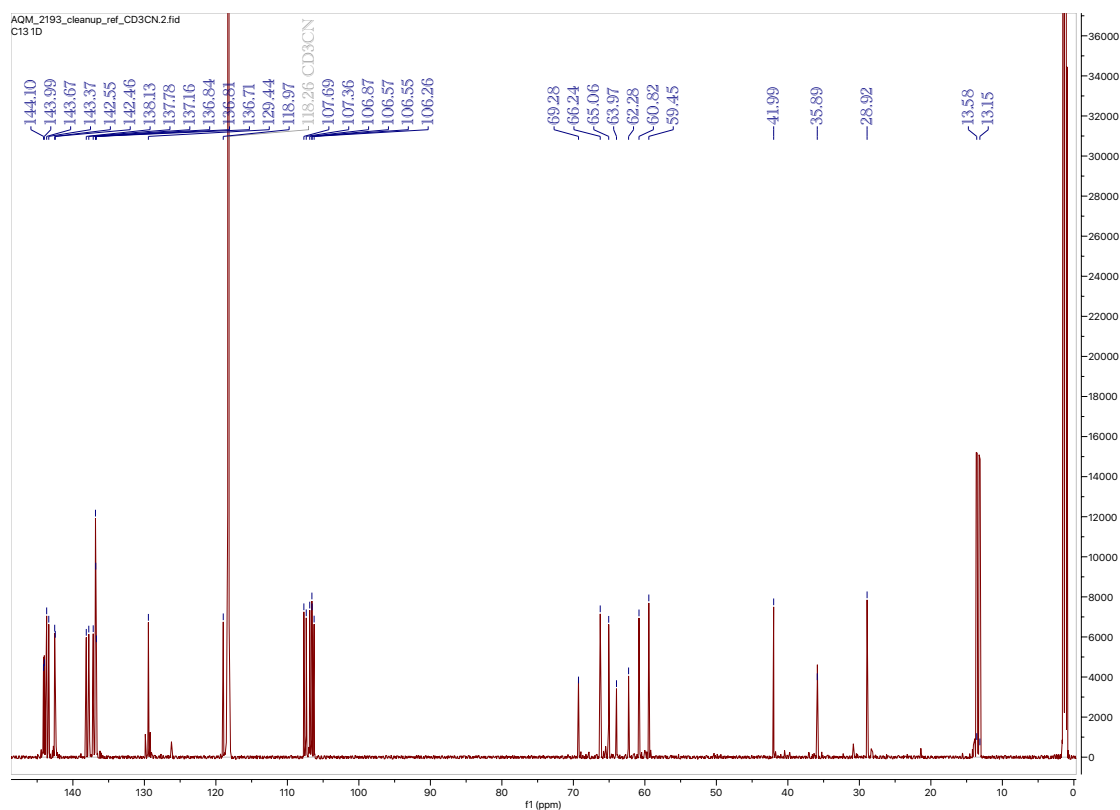
<sup>1</sup>H NMR (800 MHz, CD<sub>2</sub>CN, δ, 25 °C) of Compound **11A**



<sup>1</sup>H NMR (800 MHz, CD<sub>2</sub>CN, δ, 25 °C) of Compound **11B**

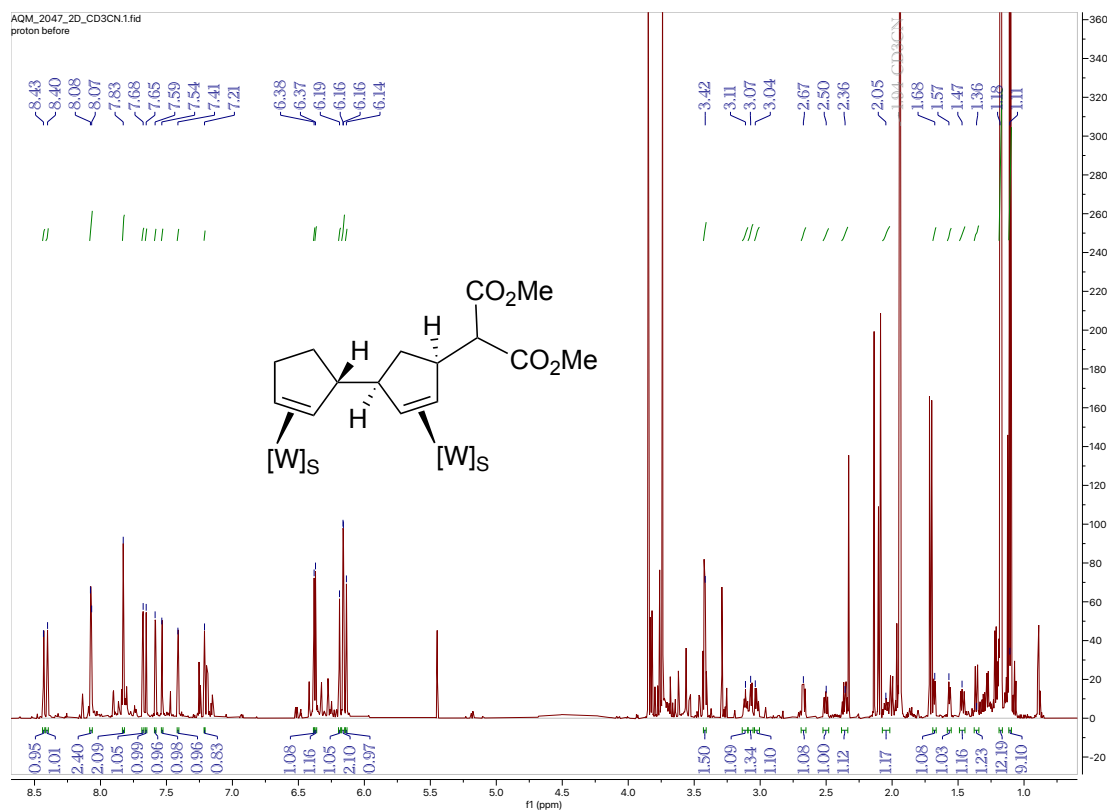


<sup>13</sup>C NMR (201 MHz, CD<sub>2</sub>CN, δ, 25 °C) of Compound **11B**

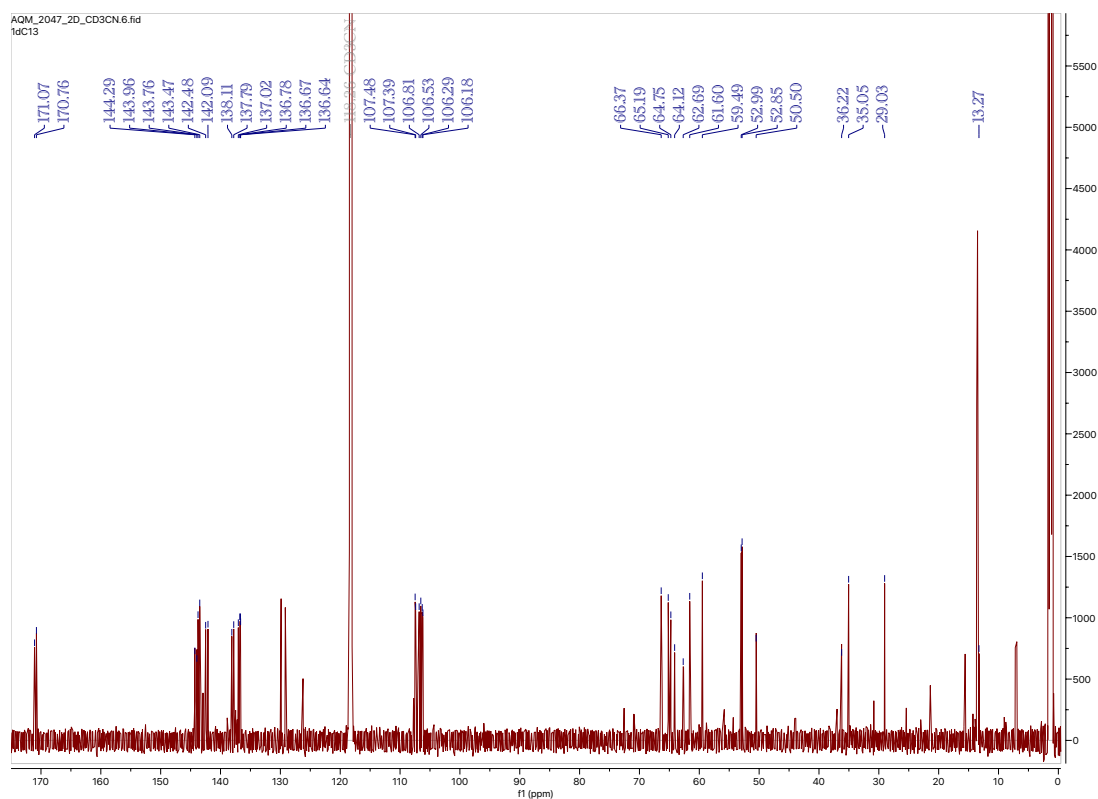




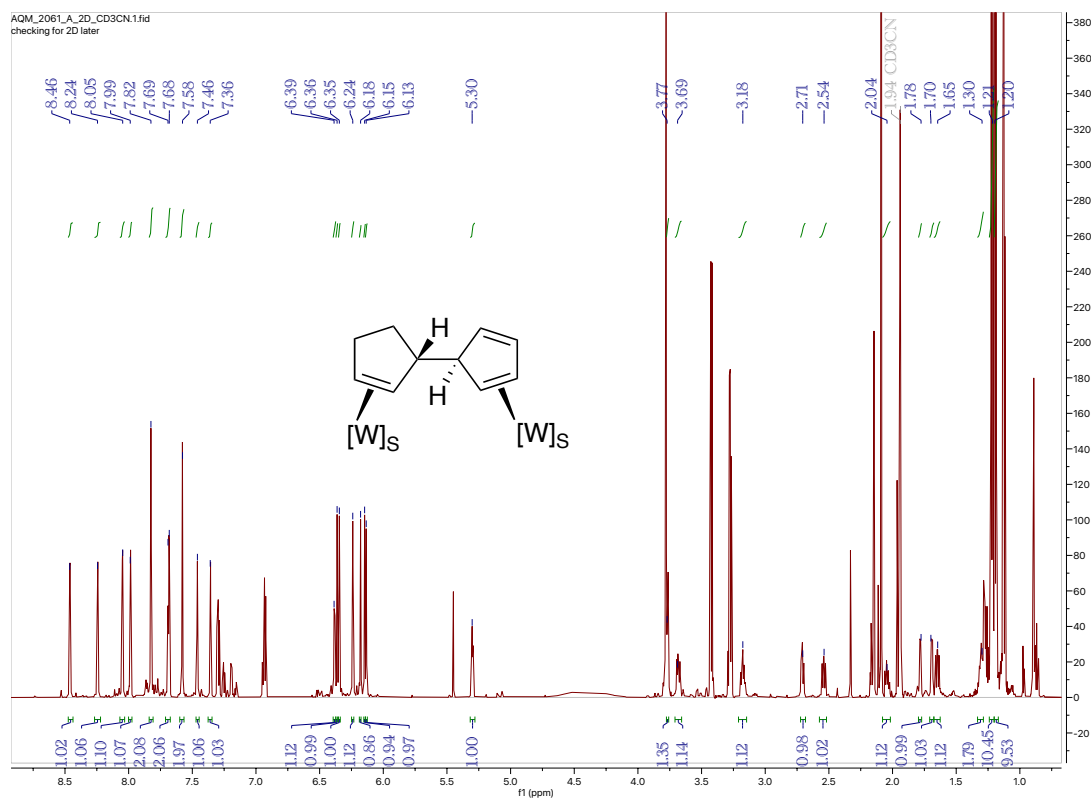
<sup>1</sup>H NMR (800 MHz, CD<sub>2</sub>CN, δ, 25 °C) of Compound **11C**



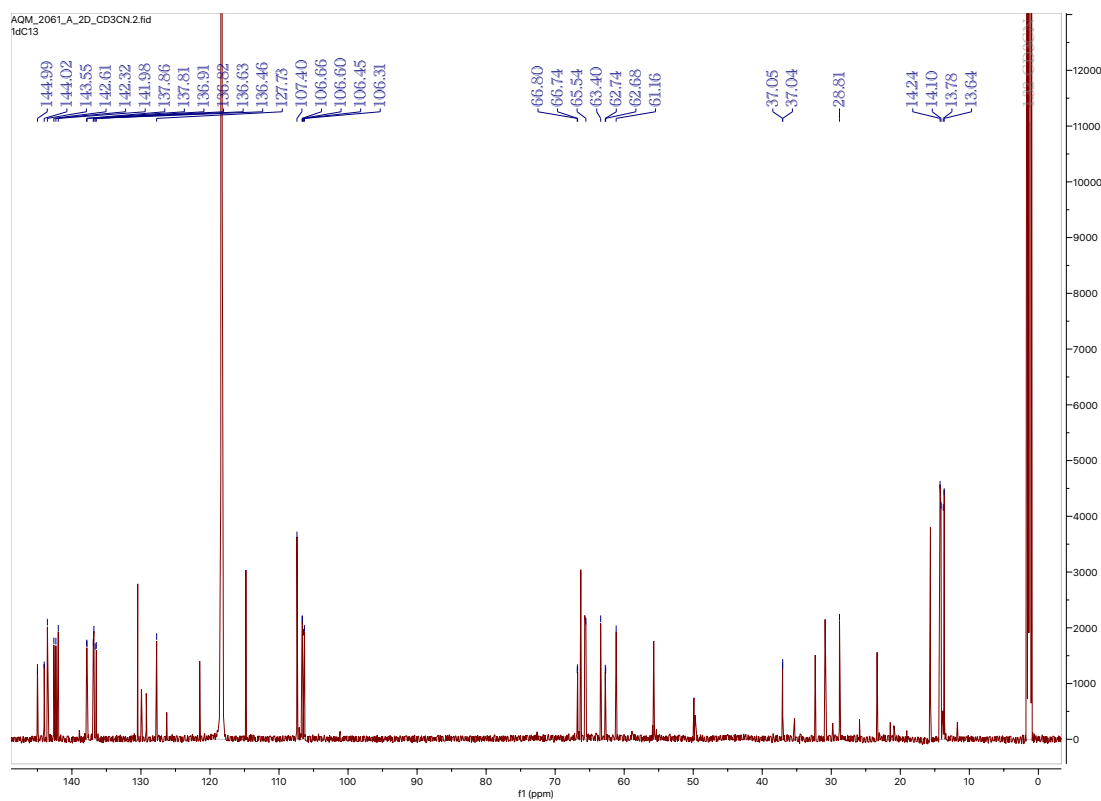
<sup>13</sup>C NMR (201 MHz, CD<sub>2</sub>CN, δ, 25 °C) of Compound **11C**



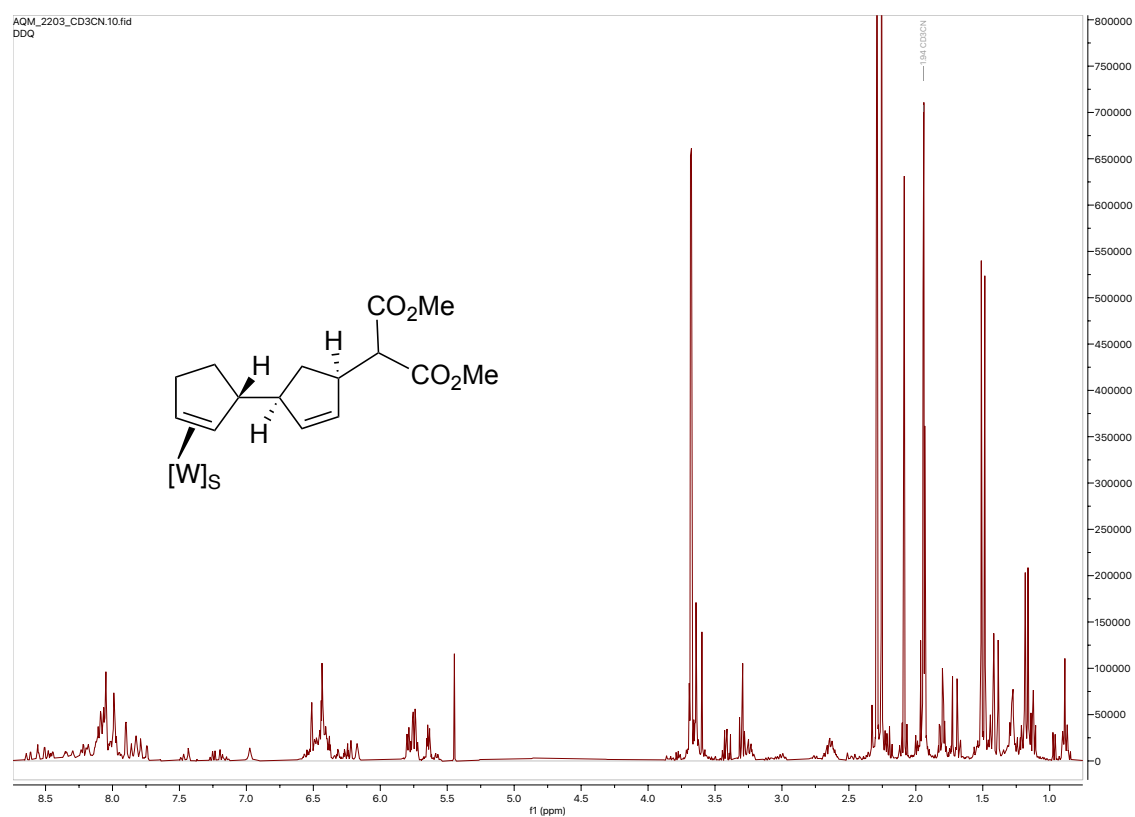
<sup>1</sup>H NMR (800 MHz, CD<sub>2</sub>CN, δ, 25 °C) of Compound **12**



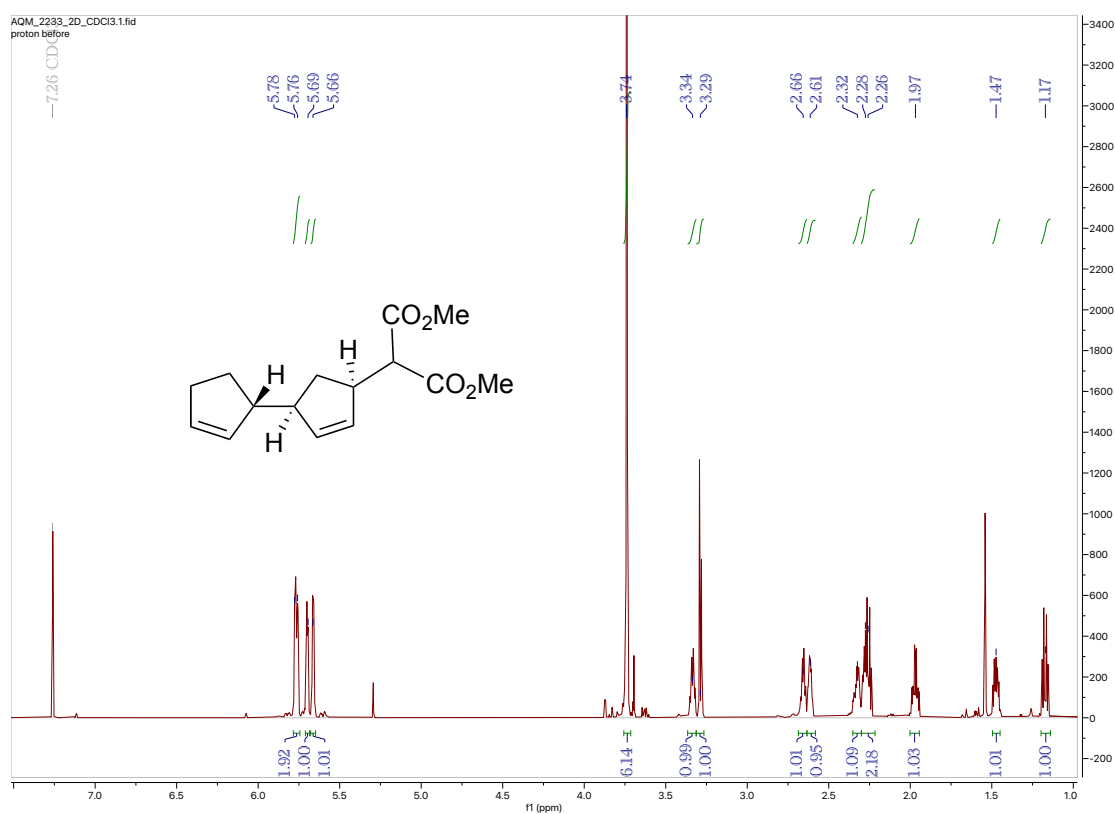
<sup>13</sup>C NMR (201 MHz, CD<sub>2</sub>CN, δ, 25 °C) of Compound **12**



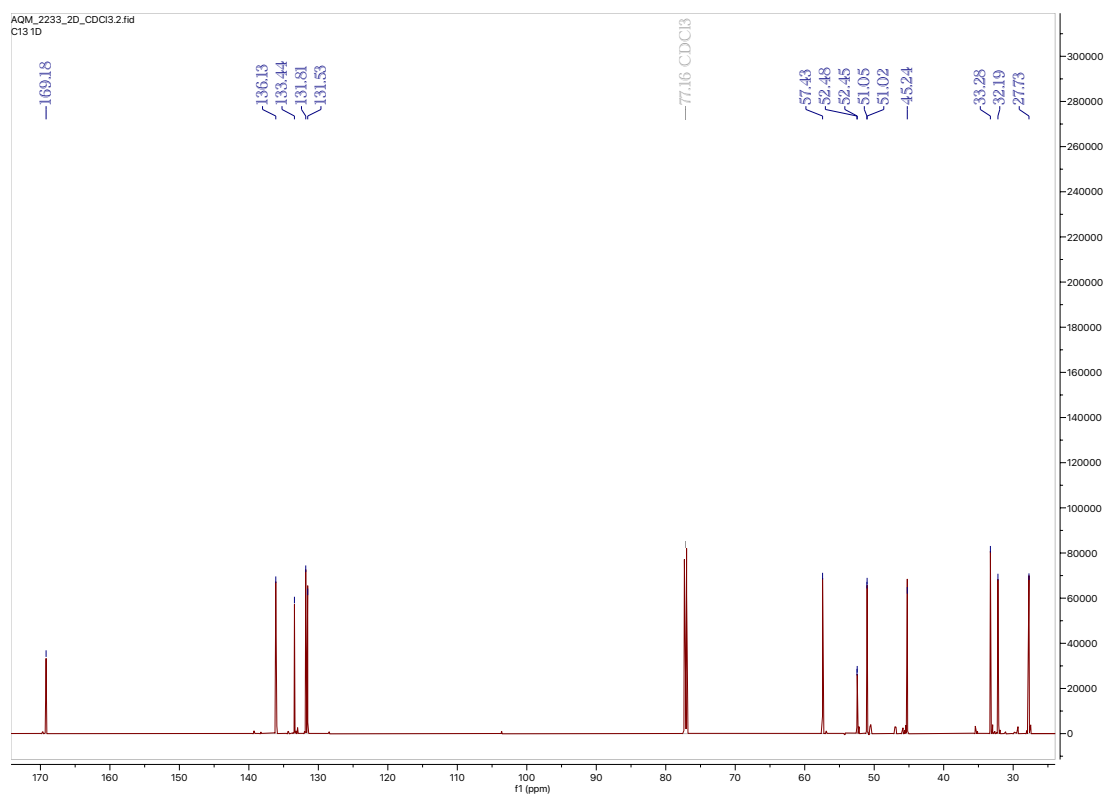
<sup>1</sup>H NMR (800 MHz, CD<sub>2</sub>CN, δ, 25 °C) of Compound **13**



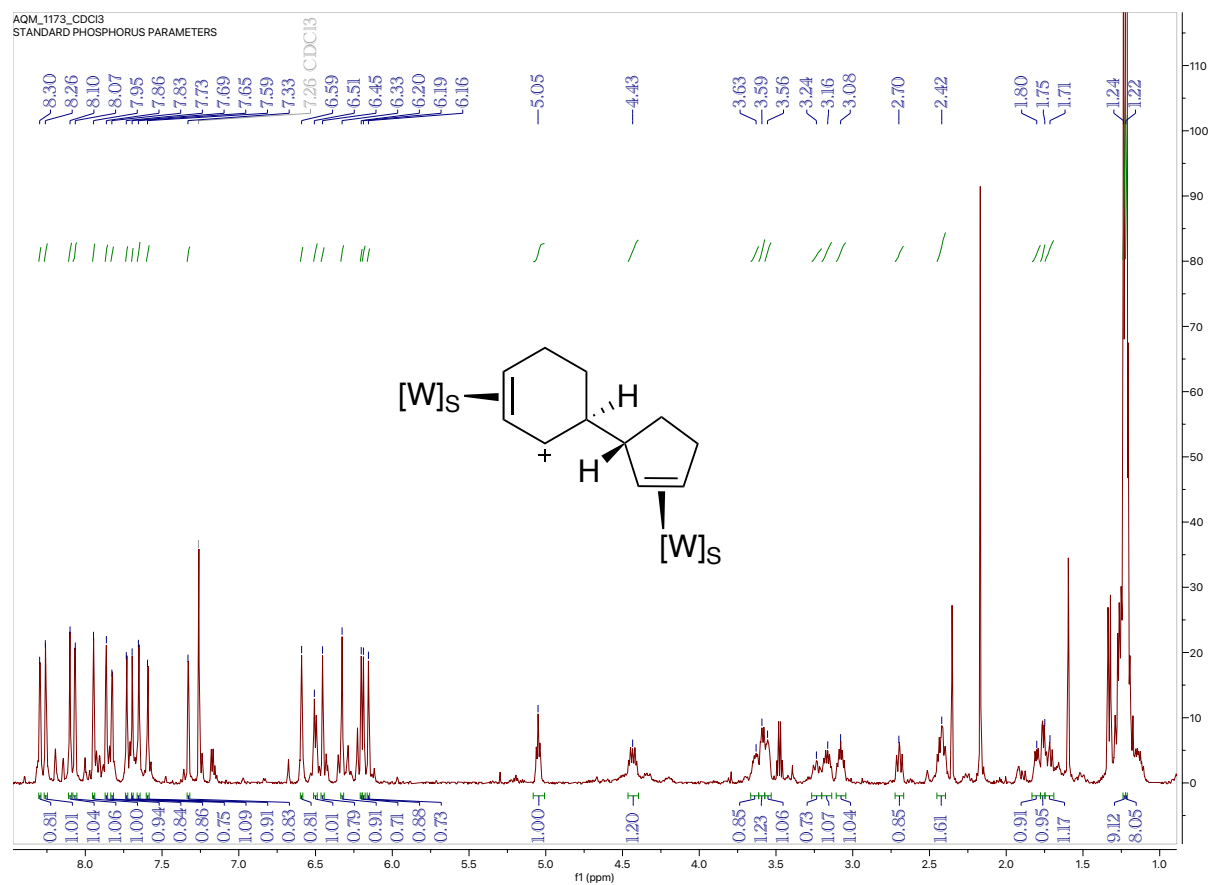
<sup>1</sup>H NMR (800 MHz, CDCl<sub>3</sub>, δ, 25 °C) of Compound **14**



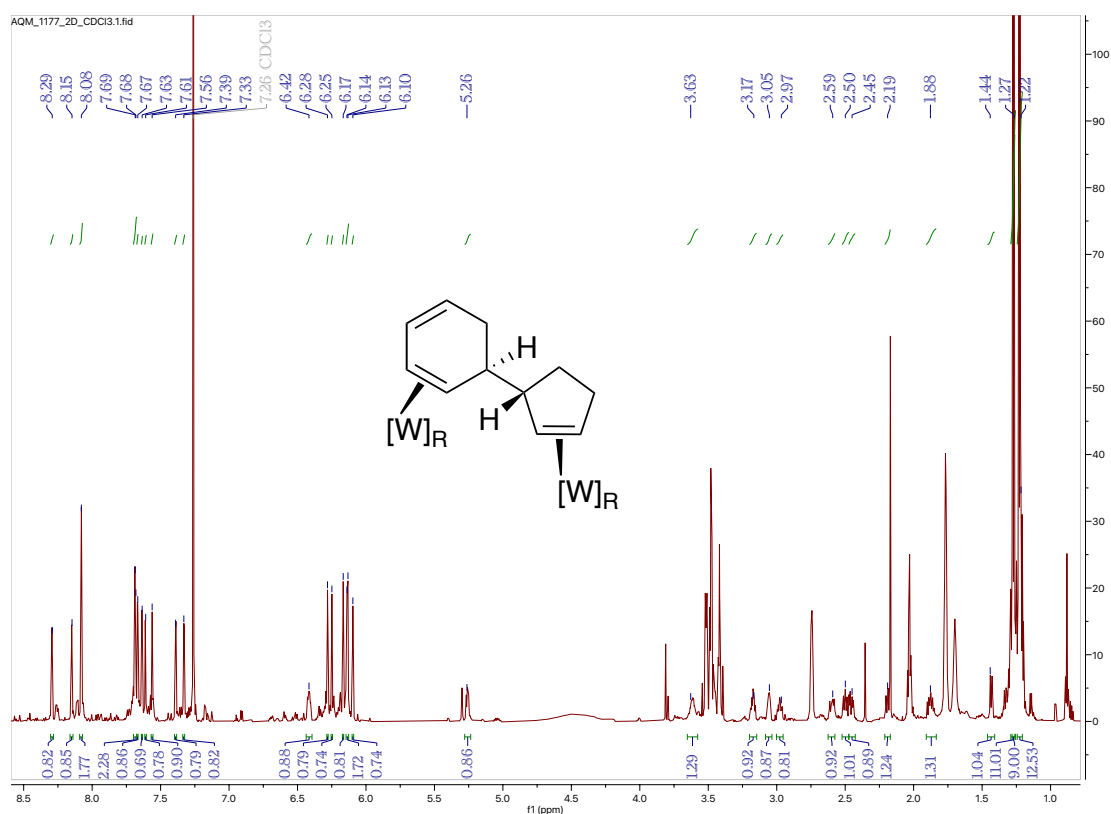
<sup>13</sup>C NMR (201 MHz, CDCl<sub>3</sub>, δ, 25 °C) of Compound **14**



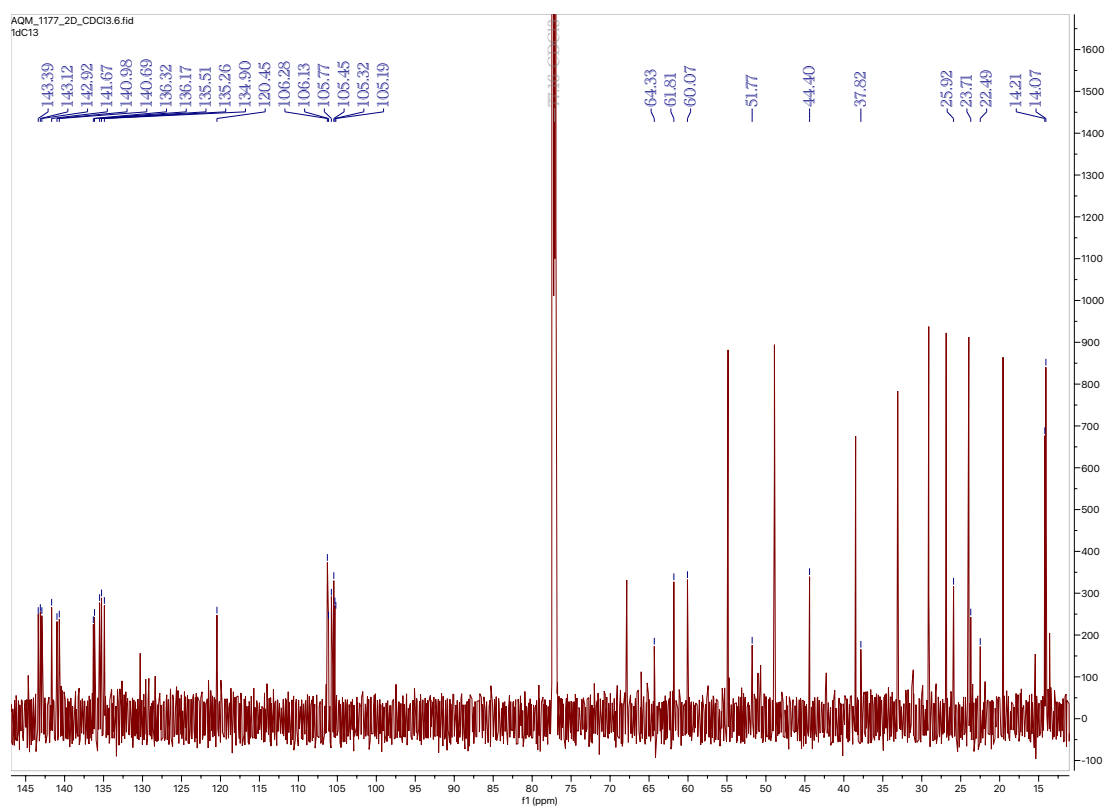
<sup>1</sup>H NMR (800 MHz, CDCl<sub>3</sub>, δ, 25 °C) of Compound **16**



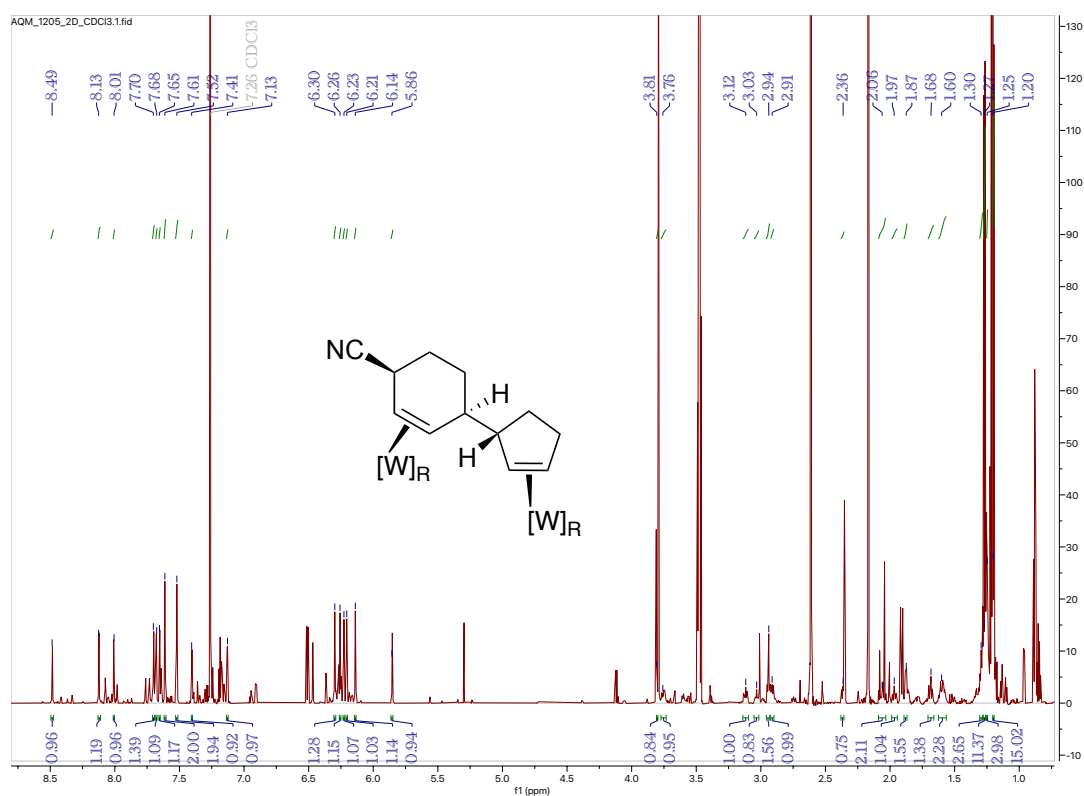
<sup>1</sup>H NMR (800 MHz, CDCl<sub>3</sub>, δ, 25 °C) of Compound **17**



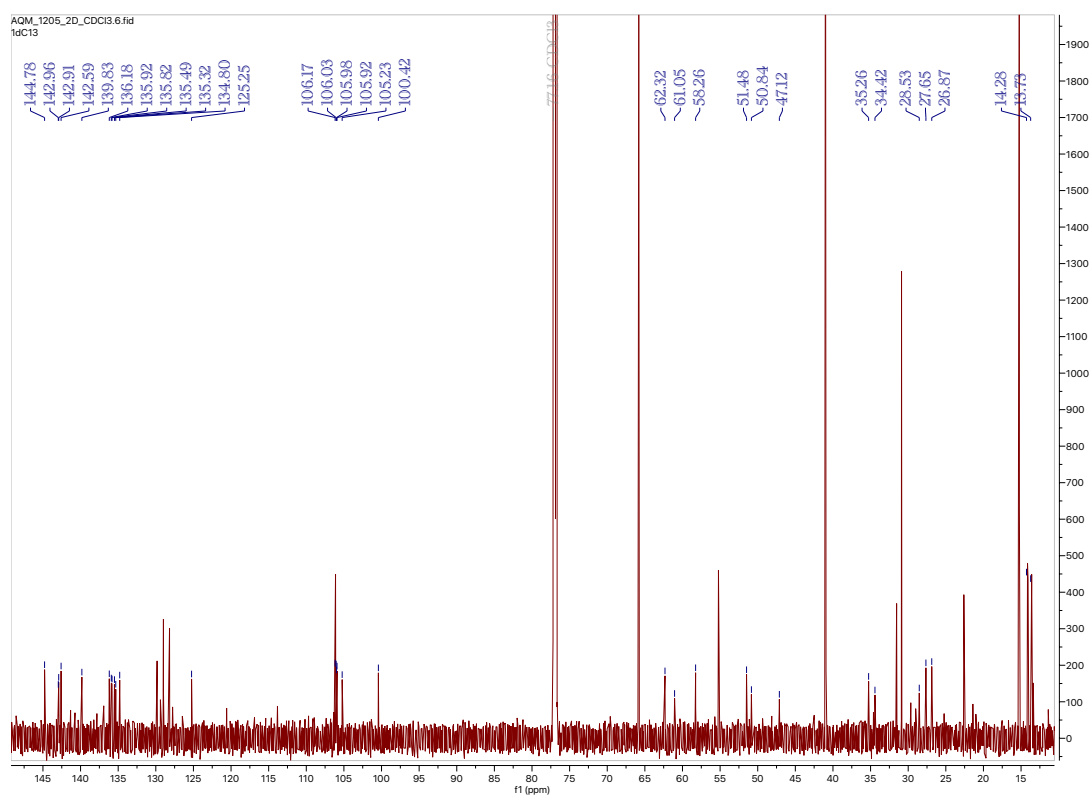
<sup>13</sup>C NMR (201 MHz, CDCl<sub>3</sub>, δ, 25 °C) of Compound **17**



<sup>1</sup>H NMR (800 MHz, CDCl<sub>3</sub>, δ, 25 °C) of Compound **18**



<sup>13</sup>C NMR (201 MHz, CDCl<sub>3</sub>, δ, 25 °C) of Compound **18**



## Crystallography.

### Structure Report for cu\_harman\_mne\_15\_16\_x2\_0m

A colourless, needle-shaped crystal of cu\_harman\_mne\_15\_16\_x2\_0m was coated with Paratone oil and mounted on a MiTeGen micromount. Data were collected at 100.00 K on a Bruker D8 VENTURE dual wavelength Mo/Cu Kappa four-circle diffractometer with a PHOTON III\_C14 detector. The diffractometer was equipped with an Oxford Cryostream 800 low temperature device and used Cu  $K_\alpha$  radiation ( $\lambda = 1.54178\text{\AA}$ ) from an Incoatec I $\mu$ S 3.0 microfocus sealed tube with a HELIOS MX double bounce multilayer mirror as monochromator.

Data collection and processing were done within the Bruker APEX6 software suite.<sup>[1]</sup> All data were integrated with SAINT V8.41 using a narrow-frame algorithm and a Multi-Scan absorption correction using SADABS 2016/2 was applied.<sup>[2]</sup> Using Olex2 as a graphical interface,<sup>[3]</sup> the structure was solved by dual methods with XT and refined by full-matrix least-squares methods against  $F^2$  using XL.<sup>[4,5]</sup> All non-hydrogen atoms were refined with anisotropic displacement parameters. The B-H hydrogen atom, as well as H10 and H11 were located in the electron density map and refined isotropically. All other hydrogen atoms were placed in calculated positions using a riding model with their  $U_{\text{iso}}$  values constrained to 1.5 times the  $U_{\text{eq}}$  of their pivot atoms for terminal  $\text{sp}^3$  carbon atoms and 1.2 times for all other carbon atoms. Disordered moieties were refined using bond lengths restraints and displacement parameter restraints.

This report and the CIF file were generated using FinalCif.<sup>[6]</sup>

### Refinement details for cu\_harman\_mne\_15\_16\_x2\_0m

The relative occupancy of the disordered atoms was freely refined. Constraints and restraints were used as needed on the anisotropic displacement parameters and/or bond lengths of the disordered atoms.



Table 6. Crystal data and structure refinement for cu\_harman\_mne\_15\_16\_x2\_0m

CCDC number	
Empirical formula	C <sub>23</sub> H <sub>32</sub> BCl <sub>3</sub> N <sub>7</sub> OPW
Formula weight	754.53
Temperature [K]	100.00
Crystal system	monoclinic
Space group (number)	<i>P</i> 2 <sub>1</sub> / <i>c</i> (14)
<i>a</i> [Å]	14.6155(17)
<i>b</i> [Å]	12.2155(12)
<i>c</i> [Å]	16.2111(14)
$\alpha$ [°]	90
$\beta$ [°]	100.628(7)
$\gamma$ [°]	90
Volume [Å <sup>3</sup> ]	2844.6(5)
<i>Z</i>	4
$\rho_{\text{calc}}$ [gcm <sup>-3</sup> ]	1.762
$\mu$ [mm <sup>-1</sup> ]	10.904
<i>F</i> (000)	1488
Crystal size [mm <sup>3</sup> ]	0.05×0.087×0.12
Crystal colour	colourless
Crystal shape	needle
Radiation	Cu <i>K</i> $\alpha$ ( $\lambda$ =1.54178 Å)
2 $\theta$ range [°]	6.15 to 138.45 (0.82 Å)
Index ranges	−16 ≤ <i>h</i> ≤ 17 −14 ≤ <i>k</i> ≤ 14 −15 ≤ <i>l</i> ≤ 19
Reflections collected	13180
Independent reflections	5133 <i>R</i> <sub>int</sub> = 0.1092 <i>R</i> <sub>sigma</sub> = 0.1201
Completeness to $\theta$ = 67.679°	98.2
Data / Restraints / Parameters	5133 / 6 / 345
Goodness-of-fit on <i>F</i> <sup>2</sup>	1.029
Final <i>R</i> indexes [ <i>I</i> ≥ 2 $\sigma$ ( <i>I</i> )]	<i>R</i> <sub>1</sub> = 0.0503 <i>wR</i> <sub>2</sub> = 0.0981
Final <i>R</i> indexes [all data]	<i>R</i> <sub>1</sub> = 0.0953 <i>wR</i> <sub>2</sub> = 0.1107
Largest peak/hole [eÅ <sup>-3</sup> ]	1.27/−1.50

Table 7. Atomic coordinates and  $U_{eq}$  [ $\text{\AA}^2$ ] for cu\_harman\_mne\_15\_16\_x2\_0m

Atom	x	y	z	$U_{eq}$
W1	0.28831(3)	0.12752(3)	0.65241(2)	0.01553(11)
P1	0.23248(16)	0.24801(19)	0.52988(13)	0.0213(5)
O1	0.2867(5)	-0.0621(5)	0.5338(4)	0.0355(16)
N1	0.3161(5)	0.2827(5)	0.7307(4)	0.0195(15)
N2	0.4058(5)	0.3075(6)	0.7674(4)	0.0204(16)
N3	0.4275(4)	0.1576(5)	0.6240(4)	0.0171(15)
N4	0.4998(5)	0.2024(6)	0.6801(4)	0.0206(16)
N5	0.3798(4)	0.0624(5)	0.7660(4)	0.0156(14)
N6	0.4572(4)	0.1172(6)	0.8058(4)	0.0205(15)
N7	0.2832(5)	0.0143(5)	0.5857(4)	0.0202(15)
C1	0.2632(6)	0.3633(7)	0.7503(5)	0.0236(18)
H1	0.197398	0.365800	0.734231	0.028
C2	0.3172(6)	0.4447(7)	0.7982(5)	0.027(2)
H2	0.296509	0.510978	0.819363	0.032
C3	0.4065(7)	0.4061(7)	0.8070(5)	0.025(2)
H3	0.460470	0.442203	0.836167	0.030
C4	0.4644(6)	0.1250(7)	0.5575(5)	0.0210(17)
H4	0.430433	0.089482	0.509314	0.025
C5	0.5579(6)	0.1503(6)	0.5691(6)	0.028(2)
H5	0.599137	0.138486	0.530931	0.034
C6	0.5785(6)	0.1961(7)	0.6477(6)	0.0220(19)
H6	0.638415	0.219655	0.674949	0.026
C7	0.3773(6)	-0.0288(7)	0.8101(5)	0.0182(18)
H7	0.330795	-0.083550	0.797040	0.022
C8	0.4513(6)	-0.0344(7)	0.8778(5)	0.0236(19)
H8	0.465154	-0.090995	0.918404	0.028
C9	0.4996(6)	0.0611(7)	0.8722(5)	0.026(2)
H9	0.554233	0.083322	0.909706	0.031
C10	0.1796(6)	0.0756(7)	0.7234(5)	0.0218(19)
H10	0.207(6)	0.104(7)	0.777(5)	0.026
C11	0.1371(6)	0.1475(7)	0.6571(5)	0.0208(19)
H11	0.123(7)	0.220(9)	0.677(6)	0.05(3)
C12	0.0535(6)	0.0806(7)	0.6087(5)	0.0242(19)
H12	0.029665	0.105754	0.549954	0.029
C13	-0.0206(6)	0.0714(7)	0.6645(5)	0.025(2)
H13	-0.080172	0.040503	0.632819	0.030
H13A	-0.077691	0.036002	0.631939	0.030
C14	-0.037(4)	0.177(2)	0.712(3)	0.037(2)
H14	-0.058169	0.244727	0.686963	0.044
C15	-0.018(5)	0.156(5)	0.794(3)	0.037(2)
H15	-0.035855	0.205003	0.833549	0.044

C16	0.033(3)	0.054(4)	0.8192(18)	0.037(2)
H16A	0.003670	0.012205	0.859543	0.044
H16B	0.098935	0.069129	0.844895	0.044
C17	0.0269(7)	-0.0086(7)	0.7362(5)	0.029(2)
H17	-0.009410	-0.077883	0.736386	0.035
H17A	-0.009084	-0.078487	0.733321	0.035
C18	0.1249(6)	-0.0304(7)	0.7118(6)	0.027(2)
H18	0.158738	-0.096538	0.738058	0.032
C19	0.0924(6)	-0.0360(7)	0.6163(5)	0.024(2)
H19A	0.144440	-0.046403	0.585717	0.029
H19B	0.043882	-0.092230	0.599130	0.029
C20	0.1542(7)	0.3608(8)	0.5428(6)	0.038(2)
H20A	0.104155	0.333758	0.570113	0.057
H20B	0.127427	0.391038	0.487628	0.057
H20C	0.189129	0.418012	0.577530	0.057
C21	0.3193(6)	0.3210(8)	0.4822(6)	0.034(2)
H21A	0.363060	0.358799	0.526098	0.051
H21B	0.287904	0.374705	0.441722	0.051
H21C	0.353222	0.268582	0.453413	0.051
C22	0.1694(7)	0.1743(8)	0.4408(5)	0.035(2)
H22A	0.210602	0.120054	0.422116	0.053
H22B	0.147485	0.225754	0.395079	0.053
H22C	0.115999	0.137056	0.456924	0.053
B1	0.4862(7)	0.2268(8)	0.7706(6)	0.022(2)
H1A	0.552(6)	0.247(7)	0.807(5)	0.026
Cl1	0.24403(17) )	0.6498(2)	0.63705(14) )	0.0448(7)
Cl2	0.27157(17) )	0.6381(2)	0.46565(15) )	0.0403(6)
Cl3	0.08906(17) )	0.6803(2)	0.50081(15) )	0.0394(6)
C23	0.2086(6)	0.7015(8)	0.5348(5)	0.029(2)
H23	0.221297	0.781959	0.535343	0.034
C14A	-0.049(3)	0.1718(18)	0.7116(18)	0.037(2)
H14A	-0.023180	0.239602	0.691347	0.044
H14B	-0.117443	0.178318	0.702701	0.044
C15A	-0.010(4)	0.154(4)	0.801(2)	0.037(2)
H15A	-0.007130	0.210001	0.842527	0.044
C16A	0.019(2)	0.053(3)	0.8175(14)	0.037(2)
H16C	0.033927	0.022770	0.872232	0.044

$U_{eq}$  is defined as 1/3 of the trace of the orthogonalized  $U_{ij}$  tensor.

Table 8. Anisotropic displacement parameters ( $\text{\AA}^2$ ) for cu\_harman\_mne\_15\_16\_x2\_0m. The anisotropic displacement factor exponent takes the form:  $-2\pi^2[h^2(a^*)^2U_{11} + k^2(b^*)^2U_{22} + \dots + 2hka^*b^*U_{12}]$

Atom	$U_{11}$	$U_{22}$	$U_{33}$	$U_{23}$	$U_{13}$	$U_{12}$
W1	0.01946(18)	0.01326(17)	0.01413(17)	-0.00131(18)	0.00376(12)	-0.0008(2)
P1	0.0222(12)	0.0226(11)	0.0168(10)	0.0013(9)	-0.0023(9)	-0.0028(10)
O1	0.044(4)	0.024(3)	0.044(4)	-0.017(3)	0.021(3)	-0.009(3)
N1	0.026(4)	0.012(3)	0.021(4)	-0.004(3)	0.007(3)	0.002(3)
N2	0.027(4)	0.014(4)	0.017(3)	-0.001(3)	-0.003(3)	-0.006(3)
N3	0.012(3)	0.021(4)	0.018(3)	0.001(3)	0.002(3)	-0.004(3)
N4	0.026(4)	0.014(3)	0.021(4)	0.005(3)	0.003(3)	-0.002(3)
N5	0.010(3)	0.014(3)	0.022(3)	0.003(3)	0.001(3)	0.000(3)
N6	0.014(3)	0.024(4)	0.024(3)	0.001(3)	0.003(3)	-0.006(3)
N7	0.023(4)	0.010(3)	0.031(4)	0.006(3)	0.016(3)	0.003(3)
C1	0.020(4)	0.023(5)	0.029(4)	-0.008(4)	0.009(3)	0.000(4)
C2	0.036(6)	0.020(5)	0.024(5)	-0.011(4)	0.006(4)	-0.001(4)
C3	0.036(5)	0.013(4)	0.027(5)	-0.006(4)	0.007(4)	-0.009(4)
C4	0.027(4)	0.020(4)	0.019(4)	0.005(4)	0.014(3)	-0.001(4)
C5	0.031(5)	0.009(4)	0.051(6)	0.004(4)	0.024(4)	0.005(4)
C6	0.010(4)	0.013(4)	0.044(5)	0.005(4)	0.006(4)	-0.002(4)
C7	0.017(4)	0.019(4)	0.019(4)	-0.003(3)	0.005(3)	0.002(4)
C8	0.028(5)	0.024(5)	0.019(4)	0.006(4)	0.004(4)	0.004(4)
C9	0.027(5)	0.030(5)	0.019(4)	0.001(4)	0.001(4)	0.005(4)
C10	0.022(5)	0.026(5)	0.018(4)	-0.004(4)	0.008(3)	-0.005(4)
C11	0.023(5)	0.021(5)	0.020(4)	0.003(4)	0.007(3)	0.004(4)
C12	0.027(5)	0.023(4)	0.024(4)	-0.004(4)	0.008(4)	0.001(4)
C13	0.023(5)	0.028(5)	0.023(4)	-0.004(4)	0.003(4)	-0.012(4)
C14	0.032(7)	0.048(4)	0.032(3)	-0.009(3)	0.013(3)	-0.013(3)
C15	0.032(7)	0.048(4)	0.032(3)	-0.009(3)	0.013(3)	-0.013(3)
C16	0.032(7)	0.048(4)	0.032(3)	-0.009(3)	0.013(3)	-0.013(3)
C17	0.036(5)	0.026(5)	0.028(5)	0.007(4)	0.013(4)	-0.007(5)
C18	0.026(5)	0.022(5)	0.035(5)	0.004(4)	0.008(4)	-0.002(4)
C19	0.019(5)	0.025(5)	0.029(5)	-0.011(4)	0.005(4)	-0.004(4)
C20	0.039(6)	0.041(6)	0.031(5)	-0.004(5)	0.000(4)	0.009(5)
C21	0.030(5)	0.032(5)	0.040(5)	0.021(5)	0.007(4)	-0.012(5)
C22	0.041(6)	0.043(6)	0.020(5)	0.002(4)	0.000(4)	-0.008(5)
B1	0.019(5)	0.018(5)	0.025(5)	-0.004(4)	-0.003(4)	-0.008(4)
Cl1	0.0324(13)	0.068(2)	0.0316(12)	0.0039(12)	0.0000(10)	-0.0045(13)
Cl2	0.0429(14)	0.0386(14)	0.0450(13)	-0.0045(12)	0.0225(11)	-0.0005(13)
Cl3	0.0301(13)	0.0528(16)	0.0334(12)	-0.0001(12)	0.0007(10)	0.0076(12)
C23	0.021(5)	0.036(5)	0.031(5)	-0.001(4)	0.009(4)	-0.007(4)
C14A	0.032(7)	0.048(4)	0.032(3)	-0.009(3)	0.013(3)	-0.013(3)
C15A	0.032(7)	0.048(4)	0.032(3)	-0.009(3)	0.013(3)	-0.013(3)
C16A	0.032(7)	0.048(4)	0.032(3)	-0.009(3)	0.013(3)	-0.013(3)

Table 9. Bond lengths and angles for cu\_harman\_mne\_15\_16\_x2\_0m

Atom–Atom	Length [Å]
W1–P1	2.486(2)
W1–N1	2.275(6)
W1–N3	2.198(6)
W1–N5	2.214(6)
W1–N7	1.749(7)
W1–C10	2.219(8)
W1–C11	2.239(9)
P1–C20	1.827(10)
P1–C21	1.834(8)
P1–C22	1.803(9)
O1–N7	1.263(9)
N1–N2	1.370(9)
N1–C1	1.326(10)
N2–C3	1.364(10)
N2–B1	1.528(12)
N3–N4	1.373(9)
N3–C4	1.351(10)
N4–C6	1.352(10)
N4–B1	1.546(12)
N5–N6	1.368(9)
N5–C7	1.327(10)
N6–C9	1.330(11)
N6–B1	1.544(12)
C1–H1	0.9500
C1–C2	1.410(12)
C2–H2	0.9500
C2–C3	1.371(13)
C3–H3	0.9500
C4–H4	0.9500
C4–C5	1.381(12)
C5–H5	0.9500
C5–C6	1.374(12)
C6–H6	0.9500
C7–H7	0.9500
C7–C8	1.393(11)
C8–H8	0.9500
C8–C9	1.374(12)
C9–H9	0.9500
C10–H10	0.95(8)
C10–C11	1.437(12)
C10–C18	1.515(12)
C11–H11	0.98(11)
C11–C12	1.556(12)
C12–H12	1.0000

C12–C13	1.538(12)
C12–C19	1.530(12)
C13–H13	1.0000
C13–H13A	1.0000
C13–C14	1.542(18)
C13–C17	1.578(12)
C13–C14A	1.541(16)
C14–H14	0.9500
C14–C15	1.325(19)
C15–H15	0.9500
C15–C16	1.478(19)
C16–H16A	0.9900
C16–H16B	0.9900
C16–C17	1.535(17)
C17–H17	1.0000
C17–H17A	1.0000
C17–C18	1.578(12)
C17–C16A	1.542(15)
C18–H18	1.0000
C18–C19	1.535(12)
C19–H19A	0.9900
C19–H19B	0.9900
C20–H20A	0.9800
C20–H20B	0.9800
C20–H20C	0.9800
C21–H21A	0.9800
C21–H21B	0.9800
C21–H21C	0.9800
C22–H22A	0.9800
C22–H22B	0.9800
C22–H22C	0.9800
B1–H1A	1.07(8)
Cl1–C23	1.761(9)
Cl2–C23	1.756(9)
Cl3–C23	1.751(9)
C23–H23	1.0000
C14A–H14A	0.9900
C14A–H14B	0.9900
C14A–C15A	1.471(18)
C15A–H15A	0.9500
C15A–C16A	1.319(18)
C16A–H16C	0.9500
Atom–Atom– Atom	Angle [°]

N1-W1-P1	87.18(18)
N3-W1-P1	85.06(17)
N3-W1-N1	84.3(2)
N3-W1-N5	78.1(2)
N3-W1-C10	159.2(3)
N3-W1-C11	161.2(3)
N5-W1-P1	159.39(17)
N5-W1-N1	79.5(2)
N5-W1-C10	81.2(3)
N5-W1-C11	117.4(3)
N7-W1-P1	90.2(2)
N7-W1-N1	170.6(3)
N7-W1-N3	86.5(3)
N7-W1-N5	100.4(3)
N7-W1-C10	98.1(3)
N7-W1-C11	100.2(3)
C10-W1-P1	115.0(2)
C10-W1-N1	91.2(3)
C10-W1-C11	37.6(3)
C11-W1-P1	77.4(2)
C11-W1-N1	88.1(3)
C20-P1-W1	118.4(3)
C20-P1-C21	100.2(5)
C21-P1-W1	118.3(3)
C22-P1-W1	112.8(3)
C22-P1-C20	103.3(5)
C22-P1-C21	101.3(5)
N2-N1-W1	119.0(5)
C1-N1-W1	134.5(6)
C1-N1-N2	106.5(7)
N1-N2-B1	122.7(6)
C3-N2-N1	108.9(7)
C3-N2-B1	127.9(7)
N4-N3-W1	123.8(5)
C4-N3-W1	129.6(5)
C4-N3-N4	105.9(6)
N3-N4-B1	119.1(7)
C6-N4-N3	109.0(7)
C6-N4-B1	130.3(7)
N6-N5-W1	122.4(5)
C7-N5-W1	132.6(5)
C7-N5-N6	105.0(6)
N5-N6-B1	120.6(6)
C9-N6-N5	110.5(7)
C9-N6-B1	128.8(7)
O1-N7-W1	173.4(6)
N1-C1-H1	124.3
N1-C1-C2	111.4(8)

C2-C1-H1	124.3
C1-C2-H2	128.1
C3-C2-C1	103.9(8)
C3-C2-H2	128.1
N2-C3-C2	109.3(8)
N2-C3-H3	125.4
C2-C3-H3	125.4
N3-C4-H4	124.6
N3-C4-C5	110.9(8)
C5-C4-H4	124.6
C4-C5-H5	127.5
C6-C5-C4	105.0(8)
C6-C5-H5	127.5
N4-C6-C5	109.1(8)
N4-C6-H6	125.4
C5-C6-H6	125.4
N5-C7-H7	124.1
N5-C7-C8	111.8(8)
C8-C7-H7	124.1
C7-C8-H8	128.1
C9-C8-C7	103.8(8)
C9-C8-H8	128.1
N6-C9-C8	108.8(8)
N6-C9-H9	125.6
C8-C9-H9	125.6
W1-C10-H10	99(5)
C11-C10-W1	71.9(5)
C11-C10-H10	120(5)
C11-C10-C18	106.5(8)
C18-C10-W1	126.3(6)
C18-C10-H10	123(5)
W1-C11-H11	112(6)
C10-C11-W1	70.5(5)
C10-C11-H11	113(6)
C10-C11-C12	104.3(7)
C12-C11-W1	127.9(6)
C12-C11-H11	117(6)
C11-C12-H12	115.0
C13-C12-C11	108.3(7)
C13-C12-H12	115.0
C19-C12-C11	101.7(7)
C19-C12-H12	115.0
C19-C12-C13	100.1(7)
C12-C13-H13	111.6
C12-C13-H13A	109.4
C12-C13-C14	115.3(19)
C12-C13-C17	102.5(7)
C12-C13-C14A	121.1(15)

C14–C13–H13	111.6
C14–C13–C17	103.7(19)
C17–C13–H13	111.6
C17–C13–H13A	109.4
C14A–C13– H13A	109.4
C14A–C13–C17	104.4(14)
C13–C14–H14	125.7
C15–C14–C13	109(4)
C15–C14–H14	125.7
C14–C15–H15	121.9
C14–C15–C16	116(5)
C16–C15–H15	121.9
C15–C16–H16A	111.1
C15–C16–H16B	111.1
C15–C16–C17	103(3)
H16A–C16– H16B	109.1
C17–C16–H16A	111.1
C17–C16–H16B	111.1
C13–C17–H17	111.4
C13–C17–H17A	109.8
C16–C17–C13	106.6(19)
C16–C17–H17	111.4
C16–C17–C18	113.1(19)
C18–C17–C13	102.5(7)
C18–C17–H17	111.4
C18–C17–H17A	109.8
C16A–C17–C13	103.6(15)
C16A–C17– H17A	109.8
C16A–C17–C18	120.6(14)
C10–C18–C17	107.9(7)
C10–C18–H18	115.5
C10–C18–C19	102.8(7)
C17–C18–H18	115.5
C19–C18–C17	97.7(7)
C19–C18–H18	115.5
C12–C19–C18	94.7(7)
C12–C19–H19A	112.8
C12–C19–H19B	112.8
C18–C19–H19A	112.8
C18–C19–H19B	112.8
H19A–C19– H19B	110.2
P1–C20–H20A	109.5
P1–C20–H20B	109.5
P1–C20–H20C	109.5

H20A–C20– H20B	109.5
H20A–C20– H20C	109.5
H20B–C20– H20C	109.5
P1–C21–H21A	109.5
P1–C21–H21B	109.5
P1–C21–H21C	109.5
H21A–C21– H21B	109.5
H21A–C21– H21C	109.5
H21B–C21– H21C	109.5
P1–C22–H22A	109.5
P1–C22–H22B	109.5
P1–C22–H22C	109.5
H22A–C22– H22B	109.5
H22A–C22– H22C	109.5
H22B–C22– H22C	109.5
N2–B1–N4	108.9(7)
N2–B1–N6	108.1(7)
N2–B1–H1A	119(5)
N4–B1–H1A	108(5)
N6–B1–N4	106.0(7)
N6–B1–H1A	106(5)
Cl1–C23–H23	108.7
Cl2–C23–Cl1	110.2(5)
Cl2–C23–H23	108.7
Cl3–C23–Cl1	110.3(5)
Cl3–C23–Cl2	110.1(5)
Cl3–C23–H23	108.7
C13–C14A– H14A	110.4
C13–C14A– H14B	110.4
H14A–C14A– H14B	108.6
C15A–C14A– C13	107(3)
C15A–C14A– H14A	110.4
C15A–C14A– H14B	110.4

C14A–C15A– H15A	123.7
C16A–C15A– C14A	113(3)
C16A–C15A– H15A	123.7
C17–C16A– H16C	124.5

C15A–C16A– C17	111(3)
C15A–C16A– H16C	124.5

Table 10. Torsion angles for cu\_harman\_mne\_15\_16\_x2\_0m

Atom–Atom– Atom–Atom	Torsion Angle [°]
W1–N1–N2–C3	176.8(5)
W1–N1–N2–B1	–10.6(10)
W1–N1–C1–C2	–176.7(6)
W1–N3–N4–C6	171.7(5)
W1–N3–N4–B1	4.2(9)
W1–N3–C4–C5	–172.7(5)
W1–N5–N6–C9	179.7(5)
W1–N5–N6–B1	–2.1(9)
W1–N5–C7–C8	179.9(5)
W1–C10–C11–C12	125.6(6)
W1–C10–C18–C17	–150.8(6)
W1–C10–C18–C19	–48.3(10)
W1–C11–C12–C13	146.6(6)
W1–C11–C12–C19	41.7(9)
N1–N2–C3–C2	1.5(9)
N1–N2–B1–N4	63.9(10)
N1–N2–B1–N6	–50.8(10)
N1–C1–C2–C3	–1.0(10)
N2–N1–C1–C2	1.9(9)
N3–N4–C6–C5	1.8(9)
N3–N4–B1–N2	–59.7(9)
N3–N4–B1–N6	56.3(9)
N3–C4–C5–C6	2.5(10)
N4–N3–C4–C5	–1.4(9)
N5–N6–C9–C8	0.7(10)
N5–N6–B1–N2	58.9(9)
N5–N6–B1–N4	–57.7(9)
N5–C7–C8–C9	0.2(9)
N6–N5–C7–C8	0.2(9)
C1–N1–N2–C3	–2.0(9)
C1–N1–N2–B1	170.6(7)
C1–C2–C3–N2	–0.3(10)
C3–N2–B1–N4	–124.9(8)
C3–N2–B1–N6	120.4(8)
C4–N3–N4–C6	–0.3(9)

C4–N3–N4–B1	–167.8(7)
C4–C5–C6–N4	–2.6(9)
C6–N4–B1–N2	135.9(8)
C6–N4–B1–N6	–108.0(9)
C7–N5–N6–C9	–0.5(9)
C7–N5–N6–B1	177.6(7)
C7–C8–C9–N6	–0.5(9)
C9–N6–B1–N2	–123.3(9)
C9–N6–B1–N4	120.0(9)
C10–C11–C12–C13	70.5(8)
C10–C11–C12–C19	–34.5(8)
C10–C18–C19–C12	–50.0(8)
C11–C10–C18–C17	–71.4(8)
C11–C10–C18–C19	31.1(9)
C11–C12–C13–C14	42(2)
C11–C12–C13–C17	–70.3(8)
C11–C12–C13– C14A	45.2(18)
C11–C12–C19–C18	50.8(7)
C12–C13–C14–C15	–119(5)
C12–C13–C17–C16	121(2)
C12–C13–C17–C18	1.9(8)
C12–C13–C17– C16A	128.2(14)
C12–C13–C14A– C15A	–108(3)
C13–C12–C19–C18	–60.5(7)
C13–C14–C15–C16	14(10)
C13–C17–C18–C10	67.6(8)
C13–C17–C18–C19	–38.5(8)
C13–C17–C16A– C15A	–9(4)
C13–C14A–C15A– C16A	–13(7)
C14–C13–C17–C16	1(2)
C14–C13–C17–C18	–118(2)
C14–C15–C16–C17	–13(10)
C15–C16–C17–C13	6(5)



C15–C16–C17–C18	118(5)
C16–C17–C18–C10	–47(2)
C16–C17–C18–C19	–153(2)
C17–C13–C14–C15	–8(6)
C17–C13–C14A– C15A	6(4)
C17–C18–C19–C12	60.3(7)
C18–C10–C11–W1	–123.5(6)
C18–C10–C11–C12	2.0(9)
C18–C17–C16A– C15A	105(4)
C19–C12–C13–C14	148(2)
C19–C12–C13–C17	35.7(8)
C19–C12–C13– C14A	151.2(17)
B1–N2–C3–C2	–170.7(8)
B1–N4–C6–C5	167.5(8)
B1–N6–C9–C8	–177.2(8)
C14A–C13–C17– C18	–125.1(16)
C14A–C13–C17– C16A	1.1(16)
C14A–C15A– C16A–C17	14(7)
C16A–C17–C18– C10	–46.7(19)
C16A–C17–C18– C19	–152.8(18)

## Crystal Structure Report for Harman\_2\_JKH\_151\_X2

A translucent pale yellow, plate-like specimen of  $C_{19}H_{28}BN_8OPW$ , approximate dimensions 0.029 mm x 0.084 mm x 0.089 mm, was coated with Paratone oil and mounted on a MiTeGen MicroLoop. The X-ray intensity data were measured on a Bruker D8 Venture Photon III Kappa four-circle diffractometer system equipped with an Incoatec  $\mu S$  3.0 micro-focus sealed X-ray tube (Mo  $K\alpha$ ,  $\lambda = 0.71073 \text{ \AA}$ ) and a HELIOS double bounce multilayer mirror monochromator.

The total exposure time was 8.76 hours. The frames were integrated with the Bruker SAINT software package<sup>5</sup> using a narrow-frame algorithm. The integration of the data using a monoclinic unit cell yielded a total of 63074 reflections to a maximum  $\theta$  angle of  $28.38^\circ$  ( $0.75 \text{ \AA}$  resolution), of which 6185 were independent (average redundancy 10.198, completeness = 99.2%,  $R_{\text{int}} = 8.87\%$ ,  $R_{\text{sig}} = 4.77\%$ ) and 4646 (75.12%) were greater than  $2\sigma(F^2)$ . The final cell constants of  $a = 15.6977(6) \text{ \AA}$ ,  $b = 12.3111(5) \text{ \AA}$ ,  $c = 25.7548(15) \text{ \AA}$ ,  $\beta = 92.2234(12)^\circ$ , volume =  $4973.5(4) \text{ \AA}^3$ , are based upon the refinement of the XYZ-centroids of 9910 reflections above  $20 \sigma(I)$  with  $5.203^\circ < 2\theta < 55.31^\circ$ . Data were corrected for absorption effects using the Multi-Scan method (SADABS).<sup>6</sup> The ratio of minimum to maximum apparent transmission was 0.858. The calculated minimum and maximum transmission coefficients (based on crystal size) are 0.6780 and 0.8750.

The structure was solved and refined using the Bruker SHELXTL Software Package<sup>7</sup> within APEX5<sup>1</sup> and OLEX2,<sup>8</sup> using the space group  $I 2/a$ , with  $Z = 8$  for the formula unit,  $C_{19}H_{28}BN_8OPW$ . Non-hydrogen atoms were refined anisotropically. The B-H hydrogen atoms and those on the Cp ligand were located in the electron density map and refined isotropically. All other hydrogen atoms were placed in geometrically calculated positions with  $U_{\text{iso}} = 1.2U_{\text{equiv}}$  of the parent atom ( $U_{\text{iso}} = 1.5U_{\text{equiv}}$  for methyl). The acetonitrile solvent molecules were refined at 50% occupancy due to the symmetry of the position. The final anisotropic full-matrix least-squares refinement on  $F^2$  with 340 variables converged at R1

---

<sup>5</sup> Bruker (2012). *Saint*; *SADABS*; *APEX5*. Bruker AXS Inc., Madison, Wisconsin, USA.

<sup>6</sup> Krause, L., Herbst-Irmer, R., Sheldrick, G. M., Stalke, D. "Comparison of silver and molybdenum microfocus X-ray sources for single-crystal structure determination" *J. Appl. Cryst.* (2015) 48, 3-10. doi:10.1107/S1600576714022985

<sup>7</sup> Sheldrick, G. M. (2015). *Acta Cryst.* A71, 3-8.

<sup>8</sup> Dolomanov, O. V.; Bourhis, L. J.; Gildea, R. J.; Howard, J. A. K.; Puschmann, H. *J. Appl. Cryst.* (2009). **42**, 339-341.

= 3.27%, for the observed data and  $wR2 = 7.89\%$  for all data. The goodness-of-fit was 1.038. The largest peak in the final difference electron density synthesis was  $1.395 \text{ e}^-/\text{\AA}^3$  and the largest hole was  $-0.816 \text{ e}^-/\text{\AA}^3$  with an RMS deviation of  $0.151 \text{ e}^-/\text{\AA}^3$ . On the basis of the final model, the calculated density was  $1.630 \text{ g/cm}^3$  and  $F(000)$ , 2400  $\text{e}^-$ .

<b>Table 1. Sample and crystal data for Harman_2_JKH_151_X2.</b>		
<b>Identification code</b>	Harman_2_JKH_151_X2	
<b>Chemical formula</b>	$\text{C}_{19}\text{H}_{28}\text{BN}_8\text{OPW}$	
<b>Formula weight</b>	610.12 g/mol	
<b>Temperature</b>	100(2) K	
<b>Wavelength</b>	0.71073 Å	
<b>Crystal size</b>	0.029 x 0.084 x 0.089 mm	
<b>Crystal habit</b>	translucent pale yellow plate	
<b>Crystal system</b>	monoclinic	
<b>Space group</b>	I 2/a	
<b>Unit cell dimensions</b>	$a = 15.6977(6) \text{ Å}$	$\alpha = 90^\circ$
	$b = 12.3111(5) \text{ Å}$	$\beta = 92.2234(12)^\circ$
	$c = 25.7548(15) \text{ Å}$	$\gamma = 90^\circ$
<b>Volume</b>	$4973.5(4) \text{ Å}^3$	
<b>Z</b>	8	
<b>Density (calculated)</b>	$1.630 \text{ g/cm}^3$	
<b>Absorption coefficient</b>	$4.736 \text{ mm}^{-1}$	
<b>F(000)</b>	2400	

<b>Table 2. Data collection and structure refinement for Harman_2_JKH_151_X2.</b>	
<b>Diffractometer</b>	Bruker D8 Venture Photon III Kappa four-circle diffractometer
<b>Radiation source</b>	Incoatec I $\mu$ S 3.0 micro-focus sealed X-ray tube (Mo K $\alpha$ , $\lambda = 0.71073 \text{ Å}$ )
<b>Theta range for data collection</b>	2.10 to $28.38^\circ$
<b>Index ranges</b>	$-20 \leq h \leq 18$ , $-16 \leq k \leq 16$ , $-34 \leq l \leq 34$
<b>Reflections collected</b>	63074
<b>Independent reflections</b>	6185 [ $R(\text{int}) = 0.0887$ ]
<b>Coverage of independent reflections</b>	99.2%
<b>Absorption correction</b>	Multi-Scan
<b>Max. and min. transmission</b>	0.8750 and 0.6780

<b>Structure solution technique</b>	direct methods	
<b>Structure solution program</b>	SHELXT 2018/2 (Sheldrick, 2018)	
<b>Refinement method</b>	Full-matrix least-squares on $F^2$	
<b>Refinement program</b>	SHELXL-2019/1 (Sheldrick, 2019)	
<b>Function minimized</b>	$\sum w(F_o^2 - F_c^2)^2$	
<b>Data / restraints / parameters</b>	6185 / 1 / 340	
<b>Goodness-of-fit on <math>F^2</math></b>	1.038	
<b><math>\Delta/\sigma_{\max}</math></b>	0.001	
<b>Final R indices</b>	4646 data; $I > 2\sigma(I)$	R1 = 0.0327, wR2 = 0.0710
	all data	R1 = 0.0556, wR2 = 0.0789
<b>Weighting scheme</b>	$w = 1/[\sigma^2(F_o^2) + (0.0396P)^2 + 2.5395P]$ where $P = (F_o^2 + 2F_c^2)/3$	
<b>Largest diff. peak and hole</b>	1.395 and -0.816 $e\text{\AA}^{-3}$	
<b>R.M.S. deviation from mean</b>	0.151 $e\text{\AA}^{-3}$	

**Table 3. Atomic coordinates and equivalent isotropic atomic displacement parameters ( $\text{\AA}^2$ ) for Harman\_2\_JKH\_151\_X2.**

U(eq) is defined as one third of the trace of the orthogonalized  $U_{ij}$  tensor.

	<b>x/a</b>	<b>y/b</b>	<b>z/c</b>	<b>U(eq)</b>
W1	0.05880(2)	0.11319(2)	0.13846(2)	0.02018(6)
P1	0.17873(7)	0.00375(10)	0.10542(5)	0.0263(3)
O1	0.1542(2)	0.3195(3)	0.11940(15)	0.0443(10)
N1	0.9426(2)	0.1198(3)	0.23570(15)	0.0248(8)
N2	0.9611(2)	0.1740(3)	0.19145(14)	0.0208(8)
N3	0.9964(2)	0.9538(3)	0.15763(15)	0.0221(8)
N4	0.9751(2)	0.9312(3)	0.20703(15)	0.0243(8)
N5	0.1240(2)	0.0923(3)	0.21538(15)	0.0239(8)
N6	0.0858(2)	0.0425(3)	0.25599(15)	0.0236(8)
N7	0.1137(2)	0.2358(3)	0.12738(15)	0.0271(9)
C1	0.9108(3)	0.2608(4)	0.18904(19)	0.0241(10)
C2	0.8586(3)	0.2635(4)	0.23152(19)	0.0280(10)
C3	0.8806(3)	0.1728(4)	0.26025(19)	0.0272(10)
C4	0.9745(3)	0.8665(3)	0.1290(2)	0.0276(10)
C5	0.9389(3)	0.7870(4)	0.1603(2)	0.0331(11)

	x/a	y/b	z/c	U(eq)
C6	0.9404(3)	0.8312(4)	0.2093(2)	0.0285(10)
C7	0.1407(3)	0.0416(4)	0.2978(2)	0.0294(11)
C8	0.2148(3)	0.0913(4)	0.2848(2)	0.0302(11)
C9	0.2022(3)	0.1224(4)	0.2331(2)	0.0291(10)
C10	0.2326(4)	0.9156(5)	0.1528(2)	0.0493(16)
C11	0.1631(3)	0.9073(4)	0.0524(2)	0.0378(13)
C12	0.2632(3)	0.0882(4)	0.0814(2)	0.0390(13)
C13	0.0175(3)	0.0872(4)	0.05563(19)	0.0277(11)
C14	0.0557(3)	0.1610(4)	0.01615(19)	0.0308(11)
C15	0.0182(3)	0.2575(5)	0.0165(2)	0.0377(12)
C16	0.9489(3)	0.2621(4)	0.0552(2)	0.0351(12)
C17	0.9548(3)	0.1501(4)	0.08089(19)	0.0276(10)
B1	0.9903(3)	0.0136(4)	0.2514(2)	0.0265(11)
N9	0.2474(10)	0.6172(10)	0.1057(5)	0.082(4)
C20	0.0936(7)	0.5539(9)	0.0826(5)	0.045(3)
C21	0.1780(10)	0.5881(9)	0.0952(5)	0.052(3)
N8	0.3719(9)	0.4564(11)	0.0698(5)	0.074(4)
C18	0.250(2)	0.3883(13)	0.9985(18)	0.121(8)
C19	0.3152(10)	0.4266(14)	0.0427(6)	0.071(4)

**Table 4. Bond lengths (Å) for Harman\_2\_JKH\_151\_X2.**

W1-N7	1.767(4)	W1-N5	2.209(4)
W1-C17	2.210(5)	W1-N2	2.221(3)
W1-C13	2.229(5)	W1-N3	2.257(4)
W1-P1	2.4916(12)	P1-C12	1.812(5)
P1-C10	1.818(6)	P1-C11	1.819(5)
O1-N7	1.232(5)	N1-C3	1.350(5)
N1-N2	1.362(5)	N1-B1	1.551(6)
N2-C1	1.329(5)	N3-C4	1.340(6)
N3-N4	1.356(5)	N4-C6	1.348(6)
N4-B1	1.540(7)	N5-C9	1.345(6)
N5-N6	1.370(5)	N6-C7	1.352(6)
N6-B1	1.541(6)	C1-C2	1.393(6)
C1-H1	0.950000	C2-C3	1.376(7)
C2-H2	0.950000	C3-H3	0.950000
C4-C5	1.398(7)	C4-H4	0.950000
C5-C6	1.374(7)	C5-H5	0.950000
C6-H6	0.950000	C7-C8	1.367(7)
C7-H7	0.950000	C8-C9	1.391(7)
C8-H8	0.950000	C9-H9	0.950000
C10-H10A	0.980000	C10-H10B	0.980000
C10-H10C	0.980000	C11-H11A	0.980000

C11-H11B	0.980000	C11-H11C	0.980000
C12-H12A	0.980000	C12-H12B	0.980000
C12-H12C	0.980000	C13-C17	1.429(7)
C13-C14	1.505(7)	C13-H13	0.98(5)
C14-C15	1.326(7)	C14-H14	1.06(5)
C15-C16	1.505(7)	C15-H15	1.04(5)
C16-C17	1.530(7)	C16-H16A	1.10(4)
C16-H16B	1.11(4)	C17-H17	1.01(6)
B1-H1A	1.18(4)	N9-C21	1.169(18)
C20-C21	1.416(18)	C20-H20A	0.980000
C20-H20B	0.980000	C20-H20C	0.980000
N8-C19	1.170(18)	C18-C19	1.57(5)
C18-H18A	0.980000	C18-H18B	0.980000
C18-H18C	0.980000		

**Table 5. Bond angles (°) for Harman\_2\_JKH\_151\_X2.**

N7-W1-N5	91.87(16)	N7-W1-C17	93.91(18)
N5-W1-C17	158.45(16)	N7-W1-N2	99.43(15)
N5-W1-N2	78.16(13)	C17-W1-N2	80.41(16)
N7-W1-C13	95.38(18)	N5-W1-C13	161.64(16)
C17-W1-C13	37.56(17)	N2-W1-C13	117.03(15)
N7-W1-N3	175.51(15)	N5-W1-N3	83.81(13)
C17-W1-N3	90.56(16)	N2-W1-N3	80.94(13)
C13-W1-N3	88.39(16)	N7-W1-P1	91.56(13)
N5-W1-P1	85.03(10)	C17-W1-P1	115.50(13)
N2-W1-P1	160.14(10)	C13-W1-P1	77.94(12)
N3-W1-P1	86.84(9)	C12-P1-C10	104.1(3)
C12-P1-C11	101.4(3)	C10-P1-C11	99.2(3)
C12-P1-W1	112.24(18)	C10-P1-W1	115.57(18)
C11-P1-W1	121.84(17)	C3-N1-N2	109.6(4)
C3-N1-B1	129.4(4)	N2-N1-B1	121.0(3)
C1-N2-N1	106.7(3)	C1-N2-W1	131.7(3)
N1-N2-W1	121.6(3)	C4-N3-N4	106.6(4)
C4-N3-W1	132.9(3)	N4-N3-W1	120.5(3)
C6-N4-N3	109.9(4)	C6-N4-B1	128.4(4)
N3-N4-B1	121.6(4)	C9-N5-N6	106.5(4)
C9-N5-W1	131.1(3)	N6-N5-W1	122.4(3)
C7-N6-N5	109.1(4)	C7-N6-B1	130.3(4)
N5-N6-B1	119.8(4)	O1-N7-W1	178.0(4)
N2-C1-C2	110.4(4)	N2-C1-H1	124.800000
C2-C1-H1	124.800000	C3-C2-C1	105.0(4)
C3-C2-H2	127.500000	C1-C2-H2	127.500000
N1-C3-C2	108.2(4)	N1-C3-H3	125.900000

C2-C3-H3	125.900000	N3-C4-C5	110.1(5)
N3-C4-H4	124.900000	C5-C4-H4	124.900000
C6-C5-C4	105.0(4)	C6-C5-H5	127.500000
C4-C5-H5	127.500000	N4-C6-C5	108.4(4)
N4-C6-H6	125.800000	C5-C6-H6	125.800000
N6-C7-C8	108.9(5)	N6-C7-H7	125.600000
C8-C7-H7	125.600000	C7-C8-C9	105.5(4)
C7-C8-H8	127.300000	C9-C8-H8	127.300000
N5-C9-C8	110.1(4)	N5-C9-H9	125.000000
C8-C9-H9	125.000000	P1-C10-H10A	109.500000
P1-C10-H10B	109.500000	H10A-C10-H10B	109.500000
P1-C10-H10C	109.500000	H10A-C10-H10C	109.500000
H10B-C10-H10C	109.500000	P1-C11-H11A	109.500000
P1-C11-H11B	109.500000	H11A-C11-H11B	109.500000
P1-C11-H11C	109.500000	H11A-C11-H11C	109.500000
H11B-C11-H11C	109.500000	P1-C12-H12A	109.500000
P1-C12-H12B	109.500000	H12A-C12-H12B	109.500000
P1-C12-H12C	109.500000	H12A-C12-H12C	109.500000
H12B-C12-H12C	109.500000	C17-C13-C14	106.3(4)
C17-C13-W1	70.5(3)	C14-C13-W1	116.8(3)
C17-C13-H13	124.(3)	C14-C13-H13	113.(3)
W1-C13-H13	120.(3)	C15-C14-C13	110.4(4)
C15-C14-H14	127.(3)	C13-C14-H14	122.(3)
C14-C15-C16	111.7(5)	C14-C15-H15	124.(3)
C16-C15-H15	124.(3)	C15-C16-C17	102.7(4)
C15-C16-H16A	113.(3)	C17-C16-H16A	116.(3)
C15-C16-H16B	108.(3)	C17-C16-H16B	111.(3)
H16A-C16-H16B	105.(4)	C13-C17-C16	108.8(4)
C13-C17-W1	71.9(3)	C16-C17-W1	120.4(3)
C13-C17-H17	116.(3)	C16-C17-H17	120.(3)
W1-C17-H17	110.(4)	N4-B1-N6	109.4(4)
N4-B1-N1	107.6(4)	N6-B1-N1	106.5(4)
N4-B1-H1A	112.(2)	N6-B1-H1A	113.(2)

N1-B1-H1A	108.(2)	C21-C20-H20A	109.500000
C21-C20-H20B	109.500000	H20A-C20-H20B	109.500000
C21-C20-H20C	109.500000	H20A-C20-H20C	109.500000
H20B-C20-H20C	109.500000	N9-C21-C20	179.4(16)
C19-C18-H18A	109.500000	C19-C18-H18B	109.500000
H18A-C18-H18B	109.500000	C19-C18-H18C	109.500000
H18A-C18-H18C	109.500000	H18B-C18-H18C	109.500000
N8-C19-C18	170.1(18)		

**Table 6. Torsion angles (°) for Harman\_2\_JKH\_151\_X2.**

C3-N1-N2-C1	0.5(5)	B1-N1-N2-C1	-179.5(4)
C3-N1-N2-W1	-179.1(3)	B1-N1-N2-W1	0.9(5)
C4-N3-N4-C6	0.0(4)	W1-N3-N4-C6	-178.8(3)
C4-N3-N4-B1	-179.6(4)	W1-N3-N4-B1	1.6(5)
C9-N5-N6-C7	-0.6(5)	W1-N5-N6-C7	-180.0(3)
C9-N5-N6-B1	170.6(4)	W1-N5-N6-B1	-8.7(5)
N1-N2-C1-C2	-0.5(5)	W1-N2-C1-C2	179.0(3)
N2-C1-C2-C3	0.3(5)	N2-N1-C3-C2	-0.2(5)
B1-N1-C3-C2	179.7(4)	C1-C2-C3-N1	-0.1(5)
N4-N3-C4-C5	0.0(5)	W1-N3-C4-C5	178.5(3)
N3-C4-C5-C6	0.1(5)	N3-N4-C6-C5	0.1(5)
B1-N4-C6-C5	179.6(4)	C4-C5-C6-N4	-0.1(5)
N5-N6-C7-C8	0.4(5)	B1-N6-C7-C8	-169.6(4)
N6-C7-C8-C9	0.0(5)	N6-N5-C9-C8	0.6(5)
W1-N5-C9-C8	179.9(3)	C7-C8-C9-N5	-0.4(5)
C17-C13-C14-C15	-1.6(6)	W1-C13-C14-C15	-77.6(5)
C13-C14-C15-C16	-1.1(6)	C14-C15-C16-C17	3.1(6)
C14-C13-C17-C16	3.5(5)	W1-C13-C17-C16	116.8(4)



C14-C13-C17-W1	-113.3(3)	C15-C16-C17-C13	-4.0(5)
C15-C16-C17-W1	75.7(5)	C6-N4-B1-N6	122.3(4)
N3-N4-B1-N6	-58.2(5)	C6-N4-B1-N1	<sup>-</sup> 122.4(4)
N3-N4-B1-N1	57.0(5)	C7-N6-B1-N4	<sup>-</sup> 128.3(5)
N5-N6-B1-N4	62.5(5)	C7-N6-B1-N1	115.7(5)
N5-N6-B1-N1	-53.4(5)	C3-N1-B1-N4	121.1(5)
N2-N1-B1-N4	-58.9(5)	C3-N1-B1-N6	<sup>-</sup> 121.7(5)
N2-N1-B1-N6	58.2(5)		

**Table 7. Anisotropic atomic displacement parameters (Å<sup>2</sup>) for Harman\_2\_JKH\_151\_X2.**

The anisotropic atomic displacement factor exponent takes the form:  $-2\pi^2 [h^2 a^{*2} U_{11} + \dots + 2 h k a^* b^* U_{12}]$

	<b>U<sub>11</sub></b>	<b>U<sub>22</sub></b>	<b>U<sub>33</sub></b>	<b>U<sub>23</sub></b>	<b>U<sub>13</sub></b>	<b>U<sub>12</sub></b>
W1	0.01424(8)	0.02216(10)	0.02411(10)	<sup>-</sup> 0.00077(8)	0.00040(6)	<sup>-</sup> 0.00067(7)
P1	0.0194(5)	0.0336(7)	0.0262(7)	0.0037(5)	0.0045(5)	0.0054(5)
O1	0.043(2)	0.046(2)	0.044(2)	0.0060(18)	<sup>-</sup> 0.0068(17)	<sup>-</sup> 0.0190(18)
N1	0.0190(17)	0.030(2)	0.025(2)	0.0006(17)	0.0041(14)	<sup>-</sup> 0.0015(15)
N2	0.0180(16)	0.0196(19)	0.025(2)	<sup>-</sup> 0.0017(15)	0.0020(14)	<sup>-</sup> 0.0011(14)
N3	0.0163(17)	0.0205(19)	0.030(2)	0.0006(16)	0.0003(15)	0.0029(14)
N4	0.0177(17)	0.0267(19)	0.028(2)	0.0027(17)	<sup>-</sup> 0.0005(15)	<sup>-</sup> 0.0001(15)
N5	0.0171(17)	0.027(2)	0.027(2)	<sup>-</sup> 0.0029(16)	<sup>-</sup> 0.0004(15)	<sup>-</sup> 0.0018(14)
N6	0.0259(19)	0.022(2)	0.023(2)	<sup>-</sup> 0.0015(16)	<sup>-</sup> 0.0001(15)	0.0029(15)
N7	0.0187(17)	0.035(2)	0.028(2)	0.0037(18)	<sup>-</sup> 0.0016(15)	<sup>-</sup> 0.0055(16)
C1	0.019(2)	0.023(2)	0.030(3)	0.0003(19)	<sup>-</sup> 0.0040(18)	0.0005(17)
C2	0.019(2)	0.028(2)	0.037(3)	-0.007(2)	0.0023(19)	0.0012(18)
C3	0.023(2)	0.032(3)	0.028(3)	-0.002(2)	0.0057(18)	<sup>-</sup> 0.0045(19)
C4	0.020(2)	0.024(3)	0.038(3)	-0.002(2)	<sup>-</sup> 0.0019(19)	<sup>-</sup> 0.0005(17)
C5	0.031(2)	0.023(2)	0.044(3)	0.003(2)	-0.006(2)	-0.002(2)

	<b>U<sub>11</sub></b>	<b>U<sub>22</sub></b>	<b>U<sub>33</sub></b>	<b>U<sub>23</sub></b>	<b>U<sub>13</sub></b>	<b>U<sub>12</sub></b>
C6	0.019(2)	0.028(3)	0.038(3)	0.005(2)	-0.0028(19)	-0.0026(19)
C7	0.037(3)	0.023(2)	0.028(3)	-0.008(2)	-0.006(2)	0.003(2)
C8	0.025(2)	0.030(3)	0.035(3)	-0.006(2)	-0.011(2)	0.0012(19)
C9	0.019(2)	0.034(3)	0.034(3)	-0.003(2)	-0.0020(18)	0.0006(19)
C10	0.047(3)	0.059(4)	0.043(4)	0.004(3)	0.012(3)	0.027(3)
C11	0.033(3)	0.036(3)	0.044(3)	-0.007(2)	0.008(2)	0.004(2)
C12	0.025(2)	0.048(3)	0.045(3)	0.001(3)	0.009(2)	-0.003(2)
C13	0.025(2)	0.030(3)	0.027(3)	-0.002(2)	-0.0062(19)	0.0004(19)
C14	0.026(2)	0.041(3)	0.025(3)	0.001(2)	0.0011(19)	-0.001(2)
C15	0.037(3)	0.043(3)	0.032(3)	0.006(2)	-0.002(2)	-0.007(2)
C16	0.032(3)	0.036(3)	0.036(3)	0.001(2)	-0.004(2)	0.011(2)
C17	0.023(2)	0.032(3)	0.028(3)	0.002(2)	-0.0029(19)	-0.001(2)
B1	0.024(2)	0.031(3)	0.025(3)	-0.001(2)	0.004(2)	0.000(2)
N9	0.095(10)	0.078(9)	0.071(9)	0.021(7)	-0.024(8)	-0.032(8)
C20	0.041(6)	0.040(6)	0.053(8)	0.019(6)	-0.009(5)	0.008(5)
C21	0.077(9)	0.034(7)	0.046(8)	0.003(5)	0.015(7)	0.002(6)
N8	0.092(9)	0.082(9)	0.049(8)	-0.009(7)	0.011(7)	-0.017(8)
C18	0.059(8)	0.122(13)	0.18(2)	0.113(19)	-0.021(10)	-0.039(15)
C19	0.068(10)	0.090(11)	0.056(10)	-0.019(9)	0.017(8)	0.002(9)

**Table 8. Hydrogen atomic coordinates and isotropic atomic displacement parameters ( $\text{\AA}^2$ ) for Harman\_2\_JKH\_151\_X2.**

	<b>x/a</b>	<b>y/b</b>	<b>z/c</b>	<b>U(eq)</b>
H1	-0.0895	0.3136	0.1621	0.029000
H2	-0.1832	0.3164	0.2390	0.034000
H3	-0.1436	0.1513	0.2919	0.033000
H4	-0.0179	-0.1404	0.0927	0.033000
H5	-0.0818	-0.2825	0.1499	0.040000
H6	-0.0797	-0.2028	0.2395	0.034000
H7	0.1296	0.0114	0.3308	0.035000
H8	0.2644	0.1023	0.3065	0.036000
H9	0.2428	0.1595	0.2133	0.035000
H10A	0.2662	-0.0402	0.1778	0.074000
H10B	0.2705	-0.1341	0.1350	0.074000
H10C	0.1902	-0.1264	0.1713	0.074000
H11A	0.1245	-0.1506	0.0630	0.057000
H11B	0.2181	-0.1243	0.0439	0.057000
H11C	0.1382	-0.0552	0.0219	0.057000

	x/a	y/b	z/c	U(eq)
H12A	0.2408	0.1322	0.0522	0.059000
H12B	0.3096	0.0421	0.0698	0.059000
H12C	0.2848	0.1362	0.1093	0.059000
H13	0.008(3)	0.014(4)	0.0424(18)	0.023(12)
H14	0.110(3)	0.138(4)	-0.005(2)	0.032(14)
H15	0.038(3)	0.324(4)	-0.005(2)	0.043(15)
H16A	<sup>-</sup> 0.046(3)	0.332(4)	0.0814(19)	0.047(16)
H16B	<sup>-</sup> 0.113(3)	0.273(4)	0.033(2)	0.051(16)
H17	<sup>-</sup> 0.099(4)	0.111(5)	0.090(3)	0.061(19)
H1A	<sup>-</sup> 0.037(3)	<sup>-</sup> 0.018(3)	0.2906(18)	0.021(11)
H20A	0.0752	0.5835	0.0486	0.068000
H20B	0.0555	0.5801	0.1091	0.068000
H20C	0.0916	0.4744	0.0813	0.068000
H18A	0.2798	0.3437	-0.0266	0.182000
H18B	0.2250	0.4518	-0.0191	0.182000
H18C	0.2048	0.3453	0.0138	0.182000

#### Structure Report for mo\_harman\_jkh\_193\_x2\_0m

A yellow, plate shaped crystal of mo\_harman\_2\_jkh\_193\_x2\_0m measuring 0.056×0.07×0.079 mm was coated with Paratone oil and mounted on a MiTeGen micromount. Data for mo\_harman\_2\_jkh\_193\_x2\_0m were measured on a Bruker D8

VENTURE dual wavelength Mo/Cu Kappa four-circle diffractometer equipped with a PHOTON III detector and an Incoatec I $\mu$ S 3.0 microfocus sealed X-ray tube (Mo  $K_{\alpha}$ ,  $\lambda=0.71073$  Å) using a HELIOS double bounce multilayer mirror as monochromator. The crystal temperature was controlled with an Oxford Cryostream 800 low temperature device. Data collection and processing were done within the Bruker APEX5 software suite.<sup>9</sup> All data were integrated with the Bruker SAINT 8.40B software using a narrow-frame algorithm. Data were corrected for absorption effects using a Multi-Scan method (SADABS).

The structure was solved by dual methods with SHELXT<sup>10</sup> and refined by full-matrix least-squares methods against  $F^2$  using XL<sup>11</sup> within OLEX2.<sup>12</sup> All non-hydrogen atoms were refined with anisotropically. Hydrogen atoms were placed in geometrically calculated positions with  $U_{iso} = 1.2U_{equiv}$  of the parent atom ( $1.5U_{equiv}$  for methyl). This report and the CIF file were generated using FinalCif.<sup>13</sup>

Table 1. Crystal data and structure refinement for mo\_harman\_2\_jkh\_193\_x2\_0m

CCDC number	
Empirical formula	C <sub>18</sub> H <sub>26</sub> BF <sub>3</sub> N <sub>7</sub> O <sub>4</sub> PSW
Formula weight	719.15
Temperature [K]	100.00
Wavelength [Å]	0.71073
Crystal size [mm <sup>3</sup> ]	0.056×0.07×0.079
Crystal habit	yellow plate
Crystal system	monoclinic
Space group	$P2_1/n$ (14)
$a$ [Å]	12.2462(9)
$b$ [Å]	9.6161(7)
$c$ [Å]	21.0198(16)
$\alpha$ [°]	90
$\beta$ [°]	97.547(3)
$\gamma$ [°]	90
Volume [Å <sup>3</sup> ]	2453.9(3)
$Z$	4
$\rho_{calc}$ [gcm <sup>-3</sup> ]	1.947
$\mu$ [mm <sup>-1</sup> ]	4.922

<sup>9</sup> APEX5, Saint, SADABS; Bruker AXS Inc. 2019.

<sup>10</sup> Sheldrick, G. M. SHELXT – Integrated space-group and crystal-structure determination. *Acta Cryst. Sect. A Found. Adv.* **2015**, 71, 3-8.

<sup>11</sup> Sheldrick, G. M. Crystal structure refinement with SHELXL. *Acta Cryst. Sect. C Struct. Chem.* **2015**, 71, 3-8.

<sup>12</sup> Dolomanov, O. V.; Bourhis, L. J.; Gildea, R. J.; Howard, J. A. K.; Puschmann, H. OLEX2: a completed structure solution, refinement and analysis program. *J. Appl. Cryst.* **2009**, 42, 339-341.

<sup>13</sup> Kratzert, D. FinalCif, <https://dkratzert.de/finalcif.html>.

$F(000)$	1408
$2\theta$ range [°]	3.91 to 56.60 (0.75 Å)
Index ranges	$-16 \leq h \leq 16$ $-12 \leq k \leq 12$ $-28 \leq l \leq 28$
Reflections collected	39898
Independent reflections	6099 [ $R_{\text{int}} = 0.1109$ ]
Data / Restraints / Parameters	6099 / 0 / 339
Goodness-of-fit on $F^2$	0.992
Final $R$ indexes [ $I \geq 2\sigma(I)$ ]	$R_1 = 0.0391$ $wR_2 = 0.0761$
Final $R$ indexes [all data]	$R_1 = 0.0730$ $wR_2 = 0.0871$
Largest peak/hole [ $\text{e}\text{\AA}^{-3}$ ]	1.11/−1.48

Table 2. Atomic coordinates and  $U_{eq}$  [Å<sup>2</sup>] for mo\_harman\_2\_jkh\_193\_x2\_0m

Atom	x	y	z	$U_{eq}$
W1	0.79523(2)	0.55390(2)	0.38709(2)	0.01456(7)
P1	0.64044(12)	0.73156(15)	0.37382(8)	0.0178(3)
O1	0.7792(3)	0.5469(4)	0.2443(2)	0.0273(10)
N1	0.8250(4)	0.2729(5)	0.4614(2)	0.0166(10)
N2	0.8678(3)	0.3492(5)	0.4155(2)	0.0163(10)
N3	0.7742(4)	0.5699(5)	0.4905(2)	0.0167(10)
N4	0.7393(3)	0.4573(5)	0.5220(2)	0.0159(9)
N5	0.6528(4)	0.4187(4)	0.3802(2)	0.0152(10)
N6	0.6307(4)	0.3356(5)	0.4295(2)	0.0169(10)
N7	0.7898(4)	0.5457(5)	0.3025(2)	0.0190(10)
C1	0.9464(4)	0.2686(6)	0.3960(3)	0.0202(13)
H1	0.989546	0.293745	0.363427	0.024
C2	0.9567(5)	0.1433(6)	0.4296(3)	0.0204(13)
H2	1.006848	0.069638	0.425208	0.025
C3	0.8783(4)	0.1504(6)	0.4704(3)	0.0164(12)
H3	0.863864	0.080452	0.500052	0.020
C4	0.7826(4)	0.6736(6)	0.5330(3)	0.0205(13)
H4	0.805048	0.765420	0.524239	0.025
C5	0.7546(5)	0.6306(6)	0.5912(3)	0.0231(14)
H5	0.754224	0.684631	0.629021	0.028
C6	0.7271(5)	0.4921(6)	0.5828(3)	0.0195(13)
H6	0.703735	0.431971	0.614230	0.023
C7	0.5420(4)	0.2583(6)	0.4101(3)	0.0191(12)
H7	0.510134	0.191805	0.435532	0.023
C8	0.5040(5)	0.2905(6)	0.3470(3)	0.0191(12)
H8	0.441931	0.252681	0.320862	0.023
C9	0.5764(5)	0.3899(6)	0.3303(3)	0.0176(12)
H9	0.572590	0.432041	0.289215	0.021
C10	0.5280(5)	0.6804(7)	0.4172(3)	0.0300(15)
H10A	0.499993	0.589223	0.401863	0.045
H10B	0.468676	0.749280	0.409848	0.045
H10C	0.554558	0.675061	0.463146	0.045
C11	0.6611(5)	0.9115(6)	0.3989(3)	0.0255(14)
H11A	0.682748	0.915220	0.445461	0.038
H11B	0.592461	0.963520	0.387670	0.038
H11C	0.719277	0.952925	0.377166	0.038
C12	0.5764(5)	0.7546(6)	0.2916(3)	0.0268(14)
H12A	0.629344	0.797089	0.266312	0.040
H12B	0.511923	0.815271	0.290915	0.040
H12C	0.553311	0.664004	0.273196	0.040
C13	0.8854(5)	0.7601(6)	0.4010(3)	0.0190(13)
H13	0.856(5)	0.823(7)	0.424(3)	0.031(19)

C14	0.9156(5)	0.8112(6)	0.3366(3)	0.0216(13)
H14A	0.955700	0.900786	0.341622	0.026
H14B	0.848932	0.823158	0.304905	0.026
C15	0.9899(5)	0.6952(6)	0.3156(3)	0.0236(14)
H15A	0.956017	0.651003	0.275217	0.028
H15B	1.063281	0.732015	0.309352	0.028
C16	0.9985(5)	0.5946(6)	0.3702(3)	0.0230(14)
H16	1.053335	0.517016	0.374069	0.028
C17	0.9619(4)	0.6513(6)	0.4227(3)	0.0204(13)
H17	0.982(5)	0.636(7)	0.465(3)	0.04(2)
B1	0.7183(5)	0.3177(7)	0.4883(3)	0.0156(13)
H1A	0.690(5)	0.239(6)	0.522(3)	0.019
S1	0.22928(11)	0.45300(16)	0.13890(7)	0.0186(3)
F1	0.3542(3)	0.4823(4)	0.2497(2)	0.0492(12)
F2	0.2591(3)	0.6639(4)	0.21935(17)	0.0362(9)
F3	0.1819(4)	0.4866(4)	0.25589(19)	0.0479(11)
O2	0.3167(4)	0.5068(5)	0.1069(2)	0.0342(11)
O3	0.2344(4)	0.3058(4)	0.1507(2)	0.0313(11)
O4	0.1226(4)	0.5063(5)	0.1161(2)	0.0336(11)
C18	0.2579(5)	0.5246(6)	0.2200(3)	0.0274(15)

$U_{eq}$  is defined as 1/3 of the trace of the orthogonalized  $U_{ij}$  tensor.

**Table 3. Anisotropic displacement parameters ( $\text{\AA}^2$ ) for mo\_harman\_2\_jkh\_193\_x2\_0m. The anisotropic displacement factor exponent takes the form:  $-2\pi^2 [h^2(a^*)^2 U_{11} + k^2(b^*)^2 U_{22} + \dots + 2hka^*b^* U_{12}]$**

Atom	$U_{11}$	$U_{22}$	$U_{33}$	$U_{23}$	$U_{13}$	$U_{12}$
W1	0.00948(11)	0.01575(11)	0.01825(12)	-0.00022(11)	0.00110(8)	-0.00040(10)
P1	0.0135(7)	0.0164(7)	0.0233(8)	0.0016(6)	0.0015(6)	0.0006(6)
O1	0.027(2)	0.033(2)	0.022(2)	-0.002(2)	0.0055(19)	-0.002(2)
N1	0.018(2)	0.016(2)	0.016(2)	0.0002(19)	0.001(2)	0.0020(19)
N2	0.005(2)	0.018(2)	0.025(3)	0.001(2)	0.002(2)	-0.0032(19)
N3	0.012(2)	0.016(2)	0.021(3)	-0.002(2)	0.0021(19)	-0.0014(19)
N4	0.008(2)	0.021(2)	0.018(2)	0.001(2)	0.0009(18)	0.000(2)
N5	0.012(2)	0.019(3)	0.015(2)	-0.0030(19)	-0.0010(19)	0.0010(18)
N6	0.011(2)	0.018(2)	0.022(3)	-0.002(2)	0.001(2)	-0.0019(19)
N7	0.014(2)	0.021(2)	0.021(3)	0.001(2)	0.001(2)	0.001(2)
C1	0.009(3)	0.026(3)	0.027(3)	0.000(3)	0.007(2)	0.002(2)
C2	0.021(3)	0.014(3)	0.026(3)	-0.003(2)	0.000(3)	0.006(2)

C3	0.016(3)	0.013(3)	0.020(3)	0.001(2)	−0.001(2)	−0.002(2)
C4	0.014(3)	0.018(3)	0.029(3)	−0.003(3)	0.003(3)	−0.001(2)
C5	0.019(3)	0.024(3)	0.026(3)	−0.004(3)	0.002(3)	0.001(2)
C6	0.015(3)	0.028(3)	0.016(3)	0.000(2)	0.002(2)	−0.002(2)
C7	0.012(3)	0.020(3)	0.025(3)	−0.007(3)	0.003(2)	−0.005(2)
C8	0.010(3)	0.023(3)	0.024(3)	−0.006(2)	0.002(2)	−0.001(2)
C9	0.017(3)	0.021(3)	0.013(3)	−0.003(2)	−0.002(2)	0.004(2)
C10	0.021(3)	0.033(4)	0.038(4)	0.008(3)	0.010(3)	0.000(3)
C11	0.020(3)	0.020(3)	0.034(4)	0.000(3)	−0.003(3)	0.001(2)
C12	0.020(3)	0.026(3)	0.031(4)	0.000(3)	−0.006(3)	0.002(3)
C13	0.020(3)	0.018(3)	0.019(3)	−0.002(3)	0.003(3)	−0.003(2)
C14	0.013(3)	0.021(3)	0.031(4)	0.000(3)	0.004(3)	−0.005(2)
C15	0.017(3)	0.030(3)	0.026(3)	0.002(3)	0.007(3)	−0.002(2)
C16	0.010(3)	0.027(3)	0.032(4)	0.000(3)	0.000(3)	0.002(2)
C17	0.008(3)	0.024(3)	0.027(4)	0.002(3)	−0.006(3)	−0.004(2)
B1	0.015(3)	0.017(3)	0.013(3)	−0.002(3)	0.000(3)	−0.003(3)
S1	0.0156(7)	0.0197(7)	0.0198(7)	−0.0008(6)	0.0002(5)	0.0007(6)
F1	0.046(3)	0.046(3)	0.046(3)	−0.007(2)	−0.027(2)	0.019(2)
F2	0.057(3)	0.0198(18)	0.028(2)	−0.0034(17)	−0.0077(19)	0.0014(18)
F3	0.069(3)	0.049(3)	0.031(2)	−0.0056(19)	0.023(2)	−0.009(2)
O2	0.027(3)	0.045(3)	0.034(3)	−0.006(2)	0.016(2)	−0.008(2)
O3	0.045(3)	0.020(2)	0.027(3)	−0.0001(19)	−0.003(2)	0.002(2)
O4	0.023(2)	0.037(3)	0.037(3)	−0.006(2)	−0.011(2)	0.003(2)
C18	0.032(4)	0.025(4)	0.024(3)	0.002(3)	−0.002(3)	0.002(3)

Table 4. Bond lengths and angles for mo\_harman\_2\_jkh\_193\_x2\_0m

Atom–Atom	Length [Å]
W1–P1	2.5398(15)
W1–N2	2.210(5)
W1–N3	2.227(5)
W1–N5	2.165(4)
W1–N7	1.772(5)
W1–C13	2.270(6)
W1–C16	2.590(6)
W1–C17	2.280(6)
P1–C10	1.816(6)
P1–C11	1.817(6)
P1–C12	1.815(6)
O1–N7	1.213(6)
N1–N2	1.371(6)
N1–C3	1.348(7)
N1–B1	1.550(8)
N2–C1	1.340(7)
N3–N4	1.367(6)



N3–C4	1.334(7)
N4–C6	1.348(7)
N4–B1	1.524(8)
N5–N6	1.364(6)
N5–C9	1.339(7)
N6–C7	1.336(7)
N6–B1	1.536(8)
C1–H1	0.9500
C1–C2	1.394(8)
C2–H2	0.9500
C2–C3	1.370(8)
C3–H3	0.9500
C4–H4	0.9500
C4–C5	1.377(8)
C5–H5	0.9500
C5–C6	1.379(8)
C6–H6	0.9500
C7–H7	0.9500
C7–C8	1.382(8)
C8–H8	0.9500
C8–C9	1.379(8)
C9–H9	0.9500
C10–H10A	0.9800
C10–H10B	0.9800
C10–H10C	0.9800
C11–H11A	0.9800
C11–H11B	0.9800
C11–H11C	0.9800
C12–H12A	0.9800
C12–H12B	0.9800
C12–H12C	0.9800
C13–H13	0.88(6)
C13–C14	1.532(8)
C13–C17	1.438(8)
C14–H14A	0.9900
C14–H14B	0.9900
C14–C15	1.540(8)
C15–H15A	0.9900
C15–H15B	0.9900
C15–C16	1.495(8)
C16–H16	1.0000
C16–C17	1.358(8)
C17–H17	0.90(7)
B1–H1A	1.13(6)
S1–O2	1.434(4)
S1–O3	1.436(4)
S1–O4	1.426(4)
S1–C18	1.829(7)

F1–C18	1.324(7)
F2–C18	1.339(7)
F3–C18	1.325(7)
<b>Atom–Atom– Atom</b>	<b>Angle [°]</b>
P1–W1–C16	126.89(14)
N2–W1–P1	153.75(11)
N2–W1–N3	83.80(17)
N2–W1–C13	124.88(19)
N2–W1–C16	79.16(17)
N2–W1–C17	88.07(19)
N3–W1–P1	83.13(12)
N3–W1–C13	86.00(19)
N3–W1–C16	111.08(18)
N3–W1–C17	82.2(2)
N5–W1–P1	79.25(12)
N5–W1–N2	77.00(16)
N5–W1–N3	84.92(17)
N5–W1–C13	155.12(19)
N5–W1–C16	149.54(17)
N5–W1–C17	161.3(2)
N7–W1–P1	89.47(15)
N7–W1–N2	101.07(19)
N7–W1–N3	171.17(18)
N7–W1–N5	88.98(19)
N7–W1–C13	97.0(2)
N7–W1–C16	77.3(2)
N7–W1–C17	105.1(2)
C13–W1–P1	76.70(16)
C13–W1–C16	54.9(2)
C13–W1–C17	36.8(2)
C17–W1–P1	112.50(16)
C17–W1–C16	31.6(2)
C10–P1–W1	111.5(2)
C10–P1–C11	101.4(3)
C11–P1–W1	122.4(2)
C12–P1–W1	114.2(2)
C12–P1–C10	104.4(3)
C12–P1–C11	100.7(3)
N2–N1–B1	121.8(4)
C3–N1–N2	110.0(4)
C3–N1–B1	127.4(5)
N1–N2–W1	119.3(3)
C1–N2–W1	135.4(4)
C1–N2–N1	105.2(4)
N4–N3–W1	120.1(3)
C4–N3–W1	134.2(4)

C4–N3–N4	105.6(4)
N3–N4–B1	121.1(4)
C6–N4–N3	110.1(5)
C6–N4–B1	128.8(5)
N6–N5–W1	122.6(3)
C9–N5–W1	130.6(4)
C9–N5–N6	106.6(4)
N5–N6–B1	119.3(4)
C7–N6–N5	109.1(5)
C7–N6–B1	129.6(5)
O1–N7–W1	175.0(4)
N2–C1–H1	124.3
N2–C1–C2	111.5(5)
C2–C1–H1	124.3
C1–C2–H2	127.8
C3–C2–C1	104.4(5)
C3–C2–H2	127.8
N1–C3–C2	108.8(5)
N1–C3–H3	125.6
C2–C3–H3	125.6
N3–C4–H4	124.3
N3–C4–C5	111.4(5)
C5–C4–H4	124.3
C4–C5–H5	127.4
C4–C5–C6	105.1(5)
C6–C5–H5	127.4
N4–C6–C5	107.8(5)
N4–C6–H6	126.1
C5–C6–H6	126.1
N6–C7–H7	125.5
N6–C7–C8	109.1(5)
C8–C7–H7	125.5
C7–C8–H8	127.7
C9–C8–C7	104.6(5)
C9–C8–H8	127.7
N5–C9–C8	110.6(5)
N5–C9–H9	124.7
C8–C9–H9	124.7
P1–C10–H10A	109.5
P1–C10–H10B	109.5
P1–C10–H10C	109.5
H10A–C10– H10B	109.5
H10A–C10– H10C	109.5
H10B–C10– H10C	109.5
P1–C11–H11A	109.5
P1–C11–H11B	109.5

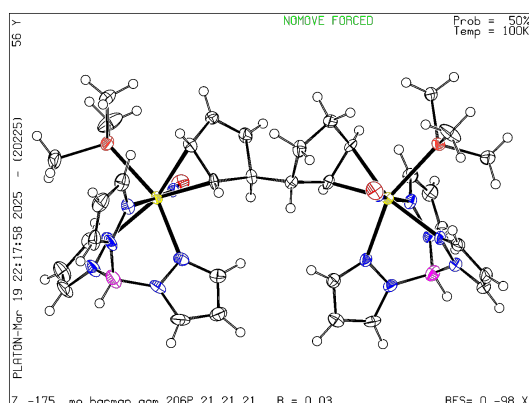
P1-C11-H11C	109.5
H11A-C11-H11B	109.5
H11A-C11-H11C	109.5
H11B-C11-H11C	109.5
P1-C12-H12A	109.5
P1-C12-H12B	109.5
P1-C12-H12C	109.5
H12A-C12-H12B	109.5
H12A-C12-H12C	109.5
H12B-C12-H12C	109.5
W1-C13-H13	116(4)
C14-C13-W1	109.6(4)
C14-C13-H13	116(4)
C17-C13-W1	72.0(3)
C17-C13-H13	128(4)
C17-C13-C14	106.9(5)
C13-C14-H14A	111.0
C13-C14-H14B	111.0
C13-C14-C15	104.0(5)
H14A-C14-H14B	109.0
C15-C14-H14A	111.0
C15-C14-H14B	111.0
C14-C15-H15A	111.1
C14-C15-H15B	111.1
H15A-C15-H15B	109.0
C16-C15-C14	103.5(5)
C16-C15-H15A	111.1
C16-C15-H15B	111.1
W1-C16-H16	121.6
C15-C16-W1	103.4(4)
C15-C16-H16	121.6
C17-C16-W1	61.6(3)
C17-C16-C15	111.5(5)
C17-C16-H16	121.6
W1-C17-H17	112(4)
C13-C17-W1	71.2(3)
C13-C17-H17	121(4)
C16-C17-W1	86.9(4)
C16-C17-C13	107.8(6)
C16-C17-H17	131(4)
N1-B1-H1A	113(3)
N4-B1-N1	108.4(4)
N4-B1-N6	109.4(5)
N4-B1-H1A	110(3)

N6–B1–N1	105.8(4)
N6–B1–H1A	110(3)
O2–S1–O3	114.7(3)
O2–S1–C18	103.8(3)
O3–S1–C18	102.2(3)
O4–S1–O2	114.8(3)
O4–S1–O3	115.4(3)
O4–S1–C18	103.4(3)
F1–C18–S1	111.9(4)
F1–C18–F2	107.6(5)
F1–C18–F3	107.2(5)
F2–C18–S1	111.6(4)
F3–C18–S1	111.3(4)
F3–C18–F2	106.9(5)

Table 5. Torsion angles for mo\_harman\_2\_jkh\_193\_x2\_0m

Atom–Atom– Atom–Atom	Torsion Angle [°]		
W1–N2–C1–C2	–177.5(4)	C4–N3–N4–C6	–0.2(6)
W1–N3–N4–C6	–176.9(3)	C4–N3–N4–B1	179.1(5)
W1–N3–N4–B1	2.4(6)	C4–C5–C6–N4	0.1(6)
W1–N3–C4–C5	176.4(4)	C6–N4–B1–N1	–124.6(6)
W1–N5–N6–C7	–176.2(4)	C6–N4–B1–N6	120.6(6)
W1–N5–N6–B1	–10.4(6)	C7–N6–B1–N1	109.8(6)
W1–N5–C9–C8	176.2(4)	C7–N6–B1–N4	–133.7(6)
W1–C13–C14–C15	–60.1(5)	C7–C8–C9–N5	–1.0(6)
W1–C13–C17–C16	80.2(4)	C9–N5–N6–C7	–0.4(6)
W1–C16–C17–C13	–69.1(4)	C9–N5–N6–B1	165.5(5)
N1–N2–C1–C2	–1.4(6)	C13–C14–C15–C16	–2.3(6)
N2–N1–C3–C2	–0.7(6)	C14–C13–C17–W1	–105.7(4)
N2–N1–B1–N4	–63.0(6)	C14–C13–C17–C16	–25.5(6)
N2–N1–B1–N6	54.2(6)	C14–C15–C16–W1	50.8(5)
N2–C1–C2–C3	1.0(7)	C14–C15–C16–C17	–13.6(7)
N3–N4–C6–C5	0.1(6)	C15–C16–C17–W1	94.0(4)
N3–N4–B1–N1	56.2(6)	C15–C16–C17–C13	24.9(7)
N3–N4–B1–N6	–58.7(6)	C17–C13–C14–C15	16.3(6)
N3–C4–C5–C6	–0.3(7)	B1–N1–N2–W1	7.5(6)
N4–N3–C4–C5	0.3(6)	B1–N1–N2–C1	–169.4(5)
N5–N6–C7–C8	–0.2(6)	B1–N1–C3–C2	169.3(5)
N5–N6–B1–N1	–52.7(6)	B1–N4–C6–C5	–179.2(5)
N5–N6–B1–N4	63.8(6)	B1–N6–C7–C8	–164.2(5)
N6–N5–C9–C8	0.9(6)	O2–S1–C18–F1	–61.5(5)
N6–C7–C8–C9	0.7(6)	O2–S1–C18–F2	59.2(5)
C1–C2–C3–N1	–0.2(6)	O2–S1–C18–F3	178.6(4)
C3–N1–N2–W1	178.1(3)	O3–S1–C18–F1	58.1(5)
C3–N1–N2–C1	1.3(6)	O3–S1–C18–F2	178.7(4)
C3–N1–B1–N4	128.1(6)	O3–S1–C18–F3	–61.9(5)
C3–N1–B1–N6	–114.7(6)	O4–S1–C18–F1	178.3(4)
		O4–S1–C18–F2	–61.1(5)
		O4–S1–C18–F3	58.3(5)

## Structure Report for mo\_harman\_aqm\_2061\_0m



A yellow, block shaped crystal of mo\_harman\_aqm\_2061\_0m measuring 0.101×0.149×0.188 mm was coated with Paratone oil and mounted on a MiTeGen micromount. Data for mo\_harman\_aqm\_2061\_0m were measured on a Bruker D8 VENTURE dual wavelength Mo/Cu Kappa four-circle diffractometer equipped with a PHOTON III detector and an Incoatec IμS 3.0 microfocus sealed X-ray tube (Mo  $K_{\alpha}$ ,  $\lambda=0.71073$  Å) using a HELIOS double bounce multilayer mirror as monochromator. The crystal temperature was controlled with an Oxford Cryostream 800low temperature device. Data collection and processing were done within the Bruker APEX4 software suite.<sup>14</sup> All data were integrated with the Bruker SAINT 8.40B software using a narrow-frame algorithm. Data were corrected for absorption effects using a Multi-Scan method (SADABS). The structure was solved by dual methods with SHELXT 2018/2<sup>15</sup> and refined by full-matrix least-squares methods against  $F^2$  using SHELXL 2018/3<sup>16</sup> within OLEX2.<sup>17</sup> All non-hydrogen atoms were refined with anisotropically. Hydrogen atoms were placed in geometrically calculated positions with  $U_{iso} = 1.2U_{equiv}$  of the parent atom ( $1.5U_{equiv}$  for methyl). This report and the CIF file were generated using FinalCif.<sup>18</sup>

<sup>14</sup> APEX4, Saint, SADABS; Bruker AXS Inc. 2019.

<sup>15</sup> Sheldrick, G. M. SHELXT – Integrated space-group and crystal-structure determination. *Acta Cryst. Sect. A Found. Adv.* **2015**, *71*, 3-8.

<sup>16</sup> Sheldrick, G. M. Crystal structure refinement with SHELXL. *Acta Cryst. Sect. C Struct. Chem.* **2015**, *71*, 3-8.

<sup>17</sup> Dolomanov, O. V.; Bourhis, L. J.; Gildea, R. J.; Howard, J. A. K.; Puschmann, H. OLEX2: a completed structure solution, refinement and analysis program. *J. Appl. Cryst.* **2009**, *42*, 339-341.

<sup>18</sup> Kratzert, D. FinalCif, <https://dkratzert.de/finalcif.html>.

Table 1. Crystal data and structure refinement for mo\_harman\_aqm\_2061\_0m

CCDC number	
Empirical formula	C <sub>34</sub> H <sub>50</sub> B <sub>2</sub> N <sub>14</sub> O <sub>2</sub> P <sub>2</sub> W <sub>2</sub>
Formula weight	1138.14
Temperature [K]	100.00
Wavelength [Å]	0.71073
Crystal size [mm <sup>3</sup> ]	0.101×0.149×0.188
Crystal habit	yellow block
Crystal system	orthorhombic
Space group	<i>P</i> 2 <sub>1</sub> 2 <sub>1</sub> 2 <sub>1</sub> (19)
<i>a</i> [Å]	13.7254(4)
<i>b</i> [Å]	14.4723(4)
<i>c</i> [Å]	20.8568(8)
α [°]	90
β [°]	90
γ [°]	90
Volume [Å <sup>3</sup> ]	4143.0(2)
<i>Z</i>	4
ρ <sub>calc</sub> [gcm <sup>-3</sup> ]	1.825
μ [mm <sup>-1</sup> ]	5.677
<i>F</i> (000)	2224
2θ range [°]	3.55 to 56.60 (0.75 Å)
Index ranges	−18 ≤ <i>h</i> ≤ 17 −19 ≤ <i>k</i> ≤ 19 −27 ≤ <i>l</i> ≤ 27
Reflections collected	69351
Independent reflections	10285 [ <i>R</i> <sub>int</sub> = 0.0879]
Data / Restraints / Parameters	10285 / 0 / 519
Goodness-of-fit on <i>F</i> <sup>2</sup>	1.026
Final <i>R</i> indexes [ <i>I</i> ≥ 2σ( <i>I</i> )]	<i>R</i> <sub>1</sub> = 0.0340 <i>wR</i> <sub>2</sub> = 0.0638
Final <i>R</i> indexes [all data]	<i>R</i> <sub>1</sub> = 0.0383 <i>wR</i> <sub>2</sub> = 0.0661
Largest peak/hole [eÅ <sup>-3</sup> ]	1.47/−0.68
Flack <i>X</i> parameter	−0.006(6)

Table 2. Atomic coordinates and  $U_{eq}$  [Å<sup>2</sup>] for mo\_harman\_aqm\_2061\_0m

Atom	x	y	z	$U_{eq}$
W1	0.88116(2)	0.25192(2)	0.37367(2)	0.01683(7)
W2	0.61328(2)	0.71992(2)	0.36070(2)	0.01589(7)
P1	0.93159(17)	0.15113(15)	0.46384(11)	0.0233(5)
P2	0.56850(16)	0.83442(14)	0.44374(10)	0.0213(4)
O1	0.6782(4)	0.1892(4)	0.4062(3)	0.0301(14)
O2	0.8108(4)	0.8083(4)	0.3627(3)	0.0290(13)
N3	0.8977(5)	0.1269(4)	0.3135(3)	0.0214(15)
N4	0.9622(6)	0.1227(5)	0.2641(4)	0.0301(18)
N1	1.0418(5)	0.2734(4)	0.3538(3)	0.0234(14)
N2	1.0792(5)	0.2466(5)	0.2958(3)	0.0254(15)
N5	0.8686(5)	0.3068(4)	0.2737(3)	0.0214(14)
N6	0.9356(5)	0.2826(5)	0.2282(3)	0.0251(15)
N7	0.7590(4)	0.2199(4)	0.3914(3)	0.0195(13)
N10	0.5677(5)	0.8318(4)	0.2942(3)	0.0194(14)
N11	0.4903(5)	0.8239(4)	0.2543(3)	0.0229(15)
N8	0.4542(4)	0.6811(4)	0.3627(3)	0.0205(13)
N9	0.3977(5)	0.6957(4)	0.3095(3)	0.0224(14)
N12	0.6032(5)	0.6483(4)	0.2662(3)	0.0199(14)
N13	0.5246(5)	0.6641(4)	0.2268(3)	0.0211(15)
N14	0.7323(4)	0.7666(4)	0.3602(3)	0.0200(13)
C1	1.1150(6)	0.3047(5)	0.3887(4)	0.0295(17)
H1	1.109382	0.327066	0.431347	0.035
C2	1.2031(6)	0.3001(6)	0.3535(5)	0.035(2)
H2	1.266369	0.318654	0.366621	0.042
C3	1.1755(6)	0.2628(6)	0.2961(4)	0.032(2)
H3	1.218374	0.250020	0.261458	0.038
C4	0.8517(6)	0.0463(5)	0.3157(4)	0.028(2)
H4	0.802774	0.030328	0.345987	0.033
C5	0.8855(7)	−0.0114(5)	0.2673(4)	0.037(2)
H5	0.864904	−0.072603	0.258124	0.044
C6	0.9543(7)	0.0385(6)	0.2359(5)	0.037(2)
H6	0.990984	0.017886	0.200047	0.044
C7	0.8114(7)	0.3706(6)	0.2459(4)	0.030(2)
H7	0.758249	0.400387	0.266538	0.035
C8	0.8401(7)	0.3873(6)	0.1834(4)	0.034(2)
H8	0.810935	0.428334	0.153426	0.041
C9	0.9193(7)	0.3320(6)	0.1741(4)	0.032(2)
H9	0.956864	0.328634	0.135910	0.038
C13	0.8951(6)	0.3566(5)	0.4529(4)	0.0197(16)
H13	0.962223	0.371483	0.468504	0.024
C14	0.8632(6)	0.3995(4)	0.3936(4)	0.0208(18)



H14	0.911135	0.441708	0.372493	0.025
C15	0.7604(5)	0.4384(5)	0.4030(4)	0.0192(17)
H15	0.714911	0.405548	0.373309	0.023
C16	0.7374(6)	0.4100(5)	0.4709(4)	0.0261(19)
H16	0.676677	0.420561	0.491531	0.031
C17	0.8142(6)	0.3675(5)	0.4985(4)	0.0207(18)
H17	0.815858	0.347317	0.541828	0.025
C18	0.6350(6)	0.6346(5)	0.4484(4)	0.0173(16)
H18	0.575859	0.621456	0.474901	0.021
C19	0.6485(5)	0.5791(5)	0.3918(4)	0.0183(16)
H19	0.596976	0.531681	0.383686	0.022
C20	0.7535(5)	0.5437(5)	0.3901(4)	0.0200(17)
H20	0.781631	0.556909	0.346880	0.024
C21	0.8062(6)	0.6012(5)	0.4391(4)	0.0250(18)
H21A	0.842740	0.651500	0.417649	0.030
H21B	0.852933	0.562570	0.463273	0.030
C22	0.7310(6)	0.6411(5)	0.4838(4)	0.0218(17)
H22A	0.746437	0.706301	0.494036	0.026
H22B	0.728383	0.605411	0.524221	0.026
C10	0.9972(6)	0.1957(6)	0.5325(4)	0.031(2)
H10A	0.957984	0.243395	0.553638	0.046
H10B	1.059120	0.222510	0.518314	0.046
H10C	1.010026	0.145317	0.562751	0.046
C11	1.0072(8)	0.0527(7)	0.4399(5)	0.053(3)
H11A	1.029900	0.019968	0.478255	0.080
H11B	1.063478	0.074878	0.415426	0.080
H11C	0.968731	0.010507	0.413263	0.080
C12	0.8298(8)	0.0959(7)	0.5026(5)	0.048(3)
H12A	0.853686	0.055545	0.536940	0.072
H12B	0.793696	0.059050	0.471191	0.072
H12C	0.786732	0.143062	0.520871	0.072
C23	0.3955(6)	0.6458(5)	0.4074(4)	0.0249(17)
H23	0.415212	0.628127	0.449331	0.030
C24	0.3004(6)	0.6387(6)	0.3835(4)	0.0293(19)
H24	0.244422	0.616456	0.405365	0.035
C25	0.3055(6)	0.6704(6)	0.3222(4)	0.0274(19)
H25	0.252447	0.674140	0.293027	0.033
C26	0.6138(7)	0.9100(5)	0.2785(4)	0.0215(16)
H26	0.671579	0.932092	0.298386	0.026
C27	0.5650(6)	0.9544(5)	0.2288(4)	0.028(2)
H27	0.581639	1.011216	0.208894	0.033
C28	0.4878(6)	0.8982(5)	0.2150(4)	0.0250(18)
H28	0.440111	0.909547	0.182984	0.030
C29	0.6644(6)	0.5959(5)	0.2333(4)	0.0229(18)
H29	0.725089	0.574043	0.248999	0.027
C30	0.6277(6)	0.5772(5)	0.1724(4)	0.0250(18)

H30	0.657390	0.542110	0.139251	0.030
C31	0.5387(6)	0.6209(5)	0.1712(4)	0.0237(18)
H31	0.494341	0.620424	0.136265	0.028
C32	0.5433(6)	0.8014(6)	0.5259(4)	0.0243(18)
H32A	0.600269	0.770005	0.543960	0.037
H32B	0.487105	0.759671	0.526926	0.037
H32C	0.528858	0.856785	0.551247	0.037
C33	0.4597(7)	0.9004(6)	0.4227(4)	0.037(2)
H33A	0.402410	0.860071	0.424831	0.055
H33B	0.466479	0.924715	0.379030	0.055
H33C	0.451740	0.951810	0.452785	0.055
C34	0.6592(7)	0.9246(6)	0.4541(5)	0.040(3)
H34A	0.637151	0.968093	0.487068	0.060
H34B	0.668104	0.957614	0.413450	0.060
H34C	0.721132	0.896898	0.467253	0.060
B1	1.0143(8)	0.2110(7)	0.2413(5)	0.034(2)
H1A	1.056(6)	0.197(6)	0.202(4)	0.03(2)
B2	0.4421(7)	0.7298(6)	0.2463(5)	0.025(2)
H2A	0.386(5)	0.732(4)	0.211(3)	0.015(18)

$U_{eq}$  is defined as 1/3 of the trace of the orthogonalized  $U_{ij}$  tensor.

**Table 3. Anisotropic displacement parameters ( $\text{\AA}^2$ ) for mo\_harman\_aqm\_2061\_0m. The anisotropic displacement factor exponent takes the form:**

$$-2\pi^2 [h^2(a^*)^2 U_{11} + k^2(b^*)^2 U_{22} + \dots + 2hka^*b^* U_{12}]$$

Atom	$U_{11}$	$U_{22}$	$U_{33}$	$U_{23}$	$U_{13}$	$U_{12}$
W1	0.01713(14)	0.01514(12)	0.01820(15)	-0.00094(11)	-0.00015(12)	0.00091(13)
W2	0.01743(14)	0.01469(12)	0.01556(14)	0.00117(10)	-0.00007(13)	0.00084(12)
P1	0.0239(12)	0.0212(10)	0.0248(13)	0.0013(9)	-0.0063(9)	0.0021(9)
P2	0.0270(11)	0.0194(10)	0.0174(11)	0.0007(8)	0.0056(9)	0.0021(9)
O1	0.016(3)	0.040(3)	0.035(4)	0.001(3)	-0.005(2)	-0.005(3)
O2	0.024(3)	0.026(3)	0.037(4)	-0.002(3)	0.005(3)	-0.008(2)
N3	0.027(4)	0.019(3)	0.019(3)	-0.005(3)	0.003(3)	-0.001(3)
N4	0.035(4)	0.025(4)	0.031(4)	-0.003(3)	0.017(3)	0.003(3)
N1	0.023(3)	0.020(3)	0.028(4)	-0.001(3)	0.004(3)	0.001(3)
N2	0.026(3)	0.023(3)	0.027(4)	-0.003(3)	0.014(3)	0.006(3)
N5	0.022(4)	0.023(3)	0.020(3)	-0.004(2)	0.000(3)	-0.005(3)
N6	0.030(4)	0.025(3)	0.020(4)	-0.009(3)	0.006(3)	-0.002(3)
N7	0.019(3)	0.017(3)	0.022(4)	-0.001(3)	-0.004(3)	0.004(3)
N10	0.024(4)	0.014(3)	0.020(4)	0.004(3)	0.003(3)	0.004(3)
N11	0.025(4)	0.023(3)	0.021(4)	0.000(3)	-0.003(3)	0.005(3)
N8	0.016(3)	0.020(3)	0.025(4)	0.004(3)	-0.002(3)	0.001(2)
N9	0.019(3)	0.023(3)	0.024(4)	0.002(3)	-0.005(3)	0.003(3)
N12	0.024(4)	0.014(3)	0.022(4)	0.000(2)	-0.005(3)	0.001(3)
N13	0.023(4)	0.023(3)	0.018(4)	0.001(3)	-0.005(3)	0.001(3)

N14	0.023(3)	0.016(3)	0.020(3)	−0.001(3)	0.001(3)	0.001(2)
C1	0.025(4)	0.028(4)	0.035(5)	0.004(3)	0.000(4)	0.002(4)
C2	0.024(4)	0.039(5)	0.041(6)	0.012(5)	−0.002(4)	0.001(4)
C3	0.024(4)	0.026(5)	0.046(6)	0.011(4)	0.011(4)	0.009(4)
C4	0.025(5)	0.027(4)	0.031(5)	0.003(4)	−0.003(4)	−0.007(3)
C5	0.039(5)	0.022(4)	0.049(6)	−0.012(4)	0.008(5)	−0.007(5)
C6	0.051(6)	0.022(4)	0.037(6)	−0.014(4)	0.009(5)	0.004(4)
C7	0.035(5)	0.031(5)	0.023(5)	−0.003(4)	−0.004(4)	0.002(4)
C8	0.054(6)	0.026(4)	0.022(5)	0.002(4)	−0.008(4)	0.001(4)
C9	0.052(6)	0.030(5)	0.014(4)	−0.002(3)	0.002(4)	−0.008(4)
C13	0.013(4)	0.021(4)	0.024(4)	−0.006(3)	−0.001(4)	−0.003(3)
C14	0.022(4)	0.008(3)	0.032(5)	−0.002(3)	0.002(3)	0.002(3)
C15	0.018(4)	0.016(4)	0.024(5)	−0.001(3)	0.001(3)	0.002(3)
C16	0.025(5)	0.027(4)	0.026(5)	0.005(4)	0.012(4)	0.006(3)
C17	0.025(4)	0.019(4)	0.018(5)	0.001(3)	0.001(3)	0.000(3)
C18	0.017(4)	0.019(3)	0.016(4)	0.007(3)	−0.003(3)	0.000(3)
C19	0.015(4)	0.017(3)	0.023(4)	0.003(3)	−0.003(3)	0.000(3)
C20	0.020(4)	0.020(4)	0.020(4)	0.002(3)	−0.001(3)	0.001(3)
C21	0.019(4)	0.021(4)	0.035(5)	−0.003(4)	−0.008(4)	0.000(3)
C22	0.025(4)	0.021(4)	0.020(4)	−0.004(3)	−0.007(3)	−0.001(3)
C10	0.035(5)	0.029(5)	0.028(5)	0.007(4)	−0.010(4)	−0.001(4)
C11	0.066(8)	0.045(6)	0.049(7)	−0.022(5)	−0.037(6)	0.035(5)
C12	0.051(7)	0.051(6)	0.042(7)	0.025(5)	−0.018(5)	−0.023(5)
C23	0.020(4)	0.030(4)	0.025(4)	0.001(3)	0.000(4)	0.000(4)
C24	0.022(4)	0.035(5)	0.031(5)	0.007(4)	0.006(4)	0.002(3)
C25	0.017(4)	0.028(4)	0.037(5)	0.000(4)	−0.007(4)	0.003(3)
C26	0.021(4)	0.023(4)	0.020(4)	−0.003(3)	−0.001(4)	0.001(4)
C27	0.037(5)	0.018(4)	0.027(5)	0.007(3)	0.009(4)	0.006(4)
C28	0.033(5)	0.024(4)	0.018(4)	0.003(3)	0.000(4)	0.005(4)
C29	0.026(4)	0.019(4)	0.024(5)	0.002(3)	0.002(4)	−0.001(3)
C30	0.026(5)	0.026(4)	0.023(4)	−0.004(3)	0.005(4)	−0.003(4)
C31	0.030(5)	0.027(4)	0.014(4)	0.002(3)	−0.005(3)	−0.006(4)
C32	0.023(4)	0.029(4)	0.021(4)	0.000(3)	0.001(3)	0.009(3)
C33	0.047(6)	0.043(5)	0.021(5)	0.005(4)	0.006(4)	0.020(5)
C34	0.051(6)	0.032(5)	0.038(6)	−0.017(4)	0.020(5)	−0.014(5)
B1	0.041(6)	0.026(5)	0.036(6)	−0.006(5)	0.012(5)	0.005(5)
B2	0.027(5)	0.021(5)	0.028(5)	0.004(4)	−0.006(4)	−0.002(4)

Table 4. Bond lengths and angles for mo\_harman\_aqm\_2061\_0m

Atom–Atom	Length [Å]
W1–P1	2.479(2)
W1–N3	2.213(6)
W1–N1	2.264(6)
W1–N5	2.238(6)
W1–N7	1.778(6)
W1–C13	2.250(7)
W1–C14	2.190(6)

W2–P2	2.475(2)
W2–N10	2.221(6)
W2–N8	2.255(6)
W2–N12	2.231(6)
W2–N14	1.768(6)
W2–C18	2.228(7)
W2–C19	2.193(7)
P1–C10	1.811(8)

P1–C11	1.832(9)
P1–C12	1.801(10)
P2–C32	1.812(8)
P2–C33	1.827(9)
P2–C34	1.817(9)
O1–N7	1.234(8)
O2–N14	1.236(7)
N3–N4	1.360(9)
N3–C4	1.328(10)
N4–C6	1.356(10)
N4–B1	1.540(13)
N1–N2	1.370(9)
N1–C1	1.321(10)
N2–C3	1.343(10)
N2–B1	1.533(13)
N5–N6	1.366(9)
N5–C7	1.344(10)
N6–C9	1.354(10)
N6–B1	1.522(12)
N10–N11	1.354(9)
N10–C26	1.338(10)
N11–C28	1.353(10)
N11–B2	1.524(11)
N8–N9	1.370(9)
N8–C23	1.336(10)
N9–C25	1.344(10)
N9–B2	1.533(11)
N12–N13	1.375(9)
N12–C29	1.323(10)
N13–C31	1.331(10)
N13–B2	1.533(11)
C1–H1	0.9500
C1–C2	1.416(12)
C2–H2	0.9500
C2–C3	1.366(13)
C3–H3	0.9500
C4–H4	0.9500
C4–C5	1.390(12)
C5–H5	0.9500
C5–C6	1.357(13)
C6–H6	0.9500
C7–H7	0.9500
C7–C8	1.384(12)
C8–H8	0.9500
C8–C9	1.364(12)
C9–H9	0.9500
C13–H13	1.0000
C13–C14	1.452(11)

C13–C17	1.470(11)
C14–H14	1.0000
C14–C15	1.532(10)
C15–H15	1.0000
C15–C16	1.508(11)
C15–C20	1.551(10)
C16–H16	0.9500
C16–C17	1.350(11)
C17–H17	0.9500
C18–H18	1.0000
C18–C19	1.440(10)
C18–C22	1.512(10)
C19–H19	1.0000
C19–C20	1.530(10)
C20–H20	1.0000
C20–C21	1.503(10)
C21–H21A	0.9900
C21–H21B	0.9900
C21–C22	1.507(11)
C22–H22A	0.9900
C22–H22B	0.9900
C10–H10A	0.9800
C10–H10B	0.9800
C10–H10C	0.9800
C11–H11A	0.9800
C11–H11B	0.9800
C11–H11C	0.9800
C12–H12A	0.9800
C12–H12B	0.9800
C12–H12C	0.9800
C23–H23	0.9500
C23–C24	1.401(11)
C24–H24	0.9500
C24–C25	1.361(12)
C25–H25	0.9500
C26–H26	0.9500
C26–C27	1.391(11)
C27–H27	0.9500
C27–C28	1.365(12)
C28–H28	0.9500
C29–H29	0.9500
C29–C30	1.391(11)
C30–H30	0.9500
C30–C31	1.376(11)
C31–H31	0.9500
C32–H32A	0.9800
C32–H32B	0.9800
C32–H32C	0.9800

C33–H33A	0.9800
C33–H33B	0.9800
C33–H33C	0.9800
C34–H34A	0.9800
C34–H34B	0.9800
C34–H34C	0.9800
B1–H1A	1.02(8)
B2–H2A	1.06(7)
<b>Atom–Atom– Atom</b>	<b>Angle [°]</b>
N3–W1–P1	85.46(18)
N3–W1–N1	84.7(2)
N3–W1–N5	76.7(2)
N3–W1–C13	163.3(3)
N1–W1–P1	87.00(18)
N5–W1–P1	159.59(17)
N5–W1–N1	81.7(2)
N5–W1–C13	116.9(2)
N7–W1–P1	87.3(2)
N7–W1–N3	90.1(3)
N7–W1–N1	172.6(3)
N7–W1–N5	102.3(3)
N7–W1–C13	95.9(3)
N7–W1–C14	96.2(3)
C13–W1–P1	79.3(2)
C13–W1–N1	87.7(3)
C14–W1–P1	117.5(2)
C14–W1–N3	156.4(3)
C14–W1–N1	90.6(3)
C14–W1–N5	79.8(3)
C14–W1–C13	38.1(3)
N10–W2–P2	83.05(17)
N10–W2–N8	85.4(2)
N10–W2–N12	76.7(2)
N10–W2–C18	162.6(2)
N8–W2–P2	85.04(17)
N12–W2–P2	156.08(17)
N12–W2–N8	80.8(3)
N14–W2–P2	88.72(19)
N14–W2–N10	88.8(3)
N14–W2–N8	171.9(2)
N14–W2–N12	103.3(3)
N14–W2–C18	95.3(3)
N14–W2–C19	98.8(3)
C18–W2–P2	80.2(2)
C18–W2–N8	88.7(3)
C18–W2–N12	118.5(2)

C19–W2–P2	118.0(2)
C19–W2–N10	157.6(3)
C19–W2–N8	88.7(2)
C19–W2–N12	81.0(2)
C19–W2–C18	38.0(3)
C10–P1–W1	122.0(3)
C10–P1–C11	102.2(4)
C11–P1–W1	114.2(4)
C12–P1–W1	112.7(3)
C12–P1–C10	100.9(5)
C12–P1–C11	102.5(6)
C32–P2–W2	122.2(3)
C32–P2–C33	102.1(4)
C32–P2–C34	102.0(4)
C33–P2–W2	112.6(3)
C34–P2–W2	113.2(3)
C34–P2–C33	102.3(5)
N4–N3–W1	122.2(5)
C4–N3–W1	130.5(6)
C4–N3–N4	107.3(7)
N3–N4–B1	119.9(7)
C6–N4–N3	108.5(7)
C6–N4–B1	130.5(8)
N2–N1–W1	119.2(5)
C1–N1–W1	133.4(6)
C1–N1–N2	107.3(6)
N1–N2–B1	122.1(7)
C3–N2–N1	108.4(7)
C3–N2–B1	129.3(7)
N6–N5–W1	120.3(5)
C7–N5–W1	133.6(6)
C7–N5–N6	105.7(7)
N5–N6–B1	121.8(7)
C9–N6–N5	109.4(7)
C9–N6–B1	128.8(7)
O1–N7–W1	173.3(6)
N11–N10–W2	122.9(5)
C26–N10–W2	129.5(6)
C26–N10–N11	107.0(6)
N10–N11–B2	118.9(6)
C28–N11–N10	109.0(7)
C28–N11–B2	129.3(7)
N9–N8–W2	119.7(5)
C23–N8–W2	133.8(6)
C23–N8–N9	106.5(6)
N8–N9–B2	121.4(6)
C25–N9–N8	109.4(7)
C25–N9–B2	129.1(7)

N13-N12-W2	119.9(5)
C29-N12-W2	133.3(6)
C29-N12-N13	106.4(6)
N12-N13-B2	121.6(6)
C31-N13-N12	109.2(7)
C31-N13-B2	129.0(7)
O2-N14-W2	172.7(5)
N1-C1-H1	124.8
N1-C1-C2	110.4(8)
C2-C1-H1	124.8
C1-C2-H2	128.2
C3-C2-C1	103.7(8)
C3-C2-H2	128.2
N2-C3-C2	110.2(8)
N2-C3-H3	124.9
C2-C3-H3	124.9
N3-C4-H4	125.0
N3-C4-C5	110.1(8)
C5-C4-H4	125.0
C4-C5-H5	127.4
C6-C5-C4	105.3(7)
C6-C5-H5	127.4
N4-C6-C5	108.9(8)
N4-C6-H6	125.5
C5-C6-H6	125.5
N5-C7-H7	124.5
N5-C7-C8	111.1(8)
C8-C7-H7	124.5
C7-C8-H8	127.5
C9-C8-C7	105.0(8)
C9-C8-H8	127.5
N6-C9-C8	108.9(8)
N6-C9-H9	125.6
C8-C9-H9	125.6
W1-C13-H13	117.5
C14-C13-W1	68.7(4)
C14-C13-H13	117.5
C14-C13-C17	106.1(7)
C17-C13-W1	118.9(5)
C17-C13-H13	117.5
W1-C14-H14	116.0
C13-C14-W1	73.2(4)
C13-C14-H14	116.0
C13-C14-C15	109.0(7)
C15-C14-W1	119.1(5)
C15-C14-H14	116.0
C14-C15-H15	108.7
C14-C15-C20	113.3(6)

C16-C15-C14	102.3(6)
C16-C15-H15	108.7
C16-C15-C20	114.7(6)
C20-C15-H15	108.7
C15-C16-H16	124.4
C17-C16-C15	111.1(7)
C17-C16-H16	124.4
C13-C17-H17	124.3
C16-C17-C13	111.3(7)
C16-C17-H17	124.3
W2-C18-H18	116.8
C19-C18-W2	69.7(4)
C19-C18-H18	116.8
C19-C18-C22	108.8(6)
C22-C18-W2	118.9(5)
C22-C18-H18	116.8
W2-C19-H19	115.6
C18-C19-W2	72.3(4)
C18-C19-H19	115.6
C18-C19-C20	109.1(6)
C20-C19-W2	120.8(5)
C20-C19-H19	115.6
C15-C20-H20	108.7
C19-C20-C15	112.5(6)
C19-C20-H20	108.7
C21-C20-C15	113.4(6)
C21-C20-C19	104.6(6)
C21-C20-H20	108.7
C20-C21-H21A	110.2
C20-C21-H21B	110.2
C20-C21-C22	107.6(6)
H21A-C21-H21B	108.5
C22-C21-H21A	110.2
C22-C21-H21B	110.2
C18-C22-H22A	110.6
C18-C22-H22B	110.6
C21-C22-C18	105.7(6)
C21-C22-H22A	110.6
C21-C22-H22B	110.6
H22A-C22-H22B	108.7
P1-C10-H10A	109.5
P1-C10-H10B	109.5
P1-C10-H10C	109.5
H10A-C10-H10B	109.5
H10A-C10-H10C	109.5

H10B–C10–H10C	109.5
P1–C11–H11A	109.5
P1–C11–H11B	109.5
P1–C11–H11C	109.5
H11A–C11–H11B	109.5
H11A–C11–H11C	109.5
H11B–C11–H11C	109.5
P1–C12–H12A	109.5
P1–C12–H12B	109.5
P1–C12–H12C	109.5
H12A–C12–H12B	109.5
H12A–C12–H12C	109.5
H12B–C12–H12C	109.5
N8–C23–H23	125.0
N8–C23–C24	109.9(7)
C24–C23–H23	125.0
C23–C24–H24	127.4
C25–C24–C23	105.2(7)
C25–C24–H24	127.4
N9–C25–C24	109.0(7)
N9–C25–H25	125.5
C24–C25–H25	125.5
N10–C26–H26	124.9
N10–C26–C27	110.2(8)
C27–C26–H26	124.9
C26–C27–H27	127.6
C28–C27–C26	104.9(7)
C28–C27–H27	127.6
N11–C28–C27	109.0(8)
N11–C28–H28	125.5
C27–C28–H28	125.5
N12–C29–H29	124.6
N12–C29–C30	110.8(8)
C30–C29–H29	124.6
C29–C30–H30	127.8
C31–C30–C29	104.4(7)
C31–C30–H30	127.8
N13–C31–C30	109.2(7)

N13–C31–H31	125.4
C30–C31–H31	125.4
P2–C32–H32A	109.5
P2–C32–H32B	109.5
P2–C32–H32C	109.5
H32A–C32–H32B	109.5
H32A–C32–H32C	109.5
H32B–C32–H32C	109.5
P2–C33–H33A	109.5
P2–C33–H33B	109.5
P2–C33–H33C	109.5
H33A–C33–H33B	109.5
H33A–C33–H33C	109.5
H33B–C33–H33C	109.5
P2–C34–H34A	109.5
P2–C34–H34B	109.5
P2–C34–H34C	109.5
H34A–C34–H34B	109.5
H34A–C34–H34C	109.5
H34B–C34–H34C	109.5
N4–B1–H1A	110(5)
N2–B1–N4	108.7(8)
N2–B1–H1A	109(5)
N6–B1–N4	106.9(8)
N6–B1–N2	108.5(7)
N6–B1–H1A	113(5)
N11–B2–N9	111.5(7)
N11–B2–N13	105.2(7)
N11–B2–H2A	111(3)
N9–B2–N13	108.8(6)
N9–B2–H2A	108(4)
N13–B2–H2A	112(4)

Table 4. Torsion angles for mo\_harman\_aqm\_2061\_0m

Atom–Atom–Atom–Atom	Torsion Angle [°]
W1–N3–N4–C6	–179.0(6)

W1–N3–N4–B1	–10.1(11)
W1–N3–C4–C5	179.0(6)
W1–N1–N2–C3	–177.6(5)

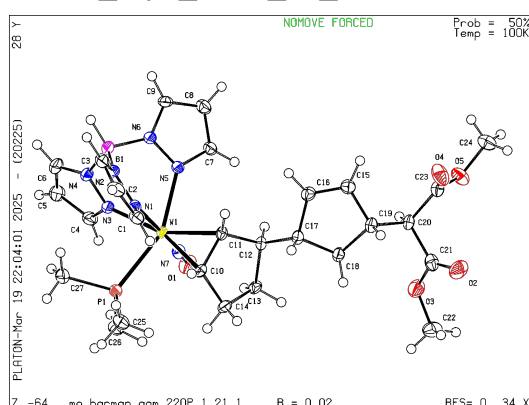
W1-N1-N2-B1	5.9(10)
W1-N1-C1-C2	177.5(5)
W1-N5-N6-C9	-173.2(5)
W1-N5-N6-B1	6.3(9)
W1-N5-C7-C8	173.0(6)
W1-C13-C14-C15	115.7(5)
W1-C13-C17-C16	-72.2(8)
W1-C14-C15-C16	78.7(7)
W1-C14-C15-C20	-157.3(5)
W2-N10-N11-C28	-173.0(5)
W2-N10-N11-B2	-10.3(9)
W2-N10-C26-C27	172.3(5)
W2-N8-N9-C25	-178.0(5)
W2-N8-N9-B2	5.6(8)
W2-N8-C23-C24	177.6(5)
W2-N12-N13-C31	174.4(5)
W2-N12-N13-B2	-0.5(9)
W2-N12-C29-C30	-172.4(5)
W2-C18-C19-C20	117.3(5)
W2-C18-C22-C21	-66.6(7)
W2-C19-C20-C15	-170.3(5)
W2-C19-C20-C21	66.1(7)
N3-N4-C6-C5	-0.4(11)
N3-N4-B1-N2	64.1(10)
N3-N4-B1-N6	-52.8(11)
N3-C4-C5-C6	0.1(11)
N4-N3-C4-C5	-0.4(10)
N1-N2-C3-C2	-0.1(10)
N1-N2-B1-N4	-61.5(10)
N1-N2-B1-N6	54.4(10)
N1-C1-C2-C3	-0.8(9)
N2-N1-C1-C2	0.7(9)
N5-N6-C9-C8	-1.3(9)
N5-N6-B1-N4	54.9(10)
N5-N6-B1-N2	-62.2(10)
N5-C7-C8-C9	-1.2(10)
N6-N5-C7-C8	0.5(9)
N10-N11-C28-C27	0.8(9)
N10-N11-B2-N9	63.3(9)
N10-N11-B2-N13	-54.4(9)
N10-C26-C27-C28	-0.7(9)
N11-N10-C26-C27	1.2(9)
N8-N9-C25-C24	-0.3(9)
N8-N9-B2-N11	-60.8(9)
N8-N9-B2-N13	54.8(9)
N8-C23-C24-C25	0.7(9)
N9-N8-C23-C24	-0.8(9)
N12-N13-C31-C30	-1.1(9)

N12-N13-B2-N11	61.3(9)
N12-N13-B2-N9	-58.3(9)
N12-C29-C30-C31	-0.9(9)
N13-N12-C29-C30	0.3(8)
C1-N1-N2-C3	-0.4(9)
C1-N1-N2-B1	-176.8(7)
C1-C2-C3-N2	0.6(10)
C3-N2-B1-N4	122.8(9)
C3-N2-B1-N6	-121.3(9)
C4-N3-N4-C6	0.5(10)
C4-N3-N4-B1	169.4(8)
C4-C5-C6-N4	0.2(12)
C6-N4-B1-N2	-129.8(10)
C6-N4-B1-N6	113.3(10)
C7-N5-N6-C9	0.5(8)
C7-N5-N6-B1	-180.0(8)
C7-C8-C9-N6	1.5(10)
C9-N6-B1-N4	-125.7(9)
C9-N6-B1-N2	117.2(9)
C13-C14-C15-C16	-2.2(8)
C13-C14-C15-C20	121.8(7)
C14-C13-C17-C16	1.9(9)
C14-C15-C16-C17	3.5(9)
C14-C15-C20-C19	173.1(7)
C14-C15-C20-C21	-68.4(9)
C15-C16-C17-C13	-3.5(10)
C15-C20-C21-C22	-102.6(7)
C16-C15-C20-C19	-69.9(9)
C16-C15-C20-C21	48.6(9)
C17-C13-C14-W1	-115.3(5)
C17-C13-C14-C15	0.4(8)
C18-C19-C20-C15	109.3(7)
C18-C19-C20-C21	-14.2(8)
C19-C18-C22-C21	10.1(8)
C19-C20-C21-C22	20.4(8)
C20-C15-C16-C17	-119.6(8)
C20-C21-C22-C18	-19.1(8)
C22-C18-C19-W2	-114.7(5)
C22-C18-C19-C20	2.6(8)
C23-N8-N9-C25	0.7(8)
C23-N8-N9-B2	-175.7(6)
C23-C24-C25-N9	-0.2(9)
C25-N9-B2-N11	123.6(8)
C25-N9-B2-N13	-120.8(8)
C26-N10-N11-C28	-1.2(9)
C26-N10-N11-B2	161.5(7)
C26-C27-C28-N11	-0.1(9)
C28-N11-B2-N9	-137.9(8)



C28–N11–B2–N13	104.3(9)
C29–N12–N13–C31	0.5(8)
C29–N12–N13–B2	–174.4(7)
C29–C30–C31–N13	1.2(9)
C31–N13–B2–N11	–112.5(9)
C31–N13–B2–N9	127.9(8)
B1–N4–C6–C5	–167.7(10)
B1–N2–C3–C2	176.0(8)
B1–N6–C9–C8	179.2(8)
B2–N11–C28–C27	–159.6(8)
B2–N9–C25–C24	175.7(7)
B2–N13–C31–C30	173.3(7)

## Structure Report for mo\_harman\_aqm\_2207\_x2\_0m



A yellow, plate shaped crystal of mo\_harman\_aqm\_2207\_x2\_0m measuring 0.044×0.089×0.158 mm was coated with Paratone oil and mounted on a MiTeGen micromount. Data for mo\_harman\_aqm\_2207\_x2\_0m were measured on a Bruker D8 VENTURE dual wavelength Mo/Cu Kappa four-circle diffractometer equipped with a PHOTON III detector and an Incoatec IμS 3.0 microfocus sealed X-ray tube (Mo  $K_{\alpha}$ ,  $\lambda=0.71073$  Å) using a HELIOS double bounce multilayer mirror as monochromator. The crystal temperature was controlled with an Oxford Cryostream 800low temperature device. Data collection and processing were done within the Bruker APEX4 software suite.<sup>19</sup> All data were integrated with the Bruker SAINT 8.40B software using a narrow-frame algorithm. Data were corrected for absorption effects using a Multi-Scan method (SADABS). The structure was solved by dual methods with SHELXT 2018/2<sup>20</sup> and refined by full-matrix least-squares methods against  $F^2$  using SHELXL 2018/3<sup>21</sup> within OLEX2.<sup>22</sup> All non-hydrogen atoms were refined with anisotropically. Hydrogen atoms were placed in geometrically calculated positions with  $U_{iso} = 1.2U_{equiv}$  of the parent atom ( $1.5U_{equiv}$  for methyl). This report and the CIF file were generated using FinalCif.<sup>23</sup>

<sup>19</sup> APEX4, Saint, SADABS; Bruker AXS Inc. 2019.

<sup>20</sup> Sheldrick, G. M. SHELXT – Integrated space-group and crystal-structure determination. *Acta Cryst. Sect. A Found. Adv.* **2015**, 71, 3-8.

<sup>21</sup> Sheldrick, G. M. Crystal structure refinement with SHELXL. *Acta Cryst. Sect. C Struct. Chem.* **2015**, 71, 3-8.

<sup>22</sup> Dolomanov, O. V.; Bourhis, L. J.; Gildea, R. J.; Howard, J. A. K.; Puschmann, H. OLEX2: a completed structure solution, refinement and analysis program. *J. Appl. Cryst.* **2009**, 42, 339-341.

<sup>23</sup> Kratzert, D. FinalCif, <https://dkratzert.de/finalcif.html>.

Table 1. Crystal data and structure refinement for mo\_harman\_aqm\_2207\_x2\_0m

CCDC number	
Empirical formula	$C_{27}H_{39}BN_7O_5PW$
Formula weight	767.28
Temperature [K]	100.00
Wavelength [Å]	0.71073
Crystal size [mm <sup>3</sup> ]	0.044×0.089×0.158
Crystal habit	yellow plate
Crystal system	monoclinic
Space group	$P2_1$ (4)
<i>a</i> [Å]	8.3017(3)
<i>b</i> [Å]	22.0514(7)
<i>c</i> [Å]	8.6547(3)
$\alpha$ [°]	90
$\beta$ [°]	104.0420(10)
$\gamma$ [°]	90
Volume [Å <sup>3</sup> ]	1537.02(9)
<i>Z</i>	2
$\rho_{\text{calc}}$ [gcm <sup>-3</sup> ]	1.658
$\mu$ [mm <sup>-1</sup> ]	3.858
<i>F</i> (000)	768
2 $\theta$ range [°]	3.69 to 56.58 (0.75 Å)
Index ranges	$-11 \leq h \leq 11$ $-29 \leq k \leq 29$ $-11 \leq l \leq 11$
Reflections collected	54603
Independent reflections	7630 [ $R_{\text{int}} = 0.0505$ ]
Data / Restraints / Parameters	7630 / 1 / 397
Goodness-of-fit on $F^2$	1.043
Final <i>R</i> indexes [ $I \geq 2\sigma(I)$ ]	$R_1 = 0.0215$ $wR_2 = 0.0448$
Final <i>R</i> indexes [all data]	$R_1 = 0.0235$ $wR_2 = 0.0455$
Largest peak/hole [eÅ <sup>-3</sup> ]	0.84/−0.43
Flack <i>X</i> parameter	−0.019(3)

Table 2. Atomic coordinates and  $U_{eq}$  [Å<sup>2</sup>] for mo\_harman\_aqm\_2207\_x2\_0m

Atom	x	y	z	$U_{eq}$
W1	0.58367(2)	0.54096(2)	0.54018(2)	0.01387(5)
P1	0.39662(15)	0.52321(5)	0.72141(14)	0.0182(3)
O1	0.2982(4)	0.5488(3)	0.2526(4)	0.0310(10)
O2	0.8046(5)	0.20667(17)	-0.1430(6)	0.0423(10)
O3	0.5841(5)	0.26593(17)	-0.1642(5)	0.0355(9)
O4	1.1386(5)	0.2910(2)	-0.0647(5)	0.0419(11)
O5	0.9828(5)	0.31949(17)	-0.3037(5)	0.0341(9)
N1	0.7876(4)	0.5467(3)	0.7645(4)	0.0176(9)
N2	0.8728(5)	0.59960(19)	0.8051(5)	0.0200(8)
N3	0.5358(6)	0.63682(19)	0.5875(5)	0.0201(10)
N4	0.6545(5)	0.67506(18)	0.6710(5)	0.0227(9)
N5	0.7726(5)	0.59113(17)	0.4466(5)	0.0171(8)
N6	0.8592(5)	0.63753(17)	0.5316(5)	0.0194(8)
N7	0.4173(4)	0.5432(3)	0.3688(4)	0.0199(7)
C1	0.8564(6)	0.5063(2)	0.8777(6)	0.0233(10)
H1	0.821375	0.465376	0.880415	0.028
C2	0.9866(6)	0.5328(4)	0.9908(5)	0.0276(15)
H2	1.055624	0.514455	1.082592	0.033
C3	0.9921(7)	0.5914(3)	0.9389(6)	0.0270(12)
H3	1.068558	0.621448	0.989977	0.032
C4	0.3969(7)	0.6692(2)	0.5406(7)	0.0264(12)
H4	0.294114	0.653990	0.479238	0.032
C5	0.4246(7)	0.7284(2)	0.5947(7)	0.0327(13)
H5	0.346508	0.760647	0.578771	0.039
C6	0.5876(7)	0.7305(2)	0.6756(7)	0.0325(13)
H6	0.644375	0.765197	0.726552	0.039
C7	0.8179(6)	0.5889(2)	0.3095(6)	0.0213(10)
H7	0.777154	0.560437	0.226972	0.026
C8	0.9332(7)	0.6341(2)	0.3036(6)	0.0274(11)
H8	0.984253	0.642871	0.219084	0.033
C9	0.9566(6)	0.6631(2)	0.4474(6)	0.0226(10)
H9	1.030207	0.696106	0.481694	0.027
C10	0.6012(6)	0.4409(2)	0.5660(6)	0.0168(10)
H10	0.659170	0.425514	0.673884	0.020

C11	0.7081(6)	0.4622(2)	0.4668(5)	0.0168(9)
H11	0.829842	0.459421	0.516735	0.020
C12	0.6523(6)	0.4334(2)	0.3012(5)	0.0173(9)
H12	0.640(7)	0.464(2)	0.212(6)	0.021
C13	0.4759(6)	0.4103(2)	0.2932(6)	0.0216(10)
H13A	0.454221	0.372185	0.231058	0.026
H13B	0.392334	0.440825	0.242496	0.026
C14	0.4685(7)	0.3992(2)	0.4672(6)	0.0226(10)
H14A	0.356(8)	0.405(3)	0.488(7)	0.027
H14B	0.483(7)	0.361(3)	0.494(7)	0.027
C15	0.9911(6)	0.3762(2)	0.1487(6)	0.0243(10)
H15	1.088807	0.386035	0.115318	0.029
C16	0.9361(6)	0.4067(2)	0.2577(6)	0.0228(10)
H16	0.993009	0.440459	0.313881	0.027
C17	0.7761(6)	0.3829(2)	0.2836(5)	0.0199(9)
H17	0.800483	0.357410	0.382114	0.024
C18	0.7184(6)	0.3411(2)	0.1369(6)	0.0215(10)
H18A	0.663846	0.304240	0.165461	0.026
H18B	0.639409	0.362537	0.050108	0.026
C19	0.8785(7)	0.3243(2)	0.0856(6)	0.0211(10)
H19	0.926059	0.286535	0.142657	0.025
C20	0.8460(6)	0.3132(2)	−0.0969(6)	0.0211(10)
H20	0.782310	0.348227	−0.155033	0.025
C21	0.7443(7)	0.2552(2)	−0.1399(6)	0.0265(11)
C22	0.4792(7)	0.2124(3)	−0.1830(7)	0.0383(14)
H22A	0.444114	0.201603	−0.296109	0.057
H22B	0.381138	0.220764	−0.142321	0.057
H22C	0.541602	0.178571	−0.123360	0.057
C23	1.0071(7)	0.3060(2)	−0.1481(6)	0.0266(11)
C24	1.1305(8)	0.3187(3)	−0.3655(8)	0.0403(14)
H24A	1.101724	0.331839	−0.477001	0.060
H24B	1.175575	0.277410	−0.358640	0.060
H24C	1.213863	0.346188	−0.302694	0.060
C25	0.4227(7)	0.4567(3)	0.8484(6)	0.0279(11)
H25A	0.334777	0.455701	0.906108	0.042
H25B	0.531205	0.458409	0.924749	0.042
H25C	0.416323	0.420142	0.782874	0.042
C26	0.1790(6)	0.5197(2)	0.6211(6)	0.0243(11)
H26A	0.158099	0.483506	0.553484	0.036
H26B	0.148383	0.555977	0.554991	0.036
H26C	0.112459	0.517767	0.700239	0.036
C27	0.4097(7)	0.5824(3)	0.8720(6)	0.0294(12)
H27A	0.353489	0.619073	0.821865	0.044
H27B	0.526538	0.591662	0.920302	0.044
H27C	0.356009	0.568301	0.954554	0.044
B1	0.8373(7)	0.6553(3)	0.6973(7)	0.0230(11)

H1A	0.919(6)	0.693(2)	0.744(6)	0.021(13)
-----	----------	----------	----------	-----------

$U_{eq}$  is defined as 1/3 of the trace of the orthogonalized  $U_{ij}$  tensor.

**Table 3. Anisotropic displacement parameters ( $\text{\AA}^2$ ) for mo\_harman\_aqm\_2207\_x2\_0m. The anisotropic displacement factor exponent takes the form:  $-2\pi^2 [h^2(a^*)^2 U_{11} + k^2(b^*)^2 U_{22} + \dots + 2hka^*b^* U_{12}]$**

Atom	$U_{11}$	$U_{22}$	$U_{33}$	$U_{23}$	$U_{13}$	$U_{12}$
W1	0.01267(7)	0.01438(7)	0.01386(7)	−0.00198(11)	0.00185(5)	−0.00051(12)
P1	0.0159(6)	0.0221(7)	0.0162(5)	−0.0014(4)	0.0034(4)	−0.0021(4)
O1	0.0225(16)	0.038(3)	0.0243(15)	−0.0045(19)	−0.0110(12)	0.002(2)
O2	0.038(3)	0.023(2)	0.065(3)	−0.0051(19)	0.012(2)	0.0036(18)
O3	0.025(2)	0.034(2)	0.045(2)	−0.0105(18)	0.0043(18)	0.0005(17)
O4	0.025(2)	0.065(3)	0.035(2)	−0.007(2)	0.0069(19)	0.012(2)
O5	0.036(2)	0.040(2)	0.031(2)	0.0087(17)	0.0174(18)	0.0042(18)
N1	0.0138(15)	0.022(3)	0.0173(14)	−0.003(2)	0.0045(12)	0.001(2)
N2	0.014(2)	0.026(2)	0.019(2)	−0.0087(17)	0.0028(17)	−0.0068(16)
N3	0.016(2)	0.020(2)	0.026(2)	−0.0054(17)	0.007(2)	−0.0020(18)
N4	0.021(2)	0.0167(19)	0.032(2)	−0.0066(17)	0.0090(18)	−0.0014(16)
N5	0.015(2)	0.0175(19)	0.0192(19)	−0.0003(15)	0.0044(16)	0.0007(15)
N6	0.016(2)	0.0187(19)	0.024(2)	−0.0028(16)	0.0068(17)	−0.0011(15)
N7	0.0201(16)	0.0177(16)	0.0214(15)	0.002(3)	0.0044(13)	0.005(3)
C1	0.019(3)	0.032(3)	0.020(2)	0.000(2)	0.006(2)	−0.001(2)
C2	0.018(2)	0.047(5)	0.0154(18)	0.002(3)	0.0005(15)	−0.005(3)
C3	0.020(3)	0.043(3)	0.018(2)	−0.011(2)	0.005(2)	−0.009(2)
C4	0.022(3)	0.023(3)	0.037(3)	0.000(2)	0.013(2)	0.000(2)
C5	0.033(3)	0.019(2)	0.050(3)	−0.001(2)	0.019(3)	0.004(2)
C6	0.035(3)	0.018(2)	0.049(3)	−0.011(2)	0.018(3)	−0.003(2)
C7	0.023(3)	0.020(2)	0.023(2)	0.0012(19)	0.010(2)	0.0001(19)
C8	0.031(3)	0.028(3)	0.027(3)	0.002(2)	0.015(2)	−0.001(2)
C9	0.017(2)	0.018(2)	0.035(3)	0.000(2)	0.011(2)	−0.0024(18)
C10	0.017(3)	0.013(2)	0.019(2)	−0.0018(17)	0.001(2)	0.0011(19)
C11	0.016(2)	0.016(2)	0.018(2)	−0.0025(18)	0.0014(18)	0.0035(18)
C12	0.019(2)	0.017(2)	0.016(2)	−0.0030(17)	0.0045(18)	0.0012(18)

C13	0.016(2)	0.023(2)	0.024(2)	−0.0082(19)	0.0008(19)	−0.0041(19)
C14	0.022(3)	0.016(2)	0.030(3)	−0.004(2)	0.006(2)	−0.0042(19)
C15	0.018(3)	0.028(3)	0.026(2)	−0.003(2)	0.004(2)	0.000(2)
C16	0.018(2)	0.024(3)	0.025(2)	−0.004(2)	0.002(2)	−0.0011(19)
C17	0.023(3)	0.018(2)	0.018(2)	−0.0026(18)	0.0058(19)	0.0010(19)
C18	0.022(3)	0.019(2)	0.024(2)	−0.0055(19)	0.006(2)	0.0000(19)
C19	0.024(3)	0.018(2)	0.021(2)	−0.002(2)	0.005(2)	0.003(2)
C20	0.025(3)	0.016(2)	0.022(2)	−0.0040(18)	0.006(2)	0.0033(19)
C21	0.026(3)	0.033(3)	0.020(2)	−0.003(2)	0.005(2)	0.004(2)
C22	0.027(3)	0.043(3)	0.043(3)	−0.004(3)	0.006(3)	−0.010(3)
C23	0.030(3)	0.023(3)	0.029(3)	−0.005(2)	0.011(2)	0.001(2)
C24	0.042(4)	0.041(3)	0.045(3)	0.001(3)	0.026(3)	−0.008(3)
C25	0.030(3)	0.032(3)	0.023(2)	0.005(2)	0.011(2)	−0.001(2)
C26	0.016(2)	0.035(3)	0.021(2)	−0.0018(18)	0.0030(19)	−0.0017(18)
C27	0.028(3)	0.035(3)	0.028(3)	−0.010(2)	0.011(2)	−0.006(2)
B1	0.021(3)	0.022(3)	0.028(3)	−0.009(2)	0.008(2)	−0.004(2)

Table 4. Bond lengths and angles for mo\_harman\_aqm\_2207\_x2\_0m

Atom–Atom	Length [Å]		
W1–P1	2.4913(11)	N3–C4	1.333(7)
W1–N1	2.249(3)	N4–C6	1.346(6)
W1–N3	2.207(4)	N4–B1	1.542(7)
W1–N5	2.226(4)	N5–N6	1.360(5)
W1–N7	1.765(3)	N5–C7	1.329(6)
W1–C10	2.219(5)	N6–C9	1.338(6)
W1–C11	2.191(4)	N6–B1	1.540(7)
P1–C25	1.813(5)	C1–H1	0.9500
P1–C26	1.806(5)	C1–C2	1.398(8)
P1–C27	1.830(5)	C2–H2	0.9500
O1–N7	1.233(4)	C2–C3	1.371(10)
O2–C21	1.184(6)	C3–H3	0.9500
O3–C21	1.317(6)	C4–H4	0.9500
O3–C22	1.453(7)	C4–C5	1.386(7)
O4–C23	1.201(7)	C5–H5	0.9500
O5–C23	1.345(6)	C5–C6	1.366(8)
O5–C24	1.452(6)	C6–H6	0.9500
N1–N2	1.365(7)	C7–H7	0.9500
N1–C1	1.344(7)	C7–C8	1.391(7)
N2–C3	1.341(7)	C8–H8	0.9500
N2–B1	1.528(7)	C8–C9	1.370(7)
N3–N4	1.363(6)	C9–H9	0.9500
		C10–H10	1.0000

C10–C11	1.454(7)
C10–C14	1.528(7)
C11–H11	1.0000
C11–C12	1.534(6)
C12–H12	1.01(5)
C12–C13	1.537(7)
C12–C17	1.548(6)
C13–H13A	0.9900
C13–H13B	0.9900
C13–C14	1.541(7)
C14–H14A	1.00(7)
C14–H14B	0.88(6)
C15–H15	0.9500
C15–C16	1.326(7)
C15–C19	1.494(7)
C16–H16	0.9500
C16–C17	1.495(7)
C17–H17	1.0000
C17–C18	1.548(6)
C18–H18A	0.9900
C18–H18B	0.9900
C18–C19	1.545(7)
C19–H19	1.0000
C19–C20	1.555(7)
C20–H20	1.0000
C20–C21	1.529(7)
C20–C23	1.516(7)
C22–H22A	0.9800
C22–H22B	0.9800
C22–H22C	0.9800
C24–H24A	0.9800
C24–H24B	0.9800
C24–H24C	0.9800
C25–H25A	0.9800
C25–H25B	0.9800
C25–H25C	0.9800
C26–H26A	0.9800
C26–H26B	0.9800
C26–H26C	0.9800
C27–H27A	0.9800
C27–H27B	0.9800
C27–H27C	0.9800
B1–H1A	1.09(5)
<b>Atom–Atom– Atom</b>	<b>Angle [°]</b>
N1–W1–P1	85.35(9)
N3–W1–P1	82.29(12)

N3–W1–N1	85.3(2)
N3–W1–N5	76.47(16)
N3–W1–C10	160.71(19)
N5–W1–P1	155.35(11)
N5–W1–N1	80.62(15)
N7–W1–P1	93.06(11)
N7–W1–N1	174.6(3)
N7–W1–N3	89.4(3)
N7–W1–N5	99.04(18)
N7–W1–C10	97.5(3)
N7–W1–C11	96.1(2)
C10–W1–P1	79.40(13)
C10–W1–N1	87.2(2)
C10–W1–N5	119.73(17)
C11–W1–P1	117.88(13)
C11–W1–N1	89.17(19)
C11–W1–N3	158.60(18)
C11–W1–N5	82.24(19)
C11–W1–C10	38.51(18)
C25–P1–W1	120.49(18)
C25–P1–C27	99.7(3)
C26–P1–W1	114.04(16)
C26–P1–C25	102.4(2)
C26–P1–C27	104.6(2)
C27–P1–W1	113.46(18)
C21–O3–C22	115.2(4)
C23–O5–C24	115.6(5)
N2–N1–W1	120.3(4)
C1–N1–W1	133.6(5)
C1–N1–N2	106.1(4)
N1–N2–B1	121.3(4)
C3–N2–N1	109.5(4)
C3–N2–B1	129.0(4)
N4–N3–W1	123.5(3)
C4–N3–W1	129.6(4)
C4–N3–N4	106.9(4)
N3–N4–B1	117.6(4)
C6–N4–N3	109.1(4)
C6–N4–B1	130.5(4)
N6–N5–W1	120.3(3)
C7–N5–W1	133.1(3)
C7–N5–N6	106.4(4)
N5–N6–B1	121.9(4)
C9–N6–N5	109.5(4)
C9–N6–B1	128.6(4)
O1–N7–W1	175.3(6)
N1–C1–H1	124.7
N1–C1–C2	110.6(6)



C2-C1-H1	124.7
C1-C2-H2	127.9
C3-C2-C1	104.2(5)
C3-C2-H2	127.9
N2-C3-C2	109.5(5)
N2-C3-H3	125.2
C2-C3-H3	125.2
N3-C4-H4	125.0
N3-C4-C5	109.9(5)
C5-C4-H4	125.0
C4-C5-H5	127.2
C6-C5-C4	105.5(5)
C6-C5-H5	127.2
N4-C6-C5	108.6(5)
N4-C6-H6	125.7
C5-C6-H6	125.7
N5-C7-H7	124.7
N5-C7-C8	110.7(4)
C8-C7-H7	124.7
C7-C8-H8	127.8
C9-C8-C7	104.4(4)
C9-C8-H8	127.8
N6-C9-C8	109.1(4)
N6-C9-H9	125.5
C8-C9-H9	125.5
W1-C10-H10	115.9
C11-C10-W1	69.7(3)
C11-C10-H10	115.9
C11-C10-C14	108.9(4)
C14-C10-W1	121.4(4)
C14-C10-H10	115.9
W1-C11-H11	115.0
C10-C11-W1	71.8(3)
C10-C11-H11	115.0
C10-C11-C12	109.2(4)
C12-C11-W1	122.9(3)
C12-C11-H11	115.0
C11-C12-H12	113(3)
C11-C12-C13	104.4(4)
C11-C12-C17	109.5(4)
C13-C12-H12	105(3)
C13-C12-C17	113.9(4)
C17-C12-H12	111(3)
C12-C13-H13A	110.6
C12-C13-H13B	110.6
C12-C13-C14	105.8(4)
H13A-C13-H13B	108.7

C14-C13-H13A	110.6
C14-C13-H13B	110.6
C10-C14-C13	104.9(4)
C10-C14-H14A	113(3)
C10-C14-H14B	114(4)
C13-C14-H14A	115(4)
C13-C14-H14B	112(4)
H14A-C14-H14B	99(5)
C16-C15-H15	124.6
C16-C15-C19	110.8(4)
C19-C15-H15	124.6
C15-C16-H16	123.2
C15-C16-C17	113.6(4)
C17-C16-H16	123.2
C12-C17-H17	108.8
C12-C17-C18	115.4(4)
C16-C17-C12	113.4(4)
C16-C17-H17	108.8
C16-C17-C18	101.3(4)
C18-C17-H17	108.8
C17-C18-H18A	110.7
C17-C18-H18B	110.7
H18A-C18-H18B	108.8
C19-C18-C17	105.2(4)
C19-C18-H18A	110.7
C19-C18-H18B	110.7
C15-C19-C18	102.5(4)
C15-C19-H19	108.7
C15-C19-C20	115.5(4)
C18-C19-H19	108.7
C18-C19-C20	112.4(4)
C20-C19-H19	108.7
C19-C20-H20	109.3
C21-C20-C19	109.2(4)
C21-C20-H20	109.3
C23-C20-C19	111.5(4)
C23-C20-H20	109.3
C23-C20-C21	108.4(4)
O2-C21-O3	125.1(5)
O2-C21-C20	123.4(5)
O3-C21-C20	111.4(4)
O3-C22-H22A	109.5
O3-C22-H22B	109.5
O3-C22-H22C	109.5
H22A-C22-H22B	109.5

H22A–C22–H22C	109.5
H22B–C22–H22C	109.5
O4–C23–O5	123.8(5)
O4–C23–C20	126.2(5)
O5–C23–C20	110.0(5)
O5–C24–H24A	109.5
O5–C24–H24B	109.5
O5–C24–H24C	109.5
H24A–C24–H24B	109.5
H24A–C24–H24C	109.5
H24B–C24–H24C	109.5
P1–C25–H25A	109.5
P1–C25–H25B	109.5
P1–C25–H25C	109.5
H25A–C25–H25B	109.5
H25A–C25–H25C	109.5
H25B–C25–H25C	109.5

P1–C26–H26A	109.5
P1–C26–H26B	109.5
P1–C26–H26C	109.5
H26A–C26–H26B	109.5
H26A–C26–H26C	109.5
H26B–C26–H26C	109.5
P1–C27–H27A	109.5
P1–C27–H27B	109.5
P1–C27–H27C	109.5
H27A–C27–H27B	109.5
H27A–C27–H27C	109.5
H27B–C27–H27C	109.5
N2–B1–N4	110.7(4)
N2–B1–N6	108.4(4)
N2–B1–H1A	112(3)
N4–B1–H1A	110(3)
N6–B1–N4	105.6(4)
N6–B1–H1A	110(3)

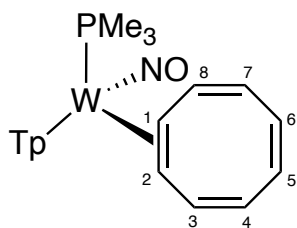
Table 5. Torsion angles for mo_harman_aqm_2207_x2_0m	
Atom–Atom–Atom–Atom	Torsion Angle [°]
W1–N1–N2–C3	–177.4(3)
W1–N1–N2–B1	–2.4(5)
W1–N1–C1–C2	177.4(3)
W1–N3–N4–C6	178.4(3)
W1–N3–N4–B1	15.5(6)
W1–N3–C4–C5	–178.4(4)
W1–N5–N6–C9	–175.9(3)
W1–N5–N6–B1	2.9(6)
W1–N5–C7–C8	174.4(4)
W1–C10–C11–C12	–119.4(3)
W1–C10–C14–C13	63.1(5)
W1–C11–C12–C13	–63.0(5)
W1–C11–C12–C17	174.7(3)
N1–N2–C3–C2	–0.8(5)
N1–N2–B1–N4	59.1(5)
N1–N2–B1–N6	–56.3(6)

N1-C1-C2-C3	0.0(6)
N2-N1-C1-C2	-0.4(5)
N3-N4-C6-C5	0.0(6)
N3-N4-B1-N2	-66.5(5)
N3-N4-B1-N6	50.6(5)
N3-C4-C5-C6	0.5(7)
N4-N3-C4-C5	-0.5(6)
N5-N6-C9-C8	0.9(6)
N5-N6-B1-N2	56.6(6)
N5-N6-B1-N4	-62.1(5)
N5-C7-C8-C9	1.0(6)
N6-N5-C7-C8	-0.5(6)
C1-N1-N2-C3	0.7(5)
C1-N1-N2-B1	175.8(4)
C1-C2-C3-N2	0.5(6)
C3-N2-B1-N4	-127.0(5)
C3-N2-B1-N6	117.7(5)
C4-N3-N4-C6	0.3(6)
C4-N3-N4-B1	-162.6(4)
C4-C5-C6-N4	-0.3(6)
C6-N4-B1-N2	134.9(5)
C6-N4-B1-N6	-108.0(6)
C7-N5-N6-C9	-0.2(5)
C7-N5-N6-B1	178.6(4)
C7-C8-C9-N6	-1.1(6)
C9-N6-B1-N2	-124.8(5)
C9-N6-B1-N4	116.5(5)
C10-C11-C12-C13	17.3(5)
C10-C11-C12-C17	-105.0(4)
C11-C10-C14-C13	-14.2(5)
C11-C12-C13-C14	-25.6(5)
C11-C12-C17-C16	-75.6(5)
C11-C12-C17-C18	168.2(4)
C12-C13-C14-C10	24.7(5)
C12-C17-C18-C19	146.4(4)
C13-C12-C17-C16	168.0(4)
C13-C12-C17-C18	51.8(5)
C14-C10-C11-W1	117.4(4)
C14-C10-C11-C12	-1.9(5)
C15-C16-C17-C12	-138.2(5)
C15-C16-C17-C18	-14.0(6)
C15-C19-C20-C21	174.2(4)
C15-C19-C20-C23	54.5(6)
C16-C15-C19-C18	17.2(6)
C16-C15-C19-C20	139.8(5)
C16-C17-C18-C19	23.5(5)
C17-C12-C13-C14	93.7(4)
C17-C18-C19-C15	-24.9(5)

C17–C18–C19–C20	–149.6(4)
C18–C19–C20–C21	–68.6(5)
C18–C19–C20–C23	171.6(4)
C19–C15–C16–C17	–2.0(6)
C19–C20–C21–O2	–91.0(6)
C19–C20–C21–O3	85.6(5)
C19–C20–C23–O4	23.0(8)
C19–C20–C23–O5	–156.7(4)
C21–C20–C23–O4	–97.2(6)
C21–C20–C23–O5	83.1(5)
C22–O3–C21–O2	5.1(8)
C22–O3–C21–C20	–171.4(4)
C23–C20–C21–O2	30.6(7)
C23–C20–C21–O3	–152.8(4)
C24–O5–C23–O4	–4.0(8)
C24–O5–C23–C20	175.7(4)
B1–N2–C3–C2	–175.3(5)
B1–N4–C6–C5	160.0(5)
B1–N6–C9–C8	–177.9(5)

## **Appendix E: Chapter 5 Data**

## Synthesis and characterization of [W(Tp)(NO)(PMe<sub>3</sub>)( $\eta^2$ -cyclooctatetraene)] (1)



To a 50 mL round bottom flask were added a stir bar, [W]-Anisole (3.00 g, 3.27 mmol), cyclooctatetraene (2.00 g, 19.2 mmol) and dried THF (6 mL). The round bottom flask was capped with a septum, and the reaction mixture was stirred for 3 hours at 55 °C in an oil bath. Afterwards, a silica column was set up with 60 mL frit packed with 1 inch of silica over a 500 mL filter flask. The reaction mixture was flushed through with ethyl acetate (300 mL) and dark red decomposition product was caught on the silica. The black-orange filtrate was reduced in vacuo to dryness. The product was redissolved in minimal DCM and precipitated with hexanes (300 mL). The orange solid was collected on a 30 mL fine porosity fritted funnel and desiccated overnight to yield **1** (2.11 g, 71%).

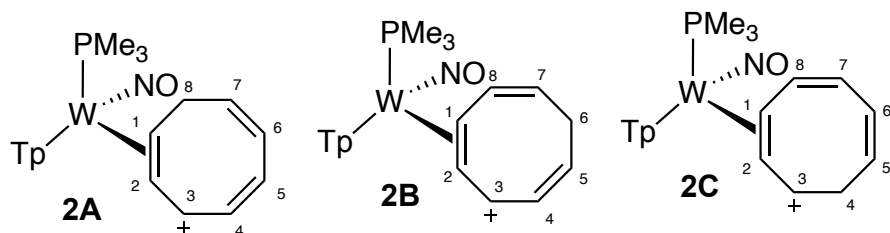
**<sup>1</sup>H NMR (800 MHz, CD<sub>3</sub>CN,  $\delta$ , 25 °C):** 8.34 (d,  $J$  = 1.90 Hz, 1H, Pz3A), 8.07 (d,  $J$  = 1.92 Hz, 1H, Pz3B), 7.86 (d,  $J$  = 2.17 Hz, 1H, Pz5C), 7.82 (d,  $J$  = 2.42 Hz, 1H, Pz5B), 7.73 (d,  $J$  = 2.42 Hz, 1H, Pz5A), 7.70 (d,  $J$  = 2.05 Hz, 1H, Pz3C), 6.42 (dd,  $J$  = 5.86, 13.05 Hz, 1H, H8), 6.37 (t,  $J$  = 2.27 Hz, 1H, Pz4B), 6.34 (t,  $J$  = 2.34 Hz, 1H, Pz4C), 6.33 (m, 1H, H3), 6.20 (t,  $J$  = 2.03 Hz, 1H, Pz4A), 5.41 (t,  $J$  = 3.40 Hz, 2H, H5/H6), 5.29 (d,  $J$  = 13.09 Hz, 1H, H4), 5.21 (d,  $J$  = 12.62 Hz, 1H, H7), 2.84-2.80 (m, 1H, H1), 1.66 (t,  $J$  = 7.71 Hz, 1H, H2), 1.13 (d,  $J$  = 8.58 Hz, 9H, PMe<sub>3</sub>).

**<sup>13</sup>C NMR (200 MHz, CD<sub>3</sub>CN,  $\delta$ , 25 °C):** 146.0 (1C, Pz3A), 143.8 (1C, Pz3B), 141.8 (1C, Pz3C), 140.5 (1C, C3), 138.1 (1C, Pz5C), 137.6 (2C, Pz5A/Pz5B), 134.7 (d,  $J_{PC}$  = 4.43 Hz, 1C, C8), 124.2 (2C, C5/C6), 120.1 (1C, C7), 118.8 (1C, C4), 107.8 (1C, Pz4B), 107.4 (1C, Pz4C), 106.3 (1C, Pz4A), 56.2 (d,  $J_{PC}$  = 9.31 Hz, 1C, C1), 56.0 (1C, C2), 13.6 (d,  $J_{PC}$  = 28.70 Hz, 3C, PMe<sub>3</sub>).

Composition of **1** confirmed by single crystal X-ray diffraction.

**CV (MeCN, 100 mV/s):** Ep,a = +0.37 V, Ep,c = -2.2V (NHE).

**Synthesis and characterization of [W(Tp)(NO)(PMe<sub>3</sub>)( $\eta^2$ -cyclooctatrienyl cation)]OTf (**2**)**



**2A:2B:1C:** In a 10 mL test tube, 0.5 mL of d-MeOH was added to compound **1** (10mg, 0.016mmol). HOTf (2.97 mg, 0.198mmol) was added and a <sup>1</sup>H NMR spectrum was obtained.

**6A:1B:0C:** In a 25 mL Erlenmeyer flask charged with a stir bar, **1** (1.00 g, 1.65 mmol) was dissolved in 10 mL dried THF. Next, HOTf (294 mg, 1.96 mmol) was syringed into a test tube with 1 mL dried THF. The HOTf solution was pipetted into the stirring solution of **1** and was let stir for 15 minutes at R.T. as orange precipitate began to form. To further induce precipitation, the crude reaction mixture was chilled at -30°C for over 12 hours. Afterwards, the orange precipitate **2A** was collected as a triflate salt on a 15 mL fine porosity fritted funnel, rinsed with dried THF, and dried in the desiccator (810 mg, 65%).

**Isomer 2A: <sup>1</sup>H NMR (800 MHz, CD<sub>3</sub>CN,  $\delta$ , 25 °C):** 8.33 (d,  $J$  = 2.02 Hz, 1H, Pz3B), 8.23 (d,  $J$  = 2.49 Hz, 1H, Pz5A), 8.00 (d,  $J$  = 2.46 Hz, 1H, Pz5B), 7.96 (d,  $J$  = 2.46 Hz, 1H, Pz5C), 7.85 (d,  $J$  = 1.88 Hz, 1H, Pz3C), 7.83 (d,  $J$  = 2.46 Hz, 1H, Pz3A), 6.88 (dd,  $J$  = 4.92, 11.64 Hz, 1H, H4), 6.52 (t,  $J$  = 2.35 Hz, 1H, Pz4C), 6.51 (t,  $J$  = 2.41 Hz, 1H, Pz4B), 6.49 (dd,  $J$  = 7.92, 10.45 Hz, 1H, H7), 6.36 (t,  $J$  = 2.45 Hz, 1H, Pz4A), 6.33 (dd,  $J$  = 4.68, 9.66 Hz, 1H, H3), 6.15 (dd,  $J$  = 3.97, 10.67 Hz, 1H, H6), 6.04 (dd,  $J$  = 3.85, 11.80 Hz, 1H, H5), 4.91 (t,  $J$  = 9.62 Hz 1H, H2), 4.40-4.35 (m,  $J$  = 8.41, 16.97, 24.16 Hz, 1H, H1), 3.60 (dt,  $J$  = 8.84, 13.07 Hz, 1H, H8), 2.48 (dt,  $J$  = 7.58, 14.09 Hz, 1H, H8), 1.16 (d,  $J$  = 9.88 Hz, 9H, PMe<sub>3</sub>).

**<sup>13</sup>C NMR (200 MHz, CD<sub>3</sub>CN,  $\delta$ , 25 °C):** 148.0 (1C, Pz5A), 146.1 (1C, Pz3B), 144.3 (1C, C7), 143.5 (1C, Pz3C), 139.7-139.5 (3C, Pz5C/Pz3C/Pz3A), 133.3 (1C, C3), 131.7 (1C, C5), 130.2 (1C, C4), 129.5 (1C, C6), 109.6-108.9 (2C, Pz4C/Pz4B), 108.1 (1C, Pz4A), 106.5 (d,  $J_{PC}$  = 13.28 Hz, 1C, C2), 73.5 (d,  $J_{PC}$  = 11.96 Hz, 1C, C1), 30.7 (d,  $J_{PC}$  = 3.73 Hz, 1C, C8), 13.3 (d,  $J_{PC}$  = 33.1 Hz, 3C, PMe<sub>3</sub>).

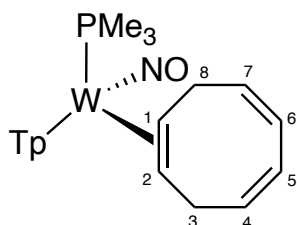
Composition of **2A** confirmed by single crystal X-ray diffraction.

**Isomer 2B: <sup>1</sup>H NMR (800 MHz, CD<sub>3</sub>CN,  $\delta$ , 25 °C):** 8.29 (d,  $J$  = 2.17 Hz, 1H, Pz3B), 8.22 (d,  $J$  = 2.84 Hz, 1H, Pz3A), 8.02 (d,  $J$  = 2.16 Hz, 1H, Pz5B), 7.97 (d,  $J$  = 2.51 Hz, 1H,

Pz5A), 7.87 (d,  $J = 2.19$  Hz, 2H, Pz3C/Pz5C), 6.78 (dd,  $J = 4.54, 10.47$  Hz, 1H, H4), 6.54 (t,  $J = 2.26$  Hz, 1H, Pz4C), 6.51 (t,  $J = 2.55$  Hz, 1H, Pz4B), 6.37 (t,  $J = 2.17$  Hz, 1H, Pz4A), 6.09 (dt,  $J = 7.75, 10.72$  Hz, 1H, H5), 6.01 (d,  $J = 9.99$  Hz, 1H, H8), 5.70 (dd,  $J = 4.64, 9.96$  Hz, 1H, H3), 5.65 (dt,  $J = 8.26, 11.95$  Hz, 1H, H7), 4.90-4.87 (m, 1H, H1), 4.78 (t,  $J = 9.69$  Hz, 1H, H2), 3.71 (dt,  $J = 7.44, 12.02$  Hz, 1H, H6), 2.94 (dt,  $J = 8.26, 11.95$  Hz, 1H, H6), 1.08 (d,  $J = 9.90$  Hz, 9H,  $\text{PMe}_3$ ).

**Isomer 2C:**  $^1\text{H}$  NMR (800 MHz, MeOD,  $\delta$ , 25 °C): too difficult to assign peaks due to overlapping signals with other two isomers.

### Synthesis and characterization of $[\text{W}(\text{Tp})(\text{NO})(\text{PMe}_3)(\eta^2\text{-cycloocta-1,4,6-triene})]$ (3)



In a 20 mL test tube charged with a stir pea, **2** (130 mg, 0.172 mmol) was dissolved in 10 mL MeOH.  $\text{NaBH}_4$  (22.6 mg, 0.598 mmol) was added to a test tube and dissolved into 2 mL MeOH. The  $\text{NaBH}_4$  solution was pipetted into the stirring solution of **2** and stirred for 15 minutes at R.T. The MeOH solution was diluted with 50 mL of chloroform, extracted 3X with 50 mL of a saturated aqueous solution of  $\text{Na}_2\text{CO}_3$ . The organic layer was collected, dried with  $\text{Na}_2\text{SO}_4$  and filtered over a 30 mL fritted disc. The solution was reduced to dryness, redissolved in minimal dichloromethane and added to 100 mL of stirring hexanes. The precipitate was discarded, and the hexanes solution was allowed to sit overnight. The mother liquor of the discarded and crystals of compound **3** were collected. (38 mg, 0.062 mmol, 36%).

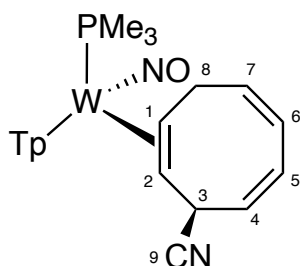
$^1\text{H}$  NMR (800 MHz,  $\text{CD}_3\text{CN}$ ,  $\delta$ , 25 °C): 8.07 (d,  $J = 2.02$  Hz, 1H, Pz3A), 7.98 (d,  $J = 2.02$  Hz, 1H, Pz3B), 7.83 (d,  $J = 2.02$  Hz, 1H, Pz5B), 7.81 (d,  $J = 2.34$  Hz, 1H, Pz5C), 7.77 (d,  $J = 2.34$  Hz, 1H, Pz5A), 7.36 (d,  $J = 2.02$  Hz, 1H, Pz3C), 6.35 (t,  $J = 2.02$  Hz, 1H, Pz4B), 6.29 (t,  $J = 2.02$  Hz, 1H, Pz4A), 6.24 (t,  $J = 2.26$  Hz, 1H, Pz4C), 5.90 – 5.78 (m, 3H, H5/H6/H7), 5.69 (ddd,  $J = 1.62, 5.44, 11.70$  Hz, 1H, H4), 3.42 – 3.31/3.10 – 3.01/2.82 – 2.73 (m, 4H, H8/H7), 2.73 – 2.62 (m, 1H, H1), 1.18 – 1.14 (d,  $J = 8.24$  Hz, 10H,  $\text{PMe}_3/\text{H}_2$ ).



**$^{13}\text{C}$  NMR (200 MHz,  $\text{CD}_3\text{CN}$ ,  $\delta$ , 25 °C):** 144.4 (1C, Pz3B), 144.0 (1C, Pz3A), 141.7 (1C, Pz3C), 138.1 - 138.0/126.5 (4C, C4 - C7), 137.6 – 137.1 (3C, Pz5A/Pz5B/P5C), 107.3 – 106.7 (3C, Pz4A/Pz4B/Pz4C), 57.8 (1C, C2), 53.7 (d,  $J_{\text{PC}}$  = 10.85 Hz, 1C, C1), 33.5 (d,  $J_{\text{PC}}$  = 3.49 Hz, 1C, C8), 32.3 (1C, C3), 13.3 (d,  $J_{\text{PC}}$  = 29.05 Hz, 3C,  $\text{PMe}_3$ ).

Composition of **3** confirmed by single crystal X-ray diffraction.

#### Synthesis and characterization of $[\text{W}(\text{Tp})(\text{NO})(\text{PMe}_3)(\eta^2\text{-3-cyano-cycloocta-1,4,6-triene})]$ (**4**)



In a 20 mL test tube charged with a stir pea, **2** (49 mg, 0.065 mmol) was dissolved in 10 mL MeCN. NaCN (38 mg, 0.776 mmol) was added to the stirring solution of **2**. 2 mL of DMSO was added to the stirring solution and stirred for 15 minutes at R.T. The acetonitrile solution was diluted with 50 mL of chloroform, extracted 3X with 50mL of a saturated aqueous solution of  $\text{Na}_2\text{CO}_3$ . The organic layer was collected, dried with  $\text{Na}_2\text{SO}_4$  and filtered over a 30mL M fritted disc. The solution was reduced to dryness, redissolved in minimal chloroform and added to 100mL of stirring hexanes. The precipitate was collected over a 15mL F fritted disc and desiccated. (15 mg, 0.024 mmol, 37%).

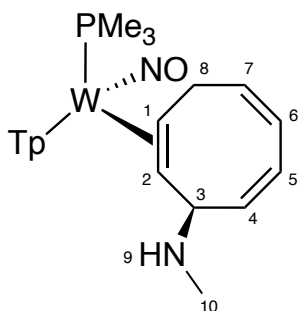
**$^1\text{H}$  NMR (800 MHz,  $\text{CD}_3\text{CN}$ ,  $\delta$ , 25 °C):** 7.98 (d,  $J$  = 1.17 Hz, 1H, Pz3B), 7.91 (s, 1H, Pz3A), 7.86 - 7.83 (m, 2H, Pz5B/Pz5C), 7.80 (d,  $J$  = 1.63 Hz, 1H, Pz5A), 7.35 (d,  $J$  = 1.58 Hz, 1H, Pz3C), 6.35 (t,  $J$  = 2.39 Hz, 1H, Pz4B), 6.34 (t,  $J$  = 2.34 Hz, 1H, Pz4A), 6.28 (t,  $J$  = 2.18 Hz, 1H, Pz4C), 6.21 (dd,  $J$  = 2.41, 10.18 Hz, 1H, H6), 6.16 (dd,  $J$  = 2.41, 10.68 Hz, 1H, H5), 5.97 (q,  $J$  = 8.27 Hz, 1H, H7), 5.89 (t,  $J$  = 9.10 Hz, 1H, H4), 4.50 (dd,  $J$  = 3.48, 8.56 Hz, 1H, H3), 3.14 (q,  $J$  = 11.77 Hz, 1H, H8), 2.95 (dt,  $J$  = 6.66, 12.85 Hz, 1H, H8), 2.49 - 2.44 (m, 1H, H1), 1.18 (d,  $J$  = 8.43 Hz, 9H,  $\text{PMe}_3$ ), 1.13 - 1.09 (m, 1H, H2).

**$^{13}\text{C}$  NMR (200 MHz,  $\text{CD}_3\text{CN}$ ,  $\delta$ , 25 °C):** 144.3 (1C, Pz3B), 144.2 (1C, Pz3A), 141.9 (1C, Pz3C), 137.8 – 137.5 (3C, Pz5B/Pz5C/Pz5A), 131.9 (1C, C5), 128.8 (1C, C4), 128.7

(1C, C6), 126.9 (1C, C9), 107.5 – 107.3 (3C, Pz4B/Pz4A/Pz4C), 58.6 (1C, C2), 47.2 (d,  $J_{PC}$  = 13.48 Hz, 1C, C1), 35.0 (1C, C3), 32.8 (d,  $J_{PC}$  = 2.86 Hz, 1C, C8), 13.2 (d,  $J_{PC}$  = 28.79 Hz 1C, PMe<sub>3</sub>).

Composition of **4** confirmed by single crystal X-ray diffraction.

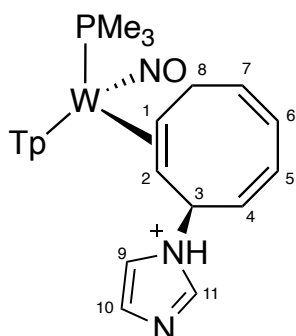
### Synthesis and characterization of [W(Tp)(NO)(PMe<sub>3</sub>)( $\eta^2$ -3-methylamine-cycloocta-1,4,6-triene) (**5**)



In a 10 mL test tube charged with a stir pea, **2** (100 mg, 0.132 mmol) was dissolved in 2 mL of d-MeCN. Methylamine (0.05 mL, 0.6 mmol) was syringed into the solution of **2**, and the reaction was stirred for 30 minutes at R.T. The solution was diluted with 50 mL of dichloromethane, extracted 3X with 50mL of Na<sub>2</sub>CO<sub>3</sub>. The organic layer was collected, dried with Na<sub>2</sub>SO<sub>4</sub> and filtered over a 30mL M fritted disc. The solution was reduced to dryness, redissolved in minimal DCM and added to 100mL of stirring hexanes. The precipitate was discarded, and the filtrate was reduced to dryness to yield a white powder **5** (65 mg, 0.102 mmol, 77%).

**<sup>1</sup>H NMR (800 MHz, CD<sub>3</sub>CN,  $\delta$ , 25 °C):** 8.10, 7.98, 7.85, 7.81, 7.35 (bs, 6H, Tp protons), 6.36, 6.28 (bs, 3H, Tp protons), 6.25 (m, 1H), 5.89 (d,  $J$  = 11.08 Hz, 1H), 5.62 (m,  $J$  = 6.16, 12.07 Hz, 1H), 5.48 (d,  $J$  = 11.08 Hz, 1H) – H4 – H7. 3.52 (t,  $J$  = 6.61 Hz, 1H), 2.98 (d,  $J$  = 14.88 Hz, 1H), 2.41 (s, 3H, H10), 2.37 (m, 1H) – H3/H8. 2.92 (ddd,  $J$  = 6.61, 13.55, 16.53 Hz, 1H, H1), 1.22 (m,  $J$  = 10.08 Hz, H2).

### Synthesis and characterization of $[W(Tp)(NO)(PMe_3)(\eta^2\text{-3-imidazole-cycloocta-1,4,6-triene})]$ (**6**)

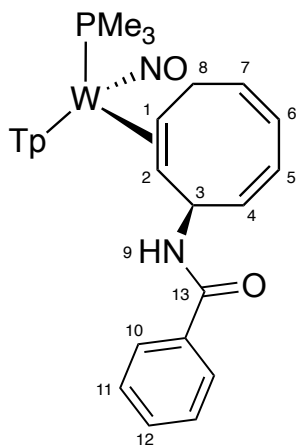


I

In a 10 mL test tube charged with a stir pea, **2** (20 mg, 0.026 mmol) was dissolved in 2 mL of d-MeCN. In a second 10 mL test tube, imidazole (18 mg, 0.265 mmol) was added to 2 mL d-MeCN. The solution of imidazole was added to the solution of **2** and a crude <sup>1</sup>H NMR was obtained.

**<sup>1</sup>H NMR (800 MHz, CD<sub>3</sub>CN, δ, 25 °C):** 8.18 – 7.86, 7.38 (d, J = 1.82; 1.82; 2.27; 2.84; 2.84; 1.82 Hz, 6H, Tp protons), 7.79, 7.54 – 7.46 (bs, H<sub>9</sub> – H<sub>11</sub>), 6.40 – 6.31 (t, J = 2.11; 2.11; 2.11 Hz, 3H, Tp protons), 6.27 – 5.39 (dd, J = 6.24, 12.40; 5.85, 11.58, 8.40; 1.41, 5.15, 12.64 Hz, 4H, H<sub>4</sub> – H<sub>7</sub>), 5.05 (ddd, J = 8.39, 10.13, 16.64 Hz, 1H, H<sub>3</sub>), 3.05 – 2.61 (m, J = 8.70, 12.93; 12.30; 8.38, 12.93 Hz, 3H, H<sub>1</sub>/H<sub>8</sub>), 1.44 (dd, 6.42, 11.89 Hz, 1H, H<sub>2</sub>), 1.00 (J = 8.38 Hz, 9H, PMe<sub>3</sub>)

### Synthesis and characterization of $[W(Tp)(NO)(PMe_3)(\eta^2\text{-3-benzamide-cycloocta-1,4,6-triene})]$ (**7**)



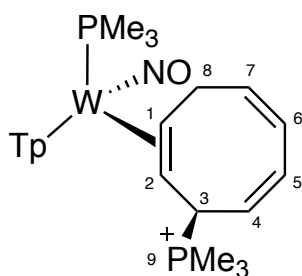
I

n a 20 mL test tube charged with a stir pea, **2** (100 mg, 0.132 mmol) was dissolved in 2 mL MeCN. In a 10 mL test tube charged with a stir pea, tBuOK (75 mg, 0.134 mmol) was added, followed by 3mL THF. In a 10mL test tube charged with a stir pea, benzamide (16 mg, 0.132) was dissolved in 1mL of MeCN. The benzamide solution was added to the base solution and stirred for 30 minutes at R.T. The solution was diluted with 50 mL of dichloromethane, extracted 3X with 50mL of H<sub>2</sub>O. The organic layer was collected, dried with Na<sub>2</sub>SO<sub>4</sub> and filtered over a 30mL M fritted disc. The solution was reduced to dryness, redissolved in minimal DCM and added to 100mL of stirring hexanes. The precipitate was discarded, and the filtrate was reduced to dryness to yield a white powder.

**<sup>1</sup>H NMR (800 MHz, CD<sub>3</sub>CN, δ, 25 °C):** 8.06 (d, *J* = 1.58 Hz, 1H, Pz3A), 8.01 (d, *J* = 2.10 Hz, 1H, Pz3B), 7.85 - 7.84 (d, *J* = 2.28 Hz, 2H, Pz5A/Pz5B), 7.77 (d, *J* = 2.80 Hz, 1H, Pz5C), 7.63 (d, *J* = 9.76 Hz, 2H, H10), 7.47 (t, *J* = 7.18 Hz, 1H, H12), 7.40 (t, *J* = 7.36 Hz, 2H, H11), 7.30 (d, *J* = 2.10 Hz, 1H, Pz3C), 7.28 (d, *J* = 10.04 Hz, 1H, H9), 6.38 (dd, *J* = 2.98, 10.16 Hz, 1H, H6), 6.35 (t, *J* = 2.10 Hz, 1H, Pz4B), 6.28 (t, *J* = 2.28 Hz, 1H, Pz4A), 6.25 (t, *J* = 2.98 Hz, 1H, Pz4C), 6.17 (dd, *J* = 7.18, 10.86 Hz, 1H, H4), 6.04 (dt, *J* = 4.38, 7.88 Hz, 1H, H3), 2.64 – 2.56 (m, 1H, H1), 1.18 (d, *J* = 8.21 Hz, 9H, PMe<sub>3</sub>), 1.14 - 1.10 (m, 1H, H2).

Composition of **7** confirmed by single crystal X-ray diffraction.

### Synthesis and characterization of [W(Tp)(NO)(PMe<sub>3</sub>)(η<sup>2</sup>-3-trimethylphosphine-cycloocta-1,4,6-triene)] (**8**)

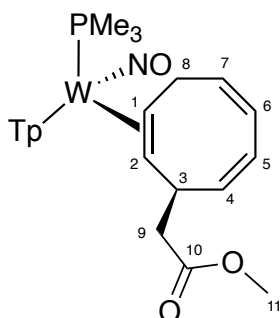


Compound **2** is left in a solution of d-MeCN overnight resulting in compound **8**.

**<sup>1</sup>H NMR (800 MHz, CD<sub>3</sub>CN, δ, 25 °C):** 7.99 – 7.43 (d, *J* = 1.59; 1.59; 2.31; 1.91; 1.59 Hz, 6H, Tp protons), 6.37 – 6.36, 6.30 (t, *J* = 1.99; 2.31; 2.31 Hz, 3H, Tp protons), 6.31 (m, 1H, H5), 6.20 (dt, *J* = 2.31, 10.50 Hz, 1H, H6), 6.05 (t, *J* = 1.91 Hz, 1H, H7), 5.80

(dt,  $J = 10.18, 15.75$  Hz, 1H, H4), 4.42 (dd,  $J = 9.86, 18.05$  Hz, 1H, H3), 3.13 (dd,  $J = 10.50, 22.03$  Hz, 1H, H8), 2.85 (dt,  $J = 5.96, 13.12$  Hz, 1H, H8), 2.63 (ddd,  $J = 5.65, 11.53, 16.70$  Hz, 1H, H1), 1.55 (d,  $J = 13.52$  Hz, 9H, H9), 1.17 (d,  $J = 8.51$  Hz, 9H,  $\text{PMe}_3$ ), 0.79 (dd,  $J = 11.45, 15.43$  Hz, 1H, H2).

### Synthesis and characterization of $[\text{W}(\text{Tp})(\text{NO})(\text{PMe}_3)(\eta^2\text{-3-enolate-cycloocta-1,4,6-triene})]$ (**9**)



In a 20 mL test tube charged with a stir pea, **2** (250 mg, 0.330 mmol) was dissolved in 10 mL MeCN. 1-(tert-butyldimethylsiloxy)-1-methoxy-ethene (93 mg, 0.494 mmol) was syringed into the solution of **2**, and the reaction was stirred for 2 hours at R.T. The reaction solution was diluted with 50 mL of DCM, extracted 3X with 50mL of a saturated aqueous solution of  $\text{Na}_2\text{CO}_3$ . The organic layer was collected, dried with  $\text{Na}_2\text{SO}_4$  and filtered over a 30mL M fritted disc. The solution was reduced to dryness, redissolved in minimal chloroform and added to 100mL of stirring hexanes. The precipitate was collected over a 15mL F fritted disc and desiccated. The filtrate was reduced dry, producing a white solid **9** (114 mg, 0.167 mmol, 50.7%).

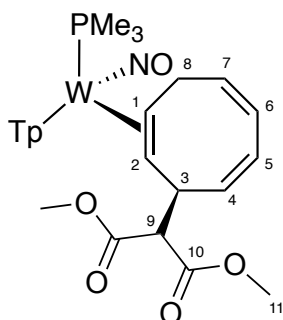
**$^1\text{H}$  NMR (800 MHz,  $\text{CD}_3\text{CN}$ ,  $\delta$ , 25 °C):**  $\delta$  8.01 (d,  $J = 2.1$  Hz, 1H, Pz), 7.97 (d,  $J = 2.0$  Hz, 1H, Pz), 7.82 (d,  $J = 2.3$  Hz, 1H, Pz), 7.82 (d,  $J = 2.6$  Hz, 1H, Pz), 7.79 (d,  $J = 2.4$ , 1H, Pz), 7.28 (d,  $J = 2.2$  Hz, 1H, Pz), 6.32 (t,  $J = 2.2$  Hz, 1H, Pz), 6.30 (t,  $J = 2.2$  Hz, 1H, Pz), 6.25 (t,  $J = 2.2$  Hz, 1H, Pz), 6.13 (dd,  $J = 10.2, 2.8$  Hz, 1H, H6), 5.90-5.85 (m, 3H, H4, H5, H7), 3.95 (m, 1H, H3), 3.44 (s, 3H, H11), 3.18 (m, 1H, H8), 3.06 (ddd,  $J = 12.7, 7.0, 5.2$  Hz, 1H, H8), 2.75 (dd,  $J = 15.3, 9.0$  Hz, 1H, H9), 2.63 (dddd,  $J = 14.2, 11.4, 9.3, 5.2$  Hz, 1H, H1), 2.36 (dd,  $J = 15.3, 5.8$  Hz, 1H, H9), 1.17 (d,  $J = 8.3$  Hz, 9H,  $\text{PMe}_3$ ), 0.77 (dd,  $J = 11.2, 4.0$ , 1H, H2).

**$^{13}\text{C}$  NMR (200 MHz,  $\text{CD}_3\text{CN}$ ,  $\delta$ , 25 °C):** 174.60 (1C, C10), 144.23 (1C, Pz), 144.10 (1C, Pz), 141.68 (1C, Pz), 137.57 (1C, Pz), 137.52 (1C, Pz), 137.33 (1C, C4 C5 or C7),

137.20 (1C, C4 C5 or C7), 137.07 (1C, Pz), 129.73 (1C, C6), 128.37 (1C, C4 C5 or C7), 107.24 (1C, Pz), 107.12 (1C, Pz), 106.84 (1C, Pz), 61.12 (1C, C2), 51.41 (1C, C11), 51.04 (d,  $J_{PC}$  = 11.5 Hz, 1C, C1), 45.73 (1C, C9), 40.35 (1C, C3), 33.68 (d,  $J_{PC}$  = 3.3 Hz, 1C, C8), 13.18 (d,  $J_{PC}$  = 27.9 Hz, 3C, PMe<sub>3</sub>).

Composition of **9** confirmed by single crystal X-ray diffraction.

### Synthesis and characterization of [W(Tp)(NO)(PMe<sub>3</sub>)( $\eta^2$ -3-dimethyl malonate-cycloocta-1,4,6-triene)] (**10**)



In a 20 mL test tube charged with a stir pea, **2** (150 mg, 0.198 mmol) was dissolved in 3 mL MeCN. In another 20 mL test tube, LiDiMM (45 mg, 0.296 mmol) was dissolved in 2 mL acetonitrile. The LiDiMM solution was pipetted into the solution of **2**, and the reaction was stirred for 5 minutes at R.T. A white solid was precipitated out of the acetonitrile and was collected on a 30 mL fine porosity fritted funnel. The white solid was washed on the frit 2X with 20 mL hexanes and dried in vacuo yielding **10** (80 mg, 0.108 mmol, 55%).

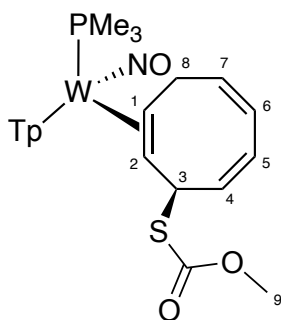
**<sup>1</sup>H NMR (800 MHz, CD<sub>3</sub>CN,  $\delta$ , 25 °C):** 8.03 (d,  $J$  = 2.1 Hz, 1H, Pz), 7.98 (d,  $J$  = 2.1 Hz, 1H, Pz), 7.74 (d,  $J$  = 2.4 Hz, 1H, Pz), 7.72 (d,  $J$  = 2.3 Hz, 2H, Pz), 7.17 (d,  $J$  = 2.2 Hz, 1H, Pz), 6.37 (t,  $J$  = 2.2 Hz, 1H, Pz), 6.31 (t,  $J$  = 2.2 Hz, 1H, Pz), 6.19 (t,  $J$  = 5.4, 3.0 Hz, 1H, Pz), 6.19 (m, 1H, H6), 6.00 (dd,  $J$  = 11.0, 8.5 Hz, 1H, H4), 5.95 (dd,  $J$  = 11.0, 2.8 Hz, 1H, H5), 5.89 (td,  $J$  = 9.5, 6.8 Hz, 1H, H7), 4.30 (d,  $J$  = 11.2 Hz, 1H, H9), 4.23 (ddt,  $J$  = 11.2, 8.8, 2.3 Hz, 1H, H3), 3.60 (s, 3H, H11), 3.19 (s, 3H, H11), 3.19 (m, 1H, H8), 2.73 (dt,  $J$  = 12.9, 6.3 Hz, 1H, H8'), 2.52 (m,  $J$  = 13.5, 10.9, 5.8 Hz, 1H, H1), 1.19 (d,  $J$  = 8.1 Hz, 9H, PMe<sub>3</sub>), 0.69 (dd,  $J$  = 11.3, 2.8 Hz, 1H, H2).

**<sup>13</sup>C NMR (200 MHz, CD<sub>3</sub>CN,  $\delta$ , 25 °C):** 169.9 - 169.8 (2C, C10), 143.6 (1C, Pz), 143.4 (1C, Pz), 140.4 (1C, Pz), 136.6 (1C, Pz), 136.6 (1C, C7), 136.5 (1C, Pz), 136.3 (1C,

Pz), 133.6 (1C, C4), 129.7 (1C, C6), 129.4 (1C, C5), 106.6 -106.2 (3C, Pz4A/Pz4B/Pz4C), 60.9 (1C, C9), 58.8 (1C, C2), 52.2 - 51.9 (2C, C11), 48.8 (d,  $J = 11.6$  Hz, 1C, C1), 44.1 (1C, C3), 32.5 (d,  $J = 3.4$  Hz, 1C, C8), 13.3 (d,  $J = 27.8$  Hz, 3C,  $\text{PMe}_3$ ). Composition of **10** confirmed by single crystal X-ray diffraction.

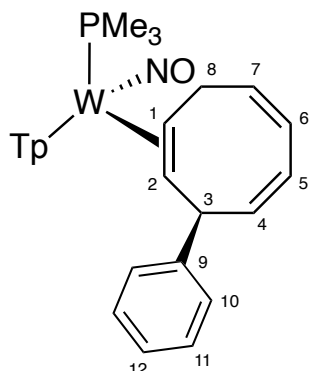
**HRMS** - Theoretical: 739.2040 m/z; Experimental: 739.2022 m/z

### Synthesis and characterization of $[\text{W}(\text{Tp})(\text{NO})(\text{PMe}_3)(\eta^2\text{-3-thioacetate-cycloocta-1,4,6-triene})]$ (**11**)



In a 10 mL test tube charged with a stir pea, **2** (50 mg, 0.066 mmol) was dissolved in 2 mL of THF. In a second 10 mL test tube, thioacetate (11 mg, 0.096 mmol) was dissolved in 2 mL of THF. The solution of thioacetate was added to the solution of **2**, and the reaction was stirred for 1 hour. The reaction solution was diluted with 50 mL of DCM, extracted 3X with 50mL of a saturated aqueous solution of  $\text{Na}_2\text{CO}_3$ . The organic layer was collected, dried with  $\text{Na}_2\text{SO}_4$  and filtered over a 30mL M fritted disc. The solution was reduced to dryness, redissolved in minimal chloroform and added to 100mL of stirring hexanes. The precipitate was collected over a 15mL F fritted disc and desiccated. The filtrate was reduced dry, producing a white solid **11** (no yield recorded).  **$^1\text{H}$  NMR (800 MHz,  $\text{CD}_3\text{CN}$ ,  $\delta$ , 25 °C):** 8.12, 8.01, 7.87, 7.84, 7.79, 7.37 (d,  $J = 1.61$ ; 2.12; 2.02; 1.71 6H, Tp protons), 6.36, 6.92, 6.26 (t,  $J = 2.11$ , 2.51, 2.51 Hz, 3H, Tp protons), 6.18, 6.14, 5.56, 5.28, 5.21 (m,  $J = 6.14$ , 12.49; 2.86, 10.31; 7.74, 10.94; 5.54, 12.64; 7.92 Hz, 5H, H3 – H7), 3.14, 2.79, 2.46, 1.23 (m,  $J = 6.93$ , 13.86; 3.33, 12.75; 5.82, 11.36 Hz, 4H, H1/H2/H8).

**Synthesis and characterization of [W(Tp)(NO)(PMe<sub>3</sub>)( $\eta^2$ -3-phenyl-cycloocta-1,4,6-triene)] (**12**)**



In a 20 mL test tube charged with a stir pea, **2** (400 mg, 0.528 mmol) was dissolved in 10 mL dried THF. PhMgBr (748 mg, 4.13 mmol) was syringed into the stirring solution of **2**, and the reaction was stirred for 30 minutes at R.T. The reaction mixture was diluted with 50 mL of DCM, extracted 3X with 50mL of a saturated aqueous solution of Na<sub>2</sub>CO<sub>3</sub>. The organic layer was collected, dried with Na<sub>2</sub>SO<sub>4</sub> and filtered over a 30mL M fritted disc. The solution was reduced to dryness, redissolved in minimal DCM and added to 100mL of stirring hexanes. The precipitate was collected over a 15mL F fritted disc and discarded. The filtrate was reduced to dryness in vacuo, yielding a white solid **12** (327 mg, 0.477 mmol, 90%).

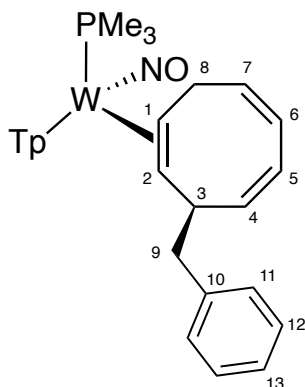
**<sup>1</sup>H NMR (800 MHz, CD<sub>3</sub>CN,  $\delta$ , 25 °C):** 7.98 (d,  $J$  = 2.0 Hz, 1H, Pz), 7.84 (d,  $J$  = 2.3 Hz, 1H, Pz), 7.79 (d,  $J$  = 2.4 Hz, 1H, Pz), 7.59 (d,  $J$  = 2.4 Hz, 1H, Pz), 7.49 (d,  $J$  = 2.2 Hz, 1H, Pz), 7.31 (d,  $J$  = 7.7 Hz, 2H, H10), 7.16 (t,  $J$  = 7.7 Hz, 2H, H11), 7.09 (m, 1H, H12), 6.93 (d,  $J$  = 2.0 Hz, 1H, Pz), 6.32 (t,  $J$  = 2.2 Hz, 1H, Pz), 6.31 (t,  $J$  = 2.2 Hz, 1H, Pz), 6.06 (dd,  $J$  = 10.9, 8.8 Hz, 1H, H4), 5.84 (dt,  $J$  = 11.5, 6.6 Hz, 1H, H7), 5.82 (t,  $J$  = 2.2 Hz, 1H, Pz), 5.73 (ddd,  $J$  = 11.3, 4.4, 2.0 Hz, 1H, H6), 5.68 (dd,  $J$  = 10.9, 4.3 Hz, 1H, H5), 4.78 (t,  $J$  = 8.0 Hz, 1H, H3), 3.57 (m, 1H, H8), 3.14 (ddd,  $J$  = 15.7, 7.2, 4.4 Hz, 1H, H8), 2.90 (m,  $J$  = 13.9, 11.2, 9.6, 4.4 Hz, 1H, H1), 1.52 (ddd,  $J$  = 11.2, 7.2, 1.6 Hz, 1H, H2), 1.14 (d,  $J$  = 8.3 Hz, 9H, PMe<sub>3</sub>).

**<sup>13</sup>C NMR (200 MHz, CD<sub>3</sub>CN,  $\delta$ , 25 °C):** 150.9 (1C, C9), 145.6 (1C, Pz), 144.0 (1C, Pz), 143.3 (1C, C4), 141.8 (1C, Pz), 138.3 (1C, C7), 137.7 (1C, Pz), 137.0 (1C, Pz), 137.0 (1C, Pz), 129.8 (2C, C10), 128.7 (2C, C11), 127.6 (1C, C6), 125.9 (1C, C12), 124.8 (1C,



C5), 107.3 (1C, Pz), 107.1 (1C, Pz), 106.2 (1C, Pz), 61.8 (1C, C2), 52.5 (d,  $J = 11.7$  Hz, 1C, C1), 49.6 (1C, C3), 35.0 (d,  $J = 3.7$  Hz, 1C, C8), 12.9 (d,  $J = 28.2$  Hz, 3C, PMe<sub>3</sub>). Composition of **12** confirmed by single crystal X-ray diffraction.

### Synthesis and characterization of [W(Tp)(NO)(PMe<sub>3</sub>)( $\eta^2$ -3-benzyl-cycloocta-1,4,6-triene)] (**13**)

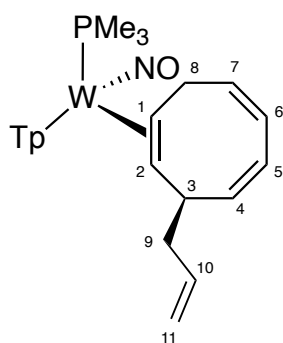


In a 20 mL test tube charged with a stir pea, **2** (400 mg, 0.528 mmol) was dissolved in 10 mL dried THF. BnMgBr (0.8 mL, 0.792 mmol) was syringed into the stirring solution of **2**, and the reaction was stirred for 30 minutes at R.T. The reaction mixture was diluted with 50 mL of DCM, extracted 3X with 50mL of H<sub>2</sub>O. The organic layer was collected, dried with Na<sub>2</sub>SO<sub>4</sub> and filtered over a 30mL M fritted disc. The solution was reduced to dryness, redissolved in minimal DCM and placed in a vial. The vial was placed in a bell jar and reduced in vacuo, inducing crystallization of product. The vial contents were washed 3X with 5 mL MeCN or until the acetonitrile wash was colorless. The vial was reduced dry with the bell jar a second time yielding crystals of **13** (233 mg, 0.333 mmol, 63%).

**<sup>1</sup>H NMR (800 MHz, CD<sub>3</sub>CN,  $\delta$ , 25 °C):** .98 (d,  $J = 2.2$  Hz, 1H, Pz), 7.97 (d,  $J = 2.5$  Hz, 1H, Pz), 7.81 (d,  $J = 2.4$  Hz, 1H, Pz), 7.80 (d,  $J = 2.3$  Hz, 1H, Pz), 7.77 (d,  $J = 2.4$  Hz, 1H, Pz), 7.31 (d,  $J = 2.2$  Hz, 1H, Pz), 7.13 (dd,  $J = 8.3, 7.0$  Hz, 2H, H12), 7.04 (m, 1H, H13), 7.02 (d, 2H, H11), 6.32 (t,  $J = 2.2$  Hz, 1H, Pz), 6.26 (t,  $J = 2.2$  Hz, 1H, Pz), 6.24 (t,  $J = 2.2$  Hz, 1H, Pz), 6.20 (dd,  $J = 10.2, 2.9$  Hz, 1H, H6), 5.92 (m, 1H, H7), 5.81 (m, 1H, H5), 5.77 (dd,  $J = 11.0, 8.4$  Hz, 1H, H4), 3.80 (m, 1H, H3), 3.26 (dt,  $J = 13.2, 9.0$  Hz, 1H, H8), 3.10 – 3.03 (m, 2H, H8 & H9), 2.73 (m, 1H, H1), 2.69 (dd,  $J = 13.6, 5.4$  Hz, 1H, H9), 1.18 (d,  $J = 8.3$  Hz, 9H, PMe<sub>3</sub>), 0.98 (dd,  $J = 11.3, 3.9$ , 1H, H2).

**$^{13}\text{C}$  NMR (200 MHz,  $\text{CD}_3\text{CN}$ ,  $\delta$ , 25 °C):** 144.3 (1C, Pz), 144.1 (1C, Pz), 144.1 (1C, C10), 141.7 (1C, Pz), 137.9 (1C, C4), 137.5 (2C, Pz), 137.1 (1C, Pz), 137.0 (1C, C7), 129.9 (2C, C11), 129.8 (1C, C6), 128.7 (2C, C12), 128.2 (1C, C5), 126.1 (1C, C13), 107.2 - 106.8 (3C, Pz4A/Pz4B/Pz4C), 62.7 (1C, C2), 51.2 (d,  $J_{\text{PC}} = 11.0$  Hz, 1C, C1), 46.7 (1C, C9), 45.3 (1C, C3), 33.9 (d,  $J_{\text{PC}} = 3.2$  Hz, 1C, C8), 13.2 (d,  $J_{\text{PC}} = 27.9$  Hz, 3C,  $\text{PMe}_3$ ).  
Composition of **13** confirmed by single crystal X-ray diffraction

### Synthesis and characterization of $[\text{W}(\text{Tp})(\text{NO})(\text{PMe}_3)(\eta^2\text{-3-allyl-cycloocta-1,4,6-triene})]$ (**14**)



In a 20 mL test tube charged with a stir pea, **2** (50 mg, 0.066 mmol) was dissolved in 2 mL dried THF. Allyl magnesium chloride (0.08 mL, 0.079 mmol) was syringed into the stirring solution of **2**, and the reaction stirred for 1 hour at R.T. The reaction mixture was then diluted with DCM, extracted 3X with 50mL of a saturated aqueous solution of  $\text{Na}_2\text{CO}_3$ . The organic layer was collected, dried with  $\text{Na}_2\text{SO}_4$  and filtered over a 30mL M fritted disc. The solution was reduced to dryness, redissolved in minimal chloroform and added to 100mL of stirring hexanes. The precipitate was collected over a 15mL F fritted disc and discarded. The filtrate was reduced in vacuo, yielding a white solid **14** (30 mg, 0.0462 mmol, 70%).

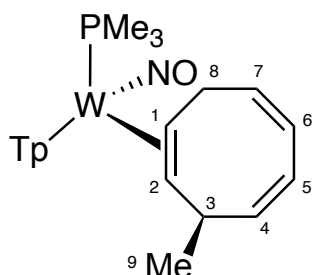
**$^1\text{H}$  NMR (800 MHz,  $\text{CD}_3\text{CN}$ ,  $\delta$ , 25 °C):** 7.96 (d,  $J = 2.0$  Hz, 1H, Pz), 7.93 (d,  $J = 2.0$  Hz, 1H, Pz), 7.83 (d,  $J = 2.3$  Hz, 1H, Pz), 7.81 (d,  $J = 2.3$ , 1H, Pz), 7.79 (d,  $J = 2.4$  Hz, 1H, Pz), 7.30 (d,  $J = 2.1$  Hz, 1H, Pz), 6.32 (t,  $J = 2.2$  Hz, 1H, Pz), 6.28 (t,  $J = 2.2$  Hz, 1H, Pz), 6.26 (t,  $J = 2.2$  Hz, 1H, Pz), 6.09 (m, 1H, H6), 5.87 (m, 2H, H5 & H7), 5.80 (dd,  $J = 10.9, 8.2$  Hz, 1H, H4), 5.67 (ddt,  $J = 17.2, 10.3, 6.9$  Hz, 1H, H10), 4.78 (m, 2H, H11), 3.47 (tt,  $J = 8.4, 4.2$  Hz, 1H, H3), 3.23 (ddd,  $J = 12.4, 7.1, 5.0$  Hz, 1H, H8), 3.18 (dt,  $J =$

13.1, 8.5 Hz, 1H, H8), 2.70 (m,  $J = 13.9, 11.5, 8.5, 5.0$  Hz, 1H, H1), 2.40 (m, 1H, H9), 2.00 (m, 1H, H9), 1.18 (d,  $J = 8.2$  Hz, 9H, PMe<sub>3</sub>), 0.82 (dd,  $J = 11.6, 4.5$  Hz, 1H, H2).

**<sup>13</sup>C NMR (200 MHz, CD<sub>3</sub>CN, δ, 25 °C):** 144.2 (1C, Pz), 144.0 (1C, Pz), 141.7 (1C, Pz), 140.4 (1C, C10), 138.7 (1C, C4), 137.6 (1C, Pz), 137.5 (1C, Pz), 137.1 (1C, C7), 137.0 (1C, Pz), 129.6 (1C, C6), 127.7 (1C, C5), 114.6 (1C, C11), 107.2 (1C, Pz), 107.1 (1C, Pz), 106.8 (1C, Pz), 61.2 (1C, C2), 52.7 (d,  $J = 11.0$  Hz, 1C, C1), 45.4 (1C, C9), 43.5 (1C, C3), 34.2 (d,  $J = 3.4$  Hz, 1C, C8), 13.2 (d,  $J = 27.9$  Hz, 3C, PMe<sub>3</sub>).

Composition of **14** confirmed by single crystal X-ray diffraction

### Synthesis and characterization of [W(Tp)(NO)(PMe<sub>3</sub>)( $\eta^2$ -3-methyl-cycloocta-1,4,6-triene)] (**15**)



In an oven dried test tube charged with a stir pea, **2** (0.591 g, 0.78 mmol) was dissolved in 50 mL dried THF. At room temperature, with a syringe, MeMgBr (1.12 mL, 1.68 mmol) was added to the solution. After 30 minutes of stirring, 2mL of H<sub>2</sub>O was added to quench the reaction. The solution was diluted with 100mL of CDCl<sub>3</sub> and extracted 3x with 100mL H<sub>2</sub>O. The organic layer was collected, dried with Na<sub>2</sub>SO<sub>4</sub> and filtered over a 60mL fritted disc and rinsed with 50mL CDCl<sub>3</sub>. The remaining solution was reduced to dryness, redissolved in minimal MeCN and precipitated into 300mL Et<sub>2</sub>O. The precipitate was collected over a 30mL fritted disc and discarded. The remaining ether filtrate was reduced to dryness to yield white powder **15** in a 20 : 1 ratio (0.326 g, 65%).

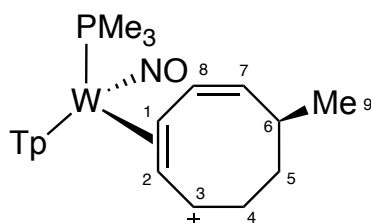
**<sup>1</sup>H NMR (800 MHz, CD<sub>3</sub>CN, δ, 25 °C):** 7.97 (d,  $J = 2.12$  Hz, 1H, Pz3A), 7.95 (d,  $J = 1.86$  Hz, 1H, Pz3B), 7.82 (d,  $J = 2.18$  Hz, 1H, Pz5C), 7.81 (d,  $J = 2.14$  Hz, 1H, Pz5B), 7.78 (d,  $J = 2.63$  Hz, 1H, Pz5A), 7.32 (d,  $J = 2.06$  Hz, 1H, Pz3C), 6.31 (t,  $J = 2.33$  Hz, 1H, Pz4B), 6.27 (t,  $J = 2.01$  Hz, 1H, Pz4A), 6.26 (t,  $J = 2.12$  Hz, 1H, Pz4C), 6.05 (dd,  $J = 3.06, 10.36$  Hz, 1H, H6), 5.87 (q,  $J = 7.71$  Hz, 1H, H7), 5.81 (dd,  $J = 7.71, 11.00$  Hz, 1H, H5), 5.79 (dd,  $J = 2.97, 10.92$  Hz, 1H, H4), 3.64 – 3.59 (m, 1H, H3), 2.78 – 2.70 (m,

$^1\text{H}$ , H1), 1.17 (d,  $J$  = 8.26 Hz, 9H,  $\text{PMe}_3$ ), 1.05 (d,  $J$  = 6.97 Hz, 3H, H9), 0.73 (dd,  $J$  = 4.18, 11.54 Hz, 1H, H2).

**$^{13}\text{C}$  NMR (201 MHz,  $\text{CD}_3\text{CN}$ ,  $\delta$ , 25 °C):** 144.1 (1C, Pz3B), 144.0 (1C, Pz3A), 141.7 (1C, Pz3C), 140.9 (1C, C4), 137.6 – 137.5 (2C, Pz5A/P5C), 137.0 (2C, Pz5B/C7), 129.3 (1C, C6), 126.3 (1C, C5), 107.2 – 106.8 (3C, Pz4B/Pz4A/Pz4C), 62.4 (1C, C2), 53.8 (d,  $J_{\text{PC}}$  = 11.62 Hz, 1C, C1), 37.8 (1C, C3), 34.1 (d,  $J_{\text{PC}}$  = 2.70 Hz, 1C, C8), 27.3 (1C, C9), 13.26 (d,  $J_{\text{PC}}$  = 27.43 Hz 1C,  $\text{PMe}_3$ ).

Composition of **15** has been confirmed by single crystal X-ray diffraction.

### Synthesis and characterization of $[\text{W}(\text{Tp})(\text{NO})(\text{PMe}_3)(\eta^2\text{-5-methyl-cycloocta-1,3-dienyl cation})]\text{OTf}$ (**16K**)



In a 20 mL test tube charged with a stir pea, **2** (500 mg, 0.661 mmol) was dissolved in 10 mL THF.  $\text{MeMgBr}$  (1.5M) (0.66 mL, 0.990 mmol) was added via syringe to the solution of **2** and stirred for 15 minutes at R.T. The THF solution was diluted with 20 mL of DCM, extracted 3X with 50mL of  $\text{H}_2\text{O}$ . The organic layer was collected, dried with  $\text{Na}_2\text{SO}_4$  and filtered over a 30mL M fritted disc. The solution was reduced to dryness, redissolved in 5 mL of MeCN and moved to a 10 mL RB flask with a stir pea. In a 10 mL test tube, HOTf (119mg, 0.793 mmol) was added, followed by 1 mL of MeCN. The acid solution was added to the RB flask and stirred for 2 minutes. The MeCN solution was reduced to dryness, redissolved in minimal DCM and added to 500 mL of stirring hexanes. The precipitate was collected over a 30 mL F fritted disc and desiccated. (435 mg, 0.545 mmol, 83%).

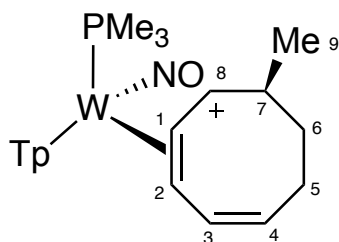
**$^1\text{H}$  NMR (800 MHz,  $\text{CD}_3\text{CN}$ ,  $\delta$ , 25 °C):** 8.35 – 7.83 (d,  $J$  = 1.66; 2.22; 2.91; 2.35; 2.22; 2.35 Hz, 6H, Tp protons), 6.52, 6.19 (t,  $J$  = 1.80; 2.22 Hz, 3H, Tp protons), 6.19 (dd,  $J$  = 2.35, 12.05 Hz, 1H, H8), 5.85 (dt,  $J$  = 8.59, 9.14 Hz, 1H, H3), 5.46 (ddd,  $J$  = 2.35, 9.14, 11.36 Hz, 1H, H7), 5.01 (t,  $J$  = 8.59 Hz, 1H, H2), 4.83 (m, 1H, H1), 3.22 (m, 1H, H4), 2.88 (dt,  $J$  = 9.69, 8.59 Hz, 1H, H6), 2.80 (m, 1H, H4), 3.28 (m, 1H, H5), 2.05 (ddd,

$J = 4.57, 9.14, 13.71$  Hz, 1H, H5), 1.47 (d,  $J = 8.03$  Hz, 3H, H9), 1.16 (d,  $J = 9.83$  Hz, 9H,  $\text{PMe}_3$ )

**$^{13}\text{C}$  NMR (201 MHz,  $\text{CD}_3\text{CN}$ ,  $\delta$ , 25 °C):** isomerized during collection.

**HRMS** - Theoretical: 624.2003 m/z; Experimental: 624.2010 m/z

**Synthesis and characterization of  $[\text{W}(\text{Tp})(\text{NO})(\text{PMe}_3)(\eta^2\text{-6-methyl-cycloocta-1,3-dienyl cation})]\text{OTf}$  (**16T'**)**



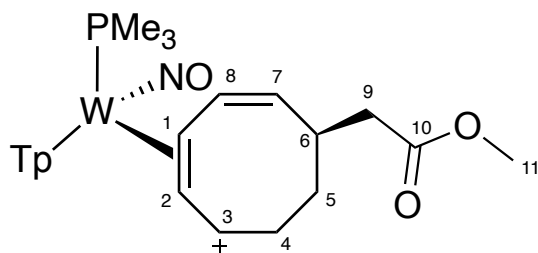
In a 20 mL RB flask charged with a stir pea, compound **16K** (230 mg, 0.289 mmol) was dissolved in 5 mL of MeCN. The solution was stirred overnight and then added to 200 mL of stirring chilled hexanes. The precipitate was collected over a 30 mL F fritted disc and desiccated (196 mg, 0.246 mmol, 85%)

**$^1\text{H}$  NMR (800 MHz,  $\text{CD}_3\text{CN}$ ,  $\delta$ , 25 °C):** 8.16 (d,  $J = 1.77$  Hz, 1H, Pz3B), 8.07 - 8.00 (d,  $J = 2.36, 2.48$  Hz, 2H, Pz5B/Pz5C), 7.396 (d,  $J = 2.54$  Hz, 1H, Pz3A), 7.94 (d,  $J = 2.11$  Hz, 1H, Pz5A), 7.80 (d,  $J = 2.30$  Hz, 1H, Pz3C), 6.51 (t,  $J = 2.39$  Hz, 2H, Pz4C/Pz4B), 6.45 (d,  $J = 10.52$  Hz, 1H, H3), 6.41 (t,  $J = 2.39$  Hz, 1H, Pz4A), 5.78 (qd,  $J = 1.95, 8.85$  Hz, 1H, H8), 5.40 (qd,  $J = 1.68, 9.78$  Hz, 1H, H4), 5.36 (t,  $J = 8.89$  Hz, 1H, H1), 3.56 (t,  $J = 8.89$  Hz, 1H, H2), 3.03 – 2.90 (m, 1H, H7), 2.75 (tt,  $J = 6.41, 7.43$  Hz, 1H, H5), 2.41 (tt,  $J = 5.39, 6.41$  Hz, 1H, H5), 1.70 - 1.59 (tt,  $J = 4.85, 5.56$  Hz, H6), 1.57 – 1.48 (m,  $J = 6.03, 6.86$  Hz, 1H, H6), 1.31 (d,  $J = 6.03$  Hz, 3H, H9), 1.10 (d,  $J = 9.23$  Hz, 9H,  $\text{PMe}_3$ ).

**$^{13}\text{C}$  NMR (201 MHz,  $\text{CD}_3\text{CN}$ ,  $\delta$ , 25 °C):** 144.8 (d,  $J_{\text{PC}} = 3.03$  Hz, 1C, Pz3B), 144.6 (1C, Pz5A), 144.0 (1C, Pz3C), 140.2 - 139.4 (3C, Pz5B/Pz5C/Pz3A), 131.7 (1C, C3), 130.6 (1C, C4), 125.4 (d,  $J_{\text{PC}} = 125.4$  Hz, 1C, C8), 109.4 – 108.1 (3C, Pz4A, Pz4B, Pz4C), 105.0 (d,  $J_{\text{PC}} = 2.16$  Hz, 1C, C1), 79.3 (d,  $J_{\text{PC}} = 3.03$  Hz, 1C, C2), 36.5 (1C, C6) 36.0 (d,  $J_{\text{PC}} = 1.04$  Hz, 1C, C7), 25.7 (1C, C5), 20.5 (1C, C9), 13.8 (d,  $J_{\text{PC}} = 32.01$  Hz 1C,  $\text{PMe}_3$ ).

**HRMS** - Theoretical: 624.2003 g/mol m/z; Experimental: 624.2010 g/mol m/z

**Synthesis and characterization of [W(Tp)(NO)(PMe<sub>3</sub>)( $\eta^2$ -5-enolate-cycloocta-1,3-dienyl cation)]OTf (**17K**)**



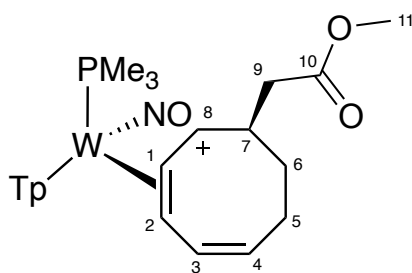
In a 20 mL RB flask charged with a stir pea, compound **2** (50 mg, 0.066 mmol) was dissolved in 5 mL of MeCN. 1-(tert-butyldimethylsiloxy)-1-methoxy-ethene (0.02 mL, 0.092 mmol) was syringed into the solution of **2**, and the reaction was stirred for 30 minutes at R.T. The reaction solution was diluted with 50 mL of DCM, extracted 3X with 50mL of a saturated aqueous solution of Na<sub>2</sub>CO<sub>3</sub>. The organic layer was collected, dried with Na<sub>2</sub>SO<sub>4</sub> and filtered over a 30mL M fritted disc. The solution was reduced to dryness, redissolved in minimal MeCN-d<sub>3</sub>. HOTf (20 mg, 0.13 mmol) was syringed into the reaction mixture, and the reaction was run for 5 minutes. A crude <sup>1</sup>H NMR was taken to observe **17K** before converting to 17T'.

**<sup>1</sup>H NMR (800 MHz, CD<sub>3</sub>CN,  $\delta$ , 25 °C):** 8.35 (d,  $J$  = 2.2 Hz, 1H, Pz), 8.12 (d,  $J$  = 2.2 Hz, 1H, Pz), 8.01 (d,  $J$  = 2.3 Hz, 1H, Pz), 7.97 (d,  $J$  = 2.3 Hz, 1H, Pz), 7.87 (d,  $J$  = 2.3 Hz, 1H, Pz), 7.83 (d,  $J$  = 2.4 Hz, 1H, Pz), 6.52 (t,  $J$  = 2.3 Hz, 2H, Pz), 6.34 (t,  $J$  = 2.3 Hz, 1H, Pz), 6.26 (dd,  $J$  = 11.9, 2.6 Hz, 1H, H8), 5.87 (m, 1H, H3), 5.45 (m, 1H, H7), 5.04 (m, 1H, H2), 4.76 (ddq,  $J$  = 14.5, 8.5, 2.1 Hz, 1H, H1), 3.65 (s, 3H, H11), 3.23 (m, 2H, H4 & H6), 3.06 (m, 1H, H9), 2.96 (dd,  $J$  = 16.4, 8.1 Hz, 1H, H9), 2.79 (dddd,  $J$  = 13.3, 7.7, 5.8, 2.7 Hz, 1H, H4), 2.06 (m, 1H, H5), 1.59 (ddd,  $J$  = 14.5, 13.1, 2.7 Hz, 1H, H5), 1.15 (d,  $J$  = 9.8 Hz, 9H, PMe<sub>3</sub>).

**<sup>13</sup>C NMR (201 MHz, CD<sub>3</sub>CN,  $\delta$ , 25 °C):** 174.1 (1C, C10), 148.1 (1C, Pz), 145.5 (d,  $J_{PC}$  = 2.9 Hz, 1C, Pz), 143.3 (1C, Pz), 139.7 (2C, Pz), 139.5 (1C, Pz), 132.9 (1C, C3), 130.5 (d,  $J_{PC}$  = 4.1 Hz, 1C, C8), 109.6 (1C, Pz), 109.0 (1C, Pz), 108.3 (d,  $J$  = 3.5 Hz, 1C, C2), 108.1 (1C, Pz), 104.6 (1C, C7), 75.1 (d,  $J_{PC}$  = 10.0 Hz, 1C, C1), 52.1 (1C, C11), 40.4 (1C, C9), 39.3 (1C, C6), 31.0 (1C, C5), 28.1 (1C, C4), 12.8 (d,  $J_{PC}$  = 32.8 Hz, 3C, PMe<sub>3</sub>)

**HRMS** - Theoretical: 682.2058g/mol m/z; Experimental: 682.2045 g/mol m/z

**Synthesis and characterization of [W(Tp)(NO)(PMe<sub>3</sub>)( $\eta^2$ -6-enolate-cycloocta-1,3-dienyl cation)]OTf (**17T'**)**



In a 20 mL RB flask charged with a stir pea, compound **2** (50 mg, 0.066 mmol) was dissolved in 5 mL of MeCN. 1-(tert-butyldimethylsiloxy)-1-methoxy-ethene (0.02 mL, 0.092 mmol) was syringed into the solution of **2**, and the reaction was stirred for 30 minutes at R.T. The reaction solution was diluted with 50 mL of DCM, extracted 3X with 50mL of a saturated aqueous solution of Na<sub>2</sub>CO<sub>3</sub>. The organic layer was collected, dried with Na<sub>2</sub>SO<sub>4</sub> and filtered over a 30mL M fritted disc. The solution was reduced to dryness, redissolved in minimal DCM. HOTf (20 mg, 0.13 mmol) was syringed into the reaction mixture, and the reaction was run for 12 hours. Afterwards, 100 mL hexanes was added, and the precipitate was collected over a 30 mL F fritted disc and desiccated (35 mg, 0.042 mmol, 64%)

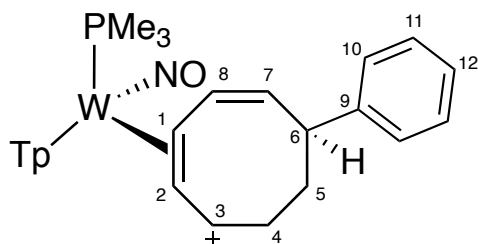
**<sup>1</sup>H NMR (800 MHz, CD<sub>3</sub>CN,  $\delta$ , 25 °C):** 8.14 (d,  $J$  = 2.2 Hz, 1H, Pz), 8.09 (d,  $J$  = 2.4 Hz, 1H, Pz), 8.00 (d,  $J$  = 2.5, 1H, Pz), 7.98 (d,  $J$  = 2.5, 1H, Pz), 7.90 (d,  $J$  = 2.1 Hz, 1H, Pz), 7.81 (d,  $J$  = 2.4 Hz, 1H, Pz), 6.52 (t,  $J$  = 2.4 Hz, 2H, Pz), 6.43 (m, 1H, H3), 6.42 (t,  $J$  = 2.4 Hz, 1H, Pz), 6.14 (m, 1H, H8), 5.41 (m, 1H, H1), 5.38 (m, 1H, H4), 3.67 (s, 3H, H11), 3.50 (m, 1H, H2), 3.24 (m, 1H, H7), 2.78 (m, 1H, H5), 2.71 (d,  $J$  = 6.0 Hz, 2H, H9), 2.43 (ddd,  $J$  = 13.4, 7.9, 4.0 Hz, 1H, H5), 1.77 (m, 1H, H6), 1.55 (m, 1H, H6), 1.09 (d,  $J$  = 9.6 Hz, 9H, PMe<sub>3</sub>).

**<sup>13</sup>C NMR (201 MHz, CD<sub>3</sub>CN,  $\delta$ , 25 °C):** 73.3 (1C, C10), 144.6 (d,  $J_{PC}$  = 3.0 Hz, 1C, Pz), 144.6 (1C, Pz), 144.0 (1C, Pz), 140.3 (1C, Pz), 139.9 (1C, Pz), 139.4 (1C, Pz), 132.0 (1C, C3), 130.3 (1C, C4), 121.1 (d,  $J_{PC}$  = 2.9 Hz, 1C, C8), 109.5 (1C, Pz), 109.0 (1C, Pz), 108.2 (1C, Pz), 104.6 (1C, C1), 78.0 (d,  $J_{PC}$  = 3.3 Hz, 1C, C2), 52.3 (1C, C11), 38.6 (1C, C7), 37.9 (1C, C9), 32.3 (1C, C6), 25.3 (1C, C5), 13.4 (d,  $J_{PC}$  = 32.5 Hz, 3C, PMe<sub>3</sub>).

Composition of **17T'** has been confirmed by single crystal X-ray diffraction.

**HRMS** - Theoretical: 682.2058 g/mol m/z; Experimental: 682.2045 g/mol m/z

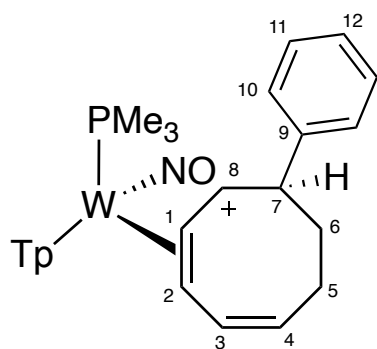
**Synthesis and characterization of [W(Tp)(NO)(PMe<sub>3</sub>)( $\eta^2$ -5-phenyl-cycloocta-1,3-dienyl cation)]OTf (**18K**)**



In a 20 mL test tube charged with a stir pea, **12** (52 mg, 0.076 mmol) was dissolved in 3 mL MeCN-d<sub>3</sub>, protonated with HOTf (13 mg, 0.087 mmol) in MeCN-d<sub>3</sub>, and left to stir for 5 minutes at R.T. A crude <sup>1</sup>H NMR was taken to observe **12A/18K** before the product isomerized into **18T'**. The first isomer seen quickly isomerizes to compounds **18K** then **18T'**. 119-JKH-3, 3-JKH-145

**18K** - <sup>1</sup>H NMR (800 MHz, CD<sub>3</sub>CN,  $\delta$ , 25 °C): 8.32 – 7.51 (d, J = 1.78; 2.20; 1.25; 2.09 Hz, 6H, Tp protons), 6.49 – 6.32 (t, J = 2.21; 2.67; 1.93 Hz, 3H, Tp protons), 6.38 – 4.15 (m, J = 7.91, 9.62; 8.77, 17.53; 9.62; 9.84; 8.77 Hz, 6H, H1 – H3, H6 – H8), 3.37 – 2.08 (m, 4H, H4 – H5), 1.13 (d, J = 9.66 Hz, 9H, PMe<sub>3</sub>).

**Synthesis and characterization of [W(Tp)(NO)(PMe<sub>3</sub>)( $\eta^2$ -6-phenyl-cycloocta-1,3-dienyl cation)]OTf (**18T'**)**



In a 20 mL test tube charged with a stir pea, **12** (52 mg, 0.076 mmol) was dissolved in 3 mL MeCN-d<sub>3</sub>, protonated with HOTf (13 mg, 0.087 mmol) in MeCN-d<sub>3</sub>, and left to stir for 12 hours at R.T. The crude reaction mixture was reduced to dryness in vacuo. Next, the reaction was redissolved in minimal DCM, and 100 mL hexanes was used to

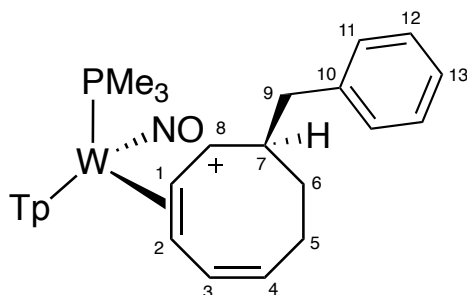


precipitate out a whitish tan solid. The solid was collected over a 15 mL F fritted disc and desiccated yielding **18T'** (43 mg, 0.051 mmol, 68%). 3-JKH-145

**<sup>1</sup>H NMR (800 MHz, CD<sub>3</sub>CN, δ, 25 °C):** 8.26 (d, *J* = 2.2 Hz, 1H, Pz), 8.10 (d, *J* = 2.2 Hz, 1H, Pz), 8.03 (d, *J* = 2.3 Hz, 1H, Pz), 7.96 (d, *J* = 2.5 Hz, 1H, Pz), 7.94 (d, *J* = 2.4 Hz, 1H, Pz), 7.79 (d, *J* = 2.4 Hz, 1H, Pz), 7.56 (m, 2H, H10), 7.43 (t, *J* = 7.6 Hz, 2H, H11), 7.33 (t, *J* = 7.4 Hz, 1H, H12), 6.95 (dt, *J* = 10.9, 1.9 Hz, 1H, H3), 6.50 (t, *J* = 2.4 Hz, 1H, Pz), 6.44 (t, *J* = 2.4 Hz, 2H, Pz), 5.86 (dtd, *J* = 10.8, 9.2, 1.8 Hz, 1H, H8), 5.61 (ddd, *J* = 10.6, 8.8, 7.2 Hz, 1H, H4), 5.51 (t, *J* = 8.8 Hz, 1H, H1), 4.33 (d, *J* = 8.9 Hz, 1H, H2), 4.18 (ddd, *J* = 11.9, 9.4, 4.9 Hz, 1H, H7), 2.95 (m, 1H, H5), 2.47 (m, 1H, H5), 1.91 (m, 1H, H6), 1.64 (tq, *J* = 14.8, 4.9 Hz, 1H, H6), 0.54 (d, *J* = 9.8 Hz, 9H, PMe<sub>3</sub>).

**<sup>13</sup>C NMR (201 MHz, CD<sub>3</sub>CN, δ, 25 °C):** 145.1 (1C, Pz), 145.0 (d, *J* = 2.6 Hz, 1C, Pz), 144.5 (1C, C9), 144.4 (1C, Pz), 140.1 (1C, Pz), 140.0 (1C, Pz), 139.4 (1C, Pz), 131.7 (1C, C3), 131.6 (1C, C4), 130.1 (2C, C11), 129.8 (2C, C10), 128.5 (1C, C12), 111.3 (d, *J* = 2.9 Hz, 1C, C1), 110.1 (d, *J* = 5.8 Hz, 1C, C8), 109.4 (1C, Pz), 108.9 (1C, Pz), 108.3 (1C, Pz), 88.9 (d, *J* = 3.7 Hz, 1C, C2), 46.9 (1C, C7), 37.9 (1C, C6), 26.1 (1C, C5), 14.0 (d, *J* = 32.9 Hz, 3C, PMe<sub>3</sub>).

### Synthesis and characterization of [W(Tp)(NO)(PMe<sub>3</sub>)(η<sup>2</sup>-6-benzyl-cycloocta-1,3-dienyl cation)]OTf (**19T'**)



In a test tube charged with a stir pea, **13** (286 mg, 0.41 mmol) was dissolved in 3 mL DCM, protonated with HOTf (70.4 mg, 0.47 mmol), and left to stir for 12 hours. Afterwards, 125 mL hexanes was added, precipitating out a whitish tan solid. The precipitate was collected on a 15 mL F fritted disc and washed with 2X 10 mL hexanes. The solid was desiccated, yielding **19T'** (314 mg, 93%).

**<sup>1</sup>H NMR (800 MHz, CD<sub>3</sub>CN, δ, 25 °C):** 8.22 (d, *J* = 2.2 Hz, 1H, Pz), 8.10 (d, *J* = 2.3 Hz, 1H, Pz), 8.02 (d, *J* = 2.5, 1H, Pz), 8.00 (d, *J* = 2.3 Hz, 1H, Pz), 7.99 (d, *J* = 2.3 Hz, 1H,

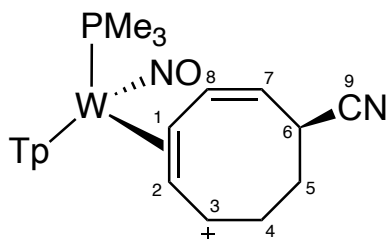
Pz), 7.84 (d,  $J = 2.3$  Hz, 1H, Pz), 7.30 (appt,  $J = 7.6$  Hz, 2H, H12), 7.25 (d,  $J = 7.5$  Hz, 2H, H11), 7.21 (m, 1H, H13), 6.53 (t,  $J = 2.3$  Hz, 2H, Pz), 6.47 (dt,  $J = 10.7, 2.7$ , 1H, H3), 6.44 (t,  $J = 2.3$  Hz, 1H, Pz), 5.87 (qd,  $J = 8.7, 2.0$  Hz, 1H, H8), 5.44 (m, 1H, H1), 5.24 (ddd,  $J = 10.6, 8.9, 7.4$  Hz, 1H, H4), 3.62 (m, 1H, H2), 3.30 (dd,  $J = 12.9, 4.0$  Hz, 1H, H9'), 3.18 (m, 1H, H7), 2.80 (m, 1H, H9), 2.75 (m, 1H, H5), 2.30 (m, 1H, H5), 1.40-1.37 (m, 2H, H6), 1.13 (d,  $J = 9.5$  Hz, 9H, PMe<sub>3</sub>).

**<sup>13</sup>C NMR (201 MHz, CD<sub>3</sub>CN, δ, 25 °C):** 144.8 (1C, Pz), 144.6 (1C, Pz), 144.0 (1C, Pz), 140.4 (1C, C10), 140.2 (1C, Pz), 139.8 (1C, Pz), 139.5 (1C, Pz), 131.7 (1C, C3), 130.6 (1C, C4), 130.5 (2C, C11), 129.3 (2C, C12), 127.2 (1C, C13), 122.3 (d,  $J_{PC} = 3.4$  Hz, 1C, C8), 109.5-108.1 (3C, Pz4A/Pz4B/Pz4C), 105.2 (d,  $J_{PC} = 2.5$  Hz, 1C, C1), 79.9 (d,  $J_{PC} = 3.2$  Hz, 1C, C2), 43.2 (1C, C7), 41.4 (1C, C9), 31.6 (1C, C6), 25.3 (1C, C5), 13.8 (d,  $J_{PC} = 32.5$  Hz).

Composition of **19T'** has been confirmed by single crystal X-ray diffraction.

**HRMS** - Theoretical: 700.2316 m/z; Experimental: 700.2290 m/z

### Synthesis and characterization of [W(Tp)(NO)(PMe<sub>3</sub>)( $\eta^2$ -5-cyano-cycloocta-1,3-dienyl cation)]OTf (**20K**)



In a 20 mL RB flask charged with a stir pea, compound **4** (75 mg, 0.118 mmol) was dissolved in 3 mL of MeCN. In a 10mL test tube, HOTf (22 mg, 0.146 mmol) was added, followed by 1 mL of MeCN. The acid solution was added to solution of compound **4**. The solution was stirred for 3 hours and then added to 200 mL of stirring ether. The precipitate was collected over a 15 mL F fritted disc and desiccated yielding compound **20K** (76 mg, 0.095 mmol, 82%) When using d-MeCN, an intermediate immediately grows and starts completely disappearing after 2 hours.

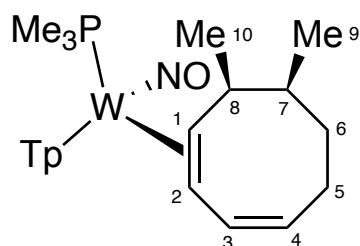
**20K <sup>1</sup>H NMR (800 MHz, CD<sub>3</sub>CN, δ, 25 °C):** 8.36 (d,  $J = 1.80$  Hz, 1H, Pz3B), 8.13 (d,  $J = 1.95$  Hz, 1H, Pz3A), 8.02 (d,  $J = 2.40$  Hz, 1H, Pz5B), 7.98 (d,  $J = 2.40$  Hz, 1H, Pz3C), 7.94 (d,  $J = 2.55$  Hz, 1H, Pz5C), 7.84 (d,  $J = 2.55$  Hz, 1H, Pz5A), 6.58 (d,  $J = 11.18$  Hz,

1H, H8), 6.54 - 6.52 (m, 2H, Pz4B/Pz4C), 6.35 (t,  $J = 1.97$  Hz, 1H, Pz4A), 5.88 (td,  $J = 9.78$  Hz, 1H, H3), 5.23 (dt,  $J = 1.55, 10.06$  Hz, 1H, H7), 5.19 (t,  $J = 8.93$  Hz, 1H, H2), 4.75 (dd,  $J = 8.18, 14.01$  Hz, 1H, H1), 3.98 (t,  $J = 7.80$  Hz, 1H, H6), 3.19 - 3.13 (m, 1H, H4), 2.92 - 2.88 (m, 1H, H4), 2.02 - 1.96 (m, 2H, H5), 1.17 (d,  $J = 9.54$  Hz, 9H, PMe<sub>3</sub>).

**<sup>20</sup>K -<sup>13</sup>C NMR (201 MHz, CD<sub>3</sub>CN, δ, 25 °C):** 148.2 (1C, Pz3A), 145.8 (1C, Pz3B), 143.2 (1C, Pz3C), 139.8 – 139.7 (3C, Pz5B/Pz5C/Pz5A), 135.0 (1C, C8), 130.6 (1C, C3), 122.3 (1C, C9), 122.1 (1C, C7), 110.3 (d,  $J_{PC} = 4.59$  Hz, 1C, C2) 109.6 – 109.1 (3C, Pz4B/Pz4A/Pz4C), 71.5 (d,  $J_{PC} = 10.54$  Hz, 1C, C1), 28.73 (1C, C5), 26.22 (1C, C4), 15.6 (1C, C6), 12.6 (d,  $J_{PC} = 31.88$  Hz 1C, PMe<sub>3</sub>).

Composition of **20K** has been confirmed by single crystal X-ray diffraction.

### Synthesis and characterization of [W(Tp)(NO)(PMe<sub>3</sub>)(η<sup>2</sup>-7,8-methyl,methyl-cycloocta-1,3-diene) (**21**)

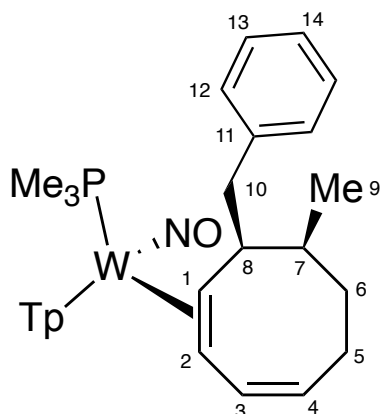


In a 20 mL test tube charged with a stir pea, compound **16T'** (50 mg, 0.065 mmol) was dissolved in 5 mL of THF. MeMgBr (1.5M) (0.47 mL, 0.071 mmol) was syringed into the test tube and stirred for 5 minutes. The reaction mixture as diluted with 10 mL dichloromethane, extracted 3X with 20mL of a saturated aqueous solution of Na<sub>2</sub>CO<sub>3</sub>. The organic layer was dried with Na<sub>2</sub>SO<sub>4</sub>, filtered over a 30mL M fritted disc and reduced to dryness. The reaction was redissolved in minimal THF and added to 100 mL of stirring chilled pentanes and collected over a 15 mL F fritted disc and desiccated yielding compound **21** (22 mg, 0.034 mmol, 52%)

**<sup>1</sup>H NMR (800 MHz, CD<sub>3</sub>CN, δ, 25 °C):** 8.04, 7.94, 7.86, 7.84, 7.81, 7.36 (d,  $J = 2.05, 2.55, 2.39$  Hz, 6H, Tp protons), 6.34, 6.30 (t,  $J = 2.16, 1.92$  Hz, Tp protons), 6.21 (d, 9.85 Hz, H3), 5.20 (m, 1H, H4), 3.62 (m, 1H, H7), 2.93 (m, 1H, H1), 2.55 (m, 1H, H8), 2.26, 2.06, 1.52, 1.47 (m, 4H, H5/H6), 1.16 (d,  $J = 2.18, 4H, H2/H9$ ), 1.33 (d,  $J = 7.59, 3H, H10$ ), 1.00 (m, 9H, PMe<sub>3</sub>).

**<sup>13</sup>C NMR (201 MHz, CD<sub>3</sub>CN, δ, 25 °C):** too dilute to solve.

**Synthesis and characterization of  $[W(Tp)(NO)(PMe_3)(\eta^2\text{-7-methyl-8-benzyl-cycloocta-1,3-diene})]$  (**22**)**

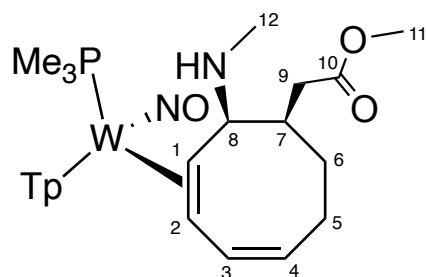


In a 20 mL test tube charged with a stir pea, compound **16T'** (100 mg, 0.129 mmol) was dissolved in 5 mL of THF.  $BnMgBr$  (1.5M) (0.65 mL, 0.975 mmol) was syringed into the test tube at R.T. and stirred for 15 minutes. The reaction mixture as diluted with 10 mL dichloromethane, extracted 3X with 20mL  $H_2O$ . The organic layer was collected, dried with  $Na_2SO_4$ , filtered over a 30mL M fritted disc and reduced to minimal solvent. The solution was transferred to a weighed vial and reduced to dryness to yield compound **22** (88 mg, 0.120 mmol, 97%)

**$^1H$  NMR (800 MHz,  $CD_3CN$ ,  $\delta$ , 25 °C):** 7.97 – 7.83 (5H, Pz3A/Pz3B/Pz5A/Pz5B/Pz5C), 7.41 (d,  $J$  = 7.40 Hz, 2H, H11), 7.26 (t,  $J$  = 8.75 Hz, 2H, H12), 7.40 (bs, 1H, Pz3C), 7.14 (t,  $J$  = 10.29 Hz, 1H, H13), 6.34 – 6.30 (t, 3H, Pz4A/Pz4B/Pz4C), 6.16 (d,  $J$  = 9.13 Hz, 1H, H3), 5.16 (bs, 1H, H4), 3.29 (d,  $J$  = 11.48 Hz, 1H, H10), 3.10 (bs, 1H, H1), 2.78 (t,  $J$  = 16.49 Hz, 1H, H10), 2.50 (t,  $J$  = 13.54 Hz, 1H, H8), 2.34 – 2.27 (m, 2H, H7/H6), 1.60 (bs, 2H, H5), 1.47 – 1.41 (m, 1H, H6), 1.17 (d,  $J$  = 9.13 Hz, 3H, H9), 0.98 (d,  $J$  = 9.13 Hz, 9H,  $PMe_3$ ).

**$^{13}C$  NMR (201 MHz,  $CD_3CN$ ,  $\delta$ , 25 °C):** 144.5 – 137.6 (6C, Tp carbons), 131.7 (1C, C3), 130.2 (2C, C11), 128.6 (2C, C12), 128.6 (1C, C14), 127.4 (1C, C4), 126.2 (1C, C13), 107.7 - 106.8 (3C, Tp carbons), 59.6 (1C, C2), 54.0 (1C, C1), 46.3 (1C, C8) 44.2 (1C, C10), 38.7 (1C, C5), 32.8 (1C, C6), 32.8 (1C, C6), 31.2 (1C, C7), 15.0 (1C, C9), 13.9 (d,  $J_{PC}$  = 26.47 Hz 3C,  $PMe_3$ ).

## Synthesis and characterization of [W(Tp)(NO)(PMe<sub>3</sub>)( $\eta^2$ -7-enolate-8-methylamine-cycloocta-1,3-diene] (**23**)

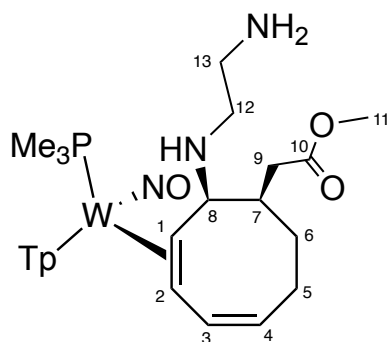


In a 20 mL test tube charged with a stir pea, compound **17T'** (50 mg, 0.060 mmol) was dissolved in 5 mL of MeCN. Methylamine (0.01 mL, 0.12 mmol) was syringed into the test tube at R.T. and stirred for 15 minutes. The reaction mixture was diluted with 10 mL dichloromethane, extracted 3X with 20mL Na<sub>2</sub>CO<sub>3</sub>. The organic layer was collected, dried with Na<sub>2</sub>SO<sub>4</sub>, filtered over a 30mL M fritted disc and reduced to minimal solvent. The solution was transferred to a weighed vial and reduced to dryness to yield compound **23** (25 mg, 0.035 mmol, 58%).

**<sup>1</sup>H NMR (800 MHz, CD<sub>3</sub>CN,  $\delta$ , 25 °C):** 7.95 (d,  $J$  = 2.0 Hz, 1H, Pz), 7.92 (d,  $J$  = 2.0 Hz, 1H, Pz), 7.76 (d,  $J$  = 2.4 Hz, 2H, Pz), 7.73 (d,  $J$  = 2.4 Hz, 1H, Pz), 7.21 (d,  $J$  = 2.1 Hz, 1H, Pz), 6.32 (t,  $J$  = 2.2 Hz, 1H, Pz), 6.26 (m, 2H, Pz), 6.17 (dt,  $J$  = 11.8, 2.3 Hz, 1H, H3), 5.23 (ddt,  $J$  = 11.2, 5.7, 2.4 Hz, 1H, H4), 3.69 (s, 3H, H11), 3.05 (m, 1H, H8), 3.03 (dd,  $J$  = 14.5, 2.9 Hz, 1H, H9), 2.96 (dt,  $J$  = 14.5, 10.1 Hz, 1H, H1), 2.55 (m, 1H, H7), 2.52 (m, 1H, H5), 2.42 – 2.35 (m, 5H, H5, H6, & H12), 2.34 (dd,  $J$  = 14.6, 11.0 Hz, 1H, H9), 1.76 (ddd,  $J$  = 12.8, 8.2, 4.1 Hz, 1H, H6), 1.34 (m, 1H, H2), 1.04 (broad s, 9H).

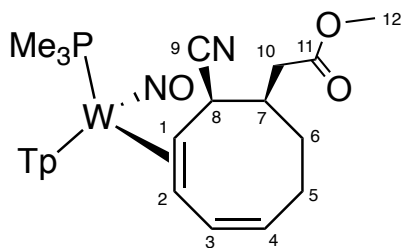
**<sup>13</sup>C NMR (201 MHz, CD<sub>3</sub>CN,  $\delta$ , 25 °C):** 75.68 (1C, C10), 143.87 (1C, Pz), 142.87 (1C, Pz), 140.09 (1C, Pz), 137.08 (1C, Pz), 136.63 (2C, Pz), 130.36 (1C, C3), 127.47 (1C, C4), 106.97 (1C, Pz), 106.71 (1C, Pz), 106.12 (1C, Pz), 63.50 (1C, C8), 58.26 (1C, C2), 55.99 (d,  $J$  = 10.5 Hz, 1C, C1), 51.59 (1C, C11), 41.03 (1C, C7), 35.69 (1C, C12), 33.93 (1C, C9), 30.96 (1C, C5), 28.72 (1C, C6), 13.69 (d,  $J$  = 27.9 Hz, 3C, PMe<sub>3</sub>).

**Synthesis and characterization of  $[W(Tp)(NO)(PMe_3)(\eta^2\text{-7-enolate-8-methylenediamine-cycloocta-1,3-diene})]$  (**24**)**



In an NMR tube, a few milligrams of compound **17T'** was dissolved in a pipette of MeCN-*d*<sub>3</sub>. A drop of ethylene diamine was syringed into the solution of **17T'**, and an <sup>1</sup>H NMR was taken of the crude reaction mixture.

**Synthesis and characterization of  $[W(Tp)(NO)(PMe_3)(\eta^2\text{-7-enolate-8-cyano-cycloocta-1,3-diene})]$  (**25**)**

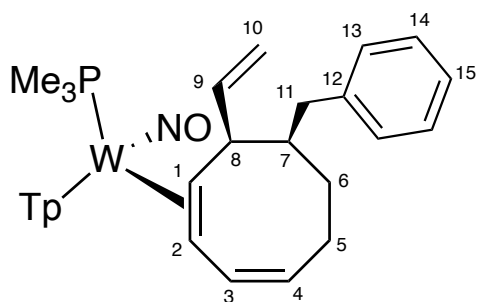


In a 20 mL test tube charged with a stir pea, compound **17T'** (100 mg, 0.120 mmol) was dissolved in 5 mL of MeCN. NaCN (59 mg, 1.20 mmol) was added into the test tube with a few drops of DMSO at R.T. and stirred for 12 hours. Afterwards, unreacted solid NaCN was filtered and discarded in a 15 mL F fritted disc. The filtrate was diluted with 10 mL dichloromethane, extracted 3X with 20mL H<sub>2</sub>O. The organic layer was collected, dried with Na<sub>2</sub>SO<sub>4</sub>, filtered over a 30mL M fritted disc and reduced to dryness. The organic layer was redissolved in a minimal DCM, and impurities were precipitated out of 100 mL hexanes. The impurities were collected and discarded on a 15 mL fritted disc, and the filtrate was reduced to a minimal volume. The solution was transferred to a weighed vial and reduced to dryness to yield compound **25** (75 mg, 0.106 mmol, 88%).

**<sup>1</sup>H NMR (800 MHz, CD<sub>2</sub>Cl<sub>2</sub>, δ, 25 °C):** 8.00 – 7.22 (d/bs, *J* = 2.83; 3.58; 2.37; 2.88 Hz, 6H, Tp protons), 6.32 – 6.26 (bs, 3H, Tp protons), 6.19 (d, *J* = 12.69 Hz, 1H, H3), 5.30 (bs, 1H, H4), 3.73 (s, 3H, H12), 3.71 (bs, 1H, H8), 2.96 (d, *J* = 13.94, 1H, H10), 2.73 (t, *J* = 11.22 Hz, 1H, H10), 2.66 (bs, 1H, H7), 2.63 (m, 1H, H1), 2.57 (bs, 1H, H5), 2.36 (bs, 2H, H5/H6), 1.75 (bs, 1H, H6), 1.32 (bs, 1H, H2), 1.09 (bs, 9H, PMe<sub>3</sub>).

**<sup>13</sup>C NMR (201 MHz, CD<sub>2</sub>Cl<sub>2</sub>, δ, 25 °C):** 173.3 (1C, C11), 143.7 – 136.8 (6C, Tp carbons), 129.6 (1C, C3), 127.0 (1C, C4), 126.9 (1C, C9), 107.0 – 106.1 (3C, Tp carbons), 57.0 (1C, C2), 52.0 (1C, C12), 44.5 (d, *J* = 10.44 Hz, 1C, C1), 43.9 (1C, C12), 37.5 – 37.2 (2C, C8/C10), 30.1 (1C, C5), 28.0 (1C, C6), 13.6 (d, *J* = 26.46 Hz, 3C, PMe<sub>3</sub>).

### Synthesis and characterization of [W(Tp)(NO)(PMe<sub>3</sub>)(η<sup>2</sup>-7-benzyl-8-vinyl-cycloocta-1,3-diene) (26)



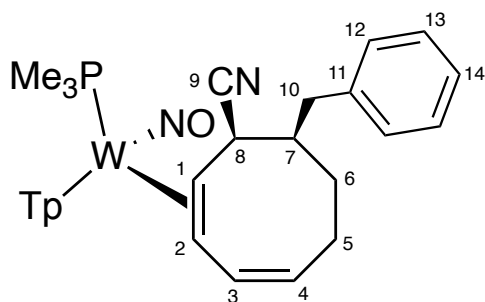
In a 20 mL test tube charged with a stir pea, compound **19T'** (50 mg, 0.059 mmol) was dissolved in 5 mL of THF. VinylMgBr (2.10 mL, 0.295 mmol) was syringed into the test tube at R.T. and stirred for 30 minutes. The reaction mixture was diluted with 10 mL dichloromethane, extracted 3X with 20mL H<sub>2</sub>O. The organic layer was collected, dried with Na<sub>2</sub>SO<sub>4</sub>, filtered over a 30mL M fritted disc and reduced to dryness. The organic layer was redissolved in minimal THF, and impurities were precipitated out of 50 mL pentanes. The impurities were collected and discarded over a 15 mL F fritted disc and, the filtrate was reduced to minimal volume. The solution was transferred to a weighed vial and reduced to dryness to yield compound **26** (40 mg, 0.055 mmol, 93%).

**<sup>1</sup>H NMR (800 MHz, CD<sub>3</sub>CN, δ, 25 °C):** 8.03 (d, *J* = 2.0 Hz, 1H, Pz), 8.02 (d, *J* = 2.0 Hz, 1H, Pz), 7.86 (d, *J* = 2.2 Hz, 1H, Pz), 7.85 (d, *J* = 2.4 Hz, 1H, Pz), 7.82 (d, *J* = 2.1 Hz, Pz), 7.40 (d, *J* = 2.2 Hz, 1H, Pz), 7.30 – 7.28 (m, 2H, H13), 7.22 (t, *J* = 7.7 Hz, 2H, H14), 7.13 (m, 1H, H15), 6.44 (m, 1H, H9), 6.42 (m, 1H, H3), 6.35 (t, *J* = 2.1 Hz, 1H, Pz), 6.30 (t, *J* = 2.2 Hz, 1H, Pz), 6.29 (t, *J* = 2.2 Hz, 1H, Pz), 5.25 (appt, *J* = 17.4, 1H, H10), 5.22

(m, 1H, H10), 5.12 (m, 1H, H4), 3.61 (m, 1H, H8), 3.07 (dd,  $J = 12.5, 3.2$  Hz, 1H, H11), 2.84 (ddd,  $J = 13.9, 11.0, 3.0$  Hz, 1H, H1), 2.66 (m, 1H, H5), 2.54 (t,  $J = 12.0$  Hz, 1H, H11), 2.49 (m, 1H, H7), 1.93 (m, 1H, H5), 1.53 (m, 1H, H6), 1.08 (d,  $J = 8.2$  Hz, 9H,  $\text{PMe}_3$ ), 1.07 - 1.03 (m, 2H, H2 & H6).

**$^{13}\text{C}$  NMR (201 MHz,  $\text{CD}_3\text{CN}$ ,  $\delta$ , 25 °C):** 147.8 (1C, C9), 144.6 (1C, Pz), 143.6 (2C, C12 or C15 & Pz), 141.4 (1C, Pz), 138.0 (1C, Pz), 137.6 (1C, Pz), 137.3 (1C, Pz), 134.7 (1C, C3), 130.6 (2C, C13), 128.8 (2C, C14), 126.3 (1C, C15 or C12), 125.2 (1C, C4), 114.3 (1C, C10), 107.5 (1C, Pz), 107.4 (1C, Pz), 106.8 (1C, Pz), 56.5 (1C, C2), 55.5 (d,  $J_{\text{PC}} = 9.7$  Hz, 1C, C1), 41.9 (1C, C11), 30.2 (1C, C6), 26.7 (1C, C5), 13.9 (d,  $J_{\text{PC}} = 27.8$  Hz, 3C,  $\text{PMe}_3$ ). Too dilute to see C7 or C8.

### Synthesis and characterization of $[\text{W}(\text{Tp})(\text{NO})(\text{PMe}_3)(\eta^2\text{-7-benzyl-8-cyano-cycloocta-1,3-diene})]$ (**27**)



In a 20 mL test tube charged with a stir pea, compound **19T'** (300 mg, 0.353 mmol) was dissolved in 5 mL MeCN. To this solution, NaCN (173 mg, 3.53 mmol) was added with a few drops of DMSO. This reaction mixture was stirred for 12 hours. The crude reaction mixture was then diluted with DCM and extracted 3x with 10 mL  $\text{H}_2\text{O}$ . The reaction was then dried with  $\text{Na}_2\text{SO}_4$  and filtered to remove drying agent. Afterwards the reaction was reduced to minimal volume. The solution was transferred to a weighed vial and reduced to dryness to yield compound **27** (220 mg, 0.303 mmol, 86%).

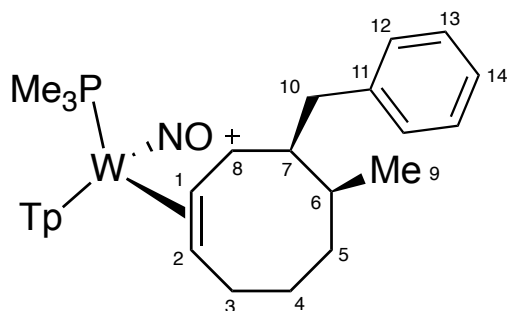
**$^1\text{H}$  NMR (800 MHz,  $\text{CD}_3\text{CN}$ ,  $\delta$ , 25 °C):** 8.03 (d,  $J = 2.0$  Hz, 1H, Pz), 7.94 (d,  $J = 2.0$  Hz, 1H, Pz), 7.89 (d,  $J = 2.3$  Hz, 1H, Pz), 7.88 (d,  $J = 2.4$  Hz, 1H, Pz), 7.84 (d,  $J = 2.5$  Hz, 1H, Pz), 7.48 (d,  $J = 2.2$  Hz, 1H, Pz), 7.36 – 7.31 (m, 4H, H12 & H13), 7.26 – 7.22 (m, 1H, H14), 6.37 (t,  $J = 2.2$  Hz, 1H, Pz), 6.36 (t,  $J = 2.2$  Hz, 1H, Pz), 6.30 (t,  $J = 2.3$  Hz, 1H, Pz), 6.19 (d,  $J = 11.7$  Hz, 1H, H3), 5.23 (dq,  $J = 9.4, 3.1$  Hz, 1H, H4), 3.74 (dd,  $J = 9.0, 3.4$  Hz, 1H, H8), 3.31 (dd,  $J = 13.0, 2.8$  Hz, 1H, H10), 2.97 (t,  $J = 12.3$  Hz, 1H, 10),



2.91 (dt,  $J = 13.1, 9.5$  Hz, 1H, H1), 2.45 (m, 1H, H5), 2.35 (q,  $J = 4.3$  Hz, 1H, H7), 2.24 – 2.15 (m, 2H, H5 & H6), 1.46 (ddd,  $J = 19.2, 10.0, 5.6$  Hz, 1H, H6), 1.23 (dt,  $J = 9.9, 2.7$  Hz, 1H, H2), 1.11 (d,  $J = 8.2$  Hz, 9H, PMe<sub>3</sub>).

**<sup>13</sup>C NMR (201 MHz, CD<sub>3</sub>CN, δ, 25 °C):** 144.2 (1C, Pz), 144.1 (1C, Pz), 142.2 (1C, C11), 141.4 (1C, Pz), 138.3 (1C, Pz), 137.8 (1C, Pz), 137.7 (1C, Pz), 130.6 (1C, C3), 130.3 (2C, C12 or C13), 129.3 (2C, C12 or C13), 128.0 (1C, C9), 127.5 (1C, C4), 126.9 (1C, C14), 107.7 (2C, Pz), 106.9 (1C, Pz), 57.1 (1C, C2), 49.3 (1C, C7), 45.6 (d,  $J_{PC} = 12.3$  Hz, 1C, C1), 39.5 (1C, C8), 38.9 (d,  $J_{PC} = 4.4$  Hz, 1C, C10), 30.0 (d,  $J_{PC} = 18.2$  Hz, 1C, C5), 27.3 (1C, C6), 13.6 (d,  $J_{PC} = 28.3$  Hz, 3C, PMe<sub>3</sub>).

### Synthesis and characterization of [W(Tp)(NO)(PMe<sub>3</sub>)( $\eta^2$ -8-benzyl-7-methyl-cyclooctenyl cation)]OTf (**28**)



In a 20 mL test tube charged with a stir pea, compound **22** (210 mg, 0.272 mmol) was dissolved in 12 mL of THF. BnMgBr (1.5M) (0.90 mL, 1.35 mmol) was syringed into the test tube at R.T. and stirred for 5 minutes. The reaction mixture was diluted with 20 mL dichloromethane, extracted 3X with 20 mL H<sub>2</sub>O. The organic layer was collected, dried with Na<sub>2</sub>SO<sub>4</sub>, filtered over a 30 mL fritted disc and reduced to minimal solvent. The solution was redissolved in 5 mL MeCN. In a 10 mL test tube, HOTf (62 mg, 0.413 mmol) was added followed by 1 mL of MeCN. The acid solution was transferred into the [W] solution and stirred for 15 minutes. The reaction was reduced with 10 mL dichloromethane, extracted 3X with 10 mL H<sub>2</sub>O, dried with Na<sub>2</sub>SO<sub>4</sub> and filtered over a 30 mL fritted disc. The filtrate was reduced to dryness, redissolved in minimal THF and added to 200 mL stirring chilled hexanes. The precipitate was collected on a 15 mL fritted disc and desiccated to yield compound **28** (173 mg, 0.202 mmol, 74%).

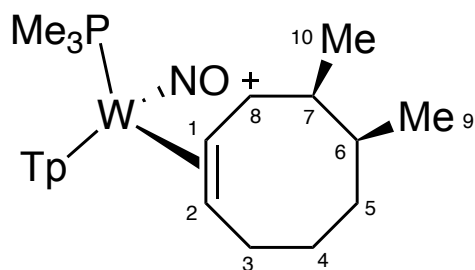
**<sup>1</sup>H NMR (800 MHz, CD<sub>3</sub>CN, δ, 25 °C):** 8.22 (d,  $J = 1.97$  Hz, 1H, Pz3B), 8.07 (d,  $J = 2.58$  Hz, 1H, Pz5B), 8.04 (d,  $J = 1.97$  Hz, 1H, Pz3A), 8.01 (d,  $J = 2.58$  Hz, 1H, Pz5C),

7.95 (d,  $J = 2.58$  Hz, 1H, Pz5A), 7.82 (d,  $J = 1.82$  Hz, 1H, Pz3C), 7.37 (d,  $J = 6.48$  Hz, 2H, H11), 7.33 (t,  $J = 8.00$  Hz, 2H, H12), 7.24 (t,  $J = 8.00$  Hz, 1H, H13), 6.52 (t,  $J = 2.36$  Hz, 2H, Pz4B/Pz4C), 6.39 (t,  $J = 2.36$  Hz, 1H, Pz4A), 5.88 (dt,  $J = 8.25, 9.37$  Hz, 1H, H8), 5.47 (t,  $J = 8.47$  Hz, 1H, H1), 3.69 – 3.63 (m, 2H, H2/H7), 3.28 – 3.21 (m, 1H, H3), 3.20 (dd,  $J = 3.89, 13.68$  Hz, 1H, H10), 2.96 (dd,  $J = 12.29, 13.53$  Hz, 1H, H10), 2.49 – 2.45 (m, 1H, H3), 1.85 – 1.80 (m, 1H, H5), 1.74 – 1.69 (m, 1H, H6), 1.66 – 1.59 (m, 2H, H4), 1.59 – 1.54 (m, 1H, H5), 1.10 (d,  $J = 9.46$  Hz, 9H, PMe<sub>3</sub>), 1.05 (d,  $J = 7.06$  Hz, 3H, H9).

**<sup>13</sup>C NMR (201 MHz, CD<sub>3</sub>CN, δ, 25 °C):** 145.0 (1C, Pz3B), 144.7 (1C, Pz3C), 143.9 (1C, Pz3A), 140.3 (1C, C14), 140.2 (1C, Pz5B), 139.6 (1C, Pz5A), 139.4 (1C, Pz5C), 130.2 (2C, C11), 129.4 (2C, C12), 127.2 (1C, C13), 119.7 (1C, C8), 109.6 (1C, C1), 109.5/108.8 (2C, Pz4B/Pz4C), 107.8 (1C, Pz4A), 85.5 (1C, C2), 46.4 (1C, C7), 38.6 (1C, C10), 37.5 (1C, C6) 33.7 (1C, C5), 32.6 (1C, C3), 28.8 (1C, C4), 15.2 (1C, C9), 14.0 (d,  $J_{PC} = 33.80$  Hz 3C, PMe<sub>3</sub>).

**HRMS** - Theoretical: 716.2629 m/z; Experimental: 716.2641 m/z

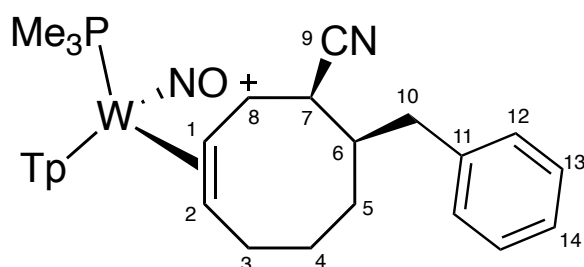
### Synthesis and characterization of [W(Tp)(NO)(PMe<sub>3</sub>)(η<sup>2</sup>-8-methyl-7-methylcyclooctenyl cation)]OTf (29)



In a 20 mL test tube charged with a stir pea, compound **22** (50 mg, 0.065 mmol) was dissolved in 5 mL of THF. MeMgBr (1.5M) (0.09 mL, 0.135 mmol) was syringed into the test tube at R.T. and stirred for 15 minutes. The reaction mixture was diluted with 10 mL dichloromethane, extracted 3X with 20mL H<sub>2</sub>O. The organic layer was collected, dried with Na<sub>2</sub>SO<sub>4</sub>, filtered over a 30mL M fritted disc and reduced to minimal solvent. The solution was redissolved in 5mL MeCN. In a 10mL test tube, HOTf (12 mg, 0.080 mmol) was added followed by 1mL of MeCN. The acid solution was transferred into the [W] solution and stirred for 5 minutes. The reaction was reduced to dryness, redissolved in

minimal DCM and added to 100 mL stirring hexanes. The precipitate was collected on a 15 mL F fritted disc and desiccated to yield compound **29** (10 mg, 0.013 mmol, 20%)  
**<sup>1</sup>H NMR (800 MHz, CD<sub>3</sub>CN, δ, 25 °C):** 8.18 – 7.78 (d, *J* = 2.36; 2.18; 2.91; 2.18; 2.19; 2.36 Hz, 6H, Tp protons), 6.51 – 6.36 (t, *J* = 2.18; 2.53, 2.18 Hz, 3H, Tp protons), 5.81 (dt, *J* = 8.73, 9.34 Hz, 1H, H8), 5.41 (t, *J* = 8.73 Hz, 1H, H1), 3.53 (dt, *J* = 8.64, 9.08 Hz, 1H, H2), 3.43 (m, 1H, H7), 3.16 (m, 1H, H3), 2.43 (dd, *J* = 7.51, 15.11 Hz, 1H, H3), 1.97 (m, 1H, H6), 1.87/1.70/1.65, 1.54 (m, 4H, H4 – H6), 1.35 (d, *J* = 6.65 Hz, 3H, H10), 1.08 (d, *J* = 9.74 Hz, 9H, PMe<sub>3</sub>), 1.03 (d, *J* = 7.02 Hz, 3H, H9).

### Synthesis and characterization of [W(Tp)(NO)(PMe<sub>3</sub>)(η<sup>2</sup>-8-cyano-7-benzyl-cyclooctenyl cation)]OTf (**30**)



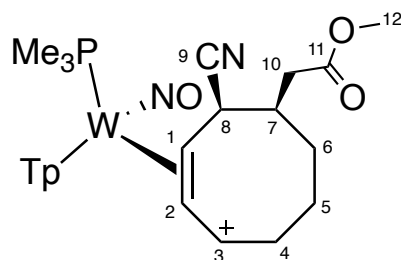
In a 20 mL test tube charged with a stir pea, **27** (193 mg, 0.27 mmol) was dissolved in 5 mL DCM, protonated with HOTf (44 mg, 0.29 mmol), and stirred for 5 minutes. Afterwards, 150 mL hexanes was added, precipitating out a white solid. The precipitated allyl complex was collected as a triflate salt on a 15 mL porosity fritted funnel. The fritted funnel was washed 2X with 10 mL hexanes, and the product was desiccated yielding **27** (224 mg, 0.256 mmol, 96%). 4-JKH-021

**<sup>1</sup>H NMR (800 MHz, CD<sub>3</sub>CN, δ, 25 °C):** 8.35 (d, *J* = 2.1 Hz, 1H, Pz), 8.09 (d, *J* = 2.3 Hz, 1H, Pz), 8.05 (d, *J* = 2.3 Hz, 1H, Pz), 8.00 (d, *J* = 2.4 Hz, 1H, Pz), 7.91 (d, *J* = 2.2 Hz, 1H, Pz), 7.88 (d, *J* = 2.4 Hz, 1H, Pz), 7.36 (t, *J* = 7.5 Hz, 2H, H13), 7.31 (d, *J* = 7.5 Hz, 2H, H12), 7.27 (t, *J* = 7.3 Hz, 1H, 14), 6.58 (t, *J* = 2.3 Hz, 1H, Pz), 6.55 (t, *J* = 2.4 Hz, 1H, Pz), 6.36 (t, *J* = 2.4 Hz, 1H, Pz), 5.60 (q, *J* = 8.9 Hz, 1H, H2), 5.50 (t, *J* = 9.2 Hz, 1H, H8), 4.46 (m, 1H, H1), 4.35 (dd, *J* = 10.9, 4.1 Hz, 1H, H7), 3.36 (dq, *J* = 14.9, 8.1 Hz, 1H, H3), 3.27 (dd, *J* = 13.4, 3.6 Hz, 1H, H10), 2.99 (dq, *J* = 13.2, 5.8 Hz, 1H, H3), 2.89 (dd, *J* = 13.4, 11.1 Hz, 1H, H10), 2.45 (m 1H, H6), 1.76 (dq, *J* = 12.1, 4.1 Hz, 2H,

H4), 1.67 (m, 1H, H5), 1.59 (dq,  $J = 21.7, 4.4$  Hz, 1H, H5), 1.20 (d,  $J = 10.0$  Hz, 9H, PMe<sub>3</sub>).

**<sup>13</sup>C NMR (201 MHz, CD<sub>3</sub>CN, δ, 25 °C):** 148.2 (1C, Pz), 146.0 (d,  $J_{PC} = 2.4$  Hz, 1C, Pz), 144.2 (1C, Pz), 140.9 (1C, C11), 139.9 (d,  $J_{PC} = 3.7$  Hz, 2C, Pz), 139.8 (1C, Pz), 130.1 (2C, C12), 129.5 (2C, C13), 128.9 (d,  $J_{PC} = 14.9$  Hz, 1C, C2), 127.4 (1C, C14), 123.4 (1C, C9), 112.6 (t,  $J_{PC} = 4.1$  Hz, 1C, C8), 109.8 (1C, Pz), 109.2 (1C, Pz), 108.3 (1C, Pz), 70.5 (dd,  $J_{PC} = 12.1, 4.2$  Hz, 1C, C1), 48.3 (d,  $J_{PC} = 11.5$  Hz, 1C, C6), 38.7 (d,  $J_{PC} = 3.5$  Hz, 1C, C10), 37.6 (1C, C7), 28.9 (d,  $J_{PC} = 3.0$  Hz, 1C, C3), 28.4 (d,  $J_{PC} = 2.6$  Hz, 1C, C5), 26.0 (1C, C4), 13.8 (d,  $J_{PC} = 33.2$  Hz, 3C, PMe<sub>3</sub>).

### Synthesis and characterization of [W(Tp)(NO)(PMe<sub>3</sub>)(η<sup>2</sup>-8-cyano-7-enolate-cyclooctenyl cation)]OTf (**31**)



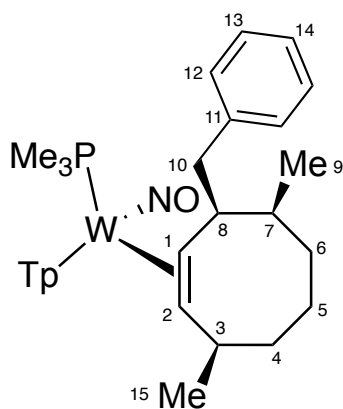
In a 20 mL test tube charged with a stir pea, compound **25** (75 mg, 0.106 mmol) was dissolved in 5 mL of DCM. In another test tube, HOTf (19 mg, 0.127 mmol) diluted with 2 mL MeCN. The solution of HOTf was pipetted into the solution of **25**, and the reaction stirred for 10 minutes. The reaction was reduced to dryness, redissolved in minimal DCM and added to 100 mL stirring hexanes. The precipitate was collected on a 15 mL F fritted disc and desiccated to yield compound **31** (56 mg, 0.065 mmol, 62%) - 3- 4- JKH-061-2D

**<sup>1</sup>H NMR (800 MHz, CD<sub>3</sub>CN, δ, 25 °C):** 8.28 (d,  $J = 2.2$  Hz, 1H, Pz), 8.06 (d,  $J = 2.4$  Hz, 1H, Pz), 8.03 (d,  $J = 2.2$  Hz, 1H, Pz), 7.95 (d,  $J = 2.5$  Hz, 1H, Pz), 7.91 (d,  $J = 2.5$  Hz, 1H, Pz), 7.79 (d,  $J = 2.5$  Hz, 1H, Pz), 6.58 (t,  $J = 2.4$  Hz, 1H, Pz), 6.53 (t,  $J = 2.3$  Hz, 1H, Pz), 6.35 (t,  $J = 2.4$  Hz, 1H, Pz), 5.58 (t,  $J = 9.0$  Hz, 1H, H2), 5.46 (m, 1H, H3), 4.59 (ddd,  $J = 14.0, 10.9, 8.0$  Hz, 1H, H1), 4.24 (dd,  $J = 10.9, 4.0$  Hz, 1H, H8), 3.73 (s, 3H, H12), 3.38 (m, 1H, H4), 2.98 (m, 1H, H4), 2.91 (dd,  $J = 15.3, 3.6$  Hz, 1H, H10), 2.76 (dd,  $J = 15.3, 9.8$  Hz, 1H, H10), 2.68 (td,  $J = 10.1, 4.2$  Hz, 1H, H7), 1.99 (m, 1H, H6), 1.93 (m, 2H, H5), 1.81 (m, 1H, H6), 1.23 (d,  $J = 9.8$  Hz, 9H, PMe<sub>3</sub>).

**$^{13}\text{C}$  NMR (201 MHz,  $\text{CD}_3\text{CN}$ ,  $\delta$ , 25 °C):** 172.7 (1C, C11), 147.0 (1C, Pz), 145.1 (d,  $J_{\text{PC}}$  = 2.7 Hz, 1C, Pz), 144.2 (1C, Pz), 139.1 (1C, Pz), 139.1 (1C, Pz), 139.0 (1C, Pz), 124.9 (1C, C3), 121.9 (1C, C9), 112.9 (d,  $J_{\text{PC}}$  = 3.8 Hz, 1C, C2), 109.3 (1C, Pz), 109.2 (1C, Pz), 107.8 (1C, Pz), 70.9 (d,  $J_{\text{PC}}$  = 11.8 Hz, 1C, C1), 52.3 (1C, C12), 42.9 (1C, C7), 36.8 (1C, C10), 36.4 (1C, C8), 28.8 (2C, C4 & C6), 26.1 (1C, C5), 14.1 (d,  $J_{\text{PC}}$  = 32.9 Hz, 3C,  $\text{PMe}_3$ ).

**HRMS** - Theoretical: 709.2167 m/z; Experimental: 709.2196m/z

**Synthesis and characterization of  $[\text{W}(\text{Tp})(\text{NO})(\text{PMe}_3)(\eta^2\text{-3-methyl-7-methyl-8-benzyl-cyclooctenene})]$  (32)**



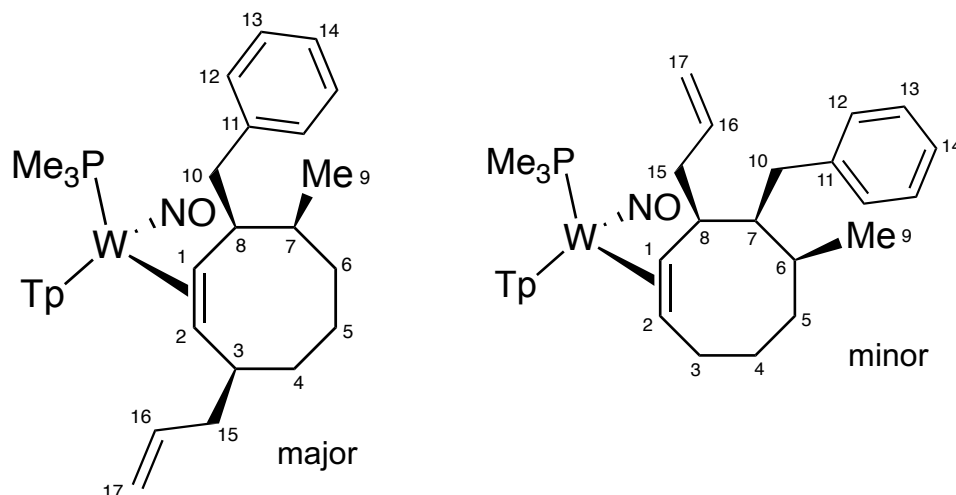
In a 10mL test tube charged with a stir pea, compound **28** (20 mg, 0.023 mmol) was dissolved in 2 mL of d-MeCN.  $\text{MeMgBr}$  (1.5M) (0.017 mL, 0.026 mmol) was syringed into the test tube at R.T. and stirred for 15 minutes. The reaction mixture as diluted with 10 mL dichloromethane, extracted 3X with 10mL  $\text{H}_2\text{O}$ . The organic layer was collected, dried with  $\text{Na}_2\text{SO}_4$ , filtered over a 30mL M fritted disc and reduced to minimal solvent. The solution was added to a basic alumina plug in a 30mL M fritted disc. The plug was flushed with 15mL hexanes, the hexanes solution was trashed. The plug was then flushed with 15mL of a 50%EtOAc/50%Hexanes solution. The solution was reduced to minimal solvent then move to a tared vial and reduced to dryness. Compound **31** was isolated in a vial (12 mg, 0.016 mmol, 71%)

**$^1\text{H}$  NMR (800 MHz,  $\text{CD}_3\text{CN}$ ,  $\delta$ , 25 °C):** 7.99 – 7.81, 7.35 (d/bs,  $J$  = 2.06; 2.54; 2.06; 2.54 Hz, 6H, Tp protons), 7.44 (d,  $J$  = 7.98 Hz, 2H, H12), 7.28 (t,  $J$  = 7.98 Hz, 2H, H13), 7.15 (t,  $J$  = 7.01 Hz, 1H, H14), 6.35 – 6.29 (t,  $J$  = 2.06; 1.93; 2.42 Hz, 3H, Tp protons), 3.57 (d,  $J$  = 11.00 Hz, 1H, H10), 3.13 (dt,  $J$  = 11.00, 16.93 Hz, 1H, H1), 2.77 (t,  $J$  = 11.00 Hz,

1H, H3), 2.73 (m, 1H, H8), 2.43 (bs, 1H, H10), 2.25 – 0.91 (m, 7H, H4 – H7), 1.15 (d, J = 8.46 Hz, 3H, H15), 1.10 (d, J = 7.01 Hz, 3H, H9), 0.99 (d, J = 7.01 Hz, 9H, PMe<sub>3</sub>), 0.73 (t, J = 9.92 Hz, 1H, H2).

<sup>13</sup>C NMR (201 MHz, CD<sub>3</sub>CN, δ, 25 °C): too dilute to solve.

### Synthesis and characterization of [W(Tp)(NO)(PMe<sub>3</sub>)(η<sup>2</sup>-3-allyl-7-methyl-8-benzyl-cyclooctenene)] (33)



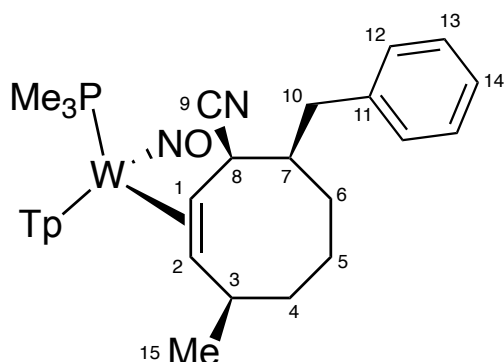
In a 10mL test tube charged with a stir pea, compound **28** (50 mg, 0.058 mmol) was dissolved in 5 mL of THF. AllylMgBr (1M) (0.18 mL, 0.180 mmol) was syringed into the test tube at R.T. and stirred for 20 minutes. The reaction was quenched with 2 mL of H<sub>2</sub>O. The mixture was diluted with 10 mL dichloromethane, extracted 3X with 10mL H<sub>2</sub>O. The organic layer was collected, dried with Na<sub>2</sub>SO<sub>4</sub>, filtered over a 30mL M fritted disc and reduced to minimal solvent. The solution was moved to a tared vial and reduced to dryness. Compound **33** was isolated in a vial in a 2:1 c.d.r. (39 mg, 0.052, 89%)

<sup>1</sup>H NMR (800 MHz, CD<sub>3</sub>CN, δ, 25 °C) - major: 7.95, 7.90, 7.88, 7.84, 7.83, 7.81 (d, J = 1.63; 1.74; 1.63; 2.04 Hz, 6H, Tp protons), 7.47 (d, J = 7.25 Hz, 2H, H12), 7.27 (t, J = 7.15 Hz, 2H, H13), 7.26 (t, J = 7.56 Hz, 1H, H14), 6.32, 6.29, 6.25 (t, J = 1.44; 2.35; 1.44 Hz), 5.53 (m, 1H, H16), 4.71 (d, 10.77 Hz, 1H, H17), 4.63 (d, J = 16.92 Hz, H17), 3.49 (bs, 1H, H10), 3.13 (m, J = 4.51, 15.24 Hz, 1H, H8), 2.74 (m, 3H, H1/H3/H10), 2.38 – 1.10 (m, 7H, H4 – H7), 1.37, 1.43 (m, 2H, H15), 1.13 (d, J = 6.75, 3H, H9), 0.97 (d, J = 7.30 Hz, 9H, PMe<sub>3</sub>), 0.85 (m, 1H, H2).

**<sup>1</sup>H NMR (800 MHz, CD<sub>3</sub>CN, δ, 25 °C) - minor:** 7.93, 7.85, 7.78, 7.40, 7.33, 7.07 (d/bs, J = 2.13 Hz, 6H, Tp protons), 7.30 (d, J = 8.72 Hz, 2H, H12), 6.94 (t, J = 7.89 Hz, 1H, H14), 6.93 (t, J = 5.19 Hz, 2H, H13), 6.33, 6.27, 6.16 (t, J = 2.23; 1.68; 2.23 Hz, 3H, Tp protons), 5.89 (m, 1H, H16), 4.94 (d, J = 10.22 Hz, 1H, H17), 4.92 (d, J = 17.94 Hz, 1H, H17), 3.31 (m, 1H, H1), 3.16 (m, 1H, H10), 2.98 (dd, J = 7.73, 14.46 Hz, H10), 2.55 (d, J = 13.96 Hz, H15), 2.37 – 1.71 (m, 8H, H3 – H7), 2.14 (m, 1H, H8), 0.94 (d, J = 8.44 Hz, 9H, PMe<sub>3</sub>), 0.88 (d, J = 6.85 Hz, 3H, H9), 0.74 (t, J = 11.76 Hz, 1H, H2).

**<sup>13</sup>C NMR (201 MHz, CD<sub>3</sub>CN, δ, 25 °C) – major/minor:** too many overlapping peaks.

### Synthesis and characterization of [W(Tp)(NO)(PMe<sub>3</sub>)(η<sup>2</sup>-3-methyl-7-benzyl-8-cyano-cyclooctenene)] (**34**)



In a 10mL test tube charged with a stir pea, compound **30** (77 mg, 0.088 mmol) was dissolved in 2 mL of dried THF. MeMgCl (0.15 mL, 0.44 mmol) was syringed into the test tube at R.T. and stirred for 15 minutes. The reaction mixture was diluted with 10 mL dichloromethane, extracted 3X with 10mL H<sub>2</sub>O. The organic layer was collected, dried with Na<sub>2</sub>SO<sub>4</sub>, filtered over a 30mL M fritted disc and reduced to minimal solvent. The solution was moved to a weighed vial and reduced to dryness. Crystals grew out of acetonitrile slowly reducing. Impurities were washed away from the crystals with more acetonitrile until colorless wash. Compound **34** was isolated in a vial (59 mg, 0.079 mmol, 90%)

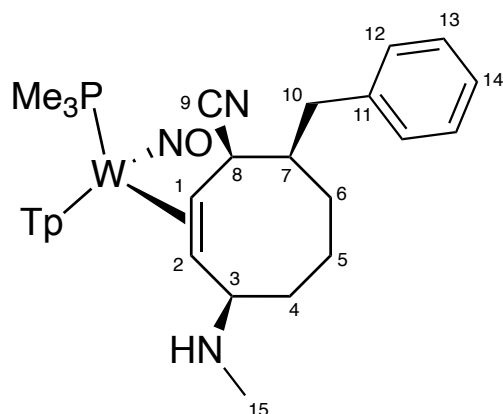
**<sup>1</sup>H NMR (800 MHz, CD<sub>3</sub>CN, δ, 25 °C):** 7.96 (s, 2H, Pz), 7.80 (d, J = 1.7 Hz, 1H, Pz), 7.75 (s, 1H, Pz), 7.73 (s, 1H, Pz), 7.31 (m, 4H, H12 & H13), 7.22 (m, 1H, H14), 7.21 (s, 1H, Pz), 6.31 (m, 1H, Pz), 6.28 (m, 1H, Pz), 6.23 (t, J = 1.9 Hz, 1H, Pz), 3.88 (m, 1H, H8), 3.43 (dd, J = 12.6, 2.8 Hz, 1H, H10), 2.99 (ddd, J = 15.8, 10.9, 7.3 Hz, 1H, H1), 2.63 (m, 2H, H3 & H10), 2.36 (m, 1H, H7), 1.96 (m, 1H, H4), 1.89 (q, J = 12.5 Hz, 1H,

H5), 1.69 (td,  $J = 12.8, 7.7$  Hz, 1H, H6), 1.58 (m, 1H, H6), 1.25 (m, 1H, H5), 1.16 (d,  $J = 8.1$  Hz, 9H,  $\text{PMe}_3$ ), 1.12 (m, 1H, H4), 0.59 (dd,  $J = 11.0, 8.3$  Hz, 1H, H2), 0.25 (d,  $J = 6.1$  Hz, 3H, H15).

**$^{13}\text{C}$  NMR (201 MHz,  $\text{CD}_3\text{CN}$ ,  $\delta$ , 25 °C):** 143.8 (1C, Pz), 143.1 (1C, Pz), 141.6 (1C, C11), 140.1 (1C, Pz), 137.6 (1C, Pz), 136.7 (1C, Pz), 136.6 (1C, Pz), 129.8 (2C, C12 or C13), 128.6 (2C, C12 or C13), 127.6 (1C, C9), 126.2 (1C, C14), 106.7 (2C, Pz), 106.6 (1C, Pz), 69.4 (1C, C2), 48.2 (1C, C1), 46.6 (1C, C7), 44.5 (1C, C4), 40.7 (1C, C8), 40.3 (1C, C10), 35.4 (1C, C3), 30.2 (1C, C6), 26.7 (1C, C15), 24.5 (1C, C5), 14.2 (d,  $J_{\text{PC}} = 27.3$  Hz, 3C,  $\text{PMe}_3$ ).

Composition of **34** has been confirmed by single crystal X-ray diffraction.

### Synthesis and characterization of $[\text{W}(\text{Tp})(\text{NO})(\text{PMe}_3)(\eta^2\text{-3-methyl-7-benzyl-8-methylamine-cyclooctenene})]$ (**35**)



In a 10mL test tube charged with a stir pea, compound **30** (40 mg, 0.046 mmol) was dissolved in 2 mL of  $\text{MeCN-d}_3$ . Methylamine (0.01 mL, 0.12 mmol) was syringed into the test tube at R.T. and stirred for 15 minutes. The reaction mixture as diluted with 10 mL dichloromethane, extracted 3X with 10mL  $\text{H}_2\text{O}$ . The organic layer was collected, dried with  $\text{Na}_2\text{SO}_4$ , filtered over a 30mL M fritted disc and reduced to minimal solvent. The solution was moved to a weighed vial and reduced to dryness. Crystals grew out of acetonitrile slowly reducing. Impurities were washed away from the crystals with more acetonitrile until colorless wash. Compound **35** was isolated in a vial (23 mg, 0.030 mmol, 67%).

**$^1\text{H}$  NMR (800 MHz,  $\text{CD}_3\text{CN}$ ,  $\delta$ , 25 °C):** 7.98 (d,  $J = 2.1$  Hz, 1H, Pz), 7.93 (d,  $J = 2.0$  Hz, 1H, Pz), 7.90 (d,  $J = 2.3$  Hz, 1H, Pz), 7.86 (d,  $J = 2.4$  Hz, 1H, Pz), 7.82 (d,  $J = 2.3$  Hz,

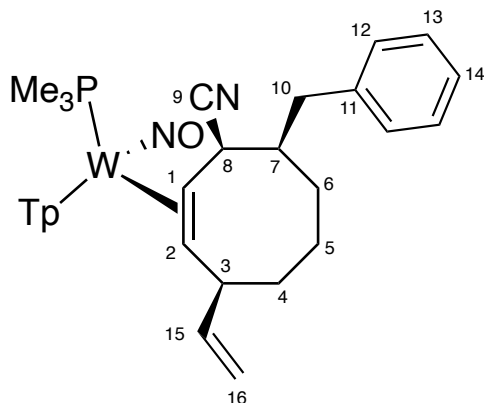


1H, Pz), 7.40 (d,  $J = 2.2$  Hz, 1H, Pz), 7.36 – 7.28 (m, 4H, H12 & H13), 7.22 (m, 1H, H14), 6.36 (t,  $J = 2.2$  Hz, 1H, Pz), 6.32 (t,  $J = 2.2$  Hz, 2H, Pz), 3.75 (m, 1H, H8), 3.35 (dd,  $J = 12.5, 2.9$  Hz, 1H, H10), 3.02 (m, 2H, H1 & H3), 2.74 (t,  $J = 12.2$  Hz, 1H, H10), 2.31 (d,  $J = 9.9$  Hz, 1H, H7), 2.15 (m, 1H, H4), 1.99 (s, 3H, H15), 1.86 (m, 1H, H5), 1.64 – 1.49 (m, 2H, H6), 1.17 (m, 1H, H5), 1.11 (d,  $J = 8.4$  Hz, 9H, PMe<sub>3</sub>), 1.00 (m, 1H, H4), 0.80 (m, 1H, H2).

**<sup>13</sup>C NMR (201 MHz, CD<sub>3</sub>CN, δ, 25 °C):** 144.9 (1C, Pz), 144.2 (1C, Pz), 142.2 (1C, C11), 141.5 (1C, Pz), 139.3 (1C, Pz), 137.9 (1C, Pz), 137.7 (1C, Pz), 130.2 (2C, C12 or C13), 129.3 (2C, C12 or C13), 127.9 (1C, C9), 126.9 (1C, C14), 107.7 (1C, Pz), 107.4 (1C, Pz), 107.3 (1C, Pz), 68.2 (1C, C2), 65.1 (1C, C3), 47.8, 47.5 (2C, C7/C1), 42.1 (1C, C4), 40.5 (1C, C8), 40.1 (1C, C10), 34.9 (1C, C15), 31.0 (1C, C6), 23.3 (1C, C5), 14.0 (d,  $J_{PC} = 28.2$  Hz, 3C, PMe<sub>3</sub>).

Composition of **35** has been confirmed by single crystal X-ray diffraction.

### Synthesis and characterization of [W(Tp)(NO)(PMe<sub>3</sub>)( $\eta^2$ -3-methyl-7-benzyl-8-vinyl-cyclooctenene) (**36**)



In a test tube charged with a stir pea, **30** (125 mg, 0.143 mmol) was dissolved in 5 mL dried THF. To the stirring solution, C<sub>2</sub>H<sub>3</sub>MgBr (3.06 mL, 0.42 mmol) was added via syringe. After reacting for 30 minutes, the crude reaction mixture was then diluted with DCM and extracted 3x with 10 mL H<sub>2</sub>O. The reaction was then dried with Na<sub>2</sub>SO<sub>4</sub> and filtered to remove drying agent. Afterwards the reaction was reduced to dryness in vacuo in a 125 mL filter flask. The remaining product on the flask was redissolved in minimal DCM, and the impurities were precipitated out of 50mL hexanes and filtered over a 15mL fritted disc. The precipitate was discarded. The hexanes filtrate was reduced to dryness, redissolved in minimal MeCN, transferred to a weighed vial, and reduced to

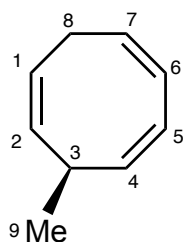
dryness again. Crystallization occurred out of the MeCN, yielding **36** (89 mg, 0.118 mmol, 83%).

**<sup>1</sup>H NMR (800 MHz, CD<sub>3</sub>CN, δ, 25 °C):** 7.93 (d, *J* = 2.1 Hz, 1H, Pz), 7.82 (d, *J* = 2.0 Hz, 1H, Pz), 7.80 (d, *J* = 2.2 Hz, 1H, Pz), 7.70 (d, *J* = 2.4 Hz, 1H, Pz), 7.64 (d, *J* = 2.4 Hz, 1H, Pz), 7.33 – 7.28 (m, 4H, H12 & H13), 7.27 (d, *J* = 2.2 Hz, 1H, Pz), 7.20 (t, *J* = 6.1, 1H, H14), 6.32 (t, *J* = 2.2 Hz, 1H, Pz), 6.26 (t, *J* = 2.2 Hz, 1H, Pz), 6.08 (t, *J* = 2.2 Hz, 1H, Pz), 5.29 (m, 1H, H15), 4.22 (d, *J* = 17.5 Hz, 1H, H16), 4.17 (m, 1H, H16), 3.74 (m, 1H, H8), 3.37 (m, 1H, H10), 2.98 (m, 2H, H1 & H3), 2.75 (appt, *J* = 12.2 Hz, 1H, H10), 2.34 (m, 1H, H7), 1.94 (m, 1H, H5), 1.85 (m, 1H, H4), 1.65 – 1.52 (m, 2H, H6), 1.25 (m, 1H, H5), 1.13 (d, *J* = 8.1 Hz, 10H, PMe<sub>3</sub> & H4), 0.93 (appt, *J* = 10.3 Hz, 1H, H2).

**<sup>13</sup>C NMR (201 MHz, CD<sub>3</sub>CN, δ, 25 °C):** 148.1 (1C, C15), 146.5 (1C, Pz), 143.1 (1C, Pz), 141.5 (1C, C11), 139.9 (1C, Pz), 137.3 (1C, Pz), 136.7 (1C, Pz), 136.5 (1C, Pz), 129.8 (2C, C12 or C13), 128.6 (2C, C12 or C13), 127.7, (1C, C9), 126.3 (1C, C14), 109.2 (1C, C16), 106.8 (1C, Pz), 106.5 (1C, Pz), 106.0 (1C, Pz), 65.5 (1C, C2), 47.4 (1C, C7), 45.9 (1C, C4), 44.2 (1C, C1), 40.1 (1C, C8), 39.4 (1C, C10), 29.9 (1C, C6), 29.5 (1C, C3), 24.2 (d, *J* = 23.8 Hz, 1C, C5), 14.2 (d, *J* = 27.2 Hz, 3C, PMe<sub>3</sub>).

Composition of **36** has been confirmed by single crystal X-ray diffraction.

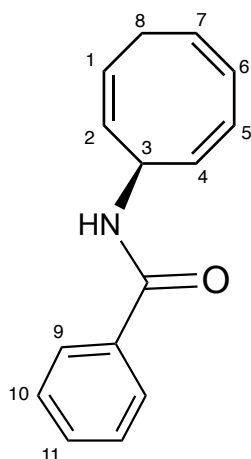
### Synthesis and characterization of 5-methyl-cyclooct-1,3,6-ene (**37**)



An NMR scale of compound **15** in d-MeCN was opened to atmospheric O<sub>2</sub>. A crude NMR was taken after 24 hours. Clean up procedure is necessary for isolation from metal byproduct.

**<sup>1</sup>H NMR (800 MHz, CD<sub>3</sub>CN, δ, 25 °C):** 6.07, 6.00 (dd, *J* = 2.45, 10.18; 2.53, 10.81 Hz, 2H, H1/H2), 5.56, 5.44, 5.34, 5.21 (m, dt, dd, *J* = 3.05, 6.16, 8.62, 10.77; 7.35, 10.70; 3.34, 10.70; 7.06, 10.18 Hz, 4H, H4 – H7), 3.06, 2.81, 2.60 (m, dt, *J* = 8.30, 14.59 Hz, 3H, H3/H8), 1.14 (d, *J* = 7.11 Hz, 3H, H9).

### Synthesis and characterization of 5-benzamide-cyclooct-1,3,6-ene (38)

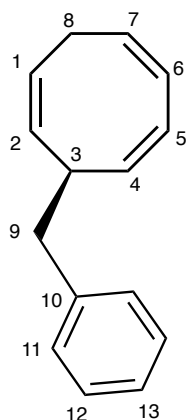


An NMR scale of compound **7** in d-MeCN was opened to atmospheric O<sub>2</sub>. A crude NMR was taken after 24 hours. Clean up procedure is necessary for isolation from metal byproduct.

**<sup>1</sup>H NMR (800 MHz, CD<sub>3</sub>CN, δ, 25 °C):** 7.81 (d, J = 6.96 Hz, 2H, H9), 7.53 (t, J = 8.29 Hz, 1H, H11), 7.46 (t, J = 6.63 Hz, 2H, H10), 6.24, 6.16 (d, J = 10.16; 10.91 Hz, 2H, H1/H2), 5.69, 5.59, 5.55, 5.44 (m, dt, dd, J = 3.17, 9.13, 11.15; 7.50, 10.38; 3.17, 10.67; 6.73, 10.28 Hz, 4H, H4 – H7), 5.31 (m, 1H, H3), 2.86, 2.67 (dt, d, J = 7.84, 16.76; 13.51 Hz, 2H, H8).

**HRMS** - Theoretical: 226.1227 m/z; Experimental: 226.1227 m/z

### Synthesis and characterization of 5-benzyl-cyclooct-1,3,6-ene (39)

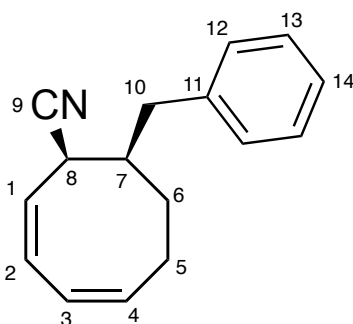


An NMR scale of compound **13** was dissolved in MeCN-d<sub>3</sub>. A few milligrams of CAN were added to the NMR tube. A crude NMR was taken after 20 minutes. Clean up procedure is necessary for isolation from metal byproduct. 3-JKH-199

**<sup>1</sup>H NMR (800 MHz, CD<sub>3</sub>CN, δ, 25 °C):** 7.25 (t, *J* = 7.6 Hz, 2H, H12), 7.19 (d, *J* = 7.4 Hz, 2H, H11), 7.15 (t, *J* = 7.3 Hz, 1H, H13) 6.09 (ddd, *J* = 24.4, 10.5, 3.4 Hz, 2H, H5 & H6), 5.61 (m, 1H, H1), 5.49 (dt, *J* = 10.5, 7.1 Hz, 1H, H7), 5.37 (dt, *J* = 10.7, 3.4 Hz, 1H, H2), 5.25 (dd, *J* = 10.4, 7.1 Hz, 1H, H4), 3.42 (m, 1H, H3), 2.85 (dt, *J* = 15.8, 7.9 Hz, 1H, H8), 2.61 (m, 1H, H8), 2.53 (d, *J* = 7.5 Hz, 2H, H9).

**<sup>13</sup>C NMR (201 MHz, CD<sub>3</sub>CN, δ, 25 °C):** 138.87 (1C, C10), 131.60 (1C, C2), 131.15 (1C, C4), 130.19 (1C, C5), 129.86 (2C, C11), 129.17 (2C, C12), 128.31 (1C, C6), 127.31 (1C, C1) 126.47 (1C, C7), 126.20 (1C, C13), 40.60 (1C, C9), 35.16 (1C, C3), 28.50 (1C, C8).

### Synthesis and characterization of *cis*-5-cyano-6-benzyl-cyclooct-1,3-ene (**40**)



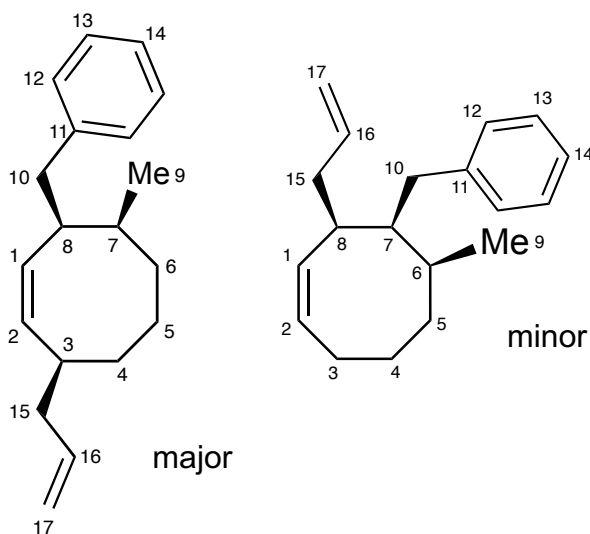
In a 20 mL test tube charged with a stir pea, **27** (17 mg, 0.023 mmol) was dissolved in 1 mL MeCN. In another test tube, CAN (15 mg, 0.027 mmol) was dissolved in 1 mL MeCN. The solution of CAN was pipetted into the solution of **27**, and the reaction stirred for 10 minutes. The crude reaction mixture was then diluted with DCM and extracted 3x with 10 mL H<sub>2</sub>O. The reaction was then dried with Na<sub>2</sub>SO<sub>4</sub> and filtered to remove drying agent. Afterwards the reaction was reduced to dryness in vacuo in a 125 mL filter flask. The remaining product on the flask was redissolved in minimal DCM, and the impurities were precipitated out of 50mL hexanes and filtered over a 15mL fritted disc. The precipitate was discarded. The hexanes filtrate was reduced via rotovap. The white solid produced was redissolved in minimal MeCN, transferred to a weighed vial, and reduced yielding **40** (no yield recorded). 4-JKH-027-2D

**<sup>1</sup>H NMR (800 MHz, CD<sub>3</sub>CN, δ, 25 °C):** 7.30 (m, 2H, 13), 7.23 (m, 1H, H14), 7.21 (m, 2H, H12), 6.12 (dd, *J* = 11.2, 4.4 Hz, 1H, H2), 5.82 (dd, *J* = 11.8, 4.3 Hz, 1H, H3), 5.73 (dt, *J* = 12.0, 6.3 Hz, 1H, H4), 5.55 (dd, *J* = 11.1, 8.2 Hz, 1H, H1), 3.84 (m, 1H, H8), 2.89 (dd, *J* = 13.6, 5.3 Hz, 1H, H10), 2.49 (dd, *J* = 13.5, 9.8 Hz, 1H, H10), 2.27 (m, 1H, H5), 2.24 (m, 1H, H7), 2.09 (m, 1H, H5), 1.57 (dtd, *J* = 14.5, 9.6, 2.0 Hz, 1H, H6), 1.40 (m, 1H, H6).

**<sup>13</sup>C NMR (201 MHz, CD<sub>3</sub>CN, δ, 25 °C):** 140.79 (1C, C11), 134.37 (1C, C4), 131.01 (1C, C2), 130.07 (2C, C12), 129.39 (2C, C13), 127.25 (1C, C14), 125.07 (1C, C3), 123.70 (1C, C1), 107.02 (1C, C9), 41.25 (1C, C10), 40.24 (1C, C7), 39.03 (1C, C5), 35.07 (1C, C8), 26.96 (1C, C6).

**HRMS** - Theoretical: 223.1361 m/z; Experimental 223.1359 m/z

### Synthesis and characterization of *cis,cis*-3-benzyl-4-methyl-8-allyl-cyclooctene (41)



Compound **33** (39mg, 0.052 mmol) was dissolved in minimal d-MeCN and opened to atmospheric O<sub>2</sub>. After 24 hours, the solution was loaded onto silica column and eluted with 100% hexanes. The hexanes solution was reduced to minimal solvent and moved to a tared round bottom flask. The solution was then reduced to dryness to yield compound **41** (12.8mg, 0.050 mmol, 97%).

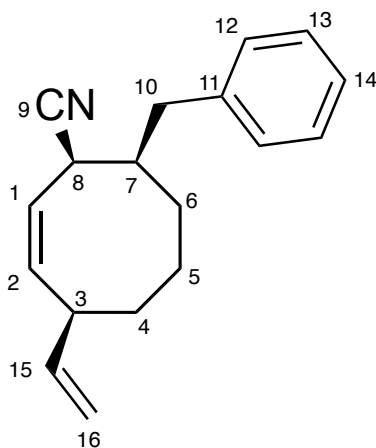
**<sup>1</sup>H NMR (800 MHz, CD<sub>3</sub>CN, δ, 25 °C) - major:** 7.25 (t, *J* = 6.62 Hz, 2H, H13), 7.21 (d, *J* = 7.24 Hz, 2H, H12), 7.15 (t, *J* = 6.56 Hz, 1H, H14), 5.67 (m, *J* = 6.35, 10.63, 13.14, 15.67 Hz, 1H, H16), 5.31 (dt, *J* = 9.08, 15.49 Hz, 2H, H17), 4.87 (m, *J* = 8.95, 10.19 Hz, 2H, H1/H2), 2.99 (m, *J* = 4.94, 9.88, 12.97 Hz, H8), 2.73 (dd, *J* = 8.52, 12.78 Hz, 1H,

H10), 2.68 (dd,  $J = 5.62, 12.78$  Hz, 1H, H10), 2.42 (m, 1H, H3), 2.01 (t,  $J = 7.84$ , 1H, H15), 1.91 (dt,  $J = 7.16$  Hz, 1H, H15), 1.73, 1.66, 1.60, 1.36, 1.27, 1.10 (m, dt, t,  $J = 3.14, 12.85; 3.41, 9.70; 13.11$  Hz, 7H, H4 – H7).

**$^1\text{H}$  NMR (800 MHz,  $\text{CD}_3\text{CN}$ ,  $\delta$ , 25 °C) - minor:** 7.27 (t,  $J = 8.01$  Hz, 2H, H13), 7.25 (d, 2H, H12), 7.16 (t, 1H, H14), 5.62, 5.59, 5.54 (m, t,  $J = 9.17$  Hz, 3H, H1/H2/H16), 4.83, 4.71 (d,  $J = 10.38; 17.12$  Hz, 2H, H17), 2.62, 2.58 (dd,  $J = 7.31, 4.66; 4.82, 9.36$  Hz, 3H, H10/H15/H7), 2.36 (m, 1H, H3), 1.92 (m, 1H, H8), 1.97 – 0.95 (m, 7H, H3 – H6).

**$^{13}\text{C}$  NMR (201 MHz,  $\text{CD}_3\text{CN}$ ,  $\delta$ , 25 °C):** too dilute/too many overlapping peaks.

### Synthesis and characterization of *cis,cis*-3-cyano-4-benzyl-8-vinyl-cyclooctene (42)



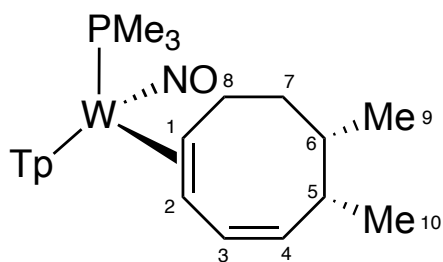
In an oven dried test tube charged with a stir pea, **36** (38 mg, 0.050 mmol) was dissolved in 1 mL acetone. In a separate test tube, cerium (IV) ammonium nitrate (33 mg, 0.060 mmol) was dissolved in 1 mL acetone. The solution of cerium (IV) ammonium nitrate was pipetted into the solution of **13**, and the reaction was stirred for 5 minutes. The crude reaction mixture was then diluted with DCM and extracted 3x with 10 mL  $\text{H}_2\text{O}$ . The reaction was then dried with  $\text{Na}_2\text{SO}_4$  and filtered to remove drying agent. Afterwards the reaction was reduced to dryness in vacuo in a 125 mL filter flask. Minimal DCM was used to redissolve the product, and 50 mL hexanes was used to precipitate out an orange solid. The solid was discarded on a fritted funnel, and the clear filtrate was transferred into a round-bottom flask and rotovapped to dryness. The resulting white solid **42** was redissolved in MeCN and transferred into a vial, which was reduced to dryness and weighed (6.0 mg, 0.024, 47%). 4-JKH-041

**<sup>1</sup>H NMR (800 MHz, CD<sub>3</sub>CN, δ, 25 °C):** 7.29 (t, *J* = 7.7 Hz, 2H, H13), 7.21 (m, 1H, H14), 7.20 (m, 2H, H12), 5.87 (ddd, *J* = 17.3, 10.3, 6.9 Hz, 1H, H15), 5.73 (m, 1H, H2), 5.60 (t, *J* = 9.9 Hz, 1H, H1), 5.07 (dd, *J* = 17.3, 1.4 Hz, 1H, H16), 4.99 (m, 1H, H16), 4.03 (m, 1H, H8), 3.12 (m, 1H, H3), 3.05 (dt, *J* = 13.5, 3.0 Hz, 1H, H10), 2.51 (t, *J* = 12.6 Hz, 1H, H10), 2.34 (dp, *J* = 12.7, 4.4 Hz, 1H, H7), 1.66 (m, 2H, H4 & H5), 1.47 (ddd, *J* = 20.3, 9.9, 4.9 Hz, 1H, H6), 1.37 – 1.19 (m, 3H, H4, H5, & H6).

**<sup>13</sup>C NMR (201 MHz, CD<sub>3</sub>CN, δ, 25 °C):** 143.13 (1C, C15), 141.10 (1C, C11), 138.08 (1C, C2), 130.01 (2C, C12), 129.32 (2C, C13), 127.11 (1C, C14), 122.53 (1C, C1), 114.23 (1C, C16), 104.97 (1C, C9), 45.64 (1C, C7), 41.96 (1C, C3), 37.44 (2C, C4 & C5), 37.06 (1C, C10), 34.22 (1C, C8), 29.55 (1C, C6).

**HRMS** - Theoretical: 251.1674 m/z; Experimental 251.1660 m/z

### Synthesis and characterization of *cis,cis*-3-cyano-4-benzyl-8-vinyl-cyclooctene (43)

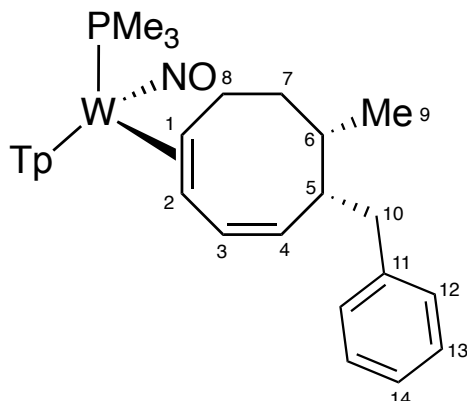


After 12 hours a sample of compound **21** in d-MeCN converted to compound **43**.

**<sup>1</sup>H NMR (800 MHz, CD<sub>3</sub>CN, δ, 25 °C):** 8.22, 8.01, 7.86, 7.83, 7.35 (d/bs, *J* = 2.19, 2.70, 1.81 Hz, 6H, Tp protons), 6.38, 6.33, 6.31 (t, *J* = 2.24, 1.51 2.24 Hz, 3H, Tp protons), 6.14 (d, *J* = 13.00 Hz, 1H, H3), 5.19 (d, *J* = 12.03 Hz, 1H, H4), 2.90 (m, *J* = 9.73, 15.24 Hz, 1H, H5), 2.60 (m, 1H, H1), 2.19 (m, 1H, H6), 2.01 – 1.30 (m, 4H, H7/H8), 1.03 – 0.95 (m, 15H, H9/H10/PMe<sub>3</sub>).

Composition of **43** has been confirmed by single crystal X-ray diffraction.

## Synthesis and characterization of *cis,cis*-3-cyano-4-benzyl-8-vinyl-cyclooctene (44)



After 12 hour a sample of compound **22** in d-MeCN converted to compound **44**.

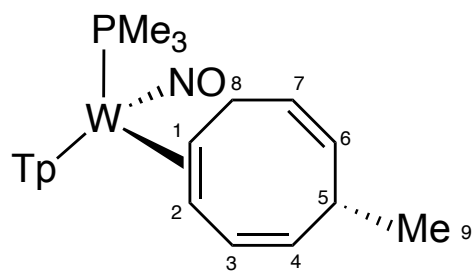
**<sup>1</sup>H NMR (800 MHz, CD<sub>3</sub>CN, δ, 25 °C):** 8.18 (d, J = 2.65 Hz, 1H, Pz3A), 7.99 (d, J = 2.65 Hz, 1H, Pz3B), 7.84 (d, J = 2.01 Hz, 1H, Pz5B), 7.80 (d, J = 2.85 Hz, 1H, Pz5C), 7.75 (d, J = 2.85 Hz, 1H, Pz5A), 7.47 (d, J = 2.18 Hz, 1H, Pz3C), 7.20 (d, J = 6.50 Hz, 2H, H12), 7.18 (t, J = 7.93 Hz, 2H, H13), 7.10 (t, J = 6.50 Hz, 1H, H13), 6.57 (d, J = 10.38 Hz, 1H, H3), 6.36 (t, J = 2.18 Hz, 1H, Pz4A), 6.26 (t, J = 2.01 Hz, 1H, Pz4C), 6.23 (t, J = 2.68 Hz, 1H, Pz4B), 5.35 (dd, J = 2.60, 8.63 Hz, 1H, H4), 3.43 (td, J = 7.78, 8.18 Hz, 1H, H5), 2.72 (d, J = 7.72 Hz, 2H, H10), 2.58 (ddd, J = 1.71, 9.71, 12.50 Hz, 1H, H1), 2.19 (dd, J = 6.87, 14.73 Hz, 1H, H8), 2.06 (m, 2H, H8/H6), 1.83 (m, 2H, H7), 1.37 (dd, 1.61, 10.77 Hz, 1H, H2), 1.08 (d, J = 8.61 Hz, 9H, PMe<sub>3</sub>), 1.00 (d, J = 7.42 Hz, 3H, H9).

**<sup>13</sup>C NMR (201 MHz, CD<sub>3</sub>CN, δ, 25 °C):** 144.1 (1C, Pz3B), 142.7 (1C, Pz3A), 141.8 (1C, Pz3C), 137.7 (2C, C4/Pz5C), 137.3 (1C, Pz5A), 137.1 (1C, Pz5B), 135.7 (1C, C3), 130.9 (1C, C11), 129.9 (1C, C12), 129.0 (1C, C11), 126.5 (1C, C13), 107.5 (1C, Pz4A), 107.0 (1C, Pz4C), 106.5 (1C, Pz4B), 63.6 (d, J = 10.70 Hz, 1H, C1), 54.9 (1C, C2), 43.8 (1C, C7), 43.5 (1C, C5), 42.1 (1C, C10), 35.8 (1C, C6), 27.9 (d, J = 4.43 Hz, 1C, C8), 15.2 (1C, C9), 12.9 (d, J = 28.32 Hz, 3C, PMe<sub>3</sub>).

Composition of **44** has been confirmed by single crystal X-ray diffraction.

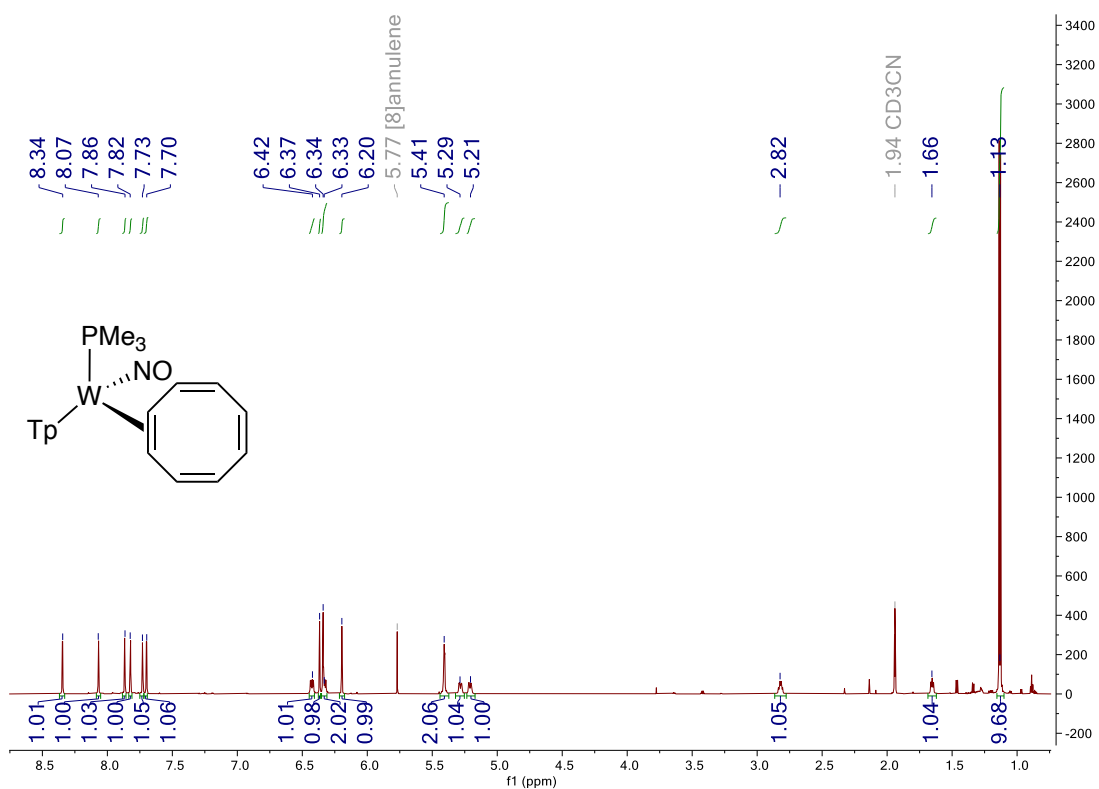


**Synthesis and characterization of cis,cis-3-cyano-4-benzyl-8-vinyl-cyclooctene  
(45)**

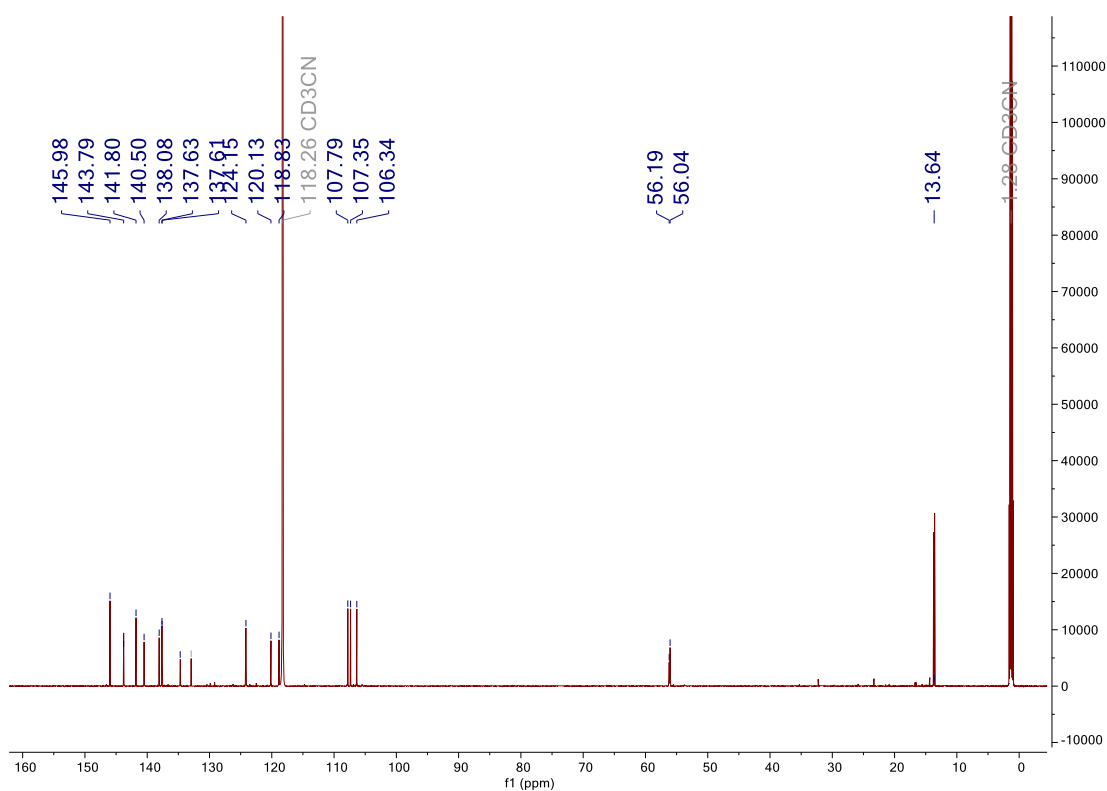


After 72 hours, a sample of compound **15** in d-MeCN grew a single crystal of compound **45**. The mother liquor of the sample after this period of time was organic compound **37**.

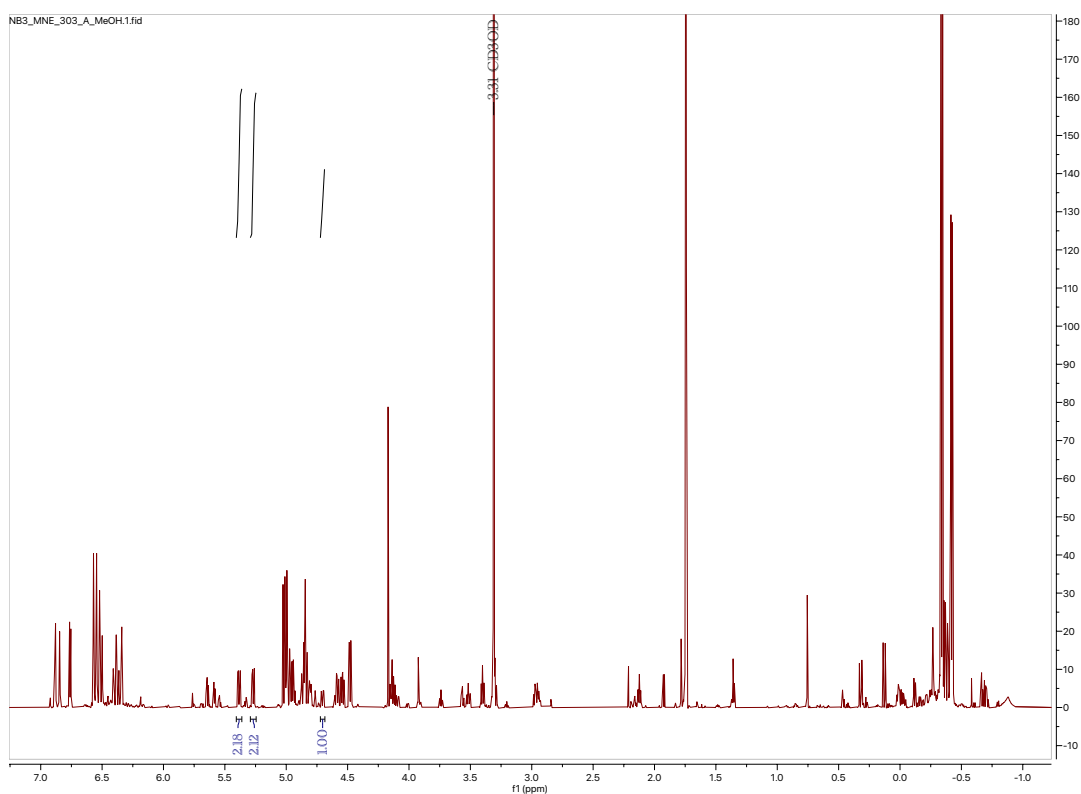
$^1\text{H}$  NMR (800 MHz,  $\text{CD}_3\text{CN}$ ,  $\delta$ , 25 °C) of Compound **1**



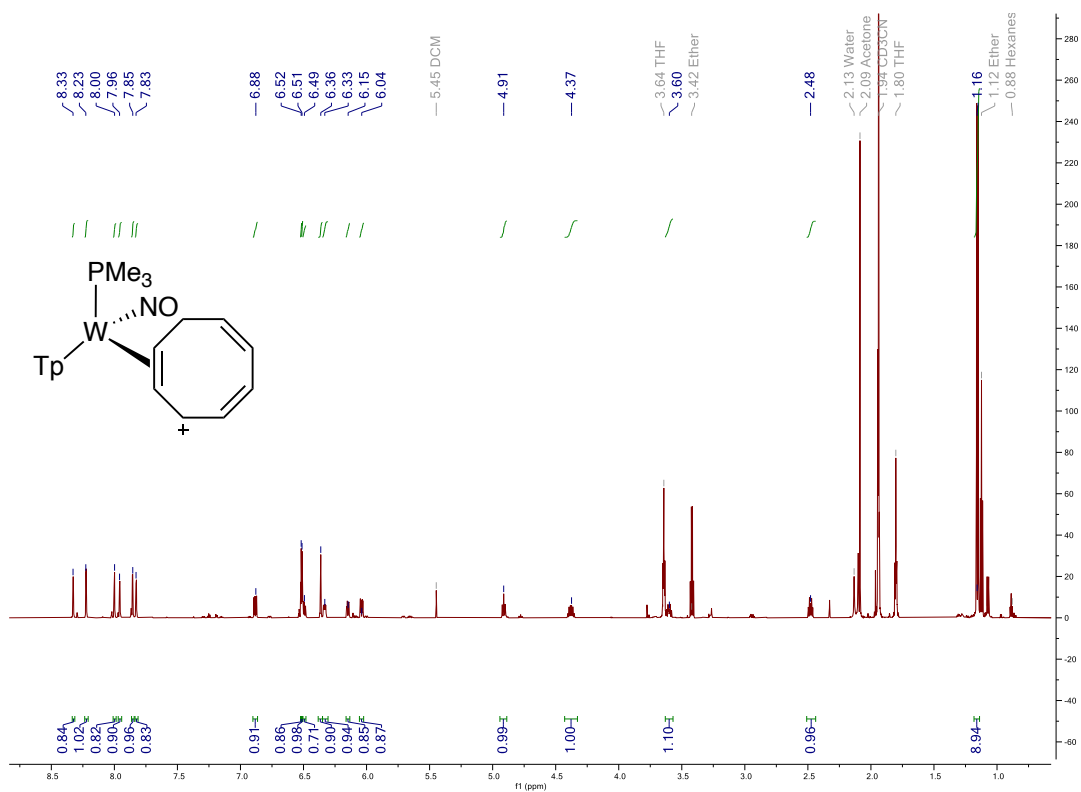
$^{13}\text{C}$  NMR (201 MHz,  $\text{CD}_3\text{CN}$ ,  $\delta$ , 25 °C) of Compound **1**



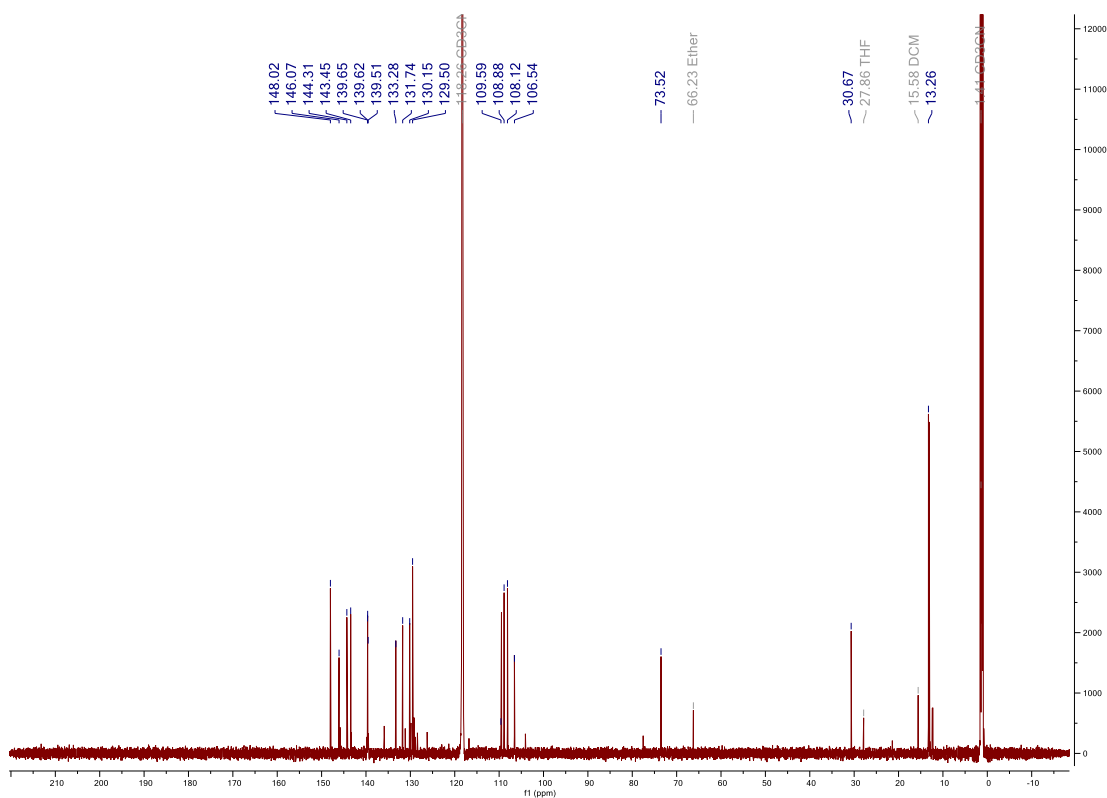
$^1\text{H}$  NMR (800 MHz, MeOD,  $\delta$ , 25 °C) of Compound **2** (**2A:2B:1C**)



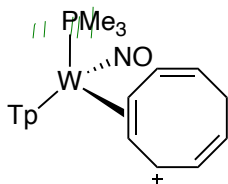
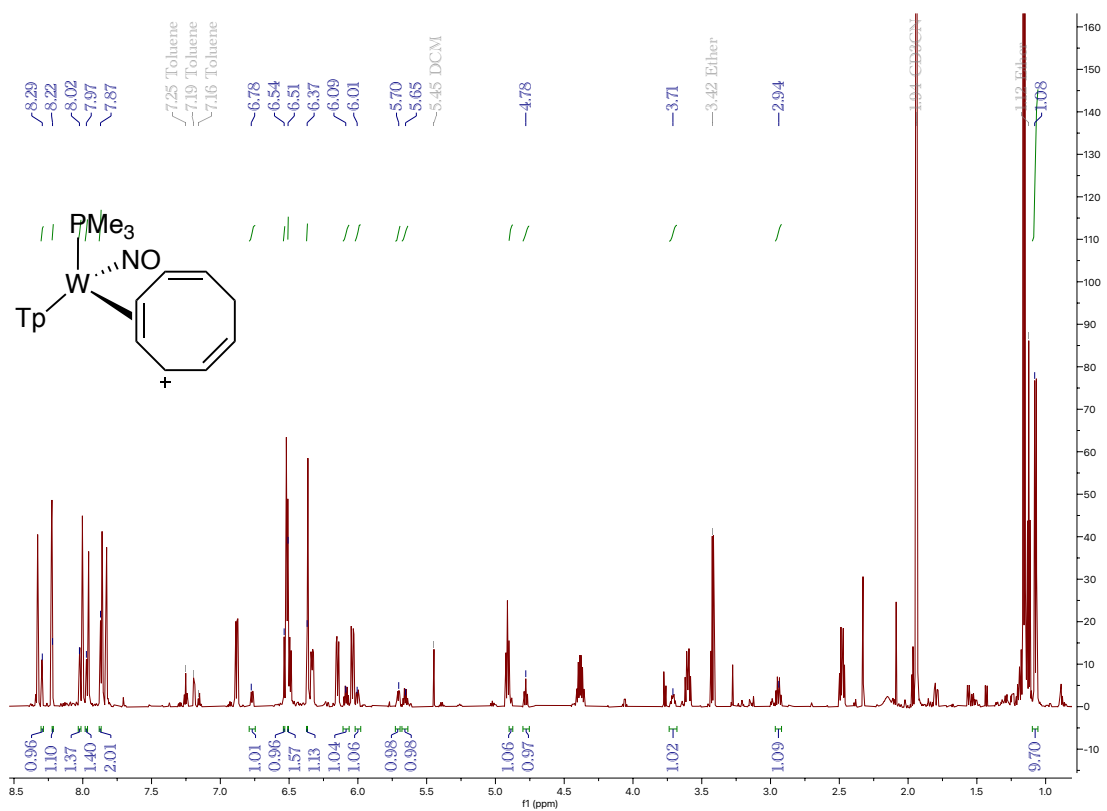
$^1\text{H}$  NMR (800 MHz, CD<sub>3</sub>CN,  $\delta$ , 25 °C) of Compound **2A** (**6A:1B:0C**)



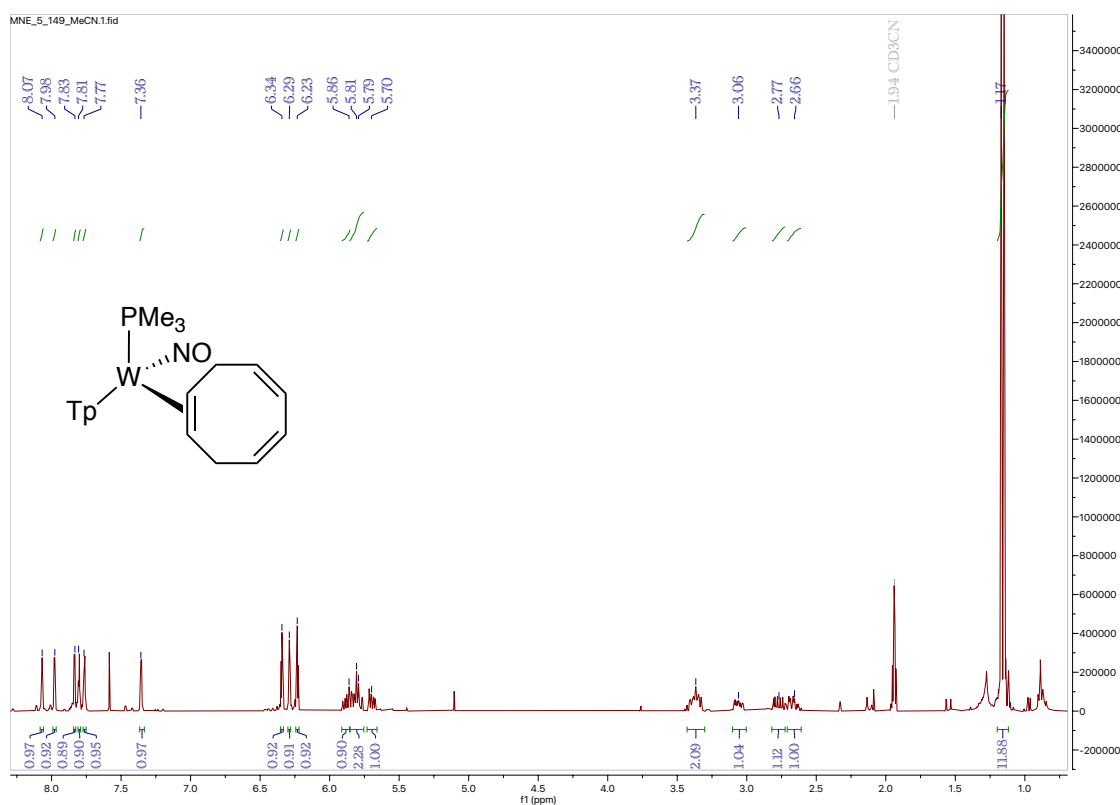
$^{13}\text{C}$  NMR (201 MHz,  $\text{CD}_3\text{CN}$ ,  $\delta$ , 25 °C) of Compound **2A** (6A:1B:0C)



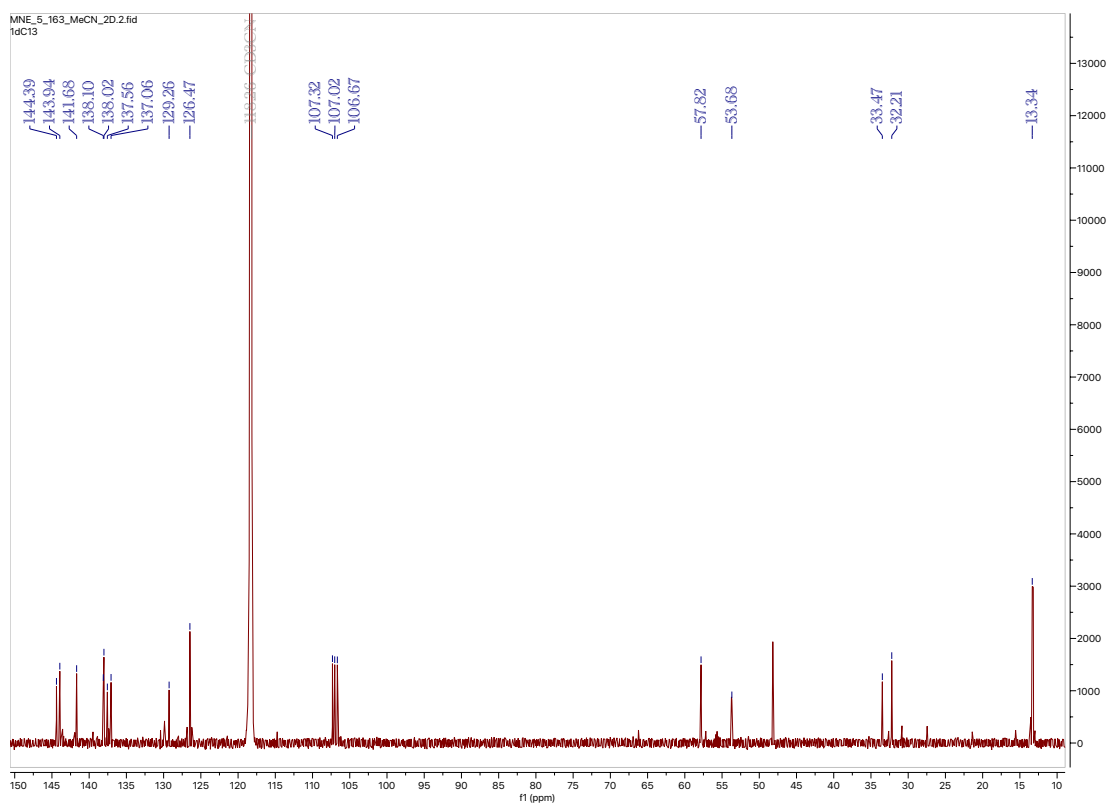
$^1\text{H}$  NMR (800 MHz,  $\text{CD}_3\text{CN}$ ,  $\delta$ , 25 °C) of Compound **2B** (6A:1B:0C)



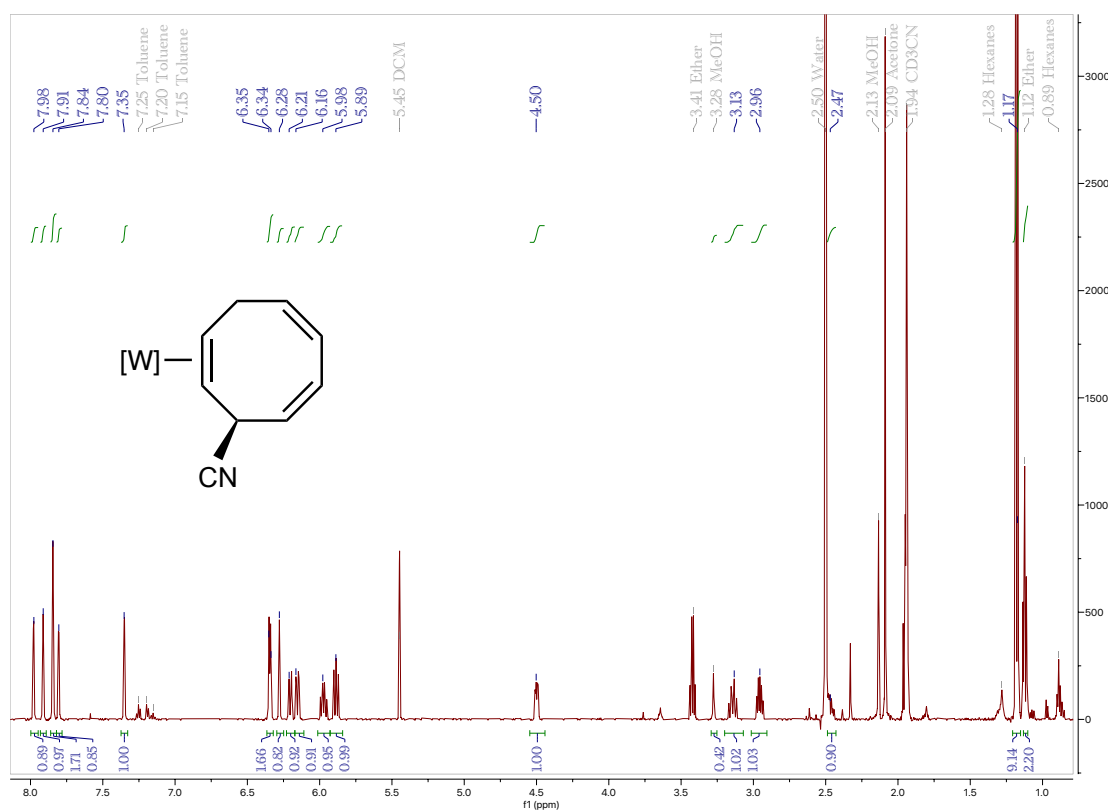
<sup>1</sup>H NMR (800 MHz, CD<sub>3</sub>CN, δ, 25 °C) of Compound **3**



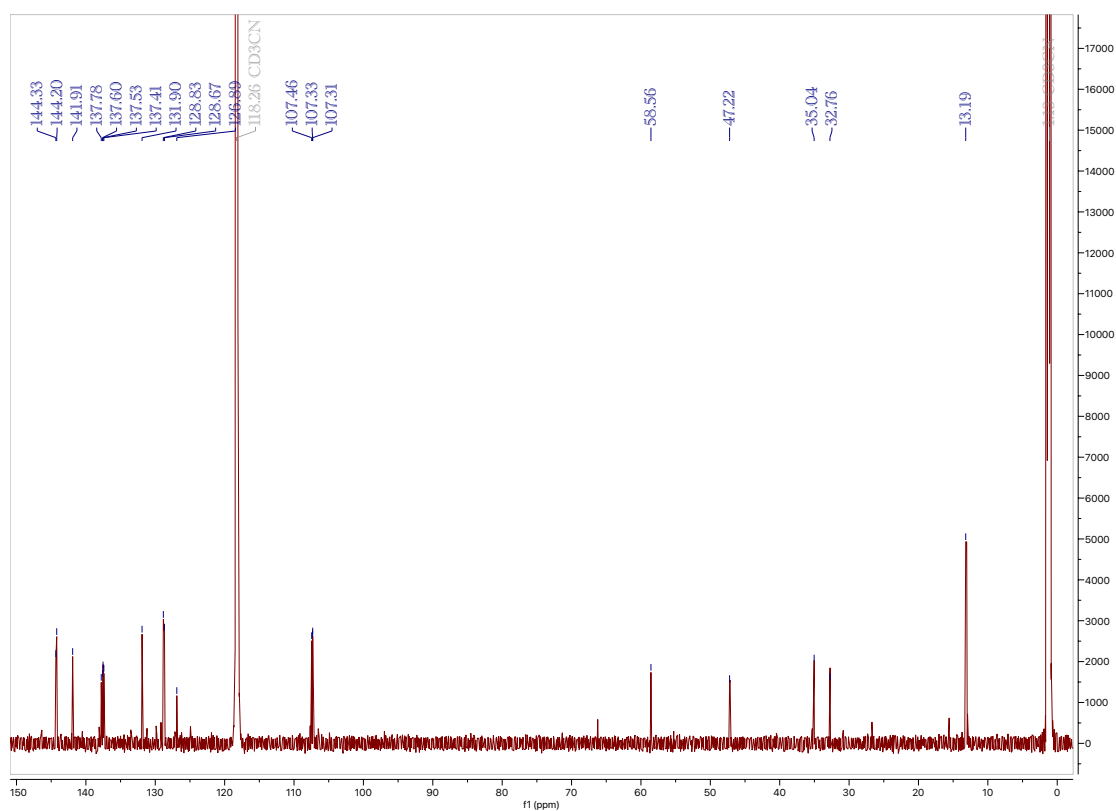
<sup>13</sup>C NMR (201 MHz, CD<sub>3</sub>CN, δ, 25 °C) of Compound **3**



<sup>1</sup>H NMR (800 MHz, CD<sub>3</sub>CN, δ, 25 °C) of Compound **4**

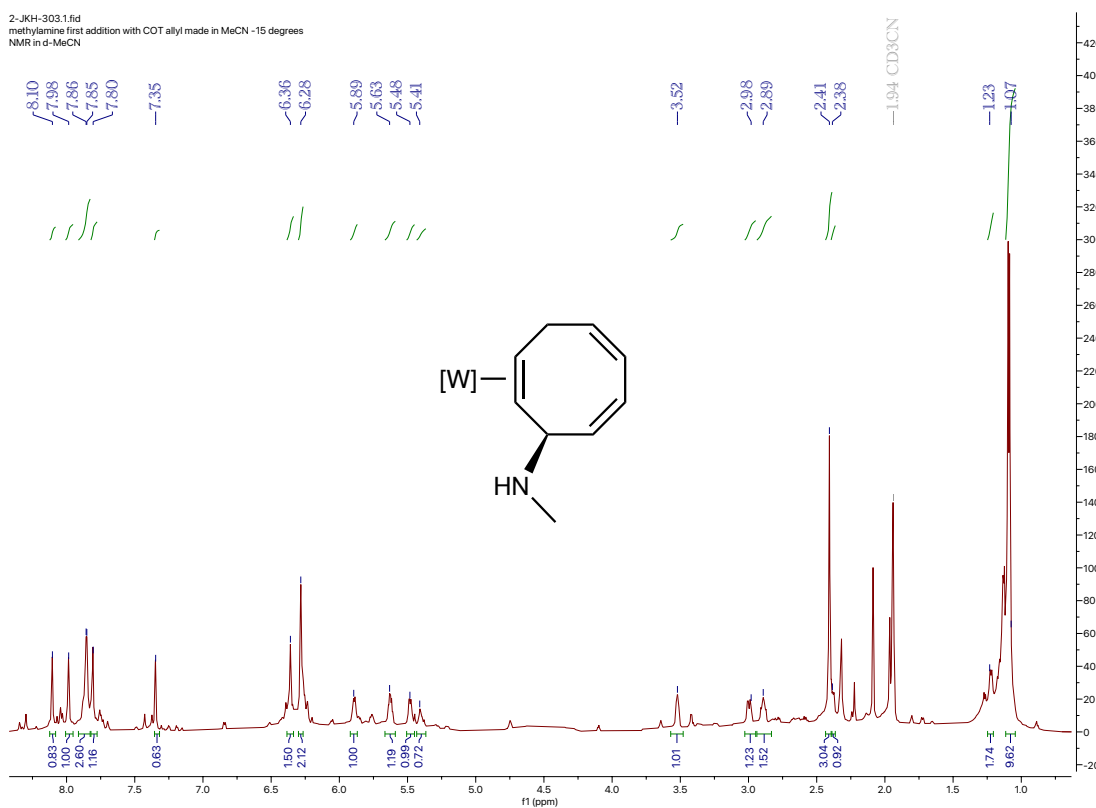


<sup>13</sup>C NMR (201 MHz, CD<sub>3</sub>CN, δ, 25 °C) of Compound **4**

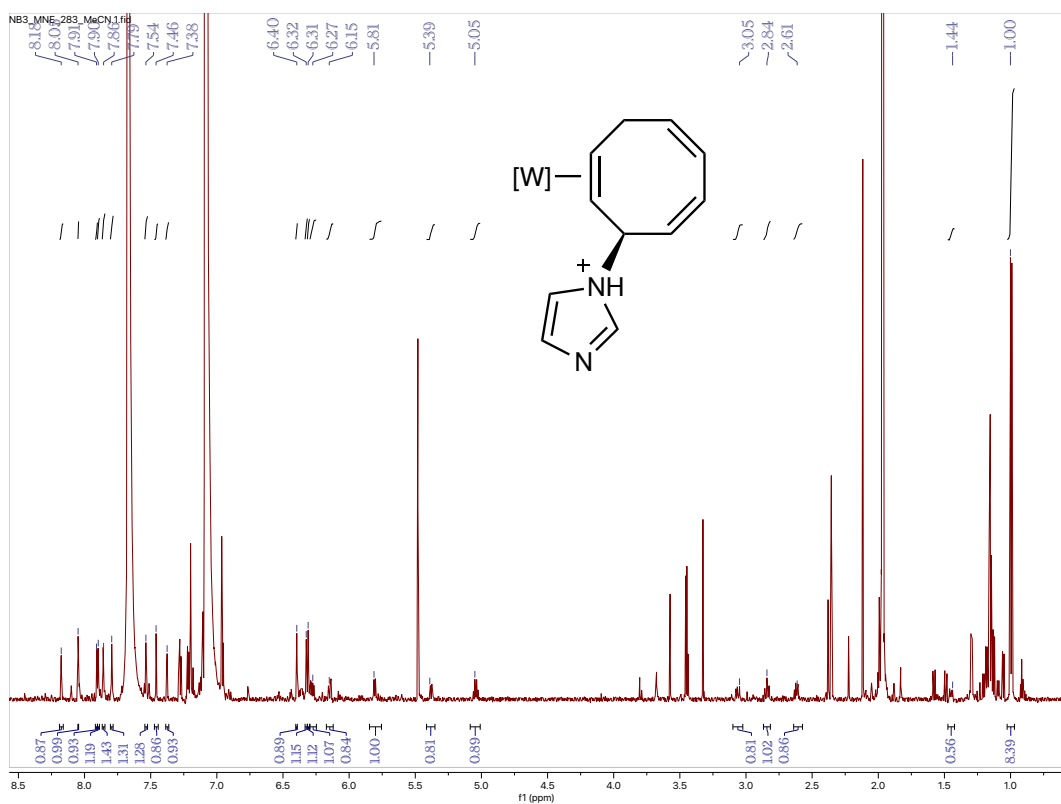


# <sup>1</sup>H NMR (800 MHz, CD<sub>3</sub>CN, δ, 25 °C) of Compound **5**

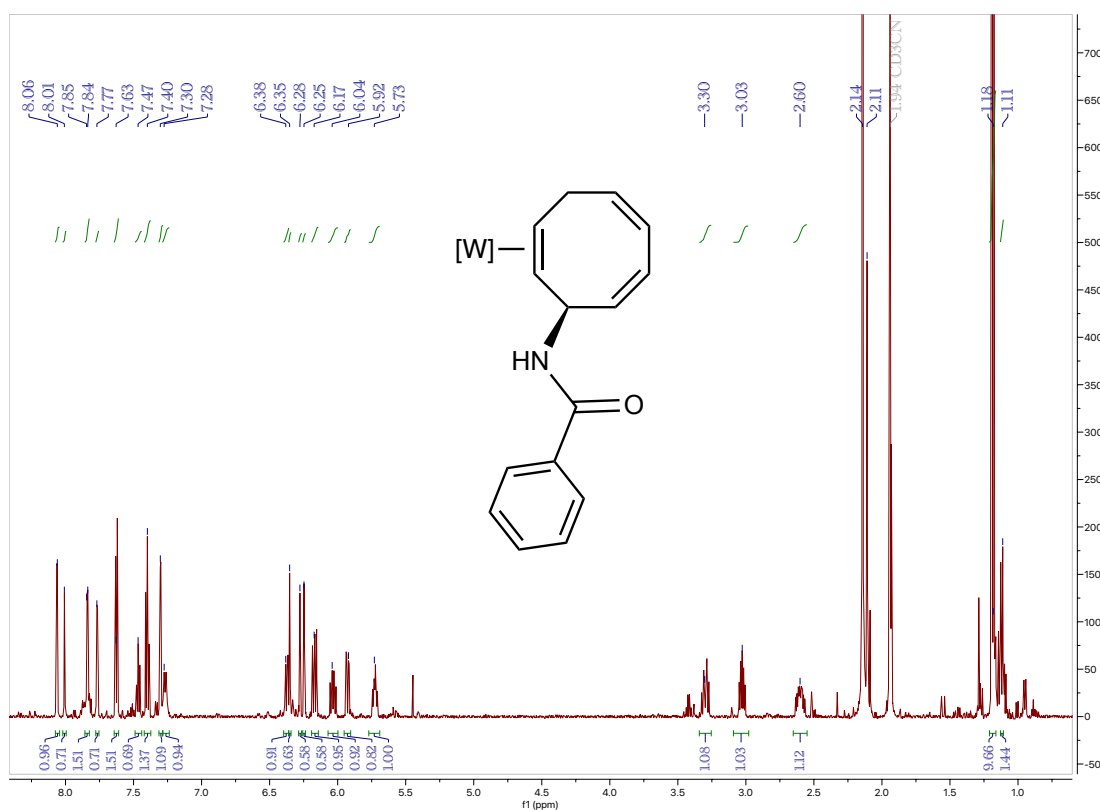
2-JKH-303.1.fid  
methylamine first addition with COT allyl made in MeCN -15 degrees  
NMR in d-MeCN



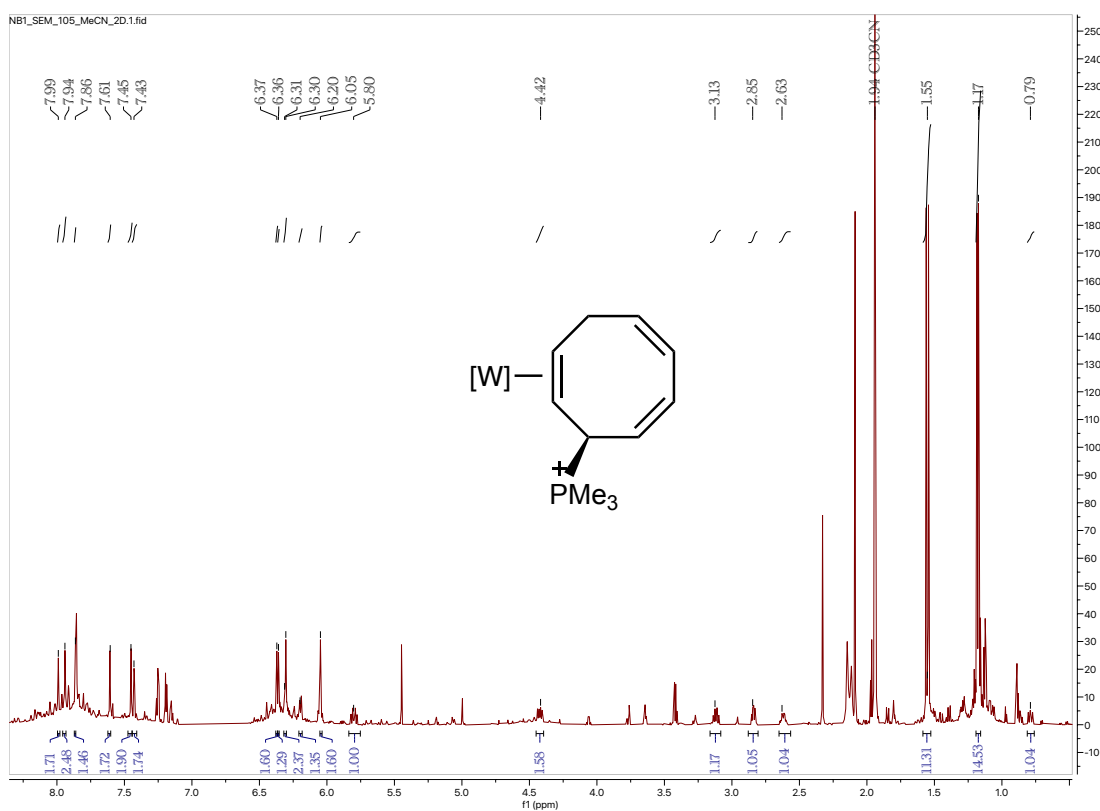
# <sup>1</sup>H NMR (800 MHz, CD<sub>3</sub>CN, δ, 25 °C) of Compound **6**



<sup>1</sup>H NMR (800 MHz, CD<sub>3</sub>CN, δ, 25 °C) of Compound 7

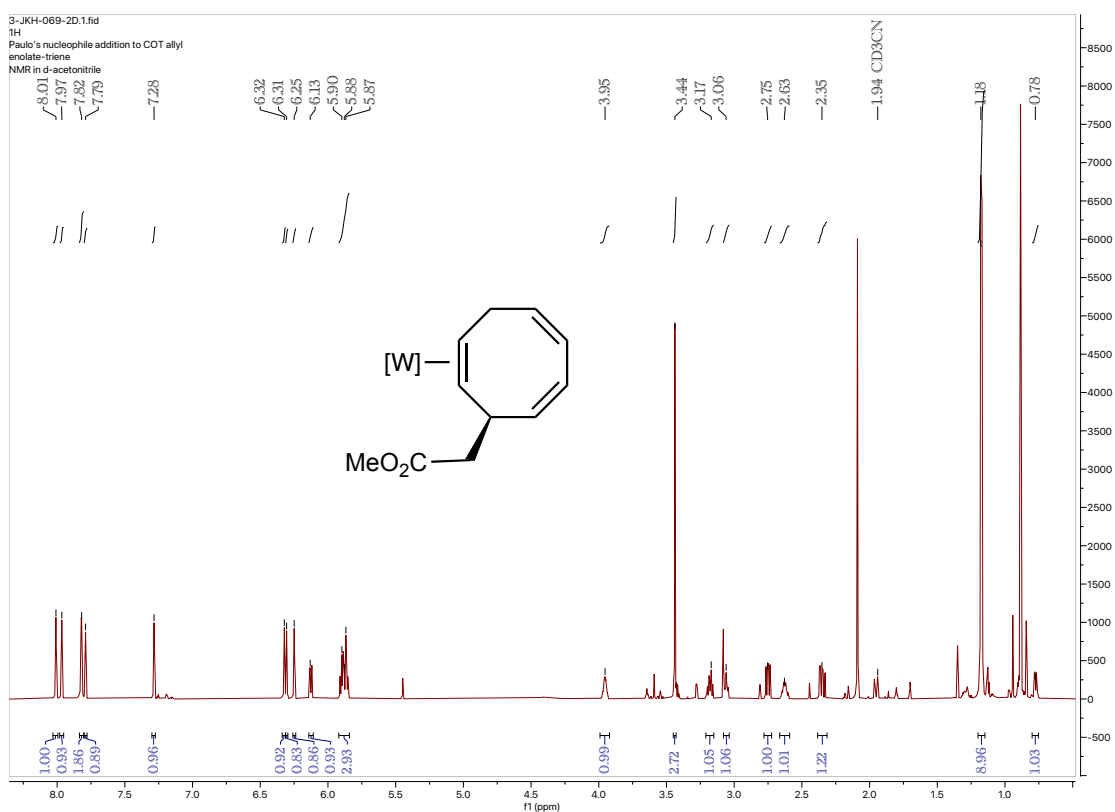


<sup>1</sup>H NMR (800 MHz, CD<sub>3</sub>CN, δ, 25 °C) of Compound 8

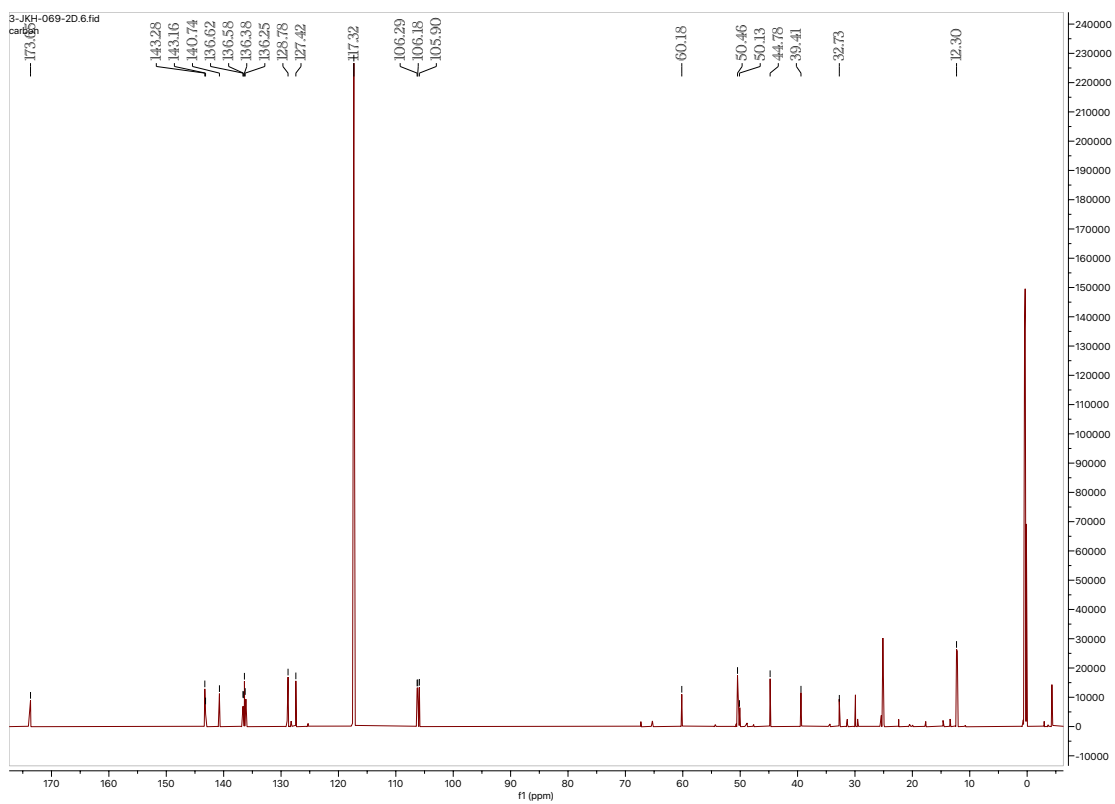




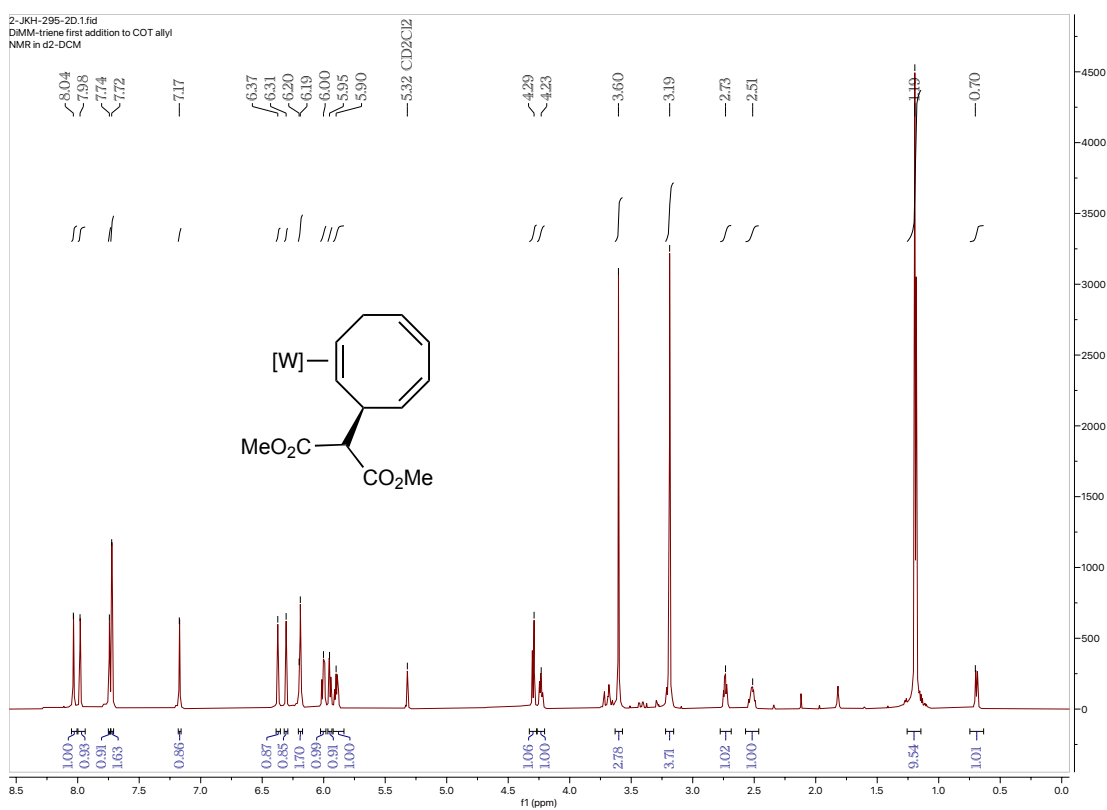
<sup>1</sup>H NMR (800 MHz, CD<sub>3</sub>CN, δ, 25 °C) of Compound **9** –



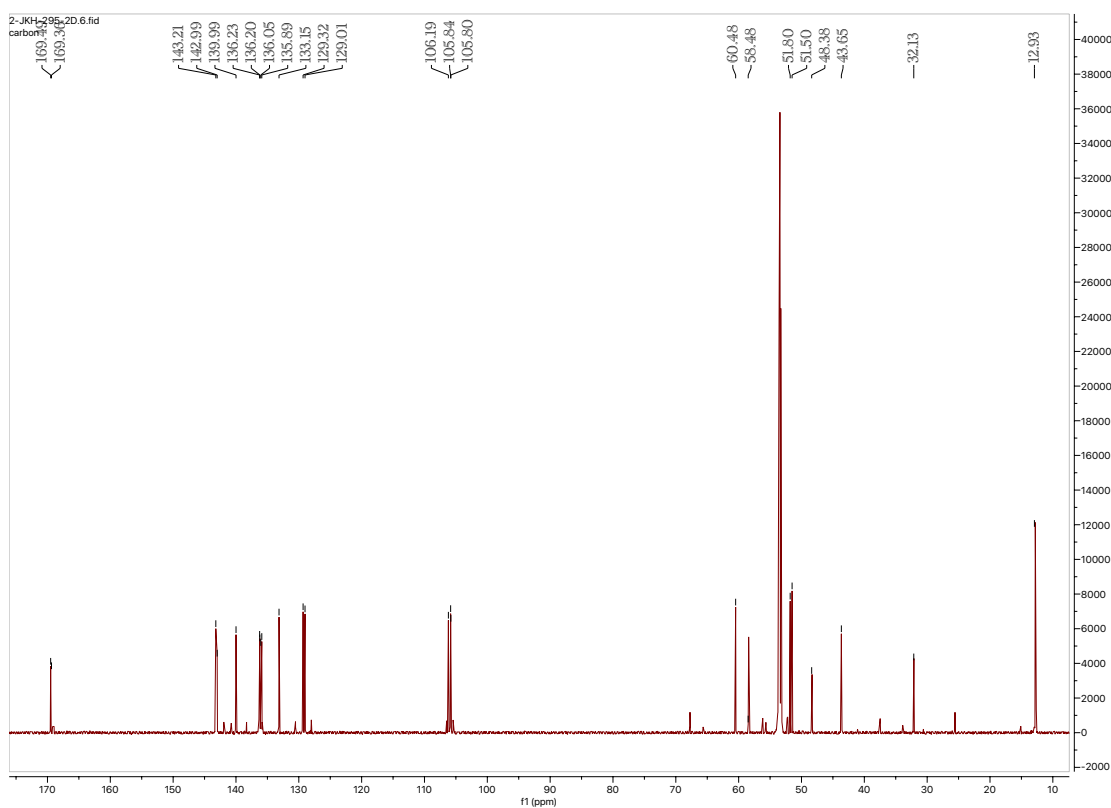
<sup>13</sup>C NMR (201 MHz, CD<sub>3</sub>CN, δ, 25 °C) of Compound **9** –



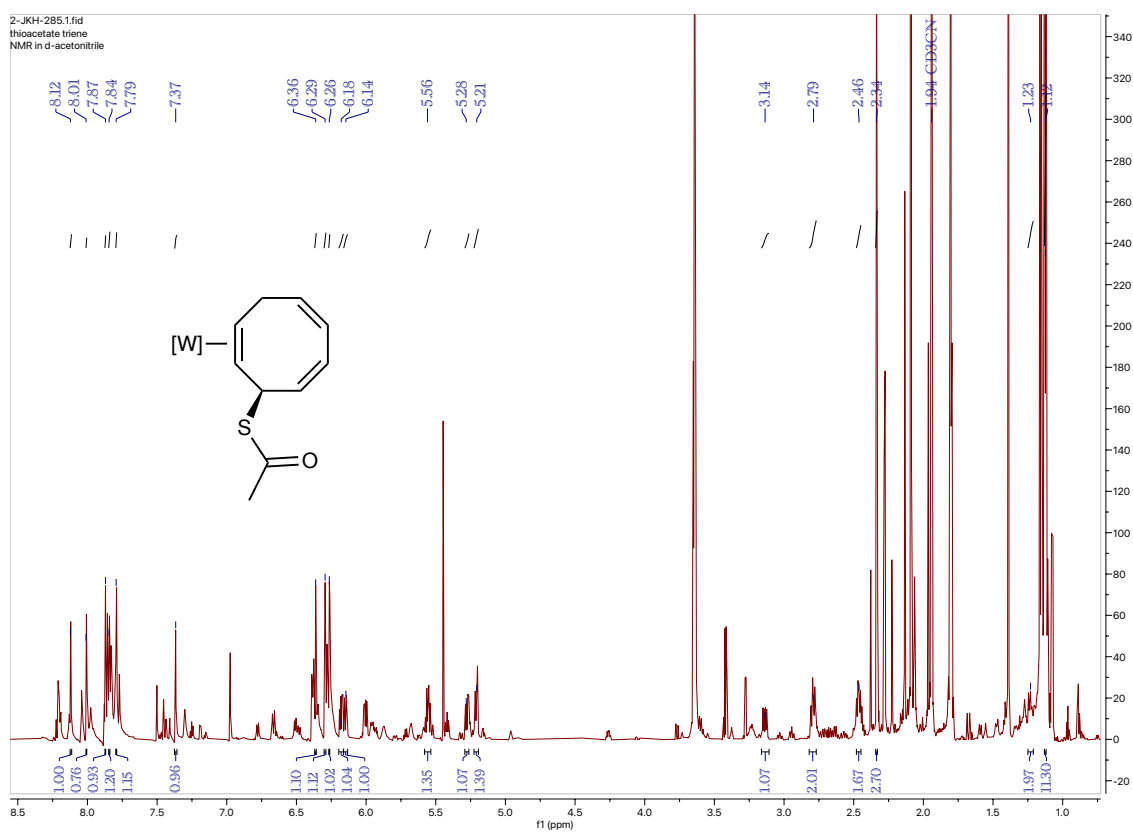
<sup>1</sup>H NMR (800 MHz, CD<sub>2</sub>Cl<sub>2</sub>, δ, 25 °C) of Compound **10** –



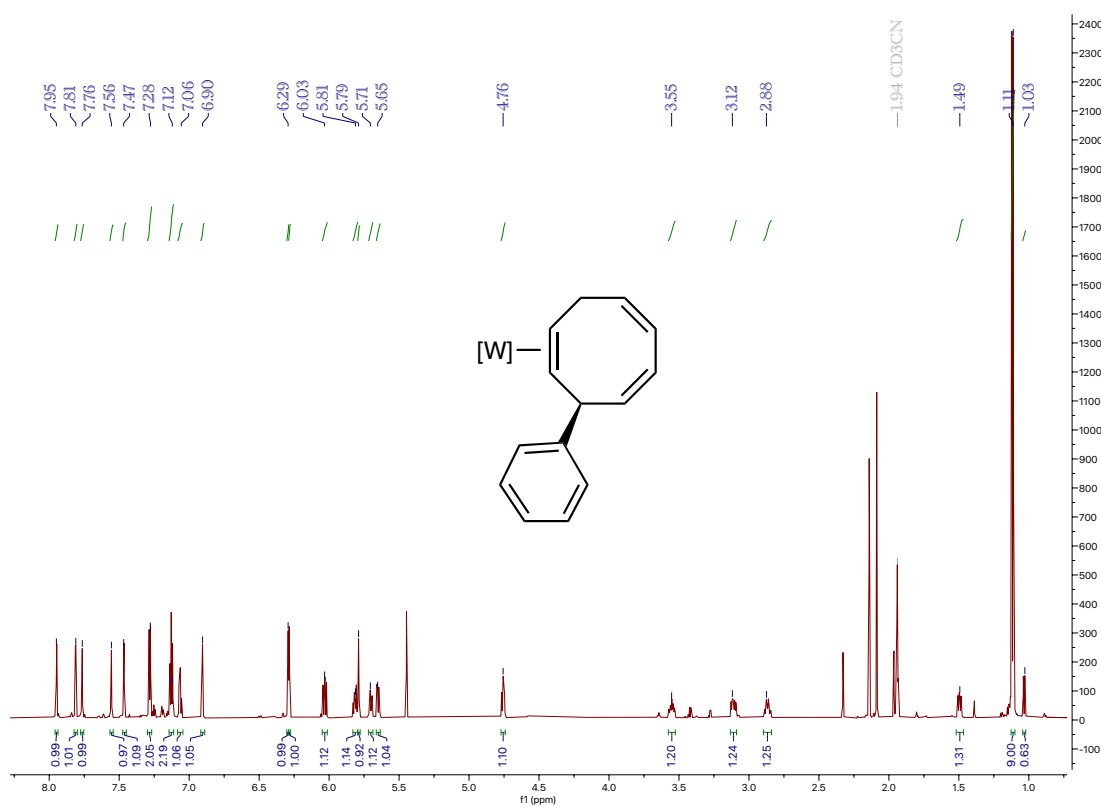
<sup>13</sup>C NMR (201 MHz, CD<sub>2</sub>Cl<sub>2</sub>, δ, 25 °C) of Compound **10** –



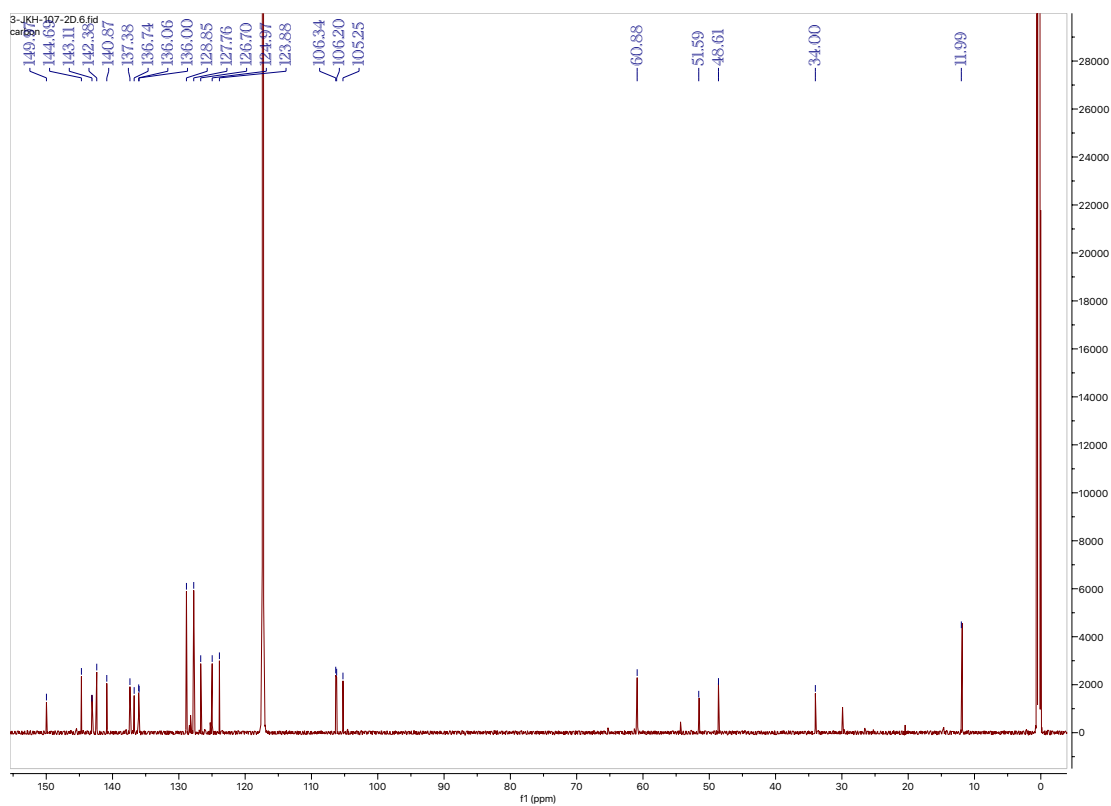
$^1\text{H}$  NMR (800 MHz,  $\text{CD}_3\text{CN}$ ,  $\delta$ , 25  $^\circ\text{C}$ ) of Compound **11** –



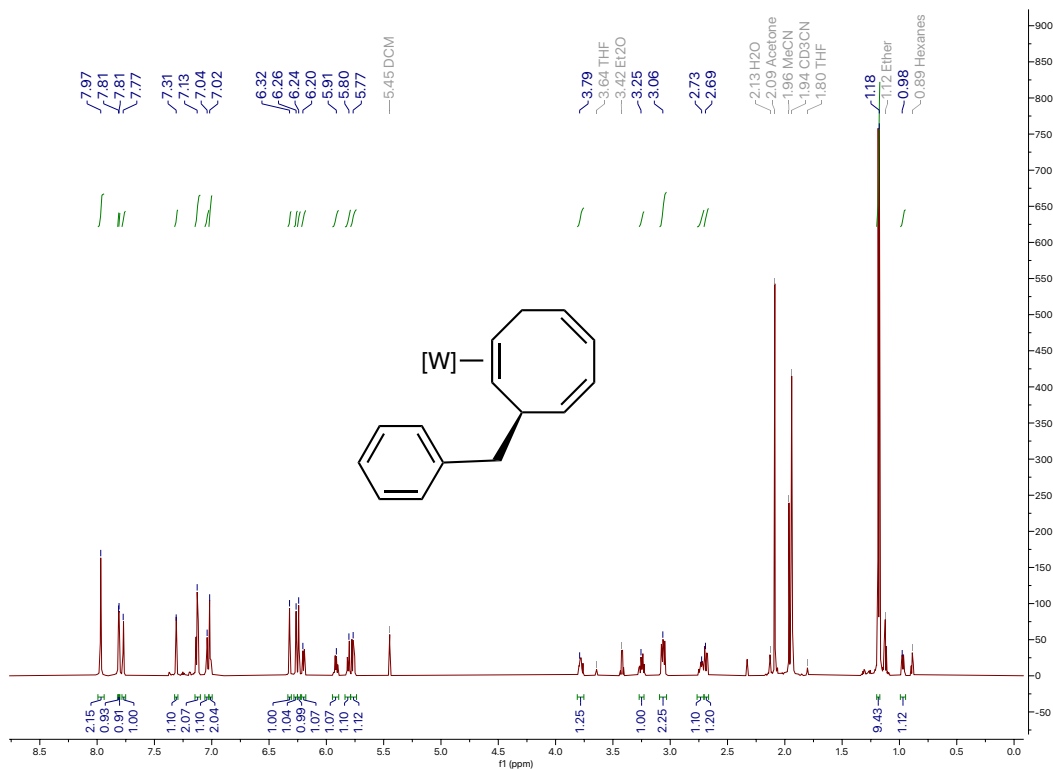
$^1\text{H}$  NMR (800 MHz,  $\text{CD}_3\text{CN}$ ,  $\delta$ , 25  $^\circ\text{C}$ ) of Compound **12** –



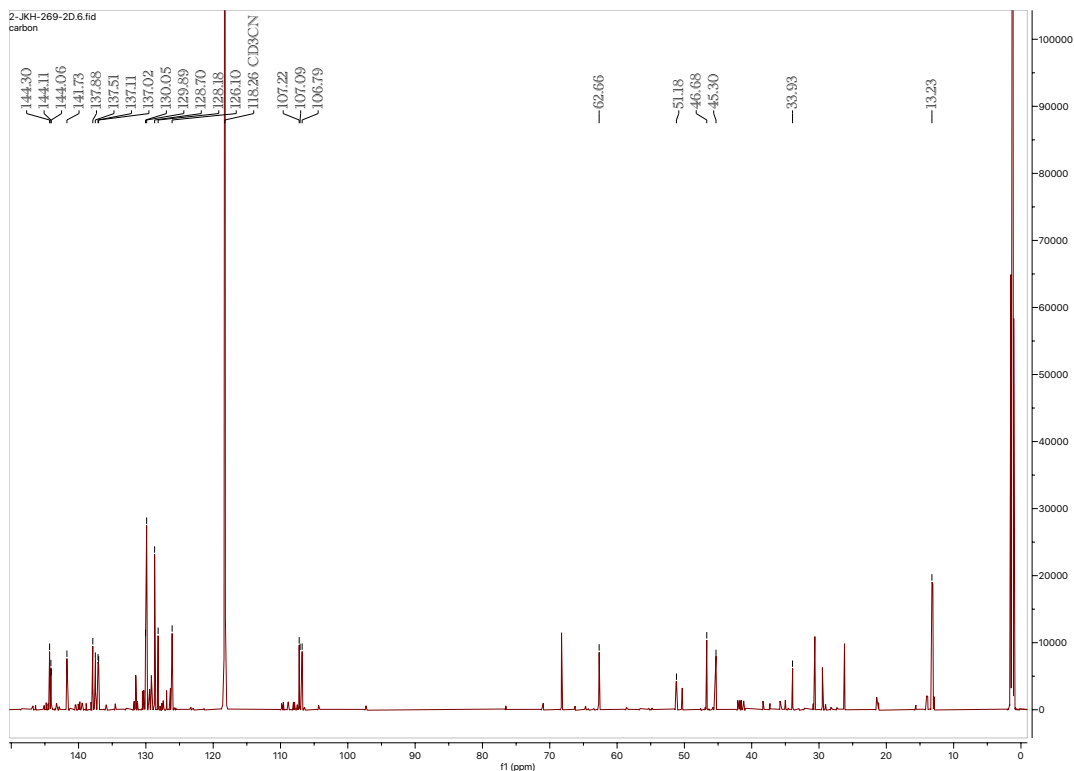
$^{13}\text{C}$  NMR (201 MHz,  $\text{CD}_3\text{CN}$ ,  $\delta$ , 25  $^\circ\text{C}$ ) of Compound **12** –



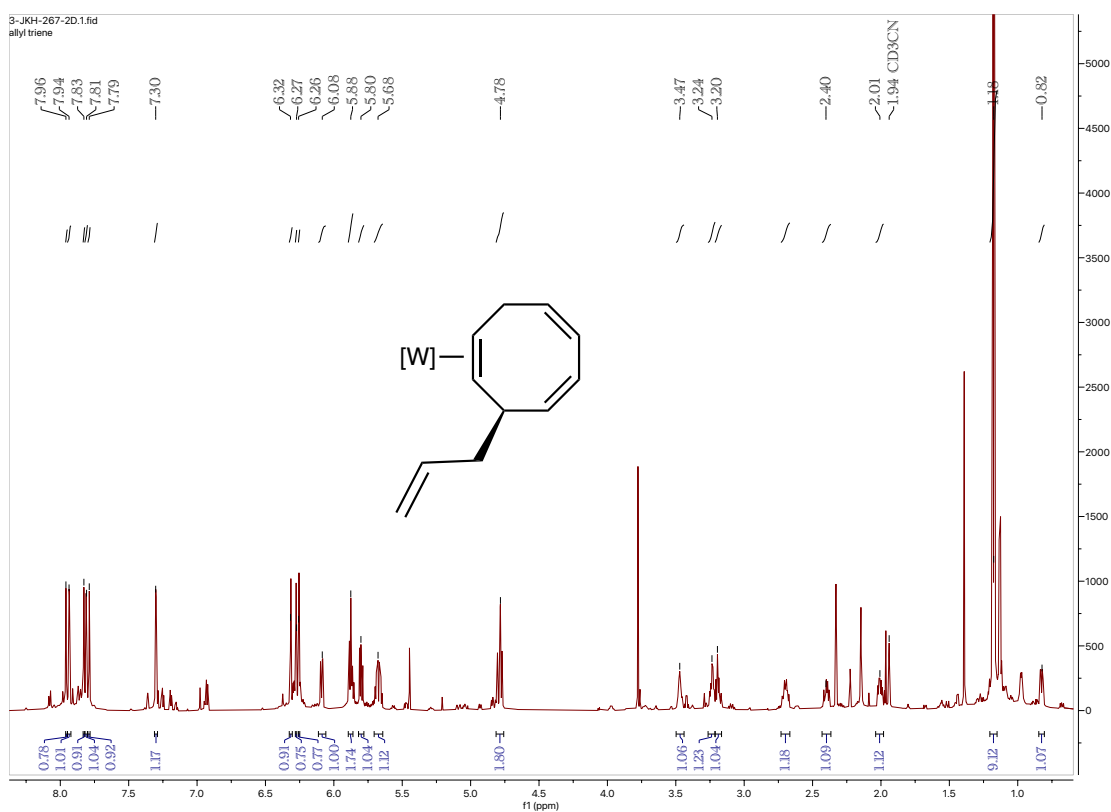
<sup>1</sup>H NMR (800 MHz, CD<sub>3</sub>CN, δ, 25 °C) of Compound **13** –



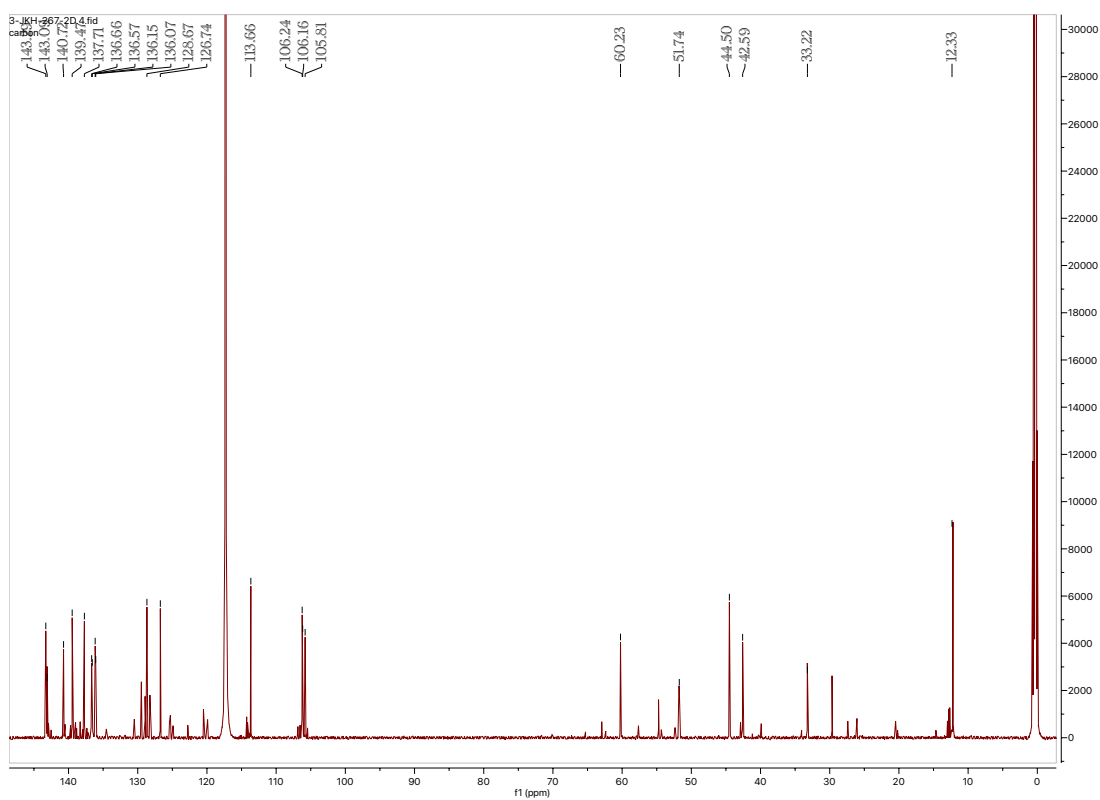
<sup>13</sup>C NMR (201 MHz, CD<sub>3</sub>CN, δ, 25 °C) of Compound **13** –



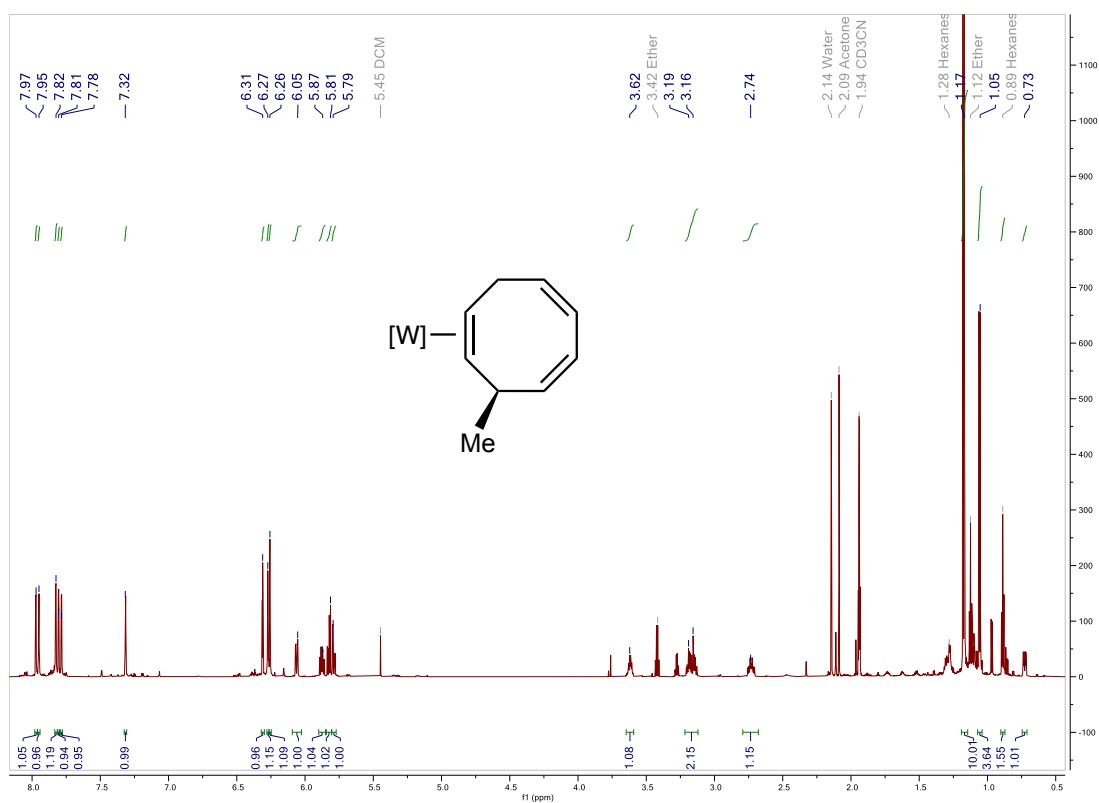
<sup>1</sup>H NMR (800 MHz, CD<sub>3</sub>CN, δ, 25 °C) of Compound **14** –



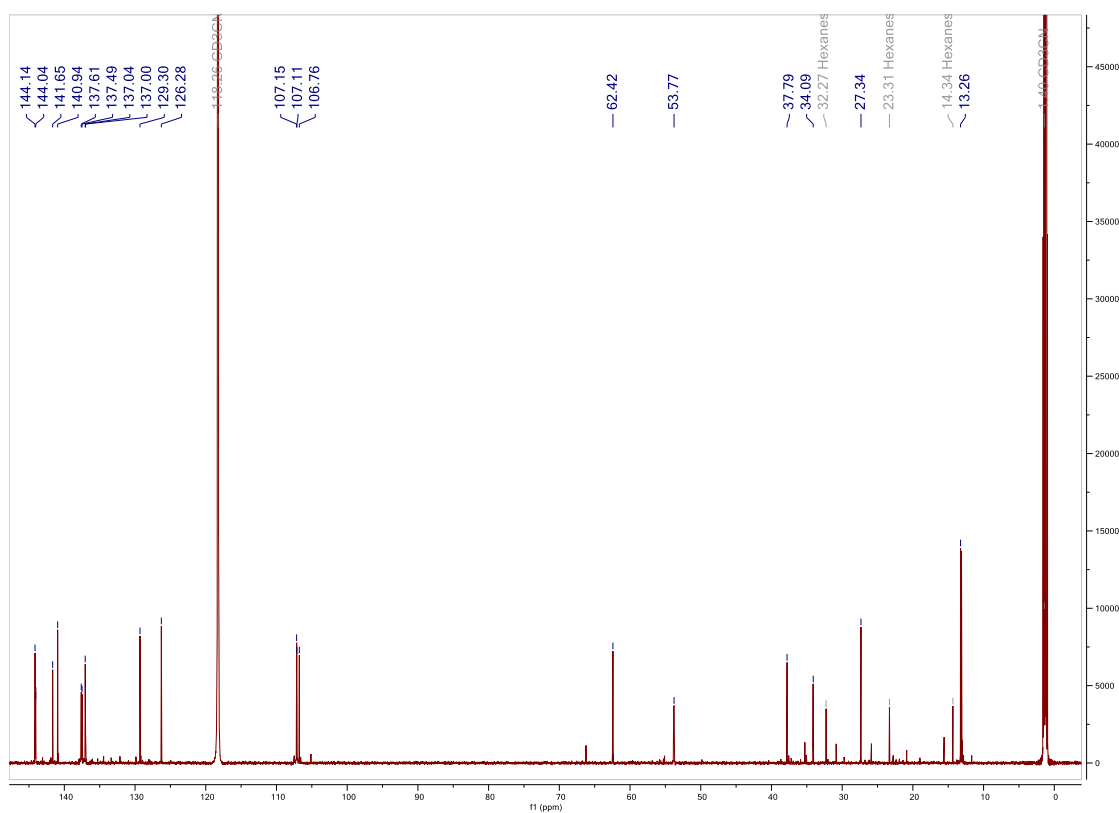
<sup>13</sup>C NMR (201 MHz, CD<sub>3</sub>CN, δ, 25 °C) of Compound **14** –



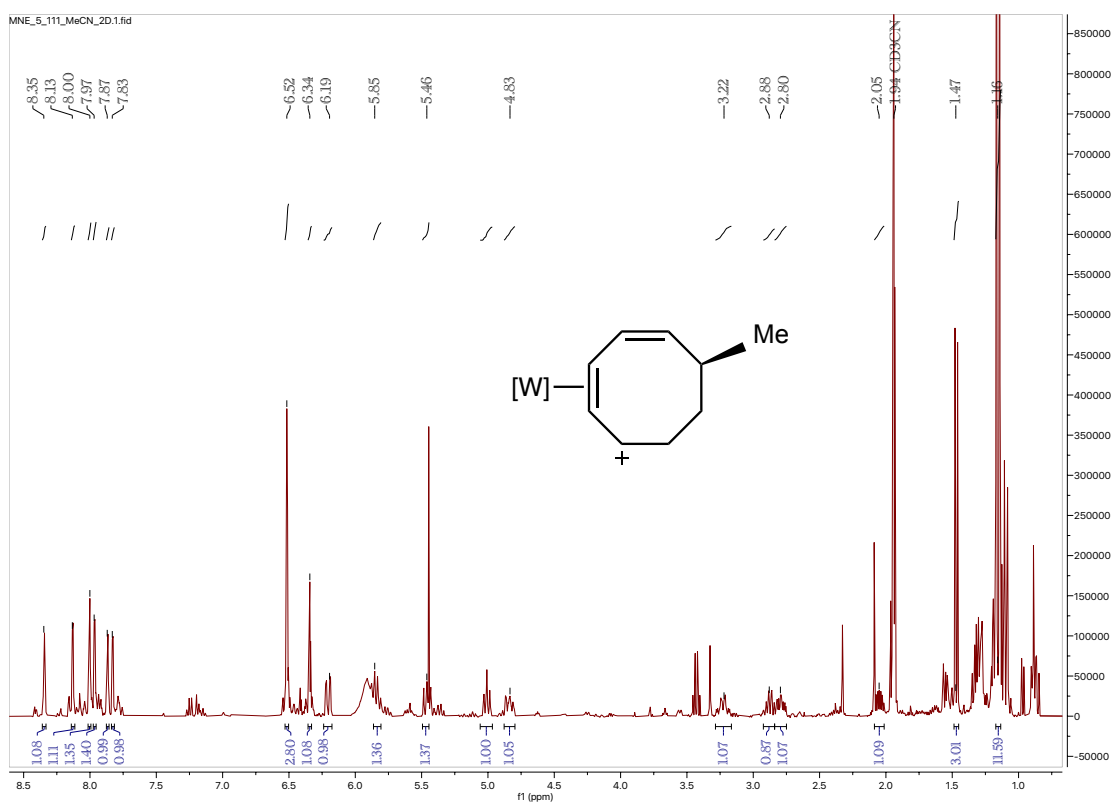
<sup>1</sup>H NMR (800 MHz, CD<sub>3</sub>CN, δ, 25 °C) of Compound **15** –



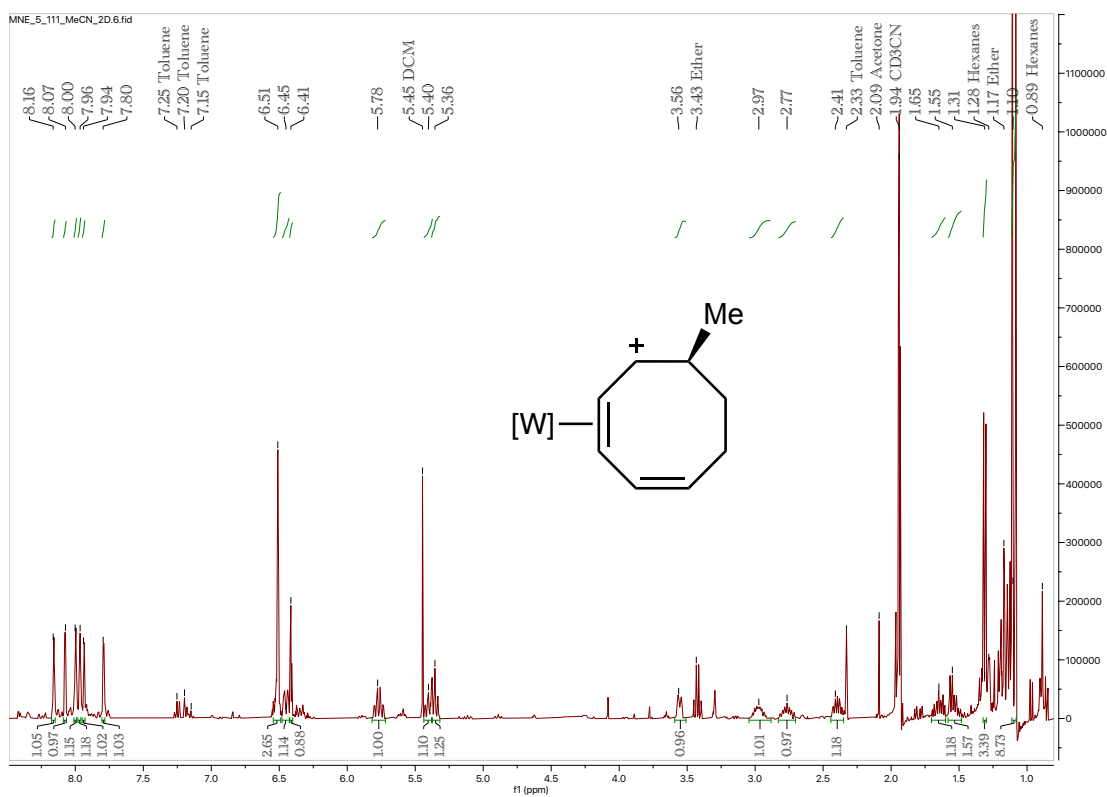
<sup>13</sup>C NMR (201 MHz, CD<sub>3</sub>CN, δ, 25 °C) of Compound **15** –



<sup>1</sup>H NMR (800 MHz, CD<sub>3</sub>CN, δ, 25 °C) of Compound **16K** –

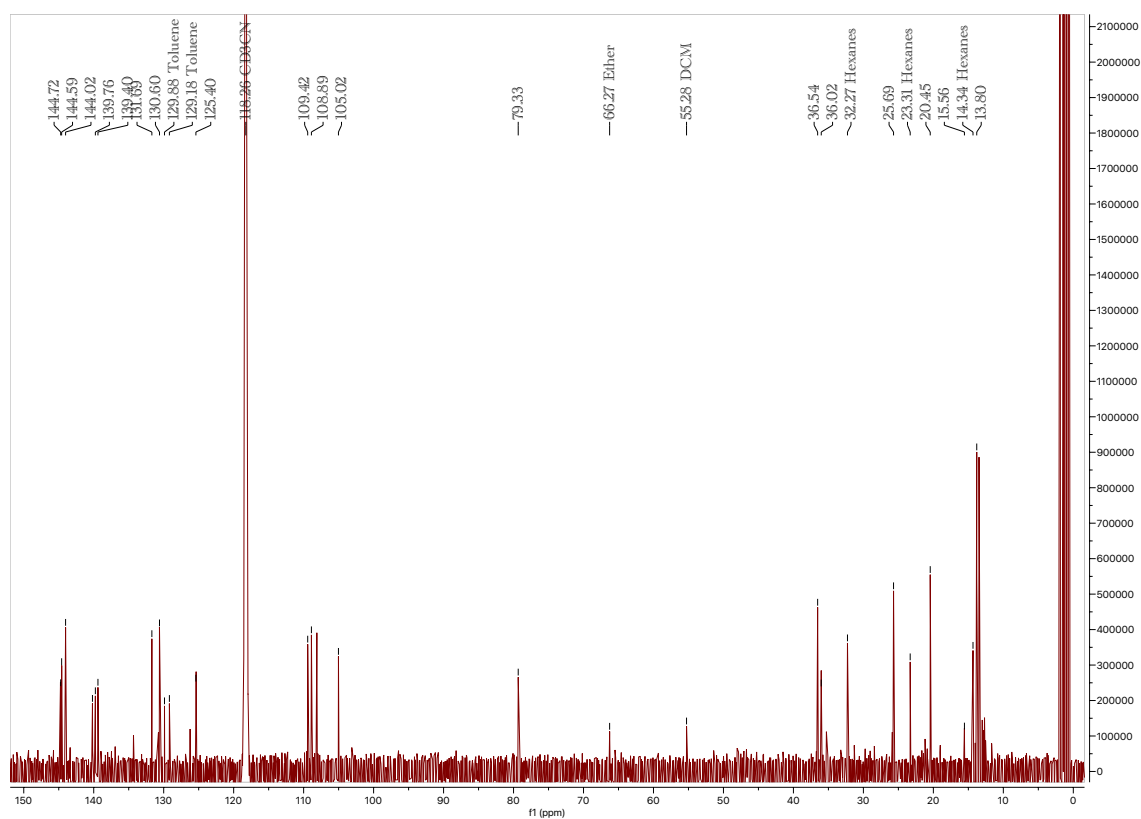


<sup>1</sup>H NMR (800 MHz, CD<sub>3</sub>CN, δ, 25 °C) of Compound **16T'** –

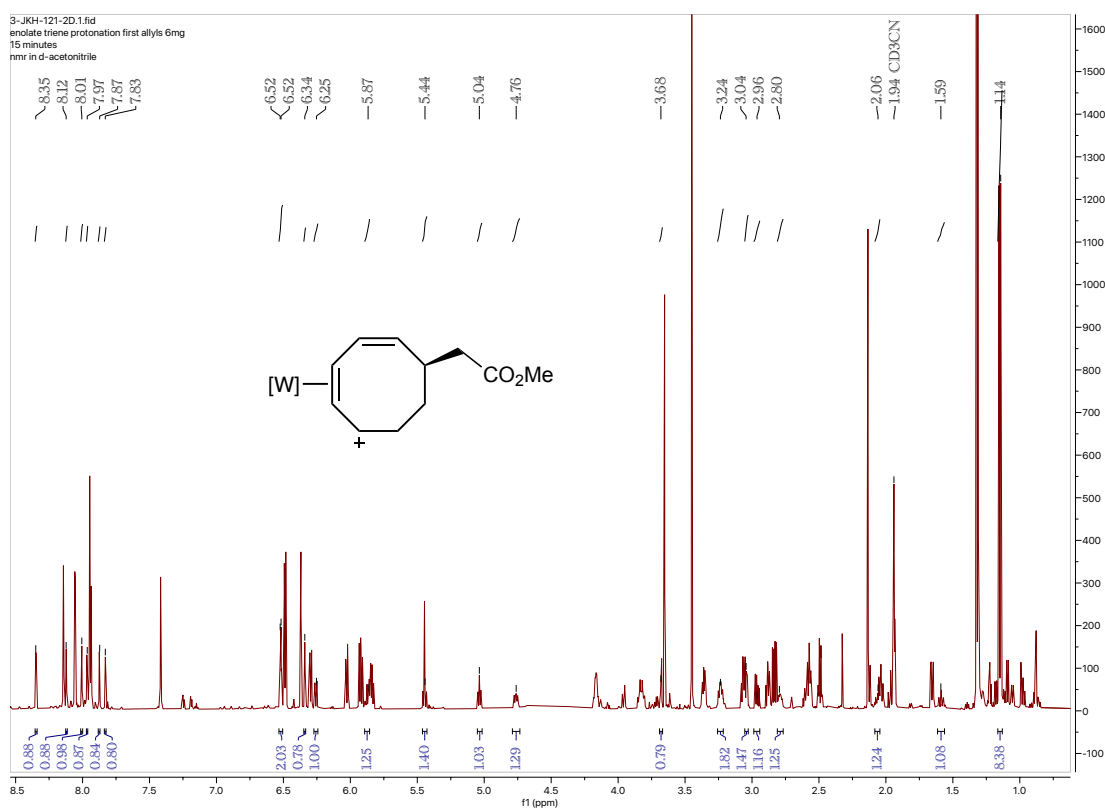




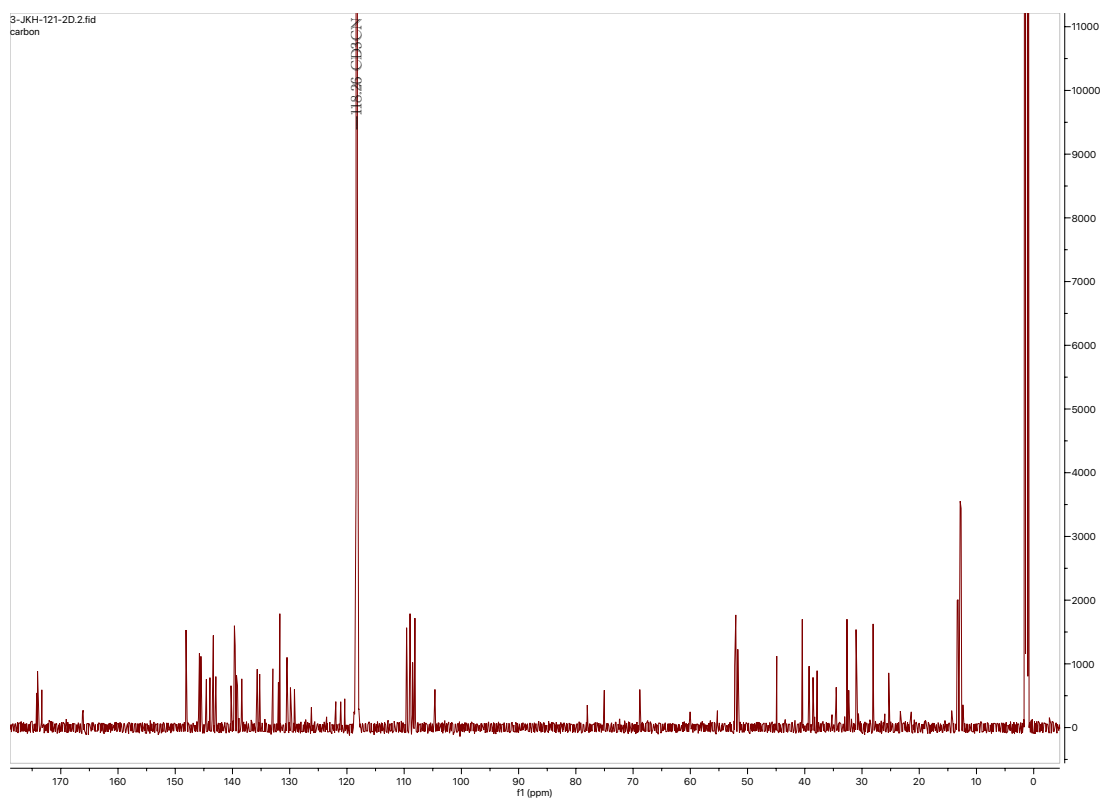
$^{13}\text{C}$  NMR (201 MHz,  $\text{CD}_3\text{CN}$ ,  $\delta$ , 25 °C) of Compound **16T'** –



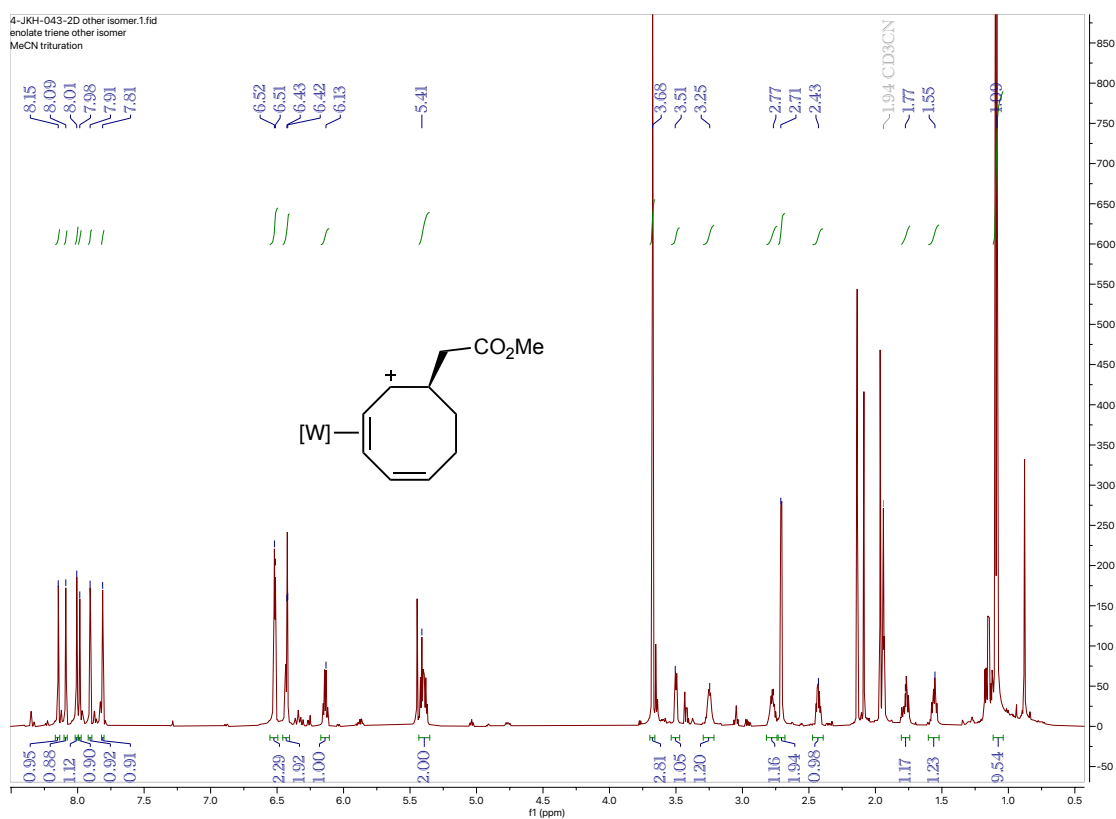
<sup>1</sup>H NMR (800 MHz, CD<sub>3</sub>CN, δ, 25 °C) of Compound **17K** –



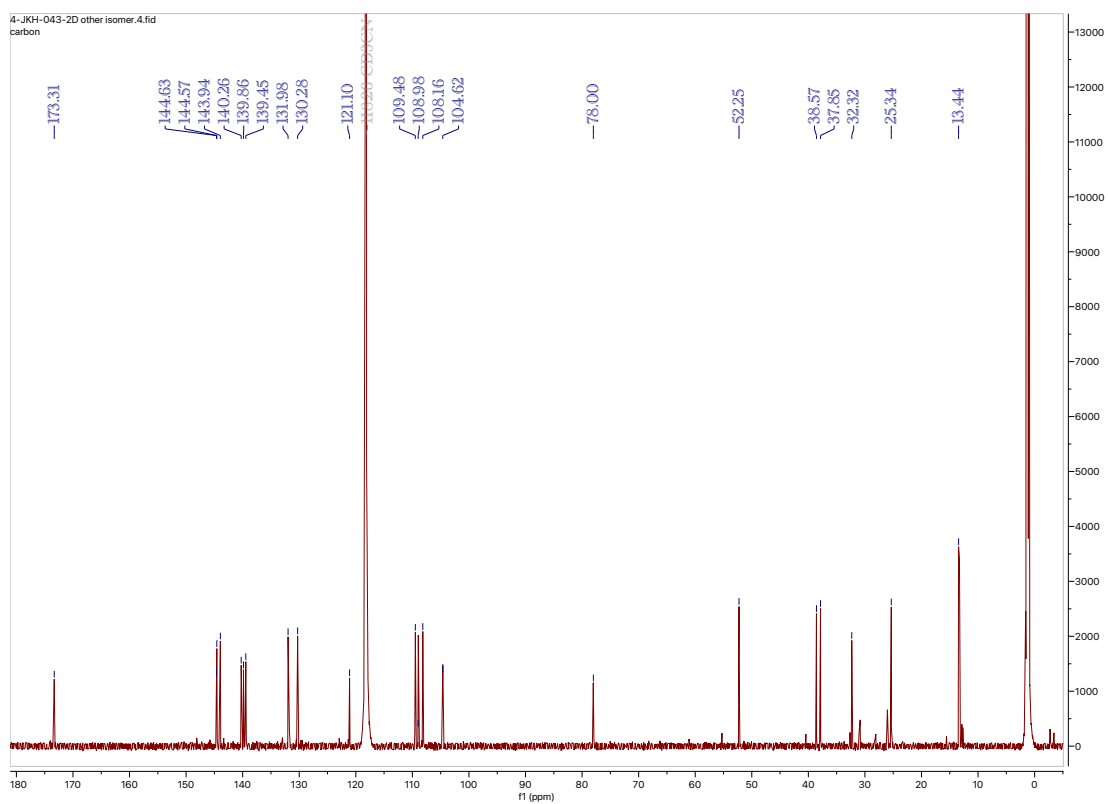
<sup>13</sup>C NMR (201 MHz, CD<sub>3</sub>CN, δ, 25 °C) of Compound **17K** –



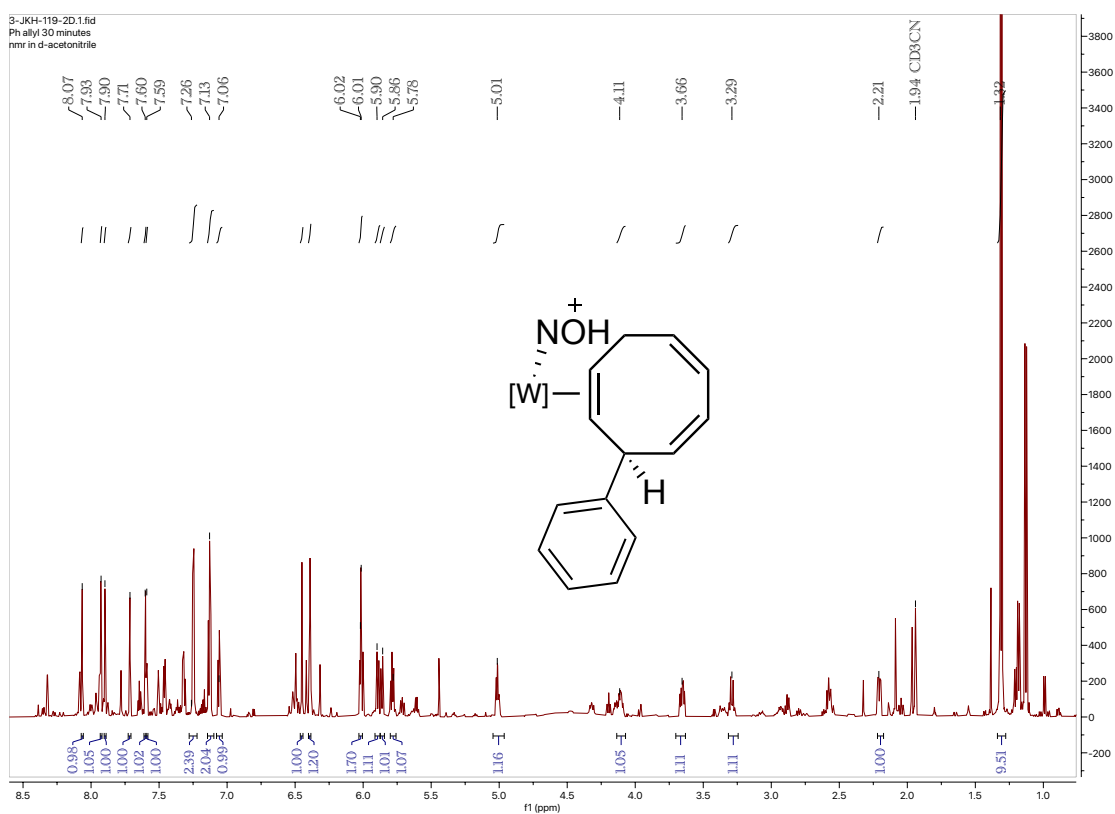
<sup>1</sup>H NMR (800 MHz, CD<sub>3</sub>CN, δ, 25 °C) of Compound **17T'** –



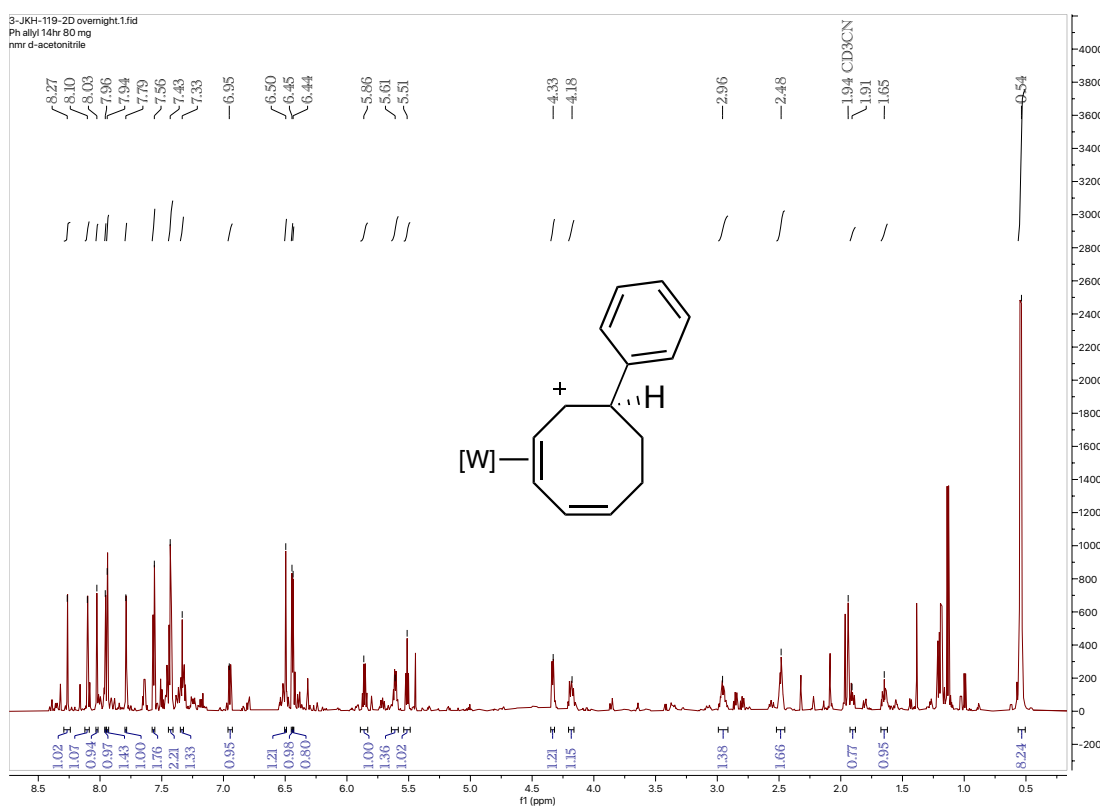
<sup>13</sup>C NMR (201 MHz, CD<sub>3</sub>CN, δ, 25 °C) of Compound **17T'** –



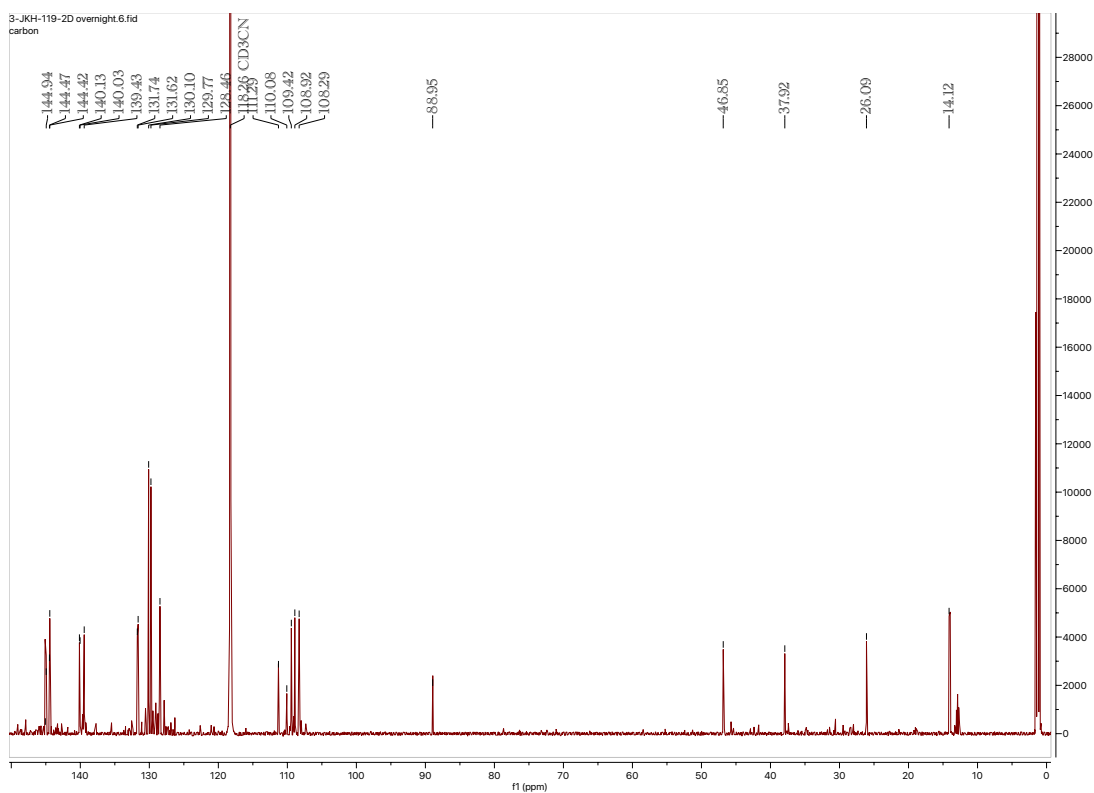
<sup>1</sup>H NMR (800 MHz, CD<sub>3</sub>CN, δ, 25 °C) of Compound **11A** –



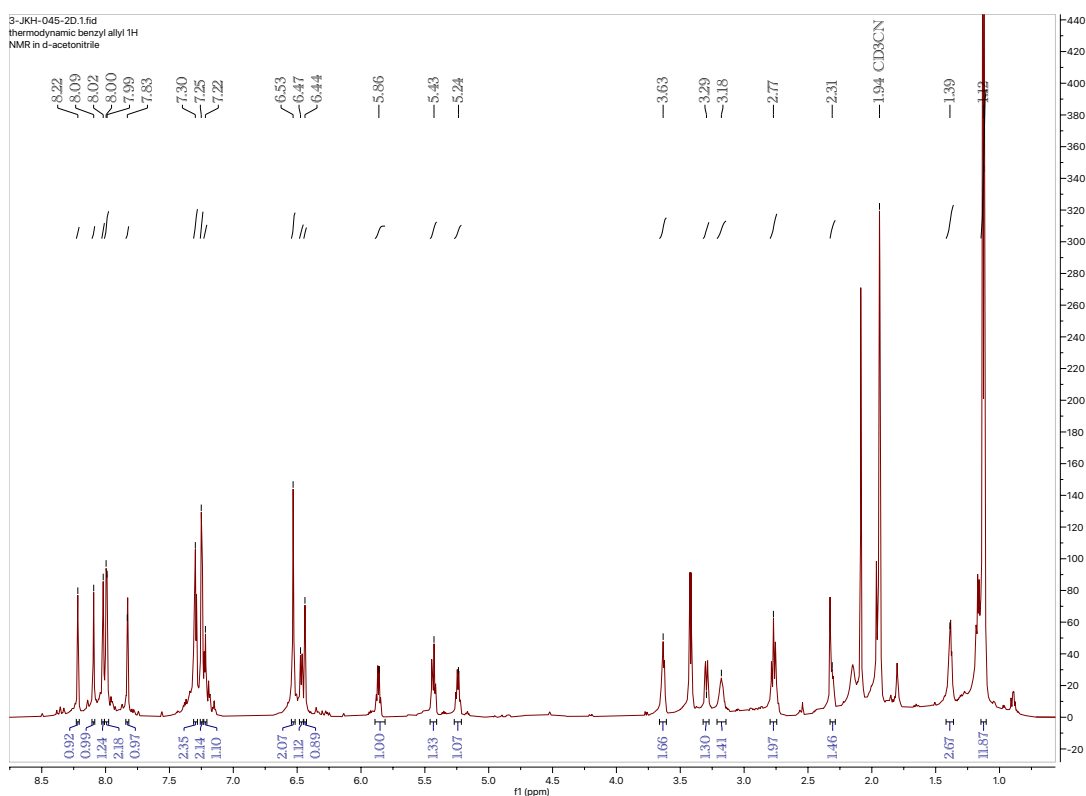
<sup>1</sup>H NMR (800 MHz, CD<sub>3</sub>CN, δ, 25 °C) of Compound **18T'** –



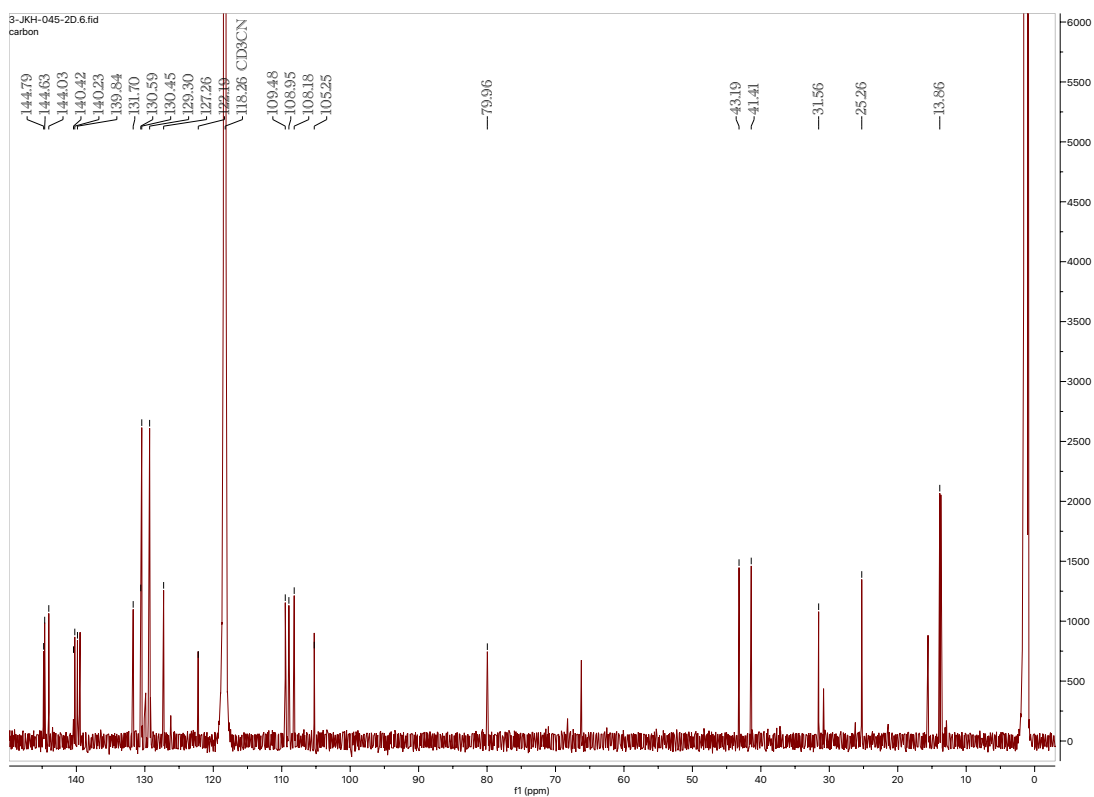
<sup>13</sup>C NMR (201 MHz, CD<sub>3</sub>CN, δ, 25 °C) of Compound **18T'** –



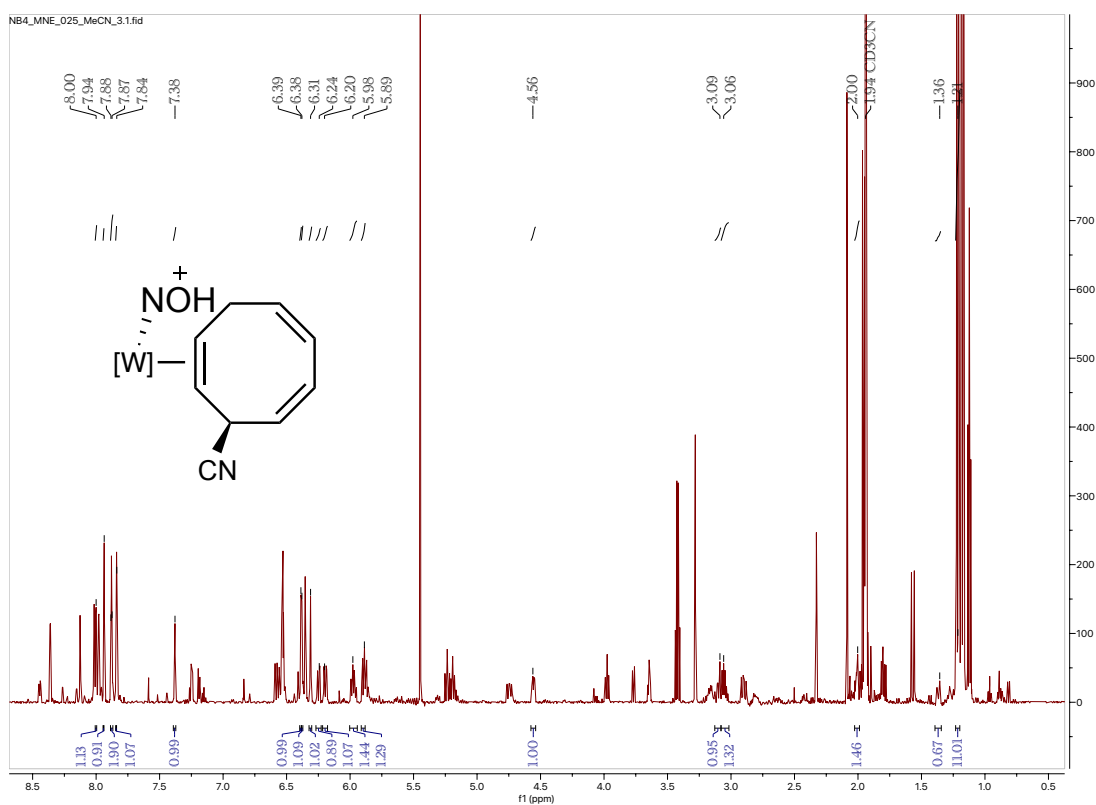
<sup>1</sup>H NMR (800 MHz, CD<sub>3</sub>CN, δ, 25 °C) of Compound **19T'** –



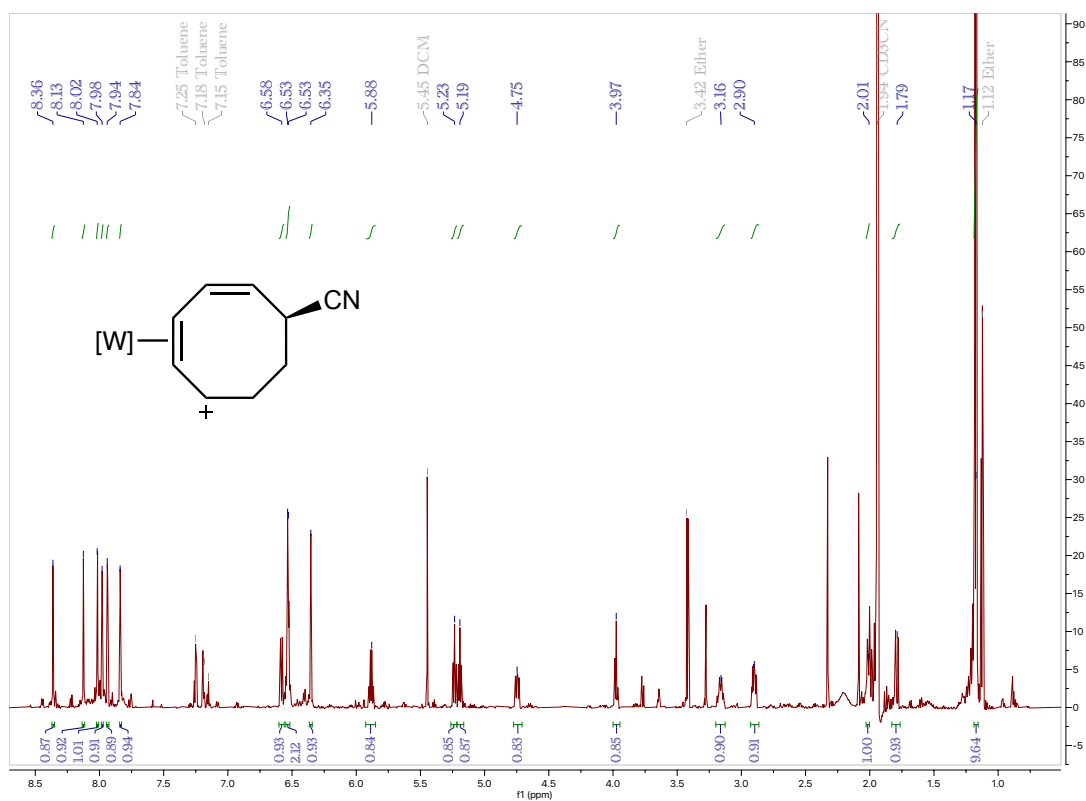
<sup>13</sup>C NMR (201 MHz, CD<sub>3</sub>CN, δ, 25 °C) of Compound **19T'** –



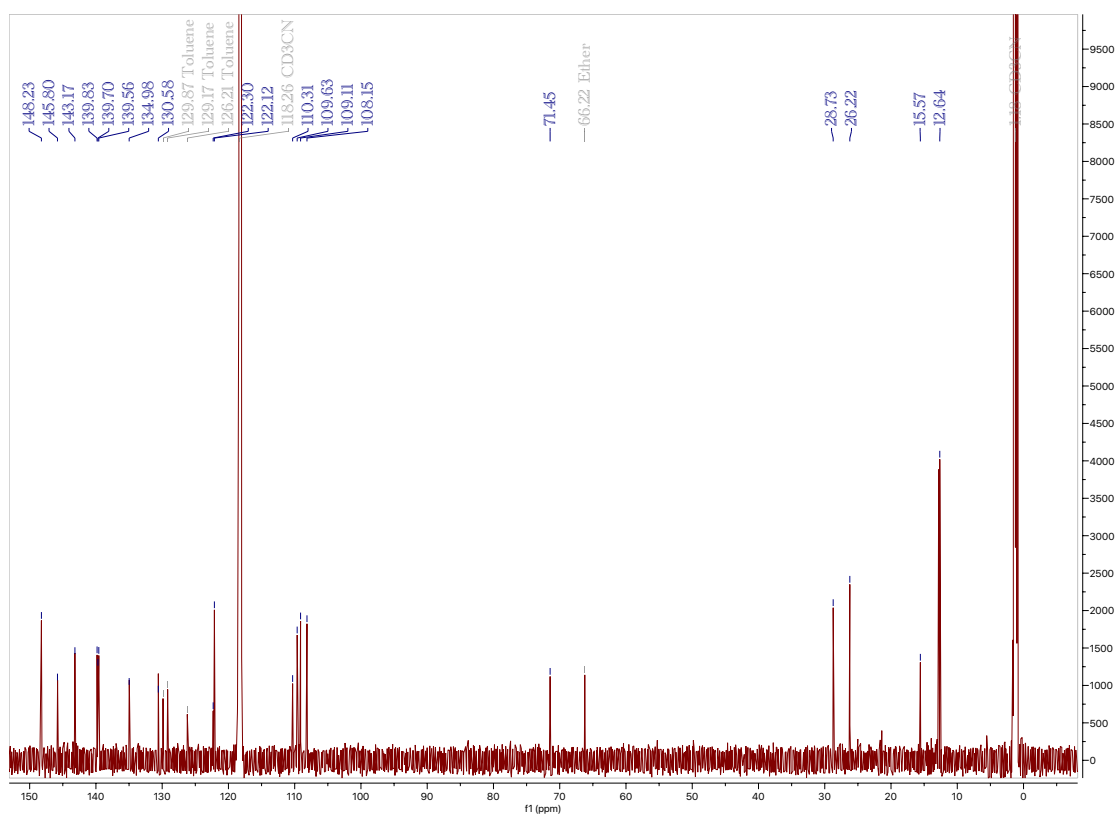
$^1\text{H}$  NMR (800 MHz,  $\text{CD}_3\text{CN}$ ,  $\delta$ , 25 °C) of Compound **4A** –



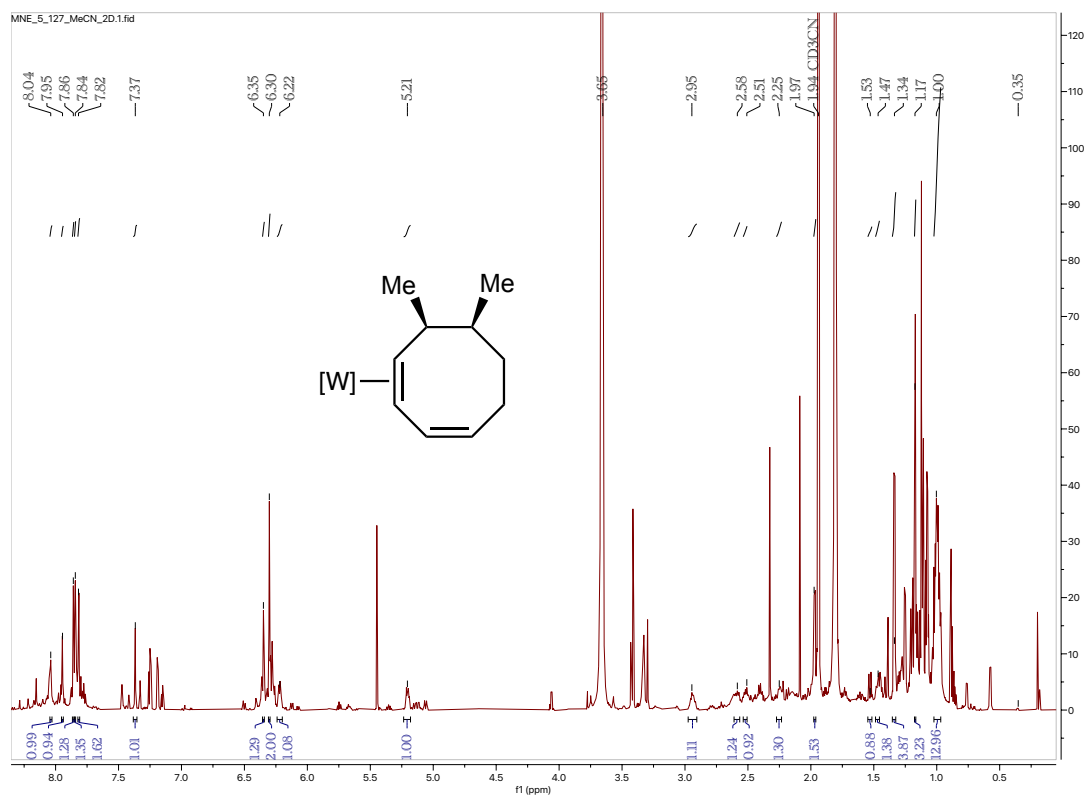
$^1\text{H}$  NMR (800 MHz,  $\text{CD}_3\text{CN}$ ,  $\delta$ , 25 °C) of Compound **20K** –



$^{13}\text{C}$  NMR (201 MHz,  $\text{CD}_3\text{CN}$ ,  $\delta$ , 25 °C) of Compound **20K** –

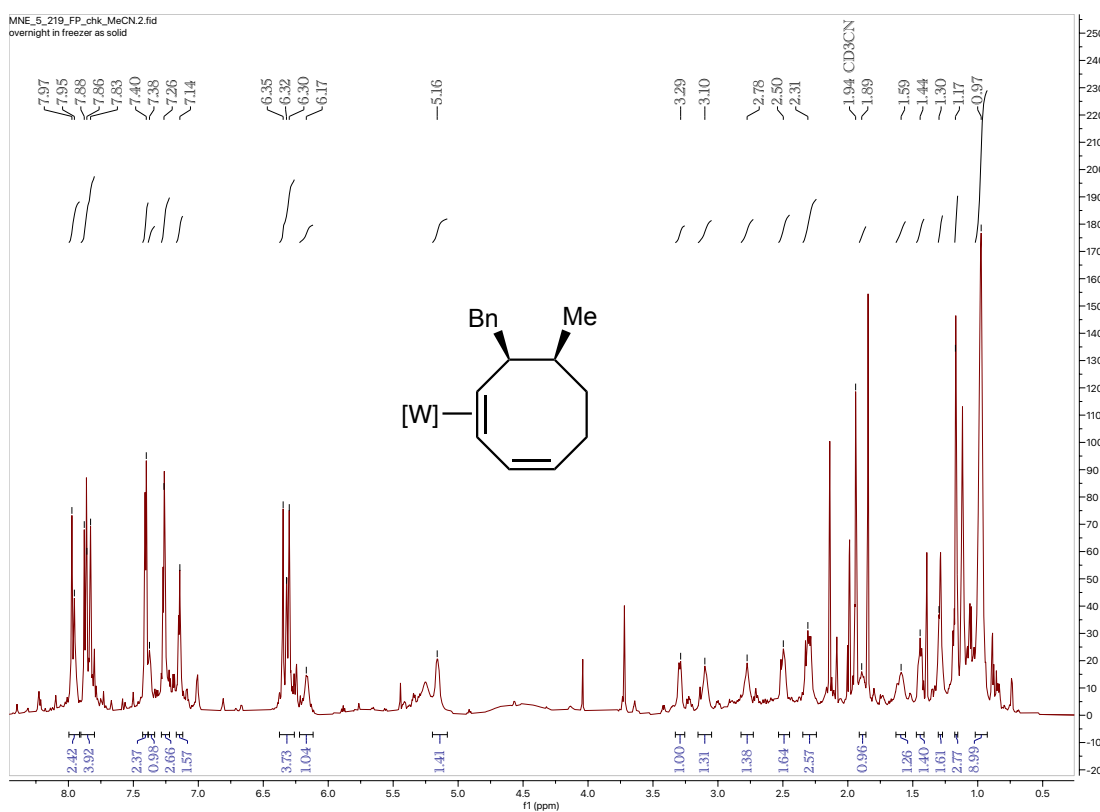


$^1\text{H}$  NMR (800 MHz,  $\text{CD}_3\text{CN}$ ,  $\delta$ , 25 °C) of Compound **21** –

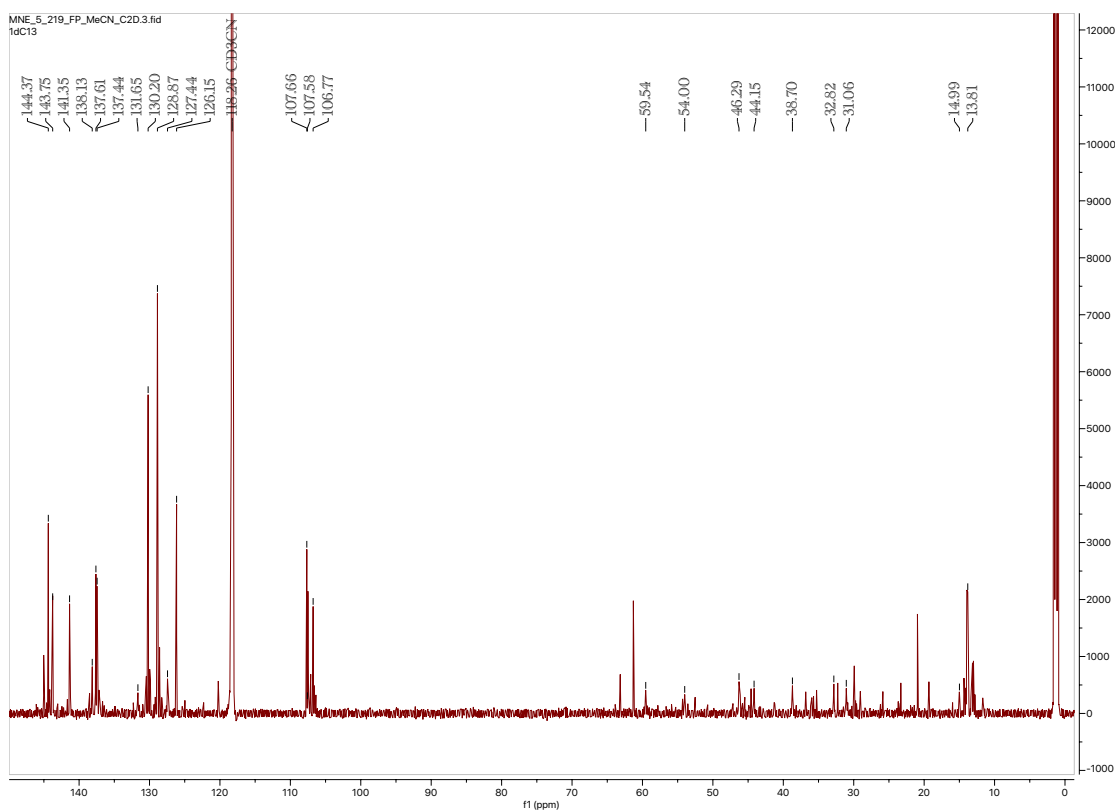




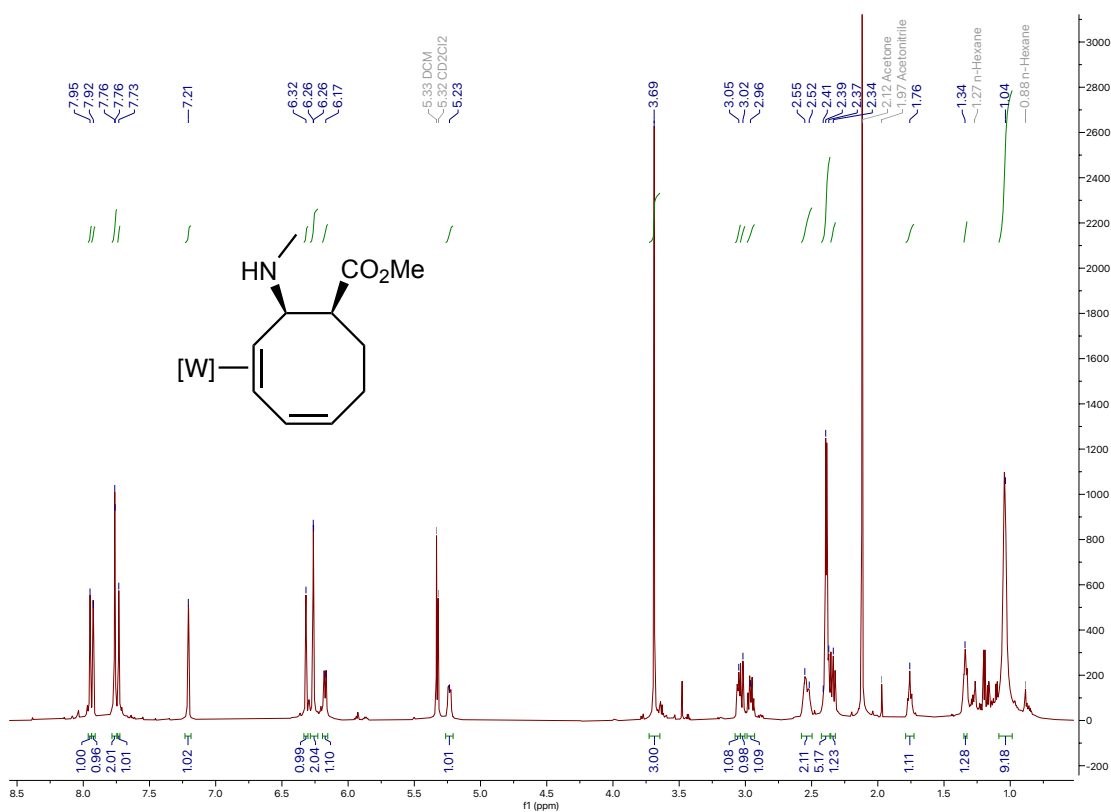
<sup>1</sup>H NMR (800 MHz, CD<sub>3</sub>CN, δ, 25 °C) of Compound **22** –



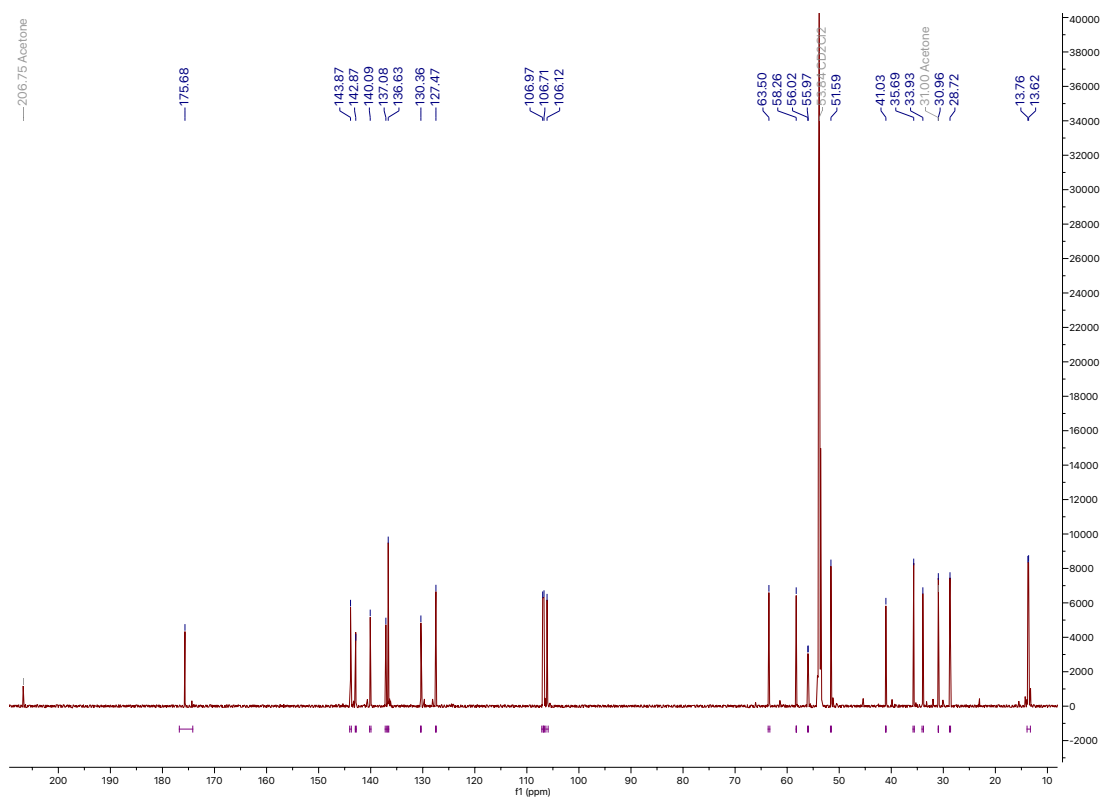
<sup>13</sup>C NMR (201 MHz, CD<sub>3</sub>CN, δ, 25 °C) of Compound **22** –



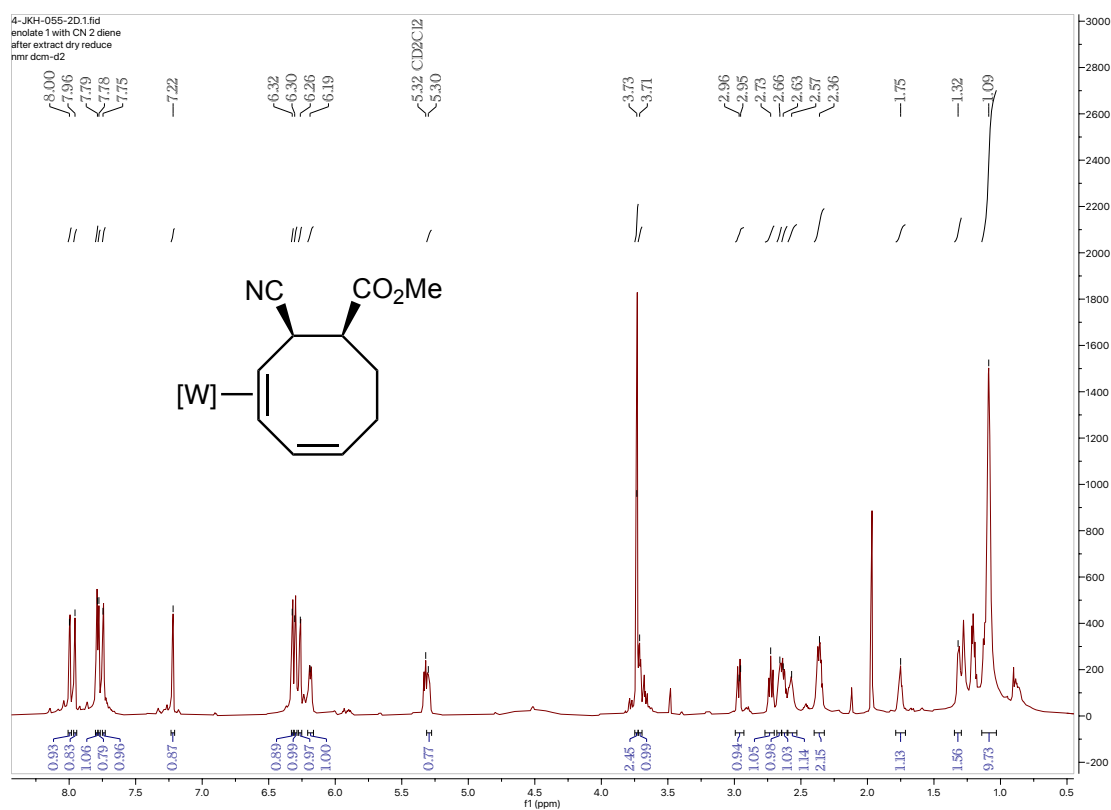
$^1\text{H}$  NMR (800 MHz,  $\text{CD}_3\text{CN}$ ,  $\delta$ , 25 °C) of Compound **23** –



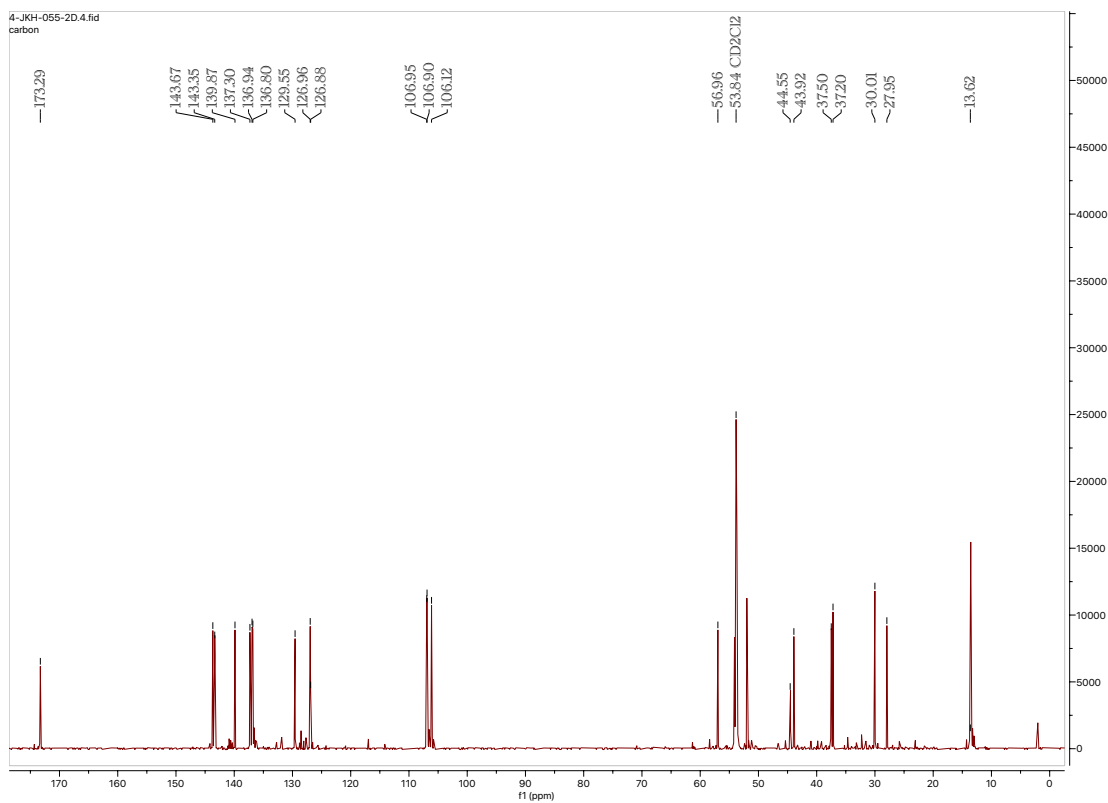
$^{13}\text{C}$  NMR (201 MHz,  $\text{CD}_3\text{CN}$ ,  $\delta$ , 25 °C) of Compound **23** –



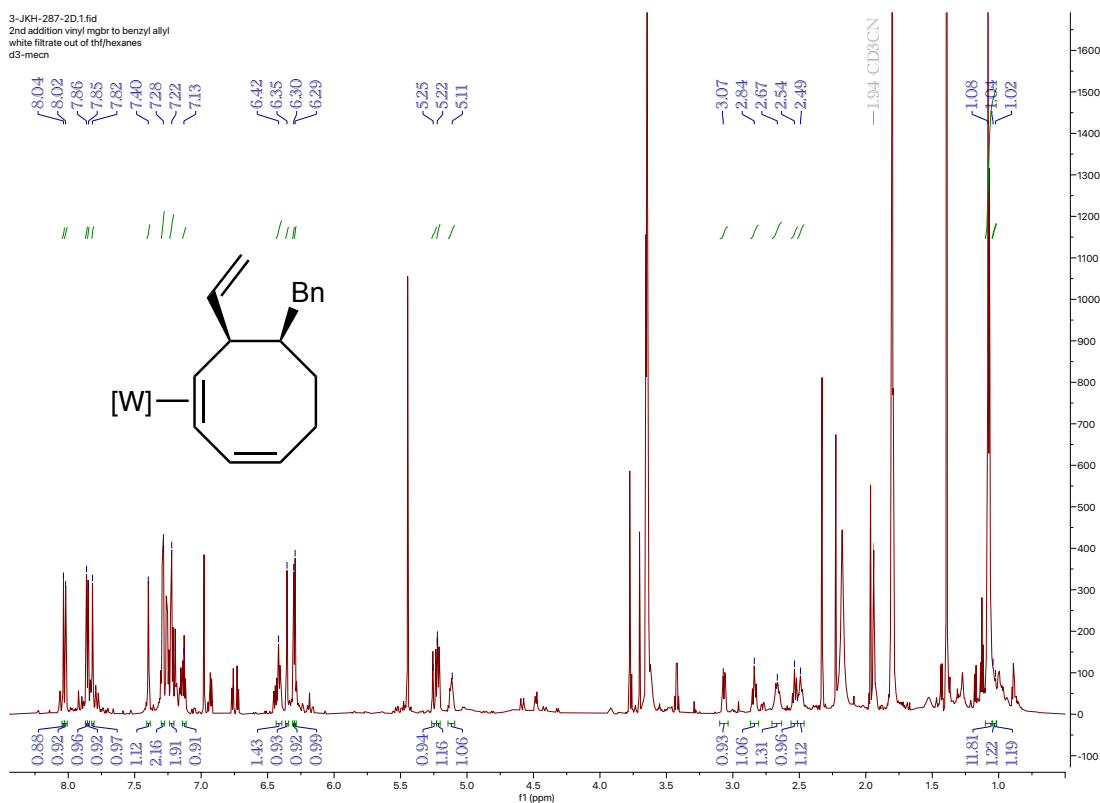
<sup>1</sup>H NMR (800 MHz, CD<sub>2</sub>Cl<sub>2</sub>, δ, 25 °C) of Compound **25** –



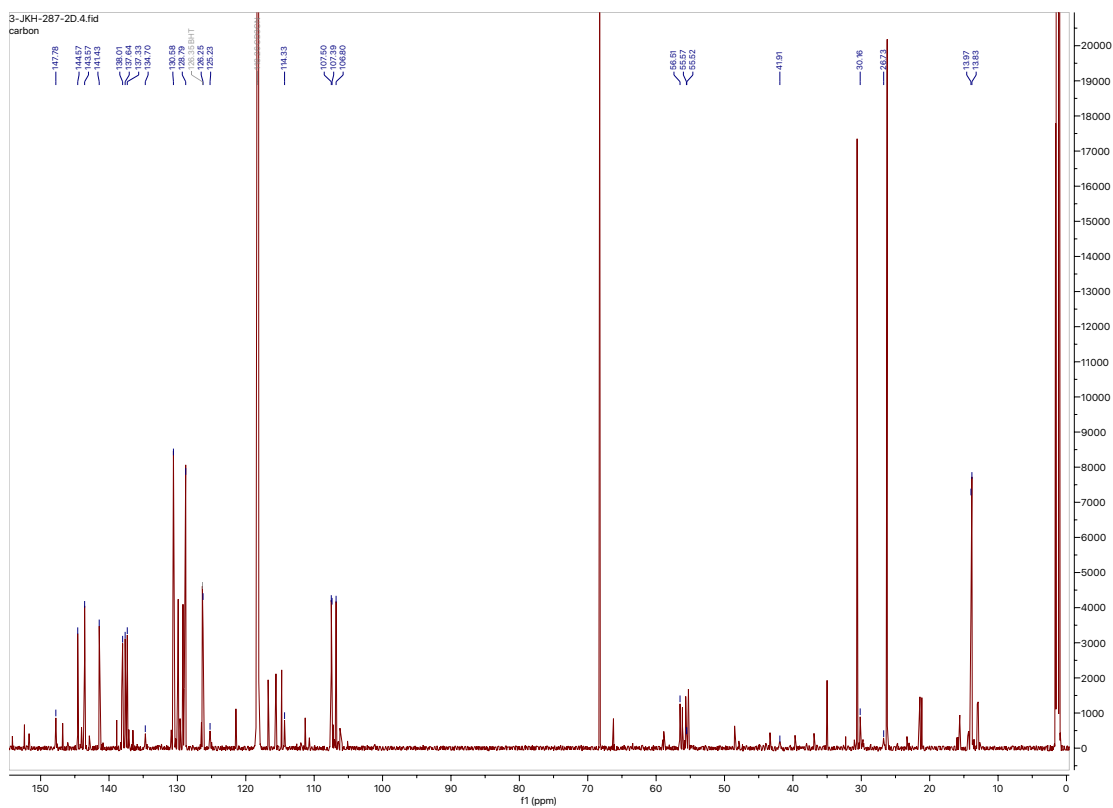
<sup>13</sup>C NMR (201 MHz, CD<sub>2</sub>Cl<sub>2</sub>, δ, 25 °C) of Compound **25** –



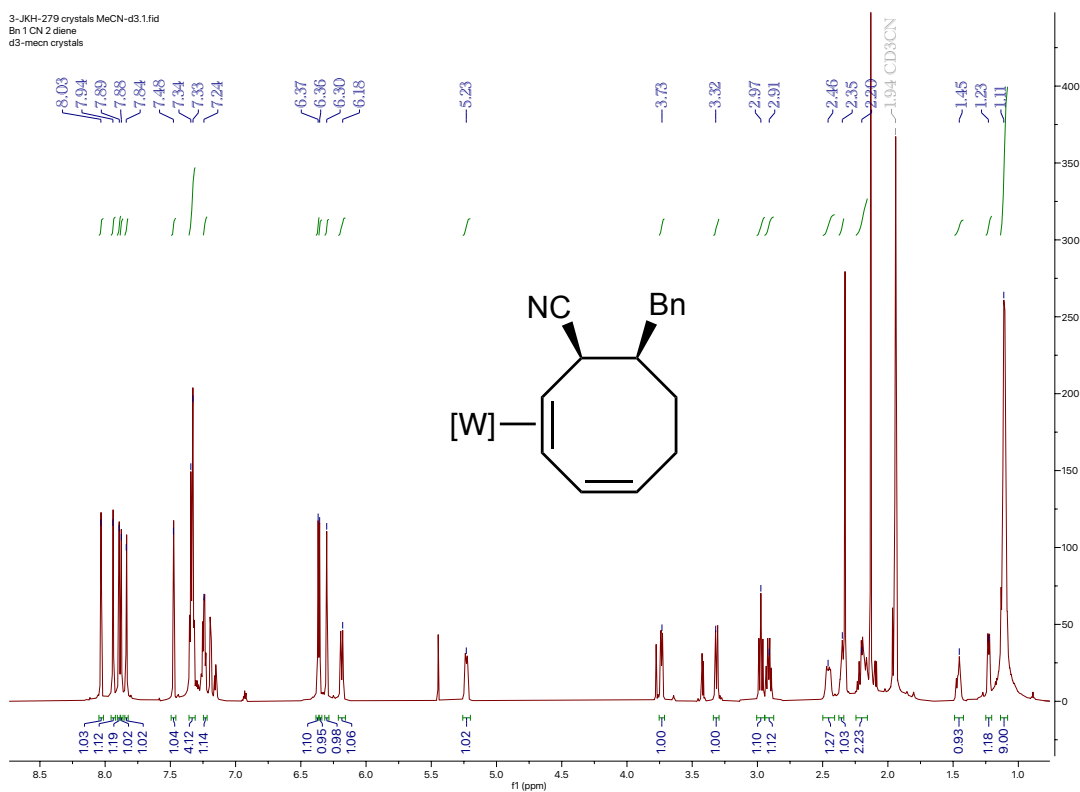
<sup>1</sup>H NMR (800 MHz, CD<sub>3</sub>CN, δ, 25 °C) of Compound **26** –



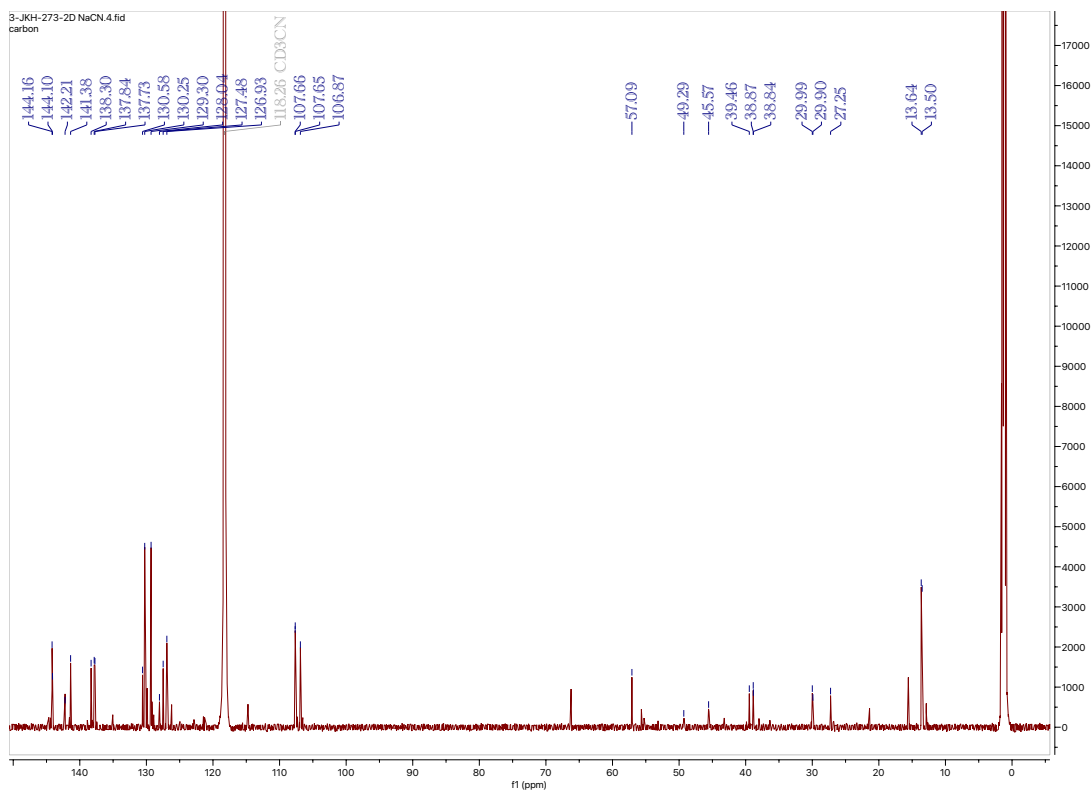
<sup>13</sup>C NMR (201 MHz, CD<sub>3</sub>CN, δ, 25 °C) of Compound **26** –



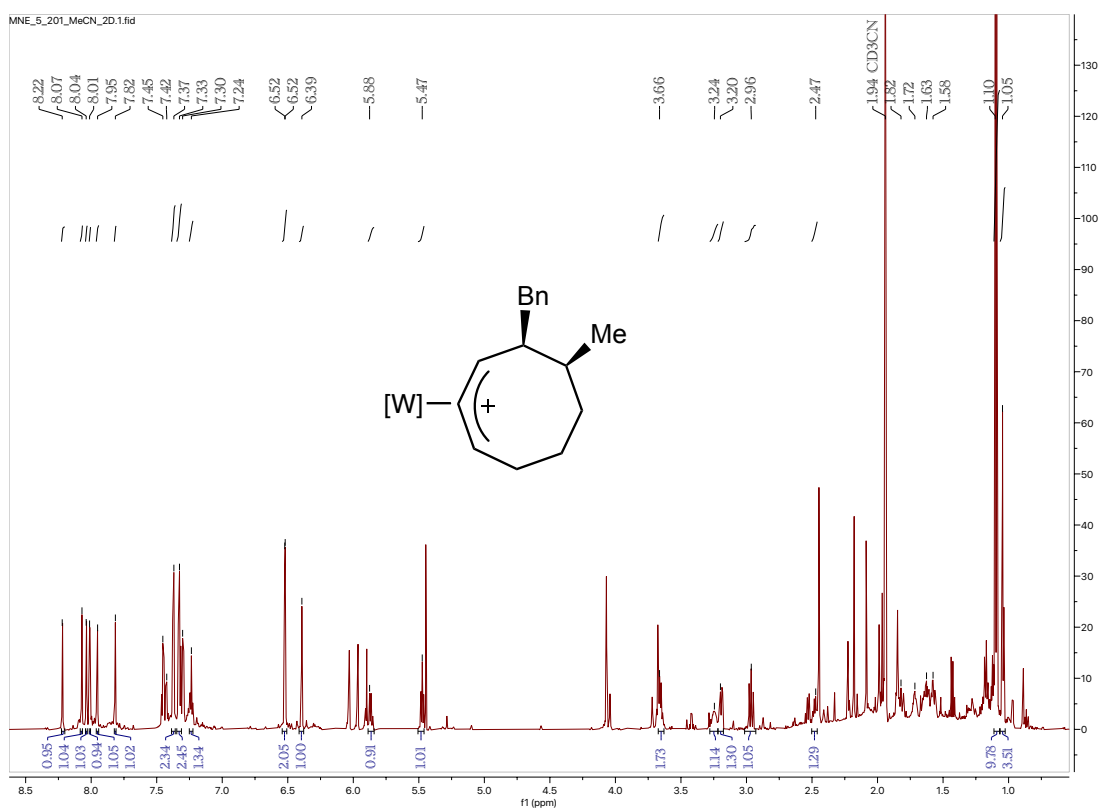
<sup>1</sup>H NMR (800 MHz, CD<sub>3</sub>CN, δ, 25 °C) of Compound **27** –



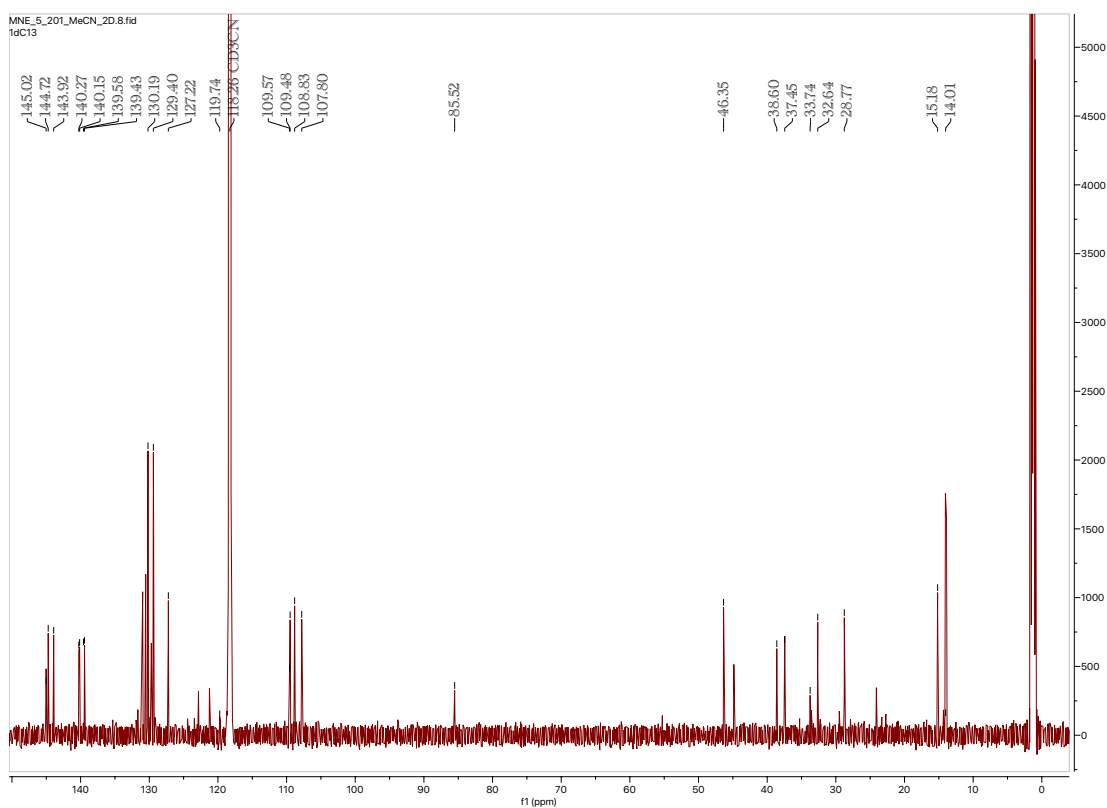
<sup>13</sup>C NMR (201 MHz, CD<sub>3</sub>CN, δ, 25 °C) of Compound **27** –



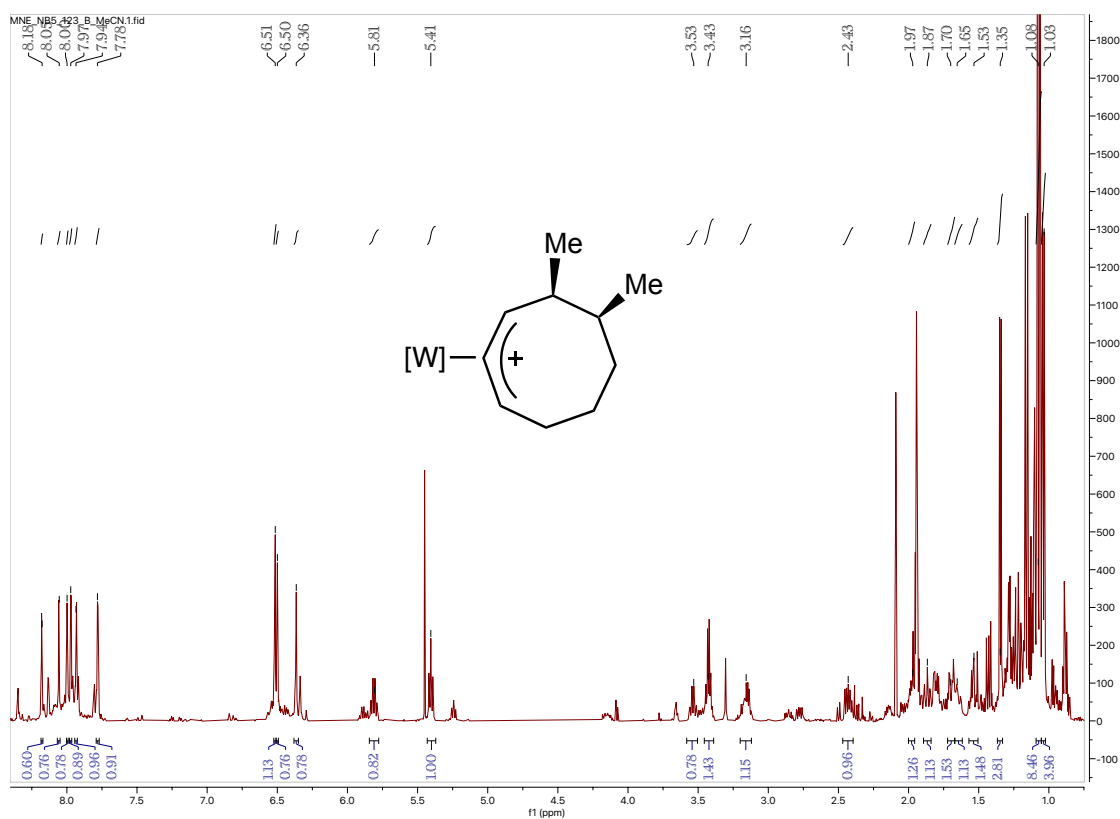
<sup>1</sup>H NMR (800 MHz, CD<sub>3</sub>CN, δ, 25 °C) of Compound **28** –



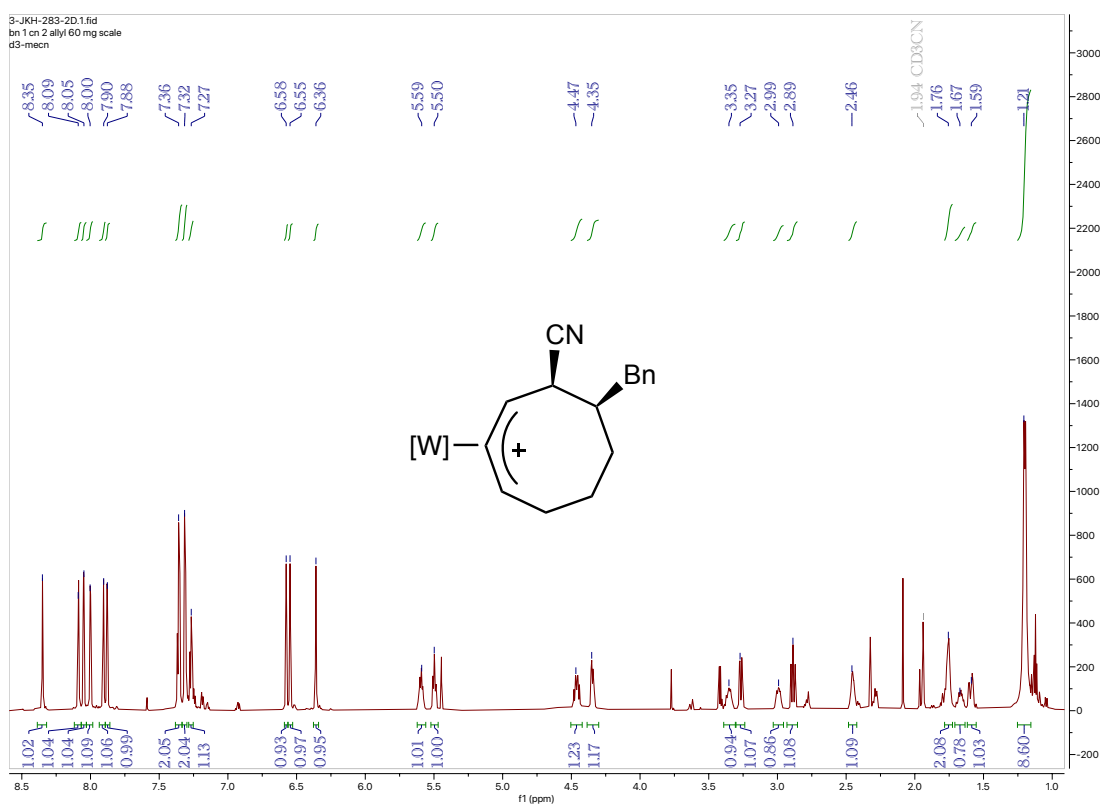
<sup>13</sup>C NMR (201 MHz, CD<sub>3</sub>CN, δ, 25 °C) of Compound **28** –



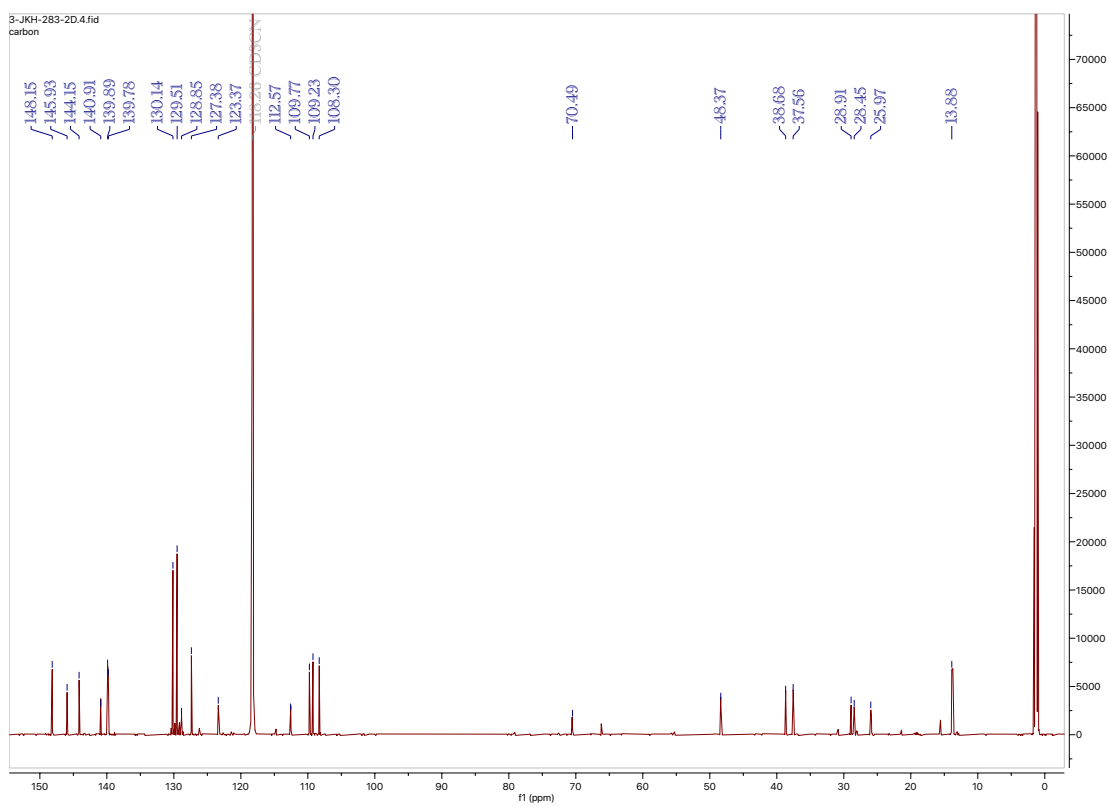
<sup>1</sup>H NMR (800 MHz, CD<sub>3</sub>CN, δ, 25 °C) of Compound **29** –



<sup>1</sup>H NMR (800 MHz, CD<sub>3</sub>CN, δ, 25 °C) of Compound **30** –

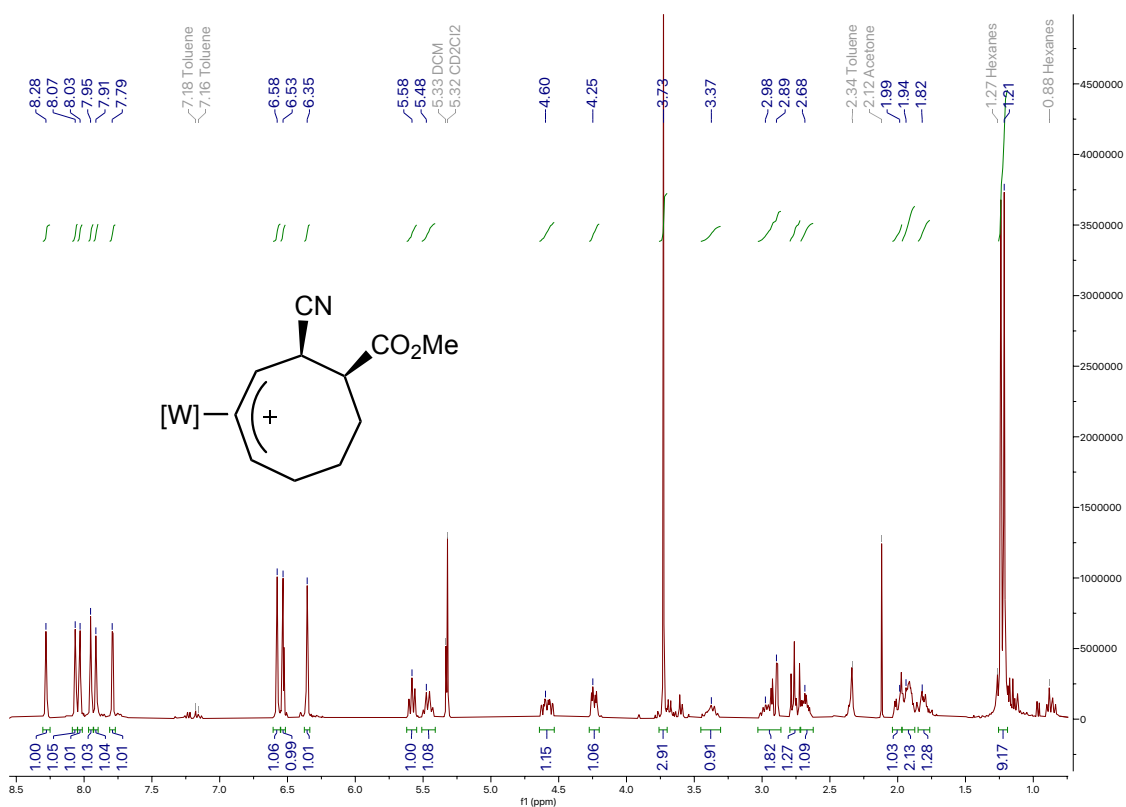


<sup>13</sup>C NMR (201 MHz, CD<sub>3</sub>CN, δ, 25 °C) of Compound **30** –

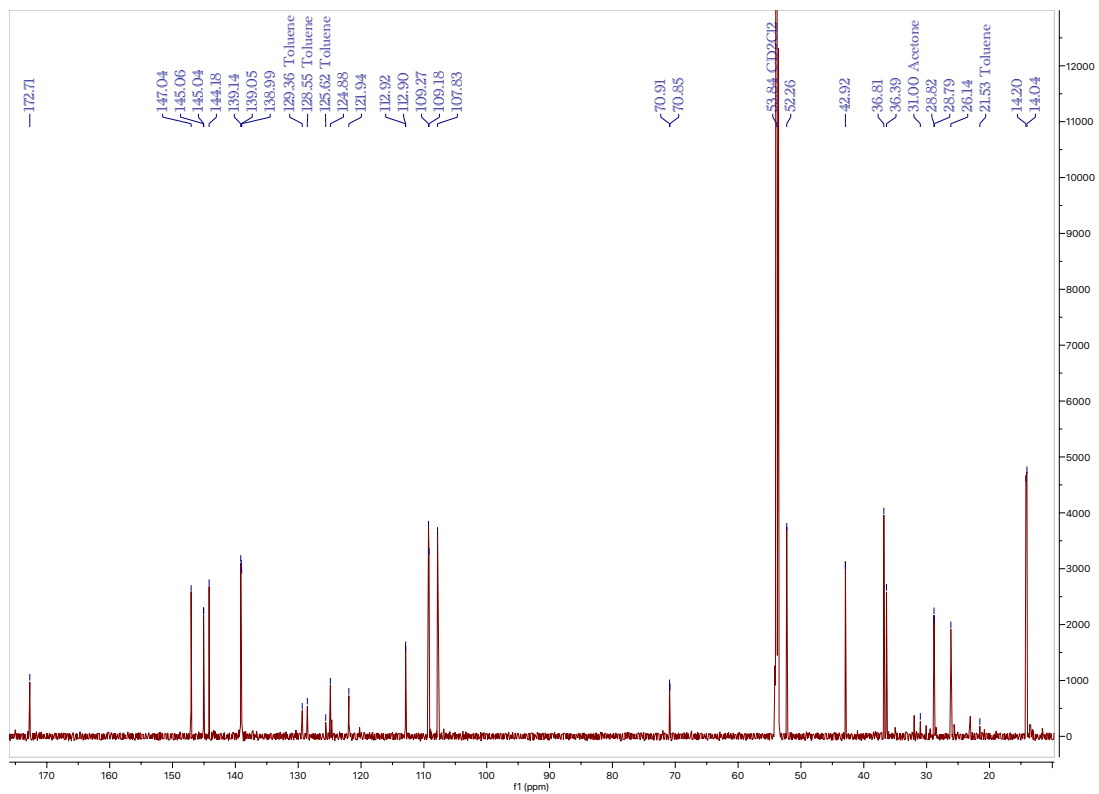




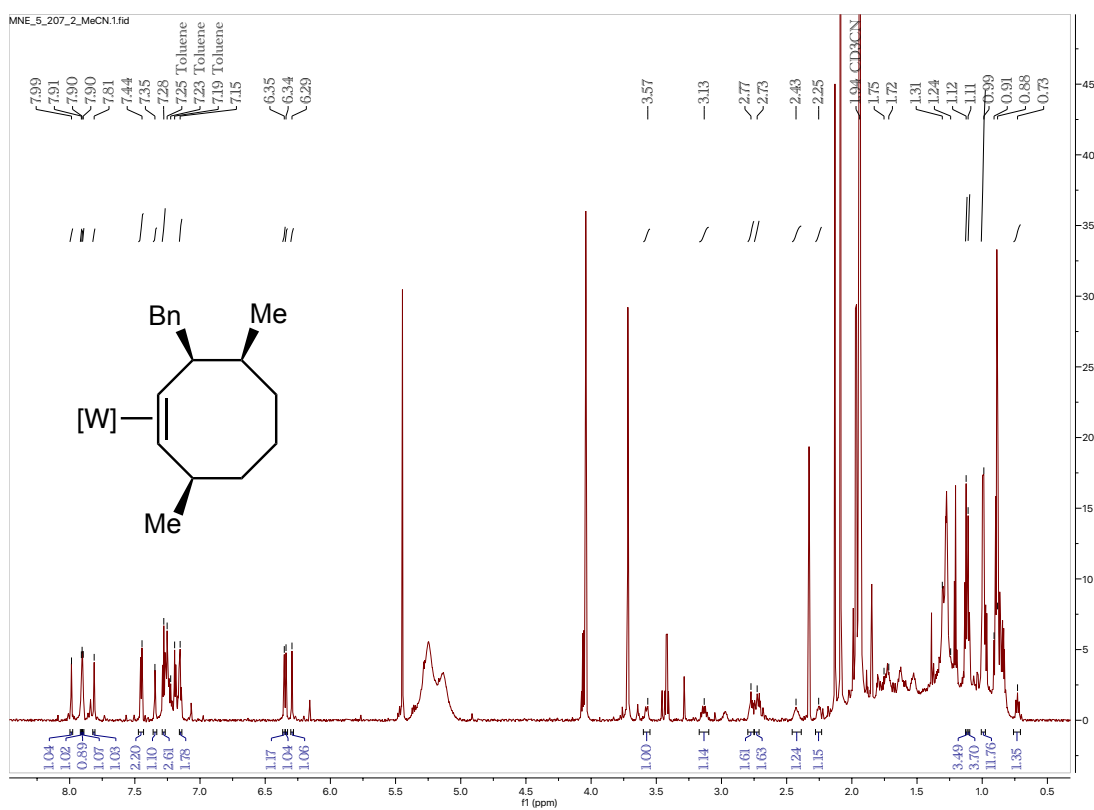
<sup>1</sup>H NMR (800 MHz, CD<sub>2</sub>Cl<sub>2</sub>, δ, 25 °C) of Compound **31** –



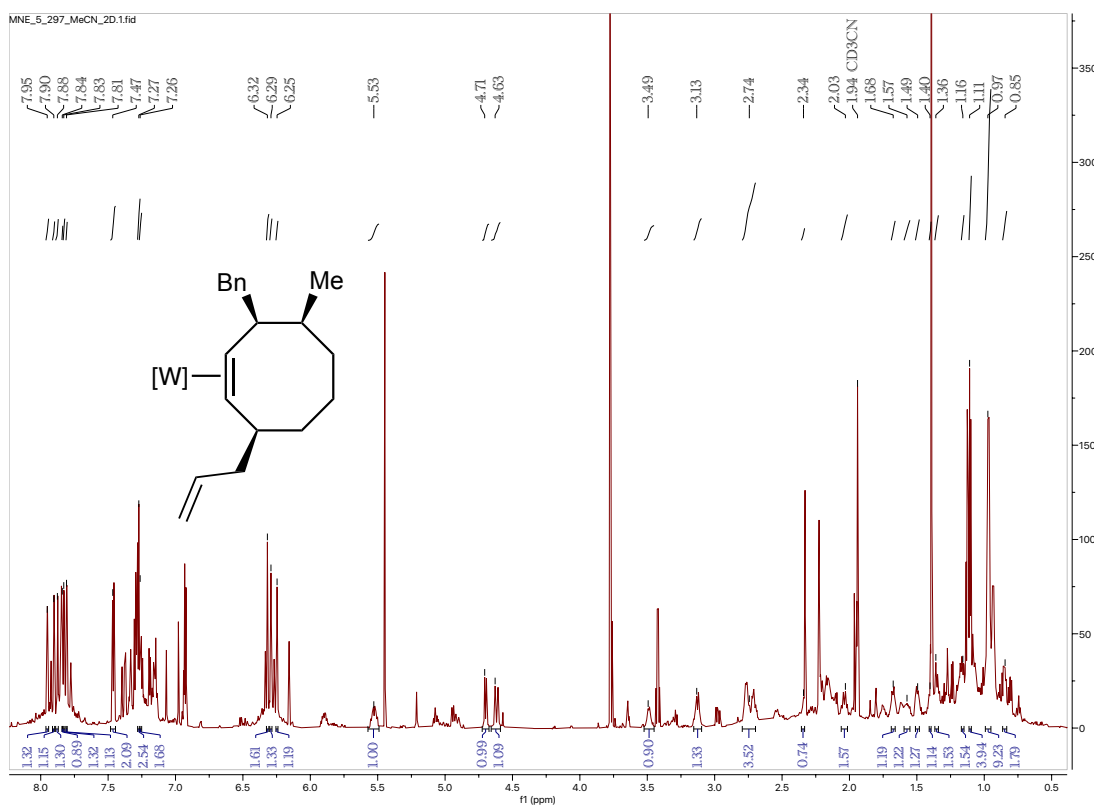
<sup>13</sup>C NMR (201 MHz, CD<sub>2</sub>Cl<sub>2</sub>, δ, 25 °C) of Compound **31** –



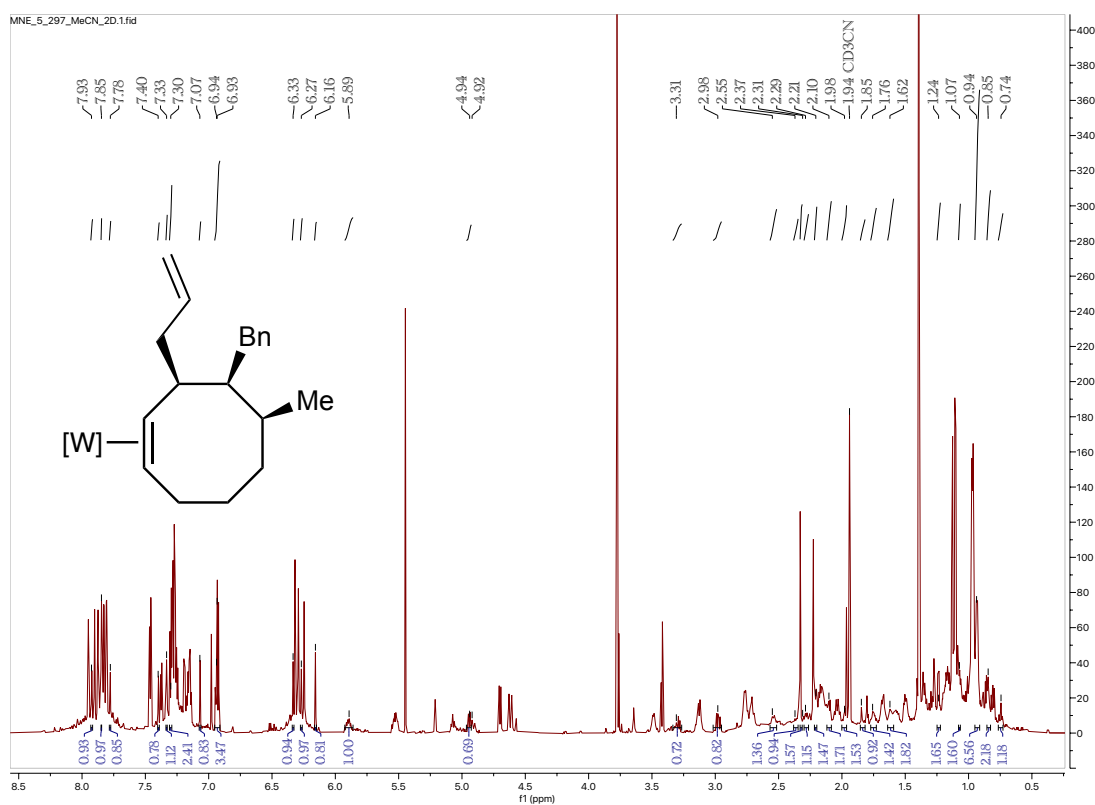
$^1\text{H}$  NMR (800 MHz,  $\text{CD}_3\text{CN}$ ,  $\delta$ , 25  $^\circ\text{C}$ ) of Compound **32** –



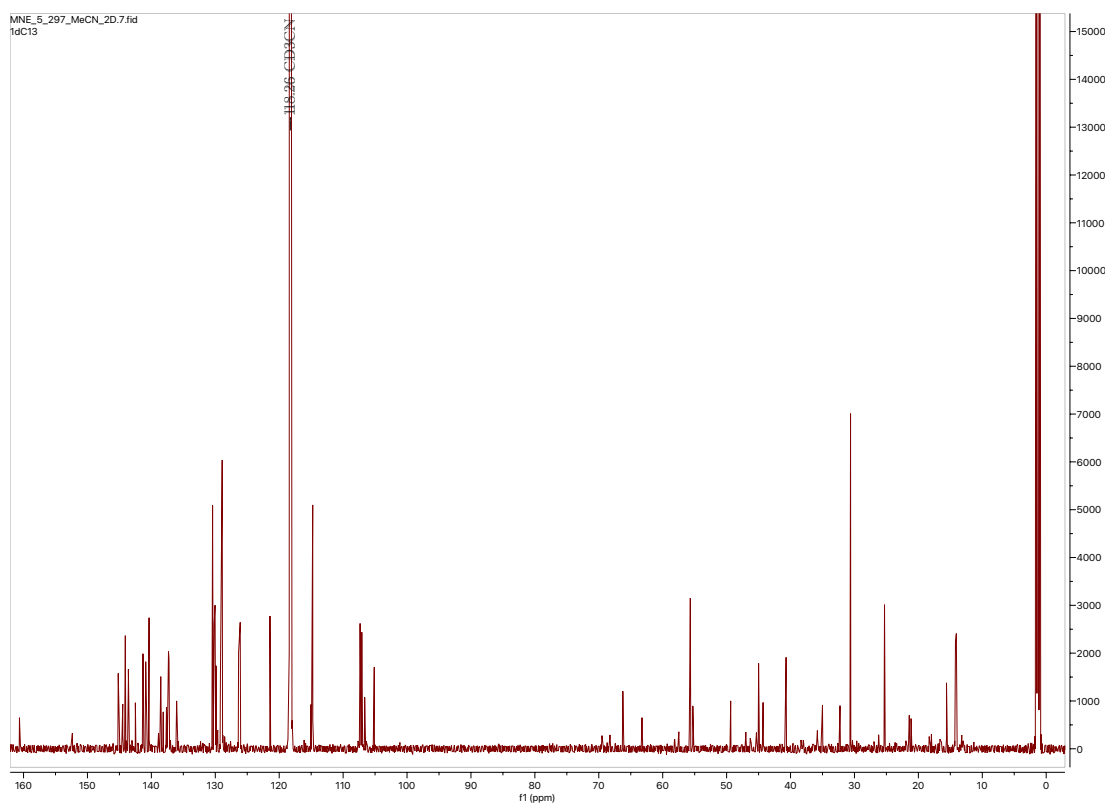
$^1\text{H}$  NMR (800 MHz,  $\text{CD}_3\text{CN}$ ,  $\delta$ , 25  $^\circ\text{C}$ ) of Compound **33** (major) –



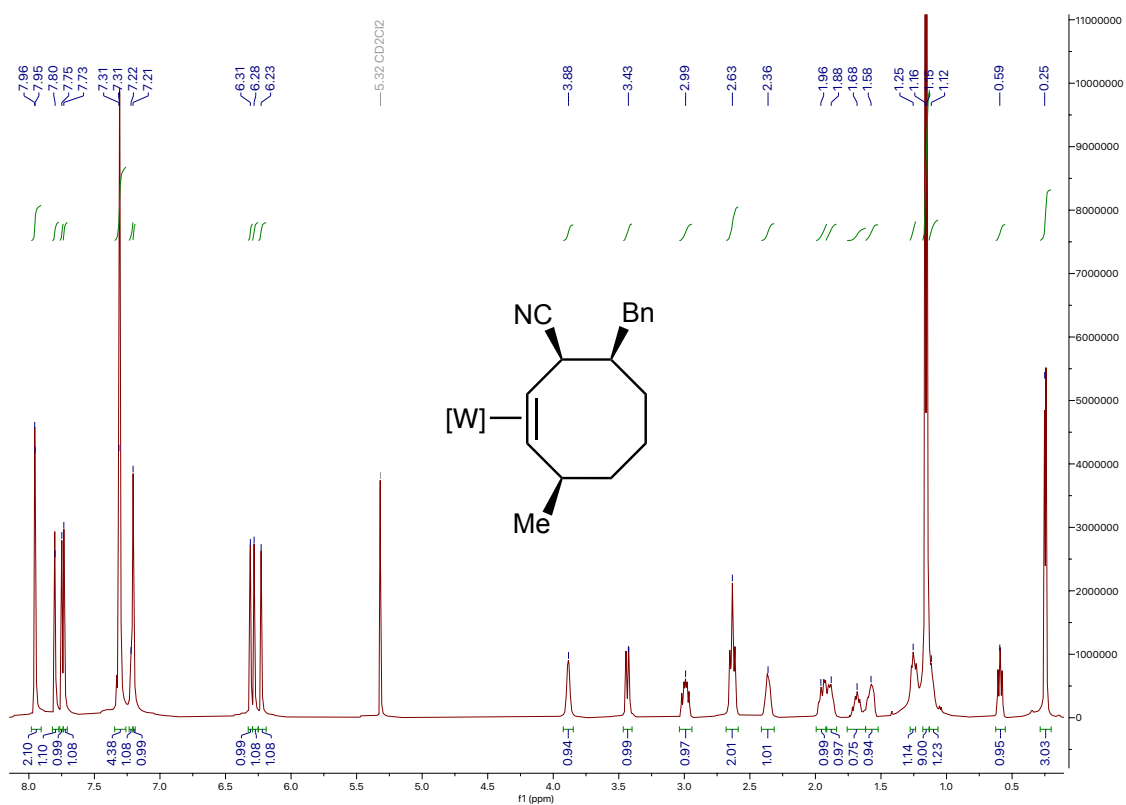
<sup>1</sup>H NMR (800 MHz, CD<sub>3</sub>CN, δ, 25 °C) of Compound **33** (minor) –



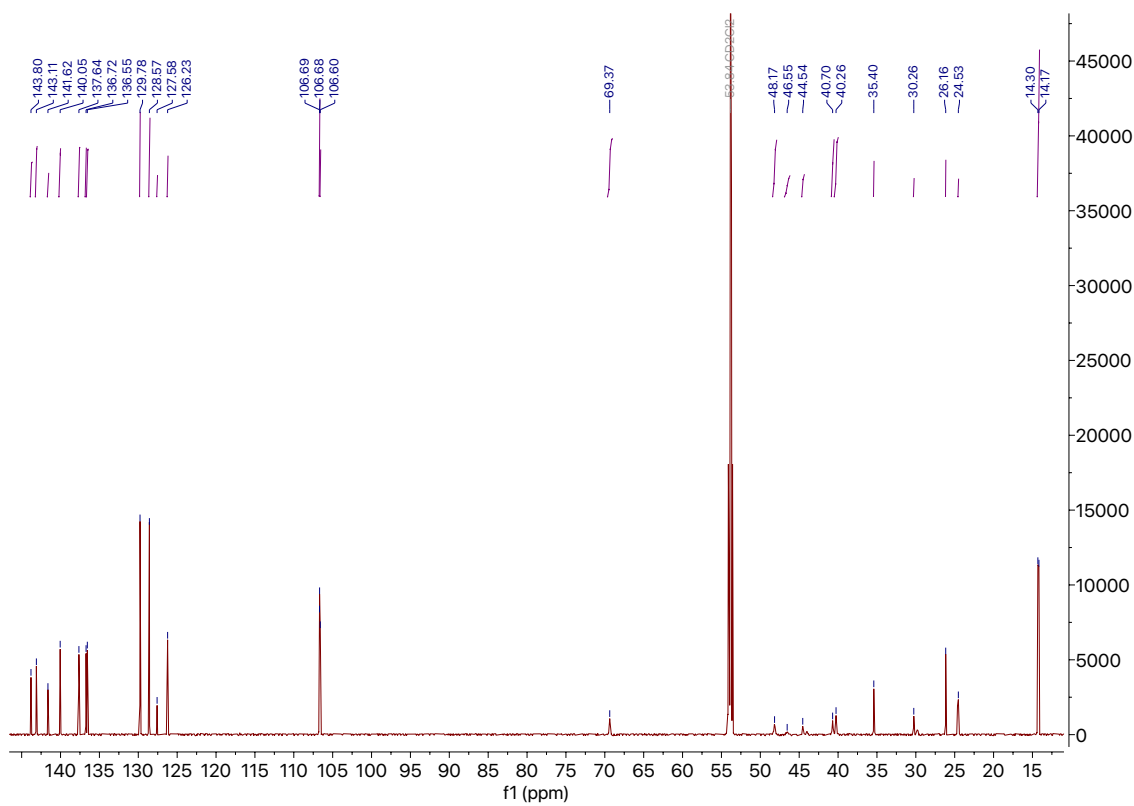
<sup>13</sup>C NMR (201 MHz, CD<sub>3</sub>CN, δ, 25 °C) of Compound **33** –



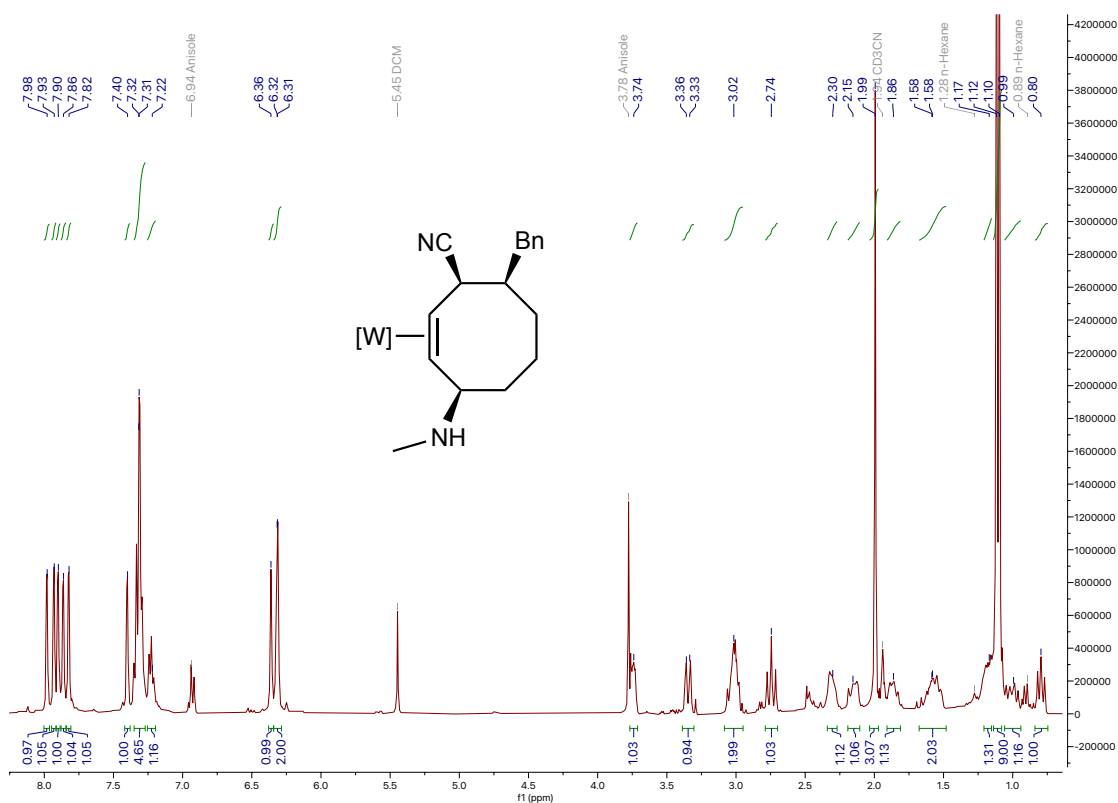
<sup>1</sup>H NMR (800 MHz, CD<sub>3</sub>CN, δ, 25 °C) of Compound **34** –



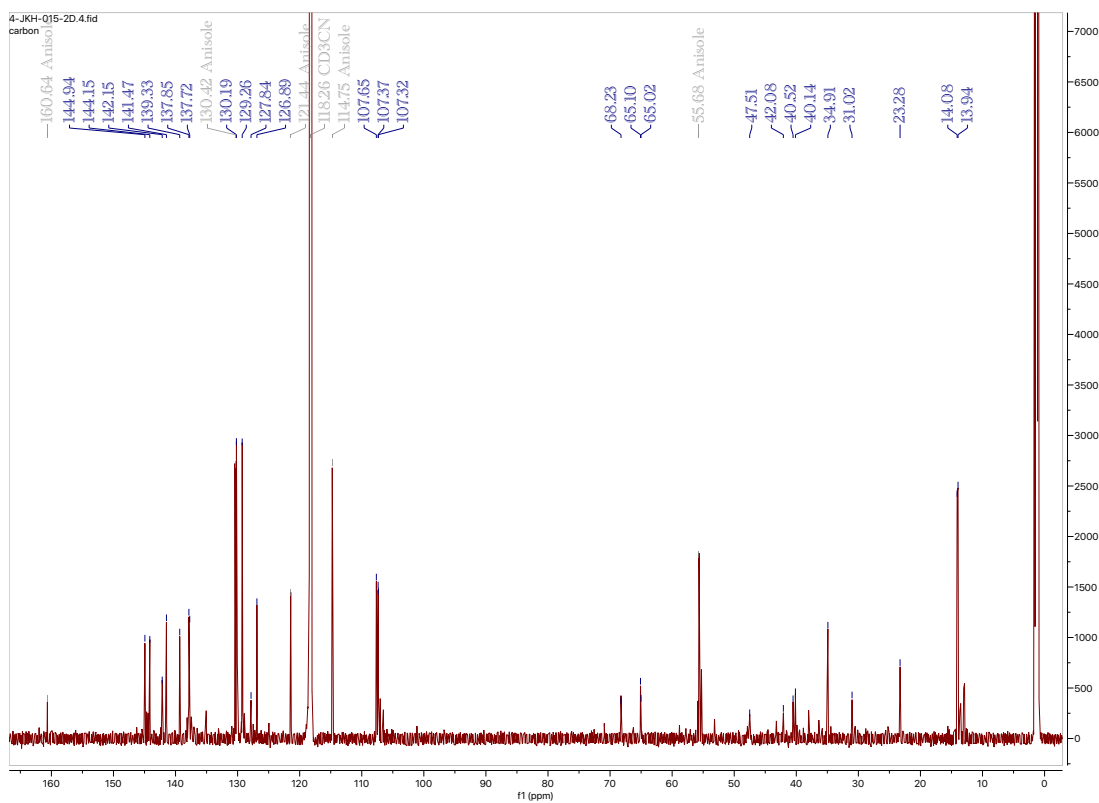
<sup>13</sup>C NMR (201 MHz, CD<sub>3</sub>CN, δ, 25 °C) of Compound **34** –



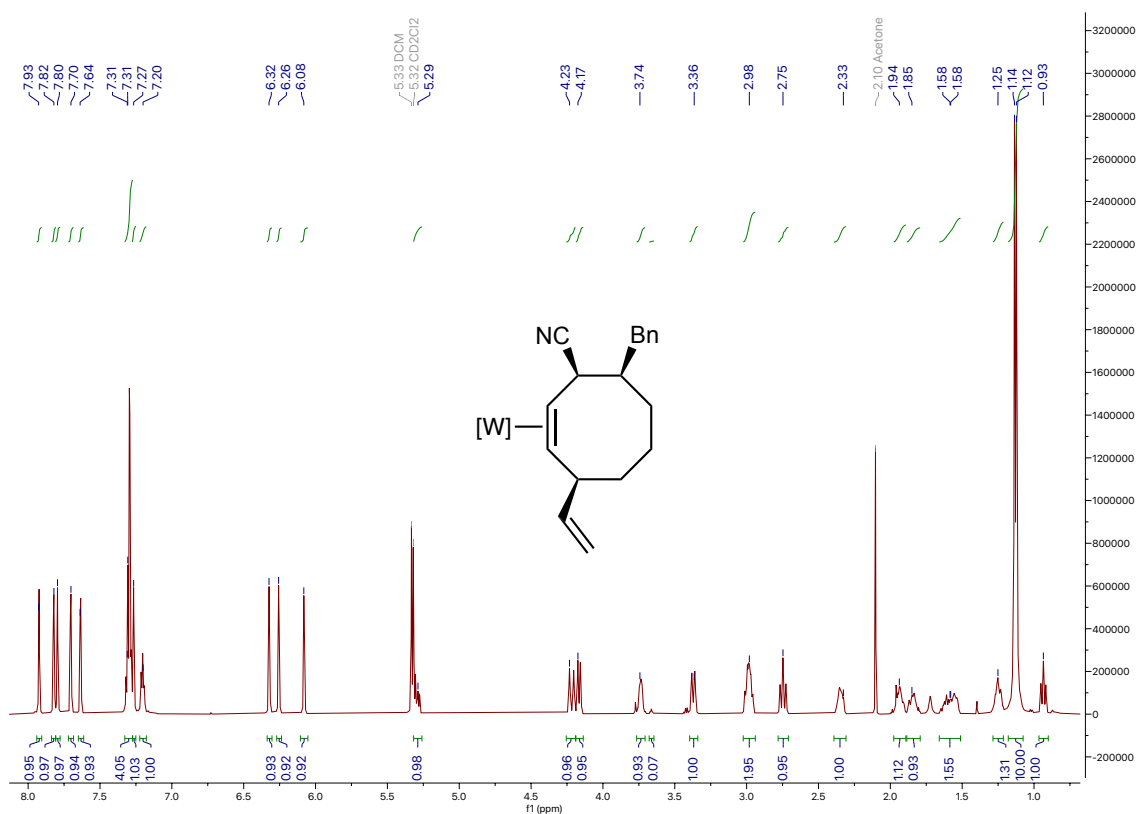
$^1\text{H}$  NMR (800 MHz,  $\text{CD}_3\text{CN}$ ,  $\delta$ , 25 °C) of Compound **35** –



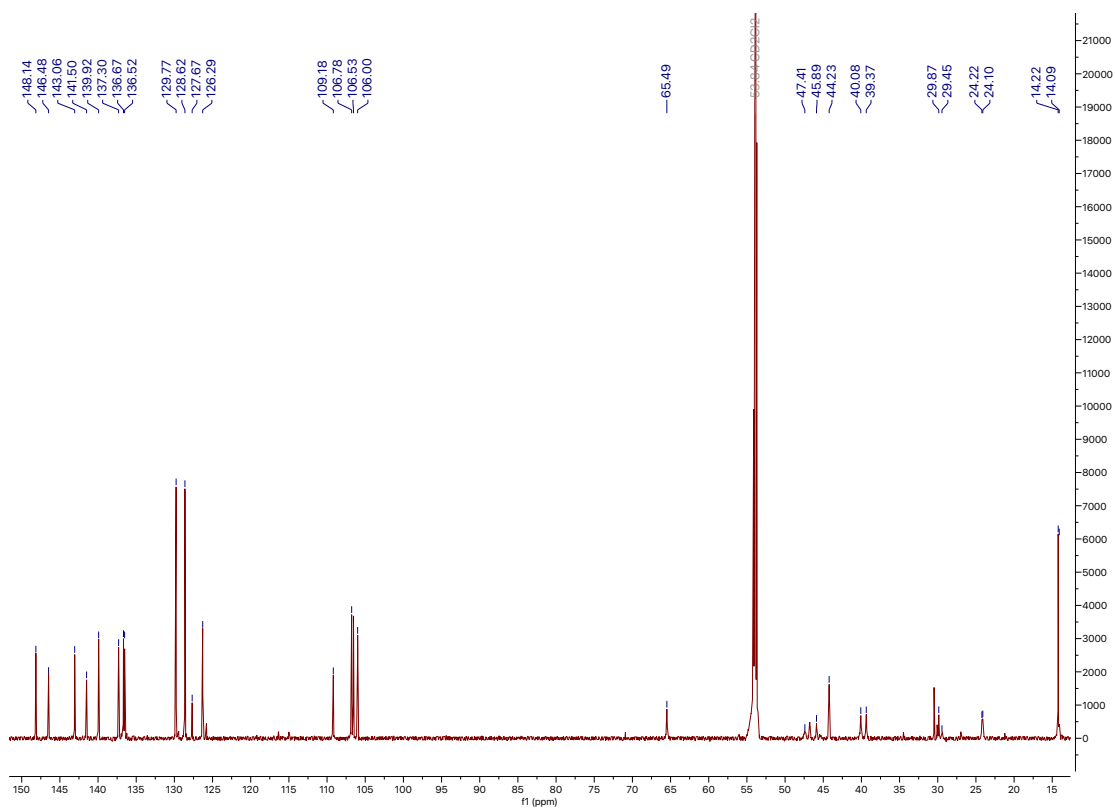
$^{13}\text{C}$  NMR (201 MHz,  $\text{CD}_3\text{CN}$ ,  $\delta$ , 25 °C) of Compound **35** –



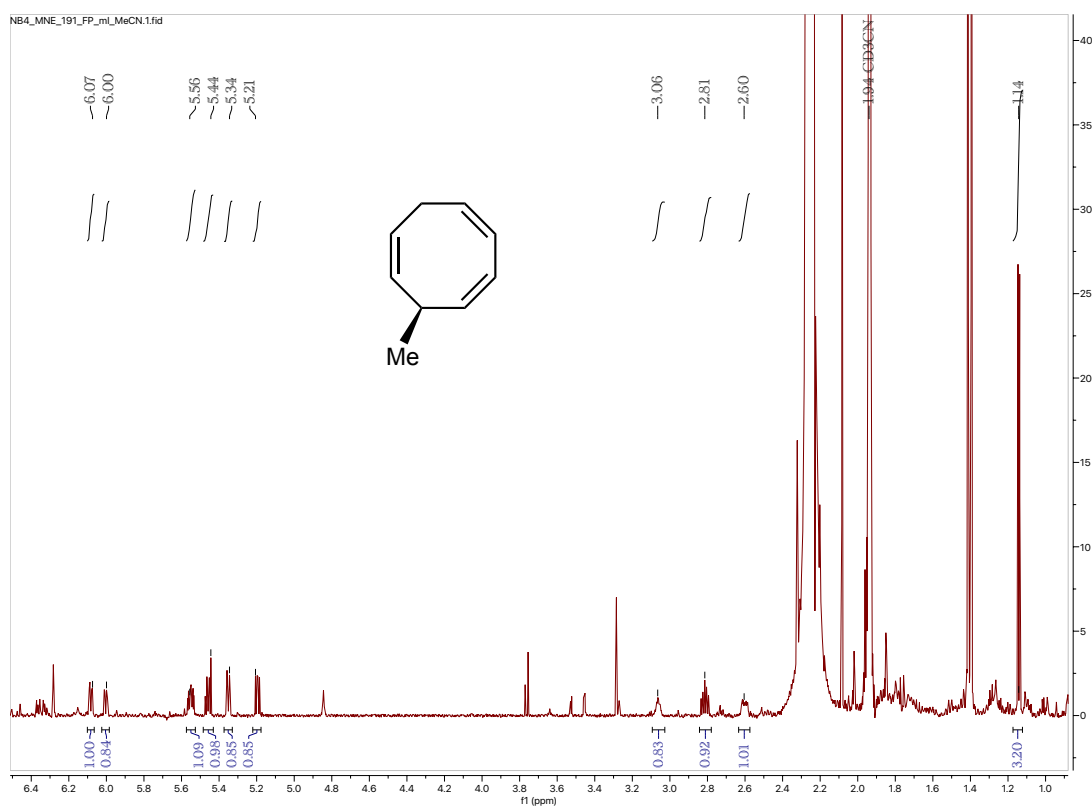
$^1\text{H}$  NMR (800 MHz,  $\text{CD}_3\text{CN}$ ,  $\delta$ , 25  $^\circ\text{C}$ ) of Compound **36** –



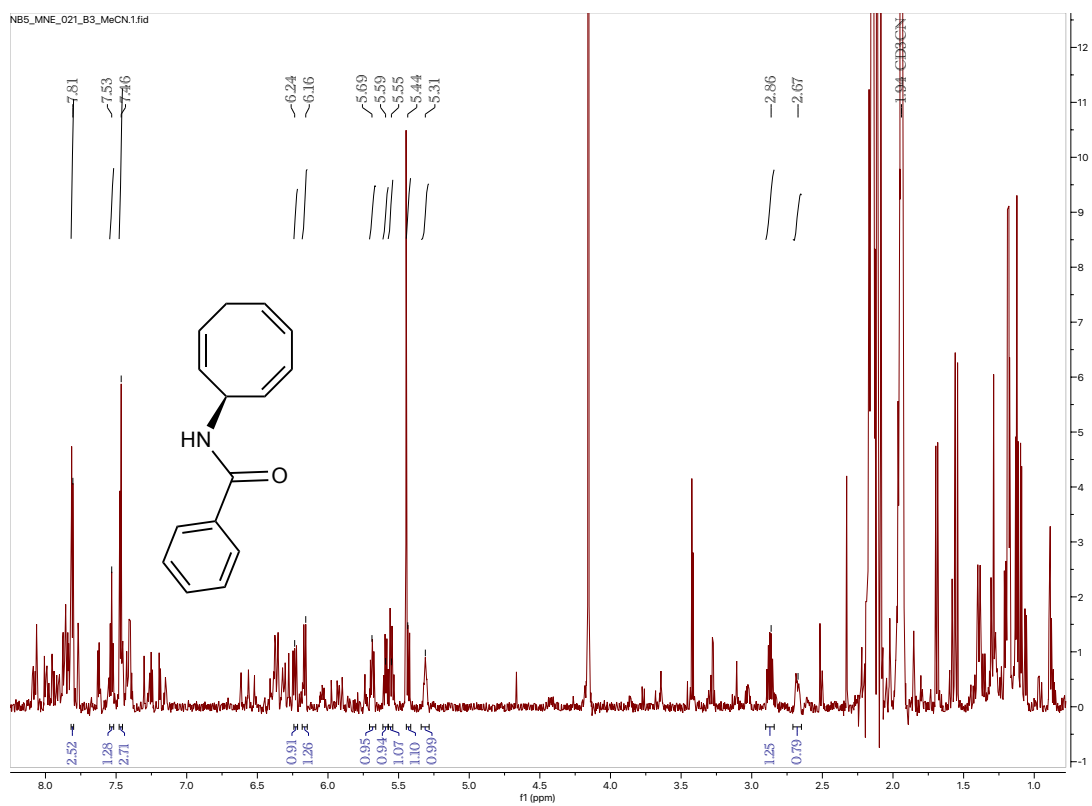
$^{13}\text{C}$  NMR (201 MHz,  $\text{CD}_3\text{CN}$ ,  $\delta$ , 25  $^\circ\text{C}$ ) of Compound **36** –



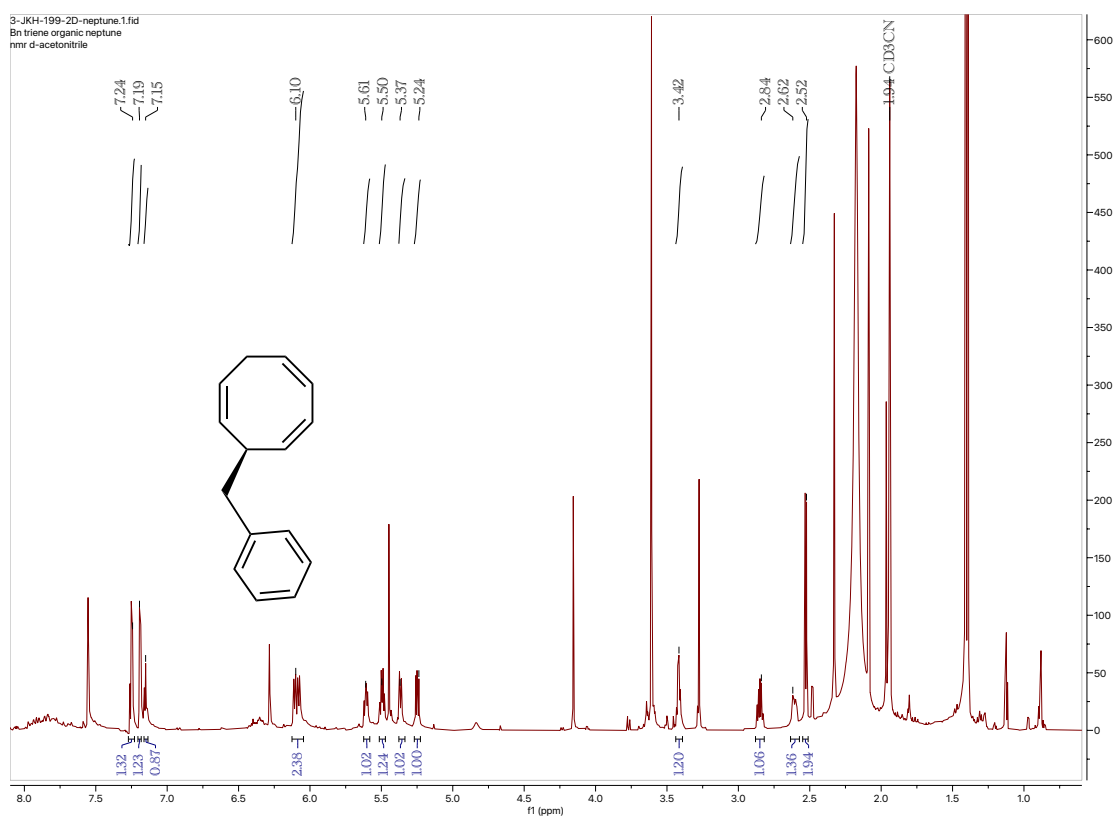
$^1\text{H}$  NMR (800 MHz,  $\text{CD}_3\text{CN}$ ,  $\delta$ , 25  $^\circ\text{C}$ ) of Compound **37** –



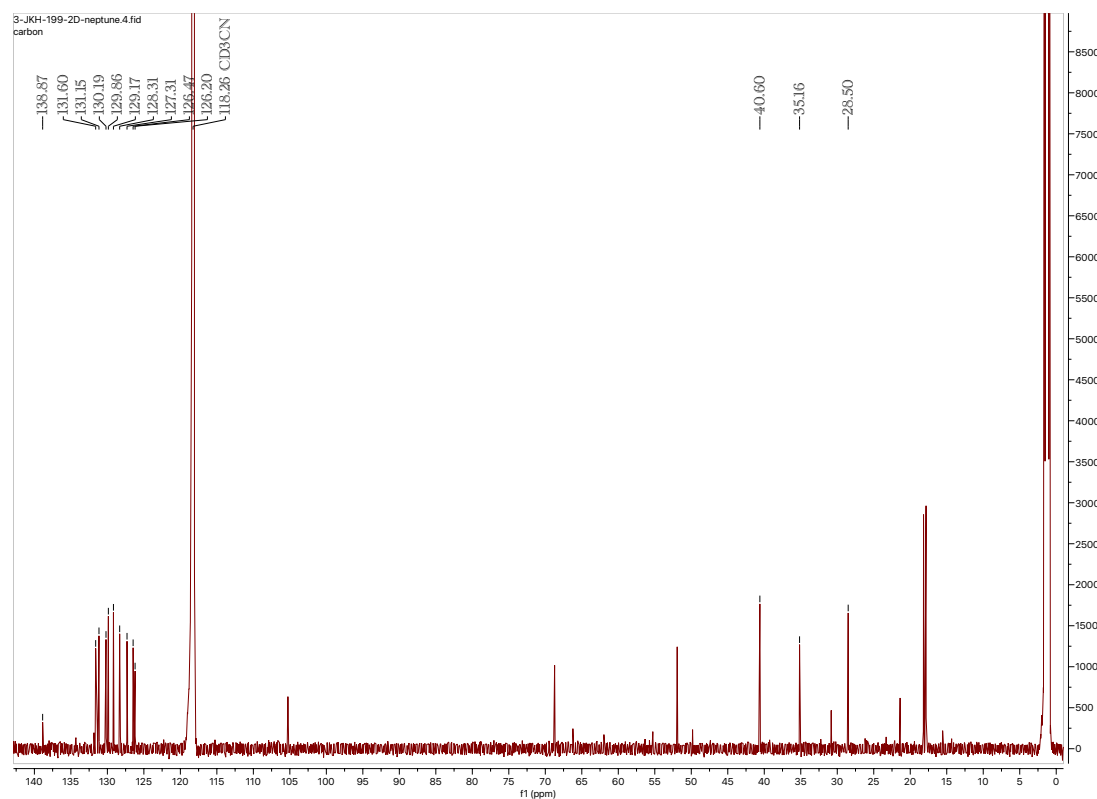
$^1\text{H}$  NMR (800 MHz,  $\text{CD}_3\text{CN}$ ,  $\delta$ , 25  $^\circ\text{C}$ ) of Compound **38** –



<sup>1</sup>H NMR (800 MHz, CD<sub>3</sub>CN, δ, 25 °C) of Compound **39** –

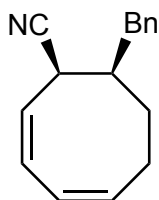


<sup>13</sup>C NMR (201 MHz, CD<sub>3</sub>CN, δ, 25 °C) of Compound **39** –

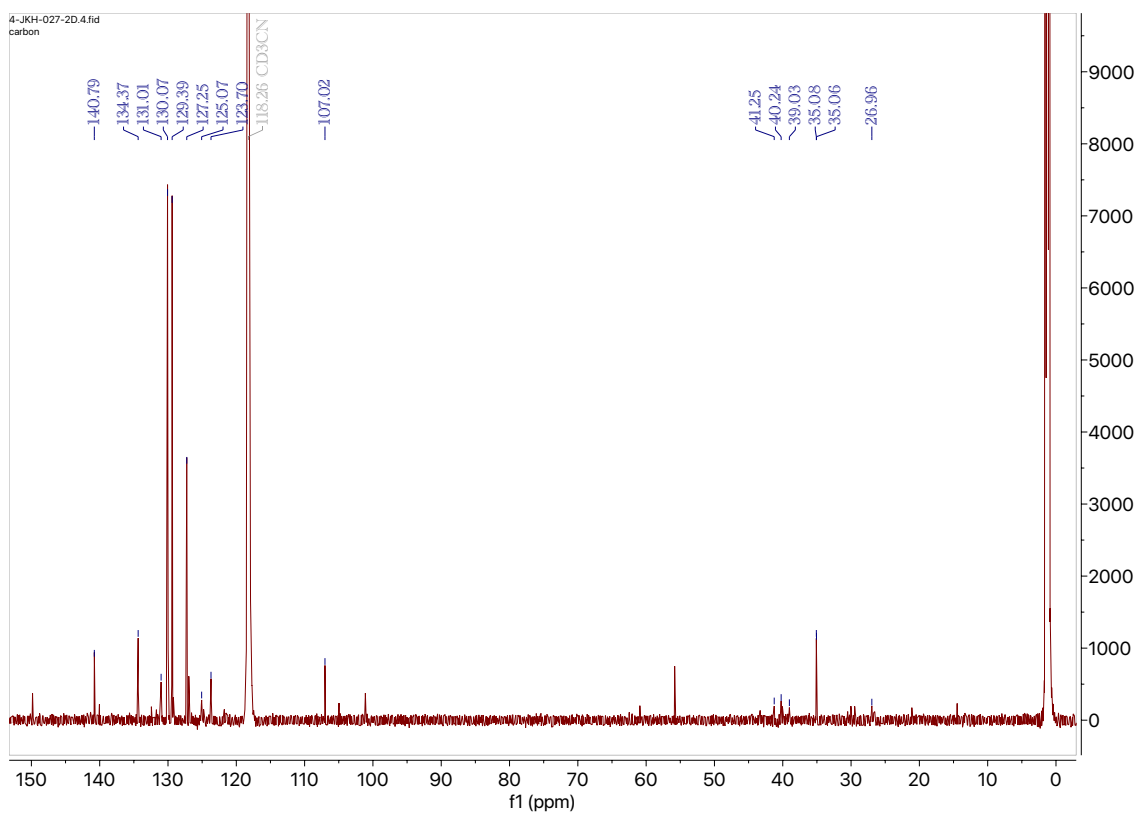




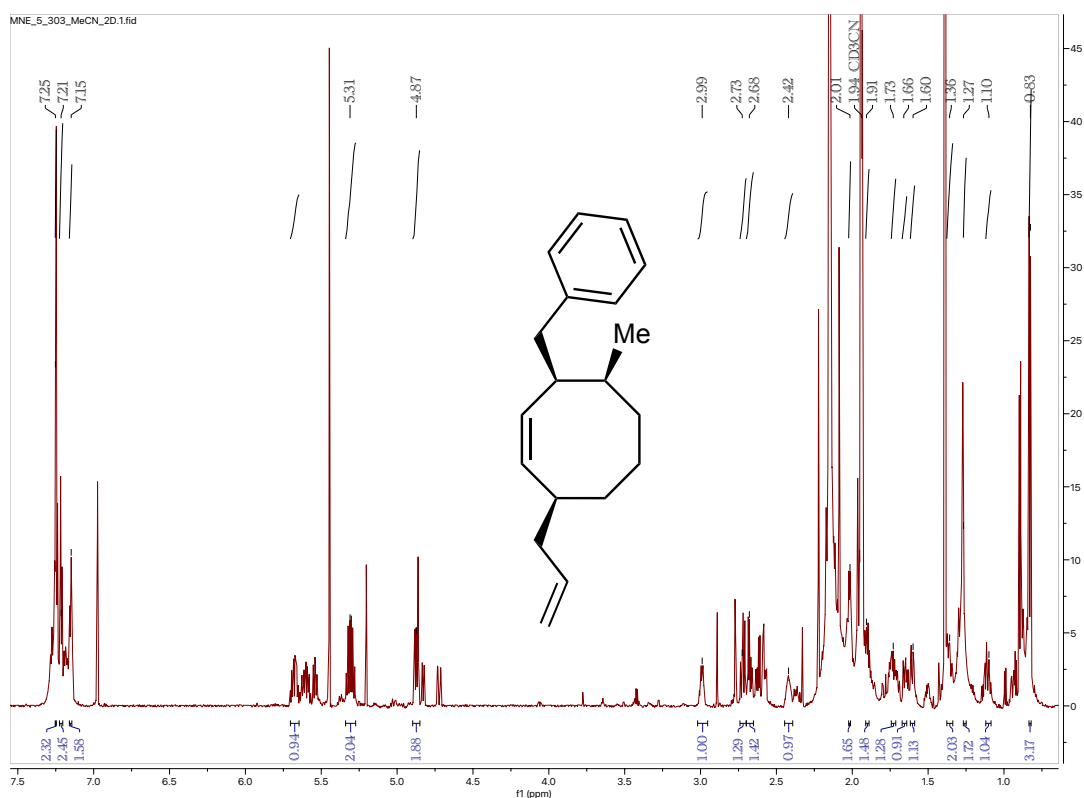
4-JKH-027 worked up.10.fid  
bn 1 cn 2 free diene  
extracted, ppted and rotovaped  
d-acetonitrile



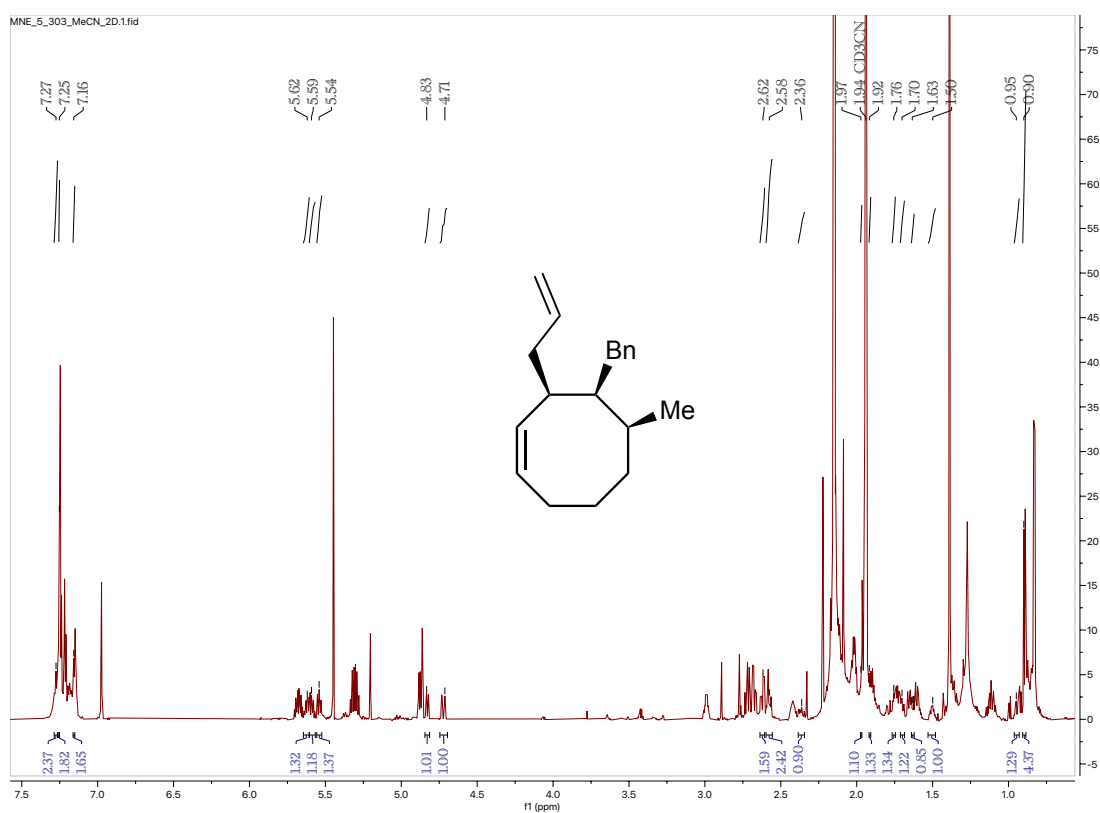
4-JKH-027-2D.4.fid  
carbon



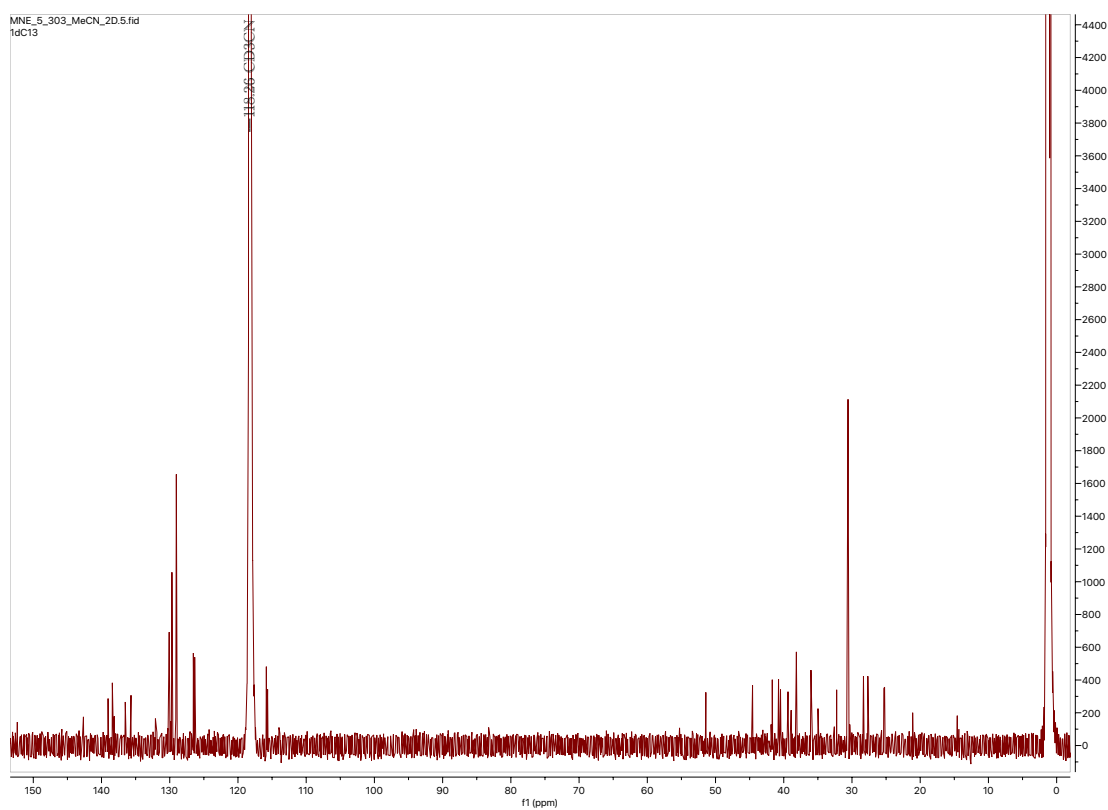
$^1\text{H}$  NMR (800 MHz,  $\text{CD}_3\text{CN}$ ,  $\delta$ , 25  $^\circ\text{C}$ ) of Compound **41** (major) –



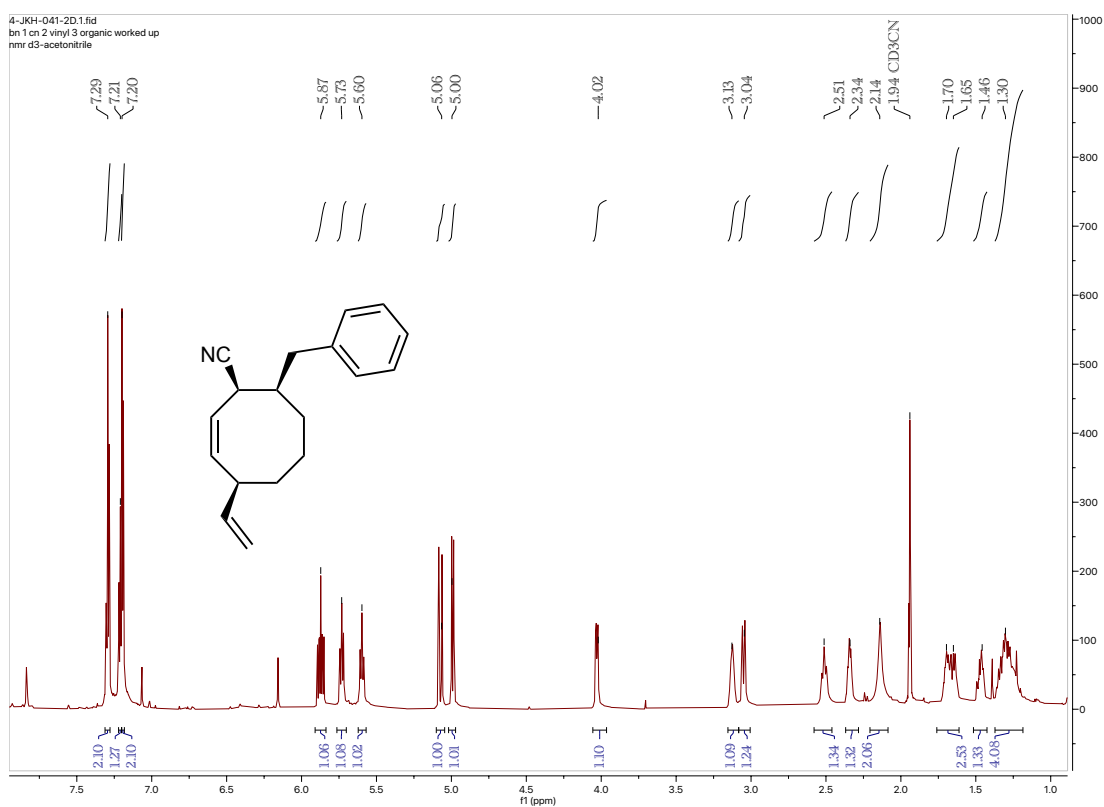
$^1\text{H}$  NMR (800 MHz,  $\text{CD}_3\text{CN}$ ,  $\delta$ , 25  $^\circ\text{C}$ ) of Compound **41** (minor) –



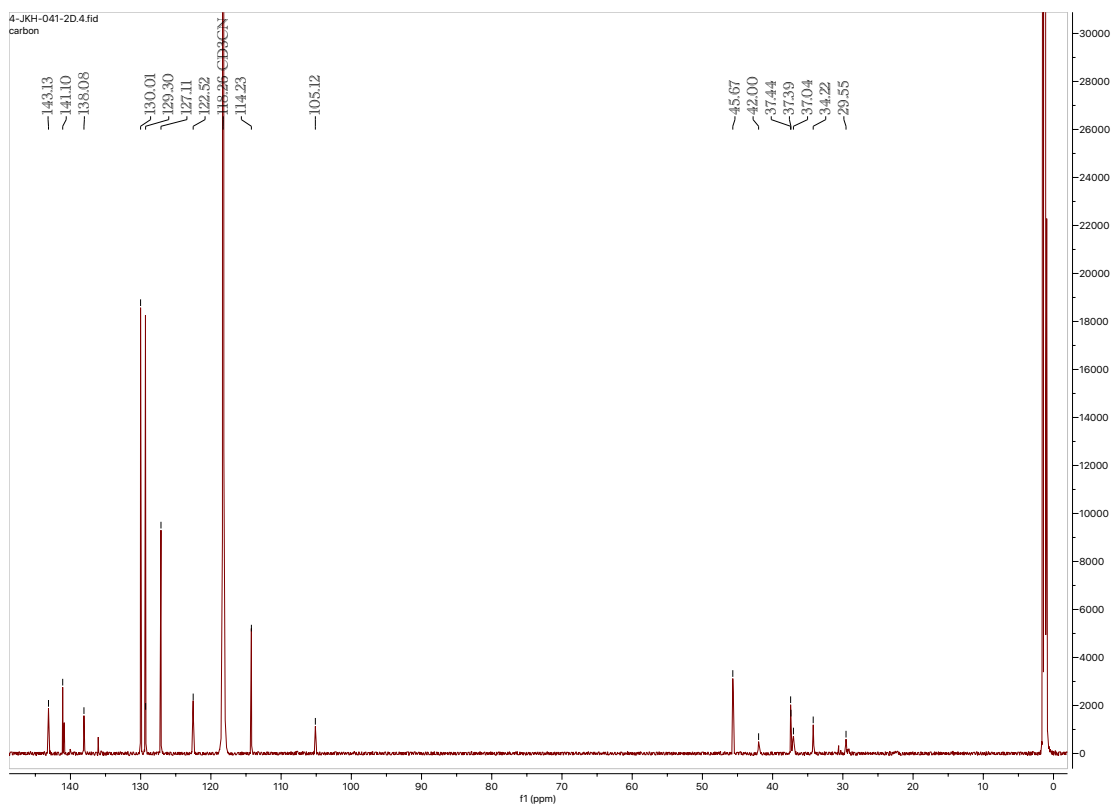
$^{13}\text{C}$  NMR (201 MHz,  $\text{CD}_3\text{CN}$ ,  $\delta$ , 25 °C) of Compound **41** –



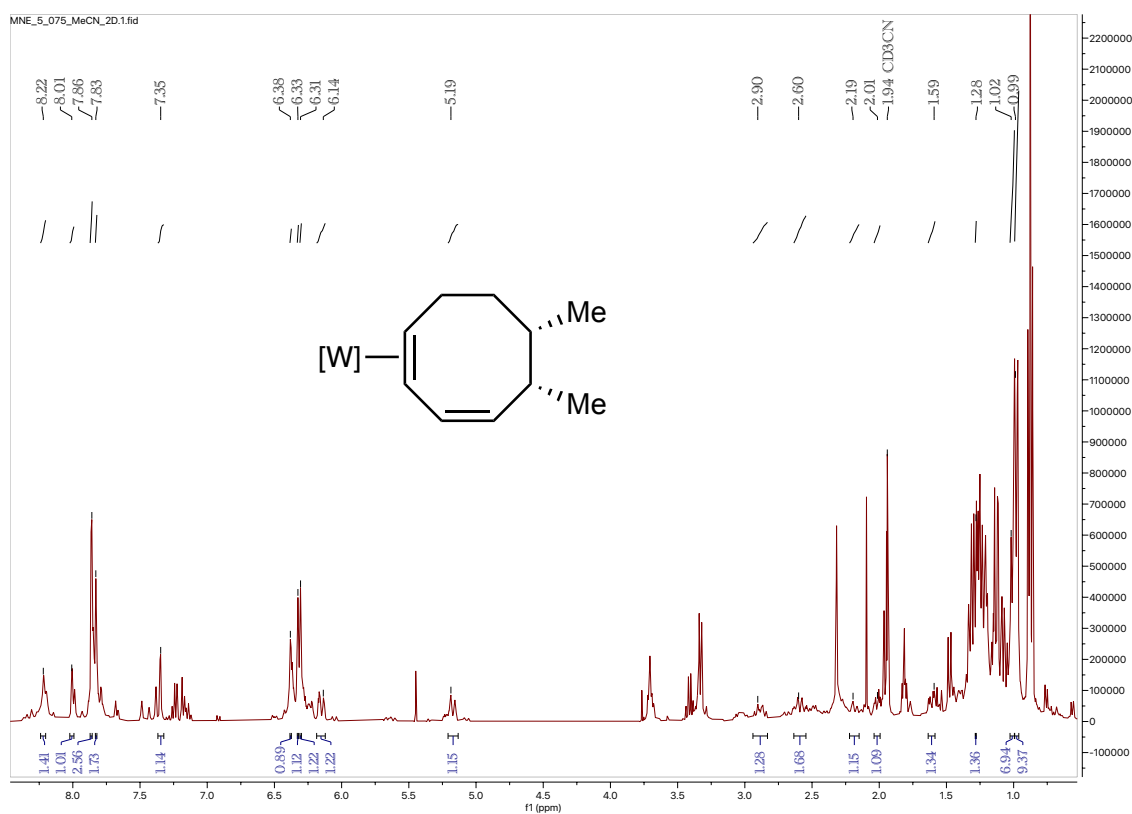
<sup>1</sup>H NMR (800 MHz, CD<sub>3</sub>CN, δ, 25 °C) of Compound **42** –



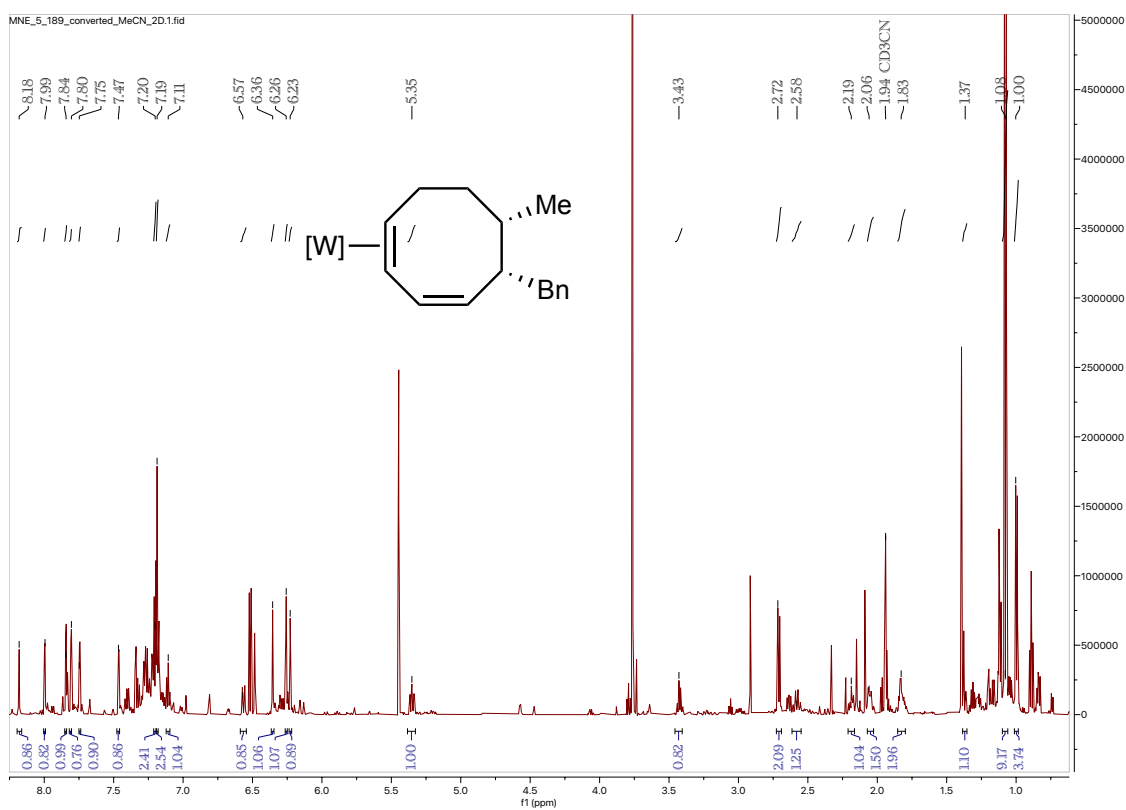
<sup>13</sup>C NMR (201 MHz, CD<sub>3</sub>CN, δ, 25 °C) of Compound **42** –



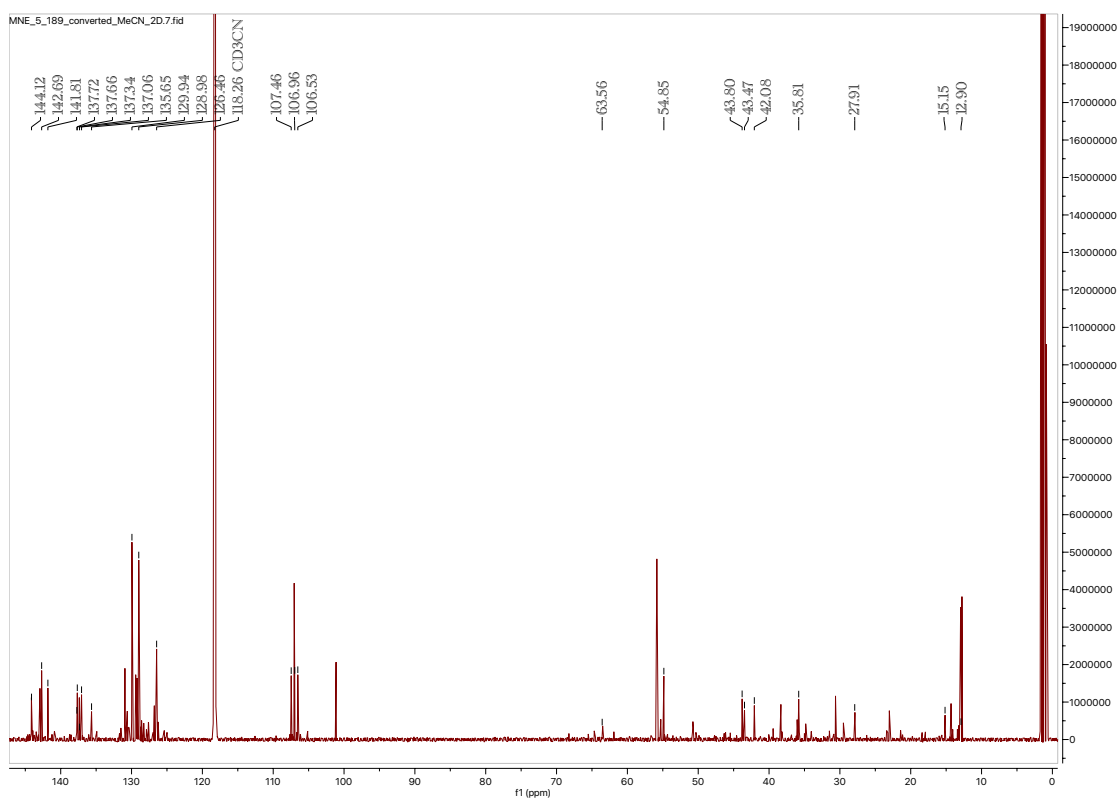
<sup>1</sup>H NMR (800 MHz, CD<sub>3</sub>CN, δ, 25 °C) of Compound **43** –



<sup>1</sup>H NMR (800 MHz, CD<sub>3</sub>CN, δ, 25 °C) of Compound **44** –

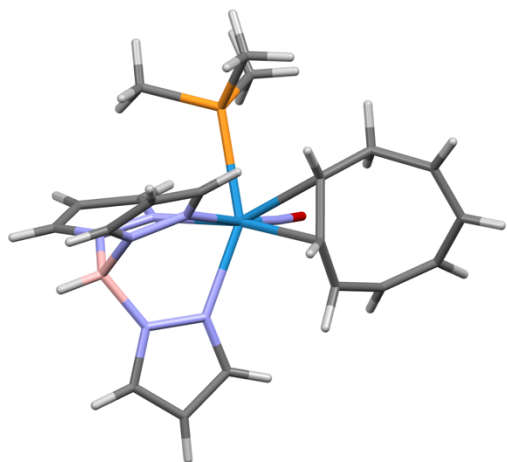


<sup>13</sup>C NMR (201 MHz, CD<sub>3</sub>CN, δ, 25 °C) of Compound **44** –



# DFT Electronic Energies + Thermal Free Energy Correction and Cartesian Coordinates

Compound 2A-D Electronic Energy: -1670.033867 Hartree

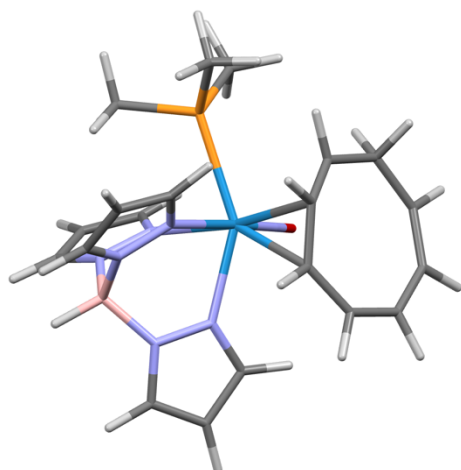


W	1.061400	1.966700	10.751400
P	0.001800	2.165300	8.444400
O	-0.930500	3.921600	11.782800
N	2.157400	3.626700	9.872400
N	3.457200	3.529500	9.501200
N	2.507100	0.614600	9.715400
N	2.798800	2.230600	12.117600
N	-0.112000	3.133000	11.403800
N	4.054900	2.346000	11.572500
N	3.786000	1.026400	9.483000
C	2.934500	2.437700	13.429700
H	2.220700	2.434800	14.056900
C	4.266500	2.659600	13.746300
H	4.635400	2.812900	14.608100
C	-1.388500	3.322200	8.421400
H	-2.166600	2.906100	8.847400
H	-1.606900	3.551800	7.494300
H	-1.144200	4.135700	8.910700
C	1.743900	4.877700	9.612800
H	0.872000	5.218000	9.774100
C	4.936200	2.609100	12.558800
H	5.870400	2.739100	12.445500
C	0.383400	0.017800	11.759400
H	1.011700	-0.759200	11.725100
C	-0.770200	1.393100	13.636000
H	-0.588700	2.234000	14.038100
C	-0.459000	0.229200	10.629000
H	-0.294400	-0.404100	9.872700
C	-1.935300	0.590000	10.834100
H	-2.000900	1.506200	11.202800

H	-2.400000	0.578700	9.959700
C	-2.612200	-0.369600	11.767200
H	-3.038400	-1.134700	11.398700
C	-2.017300	0.920300	13.784000
H	-2.559600	1.366600	14.423400
C	2.808100	5.592500	9.069000
H	2.806700	6.499000	8.784700
C	-0.589100	0.705500	7.535000
H	0.151100	0.075900	7.410700
H	-0.934000	0.982300	6.660900
H	-1.305000	0.270700	8.045500
C	3.859200	4.710200	9.030100
H	4.733900	4.909200	8.717500
C	3.630900	-1.044600	8.707000
H	3.835300	-1.884600	8.311800
C	0.354900	0.751900	12.917000
H	1.129900	0.553900	13.517000
C	1.138200	2.812300	7.173000
H	1.504900	3.671100	7.468700
H	0.650000	2.937400	6.332000
H	1.869500	2.174900	7.033600
C	4.469200	0.015800	8.883500
H	5.383800	0.044400	8.629000
C	2.418300	-0.631500	9.227400
H	1.629000	-1.159800	9.238700
C	-2.644800	-0.201100	13.078000
H	-3.104500	-0.850300	13.596500
B	4.295400	2.356700	10.047600
H	5.265200	2.484200	9.840000



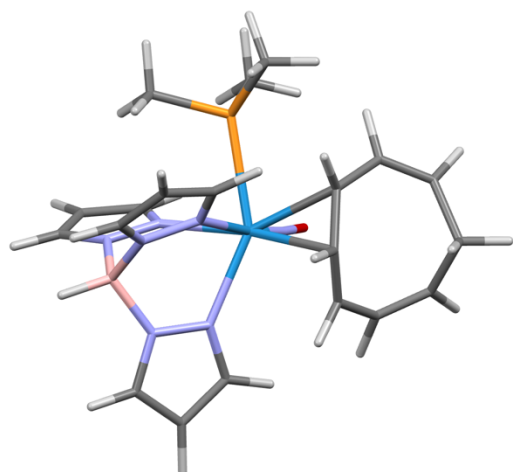
Compound 2A-P Electronic Energy: -1670.016957 Hartree



W	-0.313800	-0.063600	0.040400
O	-1.921500	0.210400	-2.430900
N	-1.376500	0.112600	-1.380900
P	0.257400	-2.562100	-0.255400
C	-0.688700	-3.425300	-1.560200
H	-1.725000	-3.569000	-1.237000
H	-0.246100	-4.405300	-1.771300
H	-0.697900	-2.828300	-2.478100
C	2.009500	-2.861100	-0.695100
H	2.249200	-2.468900	-1.686600
H	2.201200	-3.939900	-0.680000
H	2.655400	-2.373300	0.043800
C	0.136700	-3.696900	1.186200
H	0.939600	-3.460300	1.891700
H	0.283400	-4.724200	0.833100
H	-0.820500	-3.648400	1.712000
N	1.333400	0.002200	-1.421600
N	2.517000	0.389700	1.394100
N	0.350200	2.052100	-0.043100
N	2.564300	0.480900	-1.123000
N	1.654300	2.389600	0.137200
N	1.329900	-0.235400	1.595800
C	1.806900	3.707100	-0.103300
H	2.785800	4.161700	-0.021500
C	3.358800	0.119600	2.404600
H	4.353600	0.545900	2.412900
C	1.334300	-0.316400	-2.723800
H	0.434700	-0.694500	-3.196100
C	1.452700	-0.899300	2.758300
H	0.630100	-1.480600	3.156600
C	-0.299400	3.163400	-0.404900
H	-1.363000	3.126400	-0.605200
C	0.580800	4.245300	-0.441900
H	0.354100	5.272100	-0.687500
B	2.749000	1.305100	0.179400

H	3.843900	1.790500	0.222600
C	2.717200	-0.710800	3.307300
H	3.105200	-1.109000	4.233000
C	2.588800	-0.063800	-3.276300
H	2.905000	-0.216700	-4.297600
C	3.330300	0.456500	-2.228700
H	4.346200	0.828600	-2.193900
C	-1.786200	-0.489200	1.778600
H	-1.204200	-1.002700	2.544600
C	-2.353600	-1.341400	0.833600
H	-2.139800	-2.389000	1.049900
C	-1.607900	0.919600	1.721800
H	-0.883000	1.244600	2.472800
C	-3.543900	-1.284000	-0.070100
H	-3.277100	-1.821600	-0.996600
H	-4.259400	-1.976500	0.411500
C	-4.344900	-0.100800	-0.482000
C	-4.419700	1.201100	-0.159000
C	-3.662000	2.102900	0.676900
C	-2.523100	2.003200	1.394500
H	-2.199800	2.940300	1.849500
H	-4.094600	3.103900	0.693000
H	-5.230800	1.717800	-0.672900
H	-5.088100	-0.414300	-1.217300

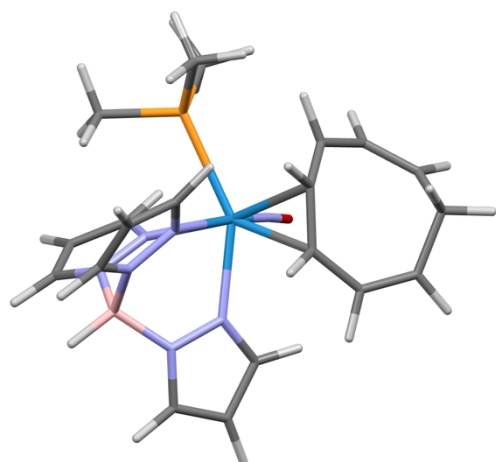
Compound 2B-D Electronic Energy: -1670.031778 Hartree



W	-0.253100	0.118600	-0.058200
O	-1.835700	0.438000	-2.545600
N	-1.208600	0.361400	-1.541300
P	-0.265400	-2.444800	-0.384700
C	-1.028900	-2.968800	-1.961000
H	-2.039200	-2.556800	-2.048000
H	-1.069100	-4.061900	-2.022600
H	-0.437600	-2.592700	-2.801200
C	-1.014900	-3.581900	0.846700
H	-0.516100	-3.458900	1.814000
H	-0.851700	-4.610800	0.507100
H	-2.088500	-3.427100	0.974300
C	1.420100	-3.162800	-0.445600
H	1.989600	-2.777400	-1.294800
H	1.341900	-4.251900	-0.536300
H	1.953700	-2.921700	0.480800
N	1.508000	-0.249500	-1.307400
N	2.772900	-0.110300	-0.840600
N	1.058300	-0.429600	1.704600
N	0.932100	2.016700	0.015700
N	2.248200	1.972100	0.358700
N	2.389200	-0.179800	1.657500
C	0.672000	3.282500	-0.337600
H	-0.317800	3.564700	-0.672400
C	1.811000	4.073200	-0.210700
H	1.909400	5.129300	-0.412900
C	1.595800	-0.534000	-2.615000
H	0.695800	-0.654700	-3.207000
C	2.787500	3.198000	0.225700
H	3.835000	3.355300	0.448000
C	2.932500	-0.604000	-3.001100
H	3.327600	-0.814300	-3.984000
C	3.641600	-0.312100	-1.847300
H	4.705900	-0.216700	-1.673800
C	2.034100	-1.296100	3.538900

H	2.178000	-1.792400	4.487200
C	2.992000	-0.688100	2.746100
H	4.059300	-0.571900	2.882500
C	0.841600	-1.103200	2.845400
H	-0.160900	-1.408300	3.123800
B	3.001100	0.630200	0.504500
H	4.171000	0.811700	0.690700
C	-1.802200	0.686100	1.613500
H	-1.218000	0.722600	2.534500
C	-2.776800	2.394800	-0.089400
H	-2.407500	3.204600	-0.719200
C	-2.125300	-0.620700	1.134300
H	-1.847900	-1.389800	1.860200
C	-4.427700	-0.378200	0.101100
H	-5.188700	-0.864200	-0.506700
C	-4.066700	2.055100	-0.202400
H	-4.670800	2.581500	-0.939200
C	-1.836200	1.884800	0.901100
H	-1.211300	2.661900	1.345200
C	-3.285300	-1.034100	0.317200
H	-3.214100	-2.037400	-0.105400
C	-4.736500	0.996800	0.618700
H	-4.384600	1.072900	1.658900
H	-5.818400	1.158700	0.633000

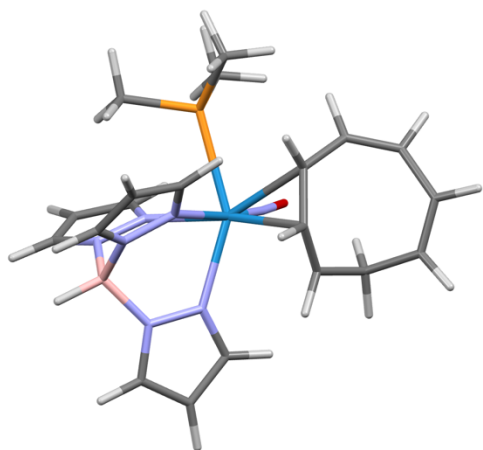
Compound 2B-P Electronic Energy: -1670.027457 Hartree



W	-0.272500	-0.050600	-0.080400
O	-1.647800	0.380000	-2.671400
N	-1.152800	0.182000	-1.612100
P	0.203700	-2.583500	-0.235500
C	-0.551100	-3.429000	-1.670300
H	-1.639000	-3.467300	-1.552500
H	-0.168200	-4.451500	-1.763900
H	-0.329300	-2.875800	-2.588700
C	1.988300	-2.971500	-0.368600
H	2.408700	-2.605400	-1.308800
H	2.126900	-4.057000	-0.311300
H	2.522300	-2.497700	0.463100
C	-0.221200	-3.675500	1.181000
H	0.449300	-3.449500	2.016400
H	-0.057100	-4.717500	0.883300
H	-1.255400	-3.574900	1.521400
N	1.583200	-0.078300	-1.262400
N	2.318400	0.372900	1.696400
N	0.461300	2.035300	-0.135000
N	2.763800	0.380100	-0.783000
N	1.722500	2.355300	0.256000
N	1.102900	-0.228900	1.719700
C	1.962600	3.648100	-0.044600
H	2.926100	4.086000	0.182000
C	2.984800	0.112600	2.833000
H	3.974600	0.521400	2.989500
C	1.784700	-0.441600	-2.536600
H	0.961800	-0.816400	-3.134800
C	1.027000	-0.866600	2.899900
H	0.139600	-1.423600	3.174600
C	-0.071100	3.129500	-0.689600
H	-1.074100	3.098300	-1.097400
C	0.838400	4.186900	-0.638700
H	0.696700	5.197300	-0.992400
B	2.763800	1.243100	0.509600

H	3.851800	1.703700	0.710600
C	2.192300	-0.685800	3.639000
H	2.421600	-1.069400	4.622100
C	3.119300	-0.241600	-2.885900
H	3.591500	-0.438500	-3.837000
C	3.697500	0.296000	-1.748000
H	4.705800	0.641900	-1.559900
C	-2.017900	-0.428600	1.425700
H	-1.596500	-0.980700	2.266400
C	-2.546300	-1.230000	0.408500
H	-2.409400	-2.301200	0.567300
C	-1.725300	0.974700	1.363100
H	-1.091500	1.288500	2.199500
C	-4.517500	-0.046300	-0.533500
C	-3.885800	2.071000	0.614800
C	-2.583400	2.082200	0.913300
H	-2.081700	3.049100	0.925000
H	-4.361200	3.013800	0.350800
H	-5.213600	0.026100	-1.367800
C	-3.520800	-0.935900	-0.630900
H	-3.468200	-1.563400	-1.520700
C	-4.755100	0.844600	0.644800
H	-5.809400	1.134400	0.685600
H	-4.539900	0.285700	1.568400

Compound 2C-D Electronic Energy: -1670.028236 Hartree

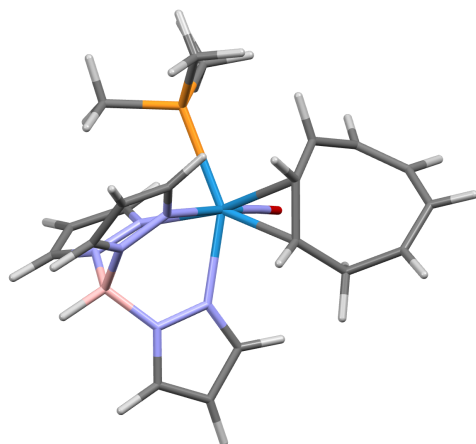


W	-0.226200	0.106000	-0.107400
O	-1.636400	0.237800	-2.711500
N	-1.078700	0.238700	-1.660900
P	-0.232500	-2.472700	-0.297200
C	-0.878200	-3.076400	-1.897200
H	-1.898300	-2.712700	-2.055900
H	-0.871900	-4.171700	-1.920900
H	-0.257900	-2.703900	-2.717400
C	-1.087800	-3.553300	0.914900
H	-0.685500	-3.384700	1.919400
H	-0.895200	-4.596700	0.641000
H	-2.168900	-3.394300	0.928900
C	1.453600	-3.184600	-0.195800
H	2.084000	-2.833600	-1.016600
H	1.386500	-4.277300	-0.241000
H	1.915100	-2.895800	0.755400
N	1.617200	-0.306400	-1.220000
N	2.848800	-0.104800	-0.690400
N	0.998000	-0.332500	1.746000
N	0.910200	2.022400	-0.081800
N	2.205400	2.037900	0.333600
N	2.318000	-0.029500	1.773700
C	0.636100	3.252500	-0.536500
H	-0.343400	3.478100	-0.940000
C	1.747200	4.081700	-0.405600
H	1.830900	5.123900	-0.675300
C	1.790700	-0.672100	-2.498900
H	0.932300	-0.851600	-3.135700
C	2.720000	3.267200	0.143500
H	3.748700	3.470800	0.411700
C	3.149200	-0.734200	-2.799900
H	3.607200	-0.998200	-3.741700
C	3.780800	-0.350400	-1.628300
H	4.830400	-0.217900	-1.398700
C	1.882000	-1.079800	3.676200
H	1.982000	-1.529600	4.652900

C	2.866300	-0.466700	2.920100
H	3.917400	-0.302600	3.119200
C	0.731800	-0.966400	2.899300
H	-0.275000	-1.299900	3.125000
B	2.979300	0.728600	0.612300
H	4.131000	0.953600	0.855400
C	-1.829400	0.726000	1.468400
H	-1.248900	0.810600	2.387500
C	-2.189300	-0.578500	1.039700
H	-1.959900	-1.346100	1.782600
C	-4.527100	-0.369100	0.014100
H	-5.269800	-0.945700	-0.541000
C	-4.326600	2.084100	0.351500
H	-4.776600	3.006300	0.714800
C	-1.885600	1.854500	0.662300
H	-1.348700	2.714400	1.061100
C	-3.334400	-0.965400	0.188000
H	-3.236700	-1.953700	-0.267200
C	-2.983600	2.174000	-0.324500
H	-2.824200	3.183400	-0.720500
H	-2.988700	1.497900	-1.185600
C	-4.988600	0.930600	0.494000
H	-5.989900	0.953300	0.925100



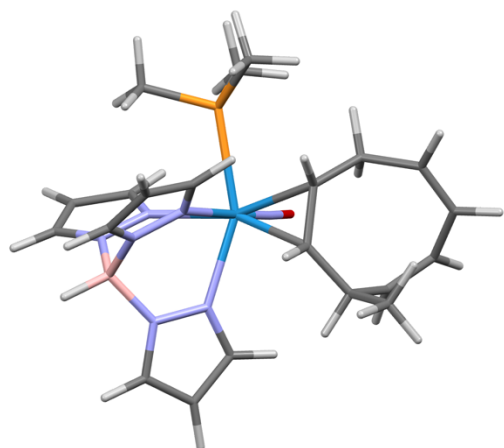
Compound 2C-P Electronic Energy: -1670.029055 Hartree



W	0.241600	-0.026900	0.115300
O	1.576900	0.192600	2.757600
N	1.085400	0.096000	1.679800
P	-0.116600	-2.580800	0.101000
C	0.628600	-3.469600	1.514300
H	1.720900	-3.419400	1.455300
H	0.319200	-4.520900	1.521300
H	0.320300	-2.997700	2.452900
C	-1.884900	-3.052900	0.152900
H	-2.349200	-2.753900	1.096300
H	-1.973400	-4.138900	0.036700
H	-2.413800	-2.559800	-0.670700
C	0.406700	-3.565400	-1.359500
H	-0.230100	-3.302600	-2.210600
H	0.262400	-4.629300	-1.139300
H	1.452000	-3.411500	-1.641100
N	-1.647700	-0.189300	1.236300
N	-2.317600	0.383000	-1.714700
N	-0.579800	2.034200	0.232100
N	-2.834500	0.240800	0.748000
N	-1.849300	2.306700	-0.164300
N	-1.068000	-0.145200	-1.741600
C	-2.130300	3.598500	0.098600
H	-3.106600	3.999500	-0.140700
C	-2.942400	0.151600	-2.880700
H	-3.950400	0.512600	-3.039000
C	-1.868000	-0.636100	2.480800
H	-1.045400	-1.006400	3.082400
C	-0.929800	-0.708400	-2.953700
H	-0.006100	-1.196900	-3.238700
C	-0.080700	3.161400	0.749700
H	0.922300	3.177400	1.155900
C	-1.022600	4.187700	0.676300
H	-0.912500	5.210300	1.005100
B	-2.835400	1.167500	-0.496500
H	-3.935900	1.592600	-0.708000

C	-2.087400	-0.552200	-3.710400
H	-2.271900	-0.890000	-4.719400
C	-3.220000	-0.518400	2.799100
H	-3.709300	-0.792000	3.722200
C	-3.790600	0.057900	1.676300
H	-4.808500	0.367600	1.476900
C	2.034000	-0.266900	-1.338000
H	1.637700	-0.772200	-2.218000
C	2.646400	-1.086000	-0.391200
H	2.554500	-2.158300	-0.579000
C	1.722000	1.116900	-1.126400
H	1.203000	1.568800	-1.975400
C	4.690100	0.030000	0.534800
C	4.977300	0.982300	-0.528300
C	4.105300	1.887000	-0.993000
H	4.429000	2.571500	-1.776100
H	6.000700	0.991500	-0.903500
H	5.453200	-0.066000	1.309300
C	3.633100	-0.802500	0.639900
H	3.612200	-1.478700	1.495500
C	2.715400	2.049500	-0.449000
H	2.381200	3.082500	-0.595800
H	2.747200	1.871700	0.634100

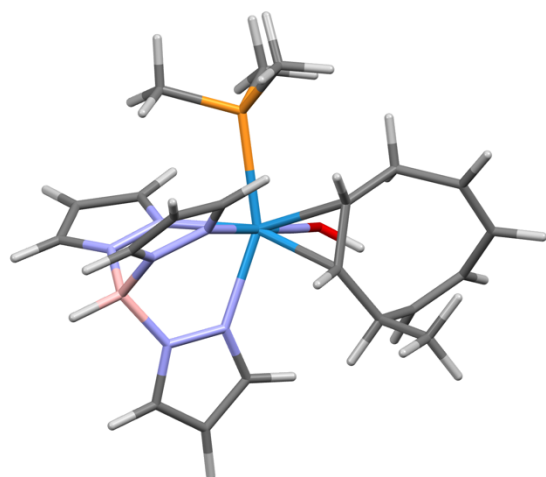
Compound 15 Electronic Energy: -1710.103451 Hartree



W	0.059000	0.100600	-0.224100
P	-0.339700	2.591400	0.005200
O	1.262700	0.361000	-2.944200
N	-1.084300	0.002300	1.755700
N	-2.283300	-0.626600	1.825100
N	-1.999300	0.200800	-1.130800
N	-0.601400	-2.045300	-0.348200
C	-3.801400	0.578700	-2.414500
H	-4.435500	0.925900	-3.218400
C	1.756300	-0.741300	0.885700
H	1.301600	-1.088100	1.824900
N	-1.823700	-2.421200	0.112300
N	-3.073900	-0.388400	-0.556900
N	0.804900	0.227600	-1.821900
C	-4.167800	-0.177700	-1.314300
H	-5.124100	-0.592800	-1.020600
C	1.915700	0.696700	0.868000
H	1.723000	1.201300	1.822100
C	-2.791300	-0.514000	3.065900
H	-3.746500	-0.963600	3.308000
C	2.760200	-1.812800	0.456800
H	2.164200	-2.721000	0.273700
C	3.568600	-1.607000	-0.803700
H	3.291800	-2.248600	-1.644900
C	4.410100	1.142800	0.480800
H	4.858600	1.828900	1.202600
C	-2.426900	0.780400	-2.256700
H	-1.727200	1.316800	-2.888700
C	2.995900	1.403700	0.053900
H	2.813100	2.487700	0.097500
H	2.898000	1.120000	-1.001100
C	-2.103800	3.024200	0.283500
H	-2.720400	2.732600	-0.572600
H	-2.201600	4.104800	0.443200
H	-2.469900	2.497500	1.174100

C	0.419500	3.567600	1.358200
H	0.079300	3.188100	2.328000
H	0.102700	4.613100	1.261500
H	1.511800	3.524400	1.324900
C	-2.039500	-3.719300	-0.182800
H	-2.969400	-4.194800	0.103800
C	-0.847300	0.504900	2.973400
H	0.069200	1.050400	3.169500
C	-0.065500	-3.118100	-0.937200
H	0.911500	-3.050500	-1.401900
C	4.659300	-0.841300	-0.968900
H	5.223300	-0.954000	-1.899200
B	-2.856700	-1.379200	0.611400
H	-3.889000	-1.918200	0.904400
C	-1.901400	0.209400	3.840700
H	-1.998700	0.478000	4.883300
C	3.667900	-2.167600	1.645200
H	4.268000	-1.309300	1.968200
H	4.355600	-2.984300	1.389000
H	3.062300	-2.494400	2.500300
C	0.094800	3.572600	-1.476200
H	1.169500	3.486500	-1.672200
H	-0.163500	4.628600	-1.331300
H	-0.446400	3.186300	-2.347100
C	5.163000	0.148600	-0.014900
H	6.217400	0.087800	0.265700
C	-0.935100	-4.210300	-0.853100
H	-0.780000	-5.212000	-1.228900

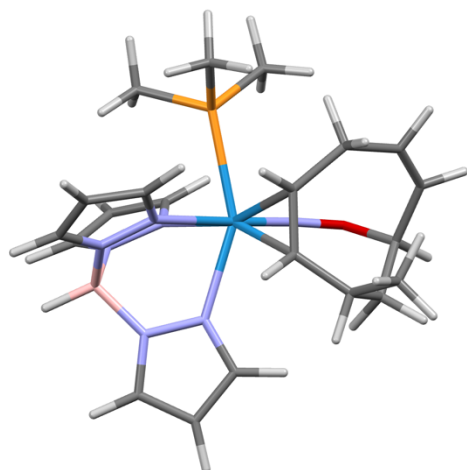
Compound I Electronic Energy: -1710.533432 Hartree



W	0.056100	0.081700	-0.206900
P	-0.328200	2.608900	-0.083600
N	-1.139200	0.121500	1.717400
N	-2.344900	-0.499800	1.795900
N	-1.961700	0.167500	-1.156900
N	-0.618500	-2.044600	-0.209100
C	-3.692800	0.470700	-2.547800
H	-4.285700	0.773000	-3.399400
C	1.708300	-0.703400	1.018000
H	1.221000	-1.026100	1.946100
N	-1.860600	-2.394100	0.217600
N	-3.061400	-0.399200	-0.608400
N	0.916100	0.060500	-1.716200
C	-4.113100	-0.229900	-1.429100
H	-5.082900	-0.630400	-1.161000
C	1.874100	0.721100	0.944400
H	1.607200	1.266600	1.852900
C	-2.872100	-0.319600	3.016500
H	-3.834200	-0.751700	3.262700
C	2.679700	-1.793300	0.577600
H	2.068900	-2.696500	0.439500
C	3.430400	-1.610800	-0.722900
H	3.120800	-2.275900	-1.535800
C	4.380200	1.114000	0.541700
H	4.868500	1.774400	1.259600
C	-2.331700	0.689600	-2.333300
H	-1.605700	1.203100	-2.954100
C	2.967600	1.429500	0.146200
H	2.814100	2.512800	0.235300
H	2.867600	1.202100	-0.919900
C	-2.098400	3.052900	0.061100
H	-2.660600	2.743500	-0.824700
H	-2.184000	4.139700	0.177500
H	-2.528300	2.564300	0.944300
C	0.365100	3.634600	1.261100

H	-0.070500	3.336700	2.220600
H	0.090300	4.677600	1.063400
H	1.453700	3.562700	1.323800
C	-2.083700	-3.692000	-0.063900
H	-3.028000	-4.150000	0.203200
C	-0.923200	0.686400	2.916300
H	-0.010400	1.236800	3.111100
C	-0.080000	-3.133500	-0.770400
H	0.906700	-3.088300	-1.215400
C	4.520600	-0.855600	-0.944500
H	5.046100	-0.985900	-1.894400
B	-2.900900	-1.321900	0.621900
H	-3.945600	-1.829400	0.915800
C	-1.993300	0.440000	3.771400
H	-2.109000	0.762300	4.796400
C	3.621100	-2.128500	1.744200
H	4.230600	-1.268400	2.039900
H	4.296900	-2.949800	1.475200
H	3.037300	-2.445000	2.617500
C	0.227400	3.455700	-1.600200
H	1.313500	3.354500	-1.701000
H	-0.035900	4.519000	-1.553500
H	-0.250400	3.002300	-2.475300
C	5.085800	0.112200	-0.002500
H	6.146600	0.013400	0.237400
C	-0.966800	-4.208900	-0.693700
H	-0.814300	-5.218200	-1.048800
O	1.557800	0.074100	-2.863800
H	2.425300	-0.357400	-2.694100

Compound II Electronic Energy: -1710.537414 Hartree

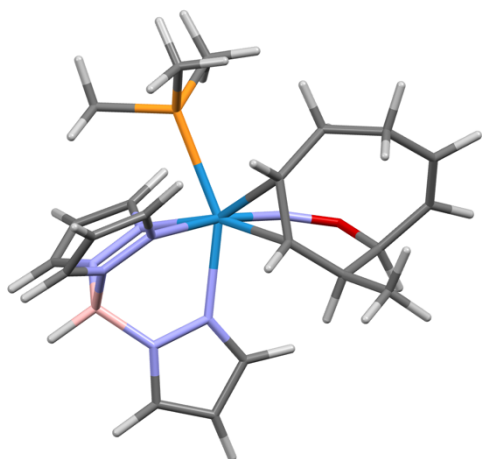


W	-0.124300	-0.002100	-0.090200
P	0.028100	-2.552100	-0.060100
N	1.389400	-0.235200	1.609300
N	2.674800	0.169200	1.420400
N	1.640500	-0.246400	-1.431400
N	0.809000	2.052500	-0.051000
C	3.005600	-0.673900	-3.156100
H	3.372500	-0.990900	-4.122000
C	-1.562800	0.946200	1.290600
H	-0.973500	1.357500	2.119200
N	2.157700	2.193200	0.059300
N	2.893900	0.130700	-1.093800
N	-1.272500	0.140900	-1.381600
C	3.731400	-0.115000	-2.116800
H	4.781400	0.137100	-2.034100
C	-1.733200	-0.477800	1.371900
H	-1.246400	-0.912000	2.248800
C	3.417200	-0.153400	2.490900
H	4.469700	0.100200	2.519000
C	-2.637700	1.942700	0.857700
H	-2.199500	2.933100	1.056400
C	-4.028800	-1.085400	0.070700
H	-4.814800	-1.835600	0.196500
C	1.695500	-0.729800	-2.678900
H	0.797700	-1.105100	-3.157500
C	1.689200	-3.203700	-0.469200
H	1.976900	-2.957000	-1.494800
H	1.678400	-4.294100	-0.353400
H	2.428900	-2.781100	0.222200
C	-0.279600	-3.507400	1.471500
H	0.571400	-3.375600	2.148400
H	-0.343800	-4.568000	1.200000
H	-1.193500	-3.218700	1.994900
C	2.485600	3.496200	0.013200
H	3.522600	3.797600	0.094600

C	1.349800	-0.811200	2.821100
H	0.424800	-1.214000	3.214400
C	0.308800	3.288600	-0.170000
H	-0.756000	3.442000	-0.274600
C	-3.446300	0.875500	-1.506500
H	-3.987800	1.287100	-2.364300
B	3.100200	0.976600	0.178500
H	4.242000	1.326800	0.276900
C	2.607600	-0.788400	3.417600
H	2.886300	-1.171200	4.389000
C	-3.845300	1.856300	1.797000
H	-4.447800	0.959500	1.620000
H	-4.501600	2.725800	1.661700
H	-3.520100	1.842400	2.844800
C	-1.056100	-3.313500	-1.313900
H	-2.104800	-3.077300	-1.101900
H	-0.919100	-4.401300	-1.321600
H	-0.801000	-2.908900	-2.300000
C	-4.249400	-0.256600	-0.955700
H	-5.158000	-0.452700	-1.525100
C	1.329000	4.238500	-0.138000
H	1.234400	5.312700	-0.210800
O	-2.244900	0.331800	-2.217100
C	-3.068300	2.054500	-0.620000
H	-2.308800	2.608200	-1.190400
H	-3.953100	2.707300	-0.627500
C	-2.994500	-1.283400	1.131200
H	-3.561900	-1.260900	2.080400
H	-2.720400	-2.346700	1.046900



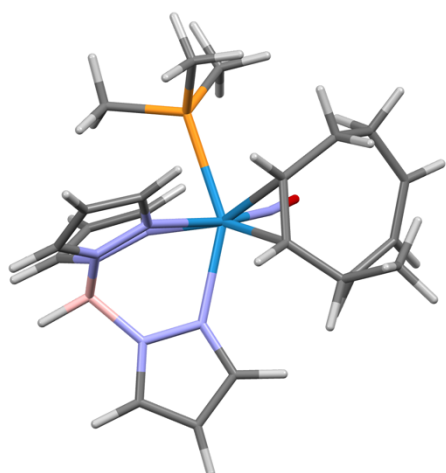
Compound III Electronic Energy: -1710.532496 Hartree



W	-0.039800	-0.045200	-0.198700
P	0.281500	-2.602100	-0.342000
N	1.170000	-0.289800	1.687700
N	2.432100	0.216500	1.740100
N	1.913400	-0.091500	-1.266900
N	0.742700	2.050900	-0.038200
C	3.568900	-0.298200	-2.761200
H	4.113200	-0.522000	-3.667700
C	-1.667600	0.648500	1.124700
H	-1.251000	0.978800	2.082100
N	2.004500	2.294100	0.404900
N	3.058700	0.360500	-0.705000
N	-1.215300	0.396900	-1.420700
C	4.066600	0.245900	-1.587700
H	5.065500	0.566700	-1.319000
C	-1.801400	-0.774100	0.977500
H	-1.496200	-1.336300	1.862700
C	3.008400	-0.116600	2.905800
H	4.017800	0.208500	3.125100
C	-2.566000	1.727500	0.548000
H	-1.923100	2.609000	0.431900
C	2.209700	-0.489500	-2.510300
H	1.434900	-0.903900	-3.146700
C	-2.895900	-1.497100	0.213500
H	-2.743600	-2.573500	0.353700
H	-2.817300	-1.338900	-0.868400
C	2.049400	-3.079500	-0.400600
H	2.539800	-2.702500	-1.302400
H	2.120300	-4.173600	-0.385900
H	2.565600	-2.679400	0.481100
C	-0.268300	-3.714800	1.001600
H	0.303300	-3.494900	1.909800
H	-0.052600	-4.745800	0.696700
H	-1.334400	-3.627300	1.221000
C	2.309700	3.592400	0.213200
H	3.283800	3.968000	0.501000

C	0.973800	-0.938200	2.846700
H	0.031700	-1.429900	3.054400
C	0.276800	3.209200	-0.521600
H	-0.704100	3.267200	-0.976300
C	-4.565000	0.857300	-0.917900
H	-5.255600	1.369400	-1.588300
B	2.993700	1.129600	0.637500
H	4.077500	1.539000	0.942600
C	2.109000	-0.862600	3.648500
H	2.252300	-1.285300	4.632600
C	-3.630500	2.167100	1.558500
H	-4.302700	1.349900	1.840100
H	-4.241600	2.987500	1.161100
H	-3.136400	2.528900	2.467500
C	-0.420200	-3.335900	-1.857000
H	-1.511100	-3.243100	-1.845900
H	-0.145000	-4.395000	-1.926000
H	-0.031200	-2.801100	-2.730600
C	-5.041800	-0.217600	-0.278500
H	-6.087300	-0.457700	-0.481000
C	1.226700	4.221100	-0.369900
H	1.134700	5.260300	-0.651900
O	-2.314400	0.919000	-1.878100
C	-3.227800	1.530900	-0.823000
H	-3.360400	2.538500	-1.235200
C	-4.337800	-1.169500	0.637000
H	-4.352700	-0.792100	1.671800
H	-4.926900	-2.094200	0.663300

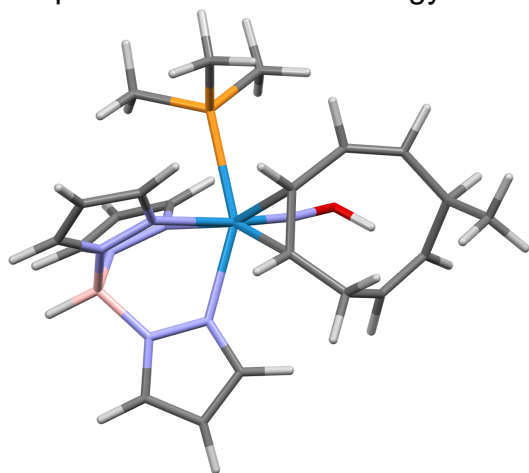
Compound III – no Nitrosyl Stabilization Electronic Energy: -1710.512786 Hartree



W	-0.186400	0.026100	-0.086400
P	-0.038900	-2.506600	0.202200
N	1.312500	-0.084300	1.627900
N	2.617400	0.229100	1.422500
N	1.576500	-0.428800	-1.380500
N	0.854000	2.074100	-0.276000
C	2.936100	-1.109400	-3.029200
H	3.295300	-1.547500	-3.949700
C	-1.528000	1.089100	1.359100
H	-0.871400	1.470200	2.147300
N	2.208700	2.129600	-0.140800
N	2.844800	-0.079600	-1.069700
N	-1.151600	-0.167100	-1.576000
C	3.679000	-0.473100	-2.048300
H	4.738800	-0.260400	-1.980400
C	-1.818200	-0.321300	1.392400
H	-1.380200	-0.790400	2.278400
C	3.325100	0.013300	2.543800
H	4.387500	0.222000	2.565700
C	-2.483800	2.130500	0.830900
H	-1.957400	3.092900	0.911400
C	1.620600	-1.048700	-2.567300
H	0.709900	-1.419600	-3.024000
C	1.677100	-3.143600	0.095800
H	2.103600	-2.975700	-0.897500
H	1.663900	-4.221100	0.298600
H	2.306200	-2.651100	0.846500
C	-0.563900	-3.327300	1.750800
H	0.048900	-2.981800	2.589700
H	-0.409000	-4.406000	1.628400
H	-1.618100	-3.148400	1.976700
C	2.635200	3.397900	-0.273900
H	3.690600	3.626400	-0.191800
C	1.220400	-0.496800	2.901500
H	0.266500	-0.795300	3.319200

C	0.456500	3.335000	-0.496900
H	-0.585500	3.581800	-0.644100
C	-3.661000	1.243500	-1.320800
H	-3.934800	1.727500	-2.260800
B	3.083300	0.880200	0.108400
H	4.241100	1.184500	0.181100
C	2.467500	-0.459000	3.522500
H	2.708000	-0.727300	4.541400
C	-3.805500	2.286800	1.574400
H	-4.465200	1.421700	1.468200
H	-4.351200	3.164300	1.206200
H	-3.606000	2.434900	2.642300
C	-0.916700	-3.478500	-1.070500
H	-1.996900	-3.428700	-0.894800
H	-0.599600	-4.526500	-1.012600
H	-0.702800	-3.088500	-2.070800
C	-4.262200	0.049400	-1.081900
H	-5.071700	-0.205200	-1.767900
C	1.542100	4.209700	-0.507100
H	1.527900	5.279200	-0.662200
O	-1.686700	-0.446500	-2.620500
C	-2.602500	1.874500	-0.637100
H	-1.975500	2.488100	-1.284300
C	-3.838200	-1.083900	-0.224600
H	-4.709500	-1.741000	-0.104200
H	-3.157600	-1.651000	-0.885000
C	-3.186700	-0.945100	1.155300
H	-3.123700	-1.983600	1.506600
H	-3.908800	-0.474900	1.838600

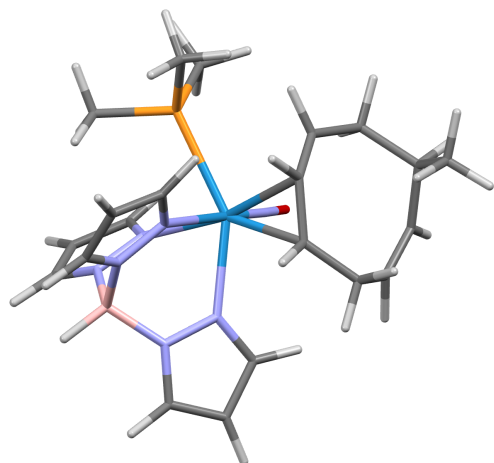
Compound IV Electronic Energy: -1710.527353 Hartree



W	-0.043400	0.011600	-0.082200
P	0.161600	-2.538200	-0.131900
N	1.451800	-0.274200	1.605100
N	2.722200	0.194600	1.483800
N	1.756700	-0.156500	-1.386300
N	0.835100	2.073100	0.024600
C	3.167600	-0.516400	-3.089800
H	3.561800	-0.804900	-4.053800
C	-1.461700	0.877600	1.359500
H	-0.847100	1.180600	2.214700
N	2.174700	2.251600	0.176800
N	2.993200	0.244200	-1.015500
N	-1.083000	0.063600	-1.469200
C	3.857400	0.040200	-2.025100
H	4.898600	0.317300	-1.915600
C	-1.712200	-0.536800	1.330600
H	-1.260100	-1.086900	2.158900
C	3.435600	-0.135000	2.571200
H	4.473400	0.164000	2.651800
C	-3.032400	2.028800	-0.353500
H	-2.571700	2.802100	-0.973700
C	-4.098000	-0.992700	0.278300
H	-4.749900	-1.870500	0.233400
C	1.849800	-0.613000	-2.642100
H	0.973100	-1.000300	-3.149500
C	1.869900	-3.123900	-0.425500
H	2.243000	-2.801100	-1.401400
H	1.878500	-4.219600	-0.384400
H	2.531000	-2.733700	0.358200
C	-0.274900	-3.583800	1.302400
H	0.425800	-3.402400	2.123700
H	-0.177700	-4.630600	0.990100
H	-1.294500	-3.415300	1.655500
C	2.463500	3.564100	0.142500
H	3.487800	3.897000	0.255800
C	1.389400	-0.897800	2.792800

H	0.467500	-1.353600	3.132600
C	0.299900	3.292700	-0.110000
H	-0.765200	3.410900	-0.253000
C	-4.012200	1.316000	-0.917800
H	-4.314300	1.600300	-1.931000
B	3.151400	1.058800	0.283100
H	4.279200	1.439600	0.417900
C	2.620000	-0.841100	3.440300
H	2.878200	-1.248400	4.407300
C	-0.806200	-3.245900	-1.503800
H	-1.870800	-3.044200	-1.340200
H	-0.642200	-4.328200	-1.562400
H	-0.501300	-2.779300	-2.446900
C	1.290000	4.272000	-0.044100
H	1.166200	5.343000	-0.118200
O	-1.822200	-0.035900	-2.544300
H	-2.618900	0.517500	-2.353700
C	-2.921100	-1.257000	0.880500
H	-2.861900	-2.307700	1.176800
C	-5.869000	0.722500	0.678500
H	-6.498500	1.487000	0.207500
H	-6.520300	-0.092000	1.018900
H	-5.397300	1.165500	1.563600
C	-2.533800	1.910400	1.054900
H	-3.383300	1.692900	1.721100
H	-2.162500	2.894400	1.368500
C	-4.817800	0.196900	-0.312700
H	-5.395000	-0.228800	-1.147500

Compound V Electronic Energy: -1710.556079 Hartree

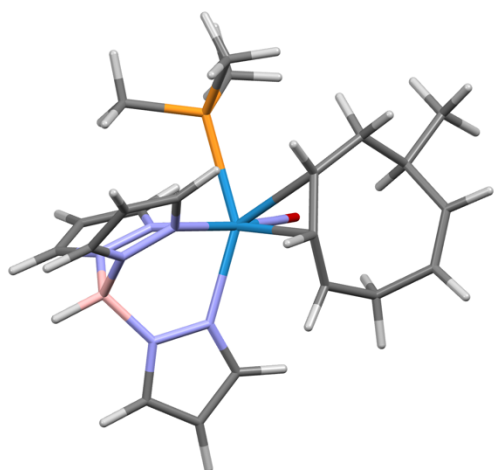


W	-0.142000	-0.030000	-0.057700
P	0.282800	-2.571100	-0.289100
O	-1.587300	0.271600	-2.630300
N	1.675200	-0.064500	-1.311700
N	2.557600	0.242300	1.613200
N	0.667200	2.048800	-0.028800
N	2.888600	0.353600	-0.880100
N	-1.064700	0.176200	-1.555900
N	1.960500	2.299900	0.302700
N	1.313800	-0.300200	1.679600
C	2.217500	3.612200	0.144300
H	3.207800	3.998600	0.350900
C	-1.827700	-0.461300	1.461700
H	-1.326700	-1.030900	2.246000
C	3.269000	-0.097200	2.700500
H	4.286200	0.255300	2.817400
C	1.810500	-0.419000	-2.596600
H	0.959000	-0.795300	-3.152800
C	1.266100	-0.983300	2.834100
H	0.372800	-1.519800	3.129500
C	-2.427700	-1.274500	0.505100
H	-2.241500	-2.333100	0.682800
C	0.127500	3.213800	-0.401800
H	-0.900800	3.255600	-0.736400
C	-1.546500	0.946600	1.425100
H	-0.927200	1.218200	2.287300
C	1.067900	4.239900	-0.297800
H	0.928300	5.288500	-0.519300
B	2.979400	1.145500	0.446900
H	4.087100	1.569000	0.616700
C	-0.579300	-3.344700	-1.695900
H	-1.658400	-3.363100	-1.509100
H	-0.220000	-4.371200	-1.834500
H	-0.388000	-2.767200	-2.607400
C	2.478100	-0.888700	3.514900
H	2.738500	-1.329200	4.466700

C	2.041500	-2.990000	-0.558100
H	2.391900	-2.651400	-1.536700
H	2.144400	-4.080200	-0.500900
H	2.655300	-2.532600	0.227000
C	3.133000	-0.243000	-3.002900
H	3.558800	-0.446700	-3.975200
C	3.777400	0.260600	-1.884600
H	4.803300	0.572800	-1.733600
C	-0.059100	-3.676500	1.132300
H	0.726400	-3.537800	1.882600
H	-0.012800	-4.710300	0.769400
H	-1.030400	-3.513500	1.606500
C	-2.501100	2.094400	1.130300
H	-3.258300	2.093000	1.931500
H	-1.929100	3.015300	1.297700
C	-3.552900	-1.093900	-0.472300
H	-3.174500	-1.057000	-1.505100
H	-4.114000	-2.038800	-0.415000
C	-3.178900	2.207600	-0.204700
H	-2.946100	3.113300	-0.769700
C	-4.041500	1.367100	-0.775700
H	-4.403900	1.639100	-1.768900
C	-4.554800	0.050900	-0.256100
H	-5.403000	-0.216300	-0.902800
C	-5.100100	0.082500	1.168900
H	-5.848100	0.876000	1.280800
H	-5.583800	-0.873500	1.407300
H	-4.323600	0.248400	1.923600



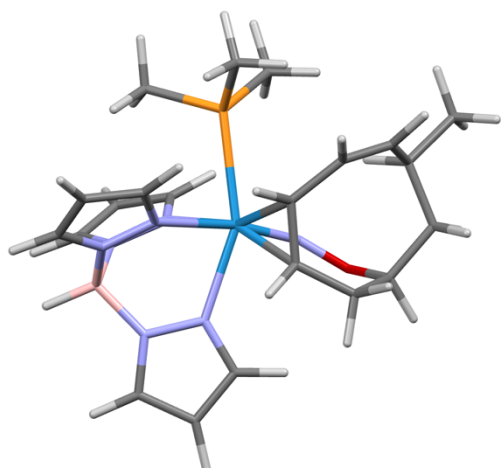
Compound VI Electronic Energy: -1710.564532 Hartree



W	-0.087500	0.130800	-0.009900
P	-0.296900	-2.439500	-0.239300
O	-1.568200	0.578100	-2.539900
N	1.601600	-0.389200	-1.326200
N	2.652400	-0.203100	1.564700
N	1.194700	1.966300	-0.126200
N	2.896400	-0.270500	-0.939000
N	-1.023800	0.417700	-1.481600
N	2.521500	1.893300	0.160300
N	1.321500	-0.440900	1.675700
C	3.092600	3.091800	-0.058500
H	4.154900	3.223900	0.105400
C	-1.502600	0.756700	1.734300
H	-0.834400	0.696000	2.595800
C	3.300000	-0.712900	2.625700
H	4.375200	-0.612700	2.707900
C	1.607100	-0.744200	-2.618900
H	0.674800	-0.888400	-3.152100
C	1.148800	-1.106000	2.828100
H	0.157300	-1.407300	3.147400
C	-2.011300	-0.488400	1.289400
H	-1.744100	-1.274800	1.997300
C	0.949900	3.220200	-0.524900
H	-0.052200	3.518600	-0.810400
C	-2.469100	2.622300	0.159100
H	-2.434200	2.256200	-0.874100
H	-2.226100	3.689600	0.106300
C	-1.425400	1.966100	1.044400
H	-0.730800	2.668200	1.505600
C	2.121100	3.976200	-0.492200
H	2.242200	5.018900	-0.749500
B	3.229600	0.527700	0.346000
H	4.412800	0.674900	0.461000
C	-1.175700	-2.946800	-1.756100
H	-2.186700	-2.524000	-1.770300

H	-1.239900	-4.040600	-1.791800
H	-0.639600	-2.593600	-2.642200
C	2.372000	-1.304500	3.465900
H	2.554500	-1.802200	4.407700
C	1.333100	-3.260800	-0.367900
H	1.870300	-2.955400	-1.269400
H	1.169000	-4.344000	-0.403400
H	1.938000	-3.022000	0.515000
C	2.917500	-0.878400	-3.073600
H	3.248000	-1.161500	-4.062800
C	3.700700	-0.553800	-1.978100
H	4.775800	-0.488300	-1.865400
C	-1.060200	-3.489200	1.050700
H	-0.546500	-3.345600	2.007300
H	-0.935800	-4.532900	0.738800
H	-2.127500	-3.289400	1.176000
C	-3.329600	-0.847300	0.628700
H	-3.194500	-1.776600	0.057100
H	-4.000800	-1.132800	1.458600
C	-4.101500	0.135700	-0.256500
H	-3.446400	0.469100	-1.072000
C	-5.291100	-0.589600	-0.876100
H	-5.886700	0.087500	-1.499700
H	-4.964400	-1.428600	-1.503400
H	-5.951700	-0.990900	-0.094600
C	-3.853300	2.437600	0.718500
H	-4.252200	3.241300	1.337700
C	-4.565700	1.326300	0.532800
H	-5.548100	1.235000	1.004700

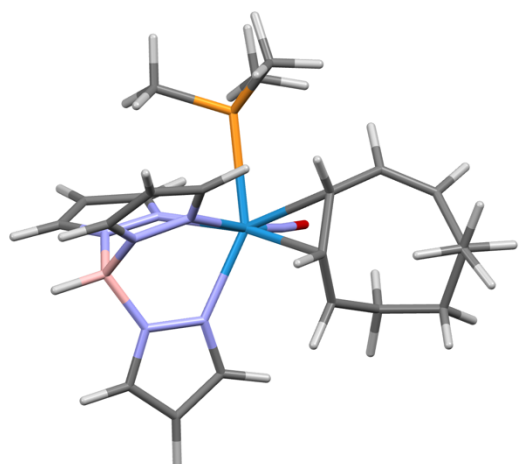
Compound VII Electronic Energy: -1710.544922 Hartree



W	0.024400	-0.138600	0.012300
P	0.596300	2.345300	-0.308700
N	-1.530000	0.660200	1.494100
N	-2.853000	0.500600	1.213600
N	-1.506700	0.355600	-1.514400
N	-1.357400	-1.889700	0.123900
C	-2.579000	0.870000	-3.413000
H	-2.776800	1.151200	-4.437600
C	1.075500	-1.272800	1.589200
H	0.352000	-1.635900	2.324800
N	-2.706000	-1.741300	0.123600
N	-2.839000	0.283500	-1.290600
N	1.144500	-1.008200	-0.995900
C	-3.502400	0.588900	-2.418400
H	-4.585200	0.575400	-2.434000
C	1.469000	0.109100	1.715400
H	0.881200	0.618000	2.479700
C	-3.596000	1.176200	2.103300
H	-4.676600	1.157700	2.033500
C	2.788500	-2.396800	-0.168500
H	2.973000	-3.452000	-0.400100
C	3.931400	0.467600	0.985300
H	4.870800	0.865700	1.380400
C	-1.339000	0.703200	-2.797400
H	-0.340100	0.821800	-3.201800
C	-0.896600	3.330500	-0.703900
H	-1.327700	3.030000	-1.663500
H	-0.620500	4.390400	-0.752300
H	-1.649300	3.193600	0.082100
C	1.324000	3.348300	1.032700
H	0.682500	3.333500	1.919500
H	1.412100	4.382400	0.678500
H	2.315500	2.971200	1.296800
C	-3.295700	-2.949700	0.092600
H	-4.375800	-3.026800	0.091700

C	-1.472900	1.450500	2.579800
H	-0.524000	1.740700	3.011700
C	-1.113800	-3.205000	0.084600
H	-0.097500	-3.576800	0.062100
B	-3.348700	-0.344200	0.026100
H	-4.544400	-0.415900	0.028300
C	-2.750600	1.803200	3.002400
H	-3.020100	2.422300	3.846000
C	1.729500	2.679400	-1.700100
H	2.734900	2.329800	-1.438400
H	1.765600	3.758500	-1.892700
H	1.397100	2.159600	-2.604400
C	-2.311000	-3.920700	0.066200
H	-2.439600	-4.993400	0.039100
O	1.920800	-2.001000	-1.317700
C	2.867800	0.582100	1.791800
H	3.065100	1.096300	2.737400
C	5.291800	0.409700	-1.078700
H	5.358100	0.056000	-2.114300
H	5.297100	1.506900	-1.091500
H	6.198400	0.080300	-0.551500
C	4.045200	-0.129700	-0.386000
H	3.169500	0.166000	-0.983700
C	2.057400	-2.366100	1.181900
H	1.536400	-3.325200	1.284000
H	2.862800	-2.398100	1.933300
C	4.101300	-1.660700	-0.349800
H	4.793600	-1.992900	0.438300
H	4.522700	-2.014800	-1.301800

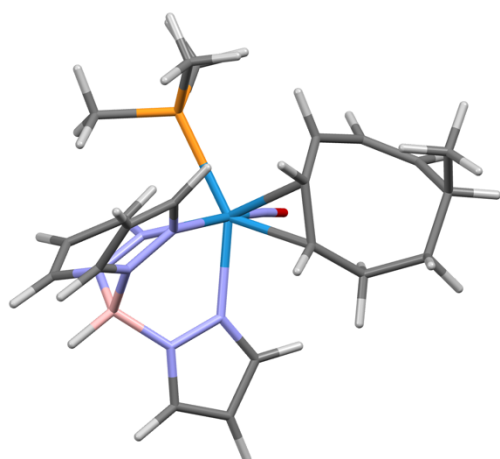
Compound 16K Electronic Energy: -1710.56756 Hartree



W	-0.053800	0.036700	-0.197500
P	0.226900	-2.532900	-0.272100
O	-1.161200	-0.010900	-2.950400
N	1.944000	-0.212700	-1.077700
N	2.266400	0.250300	1.954000
N	0.860500	2.072200	-0.122900
N	3.076100	0.157100	-0.427300
N	-0.733200	0.051400	-1.833200
N	2.093700	2.246100	0.424700
N	1.002000	-0.213400	1.790700
C	2.485900	3.520400	0.249300
H	3.452100	3.845000	0.615000
C	-1.856600	0.577900	1.168700
H	-1.391900	0.782500	2.134300
C	2.729100	-0.092600	3.167800
H	3.726100	0.199700	3.473200
C	2.307100	-0.613800	-2.304400
H	1.560600	-0.948700	-3.014700
C	0.682300	-0.851200	2.926900
H	-0.291700	-1.311900	3.045800
C	-4.266700	-0.759400	-0.408100
H	-4.859000	-1.313000	-1.139200
C	-2.008800	-0.783100	0.777400
H	-1.781100	-1.489600	1.578300
C	0.497600	3.252100	-0.643200
H	-0.456700	3.358900	-1.145400
C	-4.950700	0.456800	0.175600
H	-5.996200	0.389300	-0.155700
C	-3.050000	-1.268100	-0.157300
H	-2.803700	-2.195500	-0.680600
C	-2.959600	1.822600	-0.834900
H	-2.829200	1.058500	-1.603600
H	-2.751500	2.787000	-1.315400
C	-2.015100	1.662100	0.322500
H	-1.642000	2.600000	0.735500

C	-4.426200	1.801700	-0.392300
H	-5.018400	2.070300	-1.276500
H	-4.607600	2.592900	0.349900
C	1.490300	4.205400	-0.425000
H	1.483600	5.245700	-0.717800
B	2.968900	1.038100	0.842500
H	4.052900	1.402400	1.198500
C	-0.162600	-3.264800	-1.896500
H	-1.216300	-3.089600	-2.139100
H	0.025600	-4.344300	-1.861200
H	0.457000	-2.820400	-2.681300
C	1.743000	-0.804100	3.829700
H	1.784100	-1.222300	4.825300
C	1.947500	-3.057400	0.058800
H	2.632400	-2.699100	-0.714500
H	1.976100	-4.153100	0.076700
H	2.270700	-2.677100	1.035100
C	3.689800	-0.523300	-2.449000
H	4.281800	-0.780000	-3.315900
C	4.133500	-0.016300	-1.238500
H	5.127100	0.249400	-0.899500
C	-0.672500	-3.631300	0.879700
H	-0.451000	-3.363500	1.918300
H	-0.324800	-4.655300	0.699400
H	-1.753400	-3.597400	0.717600
C	-5.014300	0.443500	1.705100
H	-5.418300	-0.508900	2.069600
H	-4.041100	0.595700	2.182000
H	-5.677200	1.244500	2.056200

Compound 16K' Electronic Energy: -1710.56446 Hartree

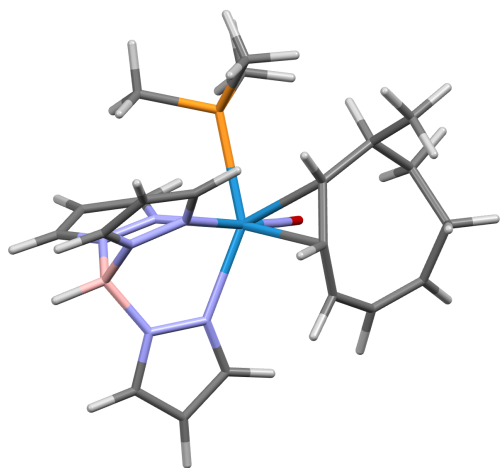


W	-0.064400	-0.046700	-0.184700
P	0.379800	-2.587800	-0.169900
O	-1.085500	0.261500	-2.954500
N	1.943800	-0.139100	-1.095100
N	2.280200	0.422300	1.909600
N	0.708100	2.046800	-0.188300
N	3.056300	0.334300	-0.484700
N	-0.725200	0.108800	-1.823400
N	1.919700	2.354400	0.342200
N	1.053000	-0.149400	1.795100
C	2.200200	3.648900	0.097600
H	3.136700	4.073700	0.437100
C	-1.979400	-0.366700	1.069100
H	-1.647400	-0.862900	1.980700
C	2.788900	0.183800	3.129400
H	3.763400	0.572200	3.398400
C	2.311100	-0.580200	-2.305500
H	1.576600	-1.010500	-2.977600
C	0.808200	-0.747300	2.971900
H	-0.117100	-1.283600	3.143400
C	-4.383300	-0.062400	-1.016200
H	-4.962400	-0.002300	-1.939100
C	-2.427900	-1.202200	0.050000
H	-2.324500	-2.274700	0.219100
C	0.242900	3.156300	-0.771900
H	-0.711600	3.147400	-1.282500
C	-4.932300	0.726400	0.147700
H	-5.908500	1.100000	-0.188900
C	-3.312400	-0.872600	-1.061500
H	-3.131400	-1.427700	-1.983600
C	-2.620600	1.985000	0.124900
H	-2.536500	1.814900	-0.955400
H	-2.239200	2.998500	0.301500
C	-1.738000	1.032400	0.913500
H	-1.329800	1.482000	1.824000

C	-4.098600	1.986600	0.508600
H	-4.552100	2.854400	0.011800
H	-4.197400	2.169100	1.589400
C	1.148400	4.206000	-0.605700
H	1.049900	5.224300	-0.954300
B	2.900500	1.235700	0.766000
H	3.957300	1.693400	1.096000
C	-0.200700	-3.443200	-1.670000
H	-1.294800	-3.409000	-1.715600
H	0.129700	-4.488500	-1.660700
H	0.204100	-2.941400	-2.555900
C	1.876000	-0.567700	3.848600
H	1.967200	-0.928900	4.863000
C	2.155200	-3.007200	-0.061600
H	2.691400	-2.723000	-0.971200
H	2.245300	-4.090400	0.082200
H	2.602900	-2.493900	0.797700
C	3.684100	-0.406700	-2.479900
H	4.279300	-0.669500	-3.342900
C	4.112300	0.188700	-1.304700
H	5.091500	0.533500	-0.996500
C	-0.252500	-3.601100	1.217700
H	0.326700	-3.370900	2.118200
H	-0.095500	-4.656200	0.963200
H	-1.313200	-3.444800	1.430900
C	-5.231900	-0.146100	1.370200
H	-5.829900	-1.022400	1.092300
H	-4.327200	-0.502900	1.873300
H	-5.805900	0.432800	2.104100



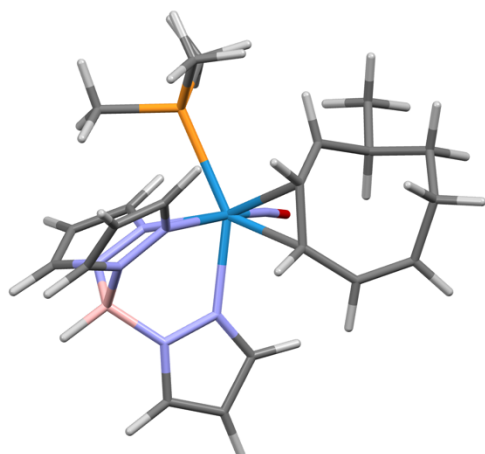
Compound 19T Electronic Energy: -1710.568368 Hartree



W	0.115600	0.178200	0.065500
P	0.390600	-2.314600	0.690700
O	1.381900	1.093200	2.588500
N	-1.663600	-0.253700	1.289000
N	-2.419800	-0.607100	-1.685800
N	-1.287700	1.914800	-0.248400
N	-2.915400	-0.297100	0.768800
N	0.910500	0.748700	1.541700
N	-2.569400	1.682700	-0.644300
N	-1.069300	-0.730700	-1.650600
C	-3.254000	2.840900	-0.651000
H	-4.300700	2.849200	-0.928400
C	1.659500	0.750300	-1.608000
H	1.093000	0.611000	-2.531800
C	-2.918900	-1.296700	-2.725300
H	-3.985500	-1.305100	-2.912300
C	-1.781000	-0.399300	2.616100
H	-0.900800	-0.388900	3.248300
C	-0.733700	-1.509000	-2.690500
H	0.304000	-1.753500	-2.885100
C	2.075100	-0.468500	-0.976300
H	1.849800	-1.297300	-1.653500
C	-1.192600	3.227800	-0.005600
H	-0.261900	3.657000	0.341900
C	4.450300	1.549800	-0.118600
H	5.487100	1.814900	0.112500
C	1.539100	2.045000	-1.103500
H	0.844500	2.650500	-1.689500
C	-2.408300	3.861700	-0.257400
H	-2.637300	4.913500	-0.161700
B	-3.163700	0.252100	-0.658500
H	-4.336400	0.282600	-0.901200
C	1.171900	-2.572700	2.319100
H	2.159500	-2.099500	2.346800
H	1.278000	-3.647500	2.508100

H	0.553200	-2.132900	3.107600
C	-1.869200	-1.895800	-3.400100
H	-1.917800	-2.517100	-4.283000
C	-1.207700	-3.196600	0.820800
H	-1.827400	-2.799400	1.628600
H	-0.999300	-4.253600	1.023200
H	-1.751000	-3.118600	-0.128400
C	-3.121700	-0.556100	2.963800
H	-3.535800	-0.700600	3.951500
C	-3.805100	-0.470100	1.761900
H	-4.864800	-0.503900	1.541200
C	1.276700	-3.488400	-0.399300
H	0.818000	-3.496600	-1.393900
H	1.170400	-4.486100	0.042300
H	2.341400	-3.264000	-0.492300
C	2.287700	2.842000	-0.147400
C	3.557000	2.679100	0.256100
H	1.768900	3.739000	0.192600
H	3.962600	3.436400	0.927700
C	4.060800	0.248100	0.607900
H	3.428200	0.480700	1.473600
H	4.966900	-0.222000	1.012900
C	3.391600	-0.800700	-0.271600
H	3.191900	-1.651200	0.396200
H	4.407000	1.393500	-1.206900
C	4.369300	-1.312500	-1.335500
H	5.324700	-1.600800	-0.879300
H	3.966600	-2.189900	-1.856900
H	4.575800	-0.550000	-2.097700

Compound 19T' Electronic Energy: -1710.573544 Hartree



W	-0.123100	0.024100	-0.092300
P	-0.012400	-2.552000	0.091200
O	-1.306300	0.350600	-2.790600
N	1.726000	-0.418500	-1.208200
N	2.513900	0.311700	1.663200
N	0.896500	1.981100	-0.356500
N	2.956800	-0.045400	-0.784100
N	-0.909900	0.193300	-1.672500
N	2.195300	2.164300	-0.007800
N	1.223200	-0.105800	1.741100
C	2.595800	3.387900	-0.403900
H	3.613700	3.709800	-0.221800
C	-1.878100	0.012900	1.409400
H	-1.529000	-0.561500	2.266700
C	3.140400	0.097800	2.831500
H	4.180100	0.376200	2.950300
C	1.878700	-1.010500	-2.400800
H	1.018000	-1.396400	-2.935600
C	1.059500	-0.580200	2.986800
H	0.106300	-0.975700	3.314600
C	-2.573900	-0.704400	0.440800
H	-2.699600	-1.770300	0.647900
C	0.495200	3.094000	-0.980200
H	-0.513000	3.170100	-1.369200
C	-4.533800	1.414400	1.176600
H	-5.491700	1.853700	1.480700
C	-1.431200	1.363500	1.230100
H	-0.745100	1.707300	2.011800
C	1.535600	4.024200	-1.022500
H	1.516300	5.017600	-1.447800
B	3.077300	0.956800	0.390400
H	4.216100	1.291500	0.551100
C	-0.783100	-3.465800	-1.284200
H	-1.873200	-3.390000	-1.208000
H	-0.491600	-4.521600	-1.234200

H	-0.464700	-3.044700	-2.244200
C	2.242900	-0.477200	3.714000
H	2.417600	-0.773700	4.738400
C	1.706700	-3.172500	0.141300
H	2.216900	-3.017300	-0.813400
H	1.677400	-4.246900	0.358200
H	2.263100	-2.663200	0.936900
C	3.228600	-1.038400	-2.749400
H	3.671900	-1.454100	-3.643000
C	3.873200	-0.403400	-1.700200
H	4.918500	-0.166800	-1.544600
C	-0.680000	-3.368900	1.586200
H	-0.061300	-3.106500	2.450600
H	-0.618800	-4.452600	1.429000
H	-1.719400	-3.103600	1.797200
C	-2.274400	2.449500	0.696600
C	-3.616300	2.493800	0.684100
H	-1.735500	3.338000	0.365600
H	-4.083800	3.392700	0.278900
C	-4.806500	0.315000	0.143000
H	-5.488700	0.690800	-0.633100
H	-5.318600	-0.528600	0.629900
C	-3.547000	-0.184100	-0.583000
H	-3.130800	0.681800	-1.107000
C	-3.900200	-1.258600	-1.598800
H	-4.642900	-0.883900	-2.312900
H	-4.328700	-2.140000	-1.101100
H	-4.106100	0.957800	2.080200
H	-3.021300	-1.582300	-2.168800

## Crystallography.

### Structure Report for mo\_harman\_mne\_octatetraene\_1\_0

A red, plate-shaped crystal of mo\_harman\_mne\_octatetraene\_1\_0 was coated with Paratone oil and mounted on a MiTeGen micromount. crystallized from hexanes filtrate. Data were collected at 100.00 K on a Bruker D8 VENTURE dual wavelength Mo/Cu Kappa four-circle diffractometer with a PHOTON III detector. The diffractometer was equipped with an Oxford Cryostream 800Plus low temperature device and used Mo  $K_{\alpha}$  radiation ( $\lambda = 0.71073\text{\AA}$ ) from an Incoatec I\ms 3.0 microfocus sealed X-ray tube with a HELIOS double bounce multilayer mirror as monochromator.

Data collection and processing were done within the Bruker APEX5 software suite.<sup>[1]</sup> All data were integrated with SAINT 8.40B using a narrow-frame algorithm and a Multi-Scan absorption correction using was applied.<sup>[2]</sup> Using Olex2 as a graphical interface,<sup>[3]</sup> the structure was solved by dual methods with SHELXT 2018/2 and refined by full-matrix least-squares methods against  $F^2$  using SHELXL 2018/3.<sup>[4,5]</sup> All non-hydrogen atoms were refined with anisotropic displacement parameters. All hydrogen atoms were refined with isotropic displacement parameters. Some of their coordinates were refined freely and some on calculated positions using a riding model with their  $U_{\text{iso}}$  values constrained to 1.5 times the  $U_{\text{eq}}$  of their pivot atoms for terminal  $\text{sp}^3$  carbon atoms and 1.2 times for all other carbon atoms.

This report and the CIF file were generated using FinalCif.<sup>[6]</sup>

Table 1. Crystal data and structure refinement for mo\_harman\_mne\_octatetraene\_1\_0

CCDC number	
Empirical formula	C <sub>20</sub> H <sub>27</sub> BN <sub>7</sub> OPW
Formula weight	607.11
Temperature [K]	100.00
Crystal system	monoclinic
Space group (numb	<i>P</i> 2 <sub>1</sub> / <i>c</i> (14)
<i>a</i> [Å]	12.2214(5)
<i>b</i> [Å]	10.1317(4)
<i>c</i> [Å]	19.2532(6)
$\alpha$ [°]	90
$\beta$ [°]	105.3930(10)
$\gamma$ [°]	90
Volume [Å <sup>3</sup> ]	2298.48(15)
<i>Z</i>	4
$\rho_{\text{calc}}$ [gcm <sup>-3</sup> ]	1.754
$\mu$ [mm <sup>-1</sup> ]	5.122
<i>F</i> (000)	1192
Crystal size [mm <sup>3</sup> ]	0.048×0.076×0.124
Crystal colour	red
Crystal shape	plate
Radiation	Mo <i>K</i> $\alpha$ ( $\lambda$ =0.71073 Å)
2 $\theta$ range [°]	4.58 to 55.08 (0.77 Å)
Index ranges	−15 ≤ <i>h</i> ≤ 15 −13 ≤ <i>k</i> ≤ 13 −25 ≤ <i>l</i> ≤ 23
Reflections collected	67248
Independent reflections	5292 <i>R</i> <sub>int</sub> = 0.0595 <i>R</i> <sub>sigma</sub> = 0.0238
Completeness to $\theta$ = 25.242°	99.9
Data / Restraints / Parameters	5292 / 0 / 295
Goodness-of-fit on <i>F</i> <sup>2</sup>	1.099
Final <i>R</i> indexes [ <i>I</i> ≥2 $\sigma$ ( <i>I</i> )]	<i>R</i> <sub>1</sub> = 0.0231 <i>wR</i> <sub>2</sub> = 0.0482
Final <i>R</i> indexes [all data]	<i>R</i> <sub>1</sub> = 0.0278 <i>wR</i> <sub>2</sub> = 0.0498
Largest peak/hole [eÅ <sup>-3</sup> ]	0.86/−1.50

Table 2. Atomic coordinates and  $U_{eq}$  [Å<sup>2</sup>] for mo\_harman\_mne\_octatetraene\_1\_0

Atom	x	y	z	$U_{eq}$
W1	0.24683(2)	0.63750(2)	0.32292(2)	0.01100(4)
P1	0.26841(7)	0.87903(8)	0.29640(4)	0.01500(16)
O1	0.0496(2)	0.5909(3)	0.19500(13)	0.0306(6)
N1	0.3818(2)	0.6742(3)	0.42522(13)	0.0145(5)
N2	0.3601(2)	0.6558(3)	0.49064(13)	0.0152(5)
N3	0.1312(2)	0.7243(3)	0.38139(13)	0.0146(5)
N4	0.1545(2)	0.7192(3)	0.45491(14)	0.0155(5)
N5	0.2033(2)	0.4707(3)	0.38485(13)	0.0146(5)
N6	0.2064(2)	0.4843(3)	0.45608(13)	0.0147(5)
N7	0.1321(2)	0.6090(3)	0.24581(14)	0.0166(5)
C1	0.4918(3)	0.7065(3)	0.43900(17)	0.0179(6)
H1	0.530434	0.724882	0.403276	0.021
C2	0.5417(3)	0.7093(3)	0.51286(17)	0.0203(7)
H2	0.618306	0.729197	0.536930	0.024
C3	0.4554(3)	0.6769(3)	0.54339(17)	0.0186(7)
H3	0.462119	0.670394	0.593573	0.022
C4	0.0365(3)	0.7967(3)	0.35886(19)	0.0202(7)
H4	-0.000023	0.816088	0.309922	0.024
C5	-0.0006(3)	0.8392(3)	0.4176(2)	0.0240(7)
H5	-0.064919	0.892555	0.416737	0.029
C6	0.0757(3)	0.7874(3)	0.47682(19)	0.0214(7)
H6	0.073202	0.798128	0.525389	0.026
C7	0.1504(3)	0.3563(3)	0.36307(17)	0.0177(6)
H7	0.135712	0.322009	0.315555	0.021
C8	0.1201(3)	0.2945(3)	0.41996(18)	0.0205(7)
H8	0.082920	0.211998	0.419326	0.025

C9	0.1557(3)	0.3795(3)	0.47712(17) )	0.0181(6)
H9	0.146032	0.366286	0.523990	0.022
C10	0.3789(3)	0.6195(3)	0.26045(17) )	0.0154(6)
H10	0.440(3)	0.672(3)	0.2836(18)	0.015(9)
C11	0.3736(3)	0.4984(3)	0.29745(16) )	0.0154(6)
H11	0.426(3)	0.497(3)	0.3433(19)	0.016(9)
C12	0.3351(3)	0.3666(3)	0.27390(18) )	0.0203(7)
H12	0.330673	0.312003	0.313164	0.024
C13	0.3038(3)	0.3012(3)	0.21056(19) )	0.0220(7)
H13	0.281971	0.212620	0.215915	0.026
C14	0.2959(3)	0.3350(3)	0.13718(18) )	0.0215(7)
H14	0.287217	0.259972	0.106631	0.026
C15	0.2982(3)	0.4502(4)	0.10130(18) )	0.0235(7)
H15	0.292254	0.437194	0.051570	0.028
C16	0.3074(3)	0.5866(4)	0.12142(17) )	0.0223(7)
H16	0.285675	0.643663	0.080914	0.027
C17	0.3395(3)	0.6535(3)	0.18401(18) )	0.0213(7)
H17	0.335457	0.746253	0.176657	0.026
C18	0.4029(3)	0.9412(3)	0.28584(19) )	0.0218(7)
H18A	0.421214	0.896381	0.245236	0.033
H18B	0.462970	0.924198	0.330000	0.033
H18C	0.396788	1.036363	0.276606	0.033
C19	0.2529(3)	0.9897(4)	0.3679(2)	0.0318(9)
H19A	0.303503	0.961129	0.413904	0.048
H19B	0.174153	0.987705	0.370973	0.048
H19C	0.272700	1.079811	0.357206	0.048
C20	0.1625(3)	0.9377(4)	0.2172(2)	0.0300(9)
H20A	0.086821	0.929363	0.225033	0.045
H20B	0.166348	0.884813	0.175262	0.045
H20C	0.177360	1.030477	0.208547	0.045
B1	0.2422(3)	0.6162(3)	0.49569(19) )	0.0156(7)
H1A	0.246(3)	0.607(4)	0.5525(19)	0.021(9)

$U_{eq}$  is defined as 1/3 of the trace of the orthogonalized  $U_{ij}$  tensor.



Table 3. Anisotropic displacement parameters ( $\text{\AA}^2$ ) for mo\_harman\_mne\_octatetraene\_1\_0. The anisotropic displacement factor exponent takes the form:  $-2\pi^2 [h^2(a^*)^2U_{11} + k^2(b^*)^2U_{22} + \dots + 2hka^*b^*U_{12}]$

Atom	$U_{11}$	$U_{22}$	$U_{33}$	$U_{23}$	$U_{13}$	$U_{12}$
W1	0.01149(6)	0.01027(6)	0.01120(6)	0.00163(4)	0.00295(4)	0.00011(5)
P1	0.0133(4)	0.0108(4)	0.0208(4)	0.0017(3)	0.0044(3)	-0.0003(3)
O1	0.0283(14)	0.0298(14)	0.0241(13)	-0.0021(11)	-0.0099(11)	-0.0083(11)
N1	0.0145(13)	0.0161(13)	0.0134(12)	0.0013(10)	0.0045(10)	-0.0007(10)
N2	0.0155(13)	0.0177(14)	0.0130(12)	0.0004(10)	0.0050(10)	0.0021(10)
N3	0.0114(13)	0.0165(13)	0.0156(12)	0.0002(10)	0.0032(10)	0.0004(10)
N4	0.0141(13)	0.0170(13)	0.0169(13)	0.0007(10)	0.0067(10)	-0.0007(10)
N5	0.0145(13)	0.0159(13)	0.0136(12)	0.0022(10)	0.0042(10)	0.0007(10)
N6	0.0134(13)	0.0179(14)	0.0132(12)	0.0040(10)	0.0039(10)	0.0004(10)
N7	0.0201(14)	0.0124(13)	0.0157(12)	0.0011(10)	0.0022(11)	-0.0009(10)
C1	0.0122(15)	0.0212(17)	0.0203(15)	0.0018(13)	0.0043(12)	0.0021(12)
C2	0.0117(15)	0.0247(18)	0.0213(16)	-0.0013(13)	-0.0013(12)	0.0009(13)
C3	0.0179(16)	0.0200(16)	0.0155(15)	0.0010(12)	0.0003(12)	0.0038(13)
C4	0.0106(15)	0.0214(17)	0.0278(17)	0.0045(14)	0.0040(13)	0.0015(13)
C5	0.0142(16)	0.0233(18)	0.037(2)	0.0044(15)	0.0113(14)	0.0056(13)
C6	0.0185(17)	0.0232(18)	0.0267(17)	-0.0009(14)	0.0135(14)	0.0005(13)
C7	0.0163(15)	0.0150(15)	0.0209(15)	0.0006(12)	0.0032(12)	0.0004(13)
C8	0.0190(17)	0.0159(16)	0.0293(18)	0.0030(13)	0.0110(14)	-0.0011(13)
C9	0.0171(15)	0.0172(16)	0.0215(16)	0.0075(12)	0.0077(12)	0.0021(12)
C10	0.0178(15)	0.0117(15)	0.0187(15)	-0.0008(12)	0.0081(12)	0.0012(12)
C11	0.0198(16)	0.0145(15)	0.0129(14)	-0.0002(12)	0.0061(12)	0.0009(12)
C12	0.0225(17)	0.0141(15)	0.0261(17)	0.0057(13)	0.0094(13)	0.0035(13)
C13	0.0149(16)	0.0170(16)	0.0336(19)	0.0006(14)	0.0056(14)	0.0011(13)
C14	0.0127(15)	0.0241(18)	0.0267(17)	-0.0096(14)	0.0033(13)	-0.0018(13)
C15	0.0155(16)	0.037(2)	0.0168(15)	-0.0066(14)	0.0027(13)	-0.0022(14)
C16	0.0224(17)	0.0299(18)	0.0154(15)	0.0051(14)	0.0064(13)	0.0027(15)
C17	0.0299(18)	0.0149(16)	0.0235(16)	0.0041(13)	0.0148(14)	0.0060(14)
C18	0.0201(17)	0.0156(16)	0.0298(18)	0.0042(13)	0.0072(14)	-0.0022(13)
C19	0.035(2)	0.0202(18)	0.046(2)	-0.0157(16)	0.0222(18)	-0.0070(16)
C20	0.0228(19)	0.0219(19)	0.039(2)	0.0158(16)	-0.0026(16)	-0.0022(14)

B1	0.0182(17)	0.0159(18)	0.0141(16)	0.0014(13)	0.0064(13)	0.0026(14)
----	------------	------------	------------	------------	------------	------------

Table 4. Bond lengths and angles for mo\_harman\_mne\_octatetraene\_1\_0

Atom–Atom	Length [Å]		
W1–P1	2.5279(8)	C12–C13	1.351(5)
W1–N1	2.239(3)	C13–H13	0.9500
W1–N3	2.209(3)	C13–C14	1.432(5)
W1–N5	2.213(3)	C14–H14	0.9500
W1–N7	1.774(3)	C14–C15	1.360(5)
W1–C10	2.262(3)	C15–H15	0.9500
W1–C11	2.243(3)	C15–C16	1.432(5)
P1–C18	1.821(3)	C16–H16	0.9500
P1–C19	1.824(4)	C16–C17	1.347(5)
P1–C20	1.818(3)	C17–H17	0.9500
O1–N7	1.218(3)	C18–H18A	0.9800
N1–N2	1.367(3)	C18–H18B	0.9800
N1–C1	1.341(4)	C18–H18C	0.9800
N2–C3	1.344(4)	C19–H19A	0.9800
N2–B1	1.523(4)	C19–H19B	0.9800
N3–N4	1.369(3)	C19–H19C	0.9800
N3–C4	1.341(4)	C20–H20A	0.9800
N4–C6	1.341(4)	C20–H20B	0.9800
N4–B1	1.552(4)	C20–H20C	0.9800
N5–N6	1.369(3)	B1–H1A	1.09(4)
N5–C7	1.339(4)		
N6–C9	1.346(4)	<b>Atom–Atom–</b>	<b>Angle [°]</b>
N6–B1	1.543(4)	<b>Atom</b>	
C1–H1	0.9500	N1–W1–P1	85.70(7)
C1–C2	1.391(4)	N1–W1–C10	91.04(11)
C2–H2	0.9500	N1–W1–C11	84.63(10)
C2–C3	1.376(5)	N3–W1–P1	80.36(7)
C3–H3	0.9500	N3–W1–N1	84.67(9)
C4–H4	0.9500	N3–W1–N5	75.64(9)
C4–C5	1.393(5)	N3–W1–C10	161.12(10)
C5–H5	0.9500	N3–W1–C11	159.04(10)
C5–C6	1.372(5)	N5–W1–P1	154.29(7)
C6–H6	0.9500	N5–W1–N1	83.06(9)
C7–H7	0.9500	N5–W1–C10	122.16(10)
C7–C8	1.395(4)	N5–W1–C11	85.21(10)
C8–H8	0.9500	N7–W1–P1	95.18(8)
C8–C9	1.373(5)	N7–W1–N1	175.59(11)
C9–H9	0.9500	N7–W1–N3	91.21(11)
C10–H10	0.93(4)	N7–W1–N5	94.41(11)
C10–C11	1.429(4)	N7–W1–C10	93.37(12)
C10–C17	1.463(4)	N7–W1–C11	98.79(12)
C11–H11	0.95(4)	C10–W1–P1	80.99(8)
C11–C12	1.447(4)	C11–W1–P1	116.69(8)
C12–H12	0.9500	C11–W1–C10	36.98(11)
		C18–P1–W1	120.19(11)

C18-P1-C19	98.59(17)
C19-P1-W1	113.92(13)
C20-P1-W1	113.37(12)
C20-P1-C18	104.82(17)
C20-P1-C19	103.8(2)
N2-N1-W1	120.67(19)
C1-N1-W1	132.9(2)
C1-N1-N2	106.3(2)
N1-N2-B1	120.9(2)
C3-N2-N1	109.5(3)
C3-N2-B1	129.7(3)
N4-N3-W1	121.74(19)
C4-N3-W1	131.8(2)
C4-N3-N4	106.3(3)
N3-N4-B1	118.4(2)
C6-N4-N3	109.6(3)
C6-N4-B1	130.1(3)
N6-N5-W1	121.07(19)
C7-N5-W1	131.1(2)
C7-N5-N6	106.5(2)
N5-N6-B1	120.8(2)
C9-N6-N5	109.2(3)
C9-N6-B1	128.9(3)
O1-N7-W1	176.6(3)
N1-C1-H1	124.7
N1-C1-C2	110.6(3)
C2-C1-H1	124.7
C1-C2-H2	127.6
C3-C2-C1	104.8(3)
C3-C2-H2	127.6
N2-C3-C2	108.9(3)
N2-C3-H3	125.6
C2-C3-H3	125.6
N3-C4-H4	124.9
N3-C4-C5	110.2(3)
C5-C4-H4	124.9
C4-C5-H5	127.5
C6-C5-C4	105.1(3)
C6-C5-H5	127.5
N4-C6-C5	108.8(3)
N4-C6-H6	125.6
C5-C6-H6	125.6
N5-C7-H7	124.8
N5-C7-C8	110.4(3)
C8-C7-H7	124.8
C7-C8-H8	127.6
C9-C8-C7	104.7(3)
C9-C8-H8	127.6

N6-C9-C8	109.1(3)
N6-C9-H9	125.5
C8-C9-H9	125.5
W1-C10-H10	107(2)
C11-C10-W1	70.78(17)
C11-C10-H10	113(2)
C11-C10-C17	131.1(3)
C17-C10-W1	115.1(2)
C17-C10-H10	111(2)
W1-C11-H11	98(2)
C10-C11-W1	72.23(18)
C10-C11-H11	111(2)
C10-C11-C12	133.6(3)
C12-C11-W1	117.5(2)
C12-C11-H11	111(2)
C11-C12-H12	111.7
C13-C12-C11	136.5(3)
C13-C12-H12	111.7
C12-C13-H13	112.7
C12-C13-C14	134.6(3)
C14-C13-H13	112.7
C13-C14-H14	112.7
C15-C14-C13	134.5(3)
C15-C14-H14	112.7
C14-C15-H15	112.7
C14-C15-C16	134.6(3)
C16-C15-H15	112.7
C15-C16-H16	112.3
C17-C16-C15	135.3(3)
C17-C16-H16	112.3
C10-C17-H17	111.9
C16-C17-C10	136.2(3)
C16-C17-H17	111.9
P1-C18-H18A	109.5
P1-C18-H18B	109.5
P1-C18-H18C	109.5
H18A-C18-H18B	109.5
H18A-C18-H18C	109.5
H18B-C18-H18C	109.5
P1-C19-H19A	109.5
P1-C19-H19B	109.5
P1-C19-H19C	109.5
H19A-C19-H19B	109.5
H19A-C19-H19C	109.5

H19B–C19– H19C	109.5
P1–C20–H20A	109.5
P1–C20–H20B	109.5
P1–C20–H20C	109.5
H20A–C20– H20B	109.5
H20A–C20– H20C	109.5

H20B–C20– H20C	109.5
N2–B1–N4	109.2(3)
N2–B1–N6	110.2(3)
N2–B1–H1A	107(2)
N4–B1–H1A	114.2(19)
N6–B1–N4	105.4(2)
N6–B1–H1A	111(2)

Table 5. Torsion angles for mo\_harman\_mne\_octatetraene\_1\_0

Atom–Atom– Atom–Atom	Torsion Angle [°]
W1–N1–N2–C3	176.6(2)
W1–N1–N2–B1	–2.9(4)
W1–N1–C1–C2	–175.9(2)
W1–N3–N4–C6	175.3(2)
W1–N3–N4–B1	–18.6(3)
W1–N3–C4–C5	–174.3(2)
W1–N5–N6–C9	168.0(2)
W1–N5–N6–B1	–0.9(4)
W1–N5–C7–C8	–167.1(2)
W1–C10–C11–C12	111.4(4)
W1–C10–C17–C16	–102.0(4)
W1–C11–C12–C13	101.7(4)
N1–N2–C3–C2	–0.1(4)
N1–N2–B1–N4	–56.4(4)
N1–N2–B1–N6	58.9(3)
N1–C1–C2–C3	0.0(4)
N2–N1–C1–C2	0.0(4)
N3–N4–C6–C5	–0.3(4)
N3–N4–B1–N2	69.5(3)
N3–N4–B1–N6	–48.9(3)
N3–C4–C5–C6	–0.8(4)
N4–N3–C4–C5	0.6(4)
N5–N6–C9–C8	0.9(4)
N5–N6–B1–N2	–57.0(3)
N5–N6–B1–N4	60.6(3)
N5–C7–C8–C9	1.1(4)
N6–N5–C7–C8	–0.6(3)

C1–N1–N2–C3	0.1(3)
C1–N1–N2–B1	–179.3(3)
C1–C2–C3–N2	0.1(4)
C3–N2–B1–N4	124.3(3)
C3–N2–B1–N6	–120.4(3)
C4–N3–N4–C6	–0.2(3)
C4–N3–N4–B1	165.8(3)
C4–C5–C6–N4	0.6(4)
C6–N4–B1–N2	–127.8(3)
C6–N4–B1–N6	113.8(3)
C7–N5–N6–C9	–0.2(3)
C7–N5–N6–B1	–169.1(3)
C7–C8–C9–N6	–1.2(4)
C9–N6–B1–N2	136.5(3)
C9–N6–B1–N4	–105.9(3)
C10–C11–C12–C13	10.5(7)
C11–C10–C17–C16	–16.2(7)
C11–C12–C13–C14	0.7(7)
C12–C13–C14–C15	–13.5(7)
C13–C14–C15–C16	–1.3(7)
C14–C15–C16–C17	16.1(7)
C15–C16–C17–C10	–0.6(7)
C17–C10–C11–W1	–107.0(4)
C17–C10–C11–C12	4.4(6)
B1–N2–C3–C2	179.2(3)
B1–N4–C6–C5	–164.2(3)
B1–N6–C9–C8	168.6(3)

## Structure Report for mo\_harman\_mne\_nb3\_303b\_0m

A yellow, plate-shaped crystal of mo\_harman\_mne\_nb3\_303b\_0m was coated with Paratone oil and mounted on a MiTeGen micromount. crystallized from acetonitrile. Data were collected at 100(2) K on a Bruker D8 VENTURE dual wavelength Mo/Cu Kappa four-circle diffractometer with a PHOTON III detector. The diffractometer was equipped with an Oxford Cryostream 800Plus low temperature device and used Mo  $K_{\alpha}$  radiation ( $\lambda = 0.71073\text{\AA}$ ) from an Incoatec  $\lambda/\text{ms}$  3.0 microfocus sealed X-ray tube with a HELIOS double bounce multilayer mirror as monochromator.

Data collection and processing were done within the Bruker APEX5 software suite.<sup>[1]</sup> All data were integrated with SAINT 8.40B using a narrow-frame algorithm and a Multi-Scan absorption correction using was applied.<sup>[2]</sup> Using [Unknown program in \_computing\_structure\_refinement] as a graphical interface,<sup>[3]</sup> the structure was solved by direct methods with SHELXT and refined by full-matrix least-squares methods against  $F^2$  using SHELXL-2019/2.<sup>[4,5]</sup> All non-hydrogen atoms were refined with anisotropic displacement parameters. All C-bound hydrogen atoms were refined isotropic on calculated positions using a riding model with their  $U_{\text{iso}}$  values constrained to 1.5 times the  $U_{\text{eq}}$  of their pivot atoms for terminal  $\text{sp}^3$  carbon atoms and 1.2 times for all other carbon atoms.

This report and the CIF file were generated using FinalCif.<sup>[6]</sup>

Table 1. Crystal data and structure refinement for mo\_harman\_mne\_nb3\_303b\_0m

CCDC number	
Empirical formula	$\text{C}_{21}\text{H}_{28}\text{BF}_3\text{N}_7\text{O}_4\text{PSW}$
Formula weight	757.19
Temperature [K]	100(2)
Crystal system	triclinic
Space group (number)	$P\bar{1}$ (2)
$a$ [ $\text{\AA}$ ]	9.5771(5)
$b$ [ $\text{\AA}$ ]	10.7462(5)
$c$ [ $\text{\AA}$ ]	13.8016(7)
$\alpha$ [ $^\circ$ ]	93.960(2)

$\beta$ [°]	109.386(2)
$\gamma$ [°]	91.001(2)
Volume [Å <sup>3</sup> ]	1335.46(12)
Z	2
$\rho_{\text{calc}}$ [gcm <sup>-3</sup> ]	1.883
$\mu$ [mm <sup>-1</sup> ]	4.527
$F(000)$	744
Crystal size [mm <sup>3</sup> ]	0.050×0.069×0.089
Crystal colour	yellow
Crystal shape	plate
Radiation	Mo $K_{\alpha}$ ( $\lambda=0.71073$ Å)
2 $\theta$ range [°]	3.80 to 56.56 (0.75 Å)
Index ranges	$-12 \leq h \leq 12$ $-14 \leq k \leq 14$ $-18 \leq l \leq 14$
Reflections collected	36468
Independent reflections	6614 $R_{\text{int}} = 0.0378$ $R_{\text{sigma}} = 0.0298$
Completeness to $\theta = 25.242^\circ$	99.7
Data / Restraints / Parameters	6614 / 0 / 355
Goodness-of-fit on $F^2$	1.046
Final $R$ indexes [ $I \geq 2\sigma(I)$ ]	$R_1 = 0.0223$ $wR_2 = 0.0511$
Final $R$ indexes [all data]	$R_1 = 0.0259$ $wR_2 = 0.0528$
Largest peak/hole [eÅ <sup>-3</sup> ]	1.40/−0.53

Table 2. Atomic coordinates and  $U_{eq}$  [ $\text{\AA}^2$ ] for mo\_harman\_mne\_nb3\_303b\_0m

Atom	x	y	z	$U_{eq}$
W1	0.51225(2)	0.26271(2)	0.82841(2)	0.01341(4)
P1	0.31686(7)	0.26396(6)	0.65066(6)	0.01549(14)
O1	0.3462(3)	0.4525(2)	0.90808(18)	0.0279(5)
N1	0.6222(2)	0.1291(2)	0.74868(19)	0.0162(5)
N2	0.7484(2)	0.1650(2)	0.73046(19)	0.0180(5)
N3	0.5963(2)	0.4103(2)	0.76103(19)	0.0169(5)
N4	0.7193(3)	0.3988(2)	0.73235(19)	0.0178(5)
N5	0.7443(2)	0.2975(2)	0.93350(19)	0.0157(4)
N6	0.8559(2)	0.3038(2)	0.89165(19)	0.0170(5)
N7	0.4163(3)	0.3767(2)	0.87928(19)	0.0187(5)
C1	0.5924(3)	0.0092(3)	0.7110(2)	0.0218(6)
H1	0.509728	-0.040001	0.712214	0.026
C2	0.6991(3)	-0.0327(3)	0.6702(3)	0.0256(6)
H2	0.704211	-0.113495	0.639298	0.031
C3	0.7952(3)	0.0679(3)	0.6844(2)	0.0224(6)
H3	0.881374	0.069004	0.664751	0.027
C4	0.5475(3)	0.5251(2)	0.7410(2)	0.0192(6)
H4	0.463129	0.558266	0.753365	0.023
C5	0.6392(3)	0.5878(3)	0.6993(2)	0.0231(6)
H5	0.630035	0.670237	0.677682	0.028
C6	0.7468(3)	0.5052(3)	0.6957(2)	0.0217(6)
H6	0.826774	0.521209	0.671355	0.026
C7	0.8073(3)	0.3266(3)	1.0347(2)	0.0190(6)
H7	0.755652	0.330691	1.082868	0.023
C8	0.9586(3)	0.3499(3)	1.0598(2)	0.0240(6)
H8	1.028862	0.371015	1.126240	0.029
C9	0.9849(3)	0.3359(3)	0.9678(2)	0.0209(6)
H9	1.078537	0.346914	0.959112	0.025
C10	0.3453(3)	0.1010(2)	0.8188(2)	0.0180(5)
H10	0.332906	0.036756	0.760323	0.022
C11	0.4743(3)	0.0884(2)	0.9057(2)	0.0183(5)
H11	0.536496	0.015326	0.902909	0.022
C12	0.5157(3)	0.1659(3)	0.9953(2)	0.0193(6)
H12	0.618474	0.151721	1.041471	0.023
C13	0.4270(3)	0.2302(3)	1.0508(2)	0.0211(6)
H13	0.462817	0.311336	1.082036	0.025
C14	0.3015(3)	0.1877(3)	1.0622(2)	0.0237(6)
H14	0.269800	0.234191	1.111614	0.028
C15	0.2069(3)	0.0782(3)	1.0081(3)	0.0239(6)
H15	0.176049	0.022184	1.048088	0.029
C16	0.1618(3)	0.0524(3)	0.9065(3)	0.0232(6)
H16	0.102713	-0.021649	0.877827	0.028

C17	0.2004(3)	0.1357(3)	0.8350(2)	0.0198(6)
H17A	0.209254	0.223467	0.864048	0.024
H17B	0.119492	0.128946	0.767671	0.024
C18	0.2180(3)	0.1213(3)	0.5808(2)	0.0212(6)
H18A	0.289306	0.061229	0.571763	0.032
H18B	0.150845	0.140530	0.513195	0.032
H18C	0.160629	0.085495	0.619974	0.032
C19	0.3897(3)	0.3145(3)	0.5530(2)	0.0244(6)
H19A	0.441212	0.396389	0.576007	0.037
H19B	0.307940	0.320536	0.488273	0.037
H19C	0.459301	0.253835	0.541994	0.037
C20	0.1730(3)	0.3717(3)	0.6490(2)	0.0204(6)
H20A	0.107966	0.337030	0.683230	0.031
H20B	0.114794	0.384882	0.577569	0.031
H20C	0.218230	0.451643	0.685439	0.031
B1	0.8251(3)	0.2934(3)	0.7753(3)	0.0187(6)
H1A	0.919139	0.303876	0.759713	0.022
S1	0.87116(8)	0.25477(7)	0.33332(6)	0.02197(15)
F1	0.8749(2)	0.2109(2)	0.51954(17)	0.0416(5)
F2	0.6576(2)	0.20130(19)	0.40635(17)	0.0367(5)
F3	0.7695(3)	0.37918(19)	0.46524(18)	0.0404(5)
O2	0.8938(3)	0.1235(2)	0.3189(2)	0.0370(6)
O3	1.0056(3)	0.3310(2)	0.3770(2)	0.0333(5)
O4	0.7578(3)	0.3065(3)	0.25116(19)	0.0373(6)
C21	0.7899(3)	0.2623(3)	0.4357(3)	0.0246(6)

$U_{eq}$  is defined as 1/3 of the trace of the orthogonalized  $U_{ij}$  tensor.

Table 3. Anisotropic displacement parameters ( $\text{\AA}^2$ ) for mo\_harman\_mne\_nb3\_303b\_0m.

The anisotropic displacement factor exponent takes the form:

$$-2\pi^2 [ h^2(a^*)^2 U_{11} + k^2(b^*)^2 U_{22} + \dots + 2hka^*b^* U_{12} ]$$

Atom	$U_{11}$	$U_{22}$	$U_{33}$	$U_{23}$	$U_{13}$	$U_{12}$
W1	0.01579(6)	0.01307(5)	0.01132(6)	0.00207(4)	0.00425(4)	0.00056(3)
P1	0.0177(3)	0.0161(3)	0.0121(3)	0.0020(2)	0.0040(3)	-0.0008(2)
O1	0.0373(12)	0.0249(11)	0.0253(13)	0.0018(9)	0.0149(10)	0.0145(9)
N1	0.0169(10)	0.0165(10)	0.0150(12)	0.0005(9)	0.0053(9)	-0.0012(8)
N2	0.0175(11)	0.0209(11)	0.0156(12)	0.0011(9)	0.0058(9)	-0.0011(9)
N3	0.0186(11)	0.0168(11)	0.0139(12)	0.0014(9)	0.0037(9)	-0.0015(8)
N4	0.0193(11)	0.0186(11)	0.0155(12)	0.0014(9)	0.0059(9)	-0.0032(9)
N5	0.0164(10)	0.0163(10)	0.0144(12)	0.0018(9)	0.0051(9)	0.0017(8)
N6	0.0173(10)	0.0172(11)	0.0169(13)	0.0007(9)	0.0065(9)	-0.0002(8)
N7	0.0229(11)	0.0181(11)	0.0143(12)	0.0042(9)	0.0047(9)	0.0009(9)
C1	0.0267(14)	0.0181(13)	0.0221(16)	-0.0010(11)	0.0108(12)	-0.0019(11)
C2	0.0328(16)	0.0218(14)	0.0261(17)	-0.0047(12)	0.0166(13)	0.0003(12)



C3	0.0247(14)	0.0250(14)	0.0202(16)	−0.0013(12)	0.0117(12)	0.0011(11)
C4	0.0259(14)	0.0168(12)	0.0123(14)	0.0011(10)	0.0031(11)	−0.0008(10)
C5	0.0336(16)	0.0170(13)	0.0176(15)	0.0027(11)	0.0070(12)	−0.0049(11)
C6	0.0263(14)	0.0218(13)	0.0170(15)	0.0030(11)	0.0074(11)	−0.0070(11)
C7	0.0226(13)	0.0181(12)	0.0153(14)	0.0003(10)	0.0049(11)	0.0050(10)
C8	0.0229(14)	0.0241(14)	0.0196(16)	−0.0021(12)	0.0008(11)	0.0019(11)
C9	0.0170(12)	0.0184(13)	0.0232(16)	−0.0001(11)	0.0015(11)	0.0005(10)
C10	0.0204(13)	0.0163(12)	0.0196(15)	0.0051(10)	0.0088(11)	0.0013(10)
C11	0.0211(13)	0.0160(12)	0.0216(15)	0.0074(10)	0.0112(11)	0.0016(10)
C12	0.0207(13)	0.0209(13)	0.0191(15)	0.0097(11)	0.0083(11)	0.0043(10)
C13	0.0279(14)	0.0214(13)	0.0135(14)	0.0038(11)	0.0055(11)	0.0046(11)
C14	0.0273(14)	0.0278(15)	0.0172(15)	0.0066(12)	0.0074(12)	0.0106(12)
C15	0.0209(13)	0.0276(15)	0.0284(17)	0.0111(12)	0.0132(12)	0.0070(11)
C16	0.0207(13)	0.0235(14)	0.0277(17)	0.0056(12)	0.0105(12)	0.0028(11)
C17	0.0170(12)	0.0223(13)	0.0193(15)	0.0021(11)	0.0048(11)	0.0028(10)
C18	0.0221(13)	0.0200(13)	0.0172(15)	−0.0017(11)	0.0019(11)	−0.0026(10)
C19	0.0286(15)	0.0298(15)	0.0148(15)	0.0021(12)	0.0074(12)	−0.0060(12)
C20	0.0198(13)	0.0200(13)	0.0203(15)	0.0036(11)	0.0048(11)	0.0019(10)
B1	0.0193(14)	0.0199(14)	0.0161(16)	0.0005(12)	0.0055(12)	−0.0032(11)
S1	0.0266(3)	0.0209(3)	0.0168(4)	0.0027(3)	0.0050(3)	−0.0023(3)
F1	0.0359(11)	0.0619(14)	0.0264(12)	0.0229(10)	0.0063(9)	−0.0019(10)
F2	0.0273(10)	0.0433(11)	0.0388(13)	−0.0050(9)	0.0122(9)	−0.0121(8)
F3	0.0628(14)	0.0290(10)	0.0364(13)	−0.0049(9)	0.0277(11)	−0.0054(9)
O2	0.0461(14)	0.0233(11)	0.0468(17)	−0.0011(11)	0.0234(12)	−0.0017(10)
O3	0.0353(12)	0.0357(13)	0.0294(14)	0.0008(10)	0.0125(10)	−0.0129(10)
O4	0.0402(14)	0.0528(16)	0.0171(13)	0.0090(11)	0.0056(10)	0.0100(11)
C21	0.0268(15)	0.0236(14)	0.0202(16)	0.0030(12)	0.0039(12)	−0.0052(11)

Table 4. Bond lengths and angles for mo\_harman\_mne\_nb3\_303b\_0m

Atom–Atom	Length [Å]
W1–N7	1.785(2)
W1–N3	2.165(2)
W1–N5	2.222(2)
W1–N1	2.233(2)
W1–C11	2.300(3)

W1–C10	2.307(3)
W1–P1	2.5452(7)
W1–C12	2.583(3)
P1–C20	1.811(3)
P1–C19	1.820(3)
P1–C18	1.820(3)

O1–N7	1.193(3)
N1–C1	1.344(3)
N1–N2	1.368(3)
N2–C3	1.345(4)
N2–B1	1.540(4)
N3–C4	1.340(4)
N3–N4	1.366(3)
N4–C6	1.338(4)
N4–B1	1.548(4)
N5–C7	1.337(4)
N5–N6	1.376(3)
N6–C9	1.350(4)
N6–B1	1.528(4)
C1–C2	1.388(4)
C1–H1	0.9500
C2–C3	1.368(4)
C2–H2	0.9500
C3–H3	0.9500
C4–C5	1.388(4)
C4–H4	0.9500
C5–C6	1.383(4)
C5–H5	0.9500
C6–H6	0.9500
C7–C8	1.387(4)
C7–H7	0.9500
C8–C9	1.373(5)
C8–H8	0.9500
C9–H9	0.9500
C10–C11	1.423(4)
C10–C17	1.526(4)
C10–H10	1.0000
C11–C12	1.380(4)
C11–H11	1.0000
C12–C13	1.471(4)
C12–H12	1.0000
C13–C14	1.340(4)
C13–H13	0.9500
C14–C15	1.469(4)
C14–H14	0.9500
C15–C16	1.330(5)
C15–H15	0.9500
C16–C17	1.504(4)
C16–H16	0.9500
C17–H17A	0.9900
C17–H17B	0.9900
C18–H18A	0.9800
C18–H18B	0.9800
C18–H18C	0.9800

C19–H19A	0.9800
C19–H19B	0.9800
C19–H19C	0.9800
C20–H20A	0.9800
C20–H20B	0.9800
C20–H20C	0.9800
B1–H1A	1.0000
S1–O4	1.436(2)
S1–O3	1.439(2)
S1–O2	1.442(2)
S1–C21	1.823(3)
F1–C21	1.337(4)
F2–C21	1.339(3)
F3–C21	1.331(4)
<b>Atom–Atom– Atom</b>	<b>Angle [°]</b>
N7–W1–N3	88.67(10)
N7–W1–N5	101.98(9)
N3–W1–N5	76.41(9)
N7–W1–N1	173.87(10)
N3–W1–N1	87.25(9)
N5–W1–N1	81.51(8)
N7–W1–C11	101.57(11)
N3–W1–C11	167.20(9)
N5–W1–C11	93.81(9)
N1–W1–C11	83.10(9)
N7–W1–C10	94.43(10)
N3–W1–C10	151.94(10)
N5–W1–C10	129.65(9)
N1–W1–C10	87.04(9)
C11–W1–C10	35.99(10)
N7–W1–P1	90.65(8)
N3–W1–P1	77.47(6)
N5–W1–P1	150.59(7)
N1–W1–P1	83.99(6)
C11–W1–P1	109.71(7)
C10–W1–P1	74.62(8)
N7–W1–C12	79.43(10)
N3–W1–C12	146.77(9)
N5–W1–C12	75.94(9)
N1–W1–C12	106.42(9)
C11–W1–C12	32.16(10)
C10–W1–C12	60.74(10)
P1–W1–C12	132.98(7)
C20–P1–C19	104.16(15)
C20–P1–C18	104.75(13)
C19–P1–C18	98.21(14)

C20-P1-W1	112.28(10)
C19-P1-W1	113.55(10)
C18-P1-W1	121.74(10)
C1-N1-N2	106.0(2)
C1-N1-W1	133.5(2)
N2-N1-W1	120.54(16)
C3-N2-N1	109.4(2)
C3-N2-B1	130.1(2)
N1-N2-B1	119.9(2)
C4-N3-N4	107.2(2)
C4-N3-W1	130.2(2)
N4-N3-W1	122.59(17)
C6-N4-N3	109.4(2)
C6-N4-B1	129.3(2)
N3-N4-B1	118.2(2)
C7-N5-N6	106.5(2)
C7-N5-W1	134.4(2)
N6-N5-W1	118.79(18)
C9-N6-N5	108.9(2)
C9-N6-B1	128.3(3)
N5-N6-B1	122.3(2)
O1-N7-W1	176.4(2)
N1-C1-C2	110.7(3)
N1-C1-H1	124.7
C2-C1-H1	124.7
C3-C2-C1	104.8(3)
C3-C2-H2	127.6
C1-C2-H2	127.6
N2-C3-C2	109.2(3)
N2-C3-H3	125.4
C2-C3-H3	125.4
N3-C4-C5	109.5(3)
N3-C4-H4	125.3
C5-C4-H4	125.3
C6-C5-C4	105.5(3)
C6-C5-H5	127.2
C4-C5-H5	127.2
N4-C6-C5	108.4(3)
N4-C6-H6	125.8
C5-C6-H6	125.8
N5-C7-C8	110.6(3)
N5-C7-H7	124.7
C8-C7-H7	124.7
C9-C8-C7	105.2(3)
C9-C8-H8	127.4
C7-C8-H8	127.4
N6-C9-C8	108.9(3)
N6-C9-H9	125.6

C8-C9-H9	125.6
C11-C10-C17	119.7(3)
C11-C10-W1	71.74(15)
C17-C10-W1	117.02(18)
C11-C10-H10	114.0
C17-C10-H10	114.0
W1-C10-H10	114.0
C12-C11-C10	124.8(3)
C12-C11-W1	85.30(17)
C10-C11-W1	72.27(16)
C12-C11-H11	117.6
C10-C11-H11	117.6
W1-C11-H11	117.6
C11-C12-C13	131.3(3)
C11-C12-W1	62.54(16)
C13-C12-W1	114.66(19)
C11-C12-H12	112.4
C13-C12-H12	112.4
W1-C12-H12	112.4
C14-C13-C12	127.5(3)
C14-C13-H13	116.3
C12-C13-H13	116.3
C13-C14-C15	128.2(3)
C13-C14-H14	115.9
C15-C14-H14	115.9
C16-C15-C14	124.1(3)
C16-C15-H15	118.0
C14-C15-H15	118.0
C15-C16-C17	122.8(3)
C15-C16-H16	118.6
C17-C16-H16	118.6
C16-C17-C10	111.8(2)
C16-C17-H17A	109.3
C10-C17-H17A	109.3
C16-C17-H17B	109.3
C10-C17-H17B	109.3
H17A-C17-H17B	107.9
P1-C18-H18A	109.5
P1-C18-H18B	109.5
H18A-C18-H18B	109.5
P1-C18-H18C	109.5
H18A-C18-H18C	109.5
H18B-C18-H18C	109.5
P1-C19-H19A	109.5
P1-C19-H19B	109.5
H19A-C19-H19B	109.5
P1-C19-H19C	109.5
H19A-C19-H19C	109.5

H19B–C19–H19C	109.5
P1–C20–H20A	109.5
P1–C20–H20B	109.5
H20A–C20–H20B	109.5
P1–C20–H20C	109.5
H20A–C20–H20C	109.5
H20B–C20–H20C	109.5
N6–B1–N2	108.5(2)
N6–B1–N4	106.0(2)
N2–B1–N4	110.2(2)
N6–B1–H1A	110.7
N2–B1–H1A	110.7
N4–B1–H1A	110.7
O4–S1–O3	115.21(16)

O4–S1–O2	116.24(16)
O3–S1–O2	114.37(15)
O4–S1–C21	101.78(15)
O3–S1–C21	103.34(14)
O2–S1–C21	103.15(15)
F3–C21–F1	107.0(3)
F3–C21–F2	106.8(3)
F1–C21–F2	106.5(3)
F3–C21–S1	112.3(2)
F1–C21–S1	112.0(2)
F2–C21–S1	111.9(2)

Table 5. Torsion angles for mo\_harman\_mne\_nb3\_303b\_0m

Atom–Atom– Atom–Atom	Torsion Angle [°]
C1–N1–N2–C3	–1.1(3)
W1–N1–N2–C3	178.36(19)
C1–N1–N2–B1	–172.8(3)
W1–N1–N2–B1	6.7(3)
C4–N3–N4–C6	0.4(3)
W1–N3–N4–C6	–178.49(19)
C4–N3–N4–B1	162.2(2)
W1–N3–N4–B1	–16.8(3)
C7–N5–N6–C9	0.3(3)
W1–N5–N6–C9	174.87(17)
C7–N5–N6–B1	–171.8(2)
W1–N5–N6–B1	2.7(3)
N2–N1–C1–C2	0.9(4)
W1–N1–C1–C2	–178.5(2)
N1–C1–C2–C3	–0.3(4)
N1–N2–C3–C2	0.9(4)
B1–N2–C3–C2	171.5(3)
C1–C2–C3–N2	–0.4(4)
N4–N3–C4–C5	0.0(3)
W1–N3–C4–C5	178.77(19)
N3–C4–C5–C6	–0.3(3)
N3–N4–C6–C5	–0.7(3)
B1–N4–C6–C5	–159.8(3)
C4–C5–C6–N4	0.6(3)
N6–N5–C7–C8	–0.9(3)
W1–N5–C7–C8	–174.2(2)
N5–C7–C8–C9	1.1(3)
N5–N6–C9–C8	0.4(3)
B1–N6–C9–C8	171.9(3)

C7–C8–C9–N6	–0.9(3)
C17–C10–C11–C12	–40.3(4)
W1–C10–C11–C12	70.9(3)
C17–C10–C11–W1	–111.3(2)
C10–C11–C12–C13	35.2(5)
W1–C11–C12–C13	99.8(3)
C10–C11–C12–W1	–64.6(3)
C11–C12–C13–C14	37.0(5)
W1–C12–C13–C14	111.2(3)
C12–C13–C14–C15	–12.2(5)
C13–C14–C15–C16	–47.8(5)
C14–C15–C16–C17	–1.6(4)
C15–C16–C17–C10	89.5(3)
C11–C10–C17–C16	–51.0(3)
W1–C10–C17–C16	–134.5(2)
C9–N6–B1–N2	128.6(3)
N5–N6–B1–N2	–60.9(3)
C9–N6–B1–N4	–113.1(3)
N5–N6–B1–N4	57.4(3)
C3–N2–B1–N6	–115.3(3)
N1–N2–B1–N6	54.4(3)
C3–N2–B1–N4	129.1(3)
N1–N2–B1–N4	–61.2(3)
C6–N4–B1–N6	108.0(3)
N3–N4–B1–N6	–49.6(3)
C6–N4–B1–N2	–134.8(3)
N3–N4–B1–N2	67.6(3)
O4–S1–C21–F3	–63.4(2)
O3–S1–C21–F3	56.4(2)
O2–S1–C21–F3	175.8(2)
O4–S1–C21–F1	176.2(2)

O3-S1-C21-F1	-64.0(2)
O2-S1-C21-F1	55.4(2)
O4-S1-C21-F2	56.8(2)
O3-S1-C21-F2	176.6(2)

O2-S1-C21-F2	-64.0(2)
--------------	----------

## Structure Report for mo\_harman\_mne\_5\_163\_0m

A yellow, block-shaped crystal of mo\_harman\_mne\_5\_163\_0m was coated with Paratone oil and mounted on a MiTeGen micromount. Crystallized from dichloromethane. Data were collected at 100.00 K on a Bruker D8 VENTURE dual wavelength Mo/Cu Kappa four-circle diffractometer with a PHOTON III\_C14 detector. The diffractometer was equipped with an Oxford Cryostream 800 low temperature device and used Mo  $K_\alpha$  radiation ( $\lambda = 0.71073 \text{ \AA}$ ) from an Incoatec I\mS 3.0 microfocus sealed tube with a HELIOS double bounce multilayer mirror as monochromator.

Data collection and processing were done within the Bruker APEX5 software suite.<sup>[1]</sup> All data were integrated with SAINT 8.41 using a narrow-frame algorithm and a numerical absorption correction using SADABS 2016/2 was applied.<sup>[2]</sup> Using Olex2 as a graphical interface,<sup>[3]</sup> the structure was solved by dual methods with XT and refined by full-matrix least-squares methods against  $F^2$  using XL.<sup>[4,5]</sup> All non-hydrogen atoms were refined with anisotropic displacement parameters. All hydrogen atoms were refined with isotropic displacement parameters. Some of their coordinates were refined freely and some on calculated positions using a riding model with their  $U_{\text{iso}}$  values constrained to 1.5 times the  $U_{\text{eq}}$  of their pivot atoms for terminal  $\text{sp}^3$  carbon atoms and 1.2 times for all other carbon atoms.

This report and the CIF file were generated using FinalCif.<sup>[6]</sup>

Table 1. Crystal data and structure refinement for mo\_harman\_mne\_5\_163\_0m

CCDC number	
Empirical formula	$C_{21}H_{31}BCl_2N_7OPW$
Formula weight	694.06
Temperature [K]	100.00
Crystal system	monoclinic
Space group (number)	$P2_1/c$ (14)
$a$ [Å]	11.5996(8)
$b$ [Å]	14.7868(10)
$c$ [Å]	15.5609(10)
$\alpha$ [°]	90
$\beta$ [°]	97.174(2)
$\gamma$ [°]	90
Volume [Å <sup>3</sup> ]	2648.1(3)
$Z$	4
$\rho_{\text{calc}}$ [gcm <sup>-3</sup> ]	1.741
$\mu$ [mm <sup>-1</sup> ]	4.653
$F(000)$	1368
Crystal size [mm <sup>3</sup> ]	0.427×0.554×0.759
Crystal colour	yellow
Crystal shape	block
Radiation	Mo $K_{\alpha}$ ( $\lambda=0.71073$ Å)
2 $\theta$ range [°]	3.81 to 65.16 (0.66 Å)
Index ranges	$-17 \leq h \leq 17$ $-22 \leq k \leq 22$ $-17 \leq l \leq 23$
Reflections collected	53960
Independent reflections	9648 $R_{\text{int}} = 0.0580$ $R_{\text{sigma}} = 0.0390$
Completeness to $\theta = 25.242^\circ$	99.8
Data / Restraints / Parameters	9648 / 0 / 322
Goodness-of-fit on $F^2$	1.050
Final $R$ indexes [ $I \geq 2\sigma(I)$ ]	$R_1 = 0.0412$ $wR_2 = 0.1126$
Final $R$ indexes [all data]	$R_1 = 0.0483$ $wR_2 = 0.1201$
Largest peak/hole [eÅ <sup>-3</sup> ]	2.07/−2.18

Table 2. Atomic coordinates and  $U_{eq}$  [Å<sup>2</sup>] for mo\_harman\_mne\_5\_163\_0m

Atom	x	y	z	$U_{eq}$
W1	0.39508(2)	0.73115(2)	0.65800(2)	0.02172(5)
P1	0.32250(9)	0.60416(6)	0.74201(6)	0.02650(17)
Cl2	0.97678(15)	0.76600(12)	0.42980(12)	0.0616(4)
Cl1	0.91233(13)	0.60822(13)	0.52519(11)	0.0608(4)
C11	0.3010(3)	0.8614(2)	0.6605(3)	0.0268(6)
N2	0.6207(3)	0.7725(2)	0.7882(2)	0.0277(6)
N1	0.5021(3)	0.7726(2)	0.7824(2)	0.0260(6)
O1	0.2725(3)	0.6697(2)	0.48638(19)	0.0334(6)
N3	0.5377(3)	0.6340(2)	0.6457(2)	0.0257(6)
N7	0.3209(2)	0.6951(2)	0.55812(19)	0.0230(5)
N5	0.5272(3)	0.8144(2)	0.6019(2)	0.0272(6)
N4	0.6502(3)	0.6503(2)	0.6818(2)	0.0299(6)
N6	0.6418(3)	0.8093(2)	0.6332(2)	0.0277(6)
C10	0.2408(3)	0.7943(3)	0.7054(3)	0.0267(6)
C1	0.4760(4)	0.8011(3)	0.8592(2)	0.0289(7)
H1	0.399245	0.807668	0.873758	0.035
C12	0.2443(4)	0.9018(3)	0.5766(3)	0.0365(9)
H12A	0.306376	0.930311	0.547664	0.044
H12B	0.212774	0.851138	0.539151	0.044
C2	0.5770(4)	0.8201(3)	0.9152(3)	0.0336(8)
H2	0.583074	0.841242	0.973261	0.040
C3	0.6658(4)	0.8010(3)	0.8668(3)	0.0315(7)
H3	0.746337	0.807171	0.886222	0.038
C9	0.7062(4)	0.8535(3)	0.5799(3)	0.0332(8)
H9	0.788394	0.859184	0.587675	0.040
C18	0.2400(4)	0.6249(3)	0.8320(3)	0.0339(8)
H18A	0.224789	0.567274	0.859728	0.051
H18B	0.166059	0.653932	0.810567	0.051
H18C	0.284649	0.664493	0.874363	0.051
C4	0.5386(4)	0.5528(3)	0.6077(3)	0.0322(8)
H4	0.472237	0.524071	0.577636	0.039
C6	0.7178(4)	0.5799(3)	0.6649(3)	0.0373(9)
H6	0.799051	0.575182	0.682339	0.045
C7	0.5215(4)	0.8629(3)	0.5288(3)	0.0298(7)
H7	0.451569	0.877604	0.493042	0.036
C8	0.6318(4)	0.8888(3)	0.5125(3)	0.0341(8)
H8	0.651583	0.923410	0.465017	0.041

C5	0.6501(4)	0.5161(3)	0.6183(3)	0.0360(9)
H5	0.674099	0.459416	0.597755	0.043
C19	0.4375(4)	0.5321(3)	0.7952(3)	0.0398(9)
H19A	0.497437	0.569749	0.827608	0.060
H19B	0.472055	0.497053	0.751405	0.060
H19C	0.404911	0.490737	0.835013	0.060
C15	0.0241(5)	0.9232(4)	0.6931(4)	0.0528(13)
H15	−0.018835	0.953827	0.732384	0.063
B1	0.6838(4)	0.7467(3)	0.7112(3)	0.0297(8)
C13	0.1498(5)	0.9695(4)	0.5779(4)	0.0495(12)
H13	0.149257	1.014641	0.534428	0.059
C20	0.2299(4)	0.5244(3)	0.6764(3)	0.0387(9)
H20A	0.271863	0.500116	0.630644	0.058
H20B	0.159449	0.555390	0.650272	0.058
H20C	0.208539	0.474794	0.713091	0.058
C17	0.1164(4)	0.7708(3)	0.6710(3)	0.0344(8)
H17A	0.105503	0.774377	0.606961	0.041
H17B	0.098808	0.708267	0.687939	0.041
C14	0.0643(5)	0.9792(4)	0.6291(5)	0.0600(16)
H14	0.023090	1.034566	0.620343	0.072
C21	1.0049(5)	0.6497(5)	0.4542(4)	0.0599(16)
H21A	0.994230	0.614037	0.399920	0.072
H21B	1.086562	0.642511	0.480636	0.072
C16	0.0367(4)	0.8349(4)	0.7069(5)	0.0597(17)
H16	−0.012200	0.809275	0.745058	0.072
H11	0.333(4)	0.903(4)	0.685(3)	0.026(12)
H1A	0.777(5)	0.755(4)	0.728(4)	0.033(14)
H10	0.246(5)	0.796(4)	0.764(4)	0.030(13)

$U_{eq}$  is defined as 1/3 of the trace of the orthogonalized  $U_{ij}$  tensor.

Table 3. Anisotropic displacement parameters ( $\text{\AA}^2$ ) for mo\_harman\_mne\_5\_163\_0m.

The anisotropic displacement factor exponent takes the form:

$$-2\pi^2[h^2(a^*)^2U_{11} + k^2(b^*)^2U_{22} + \dots + 2hka^*b^*U_{12}]$$

Atom	$U_{11}$	$U_{22}$	$U_{33}$	$U_{23}$	$U_{13}$	$U_{12}$
W1	0.02419(8)	0.01974(7)	0.02204(8)	−0.00074(4)	0.00612(5)	−0.00121(4)
P1	0.0295(4)	0.0244(4)	0.0269(4)	0.0021(3)	0.0085(3)	−0.0015(3)
Cl2	0.0512(8)	0.0749(11)	0.0576(9)	0.0027(7)	0.0029(7)	−0.0173(7)
Cl1	0.0478(7)	0.0758(10)	0.0582(8)	0.0090(7)	0.0043(6)	−0.0093(7)
C11	0.0265(15)	0.0243(14)	0.0305(17)	−0.0031(13)	0.0075(13)	−0.0026(12)
N2	0.0259(14)	0.0271(14)	0.0301(16)	−0.0025(11)	0.0031(12)	−0.0016(10)
N1	0.0262(14)	0.0267(14)	0.0256(14)	−0.0014(10)	0.0051(11)	−0.0004(10)



O1	0.0335(14)	0.0400(15)	0.0265(13)	−0.0073(11)	0.0031(11)	−0.0004(11)
N3	0.0277(13)	0.0241(13)	0.0262(14)	−0.0009(11)	0.0071(11)	−0.0007(10)
N7	0.0229(12)	0.0227(12)	0.0234(12)	−0.0005(10)	0.0031(10)	0.0004(10)
N5	0.0286(14)	0.0228(12)	0.0326(15)	−0.0014(11)	0.0132(12)	−0.0046(11)
N4	0.0297(14)	0.0262(14)	0.0355(16)	−0.0013(12)	0.0104(13)	0.0018(12)
N6	0.0256(13)	0.0254(13)	0.0335(15)	−0.0008(12)	0.0092(12)	−0.0026(11)
C10	0.0260(15)	0.0264(15)	0.0287(17)	−0.0010(13)	0.0070(13)	0.0006(12)
C1	0.0366(18)	0.0255(15)	0.0252(16)	−0.0014(13)	0.0065(14)	0.0009(14)
C12	0.041(2)	0.0288(17)	0.041(2)	0.0081(16)	0.0109(18)	0.0036(15)
C2	0.045(2)	0.0300(17)	0.0255(16)	−0.0008(14)	0.0027(15)	−0.0035(15)
C3	0.0314(17)	0.0302(17)	0.0317(18)	0.0032(15)	−0.0012(14)	−0.0027(14)
C9	0.0358(19)	0.0298(17)	0.036(2)	−0.0045(15)	0.0144(16)	−0.0082(15)
C18	0.039(2)	0.0335(18)	0.0312(18)	0.0049(15)	0.0125(16)	−0.0015(15)
C4	0.040(2)	0.0238(15)	0.0359(19)	−0.0022(14)	0.0154(16)	−0.0030(14)
C6	0.0322(18)	0.0338(19)	0.048(2)	−0.0004(17)	0.0117(17)	0.0061(15)
C7	0.0331(17)	0.0259(15)	0.0312(17)	−0.0004(13)	0.0078(14)	−0.0039(13)
C8	0.040(2)	0.0322(18)	0.0328(19)	−0.0010(15)	0.0150(16)	−0.0086(15)
C5	0.043(2)	0.0247(15)	0.044(2)	−0.0010(15)	0.0188(18)	0.0045(15)
C19	0.041(2)	0.040(2)	0.041(2)	0.0158(18)	0.0141(18)	0.0093(17)
C15	0.044(3)	0.058(3)	0.060(3)	0.000(3)	0.022(2)	0.007(2)
B1	0.0277(18)	0.0319(18)	0.030(2)	−0.0007(16)	0.0065(16)	−0.0019(15)
C13	0.042(2)	0.038(2)	0.070(4)	0.020(2)	0.012(2)	0.0057(19)
C20	0.048(2)	0.0317(19)	0.038(2)	−0.0057(16)	0.0112(18)	−0.0131(17)
C17	0.0272(17)	0.041(2)	0.036(2)	0.0031(16)	0.0056(16)	−0.0045(14)
C14	0.047(3)	0.040(2)	0.098(5)	0.009(3)	0.026(3)	0.012(2)
C21	0.038(2)	0.081(4)	0.062(4)	−0.006(3)	0.009(2)	−0.010(3)
C16	0.032(2)	0.062(3)	0.090(5)	0.029(3)	0.024(3)	0.009(2)

Table 4. Bond lengths and angles for mo\_harman\_mne\_5\_163\_0m

Atom–Atom	Length [Å]		
W1–P1	2.4937(9)	C4–C5	1.393(6)
W1–C11	2.217(4)	C6–H6	0.9500
W1–N1	2.250(4)	C6–C5	1.375(7)
W1–N3	2.217(3)	C7–H7	0.9500
W1–N7	1.763(3)	C7–C8	1.389(5)
W1–N5	2.227(3)	C8–H8	0.9500
W1–C10	2.224(4)	C5–H5	0.9500
P1–C18	1.819(4)	C19–H19A	0.9800
P1–C19	1.823(5)	C19–H19B	0.9800
P1–C20	1.820(4)	C19–H19C	0.9800
Cl2–C21	1.783(8)	C15–H15	0.9500
Cl1–C21	1.745(6)	C15–C14	1.417(8)
C11–C10	1.442(5)	C15–C16	1.329(9)
C11–C12	1.510(6)	B1–H1A	1.08(6)
C11–H11	0.80(5)	C13–H13	0.9500
N2–N1	1.368(5)	C13–C14	1.355(8)
N2–C3	1.336(5)	C20–H20A	0.9800
N2–B1	1.529(6)	C20–H20B	0.9800
N1–C1	1.337(5)	C20–H20C	0.9800
O1–N7	1.243(4)	C17–H17A	0.9900
N3–N4	1.376(5)	C17–H17B	0.9900
N3–C4	1.340(5)	C17–C16	1.480(7)
N5–N6	1.359(5)	C14–H14	0.9500
N5–C7	1.339(5)	C21–H21A	0.9900
N4–C6	1.349(5)	C21–H21B	0.9900
N4–B1	1.533(6)	C16–H16	0.9500
N6–C9	1.352(5)		
N6–B1	1.554(6)	<b>Atom–Atom–</b>	<b>Angle [°]</b>
C10–C17	1.516(6)	<b>Atom</b>	
C10–H10	0.90(5)	C11–W1–P1	116.47(10)
C1–H1	0.9500	C11–W1–N1	88.18(13)
C1–C2	1.399(6)	C11–W1–N3	159.87(12)
C12–H12A	0.9900	C11–W1–N5	83.76(13)
C12–H12B	0.9900	C11–W1–C10	37.89(13)
C12–C13	1.486(7)	N1–W1–P1	86.55(8)
C2–H2	0.9500	N3–W1–P1	82.05(8)
C2–C3	1.379(6)	N3–W1–N1	85.02(12)
C3–H3	0.9500	N3–W1–N5	76.52(12)
C9–H9	0.9500	N3–W1–C10	160.14(13)
C9–C8	1.375(7)	N7–W1–P1	94.29(10)
C18–H18A	0.9800	N7–W1–C11	95.23(14)
C18–H18B	0.9800	N7–W1–N1	175.67(12)
C18–H18C	0.9800	N7–W1–N3	90.89(13)
C4–H4	0.9500	N7–W1–N5	96.08(13)
		N7–W1–C10	95.43(14)

N5-W1-P1	156.28(9)
N5-W1-N1	81.61(12)
C10-W1-P1	78.72(10)
C10-W1-N1	88.90(13)
C10-W1-N5	121.28(13)
C18-P1-W1	121.45(14)
C18-P1-C19	100.1(2)
C18-P1-C20	102.1(2)
C19-P1-W1	113.71(15)
C20-P1-W1	114.10(15)
C20-P1-C19	102.9(2)
W1-C11-H11	119(4)
C10-C11-W1	71.3(2)
C10-C11-C12	120.4(3)
C10-C11-H11	122(4)
C12-C11-W1	119.3(3)
C12-C11-H11	104(4)
N1-N2-B1	121.6(3)
C3-N2-N1	109.6(3)
C3-N2-B1	128.7(4)
N2-N1-W1	119.9(2)
C1-N1-W1	133.8(3)
C1-N1-N2	106.2(3)
N4-N3-W1	122.1(2)
C4-N3-W1	131.8(3)
C4-N3-N4	106.1(3)
O1-N7-W1	177.6(3)
N6-N5-W1	121.2(2)
C7-N5-W1	131.7(3)
C7-N5-N6	106.1(3)
N3-N4-B1	118.5(3)
C6-N4-N3	109.3(3)
C6-N4-B1	130.1(4)
N5-N6-B1	120.6(3)
C9-N6-N5	110.1(3)
C9-N6-B1	128.6(4)
W1-C10-H10	113(4)
C11-C10-W1	70.8(2)
C11-C10-C17	119.0(4)
C11-C10-H10	120(4)
C17-C10-W1	123.8(3)
C17-C10-H10	108(3)
N1-C1-H1	124.6
N1-C1-C2	110.7(4)
C2-C1-H1	124.6
C11-C12-H12A	107.4
C11-C12-H12B	107.4

H12A-C12-H12B	106.9
C13-C12-C11	119.8(4)
C13-C12-H12A	107.4
C13-C12-H12B	107.4
C1-C2-H2	128.0
C3-C2-C1	104.1(4)
C3-C2-H2	128.0
N2-C3-C2	109.3(4)
N2-C3-H3	125.3
C2-C3-H3	125.3
N6-C9-H9	126.0
N6-C9-C8	108.0(4)
C8-C9-H9	126.0
P1-C18-H18A	109.5
P1-C18-H18B	109.5
P1-C18-H18C	109.5
H18A-C18-H18B	109.5
H18A-C18-H18C	109.5
H18B-C18-H18C	109.5
N3-C4-H4	124.6
N3-C4-C5	110.9(4)
C5-C4-H4	124.6
N4-C6-H6	125.5
N4-C6-C5	108.9(4)
C5-C6-H6	125.5
N5-C7-H7	124.6
N5-C7-C8	110.7(4)
C8-C7-H7	124.6
C9-C8-C7	105.1(4)
C9-C8-H8	127.5
C7-C8-H8	127.5
C4-C5-H5	127.6
C6-C5-C4	104.8(4)
C6-C5-H5	127.6
P1-C19-H19A	109.5
P1-C19-H19B	109.5
P1-C19-H19C	109.5
H19A-C19-H19B	109.5
H19A-C19-H19C	109.5
H19B-C19-H19C	109.5
C14-C15-H15	114.8
C16-C15-H15	114.8

C16–C15–C14	130.3(5)
N2–B1–N4	109.7(3)
N2–B1–N6	109.3(3)
N2–B1–H1A	110(3)
N4–B1–N6	106.1(3)
N4–B1–H1A	112(3)
N6–B1–H1A	109(3)
C12–C13–H13	113.8
C14–C13–C12	132.4(5)
C14–C13–H13	113.8
P1–C20–H20A	109.5
P1–C20–H20B	109.5
P1–C20–H20C	109.5
H20A–C20–H20B	109.5
H20A–C20–H20C	109.5
H20B–C20–H20C	109.5
C10–C17–H17A	109.8
C10–C17–H17B	109.8

H17A–C17–H17B	108.2
C16–C17–C10	109.4(4)
C16–C17–H17A	109.8
C16–C17–H17B	109.8
C15–C14–H14	113.5
C13–C14–C15	132.9(5)
C13–C14–H14	113.5
C12–C21–H21A	109.4
C12–C21–H21B	109.4
C11–C21–C12	111.3(4)
C11–C21–H21A	109.4
C11–C21–H21B	109.4
H21A–C21–H21B	108.0
C15–C16–C17	129.0(5)
C15–C16–H16	115.5
C17–C16–H16	115.5

Table 5. Torsion angles for mo\_harman\_mne\_5\_163\_0m

Atom–Atom–Atom–Atom	Torsion Angle [°]
W1–C11–C10–C17	–118.8(3)
W1–C11–C12–C13	159.3(3)
W1–N1–C1–C2	–178.7(3)
W1–N3–N4–C6	179.4(3)
W1–N3–N4–B1	–15.5(4)
W1–N3–C4–C5	–179.0(3)
W1–N5–N6–C9	169.5(3)
W1–N5–N6–B1	–1.7(5)
W1–N5–C7–C8	–168.1(3)
W1–C10–C17–C16	–171.4(3)
C11–C10–C17–C16	–86.1(5)
C11–C12–C13–C14	–34.2(10)
N2–N1–C1–C2	0.2(4)
N1–N2–C3–C2	0.4(4)
N1–N2–B1–N4	–59.0(5)
N1–N2–B1–N6	56.9(5)
N1–C1–C2–C3	0.0(5)
N3–N4–C6–C5	–0.7(5)
N3–N4–B1–N2	67.3(5)
N3–N4–B1–N6	–50.7(4)
N3–C4–C5–C6	–0.2(5)
N5–N6–C9–C8	0.3(4)

N5–N6–B1–N2	–56.9(5)
N5–N6–B1–N4	61.3(4)
N5–C7–C8–C9	–0.1(5)
N4–N3–C4–C5	–0.2(4)
N4–C6–C5–C4	0.5(5)
N6–N5–C7–C8	0.3(4)
N6–C9–C8–C7	–0.2(5)
C10–C11–C12–C13	74.8(5)
C10–C17–C16–C15	66.1(9)
C1–C2–C3–N2	–0.3(5)
C12–C11–C10–W1	113.7(3)
C12–C11–C10–C17	–5.1(5)
C12–C13–C14–C15	–9.0(14)
C3–N2–N1–W1	178.7(2)
C3–N2–N1–C1	–0.4(4)
C3–N2–B1–N4	124.0(4)
C3–N2–B1–N6	–120.0(4)
C9–N6–B1–N2	133.7(4)
C9–N6–B1–N4	–108.1(4)
C4–N3–N4–C6	0.5(4)
C4–N3–N4–B1	165.6(3)
C6–N4–B1–N2	–131.2(5)
C6–N4–B1–N6	110.8(5)
C7–N5–N6–C9	–0.4(4)

C7–N5–N6–B1	–171.6(3)
B1–N2–N1–W1	1.3(4)
B1–N2–N1–C1	–177.8(3)
B1–N2–C3–C2	177.6(4)
B1–N4–C6–C5	–163.5(4)

B1–N6–C9–C8	170.6(4)
C14–C15–C16–C17	13.8(13)
C16–C15–C14–C13	–20.2(14)

## Structure Report for mo\_harman\_mne\_nb4\_021\_0m

A yellow, block-shaped crystal of mo\_harman\_mne\_nb4\_021\_0m was coated with Paratone oil and mounted on a MiTeGen micromount. acetronitrile. Data were collected at 100.00 K on a Bruker D8 VENTURE dual wavelength Mo/Cu Kappa four-circle diffractometer with a PHOTON III\_C14 detector. The diffractometer was equipped with an Oxford Cryostream 800 low temperature device and used Mo  $K_\alpha$  radiation ( $\lambda = 0.71073\text{\AA}$ ) from an Incoatec IImS 3.0 microfocus sealed tube with a HELIOS double bounce multilayer mirror as monochromator.

Data collection and processing were done within the Bruker APEX6 software suite.<sup>[1]</sup> All data were integrated with SAINT 8.41 using a narrow-frame algorithm and a Multi-Scan absorption correction using SADABS 2016/2 was applied.<sup>[2]</sup> Using Olex2 as a graphical interface,<sup>[3]</sup> the structure was solved by dual methods with XT and refined by full-matrix least-squares methods against  $F^2$  using XL.<sup>[4,5]</sup> All non-hydrogen atoms were refined with anisotropic displacement parameters. All hydrogen atoms were refined with isotropic displacement parameters. Some of their coordinates were refined freely and some on calculated positions using a riding model with their  $U_{\text{iso}}$  values constrained to 1.5 times the  $U_{\text{eq}}$  of their pivot atoms for terminal  $\text{sp}^3$  carbon atoms and 1.2 times for all other carbon atoms.

This report and the CIF file were generated using FinalCif.<sup>[6]</sup>

Table 1. Crystal data and structure refinement for mo\_harman\_mne\_nb4\_021\_0m

CCDC number	
Empirical formula	C <sub>21</sub> H <sub>28</sub> BN <sub>8</sub> OPW
Formula weight	634.14
Temperature [K]	100.00
Crystal system	monoclinic
Space group (number)	<i>P</i> 2 <sub>1</sub> / <i>n</i> (14)
<i>a</i> [Å]	10.5165(4)
<i>b</i> [Å]	20.7039(6)
<i>c</i> [Å]	11.5409(3)
$\alpha$ [°]	90
$\beta$ [°]	103.2430(10)
$\gamma$ [°]	90
Volume [Å <sup>3</sup> ]	2446.01(13)
<i>Z</i>	4
$\rho_{\text{calc}}$ [gcm <sup>-3</sup> ]	1.722
$\mu$ [mm <sup>-1</sup> ]	4.818
<i>F</i> (000)	1248
Crystal size [mm <sup>3</sup> ]	0.025×0.04×0.057
Crystal colour	yellow
Crystal shape	block
Radiation	Mo <i>K</i> $\alpha$ ( $\lambda$ =0.71073 Å)
2 $\theta$ range [°]	3.93 to 56.59 (0.75 Å)
Index ranges	−13 ≤ <i>h</i> ≤ 14 −27 ≤ <i>k</i> ≤ 25 −15 ≤ <i>l</i> ≤ 15
Reflections collected	47066
Independent reflections	6055 <i>R</i> <sub>int</sub> = 0.0644 <i>R</i> <sub>sigma</sub> = 0.0411
Completeness to $\theta$ = 25.242°	100.0
Data / Restraints / Parameters	6055 / 0 / 313
Goodness-of-fit on <i>F</i> <sup>2</sup>	1.024
Final <i>R</i> indexes [ <i>I</i> ≥ 2 $\sigma$ ( <i>I</i> )]	<i>R</i> <sub>1</sub> = 0.0255 <i>wR</i> <sub>2</sub> = 0.0475
Final <i>R</i> indexes [all data]	<i>R</i> <sub>1</sub> = 0.0361 <i>wR</i> <sub>2</sub> = 0.0510
Largest peak/hole [eÅ <sup>-3</sup> ]	0.68/−0.56

Table 2. Atomic coordinates and  $U_{eq}$  [ $\text{\AA}^2$ ] for mo\_harman\_mne\_nb4\_021\_0m

Atom	x	y	z	$U_{eq}$
W1	0.32748(2)	0.64195(2)	0.64937(2)	0.01237(4)
P1	0.11684(8)	0.68462(4)	0.52592(7)	0.01732(17)
O1	0.2919(2)	0.72062(10)	0.85773(19)	0.0228(5)
N1	0.3518(3)	0.59584(12)	0.4805(2)	0.0176(6)
N2	0.4473(3)	0.61678(12)	0.4275(2)	0.0191(6)
N3	0.4078(2)	0.72999(12)	0.5835(2)	0.0151(5)
N4	0.4974(3)	0.72767(12)	0.5146(2)	0.0172(5)
N5	0.5426(3)	0.62715(11)	0.7002(2)	0.0155(5)
N6	0.6148(3)	0.63466(12)	0.6171(2)	0.0186(6)
N7	0.3080(2)	0.68597(12)	0.7752(2)	0.0157(5)
N8	0.3306(3)	0.40326(13)	0.8772(3)	0.0269(7)
C1	0.2848(3)	0.55078(15)	0.4081(3)	0.0218(7)
H1	0.212497	0.527451	0.423314	0.026
C2	0.3349(4)	0.54288(16)	0.3086(3)	0.0275(8)
H2	0.304940	0.514232	0.243810	0.033
C3	0.4378(4)	0.58552(16)	0.3235(3)	0.0258(8)
H3	0.492807	0.591821	0.269677	0.031
C4	0.3963(3)	0.79212(15)	0.6123(3)	0.0184(7)
H4	0.339824	0.807886	0.659372	0.022
C5	0.4790(3)	0.82986(15)	0.5630(3)	0.0220(7)
H5	0.489799	0.875386	0.569139	0.026
C6	0.5425(3)	0.78764(15)	0.5031(3)	0.0223(7)
H6	0.607015	0.798897	0.461004	0.027
C7	0.6278(3)	0.61657(14)	0.8028(3)	0.0185(7)
H7	0.604542	0.609267	0.876539	0.022
C8	0.7549(3)	0.61760(15)	0.7881(3)	0.0215(7)
H8	0.833318	0.611586	0.847200	0.026
C9	0.7419(3)	0.62925(15)	0.6692(3)	0.0242(7)
H9	0.811768	0.632901	0.629977	0.029
C10	0.1906(3)	0.56292(14)	0.6737(3)	0.0154(6)
H10	0.150(3)	0.5416(13)	0.600(3)	0.005(7)
C11	0.3247(3)	0.54497(15)	0.7220(3)	0.0162(6)
H11	0.355(3)	0.5186(14)	0.673(3)	0.007(8)
C12	0.3810(3)	0.52580(14)	0.8516(3)	0.0176(6)
H12	0.478064	0.526989	0.862321	0.021
C13	0.3516(3)	0.56866(15)	0.9485(3)	0.0186(7)
H13	0.411917	0.602215	0.978047	0.022
C14	0.2479(3)	0.56296(16)	0.9954(3)	0.0233(7)
H14	0.244539	0.587834	1.063798	0.028
C15	0.1378(3)	0.51962(16)	0.9455(3)	0.0242(7)

H15	0.113781	0.487284	0.994786	0.029
C16	0.0711(3)	0.52471(16)	0.8325(3)	0.0229(7)
H16	0.006039	0.493289	0.802674	0.028
C17	0.0934(3)	0.57712(15)	0.7506(3)	0.0205(7)
H17A	0.123965	0.615953	0.799065	0.025
H17B	0.008330	0.588024	0.697070	0.025
C18	0.3479(3)	0.45715(15)	0.8681(3)	0.0194(7)
C19	−0.0117(3)	0.63053(14)	0.4475(3)	0.0215(7)
H19A	0.018526	0.607859	0.384218	0.032
H19B	−0.089918	0.655759	0.412490	0.032
H19C	−0.032594	0.598976	0.503618	0.032
C20	0.1377(4)	0.73289(18)	0.4006(3)	0.0337(9)
H20A	0.190906	0.770925	0.429749	0.051
H20B	0.051977	0.746763	0.354232	0.051
H20C	0.181437	0.707072	0.350080	0.051
C21	0.0314(3)	0.73823(16)	0.6069(3)	0.0275(8)
H21A	0.010427	0.714921	0.674041	0.041
H21B	−0.049518	0.753359	0.553610	0.041
H21C	0.087137	0.775354	0.636714	0.041
B1	0.5556(4)	0.66229(17)	0.4920(3)	0.0193(8)
H1A	0.627(3)	0.6692(14)	0.440(3)	0.011(8)

$U_{eq}$  is defined as 1/3 of the trace of the orthogonalized  $U_{ij}$  tensor.

Table 3. Anisotropic displacement parameters ( $\text{\AA}^2$ ) for mo\_harman\_mne\_nb4\_021\_0m.

The anisotropic displacement factor exponent takes the form:

$$-2\pi^2 [h^2(a^*)^2 U_{11} + k^2(b^*)^2 U_{22} + \dots + 2hka^*b^* U_{12}]$$

Atom	$U_{11}$	$U_{22}$	$U_{33}$	$U_{23}$	$U_{13}$	$U_{12}$
W1	0.01218(6)	0.01302(6)	0.01254(6)	0.00131(5)	0.00413(4)	0.00096(5)
P1	0.0143(4)	0.0173(4)	0.0192(4)	0.0044(3)	0.0015(3)	0.0007(3)
O1	0.0255(13)	0.0253(12)	0.0195(11)	−0.0078(10)	0.0087(10)	0.0002(10)
N1	0.0222(15)	0.0155(12)	0.0167(13)	0.0021(11)	0.0076(11)	0.0018(11)
N2	0.0203(15)	0.0212(13)	0.0185(14)	0.0013(11)	0.0100(12)	0.0036(11)
N3	0.0128(13)	0.0157(12)	0.0182(13)	0.0014(10)	0.0066(11)	0.0002(10)
N4	0.0168(14)	0.0184(12)	0.0182(13)	0.0049(11)	0.0077(11)	0.0017(10)
N5	0.0129(13)	0.0147(12)	0.0193(13)	0.0019(10)	0.0041(11)	0.0009(10)
N6	0.0141(14)	0.0187(13)	0.0251(14)	0.0024(11)	0.0088(11)	0.0016(10)
N7	0.0136(13)	0.0157(12)	0.0187(13)	0.0007(11)	0.0060(11)	0.0000(10)
N8	0.0219(16)	0.0230(15)	0.0361(17)	0.0083(13)	0.0072(13)	0.0014(12)
C1	0.0289(19)	0.0170(15)	0.0203(16)	−0.0012(13)	0.0070(14)	−0.0011(13)
C2	0.044(2)	0.0207(16)	0.0186(17)	−0.0056(14)	0.0086(16)	0.0007(15)
C3	0.041(2)	0.0236(17)	0.0160(16)	0.0001(14)	0.0143(15)	0.0080(15)
C4	0.0154(16)	0.0203(15)	0.0176(16)	0.0006(13)	0.0003(13)	0.0034(13)



C5	0.0222(18)	0.0140(14)	0.0270(18)	0.0034(14)	−0.0004(14)	−0.0042(13)
C6	0.0197(18)	0.0231(16)	0.0233(17)	0.0043(14)	0.0036(14)	−0.0057(13)
C7	0.0204(17)	0.0138(14)	0.0201(16)	0.0014(13)	0.0020(14)	−0.0016(12)
C8	0.0147(17)	0.0193(15)	0.0270(18)	−0.0001(14)	−0.0023(14)	0.0001(13)
C9	0.0177(17)	0.0209(16)	0.036(2)	0.0029(15)	0.0095(15)	0.0036(13)
C10	0.0162(16)	0.0158(14)	0.0146(15)	0.0037(12)	0.0041(12)	0.0003(12)
C11	0.0173(16)	0.0162(14)	0.0167(15)	0.0018(13)	0.0070(13)	−0.0008(12)
C12	0.0153(16)	0.0172(15)	0.0199(16)	0.0034(13)	0.0029(13)	−0.0017(12)
C13	0.0184(17)	0.0216(15)	0.0137(15)	0.0036(13)	−0.0007(12)	0.0036(13)
C14	0.028(2)	0.0262(17)	0.0154(16)	0.0052(14)	0.0045(14)	0.0078(14)
C15	0.0216(18)	0.0245(16)	0.0313(19)	0.0099(15)	0.0160(15)	0.0046(14)
C16	0.0120(16)	0.0293(17)	0.0289(18)	0.0055(15)	0.0075(14)	0.0026(13)
C17	0.0161(17)	0.0231(15)	0.0229(16)	0.0063(14)	0.0058(13)	0.0024(13)
C18	0.0151(17)	0.0242(17)	0.0191(16)	0.0045(13)	0.0044(13)	0.0033(13)
C19	0.0192(17)	0.0208(16)	0.0231(16)	−0.0013(14)	0.0022(13)	0.0000(13)
C20	0.025(2)	0.038(2)	0.033(2)	0.0177(17)	−0.0026(16)	−0.0067(16)
C21	0.0168(18)	0.0263(17)	0.037(2)	−0.0044(16)	0.0009(15)	0.0061(14)
B1	0.0175(19)	0.0202(17)	0.0215(19)	0.0029(15)	0.0070(15)	0.0020(14)

Table 4. Bond lengths and angles for mo\_harman\_mne\_nb4\_021\_0m

Atom–Atom	Length [Å]		
W1–P1	2.5042(8)	N4–C6	1.346(4)
W1–N1	2.237(2)	N4–B1	1.533(4)
W1–N3	2.215(2)	N5–N6	1.361(4)
W1–N5	2.225(3)	N5–C7	1.329(4)
W1–N7	1.766(2)	N6–C9	1.339(4)
W1–C10	2.239(3)	N6–B1	1.546(4)
W1–C11	2.178(3)	N8–C18	1.139(4)
P1–C19	1.828(3)	C1–H1	0.9500
P1–C20	1.812(3)	C1–C2	1.379(5)
P1–C21	1.816(3)	C2–H2	0.9500
O1–N7	1.234(3)	C2–C3	1.377(5)
N1–N2	1.361(4)	C3–H3	0.9500
N1–C1	1.340(4)	C4–H4	0.9500
N2–C3	1.347(4)	C4–C5	1.385(5)
N2–B1	1.533(5)	C5–H5	0.9500
N3–N4	1.366(3)	C5–C6	1.377(5)
N3–C4	1.341(4)	C6–H6	0.9500
		C7–H7	0.9500

C7–C8	1.386(5)
C8–H8	0.9500
C8–C9	1.369(5)
C9–H9	0.9500
C10–H10	0.97(3)
C10–C11	1.441(4)
C10–C17	1.528(4)
C11–H11	0.89(3)
C11–C12	1.530(4)
C12–H12	1.0000
C12–C13	1.514(4)
C12–C18	1.486(4)
C13–H13	0.9500
C13–C14	1.329(5)
C14–H14	0.9500
C14–C15	1.473(5)
C15–H15	0.9500
C15–C16	1.336(5)
C16–H16	0.9500
C16–C17	1.492(4)
C17–H17A	0.9900
C17–H17B	0.9900
C19–H19A	0.9800
C19–H19B	0.9800
C19–H19C	0.9800
C20–H20A	0.9800
C20–H20B	0.9800
C20–H20C	0.9800
C21–H21A	0.9800
C21–H21B	0.9800
C21–H21C	0.9800
B1–H1A	1.07(3)
Atom–Atom– Atom	Angle [°]
N1–W1–P1	85.28(7)
N1–W1–C10	90.13(10)
N3–W1–P1	82.62(7)
N3–W1–N1	85.62(9)
N3–W1–N5	76.06(9)
N3–W1–C10	161.97(10)
N5–W1–P1	155.81(7)
N5–W1–N1	81.86(10)
N5–W1–C10	120.70(10)
N7–W1–P1	91.80(8)
N7–W1–N1	174.18(10)
N7–W1–N3	89.02(10)
N7–W1–N5	99.05(11)

N7–W1–C10	94.30(11)
N7–W1–C11	98.35(11)
C10–W1–P1	79.57(8)
C11–W1–P1	117.12(9)
C11–W1–N1	87.47(10)
C11–W1–N3	158.45(11)
C11–W1–N5	82.77(10)
C11–W1–C10	38.05(11)
C19–P1–W1	121.54(11)
C20–P1–W1	113.31(13)
C20–P1–C19	98.83(16)
C20–P1–C21	103.78(18)
C21–P1–W1	113.60(12)
C21–P1–C19	103.44(16)
N2–N1–W1	119.94(19)
C1–N1–W1	133.7(2)
C1–N1–N2	106.2(3)
N1–N2–B1	121.4(3)
C3–N2–N1	109.6(3)
C3–N2–B1	128.5(3)
N4–N3–W1	122.61(18)
C4–N3–W1	129.9(2)
C4–N3–N4	106.9(2)
N3–N4–B1	119.1(2)
C6–N4–N3	109.3(3)
C6–N4–B1	129.4(3)
N6–N5–W1	119.77(19)
C7–N5–W1	134.0(2)
C7–N5–N6	106.0(3)
N5–N6–B1	122.0(3)
C9–N6–N5	109.6(3)
C9–N6–B1	126.7(3)
O1–N7–W1	175.3(2)
N1–C1–H1	124.6
N1–C1–C2	110.8(3)
C2–C1–H1	124.6
C1–C2–H2	127.5
C3–C2–C1	105.0(3)
C3–C2–H2	127.5
N2–C3–C2	108.4(3)
N2–C3–H3	125.8
C2–C3–H3	125.8
N3–C4–H4	125.1
N3–C4–C5	109.8(3)
C5–C4–H4	125.1
C4–C5–H5	127.2
C6–C5–C4	105.7(3)
C6–C5–H5	127.2

N4–C6–C5	108.3(3)
N4–C6–H6	125.8
C5–C6–H6	125.8
N5–C7–H7	124.4
N5–C7–C8	111.1(3)
C8–C7–H7	124.4
C7–C8–H8	127.8
C9–C8–C7	104.3(3)
C9–C8–H8	127.8
N6–C9–C8	109.0(3)
N6–C9–H9	125.5
C8–C9–H9	125.5
W1–C10–H10	112.9(17)
C11–C10–W1	68.70(17)
C11–C10–H10	114.7(18)
C11–C10–C17	123.4(3)
C17–C10–W1	117.8(2)
C17–C10–H10	112.4(18)
W1–C11–H11	106.5(19)
C10–C11–W1	73.25(17)
C10–C11–H11	111.7(19)
C10–C11–C12	124.8(3)
C12–C11–W1	125.4(2)
C12–C11–H11	110.2(19)
C11–C12–H12	105.7
C13–C12–C11	118.1(3)
C13–C12–H12	105.7
C18–C12–C11	108.9(3)
C18–C12–H12	105.7
C18–C12–C13	111.9(3)
C12–C13–H13	117.5
C14–C13–C12	125.1(3)
C14–C13–H13	117.5
C13–C14–H14	118.7
C13–C14–C15	122.6(3)
C15–C14–H14	118.7
C14–C15–H15	119.2
C16–C15–C14	121.6(3)
C16–C15–H15	119.2
C15–C16–H16	118.2
C15–C16–C17	123.5(3)
C17–C16–H16	118.2
C10–C17–H17A	108.1

C10–C17–H17B	108.1
C16–C17–C10	116.8(3)
C16–C17–H17A	108.1
C16–C17–H17B	108.1
H17A–C17– H17B	107.3
N8–C18–C12	174.7(4)
P1–C19–H19A	109.5
P1–C19–H19B	109.5
P1–C19–H19C	109.5
H19A–C19– H19B	109.5
H19A–C19– H19C	109.5
H19B–C19– H19C	109.5
P1–C20–H20A	109.5
P1–C20–H20B	109.5
P1–C20–H20C	109.5
H20A–C20– H20B	109.5
H20A–C20– H20C	109.5
H20B–C20– H20C	109.5
P1–C21–H21A	109.5
P1–C21–H21B	109.5
P1–C21–H21C	109.5
H21A–C21– H21B	109.5
H21A–C21– H21C	109.5
H21B–C21– H21C	109.5
N2–B1–N6	108.7(3)
N2–B1–H1A	110.2(16)
N4–B1–N2	110.1(3)
N4–B1–N6	105.0(3)
N4–B1–H1A	109.6(16)
N6–B1–H1A	113.0(17)

Table 5. Torsion angles for mo\_harman\_mne\_nb4\_021\_0m

Atom–Atom– Atom–Atom	Torsion Angle [°]
-------------------------	----------------------

W1–N1–N2–C3	–175.6(2)
W1–N1–N2–B1	11.8(4)

W1–N1–C1–C2	175.0(2)
W1–N3–N4–C6	–170.9(2)
W1–N3–N4–B1	–6.4(4)
W1–N3–C4–C5	170.8(2)
W1–N5–N6–C9	174.46(19)
W1–N5–N6–B1	8.5(4)
W1–N5–C7–C8	–173.5(2)
W1–C10–C11–C12	121.8(3)
W1–C10–C17–C16	–139.4(2)
W1–C11–C12–C13	45.3(4)
W1–C11–C12–C18	174.3(2)
N1–N2–C3–C2	–0.5(4)
N1–N2–B1–N4	–65.0(4)
N1–N2–B1–N6	49.6(4)
N1–C1–C2–C3	0.3(4)
N2–N1–C1–C2	–0.6(4)
N3–N4–C6–C5	–1.5(4)
N3–N4–B1–N2	61.0(4)
N3–N4–B1–N6	–55.9(4)
N3–C4–C5–C6	–0.4(4)
N4–N3–C4–C5	–0.5(3)
N5–N6–C9–C8	0.4(4)
N5–N6–B1–N2	–62.5(4)
N5–N6–B1–N4	55.4(4)
N5–C7–C8–C9	–0.3(3)
N6–N5–C7–C8	0.5(3)
C1–N1–N2–C3	0.7(3)
C1–N1–N2–B1	–171.8(3)
C1–C2–C3–N2	0.1(4)

C3–N2–B1–N4	124.0(3)
C3–N2–B1–N6	–121.4(3)
C4–N3–N4–C6	1.2(3)
C4–N3–N4–B1	165.7(3)
C4–C5–C6–N4	1.1(4)
C6–N4–B1–N2	–138.1(3)
C6–N4–B1–N6	105.0(3)
C7–N5–N6–C9	–0.5(3)
C7–N5–N6–B1	–166.5(3)
C7–C8–C9–N6	–0.1(4)
C9–N6–B1–N2	134.1(3)
C9–N6–B1–N4	–108.0(3)
C10–C11–C12–C13	–48.3(4)
C10–C11–C12–C18	80.7(4)
C11–C10–C17–C16	–57.6(4)
C11–C12–C13–C14	88.5(4)
C12–C13–C14–C15	–9.4(5)
C13–C14–C15–C16	–57.1(5)
C14–C15–C16–C17	–5.3(5)
C15–C16–C17–C10	92.4(4)
C17–C10–C11–W1	–110.1(3)
C17–C10–C11–C12	11.7(5)
C18–C12–C13–C14	–39.2(4)
B1–N2–C3–C2	171.3(3)
B1–N4–C6–C5	–163.9(3)
B1–N6–C9–C8	165.5(3)

## Structure Report for cu\_harman\_mne\_5\_017\_01m

A white, block-shaped crystal of cu\_harman\_mne\_5\_017\_01m was coated with Paratone oil and mounted on a MiTeGen micromount. crystallized from acetonitrile solution. Data were collected at 100.00 K on a Bruker D8 VENTURE dual wavelength Mo/Cu Kappa four-circle diffractometer with a PHOTON III detector. The diffractometer was equipped with an Oxford Cryostream 800Plus low temperature device and used Cu  $K_{\alpha}$  radiation ( $\lambda = 1.54178\text{\AA}$ ) from an Incoatec  $\lambda/\text{ms}$  3.0 microfocus sealed X-ray tube with a HELIOS EF double bounce multilayer mirror as monochromator.

Data collection and processing were done within the Bruker APEX5 software suite.<sup>[1]</sup> All data were integrated with SAINT V8.40B using a narrow-frame algorithm and a Multi-

Scan absorption correction using  $\text{w}$  was applied.<sup>[2]</sup> Using Olex2 as a graphical interface,<sup>[3]</sup> the structure was solved by dual methods with SHELXT 2018/2 and refined by full-matrix least-squares methods against  $F^2$  using XL.<sup>[4,5]</sup> All non-hydrogen atoms were refined with anisotropic displacement parameters. All C-bound hydrogen atoms were refined with isotropic displacement parameters. Some of their coordinates were refined freely and some on calculated positions using a riding model with their  $U_{\text{iso}}$  values constrained to 1.5 times the  $U_{\text{eq}}$  of their pivot atoms for terminal  $\text{sp}^3$  carbon atoms and 1.2 times for all other carbon atoms.

This report and the CIF file were generated using FinalCif.<sup>[6]</sup>

Refinement details for cu\_harman\_mne\_5\_017\_01m

N-H distance was fixed; H8 and H11 were constrained to 1.2 times the  $U_{\text{eq}}$  of their pivot atoms

Table 1. Crystal data and structure refinement for cu\_harman\_mne\_5\_017\_01m

CCDC number	
Empirical formula	$\text{C}_{27}\text{H}_{34}\text{BN}_8\text{O}_2\text{PW}$
Formula weight	728.25
Temperature [K]	100.00
Crystal system	orthorhombic
Space group (number)	<i>Pbca</i> (61)
<i>a</i> [Å]	13.6181(5)
<i>b</i> [Å]	14.0892(4)
<i>c</i> [Å]	30.2413(10)
$\alpha$ [°]	90
$\beta$ [°]	90
$\gamma$ [°]	90
Volume [Å <sup>3</sup> ]	5802.3(3)
<i>Z</i>	8
$\rho_{\text{calc}}$ [gcm <sup>-3</sup> ]	1.667
$\mu$ [mm <sup>-1</sup> ]	8.226
<i>F</i> (000)	2896
Crystal size [mm <sup>3</sup> ]	0.023×0.051×0.077
Crystal colour	white
Crystal shape	block
Radiation	Cu $K_{\alpha}$ ( $\lambda=1.54178$ Å)
2 $\theta$ range [°]	5.84 to 136.64 (0.83 Å)
Index ranges	$-16 \leq h \leq 13$ $-16 \leq k \leq 15$ $-36 \leq l \leq 35$

Reflections collected	29794
Independent reflections	5305 $R_{\text{int}} = 0.1492$ $R_{\text{sigma}} = 0.0843$
Completeness to $\theta = 67.679^\circ$	99.7
Data / Restraints / Parameters	5305 / 1 / 374
Goodness-of-fit on $F^2$	0.923
Final $R$ indexes [ $I \geq 2\sigma(I)$ ]	$R_1 = 0.0447$ $wR_2 = 0.0997$
Final $R$ indexes [all data]	$R_1 = 0.0775$ $wR_2 = 0.1140$
Largest peak/hole [ $\text{e}\text{\AA}^{-3}$ ]	1.73/-1.54

Table 2. Atomic coordinates and  $U_{eq}$  [ $\text{\AA}^2$ ] for cu\_harman\_mne\_5\_017\_01m

Atom	x	y	z	$U_{eq}$
W1	0.54256(2)	0.41419(2)	0.65213(2)	0.01720(11)
P1	0.55711(13)	0.57577(13)	0.68706(5)	0.0197(4)
O1	0.5117(4)	0.3177(4)	0.73898(16)	0.0315(13)
O2	0.2181(5)	0.1671(4)	0.5737(2)	0.0475(17)
N1	0.5915(4)	0.4762(4)	0.58701(18)	0.0201(13)
N2	0.6714(4)	0.4395(4)	0.56549(19)	0.0227(13)
N3	0.7015(4)	0.4066(4)	0.66428(17)	0.0190(12)
N4	0.7683(5)	0.3880(4)	0.6311(2)	0.0227(13)
N5	0.5857(4)	0.2777(4)	0.62156(18)	0.0205(13)
N6	0.6634(4)	0.2708(4)	0.59373(18)	0.0209(13)
N7	0.5181(5)	0.3594(4)	0.7038(2)	0.0248(14)
N8	0.2506(5)	0.3175(4)	0.5946(2)	0.0276(14)
H8	0.226(6)	0.373(3)	0.587(3)	0.033
C1	0.5573(6)	0.5452(5)	0.5607(2)	0.0245(16)
H1	0.501735	0.583707	0.566983	0.029
C2	0.6144(6)	0.5524(5)	0.5230(2)	0.0263(17)
H2	0.605870	0.595870	0.499235	0.032
C3	0.6851(6)	0.4848(5)	0.5267(2)	0.0256(16)
H3	0.735241	0.471743	0.505741	0.031
C4	0.7547(6)	0.4098(5)	0.7015(2)	0.0233(15)
H4	0.727829	0.420625	0.730044	0.028
C5	0.8541(6)	0.3953(5)	0.6933(2)	0.0261(17)
H5	0.906565	0.395940	0.714021	0.031
C6	0.8589(5)	0.3800(5)	0.6492(3)	0.0253(16)
H6	0.917229	0.365768	0.633308	0.030
C7	0.5554(6)	0.1894(5)	0.6297(2)	0.0254(17)
H7	0.502041	0.173269	0.648457	0.030
C8	0.6131(6)	0.1244(5)	0.6069(3)	0.0311(18)
H8A	0.606829	0.057244	0.606859	0.037
C9	0.6811(6)	0.1778(5)	0.5842(2)	0.0288(17)
H9	0.731310	0.154140	0.565427	0.035
C10	0.3903(5)	0.4749(5)	0.6417(2)	0.0217(15)
H10	0.399(7)	0.535(7)	0.621(3)	0.06(3)
C11	0.4039(5)	0.3836(5)	0.6188(2)	0.0206(15)
H11	0.418(6)	0.392(5)	0.587(3)	0.025
C12	0.3348(6)	0.2984(5)	0.6236(2)	0.0246(16)
H12	0.370015	0.243079	0.610271	0.030
C13	0.3032(6)	0.2674(5)	0.6692(2)	0.0282(17)
H13	0.341098	0.219322	0.683146	0.034
C14	0.2266(6)	0.3019(6)	0.6917(3)	0.0304(18)
H14	0.206262	0.268888	0.717487	0.036

C15	0.1716(6)	0.3879(6)	0.6790(3)	0.0296(18)
H15	0.102535	0.383471	0.674997	0.036
C16	0.2153(6)	0.4717(6)	0.6730(3)	0.0290(17)
H16	0.176520	0.523755	0.663360	0.035
C17	0.3230(6)	0.4875(5)	0.6809(3)	0.0295(18)
H17A	0.344620	0.443409	0.704423	0.035
H17B	0.331753	0.552846	0.692292	0.035
C18	0.1969(6)	0.2525(6)	0.5731(2)	0.0298(17)
C19	0.1110(6)	0.2890(5)	0.5474(2)	0.0257(17)
C20	0.0758(6)	0.2360(6)	0.5124(2)	0.0325(18)
H20	0.105729	0.176637	0.505901	0.039
C21	-0.0011(6)	0.2665(6)	0.4867(3)	0.035(2)
H21	-0.022110	0.229255	0.462259	0.042
C22	-0.0484(6)	0.3515(6)	0.4961(3)	0.036(2)
H22	-0.102041	0.373003	0.478711	0.044
C23	-0.0144(6)	0.4041(8)	0.5320(3)	0.044(2)
H23	-0.046654	0.461623	0.539580	0.053
C24	0.0640(6)	0.3750(6)	0.5567(3)	0.036(2)
H24	0.086880	0.413569	0.580298	0.044
C25	0.4938(6)	0.6766(5)	0.6625(3)	0.0278(17)
H25A	0.496874	0.730813	0.682792	0.042
H25B	0.424963	0.659850	0.657125	0.042
H25C	0.525356	0.693418	0.634497	0.042
C26	0.6795(6)	0.6265(6)	0.6920(3)	0.0329(19)
H26A	0.712178	0.625007	0.663172	0.049
H26B	0.717878	0.589392	0.713356	0.049
H26C	0.674517	0.692261	0.702300	0.049
C27	0.5165(6)	0.5786(6)	0.7446(2)	0.0274(17)
H27A	0.557471	0.535841	0.762273	0.041
H27B	0.447818	0.558172	0.746337	0.041
H27C	0.522386	0.643430	0.756089	0.041
B1	0.7315(7)	0.3565(6)	0.5850(3)	0.028(2)
H1A	0.787400	0.338784	0.565230	0.033

$U_{eq}$  is defined as 1/3 of the trace of the orthogonalized  $U_{ij}$  tensor.

Table 3. Anisotropic displacement parameters ( $\text{\AA}^2$ ) for cu\_harman\_mne\_5\_017\_01m.

The anisotropic displacement factor exponent takes the form:

$$-2\pi^2[ h^2(a^*)^2U_{11} + k^2(b^*)^2U_{22} + \dots + 2hka^*b^*U_{12} ]$$

Atom	$U_{11}$	$U_{22}$	$U_{33}$	$U_{23}$	$U_{13}$	$U_{12}$
W1	0.01522(17)	0.01837(17)	0.01800(15)	-0.00130(13)	0.00116(13)	0.00068(13)
P1	0.0183(9)	0.0179(8)	0.0229(8)	-0.0009(7)	0.0014(7)	0.0003(7)
O1	0.041(4)	0.029(3)	0.024(3)	0.005(2)	0.010(2)	0.005(2)
O2	0.053(4)	0.029(3)	0.061(4)	-0.006(3)	-0.013(3)	-0.002(3)
N1	0.015(3)	0.026(3)	0.020(3)	0.003(2)	0.001(2)	-0.002(2)
N2	0.019(3)	0.023(3)	0.026(3)	0.000(3)	-0.003(3)	0.002(2)



N3	0.014(3)	0.024(3)	0.019(3)	0.001(2)	-0.001(2)	0.001(2)
N4	0.019(3)	0.020(3)	0.029(3)	0.001(3)	0.000(3)	0.001(2)
N5	0.018(3)	0.027(3)	0.016(3)	-0.002(2)	0.000(2)	0.003(2)
N6	0.021(3)	0.023(3)	0.018(3)	-0.003(3)	-0.003(2)	0.004(2)
N7	0.025(4)	0.020(3)	0.030(3)	-0.008(3)	0.008(3)	0.001(3)
N8	0.018(3)	0.026(3)	0.039(3)	-0.009(3)	-0.007(3)	-0.001(3)
C1	0.022(4)	0.024(4)	0.028(3)	-0.004(3)	-0.005(3)	0.001(3)
C2	0.034(5)	0.025(4)	0.020(3)	0.002(3)	-0.004(3)	0.002(3)
C3	0.023(4)	0.032(4)	0.021(3)	-0.002(3)	0.001(3)	-0.002(3)
C4	0.029(4)	0.017(3)	0.025(3)	-0.003(3)	-0.002(3)	0.001(3)
C5	0.025(4)	0.024(4)	0.029(4)	-0.001(3)	-0.010(3)	0.001(3)
C6	0.014(4)	0.022(3)	0.041(4)	0.005(3)	0.001(3)	0.003(3)
C7	0.035(5)	0.013(3)	0.027(4)	0.000(3)	-0.001(4)	-0.004(3)
C8	0.037(5)	0.017(3)	0.039(4)	0.004(3)	-0.012(4)	0.002(3)
C9	0.031(5)	0.028(4)	0.027(4)	-0.008(3)	-0.005(3)	0.013(3)
C10	0.010(3)	0.022(4)	0.033(4)	-0.006(3)	-0.007(3)	-0.002(3)
C11	0.009(3)	0.028(4)	0.024(3)	-0.005(3)	-0.005(3)	0.000(3)
C12	0.022(4)	0.021(4)	0.031(4)	-0.007(3)	-0.003(3)	0.001(3)
C13	0.026(4)	0.025(4)	0.034(4)	-0.001(3)	-0.001(3)	-0.006(3)
C14	0.029(5)	0.028(4)	0.034(4)	-0.003(3)	0.007(4)	-0.014(3)
C15	0.019(4)	0.040(5)	0.030(4)	-0.006(4)	0.000(3)	-0.003(3)
C16	0.022(4)	0.034(4)	0.032(4)	-0.005(4)	0.003(3)	-0.001(3)
C17	0.027(5)	0.023(4)	0.038(4)	-0.004(3)	0.001(4)	-0.003(3)
C18	0.029(4)	0.032(4)	0.028(4)	-0.009(4)	0.006(3)	-0.007(4)
C19	0.023(4)	0.033(4)	0.021(3)	-0.005(3)	0.006(3)	-0.009(3)
C20	0.033(5)	0.037(5)	0.027(4)	-0.005(4)	0.008(3)	-0.011(4)
C21	0.031(5)	0.048(5)	0.025(4)	-0.005(4)	0.001(3)	-0.012(4)
C22	0.020(4)	0.058(6)	0.031(4)	0.001(4)	0.006(4)	-0.007(4)
C23	0.029(5)	0.071(7)	0.034(4)	-0.013(5)	0.003(4)	0.008(5)
C24	0.028(5)	0.049(5)	0.032(4)	-0.010(4)	0.003(4)	-0.003(4)
C25	0.026(4)	0.022(4)	0.036(4)	-0.005(3)	0.000(3)	0.005(3)
C26	0.016(4)	0.026(4)	0.057(5)	0.005(4)	-0.003(4)	-0.004(3)
C27	0.032(4)	0.029(4)	0.021(3)	0.001(3)	-0.007(3)	0.004(3)
B1	0.023(5)	0.034(5)	0.026(4)	-0.003(4)	-0.001(4)	0.005(4)

Table 4. Bond lengths and angles for cu\_harman\_mne\_5\_017\_01m

Atom-Atom	Length [Å]	O2-C18	1.237(10)
W1-P1	2.5175(18)	N1-N2	1.369(8)
W1-N1	2.255(5)	N1-C1	1.341(9)
W1-N3	2.198(6)	N2-C3	1.348(9)
W1-N5	2.213(6)	N2-B1	1.544(10)
W1-N7	1.774(6)	N3-N4	1.380(8)
W1-C10	2.265(7)	N3-C4	1.339(9)
W1-C11	2.184(7)	N4-C6	1.355(9)
P1-C25	1.820(8)	N4-B1	1.546(10)
P1-C26	1.820(8)	N5-N6	1.355(8)
P1-C27	1.827(7)	N5-C7	1.333(9)
O1-N7	1.219(8)	N6-C9	1.363(9)

N6–B1	1.545(11)
N8–H8	0.87(2)
N8–C12	1.468(9)
N8–C18	1.341(9)
C1–H1	0.9500
C1–C2	1.384(10)
C2–H2	0.9500
C2–C3	1.360(10)
C3–H3	0.9500
C4–H4	0.9500
C4–C5	1.390(11)
C5–H5	0.9500
C5–C6	1.353(10)
C6–H6	0.9500
C7–H7	0.9500
C7–C8	1.391(11)
C8–H8A	0.9500
C8–C9	1.375(11)
C9–H9	0.9500
C10–H10	1.07(10)
C10–C11	1.472(10)
C10–C17	1.508(11)
C11–H11	0.99(8)
C11–C12	1.532(10)
C12–H12	1.0000
C12–C13	1.510(10)
C13–H13	0.9500
C13–C14	1.337(11)
C14–H14	0.9500
C14–C15	1.475(11)
C15–H15	0.9500
C15–C16	1.335(11)
C16–H16	0.9500
C16–C17	1.503(11)
C17–H17A	0.9900
C17–H17B	0.9900
C18–C19	1.496(11)
C19–C20	1.382(10)
C19–C24	1.399(11)
C20–H20	0.9500
C20–C21	1.374(11)
C21–H21	0.9500
C21–C22	1.389(12)
C22–H22	0.9500
C22–C23	1.394(12)
C23–H23	0.9500
C23–C24	1.365(12)
C24–H24	0.9500

C25–H25A	0.9800
C25–H25B	0.9800
C25–H25C	0.9800
C26–H26A	0.9800
C26–H26B	0.9800
C26–H26C	0.9800
C27–H27A	0.9800
C27–H27B	0.9800
C27–H27C	0.9800
B1–H1A	1.0000
<b>Atom–Atom– Atom</b>	<b>Angle [°]</b>
N1–W1–P1	89.60(15)
N1–W1–C10	90.1(2)
N3–W1–P1	84.04(15)
N3–W1–N1	82.8(2)
N3–W1–N5	76.5(2)
N3–W1–C10	160.5(2)
N5–W1–P1	160.08(17)
N5–W1–N1	83.9(2)
N5–W1–C10	120.9(2)
N7–W1–P1	92.24(19)
N7–W1–N1	173.2(3)
N7–W1–N3	91.0(3)
N7–W1–N5	92.2(2)
N7–W1–C10	96.6(3)
N7–W1–C11	99.1(3)
C10–W1–P1	77.81(18)
C11–W1–P1	116.10(19)
C11–W1–N1	85.9(2)
C11–W1–N3	156.8(2)
C11–W1–N5	82.3(2)
C11–W1–C10	38.6(2)
C25–P1–W1	119.8(3)
C25–P1–C26	99.3(4)
C25–P1–C27	103.1(3)
C26–P1–W1	117.5(3)
C26–P1–C27	100.9(4)
C27–P1–W1	113.3(3)
N2–N1–W1	120.2(4)
C1–N1–W1	134.2(5)
C1–N1–N2	105.5(6)
N1–N2–B1	121.7(6)
C3–N2–N1	110.2(6)
C3–N2–B1	128.1(6)
N4–N3–W1	122.5(4)
C4–N3–W1	132.2(5)

C4-N3-N4	105.1(6)
N3-N4-B1	119.8(6)
C6-N4-N3	108.8(6)
C6-N4-B1	129.5(7)
N6-N5-W1	121.9(4)
C7-N5-W1	130.6(5)
C7-N5-N6	106.8(6)
N5-N6-C9	109.7(6)
N5-N6-B1	121.2(6)
C9-N6-B1	127.5(7)
O1-N7-W1	172.8(6)
C12-N8-H8	128(6)
C18-N8-H8	106(6)
C18-N8-C12	126.1(7)
N1-C1-H1	124.8
N1-C1-C2	110.3(7)
C2-C1-H1	124.8
C1-C2-H2	126.9
C3-C2-C1	106.1(7)
C3-C2-H2	126.9
N2-C3-C2	107.9(7)
N2-C3-H3	126.1
C2-C3-H3	126.1
N3-C4-H4	124.1
N3-C4-C5	111.9(7)
C5-C4-H4	124.1
C4-C5-H5	127.9
C6-C5-C4	104.2(7)
C6-C5-H5	127.9
N4-C6-H6	125.0
C5-C6-N4	110.0(7)
C5-C6-H6	125.0
N5-C7-H7	124.8
N5-C7-C8	110.4(7)
C8-C7-H7	124.8
C7-C8-H8A	127.3
C9-C8-C7	105.5(7)
C9-C8-H8A	127.3
N6-C9-C8	107.6(7)
N6-C9-H9	126.2
C8-C9-H9	126.2
W1-C10-H10	107(6)
C11-C10-W1	67.7(4)
C11-C10-H10	114(5)
C11-C10-C17	123.3(7)
C17-C10-W1	119.4(5)
C17-C10-H10	116(5)
W1-C11-H11	104(5)

C10-C11-W1	73.7(4)
C10-C11-H11	112(4)
C10-C11-C12	124.3(6)
C12-C11-W1	130.0(5)
C12-C11-H11	108(5)
N8-C12-C11	106.2(6)
N8-C12-H12	106.2
N8-C12-C13	112.1(6)
C11-C12-H12	106.2
C13-C12-C11	119.1(6)
C13-C12-H12	106.2
C12-C13-H13	117.2
C14-C13-C12	125.5(7)
C14-C13-H13	117.2
C13-C14-H14	117.9
C13-C14-C15	124.3(7)
C15-C14-H14	117.9
C14-C15-H15	118.8
C16-C15-C14	122.3(7)
C16-C15-H15	118.8
C15-C16-H16	118.5
C15-C16-C17	123.1(8)
C17-C16-H16	118.5
C10-C17-H17A	108.1
C10-C17-H17B	108.1
C16-C17-C10	116.9(7)
C16-C17-H17A	108.1
C16-C17-H17B	108.1
H17A-C17-H17B	107.3
O2-C18-N8	122.0(8)
O2-C18-C19	121.7(7)
N8-C18-C19	116.3(7)
C20-C19-C18	118.8(7)
C20-C19-C24	117.6(8)
C24-C19-C18	123.5(7)
C19-C20-H20	119.1
C21-C20-C19	121.9(8)
C21-C20-H20	119.1
C20-C21-H21	119.8
C20-C21-C22	120.5(7)
C22-C21-H21	119.8
C21-C22-H22	121.2
C21-C22-C23	117.7(8)
C23-C22-H22	121.2
C22-C23-H23	119.1
C24-C23-C22	121.7(9)
C24-C23-H23	119.1

C19–C24–H24	119.7
C23–C24–C19	120.6(8)
C23–C24–H24	119.7
P1–C25–H25A	109.5
P1–C25–H25B	109.5
P1–C25–H25C	109.5
H25A–C25–H25B	109.5
H25A–C25–H25C	109.5
H25B–C25–H25C	109.5
P1–C26–H26A	109.5
P1–C26–H26B	109.5
P1–C26–H26C	109.5
H26A–C26–H26B	109.5
H26A–C26–H26C	109.5

H26B–C26–H26C	109.5
P1–C27–H27A	109.5
P1–C27–H27B	109.5
P1–C27–H27C	109.5
H27A–C27–H27B	109.5
H27A–C27–H27C	109.5
H27B–C27–H27C	109.5
N2–B1–N4	107.4(6)
N2–B1–N6	109.8(6)
N2–B1–H1A	111.3
N4–B1–H1A	111.3
N6–B1–N4	105.4(6)
N6–B1–H1A	111.3

Table 5. Torsion angles for cu\_harman\_mne\_5\_017\_01m

Atom–Atom–Atom–Atom	Torsion Angle [°]
W1–N1–N2–C3	177.8(5)
W1–N1–N2–B1	–1.0(8)
W1–N1–C1–C2	–177.8(5)
W1–N3–N4–C6	–174.9(4)
W1–N3–N4–B1	–9.3(8)
W1–N3–C4–C5	175.6(5)
W1–N5–N6–C9	172.3(5)
W1–N5–N6–B1	5.3(8)
W1–N5–C7–C8	–171.3(5)
W1–C10–C11–C12	127.6(7)
W1–C10–C17–C16	–145.1(6)
W1–C11–C12–N8	177.6(5)
W1–C11–C12–C13	49.8(9)
O2–C18–C19–C20	–22.9(11)
O2–C18–C19–C24	157.6(8)
N1–N2–C3–C2	0.7(8)
N1–N2–B1–N4	–57.5(9)
N1–N2–B1–N6	56.6(8)
N1–C1–C2–C3	0.4(9)
N2–N1–C1–C2	0.0(8)
N3–N4–C6–C5	–1.5(8)
N3–N4–B1–N2	63.9(8)
N3–N4–B1–N6	–53.1(8)
N3–C4–C5–C6	–1.9(8)
N4–N3–C4–C5	1.0(8)

N5–N6–C9–C8	–0.3(8)
N5–N6–B1–N2	–59.7(8)
N5–N6–B1–N4	55.7(8)
N5–C7–C8–C9	0.3(9)
N6–N5–C7–C8	–0.4(8)
N8–C12–C13–C14	–38.2(10)
N8–C18–C19–C20	155.9(7)
N8–C18–C19–C24	–23.7(11)
C1–N1–N2–C3	–0.5(7)
C1–N1–N2–B1	–179.3(6)
C1–C2–C3–N2	–0.6(8)
C3–N2–B1–N4	123.9(8)
C3–N2–B1–N6	–122.0(8)
C4–N3–N4–C6	0.3(7)
C4–N3–N4–B1	166.0(6)
C4–C5–C6–N4	2.0(8)
C6–N4–B1–N2	–133.8(7)
C6–N4–B1–N6	109.1(8)
C7–N5–N6–C9	0.5(8)
C7–N5–N6–B1	–166.6(6)
C7–C8–C9–N6	0.0(8)
C9–N6–B1–N2	135.8(7)
C9–N6–B1–N4	–108.8(8)
C10–C11–C12–N8	80.2(8)
C10–C11–C12–C13	–47.5(10)
C11–C10–C17–C16	–63.8(10)

C11–C12–C13–C14	86.7(10)
C12–N8–C18–O2	–4.5(12)
C12–N8–C18–C19	176.7(7)
C12–C13–C14–C15	–11.9(12)
C13–C14–C15–C16	–55.3(12)
C14–C15–C16–C17	–3.3(12)
C15–C16–C17–C10	92.1(9)
C17–C10–C11–W1	–111.5(7)
C17–C10–C11–C12	16.1(11)
C18–N8–C12–C11	148.4(7)
C18–N8–C12–C13	–79.9(9)
C18–C19–C20–C21	–178.2(7)

C18–C19–C24–C23	–179.7(8)
C19–C20–C21–C22	–2.0(12)
C20–C19–C24–C23	0.7(12)
C20–C21–C22–C23	0.5(12)
C21–C22–C23–C24	1.6(13)
C22–C23–C24–C19	–2.2(14)
C24–C19–C20–C21	1.4(11)
B1–N2–C3–C2	179.4(7)
B1–N4–C6–C5	–165.3(7)
B1–N6–C9–C8	165.7(7)

### Structure Report for mo\_harman\_2\_jkh\_295\_x2\_0m

A colourless, block shaped crystal of mo\_harman\_2\_jkh\_295\_x2\_0m measuring 0.033×0.069×0.079 mm was coated with Paratone oil and mounted on a MiTeGen micromount. Data for mo\_harman\_2\_jkh\_295\_x2\_0m were measured on a Bruker D8 VENTURE dual wavelength Mo/Cu Kappa four-circle diffractometer equipped with a PHOTON III detector and an Incoatec IpS 3.0 microfocus sealed X-ray tube (Mo  $K_{\alpha}$ ,  $\lambda=0.71073$  Å) using a HELIOS double bounce multilayer mirror as monochromator. The crystal temperature was controlled with an Oxford Cryostream 800low temperature device. Data collection and processing were done within the Bruker APEX5 software suite.<sup>24</sup> All data were integrated with the Bruker SAINT 8.40B software using a narrow-frame algorithm. Data were corrected for absorption effects using a Multi-Scan method (SADABS).

The structure was solved by dual methods with XT<sup>25</sup> and refined by full-matrix least-squares methods against  $F^2$  using XL<sup>26</sup> within OLEX2.<sup>27</sup> All non-hydrogen atoms were refined with anisotropically. The BH hydrogen was located in the electron density map and refined isotropically. All other hydrogen atoms were placed in geometrically calculated positions with  $U_{iso} = 1.2U_{equiv}$  of the parent atom ( $1.5U_{equiv}$  for methyl). This report and the CIF file were generated using FinalCif.<sup>28</sup>

<sup>24</sup> APEX5, Saint, SADABS; Bruker AXS Inc. 2019.

<sup>25</sup> Sheldrick, G. M. *SHELXT* – Integrated space-group and crystal-structure determination. *Acta Cryst. Sect. A Found. Adv.* **2015**, *71*, 3–8.

<sup>26</sup> Sheldrick, G. M. Crystal structure refinement with *SHELXL*. *Acta Cryst. Sect. C Struct. Chem.* **2015**, *71*, 3–8.

<sup>27</sup> Dolomanov, O. V.; Bourhis, L. J.; Gildea, R. J.; Howard, J. A. K.; Puschmann, H. *OLEX2*: a completed structure solution, refinement and analysis program. *J. Appl. Cryst.* **2009**, *42*, 339–341.

<sup>28</sup> Kratzert, D. FinalCif, <https://dkratzert.de/finalcif.html>.

Table 1. Crystal data and structure refinement for mo\_harman\_2\_jkh\_295\_x2\_0m

CCDC number	
Empirical formula	C <sub>25</sub> H <sub>35</sub> BN <sub>7</sub> O <sub>5</sub> PW
Formula weight	739.23
Temperature [K]	100.00
Wavelength [Å]	0.71073
Crystal size [mm <sup>3</sup> ]	0.033×0.069×0.079
Crystal habit	colourless block
Crystal system	orthorhombic
Space group	<i>Pna</i> 2 <sub>1</sub> (33)
<i>a</i> [Å]	22.7303(11)
<i>b</i> [Å]	14.2785(7)
<i>c</i> [Å]	9.0367(5)
$\alpha$ [°]	90
$\beta$ [°]	90
$\gamma$ [°]	90
Volume [Å <sup>3</sup> ]	2932.9(3)
<i>Z</i>	4
$\rho_{\text{calc}}$ [gcm <sup>-3</sup> ]	1.674
$\mu$ [mm <sup>-1</sup> ]	4.040
<i>F</i> (000)	1472
2 $\theta$ range [°]	4.58 to 56.60 (0.75 Å)
Index ranges	-30 ≤ <i>h</i> ≤ 27 -19 ≤ <i>k</i> ≤ 17 -12 ≤ <i>l</i> ≤ 12
Reflections collected	46671
Independent reflections	7278 [ <i>R</i> <sub>int</sub> = 0.1134]
Data / Restraints / Parameters	7278 / 1 / 370
Goodness-of-fit on <i>F</i> <sup>2</sup>	1.016
Final <i>R</i> indexes [ <i>I</i> ≥ 2 $\sigma$ ( <i>I</i> )]	<i>R</i> <sub>1</sub> = 0.0417 <i>wR</i> <sub>2</sub> = 0.0709
Final <i>R</i> indexes [all data]	<i>R</i> <sub>1</sub> = 0.0711 <i>wR</i> <sub>2</sub> = 0.0803
Largest peak/hole [eÅ <sup>-3</sup> ]	0.89/-1.28
Flack X parameter	-0.010(9)

Table 2. Atomic coordinates and  $U_{eq}$  [Å<sup>2</sup>] for mo\_harman\_2\_jkh\_295\_x2\_0m

Atom	x	y	z	$U_{eq}$
W1	0.64994(2)	0.26733(2)	0.68802(8)	0.01151(8)
P1	0.70404(12)	0.1598(2)	0.8596(3)	0.0167(6)
O1	0.7146(3)	0.2049(5)	0.4153(9)	0.0231(18)
O2	0.4233(3)	0.3258(5)	0.6335(8)	0.0193(17)
O3	0.4304(3)	0.1879(5)	0.7543(8)	0.0167(17)
O4	0.4352(3)	0.2548(5)	0.2662(8)	0.0213(17)
O5	0.3727(3)	0.1645(5)	0.3954(8)	0.0206(17)
N1	0.6069(3)	0.3286(6)	0.8919(9)	0.0125(18)
N2	0.6118(5)	0.4213(9)	0.9197(13)	0.016(3)
N3	0.7217(3)	0.3645(6)	0.7431(9)	0.0136(18)
N4	0.7118(4)	0.4473(6)	0.8115(9)	0.0152(19)
N5	0.6227(4)	0.4001(6)	0.5861(10)	0.0150(19)
N6	0.6232(3)	0.4821(5)	0.6619(11)	0.013(2)
N7	0.6869(3)	0.2278(6)	0.5285(9)	0.0148(18)
C1	0.5691(4)	0.2949(8)	0.9902(11)	0.018(2)
H1	0.557942	0.230910	0.997903	0.022
C2	0.5481(5)	0.3660(8)	1.0801(12)	0.018(2)
H2	0.520069	0.360817	1.157767	0.022
C3	0.5762(5)	0.4451(8)	1.0332(11)	0.016(2)
H3	0.571485	0.506156	1.073420	0.020
C4	0.7802(4)	0.3584(7)	0.7266(12)	0.021(3)
H4	0.799842	0.308343	0.678147	0.025
C5	0.8083(4)	0.4355(7)	0.7901(12)	0.019(2)
H5	0.849352	0.446625	0.798014	0.022
C6	0.7632(4)	0.4918(8)	0.8387(12)	0.018(2)
H6	0.767358	0.551548	0.883666	0.022
C7	0.6071(6)	0.4219(10)	0.4459(17)	0.015(3)
H7	0.603381	0.378193	0.367287	0.018
C8	0.5975(4)	0.5166(7)	0.4338(11)	0.016(2)
H8	0.586299	0.550109	0.347441	0.019
C9	0.6073(4)	0.5525(8)	0.5719(12)	0.016(2)
H9	0.603477	0.616428	0.599488	0.020
C10	0.5884(3)	0.1455(6)	0.7010(18)	0.011(2)
H10	0.572640	0.132833	0.802255	0.014
C11	0.5610(4)	0.2246(8)	0.6256(11)	0.022(2)
H11	0.533908	0.254198	0.699259	0.027
C12	0.5284(4)	0.2245(7)	0.4799(10)	0.012(2)
H12	0.525733	0.291479	0.448418	0.014
C13	0.5557(4)	0.1721(8)	0.3507(11)	0.015(2)
H13	0.576748	0.209122	0.281356	0.018
C14	0.5536(4)	0.0809(7)	0.3226(12)	0.015(2)
H14	0.566103	0.060958	0.227346	0.018

C15	0.5337(4)	0.0081(7)	0.4263(13)	0.020(2)
H15	0.503133	−0.033141	0.396313	0.024
C16	0.5567(4)	−0.0020(7)	0.5600(12)	0.014(2)
H16	0.541012	−0.048633	0.623800	0.017
C17	0.6064(4)	0.0571(7)	0.6139(12)	0.018(2)
H17A	0.630180	0.076701	0.527459	0.022
H17B	0.631876	0.018190	0.677934	0.022
C18	0.4368(4)	0.2437(8)	0.6337(12)	0.017(3)
C19	0.4638(4)	0.1912(7)	0.5070(11)	0.012(2)
H19	0.463786	0.122678	0.530079	0.014
C20	0.4247(4)	0.2090(7)	0.3741(12)	0.015(2)
C21	0.3274(4)	0.1838(9)	0.2838(12)	0.027(3)
H21A	0.339065	0.155894	0.189222	0.040
H21B	0.323056	0.251692	0.271859	0.040
H21C	0.289873	0.156854	0.315908	0.040
C22	0.4130(5)	0.2353(8)	0.8864(11)	0.020(2)
H22A	0.375764	0.268258	0.869006	0.030
H22B	0.443369	0.280613	0.914429	0.030
H22C	0.407761	0.189665	0.966286	0.030
C23	0.7586(5)	0.0880(8)	0.7666(14)	0.030(3)
H23A	0.779380	0.049554	0.839735	0.045
H23B	0.786913	0.128542	0.715532	0.045
H23C	0.739130	0.047312	0.694479	0.045
C24	0.7453(5)	0.2165(8)	1.0069(12)	0.026(3)
H24A	0.717926	0.247079	1.075399	0.039
H24B	0.771769	0.263462	0.964270	0.039
H24C	0.768408	0.169524	1.060496	0.039
C25	0.6659(5)	0.0773(8)	0.9759(12)	0.024(3)
H25A	0.644137	0.032802	0.914007	0.035
H25B	0.638274	0.110910	1.040155	0.035
H25C	0.694396	0.043266	1.036918	0.035
B1	0.6490(5)	0.4868(8)	0.8210(13)	0.014(2)
H1A	0.646(4)	0.558(6)	0.861(10)	0.00(2)

$U_{eq}$  is defined as 1/3 of the trace of the orthogonalized  $U_{ij}$  tensor.

Table 3. Anisotropic displacement parameters ( $\text{\AA}^2$ ) for mo\_harman\_2\_jkh\_295\_x2\_0m. The anisotropic displacement factor exponent takes the form:  $-2\pi^2[h^2(a^*)^2U_{11} + k^2(b^*)^2U_{22} + \dots + 2hka^*b^*U_{12}]$

Atom	$U_{11}$	$U_{22}$	$U_{33}$	$U_{23}$	$U_{13}$	$U_{12}$
W1	0.01134(13)	0.01074(14)	0.01246(15)	−0.0003(5)	−0.0007(4)	−0.00081(15)
P1	0.0158(13)	0.0173(15)	0.0171(15)	0.0024(12)	−0.0037(11)	−0.0015(12)
O1	0.028(4)	0.020(4)	0.021(5)	−0.005(3)	0.016(4)	0.002(3)



O2	0.024(4)	0.014(4)	0.020(4)	-0.002(3)	0.000(3)	0.006(3)
O3	0.022(4)	0.017(5)	0.011(4)	-0.001(3)	0.005(3)	-0.001(4)
O4	0.020(4)	0.025(5)	0.019(4)	0.005(3)	0.000(3)	0.000(3)
O5	0.011(3)	0.027(4)	0.023(4)	0.005(3)	-0.003(3)	-0.004(3)
N1	0.018(4)	0.012(5)	0.007(4)	-0.004(3)	0.006(3)	0.001(3)
N2	0.024(6)	0.015(7)	0.008(6)	0.001(5)	0.001(5)	-0.003(5)
N3	0.012(4)	0.016(5)	0.013(4)	0.002(3)	-0.005(3)	0.002(3)
N4	0.018(4)	0.012(5)	0.015(5)	0.002(4)	-0.001(4)	-0.005(4)
N5	0.021(5)	0.007(4)	0.017(5)	-0.001(4)	-0.002(4)	0.002(4)
N6	0.013(3)	0.010(4)	0.015(7)	-0.004(4)	-0.003(4)	0.000(3)
N7	0.017(4)	0.007(4)	0.021(5)	0.002(4)	-0.002(3)	0.002(4)
C1	0.019(5)	0.023(6)	0.013(6)	0.003(4)	0.002(4)	-0.003(4)
C2	0.018(5)	0.027(7)	0.010(5)	0.000(5)	0.001(4)	0.001(5)
C3	0.022(5)	0.017(6)	0.010(5)	0.001(4)	-0.001(4)	0.008(4)
C4	0.015(5)	0.022(6)	0.026(8)	0.010(4)	0.003(4)	0.004(4)
C5	0.011(5)	0.018(6)	0.027(6)	0.003(5)	-0.005(4)	-0.004(4)
C6	0.018(5)	0.020(6)	0.017(6)	0.006(5)	-0.006(4)	-0.008(4)
C7	0.011(6)	0.017(8)	0.018(8)	-0.003(7)	0.003(6)	-0.004(6)
C8	0.024(5)	0.015(6)	0.009(5)	0.002(4)	0.001(4)	-0.003(4)
C9	0.012(5)	0.012(6)	0.026(6)	-0.001(5)	-0.001(4)	-0.002(4)
C10	0.009(3)	0.019(5)	0.007(6)	-0.002(6)	0.000(5)	-0.006(3)
C11	0.010(4)	0.037(7)	0.019(5)	-0.007(5)	0.000(4)	0.002(5)
C12	0.010(4)	0.013(5)	0.013(5)	-0.001(4)	0.002(4)	0.000(4)
C13	0.003(4)	0.029(7)	0.012(5)	0.002(5)	-0.002(4)	0.001(4)
C14	0.010(5)	0.022(6)	0.014(6)	-0.004(4)	0.002(4)	0.002(4)
C15	0.016(5)	0.014(6)	0.030(7)	-0.011(5)	0.003(5)	0.001(4)
C16	0.014(5)	0.014(6)	0.014(6)	-0.002(4)	0.002(4)	0.006(4)
C17	0.016(5)	0.017(6)	0.022(6)	0.001(5)	-0.004(4)	0.003(4)
C18	0.013(5)	0.024(8)	0.016(5)	0.003(4)	-0.004(4)	-0.002(5)
C19	0.012(5)	0.010(5)	0.014(5)	-0.002(4)	0.000(4)	0.004(4)
C20	0.012(5)	0.019(6)	0.014(6)	0.002(4)	-0.001(4)	-0.001(4)
C21	0.013(5)	0.039(8)	0.028(7)	-0.003(6)	-0.009(5)	0.000(5)
C22	0.026(5)	0.019(6)	0.014(5)	0.003(5)	-0.001(4)	-0.002(5)
C23	0.026(6)	0.024(7)	0.040(8)	0.007(6)	-0.010(6)	0.004(5)
C24	0.028(6)	0.034(8)	0.015(6)	0.006(5)	-0.012(5)	-0.010(6)
C25	0.024(6)	0.026(7)	0.020(6)	0.008(5)	-0.011(5)	-0.007(5)
B1	0.012(5)	0.013(6)	0.015(6)	-0.002(5)	0.004(5)	0.001(5)

Table 4. Bond lengths and angles for mo\_harman\_2\_jkh\_295\_x2\_0m

Atom-Atom	Length [Å]	P1-C23	1.816(12)
W1-P1	2.505(3)	P1-C24	1.818(11)
W1-N1	2.262(8)	P1-C25	1.802(11)
W1-N3	2.199(8)	O1-N7	1.245(10)
W1-N5	2.197(8)	O2-C18	1.212(13)
W1-N7	1.761(9)	O3-C18	1.359(11)
W1-C10	2.234(8)	O3-C22	1.428(12)
W1-C11	2.186(10)	O4-C20	1.198(12)

O5–C20	1.357(11)
O5–C21	1.467(12)
N1–N2	1.353(14)
N1–C1	1.326(12)
N2–C3	1.350(15)
N2–B1	1.545(16)
N3–N4	1.353(11)
N3–C4	1.340(12)
N4–C6	1.351(12)
N4–B1	1.537(15)
N5–N6	1.357(11)
N5–C7	1.351(16)
N6–C9	1.342(13)
N6–B1	1.555(15)
C1–H1	0.9500
C1–C2	1.385(15)
C2–H2	0.9500
C2–C3	1.365(15)
C3–H3	0.9500
C4–H4	0.9500
C4–C5	1.397(14)
C5–H5	0.9500
C5–C6	1.374(15)
C6–H6	0.9500
C7–H7	0.9500
C7–C8	1.373(18)
C8–H8	0.9500
C8–C9	1.368(14)
C9–H9	0.9500
C10–H10	1.0000
C10–C11	1.459(15)
C10–C17	1.542(15)
C11–H11	1.0000
C11–C12	1.510(13)
C12–H12	1.0000
C12–C13	1.519(13)
C12–C19	1.564(13)
C13–H13	0.9500
C13–C14	1.327(14)
C14–H14	0.9500
C14–C15	1.471(15)
C15–H15	0.9500
C15–C16	1.324(15)
C16–H16	0.9500
C16–C17	1.492(14)
C17–H17A	0.9900
C17–H17B	0.9900
C18–C19	1.501(14)

C19–H19	1.0000
C19–C20	1.514(13)
C21–H21A	0.9800
C21–H21B	0.9800
C21–H21C	0.9800
C22–H22A	0.9800
C22–H22B	0.9800
C22–H22C	0.9800
C23–H23A	0.9800
C23–H23B	0.9800
C23–H23C	0.9800
C24–H24A	0.9800
C24–H24B	0.9800
C24–H24C	0.9800
C25–H25A	0.9800
C25–H25B	0.9800
C25–H25C	0.9800
B1–H1A	1.08(9)
Atom–Atom–Atom	Angle [°]
N1–W1–P1	86.9(2)
N3–W1–P1	83.3(2)
N3–W1–N1	83.8(3)
N3–W1–C10	160.7(4)
N5–W1–P1	158.0(2)
N5–W1–N1	83.4(3)
N5–W1–N3	76.1(3)
N5–W1–C10	121.1(4)
N7–W1–P1	94.4(3)
N7–W1–N1	175.5(3)
N7–W1–N3	92.0(3)
N7–W1–N5	93.9(4)
N7–W1–C10	95.2(5)
N7–W1–C11	98.1(4)
C10–W1–P1	78.3(3)
C10–W1–N1	89.3(4)
C11–W1–P1	116.3(3)
C11–W1–N1	85.3(3)
C11–W1–N3	157.0(4)
C11–W1–N5	82.6(4)
C11–W1–C10	38.5(4)
C23–P1–W1	113.3(4)
C23–P1–C24	103.7(6)
C24–P1–W1	115.7(4)
C25–P1–W1	121.7(4)
C25–P1–C23	103.3(6)
C25–P1–C24	96.5(5)

C18-O3-C22	114.9(8)
C20-O5-C21	115.2(8)
N2-N1-W1	119.6(7)
C1-N1-W1	133.3(7)
C1-N1-N2	106.5(9)
N1-N2-B1	122.0(10)
C3-N2-N1	109.8(10)
C3-N2-B1	127.9(11)
N4-N3-W1	122.1(6)
C4-N3-W1	132.0(7)
C4-N3-N4	105.8(8)
N3-N4-B1	120.0(8)
C6-N4-N3	110.5(9)
C6-N4-B1	128.3(9)
N6-N5-W1	122.1(6)
C7-N5-W1	131.7(8)
C7-N5-N6	106.0(9)
N5-N6-B1	120.5(8)
C9-N6-N5	109.8(9)
C9-N6-B1	129.0(9)
O1-N7-W1	176.3(8)
N1-C1-H1	124.8
N1-C1-C2	110.5(10)
C2-C1-H1	124.8
C1-C2-H2	127.4
C3-C2-C1	105.3(10)
C3-C2-H2	127.4
N2-C3-C2	107.9(10)
N2-C3-H3	126.0
C2-C3-H3	126.0
N3-C4-H4	124.6
N3-C4-C5	110.9(9)
C5-C4-H4	124.6
C4-C5-H5	127.7
C6-C5-C4	104.5(9)
C6-C5-H5	127.7
N4-C6-C5	108.2(9)
N4-C6-H6	125.9
C5-C6-H6	125.9
N5-C7-H7	125.0
N5-C7-C8	110.1(12)
C8-C7-H7	125.0
C7-C8-H8	127.2
C9-C8-C7	105.7(11)
C9-C8-H8	127.2
N6-C9-C8	108.4(9)
N6-C9-H9	125.8
C8-C9-H9	125.8

W1-C10-H10	114.4
C11-C10-W1	69.0(5)
C11-C10-H10	114.4
C11-C10-C17	120.6(12)
C17-C10-W1	116.4(7)
C17-C10-H10	114.4
W1-C11-H11	106.2
C10-C11-W1	72.5(5)
C10-C11-H11	106.2
C10-C11-C12	128.0(10)
C12-C11-W1	132.7(7)
C12-C11-H11	106.2
C11-C12-H12	106.1
C11-C12-C13	118.1(8)
C11-C12-C19	108.9(8)
C13-C12-H12	106.1
C13-C12-C19	110.7(8)
C19-C12-H12	106.1
C12-C13-H13	116.0
C14-C13-C12	128.1(10)
C14-C13-H13	116.0
C13-C14-H14	117.2
C13-C14-C15	125.6(10)
C15-C14-H14	117.2
C14-C15-H15	118.8
C16-C15-C14	122.5(10)
C16-C15-H15	118.8
C15-C16-H16	118.8
C15-C16-C17	122.3(10)
C17-C16-H16	118.8
C10-C17-H17A	108.4
C10-C17-H17B	108.4
C16-C17-C10	115.4(8)
C16-C17-H17A	108.4
C16-C17-H17B	108.4
H17A-C17-H17B	107.5
O2-C18-O3	122.8(10)
O2-C18-C19	125.9(10)
O3-C18-C19	111.2(9)
C12-C19-H19	109.3
C18-C19-C12	110.6(8)
C18-C19-H19	109.3
C18-C19-C20	106.3(8)
C20-C19-C12	112.1(8)
C20-C19-H19	109.3
O4-C20-O5	123.0(9)
O4-C20-C19	128.3(9)

O5–C20–C19	108.7(8)
O5–C21–H21A	109.5
O5–C21–H21B	109.5
O5–C21–H21C	109.5
H21A–C21–H21B	109.5
H21A–C21–H21C	109.5
H21B–C21–H21C	109.5
O3–C22–H22A	109.5
O3–C22–H22B	109.5
O3–C22–H22C	109.5
H22A–C22–H22B	109.5
H22A–C22–H22C	109.5
H22B–C22–H22C	109.5
P1–C23–H23A	109.5
P1–C23–H23B	109.5
P1–C23–H23C	109.5
H23A–C23–H23B	109.5
H23A–C23–H23C	109.5

H23B–C23–H23C	109.5
P1–C24–H24A	109.5
P1–C24–H24B	109.5
P1–C24–H24C	109.5
H24A–C24–H24B	109.5
H24A–C24–H24C	109.5
H24B–C24–H24C	109.5
P1–C25–H25A	109.5
P1–C25–H25B	109.5
P1–C25–H25C	109.5
H25A–C25–H25B	109.5
H25A–C25–H25C	109.5
H25B–C25–H25C	109.5
N2–B1–N6	107.5(9)
N2–B1–H1A	110(5)
N4–B1–N2	108.6(9)
N4–B1–N6	106.5(8)
N4–B1–H1A	115(5)
N6–B1–H1A	109(5)

Table 5. Torsion angles for mo\_harman\_2\_jkh\_295\_x2\_0m

Atom–Atom–Atom–Atom	Torsion Angle [°]
W1–N1–N2–C3	171.2(7)
W1–N1–N2–B1	–3.5(14)
W1–N1–C1–C2	–169.3(7)
W1–N3–N4–C6	177.2(6)
W1–N3–N4–B1	–14.2(11)
W1–N3–C4–C5	–175.0(7)
W1–N5–N6–C9	177.0(6)
W1–N5–N6–B1	6.0(12)
W1–N5–C7–C8	–175.8(7)
W1–C10–C11–C12	131.0(10)
W1–C10–C17–C16	–150.8(8)
W1–C11–C12–C13	56.2(14)
W1–C11–C12–C19	–176.5(8)
O2–C18–C19–C12	69.7(13)
O2–C18–C19–C20	–52.2(13)
O3–C18–C19–C12	–108.5(9)
O3–C18–C19–C20	129.6(9)

N1–N2–C3–C2	0.4(13)
N1–N2–B1–N4	–54.9(14)
N1–N2–B1–N6	60.0(13)
N1–C1–C2–C3	–1.3(12)
N2–N1–C1–C2	1.5(12)
N3–N4–C6–C5	–1.5(11)
N3–N4–B1–N2	66.0(11)
N3–N4–B1–N6	–49.5(11)
N3–C4–C5–C6	–3.4(12)
N4–N3–C4–C5	2.6(11)
N5–N6–C9–C8	–1.4(11)
N5–N6–B1–N2	–61.8(11)
N5–N6–B1–N4	54.4(11)
N5–C7–C8–C9	–0.4(13)
N6–N5–C7–C8	–0.5(13)
C1–N1–N2–C3	–1.2(13)
C1–N1–N2–B1	–175.9(10)
C1–C2–C3–N2	0.5(12)
C3–N2–B1–N4	131.5(12)

C3–N2–B1–N6	–113.7(13)
C4–N3–N4–C6	–0.6(11)
C4–N3–N4–B1	167.9(8)
C4–C5–C6–N4	2.9(12)
C6–N4–B1–N2	–127.7(11)
C6–N4–B1–N6	116.8(10)
C7–N5–N6–C9	1.1(11)
C7–N5–N6–B1	–169.9(9)
C7–C8–C9–N6	1.1(12)
C9–N6–B1–N2	129.0(10)
C9–N6–B1–N4	–114.8(10)
C10–C11–C12–C13	–45.5(14)
C10–C11–C12–C19	81.8(12)
C11–C10–C17–C16	–70.7(12)
C11–C12–C13–C14	81.3(13)
C11–C12–C19–C18	49.1(11)
C11–C12–C19–C20	167.6(9)
C12–C13–C14–C15	–12.3(16)
C12–C19–C20–O4	–11.2(15)
C12–C19–C20–O5	169.7(8)

C13–C12–C19–C18	–179.4(8)
C13–C12–C19–C20	–61.0(11)
C13–C14–C15–C16	–55.0(15)
C14–C15–C16–C17	–2.5(15)
C15–C16–C17–C10	93.1(13)
C17–C10–C11–W1	–109.0(8)
C17–C10–C11–C12	22.0(14)
C18–C19–C20–O4	109.8(12)
C18–C19–C20–O5	–69.3(10)
C19–C12–C13–C14	–45.3(13)
C21–O5–C20–O4	–5.9(14)
C21–O5–C20–C19	173.3(8)
C22–O3–C18–O2	–6.9(14)
C22–O3–C18–C19	171.4(8)
B1–N2–C3–C2	174.7(11)
B1–N4–C6–C5	–168.9(10)
B1–N6–C9–C8	168.7(9)

#### Structure Report for mo\_harman\_3\_jkh\_107\_x2\_0m

A yellow, plate shaped crystal of mo\_harman\_3\_jkh\_107\_x2\_0m measuring 0.099×0.108×0.196 mm was coated with Paratone oil and mounted on a MiTeGen micromount. Data for mo\_harman\_3\_jkh\_107\_x2\_0m were measured on a Bruker D8 VENTURE dual wavelength Mo/Cu Kappa four-circle diffractometer equipped with a PHOTON III detector and an Incoatec I $\mu$ S 3.0 microfocus sealed X-ray tube (Mo  $K_{\alpha}$ ,  $\lambda$ =0.71073 Å) using a HELIOS double bounce multilayer mirror as monochromator. The crystal temperature was controlled with an Oxford Cryostream 800low temperature device. Data collection and processing were done within the Bruker APEX5 software suite.<sup>29</sup> All data were integrated with the Bruker SAINT 8.40B software using a narrow-frame algorithm. Data were corrected for absorption effects using a Multi-Scan method (SADABS).

<sup>29</sup> APEX5, Saint, SADABS; Bruker AXS Inc. 2019.

The structure was solved by dual methods with SHELXT<sup>30</sup> and refined by full-matrix least-squares methods against  $F^2$  using SHELXL--2019/1<sup>31</sup> within OLEX2.<sup>32</sup> All non-hydrogen atoms were refined with anisotropically. The B-H hydrogen atom as well as H10 and H11 were located in the electron density map and refined isotropically. All other hydrogen atoms were placed in geometrically calculated positions with  $U_{iso} = 1.2U_{equiv}$  of the parent atom ( $1.5U_{equiv}$  for methyl). This report and the CIF file were generated using FinalCif.<sup>33</sup>

Table 1 Crystal data and structure refinement for mo\_harman\_3\_jkh\_107\_x2\_0m

CCDC number	
Empirical formula	C <sub>26</sub> H <sub>33</sub> BN <sub>7</sub> OPW
Formula weight	685.22
Temperature [K]	100.00
Wavelength [Å]	0.71073
Crystal size [mm <sup>3</sup> ]	0.099×0.108×0.196
Crystal habit	yellow plate
Crystal system	orthorhombic
Space group	$P2_12_12_1$ (19)
<i>a</i> [Å]	10.9926(3)
<i>b</i> [Å]	11.4079(3)
<i>c</i> [Å]	21.8156(6)
$\alpha$ [°]	90
$\beta$ [°]	90
$\gamma$ [°]	90
Volume [Å <sup>3</sup> ]	2735.73(13)
<i>Z</i>	4
$\rho_{calc}$ [gcm <sup>-3</sup> ]	1.664
$\mu$ [mm <sup>-1</sup> ]	4.314
<i>F</i> (000)	1360
2 $\theta$ range [°]	4.03 to 56.60 (0.75 Å)
Index ranges	−14 ≤ <i>h</i> ≤ 14 −15 ≤ <i>k</i> ≤ 14 −28 ≤ <i>l</i> ≤ 29
Reflections collected	35266
Independent reflections	6779 [ <i>R</i> <sub>int</sub> = 0.0303]

<sup>30</sup> Sheldrick, G. M. SHELXT – Integrated space-group and crystal-structure determination. *Acta Cryst. Sect. A Found. Adv.* **2015**, *71*, 3-8.

<sup>31</sup> Sheldrick, G. M. Crystal structure refinement with SHELXL. *Acta Cryst. Sect. C Struct. Chem.* **2015**, *71*, 3-8.

<sup>32</sup> Dolomanov, O. V.; Bourhis, L. J.; Gildea, R. J.; Howard, J. A. K.; Puschmann, H. OLEX2: a completed structure solution, refinement and analysis program. *J. Appl. Cryst.* **2009**, *42*, 339-341.

<sup>33</sup> Kratzert, D. FinalCif, <https://dkratzert.de/finalcif.html>.

Data / Restraints / Parameters	6779 / 0 / 348
Goodness-of-fit on $F^2$	1.039
Final $R$ indexes [ $I \geq 2\sigma(I)$ ]	$R_1 = 0.0158$ $wR_2 = 0.0297$
Final $R$ indexes [all data]	$R_1 = 0.0169$ $wR_2 = 0.0300$
Largest peak/hole [ $\text{e}\text{\AA}^{-3}$ ]	0.38/−0.45
Flack X parameter	−0.012(3)

Table 2. Atomic coordinates and  $U_{eq}$  [ $\text{\AA}^2$ ] for mo\_harman\_3\_jkh\_107\_x2\_0m

Atom	x	y	z	$U_{eq}$
W1	0.25933(2)	0.35579(2)	0.32294(2)	0.01030(3)
P1	0.07449(7)	0.27401(8)	0.26909(4)	0.01345(17)
O1	0.2035(2)	0.6124(2)	0.30974(11)	0.0235(6)
N1	0.30231(19)	0.1634(2)	0.32854(11)	0.0127(5)
N2	0.3976(2)	0.1174(2)	0.29572(11)	0.0130(6)
N3	0.3265(2)	0.3456(3)	0.22707(11)	0.0129(5)
N4	0.4090(2)	0.2632(3)	0.20933(12)	0.0134(6)
N5	0.46089(19)	0.3704(2)	0.33151(11)	0.0127(5)
N6	0.5343(2)	0.2910(3)	0.30193(11)	0.0145(6)
N7	0.2258(2)	0.5067(2)	0.31504(11)	0.0143(5)
C1	0.2504(3)	0.0716(3)	0.35614(11)	0.0136(5)
H1	0.181564	0.076769	0.382368	0.016
C2	0.3093(3)	-0.0316(3)	0.34171(13)	0.0147(7)
H2	0.289971	-0.108436	0.355336	0.018
C3	0.4023(3)	0.0015(3)	0.30329(13)	0.0146(7)
H3	0.460136	-0.049734	0.285144	0.018
C4	0.2946(2)	0.4044(3)	0.17665(15)	0.0155(6)
H4	0.238702	0.467857	0.175680	0.019
C5	0.3550(3)	0.3595(4)	0.12570(13)	0.0193(7)
H5	0.347742	0.384367	0.084301	0.023
C6	0.4271(3)	0.2718(3)	0.14824(14)	0.0173(7)
H6	0.481053	0.224680	0.124793	0.021
C7	0.5348(3)	0.4488(3)	0.35706(14)	0.0163(7)
H7	0.508470	0.514444	0.380338	0.020
C8	0.6562(3)	0.4215(3)	0.34501(14)	0.0200(7)
H8	0.726482	0.462804	0.358213	0.024
C9	0.6516(3)	0.3220(3)	0.30995(14)	0.0190(8)
H9	0.719956	0.281463	0.293880	0.023



C10	0.1309(3)	0.3323(3)	0.40066(13 )	0.0146(7)
H10	0.098(3)	0.259(3)	0.4025(15)	0.012(9)
C11	0.2531(3)	0.3495(3)	0.42438(11 )	0.0149(5)
H11	0.292(3)	0.278(3)	0.4372(15)	0.018
C12	0.2663(3)	0.4407(3)	0.47603(12 )	0.0163(6)
H12	0.209613	0.507225	0.467496	0.020
C13	0.2219(3)	0.3765(3)	0.53268(14 )	0.0212(7)
H13	0.282033	0.339901	0.557444	0.025
C14	0.1068(3)	0.3664(4)	0.55106(14 )	0.0250(8)
H14	0.093520	0.317825	0.585782	0.030
C15	−0.0018(3)	0.4207(4)	0.52451(17 )	0.0254(8)
H15	−0.062135	0.441995	0.553615	0.031
C16	−0.0305(3)	0.4455(3)	0.46674(18 )	0.0251(8)
H16	−0.107850	0.481566	0.462277	0.030
C17	0.0355(3)	0.4275(3)	0.40704(14 )	0.0194(7)
H17A	0.075176	0.502765	0.396513	0.023
H17B	−0.026963	0.412872	0.375251	0.023
C18	0.3923(3)	0.4902(3)	0.48755(14 )	0.0172(7)
C19	0.4109(3)	0.6100(3)	0.49110(15 )	0.0223(8)
H19	0.343922	0.661862	0.486252	0.027
C20	0.5263(3)	0.6553(4)	0.50168(15 )	0.0292(8)
H20	0.537535	0.737644	0.504495	0.035
C21	0.6248(3)	0.5812(4)	0.50813(15 )	0.0298(9)
H21	0.703731	0.612457	0.514982	0.036
C22	0.6081(3)	0.4622(4)	0.50458(15 )	0.0271(9)
H22	0.675941	0.411076	0.508319	0.033
C23	0.4920(3)	0.4157(4)	0.49550(15 )	0.0210(8)
H23	0.480740	0.333169	0.494726	0.025
C24	−0.0374(3)	0.1877(3)	0.31135(15 )	0.0186(7)
H24A	0.003489	0.122628	0.332169	0.028
H24B	−0.098194	0.156644	0.282775	0.028
H24C	−0.077683	0.237622	0.341778	0.028
C25	−0.0236(3)	0.3744(3)	0.22805(16 )	0.0233(8)

H25A	−0.056775	0.432361	0.256692	0.035
H25B	−0.090420	0.330694	0.209075	0.035
H25C	0.023399	0.414607	0.196170	0.035
C26	0.1145(3)	0.1708(3)	0.20867(14)	0.0181(7)
H26A	0.154944	0.212708	0.175183	0.027
H26B	0.040521	0.133080	0.193159	0.027
H26C	0.169498	0.110980	0.225160	0.027
B1	0.4827(3)	0.1968(3)	0.25865(16)	0.0142(7)
H1A	0.551(3)	0.150(3)	0.2383(13)	0.013(8)

$U_{eq}$  is defined as 1/3 of the trace of the orthogonalized  $U_{ij}$  tensor.

**Table 3. Anisotropic displacement parameters ( $\text{\AA}^2$ ) for mo\_harman\_3\_jkh\_107\_x2\_0m. The anisotropic displacement factor exponent takes the form:  $-2\pi^2[ h^2(a^*)^2U_{11} + k^2(b^*)^2U_{22} + \dots + 2hka^*b^*U_{12} ]$**

Atom	$U_{11}$	$U_{22}$	$U_{33}$	$U_{23}$	$U_{13}$	$U_{12}$
W1	0.00882(4)	0.01096(6)	0.01111(5)	−0.00005(5)	0.00032(4)	0.00109(5)
P1	0.0110(3)	0.0124(5)	0.0170(4)	−0.0002(3)	−0.0014(3)	0.0008(3)
O1	0.0225(11)	0.0124(14)	0.0356(14)	0.0031(10)	0.0004(9)	0.0038(9)
N1	0.0115(10)	0.0152(15)	0.0114(11)	−0.0013(11)	0.0013(9)	0.0014(9)
N2	0.0114(11)	0.0133(16)	0.0143(12)	0.0001(10)	0.0021(9)	0.0028(10)
N3	0.0123(10)	0.0133(15)	0.0131(11)	−0.0006(12)	0.0006(8)	−0.0006(12)
N4	0.0123(12)	0.0124(15)	0.0156(13)	−0.0011(11)	0.0036(10)	−0.0003(11)
N5	0.0134(10)	0.0127(15)	0.0121(12)	0.0006(11)	−0.0001(9)	0.0003(10)
N6	0.0106(11)	0.0166(16)	0.0162(12)	0.0017(11)	0.0019(9)	0.0020(11)
N7	0.0116(11)	0.0158(14)	0.0156(12)	−0.0004(10)	−0.0010(10)	0.0014(10)
C1	0.0126(12)	0.0163(15)	0.0119(11)	0.0023(11)	−0.0005(12)	−0.0023(14)
C2	0.0150(13)	0.0142(18)	0.0150(14)	0.0021(12)	−0.0050(10)	−0.0010(12)
C3	0.0170(15)	0.0128(18)	0.0141(14)	−0.0013(12)	−0.0027(11)	0.0036(12)
C4	0.0175(13)	0.0131(16)	0.0159(13)	0.0019(14)	−0.0020(13)	−0.0012(11)
C5	0.0289(15)	0.0181(18)	0.0109(14)	0.0021(16)	−0.0004(11)	−0.0034(17)
C6	0.0239(17)	0.0147(19)	0.0132(15)	−0.0023(13)	0.0038(12)	−0.0041(14)
C7	0.0202(15)	0.0161(19)	0.0126(15)	0.0014(13)	−0.0015(11)	−0.0033(14)

C8	0.0141(14)	0.028(2)	0.0178(15)	0.0033(15)	−0.0011(11)	−0.0053(14)
C9	0.0102(13)	0.026(2)	0.0207(17)	0.0065(13)	0.0005(11)	0.0009(12)
C10	0.0149(13)	0.016(2)	0.0133(14)	−0.0007(13)	0.0047(11)	0.0004(13)
C11	0.0172(12)	0.0148(15)	0.0125(11)	0.0008(12)	0.0027(11)	0.0022(19)
C12	0.0201(15)	0.0139(15)	0.0149(13)	−0.0006(12)	0.0023(12)	0.0020(14)
C13	0.0310(17)	0.0187(19)	0.0137(13)	−0.0024(13)	0.0009(12)	−0.0005(14)
C14	0.0372(18)	0.024(2)	0.0134(14)	−0.0055(16)	0.0075(12)	−0.0091(18)
C15	0.0259(17)	0.027(2)	0.0237(19)	−0.0100(17)	0.0151(14)	−0.0054(15)
C16	0.0169(15)	0.023(2)	0.036(2)	−0.0082(18)	0.0087(14)	0.0025(15)
C17	0.0162(15)	0.021(2)	0.0209(16)	−0.0006(15)	0.0037(12)	0.0037(14)
C18	0.0221(16)	0.0197(19)	0.0098(14)	0.0005(13)	0.0009(11)	−0.0003(14)
C19	0.0270(17)	0.023(2)	0.0173(16)	−0.0027(14)	0.0010(13)	−0.0017(14)
C20	0.0390(19)	0.025(2)	0.0236(17)	−0.0003(17)	−0.0019(14)	−0.0118(19)
C21	0.0259(18)	0.042(3)	0.0210(17)	−0.0008(18)	−0.0041(14)	−0.0120(18)
C22	0.0229(17)	0.041(3)	0.0176(17)	0.0037(17)	−0.0048(13)	0.0034(17)
C23	0.0267(17)	0.023(2)	0.0135(16)	0.0008(15)	−0.0020(13)	−0.0015(15)
C24	0.0118(13)	0.0203(19)	0.0238(18)	−0.0015(14)	0.0007(11)	−0.0009(12)
C25	0.0199(15)	0.019(2)	0.0315(18)	0.0036(16)	−0.0068(13)	0.0055(15)
C26	0.0189(14)	0.017(2)	0.0190(16)	−0.0032(13)	0.0003(12)	−0.0041(13)
B1	0.0135(16)	0.012(2)	0.0170(17)	0.0021(14)	0.0029(13)	0.0016(14)

Table 4. Bond lengths and angles for mo\_harman\_3\_jkh\_107\_x2\_0m

Atom–Atom	Length [Å]		
W1–P1	2.5257(8)	P1–C24	1.825(3)
W1–N1	2.248(3)	P1–C25	1.810(3)
W1–N3	2.221(2)	P1–C26	1.821(3)
W1–N5	2.230(2)	O1–N7	1.235(3)
W1–N7	1.769(3)	N1–N2	1.373(3)
W1–C10	2.222(3)	N1–C1	1.336(4)
W1–C11	2.215(2)	N2–C3	1.334(4)
		N2–B1	1.532(4)
		N3–N4	1.362(4)

N3–C4	1.335(4)
N4–C6	1.351(4)
N4–B1	1.545(4)
N5–N6	1.373(4)
N5–C7	1.331(4)
N6–C9	1.349(4)
N6–B1	1.539(5)
C1–H1	0.9500
C1–C2	1.381(4)
C2–H2	0.9500
C2–C3	1.374(4)
C3–H3	0.9500
C4–H4	0.9500
C4–C5	1.392(4)
C5–H5	0.9500
C5–C6	1.368(5)
C6–H6	0.9500
C7–H7	0.9500
C7–C8	1.395(4)
C8–H8	0.9500
C8–C9	1.369(5)
C9–H9	0.9500
C10–H10	0.92(4)
C10–C11	1.453(4)
C10–C17	1.516(4)
C11–H11	0.97(4)
C11–C12	1.540(4)
C12–H12	1.0000
C12–C13	1.517(4)
C12–C18	1.517(4)
C13–H13	0.9500
C13–C14	1.332(4)
C14–H14	0.9500
C14–C15	1.464(5)
C15–H15	0.9500
C15–C16	1.330(5)
C16–H16	0.9500
C16–C17	1.505(5)
C17–H17A	0.9900
C17–H17B	0.9900
C18–C19	1.384(5)
C18–C23	1.398(5)
C19–H19	0.9500
C19–C20	1.389(5)
C20–H20	0.9500
C20–C21	1.381(6)
C21–H21	0.9500
C21–C22	1.372(6)

C22–H22	0.9500
C22–C23	1.396(5)
C23–H23	0.9500
C24–H24A	0.9800
C24–H24B	0.9800
C24–H24C	0.9800
C25–H25A	0.9800
C25–H25B	0.9800
C25–H25C	0.9800
C26–H26A	0.9800
C26–H26B	0.9800
C26–H26C	0.9800
B1–H1A	1.03(3)
Atom–Atom– Atom	Angle [°]
N1–W1–P1	80.43(6)
N3–W1–P1	79.05(6)
N3–W1–N1	86.00(10)
N3–W1–N5	75.67(8)
N3–W1–C10	157.41(11)
N5–W1–P1	149.99(7)
N5–W1–N1	81.92(9)
N7–W1–P1	98.42(8)
N7–W1–N1	177.52(10)
N7–W1–N3	91.63(11)
N7–W1–N5	98.21(10)
N7–W1–C10	93.38(12)
N7–W1–C11	97.02(11)
C10–W1–P1	78.43(8)
C10–W1–N1	88.54(11)
C10–W1–N5	125.18(10)
C11–W1–P1	115.33(8)
C11–W1–N1	85.46(11)
C11–W1–N3	161.69(10)
C11–W1–N5	87.10(10)
C11–W1–C10	38.21(11)
C24–P1–W1	120.43(11)
C25–P1–W1	118.38(12)
C25–P1–C24	100.93(15)
C25–P1–C26	101.25(16)
C26–P1–W1	112.41(10)
C26–P1–C24	100.34(15)
N2–N1–W1	120.32(19)
C1–N1–W1	134.39(19)
C1–N1–N2	105.2(2)
N1–N2–B1	121.0(3)
C3–N2–N1	110.1(2)

C3–N2–B1	128.9(3)
N4–N3–W1	121.7(2)
C4–N3–W1	131.5(2)
C4–N3–N4	106.7(2)
N3–N4–B1	119.3(2)
C6–N4–N3	109.1(3)
C6–N4–B1	130.2(3)
N6–N5–W1	119.66(18)
C7–N5–W1	133.8(2)
C7–N5–N6	106.4(2)
N5–N6–B1	122.2(2)
C9–N6–N5	109.1(3)
C9–N6–B1	128.0(3)
O1–N7–W1	179.4(2)
N1–C1–H1	124.3
N1–C1–C2	111.4(3)
C2–C1–H1	124.3
C1–C2–H2	127.6
C3–C2–C1	104.7(3)
C3–C2–H2	127.6
N2–C3–C2	108.6(3)
N2–C3–H3	125.7
C2–C3–H3	125.7
N3–C4–H4	124.8
N3–C4–C5	110.4(3)
C5–C4–H4	124.8
C4–C5–H5	127.5
C6–C5–C4	105.0(3)
C6–C5–H5	127.5
N4–C6–C5	108.8(3)
N4–C6–H6	125.6
C5–C6–H6	125.6
N5–C7–H7	124.6
N5–C7–C8	110.8(3)
C8–C7–H7	124.6
C7–C8–H8	127.6
C9–C8–C7	104.8(3)
C9–C8–H8	127.6
N6–C9–C8	109.0(3)
N6–C9–H9	125.5
C8–C9–H9	125.5
W1–C10–H10	113(2)
C11–C10–W1	70.63(15)
C11–C10–H10	118(2)
C11–C10–C17	120.7(3)
C17–C10–W1	115.0(2)
C17–C10–H10	112(2)
W1–C11–H11	107.6(19)

C10–C11–W1	71.16(15)
C10–C11–H11	114(2)
C10–C11–C12	116.1(3)
C12–C11–W1	134.9(2)
C12–C11–H11	109(2)
C11–C12–H12	108.5
C13–C12–C11	103.9(2)
C13–C12–H12	108.5
C18–C12–C11	117.3(3)
C18–C12–H12	108.5
C18–C12–C13	109.8(2)
C12–C13–H13	116.8
C14–C13–C12	126.3(3)
C14–C13–H13	116.8
C13–C14–H14	115.9
C13–C14–C15	128.2(3)
C15–C14–H14	115.9
C14–C15–H15	114.4
C16–C15–C14	131.2(3)
C16–C15–H15	114.4
C15–C16–H16	113.7
C15–C16–C17	132.6(3)
C17–C16–H16	113.7
C10–C17–H17A	107.2
C10–C17–H17B	107.2
C16–C17–C10	120.7(3)
C16–C17–H17A	107.2
C16–C17–H17B	107.2
H17A–C17– H17B	106.8
C19–C18–C12	120.8(3)
C19–C18–C23	118.6(3)
C23–C18–C12	120.7(3)
C18–C19–H19	119.6
C18–C19–C20	120.7(4)
C20–C19–H19	119.6
C19–C20–H20	119.8
C21–C20–C19	120.4(4)
C21–C20–H20	119.8
C20–C21–H21	120.2
C22–C21–C20	119.7(3)
C22–C21–H21	120.2
C21–C22–H22	119.8
C21–C22–C23	120.4(4)
C23–C22–H22	119.8
C18–C23–H23	119.9
C22–C23–C18	120.2(4)
C22–C23–H23	119.9

P1–C24–H24A	109.5
P1–C24–H24B	109.5
P1–C24–H24C	109.5
H24A–C24–H24B	109.5
H24A–C24–H24C	109.5
H24B–C24–H24C	109.5
P1–C25–H25A	109.5
P1–C25–H25B	109.5
P1–C25–H25C	109.5
H25A–C25–H25B	109.5
H25A–C25–H25C	109.5

H25B–C25–H25C	109.5
P1–C26–H26A	109.5
P1–C26–H26B	109.5
P1–C26–H26C	109.5
H26A–C26–H26B	109.5
H26A–C26–H26C	109.5
H26B–C26–H26C	109.5
N2–B1–N4	109.7(2)
N2–B1–N6	108.3(3)
N2–B1–H1A	112(2)
N4–B1–H1A	109.9(17)
N6–B1–N4	106.1(3)
N6–B1–H1A	111.1(18)

Table 5. Torsion angles for mo\_harman\_3\_jkh\_107\_x2\_0m

Atom–Atom–Atom–Atom	Torsion Angle [°]
W1–N1–N2–C3	–176.66(19)
W1–N1–N2–B1	4.8(3)
W1–N1–C1–C2	176.0(2)
W1–N3–N4–C6	175.8(2)
W1–N3–N4–B1	–16.2(4)
W1–N3–C4–C5	–174.5(2)
W1–N5–N6–C9	175.52(19)
W1–N5–N6–B1	4.7(4)
W1–N5–C7–C8	–174.9(2)
W1–C10–C11–C12	131.6(2)
W1–C10–C17–C16	–160.4(3)
W1–C11–C12–C13	167.1(2)
W1–C11–C12–C18	–71.5(4)
N1–N2–C3–C2	–0.1(3)
N1–N2–B1–N4	–60.4(4)
N1–N2–B1–N6	55.0(3)
N1–C1–C2–C3	0.2(3)
N2–N1–C1–C2	–0.3(3)
N3–N4–C6–C5	–0.7(4)
N3–N4–B1–N2	67.6(4)
N3–N4–B1–N6	–49.2(3)
N3–C4–C5–C6	–1.2(4)
N4–N3–C4–C5	0.8(3)
N5–N6–C9–C8	0.3(4)
N5–N6–B1–N2	–61.5(4)

N5–N6–B1–N4	56.3(3)
N5–C7–C8–C9	0.6(4)
N6–N5–C7–C8	–0.4(4)
C1–N1–N2–C3	0.2(3)
C1–N1–N2–B1	–178.3(3)
C1–C2–C3–N2	0.0(3)
C3–N2–B1–N4	121.3(3)
C3–N2–B1–N6	–123.3(3)
C4–N3–N4–C6	–0.1(3)
C4–N3–N4–B1	168.0(3)
C4–C5–C6–N4	1.1(4)
C6–N4–B1–N2	–127.3(4)
C6–N4–B1–N6	115.9(4)
C7–N5–N6–C9	0.1(3)
C7–N5–N6–B1	–170.7(3)
C7–C8–C9–N6	–0.5(4)
C9–N6–B1–N2	129.6(3)
C9–N6–B1–N4	–112.7(3)
C10–C11–C12–C13	78.2(3)
C10–C11–C12–C18	–160.4(3)
C11–C10–C17–C16	–79.0(4)
C11–C12–C13–C14	–84.9(4)
C11–C12–C18–C19	129.6(3)
C11–C12–C18–C23	–51.1(4)
C12–C13–C14–C15	–5.0(6)
C12–C18–C19–C20	180.0(3)
C12–C18–C23–C22	178.4(3)
C13–C12–C18–C19	–112.2(3)
C13–C12–C18–C23	67.1(4)

C13–C14–C15–C16	34.9(7)
C14–C15–C16–C17	0.2(7)
C15–C16–C17–C10	24.7(6)
C17–C10–C11–W1	–108.2(3)
C17–C10–C11–C12	23.3(4)
C18–C12–C13–C14	148.8(3)
C18–C19–C20–C21	0.7(5)
C19–C18–C23–C22	–2.3(5)
C19–C20–C21–C22	–0.6(5)

C20–C21–C22–C23	–1.0(5)
C21–C22–C23–C18	2.5(5)
C23–C18–C19–C20	0.7(5)
B1–N2–C3–C2	178.3(3)
B1–N4–C6–C5	–167.0(3)
B1–N6–C9–C8	170.4(3)

## Structure Report for mo\_harman\_2\_jkh\_269\_x2\_0m

A colourless, plate shaped crystal of mo\_harman\_2\_jkh\_269\_x2\_0m measuring 0.083×0.091×0.096 mm was coated with Paratone oil and mounted on a MiTeGen micromount. Data for mo\_harman\_2\_jkh\_269\_x2\_0m were measured on a Bruker D8 VENTURE dual wavelength Mo/Cu Kappa four-circle diffractometer equipped with a PHOTON III detector and an Incoatec I $\mu$ S 3.0 microfocus sealed X-ray tube (Mo  $K_{\alpha}$ ,  $\lambda$ =0.71073 Å) using a HELIOS double bounce multilayer mirror as monochromator. The crystal temperature was controlled with an Oxford Cryostream 800low temperature device. Data collection and processing were done within the Bruker APEX5 software suite.<sup>34</sup> All data were integrated with the Bruker SAINT 8.40B software using a narrow-frame algorithm. Data were corrected for absorption effects using a Multi-Scan method (SADABS).

The structure was solved by dual methods with SHELXT<sup>35</sup> and refined by full-matrix least-squares methods against  $F^2$  using XL<sup>36</sup> within OLEX2.<sup>37</sup> All non-hydrogen atoms were refined with anisotropically. Hydrogen atoms were placed in geometrically calculated positions with  $U_{iso} = 1.2U_{equiv}$  of the parent atom ( $1.5U_{equiv}$  for methyl). This report and the CIF file were generated using FinalCif.<sup>38</sup>

Table 1. Crystal data and structure refinement for mo\_harman\_2\_jkh\_269\_x2\_0m

CCDC number	
-------------	--

<sup>34</sup> APEX5, Saint, SADABS; Bruker AXS Inc. 2019.

<sup>35</sup> Sheldrick, G. M. SHELXT – Integrated space-group and crystal-structure determination. *Acta Cryst. Sect. A Found. Adv.* **2015**, *71*, 3–8.

<sup>36</sup> Sheldrick, G. M. Crystal structure refinement with SHELXL. *Acta Cryst. Sect. C Struct. Chem.* **2015**, *71*, 3–8.

<sup>37</sup> Dolomanov, O. V.; Bourhis, L. J.; Gildea, R. J.; Howard, J. A. K.; Puschmann, H. OLEX2: a completed structure solution, refinement and analysis program. *J. Appl. Cryst.* **2009**, *42*, 339–341.

<sup>38</sup> Kratzert, D. FinalCif, <https://dkratzert.de/finalcif.html>.

Empirical formula	C <sub>27</sub> H <sub>35</sub> BN <sub>7</sub> OPW
Formula weight	699.25
Temperature [K]	100.00
Wavelength [Å]	0.71073
Crystal size [mm <sup>3</sup> ]	0.083×0.091×0.096
Crystal habit	colourless plate
Crystal system	triclinic
Space group	<i>P</i> $\bar{1}$ (2)
<i>a</i> [Å]	10.5971(4)
<i>b</i> [Å]	10.7598(4)
<i>c</i> [Å]	12.9648(4)
$\alpha$ [°]	91.2130(10)
$\beta$ [°]	108.2660(10)
$\gamma$ [°]	102.5090(10)
Volume [Å <sup>3</sup> ]	1364.13(8)
<i>Z</i>	2
$\rho_{\text{calc}}$ [gcm <sup>-3</sup> ]	1.702
$\mu$ [mm <sup>-1</sup> ]	4.328
<i>F</i> (000)	696
2 $\theta$ range [°]	3.90 to 63.21 (0.68 Å)
Index ranges	−15 ≤ <i>h</i> ≤ 15 −15 ≤ <i>k</i> ≤ 15 −19 ≤ <i>l</i> ≤ 18
Reflections collected	56698
Independent reflections	9125 [ <i>R</i> <sub>int</sub> = 0.0436]
Data / Restraints / Parameters	9125 / 0 / 358
Goodness-of-fit on <i>F</i> <sup>2</sup>	1.075
Final <i>R</i> indexes [ <i>I</i> ≥ 2 $\sigma$ ( <i>I</i> )]	<i>R</i> <sub>1</sub> = 0.0248 <i>wR</i> <sub>2</sub> = 0.0469
Final <i>R</i> indexes [all data]	<i>R</i> <sub>1</sub> = 0.0305 <i>wR</i> <sub>2</sub> = 0.0491
Largest peak/hole [eÅ <sup>-3</sup> ]	1.46/−0.99



Table 2. Atomic coordinates and  $U_{eq}$  [Å<sup>2</sup>] for mo\_harman\_2\_jkh\_269\_x2\_0m

Atom	x	y	z	$U_{eq}$
W1	0.69952(2)	0.20590(2)	0.24685(2)	0.01093(3)
P1	0.73854(6)	−0.01271(6)	0.28784(5)	0.01441(11)
O1	0.44595(19)	0.13262(19)	0.05196(15)	0.0252(4)
N1	0.89958(19)	0.28814(18)	0.38113(16)	0.0133(4)
N2	1.00264(19)	0.36965(18)	0.35789(16)	0.0130(4)
N3	0.8315(2)	0.19722(18)	0.14473(16)	0.0139(4)
N4	0.9524(2)	0.28410(19)	0.16375(16)	0.0138(4)
N5	0.7356(2)	0.39875(18)	0.18916(16)	0.0137(4)
N6	0.8647(2)	0.46818(18)	0.20055(16)	0.0141(4)
N7	0.5479(2)	0.15602(19)	0.13405(16)	0.0153(4)
C1	0.9445(2)	0.2831(2)	0.48949(19)	0.0165(4)
H1	0.893572	0.233344	0.529128	0.020
C2	1.0752(2)	0.3603(2)	0.5362(2)	0.0172(5)
H2	1.129938	0.373133	0.610977	0.021
C3	1.1076(2)	0.4140(2)	0.4497(2)	0.0160(4)
H3	1.190653	0.472812	0.454217	0.019
C4	0.8162(3)	0.1170(2)	0.05936(19)	0.0163(4)
H4	0.739645	0.047495	0.027406	0.020
C5	0.9294(3)	0.1503(2)	0.0242(2)	0.0191(5)
H5	0.945731	0.108282	−0.033858	0.023
C6	1.0128(3)	0.2574(2)	0.0916(2)	0.0168(4)
H6	1.097937	0.304039	0.087750	0.020
C7	0.6499(2)	0.4640(2)	0.1300(2)	0.0163(4)
H7	0.553079	0.437009	0.108309	0.020
C8	0.7208(3)	0.5773(2)	0.1039(2)	0.0188(5)
H8	0.683979	0.641366	0.063879	0.023
C9	0.8565(3)	0.5751(2)	0.1493(2)	0.0171(5)
H9	0.932002	0.638767	0.145197	0.021
C10	0.8867(3)	−0.0503(3)	0.2617(3)	0.0259(6)
H10A	0.871108	−0.056530	0.182990	0.039
H10B	0.899931	−0.132062	0.289789	0.039
H10C	0.968321	0.017409	0.298391	0.039
C11	0.6012(3)	−0.1455(2)	0.2108(2)	0.0210(5)

H11A	0.519870	−0.146739	0.231903	0.031
H11B	0.629541	−0.225891	0.226235	0.031
H11C	0.579873	−0.135732	0.132646	0.031
C12	0.7756(3)	−0.0561(2)	0.4278(2)	0.0211(5)
H12A	0.860575	0.001365	0.474453	0.032
H12B	0.785708	−0.144464	0.429791	0.032
H12C	0.700326	−0.048368	0.454351	0.032
C13	0.6015(2)	0.1599(2)	0.37436(19 )	0.0138(4)
C14	0.6042(2)	0.2914(2)	0.35269(19 )	0.0134(4)
C15	0.4779(2)	0.3482(2)	0.30750(19 )	0.0138(4)
H15	0.439392	0.325670	0.226745	0.017
C16	0.3641(2)	0.3071(2)	0.3559(2)	0.0156(4)
H16	0.367460	0.359164	0.417308	0.019
C17	0.2595(2)	0.2046(2)	0.3203(2)	0.0169(4)
H17	0.185964	0.195459	0.348883	0.020
C18	0.2547(2)	0.1061(2)	0.2388(2)	0.0185(5)
H18	0.178111	0.084731	0.173884	0.022
C19	0.3551(2)	0.0456(2)	0.2533(2)	0.0170(4)
H19	0.353648	−0.008398	0.193820	0.020
C20	0.4711(2)	0.0580(2)	0.3591(2)	0.0155(4)
H20A	0.495771	−0.025733	0.367561	0.019
H20B	0.436359	0.074470	0.419321	0.019
C21	0.5270(2)	0.4949(2)	0.33018(19 )	0.0145(4)
H21A	0.567006	0.516758	0.410110	0.017
H21B	0.600816	0.523788	0.298445	0.017
C22	0.4185(2)	0.5687(2)	0.2861(2)	0.0147(4)
C23	0.3911(2)	0.6515(2)	0.3558(2)	0.0164(4)
H23	0.436898	0.657085	0.432185	0.020
C24	0.2975(2)	0.7262(2)	0.3155(2)	0.0177(5)
H24	0.279816	0.782192	0.364109	0.021
C25	0.2307(2)	0.7184(2)	0.2046(2)	0.0189(5)
H25	0.167237	0.769646	0.176769	0.023
C26	0.2560(3)	0.6359(2)	0.1337(2)	0.0191(5)
H26	0.210187	0.630499	0.057366	0.023
C27	0.3488(2)	0.5615(2)	0.1751(2)	0.0170(4)
H27	0.365034	0.504382	0.126456	0.020
B1	0.9872(3)	0.4064(2)	0.2416(2)	0.0144(5)
H13	0.670(3)	0.149(3)	0.441(2)	0.015(7)
H1A	1.077(3)	0.470(3)	0.239(2)	0.011(7)
H14	0.677(3)	0.355(3)	0.407(2)	0.016(7)

$U_{eq}$  is defined as 1/3 of the trace of the orthogonalized  $U_{ij}$  tensor.

**Table 3. Anisotropic displacement parameters ( $\text{\AA}^2$ ) for mo\_harman\_2\_jkh\_269\_x2\_0m. The anisotropic displacement factor exponent takes the form:  $-2\pi^2[h^2(a^*)^2U_{11} + k^2(b^*)^2U_{22} + \dots + 2hka^*b^*U_{12}]$**

Atom	$U_{11}$	$U_{22}$	$U_{33}$	$U_{23}$	$U_{13}$	$U_{12}$
W1	0.00975(4)	0.00892(4)	0.01220(4)	-0.00024(3)	0.00200(3)	0.00069(3)
P1	0.0147(3)	0.0108(3)	0.0182(3)	0.0023(2)	0.0061(2)	0.0029(2)
O1	0.0173(9)	0.0319(11)	0.0160(9)	-0.0003(8)	-0.0026(7)	-0.0034(8)
N1	0.0113(8)	0.0121(8)	0.0158(9)	0.0002(7)	0.0041(7)	0.0014(7)
N2	0.0099(8)	0.0114(8)	0.0150(9)	-0.0016(7)	0.0021(7)	0.0003(7)
N3	0.0146(9)	0.0098(8)	0.0148(9)	-0.0009(7)	0.0028(7)	0.0009(7)
N4	0.0117(9)	0.0133(9)	0.0155(9)	0.0003(7)	0.0041(7)	0.0017(7)
N5	0.0124(9)	0.0113(8)	0.0165(9)	-0.0001(7)	0.0045(7)	0.0012(7)
N6	0.0127(9)	0.0113(8)	0.0164(10)	0.0001(7)	0.0041(7)	0.0002(7)
N7	0.0145(9)	0.0143(9)	0.0138(9)	0.0003(7)	0.0029(7)	-0.0005(7)
C1	0.0158(11)	0.0181(11)	0.0138(11)	0.0003(9)	0.0018(9)	0.0048(9)
C2	0.0131(10)	0.0177(11)	0.0167(11)	-0.0052(9)	-0.0005(9)	0.0041(8)
C3	0.0117(10)	0.0131(10)	0.0196(12)	-0.0045(8)	0.0016(9)	0.0012(8)
C4	0.0199(11)	0.0125(10)	0.0147(11)	-0.0014(8)	0.0030(9)	0.0040(9)
C5	0.0227(12)	0.0212(12)	0.0155(11)	-0.0011(9)	0.0062(9)	0.0099(10)
C6	0.0171(11)	0.0189(11)	0.0173(11)	0.0031(9)	0.0078(9)	0.0070(9)
C7	0.0146(10)	0.0182(11)	0.0170(11)	0.0032(9)	0.0045(9)	0.0062(9)
C8	0.0244(12)	0.0149(11)	0.0184(12)	0.0038(9)	0.0068(10)	0.0072(9)
C9	0.0225(12)	0.0106(10)	0.0179(11)	0.0006(8)	0.0071(9)	0.0023(9)
C10	0.0257(13)	0.0244(13)	0.0373(16)	0.0120(12)	0.0189(12)	0.0123(11)
C11	0.0240(13)	0.0137(11)	0.0243(13)	0.0005(9)	0.0089(10)	0.0010(9)
C12	0.0245(13)	0.0195(12)	0.0213(13)	0.0059(10)	0.0058(10)	0.0113(10)
C13	0.0132(10)	0.0131(10)	0.0142(11)	0.0005(8)	0.0035(8)	0.0027(8)
C14	0.0108(10)	0.0127(10)	0.0143(11)	-0.0010(8)	0.0019(8)	0.0012(8)
C15	0.0123(10)	0.0122(10)	0.0152(11)	-0.0001(8)	0.0027(8)	0.0022(8)
C16	0.0145(10)	0.0173(11)	0.0161(11)	0.0023(9)	0.0048(9)	0.0065(8)
C17	0.0133(10)	0.0160(11)	0.0221(12)	0.0045(9)	0.0056(9)	0.0049(8)
C18	0.0137(11)	0.0141(10)	0.0237(13)	0.0015(9)	0.0029(9)	-0.0006(8)
C19	0.0157(11)	0.0128(10)	0.0210(12)	0.0015(9)	0.0057(9)	0.0004(8)
C20	0.0147(10)	0.0141(10)	0.0182(11)	0.0042(8)	0.0057(9)	0.0037(8)
C21	0.0127(10)	0.0126(10)	0.0162(11)	-0.0020(8)	0.0029(8)	0.0021(8)
C22	0.0144(10)	0.0112(10)	0.0182(11)	0.0012(8)	0.0053(9)	0.0026(8)
C23	0.0168(11)	0.0146(10)	0.0163(11)	0.0005(8)	0.0043(9)	0.0024(8)
C24	0.0183(11)	0.0129(10)	0.0231(12)	0.0013(9)	0.0089(10)	0.0034(9)
C25	0.0155(11)	0.0142(11)	0.0273(13)	0.0054(9)	0.0069(10)	0.0037(9)
C26	0.0195(12)	0.0163(11)	0.0194(12)	0.0044(9)	0.0035(9)	0.0034(9)
C27	0.0179(11)	0.0147(10)	0.0173(11)	-0.0003(9)	0.0046(9)	0.0033(9)
B1	0.0122(11)	0.0133(11)	0.0172(12)	-0.0005(9)	0.0060(9)	0.0007(9)

**Table 4. Bond lengths and angles for mo\_harman\_2\_jkh\_269\_x2\_0m**

Atom–Atom	Length [Å]
W1–P1	2.5146(6)
W1–N1	2.2621(19)
W1–N3	2.220(2)
W1–N5	2.2164(19)
W1–N7	1.769(2)
W1–C13	2.224(2)
W1–C14	2.229(2)
P1–C10	1.829(3)
P1–C11	1.813(3)
P1–C12	1.826(3)
O1–N7	1.230(3)
N1–N2	1.362(3)
N1–C1	1.341(3)
N2–C3	1.341(3)
N2–B1	1.535(3)
N3–N4	1.361(3)
N3–C4	1.336(3)
N4–C6	1.345(3)
N4–B1	1.544(3)
N5–N6	1.370(3)
N5–C7	1.330(3)
N6–C9	1.346(3)
N6–B1	1.539(3)
C1–H1	0.9500
C1–C2	1.390(3)
C2–H2	0.9500
C2–C3	1.376(4)
C3–H3	0.9500
C4–H4	0.9500
C4–C5	1.392(3)
C5–H5	0.9500
C5–C6	1.380(3)
C6–H6	0.9500
C7–H7	0.9500
C7–C8	1.394(3)
C8–H8	0.9500
C8–C9	1.378(4)
C9–H9	0.9500
C10–H10A	0.9800
C10–H10B	0.9800
C10–H10C	0.9800
C11–H11A	0.9800
C11–H11B	0.9800
C11–H11C	0.9800
C12–H12A	0.9800
C12–H12B	0.9800
C12–H12C	0.9800

C13–C14	1.444(3)
C13–C20	1.521(3)
C13–H13	0.96(3)
C14–C15	1.544(3)
C14–H14	0.99(3)
C15–H15	1.0000
C15–C16	1.516(3)
C15–C21	1.542(3)
C16–H16	0.9500
C16–C17	1.337(3)
C17–H17	0.9500
C17–C18	1.463(3)
C18–H18	0.9500
C18–C19	1.331(3)
C19–H19	0.9500
C19–C20	1.507(3)
C20–H20A	0.9900
C20–H20B	0.9900
C21–H21A	0.9900
C21–H21B	0.9900
C21–C22	1.510(3)
C22–C23	1.392(3)
C22–C27	1.388(3)
C23–H23	0.9500
C23–C24	1.393(3)
C24–H24	0.9500
C24–C25	1.381(4)
C25–H25	0.9500
C25–C26	1.389(4)
C26–H26	0.9500
C26–C27	1.387(3)
C27–H27	0.9500
B1–H1A	1.06(3)
Atom–Atom–Atom	Angle [°]
N1–W1–P1	87.79(5)
N3–W1–P1	82.91(5)
N3–W1–N1	84.32(7)
N3–W1–C13	159.75(8)
N3–W1–C14	158.59(8)
N5–W1–P1	157.23(5)
N5–W1–N1	83.77(7)
N5–W1–N3	75.24(7)
N5–W1–C13	122.88(8)
N5–W1–C14	85.05(8)
N7–W1–P1	97.23(7)
N7–W1–N1	173.74(8)

N7–W1–N3	92.55(8)
N7–W1–N5	90.19(8)
N7–W1–C13	96.06(9)
N7–W1–C14	95.84(9)
C13–W1–P1	77.86(6)
C13–W1–N1	88.63(8)
C13–W1–C14	37.86(8)
C14–W1–P1	115.36(6)
C14–W1–N1	85.32(8)
C10–P1–W1	116.16(9)
C11–P1–W1	115.38(9)
C11–P1–C10	102.05(13)
C11–P1–C12	103.04(13)
C12–P1–W1	119.50(9)
C12–P1–C10	97.84(13)
N2–N1–W1	119.83(14)
C1–N1–W1	134.42(16)
C1–N1–N2	105.59(19)
N1–N2–B1	121.47(18)
C3–N2–N1	110.17(19)
C3–N2–B1	128.2(2)
N4–N3–W1	121.36(14)
C4–N3–W1	131.65(16)
C4–N3–N4	106.98(19)
N3–N4–B1	120.01(18)
C6–N4–N3	109.70(19)
C6–N4–B1	129.0(2)
N6–N5–W1	121.66(14)
C7–N5–W1	131.61(16)
C7–N5–N6	106.30(19)
N5–N6–B1	119.90(18)
C9–N6–N5	109.37(19)
C9–N6–B1	129.0(2)
O1–N7–W1	173.78(19)
N1–C1–H1	124.4
N1–C1–C2	111.1(2)
C2–C1–H1	124.4
C1–C2–H2	127.8
C3–C2–C1	104.4(2)
C3–C2–H2	127.8
N2–C3–C2	108.7(2)
N2–C3–H3	125.6
C2–C3–H3	125.6
N3–C4–H4	125.1
N3–C4–C5	109.8(2)
C5–C4–H4	125.1
C4–C5–H5	127.3
C6–C5–C4	105.4(2)

C6–C5–H5	127.3
N4–C6–C5	108.1(2)
N4–C6–H6	126.0
C5–C6–H6	126.0
N5–C7–H7	124.5
N5–C7–C8	111.1(2)
C8–C7–H7	124.5
C7–C8–H8	127.8
C9–C8–C7	104.4(2)
C9–C8–H8	127.8
N6–C9–C8	108.9(2)
N6–C9–H9	125.6
C8–C9–H9	125.6
P1–C10–H10A	109.5
P1–C10–H10B	109.5
P1–C10–H10C	109.5
H10A–C10– H10B	109.5
H10A–C10– H10C	109.5
H10B–C10– H10C	109.5
P1–C11–H11A	109.5
P1–C11–H11B	109.5
P1–C11–H11C	109.5
H11A–C11–H11B	109.5
H11A–C11–H11C	109.5
H11B–C11–H11C	109.5
P1–C12–H12A	109.5
P1–C12–H12B	109.5
P1–C12–H12C	109.5
H12A–C12– H12B	109.5
H12A–C12– H12C	109.5
H12B–C12– H12C	109.5
W1–C13–H13	109.1(17)
C14–C13–W1	71.27(13)
C14–C13–C20	123.9(2)
C14–C13–H13	114.3(17)
C20–C13–W1	125.07(16)
C20–C13–H13	108.7(17)
W1–C14–H14	107.9(16)
C13–C14–W1	70.87(13)
C13–C14–C15	125.9(2)
C13–C14–H14	114.9(17)
C15–C14–W1	123.38(16)
C15–C14–H14	108.8(17)

C14–C15–H15	108.6
C16–C15–C14	116.25(19)
C16–C15–H15	108.6
C16–C15–C21	107.09(19)
C21–C15–C14	107.59(18)
C21–C15–H15	108.6
C15–C16–H16	116.9
C17–C16–C15	126.1(2)
C17–C16–H16	116.9
C16–C17–H17	119.0
C16–C17–C18	122.0(2)
C18–C17–H17	119.0
C17–C18–H18	119.2
C19–C18–C17	121.6(2)
C19–C18–H18	119.2
C18–C19–H19	118.2
C18–C19–C20	123.6(2)
C20–C19–H19	118.2
C13–C20–H20A	107.8
C13–C20–H20B	107.8
C19–C20–C13	118.2(2)
C19–C20–H20A	107.8
C19–C20–H20B	107.8
H20A–C20– H20B	107.1
C15–C21–H21A	108.4
C15–C21–H21B	108.4
H21A–C21– H21B	107.5

C22–C21–C15	115.56(19)
C22–C21–H21A	108.4
C22–C21–H21B	108.4
C23–C22–C21	120.5(2)
C27–C22–C21	121.3(2)
C27–C22–C23	118.1(2)
C22–C23–H23	119.4
C22–C23–C24	121.1(2)
C24–C23–H23	119.4
C23–C24–H24	120.1
C25–C24–C23	119.7(2)
C25–C24–H24	120.1
C24–C25–H25	119.9
C24–C25–C26	120.1(2)
C26–C25–H25	119.9
C25–C26–H26	120.2
C27–C26–C25	119.5(2)
C27–C26–H26	120.2
C22–C27–H27	119.3
C26–C27–C22	121.4(2)
C26–C27–H27	119.3
N2–B1–N4	109.40(19)
N2–B1–N6	109.71(19)
N2–B1–H1A	110.6(15)
N4–B1–H1A	111.1(15)
N6–B1–N4	105.85(19)
N6–B1–H1A	110.1(15)

Table 5. Torsion angles for mo\_harman\_2\_jkh\_269\_x2\_0m

Atom–Atom– Atom–Atom	Torsion Angle [°]
W1–N1–N2–C3	175.60(15)
W1–N1–N2–B1	−0.8(3)
W1–N1–C1–C2	−175.15(16)
W1–N3–N4–C6	179.52(15)
W1–N3–N4–B1	−12.3(3)
W1–N3–C4–C5	−178.94(16)
W1–N5–N6–C9	173.90(15)
W1–N5–N6–B1	7.4(3)
W1–N5–C7–C8	−173.63(16)
W1–C13–C14–C15	117.9(2)
W1–C13–C20–C19	−41.4(3)
W1–C14–C15–C16	132.60(18)
W1–C14–C15–C21	−107.39(19)
N1–N2–C3–C2	0.6(3)

N1–N2–B1–N4	−57.3(3)
N1–N2–B1–N6	58.4(3)
N1–C1–C2–C3	0.4(3)
N2–N1–C1–C2	−0.1(3)
N3–N4–C6–C5	−0.2(3)
N3–N4–B1–N2	65.6(3)
N3–N4–B1–N6	−52.5(3)
N3–C4–C5–C6	−1.4(3)
N4–N3–C4–C5	1.3(3)
N5–N6–C9–C8	0.3(3)
N5–N6–B1–N2	−62.7(3)
N5–N6–B1–N4	55.3(3)
N5–C7–C8–C9	1.4(3)
N6–N5–C7–C8	−1.2(3)
C1–N1–N2–C3	−0.4(2)
C1–N1–N2–B1	−176.7(2)

C1–C2–C3–N2	–0.7(3)
C3–N2–B1–N4	127.1(2)
C3–N2–B1–N6	–117.2(2)
C4–N3–N4–C6	–0.7(3)
C4–N3–N4–B1	167.5(2)
C4–C5–C6–N4	0.9(3)
C6–N4–B1–N2	–128.8(2)
C6–N4–B1–N6	113.0(2)
C7–N5–N6–C9	0.6(3)
C7–N5–N6–B1	–165.9(2)
C7–C8–C9–N6	–1.0(3)
C9–N6–B1–N2	133.9(2)
C9–N6–B1–N4	–108.2(3)
C13–C14–C15–C16	43.1(3)
C13–C14–C15–C21	163.1(2)
C14–C13–C20–C19	48.5(3)
C14–C15–C16–C17	–88.6(3)
C14–C15–C21–C22	176.78(19)
C15–C16–C17–C18	10.3(4)
C15–C21–C22–C23	122.4(2)
C15–C21–C22–C27	–61.1(3)

C16–C15–C21–C22	–57.6(3)
C16–C17–C18–C19	55.5(4)
C17–C18–C19–C20	9.0(4)
C18–C19–C20–C13	–92.2(3)
C20–C13–C14–W1	–120.2(2)
C20–C13–C14–C15	–2.3(4)
C21–C15–C16–C17	151.1(2)
C21–C22–C23–C24	175.9(2)
C21–C22–C27–C26	–175.5(2)
C22–C23–C24–C25	0.0(4)
C23–C22–C27–C26	1.1(4)
C23–C24–C25–C26	0.4(4)
C24–C25–C26–C27	0.0(4)
C25–C26–C27–C22	–0.8(4)
C27–C22–C23–C24	–0.7(4)
B1–N2–C3–C2	176.7(2)
B1–N4–C6–C5	–166.9(2)
B1–N6–C9–C8	165.2(2)

#### Structure Report for mo\_harman\_3\_jkh\_267\_x3\_0m

A colourless, block-shaped crystal of mo\_harman\_3\_jkh\_267\_x3\_0m was coated with Paratone oil and mounted on a MiTeGen micromount. Data were collected at 100.00 K on a Bruker D8 VENTURE dual wavelength Mo/Cu Kappa four-circle diffractometer with a PHOTON III detector. The diffractometer was equipped with an Oxford Cryostream 800 low temperature device and used Mo  $K_\alpha$  radiation ( $\lambda = 0.71073\text{\AA}$ ) from an Incoatec I $\mu$ s 3.0 microfocus sealed X-ray tube with a HELIOS double bounce multilayer mirror as monochromator.

Data collection and processing were done within the Bruker APEX5 software suite.<sup>[1]</sup> All data were integrated with SAINT 8.40B using a narrow-frame algorithm and a Multi-Scan absorption correction using SADABS 2016/2 was applied.<sup>[2]</sup> Using Olex2 as a graphical interface,<sup>[3]</sup> the structure was solved by dual methods with SHELXT and refined by full-matrix least-squares methods against  $F^2$  using SHELXL.<sup>[4,5]</sup> All non-hydrogen atoms were refined with anisotropic displacement parameters. The B–H hydrogen atom as well as H10 and H11 were located in the electron density map and refined isotropically. All other

hydrogen atoms were refined using a riding model with their  $U_{\text{iso}}$  values constrained to 1.5 times the  $U_{\text{eq}}$  of their pivot atoms for terminal  $\text{sp}^3$  carbon atoms and 1.2 times for all other carbon atoms. Disordered moieties were refined using bond lengths restraints and displacement parameter restraints.

This report and the CIF file were generated using FinalCif.<sup>[6]</sup>

Refinement details for mo\_harman\_3\_jkh\_267\_x3\_0m

The relative occupancy of the disordered atoms was freely refined. Constraints and restraints were used as needed on the anisotropic displacement parameters and/or bond lengths of the disordered atoms .

Table 1. Crystal data and structure refinement for mo\_harman\_3\_jkh\_267\_x3\_0m

CCDC number	
Empirical formula	$\text{C}_{23}\text{H}_{33}\text{BN}_7\text{OPW}$
Formula weight	649.19
Temperature [K]	100.00
Crystal system	triclinic
Space group (number)	$P\bar{1}$ (2)
$a$ [Å]	10.4864(5)
$b$ [Å]	11.1787(6)
$c$ [Å]	13.1395(8)
$\alpha$ [°]	104.216(2)
$\beta$ [°]	96.345(2)
$\gamma$ [°]	115.115(2)
Volume [Å <sup>3</sup> ]	1310.85(13)
$Z$	2
$\rho_{\text{calc}}$ [gcm <sup>-3</sup> ]	1.645
$\mu$ [mm <sup>-1</sup> ]	4.497
$F(000)$	644
Crystal size [mm <sup>3</sup> ]	0.069×0.083×0.101
Crystal colour	colourless
Crystal shape	block
Radiation	Mo $K_{\alpha}$ ( $\lambda=0.71073$ Å)
$2\theta$ range [°]	4.26 to 56.57 (0.75 Å)
Index ranges	$-13 \leq h \leq 13$ $-14 \leq k \leq 14$ $-17 \leq l \leq 17$
Reflections collected	55191



Independent reflections	6499 $R_{\text{int}} = 0.0315$ $R_{\text{sigma}} = 0.0170$
Completeness to $\theta = 25.242^\circ$	100.0
Data / Restraints / Parameters	6499 / 10 / 350
Goodness-of-fit on $F^2$	1.056
Final $R$ indexes [ $I \geq 2\sigma(I)$ ]	$R_1 = 0.0135$ $wR_2 = 0.0312$
Final $R$ indexes [all data]	$R_1 = 0.0147$ $wR_2 = 0.0316$
Largest peak/hole [ $\text{e}\text{\AA}^{-3}$ ]	1.05/−0.54

Table 2. Atomic coordinates and  $U_{eq}$  [Å<sup>2</sup>] for mo\_harman\_3\_jkh\_267\_x3\_0m

Atom	x	y	z	$U_{eq}$
W1	0.73168(2)	0.43556(2)	0.75894(2)	0.01220(2)
P1	0.95114(5)	0.42463(5)	0.70970(4)	0.01663(9)
O1	0.77744(14)	0.36742(14)	0.96223(10)	0.0212(3)
N1	0.71017(15)	0.50846(15)	0.61482(12)	0.0155(3)
N2	0.72165(15)	0.63808(15)	0.62976(12)	0.0160(3)
N3	0.89070(15)	0.65650(15)	0.84486(11)	0.0152(3)
N4	0.88458(16)	0.76448(15)	0.81765(12)	0.0164(3)
N5	0.59546(15)	0.53591(15)	0.80848(12)	0.0153(3)
N6	0.61876(15)	0.65867(15)	0.79218(12)	0.0161(3)
N7	0.75596(15)	0.39214(15)	0.87745(11)	0.0143(3)
C1	0.67638(18)	0.4463(2)	0.50775(14)	0.0185(3)
H1	0.661319	0.354242	0.473974	0.022
C2	0.66628(19)	0.5344(2)	0.45258(15)	0.0205(4)
H2	0.644117	0.515904	0.376501	0.025
C3	0.69558(19)	0.6544(2)	0.53284(15)	0.0200(4)
H3	0.697164	0.735719	0.521648	0.024
C4	1.00686(19)	0.7132(2)	0.92835(14)	0.0196(4)
H4	1.036621	0.662097	0.964560	0.024
C5	1.0774(2)	0.8577(2)	0.95424(15)	0.0245(4)
H5	1.163179	0.922858	1.009159	0.029
C6	0.9964(2)	0.8859(2)	0.88331(15)	0.0222(4)
H6	1.016087	0.976202	0.880966	0.027
C7	0.49731(19)	0.50986(19)	0.86801(14)	0.0187(3)
H7	0.461126	0.430893	0.892078	0.022
C8	0.4554(2)	0.6148(2)	0.88987(15)	0.0213(4)
H8	0.387119	0.621279	0.929860	0.026

C9	0.53511(19) )	0.7068(2)	0.84058(15) )	0.0198(4)
H9	0.531776	0.790372	0.840614	0.024
C10	0.52152(18) )	0.25124(18) )	0.67207(14) )	0.0159(3)
H10	0.485(2)	0.278(2)	0.6145(17)	0.019(5)
C11	0.63373(18) )	0.21324(18) )	0.64963(14) )	0.0162(3)
H11	0.646(2)	0.202(2)	0.5773(17)	0.018(5)
C12	0.6637(2)	0.11152(19) )	0.69498(15) )	0.0204(4)
H12A	0.751320	0.109611	0.674979	0.024
H12B	0.685926	0.147653	0.774992	0.024
H12C	0.607448	0.023698	0.633338	0.024
H12D	0.766065	0.141038	0.691479	0.024
C17	0.39340(18) )	0.17715(18) )	0.71806(14) )	0.0173(3)
H17	0.361038	0.248149	0.747258	0.021
H17A	0.428582	0.221577	0.798482	0.021
C21	1.0442(2)	0.3694(2)	0.79838(16) )	0.0254(4)
H21A	1.080703	0.436986	0.871686	0.038
H21B	1.125795	0.364326	0.771292	0.038
H21C	0.976363	0.277237	0.799975	0.038
C22	1.0960(2)	0.5912(2)	0.71251(18) )	0.0306(5)
H22A	1.055647	0.634287	0.670936	0.046
H22B	1.169936	0.575453	0.680492	0.046
H22C	1.140314	0.653423	0.787609	0.046
C23	0.9348(2)	0.3180(2)	0.57453(15) )	0.0234(4)
H23A	0.871767	0.219365	0.564502	0.035
H23B	1.031125	0.331227	0.566190	0.035
H23C	0.892616	0.346051	0.520254	0.035
B1	0.7438(2)	0.7355(2)	0.74285(16) )	0.0169(4)
H1A	0.748(2)	0.836(2)	0.7398(16)	0.014(5)
C13	0.5413(2)	−0.0362(2)	0.65658(16) )	0.0213(4)
H13	0.537836	−0.099772	0.591925	0.026
C14	0.4378(2)	−0.0820(2)	0.70882(18) )	0.0235(4)
H14	0.367419	−0.177860	0.682336	0.028
C15	0.4282(2)	0.0097(2)	0.80556(19) )	0.0243(4)
H15	0.428035	−0.016255	0.869223	0.029

C16	0.4196(2)	0.1265(2)	0.81089(16)	0.0214(4)
H16	0.431299	0.184647	0.881161	0.026
C18	0.2642(2)	0.0604(2)	0.62254(16)	0.0197(4)
H18A	0.246716	0.100898	0.566766	0.024
H18B	0.290799	−0.012612	0.589096	0.024
C19	0.1268(2)	−0.0057(2)	0.65823(17)	0.0231(4)
H19	0.118661	−0.070782	0.695225	0.028
C20	0.0172(2)	0.0211(3)	0.6413(2)	0.0294(5)
H20A	0.022087	0.085689	0.604559	0.035
H20B	−0.066975	−0.024112	0.665895	0.035
C13A	0.659(3)	0.057(3)	0.784(2)	0.024(3)
H13A	0.732787	0.037176	0.812323	0.029
C14A	0.542(3)	0.037(3)	0.824(2)	0.024(3)
H14A	0.551657	0.073958	0.899462	0.029
C15A	0.398(3)	−0.044(3)	0.747(3)	0.024(3)
H15A	0.347536	−0.142286	0.733324	0.029
C16A	0.336(3)	0.014(3)	0.696(3)	0.024(3)
H16A	0.249597	−0.048076	0.640280	0.029
C18A	0.267(3)	0.199(3)	0.687(3)	0.024(3)
H18C	0.229509	0.157763	0.606981	0.029
H18D	0.300837	0.301032	0.705520	0.029
C19A	0.144(3)	0.138(3)	0.739(2)	0.024(3)
H19A	0.166099	0.159276	0.815235	0.029
C20A	0.008(3)	0.057(3)	0.683(3)	0.024(3)
H20C	−0.016537	0.034697	0.606869	0.029
H20D	−0.065860	0.021114	0.719835	0.029

$U_{eq}$  is defined as 1/3 of the trace of the orthogonalized  $U_{ij}$  tensor.

Table 3. Anisotropic displacement parameters ( $\text{\AA}^2$ ) for mo\_harman\_3\_jkh\_267\_x3\_0m.

The anisotropic displacement factor exponent takes the form:

$$-2\pi^2 [h^2(a^*)^2 U_{11} + k^2(b^*)^2 U_{22} + \dots + 2hka^*b^* U_{12}]$$

Atom	$U_{11}$	$U_{22}$	$U_{33}$	$U_{23}$	$U_{13}$	$U_{12}$
W1	0.01129(3)	0.01481(4)	0.01094(3)	0.00513(2)	0.00304(2)	0.00591(3)
P1	0.0137(2)	0.0187(2)	0.0154(2)	0.00331(17)	0.00514(16)	0.00657(17)
O1	0.0224(6)	0.0330(7)	0.0145(6)	0.0129(6)	0.0053(5)	0.0156(6)
N1	0.0142(7)	0.0169(7)	0.0150(7)	0.0068(6)	0.0037(5)	0.0061(6)
N2	0.0136(7)	0.0195(7)	0.0163(7)	0.0095(6)	0.0042(5)	0.0070(6)
N3	0.0151(7)	0.0168(7)	0.0143(7)	0.0048(6)	0.0036(5)	0.0081(6)
N4	0.0166(7)	0.0160(7)	0.0166(7)	0.0056(6)	0.0058(6)	0.0071(6)
N5	0.0138(7)	0.0178(7)	0.0148(7)	0.0070(6)	0.0034(5)	0.0068(6)
N6	0.0154(7)	0.0199(7)	0.0164(7)	0.0082(6)	0.0042(6)	0.0101(6)
N7	0.0128(6)	0.0169(7)	0.0135(7)	0.0044(6)	0.0033(5)	0.0077(6)

C1	0.0148(8)	0.0231(9)	0.0139(8)	0.0048(7)	0.0041(6)	0.0059(7)
C2	0.0143(8)	0.0312(10)	0.0150(8)	0.0108(7)	0.0040(6)	0.0079(7)
C3	0.0164(8)	0.0265(9)	0.0198(9)	0.0146(8)	0.0055(7)	0.0083(7)
C4	0.0175(8)	0.0237(9)	0.0157(8)	0.0027(7)	0.0016(7)	0.0105(7)
C5	0.0189(9)	0.0238(10)	0.0201(9)	−0.0008(8)	0.0003(7)	0.0059(8)
C6	0.0226(9)	0.0181(9)	0.0216(9)	0.0041(7)	0.0054(7)	0.0069(7)
C7	0.0169(8)	0.0233(9)	0.0150(8)	0.0067(7)	0.0054(6)	0.0082(7)
C8	0.0180(8)	0.0272(10)	0.0192(9)	0.0059(8)	0.0063(7)	0.0116(8)
C9	0.0179(8)	0.0247(9)	0.0200(9)	0.0065(7)	0.0037(7)	0.0135(7)
C10	0.0147(8)	0.0174(8)	0.0142(8)	0.0063(7)	0.0020(6)	0.0061(7)
C11	0.0159(8)	0.0168(8)	0.0122(8)	0.0036(6)	0.0019(6)	0.0054(7)
C12	0.0204(9)	0.0188(9)	0.0217(9)	0.0057(7)	0.0026(7)	0.0101(7)
C17	0.0141(8)	0.0173(8)	0.0183(8)	0.0058(7)	0.0038(6)	0.0056(7)
C21	0.0191(9)	0.0328(11)	0.0235(10)	0.0055(8)	0.0011(7)	0.0144(8)
C22	0.0257(10)	0.0239(10)	0.0372(12)	0.0060(9)	0.0197(9)	0.0066(8)
C23	0.0206(9)	0.0284(10)	0.0197(9)	0.0035(8)	0.0071(7)	0.0120(8)
B1	0.0156(9)	0.0193(9)	0.0187(9)	0.0080(8)	0.0054(7)	0.0093(8)
C13	0.0234(10)	0.0174(9)	0.0225(10)	0.0064(8)	0.0017(8)	0.0101(8)
C14	0.0244(10)	0.0181(10)	0.0265(11)	0.0096(8)	0.0029(8)	0.0082(8)
C15	0.0256(11)	0.0268(11)	0.0220(11)	0.0139(9)	0.0062(9)	0.0105(9)
C16	0.0194(9)	0.0247(10)	0.0163(9)	0.0069(8)	0.0043(7)	0.0069(8)
C18	0.0162(9)	0.0198(9)	0.0204(9)	0.0083(8)	0.0030(7)	0.0054(8)
C19	0.0200(9)	0.0192(10)	0.0253(10)	0.0100(8)	0.0053(8)	0.0034(8)
C20	0.0194(10)	0.0290(12)	0.0356(13)	0.0108(10)	0.0075(9)	0.0073(9)
C13A	0.029(7)	0.017(6)	0.028(7)	0.012(5)	0.005(6)	0.011(5)
C14A	0.029(7)	0.017(6)	0.028(7)	0.012(5)	0.005(6)	0.011(5)
C15A	0.029(7)	0.017(6)	0.028(7)	0.012(5)	0.005(6)	0.011(5)
C16A	0.029(7)	0.017(6)	0.028(7)	0.012(5)	0.005(6)	0.011(5)
C18A	0.029(7)	0.017(6)	0.028(7)	0.012(5)	0.005(6)	0.011(5)
C19A	0.029(7)	0.017(6)	0.028(7)	0.012(5)	0.005(6)	0.011(5)
C20A	0.029(7)	0.017(6)	0.028(7)	0.012(5)	0.005(6)	0.011(5)

Table 4. Bond lengths and angles for mo\_harman\_3\_jkh\_267\_x3\_0m

Atom–Atom	Length [Å]		
W1–P1	2.5017(5)	N2–B1	1.537(2)
W1–N1	2.2629(14)	N3–N4	1.364(2)
W1–N3	2.2076(15)	N3–C4	1.340(2)
W1–N5	2.2204(14)	N4–C6	1.346(2)
W1–N7	1.7645(14)	N4–B1	1.538(2)
W1–C10	2.1999(17)	N5–N6	1.364(2)
W1–C11	2.2468(17)	N5–C7	1.338(2)
P1–C21	1.8177(19)	N6–C9	1.349(2)
P1–C22	1.825(2)	N6–B1	1.543(2)
P1–C23	1.8232(19)	C1–H1	0.9500
O1–N7	1.2316(18)	C1–C2	1.389(3)
N1–N2	1.364(2)	C2–H2	0.9500
N1–C1	1.337(2)	C2–C3	1.374(3)
N2–C3	1.345(2)	C3–H3	0.9500
		C4–H4	0.9500

C4–C5	1.390(3)
C5–H5	0.9500
C5–C6	1.373(3)
C6–H6	0.9500
C7–H7	0.9500
C7–C8	1.397(3)
C8–H8	0.9500
C8–C9	1.375(3)
C9–H9	0.9500
C10–H10	0.98(2)
C10–C11	1.446(2)
C10–C17	1.529(2)
C11–H11	0.96(2)
C11–C12	1.531(2)
C12–H12A	0.9900
C12–H12B	0.9900
C12–H12C	0.9900
C12–H12D	0.9900
C12–C13	1.509(3)
C12–C13A	1.445(17)
C17–H17	1.0000
C17–H17A	1.0000
C17–C16	1.510(3)
C17–C18	1.560(3)
C17–C16A	1.60(3)
C17–C18A	1.48(3)
C21–H21A	0.9800
C21–H21B	0.9800
C21–H21C	0.9800
C22–H22A	0.9800
C22–H22B	0.9800
C22–H22C	0.9800
C23–H23A	0.9800
C23–H23B	0.9800
C23–H23C	0.9800
B1–H1A	1.117(19)
C13–H13	0.9500
C13–C14	1.333(3)
C14–H14	0.9500
C14–C15	1.467(3)
C15–H15	0.9500
C15–C16	1.332(3)
C16–H16	0.9500
C18–H18A	0.9900
C18–H18B	0.9900
C18–C19	1.503(3)
C19–H19	0.9500
C19–C20	1.316(3)

C20–H20A	0.9500
C20–H20B	0.9500
C13A–H13A	0.9500
C13A–C14A	1.340(19)
C14A–H14A	0.9500
C14A–C15A	1.477(19)
C15A–H15A	0.9500
C15A–C16A	1.333(18)
C16A–H16A	0.9500
C18A–H18C	0.9900
C18A–H18D	0.9900
C18A–C19A	1.509(19)
C19A–H19A	0.9500
C19A–C20A	1.321(19)
C20A–H20C	0.9500
C20A–H20D	0.9500
<b>Atom–Atom– Atom</b>	<b>Angle [°]</b>
N1–W1–P1	86.59(4)
N3–W1–P1	82.32(4)
N3–W1–N1	84.74(5)
N3–W1–N5	76.08(5)
N3–W1–C11	160.78(6)
N5–W1–P1	156.28(4)
N5–W1–N1	81.83(5)
N5–W1–C11	121.86(6)
N7–W1–P1	93.68(5)
N7–W1–N1	175.66(6)
N7–W1–N3	91.00(6)
N7–W1–N5	96.36(6)
N7–W1–C10	97.50(6)
N7–W1–C11	93.45(6)
C10–W1–P1	115.99(5)
C10–W1–N1	86.26(6)
C10–W1–N3	159.04(6)
C10–W1–N5	83.94(6)
C10–W1–C11	37.94(6)
C11–W1–P1	78.74(5)
C11–W1–N1	90.85(6)
C21–P1–W1	115.14(7)
C21–P1–C22	102.60(10)
C21–P1–C23	103.38(9)
C22–P1–W1	114.61(7)
C23–P1–W1	119.58(6)
C23–P1–C22	98.99(10)
N2–N1–W1	120.01(11)
C1–N1–W1	133.49(12)

C1-N1-N2	106.31(14)
N1-N2-B1	121.42(14)
C3-N2-N1	109.32(15)
C3-N2-B1	128.90(15)
N4-N3-W1	122.98(11)
C4-N3-W1	130.32(12)
C4-N3-N4	106.70(14)
N3-N4-B1	118.44(14)
C6-N4-N3	109.29(14)
C6-N4-B1	130.44(15)
N6-N5-W1	120.89(10)
C7-N5-W1	132.16(12)
C7-N5-N6	106.34(14)
N5-N6-B1	121.40(14)
C9-N6-N5	109.64(14)
C9-N6-B1	128.10(15)
O1-N7-W1	177.35(14)
N1-C1-H1	124.6
N1-C1-C2	110.85(17)
C2-C1-H1	124.6
C1-C2-H2	127.8
C3-C2-C1	104.46(16)
C3-C2-H2	127.8
N2-C3-C2	109.06(16)
N2-C3-H3	125.5
C2-C3-H3	125.5
N3-C4-H4	124.9
N3-C4-C5	110.12(16)
C5-C4-H4	124.9
C4-C5-H5	127.4
C6-C5-C4	105.14(17)
C6-C5-H5	127.4
N4-C6-C5	108.75(17)
N4-C6-H6	125.6
C5-C6-H6	125.6
N5-C7-H7	124.7
N5-C7-C8	110.64(16)
C8-C7-H7	124.7
C7-C8-H8	127.7
C9-C8-C7	104.59(16)
C9-C8-H8	127.7
N6-C9-C8	108.79(16)
N6-C9-H9	125.6
C8-C9-H9	125.6
W1-C10-H10	103.8(12)
C11-C10-W1	72.79(10)
C11-C10-H10	112.8(12)
C11-C10-C17	127.81(15)

C17-C10-W1	128.19(12)
C17-C10-H10	106.9(12)
W1-C11-H11	115.0(12)
C10-C11-W1	69.27(10)
C10-C11-H11	115.3(12)
C10-C11-C12	123.29(15)
C12-C11-W1	117.04(11)
C12-C11-H11	111.1(12)
C11-C12-H12A	108.5
C11-C12-H12B	108.5
C11-C12-H12C	100.6
C11-C12-H12D	100.6
H12A-C12-H12B	107.5
H12C-C12-H12D	104.3
C13-C12-C11	115.02(15)
C13-C12-H12A	108.5
C13-C12-H12B	108.5
C13A-C12-C11	145.1(12)
C13A-C12-H12C	100.6
C13A-C12-H12D	100.6
C10-C17-H17	105.3
C10-C17-H17A	105.9
C10-C17-C18	108.71(14)
C10-C17-C16A	116.7(12)
C16-C17-C10	118.61(15)
C16-C17-H17	105.3
C16-C17-C18	112.45(15)
C18-C17-H17	105.3
C16A-C17-H17A	105.9
C18A-C17-C10	113.6(10)
C18A-C17-H17A	105.9
C18A-C17-C16A	108.2(14)
P1-C21-H21A	109.5
P1-C21-H21B	109.5
P1-C21-H21C	109.5
H21A-C21-H21B	109.5
H21A-C21-H21C	109.5
H21B-C21-H21C	109.5
P1-C22-H22A	109.5

P1-C22-H22B	109.5
P1-C22-H22C	109.5
H22A-C22-H22B	109.5
H22A-C22-H22C	109.5
H22B-C22-H22C	109.5
P1-C23-H23A	109.5
P1-C23-H23B	109.5
P1-C23-H23C	109.5
H23A-C23-H23B	109.5
H23A-C23-H23C	109.5
H23B-C23-H23C	109.5
N2-B1-N4	109.62(14)
N2-B1-N6	108.52(15)
N2-B1-H1A	111.8(10)
N4-B1-N6	106.31(14)
N4-B1-H1A	110.1(10)
N6-B1-H1A	110.4(10)
C12-C13-H13	118.3
C14-C13-C12	123.30(19)
C14-C13-H13	118.3
C13-C14-H14	118.7
C13-C14-C15	122.64(19)
C15-C14-H14	118.7
C14-C15-H15	117.5
C16-C15-C14	124.94(19)
C16-C15-H15	117.5
C17-C16-H16	116.3
C15-C16-C17	127.47(19)
C15-C16-H16	116.3
C17-C18-H18A	109.1
C17-C18-H18B	109.1
H18A-C18-H18B	107.8
C19-C18-C17	112.51(16)
C19-C18-H18A	109.1
C19-C18-H18B	109.1
C18-C19-H19	118.0
C20-C19-C18	123.9(2)
C20-C19-H19	118.0
C19-C20-H20A	120.0
C19-C20-H20B	120.0
H20A-C20-H20B	120.0

C12-C13A-H13A	122.9
C14A-C13A-C12	114(2)
C14A-C13A-H13A	122.9
C13A-C14A-H14A	121.1
C13A-C14A-C15A	118(2)
C15A-C14A-H14A	121.1
C14A-C15A-H15A	118.6
C16A-C15A-C14A	123(3)
C16A-C15A-H15A	118.6
C17-C16A-H16A	116.9
C15A-C16A-C17	126(2)
C15A-C16A-H16A	116.9
C17-C18A-H18C	108.6
C17-C18A-H18D	108.6
C17-C18A-C19A	115(2)
H18C-C18A-H18D	107.6
C19A-C18A-H18C	108.6
C19A-C18A-H18D	108.6
C18A-C19A-H19A	118.5
C20A-C19A-C18A	123(3)
C20A-C19A-H19A	118.5
C19A-C20A-H20C	120.0
C19A-C20A-H20D	120.0
H20C-C20A-H20D	120.0



Table 5. Torsion angles for mo\_harman\_3\_jkh\_267\_x3\_0m

Atom–Atom– Atom–Atom	Torsion Angle [°]		
W1–N1–N2–C3	–175.89(11)	C6–N4–B1–N6	–112.3(2)
W1–N1–N2–B1	–2.18(19)	C7–N5–N6–C9	–0.40(19)
W1–N1–C1–C2	175.10(12)	C7–N5–N6–B1	169.77(15)
W1–N3–N4–C6	–179.24(12)	C7–C8–C9–N6	0.2(2)
W1–N3–N4–B1	14.59(19)	C9–N6–B1–N2	–131.96(17)
W1–N3–C4–C5	178.71(12)	C9–N6–B1–N4	110.20(18)
W1–N5–N6–C9	–172.51(11)	C10–C11–C12–C13	64.1(2)
W1–N5–N6–B1	–2.3(2)	C10–C11–C12– C13A	–30(2)
W1–N5–C7–C8	171.38(12)	C10–C17–C16–C15	–80.9(3)
W1–C10–C11–C12	109.45(16)	C10–C17–C18–C19	–172.40(15)
W1–C10–C17–C16	–55.0(2)	C10–C17–C16A– C15A	77(4)
W1–C10–C17–C18	174.87(12)	C10–C17–C18A– C19A	–174.8(18)
W1–C10–C17– C16A	–124.8(11)	C11–C10–C17–C16	42.7(3)
W1–C10–C17– C18A	108.4(14)	C11–C10–C17–C18	–87.4(2)
W1–C11–C12–C13	146.03(14)	C11–C10–C17– C16A	–27.1(11)
W1–C11–C12– C13A	52(2)	C11–C10–C17– C18A	–153.9(14)
N1–N2–C3–C2	0.08(19)	C11–C12–C13–C14	–91.3(2)
N1–N2–B1–N4	59.3(2)	C11–C12–C13A– C14A	39(4)
N1–N2–B1–N6	–56.42(19)	C12–C13–C14–C15	3.8(3)
N1–C1–C2–C3	–0.2(2)	C12–C13A–C14A– C15A	51(4)
N2–N1–C1–C2	0.25(19)	C17–C10–C11–W1	–125.38(18)
N3–N4–C6–C5	0.2(2)	C17–C10–C11–C12	–15.9(3)
N3–N4–B1–N2	–66.65(19)	C17–C18–C19–C20	103.6(2)
N3–N4–B1–N6	50.46(19)	C17–C18A–C19A– C20A	–129(3)
N3–C4–C5–C6	1.1(2)	B1–N2–C3–C2	–173.01(16)
N4–N3–C4–C5	–0.9(2)	B1–N4–C6–C5	164.20(17)
N5–N6–C9–C8	0.1(2)	B1–N6–C9–C8	–169.20(16)
N5–N6–B1–N2	59.82(19)	C13–C14–C15–C16	56.0(3)
N5–N6–B1–N4	–58.0(2)	C14–C15–C16–C17	10.8(3)
N5–C7–C8–C9	–0.4(2)	C16–C17–C18–C19	54.2(2)
N6–N5–C7–C8	0.52(19)	C18–C17–C16–C15	47.5(3)
C1–N1–N2–C3	–0.20(18)	C13A–C14A– C15A–C16A	–88(4)
C1–N1–N2–B1	173.50(15)	C14A–C15A– C16A–C17	–8(6)
C1–C2–C3–N2	0.1(2)	C16A–C17–C18A– C19A	54(3)
C3–N2–B1–N4	–128.36(17)		
C3–N2–B1–N6	115.93(18)		
C4–N3–N4–C6	0.43(19)		
C4–N3–N4–B1	–165.74(15)		
C4–C5–C6–N4	–0.8(2)		
C6–N4–B1–N2	130.59(19)		

C18A–C17–C16A– C15A	–153(4)
------------------------	---------

## Structure Report for mo\_harman\_mne\_5\_029\_0m

A yellow, block-shaped crystal of mo\_harman\_mne\_5\_029\_0m was coated with Paratone oil and mounted on a MiTeGen micromount. Data were collected at 100(2) K on a Bruker D8 VENTURE dual wavelength Mo/Cu Kappa four-circle diffractometer with a PHOTON III detector. The diffractometer was equipped with an Oxford Cryostream 800Plus low temperature device and used Mo  $K_\alpha$  radiation ( $\lambda = 0.71073\text{\AA}$ ) from an Incoatec I\ms 3.0 microfocus sealed X-ray tube with a HELIOS double bounce multilayer mirror as monochromator.

Data collection and processing were done within the Bruker APEX5 software suite.<sup>[1]</sup> All data were integrated with SAINT 8.40B using a narrow-frame algorithm and a Multi-Scan absorption correction using was applied.<sup>[2]</sup> Using [Unknown program in \_computing\_structure\_refinement] as a graphical interface,<sup>[3]</sup> the structure was solved by direct methods with SHELXT 2018/2 and refined by full-matrix least-squares methods against  $F^2$  using SHELXL-2019/2.<sup>[4,5]</sup> All non-hydrogen atoms were refined with anisotropic displacement parameters. All hydrogen atoms were refined with isotropic displacement parameters. The B-H hydrogen atom was located in the electron diffraction map and refined isotropically. All other hydrogen atoms were placed in calculated positions using a riding model with their  $U_{\text{iso}}$  values constrained to 1.5 times the  $U_{\text{eq}}$  of their pivot atoms for terminal  $\text{sp}^3$  carbon atoms and 1.2 times for all other carbon atoms. This report and the CIF file were generated using FinalCif.<sup>[6]</sup>

Table 1. Crystal data and structure refinement for mo\_harman\_mne\_5\_029\_0m

CCDC number	
Empirical formula	C <sub>22</sub> H <sub>32</sub> BCl <sub>3</sub> N <sub>7</sub> OPW
Formula weight	742.52
Temperature [K]	100(2)
Crystal system	monoclinic
Space group (number)	<i>P</i> 2 <sub>1</sub> / <i>c</i> (14)
<i>a</i> [Å]	11.6338(9)
<i>b</i> [Å]	14.6139(10)
<i>c</i> [Å]	16.7964(12)
$\alpha$ [°]	90
$\beta$ [°]	92.492(2)
$\gamma$ [°]	90
Volume [Å <sup>3</sup> ]	2852.9(4)
<i>Z</i>	4
$\rho_{\text{calc}}$ [gcm <sup>-3</sup> ]	1.729
$\mu$ [mm <sup>-1</sup> ]	4.416
<i>F</i> (000)	1464
Crystal size [mm <sup>3</sup> ]	0.043×0.054×0.072
Crystal colour	yellow
Crystal shape	block
Radiation	Mo <i>K</i> $\alpha$ ( $\lambda$ =0.71073 Å)
2 $\theta$ range [°]	3.50 to 46.52 (0.90 Å)
Index ranges	−12 ≤ <i>h</i> ≤ 12 −16 ≤ <i>k</i> ≤ 16 −17 ≤ <i>l</i> ≤ 18
Reflections collected	21647
Independent reflections	4096 <i>R</i> <sub>int</sub> = 0.1635 <i>R</i> <sub>sigma</sub> = 0.1280
Completeness to $\theta$ = 23.260°	99.9
Data / Restraints / Parameters	4096 / 0 / 332
Goodness-of-fit on <i>F</i> <sup>2</sup>	1.003
Final <i>R</i> indexes [ <i>I</i> ≥ 2 $\sigma$ ( <i>I</i> )]	<i>R</i> <sub>1</sub> = 0.0608 <i>wR</i> <sub>2</sub> = 0.1309
Final <i>R</i> indexes [all data]	<i>R</i> <sub>1</sub> = 0.1265 <i>wR</i> <sub>2</sub> = 0.1587
Largest peak/hole [eÅ <sup>-3</sup> ]	1.60/−1.57

Table 2. Atomic coordinates and  $U_{eq}$  [Å<sup>2</sup>] for mo\_harman\_mne\_5\_029\_0m

Atom	x	y	z	$U_{eq}$
W1	0.60940(6)	0.77086(4)	0.34090(3)	0.0325(2)
P1	0.6864(4)	0.9054(3)	0.2695(3)	0.0458(12)
O1	0.7208(9)	0.8162(8)	0.4992(6)	0.052(3)
N1	0.5079(11)	0.7412(7)	0.2267(6)	0.035(3)
N2	0.3901(11)	0.7446(7)	0.2257(7)	0.035(3)
N3	0.4706(12)	0.8683(8)	0.3654(7)	0.040(3)
N4	0.3605(11)	0.8555(8)	0.3373(7)	0.035(3)
N5	0.4748(11)	0.6856(8)	0.3916(6)	0.033(3)
N6	0.3619(12)	0.6921(8)	0.3653(7)	0.039(3)
N7	0.6782(10)	0.7964(7)	0.4322(7)	0.035(3)
C1	0.5372(15)	0.7174(10)	0.1541(9)	0.045(4)
H1	0.614029	0.711191	0.137919	0.054
C2	0.4416(17)	0.7033(10)	0.1063(9)	0.049(5)
H2	0.439259	0.684404	0.052104	0.058
C3	0.3528(16)	0.7209(10)	0.1499(9)	0.048(5)
H3	0.274483	0.717737	0.131516	0.058
C4	0.4690(15)	0.9462(10)	0.4081(8)	0.041(4)
H4	0.534553	0.972430	0.434994	0.050
C5	0.3598(14)	0.9828(10)	0.4079(8)	0.039(4)
H5	0.335833	1.036942	0.433671	0.046
C6	0.2943(13)	0.9243(10)	0.3627(9)	0.036(4)
H6	0.214086	0.930785	0.350877	0.044
C7	0.4762(15)	0.6343(10)	0.4573(9)	0.041(4)
H7	0.543296	0.618380	0.488587	0.050
C8	0.3637(17)	0.6073(10)	0.4734(10)	0.051(5)
H8	0.339786	0.570728	0.516460	0.061
C9	0.2967(16)	0.6448(11)	0.4140(11)	0.055(5)
H9	0.215568	0.638321	0.408007	0.066
C10	0.7674(14)	0.7088(10)	0.2891(9)	0.043(4)
H10	0.768131	0.711670	0.229634	0.052
C11	0.6934(13)	0.6367(10)	0.3198(8)	0.036(4)
H11	0.651994	0.606509	0.273404	0.043
C12	0.7234(16)	0.5639(10)	0.3818(8)	0.045(4)
H12	0.648318	0.544638	0.403244	0.055
C13	0.7959(19)	0.5888(12)	0.4514(11)	0.062(5)
H13	0.755823	0.603221	0.497882	0.075
C14	0.910(2)	0.5944(13)	0.4593(12)	0.071(6)
H14	0.945731	0.600189	0.511110	0.085
C15	0.9827(17)	0.5919(12)	0.3897(14)	0.075(6)
H15	1.038178	0.544506	0.386805	0.090
C16	0.9743(15)	0.6539(12)	0.3293(13)	0.069(6)
H16	1.023794	0.649955	0.285922	0.083

C17	0.8846(14)	0.7299(11)	0.3319(9)	0.051(4)
H17A	0.916764	0.785594	0.307835	0.061
H17B	0.871174	0.743924	0.388443	0.061
C18	0.7710(16)	0.4781(11)	0.3416(10)	0.060(5)
H18A	0.726780	0.466355	0.291598	0.091
H18B	0.764448	0.425395	0.377163	0.091
H18C	0.852011	0.487860	0.330275	0.091
C19	0.7689(15)	0.8897(10)	0.1819(10)	0.056(5)
H19A	0.842169	0.859884	0.196971	0.084
H19B	0.783930	0.949337	0.157848	0.084
H19C	0.725530	0.851248	0.143387	0.084
C20	0.7753(16)	0.9799(11)	0.3308(12)	0.076(6)
H20A	0.730649	1.003744	0.374448	0.115
H20B	0.801985	1.030973	0.298622	0.115
H20C	0.841778	0.945746	0.352934	0.115
C21	0.5755(16)	0.9810(11)	0.2287(11)	0.067(6)
H21A	0.525542	0.947214	0.190506	0.101
H21B	0.611344	1.032305	0.201565	0.101
H21C	0.529750	1.004307	0.271885	0.101
B1	0.3244(18)	0.7631(13)	0.3020(11)	0.044(5)
H1A	0.234(13)	0.759(9)	0.300(8)	0.053
Cl1	1.0850(6)	0.8373(6)	0.4912(4)	0.134(3)
Cl2	1.0300(6)	0.7400(5)	0.6282(4)	0.117(2)
Cl3	0.9365(7)	0.9146(6)	0.6080(6)	0.170(4)
C22	0.9793(17)	0.8227(13)	0.5601(17)	0.112(10)
H22	0.910194	0.796434	0.530837	0.134

$U_{eq}$  is defined as 1/3 of the trace of the orthogonalized  $U_{ij}$  tensor.

Table 3. Anisotropic displacement parameters ( $\text{\AA}^2$ ) for mo\_harman\_mne\_5\_029\_0m.

The anisotropic displacement factor exponent takes the form:

$$-2\pi^2 [h^2(a^*)^2 U_{11} + k^2(b^*)^2 U_{22} + \dots + 2hka^*b^* U_{12}]$$

Atom	$U_{11}$	$U_{22}$	$U_{33}$	$U_{23}$	$U_{13}$	$U_{12}$
W1	0.0416(4)	0.0261(3)	0.0300(3)	0.0017(3)	0.0035(3)	-0.0004(4)
P1	0.051(3)	0.032(2)	0.055(3)	0.013(2)	0.014(2)	0.000(2)
O1	0.041(7)	0.069(8)	0.047(7)	-0.008(6)	-0.007(6)	0.005(6)
N1	0.048(9)	0.030(8)	0.027(7)	0.008(6)	0.012(6)	0.014(6)
N2	0.042(9)	0.033(8)	0.031(7)	0.002(5)	0.006(6)	0.008(6)
N3	0.059(10)	0.032(7)	0.027(7)	0.000(6)	-0.016(7)	-0.021(7)
N4	0.042(9)	0.032(8)	0.031(7)	0.006(6)	-0.004(7)	-0.002(7)
N5	0.055(10)	0.017(6)	0.026(7)	0.001(6)	0.007(6)	0.004(6)
N6	0.039(9)	0.037(8)	0.042(8)	0.001(6)	-0.001(7)	-0.005(7)
N7	0.043(8)	0.025(7)	0.038(8)	0.002(6)	0.001(6)	0.003(6)
C1	0.048(11)	0.035(10)	0.050(10)	-0.009(8)	-0.011(9)	-0.001(9)
C2	0.082(14)	0.031(10)	0.033(9)	-0.005(7)	0.010(10)	0.003(9)
C3	0.066(13)	0.044(10)	0.033(9)	-0.003(8)	-0.024(9)	-0.005(10)
C4	0.063(13)	0.027(9)	0.034(9)	-0.010(7)	-0.001(8)	0.001(9)

C5	0.052(12)	0.044(10)	0.021(8)	0.000(7)	0.018(8)	0.014(9)
C6	0.027(10)	0.040(10)	0.043(10)	−0.017(8)	0.004(8)	0.001(8)
C7	0.048(12)	0.033(9)	0.044(10)	−0.008(8)	0.006(9)	−0.003(8)
C8	0.081(15)	0.034(10)	0.038(10)	0.024(8)	0.012(10)	−0.003(10)
C9	0.053(13)	0.033(10)	0.080(14)	−0.024(10)	0.030(11)	−0.014(9)
C10	0.053(11)	0.041(11)	0.036(9)	0.007(8)	0.000(8)	−0.007(9)
C11	0.050(11)	0.037(9)	0.020(8)	0.005(7)	0.000(7)	0.024(8)
C12	0.071(13)	0.045(10)	0.020(8)	0.007(7)	0.004(8)	0.014(9)
C13	0.075(16)	0.061(13)	0.052(12)	0.001(10)	0.019(11)	0.003(11)
C14	0.084(18)	0.074(14)	0.055(13)	0.001(11)	0.015(12)	0.012(13)
C15	0.063(15)	0.040(11)	0.119(19)	−0.011(12)	−0.014(14)	0.010(10)
C16	0.042(12)	0.059(13)	0.107(17)	0.022(12)	0.007(11)	0.023(10)
C17	0.064(12)	0.046(10)	0.044(10)	0.010(9)	0.001(9)	−0.016(11)
C18	0.066(14)	0.057(12)	0.058(12)	0.000(10)	0.002(10)	0.020(10)
C19	0.065(13)	0.040(10)	0.063(12)	0.034(9)	0.006(10)	0.003(9)
C20	0.065(15)	0.047(12)	0.118(18)	0.008(11)	0.020(13)	−0.039(10)
C21	0.074(15)	0.050(11)	0.082(14)	0.033(10)	0.047(11)	0.015(10)
B1	0.045(12)	0.039(11)	0.046(11)	−0.016(10)	−0.013(10)	0.005(11)
Cl1	0.092(5)	0.222(9)	0.090(5)	0.016(5)	0.018(4)	−0.040(5)
Cl2	0.093(5)	0.161(6)	0.096(4)	0.028(4)	−0.013(4)	−0.030(5)
Cl3	0.099(6)	0.165(8)	0.241(10)	−0.103(7)	−0.046(6)	0.023(5)
C22	0.040(14)	0.034(12)	0.26(3)	0.006(16)	−0.021(17)	0.001(10)

Table 4. Bond lengths and angles for mo\_harman\_mne\_5\_029\_0m

Atom–Atom	Length [Å]		
W1–N7	1.739(12)	C1–C2	1.36(2)
W1–N5	2.201(12)	C1–H1	0.9500
W1–N3	2.205(14)	C2–C3	1.32(2)
W1–C11	2.226(13)	C2–H2	0.9500
W1–N1	2.251(12)	C3–H3	0.9500
W1–C10	2.257(16)	C4–C5	1.38(2)
W1–P1	2.489(4)	C4–H4	0.9500
P1–C20	1.797(18)	C5–C6	1.355(19)
P1–C19	1.806(16)	C5–H5	0.9500
P1–C21	1.810(17)	C6–H6	0.9500
O1–N7	1.245(14)	C7–C8	1.41(2)
N1–C1	1.326(18)	C7–H7	0.9500
N1–N2	1.370(16)	C8–C9	1.35(2)
N2–C3	1.372(17)	C8–H8	0.9500
N2–B1	1.54(2)	C9–H9	0.9500
N3–C4	1.346(17)	C10–C11	1.468(19)
N3–N4	1.358(16)	C10–C17	1.54(2)
N4–C6	1.348(17)	C10–H10	1.0000
N4–B1	1.53(2)	C11–C12	1.520(18)
N5–C7	1.335(17)	C11–H11	1.0000
N5–N6	1.371(16)	C12–C13	1.46(2)
N6–C9	1.332(19)	C12–C18	1.54(2)
N6–B1	1.54(2)	C12–H12	1.0000
		C13–C14	1.33(3)

C13–H13	0.9500
C14–C15	1.47(3)
C14–H14	0.9500
C15–C16	1.36(2)
C15–H15	0.9500
C16–C17	1.53(2)
C16–H16	0.9500
C17–H17A	0.9900
C17–H17B	0.9900
C18–H18A	0.9800
C18–H18B	0.9800
C18–H18C	0.9800
C19–H19A	0.9800
C19–H19B	0.9800
C19–H19C	0.9800
C20–H20A	0.9800
C20–H20B	0.9800
C20–H20C	0.9800
C21–H21A	0.9800
C21–H21B	0.9800
C21–H21C	0.9800
B1–H1A	1.05(14)
Cl1–C22	1.74(3)
Cl2–C22	1.75(2)
Cl3–C22	1.65(2)
C22–H22	1.0000
<b>Atom–Atom– Atom</b>	<b>Angle [°]</b>
N7–W1–N5	95.1(5)
N7–W1–N3	90.6(5)
N5–W1–N3	75.8(4)
N7–W1–C11	98.1(5)
N5–W1–C11	83.5(5)
N3–W1–C11	158.2(5)
N7–W1–N1	175.7(5)
N5–W1–N1	82.2(4)
N3–W1–N1	85.5(4)
C11–W1–N1	84.9(5)
N7–W1–C10	94.3(5)
N5–W1–C10	121.8(5)
N3–W1–C10	161.1(5)
C11–W1–C10	38.2(5)
N1–W1–C10	90.0(5)
N7–W1–P1	95.4(4)
N5–W1–P1	155.5(3)
N3–W1–P1	82.0(3)
C11–W1–P1	116.7(4)

N1–W1–P1	85.9(3)
C10–W1–P1	79.4(4)
C20–P1–C19	103.3(9)
C20–P1–C21	103.3(9)
C19–P1–C21	99.5(8)
C20–P1–W1	114.4(6)
C19–P1–W1	120.5(5)
C21–P1–W1	113.5(6)
C1–N1–N2	107.2(12)
C1–N1–W1	133.4(11)
N2–N1–W1	119.4(8)
N1–N2–C3	106.2(12)
N1–N2–B1	121.8(12)
C3–N2–B1	131.8(14)
C4–N3–N4	105.5(13)
C4–N3–W1	132.3(11)
N4–N3–W1	122.2(9)
C6–N4–N3	109.3(12)
C6–N4–B1	129.2(14)
N3–N4–B1	119.8(12)
C7–N5–N6	106.4(12)
C7–N5–W1	130.9(11)
N6–N5–W1	121.6(9)
C9–N6–N5	109.2(13)
C9–N6–B1	128.6(16)
N5–N6–B1	120.5(13)
O1–N7–W1	176.0(11)
N1–C1–C2	110.3(15)
N1–C1–H1	124.9
C2–C1–H1	124.9
C3–C2–C1	106.4(14)
C3–C2–H2	126.8
C1–C2–H2	126.8
C2–C3–N2	109.9(15)
C2–C3–H3	125.0
N2–C3–H3	125.0
N3–C4–C5	111.1(15)
N3–C4–H4	124.4
C5–C4–H4	124.4
C6–C5–C4	104.7(14)
C6–C5–H5	127.7
C4–C5–H5	127.7
N4–C6–C5	109.4(14)
N4–C6–H6	125.3
C5–C6–H6	125.3
N5–C7–C8	109.8(15)
N5–C7–H7	125.1
C8–C7–H7	125.1

C9-C8-C7	104.8(15)
C9-C8-H8	127.6
C7-C8-H8	127.6
N6-C9-C8	109.8(16)
N6-C9-H9	125.1
C8-C9-H9	125.1
C11-C10-C17	119.9(13)
C11-C10-W1	69.7(8)
C17-C10-W1	117.2(10)
C11-C10-H10	114.3
C17-C10-H10	114.3
W1-C10-H10	114.3
C10-C11-C12	128.5(14)
C10-C11-W1	72.1(8)
C12-C11-W1	126.7(9)
C10-C11-H11	108.3
C12-C11-H11	108.3
W1-C11-H11	108.3
C13-C12-C11	118.9(14)
C13-C12-C18	110.5(14)
C11-C12-C18	110.2(12)
C13-C12-H12	105.4
C11-C12-H12	105.4
C18-C12-H12	105.4
C14-C13-C12	129.4(18)
C14-C13-H13	115.3
C12-C13-H13	115.3
C13-C14-C15	121(2)
C13-C14-H14	119.3
C15-C14-H14	119.3
C16-C15-C14	123.4(18)
C16-C15-H15	118.3
C14-C15-H15	118.3
C15-C16-C17	119.3(18)
C15-C16-H16	120.3
C17-C16-H16	120.3
C16-C17-C10	115.6(14)
C16-C17-H17A	108.4
C10-C17-H17A	108.4
C16-C17-H17B	108.4
C10-C17-H17B	108.4
H17A-C17-H17B	107.4
C12-C18-H18A	109.5
C12-C18-H18B	109.5
H18A-C18-H18B	109.5

C12-C18-H18C	109.5
H18A-C18-H18C	109.5
H18B-C18-H18C	109.5
P1-C19-H19A	109.5
P1-C19-H19B	109.5
H19A-C19-H19B	109.5
P1-C19-H19C	109.5
H19A-C19-H19C	109.5
H19B-C19-H19C	109.5
P1-C20-H20A	109.5
P1-C20-H20B	109.5
H20A-C20-H20B	109.5
P1-C20-H20C	109.5
H20A-C20-H20C	109.5
H20B-C20-H20C	109.5
P1-C21-H21A	109.5
P1-C21-H21B	109.5
H21A-C21-H21B	109.5
P1-C21-H21C	109.5
H21A-C21-H21C	109.5
H21B-C21-H21C	109.5
N4-B1-N6	105.3(12)
N4-B1-N2	109.9(15)
N6-B1-N2	108.7(13)
N4-B1-H1A	109(8)
N6-B1-H1A	104(8)
N2-B1-H1A	119(8)
Cl3-C22-Cl1	117.4(12)
Cl3-C22-Cl2	110.0(17)
Cl1-C22-Cl2	107.0(11)
Cl3-C22-H22	107.3
Cl1-C22-H22	107.3
Cl2-C22-H22	107.3



Table 5. Torsion angles for mo\_harman\_mne\_5\_029\_0m

Atom–Atom– Atom–Atom	Torsion Angle [°]		
C1–N1–N2–C3	0.6(15)	C7–C8–C9–N6	–0.6(18)
W1–N1–N2–C3	–178.2(8)	C17–C10–C11–C12	–12(2)
C1–N1–N2–B1	175.4(13)	W1–C10–C11–C12	–123.0(14)
W1–N1–N2–B1	–3.4(16)	C17–C10–C11–W1	110.5(13)
C4–N3–N4–C6	0.0(15)	C10–C11–C12–C13	40(2)
W1–N3–N4–C6	178.7(9)	W1–C11–C12–C13	–56(2)
C4–N3–N4–B1	–166.2(13)	C10–C11–C12–C18	–89.1(19)
W1–N3–N4–B1	12.5(17)	W1–C11–C12–C18	175.1(12)
C7–N5–N6–C9	–0.6(15)	C11–C12–C13–C14	–83(2)
W1–N5–N6–C9	–169.9(9)	C18–C12–C13–C14	46(3)
C7–N5–N6–B1	166.3(12)	C12–C13–C14–C15	12(3)
W1–N5–N6–B1	–3.1(17)	C13–C14–C15–C16	60(3)
N2–N1–C1–C2	–1.3(16)	C14–C15–C16–C17	–1(3)
W1–N1–C1–C2	177.2(9)	C15–C16–C17–C10	–93(2)
N1–C1–C2–C3	1.6(18)	C11–C10–C17–C16	66.2(19)
C1–C2–C3–N2	–1.2(18)	W1–C10–C17–C16	147.3(12)
N1–N2–C3–C2	0.4(17)	C6–N4–B1–N6	–110.9(16)
B1–N2–C3–C2	–173.7(15)	N3–N4–B1–N6	52.3(18)
N4–N3–C4–C5	0.2(16)	C6–N4–B1–N2	132.2(15)
W1–N3–C4–C5	–178.3(9)	N3–N4–B1–N2	–64.6(17)
N3–C4–C5–C6	–0.3(17)	C9–N6–B1–N4	106.2(18)
N3–N4–C6–C5	–0.2(16)	N5–N6–B1–N4	–57.9(18)
B1–N4–C6–C5	164.4(14)	C9–N6–B1–N2	–136.2(16)
C4–C5–C6–N4	0.3(17)	N5–N6–B1–N2	59.8(17)
N6–N5–C7–C8	0.2(16)	N1–N2–B1–N4	59.1(17)
W1–N5–C7–C8	168.2(10)	C3–N2–B1–N4	–127.6(16)
N5–C7–C8–C9	0.2(18)	N1–N2–B1–N6	–55.6(18)
N5–N6–C9–C8	0.7(17)	C3–N2–B1–N6	117.7(16)
B1–N6–C9–C8	–164.8(14)		

## Structure Tables

A yellow, needle-shaped crystal was mounted on a MiTeGen micromount with perfluoroether oil. Data for mo\_harman\_3\_jkh\_109\_x3\_attempt were collected from a shock-cooled single crystal at 100(2) K on a Bruker D8 VENTURE dual wavelength Mo/Cu Kappa four-circle diffractometer with a microfocus sealed X-ray tube using a HELIOS double bounce multilayer mirror as monochromator and a PHOTON III detector. The diffractometer was equipped with an Oxford Cryostream 800Plus low temperature device and used Mo  $K_{\alpha}$  radiation ( $\lambda = 0.71073 \text{ \AA}$ ). All data were integrated with SAINT 8.40B and a Multi-Scan absorption correction using was applied.<sup>[1,2]</sup> The structure was solved by direct methods with SHELXT and refined by full-matrix least-squares methods

against  $F^2$  using SHELXL-2019/1.<sup>[3,4]</sup> All non-hydrogen atoms were refined with anisotropic displacement parameters. The B-H hydrogen atom as well as H10, H11, and H17 were located in the electron density map and refined isotropically. All hydrogen atoms were refined with isotropic displacement parameters. Some of their coordinates were refined freely and some on calculated positions using a riding model with their  $U_{iso}$  values constrained to 1.5 times the  $U_{eq}$  of their pivot atoms for terminal  $sp^3$  carbon atoms and 1.2 times for all other carbon atoms. Crystallographic data for the structures reported in this paper have been deposited with the Cambridge Crystallographic Data Centre.<sup>[5]</sup> CCDC ?????? contain the supplementary crystallographic data for this paper. These data can be obtained free of charge from The Cambridge Crystallographic Data Centre via [www.ccdc.cam.ac.uk/structures](http://www.ccdc.cam.ac.uk/structures). This report and the CIF file were generated using FinalCif.<sup>[6]</sup>

Table 1. Crystal data and structure refinement for mo\_harman\_3\_jkh\_109\_x3\_attempt

CCDC number	
Empirical formula	C <sub>24</sub> H <sub>34</sub> BF <sub>3</sub> N <sub>7</sub> O <sub>6</sub> PSW
Formula weight	831.27
Temperature [K]	100(2)
Crystal system	monoclinic
Space group (number)	$P2_1/n$ (14)
$a$ [Å]	8.0695(8)
$b$ [Å]	32.869(3)
$c$ [Å]	11.5607(10)
$\alpha$ [°]	90
$\beta$ [°]	93.925(3)
$\gamma$ [°]	90
Volume [Å <sup>3</sup> ]	3059.2(5)
$Z$	4
$\rho_{calc}$ [gcm <sup>-3</sup> ]	1.805
$\mu$ [mm <sup>-1</sup> ]	3.966
$F(000)$	1648
Crystal size [mm <sup>3</sup> ]	0.066×0.069×0.197
Crystal colour	yellow
Crystal shape	needle
Radiation	Mo $K_\alpha$ ( $\lambda=0.71073$ Å)
2 $\theta$ range [°]	3.74 to 51.37 (0.82 Å)

Index ranges	$-9 \leq h \leq 9$ $-40 \leq k \leq 39$ $-14 \leq l \leq 14$
Reflections collected	36927
Independent reflections	5812 $R_{\text{int}} = 0.0652$ $R_{\text{sigma}} = 0.0423$
Completeness to $\theta = 25.242^\circ$	100.0
Data / Restraints / Parameters	5812 / 0 / 412
Goodness-of-fit on $F^2$	1.057
Final $R$ indexes [ $I \geq 2\sigma(I)$ ]	$R_1 = 0.0345$ $wR_2 = 0.0645$
Final $R$ indexes [all data]	$R_1 = 0.0486$ $wR_2 = 0.0689$
Largest peak/hole [ $\text{e}\text{\AA}^{-3}$ ]	0.84/−1.09

Table 2. Atomic coordinates and  $U_{eq}$  [ $\text{\AA}^2$ ] for mo\_harman\_3\_jkh\_109\_x3\_attempt

Atom	x	y	z	$U_{eq}$
W1	0.54304(2)	0.63906(2)	0.36974(2)	0.01781(7)
P1	0.36435(17)	0.59321(4)	0.48784(12)	0.0237(3)
O1	0.3695(5)	0.71895(11)	0.3833(3)	0.0369(10)
O2	0.4378(6)	0.65771(14)	0.8009(4)	0.0519(12)
O3	0.2723(5)	0.71103(13)	0.8165(4)	0.0444(11)
N1	0.6545(5)	0.57926(12)	0.3244(3)	0.0186(9)
N2	0.6264(5)	0.56403(12)	0.2146(3)	0.0227(9)
N3	0.3411(5)	0.62421(13)	0.2426(4)	0.0220(9)
N4	0.3605(5)	0.59979(13)	0.1493(4)	0.0242(10)
N5	0.6330(5)	0.65703(12)	0.2018(4)	0.0211(9)
N6	0.6291(5)	0.63046(12)	0.1103(4)	0.0219(9)
N7	0.4423(5)	0.68650(13)	0.3845(4)	0.0244(10)
C1	0.7523(6)	0.55232(15)	0.3827(4)	0.0233(11)
H1	0.790272	0.554891	0.461995	0.028
C2	0.7907(7)	0.52039(15)	0.3124(5)	0.0266(12)
H2	0.859072	0.497588	0.332449	0.032
C3	0.7084(7)	0.52864(15)	0.2067(5)	0.0255(12)
H3	0.709333	0.512083	0.139430	0.031
C4	0.1836(6)	0.63653(18)	0.2356(5)	0.0287(12)
H4	0.136248	0.654240	0.289312	0.034
C5	0.0990(7)	0.61981(19)	0.1390(5)	0.0363(14)
H5	-0.014973	0.623195	0.114634	0.044
C6	0.2153(7)	0.59723(17)	0.0860(5)	0.0310(13)
H6	0.196056	0.582291	0.016005	0.037
C7	0.6858(6)	0.69266(15)	0.1634(4)	0.0236(11)
H7	0.698583	0.716707	0.208746	0.028

C8	0.7194(7)	0.68956(16) )	0.0477(5)	0.0267(12)
H8	0.759954	0.710281	−0.000221	0.032
C9	0.6813(6)	0.65009(15) )	0.0171(4)	0.0250(12)
H9	0.690260	0.638520	−0.057476	0.030
C10	0.7390(6)	0.63799(16) )	0.5233(4)	0.0211(10)
H10	0.781714	0.610847	0.550632	0.025
C11	0.8113(6)	0.65566(16) )	0.4267(5)	0.0238(11)
H11	0.876(7)	0.6369(16)	0.375(5)	0.029
C12	0.8771(7)	0.69783(17) )	0.4277(5)	0.0326(13)
H12	0.884493	0.710921	0.354997	0.039
C13	0.9273(7)	0.71913(18) )	0.5240(5)	0.0355(14)
H13	0.975312	0.745069	0.512360	0.043
C14	0.9148(7)	0.70599(18) )	0.6464(5)	0.0374(15)
H14A	1.000884	0.720382	0.696003	0.045
H14B	0.938921	0.676494	0.652097	0.045
C15	0.7461(8)	0.71393(18) )	0.6934(5)	0.0370(14)
H15A	0.735495	0.743357	0.709516	0.044
H15B	0.739635	0.699145	0.767513	0.044
C16	0.6007(7)	0.70059(16) )	0.6090(5)	0.0284(12)
H16	0.609921	0.715637	0.534515	0.034
C17	0.6195(7)	0.65606(16) )	0.5846(4)	0.0239(11)
H17	0.567(6)	0.6380(15)	0.636(4)	0.020(13)
C18	0.4344(8)	0.71200(17) )	0.6565(5)	0.0349(14)
H18A	0.435492	0.741615	0.672154	0.042
H18B	0.345552	0.706866	0.594849	0.042
C19	0.3877(7)	0.69043(19) )	0.7651(5)	0.0356(14)
C20	0.2003(9)	0.6902(2)	0.9129(6)	0.0527(19)
H20A	0.146094	0.665065	0.884830	0.079
H20B	0.118270	0.707960	0.946052	0.079
H20C	0.288397	0.683625	0.972609	0.079
C21	0.1962(7)	0.61848(19) )	0.5539(5)	0.0367(14)
H21A	0.111763	0.598423	0.571819	0.055
H21B	0.146496	0.638858	0.500260	0.055
H21C	0.238917	0.631873	0.625613	0.055

C22	0.4661(7)	0.56356(17)	0.6039(5)	0.0338(14)
H22A	0.523127	0.581852	0.660497	0.051
H22B	0.547264	0.545233	0.571985	0.051
H22C	0.383145	0.547535	0.641976	0.051
C23	0.2644(8)	0.55334(18)	0.4000(5)	0.0388(15)
H23A	0.204241	0.535133	0.449586	0.058
H23B	0.348748	0.537820	0.361741	0.058
H23C	0.186284	0.565518	0.341290	0.058
B1	0.5371(8)	0.58914(18)	0.1178(5)	0.0238(13)
H1A	0.531(6)	0.5731(14)	0.034(4)	0.019(13)
S1	0.93480(18)	0.56942(4)	0.77021(11)	0.0269(3)
F1	0.6730(4)	0.53043(13)	0.8352(3)	0.0549(11)
F2	0.8573(5)	0.54461(13)	0.9731(3)	0.0530(10)
F3	0.8993(5)	0.49590(11)	0.8523(3)	0.0501(10)
O4	0.8493(6)	0.60693(12)	0.7900(4)	0.0467(12)
O5	1.1058(5)	0.56743(13)	0.8131(3)	0.0366(10)
O6	0.9020(5)	0.55267(11)	0.6553(3)	0.0275(8)
C24	0.8355(7)	0.5332(2)	0.8610(5)	0.0350(14)

$U_{eq}$  is defined as 1/3 of the trace of the orthogonalized  $U_{ij}$  tensor.

Table 3. Anisotropic displacement parameters ( $\text{\AA}^2$ ) for mo\_harman\_3\_jkh\_109\_x3\_attempt. The anisotropic displacement factor exponent takes the form:  $-2\pi^2 [h^2(a^*)^2 U_{11} + k^2(b^*)^2 U_{22} + \dots + 2hka^*b^* U_{12}]$

Atom	$U_{11}$	$U_{22}$	$U_{33}$	$U_{23}$	$U_{13}$	$U_{12}$
W1	0.01607(11)	0.01962(10)	0.01797(10)	0.00061(9)	0.00288(7)	0.00126(9)
P1	0.0191(7)	0.0299(7)	0.0222(7)	0.0057(6)	0.0017(6)	-0.0017(6)
O1	0.048(3)	0.030(2)	0.032(2)	-0.0003(18)	0.0047(19)	0.020(2)
O2	0.062(3)	0.058(3)	0.036(3)	0.009(2)	0.009(2)	0.025(3)
O3	0.042(3)	0.042(2)	0.051(3)	-0.002(2)	0.018(2)	0.003(2)
N1	0.021(2)	0.019(2)	0.016(2)	-0.0028(17)	0.0023(17)	0.0023(17)
N2	0.027(3)	0.023(2)	0.018(2)	-0.0015(18)	0.0031(18)	0.0014(19)
N3	0.014(2)	0.031(2)	0.022(2)	0.0030(18)	0.0016(17)	0.0018(18)

N4	0.022(2)	0.030(2)	0.020(2)	−0.0029(19)	−0.0032(18)	−0.0018(19)
N5	0.021(2)	0.020(2)	0.022(2)	−0.0012(18)	0.0026(18)	0.0023(18)
N6	0.021(2)	0.027(2)	0.018(2)	0.0011(18)	0.0027(17)	0.0023(18)
N7	0.025(2)	0.032(2)	0.017(2)	0.0058(19)	0.0019(18)	−0.002(2)
C1	0.025(3)	0.025(3)	0.019(3)	0.000(2)	0.000(2)	0.002(2)
C2	0.029(3)	0.022(3)	0.030(3)	0.003(2)	0.007(2)	0.006(2)
C3	0.033(3)	0.019(2)	0.026(3)	−0.005(2)	0.010(2)	0.000(2)
C4	0.020(3)	0.039(3)	0.026(3)	0.002(3)	0.000(2)	0.001(3)
C5	0.023(3)	0.054(4)	0.031(3)	0.005(3)	−0.002(2)	−0.001(3)
C6	0.021(3)	0.044(3)	0.027(3)	−0.001(3)	−0.003(2)	−0.007(3)
C7	0.025(3)	0.020(3)	0.026(3)	0.001(2)	0.006(2)	−0.001(2)
C8	0.027(3)	0.029(3)	0.026(3)	0.008(2)	0.008(2)	0.003(2)
C9	0.022(3)	0.033(3)	0.021(3)	0.006(2)	0.005(2)	0.008(2)
C10	0.020(3)	0.026(2)	0.015(2)	−0.002(2)	−0.0115(19)	0.001(2)
C11	0.016(3)	0.027(3)	0.028(3)	−0.003(2)	0.001(2)	0.000(2)
C12	0.031(3)	0.031(3)	0.035(3)	0.006(3)	0.003(3)	−0.003(3)
C13	0.032(3)	0.034(3)	0.040(3)	0.001(3)	0.000(3)	−0.009(3)
C14	0.038(4)	0.037(3)	0.036(3)	−0.002(3)	−0.004(3)	−0.008(3)
C15	0.041(4)	0.040(3)	0.029(3)	−0.012(3)	−0.002(3)	0.000(3)
C16	0.028(3)	0.029(3)	0.028(3)	−0.001(2)	0.003(2)	0.001(2)
C17	0.020(3)	0.031(3)	0.020(3)	0.001(2)	−0.002(2)	−0.002(2)
C18	0.047(4)	0.035(3)	0.023(3)	−0.002(2)	0.004(3)	0.012(3)
C19	0.030(3)	0.048(4)	0.028(3)	−0.008(3)	0.001(3)	0.009(3)
C20	0.052(5)	0.057(4)	0.053(4)	0.000(4)	0.026(4)	0.001(4)
C21	0.021(3)	0.056(4)	0.033(3)	0.007(3)	0.008(3)	0.001(3)
C22	0.034(3)	0.033(3)	0.034(3)	0.011(3)	0.001(3)	−0.004(3)
C23	0.039(4)	0.038(3)	0.039(3)	0.008(3)	−0.002(3)	−0.017(3)
B1	0.029(3)	0.026(3)	0.017(3)	−0.002(2)	0.002(2)	0.001(3)
S1	0.0317(8)	0.0305(7)	0.0187(6)	0.0015(5)	0.0029(6)	0.0048(6)
F1	0.028(2)	0.094(3)	0.043(2)	0.022(2)	0.0032(17)	−0.004(2)
F2	0.050(2)	0.090(3)	0.0199(17)	0.0100(18)	0.0086(16)	0.005(2)
F3	0.057(3)	0.042(2)	0.052(2)	0.0217(18)	0.0069(19)	0.0058(18)
O4	0.072(3)	0.038(2)	0.032(2)	−0.0030(19)	0.011(2)	0.023(2)
O5	0.028(2)	0.055(3)	0.027(2)	−0.0028(19)	−0.0016(17)	−0.0080(19)
O6	0.033(2)	0.0297(19)	0.0195(18)	−0.0005(16)	−0.0025(16)	0.0031(16)
C24	0.026(3)	0.058(4)	0.021(3)	0.010(3)	0.006(2)	0.008(3)

Table 4. Bond lengths and angles for mo\_harman\_3\_jkh\_109\_x3\_attempt

Atom–Atom	Length [Å]		
W1–N7	1.772(4)	W1–N5	2.200(4)
W1–N3	2.174(4)	W1–N1	2.239(4)
		W1–C11	2.286(5)

W1–C10	2.295(4)
W1–P1	2.5464(13)
W1–C17	2.580(5)
P1–C21	1.805(6)
P1–C22	1.809(6)
P1–C23	1.813(6)
O1–N7	1.217(5)
O2–C19	1.212(7)
O3–C19	1.324(7)
O3–C20	1.462(7)
N1–C1	1.337(6)
N1–N2	1.369(5)
N2–C3	1.344(6)
N2–B1	1.531(7)
N3–C4	1.331(7)
N3–N4	1.362(6)
N4–C6	1.341(7)
N4–B1	1.535(7)
N5–C7	1.333(6)
N5–N6	1.371(6)
N6–C9	1.347(6)
N6–B1	1.553(7)
C1–C2	1.375(7)
C1–H1	0.9500
C2–C3	1.377(8)
C2–H2	0.9500
C3–H3	0.9500
C4–C5	1.383(8)
C4–H4	0.9500
C5–C6	1.373(8)
C5–H5	0.9500
C6–H6	0.9500
C7–C8	1.387(7)
C7–H7	0.9500
C8–C9	1.374(7)
C8–H8	0.9500
C9–H9	0.9500
C10–C17	1.371(7)
C10–C11	1.419(7)
C10–H10	1.0000
C11–C12	1.484(7)
C11–H11	1.03(5)
C12–C13	1.353(8)
C12–H12	0.9500
C13–C14	1.490(8)
C13–H13	0.9500
C14–C15	1.522(8)
C14–H14A	0.9900

C14–H14B	0.9900
C15–C16	1.538(8)
C15–H15A	0.9900
C15–H15B	0.9900
C16–C17	1.500(7)
C16–C18	1.531(8)
C16–H16	1.0000
C17–H17	0.96(5)
C18–C19	1.512(8)
C18–H18A	0.9900
C18–H18B	0.9900
C20–H20A	0.9800
C20–H20B	0.9800
C20–H20C	0.9800
C21–H21A	0.9800
C21–H21B	0.9800
C21–H21C	0.9800
C22–H22A	0.9800
C22–H22B	0.9800
C22–H22C	0.9800
C23–H23A	0.9800
C23–H23B	0.9800
C23–H23C	0.9800
B1–H1A	1.10(5)
S1–O5	1.435(4)
S1–O4	1.439(4)
S1–O6	1.446(4)
S1–C24	1.810(6)
F1–C24	1.328(7)
F2–C24	1.349(6)
F3–C24	1.337(7)
Atom–Atom– Atom	Angle [°]
N7–W1–N3	86.28(18)
N7–W1–N5	91.71(17)
N3–W1–N5	74.97(15)
N7–W1–N1	171.66(17)
N3–W1–N1	86.52(15)
N5–W1–N1	82.37(14)
N7–W1–C11	101.19(19)
N3–W1–C11	154.13(18)
N5–W1–C11	80.04(18)
N1–W1–C11	83.63(17)
N7–W1–C10	103.61(19)
N3–W1–C10	164.65(17)
N5–W1–C10	115.80(17)
N1–W1–C10	84.32(17)



C11-W1-C10	36.09(18)
N7-W1-P1	100.88(14)
N3-W1-P1	78.70(11)
N5-W1-P1	149.93(11)
N1-W1-P1	81.79(11)
C11-W1-P1	123.15(14)
C10-W1-P1	87.81(13)
N7-W1-C17	78.34(18)
N3-W1-C17	144.96(16)
N5-W1-C17	136.07(17)
N1-W1-C17	110.00(15)
C11-W1-C17	60.74(18)
C10-W1-C17	31.98(17)
P1-W1-C17	73.67(13)
C21-P1-C22	104.5(3)
C21-P1-C23	104.5(3)
C22-P1-C23	100.8(3)
C21-P1-W1	115.1(2)
C22-P1-W1	118.1(2)
C23-P1-W1	112.0(2)
C19-O3-C20	115.5(5)
C1-N1-N2	106.2(4)
C1-N1-W1	134.1(3)
N2-N1-W1	119.6(3)
C3-N2-N1	109.2(4)
C3-N2-B1	128.8(4)
N1-N2-B1	121.4(4)
C4-N3-N4	107.0(4)
C4-N3-W1	129.8(4)
N4-N3-W1	123.1(3)
C6-N4-N3	109.0(4)
C6-N4-B1	130.3(4)
N3-N4-B1	118.8(4)
C7-N5-N6	107.1(4)
C7-N5-W1	131.5(3)
N6-N5-W1	121.3(3)
C9-N6-N5	108.7(4)
C9-N6-B1	129.8(4)
N5-N6-B1	120.0(4)
O1-N7-W1	173.8(4)
N1-C1-C2	110.9(5)
N1-C1-H1	124.6
C2-C1-H1	124.6
C1-C2-C3	105.0(5)
C1-C2-H2	127.5
C3-C2-H2	127.5
N2-C3-C2	108.6(4)
N2-C3-H3	125.7

C2-C3-H3	125.7
N3-C4-C5	110.1(5)
N3-C4-H4	124.9
C5-C4-H4	124.9
C6-C5-C4	105.1(5)
C6-C5-H5	127.4
C4-C5-H5	127.4
N4-C6-C5	108.7(5)
N4-C6-H6	125.7
C5-C6-H6	125.7
N5-C7-C8	110.2(5)
N5-C7-H7	124.9
C8-C7-H7	124.9
C9-C8-C7	105.2(5)
C9-C8-H8	127.4
C7-C8-H8	127.4
N6-C9-C8	108.9(5)
N6-C9-H9	125.6
C8-C9-H9	125.6
C17-C10-C11	124.9(5)
C17-C10-W1	85.5(3)
C11-C10-W1	71.6(3)
C17-C10-H10	117.5
C11-C10-H10	117.5
W1-C10-H10	117.5
C10-C11-C12	122.8(5)
C10-C11-W1	72.3(3)
C12-C11-W1	123.8(4)
C10-C11-H11	118(3)
C12-C11-H11	112(3)
W1-C11-H11	101(3)
C13-C12-C11	125.2(5)
C13-C12-H12	117.4
C11-C12-H12	117.4
C12-C13-C14	126.6(5)
C12-C13-H13	116.7
C14-C13-H13	116.7
C13-C14-C15	114.1(5)
C13-C14-H14A	108.7
C15-C14-H14A	108.7
C13-C14-H14B	108.7
C15-C14-H14B	108.7
H14A-C14-H14B	107.6
C14-C15-C16	112.8(5)
C14-C15-H15A	109.0
C16-C15-H15A	109.0
C14-C15-H15B	109.0

C16–C15–H15B	109.0
H15A–C15–H15B	107.8
C17–C16–C18	114.1(5)
C17–C16–C15	108.3(5)
C18–C16–C15	110.6(5)
C17–C16–H16	107.8
C18–C16–H16	107.8
C15–C16–H16	107.8
C10–C17–C16	127.1(5)
C10–C17–W1	62.5(3)
C16–C17–W1	111.8(3)
C10–C17–H17	114(3)
C16–C17–H17	116(3)
W1–C17–H17	112(3)
C19–C18–C16	117.2(5)
C19–C18–H18A	108.0
C16–C18–H18A	108.0
C19–C18–H18B	108.0
C16–C18–H18B	108.0
H18A–C18–H18B	107.2
O2–C19–O3	122.0(6)
O2–C19–C18	127.1(5)
O3–C19–C18	110.8(5)
O3–C20–H20A	109.5
O3–C20–H20B	109.5
H20A–C20–H20B	109.5
O3–C20–H20C	109.5
H20A–C20–H20C	109.5
H20B–C20–H20C	109.5
P1–C21–H21A	109.5
P1–C21–H21B	109.5
H21A–C21–H21B	109.5
P1–C21–H21C	109.5
H21A–C21–H21C	109.5

H21B–C21–H21C	109.5
P1–C22–H22A	109.5
P1–C22–H22B	109.5
H22A–C22–H22B	109.5
P1–C22–H22C	109.5
H22A–C22–H22C	109.5
H22B–C22–H22C	109.5
P1–C23–H23A	109.5
P1–C23–H23B	109.5
H23A–C23–H23B	109.5
P1–C23–H23C	109.5
H23A–C23–H23C	109.5
H23B–C23–H23C	109.5
N2–B1–N4	110.4(4)
N2–B1–N6	108.0(4)
N4–B1–N6	105.6(4)
N2–B1–H1A	112(3)
N4–B1–H1A	109(3)
N6–B1–H1A	111(3)
O5–S1–O4	116.4(3)
O5–S1–O6	114.3(2)
O4–S1–O6	114.4(2)
O5–S1–C24	102.9(3)
O4–S1–C24	103.6(3)
O6–S1–C24	102.8(3)
F1–C24–F3	107.4(5)
F1–C24–F2	107.2(5)
F3–C24–F2	107.5(5)
F1–C24–S1	112.6(4)
F3–C24–S1	111.8(4)
F2–C24–S1	109.9(4)

Table 5. Torsion angles for mo\_harman\_3\_jkh\_109\_x3\_attempt

Atom–Atom–Atom–Atom	Torsion Angle [°]
C1–N1–N2–C3	–0.8(5)
W1–N1–N2–C3	178.5(3)
C1–N1–N2–B1	–172.2(5)

W1–N1–N2–B1	7.1(6)
C4–N3–N4–C6	–0.1(6)
W1–N3–N4–C6	–178.5(3)
C4–N3–N4–B1	165.7(4)
W1–N3–N4–B1	–12.8(6)

C7–N5–N6–C9	0.6(5)
W1–N5–N6–C9	176.2(3)
C7–N5–N6–B1	–166.5(4)
W1–N5–N6–B1	9.1(6)
N2–N1–C1–C2	1.1(6)
W1–N1–C1–C2	–178.0(4)
N1–C1–C2–C3	–1.0(6)
N1–N2–C3–C2	0.2(6)
B1–N2–C3–C2	170.7(5)
C1–C2–C3–N2	0.4(6)
N4–N3–C4–C5	0.8(6)
W1–N3–C4–C5	179.2(4)
N3–C4–C5–C6	–1.3(7)
N3–N4–C6–C5	–0.7(6)
B1–N4–C6–C5	–164.3(5)
C4–C5–C6–N4	1.2(6)
N6–N5–C7–C8	–1.0(6)
W1–N5–C7–C8	–175.9(4)
N5–C7–C8–C9	1.0(6)
N5–N6–C9–C8	0.0(6)
B1–N6–C9–C8	165.5(5)
C7–C8–C9–N6	–0.6(6)
C17–C10–C11–C12	48.7(8)
W1–C10–C11–C12	119.3(5)
C17–C10–C11–W1	–70.6(5)
C10–C11–C12–C13	23.1(9)
W1–C11–C12–C13	112.9(6)
C11–C12–C13–C14	–5.0(10)
C12–C13–C14–C15	–83.2(8)
C13–C14–C15–C16	46.4(7)
C14–C15–C16–C17	58.2(6)
C14–C15–C16–C18	–176.0(5)
C11–C10–C17–C16	–33.7(8)
W1–C10–C17–C16	–97.5(5)

C11–C10–C17–W1	63.8(4)
C18–C16–C17–C10	167.3(5)
C15–C16–C17–C10	–69.0(7)
C18–C16–C17–W1	96.0(5)
C15–C16–C17–W1	–140.3(4)
C17–C16–C18–C19	56.0(7)
C15–C16–C18–C19	–66.5(7)
C20–O3–C19–O2	–4.7(9)
C20–O3–C19–C18	171.5(5)
C16–C18–C19–O2	–23.4(9)
C16–C18–C19–O3	160.6(5)
C3–N2–B1–N4	129.4(5)
N1–N2–B1–N4	–61.1(6)
C3–N2–B1–N6	–115.6(5)
N1–N2–B1–N6	53.9(6)
C6–N4–B1–N2	–133.3(5)
N3–N4–B1–N2	64.5(6)
C6–N4–B1–N6	110.2(6)
N3–N4–B1–N6	–52.0(5)
C9–N6–B1–N2	131.9(5)
N5–N6–B1–N2	–64.1(6)
C9–N6–B1–N4	–110.1(5)
N5–N6–B1–N4	54.0(6)
O5–S1–C24–F1	179.8(4)
O4–S1–C24–F1	58.2(5)
O6–S1–C24–F1	–61.2(5)
O5–S1–C24–F3	–59.1(5)
O4–S1–C24–F3	179.3(4)
O6–S1–C24–F3	59.9(4)
O5–S1–C24–F2	60.3(4)
O4–S1–C24–F2	–61.3(4)
O6–S1–C24–F2	179.3(4)

#### Structure Report for mo\_harman\_3\_jkh\_045\_x2\_0m

A yellow, needle shaped crystal of mo\_harman\_3\_jkh\_045\_x2\_0m measuring 0.081×0.125×0.643 mm was coated with Paratone oil and mounted on a MiTeGen micromount. Data for mo\_harman\_3\_jkh\_045\_x2\_0m were measured on a Bruker D8 VENTURE dual wavelength Mo/Cu Kappa four-circle diffractometer equipped with a PHOTON III detector and an Incoatec I $\mu$ S 3.0 microfocus sealed X-ray tube (Mo  $K_{\alpha}$ ,

$\lambda=0.71073$  Å) using a HELIOS double bounce multilayer mirror as monochromator. The crystal temperature was controlled with an Oxford Cryostream 800low temperature device. Data collection and processing were done within the Bruker APEX5 software suite.<sup>39</sup> All data were integrated with the Bruker SAINT 8.40B software using a narrow-frame algorithm. Data were corrected for absorption effects using a Multi-Scan method (SADABS).

The structure was solved by dual methods with XT<sup>40</sup> and refined by full-matrix least-squares methods against  $F^2$  using XL<sup>41</sup> within OLEX2.<sup>42</sup> All non-hydrogen atoms were refined with anisotropically. Hydrogen atoms were placed in geometrically calculated positions with  $U_{iso} = 1.2U_{equiv}$  of the parent atom ( $1.5U_{equiv}$  for methyl). This report and the CIF file were generated using FinalCif.<sup>43</sup>

---

<sup>39</sup> APEX5, Saint, SADABS; Bruker AXS Inc. 2019.

<sup>40</sup> Sheldrick, G. M. *SHELXT* – Integrated space-group and crystal-structure determination. *Acta Cryst. Sect. A Found. Adv.* **2015**, *71*, 3-8.

<sup>41</sup> Sheldrick, G. M. Crystal structure refinement with *SHELXL*. *Acta Cryst. Sect. C Struct. Chem.* **2015**, *71*, 3-8.

<sup>42</sup> Dolomanov, O. V.; Bourhis, L. J.; Gildea, R. J.; Howard, J. A. K.; Puschmann, H. *OLEX2*: a completed structure solution, refinement and analysis program. *J. Appl. Cryst.* **2009**, *42*, 339-341.

<sup>43</sup> Kratzert, D. FinalCif, <https://dkratzert.de/finalcif.html>.

Table 1. Crystal data and structure refinement for mo\_harman\_3\_jkh\_045\_x2\_0m

CCDC number	
Empirical formula	C <sub>28</sub> H <sub>36</sub> BF <sub>3</sub> N <sub>7</sub> O <sub>4</sub> PSW
Formula weight	849.33
Temperature [K]	100.00
Wavelength [Å]	0.71073
Crystal size [mm <sup>3</sup> ]	0.081×0.125×0.643
Crystal habit	yellow needle
Crystal system	triclinic
Space group	<i>P</i> $\bar{1}$ (2)
<i>a</i> [Å]	7.9337(4)
<i>b</i> [Å]	11.5592(5)
<i>c</i> [Å]	18.4212(9)
$\alpha$ [°]	75.411(2)
$\beta$ [°]	78.141(2)
$\gamma$ [°]	86.959(2)
Volume [Å <sup>3</sup> ]	1599.99(13)
<i>Z</i>	2
$\rho_{\text{calc}}$ [gcm <sup>-3</sup> ]	1.763
$\mu$ [mm <sup>-1</sup> ]	3.789
<i>F</i> (000)	844
2 $\theta$ range [°]	4.66 to 66.32 (0.65 Å)
Index ranges	-12 ≤ <i>h</i> ≤ 12 -12 ≤ <i>k</i> ≤ 17 -28 ≤ <i>l</i> ≤ 28
Reflections collected	60882
Independent reflections	12189 [ <i>R</i> <sub>int</sub> = 0.0558]
Data / Restraints / Parameters	12189 / 0 / 430
Goodness-of-fit on <i>F</i> <sup>2</sup>	1.036
Final <i>R</i> indexes [ <i>I</i> ≥ 2 $\sigma$ ( <i>I</i> )]	<i>R</i> <sub>1</sub> = 0.0289 <i>wR</i> <sub>2</sub> = 0.0637
Final <i>R</i> indexes [all data]	<i>R</i> <sub>1</sub> = 0.0323 <i>wR</i> <sub>2</sub> = 0.0651
Largest peak/hole [eÅ <sup>-3</sup> ]	1.93/-2.05

Table 2. Atomic coordinates and  $U_{eq}$  [ $\text{\AA}^2$ ] for mo\_harman\_3\_jkh\_045\_x2\_0m

Atom	x	y	z	$U_{eq}$
W1	0.39865(2)	0.56046(2)	0.76193(2)	0.00948(3)
P1	0.26289(8)	0.45038(6)	0.68451(3)	0.01271(10)
O1	0.1444(2)	0.51163(18)	0.90971(11)	0.0207(4)
N1	0.5642(3)	0.63620(18)	0.64754(11)	0.0134(3)
N2	0.5529(3)	0.75484(18)	0.61205(11)	0.0129(3)
N3	0.2085(2)	0.68883(18)	0.72148(12)	0.0129(3)
N4	0.2477(3)	0.79588(18)	0.67067(12)	0.0136(3)
N5	0.4652(3)	0.72941(18)	0.78440(11)	0.0130(3)
N6	0.4838(3)	0.83386(18)	0.72910(11)	0.0134(3)
N7	0.2493(2)	0.52372(18)	0.85082(11)	0.0126(3)
C1	0.6884(3)	0.5897(2)	0.60104(13)	0.0149(4)
H1	0.723730	0.508393	0.611155	0.018
C2	0.7574(3)	0.6776(2)	0.53618(14)	0.0175(4)
H2	0.846163	0.668888	0.494627	0.021
C3	0.6679(3)	0.7805(2)	0.54567(13)	0.0164(4)
H3	0.685053	0.857020	0.510855	0.020
C4	0.0368(3)	0.6832(2)	0.74244(14)	0.0156(4)
H4	-0.025804	0.617994	0.778103	0.019
C5	-0.0367(3)	0.7864(2)	0.70453(16)	0.0199(5)
H5	-0.155784	0.804880	0.708014	0.024
C6	0.1010(3)	0.8564(2)	0.66067(15)	0.0176(4)
H6	0.093647	0.934302	0.628713	0.021
C7	0.4833(3)	0.7560(2)	0.84928(14)	0.0172(4)
H7	0.473963	0.700166	0.897570	0.021
C8	0.5178(4)	0.8775(2)	0.83552(15)	0.0214(5)
H8	0.538589	0.919267	0.871101	0.026

C9	0.5154(3)	0.9237(2)	0.75921(15) )	0.0175(4)
H9	0.532954	1.005116	0.732237	0.021
C10	0.0696(3)	0.3678(2)	0.73793(16) )	0.0193(5)
H10A	0.101429	0.288296	0.765515	0.029
H10B	−0.003287	0.359782	0.702494	0.029
H10C	0.006200	0.410888	0.774619	0.029
C11	0.3923(3)	0.3446(2)	0.63817(15) )	0.0184(5)
H11A	0.481675	0.387751	0.596619	0.028
H11B	0.318361	0.301498	0.617249	0.028
H11C	0.446397	0.287416	0.675693	0.028
C12	0.1968(4)	0.5513(3)	0.60217(16) )	0.0222(5)
H12A	0.102983	0.602564	0.619730	0.033
H12B	0.156973	0.504661	0.571279	0.033
H12C	0.294709	0.601020	0.571127	0.033
C13	0.6029(3)	0.4108(2)	0.77526(13) )	0.0132(4)
H13	0.646(5)	0.406(3)	0.725(2)	0.020(8)
C14	0.6536(3)	0.5087(2)	0.80043(14) )	0.0142(4)
H14	0.738(4)	0.560(3)	0.7625(19)	0.016(8)
C15	0.6786(3)	0.4991(2)	0.87915(14) )	0.0173(4)
H15	0.673557	0.571470	0.895065	0.021
C16	0.7075(3)	0.3987(3)	0.93033(15) )	0.0187(5)
H16	0.723971	0.406717	0.978479	0.022
C17	0.7162(3)	0.2747(2)	0.91808(15) )	0.0178(4)
H17A	0.789573	0.224865	0.951384	0.021
H17B	0.772766	0.278688	0.864345	0.021
C18	0.5401(3)	0.2129(2)	0.93464(14) )	0.0163(4)
H18A	0.555240	0.140676	0.914297	0.020
H18B	0.499619	0.186485	0.990759	0.020
C19	0.4014(3)	0.2923(2)	0.89998(13) )	0.0131(4)
H19	0.379275	0.362711	0.922962	0.016
C20	0.4664(3)	0.3355(2)	0.81440(13) )	0.0134(4)
H20	0.434097	0.282157	0.784313	0.016
C21	0.2319(3)	0.2235(2)	0.91394(14) )	0.0155(4)
H21A	0.146885	0.278743	0.890770	0.019

H21B	0.253523	0.158649	0.886880	0.019
C22	0.1533(3)	0.1695(2)	0.99670(14)	0.0149(4)
C23	0.1779(4)	0.0497(2)	1.03063(15)	0.0214(5)
H23	0.247472	0.001140	1.001634	0.026
C24	0.1020(4)	0.0003(3)	1.10620(16)	0.0239(5)
H24	0.122240	-0.081247	1.128994	0.029
C25	-0.0028(4)	0.0690(3)	1.14856(16)	0.0251(6)
H25	-0.055855	0.034740	1.200215	0.030
C26	-0.0299(4)	0.1878(3)	1.11528(16)	0.0249(5)
H26	-0.103299	0.234956	1.144057	0.030
C27	0.0491(3)	0.2390(2)	1.04012(15)	0.0195(5)
H27	0.032281	0.321400	1.018250	0.023
B1	0.4354(3)	0.8405(2)	0.65114(15)	0.0142(4)
H1A	0.443(4)	0.929(3)	0.6141(17)	0.009(7)
S1	0.13727(8)	0.79731(5)	0.36543(3)	0.01447(10)
F1	0.0926(3)	0.8437(2)	0.50007(10)	0.0352(5)
F2	0.3580(2)	0.83239(18)	0.44651(12)	0.0333(4)
F3	0.2085(2)	0.98725(15)	0.40721(11)	0.0253(3)
O2	0.1369(3)	0.67140(17)	0.40328(11)	0.0200(4)
O3	-0.0306(3)	0.84763(19)	0.35990(12)	0.0232(4)
O4	0.2701(3)	0.83138(19)	0.29801(11)	0.0234(4)
C28	0.2027(3)	0.8686(2)	0.43331(15)	0.0187(5)

$U_{eq}$  is defined as 1/3 of the trace of the orthogonalized  $U_{ij}$  tensor.

**Table 3. Anisotropic displacement parameters ( $\text{\AA}^2$ ) for mo\_harman\_3\_jkh\_045\_x2\_0m. The anisotropic displacement factor exponent takes the form:  $-2\pi^2[ h^2(a^*)^2U_{11} + k^2(b^*)^2U_{22} + \dots + 2hka^*b^*U_{12} ]$**

Atom	$U_{11}$	$U_{22}$	$U_{33}$	$U_{23}$	$U_{13}$	$U_{12}$
------	----------	----------	----------	----------	----------	----------



W1	0.00500(4)	0.00997(4)	0.01193(4)	-0.00224(3)	0.00140(2)	-0.00080(3)
P1	0.0095(2)	0.0140(3)	0.0148(2)	-0.0045(2)	-0.00172(19)	0.0004(2)
O1	0.0175(8)	0.0212(9)	0.0171(8)	-0.0035(7)	0.0090(7)	0.0008(7)
N1	0.0100(8)	0.0120(9)	0.0160(8)	-0.0018(7)	0.0002(6)	0.0006(7)
N2	0.0113(8)	0.0123(9)	0.0127(8)	-0.0012(7)	0.0013(6)	-0.0010(7)
N3	0.0074(8)	0.0120(8)	0.0185(9)	-0.0038(7)	-0.0007(6)	0.0003(6)
N4	0.0110(8)	0.0117(8)	0.0165(8)	-0.0019(7)	-0.0014(7)	0.0014(7)
N5	0.0104(8)	0.0112(8)	0.0153(8)	-0.0023(7)	0.0009(6)	-0.0011(7)
N6	0.0118(8)	0.0121(9)	0.0147(8)	-0.0022(7)	0.0004(7)	-0.0023(7)
N7	0.0080(8)	0.0116(8)	0.0151(8)	-0.0033(7)	0.0047(6)	-0.0007(6)
C1	0.0113(9)	0.0171(11)	0.0152(9)	-0.0056(8)	0.0018(7)	0.0012(8)
C2	0.0146(10)	0.0203(12)	0.0142(9)	-0.0038(9)	0.0046(8)	-0.0014(9)
C3	0.0162(10)	0.0164(11)	0.0131(9)	-0.0010(8)	0.0025(8)	-0.0035(9)
C4	0.0075(9)	0.0163(11)	0.0223(11)	-0.0049(9)	-0.0009(8)	0.0000(8)
C5	0.0113(10)	0.0225(12)	0.0268(12)	-0.0083(10)	-0.0041(9)	0.0051(9)
C6	0.0142(10)	0.0170(11)	0.0215(11)	-0.0052(9)	-0.0039(8)	0.0055(9)
C7	0.0176(11)	0.0175(11)	0.0162(10)	-0.0057(9)	-0.0002(8)	-0.0027(9)
C8	0.0256(13)	0.0189(12)	0.0202(11)	-0.0083(9)	0.0001(9)	-0.0055(10)
C9	0.0172(11)	0.0135(10)	0.0208(11)	-0.0060(9)	0.0023(8)	-0.0059(8)
C10	0.0119(10)	0.0212(12)	0.0261(12)	-0.0083(10)	-0.0020(9)	-0.0046(9)
C11	0.0187(11)	0.0201(12)	0.0189(10)	-0.0100(9)	-0.0037(9)	0.0044(9)
C12	0.0253(13)	0.0217(12)	0.0214(11)	-0.0058(10)	-0.0094(10)	0.0039(10)
C13	0.0075(8)	0.0154(10)	0.0143(9)	-0.0020(8)	0.0007(7)	0.0020(8)
C14	0.0076(9)	0.0152(10)	0.0178(10)	-0.0017(8)	-0.0004(7)	-0.0010(8)
C15	0.0108(9)	0.0200(12)	0.0205(10)	-0.0032(9)	-0.0035(8)	-0.0031(8)
C16	0.0130(10)	0.0235(12)	0.0181(10)	-0.0021(9)	-0.0028(8)	-0.0027(9)
C17	0.0107(9)	0.0192(11)	0.0213(11)	-0.0007(9)	-0.0035(8)	0.0002(8)
C18	0.0129(10)	0.0147(10)	0.0183(10)	0.0004(8)	-0.0019(8)	-0.0003(8)
C19	0.0090(9)	0.0146(10)	0.0135(9)	-0.0014(8)	0.0001(7)	-0.0014(8)
C20	0.0107(9)	0.0106(9)	0.0166(9)	-0.0008(8)	-0.0008(7)	0.0004(7)
C21	0.0117(9)	0.0166(11)	0.0163(10)	-0.0020(8)	-0.0001(8)	-0.0030(8)
C22	0.0096(9)	0.0169(11)	0.0169(10)	-0.0037(8)	0.0001(7)	-0.0020(8)
C23	0.0203(12)	0.0165(11)	0.0214(11)	-0.0029(9)	0.0071(9)	-0.0002(9)
C24	0.0246(13)	0.0180(12)	0.0229(12)	-0.0007(10)	0.0049(10)	-0.0021(10)
C25	0.0224(13)	0.0306(15)	0.0180(11)	-0.0046(10)	0.0046(9)	-0.0016(11)
C26	0.0236(13)	0.0286(14)	0.0224(12)	-0.0123(11)	0.0019(10)	0.0044(11)
C27	0.0182(11)	0.0191(12)	0.0201(11)	-0.0059(9)	-0.0006(9)	0.0027(9)
B1	0.0116(10)	0.0129(11)	0.0154(10)	-0.0017(9)	0.0010(8)	0.0001(9)
S1	0.0125(2)	0.0123(2)	0.0174(2)	-0.0039(2)	0.00029(19)	-0.00075(19)

F1	0.0386(11)	0.0455(12)	0.0206(8)	-0.0142(8)	0.0077(7)	-0.0146(9)
F2	0.0247(9)	0.0356(11)	0.0488(12)	-0.0176(9)	-0.0209(8)	0.0074(8)
F3	0.0252(8)	0.0162(7)	0.0366(9)	-0.0100(7)	-0.0061(7)	-0.0020(6)
O2	0.0218(9)	0.0126(8)	0.0231(9)	-0.0026(7)	-0.0009(7)	-0.0006(7)
O3	0.0159(9)	0.0217(10)	0.0341(10)	-0.0093(8)	-0.0076(8)	0.0032(7)
O4	0.0254(10)	0.0218(9)	0.0201(9)	-0.0065(7)	0.0052(7)	-0.0058(8)
C28	0.0168(11)	0.0190(11)	0.0201(11)	-0.0070(9)	-0.0005(9)	-0.0002(9)

Table 4. Bond lengths and angles for mo\_harman\_3\_jkh\_045\_x2\_0m

Atom-Atom	Length [Å]		
W1-P1	2.5502(6)	C8-C9	1.376(4)
W1-N1	2.233(2)	C9-H9	0.9500
W1-N3	2.168(2)	C10-H10A	0.9800
W1-N5	2.207(2)	C10-H10B	0.9800
W1-N7	1.7807(19)	C10-H10C	0.9800
W1-C13	2.309(2)	C11-H11A	0.9800
W1-C14	2.280(2)	C11-H11B	0.9800
W1-C20	2.605(2)	C11-H11C	0.9800
P1-C10	1.815(3)	C12-H12A	0.9800
P1-C11	1.820(2)	C12-H12B	0.9800
P1-C12	1.819(3)	C12-H12C	0.9800
O1-N7	1.206(2)	C13-H13	0.94(3)
N1-N2	1.369(3)	C13-C14	1.431(3)
N1-C1	1.350(3)	C13-C20	1.383(3)
N2-C3	1.343(3)	C14-H14	0.97(3)
N2-B1	1.534(3)	C14-C15	1.480(3)
N3-N4	1.357(3)	C15-H15	0.9500
N3-C4	1.338(3)	C15-C16	1.341(4)
N4-C6	1.347(3)	C16-H16	0.9500
N4-B1	1.543(3)	C16-C17	1.502(4)
N5-N6	1.362(3)	C17-H17A	0.9900
N5-C7	1.343(3)	C17-H17B	0.9900
N6-C9	1.350(3)	C17-C18	1.542(3)
N6-B1	1.544(3)	C18-H18A	0.9900
C1-H1	0.9500	C18-H18B	0.9900
C1-C2	1.392(3)	C18-C19	1.532(3)
C2-H2	0.9500	C19-H19	1.0000
C2-C3	1.383(4)	C19-C20	1.516(3)
C3-H3	0.9500	C19-C21	1.541(3)
C4-H4	0.9500	C20-H20	1.0000
C4-C5	1.387(4)	C21-H21A	0.9900
C5-H5	0.9500	C21-H21B	0.9900
C5-C6	1.379(4)	C21-C22	1.508(3)
C6-H6	0.9500	C22-C23	1.390(4)
C7-H7	0.9500	C22-C27	1.396(3)
C7-C8	1.394(4)	C23-H23	0.9500
C8-H8	0.9500	C23-C24	1.385(4)
		C24-H24	0.9500

C24–C25	1.381(4)
C25–H25	0.9500
C25–C26	1.381(4)
C26–H26	0.9500
C26–C27	1.389(4)
C27–H27	0.9500
B1–H1A	1.07(3)
S1–O2	1.447(2)
S1–O3	1.438(2)
S1–O4	1.438(2)
S1–C28	1.828(3)
F1–C28	1.328(3)
F2–C28	1.330(3)
F3–C28	1.334(3)
Atom–Atom– Atom	Angle [°]
P1–W1–C20	75.02(6)
N1–W1–P1	82.13(6)
N1–W1–C13	85.68(8)
N1–W1–C14	84.59(8)
N1–W1–C20	111.61(7)
N3–W1–P1	78.22(6)
N3–W1–N1	85.01(7)
N3–W1–N5	74.75(7)
N3–W1–C13	165.05(8)
N3–W1–C14	153.19(8)
N3–W1–C20	145.83(7)
N5–W1–P1	149.95(6)
N5–W1–N1	82.67(7)
N5–W1–C13	115.56(8)
N5–W1–C14	79.45(8)
N5–W1–C20	134.89(8)
N7–W1–P1	100.18(7)
N7–W1–N1	170.45(8)
N7–W1–N3	86.40(8)
N7–W1–N5	91.07(8)
N7–W1–C13	103.57(9)
N7–W1–C14	101.40(9)
N7–W1–C20	77.91(8)
C13–W1–P1	88.94(6)
C13–W1–C20	31.98(7)
C14–W1–P1	124.50(6)
C14–W1–C13	36.33(9)
C14–W1–C20	60.75(8)
C10–P1–W1	113.97(9)
C10–P1–C11	104.39(13)
C10–P1–C12	104.81(13)

C11–P1–W1	119.29(9)
C12–P1–W1	112.43(10)
C12–P1–C11	100.17(13)
N2–N1–W1	120.28(14)
C1–N1–W1	133.52(17)
C1–N1–N2	106.17(19)
N1–N2–B1	121.44(19)
C3–N2–N1	109.67(19)
C3–N2–B1	128.6(2)
N4–N3–W1	124.15(15)
C4–N3–W1	128.73(17)
C4–N3–N4	107.1(2)
N3–N4–B1	118.53(19)
C6–N4–N3	109.2(2)
C6–N4–B1	130.1(2)
N6–N5–W1	121.95(15)
C7–N5–W1	131.32(17)
C7–N5–N6	106.6(2)
N5–N6–B1	120.11(19)
C9–N6–N5	109.6(2)
C9–N6–B1	129.1(2)
O1–N7–W1	173.05(19)
N1–C1–H1	124.7
N1–C1–C2	110.5(2)
C2–C1–H1	124.7
C1–C2–H2	127.7
C3–C2–C1	104.7(2)
C3–C2–H2	127.7
N2–C3–C2	109.0(2)
N2–C3–H3	125.5
C2–C3–H3	125.5
N3–C4–H4	124.9
N3–C4–C5	110.2(2)
C5–C4–H4	124.9
C4–C5–H5	127.6
C6–C5–C4	104.9(2)
C6–C5–H5	127.6
N4–C6–C5	108.7(2)
N4–C6–H6	125.7
C5–C6–H6	125.7
N5–C7–H7	124.9
N5–C7–C8	110.2(2)
C8–C7–H7	124.9
C7–C8–H8	127.5
C9–C8–C7	105.0(2)
C9–C8–H8	127.5
N6–C9–C8	108.6(2)
N6–C9–H9	125.7

C8–C9–H9	125.7
P1–C10–H10A	109.5
P1–C10–H10B	109.5
P1–C10–H10C	109.5
H10A–C10–H10B	109.5
H10A–C10–H10C	109.5
H10B–C10–H10C	109.5
P1–C11–H11A	109.5
P1–C11–H11B	109.5
P1–C11–H11C	109.5
H11A–C11–H11B	109.5
H11A–C11–H11C	109.5
H11B–C11–H11C	109.5
P1–C12–H12A	109.5
P1–C12–H12B	109.5
P1–C12–H12C	109.5
H12A–C12–H12B	109.5
H12A–C12–H12C	109.5
H12B–C12–H12C	109.5
W1–C13–H13	103(2)
C14–C13–W1	70.73(13)
C14–C13–H13	119(2)
C20–C13–W1	85.88(14)
C20–C13–H13	115(2)
C20–C13–C14	124.1(2)
W1–C14–H14	105(2)
C13–C14–W1	72.94(13)
C13–C14–H14	113(2)
C13–C14–C15	123.7(2)
C15–C14–W1	123.69(16)
C15–C14–H14	112(2)
C14–C15–H15	116.7
C16–C15–C14	126.7(2)
C16–C15–H15	116.7
C15–C16–H16	117.2
C15–C16–C17	125.6(2)
C17–C16–H16	117.2
C16–C17–H17A	108.6
C16–C17–H17B	108.6
C16–C17–C18	114.6(2)
H17A–C17–H17B	107.6
C18–C17–H17A	108.6

C18–C17–H17B	108.6
C17–C18–H18A	108.8
C17–C18–H18B	108.8
H18A–C18–H18B	107.7
C19–C18–C17	114.0(2)
C19–C18–H18A	108.8
C19–C18–H18B	108.8
C18–C19–H19	109.4
C18–C19–C21	111.7(2)
C20–C19–C18	108.50(19)
C20–C19–H19	109.4
C20–C19–C21	108.53(19)
C21–C19–H19	109.4
W1–C20–H20	113.7
C13–C20–W1	62.15(13)
C13–C20–C19	129.0(2)
C13–C20–H20	113.7
C19–C20–W1	112.62(15)
C19–C20–H20	113.7
C19–C21–H21A	108.4
C19–C21–H21B	108.4
H21A–C21–H21B	107.5
C22–C21–C19	115.4(2)
C22–C21–H21A	108.4
C22–C21–H21B	108.4
C23–C22–C21	121.2(2)
C23–C22–C27	118.7(2)
C27–C22–C21	120.1(2)
C22–C23–H23	119.6
C24–C23–C22	120.8(2)
C24–C23–H23	119.6
C23–C24–H24	119.8
C25–C24–C23	120.3(3)
C25–C24–H24	119.8
C24–C25–H25	120.3
C24–C25–C26	119.5(3)
C26–C25–H25	120.3
C25–C26–H26	119.7
C25–C26–C27	120.6(3)
C27–C26–H26	119.7
C22–C27–H27	120.0
C26–C27–C22	120.1(3)
C26–C27–H27	120.0
N2–B1–N4	109.5(2)
N2–B1–N6	108.4(2)
N2–B1–H1A	110.4(16)
N4–B1–N6	105.21(18)

N4–B1–H1A	109.2(17)
N6–B1–H1A	113.8(16)
O2–S1–C28	103.33(12)
O3–S1–O2	114.48(12)
O3–S1–O4	116.36(13)
O3–S1–C28	102.57(12)
O4–S1–O2	114.05(12)
O4–S1–C28	103.64(12)

F1–C28–S1	111.07(19)
F1–C28–F2	107.6(2)
F1–C28–F3	107.5(2)
F2–C28–S1	111.76(18)
F2–C28–F3	107.4(2)
F3–C28–S1	111.30(18)

Table 5. Torsion angles for mo\_harman\_3\_jkh\_045\_x2\_0m

Atom–Atom– Atom–Atom	Torsion Angle [°]
W1–N1–N2–C3	177.95(16)
W1–N1–N2–B1	3.6(3)
W1–N1–C1–C2	–177.67(18)
W1–N3–N4–C6	–176.90(16)
W1–N3–N4–B1	–11.7(3)
W1–N3–C4–C5	177.80(17)
W1–N5–N6–C9	176.80(16)
W1–N5–N6–B1	8.0(3)
W1–N5–C7–C8	–176.89(18)
W1–C13–C14–C15	119.5(2)
W1–C13–C20–C19	–97.6(2)
W1–C14–C15–C16	111.8(3)
N1–N2–C3–C2	0.3(3)
N1–N2–B1–N4	–58.8(3)
N1–N2–B1–N6	55.5(3)
N1–C1–C2–C3	–0.1(3)
N2–N1–C1–C2	0.3(3)
N3–N4–C6–C5	–1.3(3)
N3–N4–B1–N2	63.6(3)
N3–N4–B1–N6	–52.7(3)
N3–C4–C5–C6	–1.4(3)
N4–N3–C4–C5	0.7(3)
N5–N6–C9–C8	0.1(3)
N5–N6–B1–N2	–62.7(3)
N5–N6–B1–N4	54.4(3)
N5–C7–C8–C9	1.5(3)
N6–N5–C7–C8	–1.4(3)
C1–N1–N2–C3	–0.3(3)
C1–N1–N2–B1	–174.7(2)
C1–C2–C3–N2	–0.1(3)
C3–N2–B1–N4	128.0(3)
C3–N2–B1–N6	–117.6(3)
C4–N3–N4–C6	0.4(3)
C4–N3–N4–B1	165.6(2)
C4–C5–C6–N4	1.6(3)

C6–N4–B1–N2	–134.8(2)
C6–N4–B1–N6	108.9(3)
C7–N5–N6–C9	0.8(3)
C7–N5–N6–B1	–168.0(2)
C7–C8–C9–N6	–0.9(3)
C9–N6–B1–N2	131.0(2)
C9–N6–B1–N4	–111.9(3)
C13–C14–C15–C16	20.6(4)
C14–C13–C20–W1	63.4(2)
C14–C13–C20–C19	–34.2(4)
C14–C15–C16–C17	–1.5(4)
C15–C16–C17–C18	–84.6(3)
C16–C17–C18–C19	46.0(3)
C17–C18–C19–C20	56.8(3)
C17–C18–C19–C21	176.4(2)
C18–C19–C20–W1	–137.56(16)
C18–C19–C20–C13	–65.9(3)
C18–C19–C21–C22	57.9(3)
C19–C21–C22–C23	–98.2(3)
C19–C21–C22–C27	83.9(3)
C20–C13–C14–W1	–70.8(2)
C20–C13–C14–C15	48.7(3)
C20–C19–C21–C22	177.5(2)
C21–C19–C20–W1	100.91(18)
C21–C19–C20–C13	172.6(2)
C21–C22–C23–C24	–178.6(3)
C21–C22–C27–C26	176.9(2)
C22–C23–C24–C25	1.5(5)
C23–C22–C27–C26	–1.0(4)
C23–C24–C25–C26	–0.8(5)
C24–C25–C26–C27	–0.9(5)
C25–C26–C27–C22	1.8(4)
C27–C22–C23–C24	–0.6(4)
B1–N2–C3–C2	174.1(2)
B1–N4–C6–C5	–164.2(2)
B1–N6–C9–C8	167.6(2)
O2–S1–C28–F1	–59.8(2)

O2–S1–C28–F2	60.4(2)
O2–S1–C28–F3	–179.52(18)
O3–S1–C28–F1	59.5(2)
O3–S1–C28–F2	179.7(2)
O3–S1–C28–F3	–60.2(2)
O4–S1–C28–F1	–179.0(2)

O4–S1–C28–F2	–58.8(2)
O4–S1–C28–F3	61.2(2)

## Structure Report for mo\_harman\_mne\_nb4\_025\_0m

A yellow, block-shaped crystal of mo\_harman\_mne\_nb4\_025\_0m was coated with Paratone oil and mounted on a MiTeGen micromount. acetonitrile. Data were collected at 100.00 K on a Bruker D8 VENTURE dual wavelength Mo/Cu Kappa four-circle diffractometer with a PHOTON III\_C14 detector. The diffractometer was equipped with an Oxford Cryostream 800 low temperature device and used Mo  $K_\alpha$  radiation ( $\lambda = 0.71073\text{\AA}$ ) from an Incoatec I\ms 3.0 microfocus sealed tube with a HELIOS double bounce multilayer mirror as monochromator.

Data collection and processing were done within the Bruker APEX6 software suite.<sup>[1]</sup> All data were integrated with SAINT 8.41 using a narrow-frame algorithm and a Multi-Scan absorption correction using SADABS 2016/2 was applied.<sup>[2]</sup> Using Olex2 as a graphical interface,<sup>[3]</sup> the structure was solved by dual methods with SHELXT 2018/2 and refined by full-matrix least-squares methods against  $F^2$  using XL.<sup>[4,5]</sup> All non-hydrogen atoms were refined with anisotropic displacement parameters. All C-bound hydrogen atoms were refined with isotropic displacement parameters. Some of their coordinates were refined freely and some on calculated positions using a riding model with their  $U_{\text{iso}}$  values constrained to 1.5 times the  $U_{\text{eq}}$  of their pivot atoms for terminal  $\text{sp}^3$  carbon atoms and 1.2 times for all other carbon atoms.

This report and the CIF file were generated using FinalCif.<sup>[6]</sup>

Table 1. Crystal data and structure refinement for mo\_harman\_mne\_nb4\_025\_0m

CCDC number	
Empirical formula	C <sub>24</sub> H <sub>32</sub> BF <sub>3</sub> N <sub>9</sub> O <sub>4</sub> PSW
Formula weight	825.27
Temperature [K]	100.00
Crystal system	monoclinic
Space group (number)	<i>P</i> 2 <sub>1</sub> / <i>n</i> (14)
<i>a</i> [Å]	10.4651(4)
<i>b</i> [Å]	16.3619(5)
<i>c</i> [Å]	18.5495(7)
$\alpha$ [°]	90
$\beta$ [°]	99.7830(10)
$\gamma$ [°]	90
Volume [Å <sup>3</sup> ]	3130.02(19)
<i>Z</i>	4
$\rho_{\text{calc}}$ [gcm <sup>-3</sup> ]	1.751
$\mu$ [mm <sup>-1</sup> ]	3.873
<i>F</i> (000)	1632
Crystal size [mm <sup>3</sup> ]	0.033×0.035×0.055
Crystal colour	yellow
Crystal shape	block
Radiation	Mo <i>K</i> $\alpha$ ( $\lambda$ =0.71073 Å)
2 $\theta$ range [°]	4.19 to 54.23 (0.78 Å)
Index ranges	−13 ≤ <i>h</i> ≤ 13 −19 ≤ <i>k</i> ≤ 20 −23 ≤ <i>l</i> ≤ 23
Reflections collected	41515
Independent reflections	6901 <i>R</i> <sub>int</sub> = 0.0950 <i>R</i> <sub>sigma</sub> = 0.0688
Completeness to $\theta = 25.242^\circ$	100.0
Data / Restraints / Parameters	6901 / 0 / 409
Goodness-of-fit on <i>F</i> <sup>2</sup>	1.007
Final <i>R</i> indexes [ $\geq 2\sigma(I)$ ]	<i>R</i> <sub>1</sub> = 0.0358 <i>wR</i> <sub>2</sub> = 0.0653
Final <i>R</i> indexes [all data]	<i>R</i> <sub>1</sub> = 0.0657 <i>wR</i> <sub>2</sub> = 0.0741
Largest peak/hole [eÅ <sup>-3</sup> ]	0.88/−0.84

Table 2. Atomic coordinates and  $U_{eq}$  [ $\text{\AA}^2$ ] for mo\_harman\_mne\_nb4\_025\_0m

Atom	x	y	z	$U_{eq}$
W1	0.32325(2)	0.58272(2)	0.83567(2)	0.01472(6)
P1	0.14376(14) )	0.52858(8)	0.73586(8)	0.0205(3)
O1	0.2900(4)	0.7482(2)	0.76887(19) )	0.0284(9)
N1	0.3491(4)	0.4516(2)	0.8667(2)	0.0212(10)
N2	0.4532(4)	0.4097(2)	0.8519(2)	0.0202(9)
N3	0.4236(4)	0.5547(2)	0.7458(2)	0.0177(9)
N4	0.5127(4)	0.4923(2)	0.7497(2)	0.0215(10)
N5	0.5299(4)	0.5892(2)	0.8835(2)	0.0172(9)
N6	0.6127(4)	0.5264(2)	0.8748(2)	0.0192(9)
N7	0.3029(4)	0.6826(2)	0.7988(2)	0.0195(9)
N8	0.0496(5)	0.6134(3)	1.0675(3)	0.0333(12)
C1	0.2721(5)	0.3965(3)	0.8919(3)	0.0202(11)
H1	0.191440	0.408689	0.906392	0.024
C2	0.3268(6)	0.3200(3)	0.8936(3)	0.0268(13)
H2	0.292249	0.270500	0.908820	0.032
C3	0.4417(5)	0.3302(3)	0.8687(3)	0.0234(12)
H3	0.502798	0.288414	0.864048	0.028
C4	0.4243(5)	0.5928(3)	0.6826(3)	0.0213(11)
H4	0.372637	0.639096	0.666184	0.026
C5	0.5102(5)	0.5561(3)	0.6439(3)	0.0261(13)
H5	0.527609	0.570686	0.596977	0.031
C6	0.5650(6)	0.4937(3)	0.6882(3)	0.0288(13)
H6	0.629709	0.457296	0.677238	0.035
C7	0.6039(5)	0.6511(3)	0.9136(3)	0.0225(12)
H7	0.572535	0.703056	0.925288	0.027
C8	0.7329(6)	0.6281(3)	0.9251(3)	0.0297(13)
H8	0.805295	0.660191	0.946254	0.036
C9	0.7350(5)	0.5499(3)	0.8998(3)	0.0223(12)
H9	0.810375	0.517517	0.899962	0.027
C10	0.1359(5)	0.5904(3)	0.8886(3)	0.0228(11)
H10	0.084(5)	0.544(3)	0.890(3)	0.034(16)
C11	0.2436(5)	0.5918(3)	0.9453(3)	0.0191(11)
H11	0.275(4)	0.545(3)	0.969(2)	0.009(12)
C12	0.3322(5)	0.6544(3)	0.9589(3)	0.0234(12)
H12	0.410719	0.640021	0.995390	0.028
C13	0.3093(5)	0.7452(3)	0.9508(3)	0.0280(13)
H13A	0.270885	0.757593	0.899399	0.034
H13B	0.393341	0.774170	0.962124	0.034
C14	0.2180(6)	0.7769(3)	1.0017(3)	0.0309(14)
H14A	0.211620	0.837086	0.997100	0.037



H14B	0.256967	0.764186	1.052943	0.037
C15	0.0793(5)	0.7402(3)	0.9858(3)	0.0298(13)
H15	0.021036	0.782587	1.001538	0.036
C16	0.0305(5)	0.7261(3)	0.9058(3)	0.0283(13)
H16	-0.024669	0.767318	0.881502	0.034
C17	0.0548(5)	0.6630(3)	0.8647(3)	0.0257(12)
H17	0.015881	0.664774	0.814527	0.031
C18	0.0659(5)	0.6670(3)	1.0311(3)	0.0255(12)
C19	-0.0086(6)	0.4891(3)	0.7575(3)	0.0328(14)
H19A	-0.058285	0.534053	0.774078	0.049
H19B	0.009937	0.448031	0.796338	0.049
H19C	-0.059028	0.464060	0.713746	0.049
C20	0.1974(6)	0.4403(3)	0.6884(3)	0.0269(13)
H20A	0.125524	0.420552	0.651620	0.040
H20B	0.225428	0.396712	0.723774	0.040
H20C	0.269941	0.456314	0.664270	0.040
C21	0.0883(5)	0.6036(3)	0.6653(3)	0.0235(12)
H21A	0.019900	0.579559	0.628774	0.035
H21B	0.161066	0.620165	0.641544	0.035
H21C	0.054087	0.651477	0.687349	0.035
B1	0.5652(6)	0.4534(3)	0.8240(3)	0.0225(14)
H1A	0.637844	0.414757	0.820324	0.027
S1	0.22483(14) )	0.63089(8)	0.45591(8)	0.0228(3)
F1	0.1634(4)	0.4988(2)	0.5223(2)	0.0537(11)
F2	0.1898(3)	0.47947(17) )	0.41160(17) )	0.0340(8)
F3	0.3530(3)	0.49669(19) )	0.49540(18) )	0.0405(9)
O2	0.0883(4)	0.6467(2)	0.4394(3)	0.0496(12)
O3	0.2895(4)	0.6646(2)	0.5232(2)	0.0425(11)
O4	0.2912(4)	0.6403(2)	0.3953(2)	0.0373(10)
C22	0.2315(6)	0.5206(3)	0.4722(3)	0.0268(13)
N9	0.3225(6)	0.7875(4)	0.2067(3)	0.0530(16)
C23	0.1146(6)	0.7329(4)	0.2487(3)	0.0372(15)
H23A	0.062133	0.704179	0.207680	0.056
H23B	0.064589	0.778495	0.263989	0.056
H23C	0.138277	0.695060	0.289721	0.056
C24	0.2320(7)	0.7644(4)	0.2260(3)	0.0359(15)

$U_{eq}$  is defined as 1/3 of the trace of the orthogonalized  $U_{ij}$  tensor.

Table 3. Anisotropic displacement parameters ( $\text{\AA}^2$ ) for mo\_harman\_mne\_nb4\_025\_0m. The anisotropic displacement factor exponent takes the form:

$$-2\pi^2 [ h^2(a^*)^2 U_{11} + k^2(b^*)^2 U_{22} + \dots + 2hka^*b^* U_{12} ]$$

Atom	$U_{11}$	$U_{22}$	$U_{33}$	$U_{23}$	$U_{13}$	$U_{12}$
------	----------	----------	----------	----------	----------	----------

W1	0.01743(10)	0.01204(9)	0.01443(10)	0.00025(9)	0.00194(7)	0.00061(10)
P1	0.0223(8)	0.0179(6)	0.0195(7)	0.0034(5)	-0.0011(6)	-0.0044(6)
O1	0.042(2)	0.0163(17)	0.025(2)	0.0082(16)	0.0022(18)	0.0011(18)
N1	0.026(3)	0.017(2)	0.019(2)	0.0030(18)	0.0003(19)	0.0020(19)
N2	0.027(2)	0.0124(19)	0.022(2)	-0.0012(18)	0.0053(18)	0.0017(19)
N3	0.021(2)	0.0139(19)	0.018(2)	0.0002(17)	0.0002(18)	0.0001(17)
N4	0.025(3)	0.023(2)	0.018(2)	-0.0016(18)	0.0062(19)	0.0060(19)
N5	0.020(2)	0.017(2)	0.014(2)	0.0001(18)	0.0020(16)	0.0032(19)
N6	0.017(2)	0.022(2)	0.019(2)	0.0022(18)	0.0027(18)	0.0024(18)
N7	0.021(2)	0.021(2)	0.016(2)	-0.0010(18)	0.0021(18)	0.0006(19)
N8	0.034(3)	0.039(3)	0.028(3)	-0.001(2)	0.010(2)	0.005(2)
C1	0.026(3)	0.024(3)	0.012(3)	-0.001(2)	0.005(2)	-0.003(2)
C2	0.041(4)	0.024(3)	0.014(3)	0.001(2)	0.000(2)	-0.005(3)
C3	0.030(3)	0.015(2)	0.022(3)	-0.003(2)	-0.004(2)	0.004(2)
C4	0.019(3)	0.023(3)	0.020(3)	0.000(2)	-0.001(2)	-0.001(2)
C5	0.025(3)	0.038(3)	0.017(3)	-0.002(2)	0.007(2)	-0.002(2)
C6	0.030(3)	0.033(3)	0.025(3)	-0.008(3)	0.009(3)	0.000(3)
C7	0.021(3)	0.023(3)	0.022(3)	-0.001(2)	0.000(2)	-0.007(2)
C8	0.025(3)	0.037(3)	0.027(3)	-0.002(3)	0.005(3)	-0.007(3)
C9	0.014(3)	0.034(3)	0.017(3)	0.008(2)	0.000(2)	-0.001(2)
C10	0.023(3)	0.019(3)	0.027(3)	0.002(2)	0.006(2)	0.002(2)
C11	0.025(3)	0.020(3)	0.015(3)	0.000(2)	0.009(2)	0.005(2)
C12	0.020(3)	0.029(3)	0.023(3)	-0.003(2)	0.007(2)	0.003(2)
C13	0.030(3)	0.030(3)	0.025(3)	-0.008(3)	0.006(2)	-0.007(3)
C14	0.037(4)	0.024(3)	0.035(4)	-0.009(2)	0.017(3)	-0.003(3)
C15	0.032(3)	0.026(3)	0.034(3)	0.002(3)	0.014(3)	0.009(3)
C16	0.028(3)	0.025(3)	0.033(4)	0.005(2)	0.007(3)	0.004(2)
C17	0.019(3)	0.034(3)	0.024(3)	0.005(2)	0.002(2)	0.000(2)
C18	0.022(3)	0.030(3)	0.025(3)	-0.006(2)	0.008(2)	0.006(2)
C19	0.036(4)	0.036(3)	0.025(3)	0.001(3)	0.001(3)	-0.019(3)
C20	0.046(4)	0.013(2)	0.020(3)	0.001(2)	-0.002(3)	-0.004(2)
C21	0.019(3)	0.025(3)	0.025(3)	0.003(2)	0.000(2)	-0.001(2)
B1	0.032(4)	0.019(3)	0.017(3)	0.000(2)	0.007(3)	0.008(3)
S1	0.0276(8)	0.0171(6)	0.0247(8)	0.0019(5)	0.0075(6)	0.0026(6)
F1	0.078(3)	0.0330(18)	0.061(3)	0.0173(18)	0.044(2)	0.008(2)
F2	0.043(2)	0.0247(16)	0.0291(19)	-0.0002(14)	-0.0093(15)	-0.0089(15)
F3	0.043(2)	0.0294(17)	0.042(2)	-0.0035(16)	-0.0126(17)	0.0155(16)
O2	0.032(3)	0.036(2)	0.081(4)	0.019(2)	0.010(2)	0.013(2)
O3	0.070(3)	0.024(2)	0.032(3)	-0.0121(18)	0.002(2)	0.005(2)
O4	0.052(3)	0.026(2)	0.041(3)	0.0016(18)	0.027(2)	-0.001(2)
C22	0.038(4)	0.018(3)	0.024(3)	-0.002(2)	0.004(3)	-0.003(3)
N9	0.043(4)	0.068(4)	0.049(4)	-0.006(3)	0.013(3)	-0.008(3)

C23	0.037(4)	0.037(3)	0.036(4)	0.008(3)	0.004(3)	-0.001(3)
C24	0.048(4)	0.037(3)	0.020(3)	-0.008(3)	-0.002(3)	0.007(3)

Table 4. Bond lengths and angles for mo\_harman\_mne\_nb4\_025\_0m

Atom–Atom	Length [Å]		
W1–P1	2.5610(14)	C11–H11	0.92(4)
W1–N1	2.226(4)	C11–C12	1.376(7)
W1–N3	2.165(4)	C12–H12	1.0000
W1–N5	2.196(4)	C12–C13	1.508(7)
W1–N7	1.771(4)	C13–H13A	0.9900
W1–C10	2.340(5)	C13–H13B	0.9900
W1–C11	2.330(5)	C13–C14	1.543(7)
W1–C12	2.556(5)	C14–H14A	0.9900
P1–C19	1.827(6)	C14–H14B	0.9900
P1–C20	1.829(5)	C14–C15	1.552(8)
P1–C21	1.816(5)	C15–H15	1.0000
O1–N7	1.205(5)	C15–C16	1.502(8)
N1–N2	1.355(6)	C15–C18	1.483(8)
N1–C1	1.344(6)	C16–H16	0.9500
N2–C3	1.347(6)	C16–C17	1.334(7)
N2–B1	1.536(7)	C17–H17	0.9500
N3–N4	1.377(5)	C19–H19A	0.9800
N3–C4	1.329(6)	C19–H19B	0.9800
N4–C6	1.346(6)	C19–H19C	0.9800
N4–B1	1.533(7)	C20–H20A	0.9800
N5–N6	1.372(5)	C20–H20B	0.9800
N5–C7	1.338(6)	C20–H20C	0.9800
N6–C9	1.342(6)	C21–H21A	0.9800
N6–B1	1.548(7)	C21–H21B	0.9800
N8–C18	1.138(7)	C21–H21C	0.9800
C1–H1	0.9500	B1–H1A	1.0000
C1–C2	1.374(7)	S1–O2	1.433(4)
C2–H2	0.9500	S1–O3	1.425(4)
C2–C3	1.369(7)	S1–O4	1.427(4)
C3–H3	0.9500	S1–C22	1.829(5)
C4–H4	0.9500	F1–C22	1.312(6)
C4–C5	1.379(7)	F2–C22	1.319(6)
C5–H5	0.9500	F3–C22	1.330(6)
C5–C6	1.373(7)	N9–C24	1.133(8)
C6–H6	0.9500	C23–H23A	0.9800
C7–H7	0.9500	C23–H23B	0.9800
C7–C8	1.383(7)	C23–H23C	0.9800
C8–H8	0.9500	C23–C24	1.458(9)
C8–C9	1.364(7)		
C9–H9	0.9500	<b>Atom–Atom–</b>	<b>Angle [°]</b>
C10–H10	0.94(5)	<b>Atom</b>	
C10–C11	1.405(7)	N1–W1–P1	84.00(11)
C10–C17	1.484(7)	N1–W1–C10	90.97(17)
		N1–W1–C11	83.20(17)

N1-W1-C12	103.11(16)
N3-W1-P1	76.24(11)
N3-W1-N1	86.66(15)
N3-W1-N5	75.42(15)
N3-W1-C10	152.23(17)
N3-W1-C11	167.94(16)
N3-W1-C12	146.78(16)
N5-W1-P1	149.28(10)
N5-W1-N1	82.78(15)
N5-W1-C10	131.73(16)
N5-W1-C11	96.77(16)
N5-W1-C12	74.49(16)
N7-W1-P1	90.84(14)
N7-W1-N1	172.28(17)
N7-W1-N3	86.53(17)
N7-W1-N5	99.01(17)
N7-W1-C10	93.35(18)
N7-W1-C11	103.96(18)
N7-W1-C12	84.59(18)
C10-W1-P1	76.00(14)
C10-W1-C12	60.43(17)
C11-W1-P1	109.03(13)
C11-W1-C10	35.03(18)
C11-W1-C12	32.29(16)
C12-W1-P1	135.73(12)
C19-P1-W1	121.57(19)
C19-P1-C20	100.2(3)
C20-P1-W1	111.96(19)
C21-P1-W1	113.13(17)
C21-P1-C19	102.3(3)
C21-P1-C20	105.8(2)
N2-N1-W1	120.1(3)
C1-N1-W1	133.0(4)
C1-N1-N2	106.3(4)
N1-N2-B1	121.2(4)
C3-N2-N1	109.6(4)
C3-N2-B1	129.1(4)
N4-N3-W1	121.9(3)
C4-N3-W1	131.0(3)
C4-N3-N4	106.8(4)
N3-N4-B1	119.4(4)
C6-N4-N3	108.1(4)
C6-N4-B1	129.3(5)
N6-N5-W1	120.9(3)
C7-N5-W1	131.8(3)
C7-N5-N6	106.5(4)
N5-N6-B1	120.4(4)
C9-N6-N5	109.2(4)

C9-N6-B1	128.3(5)
O1-N7-W1	175.3(4)
N1-C1-H1	124.9
N1-C1-C2	110.3(5)
C2-C1-H1	124.9
C1-C2-H2	127.2
C3-C2-C1	105.5(5)
C3-C2-H2	127.2
N2-C3-C2	108.3(5)
N2-C3-H3	125.9
C2-C3-H3	125.9
N3-C4-H4	124.6
N3-C4-C5	110.9(5)
C5-C4-H4	124.6
C4-C5-H5	127.6
C6-C5-C4	104.8(5)
C6-C5-H5	127.6
N4-C6-C5	109.4(5)
N4-C6-H6	125.3
C5-C6-H6	125.3
N5-C7-H7	125.1
N5-C7-C8	109.9(5)
C8-C7-H7	125.1
C7-C8-H8	127.0
C9-C8-C7	105.9(5)
C9-C8-H8	127.0
N6-C9-C8	108.6(5)
N6-C9-H9	125.7
C8-C9-H9	125.7
W1-C10-H10	120(3)
C11-C10-W1	72.1(3)
C11-C10-H10	113(3)
C11-C10-C17	123.8(5)
C17-C10-W1	113.3(3)
C17-C10-H10	111(3)
W1-C11-H11	102(3)
C10-C11-W1	72.9(3)
C10-C11-H11	121(3)
C12-C11-W1	83.0(3)
C12-C11-C10	125.4(5)
C12-C11-H11	111(3)
W1-C12-H12	113.5
C11-C12-W1	64.8(3)
C11-C12-H12	113.5
C11-C12-C13	128.6(5)
C13-C12-W1	112.5(3)
C13-C12-H12	113.5
C12-C13-H13A	109.2

C12–C13–H13B	109.2
C12–C13–C14	112.0(4)
H13A–C13– H13B	107.9
C14–C13–H13A	109.2
C14–C13–H13B	109.2
C13–C14–H14A	108.7
C13–C14–H14B	108.7
C13–C14–C15	114.1(4)
H14A–C14– H14B	107.6
C15–C14–H14A	108.7
C15–C14–H14B	108.7
C14–C15–H15	105.8
C16–C15–C14	113.5(4)
C16–C15–H15	105.8
C18–C15–C14	112.3(5)
C18–C15–H15	105.8
C18–C15–C16	112.8(5)
C15–C16–H16	115.9
C17–C16–C15	128.1(5)
C17–C16–H16	115.9
C10–C17–H17	116.4
C16–C17–C10	127.1(5)
C16–C17–H17	116.4
N8–C18–C15	175.6(6)
P1–C19–H19A	109.5
P1–C19–H19B	109.5
P1–C19–H19C	109.5
H19A–C19– H19B	109.5
H19A–C19– H19C	109.5
H19B–C19– H19C	109.5
P1–C20–H20A	109.5
P1–C20–H20B	109.5
P1–C20–H20C	109.5
H20A–C20– H20B	109.5
H20A–C20– H20C	109.5

H20B–C20– H20C	109.5
P1–C21–H21A	109.5
P1–C21–H21B	109.5
P1–C21–H21C	109.5
H21A–C21– H21B	109.5
H21A–C21– H21C	109.5
H21B–C21– H21C	109.5
N2–B1–N6	109.8(4)
N2–B1–H1A	111.1
N4–B1–N2	108.5(5)
N4–B1–N6	104.8(4)
N4–B1–H1A	111.1
N6–B1–H1A	111.1
O2–S1–C22	102.9(3)
O3–S1–O2	115.2(3)
O3–S1–O4	115.2(3)
O3–S1–C22	103.8(2)
O4–S1–O2	114.4(3)
O4–S1–C22	103.1(2)
F1–C22–S1	112.0(4)
F1–C22–F2	108.9(5)
F1–C22–F3	107.1(5)
F2–C22–S1	111.4(4)
F2–C22–F3	106.6(4)
F3–C22–S1	110.6(4)
H23A–C23– H23B	109.5
H23A–C23– H23C	109.5
H23B–C23– H23C	109.5
C24–C23–H23A	109.5
C24–C23–H23B	109.5
C24–C23–H23C	109.5
N9–C24–C23	178.1(7)

Table 5. Torsion angles for mo\_harman\_mne\_nb4\_025\_0m

Atom–Atom– Atom–Atom	Torsion Angle [°]
W1–N1–N2–C3	–173.9(3)
W1–N1–N2–B1	9.1(6)

W1-N1-C1-C2	172.0(4)
W1-N3-N4-C6	-175.6(3)
W1-N3-N4-B1	-13.7(6)
W1-N3-C4-C5	175.7(3)
W1-N5-N6-C9	171.4(3)
W1-N5-N6-B1	6.6(6)
W1-N5-C7-C8	-170.3(3)
W1-C10-C11-C12	67.9(5)
W1-C10-C17-C16	-114.0(5)
W1-C11-C12-C13	99.4(5)
W1-C12-C13-C14	137.0(4)
N1-N2-C3-C2	1.2(6)
N1-N2-B1-N4	-62.9(6)
N1-N2-B1-N6	51.2(6)
N1-C1-C2-C3	0.3(6)
N2-N1-C1-C2	0.4(6)
N3-N4-C6-C5	-0.5(6)
N3-N4-B1-N2	65.6(6)
N3-N4-B1-N6	-51.7(6)
N3-C4-C5-C6	-1.4(6)
N4-N3-C4-C5	1.1(6)
N5-N6-C9-C8	0.1(5)
N5-N6-B1-N2	-60.9(6)
N5-N6-B1-N4	55.5(6)
N5-C7-C8-C9	0.8(6)
N6-N5-C7-C8	-0.8(6)
C1-N1-N2-C3	-1.0(5)
C1-N1-N2-B1	-178.0(4)
C1-C2-C3-N2	-0.9(6)
C3-N2-B1-N4	120.7(5)
C3-N2-B1-N6	-125.2(5)
C4-N3-N4-C6	-0.3(5)
C4-N3-N4-B1	161.5(4)
C4-C5-C6-N4	1.1(6)
C6-N4-B1-N2	-136.8(5)
C6-N4-B1-N6	105.8(6)
C7-N5-N6-C9	0.5(5)
C7-N5-N6-B1	-164.3(4)
C7-C8-C9-N6	-0.5(6)
C9-N6-B1-N2	137.6(5)
C9-N6-B1-N4	-106.0(5)
C10-C11-C12-W1	-63.2(5)
C10-C11-C12-C13	36.3(8)
C11-C10-C17-C16	-30.6(9)
C11-C12-C13-C14	62.1(7)
C12-C13-C14-C15	-62.8(6)
C13-C14-C15-C16	-36.0(7)
C13-C14-C15-C18	93.3(6)

C14–C15–C16–C17	82.0(7)
C15–C16–C17–C10	0.6(10)
C17–C10–C11–W1	–106.5(5)
C17–C10–C11–C12	–38.6(8)
C18–C15–C16–C17	–47.1(8)
B1–N2–C3–C2	177.9(5)
B1–N4–C6–C5	–160.0(5)
B1–N6–C9–C8	163.3(5)
O2–S1–C22–F1	–54.6(5)
O2–S1–C22–F2	67.7(5)
O2–S1–C22–F3	–174.0(4)
O3–S1–C22–F1	65.7(5)
O3–S1–C22–F2	–172.0(4)
O3–S1–C22–F3	–53.7(4)
O4–S1–C22–F1	–173.8(4)
O4–S1–C22–F2	–51.5(5)
O4–S1–C22–F3	66.8(4)

#### Structure Report for mo\_harman\_mne\_5\_219fp\_0m

A yellow, plate-shaped crystal of mo\_harman\_mne\_5\_219fp\_0m was coated with Paratone oil and mounted on a MiTeGen micromount. Data were collected at 100.00 K on a Bruker D8 VENTURE dual wavelength Mo/Cu Kappa four-circle diffractometer with a PHOTON III\_C14 detector. The diffractometer was equipped with an Oxford Cryostream 800 low temperature device and used Mo  $K_\alpha$  radiation ( $\lambda = 0.71073\text{\AA}$ ) from an Incoatec I\mS 3.0 microfocus sealed tube with a HELIOS double bounce multilayer mirror as monochromator.

Data collection and processing were done within the Bruker APEX6 software suite.<sup>[1]</sup> All data were integrated with SAINT 8.41 using a narrow-frame algorithm and a Multi-Scan absorption correction using SADABS 2016/2 was applied.<sup>[2]</sup> Using Olex2 as a graphical interface,<sup>[3]</sup> the structure was solved by dual methods with XT and refined by full-matrix least-squares methods against  $F^2$  using XL.<sup>[4,5]</sup> All non-hydrogen atoms were refined with anisotropic displacement parameters. The H atoms on the carbons bound directly to W were located in the electron density map and refined isotropically with fixed C-H distances. All other hydrogen atoms were placed in calculated positions using a riding model with their  $U_{\text{iso}}$  values constrained to 1.5 times the  $U_{\text{eq}}$  of their pivot

atoms for terminal  $sp^3$  carbon atoms and 1.2 times for all other carbon atoms. A global RIGU restraint was used to account for the poor quality of the diffraction data. An AFIX 66 constraint was applied to the pendant phenyl ring, and the C-C bonds of the pyrazolyl rings were restrained with a SADI command.

This report and the CIF file were generated using FinalCif.<sup>[6]</sup>

Refinement details for mo\_harman\_mne\_5\_219fp\_0m

Refined as a 2-component twin on HKLF 5 data, with the BASF converging to 0.40159.

Table 1. Crystal data and structure refinement for mo\_harman\_mne\_5\_219fp\_0m

CCDC number	
Empirical formula	$C_{32}H_{45}BN_9OPW$
Formula weight	797.40
Temperature [K]	100.00
Crystal system	monoclinic
Space group (number)	$P2_1/c$ (14)
$a$ [Å]	8.8445(9)
$b$ [Å]	25.523(3)
$c$ [Å]	16.0577(14)
$\alpha$ [°]	90
$\beta$ [°]	104.076(3)
$\gamma$ [°]	90
Volume [Å <sup>3</sup> ]	3515.9(6)
$Z$	4
$\rho_{\text{calc}}$ [gcm <sup>-3</sup> ]	1.506
$\mu$ [mm <sup>-1</sup> ]	3.370
$F(000)$	1608
Crystal size [mm <sup>3</sup> ]	0.098×0.164×0.17
Crystal colour	yellow
Crystal shape	plate
Radiation	Mo $K_\alpha$ ( $\lambda=0.71073$ Å)
$2\theta$ range [°]	4.13 to 51.42 (0.82 Å)
Index ranges	$-10 \leq h \leq 10$ $0 \leq k \leq 31$ $0 \leq l \leq 19$
Reflections collected	8207
Independent reflections	8207



	$R_{\text{int}} = 0.1022$ $R_{\text{sigma}} = 0.0664$
Completeness to $\theta = 25.242^\circ$	99.3
Data / Restraints / Parameters	8207 / 385 / 407
Goodness-of-fit on $F^2$	1.128
Final $R$ indexes [ $\geq 2\sigma(I)$ ]	$R_1 = 0.0818$ $wR_2 = 0.2182$
Final $R$ indexes [all data]	$R_1 = 0.1021$ $wR_2 = 0.2286$
Largest peak/hole [ $\text{e}\text{\AA}^{-3}$ ]	3.53/−5.09

Table 2. Atomic coordinates and Ueq [Å<sup>2</sup>] for mo\_harman\_mne\_5\_219fp\_0m

Atom	x	y	z	U <sub>eq</sub>
W1	0.31012(9)	0.25563(2)	0.61456(4)	0.0217(2)
P1	0.1199(5)	0.28810(18)	0.6986(2)	0.0265(9)
O1	0.6130(15)	0.2659(5)	0.7474(8)	0.040(3)
N1	0.0830(15)	0.2411(5)	0.5180(8)	0.024(2)
N2	0.0285(15)	0.1913(5)	0.5005(8)	0.026(2)
N3	0.2563(16)	0.1837(6)	0.6777(8)	0.028(3)
N4	0.1671(17)	0.1446(6)	0.6357(9)	0.031(3)
N5	0.3852(16)	0.1909(5)	0.5404(8)	0.027(3)
N6	0.2909(16)	0.1495(5)	0.5140(8)	0.029(3)
N7	0.4898(16)	0.2626(5)	0.6932(8)	0.028(3)
C1	-0.0242(17)	0.2721(6)	0.4710(9)	0.024(3)
H1	-0.016049	0.309158	0.470355	0.028
C2	-0.1483(17)	0.2446(6)	0.4233(10)	0.031(3)
H2	-0.238109	0.257977	0.383932	0.037
C3	-0.1131(18)	0.1936(6)	0.4454(9)	0.030(3)
H3	-0.178102	0.164382	0.425161	0.036
C4	0.296(2)	0.1691(7)	0.7619(10)	0.035(4)
H4	0.360709	0.188733	0.807045	0.042
C5	0.228(3)	0.1217(7)	0.7715(11)	0.057(6)
H5	0.236784	0.102840	0.823417	0.069
C6	0.145(2)	0.1073(8)	0.6909(11)	0.043(4)
H6	0.083843	0.076556	0.676754	0.052
C7	0.523(2)	0.1786(6)	0.5261(10)	0.030(3)
H7	0.612128	0.200467	0.540738	0.035
C8	0.5190(19)	0.1307(6)	0.4877(10)	0.034(3)
H8	0.600439	0.113613	0.469150	0.040
C9	0.3724(19)	0.1132(7)	0.4822(11)	0.035(3)
H9	0.332814	0.080278	0.459345	0.042
C10	0.3079(18)	0.3400(6)	0.5760(10)	0.024(3)
H10	0.209(9)	0.355(6)	0.551(10)	0.029
C11	0.3594(19)	0.3073(7)	0.5140(10)	0.026(3)
H11	0.278(14)	0.296(6)	0.467(7)	0.032
C12	0.5121(18)	0.3098(7)	0.4929(9)	0.026(3)
H12	0.552982	0.276316	0.484832	0.031
C13	0.605(2)	0.3487(7)	0.4827(10)	0.033(3)
H13	0.699950	0.337672	0.471057	0.039
C14	0.587(2)	0.4068(7)	0.4861(12)	0.041(4)
H14A	0.609585	0.421608	0.433354	0.049

H14B	0.668979	0.419952	0.535237	0.049
C15	0.427(2)	0.4298(7)	0.4946(11)	0.035(4)
H15A	0.414520	0.465215	0.468696	0.042
H15B	0.342379	0.407611	0.460301	0.042
C16	0.404(2)	0.4338(7)	0.5832(11)	0.034(3)
H16	0.489332	0.456671	0.616538	0.040
C17	0.4211(18)	0.3801(6)	0.6285(9)	0.025(3)
H17	0.528421	0.367318	0.629447	0.030
C18	0.414(2)	0.3853(7)	0.7247(10)	0.030(3)
H18A	0.312183	0.400975	0.726976	0.036
H18B	0.418947	0.349914	0.750572	0.036
C19	0.5443(11)	0.4187(4)	0.7775(7)	0.034(3)
C20	0.6971(13)	0.4012(4)	0.7907(7)	0.035(3)
H20	0.718608	0.369309	0.765201	0.042
C21	0.8183(11)	0.4302(5)	0.8411(8)	0.048(4)
H21	0.922720	0.418197	0.850043	0.057
C22	0.7868(14)	0.4768(5)	0.8783(8)	0.055(5)
H22	0.869699	0.496672	0.912762	0.066
C23	0.6341(16)	0.4944(4)	0.8652(8)	0.054(5)
H23	0.612567	0.526262	0.890640	0.064
C24	0.5128(12)	0.4654(5)	0.8148(8)	0.043(4)
H24	0.408452	0.477375	0.805797	0.051
C25	0.249(2)	0.4610(7)	0.5838(12)	0.039(4)
H25A	0.240646	0.493861	0.551407	0.059
H25B	0.245209	0.468503	0.643133	0.059
H25C	0.161805	0.437971	0.557181	0.059
C26	0.004(2)	0.3474(7)	0.6654(11)	0.035(4)
H26A	-0.080181	0.349197	0.695044	0.053
H26B	-0.040023	0.346532	0.603191	0.053
H26C	0.071222	0.378351	0.680079	0.053
C27	0.190(2)	0.2950(8)	0.8151(10)	0.039(4)
H27A	0.105782	0.309214	0.838771	0.058
H27B	0.278957	0.318915	0.828284	0.058
H27C	0.221149	0.260674	0.840769	0.058
C28	-0.044(2)	0.2423(8)	0.6929(11)	0.037(4)
H28A	-0.002865	0.207396	0.711483	0.055
H28B	-0.107044	0.240480	0.633736	0.055
H28C	-0.108371	0.254677	0.730629	0.055
B1	0.133(2)	0.1438(8)	0.5370(11)	0.029(3)
H1A	0.081775	0.110213	0.513785	0.035
N8	0.916(3)	0.3981(10)	0.3844(16)	0.078(6)
C29	0.687(3)	0.3742(11)	0.2412(19)	0.078(7)
H29A	0.710908	0.390162	0.190354	0.117
H29B	0.588267	0.388189	0.248955	0.117
H29C	0.678458	0.336115	0.233467	0.117
C30	0.820(3)	0.3871(12)	0.3221(19)	0.072(7)

N9	0.128(3)	0.4994(11)	0.8043(16)	0.088(8)
C31	-0.093(3)	0.4953(11)	0.6628(19)	0.081(8)
H31A	-0.071003	0.467495	0.625424	0.121
H31B	-0.098689	0.529076	0.633255	0.121
H31C	-0.193242	0.488184	0.676769	0.121
C32	0.033(3)	0.4970(10)	0.7432(18)	0.066(6)

$U_{eq}$  is defined as 1/3 of the trace of the orthogonalized  $U_{ij}$  tensor.

Table 3. Anisotropic displacement parameters ( $\text{\AA}^2$ ) for mo\_harman\_mne\_5\_219fp\_0m. The anisotropic displacement factor exponent takes the form:  $-2\pi^2[h^2(a^*)^2U_{11} + k^2(b^*)^2U_{22} + \dots + 2hka^*b^*U_{12}]$

Atom	$U_{11}$	$U_{22}$	$U_{33}$	$U_{23}$	$U_{13}$	$U_{12}$
W1	0.0149(3)	0.0346(4)	0.0151(3)	-0.0011(3)	0.00236(18)	-0.0011(3)
P1	0.024(2)	0.040(3)	0.0170(18)	-0.0079(17)	0.0076(16)	-0.0027(18)
O1	0.020(6)	0.052(8)	0.039(6)	-0.006(6)	-0.009(5)	0.003(5)
N1	0.015(5)	0.039(6)	0.016(5)	-0.007(4)	0.002(4)	-0.003(4)
N2	0.018(5)	0.039(6)	0.021(6)	-0.006(5)	0.003(4)	-0.003(4)
N3	0.028(7)	0.039(6)	0.015(5)	0.002(4)	0.003(4)	-0.003(5)
N4	0.034(7)	0.039(7)	0.023(5)	-0.001(4)	0.011(5)	-0.003(5)
N5	0.025(6)	0.034(6)	0.024(6)	0.001(5)	0.010(5)	0.005(4)
N6	0.030(5)	0.032(6)	0.023(6)	0.004(5)	0.005(5)	0.004(4)
N7	0.027(6)	0.034(7)	0.023(6)	-0.005(5)	0.006(4)	-0.006(5)
C1	0.021(7)	0.038(7)	0.012(6)	-0.008(5)	0.005(5)	0.003(5)
C2	0.018(6)	0.051(8)	0.022(7)	-0.008(6)	0.003(5)	0.002(5)
C3	0.022(6)	0.049(7)	0.018(7)	-0.008(6)	0.004(5)	-0.002(5)
C4	0.039(9)	0.046(9)	0.019(6)	0.006(6)	0.005(6)	-0.003(7)
C5	0.086(15)	0.057(10)	0.025(7)	0.017(7)	0.005(8)	-0.018(10)
C6	0.051(11)	0.041(9)	0.035(7)	0.008(6)	0.005(7)	-0.011(7)
C7	0.028(6)	0.039(8)	0.024(7)	0.002(6)	0.010(6)	0.005(5)
C8	0.037(7)	0.039(8)	0.024(8)	0.003(6)	0.007(6)	0.012(6)
C9	0.041(7)	0.030(7)	0.034(9)	0.004(6)	0.011(7)	0.008(5)
C10	0.024(7)	0.027(6)	0.020(6)	0.003(5)	0.001(5)	-0.003(5)
C11	0.023(7)	0.035(7)	0.019(6)	-0.003(5)	0.001(5)	-0.006(6)
C12	0.022(7)	0.040(8)	0.014(7)	-0.006(6)	-0.001(5)	-0.002(5)
C13	0.023(7)	0.048(7)	0.026(8)	0.003(7)	0.002(6)	-0.003(6)
C14	0.042(9)	0.046(8)	0.032(9)	0.002(7)	0.006(7)	-0.007(7)
C15	0.039(9)	0.035(9)	0.029(7)	0.008(6)	0.006(7)	-0.005(7)
C16	0.037(8)	0.031(7)	0.030(7)	-0.002(6)	0.003(6)	-0.005(6)
C17	0.017(7)	0.038(7)	0.021(6)	-0.001(5)	0.007(5)	-0.002(5)
C18	0.034(8)	0.032(8)	0.026(6)	-0.004(5)	0.010(6)	-0.005(6)
C19	0.044(7)	0.032(7)	0.023(7)	0.003(5)	0.004(6)	-0.007(6)
C20	0.041(7)	0.038(9)	0.021(7)	0.008(6)	-0.003(6)	-0.007(6)
C21	0.045(9)	0.053(10)	0.037(9)	0.008(7)	-0.007(7)	-0.011(7)
C22	0.071(10)	0.049(10)	0.034(10)	0.001(7)	-0.008(9)	-0.021(8)
C23	0.081(11)	0.038(10)	0.038(10)	-0.009(8)	0.007(8)	-0.011(8)
C24	0.064(10)	0.040(8)	0.024(8)	-0.003(6)	0.009(7)	-0.004(7)

C25	0.053(10)	0.022(8)	0.044(10)	0.003(7)	0.013(8)	0.003(7)
C26	0.024(8)	0.048(10)	0.036(9)	−0.004(7)	0.010(7)	0.009(7)
C27	0.032(9)	0.073(13)	0.015(7)	−0.012(7)	0.012(6)	−0.011(8)
C28	0.026(8)	0.051(10)	0.034(9)	−0.004(8)	0.011(7)	−0.019(8)
B1	0.027(6)	0.037(8)	0.020(6)	−0.006(6)	0.001(5)	−0.007(6)
N8	0.065(13)	0.097(17)	0.076(13)	0.033(12)	0.028(9)	0.008(12)
C29	0.078(17)	0.067(17)	0.089(16)	0.007(14)	0.022(12)	−0.007(14)
C30	0.057(13)	0.089(19)	0.077(13)	0.020(13)	0.032(9)	0.018(12)
N9	0.057(13)	0.12(2)	0.081(13)	−0.013(14)	0.012(9)	0.015(13)
C31	0.060(15)	0.072(18)	0.097(16)	−0.018(15)	−0.004(11)	0.028(13)
C32	0.054(13)	0.063(16)	0.081(13)	−0.005(12)	0.015(9)	0.005(11)

Table 4. Bond lengths and angles for mo\_harman\_mne\_5\_219fp\_0m

Atom–Atom	Length [Å]		
W1–P1	2.538(4)	C7–H7	0.9500
W1–N1	2.250(12)	C7–C8	1.367(15)
W1–N3	2.205(14)	C8–H8	0.9500
W1–N5	2.230(13)	C8–C9	1.353(16)
W1–N7	1.782(14)	C9–H9	0.9500
W1–C10	2.239(16)	C10–H10	0.96(2)
W1–C11	2.210(16)	C10–C11	1.45(2)
P1–C26	1.833(18)	C10–C17	1.53(2)
P1–C27	1.831(16)	C11–H11	0.95(2)
P1–C28	1.846(16)	C11–C12	1.47(2)
O1–N7	1.221(18)	C12–H12	0.9500
N1–N2	1.364(19)	C12–C13	1.32(2)
N1–C1	1.32(2)	C13–H13	0.9500
N2–C3	1.35(2)	C13–C14	1.49(3)
N2–B1	1.55(2)	C14–H14A	0.9900
N3–N4	1.348(19)	C14–H14B	0.9900
N3–C4	1.36(2)	C14–C15	1.57(3)
N4–C6	1.35(2)	C15–H15A	0.9900
N4–B1	1.54(2)	C15–H15B	0.9900
N5–N6	1.349(19)	C15–C16	1.49(2)
N5–C7	1.33(2)	C16–H16	1.0000
N6–C9	1.35(2)	C16–C17	1.54(2)
N6–B1	1.53(2)	C16–C25	1.54(3)
C1–H1	0.9500	C17–H17	1.0000
C1–C2	1.368(15)	C17–C18	1.57(2)
C2–H2	0.9500	C18–H18A	0.9900
C2–C3	1.365(16)	C18–H18B	0.9900
C3–H3	0.9500	C18–C19	1.520(18)
C4–H4	0.9500	C19–C20	1.3900
C4–C5	1.375(16)	C19–C24	1.3900
C5–H5	0.9500	C20–H20	0.9500
C5–C6	1.373(16)	C20–C21	1.3900
C6–H6	0.9500	C21–H21	0.9500
		C21–C22	1.3900

C22–H22	0.9500
C22–C23	1.3900
C23–H23	0.9500
C23–C24	1.3900
C24–H24	0.9500
C25–H25A	0.9800
C25–H25B	0.9800
C25–H25C	0.9800
C26–H26A	0.9800
C26–H26B	0.9800
C26–H26C	0.9800
C27–H27A	0.9800
C27–H27B	0.9800
C27–H27C	0.9800
C28–H28A	0.9800
C28–H28B	0.9800
C28–H28C	0.9800
B1–H1A	1.0000
N8–C30	1.18(4)
C29–H29A	0.9800
C29–H29B	0.9800
C29–H29C	0.9800
C29–C30	1.56(4)
N9–C32	1.13(3)
C31–H31A	0.9800
C31–H31B	0.9800
C31–H31C	0.9800
C31–C32	1.49(4)
<b>Atom–Atom– Atom</b>	<b>Angle [°]</b>
N1–W1–P1	79.9(3)
N3–W1–P1	77.4(4)
N3–W1–N1	85.6(5)
N3–W1–N5	75.8(5)
N3–W1–C10	160.0(6)
N3–W1–C11	159.5(5)
N5–W1–P1	148.0(4)
N5–W1–N1	80.9(5)
N5–W1–C10	123.3(5)
N7–W1–P1	100.5(4)
N7–W1–N1	176.1(6)
N7–W1–N3	90.7(6)
N7–W1–N5	97.0(6)
N7–W1–C10	92.7(6)
N7–W1–C11	99.1(6)
C10–W1–P1	82.6(4)
C10–W1–N1	91.2(5)

C11–W1–P1	117.9(4)
C11–W1–N1	84.0(5)
C11–W1–N5	85.1(5)
C11–W1–C10	38.2(6)
C26–P1–W1	120.7(6)
C26–P1–C28	97.7(9)
C27–P1–W1	118.2(6)
C27–P1–C26	104.1(9)
C27–P1–C28	100.1(8)
C28–P1–W1	112.4(6)
N2–N1–W1	120.4(10)
C1–N1–W1	133.8(11)
C1–N1–N2	105.8(12)
N1–N2–B1	120.1(12)
C3–N2–N1	108.6(13)
C3–N2–B1	131.1(14)
N4–N3–W1	123.5(9)
N4–N3–C4	105.8(13)
C4–N3–W1	130.6(11)
N3–N4–B1	117.9(13)
C6–N4–N3	110.7(13)
C6–N4–B1	130.3(15)
N6–N5–W1	120.4(10)
C7–N5–W1	132.1(11)
C7–N5–N6	106.5(13)
N5–N6–B1	121.8(13)
C9–N6–N5	108.0(14)
C9–N6–B1	128.9(15)
O1–N7–W1	178.2(13)
N1–C1–H1	123.8
N1–C1–C2	112.4(14)
C2–C1–H1	123.8
C1–C2–H2	128.0
C3–C2–C1	103.9(14)
C3–C2–H2	128.0
N2–C3–C2	109.2(14)
N2–C3–H3	125.4
C2–C3–H3	125.4
N3–C4–H4	125.1
N3–C4–C5	109.7(14)
C5–C4–H4	125.1
C4–C5–H5	126.9
C6–C5–C4	106.1(16)
C6–C5–H5	126.9
N4–C6–C5	107.6(15)
N4–C6–H6	126.2
C5–C6–H6	126.2
N5–C7–H7	124.2

N5-C7-C8	111.5(15)
C8-C7-H7	124.2
C7-C8-H8	128.0
C9-C8-C7	103.9(15)
C9-C8-H8	128.0
N6-C9-C8	110.0(15)
N6-C9-H9	125.0
C8-C9-H9	125.0
W1-C10-H10	117(10)
C11-C10-W1	69.8(9)
C11-C10-H10	111(10)
C11-C10-C17	119.2(14)
C17-C10-W1	121.9(10)
C17-C10-H10	112(10)
W1-C11-H11	98(10)
C10-C11-W1	72.0(9)
C10-C11-H11	114(10)
C10-C11-C12	126.2(14)
C12-C11-W1	123.4(11)
C12-C11-H11	113(10)
C11-C12-H12	113.1
C13-C12-C11	133.8(17)
C13-C12-H12	113.1
C12-C13-H13	114.0
C12-C13-C14	132.0(17)
C14-C13-H13	114.0
C13-C14-H14A	107.7
C13-C14-H14B	107.7
C13-C14-C15	118.5(15)
H14A-C14-H14B	107.1
C15-C14-H14A	107.7
C15-C14-H14B	107.7
C14-C15-H15A	108.2
C14-C15-H15B	108.2
H15A-C15-H15B	107.4
C16-C15-C14	116.3(15)
C16-C15-H15A	108.2
C16-C15-H15B	108.2
C15-C16-H16	107.0
C15-C16-C17	111.7(14)
C15-C16-C25	111.4(15)
C17-C16-H16	107.0
C25-C16-H16	107.0
C25-C16-C17	112.6(14)
C10-C17-C16	111.0(12)
C10-C17-H17	106.3

C10-C17-C18	114.8(13)
C16-C17-H17	106.3
C16-C17-C18	111.5(13)
C18-C17-H17	106.3
C17-C18-H18A	109.0
C17-C18-H18B	109.0
H18A-C18-H18B	107.8
C19-C18-C17	112.8(13)
C19-C18-H18A	109.0
C19-C18-H18B	109.0
C20-C19-C18	118.9(10)
C20-C19-C24	120.0
C24-C19-C18	121.0(10)
C19-C20-H20	120.0
C19-C20-C21	120.0
C21-C20-H20	120.0
C20-C21-H21	120.0
C22-C21-C20	120.0
C22-C21-H21	120.0
C21-C22-H22	120.0
C21-C22-C23	120.0
C23-C22-H22	120.0
C22-C23-H23	120.0
C24-C23-C22	120.0
C24-C23-H23	120.0
C19-C24-H24	120.0
C23-C24-C19	120.0
C23-C24-H24	120.0
C16-C25-H25A	109.5
C16-C25-H25B	109.5
C16-C25-H25C	109.5
H25A-C25-H25B	109.5
H25A-C25-H25C	109.5
H25B-C25-H25C	109.5
P1-C26-H26A	109.5
P1-C26-H26B	109.5
P1-C26-H26C	109.5
H26A-C26-H26B	109.5
H26A-C26-H26C	109.5
H26B-C26-H26C	109.5
P1-C27-H27A	109.5
P1-C27-H27B	109.5

P1–C27–H27C	109.5
H27A–C27–H27B	109.5
H27A–C27–H27C	109.5
H27B–C27–H27C	109.5
P1–C28–H28A	109.5
P1–C28–H28B	109.5
P1–C28–H28C	109.5
H28A–C28–H28B	109.5
H28A–C28–H28C	109.5
H28B–C28–H28C	109.5
N2–B1–H1A	110.6
N4–B1–N2	109.1(14)
N4–B1–H1A	110.6
N6–B1–N2	109.3(14)
N6–B1–N4	106.7(13)
N6–B1–H1A	110.6

H29A–C29–H29B	109.5
H29A–C29–H29C	109.5
H29B–C29–H29C	109.5
C30–C29–H29A	109.5
C30–C29–H29B	109.5
C30–C29–H29C	109.5
N8–C30–C29	177(3)
H31A–C31–H31B	109.5
H31A–C31–H31C	109.5
H31B–C31–H31C	109.5
C32–C31–H31A	109.5
C32–C31–H31B	109.5
C32–C31–H31C	109.5
N9–C32–C31	179(3)

Table 5. Torsion angles for mo\_harman\_mne\_5\_219fp\_0m

Atom–Atom–Atom–Atom	Torsion Angle [°]
W1–N1–N2–C3	175.9(10)
W1–N1–N2–B1	–8.8(17)
W1–N1–C1–C2	–177.2(11)
W1–N3–N4–C6	–175.9(13)
W1–N3–N4–B1	15(2)
W1–N3–C4–C5	176.6(15)
W1–N5–N6–C9	–171.3(10)
W1–N5–N6–B1	–2.9(18)
W1–N5–C7–C8	170.5(11)
W1–C10–C11–C12	–118.6(16)
W1–C10–C17–C16	174.9(11)
W1–C10–C17–C18	–57.6(18)
W1–C11–C12–C13	–131.1(17)
N1–N2–C3–C2	3.0(17)
N1–N2–B1–N4	64.1(18)
N1–N2–B1–N6	–52.2(18)
N1–C1–C2–C3	1.4(18)
N2–N1–C1–C2	0.3(17)
N3–N4–C6–C5	–2(2)
N3–N4–B1–N2	–67.5(18)
N3–N4–B1–N6	50.4(19)

N3–C4–C5–C6	0(3)
N4–N3–C4–C5	–1(2)
N5–N6–C9–C8	0.0(19)
N5–N6–B1–N2	60.1(18)
N5–N6–B1–N4	–57.7(19)
N5–C7–C8–C9	–2.3(19)
N6–N5–C7–C8	2.3(18)
C1–N1–N2–C3	–2.1(16)
C1–N1–N2–B1	173.2(13)
C1–C2–C3–N2	–2.7(17)
C3–N2–B1–N4	–121.9(17)
C3–N2–B1–N6	121.8(17)
C4–N3–N4–C6	2(2)
C4–N3–N4–B1	–166.9(15)
C4–C5–C6–N4	1(3)
C6–N4–B1–N2	126(2)
C6–N4–B1–N6	–116(2)
C7–N5–N6–C9	–1.4(17)
C7–N5–N6–B1	167.0(14)
C7–C8–C9–N6	1.3(19)
C9–N6–B1–N2	–134.1(16)
C9–N6–B1–N4	108.0(18)
C10–C11–C12–C13	–40(3)



C10–C17–C18–C19	170.9(13)
C11–C10–C17–C16	91.7(17)
C11–C10–C17–C18	–140.8(15)
C11–C12–C13–C14	–2(3)
C12–C13–C14–C15	–7(3)
C13–C14–C15–C16	85(2)
C14–C15–C16–C17	–58(2)
C14–C15–C16–C25	175.2(15)
C15–C16–C17–C10	–56.3(18)
C15–C16–C17–C18	174.4(14)
C16–C17–C18–C19	–61.9(18)
C17–C10–C11–W1	116.1(13)
C17–C10–C11–C12	–3(2)
C17–C18–C19–C20	–65.2(15)
C17–C18–C19–C24	116.9(13)
C18–C19–C20–C21	–177.9(12)

C18–C19–C24–C23	177.8(12)
C19–C20–C21–C22	0.0
C20–C19–C24–C23	0.0
C20–C21–C22–C23	0.0
C21–C22–C23–C24	0.0
C22–C23–C24–C19	0.0
C24–C19–C20–C21	0.0
C25–C16–C17–C10	69.9(18)
C25–C16–C17–C18	–59.5(18)
B1–N2–C3–C2	–171.5(15)
B1–N4–C6–C5	165.2(19)
B1–N6–C9–C8	–167.3(15)

## Structure Report for 3-jkh-273

A yellow, block-shaped crystal of 3-jkh-273 was coated with Paratone oil and mounted on a MiTeGen micromount. Data were collected at 100(2) K on a Bruker D8 VENTURE dual wavelength Mo/Cu Kappa four-circle diffractometer with a PHOTON III detector. The diffractometer was equipped with an Oxford Cryostream 800Plus low temperature device and used Mo  $K_\alpha$  radiation ( $\lambda = 0.71073\text{\AA}$ ) from an Incoatec  $\lambda$ ms 3.0 microfocus sealed X-ray tube with a HELIOS double bounce multilayer mirror as monochromator.

Data collection and processing were done within the Bruker APEX5 software suite.<sup>[1]</sup> All data were integrated with SAINT 8.40B using a narrow-frame algorithm and a Multi-Scan absorption correction using was applied.<sup>[2]</sup> Using [Unknown program in \_computing\_structure\_refinement] as a graphical interface,<sup>[3]</sup> the structure was solved by direct methods with SHELXT and refined by full-matrix least-squares methods against  $F^2$  using SHELXL-2019/1.<sup>[4,5]</sup> All non-hydrogen atoms were refined with anisotropic displacement parameters. The B-H hydrogen, as well as H10 and H11, were located in the electron density map and refined isotropically. All other hydrogen atoms, were placed in geometrically calculated positions with  $U_{iso} = 1.2U_{equiv}$  of the parent atom ( $1.5U_{equiv}$  for methyl).

This report and the CIF file were generated using FinalCif.<sup>[6]</sup>

Table 1. Crystal data and structure refinement for 3-jkh-273

CCDC number	
Empirical formula	$\text{C}_{30}\text{H}_{39}\text{BN}_9\text{OPW}$
Formula weight	767.33
Temperature [K]	100(2)
Crystal system	monoclinic
Space group (number)	$P2_1/c$ (14)
$a$ [Å]	16.3086(7)
$b$ [Å]	14.2555(6)
$c$ [Å]	14.4785(7)
$\alpha$ [°]	90
$\beta$ [°]	105.979(2)
$\gamma$ [°]	90
Volume [Å <sup>3</sup> ]	3236.0(3)
$Z$	4
$\rho_{\text{calc}}$ [gcm <sup>-3</sup> ]	1.575
$\mu$ [mm <sup>-1</sup> ]	3.658
$F(000)$	1536
Crystal size [mm <sup>3</sup> ]	0.126×0.134×0.184
Crystal colour	yellow
Crystal shape	block
Radiation	Mo $K_{\alpha}$ ( $\lambda=0.71073$ Å)
2 $\theta$ range [°]	5.72 to 66.26 (0.65 Å)
Index ranges	$-25 \leq h \leq 24$ $-21 \leq k \leq 19$ $-22 \leq l \leq 22$
Reflections collected	77585
Independent reflections	12304 $R_{\text{int}} = 0.0418$ $R_{\text{sigma}} = 0.0289$
Completeness to $\theta = 25.242^\circ$	99.8
Data / Restraints / Parameters	12304 / 0 / 403
Goodness-of-fit on $F^2$	1.024
Final $R$ indexes [ $\geq 2\sigma(I)$ ]	$R_1 = 0.0212$ $wR_2 = 0.0409$
Final $R$ indexes [all data]	$R_1 = 0.0275$ $wR_2 = 0.0426$
Largest peak/hole [eÅ <sup>-3</sup> ]	0.64/−0.78

Table 2. Atomic coordinates and  $U_{eq}$  [ $\text{\AA}^2$ ] for 3-jkh-273

Atom	x	y	z	$U_{eq}$
W1	0.18213(2)	0.42681(2)	0.36153(2)	0.00886(2)
P1	0.18943(3)	0.35821(3)	0.20327(3)	0.01211(7)
O1	0.10943(9)	0.25569(9)	0.43093(10)	0.0211(3)
N1	0.22623(9)	0.55753(9)	0.30325(10)	0.0122(2)
N2	0.17607(9)	0.63528(10)	0.28507(10)	0.0136(3)
N3	0.05426(9)	0.46651(10)	0.26822(10)	0.0118(2)
N4	0.03207(9)	0.55779(9)	0.24725(10)	0.0129(3)
N5	0.13112(9)	0.52638(10)	0.44908(10)	0.0119(2)
N6	0.09910(9)	0.61161(10)	0.41233(10)	0.0138(3)
N7	0.14139(9)	0.32514(10)	0.40396(10)	0.0122(2)
N8	0.27294(10)	0.13203(11)	0.34939(12)	0.0206(3)
C1	0.29883(11)	0.57999(12)	0.28164(12)	0.0149(3)
H1	0.345780	0.538752	0.287712	0.018
C2	0.29555(12)	0.67217(13)	0.24910(13)	0.0185(3)
H2	0.338104	0.705442	0.229003	0.022
C3	0.21666(12)	0.70443(12)	0.25255(13)	0.0190(3)
H3	0.194676	0.765533	0.234830	0.023
C4	-0.04869(11)	0.56225(13)	0.19038(13)	0.0181(3)
H4	-0.078954	0.618010	0.166246	0.022
C5	-0.07981(11)	0.47221(13)	0.17325(13)	0.0201(3)
H5	-0.134614	0.453434	0.135240	0.024
C6	-0.01362(11)	0.41471(12)	0.22367(12)	0.0159(3)
H6	-0.016207	0.348216	0.226138	0.019
C7	0.11484(11)	0.51807(13)	0.53457(12)	0.0167(3)
H7	0.129105	0.465075	0.575651	0.020
C8	0.07392(11)	0.59848(14)	0.55455(13)	0.0208(4)

H8	0.056340	0.611178	0.610626	0.025
C9	0.06458(11 )	0.65517(13 )	0.47581(13 )	0.0184(3)
H9	0.038200	0.715162	0.467229	0.022
C10	0.31669(10 )	0.37699(11 )	0.40863(11 )	0.0115(3)
H10	0.3497(13)	0.3977(14)	0.3680(15)	0.014
C11	0.30253(11 )	0.44679(11 )	0.47602(12 )	0.0126(3)
H11	0.3170(12)	0.5060(14)	0.4624(14)	0.011(5)
C12	0.31120(10 )	0.43139(12 )	0.57958(11 )	0.0137(3)
H12	0.265869	0.456828	0.601144	0.016
C13	0.37109(11 )	0.38830(12 )	0.64789(12 )	0.0148(3)
H13	0.359452	0.387272	0.708666	0.018
C14	0.45351(11 )	0.34099(13 )	0.64763(12 )	0.0170(3)
H14A	0.450139	0.275280	0.668419	0.020
H14B	0.499597	0.371722	0.697540	0.020
C15	0.48161(10 )	0.33847(12 )	0.55522(12 )	0.0146(3)
H15A	0.469486	0.400207	0.523038	0.017
H15B	0.544054	0.328466	0.572189	0.017
C16	0.43792(10 )	0.26216(11 )	0.48455(11 )	0.0125(3)
H16	0.447674	0.200945	0.519612	0.015
C17	0.33962(10 )	0.27898(11 )	0.45029(11 )	0.0115(3)
H17	0.319289	0.275923	0.509382	0.014
C18	0.29963(11 )	0.19900(12 )	0.39014(12 )	0.0147(3)
C19	0.47592(10 )	0.25398(13 )	0.39838(12 )	0.0151(3)
H19A	0.444878	0.204608	0.354373	0.018
H19B	0.467362	0.314066	0.362719	0.018
C20	0.56980(10 )	0.23065(12 )	0.42814(12 )	0.0146(3)
C21	0.59786(12 )	0.13854(13 )	0.44682(14 )	0.0205(4)
H21	0.557532	0.088924	0.437698	0.025
C22	0.68505(13 )	0.11866(15 )	0.47893(15 )	0.0264(4)
H22	0.703849	0.055729	0.491948	0.032
C23	0.74399(12 )	0.19081(16 )	0.49175(14 )	0.0259(4)
H23	0.803205	0.177373	0.514422	0.031

C24	0.71685(12) )	0.28252(15) )	0.47160(14) )	0.0230(4)
H24	0.757360	0.331863	0.479607	0.028
C25	0.63054(11) )	0.30197(13) )	0.43977(13) )	0.0182(3)
H25	0.612255	0.364917	0.425587	0.022
C26	0.29180(11) )	0.33717(14) )	0.17988(13) )	0.0190(3)
H26A	0.322754	0.288487	0.223537	0.028
H26B	0.325247	0.395246	0.190240	0.028
H26C	0.282586	0.316444	0.113268	0.028
C27	0.13560(12) )	0.24673(12) )	0.16954(13) )	0.0182(3)
H27A	0.078550	0.249520	0.179368	0.027
H27B	0.168564	0.196630	0.209332	0.027
H27C	0.130648	0.233878	0.101729	0.027
C28	0.13981(12) )	0.43400(13) )	0.10129(12) )	0.0200(3)
H28A	0.168375	0.495150	0.109933	0.030
H28B	0.079330	0.442466	0.097446	0.030
H28C	0.145147	0.405004	0.041847	0.030
B1	0.08870(12) )	0.63588(13) )	0.30613(14) )	0.0145(3)
H1A	0.0578(13)	0.7046(15)	0.2900(15)	0.017(5)
N9	0.51106(16) )	0.56074(17) )	0.7901(2)	0.0596(8)
C29	0.35356(17) )	0.58497(15) )	0.79132(17) )	0.0361(5)
H29A	0.350247	0.635041	0.836538	0.054
H29B	0.331396	0.526563	0.810875	0.054
H29C	0.319486	0.602331	0.726649	0.054
C30	0.44202(18) )	0.57157(16) )	0.79119(18) )	0.0387(6)

$U_{eq}$  is defined as 1/3 of the trace of the orthogonalized  $U_{ij}$  tensor.

Table 3. Anisotropic displacement parameters ( $\text{\AA}^2$ ) for 3-jkh-273. The anisotropic displacement factor exponent takes the form:

$$-2\pi^2 [h^2(a^*)^2 U_{11} + k^2(b^*)^2 U_{22} + \dots + 2hka^*b^* U_{12}]$$

Atom	$U_{11}$	$U_{22}$	$U_{33}$	$U_{23}$	$U_{13}$	$U_{12}$
W1	0.00974(3)	0.00836(3)	0.00859(3)	−0.00028(2)	0.00271(2)	−0.00008(2)
P1	0.01333(18)	0.01335(18)	0.01011(17)	−0.00163(14)	0.00401(14)	0.00022(15)
O1	0.0297(7)	0.0148(6)	0.0223(6)	0.0009(5)	0.0129(6)	−0.0079(5)
N1	0.0124(6)	0.0107(6)	0.0137(6)	0.0006(5)	0.0038(5)	0.0003(5)
N2	0.0155(6)	0.0101(6)	0.0149(6)	0.0014(5)	0.0037(5)	0.0009(5)

N3	0.0131(6)	0.0106(6)	0.0119(6)	−0.0004(5)	0.0036(5)	0.0004(5)
N4	0.0139(6)	0.0110(6)	0.0130(6)	0.0002(5)	0.0021(5)	0.0028(5)
N5	0.0117(6)	0.0129(6)	0.0113(6)	−0.0011(5)	0.0033(5)	−0.0004(5)
N6	0.0117(6)	0.0134(6)	0.0157(6)	−0.0033(5)	0.0030(5)	0.0017(5)
N7	0.0148(6)	0.0114(6)	0.0110(6)	0.0000(5)	0.0045(5)	−0.0010(5)
N8	0.0196(7)	0.0168(7)	0.0248(8)	−0.0024(6)	0.0049(6)	0.0002(6)
C1	0.0158(7)	0.0138(7)	0.0163(7)	0.0005(6)	0.0062(6)	−0.0012(6)
C2	0.0198(8)	0.0164(8)	0.0203(8)	0.0035(6)	0.0072(7)	−0.0033(7)
C3	0.0226(9)	0.0116(7)	0.0227(8)	0.0049(6)	0.0061(7)	−0.0002(6)
C4	0.0148(7)	0.0199(8)	0.0166(7)	0.0000(6)	−0.0008(6)	0.0054(7)
C5	0.0133(8)	0.0224(9)	0.0208(8)	−0.0030(7)	−0.0015(6)	0.0002(7)
C6	0.0144(7)	0.0163(8)	0.0163(7)	−0.0029(6)	0.0028(6)	−0.0023(6)
C7	0.0134(7)	0.0248(9)	0.0132(7)	−0.0017(6)	0.0058(6)	−0.0015(7)
C8	0.0145(8)	0.0310(10)	0.0182(8)	−0.0094(7)	0.0068(6)	−0.0011(7)
C9	0.0109(7)	0.0218(8)	0.0221(8)	−0.0106(7)	0.0036(6)	0.0017(6)
C10	0.0119(7)	0.0112(7)	0.0110(6)	0.0000(5)	0.0024(5)	0.0000(6)
C11	0.0142(7)	0.0105(7)	0.0119(7)	−0.0005(5)	0.0018(6)	0.0008(6)
C12	0.0141(7)	0.0143(7)	0.0123(6)	−0.0029(6)	0.0030(5)	0.0009(6)
C13	0.0178(8)	0.0159(7)	0.0108(7)	−0.0019(6)	0.0040(6)	0.0005(6)
C14	0.0164(8)	0.0233(9)	0.0099(7)	−0.0013(6)	0.0015(6)	0.0041(7)
C15	0.0108(7)	0.0202(8)	0.0122(7)	−0.0029(6)	0.0021(6)	0.0002(6)
C16	0.0123(7)	0.0138(7)	0.0114(7)	−0.0001(5)	0.0032(5)	0.0018(6)
C17	0.0122(7)	0.0113(7)	0.0109(6)	−0.0005(5)	0.0029(5)	0.0006(6)
C18	0.0135(7)	0.0137(7)	0.0169(7)	0.0022(6)	0.0045(6)	0.0025(6)
C19	0.0126(7)	0.0206(8)	0.0119(7)	−0.0030(6)	0.0032(6)	0.0015(6)
C20	0.0126(7)	0.0191(8)	0.0122(7)	−0.0024(6)	0.0039(6)	0.0011(6)
C21	0.0206(9)	0.0198(8)	0.0229(9)	0.0002(7)	0.0087(7)	0.0017(7)
C22	0.0260(10)	0.0288(10)	0.0265(10)	0.0071(8)	0.0109(8)	0.0121(8)
C23	0.0132(8)	0.0424(12)	0.0214(9)	0.0031(8)	0.0035(7)	0.0055(8)
C24	0.0151(8)	0.0325(10)	0.0207(9)	−0.0060(8)	0.0039(7)	−0.0033(8)
C25	0.0168(8)	0.0200(8)	0.0182(8)	−0.0052(6)	0.0057(6)	−0.0007(7)
C26	0.0178(8)	0.0247(9)	0.0167(8)	−0.0041(7)	0.0087(6)	0.0003(7)
C27	0.0201(8)	0.0170(8)	0.0166(8)	−0.0051(6)	0.0038(6)	−0.0029(7)
C28	0.0249(9)	0.0231(9)	0.0123(7)	0.0025(7)	0.0054(6)	0.0032(7)
B1	0.0135(8)	0.0119(8)	0.0171(8)	0.0004(6)	0.0026(7)	0.0028(7)
N9	0.0420(14)	0.0432(14)	0.080(2)	0.0136(13)	−0.0059(13)	−0.0172(11)
C29	0.0615(16)	0.0211(10)	0.0303(11)	0.0003(8)	0.0201(11)	0.0006(10)
C30	0.0525(15)	0.0224(10)	0.0337(12)	0.0038(9)	−0.0008(11)	−0.0131(11)

Table 4. Bond lengths and angles for 3-jkh-273

Atom–Atom	Length [Å]	W1–C10	2.2274(16)
W1–N7	1.7732(13)	W1–N1	2.2442(13)
W1–C11	2.2119(17)	W1–P1	2.5241(4)
W1–N5	2.2123(13)	P1–C27	1.8162(18)
W1–N3	2.2234(14)	P1–C26	1.8174(17)

P1–C28	1.8287(18)
O1–N7	1.2314(17)
N1–C1	1.344(2)
N1–N2	1.3596(19)
N2–C3	1.343(2)
N2–B1	1.537(2)
N3–C6	1.339(2)
N3–N4	1.3624(19)
N4–C4	1.349(2)
N4–B1	1.544(2)
N5–C7	1.341(2)
N5–N6	1.371(2)
N6–C9	1.354(2)
N6–B1	1.539(2)
N8–C18	1.144(2)
C1–C2	1.392(2)
C1–H1	0.9500
C2–C3	1.380(3)
C2–H2	0.9500
C3–H3	0.9500
C4–C5	1.377(3)
C4–H4	0.9500
C5–C6	1.392(2)
C5–H5	0.9500
C6–H6	0.9500
C7–C8	1.396(3)
C7–H7	0.9500
C8–C9	1.371(3)
C8–H8	0.9500
C9–H9	0.9500
C10–C11	1.456(2)
C10–C17	1.527(2)
C10–H10	0.95(2)
C11–C12	1.483(2)
C11–H11	0.91(2)
C12–C13	1.333(2)
C12–H12	0.9500
C13–C14	1.505(2)
C13–H13	0.9500
C14–C15	1.529(2)
C14–H14A	0.9900
C14–H14B	0.9900
C15–C16	1.529(2)
C15–H15A	0.9900
C15–H15B	0.9900
C16–C19	1.543(2)
C16–C17	1.561(2)
C16–H16	1.0000

C17–C18	1.473(2)
C17–H17	1.0000
C19–C20	1.509(2)
C19–H19A	0.9900
C19–H19B	0.9900
C20–C21	1.392(2)
C20–C25	1.397(2)
C21–C22	1.398(3)
C21–H21	0.9500
C22–C23	1.385(3)
C22–H22	0.9500
C23–C24	1.385(3)
C23–H23	0.9500
C24–C25	1.383(3)
C24–H24	0.9500
C25–H25	0.9500
C26–H26A	0.9800
C26–H26B	0.9800
C26–H26C	0.9800
C27–H27A	0.9800
C27–H27B	0.9800
C27–H27C	0.9800
C28–H28A	0.9800
C28–H28B	0.9800
C28–H28C	0.9800
B1–H1A	1.10(2)
N9–C30	1.141(4)
C29–C30	1.456(4)
C29–H29A	0.9800
C29–H29B	0.9800
C29–H29C	0.9800
Atom–Atom– Atom	Angle [°]
N7–W1–C11	100.70(6)
N7–W1–N5	95.17(6)
C11–W1–N5	83.35(5)
N7–W1–N3	92.31(6)
C11–W1–N3	155.96(5)
N5–W1–N3	75.35(5)
N7–W1–C10	93.72(6)
C11–W1–C10	38.29(6)
N5–W1–C10	121.55(5)
N3–W1–C10	161.35(5)
N7–W1–N1	176.81(6)
C11–W1–N1	82.21(6)
N5–W1–N1	83.84(5)
N3–W1–N1	84.51(5)

C10-W1-N1	89.38(5)
N7-W1-P1	96.53(4)
C11-W1-P1	118.44(4)
N5-W1-P1	152.61(4)
N3-W1-P1	79.50(4)
C10-W1-P1	82.28(4)
N1-W1-P1	83.12(4)
C27-P1-C26	101.91(9)
C27-P1-C28	103.08(9)
C26-P1-C28	99.91(9)
C27-P1-W1	116.29(6)
C26-P1-W1	120.55(6)
C28-P1-W1	112.53(6)
C1-N1-N2	106.41(13)
C1-N1-W1	132.80(11)
N2-N1-W1	120.78(10)
C3-N2-N1	109.75(14)
C3-N2-B1	129.71(15)
N1-N2-B1	120.49(13)
C6-N3-N4	106.60(14)
C6-N3-W1	131.68(11)
N4-N3-W1	121.71(10)
C4-N4-N3	109.62(14)
C4-N4-B1	129.64(14)
N3-N4-B1	118.92(13)
C7-N5-N6	106.59(13)
C7-N5-W1	132.34(12)
N6-N5-W1	120.63(10)
C9-N6-N5	109.17(14)
C9-N6-B1	128.55(15)
N5-N6-B1	120.82(13)
O1-N7-W1	177.07(13)
N1-C1-C2	110.45(15)
N1-C1-H1	124.8
C2-C1-H1	124.8
C3-C2-C1	104.58(15)
C3-C2-H2	127.7
C1-C2-H2	127.7
N2-C3-C2	108.82(15)
N2-C3-H3	125.6
C2-C3-H3	125.6
N4-C4-C5	108.39(15)
N4-C4-H4	125.8
C5-C4-H4	125.8
C4-C5-C6	105.09(16)
C4-C5-H5	127.5
C6-C5-H5	127.5
N3-C6-C5	110.30(16)

N3-C6-H6	124.9
C5-C6-H6	124.9
N5-C7-C8	110.26(16)
N5-C7-H7	124.9
C8-C7-H7	124.9
C9-C8-C7	105.17(15)
C9-C8-H8	127.4
C7-C8-H8	127.4
N6-C9-C8	108.80(16)
N6-C9-H9	125.6
C8-C9-H9	125.6
C11-C10-C17	115.30(13)
C11-C10-W1	70.28(9)
C17-C10-W1	121.75(11)
C11-C10-H10	115.2(13)
C17-C10-H10	114.3(13)
W1-C10-H10	113.0(13)
C10-C11-C12	126.00(14)
C10-C11-W1	71.43(9)
C12-C11-W1	123.81(11)
C10-C11-H11	112.9(12)
C12-C11-H11	113.4(13)
W1-C11-H11	100.8(13)
C13-C12-C11	131.65(15)
C13-C12-H12	114.2
C11-C12-H12	114.2
C12-C13-C14	132.62(15)
C12-C13-H13	113.7
C14-C13-H13	113.7
C13-C14-C15	119.72(14)
C13-C14-H14A	107.4
C15-C14-H14A	107.4
C13-C14-H14B	107.4
C15-C14-H14B	107.4
H14A-C14-H14B	106.9
C16-C15-C14	113.93(14)
C16-C15-H15A	108.8
C14-C15-H15A	108.8
C16-C15-H15B	108.8
C14-C15-H15B	108.8
H15A-C15-H15B	107.7
C15-C16-C19	112.21(13)
C15-C16-C17	110.62(13)
C19-C16-C17	111.15(13)
C15-C16-H16	107.5
C19-C16-H16	107.5
C17-C16-H16	107.5



C18–C17–C10	117.01(13)
C18–C17–C16	108.53(13)
C10–C17–C16	112.62(13)
C18–C17–H17	106.0
C10–C17–H17	106.0
C16–C17–H17	106.0
N8–C18–C17	174.08(18)
C20–C19–C16	112.81(13)
C20–C19–H19A	109.0
C16–C19–H19A	109.0
C20–C19–H19B	109.0
C16–C19–H19B	109.0
H19A–C19– H19B	107.8
C21–C20–C25	118.60(16)
C21–C20–C19	121.12(16)
C25–C20–C19	120.27(16)
C20–C21–C22	120.38(18)
C20–C21–H21	119.8
C22–C21–H21	119.8
C23–C22–C21	119.93(19)
C23–C22–H22	120.0
C21–C22–H22	120.0
C22–C23–C24	120.19(18)
C22–C23–H23	119.9
C24–C23–H23	119.9
C25–C24–C23	119.75(18)
C25–C24–H24	120.1
C23–C24–H24	120.1
C24–C25–C20	121.13(18)
C24–C25–H25	119.4
C20–C25–H25	119.4
P1–C26–H26A	109.5
P1–C26–H26B	109.5
H26A–C26– H26B	109.5
P1–C26–H26C	109.5
H26A–C26– H26C	109.5

H26B–C26– H26C	109.5
P1–C27–H27A	109.5
P1–C27–H27B	109.5
H27A–C27– H27B	109.5
P1–C27–H27C	109.5
H27A–C27– H27C	109.5
H27B–C27– H27C	109.5
P1–C28–H28A	109.5
P1–C28–H28B	109.5
H28A–C28– H28B	109.5
P1–C28–H28C	109.5
H28A–C28– H28C	109.5
H28B–C28– H28C	109.5
N2–B1–N6	110.10(14)
N2–B1–N4	109.43(14)
N6–B1–N4	105.91(14)
N2–B1–H1A	111.0(11)
N6–B1–H1A	109.3(11)
N4–B1–H1A	110.9(11)
C30–C29–H29A	109.5
C30–C29–H29B	109.5
H29A–C29– H29B	109.5
C30–C29–H29C	109.5
H29A–C29– H29C	109.5
H29B–C29– H29C	109.5
N9–C30–C29	179.3(3)

Table 5. Torsion angles for 3-jkh-273

Atom–Atom– Atom–Atom	Torsion Angle [°]
C1–N1–N2–C3	0.20(18)
W1–N1–N2–C3	178.86(11)
C1–N1–N2–B1	–177.37(15)
W1–N1–N2–B1	1.29(19)

C6–N3–N4–C4	0.03(18)
W1–N3–N4–C4	–179.46(11)
C6–N3–N4–B1	166.17(14)
W1–N3–N4–B1	–13.32(18)
C7–N5–N6–C9	0.76(18)
W1–N5–N6–C9	174.06(11)

C7–N5–N6–B1	–166.56(15)
W1–N5–N6–B1	6.74(19)
N2–N1–C1–C2	–0.24(19)
W1–N1–C1–C2	–178.68(12)
N1–C1–C2–C3	0.2(2)
N1–N2–C3–C2	–0.1(2)
B1–N2–C3–C2	177.20(17)
C1–C2–C3–N2	–0.1(2)
N3–N4–C4–C5	–0.4(2)
B1–N4–C4–C5	–164.59(17)
N4–C4–C5–C6	0.6(2)
N4–N3–C6–C5	0.34(19)
W1–N3–C6–C5	179.76(12)
C4–C5–C6–N3	–0.6(2)
N6–N5–C7–C8	–1.25(19)
W1–N5–C7–C8	–173.45(12)
N5–C7–C8–C9	1.3(2)
N5–N6–C9–C8	0.02(19)
B1–N6–C9–C8	166.07(16)
C7–C8–C9–N6	–0.8(2)
C17–C10–C11–C12	2.1(2)
W1–C10–C11–C12	118.78(17)
C17–C10–C11–W1	–116.67(13)
C10–C11–C12–C13	45.0(3)
W1–C11–C12–C13	135.75(17)
C11–C12–C13–C14	1.7(3)
C12–C13–C14–C15	1.0(3)
C13–C14–C15–C16	–80.4(2)
C14–C15–C16–C19	–172.92(14)
C14–C15–C16–C17	62.33(18)
C11–C10–C17–C18	138.67(15)
W1–C10–C17–C18	57.09(17)

C11–C10–C17–C16	–94.55(16)
W1–C10–C17–C16	–176.14(10)
C15–C16–C17–C18	–174.49(13)
C19–C16–C17–C18	60.15(17)
C15–C16–C17–C10	54.33(17)
C19–C16–C17–C10	–71.03(17)
C15–C16–C19–C20	59.73(19)
C17–C16–C19–C20	–175.81(14)
C16–C19–C20–C21	82.5(2)
C16–C19–C20–C25	–95.88(19)
C25–C20–C21–C22	1.6(3)
C19–C20–C21–C22	–176.81(16)
C20–C21–C22–C23	–0.4(3)
C21–C22–C23–C24	–0.9(3)
C22–C23–C24–C25	0.8(3)
C23–C24–C25–C20	0.5(3)
C21–C20–C25–C24	–1.7(3)
C19–C20–C25–C24	176.76(16)
C3–N2–B1–N6	–120.47(19)
N1–N2–B1–N6	56.56(19)
C3–N2–B1–N4	123.52(18)
N1–N2–B1–N4	–59.45(19)
C9–N6–B1–N2	133.40(17)
N5–N6–B1–N2	–61.97(19)
C9–N6–B1–N4	–108.39(18)
N5–N6–B1–N4	56.24(18)
C4–N4–B1–N2	–130.29(17)
N3–N4–B1–N2	66.75(18)
C4–N4–B1–N6	111.05(18)
N3–N4–B1–N6	–51.90(18)

## Structure Report for 4-jkh-033

A colourless, needle-shaped crystal of 4-jkh-033 was coated with Paratone oil and mounted on a MiTeGen micromount. Data were collected at 100(2) K on a Bruker D8 VENTURE dual wavelength Mo/Cu Kappa four-circle diffractometer with a PHOTON III detector. The diffractometer was equipped with an Oxford Cryostream 800Plus low temperature device and used Mo  $K_\alpha$  radiation ( $\lambda = 0.71073\text{\AA}$ ) from an Incoatec  $\lambda/\text{ms}$  3.0 microfocus sealed X-ray tube with a HELIOS double bounce multilayer mirror as monochromator.

Data collection and processing were done within the Bruker APEX5 software suite.<sup>[1]</sup> All data were integrated with SAINT 8.40B using a narrow-frame algorithm and a Multi-Scan absorption correction using was applied.<sup>[2]</sup> Using [Unknown program in \_computing\_structure\_refinement] as a graphical interface,<sup>[3]</sup> the structure was solved by direct methods with SHELXT and refined by full-matrix least-squares methods against  $F^2$  using SHELXL-2019/2.<sup>[4,5]</sup> All non-hydrogen atoms were refined with anisotropic displacement parameters. The B-H hydrogen was located in the electron density map and refined isotropically. All other hydrogen atoms were refined with isotropic displacement parameters. Some of their coordinates were refined freely and some on calculated positions using a riding model with their  $U_{\text{iso}}$  values constrained to 1.5 times the  $U_{\text{eq}}$  of their pivot atoms for terminal  $\text{sp}^3$  carbon atoms and 1.2 times for all other carbon atoms.

This report and the CIF file were generated using FinalCif.<sup>[6]</sup>

Table 1. Crystal data and structure refinement for 4-jkh-033

CCDC number	
Empirical formula	$\text{C}_{29}\text{H}_{40}\text{BN}_8\text{OPW}$
Formula weight	742.32
Temperature [K]	100(2)
Crystal system	monoclinic
Space group (number)	$P2_1/c$ (14)
$a$ [Å]	17.3257(8)
$b$ [Å]	17.5232(9)
$c$ [Å]	10.2765(4)
$\alpha$ [°]	90
$\beta$ [°]	96.688(2)
$\gamma$ [°]	90
Volume [Å <sup>3</sup> ]	3098.7(2)
$Z$	4
$\rho_{\text{calc}}$ [gcm <sup>-3</sup> ]	1.591
$\mu$ [mm <sup>-1</sup> ]	3.816
$F(000)$	1488
Crystal size [mm <sup>3</sup> ]	0.040×0.103×0.165
Crystal colour	colourless
Crystal shape	needle
Radiation	Mo $K_{\alpha}$ ( $\lambda=0.71073$ Å)
2 $\theta$ range [°]	5.22 to 57.43 (0.74 Å)

Index ranges	$-22 \leq h \leq 23$ $-23 \leq k \leq 23$ $-13 \leq l \leq 13$
Reflections collected	43547
Independent reflections	8007 $R_{\text{int}} = 0.0766$ $R_{\text{sigma}} = 0.0611$
Completeness to $\theta = 25.242^\circ$	99.9
Data / Restraints / Parameters	8007 / 0 / 378
Goodness-of-fit on $F^2$	0.995
Final $R$ indexes [ $I \geq 2\sigma(I)$ ]	$R_1 = 0.0359$ $wR_2 = 0.0717$
Final $R$ indexes [all data]	$R_1 = 0.0609$ $wR_2 = 0.0800$
Largest peak/hole [ $\text{e}\text{\AA}^{-3}$ ]	1.70/-0.68

Table 2. Atomic coordinates and  $U_{eq}$  [ $\text{\AA}^2$ ] for 4-jkh-033

Atom	x	y	z	$U_{eq}$
W1	0.29573(2)	0.46867(2)	0.67318(2)	0.01799(6)
P1	0.15304(7)	0.43448(7)	0.66474(11)	0.0243(2)
O1	0.3226(2)	0.44493(18)	0.3935(3)	0.0354(8)
N1	0.2872(2)	0.48652(19)	0.8860(3)	0.0208(8)
N2	0.3339(2)	0.4457(2)	0.9781(3)	0.0249(8)
N3	0.3026(2)	0.34569(19)	0.7307(3)	0.0241(8)
N4	0.3396(2)	0.3250(2)	0.8508(3)	0.0288(9)
N5	0.4182(2)	0.4443(2)	0.7280(3)	0.0226(8)
N6	0.4459(2)	0.4180(2)	0.8494(3)	0.0273(8)
N7	0.3085(2)	0.45410(18)	0.5071(3)	0.0208(7)
N8	0.1277(2)	0.5269(2)	0.3395(4)	0.0328(9)
C1	0.2445(3)	0.5328(2)	0.9515(4)	0.0249(9)
H1	0.207028	0.567921	0.912101	0.030
C2	0.2626(3)	0.5226(3)	1.0861(4)	0.0315(11)
H2	0.240477	0.547921	1.154592	0.038
C3	0.3197(3)	0.4674(3)	1.0977(4)	0.0316(11)
H3	0.344896	0.447973	1.177858	0.038
C4	0.2757(3)	0.2807(3)	0.6724(5)	0.0339(11)
H4	0.247390	0.277833	0.587622	0.041
C5	0.2949(3)	0.2194(3)	0.7519(5)	0.0384(13)
H5	0.282115	0.167360	0.734302	0.046
C6	0.3362(3)	0.2486(2)	0.8621(5)	0.0363(12)
H6	0.358879	0.219723	0.934929	0.044
C7	0.4778(3)	0.4426(3)	0.6561(5)	0.0295(10)
H7	0.474706	0.456842	0.566488	0.035
C8	0.5442(3)	0.4172(3)	0.7302(5)	0.0373(12)
H8	0.594429	0.411474	0.703142	0.045
C9	0.5222(3)	0.4021(3)	0.8509(5)	0.0366(11)
H9	0.555330	0.383437	0.924170	0.044
C10	0.2498(2)	0.5850(2)	0.6285(4)	0.0186(8)
H10	0.211936	0.602952	0.688135	0.022
C11	0.3308(3)	0.5903(2)	0.6848(4)	0.0217(9)
H11	0.332950	0.607864	0.777743	0.026
C12	0.4000(2)	0.6244(2)	0.6237(4)	0.0215(9)
H12	0.408196	0.594141	0.543857	0.026
C13	0.3973(3)	0.7099(3)	0.5876(5)	0.0315(10)
H13A	0.392783	0.738335	0.669578	0.038

H13B	0.448774	0.722902	0.560637	0.038
C14	0.3367(3)	0.7429(3)	0.4839(4)	0.0294(10)
H14A	0.333628	0.710290	0.404806	0.035
H14B	0.353806	0.794271	0.459204	0.035
C15	0.2557(3)	0.7493(2)	0.5277(5)	0.0316(11)
H15A	0.260544	0.744355	0.624230	0.038
H15B	0.235226	0.801005	0.505217	0.038
C16	0.1972(2)	0.6913(2)	0.4688(4)	0.0258(10)
H16	0.187832	0.701699	0.372539	0.031
C17	0.2292(2)	0.6086(2)	0.4859(4)	0.0203(9)
H17	0.278542	0.607091	0.444291	0.024
C18	0.1737(3)	0.5595(3)	0.4070(4)	0.0257(9)
C19	0.1187(3)	0.7004(2)	0.5240(5)	0.0294(10)
H19A	0.087059	0.654189	0.501267	0.035
H19B	0.128638	0.702946	0.620728	0.035
C20	0.0722(3)	0.7692(3)	0.4758(4)	0.0279(10)
C21	0.0733(3)	0.8357(3)	0.5474(5)	0.0341(11)
H21	0.106107	0.839921	0.627894	0.041
C22	0.0263(3)	0.8970(3)	0.5018(6)	0.0481(15)
H22	0.027701	0.943188	0.550412	0.058
C23	-0.0216(3)	0.8904(4)	0.3877(7)	0.0582(19)
H23	-0.055338	0.931345	0.358984	0.070
C24	-0.0217(3)	0.8267(4)	0.3153(6)	0.0524(16)
H24	-0.053993	0.823718	0.234220	0.063
C25	0.0247(3)	0.7652(3)	0.3573(5)	0.0415(13)
H25	0.024207	0.720364	0.305229	0.050
C26	0.4731(3)	0.6176(3)	0.7232(5)	0.0340(11)
H26A	0.472805	0.658039	0.788899	0.051
H26B	0.519463	0.622596	0.677667	0.051
H26C	0.473476	0.567685	0.766385	0.051
C27	0.0796(3)	0.5074(3)	0.6695(5)	0.0345(11)
H27A	0.096165	0.543865	0.739594	0.052
H27B	0.030466	0.483739	0.686226	0.052
H27C	0.072329	0.534257	0.585281	0.052
C28	0.1116(3)	0.3763(3)	0.5267(4)	0.0341(11)
H28A	0.126734	0.397473	0.445081	0.051
H28B	0.054831	0.376257	0.522866	0.051
H28C	0.131026	0.323894	0.537893	0.051
C29	0.1343(3)	0.3767(3)	0.8058(4)	0.0335(11)
H29A	0.165809	0.330143	0.808435	0.050
H29B	0.079112	0.362965	0.798037	0.050
H29C	0.147907	0.405941	0.886451	0.050
B1	0.3879(3)	0.3841(3)	0.9371(5)	0.0298(12)
H1A	0.414(3)	0.358(2)	1.018(4)	0.030(12)

$U_{eq}$  is defined as 1/3 of the trace of the orthogonalized  $U_{ij}$  tensor.

Table 3. Anisotropic displacement parameters ( $\text{\AA}^2$ ) for 4-jkh-033. The anisotropic displacement factor exponent takes the form:

$$-2\pi^2 [h^2(a^*)^2U_{11} + k^2(b^*)^2U_{22} + \dots + 2hka^*b^*U_{12}]$$

Atom	$U_{11}$	$U_{22}$	$U_{33}$	$U_{23}$	$U_{13}$	$U_{12}$
W1	0.02287(9)	0.01622(8)	0.01549(8)	0.00040(7)	0.00488(6)	0.00023(8)
P1	0.0258(6)	0.0234(6)	0.0244(6)	-0.0005(4)	0.0057(5)	-0.0042(5)
O1	0.055(2)	0.0369(18)	0.0169(15)	-0.0043(13)	0.0143(15)	-0.0003(17)
N1	0.027(2)	0.0211(19)	0.0149(16)	0.0006(13)	0.0038(14)	0.0007(15)
N2	0.032(2)	0.0252(19)	0.0181(17)	0.0045(14)	0.0046(15)	-0.0025(16)
N3	0.030(2)	0.0191(18)	0.0245(18)	0.0024(15)	0.0091(16)	0.0031(16)
N4	0.038(2)	0.025(2)	0.0254(19)	0.0052(15)	0.0140(17)	0.0067(17)
N5	0.0213(19)	0.0227(18)	0.0242(18)	0.0045(14)	0.0047(15)	0.0053(15)
N6	0.027(2)	0.030(2)	0.0239(18)	0.0078(15)	0.0015(16)	0.0067(17)
N7	0.0226(19)	0.0165(18)	0.0238(17)	-0.0007(13)	0.0052(15)	-0.0060(14)
N8	0.031(2)	0.043(2)	0.0243(19)	-0.0027(17)	0.0016(17)	-0.0045(19)
C1	0.032(2)	0.021(2)	0.024(2)	-0.0047(17)	0.0115(18)	-0.004(2)
C2	0.045(3)	0.034(3)	0.018(2)	-0.0083(18)	0.009(2)	-0.008(2)
C3	0.044(3)	0.035(3)	0.017(2)	0.0025(19)	0.0073(19)	-0.006(2)
C4	0.041(3)	0.027(2)	0.036(3)	-0.004(2)	0.015(2)	-0.002(2)
C5	0.058(4)	0.017(2)	0.044(3)	-0.003(2)	0.021(3)	0.000(2)
C6	0.055(3)	0.019(2)	0.039(3)	0.012(2)	0.019(2)	0.011(2)
C7	0.033(3)	0.027(2)	0.031(2)	0.0079(19)	0.012(2)	0.000(2)
C8	0.026(3)	0.044(3)	0.042(3)	0.003(2)	0.007(2)	0.009(2)
C9	0.027(3)	0.042(3)	0.038(3)	0.004(2)	-0.004(2)	0.007(2)
C10	0.021(2)	0.018(2)	0.0166(18)	-0.0017(15)	0.0005(16)	0.0009(17)
C11	0.026(2)	0.018(2)	0.021(2)	-0.0035(16)	0.0022(17)	-0.0021(18)
C12	0.020(2)	0.020(2)	0.025(2)	0.0028(16)	0.0045(17)	-0.0010(17)
C13	0.028(3)	0.028(2)	0.038(3)	0.008(2)	0.000(2)	-0.004(2)
C14	0.027(2)	0.022(2)	0.038(3)	0.0116(19)	0.002(2)	-0.0032(19)
C15	0.034(3)	0.020(2)	0.040(3)	0.0065(19)	0.000(2)	0.003(2)
C16	0.025(2)	0.025(2)	0.027(2)	0.0110(18)	0.0016(18)	0.0076(19)
C17	0.018(2)	0.023(2)	0.0189(19)	0.0008(16)	-0.0012(16)	-0.0012(17)
C18	0.028(2)	0.029(2)	0.020(2)	0.0031(17)	0.0046(19)	-0.001(2)
C19	0.027(2)	0.022(2)	0.040(3)	0.0065(19)	0.004(2)	0.0064(19)
C20	0.028(2)	0.027(2)	0.030(2)	0.0101(19)	0.010(2)	0.004(2)
C21	0.035(3)	0.031(3)	0.038(3)	0.007(2)	0.009(2)	0.007(2)
C22	0.054(4)	0.031(3)	0.064(4)	0.020(3)	0.028(3)	0.017(3)

C23	0.040(3)	0.058(4)	0.081(5)	0.048(4)	0.025(3)	0.021(3)
C24	0.036(3)	0.069(4)	0.051(3)	0.034(3)	−0.002(3)	0.002(3)
C25	0.034(3)	0.051(3)	0.038(3)	0.013(2)	−0.001(2)	−0.006(3)
C26	0.025(3)	0.033(3)	0.042(3)	0.006(2)	−0.004(2)	−0.004(2)
C27	0.026(3)	0.041(3)	0.038(3)	−0.001(2)	0.010(2)	−0.004(2)
C28	0.036(3)	0.036(3)	0.030(2)	−0.007(2)	0.001(2)	−0.010(2)
C29	0.035(3)	0.032(3)	0.035(3)	0.004(2)	0.011(2)	−0.009(2)
B1	0.039(3)	0.030(3)	0.021(2)	0.012(2)	0.005(2)	0.003(2)

Table 4. Bond lengths and angles for 4-jkh-033

Atom–Atom	Length [Å]		
W1–N7	1.765(3)	C9–H9	0.9500
W1–N5	2.174(4)	C10–C11	1.456(6)
W1–C11	2.216(4)	C10–C17	1.524(5)
W1–C10	2.217(4)	C10–H10	1.0000
W1–N1	2.231(3)	C11–C12	1.538(6)
W1–N3	2.234(3)	C11–H11	1.0000
W1–P1	2.5353(12)	C12–C26	1.536(6)
P1–C27	1.809(5)	C12–C13	1.543(6)
P1–C28	1.825(4)	C12–H12	1.0000
P1–C29	1.828(4)	C13–C14	1.521(6)
O1–N7	1.230(4)	C13–H13A	0.9900
N1–C1	1.332(5)	C13–H13B	0.9900
N1–N2	1.372(5)	C14–C15	1.526(6)
N2–C3	1.337(5)	C14–H14A	0.9900
N2–B1	1.522(7)	C14–H14B	0.9900
N3–C4	1.344(6)	C15–C16	1.512(6)
N3–N4	1.372(5)	C15–H15A	0.9900
N4–C6	1.346(5)	C15–H15B	0.9900
N4–B1	1.544(7)	C16–C19	1.541(6)
N5–C7	1.337(5)	C16–C17	1.554(6)
N5–N6	1.363(5)	C16–H16	1.0000
N6–C9	1.351(6)	C17–C18	1.463(6)
N6–B1	1.544(6)	C17–H17	1.0000
N8–C18	1.146(6)	C19–C20	1.503(6)
C1–C2	1.394(6)	C19–H19A	0.9900
C1–H1	0.9500	C19–H19B	0.9900
C2–C3	1.377(7)	C20–C21	1.377(6)
C2–H2	0.9500	C20–C25	1.390(6)
C3–H3	0.9500	C21–C22	1.395(6)
C4–C5	1.368(6)	C21–H21	0.9500
C4–H4	0.9500	C22–C23	1.360(8)
C5–C6	1.368(7)	C22–H22	0.9500
C5–H5	0.9500	C23–C24	1.342(9)
C6–H6	0.9500	C23–H23	0.9500
C7–C8	1.377(6)	C24–C25	1.382(7)
C7–H7	0.9500	C24–H24	0.9500
C8–C9	1.365(6)	C25–H25	0.9500
C8–H8	0.9500	C26–H26A	0.9800
		C26–H26B	0.9800



C26–H26C	0.9800
C27–H27A	0.9800
C27–H27B	0.9800
C27–H27C	0.9800
C28–H28A	0.9800
C28–H28B	0.9800
C28–H28C	0.9800
C29–H29A	0.9800
C29–H29B	0.9800
C29–H29C	0.9800
B1–H1A	1.01(4)
Atom–Atom– Atom	Angle [°]
N7–W1–N5	89.61(15)
N7–W1–C11	97.27(14)
N5–W1–C11	85.51(15)
N7–W1–C10	90.86(14)
N5–W1–C10	123.36(14)
C11–W1–C10	38.36(15)
N7–W1–N1	176.60(14)
N5–W1–N1	87.01(13)
C11–W1–N1	82.04(13)
C10–W1–N1	90.63(13)
N7–W1–N3	96.16(13)
N5–W1–N3	73.85(13)
C11–W1–N3	155.22(15)
C10–W1–N3	161.57(14)
N1–W1–N3	83.32(12)
N7–W1–P1	99.48(11)
N5–W1–P1	151.79(9)
C11–W1–P1	119.28(12)
C10–W1–P1	83.43(11)
N1–W1–P1	83.73(9)
N3–W1–P1	78.63(10)
C27–P1–C28	101.6(2)
C27–P1–C29	100.3(2)
C28–P1–C29	102.5(2)
C27–P1–W1	121.23(17)
C28–P1–W1	116.89(16)
C29–P1–W1	111.49(16)
C1–N1–N2	106.6(3)
C1–N1–W1	133.3(3)
N2–N1–W1	120.1(2)
C3–N2–N1	109.2(4)
C3–N2–B1	129.9(4)
N1–N2–B1	120.8(3)
C4–N3–N4	106.2(4)

C4–N3–W1	134.0(3)
N4–N3–W1	119.8(3)
C6–N4–N3	108.6(4)
C6–N4–B1	130.0(4)
N3–N4–B1	120.4(3)
C7–N5–N6	106.6(4)
C7–N5–W1	130.9(3)
N6–N5–W1	122.1(3)
C9–N6–N5	108.6(3)
C9–N6–B1	128.0(4)
N5–N6–B1	118.8(4)
O1–N7–W1	175.8(3)
N1–C1–C2	110.4(4)
N1–C1–H1	124.8
C2–C1–H1	124.8
C3–C2–C1	104.6(4)
C3–C2–H2	127.7
C1–C2–H2	127.7
N2–C3–C2	109.1(4)
N2–C3–H3	125.5
C2–C3–H3	125.5
N3–C4–C5	110.6(4)
N3–C4–H4	124.7
C5–C4–H4	124.7
C6–C5–C4	105.5(4)
C6–C5–H5	127.3
C4–C5–H5	127.3
N4–C6–C5	109.0(4)
N4–C6–H6	125.5
C5–C6–H6	125.5
N5–C7–C8	110.5(4)
N5–C7–H7	124.7
C8–C7–H7	124.7
C9–C8–C7	105.2(4)
C9–C8–H8	127.4
C7–C8–H8	127.4
N6–C9–C8	109.0(4)
N6–C9–H9	125.5
C8–C9–H9	125.5
C11–C10–C17	118.2(3)
C11–C10–W1	70.8(2)
C17–C10–W1	119.1(3)
C11–C10–H10	114.0
C17–C10–H10	114.0
W1–C10–H10	114.0
C10–C11–C12	128.6(4)
C10–C11–W1	70.9(2)
C12–C11–W1	125.0(3)

C10–C11–H11	109.1
C12–C11–H11	109.1
W1–C11–H11	109.1
C26–C12–C11	108.6(3)
C26–C12–C13	103.6(3)
C11–C12–C13	118.1(4)
C26–C12–H12	108.7
C11–C12–H12	108.7
C13–C12–H12	108.7
C14–C13–C12	122.5(4)
C14–C13–H13A	106.7
C12–C13–H13A	106.7
C14–C13–H13B	106.7
C12–C13–H13B	106.7
H13A–C13– H13B	106.6
C13–C14–C15	113.9(4)
C13–C14–H14A	108.8
C15–C14–H14A	108.8
C13–C14–H14B	108.8
C15–C14–H14B	108.8
H14A–C14– H14B	107.7
C16–C15–C14	115.4(4)
C16–C15–H15A	108.4
C14–C15–H15A	108.4
C16–C15–H15B	108.4
C14–C15–H15B	108.4
H15A–C15– H15B	107.5
C15–C16–C19	111.3(4)
C15–C16–C17	111.6(3)
C19–C16–C17	111.9(3)
C15–C16–H16	107.3
C19–C16–H16	107.3
C17–C16–H16	107.3
C18–C17–C10	116.0(3)
C18–C17–C16	106.4(3)
C10–C17–C16	113.7(3)
C18–C17–H17	106.7
C10–C17–H17	106.7
C16–C17–H17	106.7
N8–C18–C17	173.8(5)
C20–C19–C16	115.1(3)
C20–C19–H19A	108.5
C16–C19–H19A	108.5
C20–C19–H19B	108.5
C16–C19–H19B	108.5

H19A–C19– H19B	107.5
C21–C20–C25	118.8(5)
C21–C20–C19	122.0(4)
C25–C20–C19	119.2(4)
C20–C21–C22	120.0(5)
C20–C21–H21	120.0
C22–C21–H21	120.0
C23–C22–C21	119.9(6)
C23–C22–H22	120.1
C21–C22–H22	120.1
C24–C23–C22	120.6(5)
C24–C23–H23	119.7
C22–C23–H23	119.7
C23–C24–C25	120.9(6)
C23–C24–H24	119.6
C25–C24–H24	119.6
C24–C25–C20	119.8(5)
C24–C25–H25	120.1
C20–C25–H25	120.1
C12–C26–H26A	109.5
C12–C26–H26B	109.5
H26A–C26– H26B	109.5
C12–C26–H26C	109.5
H26A–C26– H26C	109.5
H26B–C26– H26C	109.5
P1–C27–H27A	109.5
P1–C27–H27B	109.5
H27A–C27– H27B	109.5
P1–C27–H27C	109.5
H27A–C27– H27C	109.5
H27B–C27– H27C	109.5
P1–C28–H28A	109.5
P1–C28–H28B	109.5
H28A–C28– H28B	109.5
P1–C28–H28C	109.5
H28A–C28– H28C	109.5
H28B–C28– H28C	109.5
P1–C29–H29A	109.5
P1–C29–H29B	109.5

H29A–C29– H29B	109.5
P1–C29–H29C	109.5
H29A–C29– H29C	109.5
H29B–C29– H29C	109.5
N2–B1–N4	109.0(4)

N2–B1–N6	110.5(4)
N4–B1–N6	105.6(4)
N2–B1–H1A	109(2)
N4–B1–H1A	109(2)
N6–B1–H1A	113(3)

Table 5. Torsion angles for 4-jkh-033

Atom–Atom– Atom–Atom	Torsion Angle [°]
C1–N1–N2–C3	–0.2(5)
W1–N1–N2–C3	178.5(3)
C1–N1–N2–B1	177.0(4)
W1–N1–N2–B1	–4.3(5)
C4–N3–N4–C6	1.4(5)
W1–N3–N4–C6	–179.8(3)
C4–N3–N4–B1	171.2(4)
W1–N3–N4–B1	–10.0(5)
C7–N5–N6–C9	1.3(5)
W1–N5–N6–C9	174.8(3)
C7–N5–N6–B1	–156.7(4)
W1–N5–N6–B1	16.9(5)
N2–N1–C1–C2	–0.2(5)
W1–N1–C1–C2	–178.7(3)
N1–C1–C2–C3	0.6(5)
N1–N2–C3–C2	0.6(5)
B1–N2–C3–C2	–176.3(4)
C1–C2–C3–N2	–0.7(5)
N4–N3–C4–C5	–0.2(5)
W1–N3–C4–C5	–178.7(3)
N3–C4–C5–C6	–1.0(6)
N3–N4–C6–C5	–2.0(5)
B1–N4–C6–C5	–170.6(4)
C4–C5–C6–N4	1.9(6)
N6–N5–C7–C8	–1.4(5)
W1–N5–C7–C8	–174.2(3)
N5–C7–C8–C9	1.0(6)
N5–N6–C9–C8	–0.7(6)
B1–N6–C9–C8	154.7(5)
C7–C8–C9–N6	–0.2(6)
C17–C10–C11–C12	6.5(6)
W1–C10–C11–C12	119.9(4)
C17–C10–C11–W1	–113.5(3)
C10–C11–C12–C26	179.0(4)
W1–C11–C12–C26	–88.3(4)

C10–C11–C12–C13	61.6(6)
W1–C11–C12–C13	154.2(3)
C26–C12–C13–C14	176.0(4)
C11–C12–C13–C14	–63.9(6)
C12–C13–C14–C15	73.9(6)
C13–C14–C15–C16	–106.0(5)
C14–C15–C16–C19	177.4(4)
C14–C15–C16–C17	51.7(5)
C11–C10–C17–C18	138.2(4)
W1–C10–C17–C18	55.7(4)
C11–C10–C17–C16	–97.8(4)
W1–C10–C17–C16	179.6(3)
C15–C16–C17–C18	–170.7(3)
C19–C16–C17–C18	63.9(4)
C15–C16–C17–C10	60.3(5)
C19–C16–C17–C10	–65.1(5)
C15–C16–C19–C20	72.5(5)
C17–C16–C19–C20	–161.9(4)
C16–C19–C20–C21	–97.6(5)
C16–C19–C20–C25	84.4(5)
C25–C20–C21–C22	1.2(7)
C19–C20–C21–C22	–176.9(4)
C20–C21–C22–C23	1.1(8)
C21–C22–C23–C24	–2.9(8)
C22–C23–C24–C25	2.4(9)
C23–C24–C25–C20	0.0(8)
C21–C20–C25–C24	–1.7(7)
C19–C20–C25–C24	176.4(4)
C3–N2–B1–N4	120.2(5)
N1–N2–B1–N4	–56.4(5)
C3–N2–B1–N6	–124.2(5)
N1–N2–B1–N6	59.2(5)
C6–N4–B1–N2	–127.3(5)
N3–N4–B1–N2	65.3(5)
C6–N4–B1–N6	113.9(5)
N3–N4–B1–N6	–53.4(5)
C9–N6–B1–N2	139.6(5)

N5–N6–B1–N2	–67.3(5)
C9–N6–B1–N4	–102.7(5)
N5–N6–B1–N4	50.4(5)

### SC-XRD 35 – Dr. Dickie is finishing solving this data.

#### Structure Report for 4-jkh-013-x2

A colourless, needle-shaped crystal of 4-jkh-013-x2 was coated with Paratone oil and mounted on a MiTeGen micromount. Data were collected at 100.00 K on a Bruker D8 VENTURE dual wavelength Mo/Cu Kappa four-circle diffractometer with a PHOTON III detector. The diffractometer was equipped with an Oxford Cryostream 800 low temperature device and used Mo  $K_\alpha$  radiation ( $\lambda = 0.71073\text{\AA}$ ) from an Incoatec  $\lambda/\text{ms}$  3.0 microfocus sealed X-ray tube with a HELIOS double bounce multilayer mirror as monochromator.

Data collection and processing were done within the Bruker APEX5 software suite.<sup>[1]</sup> All data were integrated with SAINT 8.40B using a narrow-frame algorithm and a Multi-Scan absorption correction using SADABS 2016/2 was applied.<sup>[2]</sup> Using Olex2 as a graphical interface,<sup>[3]</sup> the structure was solved by dual methods with SHELXT and refined by full-matrix least-squares methods against  $F^2$  using SHELXL.<sup>[4,5]</sup> All non-hydrogen atoms were refined with anisotropic displacement parameters. The B–H hydrogen atom as well as H10 and H11 were located in the electron density map and refined isotropically. All other hydrogen atoms were refined with isotropic displacement parameters using a riding model with their  $U_{\text{iso}}$  values constrained to 1.5 times the  $U_{\text{eq}}$  of their pivot atoms for terminal  $\text{sp}^3$  carbon atoms and 1.2 times for all other carbon atoms.

This report and the CIF file were generated using FinalCif.<sup>[6]</sup>

Table 1. Crystal data and structure refinement for 4-jkh-013-x2

CCDC number	
Empirical formula	$\text{C}_{30}\text{H}_{40}\text{BN}_8\text{OPW}$
Formula weight	754.33
Temperature [K]	100.00
Crystal system	monoclinic

Space group (number)	$P2_1/c$ (14)
$a$ [Å]	16.8919(6)
$b$ [Å]	18.6996(6)
$c$ [Å]	10.1419(4)
$\alpha$ [°]	90
$\beta$ [°]	97.0400(10)
$\gamma$ [°]	90
Volume [Å <sup>3</sup> ]	3179.4(2)
$Z$	4
$\rho_{\text{calc}}$ [gcm <sup>-3</sup> ]	1.576
$\mu$ [mm <sup>-1</sup> ]	3.721
$F(000)$	1512
Crystal size [mm <sup>3</sup> ]	0.059×0.081×0.151
Crystal colour	colourless
Crystal shape	needle
Radiation	Mo $K_{\alpha}$ ( $\lambda=0.71073$ Å)
$2\theta$ range [°]	4.60 to 61.19 (0.70 Å)
Index ranges	$-24 \leq h \leq 24$ $-20 \leq k \leq 26$ $-14 \leq l \leq 14$
Reflections collected	71130
Independent reflections	9765 $R_{\text{int}} = 0.0909$ $R_{\text{sigma}} = 0.0619$
Completeness to $\theta = 25.242^\circ$	99.9
Data / Restraints / Parameters	9765 / 0 / 400
Goodness-of-fit on $F^2$	1.005
Final $R$ indexes [ $I \geq 2\sigma(I)$ ]	$R_1 = 0.0367$ $wR_2 = 0.0724$
Final $R$ indexes [all data]	$R_1 = 0.0627$ $wR_2 = 0.0813$
Largest peak/hole [eÅ <sup>-3</sup> ]	1.14/−1.24

Table 2. Atomic coordinates and  $U_{eq}$  [ $\text{\AA}^2$ ] for 4-jkh-013-x2

Atom	x	y	z	$U_{eq}$
W1	0.30076(2)	0.49324(2)	0.67598(2)	0.01542(4)
P1	0.15734(6)	0.45050(5)	0.65278(10)	0.0197(2)
O1	0.31978(19)	0.47732(17)	0.3885(3)	0.0340(7)
N1	0.28015(18)	0.49815(14)	0.8891(3)	0.0171(6)
N2	0.31465(19)	0.45012(15)	0.9786(3)	0.0192(6)
N3	0.31271(19)	0.37635(16)	0.7074(3)	0.0191(7)
N4	0.3400(2)	0.34776(16)	0.8290(3)	0.0227(7)
N5	0.42603(19)	0.47367(16)	0.7596(3)	0.0197(6)
N6	0.4437(2)	0.43828(16)	0.8790(3)	0.0226(7)
N7	0.31343(19)	0.48493(16)	0.5062(3)	0.0206(6)
N8	0.1179(2)	0.55345(18)	0.3481(3)	0.0267(7)
C1	0.2300(2)	0.53664(19)	0.9545(4)	0.0193(7)
H1	0.197983	0.575004	0.916804	0.023
C2	0.2313(2)	0.5128(2)	1.0838(4)	0.0247(8)
H2	0.201402	0.530611	1.150097	0.030
C3	0.2854(3)	0.4578(2)	1.0950(4)	0.0248(9)
H3	0.299841	0.429797	1.172405	0.030
C4	0.2997(3)	0.3215(2)	0.6229(4)	0.0269(9)
H4	0.281010	0.325743	0.531011	0.032
C5	0.3175(3)	0.2574(2)	0.6890(5)	0.0373(12)
H5	0.312530	0.210388	0.653249	0.045
C6	0.3439(3)	0.2769(2)	0.8182(4)	0.0328(10)
H6	0.361911	0.244882	0.888250	0.039
C7	0.4938(2)	0.4760(2)	0.7056(4)	0.0248(8)
H7	0.499275	0.497000	0.621930	0.030
C8	0.5557(3)	0.4438(2)	0.7876(5)	0.0297(9)
H8	0.609821	0.438967	0.772314	0.036
C9	0.5216(2)	0.4206(2)	0.8944(4)	0.0272(9)
H9	0.548530	0.395809	0.968464	0.033
C10	0.2455(2)	0.60012(18)	0.6444(4)	0.0186(7)
H10	0.206(2)	0.611(2)	0.707(4)	0.022

C11	0.3285(2)	0.60820(19) )	0.7019(4)	0.0195(8)
H11	0.335(2)	0.615(2)	0.792(4)	0.023
C12	0.3857(2)	0.65699(19) )	0.6392(4)	0.0241(8)
H12	0.370891	0.655936	0.540641	0.029
C13	0.3766(3)	0.7349(2)	0.6874(4)	0.0293(9)
H13A	0.397254	0.737253	0.783017	0.035
H13B	0.410665	0.766220	0.639387	0.035
C14	0.2912(3)	0.7651(2)	0.6689(4)	0.0318(10)
H14A	0.258040	0.737124	0.724403	0.038
H14B	0.292470	0.815131	0.700892	0.038
C15	0.2523(3)	0.7633(2)	0.5258(4)	0.0308(10)
H15A	0.294949	0.757544	0.467800	0.037
H15B	0.226976	0.810359	0.504939	0.037
C16	0.1895(2)	0.70521(19) )	0.4886(4)	0.0220(8)
H16	0.171818	0.711772	0.391555	0.026
C17	0.2224(2)	0.62739(18) )	0.5034(4)	0.0200(8)
H17	0.272339	0.626765	0.459670	0.024
C18	0.1135(2)	0.7142(2)	0.5577(4)	0.0255(9)
H18A	0.081798	0.669555	0.547205	0.031
H18B	0.129049	0.722129	0.653848	0.031
C19	0.0625(2)	0.77588(19) )	0.5014(4)	0.0230(8)
C20	0.0637(3)	0.8416(2)	0.5648(4)	0.0271(9)
H20	0.097306	0.848458	0.645958	0.033
C21	0.0164(3)	0.8975(2)	0.5111(5)	0.0321(11)
H21	0.018304	0.942280	0.555775	0.039
C22	−0.0329(3)	0.8893(2)	0.3950(5)	0.0354(11)
H22	−0.065305	0.927783	0.358962	0.042
C23	−0.0349(3)	0.8242(3)	0.3308(5)	0.0385(11)
H23	−0.069364	0.817863	0.250327	0.046
C24	0.0128(3)	0.7679(2)	0.3822(4)	0.0309(9)
H24	0.011577	0.723732	0.335779	0.037
C25	0.1639(2)	0.58286(19) )	0.4195(4)	0.0212(8)
C26	0.4722(2)	0.6377(2)	0.6684(5)	0.0270(9)
H26	0.491713	0.623996	0.756673	0.032
C27	0.5228(3)	0.6385(2)	0.5796(6)	0.0377(12)
C28	0.0761(2)	0.5125(2)	0.6704(4)	0.0268(8)
H28A	0.088548	0.540196	0.752369	0.040
H28B	0.026624	0.485637	0.674140	0.040
H28C	0.069426	0.545093	0.594134	0.040
C29	0.1203(3)	0.4008(2)	0.5024(4)	0.0272(9)

H29A	0.128952	0.429065	0.423982	0.041
H29B	0.063155	0.391520	0.501531	0.041
H29C	0.148972	0.355334	0.501027	0.041
C30	0.1411(2)	0.3852(2)	0.7806(4)	0.0260(9)
H30A	0.175241	0.343462	0.772745	0.039
H30B	0.085027	0.370268	0.769099	0.039
H30C	0.154170	0.406847	0.868580	0.039
B1	0.3779(3)	0.3984(2)	0.9404(5)	0.0224(9)
H1A	0.408(2)	0.368(2)	1.030(4)	0.024(11)
H27A	0.502(2)	0.647(2)	0.487(4)	0.027(13)
H27B	0.577(3)	0.624(3)	0.597(5)	0.052(16)

$U_{eq}$  is defined as 1/3 of the trace of the orthogonalized  $U_{ij}$  tensor.

Table 3. Anisotropic displacement parameters ( $\text{\AA}^2$ ) for 4-jkh-013-x2. The anisotropic displacement factor exponent takes the form:

$$-2\pi^2 [h^2(a^*)^2 U_{11} + k^2(b^*)^2 U_{22} + \dots + 2hka^*b^* U_{12}]$$

Atom	$U_{11}$	$U_{22}$	$U_{33}$	$U_{23}$	$U_{13}$	$U_{12}$
W1	0.01754(7)	0.01763(7)	0.01119(7)	0.00019(6)	0.00214(5)	0.00078(6)
P1	0.0198(5)	0.0225(5)	0.0167(5)	-0.0002(4)	0.0021(4)	-0.0018(4)
O1	0.0373(18)	0.0544(18)	0.0105(14)	-0.0033(13)	0.0036(13)	0.0084(15)
N1	0.0191(15)	0.0187(14)	0.0133(14)	-0.0014(11)	0.0015(11)	0.0004(12)
N2	0.0231(17)	0.0211(15)	0.0135(16)	0.0017(11)	0.0028(13)	0.0007(12)
N3	0.0191(17)	0.0237(15)	0.0142(16)	-0.0003(11)	0.0010(13)	0.0002(12)
N4	0.0286(19)	0.0213(15)	0.0195(17)	0.0042(12)	0.0073(14)	0.0040(13)
N5	0.0198(16)	0.0226(15)	0.0163(16)	0.0005(12)	0.0009(13)	0.0033(12)
N6	0.0238(18)	0.0265(16)	0.0165(17)	0.0014(12)	-0.0021(14)	0.0028(13)
N7	0.0211(16)	0.0263(16)	0.0147(15)	0.0013(12)	0.0039(12)	0.0039(13)
N8	0.0274(19)	0.0339(18)	0.0189(18)	0.0006(14)	0.0026(15)	0.0012(15)
C1	0.022(2)	0.0184(16)	0.0177(19)	0.0002(13)	0.0035(15)	0.0006(14)
C2	0.029(2)	0.0270(19)	0.0189(19)	-0.0049(15)	0.0076(16)	-0.0037(16)
C3	0.036(2)	0.0262(19)	0.0126(18)	0.0001(14)	0.0054(17)	-0.0038(16)
C4	0.036(3)	0.027(2)	0.019(2)	-0.0047(15)	0.0066(18)	0.0032(17)
C5	0.062(4)	0.0182(18)	0.032(3)	-0.0042(17)	0.009(2)	0.0043(19)
C6	0.047(3)	0.0223(19)	0.030(2)	0.0059(17)	0.011(2)	0.0064(18)
C7	0.022(2)	0.0252(19)	0.029(2)	-0.0040(16)	0.0079(17)	0.0006(15)
C8	0.020(2)	0.030(2)	0.039(3)	-0.0038(18)	0.0032(19)	0.0032(16)



C9	0.019(2)	0.033(2)	0.028(2)	−0.0007(17)	−0.0037(17)	0.0070(16)
C10	0.022(2)	0.0188(16)	0.0157(19)	0.0016(13)	0.0050(15)	0.0006(14)
C11	0.022(2)	0.0195(17)	0.0173(19)	−0.0002(14)	0.0025(16)	0.0003(14)
C12	0.025(2)	0.0227(18)	0.024(2)	0.0002(15)	0.0007(17)	−0.0075(15)
C13	0.030(2)	0.0224(19)	0.035(3)	−0.0008(17)	0.003(2)	−0.0035(16)
C14	0.040(3)	0.027(2)	0.030(2)	−0.0019(17)	0.009(2)	−0.0018(18)
C15	0.039(3)	0.0228(19)	0.031(2)	0.0053(17)	0.007(2)	0.0039(17)
C16	0.022(2)	0.0229(18)	0.021(2)	0.0060(14)	0.0029(16)	0.0038(15)
C17	0.022(2)	0.0225(17)	0.0161(19)	0.0011(14)	0.0029(15)	−0.0004(14)
C18	0.029(2)	0.0265(19)	0.021(2)	0.0056(15)	0.0045(17)	0.0024(16)
C19	0.022(2)	0.0236(18)	0.024(2)	0.0050(15)	0.0054(17)	0.0001(15)
C20	0.036(3)	0.0251(19)	0.021(2)	−0.0003(15)	0.0057(18)	0.0019(17)
C21	0.040(3)	0.0208(19)	0.038(3)	0.0038(17)	0.017(2)	0.0049(17)
C22	0.027(2)	0.036(2)	0.045(3)	0.019(2)	0.011(2)	0.0101(18)
C23	0.035(3)	0.052(3)	0.027(3)	0.012(2)	−0.006(2)	0.003(2)
C24	0.033(3)	0.031(2)	0.028(2)	−0.0003(17)	−0.0004(19)	−0.0010(18)
C25	0.028(2)	0.0228(18)	0.0137(18)	0.0057(14)	0.0066(16)	0.0070(15)
C26	0.024(2)	0.0210(18)	0.035(3)	−0.0004(16)	−0.0006(18)	−0.0021(15)
C27	0.028(3)	0.033(2)	0.053(4)	0.001(2)	0.012(2)	−0.0019(19)
C28	0.023(2)	0.034(2)	0.024(2)	−0.0008(16)	0.0043(16)	0.0037(17)
C29	0.029(2)	0.030(2)	0.021(2)	−0.0038(16)	−0.0054(17)	−0.0020(17)
C30	0.026(2)	0.028(2)	0.024(2)	0.0014(16)	0.0046(17)	−0.0064(16)
B1	0.023(2)	0.024(2)	0.019(2)	0.0044(16)	0.0004(18)	0.0022(17)

Table 3. Bond lengths and angles for 4-jkh-013-x2

Atom–Atom	Length [Å]
W1–P1	2.5345(10)
W1–N1	2.233(3)
W1–N3	2.215(3)
W1–N5	2.211(3)
W1–N7	1.768(3)
W1–C10	2.213(4)
W1–C11	2.209(4)
P1–C28	1.822(4)
P1–C29	1.829(4)
P1–C30	1.826(4)

O1–N7	1.220(4)
N1–N2	1.356(4)
N1–C1	1.346(4)
N2–C3	1.342(5)
N2–B1	1.526(5)
N3–N4	1.371(4)
N3–C4	1.338(5)
N4–C6	1.332(5)
N4–B1	1.551(6)
N5–N6	1.381(4)
N5–C7	1.329(5)

N6–C9	1.347(5)
N6–B1	1.532(5)
N8–C25	1.136(5)
C1–H1	0.9500
C1–C2	1.382(5)
C2–H2	0.9500
C2–C3	1.371(6)
C3–H3	0.9500
C4–H4	0.9500
C4–C5	1.388(6)
C5–H5	0.9500
C5–C6	1.380(6)
C6–H6	0.9500
C7–H7	0.9500
C7–C8	1.391(6)
C8–H8	0.9500
C8–C9	1.358(6)
C9–H9	0.9500
C10–H10	0.99(4)
C10–C11	1.459(6)
C10–C17	1.524(5)
C11–H11	0.91(4)
C11–C12	1.524(5)
C12–H12	1.0000
C12–C13	1.550(5)
C12–C26	1.499(6)
C13–H13A	0.9900
C13–H13B	0.9900
C13–C14	1.540(6)
C14–H14A	0.9900
C14–H14B	0.9900
C14–C15	1.519(6)
C15–H15A	0.9900
C15–H15B	0.9900
C15–C16	1.533(6)
C16–H16	1.0000
C16–C17	1.558(5)
C16–C18	1.545(5)
C17–H17	1.0000
C17–C25	1.479(5)
C18–H18A	0.9900
C18–H18B	0.9900
C18–C19	1.509(5)
C19–C20	1.386(5)
C19–C24	1.393(6)
C20–H20	0.9500
C20–C21	1.386(6)
C21–H21	0.9500

C21–C22	1.365(6)
C22–H22	0.9500
C22–C23	1.378(7)
C23–H23	0.9500
C23–C24	1.388(6)
C24–H24	0.9500
C26–H26	0.9500
C26–C27	1.315(6)
C27–H27A	0.97(4)
C27–H27B	0.95(5)
C28–H28A	0.9800
C28–H28B	0.9800
C28–H28C	0.9800
C29–H29A	0.9800
C29–H29B	0.9800
C29–H29C	0.9800
C30–H30A	0.9800
C30–H30B	0.9800
C30–H30C	0.9800
B1–H1A	1.13(4)
<b>Atom–Atom– Atom</b>	<b>Angle [°]</b>
N1–W1–P1	80.92(8)
N3–W1–P1	76.78(8)
N3–W1–N1	85.61(11)
N5–W1–P1	147.38(8)
N5–W1–N1	83.75(11)
N5–W1–N3	73.46(11)
N5–W1–C10	124.89(13)
N7–W1–P1	96.33(11)
N7–W1–N1	176.66(12)
N7–W1–N3	91.93(12)
N7–W1–N5	97.73(13)
N7–W1–C10	92.15(14)
N7–W1–C11	98.76(14)
C10–W1–P1	83.67(10)
C10–W1–N1	89.43(12)
C10–W1–N3	160.36(13)
C11–W1–P1	120.28(10)
C11–W1–N1	84.30(12)
C11–W1–N3	158.30(14)
C11–W1–N5	86.36(13)
C11–W1–C10	38.53(14)
C28–P1–W1	120.87(14)
C28–P1–C29	102.72(19)
C28–P1–C30	100.09(19)
C29–P1–W1	117.57(14)

C30-P1-W1	111.74(14)
C30-P1-C29	100.76(19)
N2-N1-W1	121.0(2)
C1-N1-W1	132.9(2)
C1-N1-N2	105.6(3)
N1-N2-B1	120.4(3)
C3-N2-N1	110.1(3)
C3-N2-B1	129.5(3)
N4-N3-W1	121.9(2)
C4-N3-W1	131.3(3)
C4-N3-N4	106.7(3)
N3-N4-B1	118.7(3)
C6-N4-N3	109.2(3)
C6-N4-B1	130.4(4)
N6-N5-W1	120.6(2)
C7-N5-W1	132.0(3)
C7-N5-N6	105.8(3)
N5-N6-B1	120.0(3)
C9-N6-N5	108.8(3)
C9-N6-B1	125.5(3)
O1-N7-W1	177.5(3)
N1-C1-H1	124.6
N1-C1-C2	110.9(3)
C2-C1-H1	124.6
C1-C2-H2	127.6
C3-C2-C1	104.7(3)
C3-C2-H2	127.6
N2-C3-C2	108.7(3)
N2-C3-H3	125.7
C2-C3-H3	125.7
N3-C4-H4	124.9
N3-C4-C5	110.1(4)
C5-C4-H4	124.9
C4-C5-H5	127.6
C6-C5-C4	104.8(4)
C6-C5-H5	127.6
N4-C6-C5	109.1(4)
N4-C6-H6	125.4
C5-C6-H6	125.4
N5-C7-H7	124.4
N5-C7-C8	111.2(4)
C8-C7-H7	124.4
C7-C8-H8	127.7
C9-C8-C7	104.7(4)
C9-C8-H8	127.7
N6-C9-C8	109.5(4)
N6-C9-H9	125.3
C8-C9-H9	125.3

W1-C10-H10	113(2)
C11-C10-W1	70.6(2)
C11-C10-H10	114(2)
C11-C10-C17	117.6(3)
C17-C10-W1	119.6(2)
C17-C10-H10	115(2)
W1-C11-H11	105(2)
C10-C11-W1	70.9(2)
C10-C11-H11	114(3)
C10-C11-C12	121.5(3)
C12-C11-W1	132.0(3)
C12-C11-H11	109(3)
C11-C12-H12	108.2
C11-C12-C13	109.8(3)
C13-C12-H12	108.2
C26-C12-C11	115.2(3)
C26-C12-H12	108.2
C26-C12-C13	107.2(3)
C12-C13-H13A	108.4
C12-C13-H13B	108.4
H13A-C13-H13B	107.4
C14-C13-C12	115.7(3)
C14-C13-H13A	108.4
C14-C13-H13B	108.4
C13-C14-H14A	108.9
C13-C14-H14B	108.9
H14A-C14-H14B	107.7
C15-C14-C13	113.4(4)
C15-C14-H14A	108.9
C15-C14-H14B	108.9
C14-C15-H15A	108.0
C14-C15-H15B	108.0
C14-C15-C16	117.1(3)
H15A-C15-H15B	107.3
C16-C15-H15A	108.0
C16-C15-H15B	108.0
C15-C16-H16	105.6
C15-C16-C17	114.2(3)
C15-C16-C18	113.6(3)
C17-C16-H16	105.6
C18-C16-H16	105.6
C18-C16-C17	111.4(3)
C10-C17-C16	116.8(3)
C10-C17-H17	106.2
C16-C17-H17	106.2
C25-C17-C10	115.3(3)

C25–C17–C16	105.4(3)
C25–C17–H17	106.2
C16–C18–H18A	109.1
C16–C18–H18B	109.1
H18A–C18– H18B	107.9
C19–C18–C16	112.3(3)
C19–C18–H18A	109.1
C19–C18–H18B	109.1
C20–C19–C18	121.9(4)
C20–C19–C24	118.0(4)
C24–C19–C18	120.1(4)
C19–C20–H20	119.6
C21–C20–C19	120.8(4)
C21–C20–H20	119.6
C20–C21–H21	119.5
C22–C21–C20	121.0(4)
C22–C21–H21	119.5
C21–C22–H22	120.5
C21–C22–C23	119.0(4)
C23–C22–H22	120.5
C22–C23–H23	119.6
C22–C23–C24	120.8(4)
C24–C23–H23	119.6
C19–C24–H24	119.8
C23–C24–C19	120.3(4)
C23–C24–H24	119.8
N8–C25–C17	174.3(4)
C12–C26–H26	118.0
C27–C26–C12	124.1(5)
C27–C26–H26	118.0
C26–C27–H27A	118(3)
C26–C27–H27B	124(3)
H27A–C27– H27B	117(4)

P1–C28–H28A	109.5
P1–C28–H28B	109.5
P1–C28–H28C	109.5
H28A–C28– H28B	109.5
H28A–C28– H28C	109.5
H28B–C28– H28C	109.5
P1–C29–H29A	109.5
P1–C29–H29B	109.5
P1–C29–H29C	109.5
H29A–C29– H29B	109.5
H29A–C29– H29C	109.5
H29B–C29– H29C	109.5
P1–C30–H30A	109.5
P1–C30–H30B	109.5
P1–C30–H30C	109.5
H30A–C30– H30B	109.5
H30A–C30– H30C	109.5
H30B–C30– H30C	109.5
N2–B1–N4	109.4(3)
N2–B1–N6	111.1(3)
N2–B1–H1A	112(2)
N4–B1–H1A	112(2)
N6–B1–N4	104.9(3)
N6–B1–H1A	107(2)

Table 5. Torsion angles for 4-jkh-013-x2

Atom–Atom– Atom–Atom	Torsion Angle [°]
W1–N1–N2–C3	–171.9(2)
W1–N1–N2–B1	9.0(4)
W1–N1–C1–C2	170.9(3)
W1–N3–N4–C6	–177.7(3)
W1–N3–N4–B1	–11.4(4)
W1–N3–C4–C5	178.5(3)
W1–N5–N6–C9	167.7(2)
W1–N5–N6–B1	13.0(4)

W1–N5–C7–C8	–166.1(3)
W1–C10–C11–C12	128.2(3)
W1–C10–C17–C16	–175.7(2)
W1–C10–C17–C25	59.8(4)
W1–C11–C12–C13	176.2(3)
W1–C11–C12–C26	–62.7(5)
N1–N2–C3–C2	–1.0(4)
N1–N2–B1–N4	–64.0(4)
N1–N2–B1–N6	51.3(5)
N1–C1–C2–C3	0.4(4)

N2–N1–C1–C2	–1.0(4)
N3–N4–C6–C5	–1.3(5)
N3–N4–B1–N2	65.2(4)
N3–N4–B1–N6	–54.0(4)
N3–C4–C5–C6	–1.4(5)
N4–N3–C4–C5	0.7(5)
N5–N6–C9–C8	0.1(4)
N5–N6–B1–N2	–64.8(4)
N5–N6–B1–N4	53.3(4)
N5–C7–C8–C9	0.8(5)
N6–N5–C7–C8	–0.7(4)
C1–N1–N2–C3	1.2(4)
C1–N1–N2–B1	–177.9(3)
C1–C2–C3–N2	0.4(4)
C3–N2–B1–N4	117.1(4)
C3–N2–B1–N6	–127.6(4)
C4–N3–N4–C6	0.4(4)
C4–N3–N4–B1	166.7(3)
C4–C5–C6–N4	1.6(5)
C6–N4–B1–N2	–131.8(4)
C6–N4–B1–N6	108.9(4)
C7–N5–N6–C9	0.4(4)
C7–N5–N6–B1	–154.4(3)
C7–C8–C9–N6	–0.5(5)
C9–N6–B1–N2	144.9(4)
C9–N6–B1–N4	–97.0(4)
C10–C11–C12–C13	84.3(4)
C10–C11–C12–C26	–154.7(4)
C11–C10–C17–C16	–93.4(4)
C11–C10–C17–C25	142.1(3)
C11–C12–C13–C14	–53.1(5)

C11–C12–C26–C27	137.5(4)
C12–C13–C14–C15	–57.3(5)
C13–C12–C26–C27	–100.0(5)
C13–C14–C15–C16	104.1(4)
C14–C15–C16–C17	–63.2(5)
C14–C15–C16–C18	65.9(5)
C15–C16–C17–C10	70.8(4)
C15–C16–C17–C25	–159.8(3)
C15–C16–C18–C19	72.5(4)
C16–C18–C19–C20	–100.3(4)
C16–C18–C19–C24	79.2(5)
C17–C10–C11–W1	–114.0(3)
C17–C10–C11–C12	14.2(5)
C17–C16–C18–C19	–156.9(3)
C18–C16–C17–C10	–59.5(4)
C18–C16–C17–C25	69.9(4)
C18–C19–C20–C21	179.9(4)
C18–C19–C24–C23	179.3(4)
C19–C20–C21–C22	0.4(7)
C20–C19–C24–C23	–1.2(6)
C20–C21–C22–C23	–0.3(7)
C21–C22–C23–C24	–0.6(7)
C22–C23–C24–C19	1.3(7)
C24–C19–C20–C21	0.4(6)
C26–C12–C13–C14	–178.9(4)
B1–N2–C3–C2	178.0(4)
B1–N4–C6–C5	–165.4(4)
B1–N6–C9–C8	153.1(4)

# Structure Report for mo\_harman\_mne\_5\_synmebn\_diene\_\_sq

A yellow, needle-shaped crystal of mo\_harman\_mne\_5\_synmebn\_diene\_\_sq was coated with Paratone oil and mounted on a MiTeGen micromount. Data were collected at 100.00 K on a Bruker D8 VENTURE dual wavelength Mo/Cu Kappa four-circle diffractometer with a PHOTON III\_C14 detector. The diffractometer was equipped with an Oxford Cryostream 800 low temperature device and used Mo  $K_\alpha$  radiation ( $\lambda = 0.71073\text{\AA}$ ) from an Incoatec I $\mu$ S 3.0 microfocus sealed tube with a HELIOS double bounce multilayer mirror as monochromator.

Data collection and processing were done within the Bruker APEX6 software suite.<sup>[1]</sup> All data were integrated with SAINT 8.41 using a narrow-frame algorithm and a Multi-Scan absorption correction using  $\text{w}$  was applied.<sup>[2]</sup> Using Olex2 as a graphical interface,<sup>[3]</sup> the structure was solved by direct methods with SHELXT and refined by full-matrix least-squares methods against  $F^2$  using XL.<sup>[4,5]</sup> All non-hydrogen atoms were refined with anisotropic displacement parameters. All C-bound hydrogen atoms were refined with isotropic displacement parameters. Some of their coordinates were refined freely and some on calculated positions using a riding model with their  $U_{\text{iso}}$  values constrained to 1.5 times the  $U_{\text{eq}}$  of their pivot atoms for terminal  $\text{sp}^3$  carbon atoms and 1.2 times for all other carbon atoms.

This report and the CIF file were generated using FinalCif.<sup>[6]</sup>

Refinement details for mo\_harman\_mne\_5\_synmebn\_diene\_\_sq

'Disordered solvent located in the crystal lattice could not be adequately modeled with or without restraints. Therefore, the solvent was accounted for using the Platon SQUEEZE method. A void space of 450 Å<sup>3</sup> containing 80 electrons was found. This corresponds to a combination of dichloromethane and acetonitrile.'

Table 1. Crystal data and structure refinement for  
mo\_harman\_mne\_5\_synmebn\_diene\_\_sq

CCDC number	
Empirical formula	C <sub>22</sub> H <sub>35</sub> BN <sub>7</sub> OPW
Formula weight	639.20
Temperature [K]	100.00
Crystal system	monoclinic
Space group (number)	$P2_1/c$ (14)
$a$ [Å]	12.3841(5)
$b$ [Å]	14.8966(4)
$c$ [Å]	15.4059(6)
$\alpha$ [°]	90
$\beta$ [°]	91.9640(10)
$\gamma$ [°]	90
Volume [Å <sup>3</sup> ]	2840.43(18)
$Z$	4
$\rho_{\text{calc}}$ [gcm <sup>-3</sup> ]	1.495
$\mu$ [mm <sup>-1</sup> ]	4.149
$F(000)$	1272
Crystal size [mm <sup>3</sup> ]	0.07×0.097×0.106
Crystal colour	yellow

Crystal shape	needle
Radiation	Mo $K_{\alpha}$ ( $\lambda=0.71073$ Å)
2 $\theta$ range [°]	3.80 to 55.01 (0.77 Å)
Index ranges	$-16 \leq h \leq 16$ $-19 \leq k \leq 16$ $-19 \leq l \leq 19$
Reflections collected	42549
Independent reflections	6502 $R_{\text{int}} = 0.0451$ $R_{\text{sigma}} = 0.0298$
Completeness to $\theta = 25.242^{\circ}$	99.8
Data / Restraints / Parameters	6502 / 0 / 311
Goodness-of-fit on $F^2$	1.001
Final $R$ indexes [ $I \geq 2\sigma(I)$ ]	$R_1 = 0.0289$ $wR_2 = 0.0697$
Final $R$ indexes [all data]	$R_1 = 0.0423$ $wR_2 = 0.0766$
Largest peak/hole [ $\text{e}\text{\AA}^{-3}$ ]	2.30/−0.74

Table 2. Atomic coordinates and  $U_{eq}$  [Å<sup>2</sup>] for mo\_harman\_mne\_5\_synmebn\_diene\_\_sq

Atom	x	y	z	$U_{eq}$
W1	0.40448(2)	0.76720(2)	0.33290(2)	0.02892(6)
P1	0.33871(9)	0.89325(7)	0.23862(7)	0.0346(2)
O1	0.2861(2)	0.82235(19)	0.49068(19)	0.0419(7)
N1	0.5108(3)	0.7292(2)	0.2227(2)	0.0319(7)
N2	0.6207(3)	0.7313(2)	0.2340(2)	0.0331(7)
N3	0.5347(3)	0.8653(2)	0.3661(2)	0.0318(7)
N4	0.6397(3)	0.8492(2)	0.3507(2)	0.0341(7)
N5	0.5259(3)	0.6835(2)	0.4069(2)	0.0301(7)
N6	0.6327(3)	0.6893(2)	0.3913(2)	0.0340(7)
N7	0.3314(3)	0.7992(2)	0.4239(2)	0.0319(7)
C1	0.4916(4)	0.7017(3)	0.1410(3)	0.0364(9)
H1	0.421543	0.694388	0.114765	0.044
C2	0.5870(4)	0.6854(3)	0.0996(3)	0.0404(10)
H2	0.595443	0.665006	0.041829	0.048
C3	0.6664(4)	0.7051(3)	0.1604(3)	0.0378(9)
H3	0.741856	0.700998	0.151888	0.045
C4	0.5312(4)	0.9461(2)	0.4036(3)	0.0340(9)
H4	0.467287	0.974767	0.421763	0.041
C5	0.6343(4)	0.9823(3)	0.4122(3)	0.0376(9)
H5	0.654531	1.038727	0.436418	0.045
C6	0.7003(4)	0.9189(3)	0.3784(3)	0.0378(9)
H6	0.776601	0.923331	0.375010	0.045
C7	0.5179(3)	0.6300(2)	0.4759(3)	0.0339(8)
H7	0.451877	0.613928	0.501326	0.041
C9	0.6888(4)	0.6397(3)	0.4509(3)	0.0401(10)
H9	0.765077	0.632880	0.454027	0.048
C10	0.2638(3)	0.7032(3)	0.2628(3)	0.0343(8)
H10	0.274(3)	0.702(3)	0.199(3)	0.032(10)
C11	0.3222(4)	0.6378(3)	0.3147(3)	0.0377(9)
H11	0.363(3)	0.592(3)	0.279(3)	0.041(12)
C12	0.2682(4)	0.5910(3)	0.3865(3)	0.0464(11)
H12	0.298426	0.598950	0.443436	0.056
C13	0.1823(4)	0.5396(3)	0.3781(4)	0.0561(13)
H13	0.154916	0.513972	0.429356	0.067
C14	0.1240(5)	0.5185(3)	0.2932(4)	0.0643(15)
H14	0.176796	0.524675	0.245844	0.077
C15	0.0305(4)	0.5832(4)	0.2738(4)	0.0609(14)
H15	-0.017091	0.553018	0.228961	0.073
C16	0.0629(4)	0.6731(3)	0.2345(4)	0.0549(13)
H16A	0.089116	0.661413	0.175569	0.066
H16B	-0.002947	0.710456	0.227651	0.066



C17	0.1489(4)	0.7284(3)	0.2840(3)	0.0421(10)
H17A	0.137345	0.792679	0.270336	0.051
H17B	0.139563	0.720390	0.347071	0.051
C18	0.0854(5)	0.4201(4)	0.2947(6)	0.089(2)
H18A	0.029902	0.413280	0.338015	0.133
H18B	0.146715	0.380763	0.309688	0.133
H18C	0.055128	0.403640	0.237255	0.133
C19	−0.0386(5)	0.5970(4)	0.3523(5)	0.0763(18)
H19A	0.002940	0.630027	0.397172	0.114
H19B	−0.059936	0.538510	0.375232	0.114
H19C	−0.103308	0.631341	0.335058	0.114
C20	0.2644(4)	0.8727(3)	0.1370(3)	0.0438(10)
H20A	0.305573	0.831587	0.101123	0.066
H20B	0.253169	0.929579	0.106024	0.066
H20C	0.194193	0.845832	0.148988	0.066
C21	0.4469(4)	0.9634(3)	0.2001(3)	0.0484(11)
H21A	0.479579	0.997057	0.248948	0.073
H21B	0.417686	1.005483	0.156404	0.073
H21C	0.501919	0.925553	0.174145	0.073
C22	0.2526(4)	0.9729(3)	0.2924(3)	0.0514(12)
H22A	0.186455	0.942667	0.309768	0.077
H22B	0.233830	1.022180	0.252500	0.077
H22C	0.290951	0.996983	0.344024	0.077
C23	0.6187(4)	0.6013(3)	0.5053(3)	0.0390(9)
H23	0.635187	0.562959	0.553237	0.047
B1	0.6743(4)	0.7545(3)	0.3220(3)	0.0352(10)
H1A	0.754721	0.750640	0.319091	0.042

$U_{eq}$  is defined as 1/3 of the trace of the orthogonalized  $U_{ij}$  tensor.

Table 3. Anisotropic displacement parameters ( $\text{\AA}^2$ ) for mo\_harman\_mne\_5\_synmebn\_diene\_sq. The anisotropic displacement factor exponent takes the form:  $-2\pi^2 [h^2(a^*)^2U_{11} + k^2(b^*)^2U_{22} + \dots + 2hka^*b^*U_{12}]$

Atom	$U_{11}$	$U_{22}$	$U_{33}$	$U_{23}$	$U_{13}$	$U_{12}$
W1	0.03745(10)	0.02194(8)	0.02718(9)	0.00020(6)	−0.00156(6)	0.00089(6)
P1	0.0421(6)	0.0279(5)	0.0334(6)	0.0033(4)	−0.0034(4)	0.0015(4)
O1	0.0506(18)	0.0421(17)	0.0333(16)	−0.0051(12)	0.0069(13)	−0.0014(13)
N1	0.0407(18)	0.0254(15)	0.0296(17)	−0.0015(13)	−0.0010(14)	0.0033(13)
N2	0.0390(18)	0.0277(16)	0.0326(18)	0.0007(13)	0.0036(14)	0.0027(13)
N3	0.0414(19)	0.0250(15)	0.0288(17)	0.0003(12)	−0.0029(14)	0.0007(13)
N4	0.0404(19)	0.0284(16)	0.0333(18)	0.0014(13)	−0.0006(14)	−0.0019(13)

N5	0.0371(17)	0.0255(16)	0.0275(16)	0.0004(12)	−0.0044(13)	0.0021(13)
N6	0.0394(18)	0.0268(16)	0.0354(18)	0.0001(13)	−0.0029(14)	0.0041(13)
N7	0.0375(18)	0.0257(15)	0.0321(17)	0.0023(13)	−0.0034(14)	−0.0030(13)
C1	0.051(2)	0.0280(18)	0.030(2)	−0.0002(16)	−0.0005(17)	0.0012(17)
C2	0.061(3)	0.032(2)	0.029(2)	−0.0010(16)	0.0035(19)	0.0034(19)
C3	0.049(2)	0.0299(19)	0.035(2)	0.0001(17)	0.0091(18)	0.0007(18)
C4	0.052(2)	0.0218(18)	0.028(2)	−0.0009(14)	−0.0008(17)	0.0006(16)
C5	0.055(3)	0.0272(19)	0.030(2)	0.0026(15)	−0.0006(18)	−0.0042(17)
C6	0.048(2)	0.033(2)	0.032(2)	0.0040(16)	0.0004(18)	−0.0085(18)
C7	0.047(2)	0.0259(18)	0.029(2)	0.0004(15)	0.0012(17)	−0.0010(16)
C9	0.049(2)	0.030(2)	0.041(2)	−0.0026(17)	−0.0089(19)	0.0051(17)
C10	0.035(2)	0.0324(19)	0.035(2)	−0.0010(17)	−0.0033(17)	−0.0022(16)
C11	0.043(2)	0.029(2)	0.041(2)	−0.0053(17)	−0.0055(18)	−0.0008(17)
C12	0.047(3)	0.033(2)	0.058(3)	0.013(2)	−0.008(2)	−0.0041(18)
C13	0.056(3)	0.042(3)	0.070(4)	0.016(2)	−0.005(3)	−0.002(2)
C14	0.058(3)	0.044(3)	0.090(4)	−0.013(3)	0.005(3)	−0.009(2)
C15	0.046(3)	0.061(3)	0.076(4)	−0.002(3)	0.001(3)	−0.011(2)
C16	0.043(3)	0.056(3)	0.065(3)	0.005(2)	−0.009(2)	0.001(2)
C17	0.044(2)	0.037(2)	0.046(3)	0.0000(18)	0.0030(19)	0.0024(18)
C18	0.067(4)	0.048(3)	0.151(7)	−0.016(4)	0.010(4)	−0.007(3)
C19	0.065(4)	0.068(4)	0.096(5)	−0.002(3)	0.013(3)	0.006(3)
C20	0.051(3)	0.041(2)	0.039(2)	0.0081(18)	−0.007(2)	0.0025(19)
C21	0.061(3)	0.041(2)	0.042(3)	0.0144(19)	−0.010(2)	−0.012(2)
C22	0.063(3)	0.035(2)	0.056(3)	−0.005(2)	−0.012(2)	0.014(2)
C23	0.055(3)	0.0291(19)	0.032(2)	0.0026(16)	−0.0059(19)	0.0038(18)
B1	0.040(2)	0.028(2)	0.038(3)	−0.0005(18)	−0.002(2)	0.0012(17)

Table 4. Bond lengths and angles for mo\_harman\_mne\_5\_synmebn\_diene\_\_sq

Atom–Atom	Length [Å]		
W1–P1	2.4935(10)	W1–N5	2.236(3)
W1–N1	2.257(3)	W1–N7	1.761(3)
W1–N3	2.223(3)	W1–C10	2.231(4)
		W1–C11	2.193(4)

P1–C20	1.815(4)
P1–C21	1.815(5)
P1–C22	1.815(5)
O1–N7	1.237(4)
N1–N2	1.366(5)
N1–C1	1.338(5)
N2–C3	1.343(5)
N2–B1	1.528(6)
N3–N4	1.351(5)
N3–C4	1.338(5)
N4–C6	1.342(5)
N4–B1	1.544(5)
N5–N6	1.355(5)
N5–C7	1.334(5)
N6–C9	1.352(5)
N6–B1	1.545(6)
C1–H1	0.9500
C1–C2	1.383(6)
C2–H2	0.9500
C2–C3	1.366(6)
C3–H3	0.9500
C4–H4	0.9500
C4–C5	1.388(6)
C5–H5	0.9500
C5–C6	1.364(6)
C6–H6	0.9500
C7–H7	0.9500
C7–C23	1.381(6)
C9–H9	0.9500
C9–C23	1.355(6)
C10–H10	1.00(4)
C10–C11	1.438(6)
C10–C17	1.519(6)
C11–H11	1.02(4)
C11–C12	1.486(6)
C12–H12	0.9500
C12–C13	1.313(6)
C13–H13	0.9500
C13–C14	1.505(8)
C14–H14	1.0000
C14–C15	1.528(8)
C14–C18	1.542(7)
C15–H15	1.0000
C15–C16	1.530(7)
C15–C19	1.518(8)
C16–H16A	0.9900
C16–H16B	0.9900
C16–C17	1.528(6)

C17–H17A	0.9900
C17–H17B	0.9900
C18–H18A	0.9800
C18–H18B	0.9800
C18–H18C	0.9800
C19–H19A	0.9800
C19–H19B	0.9800
C19–H19C	0.9800
C20–H20A	0.9800
C20–H20B	0.9800
C20–H20C	0.9800
C21–H21A	0.9800
C21–H21B	0.9800
C21–H21C	0.9800
C22–H22A	0.9800
C22–H22B	0.9800
C22–H22C	0.9800
C23–H23	0.9500
B1–H1A	1.0000
Atom–Atom– Atom	Angle [°]
N1–W1–P1	86.44(8)
N3–W1–P1	81.89(8)
N3–W1–N1	84.27(12)
N3–W1–N5	77.26(11)
N3–W1–C10	160.09(14)
N5–W1–P1	156.59(9)
N5–W1–N1	81.04(12)
N7–W1–P1	95.37(11)
N7–W1–N1	175.21(13)
N7–W1–N3	91.59(13)
N7–W1–N5	95.72(13)
N7–W1–C10	95.00(15)
N7–W1–C11	95.19(16)
C10–W1–P1	78.81(11)
C10–W1–N1	89.70(14)
C10–W1–N5	120.56(14)
C11–W1–P1	116.49(11)
C11–W1–N1	87.94(14)
C11–W1–N3	159.58(14)
C11–W1–N5	82.90(13)
C11–W1–C10	37.93(15)
C20–P1–W1	121.42(15)
C20–P1–C21	100.0(2)
C20–P1–C22	102.4(2)
C21–P1–W1	113.20(16)
C21–P1–C22	103.0(2)

C22-P1-W1	114.32(17)
N2-N1-W1	120.2(2)
C1-N1-W1	134.0(3)
C1-N1-N2	105.8(3)
N1-N2-B1	121.3(3)
C3-N2-N1	109.4(3)
C3-N2-B1	129.2(4)
N4-N3-W1	122.6(2)
C4-N3-W1	131.1(3)
C4-N3-N4	106.3(3)
N3-N4-B1	119.3(3)
C6-N4-N3	109.8(3)
C6-N4-B1	129.8(4)
N6-N5-W1	121.1(2)
C7-N5-W1	132.3(3)
C7-N5-N6	106.2(3)
N5-N6-C9	109.0(3)
N5-N6-B1	120.9(3)
C9-N6-B1	129.6(4)
O1-N7-W1	176.1(3)
N1-C1-H1	124.5
N1-C1-C2	111.1(4)
C2-C1-H1	124.5
C1-C2-H2	127.7
C3-C2-C1	104.7(4)
C3-C2-H2	127.7
N2-C3-C2	109.1(4)
N2-C3-H3	125.5
C2-C3-H3	125.5
N3-C4-H4	124.8
N3-C4-C5	110.3(4)
C5-C4-H4	124.8
C4-C5-H5	127.6
C6-C5-C4	104.9(4)
C6-C5-H5	127.6
N4-C6-C5	108.7(4)
N4-C6-H6	125.6
C5-C6-H6	125.6
N5-C7-H7	124.6
N5-C7-C23	110.9(4)
C23-C7-H7	124.6
N6-C9-H9	125.5
N6-C9-C23	109.0(4)
C23-C9-H9	125.5
W1-C10-H10	111(2)
C11-C10-W1	69.6(2)
C11-C10-H10	117(2)
C11-C10-C17	120.3(4)

C17-C10-W1	120.8(3)
C17-C10-H10	112(2)
W1-C11-H11	115(2)
C10-C11-W1	72.5(2)
C10-C11-H11	114(3)
C10-C11-C12	120.1(4)
C12-C11-W1	122.4(3)
C12-C11-H11	109(3)
C11-C12-H12	117.1
C13-C12-C11	125.8(5)
C13-C12-H12	117.1
C12-C13-H13	117.6
C12-C13-C14	124.7(5)
C14-C13-H13	117.6
C13-C14-H14	108.0
C13-C14-C15	112.0(5)
C13-C14-C18	109.0(5)
C15-C14-H14	108.0
C15-C14-C18	111.7(5)
C18-C14-H14	108.0
C14-C15-H15	106.0
C14-C15-C16	115.0(4)
C16-C15-H15	106.0
C19-C15-C14	112.0(5)
C19-C15-H15	106.0
C19-C15-C16	111.1(5)
C15-C16-H16A	107.9
C15-C16-H16B	107.9
H16A-C16-H16B	107.2
C17-C16-C15	117.5(4)
C17-C16-H16A	107.9
C17-C16-H16B	107.9
C10-C17-C16	113.7(4)
C10-C17-H17A	108.8
C10-C17-H17B	108.8
C16-C17-H17A	108.8
C16-C17-H17B	108.8
H17A-C17-H17B	107.7
C14-C18-H18A	109.5
C14-C18-H18B	109.5
C14-C18-H18C	109.5
H18A-C18-H18B	109.5
H18A-C18-H18C	109.5
H18B-C18-H18C	109.5

C15–C19–H19A	109.5
C15–C19–H19B	109.5
C15–C19–H19C	109.5
H19A–C19–H19B	109.5
H19A–C19–H19C	109.5
H19B–C19–H19C	109.5
P1–C20–H20A	109.5
P1–C20–H20B	109.5
P1–C20–H20C	109.5
H20A–C20–H20B	109.5
H20A–C20–H20C	109.5
H20B–C20–H20C	109.5
P1–C21–H21A	109.5
P1–C21–H21B	109.5
P1–C21–H21C	109.5
H21A–C21–H21B	109.5

H21A–C21–H21C	109.5
H21B–C21–H21C	109.5
P1–C22–H22A	109.5
P1–C22–H22B	109.5
P1–C22–H22C	109.5
H22A–C22–H22B	109.5
H22A–C22–H22C	109.5
H22B–C22–H22C	109.5
C7–C23–H23	127.6
C9–C23–C7	104.9(4)
C9–C23–H23	127.6
N2–B1–N4	110.2(3)
N2–B1–N6	109.0(3)
N2–B1–H1A	110.6
N4–B1–N6	105.9(3)
N4–B1–H1A	110.6
N6–B1–H1A	110.6

Table 5. Torsion angles for mo\_harman\_mne\_5\_synmebn\_diene\_\_sq

Atom–Atom–Atom–Atom	Torsion Angle [°]
W1–N1–N2–C3	179.3(2)
W1–N1–N2–B1	3.1(4)
W1–N1–C1–C2	–178.9(3)
W1–N3–N4–C6	–179.0(3)
W1–N3–N4–B1	–9.5(5)
W1–N3–C4–C5	179.1(3)
W1–N5–N6–C9	173.2(2)
W1–N5–N6–B1	0.2(4)
W1–N5–C7–C23	–172.2(3)
W1–C10–C11–C12	117.9(4)
W1–C10–C17–C16	–175.8(3)
W1–C11–C12–C13	148.3(4)
N1–N2–C3–C2	–0.1(4)
N1–N2–B1–N4	–59.6(5)
N1–N2–B1–N6	56.2(4)
N1–C1–C2–C3	–0.5(5)
N2–N1–C1–C2	0.4(4)
N3–N4–C6–C5	–0.3(4)
N3–N4–B1–N2	63.5(5)
N3–N4–B1–N6	–54.2(5)

N3–C4–C5–C6	–0.3(5)
N4–N3–C4–C5	0.1(4)
N5–N6–C9–C23	0.1(5)
N5–N6–B1–N2	–58.6(5)
N5–N6–B1–N4	59.9(4)
N5–C7–C23–C9	–0.1(4)
N6–N5–C7–C23	0.1(4)
N6–C9–C23–C7	0.0(5)
C1–N1–N2–C3	–0.2(4)
C1–N1–N2–B1	–176.4(3)
C1–C2–C3–N2	0.3(5)
C3–N2–B1–N4	125.1(4)
C3–N2–B1–N6	–119.1(4)
C4–N3–N4–C6	0.1(4)
C4–N3–N4–B1	169.6(3)
C4–C5–C6–N4	0.4(4)
C6–N4–B1–N2	–129.4(4)
C6–N4–B1–N6	112.8(4)
C7–N5–N6–C9	–0.1(4)
C7–N5–N6–B1	–173.1(3)
C9–N6–B1–N2	130.0(4)
C9–N6–B1–N4	–111.5(4)

C10–C11–C12–C13	60.8(7)
C11–C10–C17–C16	–92.7(5)
C11–C12–C13–C14	0.7(8)
C12–C13–C14–C15	–93.3(7)
C12–C13–C14–C18	142.6(5)
C13–C14–C15–C16	81.7(6)
C13–C14–C15–C19	–46.3(6)
C14–C15–C16–C17	–54.9(7)
C15–C16–C17–C10	86.0(6)
C17–C10–C11–W1	–114.6(4)
C17–C10–C11–C12	3.3(6)
C18–C14–C15–C16	–155.7(6)
C18–C14–C15–C19	76.3(7)
C19–C15–C16–C17	73.6(6)
B1–N2–C3–C2	175.7(4)
B1–N4–C6–C5	–168.4(4)
B1–N6–C9–C23	172.3(4)

**SC-XRD 41 – Dr. Dickie finishing solving data.**

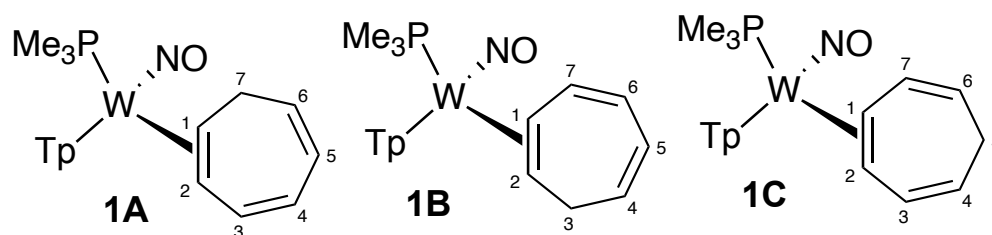
## Bibliography

- [1] Bruker, *SAINT*, 8.41, Bruker AXS Inc., Madison, Wisconsin, USA.
- [2] Unknown Reference, please add.
- [3] O. V. Dolomanov, L. J. Bourhis, R. J. Gildea, J. A. K. Howard, H. Puschmann, *J. Appl. Cryst.* **2009**, 42, 339-341, doi:10.1107/S0021889808042726.
- [4] G. M. Sheldrick, *Acta Cryst.* **2015**, A71, 3–8, doi:10.1107/S2053273314026370.
- [5] G. M. Sheldrick, *Acta Cryst.* **2015**, C71, 3–8, doi:10.1107/S2053229614024218.
- [6] D. Kratzert, *FinalCif*, V149, <https://dkratzert.de/finalcif.html>.

## **Appendix F: Chapter 6 Data**



## Synthesis and characterization of W(Tp)(NO)(PMe<sub>3</sub>)( $\eta^2$ -cycloheptatriene) (1)



In an oven-dried round-bottom flask charged with a stir bar, W(Tp)(NO)(PMe<sub>3</sub>)( $\eta^2$ -anisole) (2.5 g, 4.1 mmol) was combined with 1,3,5-cycloheptatriene (7.5 mL, 72.5 mmol) and 5 mL of DME. The round-bottom was capped with a septum and stirred in an oil bath at 60 °C for 1.5 h. A reaction precipitate was collected on a 30 mL fine porosity (F) frit. The remaining filtrate was precipitated in 1 L of chilled hexanes. The precipitate was filtered on a 60 mL F frit. The hexanes filtrate was evaporated in vacuo and the resulting precipitate was collected on a 30 mL F frit. The solids were desiccated (2.094 g, 3.51 mmol, 85% yield).

**IR(ATR, cm<sup>-1</sup>):**  $\nu(\text{NO}) = 1561 \text{ cm}^{-1}$

**CV (MeCN, 100 mV/s):**  $E_{p,a} +0.37 \text{ V (NHE)}$

**APCI-HRMS (m/z):**  $[M]^{+H}$  calculated for C<sub>19</sub>H<sub>28</sub>BN<sub>7</sub>OPW<sup>+</sup>, 596.1690 ; found 596.1673.

**1A:** To a 4-dram vial charged with a stir bar, compound 1 (100 mg, 0.17 mmol) dissolved in CHCl<sub>3</sub> was left to stir outside of the glovebox for a full 24 h covered with an unscrewed cap to prevent evaporation. The reaction mixture was precipitated in hexanes. A brown precipitate was filtered, and the hexanes filtrate was reduced by 75%. The white solid formed from the filtrate was filtered over a 30 mL F frit and placed in the desiccator (48 mg, 0.08 mmol, 48% yield).

**<sup>1</sup>H NMR (800 MHz, CDCl<sub>3</sub>,  $\delta$ , 25 °C):** 8.31 (d,  $J = 1.4 \text{ Hz}$ , 1H, PzA3), 8.04 (d,  $J = 1.4 \text{ Hz}$ , 1H, PzB3), 7.70 (d,  $J = 2.4 \text{ Hz}$ , 1H, Pz5B), 7.69 (d,  $J = 1.7 \text{ Hz}$ , 1H, Pz5C), 7.64 (d,  $J = 2.4 \text{ Hz}$ , 1H, PzA5), 7.21 (d,  $J = 1.7 \text{ Hz}$ , 1H, PzC3), 6.28 (d,  $J = 2.2 \text{ Hz}$ , 1H, PzB4), 6.25 (d,  $J = 2.2 \text{ Hz}$ , 1H, PzA4), 6.15 (d,  $J = 2.2 \text{ Hz}$ , 1H, PzC4), 7.03 (dd,  $J = 11.0, 3.5 \text{ Hz}$ , 1H, H3), 6.21-6.18 (m, 1H, H5), 6.10-6.06 (m, 1H, H6), 5.76 (dd,  $J = 11.0, 5.4 \text{ Hz}$ , 1H, H4), 3.18-3.08 (m, 2H, H7), 2.83-2.77 (m, 1H, H1), 1.46-1.41 (m, 1H, H2), 1.26 (d,  $J_{PH} = 8.1 \text{ Hz}$ , 9H, PMe<sub>3</sub>)

**<sup>13</sup>C NMR (800 MHz, CDCl<sub>3</sub>,  $\delta$ , 25 °C):** 143.8 (PzA3), 143.5 (PzB3), 137.5-135.0 (2C, PzB5/PzC5), 136.2 (PzA5), 139.9 (PzC3), 107.7-105.0 (3C, PzB4/PzA4/PzC4),

141.90 (C3), 128.6 (C5), 128.70 (C6), 122.74 (C4), 34.0 (C7), 55.6 (C1), 55.0 (C2), 14.2 (d,  $J_{PC} = 27.3$  Hz, 3C,  $\text{PMe}_3$ ).

**$^{31}\text{P}$  NMR** (500 MHz, DME,  $\delta$ , 25 °C): :  $J_{WP} = 144.8$  Hz

**1B:** attempts to isolate this complex from its isomers were unsuccessful.

**$^1\text{H}$  NMR (800 MHz,  $\text{CDCl}_3$ ,  $\delta$ , 25°C):** 8.15 (d,  $J = 2.0$  Hz, 1H, PzA3), 8.06 (d,  $J = 1.7$  Hz, 1H, PzB3), 7.70 (d,  $J = 1.7$  Hz, 1H, Pz5B), 7.61 (d,  $J = 2.4$  Hz, 1H, Pz5C), 7.26, 7.23 (d,  $J = 2.0$  Hz, 2H, PzA5/PzC3), 6.28 (d,  $J = 2.2$  Hz, 1H, PzB4), 6.22 (d,  $J = 2.2$  Hz, 1H, PzA4), 6.17 (d,  $J = 2.2$  Hz, 1H, PzC4), 6.86 (dd,  $J = 11.3, 4.5$  Hz, 1H, H7), 6.10-6.05 (m, 1H, H5), 6.05-6.01 (m, 1H, H4), 5.61 (dd,  $J = 11.5, 5.6$  Hz, 1H, H6), 3.54 (td,  $J = 14.5, 4.5$  Hz, 1H, H3), 3.21-3.17 (m, 1H, H3), 2.80 (m, 1H, H1), 1.87-1.83 (m, 1H, H2), 1.26 (d,  $J_{PH} = 8.1$  Hz, 9H,  $\text{PMe}_3$ )

**$^{13}\text{C}$  NMR (800 MHz,  $\text{CDCl}_3$ ,  $\delta$ , 25°C):** 142.8 (PzA3), 143.9 (PzB3), 137.5-135.0 (PzB5), 135.6, (PzC5) 135.4 (PzA5), 140.0 (PzC3), 106.6-105.0 (3C, PzB4/PzA4/PzC4), 140.3 (C7), 137.0 (C5), 135.4 (C4), 123.3 (C6), 32.1 (C3), 55.9 (C1), 67.4 (C2), 13.6 (d,  $J_{PC} = 17.6$  Hz, 3C,  $\text{PMe}_3$ ).

**$^{31}\text{P}$  NMR (500 MHz, DME,  $\delta$ , 25°C):**  $J_{WP} = 145.1$  Hz

**1C:** In a test tube charged with a stir bar, compound 2 (160 mg, 0.21 mmol) was dissolved in 3 mL  $\text{CHCl}_3$  and allowed to stir at -15 °C. Another test tube containing triethylamine (TEA) (0.30 mL, 2.15 mmol) dissolved in 1 mL  $\text{CHCl}_3$  was also chilled at -15 °C. After 10 minutes, the TEA test tube was added to the test tube containing the complex and the solution was allowed to stir for 15 minutes. Upon removal from the bath, the solution was diluted with 30 mL of  $\text{CHCl}_3$  and extracted 5x with 30 mL of 1 M NaOH. The organic layer was dried with  $\text{Na}_2\text{SO}_4$ , filtered, and evaporated in vacuo until dryness. The dark brown material was redissolved in  $\text{CHCl}_3$  and evaporated three times to remove excess TEA. The remaining material was dissolved in  $\text{CHCl}_3$  and precipitated in 300 mL chilled hexanes. The black precipitate was collected on a 15 mL F frit and discarded. The hexanes filtrate was reduced by 150 mL. The white precipitate formed was filtered, dried in the desiccator, and collected on a 15 mL F frit (45 mg, 0.08 mmol 35%).

**$^1\text{H}$  NMR (800 MHz,  $\text{CDCl}_3$ ,  $\delta$ , 25°C):** 8.51 (d,  $J = 2.0$  Hz, 1H, PzA3), 8.06 (d,  $J = 2.0$  Hz, 1H, PzB3), 7.70 (d,  $J = 2.3$  Hz, 1H, PzB5), 7.68 (d,  $J = 2.4$  Hz, 1H, PzA5), 7.59 (d,  $J = 2.4$  Hz, 1H, PzC5), 7.31 (d,  $J = 2.2$  Hz, 1H, PzC3), 6.62-6.56 (m, 2H, H3/H4), 6.28

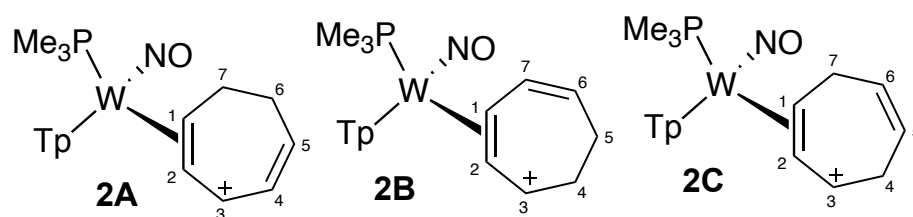
(t,  $J = 2.1$  Hz, 1H, PzB4), 6.20 (t,  $J = 2.2$  Hz, 1H, PzC4), 6.17 (t,  $J = 2.2$  Hz, 1H, PzA4), 5.24 (dtd,  $J = 6.9, 4.0, 1.4$  Hz, 1H, H6), 5.19 (dtd,  $J = 6.9, 4.0, 1.4$  Hz, 1H, H7), 4.36 (dq,  $J = 20.9, 2.9$  Hz, 1H, H5), 2.79 – 2.73 (m, 1H, H1), 2.72 (dt,  $J = 21.0, 6.9$  Hz, 1H, H5), 1.53 – 1.44 (m, 1H, H2), 1.25 (d,  $J_{PH} = 8.3$  Hz, 9H, PMe3).

**$^{13}\text{C}$  NMR (800 MHz,  $\text{CDCl}_3$ ,  $\delta$ , 25°C):** 143.6 (PzA3), 143.4 (PzB3), 137.5-135.0 (2C, PzB5/PzA5), 137.8 (PzC5), 140.3 (PzC3), 107.7-105.0 (3C, PzB4/PzA4/PzC4), 137.5/133.7 (C3/C4), 122.5 (C7), 123.4 (C1), 30.1 (C5), 55.6 (C1), 53.85 (C2), 13.8 (d,  $J_{PC} = 17.8$  Hz, 3C, PMe3).

**$^{31}\text{P}$  NMR (500 MHz, DME,  $\delta$ , 25°C):**  $J_{WP} = 147.5$  Hz

Composition of **1C** confirmed by single crystal X-ray diffraction.

### Synthesis and characterization of $[\text{W}(\text{Tp})(\text{NO})(\text{PMe}_3)(\eta^2\text{-cycloheptadienyl cation})]\text{OTf}$ (**2**)



To a 4-dram vial charged with a stir bar, compound **1** (150 mg, 0.25 mmol) was dissolved in  $\text{CHCl}_3$ . HOTf diluted in MeCN was added (0.6 mM, 0.30 mmol) and the solution was allowed to stir at 25 °C for 24 h. The solution was pipetted into chilled hexanes. The precipitate obtained was dried in the desiccator and collected on a 30 mL F frit (164.4 g, 0.22 mmol, 87.5% yield, cdr = 6:1 **2A:2B**). Immediate precipitation produced another allyl complex (**2C**) in a cdr of 3:3:1 for **2A:2C:2B**.

**2A:  $^1\text{H}$  NMR (800 MHz,  $\text{CDCl}_3$ ,  $\delta$ , 25 °C):** 8.28 (d,  $J = 2.2$  Hz, 1H, PzB3), 8.19 (d,  $J = 2.4$  Hz, 1H, PzC3), 8.07 (d,  $J = 2.2$  Hz, 1H, PzA3), 7.86 (d,  $J = 2.4$  Hz, 1H, PzC5), 7.83 (d,  $J = 2.5$  Hz, 1H, PzB5), 7.70 (d,  $J = 2.5$  Hz, 1H, PzA5), 6.61 (t,  $J = 2.3$  Hz, 1H, PzC4), 6.54 (ddd,  $J = 10.5, 5.6, 2.6$  Hz, 1H, H4), 6.48 (t,  $J = 2.3$  Hz, 1H, PzB4), 6.36 (td,  $J = 9.5, 4.3$  Hz, 1H, H5), 6.31 (t,  $J = 2.3$  Hz, 1H, PzA4), 6.13 (dd,  $J = 6.5, 7.5$  Hz, 1H, H3), 5.24 (t,  $J = 9.0$  Hz, 1H, H2), 4.99 – 4.92 (m, 1H, H1), 3.17 (td,  $J = 10.9, 5.2$  Hz, 1H, H7), 3.02 (t,  $J = 13.3$  Hz, 1H, H7), 2.63 – 2.57 (m, 1H, H6), 2.37-2.32 (m, 1H, H6), 1.30 – 1.24 (m, 1H), 1.21 (d,  $J_{PC} = 9.3$  Hz, 9H, PMe3).

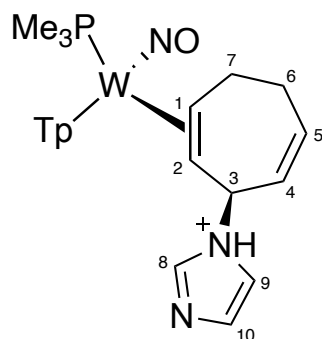
**<sup>13</sup>C NMR (800 MHz, CDCl<sub>3</sub>, δ, 25 °C):** 145.0 (PzB3), 143.5 (PzC3), 146.9 (PzA3), 137.9-138.5 (3C PzC5/PzB5/PzA5), 109.3 (PzC4), 108.6 (PzB4), 107.4 (PzA4), 124.4 (C4), 138.4 (C5), 126.8 (C3), 109.5 (C2), 77.9 (C1), 36.8 (C7), 31.3 (C6). 14.1 (9C, *J*<sub>PH</sub> = 32.2 Hz, PMe<sub>3</sub>).

Composition of **2A** confirmed by single crystal X-ray diffraction.

**2B: <sup>1</sup>H NMR (800 MHz, CDCl<sub>3</sub>, δ, 25 °C):** 8.27 (d, *J* = 2.2 Hz, 1H, PzB3) 8.12 (d, *J* = 2.2 Hz, 1H, PzC3), 7.99 (d, *J* = 2.2 Hz, 1H, PzA3), 7.87 (d, *J* = 2.2 Hz, 1H, PzB5), 7.85 (d, *J* = 2.4 Hz, 1H, PzC5), 7.70-7.69 (d, 1H, PzA5), 6.60-6.58 (t, 1 H, PzC4), 6.48 (d, *J* = 2.4 Hz, 1H, PzB4), 6.31 (d, *J* = 2.4 Hz, 1H, PzA4), 5.78-5.74 (m, 1H, H7), 5.72 (t, *J* = 8.50 Hz, 1H, H3), 5.66-5.62 (m, 1H, H6), 5.39-5.34 (m, 1H, H1), 5.29-5.27 (m, 1H, H2), 3.99-3.93 (m, 1H, H4), 3.40-3.33 (m, 1H, H4), 2.80-2.75 (m, 1H, H5), 2.37-2.32 (m, 1H, H5), 1.20 (d, *J*<sub>PH</sub> = 9.7 Hz, PMe<sub>3</sub>).

**2C: <sup>1</sup>H NMR (800 MHz, CDCl<sub>3</sub>, δ, 25 °C):** 8.27 (d, *J* = 2.1 Hz, 1H, PzB3), 8.07 (d, *J* = 2.1 Hz, 1H, PzA3), 8.05 (d, *J* = 2.1 Hz, 1H, PzC3), 8.03 (d, *J* = 2.1 Hz, 1H, PzC5), 7.85-7.83 (d, 1H, PzB5), 7.69 (d, *J* = 2.1 Hz, 1H, PzA5), 6.59 (d, *J* = 2.3 Hz, 1H, PzC4), 6.47 (d, *J* = 2.3 Hz, 1H, PzB4), 6.32 (d, *J* = 2.1 Hz, 1H, PzA4), 5.83-5.79 (m, 1H, H3), 5.61-5.53 (m, 2H, H5/H6), 4.96 (t, *J* = 9.5 Hz, 1H, H2), 4.87-4.79 (m, 1H, H1), 4.60 (d, *J* = 21.0 Hz, 1H, H7), 4.35 (d, *J* = 23.5 Hz, 1H, H4), 4.25 (d, *J* = 23.5 Hz, 1H, H4), 3.30 (d, *J* = 21.0 Hz, 1H, H7), 1.18 (d, *J*<sub>PH</sub> = 9.6 Hz, PMe<sub>3</sub>).

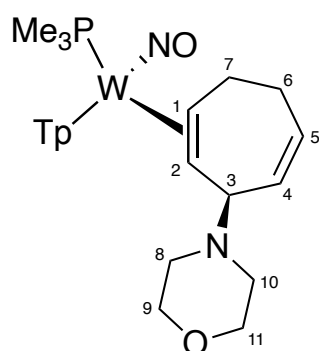
### Synthesis and characterization of W(Tp)(NO)(PMe<sub>3</sub>)(η<sup>2</sup>-3-imidazole-cyclohepta,1,4-diene) (**3A**)



At an NMR scale, compound **2A** was dissolved in d-MeCN. Imidazole is added to the reaction.

**<sup>1</sup>H NMR (800 MHz, CD<sub>3</sub>CN, δ, 25 °C):** 8.21, 8.07, 7.88, 7.79, 7.75 (d, J = 1.79, 1.95, 1.74, 1.74, 2.16 Hz, 6H, Tp protons), 8.19, 7.50, 7.12 (bs, 3H, H<sub>8</sub> – H<sub>10</sub>), 6.39, 6.27 (t, J = 2.09, 2.29, 2.09 Hz, 3H, Tp protons), 5.65 (d, J = 6.08 Hz, 1H, H<sub>4</sub> or H<sub>5</sub>), 4.93 (dd, J = 5.90, 11.80 Hz, 1H, H<sub>4</sub> or H<sub>5</sub>), 2.92, (t, J = 11.50 Hz, 1H), 2.83 (t, J = 11.20 Hz, 1H), 2.31 (d, J = 17.56 Hz, 1H), 2.04 (m, 1H), 2.01 (m, 1H), 1.73 (m, 1H), 1.52 (m, 1H) – H<sub>1</sub> – H<sub>3</sub>, H<sub>6</sub> – H<sub>7</sub>), 1.18 (d, J = 7.57, 9H, PMe<sub>3</sub>).

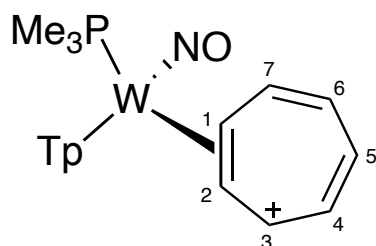
### Synthesis and characterization of W(Tp)(NO)(PMe<sub>3</sub>)(η<sup>2</sup>-3-morpholine-cyclohepta,1,4-diene) (3B)



At an NMR scale, compound **2A** was dissolved in CDCl<sub>3</sub>. Morpholine is added to the reaction.

**<sup>1</sup>H NMR (800 MHz, CD<sub>3</sub>CN, δ, 25 °C):** 8.17, 7.95, 7.66, 7.64, 7.58, 7.24 (d, J = 1.82, 1.82, 2.16, 2.16, 2.51, 2.16 Hz, 6H, Tp protons), 6.44 (d, J = 12.20, 1H), 2.06 (d, J = 12.20 Hz, 1H) – H<sub>4</sub> – H<sub>5</sub>. 6.23, 6.17, 6.16 (t, J = 2.10, 2.61, 2.10 Hz, 3H, Tp protons), 3.68, 3.46, 2.69, 2.66, 2.59, 2.51, 2.10, 1.68 (m, 15H, H<sub>1</sub> – H<sub>3</sub>, H<sub>6</sub> – H<sub>7</sub>, H<sub>8</sub> – H<sub>11</sub>), 1.19 (d, J = 8.11 Hz, 9H, PMe<sub>3</sub>).

### Synthesis and characterization of [W(Tp)(NO)(PMe<sub>3</sub>)(η<sup>2</sup>-cycloheptatrieny)]DDQ radical anion (4)



In a test tube charged with a stir bar, **1** (100 mg, 0.17 mmol) was dissolved in 2.0 mL MeCN and allowed to stir at RT. Another test tube containing 3,6-dichloro-1,2,4,5-tetrazine (51mg, 0.34 mmol) dissolved in 2 mL MeCN was chilled at -30 °C. After 10 minutes, the 3,6-dichloro-1,2,4,5-tetrazine solution was added to the complex. After 15 minutes hours, the reaction mixture was added to a stirring solution of diethyl ether (100 mL) and triflic acid (126 mg, 0.84 mmol). A dark grey solid was immediately precipitated in diethyl ether solution. The precipitate was collected on a fritted disk, washed with diethyl ether (50mL), then washed through the fritted disk with acetone into a clean filter flask. The acetone solution was added to stirring diethyl ether (100 mL), precipitating a light grey solid which was collected and dried desiccated under active vacuum. (90 mg, 0.12 mmol, 72% yield).

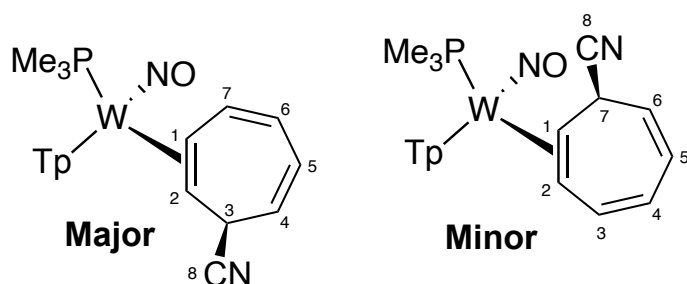
**<sup>1</sup>H NMR (800 MHz, CD<sub>3</sub>CN, δ, 25 °C):** 8.14 (d, *J* = 2.1 Hz, 1H, PzB3), 8.09 (d, *J* = 2.3 Hz, 1H, PzC5), 8.01 (d, *J* = 2.2 Hz, 1H, PzB5), 7.87 (d, *J* = 2.2 Hz, 1H, PzA5), 7.85 (d, *J* = 2.2 Hz, 1H, PzA3), 7.74 (d, *J* = 2.2 Hz, 1H, PzC3), 6.53 (t, *J* = 2.3 Hz, 1H, PzC4), 6.45 (t, *J* = 2.3 Hz, 1H, PzB4), 6.32 (t, *J* = 2.3 Hz, 1H, PzA4), 5.67 (d, *J<sub>PH</sub>* = 2.0 Hz, *J<sub>WH</sub>* = 20.0 Hz, 7H, H1-7) 1.21 (d, *J<sub>PH</sub>* = 9.6 Hz, 9H, PMe<sub>3</sub>).

**<sup>13</sup>C NMR (201 MHz, CD<sub>3</sub>CN, δ, 25 °C):** 146.6 (1C, PzB3), 145.2 (1C, PzA3), 142.6 (1C, PzC3), 139.4 (1C, PzB5), 139.1 (1C, PzA5), 139.7 (1C, PzC5), 123.3 (7C, C1-7), 108.6 (1C, PzC4), 108.9 (1C, PzB4), 107.6 (1C, PzA4), 12.9 (d, *J<sub>PC</sub>* = 32.0 Hz, 3C, PMe<sub>3</sub>).

**IR (ATR, cm<sup>-1</sup>):** ν(NO) = 1636 cm<sup>-1</sup>, DDQ anion ν(CN) = 2220 cm<sup>-1</sup>, triflate anion ν(CF<sub>3</sub>SO<sub>3</sub>) = 636 cm<sup>-1</sup>.

Composition of **4** confirmed by single crystal X-ray diffraction.

### Synthesis and characterization of W(Tp)(NO)(PMe<sub>3</sub>)(η<sup>2</sup>-7-cyano-cyclohepta,1,3,5-triene) (**5A**)

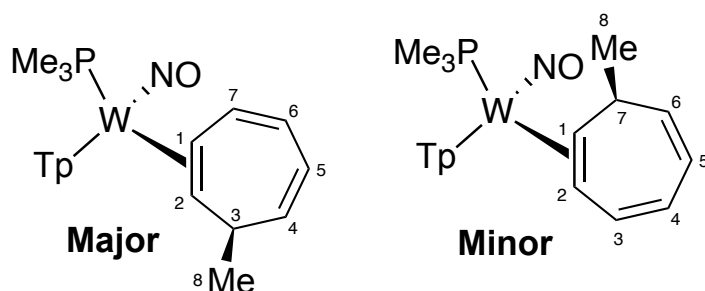


In a test tube charged with a stir bar, compound **4** (100 mg, 0.12 mmol) was dissolved in 2 mL MeOH and allowed to stir at -60 °C. Another test tube containing NaCN (29.8 mg, 0.61 mmol) dissolved in 1 mL MeOH was also chilled at -60 °C. After 15 minutes, the NaCN solution was added to the complex and allowed to stir overnight. The reaction solution was diluted with 25 mL of DCM and extracted with 3x 30 mL of H<sub>2</sub>O. The organic layer was dried with Na<sub>2</sub>SO<sub>4</sub>, filtered, and evaporated to dryness. The product was redissolved in minimal DCM and precipitated in 300 mL of chilled hexanes. The precipitate was filtered over a 15 mL F frit and dried in the desiccator (50 mg, 0.08 mmol, 66% yield).

**Major: <sup>1</sup>H NMR (800 MHz, CD<sub>3</sub>CN, δ, 25 °C):** 7.99, 7.86, 7.81, 7.78, 7.40 (t, *J* = 2.1, 3.4, 2.5, 2.0, 2.2, 2.3 Hz, 6H, Tp protons), 6.35, 6.30, 6.29 (t, *J* = 2.2, 2.2, 2.3 Hz, 3H, Tp protons), 7.02 (dd, *J* = 11.7, 7.2 Hz), 6.08 (dd, *J* = 10.5, 6.5 Hz), 5.66 (t, *J* = 9.5 Hz), 5.25 (dd, *J* = 11.7, 6.5 Hz) – H<sub>4</sub> – H<sub>7</sub>. 3.97 (dd, *J* = 8.8, 4.8 Hz), 2.96 – 2.90 (m), 2.13-2.10 (m) – H<sub>1</sub> – H<sub>3</sub>. 1.20 (d, *J*<sub>PH</sub> = 8.8 Hz, 9H, PMe<sub>3</sub>).

**Minor: <sup>1</sup>H NMR (800 MHz, CD<sub>3</sub>CN, δ, 25 °C):** 8.20 - 6.85 (d, 6H, Tp protons), 6.40 – 6.30 (t, 3H, Tp protons), 7.02 (dd, *J* = 11.7, 7.0 Hz), 6.16 (dd, *J* = 10.5, 6.5 Hz), 5.59 (t, *J* = 9.5 Hz), 5.47 (dd, *J* = 11.7, 6.5 Hz) – H<sub>3</sub> – H<sub>6</sub>. 4.24 (dd, *J* = 8.8, 4.8 Hz), 3.65-3.59 (m), 1.48-1.45 (m) – H<sub>1</sub>/H<sub>2</sub>/H<sub>7</sub>. 1.17 (d, *J*<sub>PH</sub> = 8.60 Hz, 9H, PMe<sub>3</sub>).

### Synthesis and characterization of W(Tp)(NO)(PMe<sub>3</sub>)( $\eta^2$ -7-methyl-cyclohepta,1,3,5-triene) (**5B**)

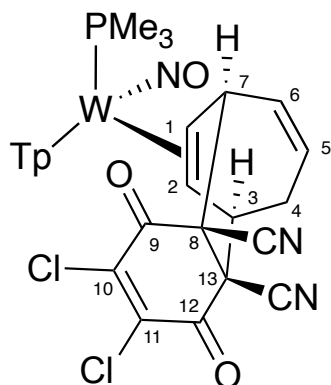


In a test tube, compound **4** (10mg, 0.16 mmol) was dissolved in 2 mL THF. At room temperature, MeMgCl (3M) was added (0.02 mL, 0.061 mmol) was added and stirred for 15 minutes. The reaction was diluted with 10mL of DCM, extracted 3X with 10mL of a saturated aqueous solution of Na<sub>2</sub>CO<sub>3</sub>. The organic layer was collected and dried with Na<sub>2</sub>SO<sub>4</sub>, filtered over a 15mL M fritted disc and dissolved to dryness to yield compound **5B**.

**Major:  $^1\text{H}$  NMR (800 MHz,  $\text{CD}_3\text{CN}$ ,  $\delta$ , 25 °C):** 7.97, 7.84, 7.83, 7.76, 7.35 (d,  $J$  = 2.57, 2.20, 2.47, 2.20, 2.54, 2.00 Hz, 6H, Tp protons), 6.35, 6.33, 6.27 (t,  $J$  = 2.20, 2.27, 1.94 Hz, 3H, Tp protons), 6.27 (m), 6.72 (dt,  $J$  = 7.54, 11.42 Hz), 5.73 (m,  $J$  = 5.95, 11.61, 18.29 Hz), 5.70 (m,  $J$  = 5.52, 11.47, 17.57 Hz) – H4 – H7. 3.28 (m,  $J$  = 7.12, 12.60 Hz), 3.04 (bs), 1.80 (m) – H1 – H3. 1.41 (d,  $J$  = 6.98 Hz, 3H, H8), 1.23 (d,  $J$  = 8.31 Hz, 9H,  $\text{PMe}_3$ ).

**Minor:  $^1\text{H}$  NMR (800 MHz,  $\text{CD}_3\text{CN}$ ,  $\delta$ , 25 °C):** 8.30, 8.01, 7.85, 7.73, 7.41 (d,  $J$  = 1.71, 2.07, 2.15, 2.42, 2.31, 2.17 Hz, 6H, Tp protons), 6.27, 6.20, 6.16 (t,  $J$  = 2.21, 2.08 Hz, 3H, Tp protons), 6.37 (bs), 5.56 (dd,  $J$  = 8.25, 10.67 Hz), 5.18 (dd,  $J$  = 6.42, 10.86 Hz), 5.00 (dd,  $J$  = 6.42, 11.47 Hz) – H3 – H6. 3.35 (m), 2.99 (m,  $J$  = 7.56, 10.44), 1.73 (dd,  $J$  = 4.55, 11.87 Hz) – H1/H2/H7. 1.57 (d,  $J$  = 6.61 Hz, 3H, H8), 1.17 (d,  $J$  = 8.42, 9H,  $\text{PMe}_3$ ).

**Synthesis and characterization of  $\text{W}(\text{Tp})(\text{NO})(\text{PMe}_3)(1,2\text{-}\eta^2\text{-(10,11-dichloro-8,13-dicyano-tricyclo[5.2.2.0(8,13)]tetradeca-1,5,10-triene-9,12-dione})$  (6B)**



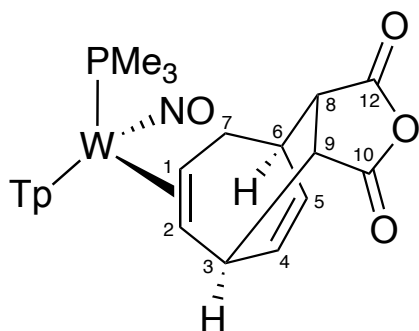
In a test tube charged with a stir bar, compound **1** (40 mg, 0.07 mmol) was dissolved in 1.5 mL MeCN and allowed to stir at -15 °C. Another test tube containing DDQ (16.8 mg, 0.07 mmol) dissolved in 1 mL MeCN was also chilled at -15 °C. After 10 minutes, the DDQ solution was added to the complex. After 12 hours, the reaction solution was precipitated in 200 mL ether. It was filtered to remove compound **3** and the remaining filtrate was evaporated until a precipitate was formed (~150 mL). This precipitate was then filtered and dried in the desiccator (17 mg, 0.02 mmol, 30% yield).

**$^1\text{H}$  NMR (800 MHz,  $\text{CD}_3\text{CN}$ ,  $\delta$ , 25 °C):** 7.99, 7.90, 7.87, 7.81, 7.72, 7.28 (d,  $J$  = 2.0, 2.3, 2.4, 2.2, 2.0, 2.3 Hz, 6H, Tp protons), 6.41 (m, 1H, H6), 6.37, 6.35 (t,  $J$  = 2.2 Hz, 3H, Tp protons), 4.87 (dd,  $J$  = 9.0, 11.0 Hz, 1H, H5), 4.04 (t,  $J$  = 5.7 Hz, 1H, H3), 3.93



(m, 1H, H7), 2.75 (d,  $J = 12.9$  Hz, H4), 2.67 (dt,  $J = 13.2, 6.8$  Hz, 1H, H4), 2.40 (td,  $J = 5.0, 11.0$  Hz, 1H, H1), 1.10 (d,  $J = 8.7$  Hz, 9H, PMe<sub>3</sub>), 0.97 (m, 1H, H2).

### Synthesis and characterization of W(Tp)(NO)(PMe<sub>3</sub>)(1,2- $\eta^2$ -11-oxatricyclo[5.2.2.0(8,9)]dodeca-1,4-diene-10,12-dione) (7A)

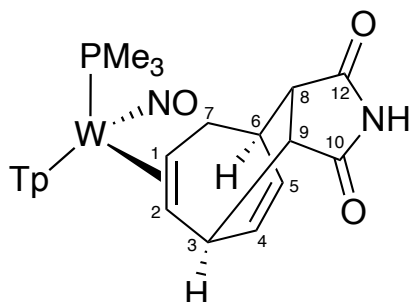


In an oven-dried round-bottom flask charged with a stir egg, W(Tp)(NO)(PMe<sub>3</sub>)( $\eta^2$ -cycloheptatriene) (150 mg, 0.25 mmol) was combined with maleic anhydride (150 mg, 1.53 mmol) in 5 mL of DME. The reaction was allowed to stir in an oil bath at 80 °C for 2 h. The reaction solution was then diluted with 30 mL of DCM and extracted 3x with 30 mL of H<sub>2</sub>O. The resulting organic layer was dried with Na<sub>2</sub>SO<sub>4</sub>, filtered, and evaporated in vacuo until dryness. The product was then redissolved in 2 mL of DCM and precipitated in 500 mL of chilled hexanes. The precipitate was collected on a 30 mL F frit and desiccated (113 mg, 0.16 mmol, 63% yield).

**<sup>1</sup>H NMR (800 MHz, CD<sub>3</sub>CN,  $\delta$ , 25 °C):** 8.04, 8.03, 7.86, 7.81, 7.76, 7.25 (d,  $J = 2.0, 2.0, 2.4, 2.4, 2.4, 2.0$  Hz, 6H, Tp protons), 6.40 (dd,  $J = 9.0, 7.2$  Hz, 1H, H4), 6.37, 6.33, 6.24 (t,  $J = 2.2$  Hz, 2.2, 2.2 Hz, 3H, Tp protons), 6.04 (dd,  $J = 9.0, 7.2$  Hz, 1H, H5), 3.93 (dd,  $J = 9.0, 2.4$  Hz, 1H, H9), 3.80 (dd,  $J = 9.0, 1.5$  Hz, 1H, H8), 3.52 (dddd,  $J = 7.1, 4.7, 2.4, 1.2$  Hz, 1H, H3), 3.13 (td,  $J = 14.0, 2.4$  Hz 1H, H7), 3.04 (ddd,  $J = 14.0, 9.8, 5.0$  Hz, 1H, H7), 2.87 (td,  $J = 5.1, 2.5$  Hz, 1H, H6), 2.58 (dddd,  $J = 15.2, 12.7, 9.8, 3.1$  Hz, 1H, H1), 1.12-1.10 (m, 1H, H2) 1.11 (d,  $J_{PH} = 8.3$  Hz, 9H, PMe<sub>3</sub>).

**<sup>13</sup>C NMR: (800 MHz, CD<sub>3</sub>CN,  $\delta$ , 25 °C):** 177.3, 176.2 (2C, C10/C12), 144.9, 141.1, 137.9, 137.6, 137.2, 137.0 (6C, Tp carbons), 135.9 (C4), 132.7 (C5), 107.5, 107.1, 107.0 (3C, Tp carbons), 59.2 (C2), 54.9 (C9), 47.6 (d,  $J = 10.86$  Hz, 1C, C1), 46.7 (C8), 41.1 (C3), 37.9 (C6), 34.0 (C7), 13.7 (d,  $J_{PC} = 28.3$  Hz, 3C, PMe<sub>3</sub>)

**Synthesis and characterization of  $W(Tp)(NO)(PMe_3)(1,2-\eta^2-11-azatricyclo[5.2.2.0(8,9)]dodeca-1,4-diene-10,12-dione)$  (7B)**

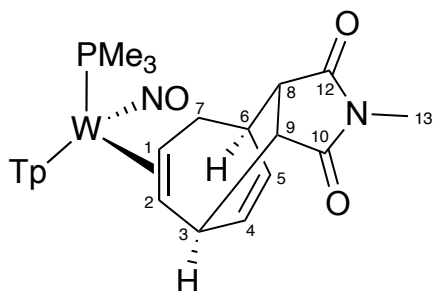


In an oven-dried round-bottom flask charged with a stir egg, compound **1** (150 mg, 0.25 mmol) was combined with maleimide (293 mg, 3.02 mmol) in 5 mL of diglyme. The reaction was allowed to stir in an oil bath at 110 °C for 6 h. The reaction solution was then diluted with 30 mL of DCM and extracted 3x with 30 mL of H<sub>2</sub>O. The resulting organic layer was dried with Na<sub>2</sub>SO<sub>4</sub>, filtered, and evaporated to dryness. The product was then redissolved in 2 mL of DCM and precipitated in 500 mL of chilled hexanes. The precipitate was collected on a 30 mL F frit and desiccated (127 mg, 0.18 mmol, 71% yield)

**<sup>1</sup>H NMR (800 MHz, CD<sub>3</sub>CN,  $\delta$ , 25 °C):** 8.04, 7.85, 7.80, 7.75, 7.25 (d,  $J$  = 2.35, 1.57, 2.55, 1.76 Hz, 6H, Tp protons), 6.37, 6.33, 6.23 (t,  $J$  = 1.69, 2.21, 2.72 Hz, 3H, Tp protons), 6.28 (dd,  $J$  = 8.5, 7.5 Hz, 1H, H<sub>4</sub>), 5.94 (dd,  $J$  = 8.0, 7.0 Hz, 1H, H<sub>5</sub>), 3.55 (dd,  $J$  = 8.3, 2.4 Hz, 1H, H<sub>9</sub>), 3.45 – 3.41 (m, 2H, H<sub>3</sub>/H<sub>8</sub>), 3.12 (dt,  $J$  = 14.1, 2.8 Hz, 1H, H<sub>7</sub>), 3.00 (ddd,  $J$  = 14.3, 9.8, 5.0 Hz, 1H, H<sub>7</sub>), 2.78 (td,  $J$  = 5.1, 2.5 Hz, 1H, H<sub>6</sub>), 2.60 (dddd,  $J$  = 15.1, 12.5, 9.8, 2.9 Hz, 1H, H<sub>1</sub>), 1.12 (d,  $J_{PH}$  = 8.3 Hz, 9H), 1.07 (dd,  $J$  = 12.2, 4.8, 1.2, 1H, H<sub>2</sub>).

**<sup>13</sup>C NMR: (800 MHz, CD<sub>3</sub>CN,  $\delta$ , 25 °C):** 182.4, 181.7 (2C, C<sub>10</sub>/C<sub>12</sub>), 144.8, 143.7, 141.1, 137.6, 137.1, 136.9 (6C, Tp carbons), 134.5 (C<sub>4</sub>), 132.3 (C<sub>5</sub>), 107.5, 107.0, 106.9 (3C, Tp carbons), 60.0 (C<sub>2</sub>), 55.7 (C<sub>9</sub>), 48.2 (d,  $J$  = 10.57 Hz, C<sub>1</sub>), 47.4, 40.1 (C<sub>3</sub>/C<sub>8</sub>), 37.4 (C<sub>6</sub>), 34.4 (C<sub>7</sub>), 12.6 (d,  $J_{PC}$  = 27.8 Hz, 3C, PMe<sub>3</sub>).

**Synthesis and characterization of  $W(Tp)(NO)(PMe_3)(1,2-\eta^2-13\text{-methyl-13-aza-tricyclo}[5.2.2.0(8,9)]\text{dodeca-1,4-diene-10,12-dione})$  (7C)**

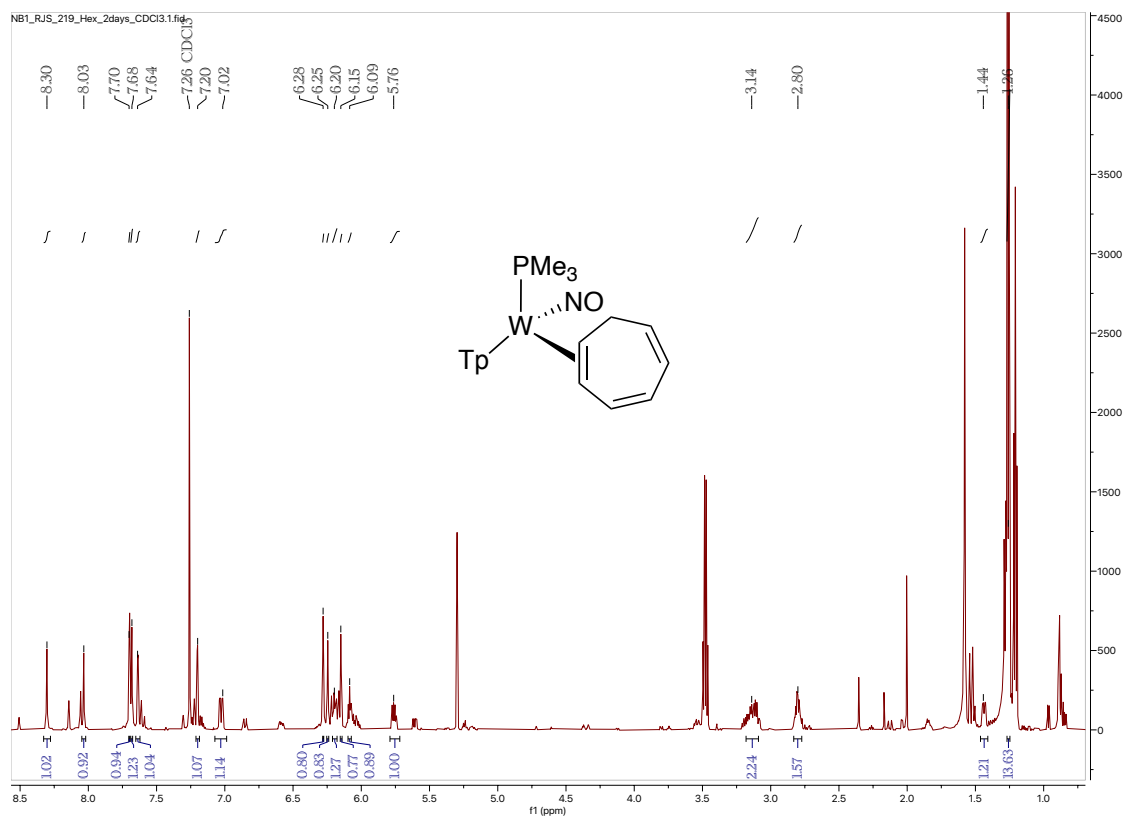


In an oven-dried round-bottom flask charged with a stir egg, compound **1** (150 mg, 0.25 mmol) was combined with N-methylmaleimide (167.7 mg, 1.51 mmol) in 5 mL of diglyme. The reaction was allowed to stir in an oil bath at 110 °C for 6 h. The reaction solution was then diluted with 30 mL of DCM and extracted 3x with 30mL of H<sub>2</sub>O. The resulting organic layer was dried with Na<sub>2</sub>SO<sub>4</sub>, filtered, and evaporated in vacuo until dryness. The product was then redissolved in 2 mL of DCM and precipitated in 500 mL of chilled hexanes. The precipitate was collected on a 30 mL F frit and desiccated (102 mg, 0.14 mmol, 57% yield)

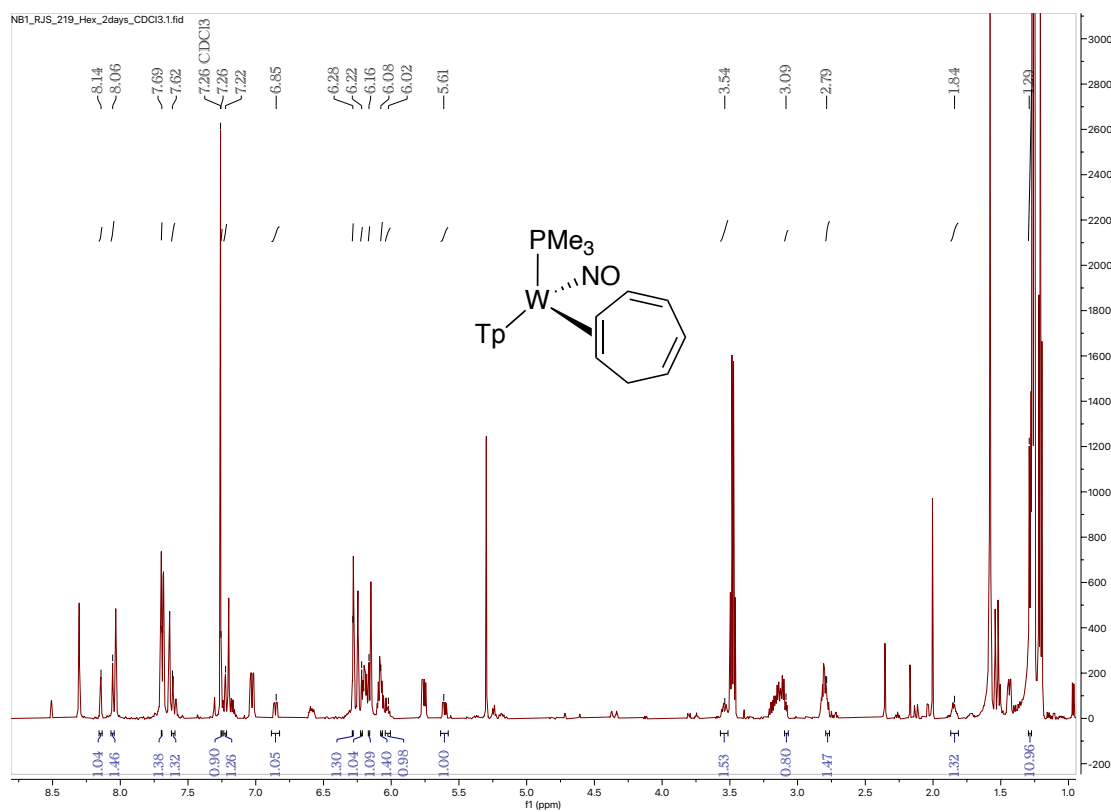
**<sup>1</sup>H NMR (800 MHz, CD<sub>3</sub>CN, δ, 25 °C):** 8.03, 7.85, 7.80, 7.75, 7.25 (d, *J* = 2.39, 2.39, 2.39, 1.43 Hz, 6H, Tp protons), 6.37, 6.33, 6.23 (t, *J* = 2.24, 2.16, 2.16 Hz, 3H, Tp protons), 6.22 (dd, *J* = 9.0, 7.0 Hz, 1H, H<sub>4</sub>), 5.87 (dd, *J* = 9.0, 7.0 Hz, 1H, H<sub>5</sub>), 3.52 (dd, *J* = 8.5, 2.4 Hz, 1H, H<sub>9</sub>), 3.46 (m, 1H, H<sub>3</sub>), 3.43 (dd, *J* = 8.5, 1.2 Hz, 1H, H<sub>8</sub>), 3.11 (td, *J* = 14.0, 2.5 Hz, 1H, H<sub>7</sub>), 3.00 (ddd, *J* = 14, 9.8, 5.0 Hz, 1H, H<sub>7</sub>), 2.83 (s, 3H, H<sub>13</sub>), 2.82-2.80 (m, 1H, H<sub>6</sub>), 2.62 (ddd, *J* = 7.1, 4.7, 2.4 Hz, 1H, H<sub>1</sub>), 1.12 (d, *J*<sub>PH</sub> = 8.36 Hz, 9H, PMe<sub>3</sub>) 1.12-1.11 (m, 1H, H<sub>2</sub>).

**<sup>13</sup>C NMR: (800 MHz, CD<sub>3</sub>CN, δ, 25 °C):** 182.1, 181.3 (C<sub>10</sub>/C<sub>12</sub>), 144.8, 143.7, 141.1, 137.6, 137.1, 136.9 (6C, Tp carbons), 134.5 (C<sub>4</sub>), 132.3 (C<sub>5</sub>), 107.5, 107.0, 106.9 (3C, Tp carbons), 60.0 (C<sub>2</sub>), 54.5 (C<sub>9</sub>), 51.8 (C<sub>8</sub>), 48.3 (d, *J* = 11.13 Hz, C<sub>1</sub>), 46.1 (C<sub>3</sub>), 37.4 (C<sub>6</sub>), 34.3 (d, *J* = 3.71 Hz, C<sub>7</sub>), 24.8 (C<sub>13</sub>), 12.1 (d, *J*<sub>PC</sub> = 27.9 Hz, 3C, PMe<sub>3</sub>).

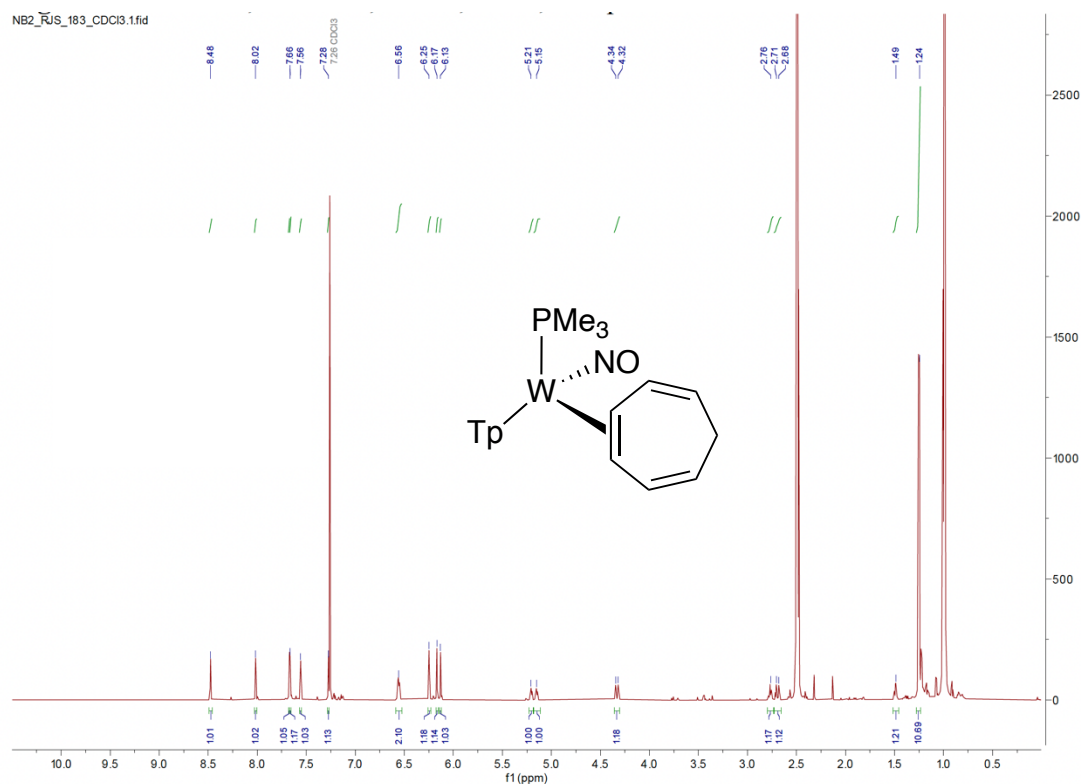
<sup>1</sup>H NMR (800 MHz, CD<sub>2</sub>CN, δ, 25 °C) of Compound **1A**



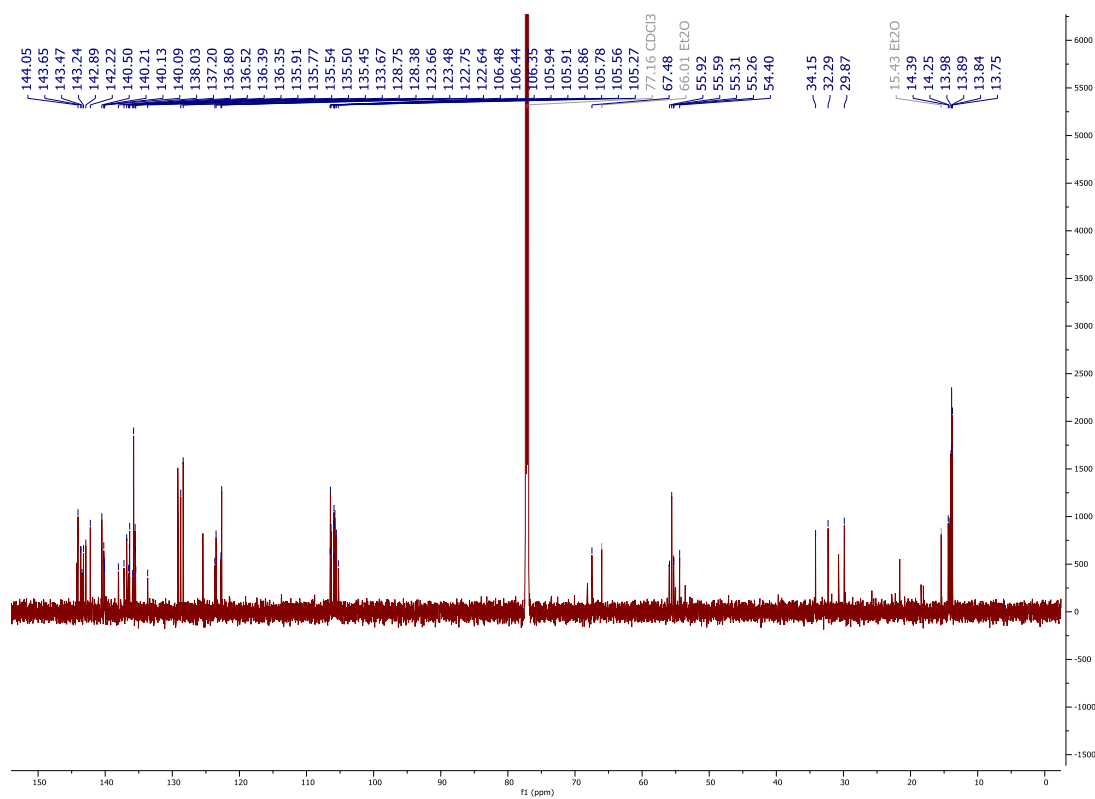
<sup>1</sup>H NMR (800 MHz, CD<sub>2</sub>CN, δ, 25 °C) of Compound **1B**



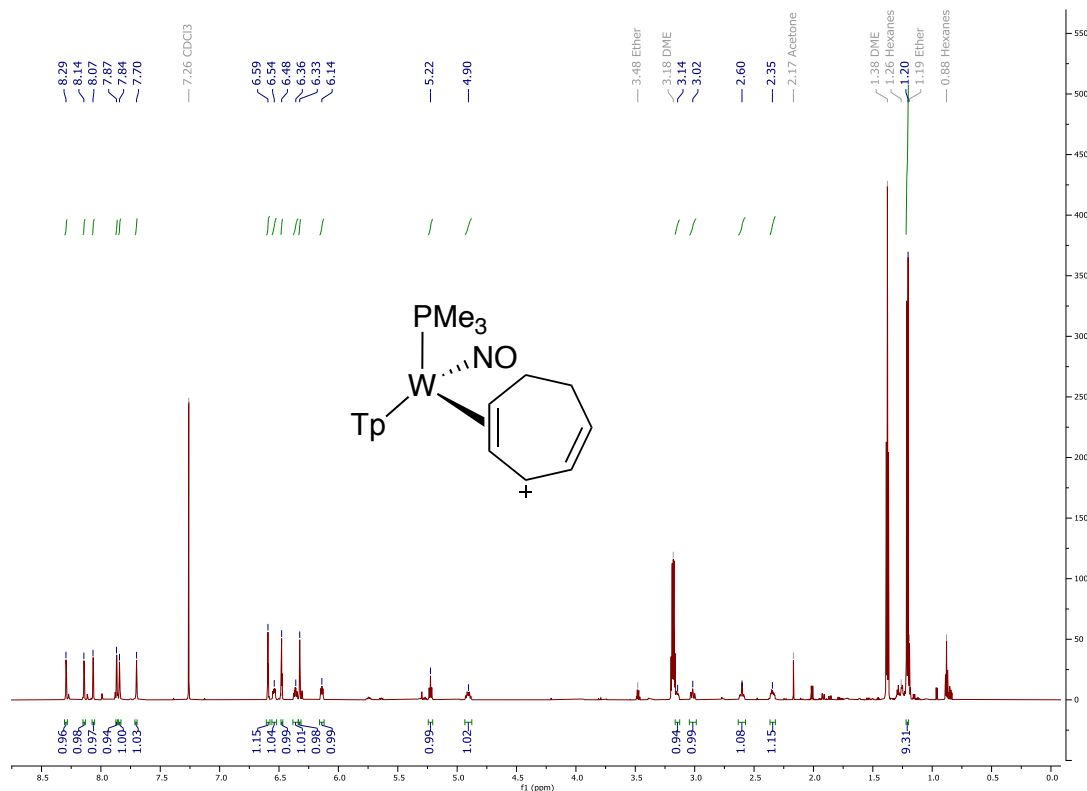
<sup>1</sup>H NMR (800 MHz, CD<sub>2</sub>CN, δ, 25 °C) of Compound **1C**



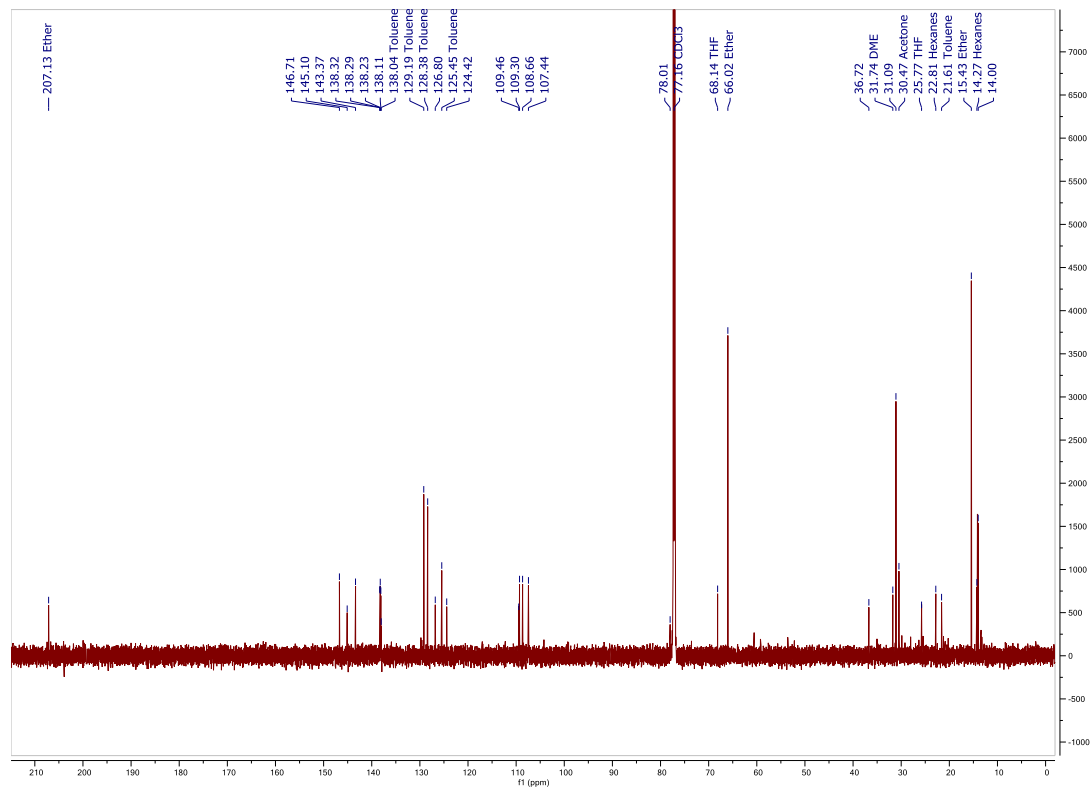
<sup>13</sup>C NMR (201 MHz, CD<sub>2</sub>CN, δ, 25 °C) of Compound **1A/1B/1C**



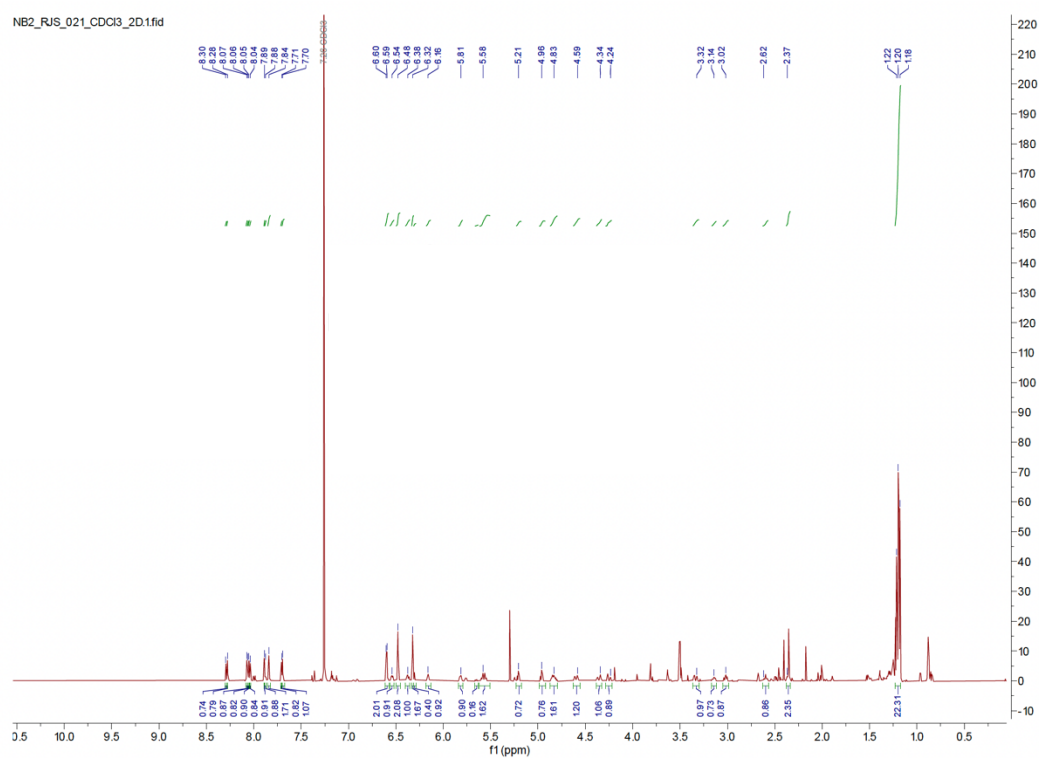
<sup>1</sup>H NMR (800 MHz, CD<sub>2</sub>CN, δ, 25 °C) of Compound **2A**



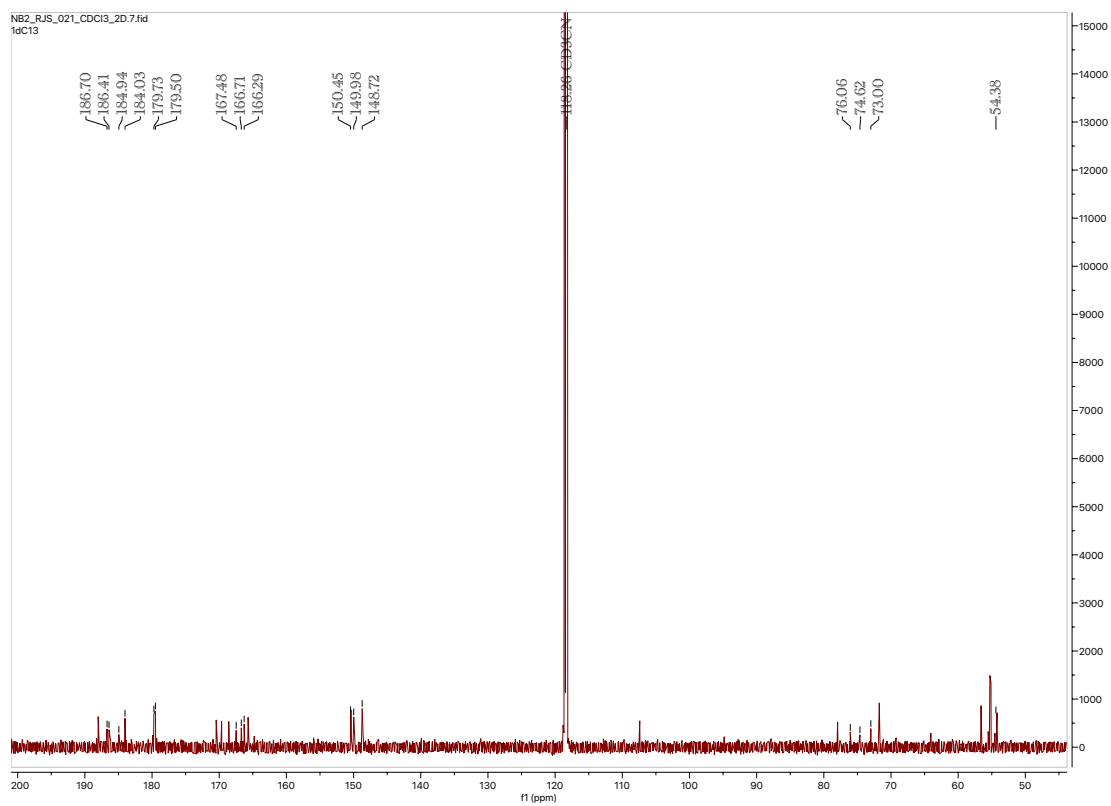
<sup>13</sup>C NMR (201 MHz, CD<sub>2</sub>CN, δ, 25 °C) of Compound **2A**



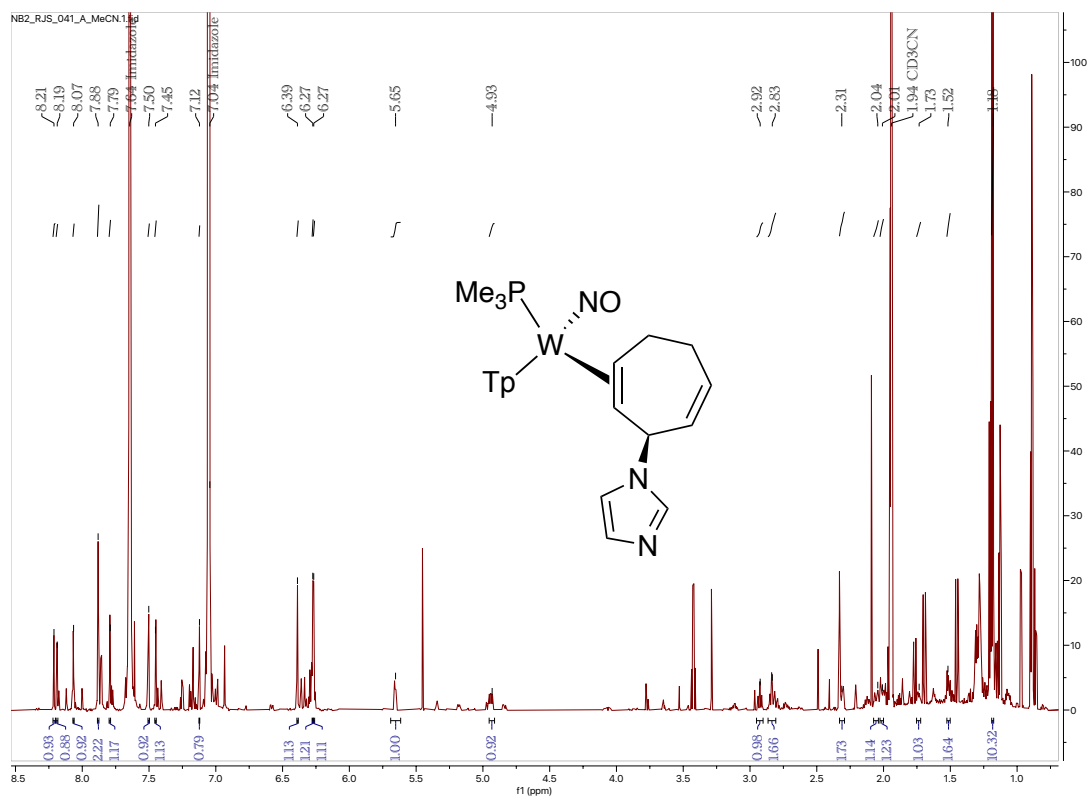
$^1\text{H}$  NMR (800 MHz,  $\text{CD}_2\text{CN}$ ,  $\delta$ , 25 °C) of Compound **2A/2B/2C**



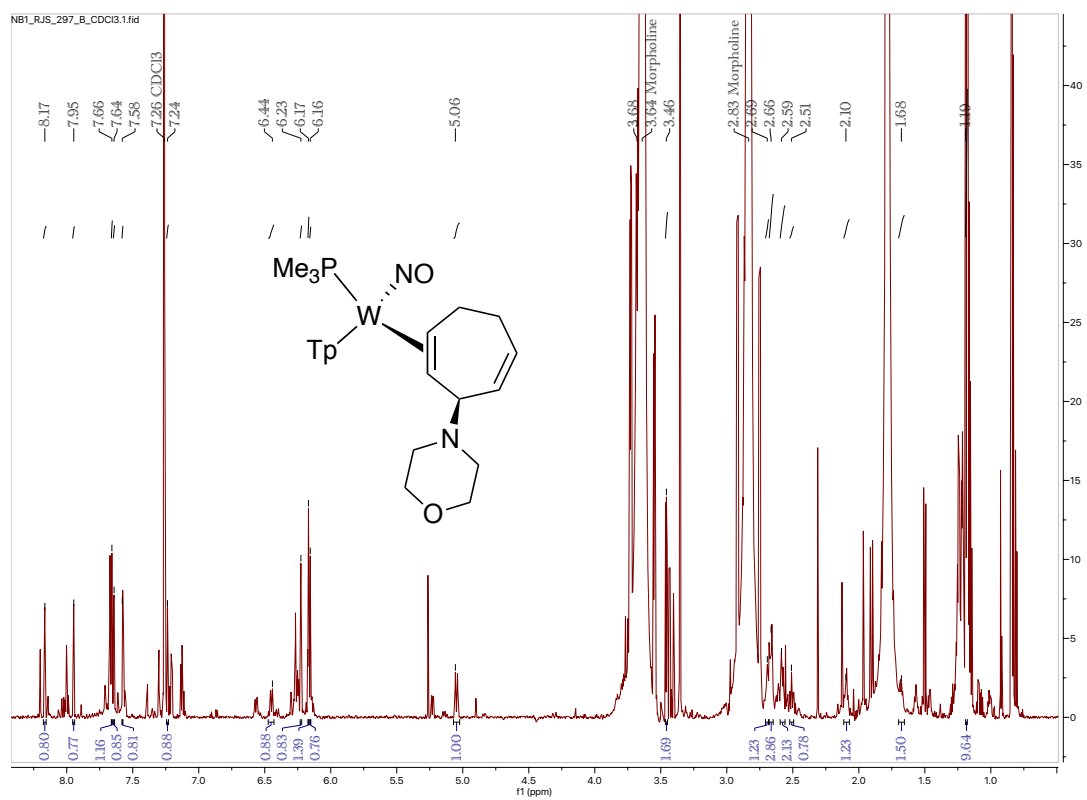
$^{13}\text{C}$  NMR (201 MHz,  $\text{CD}_2\text{CN}$ ,  $\delta$ , 25 °C) of Compound **2A/2B**



<sup>1</sup>H NMR (800 MHz, CD<sub>2</sub>CN, δ, 25 °C) of Compound **3A**

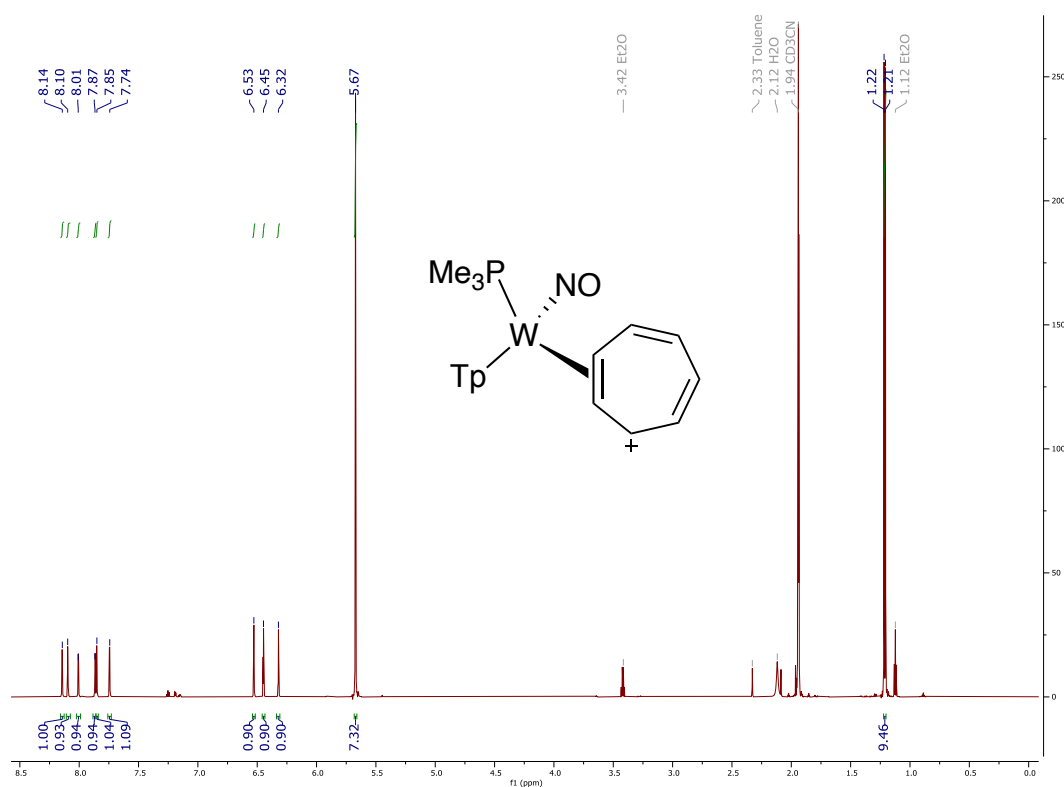


<sup>1</sup>H NMR (800 MHz, CD<sub>2</sub>CN, δ, 25 °C) of Compound **3B**

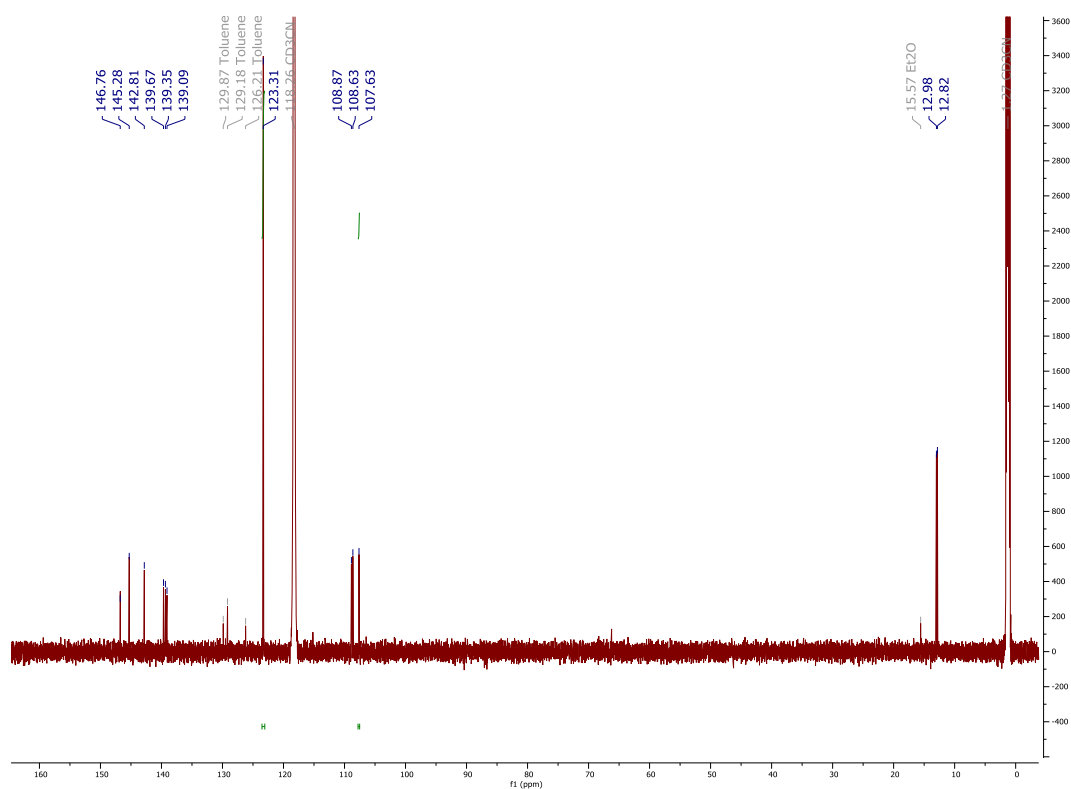




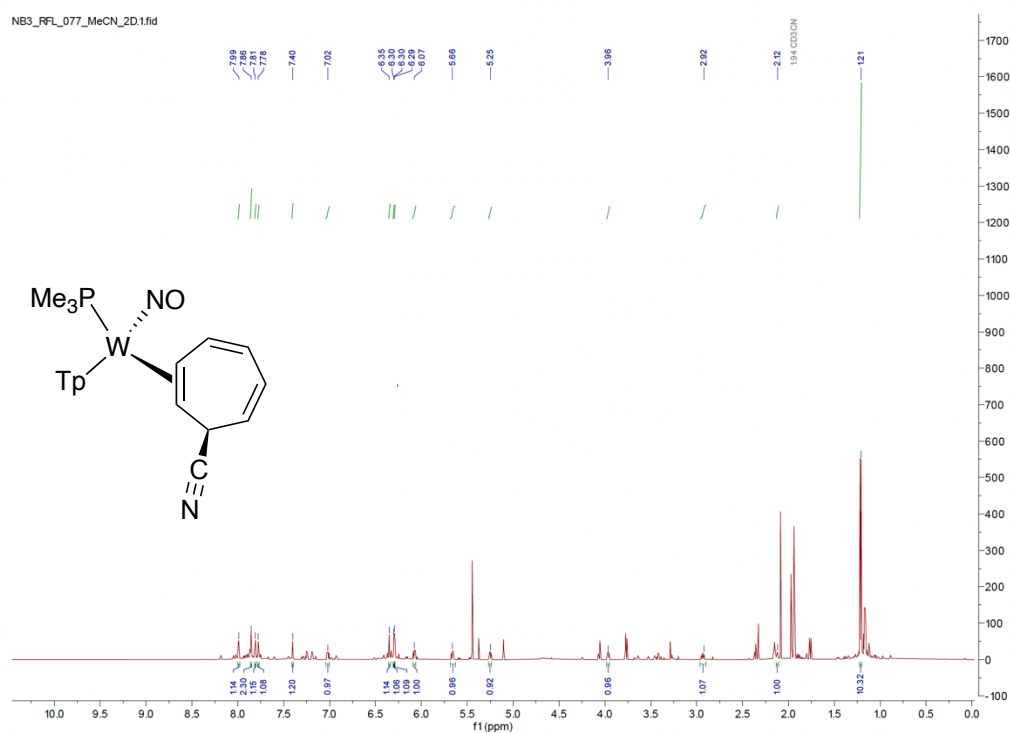
<sup>1</sup>H NMR (800 MHz, CD<sub>2</sub>CN, δ, 25 °C) of Compound **4**



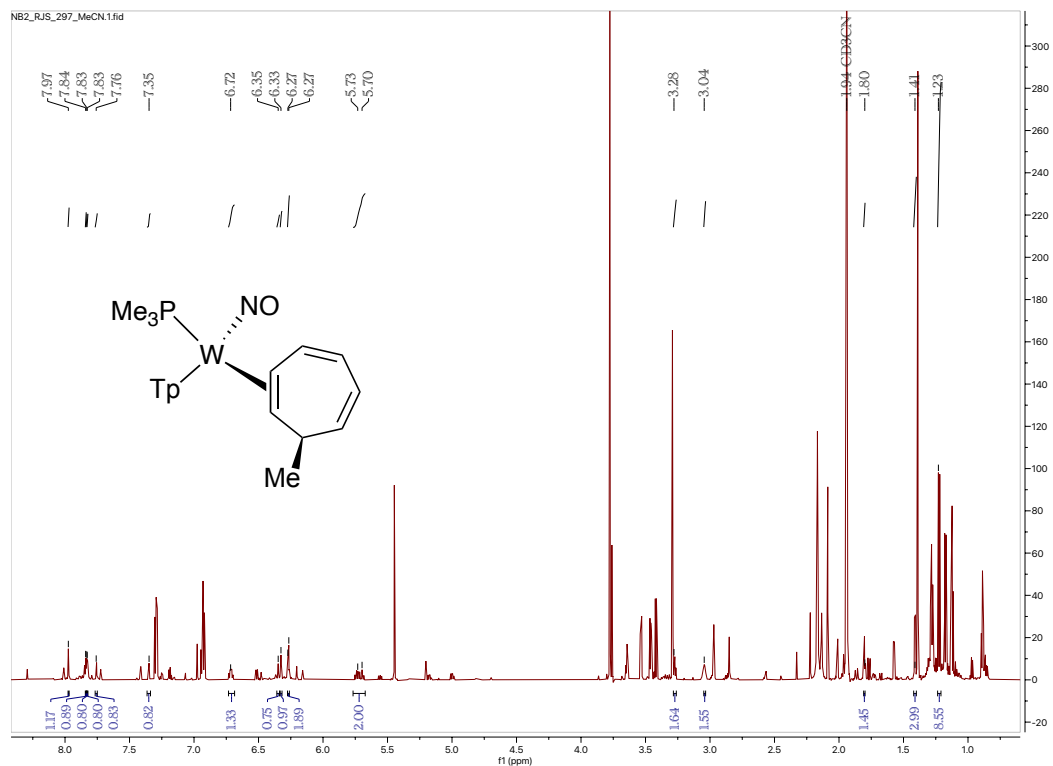
<sup>13</sup>C NMR (201 MHz, CD<sub>2</sub>CN, δ, 25 °C) of Compound **4**



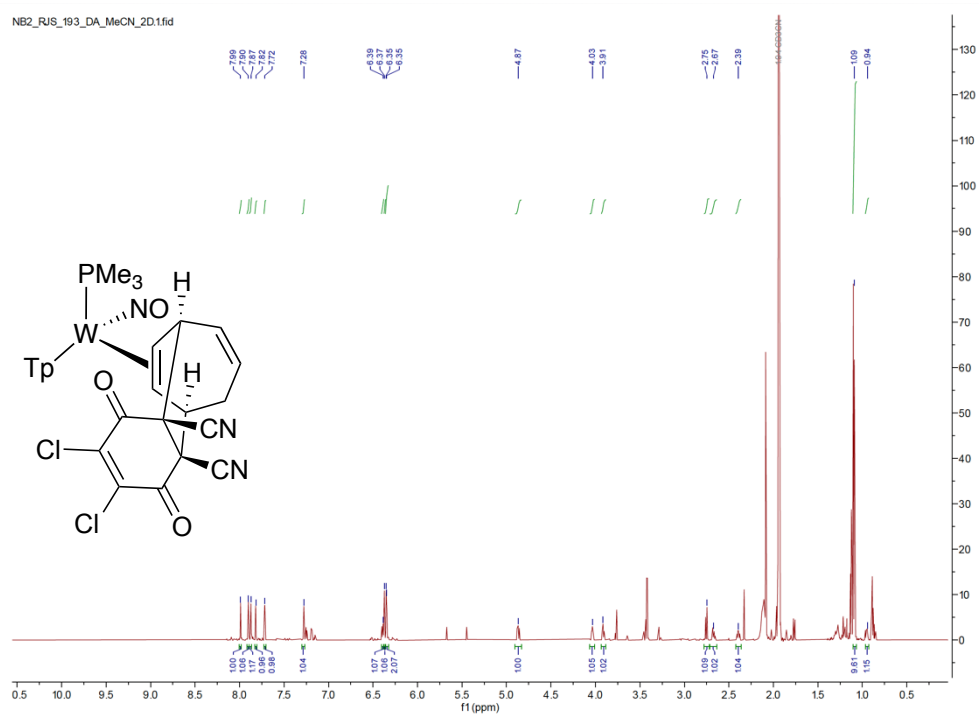
<sup>1</sup>H NMR (800 MHz, CD<sub>2</sub>CN, δ, 25 °C) of Compound **5A**



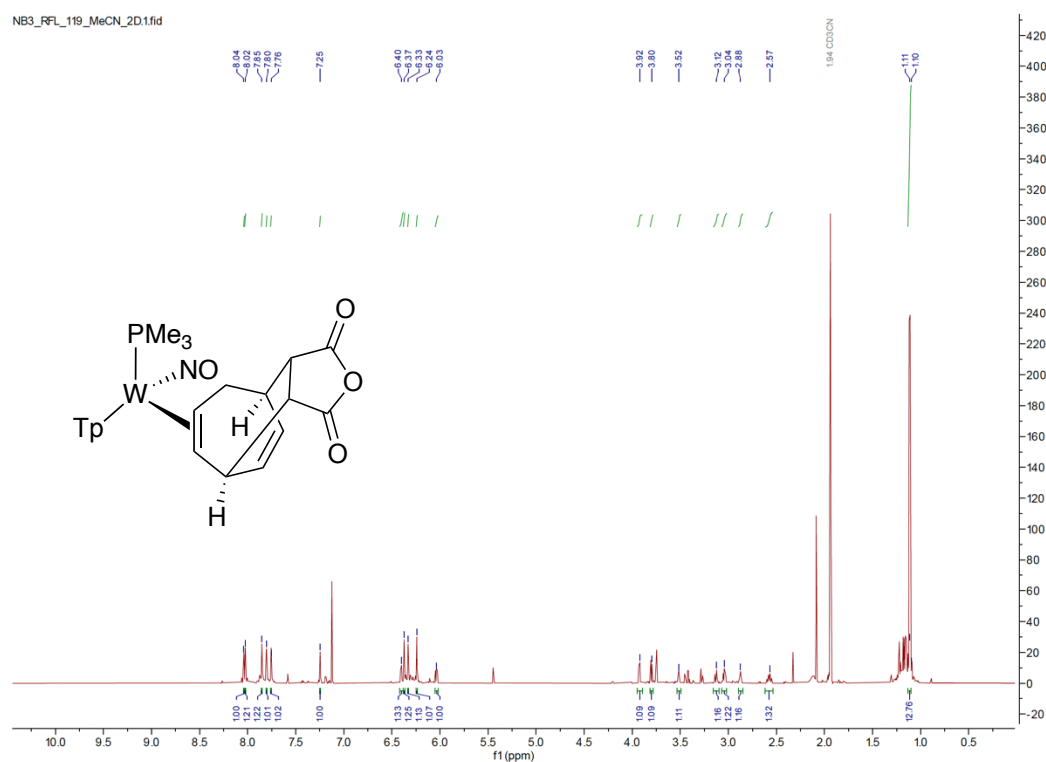
<sup>1</sup>H NMR (800 MHz, CD<sub>2</sub>CN, δ, 25 °C) of Compound **5B**



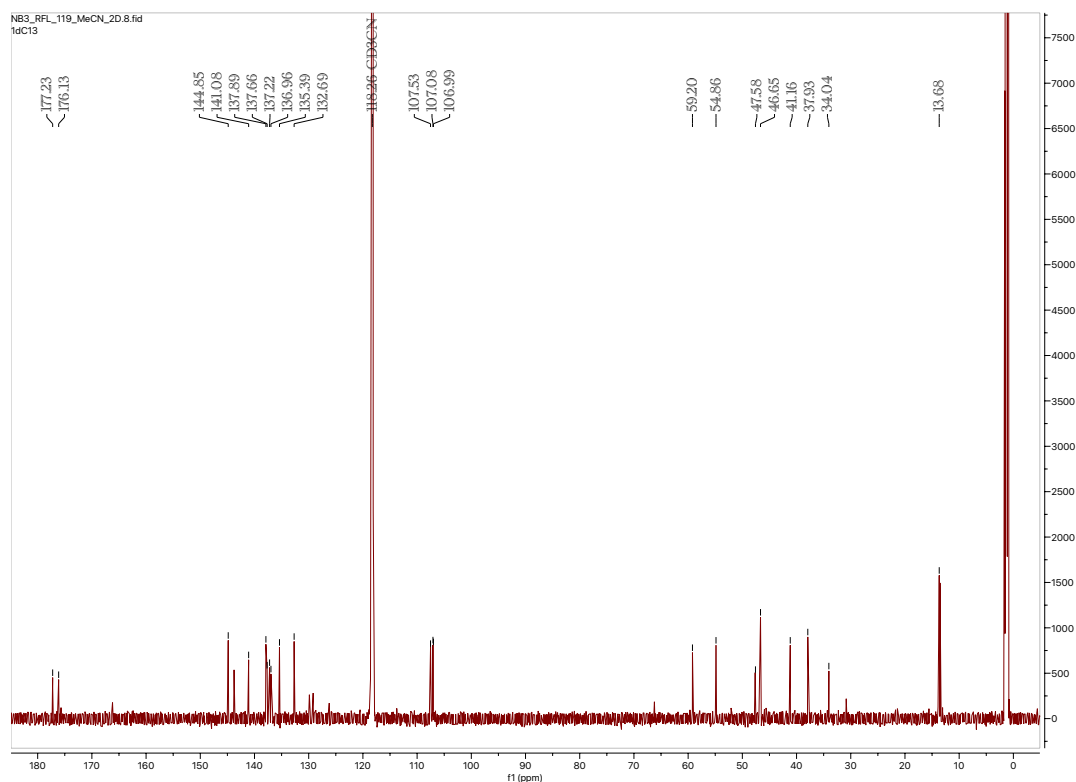
$^1\text{H}$  NMR (800 MHz,  $\text{CD}_2\text{CN}$ ,  $\delta$ , 25 °C) of Compound **6B**



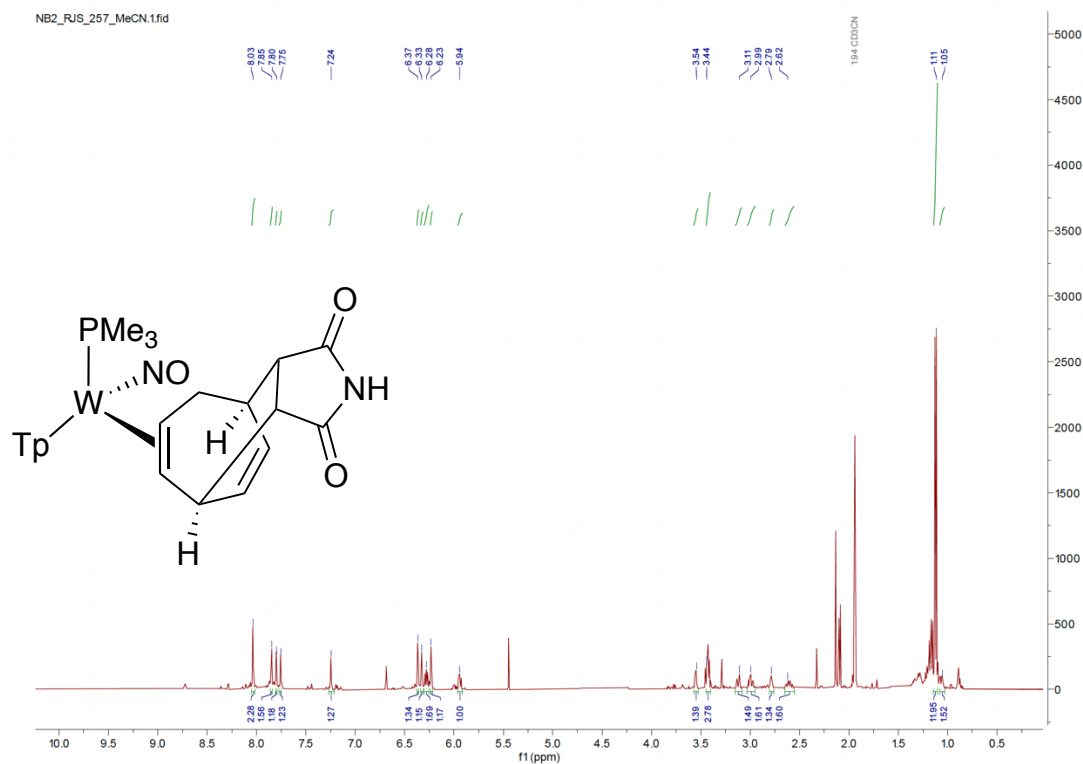
<sup>1</sup>H NMR (800 MHz, CD<sub>2</sub>CN, δ, 25 °C) of Compound **7A**



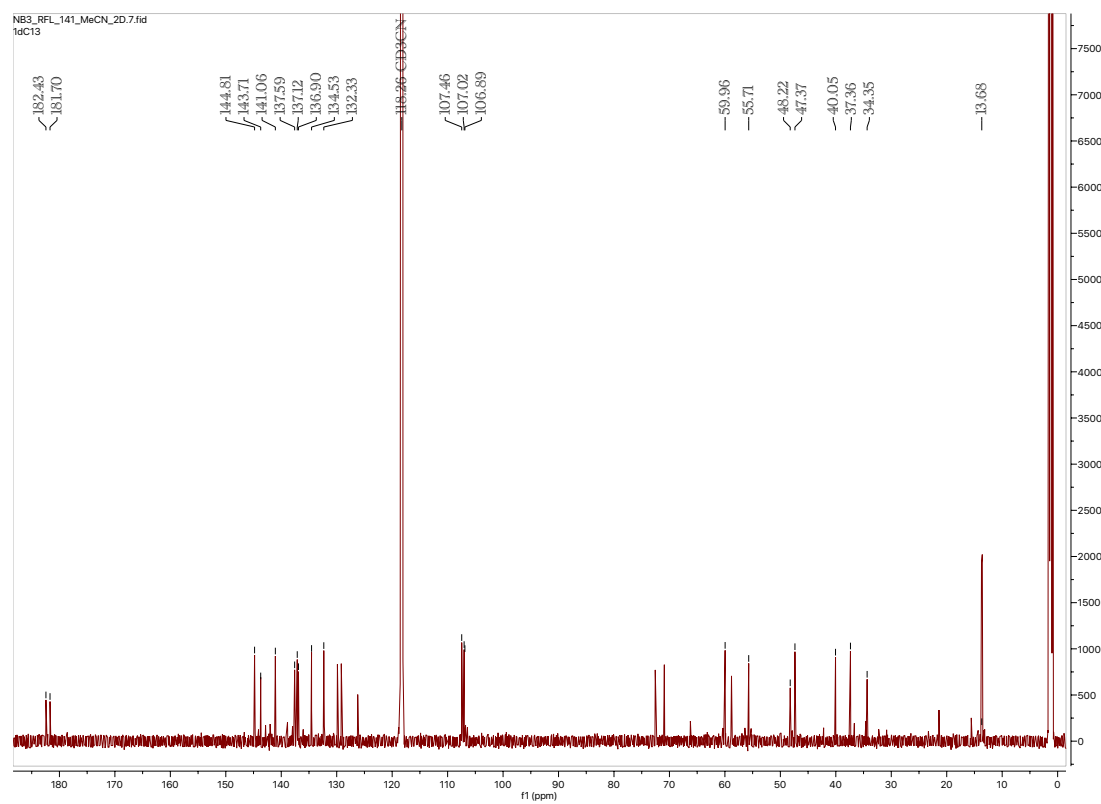
<sup>13</sup>C NMR (201 MHz, CD<sub>2</sub>CN, δ, 25 °C) of Compound **7A**



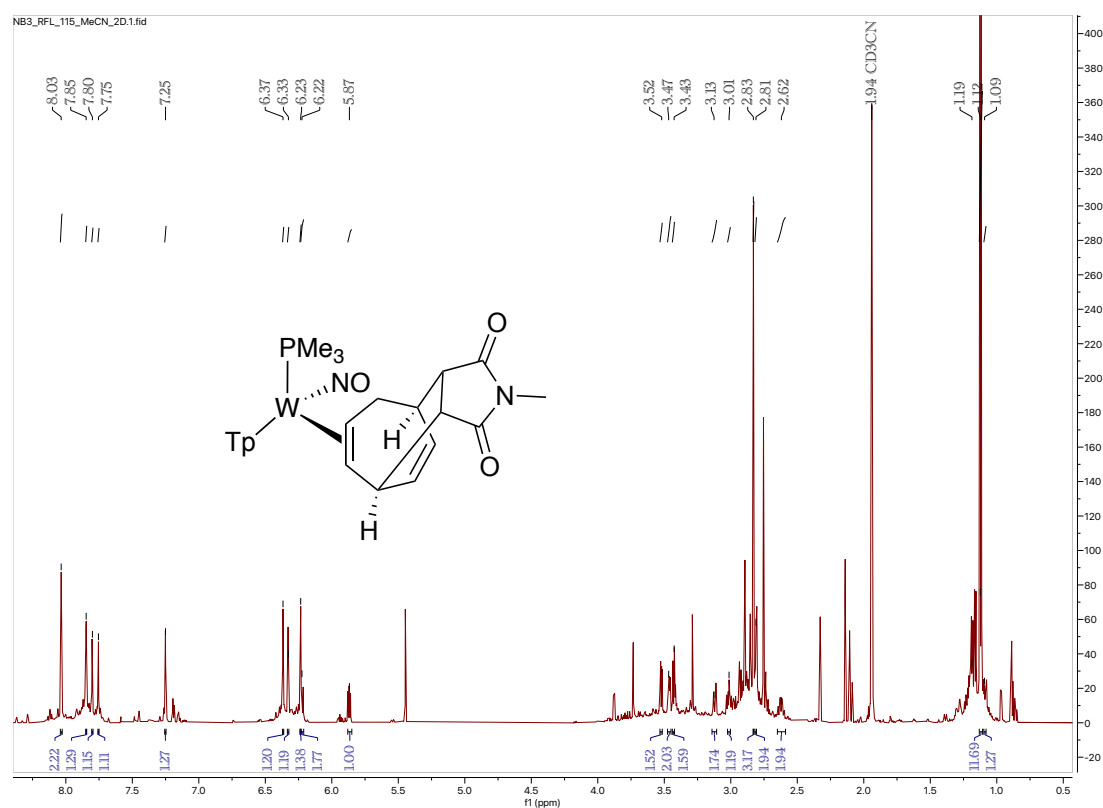
<sup>1</sup>H NMR (800 MHz, CD<sub>2</sub>CN, δ, 25 °C) of Compound **7B**



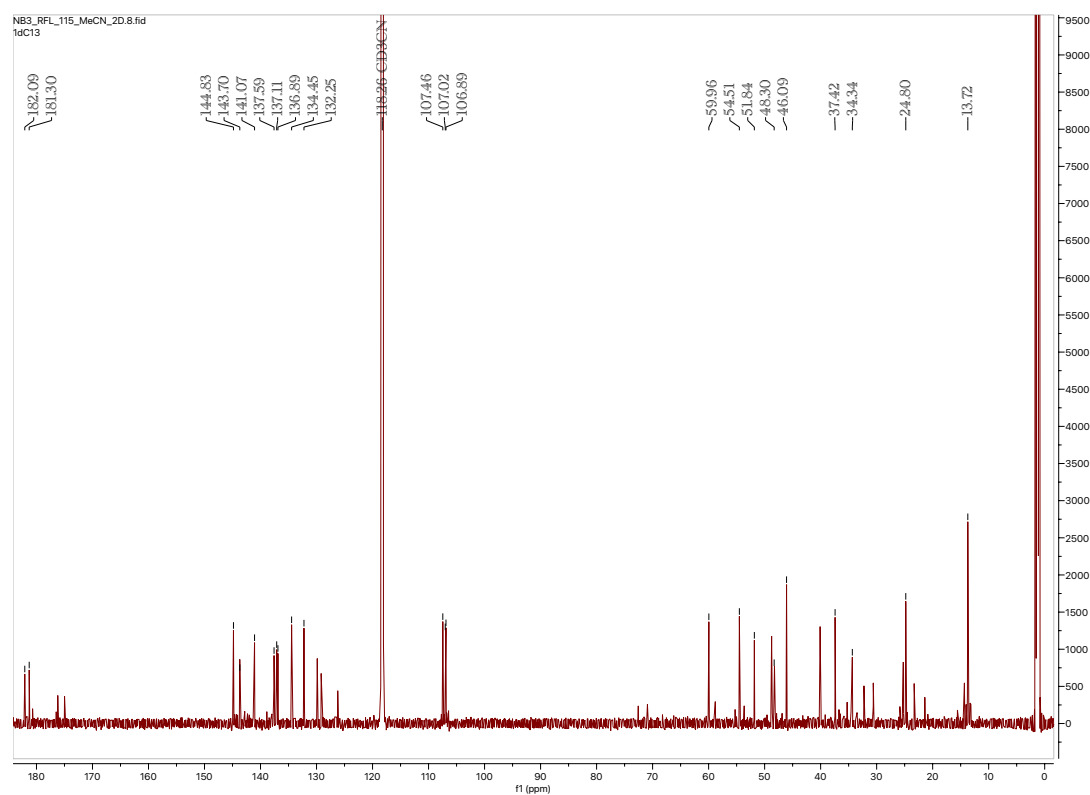
<sup>13</sup>C NMR (201 MHz, CD<sub>2</sub>CN, δ, 25 °C) of Compound **7B**



<sup>1</sup>H NMR (800 MHz, CD<sub>2</sub>CN, δ, 25 °C) of Compound **7C**



<sup>13</sup>C NMR (201 MHz, CD<sub>2</sub>CN, δ, 25 °C) of Compound **7C**



## Crystallography.

### Structure Report for mo\_harman\_nb4\_rjs\_allyl\_0m\_4

A yellow, block-shaped crystal of mo\_harman\_nb4\_rjs\_allyl\_0m\_4 was coated with Paratone oil and mounted on a MiTeGen micromount. Data were collected at 100(2) K on a Bruker D8 VENTURE dual wavelength Mo/Cu Kappa four-circle diffractometer with a PHOTON III detector. The diffractometer was equipped with an Oxford Cryostream 800Plus low temperature device and used Mo  $K_\alpha$  radiation ( $\lambda = 0.71073\text{\AA}$ ) from an Incoatec I $\mu$ s 3.0 microfocus sealed X-ray tube with a HELIOS double bounce multilayer mirror as monochromator.

Data collection and processing were done within the Bruker APEX5 software suite.<sup>[1]</sup> All data were integrated with SAINT 8.40B using a narrow-frame algorithm and a Multi-Scan absorption correction using TWINABS was applied.<sup>[2]</sup> Using OLEX2 as a graphical interface,<sup>[3]</sup> the structure was solved by dual methods with SHELXT and refined by full-matrix least-squares methods against  $F^2$  using SHELXL-2019/2.<sup>[4,5]</sup> All non-hydrogen atoms were refined with anisotropic displacement parameters. All hydrogen atoms were refined with isotropic displacement parameters. Some of their coordinates were refined freely and some on calculated positions using a riding model with their  $U_{\text{iso}}$  values constrained to 1.5 times the  $U_{\text{eq}}$  of their pivot atoms for terminal  $\text{sp}^3$  carbon atoms and 1.2 times for all other carbon atoms.

This report and the CIF file were generated using FinalCif.<sup>[6]</sup>

### Refinement details for mo\_harman\_nb4\_rjs\_allyl\_0m\_4

Refined as a 2-component twin on HKLF5 data. The BASF parameter refined to 0.397(4).

Table 11. Crystal data and structure refinement for mo\_harman\_nb4\_rjs\_allyl\_0m\_4

CCDC number	
Empirical formula	$\text{C}_{20}\text{H}_{28}\text{BF}_3\text{N}_7\text{O}_4\text{PSW}$
Formula weight	745.18
Temperature [K]	100(2)
Crystal system	triclinic
Space group (number)	$P\bar{1}$ (2)

<i>a</i> [Å]	10.0480(5)
<i>b</i> [Å]	10.4236(6)
<i>c</i> [Å]	12.7780(8)
$\alpha$ [°]	85.658(2)
$\beta$ [°]	86.388(2)
$\gamma$ [°]	82.542(2)
Volume [Å <sup>3</sup> ]	1321.28(13)
<i>Z</i>	2
$\rho_{\text{calc}}$ [gcm <sup>-3</sup> ]	1.873
$\mu$ [mm <sup>-1</sup> ]	4.574
<i>F</i> (000)	732
Crystal size [mm <sup>3</sup> ]	0.006×0.008×0.096
Crystal colour	yellow
Crystal shape	block
Radiation	Mo <i>K</i> <sub>α</sub> ( $\lambda$ =0.71073 Å)
2 $\theta$ range [°]	4.09 to 50.07 (0.84 Å)
Index ranges	−11 ≤ <i>h</i> ≤ 11 −12 ≤ <i>k</i> ≤ 12 0 ≤ <i>l</i> ≤ 15
Reflections collected	4657
Independent reflections	4657 <i>R</i> <sub>int</sub> = 0.1535 <i>R</i> <sub>sigma</sub> = 0.0668
Completeness to $\theta$ = 25.037°	99.8
Data / Restraints / Parameters	4657 / 3 / 360
Goodness-of-fit on <i>F</i> <sup>2</sup>	1.083
Final <i>R</i> indexes [ $\geq 2\sigma(I)$ ]	<i>R</i> <sub>1</sub> = 0.0548 <i>wR</i> <sub>2</sub> = 0.1230
Final <i>R</i> indexes [all data]	<i>R</i> <sub>1</sub> = 0.0741 <i>wR</i> <sub>2</sub> = 0.1331
Largest peak/hole [eÅ <sup>-3</sup> ]	3.03/−0.80



Table 12. Atomic coordinates and Ueq [Å<sup>2</sup>] for mo\_harman\_nb4\_rjs\_allyl\_0m\_4

Atom	x	y	z	U <sub>eq</sub>
W1	0.46247(4)	0.30101(4)	0.20197(3)	0.03754(17)
P1	0.3097(3)	0.2945(3)	0.3684(2)	0.0414(6)
O1	0.4692(8)	0.0137(7)	0.2073(6)	0.0481(17)
N1	0.4493(7)	0.5086(8)	0.2293(6)	0.0374(18)
N2	0.5634(8)	0.5614(8)	0.2568(6)	0.0387(18)
N3	0.6074(8)	0.2673(8)	0.3224(6)	0.0419(19)
N4	0.6826(8)	0.3593(8)	0.3462(7)	0.043(2)
N5	0.6582(8)	0.3330(8)	0.1196(6)	0.0421(19)
N6	0.7370(8)	0.4129(8)	0.1585(6)	0.0388(18)
N7	0.4704(7)	0.1321(9)	0.2002(6)	0.041(2)
C1	0.3512(11)	0.6066(11)	0.2347(8)	0.047(2)
H1	0.260163	0.599331	0.222795	0.056
C2	0.3956(10)	0.7211(10)	0.2596(8)	0.047(2)
H2	0.344244	0.803600	0.265875	0.056
C3	0.5319(11)	0.6875(10)	0.2732(7)	0.045(2)
H3	0.592548	0.744081	0.291003	0.055
C4	0.6491(10)	0.1625(10)	0.3862(8)	0.045(2)
H4	0.615403	0.081499	0.386278	0.054
C5	0.7440(10)	0.1860(11)	0.4496(8)	0.048(2)
H5	0.786852	0.128255	0.501916	0.057
C6	0.7649(10)	0.3109(11)	0.4222(7)	0.043(2)
H6	0.827635	0.356435	0.452028	0.051
C7	0.7302(10)	0.2790(10)	0.0368(8)	0.043(2)
H7	0.701786	0.216593	−0.004502	0.052
C8	0.8513(10)	0.3291(11)	0.0224(8)	0.049(3)
H8	0.920000	0.310257	−0.030822	0.059
C9	0.8516(10)	0.4122(10)	0.1012(8)	0.046(2)
H9	0.922275	0.460941	0.112567	0.055
C10	0.2412(10)	0.3368(11)	0.1438(8)	0.046(2)
H10	0.176(9)	0.412(9)	0.179(8)	0.055
C11	0.3283(10)	0.3824(11)	0.0636(8)	0.046(2)
H11	0.324(11)	0.484(7)	0.045(9)	0.055
C12	0.4261(10)	0.3037(11)	0.0071(8)	0.047(2)
H12	0.496(9)	0.354(10)	−0.040(8)	0.056
C13	0.4179(11)	0.1735(10)	−0.0239(8)	0.045(2)
H13	0.498377	0.123508	−0.047807	0.054
C14	0.3017(12)	0.1196(13)	−0.0206(9)	0.061(3)
H14	0.303743	0.043705	−0.057743	0.073
C15	0.1767(12)	0.1638(14)	0.0323(10)	0.066(3)
H15A	0.121718	0.091136	0.038080	0.079
H15B	0.130084	0.233458	−0.014145	0.079

C16	0.1737(10)	0.2148(11)	0.1406(9)	0.048(3)
H16A	0.218615	0.146197	0.188852	0.058
H16B	0.078915	0.233337	0.166991	0.058
C17	0.1352(10)	0.3675(11)	0.3763(8)	0.049(3)
H17A	0.130218	0.460490	0.356093	0.073
H17B	0.097672	0.354837	0.448468	0.073
H17C	0.083607	0.326414	0.328589	0.073
C18	0.3757(11)	0.3738(11)	0.4718(8)	0.052(3)
H18A	0.463861	0.328172	0.489276	0.077
H18B	0.313980	0.372183	0.534310	0.077
H18C	0.384854	0.463915	0.447795	0.077
C19	0.2959(11)	0.1309(11)	0.4215(9)	0.053(3)
H19A	0.238892	0.090184	0.377701	0.079
H19B	0.255718	0.132882	0.493351	0.079
H19C	0.385440	0.080921	0.422192	0.079
B1	0.6974(11)	0.4748(12)	0.2641(9)	0.044(3)
H1A	0.783(10)	0.536(10)	0.287(8)	0.05(3)
S1	1.0380(3)	0.2512(3)	0.6974(2)	0.0456(6)
F1	0.9996(8)	0.0138(8)	0.6684(7)	0.086(2)
F2	0.8782(7)	0.0971(8)	0.7953(8)	0.091(3)
F3	1.0858(7)	0.0319(8)	0.8136(6)	0.077(2)
O2	0.9454(8)	0.2895(9)	0.6172(6)	0.063(2)
O3	1.1755(7)	0.2252(8)	0.6606(6)	0.0550(19)
O4	1.0147(8)	0.3242(8)	0.7886(6)	0.0551(19)
C20	0.9983(13)	0.0904(12)	0.7457(11)	0.063(3)

$U_{eq}$  is defined as 1/3 of the trace of the orthogonalized  $U_{ij}$  tensor.

Table 13. Anisotropic displacement parameters ( $\text{\AA}^2$ ) for mo\_harman\_nb4\_rjs\_allyl\_0m\_4.

The anisotropic displacement factor exponent takes the form:

$$-2\pi^2 [ h^2(a^*)^2 U_{11} + k^2(b^*)^2 U_{22} + \dots + 2hka^*b^* U_{12} ]$$

Atom	$U_{11}$	$U_{22}$	$U_{33}$	$U_{23}$	$U_{13}$	$U_{12}$
W1	0.0356(2)	0.0448(3)	0.0328(2)	−0.00339(15)	−0.00064(15)	−0.00757(15)
P1	0.0414(14)	0.0500(15)	0.0337(14)	−0.0023(11)	0.0006(11)	−0.0104(11)
O1	0.066(5)	0.037(4)	0.041(4)	−0.003(3)	−0.001(3)	−0.006(3)
N1	0.030(4)	0.047(5)	0.034(4)	0.001(4)	0.005(3)	−0.004(3)
N2	0.038(4)	0.048(5)	0.032(4)	−0.004(4)	−0.001(3)	−0.010(4)
N3	0.036(4)	0.054(5)	0.039(5)	−0.007(4)	−0.004(4)	−0.012(4)
N4	0.045(5)	0.047(5)	0.039(5)	−0.007(4)	0.011(4)	−0.015(4)
N5	0.043(5)	0.047(5)	0.036(5)	0.001(4)	−0.001(4)	−0.007(4)
N6	0.035(4)	0.048(5)	0.034(4)	−0.008(4)	0.004(3)	−0.010(3)
N7	0.031(4)	0.073(7)	0.020(4)	−0.006(4)	0.002(3)	−0.009(4)
C1	0.054(6)	0.056(6)	0.033(5)	0.003(5)	−0.004(5)	−0.015(5)
C2	0.049(6)	0.043(6)	0.045(6)	−0.002(5)	0.001(5)	0.002(5)
C3	0.056(6)	0.048(6)	0.032(6)	−0.006(5)	0.001(5)	−0.004(5)

C4	0.035(5)	0.048(6)	0.052(6)	-0.004(5)	0.002(5)	-0.007(4)
C5	0.047(6)	0.057(7)	0.038(6)	0.007(5)	-0.015(5)	-0.006(5)
C6	0.038(5)	0.060(7)	0.031(5)	-0.003(5)	-0.003(4)	-0.006(5)
C7	0.041(5)	0.053(6)	0.034(5)	0.003(5)	-0.004(4)	0.001(4)
C8	0.035(5)	0.064(7)	0.043(6)	0.010(5)	0.007(4)	0.000(5)
C9	0.048(6)	0.050(6)	0.041(6)	-0.003(5)	-0.002(5)	-0.008(5)
C10	0.039(5)	0.057(6)	0.044(6)	-0.005(5)	-0.010(5)	-0.004(5)
C11	0.042(6)	0.050(6)	0.047(6)	0.000(5)	-0.012(5)	-0.010(5)
C12	0.041(5)	0.058(7)	0.040(6)	-0.001(5)	0.001(4)	-0.002(5)
C13	0.052(6)	0.043(6)	0.040(6)	-0.009(5)	-0.001(5)	-0.006(5)
C14	0.059(7)	0.076(8)	0.054(7)	-0.023(6)	0.004(6)	-0.025(6)
C15	0.052(7)	0.082(9)	0.070(8)	-0.025(7)	0.006(6)	-0.028(6)
C16	0.036(5)	0.053(6)	0.056(7)	-0.008(5)	-0.007(5)	-0.005(5)
C17	0.038(5)	0.066(7)	0.041(6)	-0.007(5)	0.003(4)	-0.002(5)
C18	0.049(6)	0.061(7)	0.045(6)	-0.010(5)	0.012(5)	-0.015(5)
C19	0.054(6)	0.059(7)	0.046(6)	0.000(5)	0.002(5)	-0.014(5)
B1	0.039(6)	0.059(7)	0.035(6)	-0.005(5)	-0.003(5)	-0.013(5)
S1	0.0439(14)	0.0567(16)	0.0376(14)	-0.0041(1 2)	-0.0004(1 1)	-0.0116(1 2)
F1	0.088(6)	0.067(5)	0.108(7)	-0.017(5)	-0.022(5)	-0.016(4)
F2	0.051(4)	0.080(5)	0.136(8)	0.020(5)	0.016(5)	-0.015(4)
F3	0.070(5)	0.076(5)	0.083(5)	0.020(4)	-0.015(4)	-0.007(4)
O2	0.067(5)	0.075(6)	0.048(5)	0.001(4)	-0.006(4)	-0.009(4)
O3	0.051(4)	0.070(5)	0.046(4)	-0.006(4)	0.005(3)	-0.018(4)
O4	0.059(5)	0.071(5)	0.037(4)	-0.010(4)	0.012(3)	-0.020(4)
C20	0.059(8)	0.058(7)	0.076(9)	0.001(7)	-0.020(7)	-0.014(6)

Table 14. Bond lengths and angles for mo\_harman\_nb4\_rjs\_allyl\_0m\_4

Atom-Atom	Length [Å]
W1-N7	1.754(10)
W1-N3	2.163(8)
W1-N1	2.204(8)
W1-N5	2.223(8)
W1-C11	2.332(10)
W1-C10	2.363(10)
W1-C12	2.536(11)
W1-P1	2.545(3)
P1-C19	1.806(11)
P1-C18	1.813(11)
P1-C17	1.819(10)
O1-N7	1.232(11)
N1-C1	1.327(14)
N1-N2	1.408(11)
N2-C3	1.340(13)
N2-B1	1.525(15)
N3-C4	1.350(13)
N3-N4	1.358(11)
N4-C6	1.341(13)

N4-B1	1.552(15)
N5-C7	1.359(13)
N5-N6	1.360(11)
N6-C9	1.324(13)
N6-B1	1.547(14)
C1-C2	1.393(15)
C1-H1	0.9500
C2-C3	1.387(15)
C2-H2	0.9500
C3-H3	0.9500
C4-C5	1.347(14)
C4-H4	0.9500
C5-C6	1.362(15)
C5-H5	0.9500
C6-H6	0.9500
C7-C8	1.382(14)
C7-H7	0.9500
C8-C9	1.377(15)
C8-H8	0.9500
C9-H9	0.9500

C10–C11	1.401(15)
C10–C16	1.521(15)
C10–H10	1.06(6)
C11–C12	1.396(15)
C11–H11	1.06(6)
C12–C13	1.456(15)
C12–H12	1.06(6)
C13–C14	1.357(15)
C13–H13	0.9500
C14–C15	1.427(16)
C14–H14	0.9500
C15–C16	1.516(16)
C15–H15A	0.9900
C15–H15B	0.9900
C16–H16A	0.9900
C16–H16B	0.9900
C17–H17A	0.9800
C17–H17B	0.9800
C17–H17C	0.9800
C18–H18A	0.9800
C18–H18B	0.9800
C18–H18C	0.9800
C19–H19A	0.9800
C19–H19B	0.9800
C19–H19C	0.9800
B1–H1A	1.20(11)
S1–O2	1.427(9)
S1–O3	1.430(8)
S1–O4	1.430(8)
S1–C20	1.826(13)
F1–C20	1.315(15)
F2–C20	1.323(15)
F3–C20	1.332(14)
<b>Atom–Atom– Atom</b>	<b>Angle [°]</b>
N7–W1–N3	87.5(3)
N7–W1–N1	171.6(3)
N3–W1–N1	86.8(3)
N7–W1–N5	100.7(3)
N3–W1–N5	74.8(3)
N1–W1–N5	83.8(3)
N7–W1–C11	104.4(4)
N3–W1–C11	166.6(3)
N1–W1–C11	82.0(3)
N5–W1–C11	96.5(3)
N7–W1–C10	92.9(4)
N3–W1–C10	153.2(3)

N1–W1–C10	89.4(3)
N5–W1–C10	131.2(3)
C11–W1–C10	34.7(4)
N7–W1–C12	85.1(4)
N3–W1–C12	145.9(3)
N1–W1–C12	103.0(3)
N5–W1–C12	74.0(3)
C11–W1–C12	33.0(4)
C10–W1–C12	60.6(3)
N7–W1–P1	89.6(2)
N3–W1–P1	78.5(2)
N1–W1–P1	83.2(2)
N5–W1–P1	150.8(2)
C11–W1–P1	107.4(3)
C10–W1–P1	74.7(3)
C12–W1–P1	134.6(2)
C19–P1–C18	105.6(5)
C19–P1–C17	101.6(5)
C18–P1–C17	100.2(5)
C19–P1–W1	112.4(4)
C18–P1–W1	111.0(3)
C17–P1–W1	124.1(4)
C1–N1–N2	103.9(8)
C1–N1–W1	135.5(7)
N2–N1–W1	120.4(6)
C3–N2–N1	110.4(8)
C3–N2–B1	130.0(8)
N1–N2–B1	119.5(8)
C4–N3–N4	104.4(8)
C4–N3–W1	132.9(7)
N4–N3–W1	122.6(7)
C6–N4–N3	109.6(8)
C6–N4–B1	128.6(8)
N3–N4–B1	117.9(8)
C7–N5–N6	106.3(8)
C7–N5–W1	133.3(7)
N6–N5–W1	120.1(6)
C9–N6–N5	110.1(8)
C9–N6–B1	128.5(8)
N5–N6–B1	120.9(7)
O1–N7–W1	174.3(7)
N1–C1–C2	112.9(10)
N1–C1–H1	123.5
C2–C1–H1	123.5
C3–C2–C1	104.4(10)
C3–C2–H2	127.8
C1–C2–H2	127.8
N2–C3–C2	108.3(9)

N2-C3-H3	125.9
C2-C3-H3	125.9
C5-C4-N3	112.3(9)
C5-C4-H4	123.9
N3-C4-H4	123.9
C4-C5-C6	104.7(9)
C4-C5-H5	127.6
C6-C5-H5	127.6
N4-C6-C5	108.9(9)
N4-C6-H6	125.5
C5-C6-H6	125.5
N5-C7-C8	109.2(9)
N5-C7-H7	125.4
C8-C7-H7	125.4
C9-C8-C7	105.6(9)
C9-C8-H8	127.2
C7-C8-H8	127.2
N6-C9-C8	108.8(9)
N6-C9-H9	125.6
C8-C9-H9	125.6
C11-C10-C16	124.4(10)
C11-C10-W1	71.4(6)
C16-C10-W1	114.8(7)
C11-C10-H10	114(6)
C16-C10-H10	111(6)
W1-C10-H10	116(6)
C12-C11-C10	124.6(10)
C12-C11-W1	81.6(6)
C10-C11-W1	73.8(6)
C12-C11-H11	116(6)
C10-C11-H11	119(6)
W1-C11-H11	115(6)
C11-C12-C13	127.3(10)
C11-C12-W1	65.5(6)
C13-C12-W1	111.0(7)
C11-C12-H12	115(6)
C13-C12-H12	114(6)
W1-C12-H12	113(6)
C14-C13-C12	123.7(10)
C14-C13-H13	118.2
C12-C13-H13	118.2
C13-C14-C15	127.4(11)
C13-C14-H14	116.3
C15-C14-H14	116.3
C14-C15-C16	120.4(10)
C14-C15-H15A	107.2
C16-C15-H15A	107.2
C14-C15-H15B	107.2

C16-C15-H15B	107.2
H15A-C15-H15B	106.9
C15-C16-C10	114.3(10)
C15-C16-H16A	108.7
C10-C16-H16A	108.7
C15-C16-H16B	108.7
C10-C16-H16B	108.7
H16A-C16-H16B	107.6
P1-C17-H17A	109.5
P1-C17-H17B	109.5
H17A-C17-H17B	109.5
P1-C17-H17C	109.5
H17A-C17-H17C	109.5
H17B-C17-H17C	109.5
P1-C18-H18A	109.5
P1-C18-H18B	109.5
H18A-C18-H18B	109.5
P1-C18-H18C	109.5
H18A-C18-H18C	109.5
H18B-C18-H18C	109.5
P1-C19-H19A	109.5
P1-C19-H19B	109.5
H19A-C19-H19B	109.5
P1-C19-H19C	109.5
H19A-C19-H19C	109.5
H19B-C19-H19C	109.5
N2-B1-N6	110.0(8)
N2-B1-N4	109.8(8)
N6-B1-N4	105.4(9)
N2-B1-H1A	110(5)
N6-B1-H1A	111(5)
N4-B1-H1A	111(5)
O2-S1-O3	115.0(5)
O2-S1-O4	114.7(5)
O3-S1-O4	115.3(5)
O2-S1-C20	103.5(5)
O3-S1-C20	102.4(5)
O4-S1-C20	103.3(6)

F1–C20–F2	108.1(10)
F1–C20–F3	107.0(11)
F2–C20–F3	106.7(11)
F1–C20–S1	111.4(9)

F2–C20–S1	111.2(9)
F3–C20–S1	112.2(8)

Table 15. Torsion angles for mo\_harman\_nb4\_rjs\_allyl\_0m\_4

Atom–Atom– Atom–Atom	Torsion Angle [°]
C1–N1–N2–C3	–2.4(10)
W1–N1–N2–C3	–177.9(6)
C1–N1–N2–B1	177.3(8)
W1–N1–N2–B1	1.9(11)
C4–N3–N4–C6	–0.6(10)
W1–N3–N4–C6	–179.0(6)
C4–N3–N4–B1	159.4(9)
W1–N3–N4–B1	–19.0(11)
C7–N5–N6–C9	1.8(11)
W1–N5–N6–C9	176.4(7)
C7–N5–N6–B1	–170.3(9)
W1–N5–N6–B1	4.4(12)
N2–N1–C1–C2	2.5(11)
W1–N1–C1–C2	176.9(7)
N1–C1–C2–C3	–1.8(12)
N1–N2–C3–C2	1.4(11)
B1–N2–C3–C2	–178.3(10)
C1–C2–C3–N2	0.1(11)
N4–N3–C4–C5	1.3(11)
W1–N3–C4–C5	179.5(7)
N3–C4–C5–C6	–1.5(12)
N3–N4–C6–C5	–0.3(11)
B1–N4–C6–C5	–157.6(10)
C4–C5–C6–N4	1.1(12)
N6–N5–C7–C8	–2.2(11)
W1–N5–C7–C8	–175.8(7)
N5–C7–C8–C9	1.8(12)
N5–N6–C9–C8	–0.6(12)
B1–N6–C9–C8	170.6(10)
C7–C8–C9–N6	–0.7(12)
C16–C10–C11–C12	–40.5(16)
W1–C10–C11–C12	67.3(10)
C16–C10–C11–W1	–107.8(10)
C10–C11–C12–C13	34.8(17)
W1–C11–C12–C13	98.4(11)
C10–C11–C12–W1	–63.6(9)
C11–C12–C13–C14	14.1(18)
W1–C12–C13–C14	88.6(12)
C12–C13–C14–C15	–14(2)

C13–C14–C15–C16	–40(2)
C14–C15–C16–C10	63.4(16)
C11–C10–C16–C15	–15.7(15)
W1–C10–C16–C15	–99.4(10)
C3–N2–B1–N6	–123.3(10)
N1–N2–B1–N6	57.0(11)
C3–N2–B1–N4	121.2(10)
N1–N2–B1–N4	–58.5(11)
C9–N6–B1–N2	128.1(10)
N5–N6–B1–N2	–61.5(12)
C9–N6–B1–N4	–113.7(11)
N5–N6–B1–N4	56.8(11)
C6–N4–B1–N2	–134.9(10)
N3–N4–B1–N2	69.5(11)
C6–N4–B1–N6	106.7(11)
N3–N4–B1–N6	–49.0(11)
O2–S1–C20–F1	52.8(10)
O3–S1–C20–F1	–67.1(9)
O4–S1–C20–F1	172.7(8)
O2–S1–C20–F2	–67.8(10)
O3–S1–C20–F2	172.3(9)
O4–S1–C20–F2	52.1(10)
O2–S1–C20–F3	172.7(9)
O3–S1–C20–F3	52.8(11)
O4–S1–C20–F3	–67.3(10)

## Structure Report for mo\_harman\_nb2\_rjs\_triene\_0m

A yellow, needle-shaped crystal of mo\_harman\_nb2\_rjs\_triene\_0m was coated with Paratone oil and mounted on a MiTeGen micromount. crystallized from chloroform. Data were collected at 100.00 K on a Bruker D8 VENTURE dual wavelength Mo/Cu Kappa four-circle diffractometer with a PHOTON III detector. The diffractometer was equipped with an Oxford Cryostream 800Plus low temperature device and used Mo  $K_\alpha$  radiation ( $\lambda = 0.71073\text{\AA}$ ) from an Incoatec l\ms 3.0 microfocus sealed X-ray tube with a HELIOS double bounce multilayer mirror as monochromator.

Data collection and processing were done within the Bruker APEX5 software suite.<sup>[1]</sup> All data were integrated with SAINT 8.40B using a narrow-frame algorithm and a Multi-Scan absorption correction using was applied.<sup>[2]</sup> Using Olex2 as a graphical interface,<sup>[3]</sup> the structure was solved by dual methods with XT and refined by full-matrix least-squares methods against  $F^2$  using XL.<sup>[4,5]</sup> All non-hydrogen atoms were refined with anisotropic displacement parameters. All C-bound hydrogen atoms were refined with isotropic displacement parameters. Some of their coordinates were refined freely and some on calculated positions using a riding model with their  $U_{\text{iso}}$  values constrained to 1.5 times the  $U_{\text{eq}}$  of their pivot atoms for terminal  $\text{sp}^3$  carbon atoms and 1.2 times for all other carbon atoms.

This report and the CIF file were generated using FinalCif.<sup>[6]</sup>

Table 1. Crystal data and structure refinement for mo\_harman\_nb2\_rjs\_triene\_0m

CCDC number	
Empirical formula	C <sub>20</sub> H <sub>27</sub> BCl <sub>3</sub> N <sub>7</sub> OPW
Formula weight	713.46
Temperature [K]	100.00
Crystal system	monoclinic
Space group (number)	<i>P</i> 2 <sub>1</sub> / <i>n</i> (14)
<i>a</i> [Å]	10.3682(7)
<i>b</i> [Å]	12.4816(9)
<i>c</i> [Å]	20.3456(17)
$\alpha$ [°]	90
$\beta$ [°]	90.196(3)
$\gamma$ [°]	90
Volume [Å <sup>3</sup> ]	2632.9(3)
<i>Z</i>	4
$\rho_{\text{calc}}$ [gcm <sup>-3</sup> ]	1.800
$\mu$ [mm <sup>-1</sup> ]	4.781
<i>F</i> (000)	1396
Crystal size [mm <sup>3</sup> ]	0.066×0.12×0.125
Crystal colour	yellow
Crystal shape	needle
Radiation	Mo <i>K</i> $\alpha$ ( $\lambda$ =0.71073 Å)
2 $\theta$ range [°]	4.42 to 55.00 (0.77 Å)
Index ranges	−13 ≤ <i>h</i> ≤ 13 −16 ≤ <i>k</i> ≤ 13 −23 ≤ <i>l</i> ≤ 26
Reflections collected	34497
Independent reflections	6027 <i>R</i> <sub>int</sub> = 0.1138 <i>R</i> <sub>sigma</sub> = 0.0823
Completeness to $\theta$ = 25.242°	99.9
Data / Restraints / Parameters	6027 / 0 / 317
Goodness-of-fit on <i>F</i> <sup>2</sup>	1.017
Final <i>R</i> indexes [ <i>I</i> ≥ 2 $\sigma$ ( <i>I</i> )]	<i>R</i> <sub>1</sub> = 0.0443 <i>wR</i> <sub>2</sub> = 0.0882
Final <i>R</i> indexes [all data]	<i>R</i> <sub>1</sub> = 0.0786 <i>wR</i> <sub>2</sub> = 0.1008
Largest peak/hole [eÅ <sup>-3</sup> ]	1.39/−1.50



Table 2. Atomic coordinates and  $U_{eq}$  [Å<sup>2</sup>] for mo\_harman\_nb2\_rjs\_triene\_0m

Atom	x	y	z	$U_{eq}$
W1	0.55955(2)	0.62395(2)	0.66731(2)	0.01663(9)
P3	0.59923(17)	0.43968(15)	0.71011(9)	0.0211(4)
O1	0.8346(4)	0.6701(4)	0.7013(3)	0.0321(13)
N1	0.3474(5)	0.5854(5)	0.6610(3)	0.0207(13)
N2	0.2601(5)	0.6459(4)	0.6951(3)	0.0198(13)
N3	0.5151(5)	0.6621(4)	0.7706(3)	0.0201(13)
N4	0.3986(5)	0.7019(4)	0.7897(3)	0.0205(12)
N5	0.4883(5)	0.7913(5)	0.6625(3)	0.0213(13)
N6	0.3781(5)	0.8219(5)	0.6949(3)	0.0210(13)
N7	0.7228(5)	0.6528(4)	0.6837(3)	0.0222(13)
C1	0.2781(7)	0.5118(6)	0.6271(4)	0.0263(16)
H1	0.313687	0.458362	0.599331	0.032
C2	0.1480(6)	0.5259(6)	0.6387(4)	0.0262(17)
H2	0.078879	0.485238	0.620802	0.031
C3	0.1391(7)	0.6108(6)	0.6816(4)	0.0284(17)
H3	0.061524	0.639824	0.698809	0.034
C4	0.5896(7)	0.6623(6)	0.8248(4)	0.0259(16)
H4	0.676831	0.638994	0.826072	0.031
C5	0.5223(7)	0.7010(6)	0.8788(4)	0.0295(17)
H5	0.552248	0.708123	0.922748	0.035
C6	0.4053(8)	0.7261(6)	0.8548(4)	0.0307(18)
H6	0.337059	0.756401	0.879660	0.037
C7	0.5413(7)	0.8814(6)	0.6406(3)	0.0264(15)
H7	0.619164	0.884655	0.616181	0.032
C8	0.4676(7)	0.9706(6)	0.6579(4)	0.0299(18)
H8	0.484594	1.043710	0.648191	0.036
C9	0.3662(7)	0.9297(6)	0.6918(4)	0.0285(17)
H9	0.297896	0.970325	0.710335	0.034
C10	0.5905(7)	0.5335(6)	0.5732(4)	0.0258(16)
H10	0.520(7)	0.481(6)	0.569(3)	0.031
C11	0.5586(7)	0.6438(6)	0.5589(4)	0.0258(17)
H11	0.466(7)	0.649(6)	0.549(4)	0.03(2)
C12	0.6437(8)	0.7213(6)	0.5258(4)	0.0332(19)
H12	0.600516	0.781486	0.507528	0.040
C13	0.7692(8)	0.7212(7)	0.5174(4)	0.043(2)
H13	0.802633	0.781946	0.495036	0.051
C14	0.8656(8)	0.6411(8)	0.5374(5)	0.047(2)
H14A	0.899527	0.662738	0.580970	0.056
H14B	0.938301	0.645627	0.506075	0.056
C15	0.8272(7)	0.5272(7)	0.5420(4)	0.035(2)
H15	0.894455	0.477271	0.533840	0.042

C16	0.7150(7)	0.4845(6)	0.5554(4)	0.0294(17)
H16	0.713574	0.408436	0.553407	0.035
C17	0.5360(7)	0.4105(6)	0.7924(4)	0.0294(18)
H17A	0.579510	0.456141	0.824840	0.044
H17B	0.551596	0.335086	0.803127	0.044
H17C	0.443052	0.424864	0.793247	0.044
C18	0.7695(7)	0.4120(6)	0.7193(4)	0.0309(18)
H18A	0.809389	0.406877	0.675838	0.046
H18B	0.781063	0.344098	0.742835	0.046
H18C	0.810437	0.469949	0.744320	0.046
C19	0.5413(7)	0.3226(6)	0.6659(4)	0.0311(18)
H19A	0.447109	0.325602	0.662295	0.047
H19B	0.566576	0.257599	0.689708	0.047
H19C	0.579049	0.321371	0.621788	0.047
B1	0.3030(8)	0.7398(7)	0.7377(4)	0.0257(19)
H1A	0.226895	0.774824	0.758805	0.031
Cl1	0.1907(3)	0.7616(2)	0.54650(12)	0.0571(7)
Cl2	0.3327(3)	0.8906(3)	0.45552(13)	0.0730(9)
Cl3	0.1572(4)	0.9867(3)	0.54678(19)	0.1049(13)
C20	0.2668(9)	0.8848(7)	0.5337(4)	0.045(2)

$U_{eq}$  is defined as 1/3 of the trace of the orthogonalized  $U_{ij}$  tensor.

Table 3. Anisotropic displacement parameters ( $\text{\AA}^2$ ) for mo\_harman\_nb2\_rjs\_triene\_0m.

The anisotropic displacement factor exponent takes the form:

$$-2\pi^2 [h^2(a^*)^2 U_{11} + k^2(b^*)^2 U_{22} + \dots + 2hka^*b^* U_{12}]$$

Atom	$U_{11}$	$U_{22}$	$U_{33}$	$U_{23}$	$U_{13}$	$U_{12}$
W1	0.01419(13)	0.01989(14)	0.01581(14)	-0.00168(14)	0.00036(9)	0.00156(13)
P3	0.0174(8)	0.0212(9)	0.0248(10)	-0.0003(8)	0.0000(7)	0.0018(7)
O1	0.016(2)	0.033(3)	0.048(4)	-0.009(3)	-0.007(2)	-0.002(2)
N1	0.015(3)	0.024(3)	0.023(3)	0.003(3)	0.002(2)	0.006(2)
N2	0.014(3)	0.025(3)	0.020(3)	0.003(2)	0.002(2)	0.003(2)
N3	0.019(3)	0.022(3)	0.020(3)	-0.005(2)	0.000(2)	0.002(2)
N4	0.020(3)	0.021(3)	0.021(3)	-0.002(3)	0.001(2)	0.002(2)
N5	0.023(3)	0.024(3)	0.017(3)	0.001(3)	0.001(2)	0.004(3)
N6	0.020(3)	0.024(3)	0.019(3)	0.000(3)	-0.002(2)	0.007(3)
N7	0.029(3)	0.018(3)	0.020(3)	-0.007(2)	-0.001(3)	0.000(2)
C1	0.024(4)	0.025(4)	0.030(4)	-0.001(3)	-0.001(3)	-0.003(3)
C2	0.019(3)	0.032(4)	0.028(4)	0.010(3)	-0.010(3)	-0.009(3)
C3	0.025(4)	0.032(4)	0.029(4)	0.012(4)	0.003(3)	0.003(3)
C4	0.027(4)	0.023(4)	0.028(4)	0.000(3)	-0.005(3)	-0.006(3)
C5	0.041(5)	0.033(4)	0.015(4)	0.001(3)	0.000(3)	-0.001(4)
C6	0.040(5)	0.031(4)	0.021(4)	-0.003(3)	0.009(3)	0.009(4)
C7	0.032(4)	0.022(4)	0.025(4)	-0.003(4)	0.006(3)	-0.001(4)

C8	0.030(4)	0.022(4)	0.038(5)	0.000(3)	0.001(4)	-0.006(3)
C9	0.030(4)	0.027(4)	0.029(4)	-0.004(4)	-0.005(3)	0.008(3)
C10	0.024(4)	0.032(4)	0.022(4)	-0.007(3)	0.001(3)	-0.003(3)
C11	0.021(3)	0.035(5)	0.022(4)	0.000(3)	0.002(3)	0.007(3)
C12	0.054(5)	0.027(4)	0.019(4)	-0.004(3)	0.001(4)	0.005(4)
C13	0.045(5)	0.042(5)	0.042(5)	0.011(4)	0.018(4)	-0.011(4)
C14	0.028(4)	0.061(7)	0.052(6)	-0.005(5)	0.014(4)	-0.004(4)
C15	0.025(4)	0.043(5)	0.038(5)	-0.009(4)	0.004(4)	0.006(4)
C16	0.035(4)	0.029(4)	0.025(4)	0.000(3)	0.004(3)	0.002(3)
C17	0.027(4)	0.029(4)	0.032(5)	0.002(3)	0.001(3)	-0.002(3)
C18	0.023(4)	0.027(4)	0.043(5)	0.008(4)	-0.005(3)	0.006(3)
C19	0.029(4)	0.024(4)	0.041(5)	-0.004(4)	0.001(4)	-0.004(3)
B1	0.027(4)	0.026(4)	0.024(5)	-0.006(4)	0.005(4)	0.003(4)
Cl1	0.0689(17)	0.0533(15)	0.0488(15)	0.0159(12)	-0.0201(13)	-0.0162(13)
Cl2	0.0610(16)	0.117(3)	0.0411(15)	0.0104(16)	0.0104(12)	-0.0151(17)
Cl3	0.132(3)	0.064(2)	0.120(3)	0.010(2)	0.028(2)	0.050(2)
C20	0.054(5)	0.037(5)	0.044(5)	-0.006(4)	0.005(4)	-0.005(5)

Table 4. Bond lengths and angles for mo\_harman\_nb2\_rjs\_triene\_0m

Atom-Atom	Length [Å]
W1-P3	2.4931(18)
W1-N1	2.255(5)
W1-N3	2.205(6)
W1-N5	2.217(6)
W1-N7	1.761(6)
W1-C10	2.247(7)
W1-C11	2.220(7)
P3-C17	1.837(7)
P3-C18	1.808(7)
P3-C19	1.817(7)
O1-N7	1.231(7)
N1-N2	1.369(7)
N1-C1	1.354(9)
N2-C3	1.356(9)
N2-B1	1.524(10)
N3-N4	1.365(7)
N3-C4	1.344(9)
N4-C6	1.359(9)
N4-B1	1.523(10)
N5-N6	1.375(7)
N5-C7	1.330(9)
N6-C9	1.353(9)
N6-B1	1.555(10)
C1-H1	0.9500
C1-C2	1.381(9)
C2-H2	0.9500

C2-C3	1.376(10)
C3-H3	0.9500
C4-H4	0.9500
C4-C5	1.390(10)
C5-H5	0.9500
C5-C6	1.343(10)
C6-H6	0.9500
C7-H7	0.9500
C7-C8	1.397(10)
C8-H8	0.9500
C8-C9	1.359(10)
C9-H9	0.9500
C10-H10	0.98(7)
C10-C11	1.445(10)
C10-C16	1.475(10)
C11-H11	0.98(7)
C11-C12	1.473(11)
C12-H12	0.9500
C12-C13	1.312(11)
C13-H13	0.9500
C13-C14	1.471(12)
C14-H14A	0.9900
C14-H14B	0.9900
C14-C15	1.479(12)
C15-H15	0.9500
C15-C16	1.310(10)
C16-H16	0.9500

C17–H17A	0.9800
C17–H17B	0.9800
C17–H17C	0.9800
C18–H18A	0.9800
C18–H18B	0.9800
C18–H18C	0.9800
C19–H19A	0.9800
C19–H19B	0.9800
C19–H19C	0.9800
B1–H1A	1.0000
Cl1–C20	1.748(9)
Cl2–C20	1.734(9)
Cl3–C20	1.727(9)
<b>Atom–Atom– Atom</b>	<b>Angle [°]</b>
N1–W1–P3	89.00(15)
N3–W1–P3	84.31(15)
N3–W1–N1	83.9(2)
N3–W1–N5	76.6(2)
N3–W1–C10	162.1(3)
N3–W1–C11	157.3(2)
N5–W1–P3	159.86(15)
N5–W1–N1	82.8(2)
N5–W1–C10	119.0(2)
N5–W1–C11	81.4(2)
N7–W1–P3	87.98(19)
N7–W1–N1	172.3(2)
N7–W1–N3	88.8(2)
N7–W1–N5	97.8(2)
N7–W1–C10	97.1(3)
N7–W1–C11	99.6(3)
C10–W1–P3	79.1(2)
C10–W1–N1	89.2(2)
C11–W1–P3	116.8(2)
C11–W1–N1	88.1(2)
C11–W1–C10	37.7(3)
C17–P3–W1	116.2(3)
C18–P3–W1	111.9(3)
C18–P3–C17	102.7(4)
C18–P3–C19	102.6(4)
C19–P3–W1	121.0(3)
C19–P3–C17	100.0(4)
N2–N1–W1	120.0(4)
C1–N1–W1	133.6(5)
C1–N1–N2	106.4(5)
N1–N2–B1	121.4(5)
C3–N2–N1	109.4(6)

C3–N2–B1	129.2(6)
N4–N3–W1	122.6(4)
C4–N3–W1	131.4(5)
C4–N3–N4	105.8(6)
N3–N4–B1	119.3(6)
C6–N4–N3	108.4(6)
C6–N4–B1	129.7(6)
N6–N5–W1	121.2(4)
C7–N5–W1	132.4(5)
C7–N5–N6	105.7(5)
N5–N6–B1	120.2(6)
C9–N6–N5	109.3(6)
C9–N6–B1	129.4(6)
O1–N7–W1	173.9(5)
N1–C1–H1	125.0
N1–C1–C2	110.1(7)
C2–C1–H1	125.0
C1–C2–H2	127.0
C3–C2–C1	105.9(6)
C3–C2–H2	127.0
N2–C3–C2	108.2(6)
N2–C3–H3	125.9
C2–C3–H3	125.9
N3–C4–H4	124.4
N3–C4–C5	111.1(7)
C5–C4–H4	124.4
C4–C5–H5	127.8
C6–C5–C4	104.4(7)
C6–C5–H5	127.8
N4–C6–H6	124.9
C5–C6–N4	110.2(7)
C5–C6–H6	124.9
N5–C7–H7	124.4
N5–C7–C8	111.3(6)
C8–C7–H7	124.4
C7–C8–H8	127.7
C9–C8–C7	104.7(7)
C9–C8–H8	127.7
N6–C9–C8	109.1(7)
N6–C9–H9	125.5
C8–C9–H9	125.5
W1–C10–H10	108(4)
C11–C10–W1	70.1(4)
C11–C10–H10	116(4)
C11–C10–C16	123.1(7)
C16–C10–W1	123.0(5)
C16–C10–H10	111(4)
W1–C11–H11	102(4)

C10–C11–W1	72.2(4)
C10–C11–H11	109(4)
C10–C11–C12	125.4(7)
C12–C11–W1	121.8(5)
C12–C11–H11	117(4)
C11–C12–H12	114.5
C13–C12–C11	130.9(8)
C13–C12–H12	114.5
C12–C13–H13	115.2
C12–C13–C14	129.6(8)
C14–C13–H13	115.2
C13–C14–H14A	107.5
C13–C14–H14B	107.5
C13–C14–C15	119.2(7)
H14A–C14–H14B	107.0
C15–C14–H14A	107.5
C15–C14–H14B	107.5
C14–C15–H15	114.9
C16–C15–C14	130.1(8)
C16–C15–H15	114.9
C10–C16–H16	114.3
C15–C16–C10	131.4(8)
C15–C16–H16	114.3
P3–C17–H17A	109.5
P3–C17–H17B	109.5
P3–C17–H17C	109.5
H17A–C17–H17B	109.5
H17A–C17–H17C	109.5

H17B–C17–H17C	109.5
P3–C18–H18A	109.5
P3–C18–H18B	109.5
P3–C18–H18C	109.5
H18A–C18–H18B	109.5
H18A–C18–H18C	109.5
H18B–C18–H18C	109.5
P3–C19–H19A	109.5
P3–C19–H19B	109.5
P3–C19–H19C	109.5
H19A–C19–H19B	109.5
H19A–C19–H19C	109.5
H19B–C19–H19C	109.5
N2–B1–N6	109.4(6)
N2–B1–H1A	110.5
N4–B1–N2	110.2(6)
N4–B1–N6	105.6(6)
N4–B1–H1A	110.5
N6–B1–H1A	110.5
Cl2–C20–Cl1	110.7(5)
Cl3–C20–Cl1	109.1(5)
Cl3–C20–Cl2	111.9(5)

Table 5. Torsion angles for mo\_harman\_nb2\_rjs\_triene\_0m

Atom–Atom–Atom–Atom	Torsion Angle [°]
W1–N1–N2–C3	177.4(4)
W1–N1–N2–B1	–0.1(8)
W1–N1–C1–C2	–177.1(5)
W1–N3–N4–C6	–174.5(5)
W1–N3–N4–B1	–10.9(8)
W1–N3–C4–C5	174.8(5)
W1–N5–N6–C9	171.4(5)
W1–N5–N6–B1	2.1(8)
W1–N5–C7–C8	–169.9(5)
W1–C10–C11–C12	116.7(7)
W1–C10–C16–C15	–65.9(11)
W1–C11–C12–C13	70.4(11)

N1–N2–C3–C2	0.5(8)
N1–N2–B1–N4	–57.6(8)
N1–N2–B1–N6	58.1(8)
N1–C1–C2–C3	–0.3(8)
N2–N1–C1–C2	0.6(8)
N3–N4–C6–C5	–1.3(8)
N3–N4–B1–N2	64.4(8)
N3–N4–B1–N6	–53.7(8)
N3–C4–C5–C6	–1.2(9)
N4–N3–C4–C5	0.4(8)
N5–N6–C9–C8	–0.2(8)
N5–N6–B1–N2	–59.6(8)
N5–N6–B1–N4	58.9(8)
N5–C7–C8–C9	–0.1(9)

N6–N5–C7–C8	0.0(8)
C1–N1–N2–C3	–0.6(7)
C1–N1–N2–B1	–178.2(6)
C1–C2–C3–N2	–0.1(8)
C3–N2–B1–N4	125.4(7)
C3–N2–B1–N6	–119.0(7)
C4–N3–N4–C6	0.5(7)
C4–N3–N4–B1	164.1(6)
C4–C5–C6–N4	1.5(9)
C6–N4–B1–N2	–136.0(7)
C6–N4–B1–N6	106.0(8)
C7–N5–N6–C9	0.1(8)
C7–N5–N6–B1	–169.2(6)
C7–C8–C9–N6	0.1(9)
C9–N6–B1–N2	133.4(7)
C9–N6–B1–N4	–108.0(8)
C10–C11–C12–C13	–19.5(14)
C11–C10–C16–C15	20.6(13)
C11–C12–C13–C14	1.5(16)
C12–C13–C14–C15	29.5(15)
C13–C14–C15–C16	–29.2(14)
C14–C15–C16–C10	–2.8(16)
C16–C10–C11–W1	–117.1(7)
C16–C10–C11–C12	–0.4(12)
B1–N2–C3–C2	177.8(7)
B1–N4–C6–C5	–162.6(7)
B1–N6–C9–C8	167.9(7)

## Structure Report for mo\_harman\_rfl\_3\_137\_0m

A orange, needle-shaped crystal of mo\_harman\_rfl\_3\_137\_0m was coated with Paratone oil and mounted on a MiTeGen micromount. evaporation of Et<sub>2</sub>O/HOTf solution. Data were collected at 100(2) K on a Bruker D8 VENTURE dual wavelength Mo/Cu Kappa four-circle diffractometer with a PHOTON III detector. The diffractometer was equipped with an Oxford Cryostream 800Plus low temperature device and used Mo  $K_{\alpha}$  radiation ( $\lambda = 0.71073\text{\AA}$ ) from an Incoatec  $\lambda$ ms 3.0 microfocus sealed X-ray tube with a HELIOS double bounce multilayer mirror as monochromator.

Data collection and processing were done within the Bruker APEX5 software suite.<sup>[1]</sup> All data were integrated with SAINT 8.40B using a narrow-frame algorithm and a Multi-Scan absorption correction using was applied.<sup>[2]</sup> Using [Unknown program in \_computing\_structure\_refinement] as a graphical interface,<sup>[3]</sup> the structure was solved by direct methods with SHELXT and refined by full-matrix least-squares methods against  $F^2$  using SHELXL-2019/2.<sup>[4,5]</sup> All non-hydrogen atoms were refined with anisotropic displacement parameters. All hydrogen atoms were refined with isotropic displacement parameters. Some of their coordinates were refined freely and some on calculated positions using a riding model with their  $U_{\text{iso}}$  values constrained to 1.5 times the  $U_{\text{eq}}$  of their pivot atoms for terminal sp<sup>3</sup> carbon atoms and 1.2 times for all other carbon atoms. This report and the CIF file were generated using FinalCif.<sup>[6]</sup>

Table 1. Crystal data and structure refinement for mo\_harman\_rfl\_3\_137\_0m

CCDC number	
Empirical formula	C <sub>20</sub> H <sub>26</sub> BF <sub>3</sub> N <sub>7</sub> O <sub>4</sub> PSW
Formula weight	743.17
Temperature [K]	100(2)
Crystal system	monoclinic
Space group (number)	$P2_1/n$ (14)
$a$ [Å]	14.6316(6)
$b$ [Å]	10.9406(3)
$c$ [Å]	18.1297(7)
$\alpha$ [°]	90
$\beta$ [°]	113.3850(10)

$\gamma$ [°]	90
Volume [Å <sup>3</sup> ]	2663.79(17)
Z	4
$\rho_{\text{calc}}$ [gcm <sup>-3</sup> ]	1.853
$\mu$ [mm <sup>-1</sup> ]	4.537
<i>F</i> (000)	1456
Crystal size [mm <sup>3</sup> ]	0.128×0.235×0.478
Crystal colour	orange
Crystal shape	needle
Radiation	Mo <i>K</i> <sub>α</sub> ( $\lambda$ =0.71073 Å)
2 $\theta$ range [°]	4.46 to 59.18 (0.72 Å)
Index ranges	-20 ≤ <i>h</i> ≤ 20 -15 ≤ <i>k</i> ≤ 11 -25 ≤ <i>l</i> ≤ 25
Reflections collected	47564
Independent reflections	7467 <i>R</i> <sub>int</sub> = 0.0453 <i>R</i> <sub>sigma</sub> = 0.0281
Completeness to $\theta = 25.242^\circ$	99.9
Data / Restraints / Parameters	7467 / 0 / 358
Goodness-of-fit on <i>F</i> <sup>2</sup>	1.051
Final <i>R</i> indexes [ <i>I</i> ≥2 $\sigma$ ( <i>I</i> )]	<i>R</i> <sub>1</sub> = 0.0213 <i>wR</i> <sub>2</sub> = 0.0505
Final <i>R</i> indexes [all data]	<i>R</i> <sub>1</sub> = 0.0243 <i>wR</i> <sub>2</sub> = 0.0520
Largest peak/hole [eÅ <sup>-3</sup> ]	0.94/-1.03



Table 2. Atomic coordinates and  $U_{eq}$  [Å<sup>2</sup>] for mo\_harman\_rfl\_3\_137\_0m

Atom	x	y	z	$U_{eq}$
W1	0.32810(2)	0.38029(2)	0.66498(2)	0.01666(3)
P1	0.49566(4)	0.37625(5)	0.65455(3)	0.01961(11)
O1	0.40278(12)	0.21112(14)	0.80558(9)	0.0232(3)
N1	0.28785(14)	0.50161(18)	0.55713(11)	0.0216(4)
N2	0.22715(13)	0.45740(17)	0.48332(11)	0.0206(4)
N3	0.31109(13)	0.22804(17)	0.58452(11)	0.0190(3)
N4	0.24643(13)	0.23088(17)	0.50562(11)	0.0193(3)
N5	0.16615(13)	0.34432(18)	0.61379(11)	0.0208(3)
N6	0.11575(13)	0.34159(17)	0.53208(11)	0.0204(3)
N7	0.36945(13)	0.27796(16)	0.74809(11)	0.0187(3)
C1	0.31287(17)	0.61541(19)	0.54481(14)	0.0227(4)
H1	0.355035	0.668187	0.585812	0.027
C2	0.26840(18)	0.6455(2)	0.46346(14)	0.0260(5)
H2	0.273805	0.720181	0.438737	0.031
C3	0.21479(16)	0.5428(2)	0.42685(14)	0.0233(4)
H3	0.175646	0.533998	0.370995	0.028
C4	0.35260(17)	0.11641(18)	0.59880(14)	0.0206(4)
H4	0.399991	0.088949	0.649177	0.025
C5	0.31584(17)	0.0470(2)	0.52881(14)	0.0232(4)
H5	0.333441	-0.034461	0.521736	0.028
C6	0.24830(17)	0.1219(2)	0.47185(14)	0.0227(4)
H6	0.209453	0.100043	0.417646	0.027
C7	0.09781(17)	0.3234(2)	0.64493(14)	0.0236(4)
H7	0.111778	0.319081	0.700704	0.028
C8	0.00431(17)	0.3091(2)	0.58388(15)	0.0256(5)
H8	-0.056719	0.294184	0.589244	0.031

C9	0.01890(16 )	0.3213(2)	0.51373(14 )	0.0233(4)
H9	-0.031499	0.316213	0.460941	0.028
C10	0.40933(17 )	0.5403(2)	0.74104(14 )	0.0223(4)
H10	0.430(2)	0.593(3)	0.7122(18)	0.027(7)
C11	0.30527(18 )	0.5574(2)	0.72669(14 )	0.0230(4)
H11	0.268(2)	0.609(2)	0.6863(18)	0.026(7)
C12	0.25414(18 )	0.4982(2)	0.76502(14 )	0.0237(4)
H12	0.183750	0.499723	0.737342	0.028
C13	0.29017(18 )	0.4338(2)	0.84099(14 )	0.0257(5)
H13	0.241466	0.393098	0.854384	0.031
C14	0.38509(19 )	0.4252(2)	0.89477(14 )	0.0266(5)
H14	0.394676	0.384883	0.943715	0.032
C15	0.47425(18 )	0.4694(2)	0.88750(14 )	0.0268(5)
H15	0.533849	0.462774	0.934537	0.032
C16	0.48419(18 )	0.5186(2)	0.82325(14 )	0.0252(5)
H16	0.549922	0.543496	0.832072	0.030
C17	0.56593(18 )	0.5165(2)	0.66354(15 )	0.0263(5)
H17A	0.585000	0.550228	0.717702	0.039
H17B	0.524719	0.576009	0.623855	0.039
H17C	0.625960	0.498959	0.653920	0.039
C18	0.48622(19 )	0.3242(3)	0.55617(15 )	0.0308(5)
H18A	0.466082	0.238096	0.548915	0.046
H18B	0.551005	0.333039	0.552628	0.046
H18C	0.436505	0.373445	0.514133	0.046
C19	0.58498(17 )	0.2753(2)	0.72664(15 )	0.0281(5)
H19A	0.598880	0.304150	0.781216	0.042
H19B	0.646791	0.274775	0.717708	0.042
H19C	0.557596	0.192343	0.719989	0.042
B1	0.17129(18 )	0.3366(2)	0.47534(14 )	0.0207(4)
H1A	0.1204(18)	0.320(2)	0.4140(14)	0.014(6)
S1	0.53750(4)	0.86466(5)	0.71881(3)	0.02094(10 )
F1	0.62437(14 )	0.79320(15 )	0.62435(11 )	0.0438(4)

F2	0.56012(13) )	0.97355(17) )	0.59813(10) )	0.0436(4)
F3	0.69626(12) )	0.94434(16) )	0.70059(11) )	0.0429(4)
O2	0.44378(13) )	0.81910(17) )	0.66112(11) )	0.0310(4)
O3	0.53153(13) )	0.98319(15) )	0.75149(10) )	0.0271(3)
O4	0.59792(13) )	0.77586(15) )	0.77608(10) )	0.0282(4)
C20	0.60786(19) )	0.8951(2)	0.65712(16) )	0.0281(5)

$U_{eq}$  is defined as 1/3 of the trace of the orthogonalized  $U_{ij}$  tensor.

Table 3. Anisotropic displacement parameters ( $\text{\AA}^2$ ) for mo\_harman\_rfl\_3\_137\_0m. The anisotropic displacement factor exponent takes the form:

$$-2\pi^2 [h^2(a^*)^2 U_{11} + k^2(b^*)^2 U_{22} + \dots + 2hka^*b^* U_{12}]$$

Atom	$U_{11}$	$U_{22}$	$U_{33}$	$U_{23}$	$U_{13}$	$U_{12}$
W1	0.01646(5)	0.01816(5)	0.01478(5)	-0.00011(3)	0.00558(3)	0.00005(3)
P1	0.0182(2)	0.0213(3)	0.0190(3)	-0.00067(19)	0.0070(2)	-0.00186(19)
O1	0.0260(8)	0.0226(8)	0.0188(7)	0.0035(6)	0.0064(6)	0.0007(6)
N1	0.0195(9)	0.0254(9)	0.0179(9)	0.0012(7)	0.0054(7)	0.0008(7)
N2	0.0181(8)	0.0253(9)	0.0165(8)	0.0006(7)	0.0048(7)	-0.0002(7)
N3	0.0169(8)	0.0232(9)	0.0155(8)	-0.0006(7)	0.0051(7)	0.0000(7)
N4	0.0182(8)	0.0237(9)	0.0151(8)	-0.0017(7)	0.0056(7)	-0.0012(7)
N5	0.0186(8)	0.0269(9)	0.0174(8)	-0.0011(7)	0.0078(7)	-0.0005(7)
N6	0.0186(8)	0.0241(9)	0.0171(8)	-0.0006(7)	0.0055(7)	-0.0001(7)
N7	0.0197(8)	0.0187(8)	0.0182(8)	-0.0014(7)	0.0081(7)	-0.0009(6)
C1	0.0217(10)	0.0222(11)	0.0228(11)	0.0032(8)	0.0074(9)	0.0003(8)
C2	0.0246(11)	0.0276(11)	0.0257(11)	0.0086(9)	0.0098(9)	0.0024(9)
C3	0.0188(10)	0.0294(11)	0.0207(10)	0.0050(9)	0.0067(8)	0.0023(8)
C4	0.0219(10)	0.0204(10)	0.0211(10)	0.0008(8)	0.0103(8)	-0.0014(7)
C5	0.0258(11)	0.0230(10)	0.0226(11)	-0.0029(8)	0.0115(9)	-0.0017(8)
C6	0.0234(11)	0.0276(12)	0.0178(10)	-0.0030(8)	0.0090(8)	-0.0033(8)
C7	0.0227(11)	0.0269(11)	0.0245(11)	-0.0005(9)	0.0129(9)	-0.0001(8)
C8	0.0190(10)	0.0285(11)	0.0314(12)	-0.0004(9)	0.0123(9)	-0.0016(8)
C9	0.0173(10)	0.0253(11)	0.0253(11)	-0.0027(8)	0.0064(8)	-0.0005(8)
C10	0.0253(11)	0.0172(9)	0.0240(11)	-0.0001(8)	0.0094(9)	-0.0005(8)
C11	0.0284(11)	0.0186(10)	0.0189(10)	-0.0020(8)	0.0060(9)	0.0056(8)
C12	0.0245(11)	0.0213(10)	0.0236(10)	-0.0045(8)	0.0077(9)	0.0030(8)
C13	0.0329(12)	0.0241(11)	0.0245(11)	-0.0009(9)	0.0160(10)	0.0042(9)
C14	0.0381(13)	0.0240(11)	0.0185(10)	-0.0008(9)	0.0121(10)	0.0061(10)
C15	0.0276(12)	0.0262(11)	0.0210(11)	-0.0052(9)	0.0038(9)	0.0037(9)
C16	0.0244(11)	0.0222(11)	0.0265(11)	-0.0058(9)	0.0075(9)	-0.0003(8)
C17	0.0233(11)	0.0241(11)	0.0314(12)	0.0012(9)	0.0107(10)	-0.0037(8)

C18	0.0291(12)	0.0403(14)	0.0282(12)	−0.0076(10)	0.0170(10)	−0.0087(10)
C19	0.0193(10)	0.0259(11)	0.0339(13)	0.0045(10)	0.0051(10)	0.0016(8)
B1	0.0187(11)	0.0253(12)	0.0165(10)	−0.0005(9)	0.0052(9)	−0.0001(9)
S1	0.0241(3)	0.0206(2)	0.0183(2)	−0.00068(19)	0.0086(2)	−0.00129(19)
F1	0.0623(11)	0.0389(9)	0.0473(10)	−0.0070(7)	0.0398(9)	−0.0017(8)
F2	0.0457(10)	0.0539(11)	0.0386(9)	0.0209(8)	0.0245(8)	0.0084(8)
F3	0.0258(8)	0.0457(10)	0.0575(11)	−0.0001(8)	0.0169(8)	−0.0075(7)
O2	0.0263(9)	0.0330(9)	0.0309(9)	−0.0037(7)	0.0083(7)	−0.0093(7)
O3	0.0336(9)	0.0235(8)	0.0217(8)	−0.0019(6)	0.0084(7)	0.0039(7)
O4	0.0373(10)	0.0231(8)	0.0227(8)	0.0019(6)	0.0104(7)	0.0051(7)
C20	0.0284(12)	0.0292(12)	0.0303(12)	0.0021(9)	0.0154(10)	−0.0014(9)

Table 4. Bond lengths and angles for mo\_harman\_rfl\_3\_137\_0m

Atom–Atom	Length [Å]		
W1–N7	1.7792(18)	C7–C8	1.385(3)
W1–N3	2.1626(18)	C7–H7	0.9500
W1–N5	2.2103(18)	C8–C9	1.377(3)
W1–N1	2.2401(19)	C8–H8	0.9500
W1–C10	2.253(2)	C9–H9	0.9500
W1–C11	2.327(2)	C10–C11	1.451(3)
W1–P1	2.5331(6)	C10–C16	1.477(3)
P1–C19	1.811(2)	C10–H10	0.90(3)
P1–C17	1.818(2)	C11–C12	1.369(3)
P1–C18	1.825(2)	C11–H11	0.92(3)
O1–N7	1.206(2)	C12–C13	1.447(3)
N1–C1	1.341(3)	C12–H12	0.9500
N1–N2	1.368(3)	C13–C14	1.347(3)
N2–C3	1.344(3)	C13–H13	0.9500
N2–B1	1.531(3)	C14–C15	1.446(4)
N3–C4	1.343(3)	C14–H14	0.9500
N3–N4	1.367(2)	C15–C16	1.343(3)
N4–C6	1.346(3)	C15–H15	0.9500
N4–B1	1.539(3)	C16–H16	0.9500
N5–C7	1.349(3)	C17–H17A	0.9800
N5–N6	1.368(2)	C17–H17B	0.9800
N6–C9	1.339(3)	C17–H17C	0.9800
N6–B1	1.545(3)	C18–H18A	0.9800
C1–C2	1.395(3)	C18–H18B	0.9800
C1–H1	0.9500	C18–H18C	0.9800
C2–C3	1.380(3)	C19–H19A	0.9800
C2–H2	0.9500	C19–H19B	0.9800
C3–H3	0.9500	C19–H19C	0.9800
C4–C5	1.391(3)	B1–H1A	1.08(2)
C4–H4	0.9500	S1–O4	1.4404(17)
C5–C6	1.380(3)	S1–O3	1.4427(17)
C5–H5	0.9500	S1–O2	1.4438(18)
C6–H6	0.9500	S1–C20	1.826(3)
		F1–C20	1.330(3)

F2–C20	1.332(3)
F3–C20	1.332(3)
<b>Atom–Atom– Atom</b>	<b>Angle [°]</b>
N7–W1–N3	89.77(7)
N7–W1–N5	101.02(8)
N3–W1–N5	76.26(7)
N7–W1–N1	174.39(7)
N3–W1–N1	86.99(7)
N5–W1–N1	82.67(7)
N7–W1–C10	92.93(8)
N3–W1–C10	154.52(8)
N5–W1–C10	127.77(8)
N1–W1–C10	88.05(8)
N7–W1–C11	100.50(8)
N3–W1–C11	164.96(8)
N5–W1–C11	90.89(8)
N1–W1–C11	83.58(7)
C10–W1–C11	36.90(8)
N7–W1–P1	92.20(6)
N3–W1–P1	77.98(5)
N5–W1–P1	150.88(5)
N1–W1–P1	82.65(5)
C10–W1–P1	76.60(6)
C11–W1–P1	112.23(6)
C19–P1–C17	103.27(11)
C19–P1–C18	105.54(13)
C17–P1–C18	99.90(12)
C19–P1–W1	113.54(8)
C17–P1–W1	120.55(8)
C18–P1–W1	112.24(8)
C1–N1–N2	106.24(18)
C1–N1–W1	134.49(16)
N2–N1–W1	119.22(14)
C3–N2–N1	109.75(19)
C3–N2–B1	128.55(19)
N1–N2–B1	120.87(17)
C4–N3–N4	107.14(18)
C4–N3–W1	130.42(15)
N4–N3–W1	122.34(13)
C6–N4–N3	108.99(18)
C6–N4–B1	130.11(19)
N3–N4–B1	119.36(17)
C7–N5–N6	106.20(18)
C7–N5–W1	134.74(15)
N6–N5–W1	119.06(13)
C9–N6–N5	109.58(18)

C9–N6–B1	127.82(19)
N5–N6–B1	121.46(17)
O1–N7–W1	176.35(16)
N1–C1–C2	110.6(2)
N1–C1–H1	124.7
C2–C1–H1	124.7
C3–C2–C1	104.7(2)
C3–C2–H2	127.6
C1–C2–H2	127.6
N2–C3–C2	108.7(2)
N2–C3–H3	125.6
C2–C3–H3	125.6
N3–C4–C5	109.8(2)
N3–C4–H4	125.1
C5–C4–H4	125.1
C6–C5–C4	105.1(2)
C6–C5–H5	127.4
C4–C5–H5	127.4
N4–C6–C5	108.9(2)
N4–C6–H6	125.6
C5–C6–H6	125.6
N5–C7–C8	110.2(2)
N5–C7–H7	124.9
C8–C7–H7	124.9
C9–C8–C7	105.1(2)
C9–C8–H8	127.4
C7–C8–H8	127.4
N6–C9–C8	108.9(2)
N6–C9–H9	125.6
C8–C9–H9	125.6
C11–C10–C16	120.4(2)
C11–C10–W1	74.30(13)
C16–C10–W1	119.52(15)
C11–C10–H10	112.1(19)
C16–C10–H10	113.9(19)
W1–C10–H10	110.8(19)
C12–C11–C10	126.4(2)
C12–C11–W1	93.57(14)
C10–C11–W1	68.80(12)
C12–C11–H11	115.0(19)
C10–C11–H11	118.5(19)
W1–C11–H11	106.5(18)
C11–C12–C13	130.3(2)
C11–C12–H12	114.8
C13–C12–H12	114.8
C14–C13–C12	127.2(2)
C14–C13–H13	116.4
C12–C13–H13	116.4

C13–C14–C15	128.3(2)
C13–C14–H14	115.9
C15–C14–H14	115.9
C16–C15–C14	128.7(2)
C16–C15–H15	115.6
C14–C15–H15	115.6
C15–C16–C10	130.4(2)
C15–C16–H16	114.8
C10–C16–H16	114.8
P1–C17–H17A	109.5
P1–C17–H17B	109.5
H17A–C17– H17B	109.5
P1–C17–H17C	109.5
H17A–C17– H17C	109.5
H17B–C17– H17C	109.5
P1–C18–H18A	109.5
P1–C18–H18B	109.5
H18A–C18– H18B	109.5
P1–C18–H18C	109.5
H18A–C18– H18C	109.5
H18B–C18– H18C	109.5
P1–C19–H19A	109.5
P1–C19–H19B	109.5

H19A–C19– H19B	109.5
P1–C19–H19C	109.5
H19A–C19– H19C	109.5
H19B–C19– H19C	109.5
N2–B1–N4	109.65(18)
N2–B1–N6	107.98(18)
N4–B1–N6	106.22(18)
N2–B1–H1A	111.5(13)
N4–B1–H1A	110.2(13)
N6–B1–H1A	111.2(13)
O4–S1–O3	115.48(10)
O4–S1–O2	115.09(11)
O3–S1–O2	114.39(11)
O4–S1–C20	103.33(11)
O3–S1–C20	103.21(11)
O2–S1–C20	102.91(11)
F1–C20–F3	107.3(2)
F1–C20–F2	108.2(2)
F3–C20–F2	106.9(2)
F1–C20–S1	111.56(17)
F3–C20–S1	111.24(18)
F2–C20–S1	111.44(17)

Table 5. Torsion angles for mo\_harman\_rfl\_3\_137\_0m

Atom–Atom– Atom–Atom	Torsion Angle [°]
C1–N1–N2–C3	–0.3(2)
W1–N1–N2–C3	–178.14(14)
C1–N1–N2–B1	–170.74(19)
W1–N1–N2–B1	11.4(3)
C4–N3–N4–C6	0.0(2)
W1–N3–N4–C6	–176.93(14)
C4–N3–N4–B1	167.23(18)
W1–N3–N4–B1	–9.7(2)
C7–N5–N6–C9	0.9(2)
W1–N5–N6–C9	–178.62(14)
C7–N5–N6–B1	–167.83(19)
W1–N5–N6–B1	12.7(3)
N2–N1–C1–C2	0.3(3)
W1–N1–C1–C2	177.60(16)
N1–C1–C2–C3	–0.1(3)
N1–N2–C3–C2	0.2(3)
B1–N2–C3–C2	169.7(2)
C1–C2–C3–N2	–0.1(3)
N4–N3–C4–C5	0.8(2)
W1–N3–C4–C5	177.36(15)
N3–C4–C5–C6	–1.2(2)
N3–N4–C6–C5	–0.8(2)
B1–N4–C6–C5	–166.2(2)
C4–C5–C6–N4	1.2(2)
N6–N5–C7–C8	–0.8(3)
W1–N5–C7–C8	178.54(17)
N5–C7–C8–C9	0.5(3)
N5–N6–C9–C8	–0.6(3)
B1–N6–C9–C8	167.2(2)
C7–C8–C9–N6	0.1(3)
C16–C10–C11–C12	–37.1(3)
W1–C10–C11–C12	78.3(2)
C16–C10–C11–W1	–115.4(2)
C10–C11–C12–C13	19.6(4)
W1–C11–C12–C13	85.8(2)
C11–C12–C13–C14	5.1(4)
C12–C13–C14–C15	–5.2(4)
C13–C14–C15–C16	–6.9(4)
C14–C15–C16–C10	–1.4(4)
C11–C10–C16–C15	26.5(4)
W1–C10–C16–C15	–61.9(3)
C3–N2–B1–N4	127.2(2)
N1–N2–B1–N4	–64.3(2)
C3–N2–B1–N6	–117.4(2)
N1–N2–B1–N6	51.0(3)
C6–N4–B1–N2	–132.4(2)

N3–N4–B1–N2	63.5(2)
C6–N4–B1–N6	111.2(2)
N3–N4–B1–N6	–52.9(2)
C9–N6–B1–N2	126.8(2)
N5–N6–B1–N2	–66.7(2)
C9–N6–B1–N4	–115.7(2)
N5–N6–B1–N4	50.8(3)
O4–S1–C20–F1	56.7(2)
O3–S1–C20–F1	177.37(18)
O2–S1–C20–F1	–63.4(2)
O4–S1–C20–F3	–63.05(19)
O3–S1–C20–F3	57.59(19)
O2–S1–C20–F3	176.86(17)
O4–S1–C20–F2	177.76(18)
O3–S1–C20–F2	–61.6(2)
O2–S1–C20–F2	57.7(2)

#### Structure Report for cu\_harman\_rfl\_3\_191\_0m

A yellow, block-shaped crystal of cu\_harman\_rfl\_3\_191\_0m was coated with Paratone oil and mounted on a MiTeGen micromount. Data were collected at 100.00 K on a Bruker D8 VENTURE dual wavelength Mo/Cu Kappa four-circle diffractometer with a PHOTON III\_C14 detector. The diffractometer was equipped with an Oxford Cryostream 800Plus low temperature device and used Cu  $K_\alpha$  radiation ( $\lambda = 1.54178\text{\AA}$ ) from an Incoatec I\mS 3.0 microfocus sealed tube with a HELIOS EF double bounce multilayer mirror as monochromator.

Data collection and processing were done within the Bruker APEX6 software suite.<sup>[1]</sup> All data were integrated with SAINT V8.41 using a narrow-frame algorithm and a Multi-Scan absorption correction using was applied.<sup>[2]</sup> Using Olex2 as a graphical interface,<sup>[3]</sup> the structure was solved by dual methods with XT and refined by full-matrix least-squares methods against  $F^2$  using XL.<sup>[4,5]</sup> All non-hydrogen atoms were refined with anisotropic displacement parameters. All C-bound hydrogen atoms were refined with isotropic displacement parameters. Some of their coordinates were refined freely and some on calculated positions using a riding model with their  $U_{\text{iso}}$  values constrained to 1.5 times the  $U_{\text{eq}}$  of their pivot atoms for terminal  $\text{sp}^3$  carbon atoms and 1.2 times for all other carbon atoms.

This report and the CIF file were generated using FinalCif.<sup>[6]</sup>



Table 1. Crystal data and structure refinement for cu\_harman\_rfl\_3\_191\_0m

CCDC number	
Empirical formula	C <sub>24</sub> H <sub>32</sub> BN <sub>8</sub> O <sub>3</sub> PW
Formula weight	706.20
Temperature [K]	100.00
Crystal system	monoclinic
Space group (number)	<i>P</i> 2 <sub>1</sub> / <i>n</i> (14)
<i>a</i> [Å]	7.6769(3)
<i>b</i> [Å]	19.3965(7)
<i>c</i> [Å]	17.6818(7)
$\alpha$ [°]	90
$\beta$ [°]	92.138(3)
$\gamma$ [°]	90
Volume [Å <sup>3</sup> ]	2631.07(17)
<i>Z</i>	4
$\rho_{\text{calc}}$ [gcm <sup>-3</sup> ]	1.783
$\mu$ [mm <sup>-1</sup> ]	9.076
<i>F</i> (000)	1400
Crystal size [mm <sup>3</sup> ]	0.077×0.085×0.092
Crystal colour	yellow
Crystal shape	block
Radiation	Cu <i>K</i> $\alpha$ ( $\lambda$ =1.54178 Å)
2 $\theta$ range [°]	6.77 to 136.88 (0.83 Å)
Index ranges	−9 ≤ <i>h</i> ≤ 9 −23 ≤ <i>k</i> ≤ 23 −21 ≤ <i>l</i> ≤ 21
Reflections collected	27058
Independent reflections	4826 <i>R</i> <sub>int</sub> = 0.1364 <i>R</i> <sub>sigma</sub> = 0.0893
Completeness to $\theta = 67.679^\circ$	99.9
Data / Restraints / Parameters	4826 / 0 / 355
Goodness-of-fit on <i>F</i> <sup>2</sup>	1.023
Final <i>R</i> indexes [ $\geq 2\sigma(I)$ ]	<i>R</i> <sub>1</sub> = 0.0540 <i>wR</i> <sub>2</sub> = 0.1277
Final <i>R</i> indexes [all data]	<i>R</i> <sub>1</sub> = 0.0874 <i>wR</i> <sub>2</sub> = 0.1475
Largest peak/hole [eÅ <sup>-3</sup> ]	2.36/−1.81

Table 2. Atomic coordinates and  $U_{eq}$  [Å<sup>2</sup>] for cu\_harman\_rfl\_3\_191\_0m

Atom	x	y	z	$U_{eq}$
B1	0.2455(14)	0.8905(6)	0.4892(7)	0.038(2)
H1	0.259668	0.936444	0.464437	0.045
C1	0.4516(11)	0.7342(5)	0.4221(5)	0.0311(18)
H1A	0.485707	0.687256	0.426647	0.037
N1	0.3602(10)	0.7685(4)	0.4731(4)	0.0308(15)
O1	-0.0587(10)	0.7027(4)	0.6878(4)	0.0522(18)
P1	0.0425(3)	0.66021(12)	0.48199(13)	0.0326(5)
W1	0.20513(5)	0.73616(2)	0.57351(2)	0.03157(15)
C2	0.4898(13)	0.7768(5)	0.3615(6)	0.044(2)
H2	0.552756	0.765117	0.318058	0.052
N2	0.3403(10)	0.8337(4)	0.4448(4)	0.0324(17)
O2	0.7432(12)	0.5143(4)	0.8158(5)	0.067(3)
C3	0.4166(13)	0.8392(5)	0.3783(6)	0.040(2)
H3	0.419673	0.879540	0.347893	0.048
N3	0.3100(11)	0.8358(4)	0.6189(5)	0.0370(18)
O3	0.3869(11)	0.4183(3)	0.6340(5)	0.0506(19)
C4	0.3638(15)	0.8574(5)	0.6868(6)	0.048(3)
H4	0.370542	0.829582	0.731014	0.057
N4	0.3216(11)	0.8920(4)	0.5717(5)	0.0376(19)
C5	0.4092(17)	0.9271(6)	0.6841(7)	0.056(3)
H5	0.450953	0.954984	0.725075	0.067
N5	0.0111(10)	0.8138(4)	0.5334(4)	0.0348(18)
C6	0.3814(14)	0.9466(5)	0.6113(7)	0.047(3)
H6	0.400960	0.991312	0.591474	0.056
N6	0.0528(10)	0.8725(4)	0.4940(5)	0.0347(18)
C7	-0.1605(13)	0.8169(5)	0.5424(6)	0.042(2)
H7	-0.226624	0.783121	0.567525	0.050
N7	0.0596(11)	0.7148(4)	0.6447(4)	0.0383(18)
C8	-0.2278(14)	0.8761(6)	0.5100(7)	0.051(3)
H8	-0.345887	0.890758	0.508877	0.061
N8	0.5686(11)	0.4522(4)	0.7334(5)	0.0388(19)
C9	-0.0886(13)	0.9097(5)	0.4794(6)	0.044(2)
H9	-0.093613	0.952105	0.452521	0.053
C10	0.3677(14)	0.6424(5)	0.5824(6)	0.036(2)
H10	0.432(11)	0.628(4)	0.541(5)	0.02(2)
C11	0.4492(12)	0.6968(5)	0.6275(6)	0.034(2)

H11	0.534(15)	0.720(5)	0.611(6)	0.04(3)
C12	0.4889(15)	0.6946(5)	0.7135(6)	0.045(2)
H12A	0.605251	0.715295	0.723647	0.055
H12B	0.402799	0.724164	0.738342	0.055
C13	0.4868(14)	0.6236(5)	0.7513(6)	0.042(2)
H13	0.536246	0.627877	0.804235	0.050
C14	0.2993(15)	0.5994(6)	0.7540(6)	0.046(2)
H14	0.239988	0.599594	0.800174	0.055
C15	0.2209(15)	0.5782(5)	0.6912(7)	0.047(3)
H15	0.100870	0.566130	0.690104	0.056
C16	0.3246(13)	0.5733(5)	0.6203(6)	0.037(2)
H16	0.257962	0.544171	0.582641	0.045
C17	0.5998(14)	0.5712(5)	0.7070(6)	0.042(2)
H17	0.707292	0.594048	0.688954	0.051
C18	0.4975(13)	0.5372(5)	0.6406(6)	0.038(2)
H18	0.571387	0.537190	0.595247	0.046
C19	0.4713(13)	0.4629(5)	0.6664(6)	0.040(2)
C20	0.6468(15)	0.5124(6)	0.7596(6)	0.047(3)
C21	0.5826(16)	0.3864(5)	0.7727(7)	0.048(3)
H21B	0.507530	0.386852	0.816321	0.073
H21A	0.703831	0.378897	0.790145	0.073
H21C	0.546026	0.349224	0.738149	0.073
C22	0.1481(15)	0.5933(5)	0.4285(6)	0.044(2)
H22A	0.230289	0.614357	0.394278	0.065
H22B	0.059857	0.567259	0.398896	0.065
H22C	0.211060	0.562018	0.463432	0.065
C23	−0.0628(13 )	0.7053(6)	0.4030(6)	0.043(2)
H23A	−0.130165	0.744147	0.421980	0.065
H23B	−0.141055	0.673620	0.375073	0.065
H23C	0.025829	0.722517	0.369299	0.065
C24	−0.1352(13 )	0.6124(5)	0.5244(6)	0.041(2)
H24A	−0.086876	0.580640	0.562845	0.061
H24B	−0.199254	0.586144	0.485012	0.061
H24C	−0.214568	0.644839	0.548024	0.061

$U_{eq}$  is defined as 1/3 of the trace of the orthogonalized  $U_{ij}$  tensor.

Table 3. Anisotropic displacement parameters ( $\text{\AA}^2$ ) for cu\_harman\_rfl\_3\_191\_0m. The anisotropic displacement factor exponent takes the form:

$$-2\pi^2 [h^2(a^*)^2 U_{11} + k^2(b^*)^2 U_{22} + \dots + 2hka^*b^* U_{12}]$$

Atom	$U_{11}$	$U_{22}$	$U_{33}$	$U_{23}$	$U_{13}$	$U_{12}$
B1	0.034(5)	0.034(6)	0.044(6)	−0.002(5)	−0.007(5)	0.009(4)
C1	0.030(4)	0.032(4)	0.031(4)	0.002(4)	−0.002(4)	0.002(4)
N1	0.036(4)	0.028(4)	0.028(4)	0.005(3)	0.007(3)	−0.002(3)
O1	0.053(4)	0.065(5)	0.039(4)	0.003(4)	0.012(4)	0.001(4)

P1	0.0385(12)	0.0334(12)	0.0260(11)	-0.0036(9)	0.0016(10)	-0.0006(10)
W1	0.0348(2)	0.0308(2)	0.0290(2)	-0.00230(18)	0.00102(15)	0.00021(19)
C2	0.038(5)	0.054(7)	0.039(5)	0.003(5)	0.004(4)	-0.005(5)
N2	0.032(4)	0.032(4)	0.033(4)	0.009(3)	0.002(3)	0.001(3)
O2	0.076(6)	0.051(5)	0.070(6)	0.000(4)	-0.034(5)	0.009(4)
C3	0.043(5)	0.041(6)	0.036(5)	0.011(4)	0.003(4)	-0.006(4)
N3	0.043(4)	0.033(4)	0.035(4)	-0.008(3)	-0.006(4)	0.003(3)
O3	0.063(5)	0.033(4)	0.054(5)	-0.004(3)	-0.017(4)	0.004(3)
C4	0.057(7)	0.042(6)	0.043(6)	-0.018(5)	-0.015(5)	0.016(5)
N4	0.039(4)	0.028(4)	0.045(5)	-0.006(3)	-0.010(4)	0.002(3)
C5	0.064(8)	0.041(6)	0.062(8)	-0.020(5)	-0.013(6)	0.002(5)
N5	0.040(4)	0.034(4)	0.031(4)	-0.011(3)	0.001(3)	0.007(3)
C6	0.038(5)	0.030(5)	0.073(8)	-0.010(5)	-0.006(5)	0.002(4)
N6	0.038(4)	0.025(4)	0.040(4)	0.001(3)	0.001(4)	0.007(3)
C7	0.035(5)	0.048(6)	0.042(6)	-0.019(5)	0.005(4)	-0.006(4)
N7	0.044(4)	0.041(5)	0.030(4)	0.002(3)	0.007(4)	0.007(4)
C8	0.035(5)	0.054(7)	0.062(7)	-0.020(5)	-0.006(5)	0.006(5)
N8	0.051(5)	0.032(4)	0.033(4)	0.001(3)	-0.001(4)	0.012(4)
C9	0.041(6)	0.046(6)	0.045(6)	-0.002(5)	-0.016(5)	0.008(4)
C10	0.045(5)	0.035(5)	0.029(5)	0.003(4)	0.006(4)	0.001(4)
C11	0.027(4)	0.036(5)	0.039(5)	0.002(4)	0.001(4)	-0.004(4)
C12	0.050(6)	0.049(6)	0.036(5)	-0.010(4)	-0.009(5)	0.006(5)
C13	0.051(6)	0.041(6)	0.033(5)	-0.001(4)	-0.010(5)	0.003(4)
C14	0.048(6)	0.048(6)	0.042(6)	0.006(5)	0.003(5)	0.008(5)
C15	0.045(6)	0.040(6)	0.056(7)	0.004(5)	0.001(5)	0.003(5)
C16	0.042(5)	0.028(5)	0.041(5)	0.000(4)	-0.003(5)	-0.001(4)
C17	0.044(6)	0.036(5)	0.046(6)	0.000(4)	-0.007(5)	-0.001(4)
C18	0.040(5)	0.041(5)	0.035(5)	0.001(4)	0.006(4)	0.009(4)
C19	0.040(5)	0.035(5)	0.043(6)	-0.008(4)	-0.001(5)	0.007(4)
C20	0.045(6)	0.057(7)	0.038(6)	-0.006(5)	-0.010(5)	0.005(5)
C21	0.059(7)	0.035(5)	0.050(6)	0.005(5)	-0.003(5)	0.000(5)
C22	0.051(6)	0.041(6)	0.039(5)	-0.010(4)	0.001(5)	0.005(5)
C23	0.042(5)	0.051(6)	0.037(5)	-0.005(5)	-0.002(4)	-0.004(5)
C24	0.043(5)	0.036(5)	0.042(6)	-0.005(4)	0.001(5)	0.002(4)

Table 4. Bond lengths and angles for cu\_harman\_rfl\_3\_191\_0m

Atom-Atom	Length [Å]
B1-H1	1.0000
B1-N2	1.550(14)
B1-N4	1.552(14)
B1-N6	1.526(14)
C1-H1A	0.9500
C1-N1	1.341(12)
C1-C2	1.392(14)
N1-W1	2.263(7)
N1-N2	1.367(10)

O1-N7	1.229(11)
P1-W1	2.489(2)
P1-C22	1.815(10)
P1-C23	1.812(10)
P1-C24	1.833(11)
W1-N3	2.231(8)
W1-N5	2.216(8)
W1-N7	1.764(8)
W1-C10	2.207(10)
W1-C11	2.208(9)

C2–H2	0.9500
C2–C3	1.373(15)
N2–C3	1.336(13)
O2–C20	1.216(13)
C3–H3	0.9500
N3–C4	1.324(13)
N3–N4	1.378(12)
O3–C19	1.211(12)
C4–H4	0.9500
C4–C5	1.396(16)
N4–C6	1.340(13)
C5–H5	0.9500
C5–C6	1.352(18)
N5–N6	1.378(11)
N5–C7	1.334(13)
C6–H6	0.9500
N6–C9	1.321(12)
C7–H7	0.9500
C7–C8	1.374(16)
C8–H8	0.9500
C8–C9	1.379(16)
N8–C19	1.393(13)
N8–C20	1.386(14)
N8–C21	1.455(13)
C9–H9	0.9500
C10–H10	0.93(9)
C10–C11	1.451(14)
C10–C16	1.540(13)
C11–H11	0.85(12)
C11–C12	1.540(14)
C12–H12A	0.9900
C12–H12B	0.9900
C12–C13	1.530(15)
C13–H13	1.0000
C13–C14	1.517(15)
C13–C17	1.565(15)
C14–H14	0.9500
C14–C15	1.309(16)
C15–H15	0.9500
C15–C16	1.512(16)
C16–H16	1.0000
C16–C18	1.532(13)
C17–H17	1.0000
C17–C18	1.536(14)
C17–C20	1.506(15)
C18–H18	1.0000
C18–C19	1.526(14)
C21–H21B	0.9800

C21–H21A	0.9800
C21–H21C	0.9800
C22–H22A	0.9800
C22–H22B	0.9800
C22–H22C	0.9800
C23–H23A	0.9800
C23–H23B	0.9800
C23–H23C	0.9800
C24–H24A	0.9800
C24–H24B	0.9800
C24–H24C	0.9800
<b>Atom–Atom– Atom</b>	<b>Angle [°]</b>
N2–B1–H1	110.5
N2–B1–N4	108.8(7)
N4–B1–H1	110.5
N6–B1–H1	110.5
N6–B1–N2	109.9(8)
N6–B1–N4	106.5(9)
N1–C1–H1A	124.6
N1–C1–C2	110.7(8)
C2–C1–H1A	124.6
C1–N1–W1	134.0(6)
C1–N1–N2	105.5(7)
N2–N1–W1	119.3(6)
C22–P1–W1	122.6(4)
C22–P1–C24	101.8(5)
C23–P1–W1	114.4(4)
C23–P1–C22	98.0(5)
C23–P1–C24	104.0(5)
C24–P1–W1	113.4(3)
N1–W1–P1	85.4(2)
N3–W1–N1	81.3(3)
N3–W1–P1	155.7(2)
N5–W1–N1	85.9(3)
N5–W1–P1	83.1(2)
N5–W1–N3	75.8(3)
N7–W1–N1	172.4(3)
N7–W1–P1	90.5(3)
N7–W1–N3	100.2(4)
N7–W1–N5	87.3(3)
N7–W1–C10	97.3(4)
N7–W1–C11	99.2(4)
C10–W1–N1	88.4(3)
C10–W1–P1	80.1(3)
C10–W1–N3	119.5(3)
C10–W1–N5	162.6(3)

C10-W1-C11	38.4(4)
C11-W1-N1	88.4(3)
C11-W1-P1	118.3(3)
C11-W1-N3	81.7(3)
C11-W1-N5	157.4(3)
C1-C2-H2	127.6
C3-C2-C1	104.9(9)
C3-C2-H2	127.6
N1-N2-B1	121.3(8)
C3-N2-B1	128.2(8)
C3-N2-N1	110.5(8)
C2-C3-H3	125.8
N2-C3-C2	108.4(9)
N2-C3-H3	125.8
C4-N3-W1	134.2(8)
C4-N3-N4	105.9(8)
N4-N3-W1	119.9(6)
N3-C4-H4	124.9
N3-C4-C5	110.2(11)
C5-C4-H4	124.9
N3-N4-B1	121.6(8)
C6-N4-B1	128.0(9)
C6-N4-N3	109.7(9)
C4-C5-H5	127.1
C6-C5-C4	105.8(10)
C6-C5-H5	127.1
N6-N5-W1	123.8(6)
C7-N5-W1	130.4(7)
C7-N5-N6	105.8(8)
N4-C6-C5	108.4(10)
N4-C6-H6	125.8
C5-C6-H6	125.8
N5-N6-B1	117.5(7)
C9-N6-B1	130.9(9)
C9-N6-N5	110.2(9)
N5-C7-H7	124.9
N5-C7-C8	110.2(10)
C8-C7-H7	124.9
O1-N7-W1	171.6(7)
C7-C8-H8	127.1
C7-C8-C9	105.9(9)
C9-C8-H8	127.1
C19-N8-C21	124.4(9)
C20-N8-C19	111.8(8)
C20-N8-C21	123.8(9)
N6-C9-C8	107.9(10)
N6-C9-H9	126.0
C8-C9-H9	126.0

W1-C10-H10	120(5)
C11-C10-W1	70.8(5)
C11-C10-H10	114(5)
C11-C10-C16	119.3(8)
C16-C10-W1	128.2(7)
C16-C10-H10	102(5)
W1-C11-H11	109(7)
C10-C11-W1	70.8(5)
C10-C11-H11	121(8)
C10-C11-C12	126.0(9)
C12-C11-W1	124.8(7)
C12-C11-H11	103(8)
C11-C12-H12A	108.1
C11-C12-H12B	108.1
H12A-C12-H12B	107.3
C13-C12-C11	116.8(8)
C13-C12-H12A	108.1
C13-C12-H12B	108.1
C12-C13-H13	108.9
C12-C13-C17	110.6(9)
C14-C13-C12	108.5(8)
C14-C13-H13	108.9
C14-C13-C17	111.0(8)
C17-C13-H13	108.9
C13-C14-H14	120.7
C15-C14-C13	118.5(11)
C15-C14-H14	120.7
C14-C15-H15	120.6
C14-C15-C16	118.8(10)
C16-C15-H15	120.6
C10-C16-H16	108.4
C15-C16-C10	115.7(8)
C15-C16-H16	108.4
C15-C16-C18	108.2(8)
C18-C16-C10	107.6(8)
C18-C16-H16	108.4
C13-C17-H17	110.5
C18-C17-C13	112.6(8)
C18-C17-H17	110.5
C20-C17-C13	107.9(9)
C20-C17-H17	110.5
C20-C17-C18	104.6(8)
C16-C18-C17	113.4(8)
C16-C18-H18	108.9
C17-C18-H18	108.9
C19-C18-C16	112.3(8)
C19-C18-C17	104.3(8)

C19–C18–H18	108.9
O3–C19–N8	123.7(9)
O3–C19–C18	127.4(10)
N8–C19–C18	108.8(8)
O2–C20–N8	122.8(10)
O2–C20–C17	127.3(10)
N8–C20–C17	109.9(8)
N8–C21–H21B	109.5
N8–C21–H21A	109.5
N8–C21–H21C	109.5
H21B–C21–H21A	109.5
H21B–C21–H21C	109.5
H21A–C21–H21C	109.5
P1–C22–H22A	109.5
P1–C22–H22B	109.5
P1–C22–H22C	109.5
H22A–C22–H22B	109.5
H22A–C22–H22C	109.5

H22B–C22–H22C	109.5
P1–C23–H23A	109.5
P1–C23–H23B	109.5
P1–C23–H23C	109.5
H23A–C23–H23B	109.5
H23A–C23–H23C	109.5
H23B–C23–H23C	109.5
P1–C24–H24A	109.5
P1–C24–H24B	109.5
P1–C24–H24C	109.5
H24A–C24–H24B	109.5
H24A–C24–H24C	109.5
H24B–C24–H24C	109.5

Table 5. Torsion angles for cu\_harman\_rfl\_3\_191\_0m

Atom–Atom–Atom–Atom	Torsion Angle [°]
B1–N2–C3–C2	177.8(9)
B1–N4–C6–C5	170.3(10)
B1–N6–C9–C8	–165.4(10)
C1–N1–N2–B1	–178.0(8)
C1–N1–N2–C3	0.2(10)
C1–C2–C3–N2	0.1(11)
N1–C1–C2–C3	0.0(11)
N1–N2–C3–C2	–0.2(11)
W1–N1–N2–B1	13.1(10)
W1–N1–N2–C3	–168.8(6)
W1–N3–C4–C5	–177.0(8)
W1–N3–N4–B1	6.6(12)
W1–N3–N4–C6	177.7(7)
W1–N5–N6–B1	–10.4(11)
W1–N5–N6–C9	–178.4(6)
W1–N5–C7–C8	177.8(7)
W1–C10–C11–C12	119.6(10)
W1–C10–C16–C15	–35.8(12)
W1–C10–C16–C18	–156.9(7)
W1–C11–C12–C13	107.5(10)
C2–C1–N1–W1	166.4(7)

C2–C1–N1–N2	–0.1(10)
N2–B1–N4–N3	–61.7(12)
N2–B1–N4–C6	128.9(11)
N2–B1–N6–N5	64.0(11)
N2–B1–N6–C9	–130.8(11)
N3–C4–C5–C6	–0.4(14)
N3–N4–C6–C5	–0.1(13)
C4–N3–N4–B1	–171.2(9)
C4–N3–N4–C6	–0.1(11)
C4–C5–C6–N4	0.3(14)
N4–B1–N2–N1	49.2(12)
N4–B1–N2–C3	–128.6(10)
N4–B1–N6–N5	–53.6(10)
N4–B1–N6–C9	111.5(11)
N4–N3–C4–C5	0.3(12)
N5–N6–C9–C8	0.6(11)
N5–C7–C8–C9	0.6(12)
N6–B1–N2–N1	–67.0(10)
N6–B1–N2–C3	115.2(11)
N6–B1–N4–N3	56.7(11)
N6–B1–N4–C6	–112.7(11)
N6–N5–C7–C8	–0.3(11)

C7–N5–N6–B1	167.9(8)
C7–N5–N6–C9	–0.2(10)
C7–C8–C9–N6	–0.7(12)
C10–C11–C12–C13	16.9(15)
C10–C16–C18–C17	71.8(11)
C10–C16–C18–C19	–170.3(8)
C11–C10–C16–C15	52.0(13)
C11–C10–C16–C18	–69.1(12)
C11–C12–C13–C14	–72.3(12)
C11–C12–C13–C17	49.6(12)
C12–C13–C14–C15	74.1(12)
C12–C13–C17–C18	–85.4(11)
C12–C13–C17–C20	159.7(8)
C13–C14–C15–C16	4.9(15)
C13–C17–C18–C16	13.7(12)
C13–C17–C18–C19	–108.7(9)
C13–C17–C20–O2	–68.1(16)
C13–C17–C20–N8	114.4(10)
C14–C13–C17–C18	35.0(12)
C14–C13–C17–C20	–79.8(10)
C14–C15–C16–C10	–74.4(12)
C14–C15–C16–C18	46.4(12)
C15–C16–C18–C17	–53.9(11)
C15–C16–C18–C19	64.0(10)
C16–C10–C11–W1	–123.7(9)
C16–C10–C11–C12	–4.1(15)
C16–C18–C19–O3	51.5(15)
C16–C18–C19–N8	–131.3(9)
C17–C13–C14–C15	–47.5(13)
C17–C18–C19–O3	174.6(11)
C17–C18–C19–N8	–8.2(11)
C18–C17–C20–O2	171.9(12)
C18–C17–C20–N8	–5.6(12)
C19–N8–C20–O2	–177.1(11)
C19–N8–C20–C17	0.5(13)
C20–N8–C19–O3	–177.7(11)
C20–N8–C19–C18	5.0(12)
C20–C17–C18–C16	130.5(9)
C20–C17–C18–C19	8.1(11)
C21–N8–C19–O3	0.5(17)
C21–N8–C19–C18	–176.8(9)
C21–N8–C20–O2	4.7(18)
C21–N8–C20–C17	–177.7(10)



## Bibliography

- [1] Bruker, *SAINT*, V8.41, Bruker AXS Inc., Madison, Wisconsin, USA.
- [2] Unknown Reference, please add.
- [3] O. V. Dolomanov, L. J. Bourhis, R. J. Gildea, J. A. K. Howard, H. Puschmann, *J. Appl. Cryst.* **2009**, 42, 339-341, doi:10.1107/S0021889808042726.
- [4] G. M. Sheldrick, *Acta Cryst.* **2015**, A71, 3–8, doi:10.1107/S2053273314026370.
- [5] G. M. Sheldrick, *Acta Cryst.* **2015**, C71, 3–8, doi:10.1107/S2053229614024218.
- [6] D. Kratzert, *FinalCif*, V149, <https://dkratzert.de/finalcif.html>.

## **Appendix G: Chapter 7 Data**

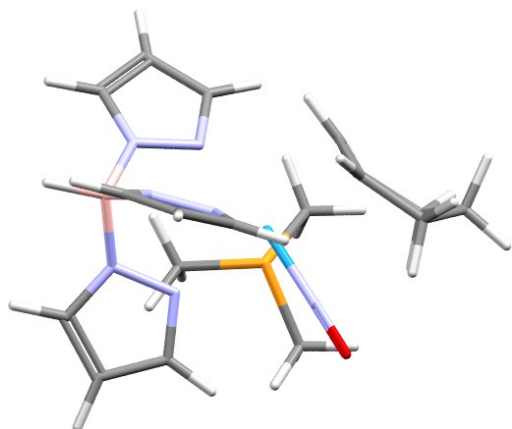
**Computational Methods.** Ground-state structures were optimized at the M06 level of theory using the 6-31G\*\*[LANL2DZ for W] basis set in Gaussian 16. Previous literature demonstrates that this functional and basis set choice accurately corroborates experimental results. Vibrational frequency analysis verified that optimized structures were minima, and rigid-rotor-harmonic oscillator thermochemical chemical corrections were applied at 298 K and 1 atm utilizing Gaussian's default implementation. When solvent corrections were applied to estimate DG<sub>solv</sub>, optimization and frequency calculations were performed using the SMD continuum solvent model with the appropriate solvent's parameters from Gaussian.

### Energies and Cartesian Coordinates:

#### Parent Allyl Distal Boat Conformation of [WTp(NO)(PMe<sub>3</sub>)(C<sub>6</sub>H<sub>9</sub>)]<sup>+</sup> Energies in MeCN

Electronic Energy: -1594.42334696 Hartree

Electronic Energy + Free Energy Correction: -1594.016150 Hartree



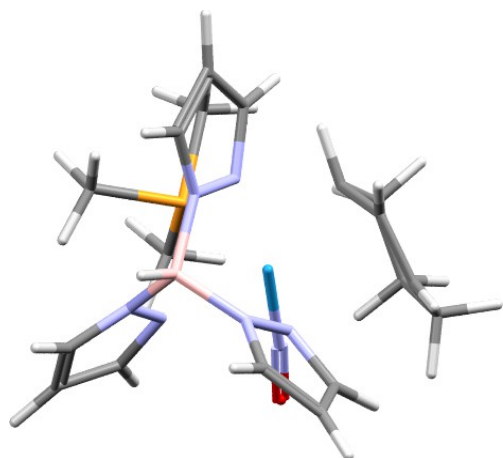
W	-0.36887600	0.26000800	-0.06018800
P	-1.11477700	-2.18552600	-0.37179300
O	-1.81811200	1.02571600	-2.53622900
N	0.79729900	-0.61667000	1.67748000
N	2.15284500	-0.64145300	1.64428900
N	2.51956600	-0.68553300	-0.84338600
N	1.24921300	-0.55874800	-1.30355000
N	2.49669800	1.48280800	0.32939400
N	1.21960500	1.82333900	0.00445100
N	-1.22808300	0.75026400	-1.52968700
C	0.43395300	-1.24897100	2.80327100
H	-0.61264400	-1.35515300	3.06424600

C	1.55729300	-1.68906600	3.50155300
H	1.58531500	-2.22446900	4.43983200
C	2.62884900	-1.27948600	2.72659600
H	3.69666200	-1.39084900	2.86832600
C	2.54658100	-1.29258100	-2.97804800
H	2.87422900	-1.63380000	-3.94967600
C	3.31324500	-1.11986500	-1.83699300
H	4.37295600	-1.26038800	-1.66317700
C	1.24637300	3.10814200	-0.37527500
H	0.33927300	3.60287300	-0.70204300
C	2.54096800	3.61597700	-0.28253900
H	2.87527700	4.61861500	-0.50817600
C	3.30066500	2.54787400	0.16068000
H	4.36101800	2.46392400	0.36449800
C	0.29463100	-3.35157800	-0.39163900
H	-0.09632600	-4.37373100	-0.45551600
H	0.95017900	-3.16882700	-1.24797900
C	-2.22144200	-3.00833100	0.82655000
H	-1.78488300	-2.99639500	1.83054900
H	-3.20590600	-2.53163000	0.85001300
C	-1.98206800	-2.49490900	-1.94652900
H	-2.19660300	-3.56658300	-2.03540300
H	-2.92620400	-1.93899100	-1.95979700
B	2.92349900	0.00076200	0.48609100
H	4.10547600	-0.08238500	0.66199500
C	-2.26132600	0.07120600	1.22340400
H	-2.25090300	-0.75311800	1.93418300
C	-1.55878300	1.24314000	1.65006500
H	-0.86217100	1.21696000	2.48750000
C	1.26159200	-0.91246700	-2.59675400
H	0.35071700	-0.87886800	-3.18300100
H	-2.34320800	-4.05057600	0.50856200
H	0.87370100	-3.24858300	0.53378300
H	-1.37512200	-2.18130100	-2.80055500
C	-2.84161300	2.66612300	0.02505500
H	-2.63997000	2.64338000	-1.05504600
H	-3.12263300	3.70629400	0.24117900
C	-3.98553100	1.72666600	0.40253400
H	-4.82676800	1.85808100	-0.28776300
H	-4.34261800	2.01772100	1.40101900
C	-3.56866300	0.25770500	0.45373500
H	-3.50226600	-0.14729000	-0.56534500
H	-4.35760400	-0.31936700	0.95524800
C	-1.62375500	2.36836200	0.84529400
H	-0.92891200	3.18155800	1.04406400

**Parent Allyl Distal Chair Conformation of [WTp(NO)(PMe<sub>3</sub>)(C<sub>6</sub>H<sub>9</sub>)]<sup>+</sup> Energies in MeCN**

Electronic Energy: -1594.42173935 Hartree

Electronic Energy + Free Energy Correction: -1594.015248 Hartree



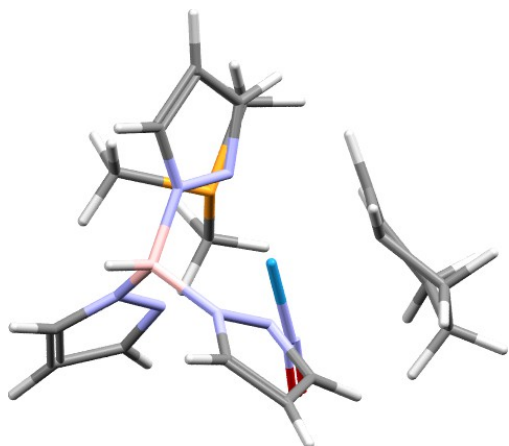
W	-0.36546300	0.28291100	-0.01255900
P	-1.28405900	-2.07540000	-0.43355800
O	-1.55759200	1.33591500	-2.51949600
N	0.81324500	-0.75090500	1.63253500
N	2.16320300	-0.85255800	1.54372400
N	2.44666400	-0.77099800	-0.95143500
N	1.16807800	-0.55653100	-1.34859300
N	2.58032700	1.32348200	0.34778800
N	1.31205000	1.74933700	0.09894300
N	-1.13650000	0.94018800	-1.46865100
C	0.45810100	-1.40966800	2.74607400
H	-0.58057200	-1.46624000	3.04842300
C	1.57890900	-1.94546500	3.37786700
H	1.61058700	-2.52272300	4.29088200
C	2.64188400	-1.56421800	2.57759000
H	3.70596900	-1.74282400	2.67005800
C	2.35633800	-1.25754300	-3.11470000
H	2.62598400	-1.56022000	-4.11650000
C	3.17658600	-1.18730400	-2.00035600
H	4.23380000	-1.38947400	-1.88043000
C	1.39368900	3.05289300	-0.20053900
H	0.50405300	3.61341300	-0.46306000
C	2.71634800	3.48678300	-0.12933500
H	3.09554400	4.48344400	-0.30502800
C	3.43362400	2.35433800	0.21325000
H	4.49498500	2.20230200	0.36612000
C	0.02694000	-3.32720900	-0.68643900

H	-0.44376800	-4.31114100	-0.79653200
H	0.62337100	-3.11673700	-1.57830400
C	-2.30099700	-2.93659400	0.81696600
H	-1.74997000	-3.03138900	1.75844700
H	-3.24613200	-2.41798700	0.99915600
C	-2.32302000	-2.17711600	-1.92818100
H	-2.67025800	-3.20776100	-2.06748400
H	-3.18943400	-1.51579000	-1.81327500
B	2.93130300	-0.18600100	0.39804800
H	4.11211100	-0.34132700	0.52739000
C	-2.17561500	0.13376100	1.36359000
H	-2.13334800	-0.70611200	2.05658000
C	-1.41271300	1.28296400	1.76547900
H	-0.66420700	1.24132200	2.55670300
C	1.10868100	-0.83734500	-2.65755800
H	0.17590000	-0.73060400	-3.19863700
H	-2.51921500	-3.94092100	0.43508100
H	0.68612800	-3.34414400	0.19022000
H	-1.75806500	-1.86704300	-2.81295600
C	-1.53983800	2.43156700	1.01076100
H	-0.85001500	3.25092300	1.20785900
C	-2.75750500	2.76467600	0.21682700
H	-3.28378400	3.50661400	0.84121800
H	-2.48069500	3.31223400	-0.69470700
C	-3.57716300	0.40942100	0.84654300
H	-3.99786300	-0.48393100	0.36526800
H	-4.20740500	0.59742800	1.73079700
C	-3.67818100	1.58758700	-0.12036300
H	-3.45477300	1.24176300	-1.13418100
H	-4.71548200	1.94191600	-0.14970300

# **Parent Allyl Proximal Chair Conformation of [Wtp(NO)(PMe<sub>3</sub>)(C<sub>6</sub>H<sub>9</sub>)]<sup>+</sup> Energies in MeCN**

Electronic Energy: -1594.41887250 Hartree

Electronic Energy + Free Energy Correction: -1594.013116 Hartree



W	-0.43526400	0.15519000	-0.03418600
P	-1.02128100	-2.34510200	-0.20351400
O	-1.79268800	0.87957700	-2.57535800
N	0.93452100	-0.55111900	1.64109500
N	2.28138100	-0.42239500	1.51954300
N	2.50806300	-0.52118000	-0.97754100
N	1.20568300	-0.53224100	-1.34833600
N	2.32750400	1.67352600	0.13356200
N	1.00393000	1.84994200	-0.10376600
N	-1.29827000	0.62557000	-1.51340100
C	0.72249200	-1.16970700	2.81313400
H	-0.28192400	-1.39670400	3.14781000
C	1.92958300	-1.44613300	3.45132900
H	2.07814300	-1.93276800	4.40473000
C	2.89424600	-0.95148300	2.59096600
H	3.97448700	-0.93293100	2.66454000
C	2.44329400	-1.27422200	-3.06279900
H	2.73196400	-1.65696000	-4.03139600
C	3.26871800	-0.95800300	-1.99628400
H	4.34584200	-0.99863200	-1.89192100
C	0.83056800	3.13368400	-0.43331900
H	-0.15684800	3.50522300	-0.68030700
C	2.05261700	3.80849800	-0.40092800
H	2.23693300	4.85223300	-0.61267300
C	2.97406000	2.84160900	-0.04166100
H	4.04663500	2.89408300	0.09792900
C	0.45327000	-3.41074200	-0.37366200
H	0.13725200	-4.45980400	-0.33389300

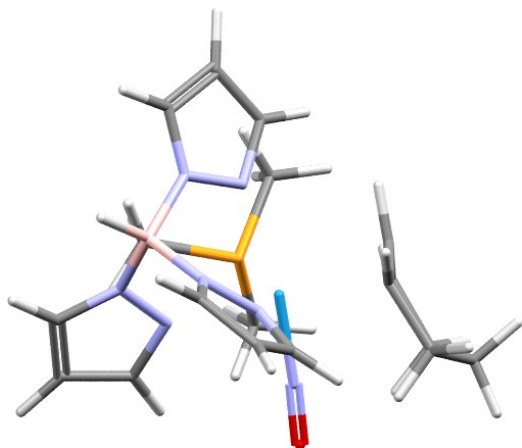
H	0.96635500	-3.22817000	-1.32238500
C	-1.86684400	-3.16446600	1.19533200
H	-1.20569000	-3.17853900	2.06812500
H	-2.80837700	-2.67836900	1.46665700
C	-2.06025800	-2.75421300	-1.64373800
H	-2.23467300	-3.83573500	-1.68727900
H	-3.02110100	-2.23312000	-1.56176700
B	2.91898600	0.25413400	0.29681400
H	4.11125400	0.29541500	0.40787200
C	-2.02867800	0.28845400	1.59473000
H	-1.80407600	-0.48509900	2.32628500
C	-1.32348200	1.53684800	1.50331700
H	-0.58811900	1.71641600	2.29143700
C	1.15779800	-0.97550200	-2.61194000
H	0.20795400	-1.06529200	-3.12634100
H	-2.07881600	-4.19965400	0.90226600
H	1.14673300	-3.21322600	0.45275400
H	-1.56415200	-2.43153600	-2.56528900
C	-3.06917300	2.51195900	-0.07171900
H	-2.49403100	2.64238200	-0.99501200
H	-3.85232500	3.27914500	-0.09537500
C	-3.72575400	1.12823000	-0.08703100
H	-3.96052500	0.81874800	-1.11466900
H	-4.70120900	1.15321300	0.42884700
C	-2.15572000	2.74715700	1.12754800
H	-2.76030200	3.01012200	2.01073000
H	-1.51429700	3.61726600	0.94093700
C	-2.99248300	0.04431700	0.62689900
H	-3.44694600	-0.94497200	0.56955700



**Parent Allyl Proximal Boat Conformation of [Wtp(NO)(PMe<sub>3</sub>)(C<sub>6</sub>H<sub>9</sub>)]<sup>+</sup> Energies in MeCN**

Electronic Energy: -1594.41822228 Hartree

Electronic Energy + Free Energy Correction: -1594.011677 Hartree



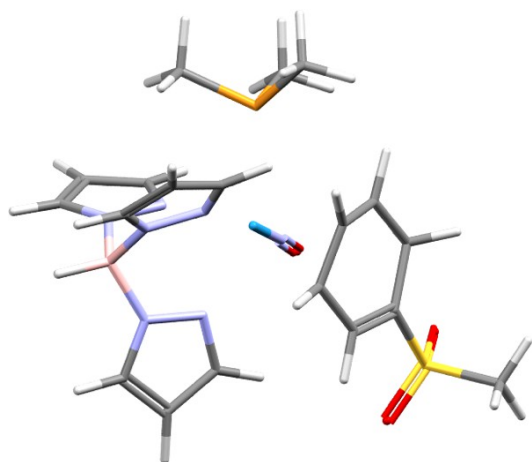
W	-0.40878100	0.19455800	-0.03568800
P	-1.00552200	-2.30114000	-0.23091000
O	-1.80845500	0.95224500	-2.53774900
N	0.93673300	-0.56166300	1.64628600
N	2.28775000	-0.51245900	1.50164600
N	2.51300900	-0.52664500	-1.00449800
N	1.20988700	-0.47283100	-1.36848300
N	2.40909600	1.62188500	0.19164100
N	1.09057400	1.86821700	-0.02005600
N	-1.27194100	0.66892400	-1.50327500
C	0.70864400	-1.22518600	2.79103700
H	-0.30204500	-1.40922800	3.13471300
C	1.90718900	-1.60588600	3.38970800
H	2.04270600	-2.14427800	4.31683200
C	2.88503800	-1.12988500	2.53346500
H	3.96550900	-1.18004400	2.58640300
C	2.41657800	-1.14230300	-3.13337700
H	2.68950600	-1.47372700	-4.12516400
C	3.25552100	-0.92056300	-2.05323200
H	4.33126900	-1.00130800	-1.95797100
C	0.97136800	3.18556300	-0.22347700
H	0.00104600	3.62735500	-0.41277100
C	2.21823300	3.80476300	-0.14104400
H	2.44304900	4.85552400	-0.25724700
C	3.10129100	2.77270700	0.12132100
H	4.17502300	2.76888900	0.26177400
C	0.40665200	-3.35018900	-0.72812800
H	0.10045500	-4.39948800	-0.64050500
H	0.71345200	-3.15460200	-1.75876300

C	-1.53878200	-3.22726400	1.25658300
H	-0.66214700	-3.42208700	1.88316700
H	-2.29300600	-2.71077300	1.85554800
C	-2.28451100	-2.64908700	-1.48057500
H	-2.36051000	-3.73033400	-1.64495500
H	-3.25396700	-2.26758400	-1.14253000
B	2.94907900	0.17938800	0.29940800
H	4.14190000	0.17329700	0.41126600
C	-1.94214200	0.55791900	1.66817300
H	-1.53705900	0.04750700	2.53859900
C	-1.43293300	1.81140700	1.23908400
H	-0.71153700	2.28673600	1.90430500
C	1.14313600	-0.83395700	-2.65737800
H	0.18693800	-0.87020200	-3.16735000
H	-1.94801700	-4.18898300	0.92417500
H	1.25438600	-3.16856700	-0.05617300
H	-2.02115100	-2.15577600	-2.42293800
C	-3.76530000	2.16245800	0.34819900
H	-4.24797800	2.26708500	1.33060600
H	-4.36107900	2.74538300	-0.36364400
C	-3.79428200	0.68150100	-0.02942900
H	-3.61930400	0.53658300	-1.10343500
H	-4.79556700	0.26875100	0.15601500
C	-2.35283400	2.73521500	0.44803900
H	-2.39301600	3.70642900	0.95987600
H	-1.96362300	2.94294700	-0.55764900
C	-2.83966900	-0.09816100	0.83023200
H	-3.12531900	-1.11690600	1.07928200

### Compound 2A Energies in Gas Phase

Electronic Energy: -2180.88192679 Hartree

Electronic Energy + Free Energy Correction: -2180.469184 Hartree



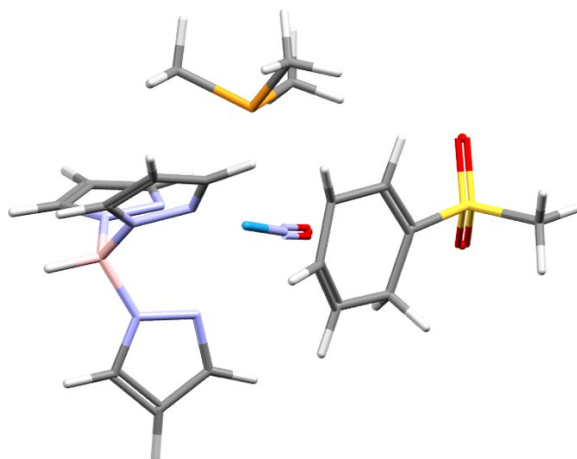
W	0.27912800	-0.23303100	0.03199300
P	1.50950800	-2.45191600	-0.40129900
O	-1.62528400	-0.31230500	-2.24230000
N	1.90030000	0.07088600	1.58700300
N	2.79368700	1.08026500	1.42998600
N	2.80031500	1.27722300	-1.07550200
N	1.80395200	0.42192200	-1.40591800
N	1.29983300	2.72555500	0.24487900
N	0.18664000	1.97282900	0.05208500
N	-0.88025700	-0.31894800	-1.32260900
C	2.26406400	-0.57503000	2.70836800
H	1.70057700	-1.42592300	3.07081400
C	3.39295000	0.00815900	3.27469500
H	3.91026100	-0.28444300	4.17627800
C	3.69272000	1.06019000	2.42662100
H	4.47986700	1.80209400	2.46434900
C	3.02234300	0.83491000	-3.24117300
H	3.37788900	0.82832000	-4.26091900
C	3.53867700	1.54206900	-2.16778800
H	4.37082200	2.23160500	-2.10671600
C	-0.82157600	2.81168500	-0.21623700
H	-1.81713400	2.43415100	-0.42738200
C	-0.36664700	4.13007500	-0.18131000
H	-0.94232300	5.02819400	-0.34873100
C	0.98111000	4.02810000	0.10402200
H	1.74504500	4.78714700	0.21252500
C	3.29978900	-2.22344900	-0.70099900
H	3.78543700	-3.20168500	-0.78973400
H	3.47304500	-1.65224500	-1.61735700

C	1.55554700	-3.71738300	0.92666500
H	2.10777300	-3.32396800	1.78642700
H	0.55883500	-4.02535000	1.25516600
C	0.91174400	-3.38171700	-1.85699400
H	1.49762700	-4.29577000	-2.00513100
H	-0.14350900	-3.64482900	-1.72638700
B	2.69575000	2.07169800	0.25522300
H	3.56366400	2.89449300	0.32723300
C	-0.86757300	-1.27728200	1.72892500
H	-0.14687600	-1.73039300	2.40433600
C	-1.16319300	0.13122600	1.72955200
H	-0.70416600	0.74302000	2.50472200
C	1.92039600	0.16286500	-2.71690800
H	1.19991400	-0.47619500	-3.21475100
H	2.08460600	-4.60341000	0.55764500
H	3.74094600	-1.67729900	0.14077900
H	0.99313000	-2.75923800	-2.75362900
C	-3.27403900	-0.31676300	0.56817300
C	-2.83919700	-1.70002400	0.19103900
H	-2.85915400	-1.81205600	-0.90460300
H	-3.55407200	-2.46251000	0.54941900
C	-1.51013200	-2.05457800	0.77672000
H	-1.20196200	-3.09285700	0.65108800
C	-2.49648700	0.52366000	1.26203800
H	-2.84458500	1.53843500	1.44974400
S	-4.77232200	0.31041500	-0.15587800
O	-4.96399000	-0.41465800	-1.40802300
O	-4.69029600	1.76915200	-0.11819300
C	-6.06129100	-0.19035500	0.97135300
H	-7.00571600	0.14566700	0.53456100
H	-6.06186400	-1.28015600	1.05917200
H	-5.89772800	0.28934300	1.93913000

### Compound 2B Energies in Gas Phase

Electronic Energy: -2180.88945198 Hartree

Electronic Energy + Free Energy Correction: -2180.473959 Hartree



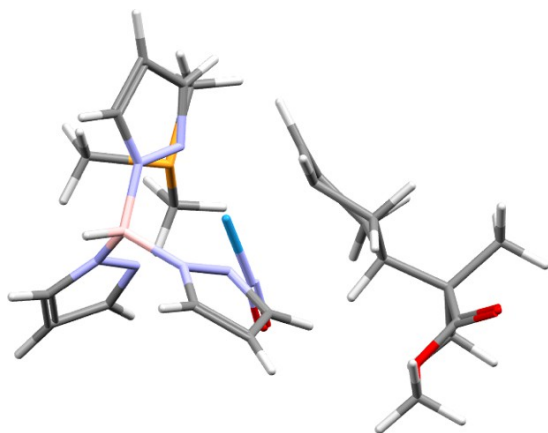
W	-0.30164000	0.14916400	-0.08091700
P	0.14223100	-2.34178000	0.38632900
O	1.62492000	0.78535300	2.08289000
N	-1.85607000	-0.60787300	-1.54821000
N	-3.17062000	-0.38486200	-1.30192900
N	-3.12887700	-0.18392700	1.20707900
N	-1.79748100	-0.26036600	1.45241500
N	-2.92055800	1.85360100	-0.17416000
N	-1.56894200	1.97007900	-0.07003500
N	0.85361200	0.57313400	1.20803500
C	-1.80682600	-1.35039400	-2.66656600
H	-0.85715100	-1.65168900	-3.09088400
C	-3.08802500	-1.61389200	-3.14303200
H	-3.36628600	-2.17709200	-4.02140600
C	-3.92423900	-0.97742000	-2.24294100
H	-5.00302300	-0.89753600	-2.20730000
C	-2.89447700	-0.59443200	3.37830600
H	-3.10632300	-0.77975600	4.42094000
C	-3.80227700	-0.37691100	2.35416900
H	-4.88370100	-0.32897600	2.36370300
C	-1.31159000	3.26350600	0.17306200
H	-0.29445100	3.59841200	0.33549100
C	-2.49206200	4.00025800	0.20439300
H	-2.60631000	5.06130100	0.36918100
C	-3.48609700	3.06330600	-0.01113600
H	-4.56262800	3.16803900	-0.05366100
C	-1.33858000	-3.25968900	0.95307700
H	-1.08699600	-4.31937800	1.07128600
H	-1.71678900	-2.87530000	1.90343100

C	0.68912000	-3.45962000	-0.95956100
H	-0.05295300	-3.47242800	-1.76487600
H	1.66186100	-3.17269300	-1.36589200
C	1.40942600	-2.60283200	1.67451900
H	1.55080800	-3.67474800	1.85248500
H	2.36421900	-2.15812500	1.36546600
B	-3.61862800	0.47223500	-0.11102600
H	-4.81020900	0.59776500	-0.10200900
C	1.23756300	-0.43466700	-1.66133600
H	0.95367000	-1.23595100	-2.33957400
C	0.76704300	0.88971500	-1.98721300
H	-0.03741600	1.05418200	-2.70226300
C	-1.64878400	-0.49396300	2.76546800
H	-0.65816400	-0.57187000	3.19857100
H	0.77453300	-4.47392200	-0.55396800
H	-2.12778500	-3.16261300	0.19756800
H	1.10716500	-2.12475300	2.61122600
C	1.29518900	1.94882000	-1.27862200
H	0.82941000	2.92569000	-1.39980800
C	2.63739500	1.92244300	-0.61907900
H	2.60281700	2.30498400	0.41330600
C	3.23734200	0.55052000	-0.62824200
H	3.27511000	2.64938900	-1.15286200
C	2.58938000	-0.52325300	-1.09355200
H	3.06939200	-1.49841700	-1.00175700
O	4.84487200	-1.12843500	0.56626800
S	4.77167000	0.29565400	0.23846900
C	6.03217000	0.63855600	-0.97647000
H	6.99376400	0.53299200	-0.46672700
H	5.95179200	-0.08350100	-1.79229800
H	5.91578000	1.66429400	-1.33656900
O	4.85104800	1.32306300	1.27058100

**Compound 5E (Proximal Chair) in MeCN**

Electronic Energy: -1940.03549747 Hartree

Electronic Energy + Free Energy Correction: -1939.511278 Hartree



W	0.55399000	-0.30716800	-0.01316400
P	2.17716700	-2.26611000	-0.39013200
O	-1.01219300	-0.79312100	-2.49206700
N	2.02336100	0.27529600	1.62173200
N	2.71587300	1.44033800	1.53387000
N	2.80517800	1.70102600	-0.95883100
N	2.02076700	0.66826400	-1.34938000
N	0.99330200	2.80127600	0.30449700
N	0.05174800	1.85745900	0.05550200
N	-0.43186500	-0.62273300	-1.45705100
C	2.43944400	-0.32408500	2.74802900
H	2.03150900	-1.27979900	3.05331100
C	3.40636900	0.44758100	3.38894800
H	3.92413300	0.22765000	4.31169600
C	3.54902400	1.56161900	2.58041500
H	4.18078900	2.43606500	2.67458900
C	3.27182100	1.31470700	-3.09262900
H	3.70423800	1.37188300	-4.08140600
C	3.56036600	2.10753500	-1.99409200
H	4.23948600	2.94284000	-1.87680300
C	-1.09246200	2.49966900	-0.20199600
H	-1.99039800	1.94428100	-0.45200200
C	-0.90090500	3.87975700	-0.10791900
H	-1.63500600	4.65965600	-0.25531100
C	0.43772000	4.02451300	0.20912700
H	1.04218800	4.90880800	0.36820400
C	3.90774800	-1.72774200	-0.61931700
H	4.55139800	-2.61414100	-0.66283500
H	4.02441100	-1.15620000	-1.54476400
C	2.37996600	-3.52249800	0.92191800
H	2.80671700	-3.06009300	1.81812500

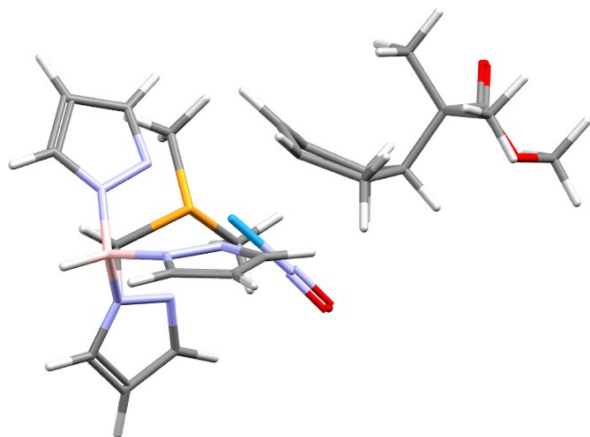
H	1.43660400	-4.01062500	1.18268400
C	1.79000100	-3.25038700	-1.87426900
H	2.53978800	-4.03837700	-2.01186000
H	0.79921900	-3.70529800	-1.75977100
B	2.49234200	2.42194800	0.37419600
H	3.17537600	3.39733100	0.50488900
C	-0.41529000	-1.61234500	1.58902300
H	0.38720300	-1.98257600	2.22368000
C	-0.95193800	-0.27992800	1.65497300
H	-0.56974100	0.34161300	2.46787200
C	2.28811400	0.43514800	-2.64157700
H	1.77078200	-0.35408000	-3.17503200
H	3.07803600	-4.28445800	0.55490300
H	4.21320200	-1.10313700	0.22883400
H	1.77728800	-2.60502200	-2.75912900
C	-2.91984800	-0.87313000	0.15900600
H	-2.58619000	-0.27450800	-0.69520100
C	-2.27858300	-2.25812500	-0.00232000
H	-2.26605300	-2.55574900	-1.06014200
H	-2.87323500	-3.03869600	0.50415600
C	-2.43997400	-0.14693000	1.41546100
H	-2.71596500	0.91614000	1.35861500
C	-0.92203200	-2.43166400	0.59189000
H	-0.45213900	-3.39785300	0.40356800
C	-5.15689700	-1.74196700	1.10533900
H	-4.92496400	-1.39912100	2.11903600
H	-6.24458100	-1.68585300	0.98264100
H	-4.87106100	-2.79634000	1.02105500
C	-4.46736900	-0.90527800	0.03313600
C	-4.86988900	-1.42606300	-1.35210000
H	-5.94232400	-1.27370700	-1.52768400
H	-4.31532800	-0.92261900	-2.15257100
H	-4.67689500	-2.50281000	-1.42420200
C	-4.94596900	0.53501200	0.17067800
O	-5.68103500	0.95477800	1.03650300
O	-4.43430500	1.32508100	-0.78920800
C	-4.75596500	2.71304700	-0.68069100
H	-4.24037200	3.20980300	-1.50483200
H	-5.83555300	2.87105200	-0.76499900
H	-4.41049600	3.11567800	0.27843800
H	-2.95555400	-0.54049700	2.30701300



### Compound 5E (Proximal Boat) in MeCN

Electronic Energy: -1940.02794219 Hartree

Electronic Energy + Free Energy Correction: -1939.505976 Hartree



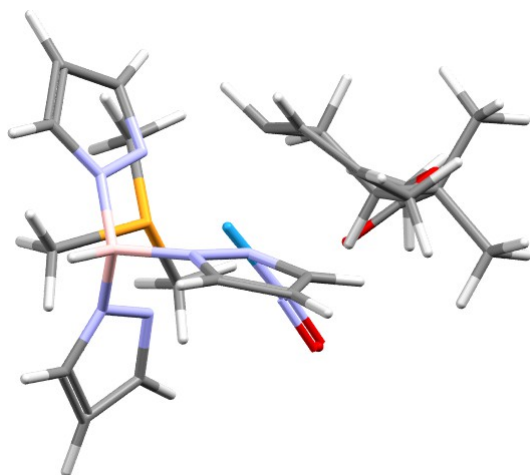
W	0.58991100	-0.02005300	-0.11813200
P	0.87727300	-2.57012200	0.05895200
O	-0.82070000	-0.10811100	-2.72654200
N	1.98053000	-0.04159200	1.69361700
N	3.25043200	0.42864000	1.57316500
N	3.64984200	0.15922200	-0.89791100
N	2.43078700	-0.27298700	-1.29781100
N	2.76068900	2.28633700	-0.03264600
N	1.45009000	2.05236200	-0.30282900
N	-0.28140700	-0.05930700	-1.65625100
C	1.89307700	-0.56539600	2.92683400
H	0.97304200	-1.01682200	3.27718400
C	3.10240800	-0.43754900	3.60597600
H	3.33389900	-0.75798300	4.61171500
C	3.93594000	0.20260100	2.70534800
H	4.96762000	0.52088600	2.78950600
C	3.91751100	-0.74135600	-2.90712900
H	4.35627300	-1.09693900	-3.82852300
C	4.55623500	-0.10676600	-1.85394700
H	5.58968100	0.18847200	-1.72106900
C	0.92138200	3.22181700	-0.68280900
H	-0.12479400	3.29306300	-0.95147400
C	1.88904700	4.22544100	-0.65770300
H	1.76469500	5.26925300	-0.90890200
C	3.04192100	3.58457400	-0.24114300
H	4.04692200	3.95423300	-0.07972200
C	2.59712900	-3.12777300	-0.20900100
H	2.64953100	-4.19768200	0.02548900
H	2.91346900	-2.97515600	-1.24409700
C	0.54848600	-3.40951600	1.65339300

H	1.37527600	-3.19857600	2.33966800
H	-0.38942300	-3.11216700	2.12966700
C	-0.09089400	-3.50723300	-1.16741900
H	0.22128500	-4.55814000	-1.16208800
H	-1.15836300	-3.44854800	-0.92957100
B	3.73454800	1.13473400	0.29700700
H	4.85207100	1.54326200	0.43769900
C	-1.10324600	-0.01130700	1.46137900
H	-0.62075600	-0.25345100	2.40535800
C	-1.01323700	1.27929500	0.88279300
H	-0.55349200	2.04974000	1.50295500
C	2.58130300	-0.81116400	-2.51601700
H	1.72936400	-1.23374900	-3.03702700
H	0.52267400	-4.48938600	1.46356200
H	3.27194500	-2.58234500	0.46175300
H	0.07132600	-3.08481600	-2.16534200
C	-3.24408600	0.73203800	-0.31858900
H	-3.61381700	0.92707100	-1.33317400
C	-2.75316500	-0.73230700	-0.30596900
H	-2.45207000	-1.03769200	-1.31647900
H	-3.57846200	-1.41708600	-0.05535500
C	-2.11018300	1.74664000	-0.06415200
H	-1.69020300	2.03135500	-1.03643700
C	-1.68076900	-1.01764700	0.69923100
H	-1.63178200	-2.04010400	1.06552800
C	-4.48073600	0.94802600	0.60565900
C	-4.16963400	0.79459900	2.08947100
H	-5.07267900	0.97302300	2.68461600
H	-3.80848900	-0.20980700	2.33769200
H	-3.41393300	1.52541600	2.40023900
C	-5.10596400	2.33011400	0.36585700
H	-6.08634200	2.39419900	0.85549300
H	-4.48163400	3.12230300	0.79372500
H	-5.24384400	2.53457200	-0.70162800
C	-5.54673300	-0.07573600	0.23013000
O	-6.07077400	-0.85970700	0.99178600
O	-5.86515600	-0.00695700	-1.07049200
C	-6.85314200	-0.93752800	-1.51472400
H	-6.98857600	-0.75067900	-2.58110700
H	-6.51543500	-1.96672800	-1.35482400
H	-7.79839300	-0.78562900	-0.98457600
H	-2.53144100	2.67501500	0.34384900

**Compound 5F (Distal Chair) in MeCN**

Electronic Energy: -1940.03648027 Hartree

Electronic Energy + Free Energy Correction: -1939.513931 Hartree



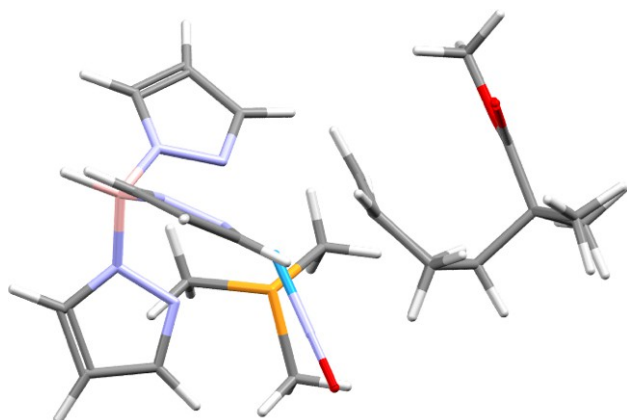
W	0.61429800	0.19334600	0.04416000
P	-0.06515500	-2.26739200	-0.17526400
O	-0.96857600	0.99839300	-2.33673300
N	2.08689800	-0.59809800	1.59276200
N	3.42152400	-0.52374300	1.35686000
N	3.43027400	-0.54195200	-1.15398400
N	2.09952000	-0.52735000	-1.41476000
N	3.41822100	1.62032500	0.03921000
N	2.08587600	1.86434000	-0.08762900
N	-0.38150900	0.68637400	-1.33892400
C	1.94877500	-1.24311600	2.76153300
H	0.96822200	-1.42519300	3.18339600
C	3.19358700	-1.59236800	3.28143300
H	3.40193700	-2.11438800	4.20449500
C	4.10172200	-1.11320500	2.35383900
H	5.18397300	-1.14359400	2.33131500
C	3.18468500	-1.17994700	-3.26481700
H	3.38824600	-1.51096700	-4.27322300
C	4.09840000	-0.92607700	-2.25471500
H	5.18013400	-0.97702300	-2.24333200
C	1.96080700	3.15190400	-0.43728500
H	0.98264900	3.57885300	-0.62424600
C	3.21318800	3.75789900	-0.52032100
H	3.43483600	4.78608600	-0.76861400
C	4.10725000	2.74607300	-0.21842300
H	5.18933700	2.74108900	-0.17415500
C	1.33637200	-3.37675100	-0.57238800
H	0.97922100	-4.41309200	-0.56243900
H	1.76357200	-3.15843100	-1.55473700

C	-0.79082600	-3.18767600	1.22760900
H	-0.09123900	-3.21010000	2.06996400
H	-1.74085300	-2.75771600	1.55485200
C	-1.27739900	-2.53484400	-1.50929500
H	-1.47431800	-3.60789700	-1.62128600
H	-2.21474700	-2.01562000	-1.26963000
B	3.96932100	0.17392500	0.10830400
H	5.16731700	0.17856200	0.11255200
C	-0.97047700	-0.09184000	1.65477600
H	-0.70528800	-0.85080600	2.38966800
C	-0.35260600	1.19096300	1.86162800
H	0.48521900	1.34459300	2.54192300
C	1.94489700	-0.90243000	-2.69258500
H	0.95556400	-0.96959000	-3.12965800
H	-0.96807900	-4.21678700	0.89332200
H	2.11637200	-3.26134200	0.19074400
H	-0.89175300	-2.13913700	-2.45442400
C	-0.78167900	2.22662000	1.05631600
H	-0.23044400	3.16559300	1.08683000
C	-2.12180800	2.27677400	0.40313900
H	-2.03821300	2.76799800	-0.57664900
C	-2.45966400	-0.05611500	1.35958000
H	-2.82614700	-1.05262200	1.07925000
H	-2.95979400	0.19796700	2.30861700
C	-2.85860200	0.93711800	0.27059900
H	-2.55643400	0.49542100	-0.68338000
C	-4.39057000	1.10602400	0.14368500
C	-5.06233300	1.58789600	1.42811600
H	-6.10929500	1.84966700	1.24390400
H	-5.04616200	0.82954400	2.21853100
H	-4.56038200	2.48582900	1.80838700
C	-4.71262600	2.08650700	-0.99736600
H	-4.44127200	3.10985800	-0.71376500
H	-4.16656700	1.82216400	-1.91261700
H	-5.78658300	2.08032900	-1.22040100
C	-4.96924900	-0.22508500	-0.32692200
O	-4.39124000	-1.02342300	-1.03693100
O	-6.23662100	-0.39633500	0.06117000
C	-6.87910400	-1.57823200	-0.42255700
H	-6.35640500	-2.47387100	-0.07332700
H	-7.89332700	-1.55653900	-0.02128100
H	-6.90811300	-1.58417200	-1.51646100
H	-2.68908900	2.99005500	1.02724100

**Compound 5F (Distal Boat) in MeCN**

Electronic Energy: -1940.03372083 Hartree

Electronic Energy + Free Energy Correction: -1939.508794 Hartree



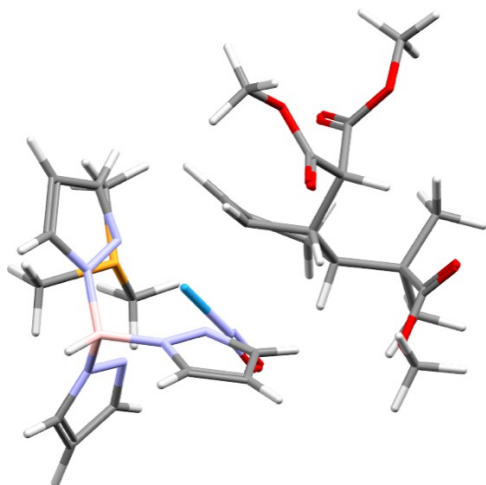
W	0.51805700	0.01024100	-0.35884300
P	0.73147700	-2.54506400	-0.15211700
O	-0.12614300	-0.24963600	-3.24687300
N	1.18369800	-0.04458800	1.80906600
N	2.39001000	0.46303700	2.16383500
N	3.63133900	0.16048000	-0.00144800
N	2.64609700	-0.30368200	-0.81091500
N	2.49882400	2.30612600	0.44728500
N	1.39047200	2.05960500	-0.30306600
N	0.13237200	-0.11294900	-2.08324000
C	0.65333800	-0.57484500	2.92097600
H	-0.32325500	-1.04420000	2.89706000
C	1.52019000	-0.41480800	4.00088100
H	1.37073900	-0.73348000	5.02265600
C	2.61221500	0.25181300	3.47192700
H	3.53009700	0.59628100	3.93173700
C	4.62451400	-0.73725900	-1.77190100
H	5.37323400	-1.08082900	-2.47132600
C	4.82592300	-0.08641200	-0.56547700
H	5.73547100	0.23379600	-0.07242300
C	1.14314700	3.17356800	-1.00570700
H	0.31183300	3.21043800	-1.69988600
C	2.08145700	4.15845300	-0.70221700
H	2.13781300	5.16246400	-1.09808400
C	2.92526400	3.56079200	0.21716100
H	3.80672200	3.93475100	0.72318500
C	2.33611100	-3.06310000	0.55719000
H	2.33138300	-4.15252900	0.67899900
H	3.16861900	-2.78293500	-0.09470200
C	-0.42446000	-3.51664600	0.87604600

H	-0.40221900	-3.17132700	1.91508200
H	-1.44682700	-3.45226200	0.49172000
C	0.63756700	-3.42144900	-1.74961800
H	0.81206100	-4.49152000	-1.58562800
H	-0.35865700	-3.28401900	-2.18481100
B	3.28435600	1.15859700	1.13214500
H	4.28197700	1.57782800	1.64578900
C	-1.53944100	-0.66624900	0.36496100
H	-1.53751500	-1.27543100	1.26726600
C	-1.43713400	0.74472900	0.59084100
H	-1.10939700	1.15610900	1.54517600
C	3.23965500	-0.83671700	-1.88824600
H	2.64289400	-1.26517900	-2.68482500
H	-0.10191300	-4.56406900	0.84547900
H	2.47486500	-2.59540900	1.53924100
H	1.38550600	-3.04171000	-2.45212500
C	-2.49699400	1.19841300	-1.64159000
H	-1.91460400	1.03374100	-2.55926800
C	-3.35405100	-0.04762900	-1.35608500
H	-3.70319400	-0.42028400	-2.33102000
C	-2.48231500	-1.15524900	-0.73660700
H	-1.92116200	-1.63022100	-1.55188300
H	-3.11629900	-1.94771800	-0.32207200
C	-1.62250500	1.58229300	-0.49131400
H	-1.35163400	2.63093700	-0.38636500
C	-4.69491600	0.24187200	-0.59441600
C	-5.57593900	-1.01089700	-0.62480900
H	-5.11216300	-1.88490000	-0.16123600
H	-6.52131900	-0.82448500	-0.10090100
H	-5.81416700	-1.25927400	-1.66696700
C	-5.47133700	1.35728700	-1.29643600
H	-5.00678000	2.33897600	-1.17522100
H	-5.55833300	1.13588500	-2.36770000
H	-6.48504900	1.42658700	-0.88333500
C	-4.43377300	0.68249000	0.83874400
O	-4.34959400	1.83516300	1.20749900
O	-4.29393700	-0.35629900	1.67489800
C	-3.97585300	-0.02695900	3.02634300
H	-3.87237700	-0.97685700	3.55393000
H	-3.03783500	0.53665300	3.08173400
H	-4.77414000	0.56838100	3.48053300
H	-3.12082300	2.07000300	-1.87308200

**Compound 7B (Proximal Chair) in MeCN**

Electronic Energy: -2434.83460798 Hartree

Electronic Energy + Free Energy Correction: -2434.208128 Hartree



W	-1.19116500	-0.11214000	-0.41120800
P	-2.59214500	0.98134200	-2.27062800
O	-0.56114500	-2.57094400	-1.95779200
N	-2.02069100	1.58758800	0.85770300
N	-2.84494000	1.31614900	1.90274000
N	-3.86846900	-0.83248700	1.10626000
N	-3.15735400	-1.04857000	-0.02628600
N	-1.87664000	-0.90832900	2.56226300
N	-0.98550000	-1.11422100	1.56084000
N	-0.76038200	-1.56086800	-1.34425400
C	-1.90462700	2.92418300	0.81069000
H	-1.28962100	3.40605400	0.06079500
C	-2.65689400	3.52060200	1.82025000
H	-2.75987800	4.57500500	2.03358700
C	-3.23700500	2.45799600	2.49075000
H	-3.89752800	2.42990500	3.34846900
C	-5.02573500	-2.28309100	-0.10904400
H	-5.79136900	-2.96594000	-0.44882100
C	-4.99201000	-1.57014800	1.07802200
H	-5.68002800	-1.54470000	1.91400100
C	-0.10964500	-2.02727100	1.99403700
H	0.68702400	-2.37604000	1.34537500
C	-0.42063200	-2.41077000	3.30013900
H	0.10194000	-3.12444100	3.92162000
C	-1.55243800	-1.68117600	3.61631300
H	-2.16026200	-1.65935500	4.51223600
C	-4.32798900	1.26599900	-1.77843400
H	-4.83521400	1.82252300	-2.57526300
H	-4.85204300	0.31968100	-1.61457600

C	-2.12433800	2.64262300	-2.87074800
H	-2.20831900	3.37120200	-2.05770200
H	-1.10746500	2.66850400	-3.27297000
C	-2.69091000	-0.01233900	-3.79481400
H	-3.33044800	0.48991500	-4.53014500
H	-1.68567100	-0.13980600	-4.21272100
B	-3.18723200	-0.12600300	2.30274000
H	-3.89434600	-0.14276300	3.26949600
C	0.43556800	1.37954300	-0.97638600
H	-0.01486700	2.36849200	-1.01580800
C	0.79308100	0.69861800	0.23850800
H	0.61421200	1.26352800	1.15748300
C	-3.84424200	-1.93330800	-0.76184600
H	-3.46167300	-2.26440500	-1.72044000
H	-2.82249000	2.92411600	-3.66805500
H	-4.35540100	1.85579800	-0.85419900
H	-3.10511900	-1.00142600	-3.57400800
C	2.18161500	-1.01811300	-0.99183700
H	1.45221000	-1.80195100	-0.76228900
C	1.68241900	-0.37978300	-2.29496200
H	1.32010100	-1.16014700	-2.97843300
H	2.49422300	0.13000000	-2.83866800
C	2.08495900	-0.10368000	0.25183200
H	2.04047700	-0.77429300	1.12412600
C	0.65478300	0.68666700	-2.15476000
H	0.27166700	1.09112800	-3.09239300
C	3.29906700	0.80273500	0.60859700
H	4.13520700	0.15144000	0.89765800
C	4.70425600	-1.03570300	-1.70260700
H	5.08509100	-0.29133400	-0.99948700
H	5.53279400	-1.72652200	-1.89960800
H	4.46601600	-0.53668300	-2.64864200
C	3.81387700	1.74152600	-0.45969000
C	2.94226800	1.55527800	1.87685500
O	2.75575800	1.01151800	2.94106800
O	3.23106600	2.10503000	-1.45551600
O	2.79620200	2.86419700	1.66539500
C	2.35029500	3.62914000	2.79125200
H	2.31060900	4.66549900	2.45463200
H	1.35515600	3.29629200	3.10534800
H	3.04757100	3.52937000	3.62771700
O	5.06113100	2.11927100	-0.15684900
C	5.68820600	2.98638400	-1.10510900
H	5.12597900	3.91915300	-1.21005500
H	6.68592200	3.19074000	-0.71481000
H	5.75986700	2.49551700	-2.08162400
C	3.50280400	-1.82497100	-1.18436400
C	3.24331600	-2.97524200	-2.17073000

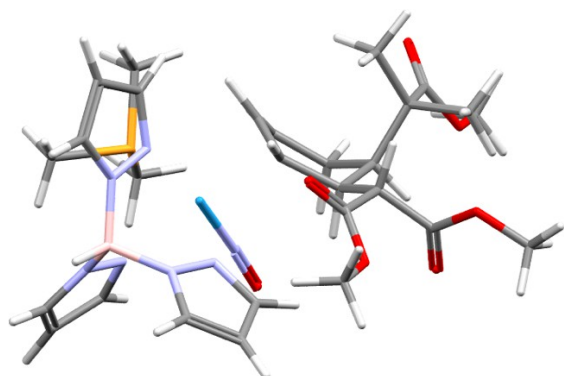


H	4.08522000	-3.67862300	-2.16537200
H	2.33096000	-3.52989900	-1.92731100
H	3.15065600	-2.58570100	-3.19099500
C	3.85847800	-2.42590700	0.17020000
O	4.84605800	-2.15955300	0.82135900
O	2.92507800	-3.29077700	0.59435500
C	3.12476600	-3.82185300	1.90768500
H	2.29387500	-4.50644500	2.08710100
H	4.07444100	-4.36115600	1.96875100
H	3.11995000	-3.01641500	2.65127500

**Compound 7B (Proximal Boat) in MeCN**

Electronic Energy: -2434.82417555 Hartree

Electronic Energy + Free Energy Correction: -2434.197932 Hartree



W	1.19150400	-0.43069100	-0.22332800
P	2.46545800	-2.64532300	0.09742000
O	0.15915500	-0.86636000	-2.97257900
N	2.22907000	0.13795700	1.72040000
N	3.14858000	1.13799900	1.72724700
N	3.99111300	0.97653000	-0.63592600
N	3.13488200	0.06415400	-1.15395600
N	2.18671300	2.56438400	-0.11406000
N	1.16662400	1.77672800	-0.54142900
N	0.55198200	-0.73051100	-1.84819500
C	2.19269600	-0.34361300	2.97296100
H	1.53263600	-1.15982500	3.23913700
C	3.08926100	0.33963200	3.79128800
H	3.28015700	0.17844000	4.84262800
C	3.67471200	1.27397400	2.95526500
H	4.42632000	2.03014900	3.14433800
C	4.91635300	0.21661800	-2.50395400
H	5.59998700	0.05400000	-3.32502100
C	5.06514500	1.08791100	-1.43732000
H	5.85224200	1.79166800	-1.19670900
C	0.39349100	2.53141300	-1.33018600
H	-0.49419100	2.12177500	-1.79905900
C	0.90899000	3.82645100	-1.41662900
H	0.49858700	4.66339100	-1.96440300
C	2.04897600	3.79922300	-0.63584900
H	2.78208000	4.56519200	-0.41583900
C	4.25702300	-2.40200500	0.35793200
H	4.71080200	-3.37259100	0.59057900
H	4.73577800	-1.98929500	-0.53478300
C	2.06202300	-3.70024200	1.53459200
H	2.31253100	-3.17137000	2.46020500
H	1.01005400	-3.99657300	1.56548100

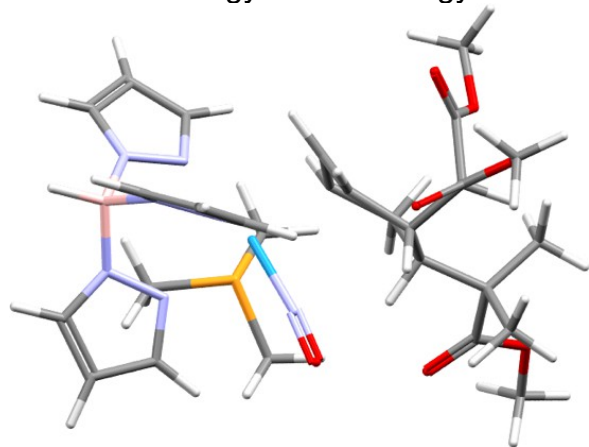
C	2.35033400	-3.77668100	-1.32584800
H	2.94437400	-4.67889600	-1.13874100
H	1.30286400	-4.05520400	-1.48649400
B	3.47973000	1.94050500	0.46441200
H	4.29425500	2.78652000	0.70024500
C	-0.41861900	-1.30256000	1.13298300
H	0.08872700	-1.61799200	2.04158600
C	-0.73528100	0.06406000	0.85083000
H	-0.53818300	0.76547900	1.66073700
C	3.68043300	-0.39296800	-2.28918600
H	3.16531800	-1.14036200	-2.88213000
H	2.67831700	-4.60492600	1.47067800
H	4.41791400	-1.72019300	1.20158100
H	2.72342000	-3.27992800	-2.22775700
C	-2.83023300	-0.88797400	-0.29514600
H	-3.45590700	-0.63823300	-1.16084200
C	-1.86583200	-1.99311600	-0.78496700
H	-1.53158900	-1.75427200	-1.80418900
H	-2.37724900	-2.95693600	-0.90595100
C	-1.96262400	0.37537500	-0.01269000
H	-1.63541100	0.67174300	-1.01909300
C	-0.72419900	-2.23236800	0.15075800
H	-0.35124100	-3.25242900	0.22685000
C	-2.75213700	1.59632700	0.51566300
H	-3.22851800	1.34938000	1.47236500
C	-3.84514100	-1.39903500	0.79211300
C	-3.29749800	-1.53916700	2.21055300
H	-4.10666900	-1.84896900	2.88314400
H	-2.51051500	-2.29435700	2.28513500
H	-2.90517700	-0.58577800	2.58080100
C	-5.12167600	-0.53889800	0.85030400
H	-5.91328000	-1.09244300	1.37203700
H	-4.96757100	0.38472600	1.41427400
H	-5.49822800	-0.28900600	-0.14797600
C	-1.90112100	2.81356300	0.87157400
C	-3.82390800	2.01932700	-0.47205100
C	-4.31275800	-2.78094600	0.33985700
O	-1.16471600	2.87267600	1.83014200
O	-3.77817000	1.83953700	-1.66805100
O	-4.13653400	-3.81751900	0.94169300
O	-2.12135500	3.83871400	0.04588300
O	-4.82710900	2.63617100	0.15410600
O	-4.96082000	-2.72296600	-0.83232100
C	-5.39315300	-3.97741500	-1.36119100
H	-5.89236700	-3.75316100	-2.30499800
H	-4.53751900	-4.63823400	-1.53821800
H	-6.08926600	-4.47055500	-0.67597500

C	-5.88166000	3.10926700	-0.68820100
H	-6.35142000	2.27637000	-1.22129300
H	-6.60579100	3.58681400	-0.02715300
H	-5.49926900	3.83291900	-1.41445300
C	-1.52291800	5.08400500	0.42467700
H	-0.44006100	4.97876600	0.53392600
H	-1.75531100	5.78514600	-0.37794100
H	-1.95387300	5.43381500	1.36785600

### Compound 7C (Distal Chair) Energies in MeCN

Electronic Energy: -2434.83185845 Hartree

Electronic Energy + Free Energy Correction: -2434.205988 Hartree



W	-1.11676900	0.07744900	-0.07071100
P	-1.63319100	2.51342900	0.56764800
O	0.17411400	0.90708700	-2.61218000
N	-2.52929700	-0.39415200	1.64313400
N	-3.71769100	-1.00371400	1.40615500
N	-4.12875500	-0.22984800	-0.94376700
N	-2.97296200	0.43138200	-1.20005800
N	-3.00796100	-2.39305900	-0.57143700
N	-1.73488600	-1.95443400	-0.76667800
N	-0.26926600	0.57088200	-1.55369200
C	-2.49487900	-0.13348700	2.95930300
H	-1.63380800	0.34818600	3.40668500
C	-3.66543600	-0.56983900	3.57627600
H	-3.92660400	-0.50165000	4.62269100
C	-4.41384100	-1.11813400	2.54893500
H	-5.39012600	-1.58654200	2.54740700
C	-4.50492300	1.05549300	-2.71284100
H	-4.98310200	1.54806500	-3.54741700
C	-5.05858400	0.12789100	-1.84488200
H	-6.04610800	-0.31538800	-1.81176900
C	-1.12889300	-2.86088800	-1.54770600
H	-0.09721600	-2.72591000	-1.85459400
C	-2.00301500	-3.90352100	-1.84912700
H	-1.80136400	-4.78265300	-2.44450100
C	-3.18402900	-3.56043800	-1.21547300
H	-4.14400500	-4.06031100	-1.17850900
C	-3.43125000	2.84720400	0.64997500
H	-3.57858300	3.87884600	0.99033500
H	-3.91085700	2.72297000	-0.32476400
C	-1.10755200	3.23101500	2.16391000

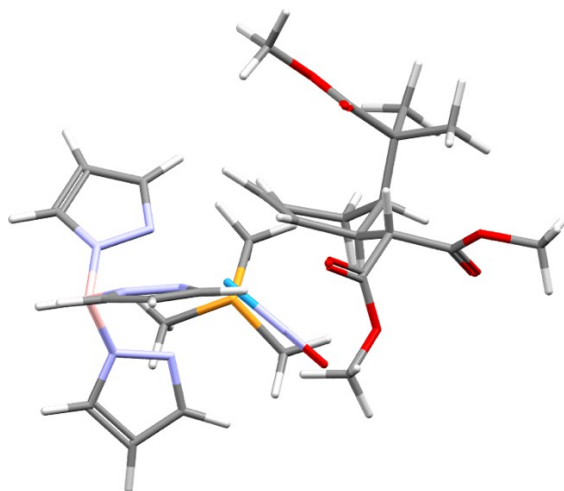
H	-1.51969800	2.65431700	2.99851300
H	-0.01847500	3.27324600	2.25156100
C	-0.98864800	3.71433000	-0.64061200
H	-1.23965400	4.73073200	-0.31416900
H	0.10064000	3.61195900	-0.72277300
B	-4.10561800	-1.45929600	-0.00400700
H	-5.16937400	-2.00991000	0.00173000
C	0.46769900	0.61535900	1.57435400
H	0.03118100	0.98674400	2.50012900
C	0.41550900	-0.79309700	1.38372400
H	-0.18613000	-1.45236900	2.00960900
C	-3.19042300	1.20200700	-2.27580700
H	-2.39777700	1.82548100	-2.67243200
H	-1.50317000	4.25230300	2.21399800
H	-3.89905300	2.16471800	1.37003200
H	-1.43284300	3.53924600	-1.62577400
C	0.96782400	-1.27633000	0.20472700
H	0.80323700	-2.32346900	-0.03584100
C	2.21714000	-0.67722600	-0.40436600
H	2.16763900	-0.81106300	-1.49461900
C	1.75294300	1.31659800	1.18056600
H	1.59475300	2.40309100	1.12141800
H	2.45943400	1.15449400	2.00849000
C	2.34313100	0.84706800	-0.14915100
H	1.68560900	1.27215400	-0.90843600
C	3.36957600	-1.63189700	0.03855900
H	4.33828300	-1.13851300	-0.08809700
C	3.69092000	1.53768500	-0.48979300
C	4.78393700	1.42486800	0.57378700
H	5.70924600	1.88815500	0.21761900
H	4.49997100	1.92802500	1.50522900
H	5.00835300	0.38515600	0.82221600
C	3.25325800	-2.06165100	1.48889500
C	3.40038500	-2.88172100	-0.82203700
O	2.87388700	-3.15045900	1.85672800
O	2.51236300	-3.25842500	-1.55458100
O	4.56056900	-3.51497800	-0.67011000
O	3.57662000	-1.06263600	2.30761100
C	3.34561100	-1.29175200	3.70228800
H	3.61721600	-0.36342600	4.20709800
H	2.29055600	-1.52447800	3.88011200
H	3.96623300	-2.11519500	4.06709200
C	4.70254700	-4.73878000	-1.40048300
H	4.63118000	-4.55454800	-2.47648200
H	5.69115000	-5.12518700	-1.15050700
H	3.93101000	-5.45485900	-1.10277700
C	4.21607200	1.05012500	-1.85321800
H	4.57799100	0.01675100	-1.80771200

H	3.43033300	1.10669200	-2.61744600
H	5.05803400	1.67260400	-2.18062100
C	3.36389500	3.01372400	-0.75678700
O	2.33749800	3.41460500	-1.26737400
O	4.37440900	3.82947900	-0.44810800
C	4.17753300	5.20930400	-0.76776300
H	3.31568900	5.61252900	-0.22767500
H	5.08827900	5.72345400	-0.45748700
H	4.01975300	5.33911400	-1.84268300

**Compound 7C (Distal Boat) in MeCN**

Electronic Energy: -2434.83233371 Hartree

Electronic Energy + Free Energy Correction: -2434.203519 Hartree



W	-1.13571500	-0.05734600	-0.25208000
P	-2.11602100	1.32419000	-2.18589900
O	0.33092600	-1.74015200	-2.21182200
N	-2.51391600	1.26146200	0.99372700
N	-3.60318000	0.72079900	1.59536300
N	-4.00581300	-1.27398300	0.11662500
N	-2.95608300	-1.18238800	-0.73717800
N	-2.58617100	-1.51372300	2.12079000
N	-1.37974400	-1.42917400	1.49462000
N	-0.23998100	-1.08001300	-1.39002600
C	-2.56565400	2.58022400	1.23666100
H	-1.79189500	3.24241700	0.86789700
C	-3.69332600	2.89660700	1.99180000
H	-4.00184300	3.87073100	2.34360500
C	-4.32276400	1.68132300	2.19857200
H	-5.22740300	1.42755300	2.73708500
C	-4.49125200	-2.54732200	-1.63453500
H	-4.99829500	-3.21694600	-2.31448600
C	-4.93462100	-2.09381600	-0.40237400
H	-5.84046000	-2.30811300	0.15117600
C	-0.58757100	-2.34843500	2.06536500
H	0.43333300	-2.48833500	1.73110200
C	-1.27116700	-3.02449800	3.07353000
H	-0.89526700	-3.80965300	3.71393600
C	-2.53653800	-2.46558400	3.06822600
H	-3.41274700	-2.67890700	3.66789700
C	-3.94452500	1.35216200	-2.17864500
H	-4.28599800	2.00601400	-2.98965200



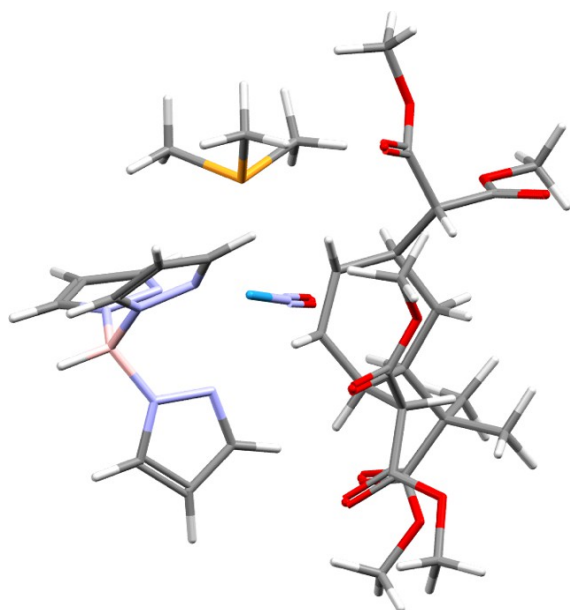
H	-4.36190400	0.35250000	-2.32920200
C	-1.75468800	3.10617000	-2.35658800
H	-2.05424300	3.65222900	-1.45597000
H	-0.69232200	3.27850800	-2.55268600
C	-1.67322400	0.68875800	-3.83658700
H	-2.16948800	1.29710300	-4.60208200
H	-0.58839800	0.75431300	-3.97573500
B	-3.84388900	-0.79221300	1.57732600
H	-4.80930700	-1.07859900	2.22599500
C	0.22559800	1.78005600	-0.38100300
H	-0.29159500	2.73378800	-0.29388600
C	0.49044400	1.11061800	0.85626200
H	-0.00485500	1.37701900	1.79023800
C	-3.23925700	-1.95848800	-1.79429100
H	-2.53454900	-2.04779800	-2.61261800
H	-2.33441900	3.48413400	-3.20701300
H	-4.30280000	1.75265200	-1.22276400
H	-1.98402900	-0.35359400	-3.95392400
C	2.38320700	-0.13781600	-0.25721200
H	2.01402800	-0.72725700	-1.10874000
C	2.68771700	1.25281500	-0.87805900
H	3.32303900	1.07075100	-1.75428800
C	1.33880300	1.74777100	-1.42888000
H	1.07943200	1.09035800	-2.27039100
H	1.44876200	2.74469200	-1.86719500
C	1.31580800	0.00326800	0.80654800
H	1.39620800	-0.61305900	1.70085200
C	3.55353400	-0.98239100	0.28713800
C	3.01626400	-2.35238800	0.66534500
O	2.76764500	-2.70591900	1.79758700
O	2.79624000	-3.09041100	-0.41982100
C	2.17241200	-4.36339100	-0.21287900
H	1.15951300	-4.23050300	0.18143300
H	2.13044300	-4.83878500	-1.19316400
H	2.75844000	-4.97327000	0.48026200
C	3.50780500	2.29511000	-0.03111900
H	3.96568400	-0.54650900	1.20280700
C	4.65742700	-1.16723700	-0.73498100
O	4.57122000	-0.96083200	-1.92283800
O	5.75685000	-1.62349200	-0.13017300
C	6.88870500	-1.82890900	-0.98342900
H	7.18446600	-0.88529700	-1.45339500
H	7.68916800	-2.19542100	-0.34002200
H	6.65996600	-2.56477600	-1.75975100
C	3.38831000	3.68638400	-0.65664300
H	2.38004200	4.10381600	-0.59289200
H	4.06676900	4.38367800	-0.15094800
H	3.68107200	3.64064900	-1.71345400

C	5.00070300	1.92963100	-0.06453300
H	5.22970400	0.98082700	0.42606200
H	5.35070000	1.88435000	-1.10289300
H	5.58508800	2.70004900	0.45342000
C	3.10518200	2.32048000	1.44007200
O	3.48864600	1.51477200	2.26566200
O	2.29753000	3.33759100	1.75473300
C	1.88837300	3.40500000	3.12278000
H	1.18372700	4.23564500	3.18625000
H	1.40387500	2.47332700	3.43241200
H	2.74856400	3.59160200	3.77316700

### Compound 8 in Gas Phase

Electronic Energy: -2930.38960927 Hartree

Electronic Energy + Free Energy Correction: -2929.651543 Hartree



O	-0.57394300	0.20567200	-3.17817100
N	-0.82100200	-2.63317000	-0.31806700
N	-1.63648400	-3.53123200	0.29695900
N	-2.20621700	-0.92574300	1.70245500
N	-2.89545100	-2.07407500	1.91627300
N	-3.17684600	-1.52883700	-1.11777000
N	-3.77661200	-2.51915500	-0.41408900
N	-0.85866800	-0.07379400	-2.02616300
C	-1.15897700	-4.77857400	0.11209700
C	-0.00397300	-4.70238900	-0.64228500
C	0.15833200	-3.33602600	-0.89508400
C	-3.25170300	-2.16345500	3.21030800
C	-2.78739200	-1.04031000	3.87243600
C	-2.13554500	-0.30028700	2.88409000
C	-4.78835700	-3.03850600	-1.13764100
C	-4.86009400	-2.36422500	-2.34395200
C	-3.81671600	-1.43546800	-2.28609200
B	-3.04333300	-3.12638500	0.80587000
H	-3.63415800	-4.08721800	1.21787500
H	-1.68542900	-5.62865800	0.52842600
H	0.62880600	-5.51552700	-0.97039600
H	0.92232200	-2.83832500	-1.48343600
H	-3.80548800	-3.02361800	3.56591000
H	-2.90167900	-0.79414200	4.91873200
H	-1.62399000	0.65223600	2.96994500

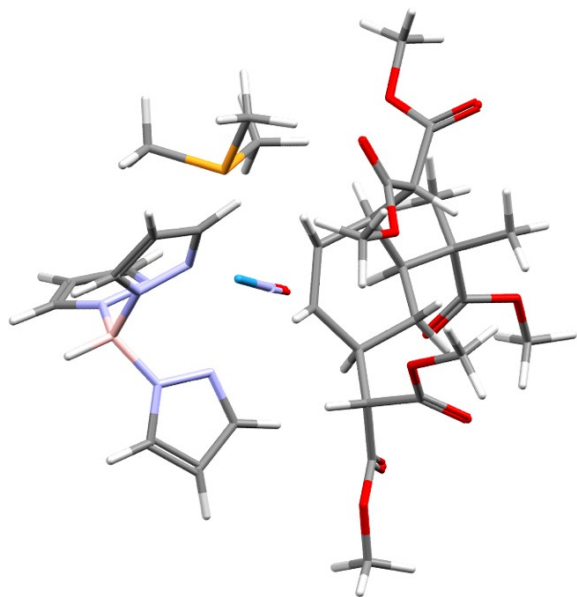
H	-5.37429100	-3.86028200	-0.74443500
H	-5.56092400	-2.52598800	-3.15101000
H	-3.50206400	-0.69626700	-3.01580200
C	-4.72954400	1.11236200	-0.69346700
H	-5.35411700	1.98741300	-0.47578900
H	-4.84890500	0.84857800	-1.74786900
H	-5.06495900	0.26972300	-0.07534100
C	-2.66386100	2.86899900	-1.48778100
H	-2.60539800	2.43683900	-2.49447200
H	-3.48413300	3.59752900	-1.45584300
H	-1.72208100	3.38536800	-1.27552800
W	-1.36295800	-0.44059100	-0.37343600
P	-2.97990300	1.51505000	-0.29909800
C	-3.27652000	2.35795100	1.29926900
H	-3.94344400	3.21279100	1.13045800
H	-3.78449300	1.65643300	1.97108400
H	-2.35532000	2.69884200	1.77910300
C	2.11805000	1.67111800	-0.82945500
C	0.73065900	2.12964700	-0.32458700
C	0.00638700	1.10113900	0.55471500
C	0.54803000	-0.23895400	0.67252000
C	1.92194400	-0.61214000	0.14072800
C	2.22123800	0.18654900	-1.13665500
H	-0.39550000	1.53349300	1.47560900
H	0.35904200	-0.72055200	1.63912400
H	1.40685800	-0.07100000	-1.82421600
H	2.37578100	2.26059300	-1.71978900
H	1.90576300	-1.68273600	-0.10143600
C	3.02828600	-0.48220800	1.24586600
C	3.73658300	-1.80075300	1.48618600
O	3.24362100	-2.89855900	1.36452000
O	4.98942300	-1.58751100	1.90097600
C	5.74779400	-2.76164800	2.20185100
H	6.72799100	-2.41389600	2.53067600
H	5.26721800	-3.34025400	2.99652700
H	5.85216300	-3.39010800	1.31131200
H	2.87117500	1.92901800	-0.06783000
H	0.12292500	2.36457200	-1.20969000
C	3.50911600	-0.18453200	-1.94769200
C	4.83428100	0.32529300	-1.37928600
H	5.64540000	0.10601800	-2.08476900
H	4.79841200	1.41364500	-1.25309200
H	5.11604600	-0.12453300	-0.42406800
C	3.36846000	0.37846000	-3.37046400
H	4.16924700	-0.00633800	-4.01462600
H	2.40710200	0.10481300	-3.81758300
H	3.45230600	1.47099600	-3.36415300
C	3.48446900	-1.69805300	-2.08831300

O	2.65687600	-2.29829300	-2.74609500
O	4.44493600	-2.32350000	-1.39954300
C	4.39826400	-3.75249700	-1.44519200
H	4.44614100	-4.10712300	-2.47888200
H	5.26854900	-4.10366400	-0.88795700
H	3.48019100	-4.11815400	-0.97346400
C	1.00538900	3.46767700	0.42105900
H	1.70167000	3.24018700	1.23795800
C	1.72232200	4.46630300	-0.47003300
O	2.69933200	5.09168700	-0.12214900
O	1.16866000	4.57063500	-1.68005300
C	-0.17584700	4.11806300	1.10528300
O	-0.48145800	3.91125500	2.26120200
C	1.82871200	5.46022900	-2.58286800
H	2.85777500	5.13133200	-2.76223200
H	1.25815500	5.42665800	-3.51186200
H	1.84086300	6.47975300	-2.18575000
O	-0.82344900	4.97381300	0.31161000
C	-1.90070500	5.70680600	0.90472800
H	-2.30760600	6.33429500	0.11065100
H	-2.67418000	5.03387300	1.28545300
H	-1.52996200	6.32949700	1.72465200
H	3.77368600	0.26925500	0.96827300
C	2.48797100	-0.04157300	2.59100100
O	2.20823400	-0.78448400	3.50657900
O	2.36240900	1.28628800	2.64962600
C	1.70867600	1.78773100	3.81903100
H	1.56687100	2.85705200	3.65551000
H	0.73594600	1.30049100	3.94949900
H	2.32123800	1.61264900	4.70880100

### Compound 9 in Gas Phase

Electronic Energy: -2930.38794548 Hartree

Electronic Energy + Free Energy Correction: -2929.650549 Hartree



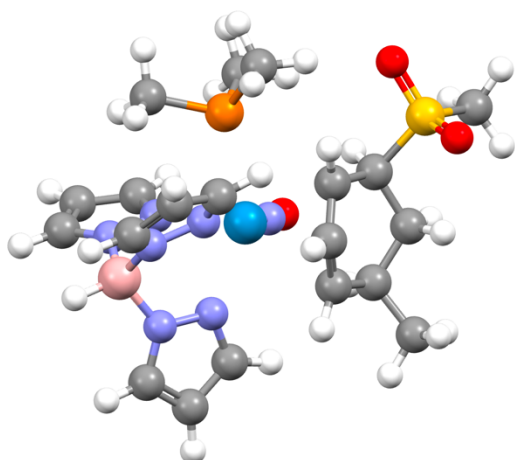
O	-0.30159300	-0.28421800	3.18875800
N	-2.23873100	1.88304100	0.41260200
N	-3.47777300	2.15585600	-0.07083600
N	-2.65020500	-0.38702100	-1.51307900
N	-3.86998600	0.19848700	-1.61094900
N	-3.48549900	-0.37931600	1.38281000
N	-4.59965500	0.12163800	0.79884400
N	-0.71222100	-0.21738400	2.04370000
C	-3.74017100	3.47159500	0.06416900
C	-2.64773800	4.08072800	0.65346800
C	-1.73970100	3.03804700	0.86131200
C	-4.40535600	-0.04807200	-2.82007000
C	-3.51503400	-0.81999400	-3.54550200
C	-2.43325000	-1.00392200	-2.68230600
C	-5.65751300	-0.05250100	1.61520700
C	-5.22620800	-0.69208500	2.76439200
C	-3.85185800	-0.86360600	2.57270500
B	-4.46028800	1.02099100	-0.45172600
H	-5.52587800	1.47673600	-0.76595000
H	-4.69116700	3.87301000	-0.26358000
H	-2.52623200	5.12530600	0.90547900
H	-0.75845800	3.06682300	1.32099200
H	-5.38073000	0.34703800	-3.07607800
H	-3.63082500	-1.19439800	-4.55287200
H	-1.51525200	-1.55601000	-2.85238100
H	-6.63759600	0.30365300	1.32233600

H	-5.81905700	-0.98484800	3.61970800
H	-3.11078800	-1.31820600	3.22206300
C	-3.32099800	-3.42421500	0.60705600
H	-3.31298600	-4.50856000	0.44312100
H	-3.74030100	-3.21807100	1.59602400
H	-3.95976300	-2.95081900	-0.15027300
C	-0.75819000	-3.56103800	1.87115900
H	-1.02743000	-3.05202200	2.80342100
H	-1.03597500	-4.62028900	1.93698900
H	0.32872600	-3.48839400	1.74126300
W	-1.45357200	-0.23530600	0.43917600
P	-1.61159700	-2.76538700	0.46041400
C	-1.04665600	-3.76715300	-0.96760900
H	-1.06771500	-4.82629500	-0.68022500
H	-1.74049800	-3.62242200	-1.80395000
H	-0.03661900	-3.51098500	-1.29544100
C	2.33573000	-0.33449100	0.81087400
C	1.65917200	-1.35061700	-0.13304200
C	0.37446700	-0.74703900	-0.70922600
C	0.16809500	0.68235800	-0.74466700
C	1.17504000	1.65157700	-0.12518600
C	2.53960300	0.98524100	0.06755000
H	0.04515400	-1.27316500	-1.60741100
H	-0.28558500	1.05709900	-1.67076800
H	3.19995100	1.66359600	0.62617500
H	1.58478400	-0.14042400	1.58692400
H	0.85491900	1.92788100	0.88974100
C	1.23869900	2.99158700	-0.90464700
C	1.31359700	4.20088100	0.00668500
O	1.58639500	4.19298000	1.18523400
O	1.01666900	5.30924500	-0.67807500
C	1.06453900	6.52784200	0.06862400
H	0.80331300	7.32257400	-0.63134200
H	0.34510500	6.50245900	0.89338000
H	2.06789800	6.69646900	0.47140700
H	0.33397700	3.10466200	-1.51682900
H	1.38998200	-2.23313800	0.45594300
C	2.44122400	3.06246500	-1.81834100
O	3.49598800	3.57472800	-1.51103400
O	2.22208300	2.46088000	-2.98882100
C	3.36576300	2.38794600	-3.84788100
H	3.02971500	1.91354800	-4.77107500
H	3.75183400	3.38872300	-4.06152500
H	4.15490800	1.78763200	-3.38321900
C	2.61376100	-1.87643700	-1.27045600
H	3.50250100	-1.24084300	-1.34391200
C	3.12115000	-3.29368700	-1.08050400
O	4.20568500	-3.67310000	-1.46504100

O	2.23511300	-4.08568500	-0.47393000
C	1.96926500	-1.83361200	-2.64027400
O	1.43845800	-2.77687100	-3.18980600
O	2.04394100	-0.61072800	-3.16184200
C	1.24872500	-0.38002900	-4.32635400
H	0.25272300	-0.81932100	-4.20746700
H	1.16260700	0.70331900	-4.42380900
H	1.72598800	-0.80921000	-5.21333400
C	2.63263000	-5.44404100	-0.27822400
H	3.52470700	-5.49487500	0.35448300
H	1.79199000	-5.93260400	0.21810500
H	2.83987400	-5.92896700	-1.23680800
C	3.56370100	-0.80055400	1.63396800
C	3.23182600	-2.10035700	2.38697300
H	4.02350400	-2.34840000	3.10440100
H	2.28513300	-1.99836500	2.93607400
H	3.13956100	-2.94597400	1.69376400
C	4.86329400	-0.97777600	0.84707300
H	4.80180200	-1.82212300	0.15520500
H	5.12180600	-0.07827000	0.27405800
H	5.69527100	-1.18773300	1.52513200
C	3.76241800	0.23221700	2.75297500
O	2.89674800	0.93842600	3.22138100
O	5.01275000	0.22135500	3.23968900
C	5.24729000	1.08607700	4.35079900
H	4.61181200	0.81250900	5.19905000
H	6.29840600	0.96018100	4.61571300
H	5.05127200	2.12860500	4.08153100
H	3.02009200	0.80418400	-0.90877800



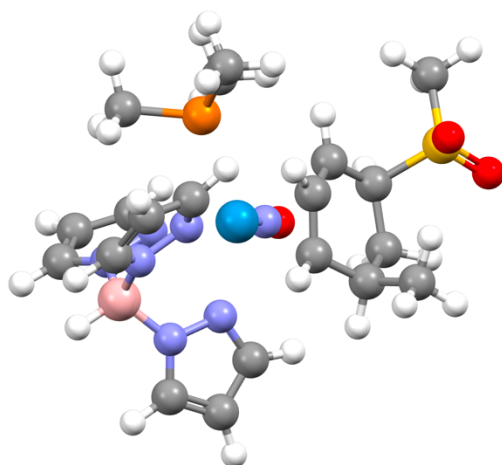
ID Electronic Energy: -2221.027764 Hartree



W	0.327800	0.193700	-0.112200
O	-0.773900	0.988500	-2.750000
N	-0.349400	0.698000	-1.668600
P	-0.246400	-2.302500	-0.493100
C	1.242700	-3.364700	-0.512000
H	0.916200	-4.406300	-0.611400
H	1.908300	-3.122900	-1.344400
C	-1.289900	-3.240100	0.674600
H	-0.901700	-3.160700	1.695200
H	-2.329700	-2.901300	0.640100
C	-1.062500	-2.613800	-2.091900
H	-1.219300	-3.691900	-2.216300
H	-2.034500	-2.106900	-2.110800
H	-1.253400	-4.292100	0.367900
H	1.785700	-3.253000	0.434100
H	-0.449500	-2.242400	-2.919100
N	1.363800	-0.663200	1.703400
N	2.718600	-0.682400	1.773100
N	3.296200	-0.663500	-0.678900
N	2.063000	-0.545300	-1.230100
N	3.130900	1.469800	0.531700
N	1.879300	1.785200	0.103600
C	0.916200	-1.314300	2.787900
H	-0.148700	-1.424500	2.960800
C	1.984200	-1.761400	3.563300
H	1.943500	-2.310500	4.493100
C	3.110700	-1.335200	2.879700
H	4.164700	-1.443300	3.103900
C	3.495700	-1.192500	-2.825600
H	3.902300	-1.493900	-3.780300
C	4.171500	-1.044400	-1.624800
H	5.218500	-1.168500	-1.377300

C	1.896400	3.082900	-0.227900
H	1.002600	3.564300	-0.608000
C	3.161500	3.623100	-0.004800
H	3.482900	4.642100	-0.166800
C	3.912900	2.562100	0.469600
H	4.953400	2.500700	0.763600
B	3.575900	-0.005200	0.695700
H	4.739300	-0.072100	0.970600
C	2.177000	-0.853300	-2.530000
H	1.308400	-0.823500	-3.177900
C	-1.810800	-0.042900	0.801900
H	-1.990500	-0.947100	1.380900
C	-1.151900	1.006400	1.499300
H	-0.662100	0.814800	2.452300
C	-1.874100	2.734200	-0.197800
H	-1.420200	2.778800	-1.196500
C	-3.134600	1.863400	-0.238800
H	-3.729400	2.127700	-1.121000
H	-3.728000	2.125800	0.651500
C	-2.890200	0.352900	-0.198700
H	-2.715500	-0.063100	-1.201400
C	-0.906300	2.190500	0.822600
H	-0.228600	2.905000	1.288300
C	-2.245600	4.161700	0.195000
H	-1.367400	4.818000	0.171100
H	-2.994000	4.568400	-0.495500
H	-2.666300	4.191200	1.208800
S	-4.425800	-0.483500	0.313700
O	-4.796700	-0.029600	1.659700
O	-4.231200	-1.926000	0.094900
C	-5.653500	0.070200	-0.846000
H	-5.287700	-0.097800	-1.863300
H	-6.542400	-0.541200	-0.663400
H	-5.882400	1.124900	-0.677000

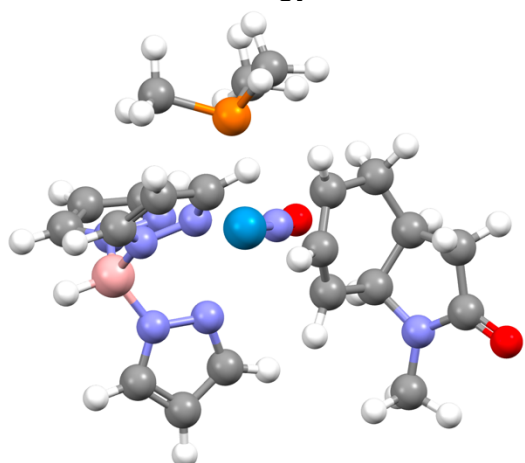
IP Electronic Energy: -2221.020150 Hartree



W	0.320500	0.014300	-0.122000
O	-0.816300	0.173600	-2.860900
N	-0.428300	0.125400	-1.730900
P	0.269800	-2.555600	0.061900
C	1.930500	-3.310500	0.134700
H	1.816100	-4.384700	0.322300
H	2.476000	-3.168500	-0.802400
C	-0.504400	-3.325700	1.528000
H	0.088600	-3.091700	2.418200
H	-1.536400	-3.003900	1.691900
C	-0.553700	-3.351400	-1.354900
H	-0.506300	-4.442000	-1.255600
H	-1.602700	-3.033700	-1.395500
H	-0.496200	-4.411900	1.378100
H	2.501200	-2.862500	0.956900
H	-0.059800	-3.051200	-2.285500
N	1.624500	-0.154000	1.737500
N	2.931400	0.216200	1.682800
N	3.412800	-0.188100	-0.745100
N	2.177500	-0.516800	-1.192200
N	2.720300	2.060200	-0.009500
N	1.418600	1.928300	-0.367400
C	1.423100	-0.621100	2.981200
H	0.453100	-0.983800	3.296500
C	2.595700	-0.559000	3.728900
H	2.741000	-0.859500	4.756700
C	3.528600	-0.018100	2.861800
H	4.575600	0.222500	2.998400
C	3.688600	-1.218300	-2.690000
H	4.134500	-1.664600	-3.567500
C	4.334400	-0.596000	-1.634300

H	5.384600	-0.400100	-1.456600
C	1.051900	3.073900	-0.951300
H	0.047500	3.192000	-1.339700
C	2.120600	3.971800	-0.962100
H	2.133800	4.978100	-1.355900
C	3.159000	3.283500	-0.361700
H	4.184800	3.568900	-0.163900
B	3.547500	0.825400	0.416400
H	4.694400	1.117900	0.598700
C	2.333700	-1.130300	-2.373700
H	1.472700	-1.489100	-2.926400
C	-1.412900	0.093800	1.375700
H	-1.107400	-0.494600	2.237300
C	-0.972600	1.426000	1.119300
H	-0.367000	1.884000	1.905500
C	-2.695900	1.730700	-0.716700
H	-2.094900	1.859100	-1.622200
H	-3.634300	2.263700	-0.913900
C	-2.989400	0.229200	-0.588300
H	-2.996200	-0.231200	-1.588200
C	-1.974900	2.367300	0.474600
H	-1.441700	3.250900	0.098600
C	-2.115100	-0.538300	0.355000
H	-2.341100	-1.599000	0.450100
C	-2.956000	2.848500	1.544000
H	-2.427300	3.308200	2.388100
H	-3.646800	3.594200	1.130200
H	-3.552900	2.012800	1.933100
S	-4.732600	-0.059100	-0.041300
C	-5.082700	-1.702900	-0.622800
H	-4.400700	-2.420200	-0.157600
H	-6.111700	-1.923200	-0.322300
H	-4.994800	-1.724800	-1.712000
O	-5.587900	0.875500	-0.781200
O	-4.797700	-0.065700	1.426100

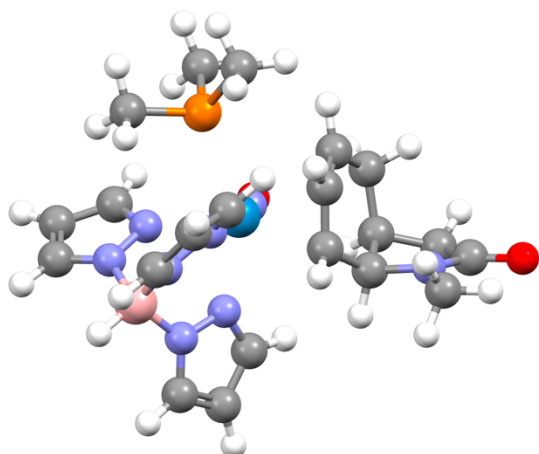
IIID Electronic Energy: -1839.943947 Hartree



W	0.182000	-0.124400	-0.132400
O	-0.981500	-0.575200	-2.827500
N	-0.555200	-0.356000	-1.730100
P	1.257000	-2.474400	-0.276500
C	3.069200	-2.411200	-0.037200
H	3.454800	-3.437300	-0.038100
H	3.557500	-1.849400	-0.838600
C	0.807300	-3.825700	0.868100
H	0.960200	-3.523300	1.909300
H	-0.232200	-4.136300	0.724000
C	1.041900	-3.288200	-1.894800
H	1.586100	-4.240100	-1.887200
H	-0.021200	-3.486900	-2.068900
H	1.461400	-4.677800	0.648400
H	3.302500	-1.943200	0.926500
H	1.425800	-2.668100	-2.709400
N	1.400700	-0.013000	1.768900
N	2.439000	0.853800	1.867700
N	3.072500	1.027500	-0.558500
N	2.087800	0.298200	-1.141900
N	1.511700	2.675800	0.388700
N	0.375400	2.097700	-0.085400
C	1.399600	-0.736400	2.899200
H	0.653400	-1.505700	3.062600
C	2.442400	-0.338600	3.733900
H	2.695300	-0.729500	4.709100
C	3.076800	0.675600	3.036600
H	3.934200	1.287300	3.288500
C	3.749300	0.570000	-2.622200
H	4.337500	0.516700	-3.527100
C	4.075300	1.205300	-1.434800
H	4.945300	1.785900	-1.153800
C	-0.387600	3.084400	-0.574400

H	-1.350200	2.862100	-1.021100
C	0.245100	4.315000	-0.408100
H	-0.122200	5.290900	-0.692100
C	1.449000	4.006100	0.200300
H	2.273300	4.636400	0.510300
B	2.763400	1.829600	0.730700
H	3.686000	2.534700	1.023800
C	2.485800	0.029700	-2.394000
H	1.848100	-0.534900	-3.063600
C	-1.337700	-1.566700	0.934300
H	-0.912300	-2.250400	1.664600
C	-1.558400	-0.247800	1.397100
H	-1.141300	0.096200	2.342400
C	-3.099700	0.263300	-0.540600
H	-2.804000	0.551500	-1.557700
C	-3.464800	-1.233700	-0.426900
H	-3.878800	-1.540700	-1.395700
C	-2.316100	-2.175300	-0.058500
H	-1.807700	-2.524300	-0.965600
H	-2.749800	-3.076900	0.398800
C	-2.070700	0.674100	0.491500
H	-2.084000	1.721000	0.789200
C	-4.601900	-1.225800	0.597100
H	-5.338100	-2.019900	0.440500
H	-4.224100	-1.328600	1.625500
N	-4.360700	0.925700	-0.221800
C	-5.239600	0.137400	0.464200
O	-6.328800	0.494100	0.888300
C	-4.588300	2.320100	-0.501900
H	-5.628700	2.550800	-0.257900
H	-3.937800	2.972500	0.096700
H	-4.410500	2.530800	-1.563900

IIIP Electronic Energy: -1839.943133 Hartree

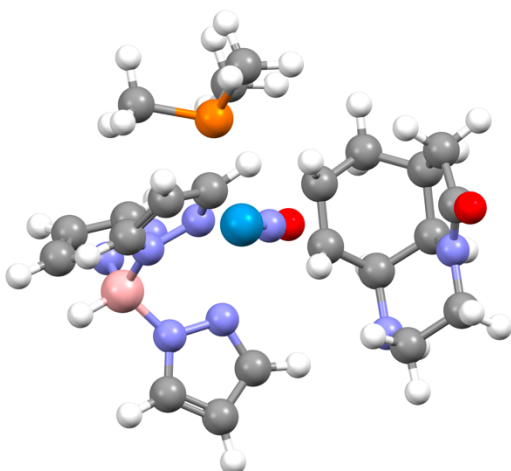


W	0.213200	-0.229400	-0.184700
O	-0.600700	-0.917500	-2.957900
N	-0.335400	-0.643800	-1.822500
P	1.353700	-2.494000	0.285400
C	3.145200	-2.337700	0.604400
H	3.536800	-3.321500	0.888300
H	3.676900	-1.985200	-0.284200
C	0.837000	-3.469500	1.741800
H	1.060600	-2.912800	2.657800
H	-0.226200	-3.724300	1.726900
C	1.226700	-3.667400	-1.102100
H	1.747200	-4.600300	-0.855700
H	0.172000	-3.880600	-1.309400
H	1.418600	-4.399100	1.746800
H	3.313300	-1.633900	1.428300
H	1.677400	-3.230700	-1.999600
N	1.205500	0.368800	1.770600
N	2.178800	1.316700	1.776200
N	3.088000	1.034000	-0.547200
N	2.214000	0.131500	-1.054000
N	1.336100	2.717300	-0.133300
N	0.305000	1.956100	-0.577300
C	1.089100	-0.054700	3.039300
H	0.372200	-0.820300	3.308300
C	1.988400	0.613500	3.867000
H	2.126500	0.488400	4.931400
C	2.659800	1.477400	3.019500
H	3.443700	2.199600	3.210300
C	4.049300	0.148000	-2.339400
H	4.755200	-0.081500	-3.124900
C	4.194500	1.063400	-1.310000
H	5.001000	1.745600	-1.071500
C	-0.486500	2.750400	-1.305700

H	-1.372800	2.350000	-1.783500
C	0.024500	4.049300	-1.327700
H	-0.391200	4.914400	-1.824600
C	1.184300	3.979200	-0.577400
H	1.921200	4.733200	-0.330400
B	2.586800	2.060500	0.497200
H	3.429100	2.879000	0.731900
C	2.782600	-0.401100	-2.144500
H	2.261100	-1.153700	-2.724800
C	-1.495900	-0.965600	1.142200
H	-1.065900	-1.297900	2.084300
C	-1.686500	0.417200	0.790200
H	-1.464700	1.142200	1.577200
C	-3.213100	-0.211300	-1.188600
H	-2.681500	0.132700	-2.080600
C	-2.820500	-1.669100	-0.896800
H	-2.517700	-2.172300	-1.825400
H	-3.699700	-2.239800	-0.547700
C	-2.920200	0.738700	-0.016900
H	-2.850200	1.775800	-0.387200
C	-1.820000	-1.905200	0.177400
H	-1.557200	-2.949700	0.345200
C	-4.724900	-0.075200	-1.352500
H	-4.983700	0.785000	-1.985500
H	-5.218100	-0.957400	-1.773600
N	-4.148400	0.619700	0.783900
C	-4.281700	1.228400	2.082800
H	-3.669900	0.713700	2.833600
H	-3.979500	2.284900	2.053800
H	-5.332100	1.166500	2.380100
C	-5.226100	0.228000	0.043600
O	-6.381800	0.169100	0.439600



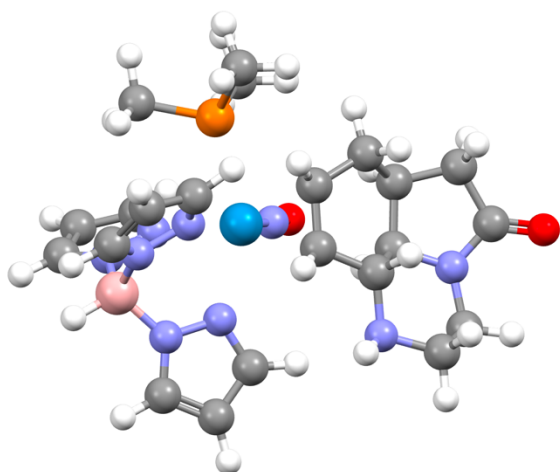
VII Electronic Energy: -1934.062356 Hartree



W	0.519500	-0.172100	-0.405500
O	0.106200	-0.805600	-3.292200
N	0.270200	-0.522100	-2.117400
P	1.236700	-2.535900	0.140100
C	2.934500	-2.667400	0.829200
H	3.149200	-3.710600	1.090500
H	3.681800	-2.318400	0.109600
C	0.337400	-3.533100	1.387300
H	0.392600	-3.041200	2.364800
H	-0.714000	-3.666600	1.117100
C	1.290000	-3.657400	-1.303100
H	1.663000	-4.646600	-1.011000
H	0.285300	-3.760600	-1.727900
H	0.813300	-4.518200	1.464300
H	3.005400	-2.051800	1.735100
H	1.947500	-3.236100	-2.071900
N	1.020900	0.203500	1.806800
N	2.089500	0.977200	2.128700
N	3.524000	0.805000	0.051900
N	2.728900	0.056500	-0.745400
N	1.854300	2.629100	0.262500
N	0.800400	2.071500	-0.392000
C	0.531900	-0.265000	2.961800
H	-0.340200	-0.908800	2.966600
C	1.286700	0.197900	4.041600
H	1.136000	-0.005700	5.092400
C	2.264900	0.987000	3.462600
H	3.070200	1.561900	3.903000
C	4.838700	-0.075500	-1.499800
H	5.703000	-0.339800	-2.092900
C	4.796100	0.745600	-0.385600
H	5.575200	1.303100	0.119800

C	0.122900	3.075100	-0.958200
H	-0.804700	2.862600	-1.484900
C	0.740500	4.298300	-0.678100
H	0.429200	5.285000	-0.992200
C	1.832500	3.966000	0.102600
H	2.596100	4.581000	0.563100
B	2.865100	1.773100	1.057100
H	3.694800	2.468000	1.578200
C	3.512500	-0.475000	-1.689600
H	3.084500	-1.123300	-2.446700
C	-1.399100	-1.066300	0.223100
H	-1.403800	-1.356800	1.279000
C	-1.590600	0.345100	-0.060100
H	-1.683100	0.999100	0.814700
C	-3.866000	-0.170100	-1.023200
H	-4.451300	-0.052200	-1.952600
C	-3.664400	-1.663100	-0.664300
H	-4.179600	-2.279600	-1.410800
C	-2.174000	-2.021700	-0.663300
H	-1.804500	-1.981300	-1.697800
H	-2.054700	-3.065000	-0.337200
C	-4.334500	-1.842300	0.706000
H	-5.155700	-2.568600	0.693100
H	-3.633400	-2.176300	1.482600
N	-4.639000	0.369700	0.083400
C	-4.889100	-0.491200	1.101500
O	-5.469000	-0.214700	2.145500
C	-2.570600	0.655300	-1.183600
H	-2.128400	0.373600	-2.150400
N	-2.902000	2.087200	-1.290000
H	-3.444700	2.217600	-2.143400
C	-3.693900	2.589700	-0.167800
H	-3.068900	2.583500	0.735800
H	-3.957000	3.635600	-0.366600
C	-4.961000	1.778600	0.082100
H	-5.690700	1.978700	-0.720000
H	-5.428700	2.023300	1.042200

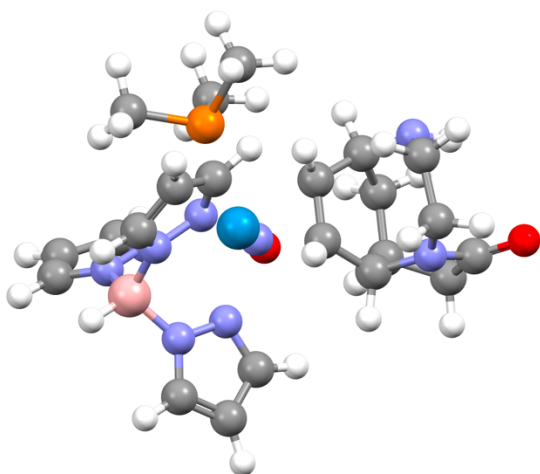
VI Electronic Energy: -1934.061306 Hartree



W	0.423700	-0.156900	-0.090700
O	-1.019500	-0.703000	-2.640900
N	-0.493600	-0.460400	-1.567100
P	1.191700	-2.563700	0.067100
C	3.007500	-2.792900	-0.083500
H	3.262200	-3.848300	0.071500
H	3.365000	-2.480800	-1.069600
C	0.893100	-3.557800	1.576800
H	1.407800	-3.103900	2.430700
H	-0.173300	-3.635600	1.806200
C	0.519800	-3.639600	-1.248700
H	0.959800	-4.642600	-1.191900
H	-0.567900	-3.716300	-1.134500
H	1.297100	-4.565200	1.420200
H	3.512500	-2.188100	0.680700
H	0.732600	-3.203700	-2.230800
N	1.890400	0.163200	1.653500
N	3.005000	0.915700	1.469800
N	3.360900	0.704100	-1.018400
N	2.271100	-0.016400	-1.367400
N	2.020200	2.587300	-0.121400
N	0.771100	2.068400	-0.258800
C	1.962200	-0.318100	2.901300
H	1.174000	-0.951000	3.292500
C	3.129300	0.116300	3.532200
H	3.461200	-0.103200	4.537200
C	3.760300	0.900600	2.582800
H	4.689300	1.456100	2.618800
C	3.808500	-0.199000	-2.992000
H	4.304700	-0.482300	-3.909800
C	4.296200	0.613700	-1.982700
H	5.234400	1.146300	-1.885600

C	-0.039700	3.087900	-0.558000
H	-1.105900	2.907600	-0.664200
C	0.682900	4.283600	-0.618900
H	0.307700	5.274700	-0.833400
C	1.985300	3.916700	-0.333600
H	2.893500	4.502700	-0.262200
B	3.248500	1.693100	0.161200
H	4.245000	2.357400	0.252300
C	2.528500	-0.560100	-2.561500
H	1.785800	-1.185900	-3.044300
C	-1.026300	-0.983700	1.358500
H	-0.514200	-1.350800	2.253600
C	-1.213700	0.454600	1.261600
H	-0.781500	1.057700	2.072400
C	-3.161100	0.122300	-0.280200
H	-2.614600	0.486200	-1.161700
C	-3.086400	-1.411900	-0.157800
H	-2.645600	-1.789400	-1.088200
N	-4.571400	0.427000	-0.443900
C	-5.407800	-0.627300	-0.270800
O	-6.632100	-0.580200	-0.275900
C	-4.552700	-1.863500	-0.059900
H	-4.832200	-2.628000	-0.793600
H	-4.800700	-2.274000	0.928900
C	-2.631900	0.861800	0.934000
H	-3.271400	0.526300	1.789000
C	-4.303100	2.560600	0.685000
H	-4.796800	2.234800	1.621800
H	-4.469500	3.638600	0.575700
N	-2.867100	2.287900	0.708000
H	-2.433100	2.823100	1.457700
C	-4.953300	1.821800	-0.479000
H	-4.618700	2.264400	-1.429600
H	-6.045700	1.880300	-0.431000
C	-2.221900	-1.865500	1.026700
H	-2.865900	-1.895100	1.925000
H	-1.915100	-2.909100	0.858900

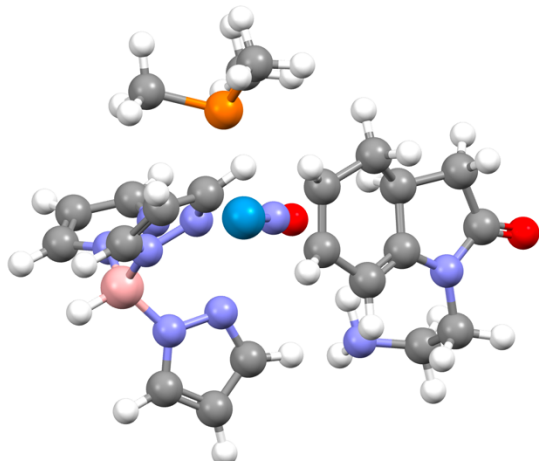
VIII Electronic Energy: -1934.043481 Hartree



W	0.411600	-0.083800	-0.302000
O	-0.271500	-0.187500	-3.199900
N	-0.062600	-0.140000	-2.000500
P	0.938400	-2.561000	-0.177600
C	2.687800	-2.927900	0.243500
H	2.824100	-4.010200	0.356700
H	3.364800	-2.562400	-0.535100
C	0.096900	-3.640600	1.038900
H	0.319200	-3.301200	2.056600
H	-0.987700	-3.640100	0.893600
C	0.686800	-3.465600	-1.745600
H	0.989900	-4.514200	-1.639100
H	-0.372100	-3.422400	-2.025900
H	0.471600	-4.664500	0.921500
H	2.943200	-2.434500	1.190000
H	1.276200	-2.999500	-2.542800
N	1.324300	-0.019800	1.805900
N	2.467600	0.676600	2.027600
N	3.520800	0.623400	-0.259700
N	2.553700	-0.006000	-0.966000
N	2.065400	2.530600	0.376800
N	0.916000	2.104600	-0.206900
C	1.007200	-0.604000	2.968800
H	0.117300	-1.217500	3.051300
C	1.949800	-0.293400	3.950400
H	1.962900	-0.614200	4.982500
C	2.859500	0.525900	3.305400
H	3.755000	1.018900	3.663200
C	4.490200	-0.175400	-2.086500
H	5.221400	-0.427700	-2.841700
C	4.692900	0.538100	-0.917400
H	5.582200	1.003800	-0.511000

C	0.308400	3.188000	-0.699000
H	-0.634200	3.088400	-1.225100
C	1.060800	4.335200	-0.431000
H	0.830000	5.357000	-0.698100
C	2.168400	3.868400	0.252700
H	3.027000	4.387900	0.660200
B	3.114800	1.531600	0.922800
H	4.069900	2.117600	1.354000
C	3.126900	-0.483900	-2.075200
H	2.531600	-1.027100	-2.801200
C	-1.442300	-0.857000	0.613600
H	-1.210200	-1.359700	1.555500
C	-1.461700	0.590300	0.626700
H	-1.196200	1.088000	1.567000
C	-2.953300	0.685800	-1.470500
H	-2.262600	1.047700	-2.240600
C	-2.937800	-0.861600	-1.443700
H	-2.222100	-1.213700	-2.195600
H	-3.917100	-1.250800	-1.765000
C	-2.590900	1.267500	-0.099700
H	-2.375700	2.344900	-0.205900
C	-4.365800	1.234900	-1.662400
H	-4.350500	2.300500	-1.935300
H	-4.973100	0.700100	-2.400000
N	-3.903000	1.147700	0.603400
C	-4.945000	1.078100	-0.273100
O	-6.118800	0.883700	0.024600
C	-2.590500	-1.530900	-0.105300
H	-2.289600	-2.562800	-0.367300
N	-3.766100	-1.656100	0.800600
H	-4.629700	-1.588400	0.270600
C	-4.062500	0.644600	1.944400
H	-3.368100	1.160900	2.617200
H	-5.078700	0.911100	2.254800
C	-3.869700	-0.904000	2.035500
H	-4.724800	-1.317500	2.587100
H	-2.990900	-1.113500	2.656200

V Electronic Energy: -1934.061200 Hartree

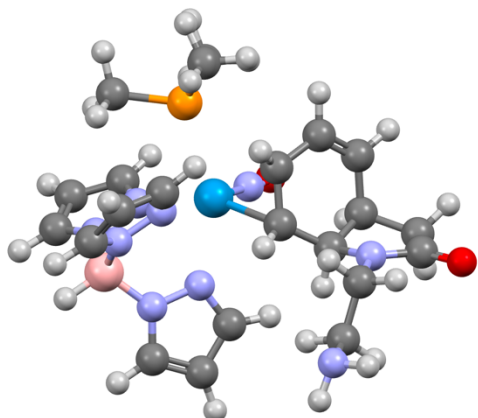


W	0.467400	-0.181900	-0.003100
O	-1.540700	0.090800	-2.195100
N	-0.740500	-0.049200	-1.279300
P	1.245000	-2.499800	-0.648400
C	3.015500	-2.590600	-1.127800
H	3.303500	-3.634600	-1.300600
H	3.206300	-2.012600	-2.037200
C	1.182900	-3.890400	0.542800
H	1.826100	-3.672400	1.402600
H	0.164800	-4.071400	0.898700
C	0.378600	-3.184700	-2.105400
H	0.787700	-4.164600	-2.379700
H	-0.689400	-3.288000	-1.879700
H	1.553900	-4.796800	0.049600
H	3.631400	-2.178500	-0.317800
H	0.485600	-2.497400	-2.952300
N	2.182600	-0.245800	1.523100
N	3.206000	0.640100	1.426100
N	3.170000	1.145500	-1.041800
N	2.087300	0.433800	-1.433000
N	1.899300	2.592800	0.524500
N	0.676900	2.025300	0.356100
C	2.481200	-1.055700	2.547200
H	1.806800	-1.855100	2.831000
C	3.704900	-0.700400	3.117200
H	4.206000	-1.164500	3.955000
C	4.128300	0.385300	2.371300
H	5.017100	0.999700	2.445600
C	3.371600	0.839700	-3.228500
H	3.740500	0.858200	-4.244500
C	3.953500	1.404400	-2.106300
H	4.862000	1.982100	-1.988100

C	-0.217200	3.019000	0.354100
H	-1.273100	2.806400	0.201500
C	0.425400	4.248900	0.532100
H	-0.025200	5.230600	0.578400
C	1.766900	3.929700	0.633000
H	2.641500	4.553600	0.771100
B	3.197500	1.765400	0.375300
H	4.163200	2.466600	0.508500
C	2.196000	0.251500	-2.752900
H	1.430800	-0.300400	-3.288500
C	-0.735600	-1.414000	1.409400
H	-0.081700	-1.945200	2.107400
C	-0.932600	-0.007500	1.702800
H	-0.373000	0.414800	2.544000
C	-3.000700	-1.474500	0.270700
H	-2.656100	-1.348400	-0.768300
C	-5.285300	-0.780500	0.102900
O	-6.453700	-0.709000	-0.246400
C	-3.204100	-0.093800	0.826200
N	-4.515300	0.290300	0.493700
C	-2.262600	0.590600	1.488900
H	-2.450400	1.602200	1.848500
C	-5.023900	1.649500	0.501900
H	-6.095300	1.599200	0.726900
H	-4.529600	2.204200	1.308600
C	-4.814100	2.343400	-0.832800
H	-5.378100	1.781800	-1.599800
H	-5.272600	3.339400	-0.771400
N	-3.397300	2.500500	-1.145500
H	-2.980400	1.593000	-1.363300
H	-3.306300	3.047500	-1.997900
C	-1.960600	-2.248200	1.062900
H	-2.429300	-2.580200	2.008200
H	-1.692400	-3.167600	0.521700
C	-4.426300	-2.023800	0.228900
H	-4.633800	-2.724800	-0.584500
H	-4.690700	-2.519100	1.176200



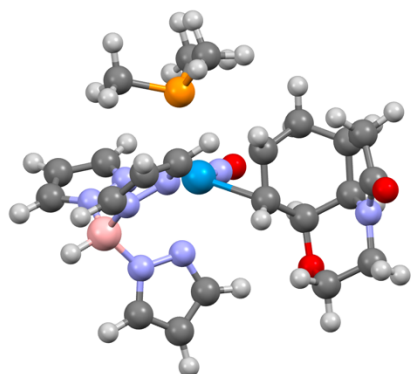
IX Electronic Energy: -1934.055962 Hartree



W	0.543300	-0.365100	-0.203900
O	0.105100	-2.044200	-2.628200
N	0.244800	-1.356800	-1.635100
C	-1.049000	-1.295800	1.066600
H	-0.806000	-1.251100	2.131200
C	-1.533400	-0.093200	0.417200
H	-1.564100	0.805200	1.044700
C	-2.876600	-1.534800	-1.252500
H	-2.288600	-1.509700	-2.181300
C	-2.723500	-0.200100	-0.498600
H	-2.718900	0.625100	-1.231100
C	-1.611300	-2.581800	0.629200
H	-1.334800	-3.475900	1.193000
C	-4.378800	-1.584500	-1.534700
H	-4.638800	-1.043000	-2.455700
H	-4.790300	-2.596400	-1.618700
N	-4.011200	-0.127900	0.233000
C	-5.003100	-0.833100	-0.379600
O	-6.186900	-0.829700	-0.061800
N	-4.635300	3.261600	1.649400
H	-4.585800	4.201100	1.265300
H	-5.602300	3.134900	1.941100
C	-4.302800	0.893600	1.211400
H	-3.573300	0.854600	2.031700
H	-5.289100	0.659000	1.632500
C	-4.323200	2.290700	0.609700
H	-5.026700	2.288400	-0.244800
H	-3.331200	2.528500	0.196600
C	-2.441600	-2.703800	-0.415000
H	-2.824400	-3.684000	-0.704600
P	1.889900	-2.164300	0.967800
C	3.595400	-1.646300	1.405500

H	4.103100	-2.455400	1.944200
H	4.173600	-1.395100	0.510600
C	1.351700	-2.857300	2.574700
H	1.268800	-2.060500	3.322000
H	0.385800	-3.362600	2.484000
C	2.141000	-3.668400	-0.038800
H	2.760300	-4.396900	0.498300
H	1.166700	-4.116100	-0.266300
H	2.099700	-3.583000	2.916300
H	3.548500	-0.761200	2.052900
H	2.629600	-3.406000	-0.983600
N	1.128000	0.921900	1.597100
N	1.931700	2.001700	1.428900
N	3.177100	1.359400	-0.667700
N	2.575700	0.186600	-0.975900
N	1.090000	2.686300	-0.842000
N	0.251200	1.660300	-1.139100
C	0.899900	0.821400	2.912800
H	0.268400	0.030800	3.301000
C	1.562400	1.835800	3.606600
H	1.567500	2.016900	4.672200
C	2.204300	2.563800	2.620200
H	2.830700	3.445500	2.676900
C	4.564400	0.271200	-2.012200
H	5.418200	0.006100	-2.619900
C	4.371900	1.433300	-1.284200
H	4.992000	2.313900	-1.169800
C	-0.603500	2.116100	-2.059600
H	-1.359000	1.457800	-2.472300
C	-0.333000	3.454300	-2.360200
H	-0.851800	4.094500	-3.059800
C	0.753100	3.772100	-1.565800
H	1.318400	4.690300	-1.464000
B	2.354900	2.470700	0.025900
H	2.993600	3.484600	0.099500
C	3.402100	-0.473700	-1.793800
H	3.121800	-1.449500	-2.175600

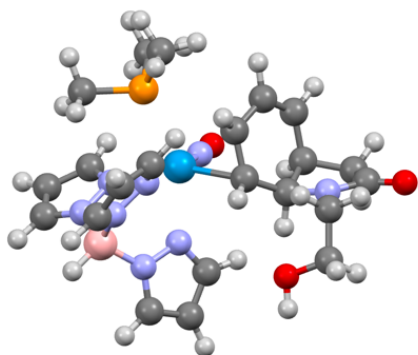
Compound 10 Electronic Energy: -1953.940675 Hartree



W	0.521200	-0.191000	-0.398900
O	0.101300	-0.836200	-3.282000
N	0.269400	-0.551300	-2.108700
C	-1.387900	-1.102900	0.238500
H	-1.388900	-1.393100	1.294400
C	-1.581100	0.309700	-0.039700
H	-1.678900	0.961300	0.835100
C	-3.852800	-0.189300	-1.033800
H	-4.415900	-0.074900	-1.974600
C	-3.662000	-1.677200	-0.648800
H	-4.185400	-2.300700	-1.383300
C	-2.174500	-2.053600	-0.643700
H	-1.804600	-2.025300	-1.678800
H	-2.069100	-3.095700	-0.309700
C	-4.333600	-1.822900	0.725600
H	-5.158100	-2.545400	0.727500
H	-3.633900	-2.143100	1.508900
N	-4.634400	0.374200	0.052200
C	-4.879600	-0.460500	1.094700
O	-5.448800	-0.153700	2.134900
C	-2.549900	0.615700	-1.168900
H	-2.100900	0.358900	-2.138600
C	-3.606100	2.540000	-0.205400
H	-2.994200	2.521600	0.711100
H	-3.804800	3.589300	-0.450800
C	-4.908000	1.792100	0.024700
H	-5.611200	2.009000	-0.793800
H	-5.373800	2.077000	0.974000
O	-2.894200	1.999600	-1.304200
P	1.273100	-2.542300	0.152500
C	2.969600	-2.644000	0.848900
H	3.199700	-3.681300	1.120300
H	3.714000	-2.289500	0.128900
C	0.379400	-3.552700	1.392000
H	0.407900	-3.056300	2.368300

H	-0.664300	-3.709700	1.104400
C	1.344500	-3.662600	-1.290500
H	1.727400	-4.647800	-0.997900
H	0.340900	-3.775800	-1.715900
H	0.874800	-4.527100	1.480300
H	3.027700	-2.018400	1.749000
H	1.998200	-3.234200	-2.058600
N	1.015200	0.216100	1.806000
N	2.056600	1.028400	2.121000
N	3.494900	0.869000	0.048400
N	2.724000	0.082600	-0.736700
N	1.776100	2.652300	0.234200
N	0.748600	2.055200	-0.425200
C	0.541300	-0.258000	2.965000
H	-0.308400	-0.931300	2.975000
C	1.278800	0.240600	4.040700
H	1.134300	0.041800	5.093300
C	2.230400	1.056700	3.454800
H	3.015800	1.662400	3.890100
C	4.838800	-0.002800	-1.483300
H	5.712200	-0.253500	-2.069000
C	4.769500	0.837500	-0.384900
H	5.530800	1.426300	0.111900
C	0.047100	3.030800	-1.010500
H	-0.855000	2.787700	-1.561900
C	0.621800	4.275800	-0.737400
H	0.284300	5.248300	-1.068100
C	1.714600	3.986200	0.059300
H	2.454200	4.629800	0.519700
B	2.809600	1.833100	1.040200
H	3.619500	2.557200	1.552100
C	3.525300	-0.443600	-1.668800
H	3.118400	-1.118300	-2.414500

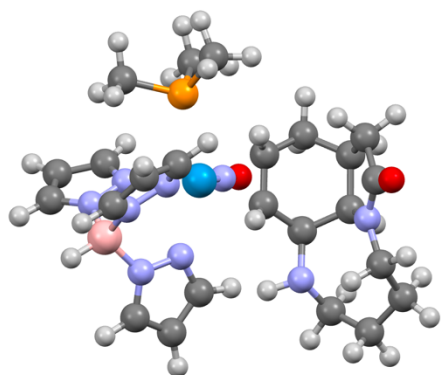
Compound 11 Electronic Energy: -1953.931793 Hartree



W	0.494500	-0.354100	-0.219700
O	-0.073800	-1.796500	-2.766200
N	0.117600	-1.205300	-1.721100
C	-1.115700	-1.308600	1.011200
H	-0.846200	-1.369900	2.068700
C	-1.550300	-0.031100	0.482700
H	-1.519000	0.814500	1.177300
C	-2.994100	-1.242600	-1.276900
H	-2.420600	-1.156700	-2.211200
C	-2.766100	0.004800	-0.402400
H	-2.742700	0.901300	-1.041500
C	-1.752800	-2.520300	0.474400
H	-1.513000	-3.474900	0.949000
C	-4.501300	-1.197100	-1.530200
H	-4.752700	-0.542900	-2.377600
H	-4.960200	-2.174200	-1.717700
N	-4.036400	0.051100	0.368200
C	-4.280300	0.890600	1.519900
H	-3.462000	0.774500	2.242200
H	-5.200700	0.526200	1.990600
C	-5.065400	-0.561100	-0.279200
O	-6.237100	-0.567400	0.083800
C	-2.604300	-2.505000	-0.560000
H	-3.041100	-3.434800	-0.928800
C	-4.456700	2.352700	1.177800
H	-5.241700	2.445200	0.407700
H	-4.811800	2.887600	2.075300
O	-3.221800	2.867200	0.725200
H	-3.369200	3.761300	0.396800
P	1.771300	-2.311200	0.760300
C	3.513800	-1.921300	1.185700
H	3.983200	-2.787800	1.666700
H	4.087100	-1.655200	0.292100

C	1.239300	-3.106100	2.321500
H	1.245100	-2.376900	3.138900
H	0.234700	-3.528900	2.228700
C	1.912700	-3.739100	-0.371300
H	2.513600	-4.536600	0.082100
H	0.909500	-4.120800	-0.593900
H	1.941400	-3.912300	2.566200
H	3.534400	-1.071800	1.880500
H	2.378900	-3.425200	-1.311700
N	1.186000	0.749800	1.661800
N	2.028800	1.807600	1.558700
N	3.198800	1.276600	-0.610800
N	2.535300	0.161300	-0.995400
N	1.175800	2.709400	-0.632600
N	0.283200	1.749300	-0.987800
C	0.986300	0.551000	2.970800
H	0.334700	-0.245500	3.311400
C	1.706500	1.479100	3.725400
H	1.745600	1.572100	4.801600
C	2.353300	2.259700	2.783300
H	3.017300	3.108200	2.893400
C	4.504700	0.234700	-2.068800
H	5.332500	-0.021300	-2.715100
C	4.383500	1.343100	-1.247600
H	5.047800	2.181800	-1.079200
C	-0.560800	2.310100	-1.857900
H	-1.357000	1.720800	-2.298000
C	-0.229200	3.652100	-2.067000
H	-0.726100	4.365600	-2.709500
C	0.882500	3.859400	-1.271500
H	1.493400	4.739900	-1.114500
B	2.444600	2.367000	0.186500
H	3.133100	3.340800	0.324100
C	3.312400	-0.470000	-1.881600
H	2.978400	-1.399300	-2.330600

Compound 12 Electronic Energy: -2012.565689 Hartree

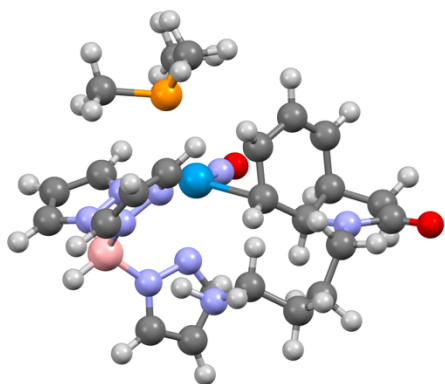


W	0.816600	-0.169100	-0.396900
O	0.344500	-0.229900	-3.343700
N	0.542200	-0.203400	-2.141800
P	1.873500	-2.464900	-0.296500
C	3.525900	-2.490500	0.505000
H	3.897400	-3.520300	0.568600
H	4.244500	-1.886000	-0.057300
C	1.067700	-3.840600	0.604500
H	0.932200	-3.574000	1.658600
H	0.091200	-4.075500	0.169300
C	2.182300	-3.216900	-1.934700
H	2.681500	-4.187800	-1.830000
H	1.226600	-3.354900	-2.454000
H	1.706900	-4.729800	0.545600
H	3.440800	-2.078300	1.518900
H	2.809400	-2.552200	-2.539000
N	1.258400	-0.074700	1.837400
N	2.101000	0.868600	2.326200
N	3.581100	1.230000	0.318800
N	2.971300	0.453000	-0.608000
N	1.618100	2.705100	0.656200
N	0.781100	2.067600	-0.200200
C	0.873100	-0.819000	2.880900
H	0.181500	-1.641800	2.738500
C	1.472300	-0.362900	4.057100
H	1.356700	-0.757000	5.057000
C	2.244100	0.713200	3.655200
H	2.882200	1.383600	4.217600
C	5.092100	0.816100	-1.250400
H	6.009800	0.796800	-1.821400
C	4.855200	1.464000	-0.050300
H	5.495600	2.086300	0.562700
C	0.149300	3.013200	-0.902000

H	-0.564300	2.732900	-1.670400
C	0.561500	4.284800	-0.489400
H	0.225900	5.243200	-0.860100
C	1.499800	4.039500	0.496100
H	2.099600	4.714900	1.093600
B	2.731700	1.929900	1.408300
H	3.409600	2.685800	2.048900
C	3.874000	0.205100	-1.562400
H	3.605600	-0.405100	-2.418000
C	-0.945200	-1.437300	0.033300
H	-0.854300	-2.033300	0.947000
C	-1.301400	-0.044800	0.196500
H	-1.386300	0.324100	1.226700
C	-3.610000	-0.470500	-0.745000
H	-4.249300	-0.154000	-1.583600
C	-3.194400	-1.961400	-0.941100
H	-3.687200	-2.340500	-1.844900
C	-1.678300	-2.142800	-1.091400
H	-1.363200	-1.754500	-2.068900
H	-1.455500	-3.220400	-1.104800
C	-4.528400	-1.691900	1.076400
O	-5.177400	-1.925300	2.091300
C	-2.401700	0.490000	-0.692800
H	-2.044000	0.539300	-1.745400
N	-2.805800	1.807300	-0.222500
H	-1.967500	2.344300	-0.029500
N	-4.417500	-0.476100	0.474900
C	-3.741400	-2.700100	0.282800
H	-4.401400	-3.537100	0.027500
H	-2.946500	-3.112000	0.920000
C	-3.695900	2.555900	-1.106500
H	-3.250800	3.536700	-1.332200
H	-3.798300	2.041100	-2.078300
C	-5.069900	2.775800	-0.489900
H	-5.674600	3.383600	-1.178700
H	-4.942400	3.378300	0.423300
C	-5.228900	0.636300	0.959700
H	-6.020200	0.164200	1.554300
H	-4.643800	1.261300	1.648500
C	-5.850500	1.515700	-0.127700
H	-6.055000	0.913400	-1.025300
H	-6.835300	1.833500	0.239600



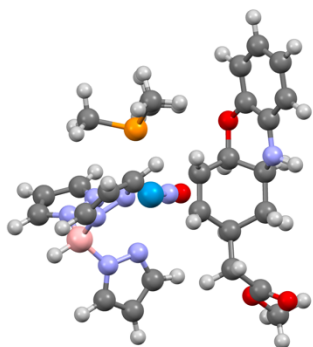
Compound 13 Electronic Energy: -2012.568747 Hartree



W	0.657000	-0.534500	-0.192200
O	0.449600	-2.610800	-2.322400
N	0.504200	-1.767800	-1.448000
C	-0.910300	-1.388400	1.163800
H	-0.719600	-1.146300	2.212100
C	-1.453900	-0.354500	0.307300
H	-1.577400	0.624500	0.781000
C	-2.658000	-2.152500	-1.107600
H	-2.060500	-2.258800	-2.025000
C	-2.594700	-0.694600	-0.613800
H	-2.590800	-0.024200	-1.489200
C	-1.360500	-2.769100	0.938200
H	-1.029900	-3.534000	1.645100
C	-4.151800	-2.345200	-1.380700
H	-4.428000	-2.013900	-2.392000
H	-4.501600	-3.377000	-1.264300
N	-3.907700	-0.540700	0.051800
C	-4.233100	0.611800	0.864200
H	-3.558200	0.638000	1.731700
H	-5.246100	0.450400	1.251600
C	-4.840700	-1.421900	-0.397200
O	-6.024800	-1.442100	-0.079500
C	-2.157700	-3.125400	-0.078000
H	-2.460000	-4.166800	-0.202800
C	-4.160500	1.929500	0.093500
H	-3.324000	1.900900	-0.620800
H	-5.066200	2.033100	-0.519400
C	-3.997500	3.141300	1.006800
H	-4.189600	4.057900	0.431600
H	-4.754400	3.102900	1.805100
C	-2.617400	3.261300	1.642600
H	-2.615600	4.131100	2.313000

H	-2.425000	2.381900	2.287300
N	-1.576800	3.474400	0.634900
H	-0.692400	3.659600	1.105100
H	-1.420700	2.613000	0.112400
P	2.094100	-1.977100	1.317000
C	3.729000	-1.241300	1.710200
H	4.266700	-1.884400	2.417200
H	4.334500	-1.119900	0.806700
C	1.537200	-2.420500	3.003500
H	1.361100	-1.514300	3.593500
H	0.616600	-3.010800	2.974100
C	2.513700	-3.606300	0.604400
H	3.173800	-4.166900	1.277200
H	1.590900	-4.175800	0.442800
H	2.321100	-3.011400	3.492400
H	3.579800	-0.254400	2.166700
H	3.012000	-3.472400	-0.362200
N	1.015600	1.092700	1.383500
N	1.691000	2.221600	1.053600
N	3.125900	1.362700	-0.836600
N	2.665100	0.096000	-0.965400
N	0.934400	2.407700	-1.339300
N	0.220400	1.260700	-1.481800
C	0.694200	1.209300	2.678500
H	0.136100	0.427000	3.179800
C	1.163800	2.418200	3.196300
H	1.060500	2.792300	4.205100
C	1.791200	3.030200	2.124900
H	2.300800	3.982500	2.044100
C	4.698300	0.222600	-1.906800
H	5.611600	-0.045600	-2.419300
C	4.344900	1.461800	-1.400500
H	4.866000	2.411100	-1.411400
C	-0.606500	1.449000	-2.515900
H	-1.264300	0.650000	-2.838000
C	-0.446300	2.733100	-3.044500
H	-0.974600	3.178500	-3.875700
C	0.546000	3.303200	-2.268300
H	1.010600	4.280600	-2.309100
B	2.156400	2.482000	-0.390400
H	2.685400	3.556600	-0.469700
C	3.604300	-0.597500	-1.617000
H	3.449800	-1.649300	-1.832600

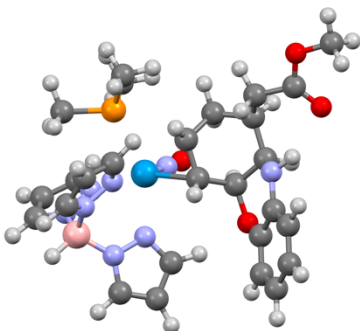
Compound 14 Electronic Energy: -2221.859302 Hartree



W	0.762100	-0.321700	-0.303700
O	0.304800	0.708100	-3.067000
N	0.494600	0.282300	-1.941700
P	-0.208300	-2.626400	-0.753500
C	0.998600	-4.006900	-0.630000
H	0.469100	-4.965400	-0.691200
H	1.742800	-3.961600	-1.430100
C	-1.519700	-3.312300	0.325900
H	-1.112000	-3.486600	1.328300
H	-2.376800	-2.639600	0.400700
C	-0.903400	-2.829000	-2.431800
H	-1.242400	-3.860700	-2.587900
H	-1.751400	-2.144200	-2.549900
H	-1.851800	-4.273100	-0.087000
H	1.518100	-3.946000	0.335400
H	-0.139400	-2.583000	-3.178100
N	1.214300	-1.119400	1.781300
N	2.496300	-1.216300	2.214000
N	3.689200	-1.528700	0.009700
N	2.670500	-1.368400	-0.868900
N	3.467600	0.745800	0.954800
N	2.400400	1.130100	0.209200
C	0.440500	-1.562700	2.779200
H	-0.638200	-1.572500	2.669400
C	1.221100	-1.955600	3.868500
H	0.886000	-2.354200	4.815700
C	2.522500	-1.715700	3.463200
H	3.466700	-1.860800	3.973600
C	4.363300	-2.411800	-1.909900
H	4.955500	-2.902100	-2.669900
C	4.718700	-2.149700	-0.598100
H	5.634600	-2.347400	-0.054700
C	2.654300	2.368300	-0.221800
H	1.935700	2.883900	-0.850400

C	3.891400	2.809600	0.259600
H	4.364400	3.767300	0.092700
C	4.374500	1.743400	0.995300
H	5.300900	1.614500	1.541200
B	3.672400	-0.741300	1.343300
H	4.710100	-0.884000	1.930000
C	3.071800	-1.890400	-2.031400
H	2.406600	-1.878800	-2.888600
C	-1.347000	0.003400	0.281400
H	-1.744700	-0.646600	1.067600
C	-0.544000	1.137800	0.700700
H	-0.302700	1.172000	1.771100
C	-2.441600	2.714600	0.133400
H	-2.687800	3.583300	-0.493600
C	-3.272000	1.501500	-0.309500
H	-3.917900	1.774600	-1.163800
C	-2.377700	0.347300	-0.767700
H	-1.891000	0.660600	-1.700600
C	-0.913500	2.501200	0.135800
H	-0.555600	2.589200	-0.902400
H	-2.748700	2.976800	1.157800
C	-0.532600	4.983500	0.402300
O	-1.209400	5.842000	0.925200
O	0.062800	5.144800	-0.791200
C	-0.167300	6.400600	-1.430700
H	0.376500	6.365300	-2.376000
H	-1.235300	6.550500	-1.619000
H	0.205500	7.225600	-0.815500
O	-3.174100	-0.781600	-1.154400
N	-4.081000	1.011700	0.801400
H	-4.646400	1.726300	1.248300
C	-6.531000	-1.764400	1.075500
C	-6.038700	-2.639900	0.110100
C	-4.905800	-2.288900	-0.620200
C	-5.896300	-0.546700	1.300900
H	-7.414900	-2.024200	1.654100
H	-6.528200	-3.593200	-0.074800
H	-4.487400	-2.951400	-1.377700
H	-6.277000	0.148200	2.049300
C	-4.269100	-1.071900	-0.396800
C	-4.759300	-0.179500	0.575000
C	-0.263000	3.617800	0.960600
H	0.821700	3.463100	1.013300
H	-0.657400	3.593300	1.984200

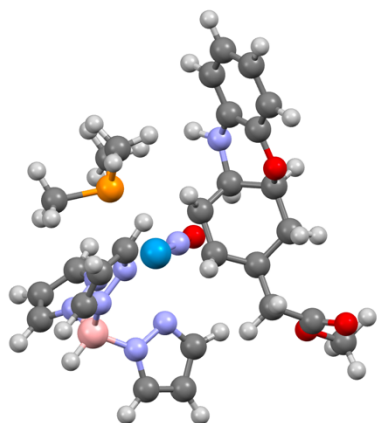
Compound 15 Electronic Energy: -2221.855662 Hartree



W	1.169200	-0.311900	-0.407400
O	0.876400	-0.904300	-3.317700
N	0.994000	-0.638400	-2.134100
C	-0.838700	-1.078000	0.108000
H	-0.939500	-1.395700	1.151400
C	-0.902700	0.348200	-0.159000
H	-1.016600	1.018200	0.702400
C	-3.215700	0.081200	-1.099300
H	-3.803100	0.281700	-2.012600
C	-3.116800	-1.466400	-0.901400
H	-3.587300	-1.933400	-1.778900
C	-1.642200	-1.922000	-0.861800
H	-1.222800	-1.847900	-1.873800
H	-1.605500	-2.990100	-0.605200
N	-3.817000	0.762300	0.042000
C	-1.819000	0.690100	-1.312600
H	-1.421700	0.301100	-2.257500
O	-1.931900	2.097700	-1.551700
H	-4.770600	0.452700	0.211700
C	-3.837600	-2.012200	0.336800
H	-3.567800	-1.430900	1.230500
H	-3.512800	-3.041500	0.528100
C	-5.334000	-2.004200	0.239800
O	-6.001000	-1.146500	-0.308900
O	-5.874900	-3.059000	0.854700
C	-7.304100	-3.111400	0.858000
H	-7.571600	-4.012700	1.411400
H	-7.723800	-2.229100	1.350700
H	-7.691700	-3.170000	-0.163600
C	-4.461400	2.921600	0.966400
C	-3.672300	2.143200	0.112800
C	-2.692300	2.792500	-0.659800
C	-2.510000	4.167600	-0.566700
C	-3.307100	4.928900	0.285600

C	-4.284200	4.299200	1.053200
H	-5.224100	2.421500	1.563200
H	-1.743600	4.627800	-1.188900
H	-3.161100	6.004800	0.347700
H	-4.915200	4.879400	1.723100
P	1.690900	-2.718800	0.164900
C	3.318600	-2.957700	0.980300
H	3.448200	-4.011300	1.255400
H	4.137500	-2.657600	0.318900
C	0.631800	-3.665300	1.321500
H	0.628800	-3.182200	2.304700
H	-0.397600	-3.734700	0.957400
C	1.780800	-3.828200	-1.285200
H	2.050600	-4.846200	-0.979300
H	0.809600	-3.847300	-1.792800
H	1.040200	-4.677300	1.430100
H	3.359000	-2.343300	1.888900
H	2.531200	-3.452700	-1.989800
N	1.550000	0.033500	1.829100
N	2.632900	0.752600	2.221300
N	4.184400	0.496000	0.241800
N	3.405800	-0.217700	-0.603100
N	2.609000	2.412000	0.343300
N	1.592300	1.904600	-0.402200
C	0.965000	-0.409700	2.949000
H	0.063700	-1.009200	2.896300
C	1.671000	0.015100	4.076100
H	1.443300	-0.180500	5.114600
C	2.722800	0.754000	3.563600
H	3.526300	1.287700	4.056000
C	5.550900	-0.465300	-1.214800
H	6.437500	-0.778600	-1.748000
C	5.477700	0.366400	-0.109900
H	6.249900	0.886500	0.443600
C	1.033900	2.934700	-1.044300
H	0.172100	2.765700	-1.680100
C	1.689900	4.126000	-0.720200
H	1.467500	5.122600	-1.076200
C	2.681100	3.745100	0.166000
H	3.434000	4.323300	0.687800
B	3.516400	1.503200	1.203100
H	4.347800	2.153300	1.776200
C	4.221300	-0.796800	-1.490600
H	3.810700	-1.426900	-2.272300

Compound 16 Electronic Energy: -2221.858350 Hartree



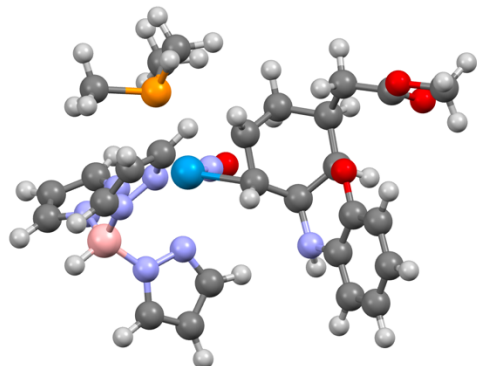
W	0.755400	-0.320400	-0.324200
O	0.327300	0.662800	-3.110200
N	0.499200	0.251800	-1.976200
P	-0.021600	-2.710100	-0.701500
C	1.225600	-3.966800	-0.209900
H	0.803100	-4.971900	-0.328400
H	2.131100	-3.887300	-0.819100
C	-1.476600	-3.390100	0.177200
H	-1.300900	-3.356400	1.258300
H	-2.384300	-2.824500	-0.046900
C	-0.354100	-3.133200	-2.450500
H	-0.696800	-4.170700	-2.544400
H	-1.112400	-2.458800	-2.864800
H	-1.618500	-4.435700	-0.121700
H	1.496100	-3.816500	0.843100
H	0.565000	-3.005900	-3.033700
N	1.200100	-1.062400	1.782700
N	2.476600	-1.109600	2.236800
N	3.724700	-1.396200	0.060000
N	2.721800	-1.289300	-0.843800
N	3.383800	0.879000	0.968500
N	2.317000	1.207700	0.195400
C	0.426600	-1.537100	2.766400
H	-0.649100	-1.588300	2.637800
C	1.203700	-1.903200	3.867600
H	0.868500	-2.315600	4.808800
C	2.501500	-1.611400	3.485200
H	3.441800	-1.719500	4.011700
C	4.473900	-2.293200	-1.824600
H	5.100900	-2.775900	-2.561300
C	4.789500	-1.992000	-0.511000

H	5.699100	-2.145200	0.056800
C	2.528700	2.448400	-0.251200
H	1.800400	2.927100	-0.897600
C	3.737000	2.947300	0.247100
H	4.173400	3.921200	0.074100
C	4.248200	1.913800	1.009500
H	5.168100	1.832000	1.575300
B	3.646700	-0.592300	1.382100
H	4.678400	-0.681100	1.989600
C	3.168100	-1.820800	-1.986200
H	2.526500	-1.844200	-2.860400
C	-1.387700	-0.062700	0.199000
H	-1.786500	-0.750000	0.953400
C	-0.620800	1.077600	0.667300
H	-0.401000	1.093300	1.742700
C	-2.524800	2.635100	0.103300
H	-2.782100	3.514200	-0.504100
C	-3.310500	1.421600	-0.382500
H	-4.001000	1.694800	-1.197000
C	-2.410900	0.285400	-0.874200
H	-1.902200	0.658100	-1.774600
C	-0.996300	2.447400	0.126400
H	-0.623200	2.561700	-0.903800
H	-2.868300	2.852600	1.125300
C	-0.374500	3.556900	0.982600
H	0.706800	3.397700	1.075700
H	-0.808700	3.530100	1.989900
C	-0.614700	4.925200	0.417300
O	-1.309400	5.786400	0.911500
O	0.034200	5.086200	-0.748600
C	-0.159600	6.344400	-1.395400
H	0.423000	6.306100	-2.317100
H	-1.217500	6.502900	-1.628100
H	0.193500	7.165800	-0.763900
C	-6.558700	-1.701200	1.180000
C	-6.161000	-2.603800	0.197200
C	-5.073500	-2.313000	-0.621600
C	-5.863600	-0.501700	1.329300
H	-7.406000	-1.921000	1.825200
H	-6.693700	-3.543400	0.065600
H	-4.750400	-3.017500	-1.388700
H	-6.147700	0.228100	2.085400
C	-4.362700	-1.115500	-0.479700
C	-4.776300	-0.207400	0.516400
N	-3.292400	-0.790000	-1.292600
H	-2.874300	-1.557700	-1.803300



O    -4.107000    0.962600    0.723900

Compound 17 Electronic Energy: -2221.857058 Hartree

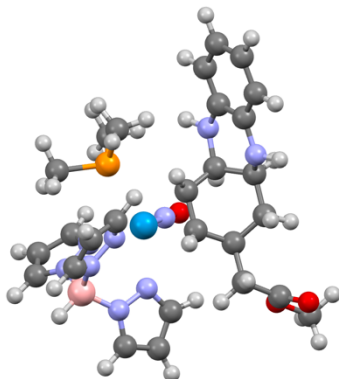


W	1.283400	-0.268900	-0.389600
O	1.088100	-1.017900	-3.272500
N	1.170300	-0.697100	-2.099300
C	-0.661800	-1.196500	0.122800
H	-0.750100	-1.513800	1.167300
C	-0.842400	0.214600	-0.156700
H	-0.985700	0.870500	0.710800
C	-3.090600	-0.287800	-1.082200
H	-3.800400	-0.056700	-1.893800
C	-2.839800	-1.806300	-1.017200
H	-3.184600	-2.222400	-1.974100
C	-1.341700	-2.127900	-0.862600
H	-0.870600	-2.039500	-1.850200
H	-1.229000	-3.182400	-0.570200
C	-1.814300	0.543100	-1.281800
H	-1.393000	0.287200	-2.264300
C	-3.656800	-2.478400	0.083700
H	-3.310300	-2.183800	1.080100
H	-3.520900	-3.566900	0.005000
C	-5.128400	-2.208300	-0.034800
O	-5.729100	-2.076600	-1.080400
O	-5.726300	-2.168100	1.164100
C	-7.134600	-1.939700	1.137000
H	-7.456900	-1.897900	2.178800
H	-7.365900	-0.994400	0.635400
H	-7.653800	-2.752500	0.618500
C	-5.039300	1.876600	1.017300
C	-3.999000	1.457100	0.196200
C	-3.268200	2.381400	-0.573800
C	-3.657800	3.726200	-0.531700

C	-4.712100	4.141300	0.274100
C	-5.396800	3.221100	1.067700
H	-5.566400	1.121800	1.599500
H	-3.104200	4.444100	-1.136600
H	-4.991900	5.192600	0.289600
H	-6.213900	3.542800	1.709200
N	-2.175100	1.957400	-1.315700
H	-2.046300	2.434900	-2.198400
O	-3.702600	0.127400	0.147800
P	2.015400	-2.576600	0.337500
C	3.612800	-2.601800	1.244300
H	3.832400	-3.619500	1.588900
H	4.432800	-2.255200	0.607400
C	0.999500	-3.581200	1.483400
H	0.882300	-3.057100	2.438300
H	0.008900	-3.781800	1.064800
C	2.295100	-3.736500	-1.048000
H	2.667400	-4.700600	-0.680800
H	1.352000	-3.893000	-1.584200
H	1.508600	-4.535100	1.667100
H	3.542700	-1.936500	2.114700
H	3.022600	-3.310600	-1.748000
N	1.550700	0.266400	1.818900
N	2.509400	1.151800	2.190200
N	4.164000	0.901200	0.300900
N	3.510200	0.035300	-0.508300
N	2.403200	2.641600	0.163400
N	1.519600	1.957200	-0.607900
C	0.981200	-0.171900	2.948300
H	0.171900	-0.892200	2.908400
C	1.574500	0.424900	4.062700
H	1.330600	0.274400	5.104900
C	2.540300	1.261300	3.530800
H	3.244800	1.931600	4.007600
C	5.698300	-0.021900	-1.006500
H	6.639300	-0.278400	-1.472900
C	5.480100	0.886500	0.015400
H	6.162900	1.534000	0.551700
C	0.994500	2.835200	-1.465200
H	0.257000	2.507200	-2.187100
C	1.531000	4.108700	-1.252700
H	1.300800	5.022700	-1.782300
C	2.422800	3.936500	-0.209800
H	3.074500	4.638900	0.295200
B	3.349600	1.910000	1.145400
H	4.082000	2.691500	1.688500

C	4.427400	-0.521300	-1.305900
H	4.127700	-1.257800	-2.043700

Compound 18 Electronic Energy: -2201.980776 Hartree

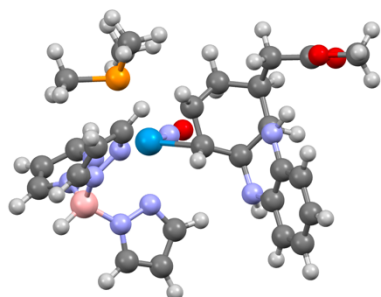


W	0.767300	-0.317800	-0.317500
O	0.293900	0.620600	-3.111800
N	0.481100	0.228700	-1.973300
P	-0.031200	-2.708900	-0.637300
C	1.214600	-3.963600	-0.136700
H	0.788300	-4.968700	-0.241800
H	2.117300	-3.893900	-0.751300
C	-1.479000	-3.360100	0.273700
H	-1.286700	-3.307200	1.351200
H	-2.384200	-2.789500	0.052000
C	-0.384700	-3.168100	-2.373600
H	-0.753100	-4.198900	-2.439000
H	-1.127300	-2.486000	-2.803300
H	-1.634000	-4.410100	-0.002800
H	1.490300	-3.802600	0.913200
H	0.534700	-3.079900	-2.963700
N	1.254900	-1.031600	1.790800
N	2.541100	-1.082400	2.216400
N	3.739100	-1.407200	0.017200
N	2.716100	-1.308700	-0.864700
N	3.432100	0.882400	0.900400
N	2.351400	1.206100	0.144500
C	0.500800	-1.488200	2.797800
H	-0.577900	-1.533300	2.694400
C	1.300300	-1.846400	3.885600
H	0.983700	-2.244600	4.839300
C	2.591000	-1.568900	3.470100
H	3.542300	-1.677100	3.976400
C	4.440500	-2.336300	-1.870200

H	5.048100	-2.832900	-2.613800
C	4.787700	-2.016900	-0.569000
H	5.709300	-2.166300	-0.019900
C	2.563700	2.436700	-0.328600
H	1.826000	2.907500	-0.969800
C	3.786100	2.934800	0.134700
H	4.226400	3.901700	-0.065100
C	4.305300	1.910700	0.904400
H	5.236500	1.831300	1.451700
B	3.694900	-0.584600	1.329100
H	4.739300	-0.671400	1.914900
C	3.133400	-1.859700	-2.008800
H	2.471600	-1.892200	-2.867700
C	-1.362700	-0.040100	0.252700
H	-1.745300	-0.715100	1.026500
C	-0.578300	1.102800	0.683500
H	-0.330200	1.132700	1.752700
C	-2.502600	2.645100	0.196900
H	-2.791500	3.551800	-0.354500
C	-3.309600	1.443900	-0.313100
H	-3.932000	1.750100	-1.174000
C	-2.407700	0.298400	-0.801600
H	-1.906500	0.663100	-1.709400
C	-0.974700	2.466800	0.141900
H	-0.651300	2.572100	-0.906000
H	-2.777300	2.821300	1.249000
C	-0.618900	4.952000	0.417900
O	-1.281200	5.803600	0.970300
O	-0.069500	5.123700	-0.796200
C	-0.331700	6.380600	-1.420700
H	0.175700	6.352700	-2.386300
H	-1.406900	6.524800	-1.567700
H	0.059300	7.205600	-0.816800
C	-6.670800	-1.790200	1.034600
C	-6.191000	-2.678600	0.077600
C	-5.052400	-2.354900	-0.659700
C	-6.006000	-0.581800	1.246700
H	-7.559100	-2.027700	1.616100
H	-6.695900	-3.625900	-0.100600
H	-4.666100	-3.041200	-1.414600
H	-6.368300	0.125300	1.993500
C	-4.379700	-1.146300	-0.458900
C	-4.863400	-0.247400	0.521300
C	-0.317800	3.585800	0.958500
H	0.769800	3.446800	0.982100
H	-0.685000	3.549100	1.991900

N	-3.276100	-0.790400	-1.215500
H	-2.853900	-1.531400	-1.759900
N	-4.149900	0.924900	0.764100
H	-4.694900	1.640000	1.234600

Compound 19 Electronic Energy: -2201.976988 Hartree

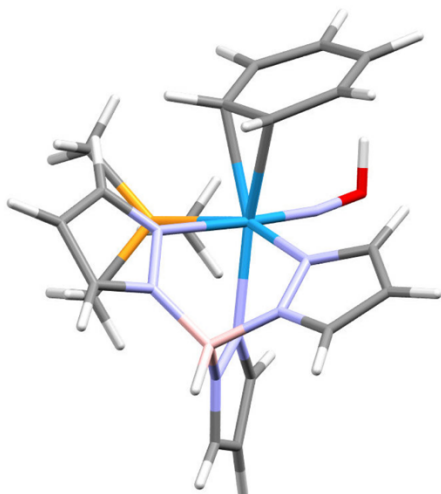


W	1.270700	-0.308400	-0.371600
O	0.998500	-1.210400	-3.204200
N	1.110000	-0.826800	-2.052300
C	-0.684300	-1.162600	0.238800
H	-0.754600	-1.428800	1.299200
C	-0.837100	0.234800	-0.106900
H	-0.929400	0.933600	0.733400
C	-3.147100	-0.247800	-0.912900
H	-3.857100	-0.034800	-1.735000
C	-2.896400	-1.775400	-0.871400
H	-3.204200	-2.157100	-1.855200
C	-1.403000	-2.120000	-0.690200
H	-0.935800	-2.092300	-1.683000
H	-1.312500	-3.161700	-0.348100
N	-3.674500	0.292900	0.341000
C	-1.848300	0.539400	-1.203600
H	-1.476200	0.224600	-2.189300
H	-4.443100	-0.224400	0.752400
C	-3.760200	-2.510900	0.153500
H	-3.525600	-2.210700	1.181800
H	-3.541300	-3.585500	0.080400
C	-5.231100	-2.360100	-0.120500
O	-5.744000	-2.445400	-1.214700
O	-5.926700	-2.112800	1.001500
C	-7.338400	-1.955900	0.831300
H	-7.745300	-1.776700	1.827500
H	-7.555800	-1.104700	0.178500
H	-7.780300	-2.860200	0.402100

C	-4.919800	2.231700	1.140100
C	-3.933200	1.665700	0.330200
C	-3.176400	2.500200	-0.524000
C	-3.462900	3.868900	-0.557100
C	-4.459600	4.417900	0.244300
C	-5.183700	3.598600	1.108100
H	-5.497400	1.570600	1.787800
H	-2.878600	4.500900	-1.226300
H	-4.661900	5.486000	0.197100
H	-5.960600	4.015000	1.745700
N	-2.151600	1.962900	-1.293300
H	-2.025700	2.394500	-2.198900
P	1.964800	-2.591600	0.458500
C	3.590500	-2.616800	1.314100
H	3.792300	-3.620600	1.706700
H	4.398500	-2.330400	0.633400
C	0.959400	-3.503300	1.688600
H	0.875600	-2.920400	2.612500
H	-0.045100	-3.707200	1.306000
C	2.166800	-3.833700	-0.868200
H	2.524100	-4.786800	-0.459700
H	1.203400	-3.991600	-1.366400
H	1.453400	-4.455400	1.917500
H	3.569200	-1.903900	2.148700
H	2.882900	-3.467900	-1.612500
N	1.603400	0.341100	1.796200
N	2.587600	1.225200	2.096700
N	4.191300	0.837900	0.186900
N	3.500600	-0.057700	-0.556700
N	2.463300	2.605100	-0.006400
N	1.550100	1.897500	-0.720400
C	1.052000	-0.022700	2.960500
H	0.227000	-0.726000	2.978200
C	1.682700	0.621500	4.026800
H	1.460300	0.533400	5.080900
C	2.652100	1.407200	3.428200
H	3.380400	2.088000	3.851400
C	5.674200	-0.187500	-1.103300
H	6.598000	-0.489200	-1.576800
C	5.499200	0.780200	-0.128700
H	6.207600	1.442000	0.354400
C	1.026600	2.736600	-1.616700
H	0.268800	2.383800	-2.305100
C	1.593800	4.008100	-1.487700
H	1.371800	4.895500	-2.064000
C	2.502500	3.875900	-0.453600

H	3.179100	4.591100	-0.002300
B	3.417500	1.908000	0.993000
H	4.178100	2.702300	1.475600
C	4.386700	-0.676400	-1.343700
H	4.055400	-1.446900	-2.031700

**Compound 20H Electronic Energy in DCM: - 1592.79908 Hartree**

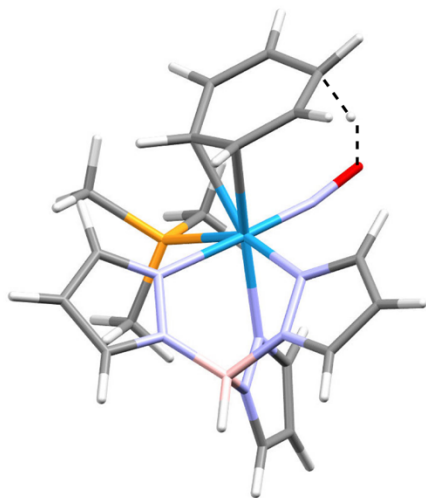


W	-0.37180	0.15270	-0.14030
P	-1.02920	-2.30900	-0.10880
N	0.89160	-0.45680	1.64430
N	2.24410	-0.33600	1.57950
N	2.60270	-0.53770	-0.89720
N	1.31910	-0.61270	-1.32130
N	2.35730	1.70310	0.12060
N	1.03340	1.87450	-0.12400
N	-1.39080	0.55700	-1.48750
C	0.61500	-0.99010	2.84470
H	-0.40950	-1.17810	3.14180
C	1.78670	-1.22370	3.55830
H	1.88610	-1.64070	4.55010
C	2.79630	-0.79090	2.71470
H	3.87120	-0.76860	2.84350
C	2.64800	-1.47240	-2.90760
H	2.98870	-1.92760	-3.82650
C	3.41720	-1.04940	-1.83630
H	4.48790	-1.06540	-1.67610
C	0.86100	3.15490	-0.46850
H	-0.12720	3.51870	-0.72300
C	2.08200	3.83110	-0.43930

H	2.26650	4.87250	-0.66150
C	3.00240	2.87070	-0.06070
H	4.07240	2.92950	0.09520
C	0.41620	-3.43000	-0.14030
H	0.07170	-4.46960	-0.09300
H	1.00490	-3.28880	-1.05190
C	-2.00240	-3.04100	1.25600
H	-1.45700	-2.96620	2.20270
H	-2.97860	-2.55900	1.36440
C	-2.00960	-2.76970	-1.57690
H	-2.20860	-3.84780	-1.57610
H	-2.96240	-2.22770	-1.55890
B	2.94380	0.29500	0.36000
H	4.12840	0.34400	0.53110
C	-2.15070	0.23550	1.29510
H	-2.00830	-0.49210	2.09370
C	-1.43620	1.49630	1.33670
H	-0.69700	1.64580	2.12610
C	-2.10360	2.68670	0.84970
H	-1.63150	3.65220	1.02360
C	-3.99810	1.35890	0.12580
C	-3.45500	0.22930	0.66130
H	-4.02650	-0.69910	0.65580
C	1.33760	-1.17000	-2.54020
H	0.41240	-1.32610	-3.08250
H	-2.16040	-4.10250	1.03090
H	1.05610	-3.22600	0.72710
H	-1.47520	-2.50210	-2.49420
C	-3.31630	2.62080	0.24180
H	-4.99590	1.32750	-0.30960
H	-3.80710	3.52500	-0.11100
O	-2.28680	0.83700	-2.39950
H	-3.12070	1.01320	-1.89800



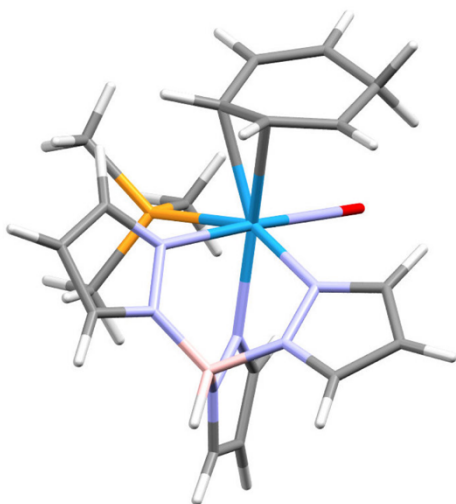
**TS for 20H to 21 Electronic Energy in DCM: - 1592.78603 Hartree**



O	-2.12300	1.58040	-2.07690
N	1.14050	1.82950	-0.01600
N	2.44580	1.55340	0.23590
N	0.86370	-0.58740	1.64760
N	2.21980	-0.56490	1.56130
N	1.24650	-0.58760	-1.35040
N	2.53590	-0.62510	-0.93490
N	-1.32690	0.88800	-1.40430
C	3.17390	2.67900	0.12100
C	2.32990	3.72160	-0.21670
C	1.06680	3.13530	-0.29850
C	2.75940	-1.13440	2.65100
C	1.73610	-1.54720	3.48640
C	0.57200	-1.17940	2.81630
C	3.31450	-1.06920	-1.93590
C	2.51700	-1.33260	-3.03820
C	1.22770	-1.00450	-2.62420
B	2.94000	0.09490	0.37510
H	4.12780	0.05850	0.52680
H	4.24380	2.65240	0.28600
H	2.59090	4.75680	-0.38380
H	0.11670	3.58430	-0.56260
H	3.83520	-1.19990	2.75470
H	1.82100	-2.03730	4.44560
H	-0.45590	-1.31360	3.13040
H	4.38480	-1.15380	-1.79480
H	2.82760	-1.70150	-4.00520
H	0.29090	-1.05100	-3.16740
C	0.26230	-3.41810	-0.51420

H	-0.13350	-4.44040	-0.52050
H	0.81020	-3.24190	-1.44420
H	0.95520	-3.30860	0.32950
C	-2.18690	-2.50540	-1.77180
H	-2.47690	-3.56020	-1.84560
H	-3.08510	-1.88440	-1.67680
H	-1.65620	-2.21180	-2.68350
W	-0.37100	0.19920	-0.10240
P	-1.12270	-2.23910	-0.31560
C	-2.05350	-3.05470	1.02900
H	-2.25020	-4.09080	0.72930
H	-1.46070	-3.06590	1.94940
H	-3.00910	-2.55870	1.21920
C	-3.99840	1.25070	0.21260
C	-3.47350	0.15060	0.78470
C	-2.10650	0.12170	1.31320
C	-1.43260	1.41470	1.47890
C	-2.01990	2.54350	0.86300
C	-3.19640	2.47650	0.09190
H	-4.08690	-0.74280	0.89780
H	-1.94810	-0.60360	2.11010
H	-0.72390	1.58350	2.28930
H	-1.54530	3.51510	0.99960
H	-3.71370	3.42090	-0.08780
H	-5.01200	1.25210	-0.18050
H	-2.69150	2.24030	-1.13310

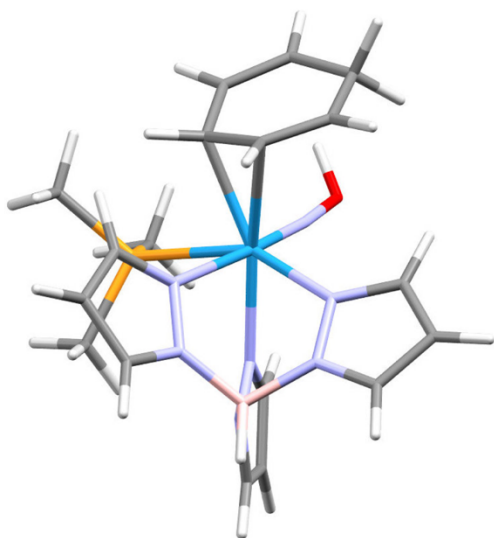
**Compound 21 Electronic Energy in DCM: - 1592.81301 Hartree**



W	-0.37630	0.28470	-0.02260
P	-1.30000	-2.08400	-0.38090
N	0.79990	-0.70670	1.64260
N	2.14760	-0.82110	1.54300
N	2.40720	-0.79920	-0.96040
N	1.12780	-0.58260	-1.35510
N	2.56360	1.32410	0.28950
N	1.29710	1.75040	0.03250
N	-1.24870	0.89890	-1.44030
C	0.44980	-1.33310	2.77590
H	-0.58690	-1.37160	3.08860
C	1.57240	-1.86080	3.41130
H	1.60890	-2.41360	4.33910
C	2.63050	-1.50880	2.59120
H	3.69390	-1.69340	2.67910
C	2.29970	-1.32450	-3.11460
H	2.56230	-1.64510	-4.11260
C	3.12690	-1.24010	-2.00630
H	4.18340	-1.44770	-1.88970
C	1.38360	3.04750	-0.29170
H	0.49600	3.60540	-0.56630
C	2.70750	3.47790	-0.22790
H	3.09100	4.46910	-0.42320
C	3.42040	2.34930	0.13600
H	4.48110	2.19660	0.29160
C	0.00750	-3.34490	-0.59840
H	-0.46310	-4.33030	-0.69460
H	0.61200	-3.15180	-1.48890

C	-2.32830	-2.90110	0.89080
H	-1.79900	-2.94370	1.84830
H	-3.28540	-2.38980	1.02630
C	-2.34340	-2.22170	-1.86950
H	-2.70500	-3.25120	-1.97680
H	-3.19990	-1.54480	-1.77300
B	2.90710	-0.18570	0.37250
H	4.08810	-0.34490	0.49430
C	-2.19100	0.19390	1.35800
H	-2.19980	-0.63340	2.06520
C	-1.41410	1.34660	1.74330
H	-0.67690	1.30810	2.54400
C	-1.54850	2.49070	0.98780
H	-0.85350	3.31000	1.16380
C	-3.76150	1.67860	0.16640
C	-3.48390	0.48230	0.69640
H	-4.22780	-0.31390	0.66760
C	1.05820	-0.88620	-2.65880
H	0.12330	-0.77530	-3.19570
H	-2.52690	-3.92620	0.55610
H	0.66120	-3.34710	0.28250
H	-1.78050	-1.94610	-2.76670
H	-4.72690	1.87290	-0.29600
O	-1.83440	1.27010	-2.41490
C	-2.76220	2.79270	0.17360
H	-2.48800	3.07870	-0.85520
H	-3.20310	3.71260	0.59430

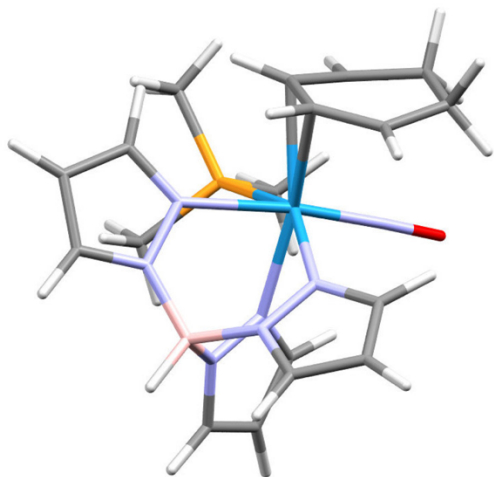
**Compound 21H Electronic Energy in DCM: - 1593.19866 Hartree**



W	-0.37650	0.22730	-0.08620
P	-0.93460	-2.30360	-0.14520
N	0.87650	-0.47190	1.64290
N	2.23310	-0.45030	1.53360
N	2.49490	-0.59030	-0.96240
N	1.19400	-0.57010	-1.34870
N	2.40720	1.61530	0.13740
N	1.08570	1.85420	-0.07240
N	-1.37440	0.59610	-1.45860
C	0.60160	-0.99700	2.85120
H	-0.42020	-1.11330	3.18960
C	1.77530	-1.32130	3.51940
H	1.87670	-1.75300	4.50450
C	2.78610	-0.95420	2.64570
H	3.86340	-1.00930	2.73940
C	2.42770	-1.30890	-3.06280
H	2.71880	-1.67810	-4.03550
C	3.24970	-1.02840	-1.98210
H	4.32460	-1.09430	-1.87000
C	0.96370	3.15480	-0.38560
H	-0.00820	3.57520	-0.61600
C	2.21030	3.76890	-0.36350
H	2.43900	4.80620	-0.56090
C	3.09480	2.75470	-0.03040
H	4.16970	2.76260	0.10020
C	0.55190	-3.35220	-0.23790
H	0.22890	-4.39890	-0.19520
H	1.10330	-3.19000	-1.16790
C	-1.84550	-3.07310	1.23220

H	-1.31490	-2.93400	2.17950
H	-2.86360	-2.68180	1.31710
C	-1.94100	-2.73700	-1.59900
H	-2.11450	-3.81950	-1.60370
H	-2.90610	-2.22170	-1.54250
B	2.93110	0.16940	0.31360
H	4.11900	0.14940	0.43850
C	-2.13380	0.07120	1.27830
H	-2.05890	-0.68490	2.05770
C	-1.54190	1.36830	1.59850
H	-0.77400	1.46120	2.36660
C	-2.01990	2.51160	1.00680
H	-1.52950	3.46140	1.22100
C	-3.95070	1.23970	0.07250
C	-3.43860	0.11090	0.58410
H	-3.99830	-0.82160	0.52070
C	1.14720	-0.99290	-2.62380
H	0.20130	-1.05030	-3.14910
H	-1.90310	-4.14700	1.01860
H	1.20700	-3.14770	0.61660
H	-1.43630	-2.45160	-2.52720
H	-4.93080	1.23790	-0.39980
C	-3.24050	2.54950	0.17990
H	-3.00700	2.98370	-0.80830
H	-3.89570	3.31930	0.62460
O	-2.17360	0.79170	-2.45860
H	-3.07820	0.52490	-2.16070

**Compound 5 Electronic Energy in DCM: - 1593.22091 Hartree**

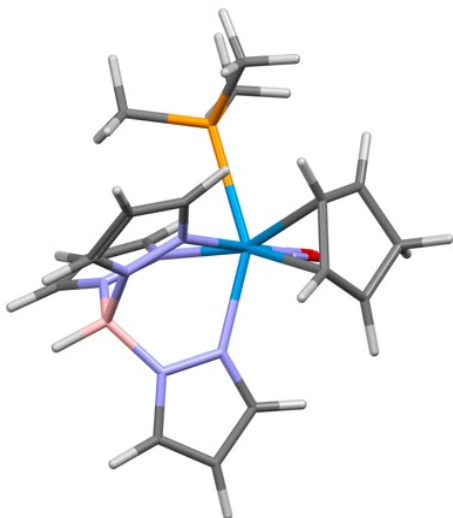


W	-0.41760	0.25180	0.00960
P	-1.16800	-2.19540	-0.46050
N	0.80000	-0.73560	1.62670
N	2.15420	-0.77960	1.52340
N	2.38910	-0.69170	-0.97400
N	1.09740	-0.50900	-1.35190
N	2.47120	1.39790	0.31410
N	1.18500	1.74170	0.03700
N	-1.24040	0.96560	-1.41040
C	0.49230	-1.38090	2.76700
H	-0.53320	-1.48530	3.09650
C	1.64230	-1.84660	3.39370
H	1.71220	-2.39630	4.32110
C	2.67600	-1.43910	2.56790
H	3.74810	-1.56620	2.65040
C	2.28520	-1.10520	-3.15420
H	2.55290	-1.36320	-4.16860
C	3.11560	-1.04380	-2.04620
H	4.18100	-1.21060	-1.94650
C	1.19180	3.03010	-0.34060
H	0.27210	3.52250	-0.63740
C	2.48490	3.53820	-0.28130
H	2.80940	4.54340	-0.50820
C	3.26290	2.46620	0.12410
H	4.33080	2.38270	0.28290
C	0.21930	-3.35110	-0.68620
H	-0.19610	-4.36340	-0.75360
H	0.77830	-3.13680	-1.60060
C	-2.12080	-3.04460	0.84270

H	-1.50800	-3.14830	1.74400
H	-3.06180	-2.54920	1.09430
C	-2.19700	-2.33690	-1.95360
H	-2.54960	-3.36930	-2.05910
H	-3.05580	-1.65990	-1.87780
B	2.88570	-0.09530	0.36790
H	4.07050	-0.21030	0.47530
C	-2.11580	0.13860	1.55490
H	-2.03400	-0.76480	2.15280
C	-1.35670	1.33630	1.86720
H	-0.60860	1.33360	2.65630
C	-1.60980	2.48710	1.15550
H	-0.94510	3.33540	1.31670
C	-3.06640	0.21940	0.54590
H	-3.57780	-0.69250	0.23570
C	1.03170	-0.74410	-2.67410
H	0.09200	-0.65390	-3.20620
H	-2.35430	-4.04840	0.46750
H	0.89260	-3.29890	0.17740
H	-1.61420	-2.06720	-2.84010
O	-1.74290	1.43180	-2.37290
C	-2.80660	2.73090	0.31860
H	-2.51030	3.23580	-0.61080
H	-3.39420	3.48610	0.86190
C	-3.63930	1.48160	0.02990
H	-3.86350	1.38360	-1.03960
H	-4.62860	1.53550	0.51230



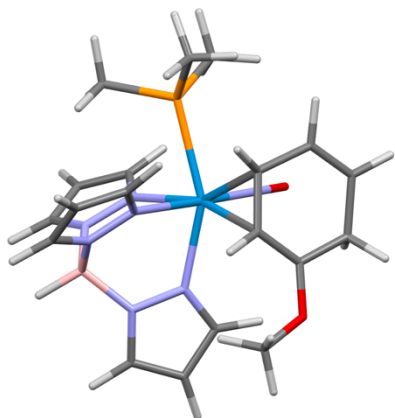
**Dicationic Cyclopentene Electronic Energy: -1553.730555 Hartree**



O	-1.294200	1.898400	-2.451800
N	-0.923600	1.365900	-1.475200
W	-0.356400	0.485000	-0.008700
N	1.644600	1.319700	-0.002700
N	2.733700	0.548800	0.267900
N	0.445600	-0.831700	1.633500
N	1.693400	-1.360000	1.514000
N	0.749900	-0.790400	-1.355100
N	1.904700	-1.404900	-0.984500
C	3.844200	1.287500	0.115200
C	3.487500	2.573300	-0.261800
C	2.103500	2.541000	-0.342900
C	1.961800	-2.159200	2.556800
C	0.864300	-2.171100	3.402100
C	-0.050200	-1.328100	2.788300
C	2.430400	-2.029600	-2.049400
C	1.603500	-1.833600	-3.147300
C	0.575700	-1.033700	-2.671500
B	2.604500	-0.992100	0.339500
H	3.673300	-1.514500	0.437700
H	4.818700	0.844000	0.277200
H	4.142000	3.409700	-0.459000
H	1.422300	3.327200	-0.643400
H	2.919700	-2.658800	2.630300
H	0.752400	-2.703400	4.335300
H	-1.032800	-1.057700	3.151300
H	3.370600	-2.559700	-1.959400
H	1.744100	-2.200700	-4.153700
H	-0.266300	-0.613300	-3.208200

C	-1.023900	-3.145900	-0.448200
H	-1.750400	-3.963700	-0.514700
H	-0.363500	-3.189800	-1.318300
H	-0.429900	-3.270700	0.463600
C	-2.897400	-1.481600	-1.932600
H	-2.241300	-1.486100	-2.807100
H	-3.560800	-2.351600	-1.997700
H	-3.505000	-0.570700	-1.958200
P	-1.929700	-1.567000	-0.388900
C	-3.197000	-1.896300	0.889300
H	-3.771700	-2.776500	0.577600
H	-2.725100	-2.129800	1.849200
H	-3.900300	-1.067900	1.015200
C	-2.693200	1.552500	0.612700
C	-1.915100	1.016900	1.634900
C	-0.776800	1.905200	1.833000
C	-0.910600	2.958500	0.947800
H	-3.607000	1.108700	0.225000
H	-2.199600	0.179900	2.258100
H	0.005400	1.784200	2.575800
H	-0.196100	3.770000	0.847600
C	-2.264200	2.951000	0.316000
H	-2.925000	3.646900	0.866500
H	-2.315300	3.260700	-0.733800

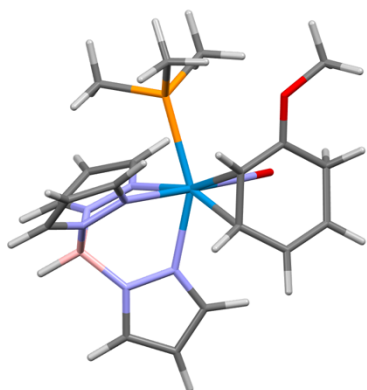
**Compound 28D Electronic Energy: -1707.680460 Hartree**



O	-1.396200	-1.177600	-2.724200
N	-0.918900	-0.830300	-1.678100
W	-0.195800	-0.299100	-0.151200
N	-0.470700	1.853100	-0.551500
N	0.455900	2.758200	-0.138800
N	0.850200	0.402100	1.726100
N	1.661700	1.487500	1.683200
N	1.662100	0.305800	-1.170600
N	2.407000	1.344900	-0.715200
C	0.115200	3.978900	-0.594600
C	-1.061100	3.875900	-1.316100
C	-1.378700	2.517600	-1.275400
C	2.225800	1.687400	2.886400
C	1.772500	0.707500	3.753200
C	0.913000	-0.070800	2.978800
C	3.420600	1.573700	-1.569700
C	3.346100	0.659300	-2.606900
C	2.215500	-0.104500	-2.318000
B	1.840400	2.284200	0.383200
H	2.569300	3.219700	0.555300
H	0.745800	4.833100	-0.381300
H	-1.604000	4.668100	-1.811500
H	-2.215400	1.989500	-1.719200
H	2.907600	2.514800	3.038600
H	2.025300	0.578500	4.795900
H	0.338500	-0.944500	3.264600
H	4.114700	2.384100	-1.384400
H	4.007700	0.567900	-3.456400
H	1.773400	-0.924400	-2.872200
C	3.019900	-2.062900	0.304300

H	3.548000	-3.000100	0.515800
H	3.435100	-1.617600	-0.604400
H	3.174700	-1.368300	1.139400
C	1.108800	-3.543800	-1.294700
H	1.410700	-3.039700	-2.218600
H	1.750500	-4.418700	-1.136800
H	0.068300	-3.871100	-1.403100
P	1.230800	-2.404500	0.124900
C	0.962200	-3.519300	1.548900
H	1.696000	-4.332200	1.492900
H	1.111200	-2.979900	2.490500
H	-0.041700	-3.953500	1.536000
C	-1.504400	-1.564800	1.114600
C	-2.049300	-0.208400	1.197800
C	-3.097600	0.163700	0.366000
C	-3.757500	-0.777300	-0.584100
H	-1.063500	-1.915600	2.048800
H	-1.788500	0.429300	2.039700
H	-4.842300	-0.629300	-0.479700
H	-3.530300	-0.468700	-1.619800
C	-2.336000	-2.556100	0.406500
H	-2.081800	-3.609700	0.526000
O	-3.658800	1.352300	0.374700
C	-3.260700	2.324900	1.352100
H	-3.801400	3.236900	1.096800
H	-3.551100	1.985800	2.352000
H	-2.181800	2.511100	1.314100
C	-3.368400	-2.207100	-0.368200
H	-3.954500	-2.957800	-0.893000

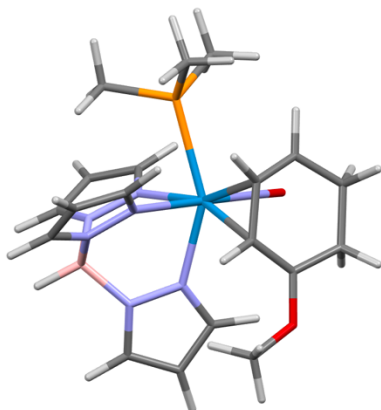
**Compound 28P Electronic Energy: -1707.672751 Hartree**



O	-1.462700	1.275200	-2.526000
N	-0.939600	0.872300	-1.516600
W	-0.132900	0.244900	-0.071700
C	-3.413200	1.872100	-0.176100
C	-3.053600	0.667200	0.615500
C	-1.876800	0.568600	1.373100
C	-0.941000	1.695500	1.355700
C	-1.452000	2.979900	0.855500
H	-1.884700	-0.168900	2.173800
H	-0.284900	1.755400	2.226700
H	-0.877500	3.876000	1.084800
H	-3.339400	1.623800	-1.253100
H	-4.481100	2.080100	-0.013000
O	-3.892400	-0.337500	0.694900
C	-5.105500	-0.365700	-0.074700
H	-4.910300	-0.145300	-1.128400
H	-5.487800	-1.382100	0.026500
H	-5.830500	0.343700	0.336100
C	-2.580100	3.073900	0.144800
H	-2.937700	4.028400	-0.232800
N	1.546300	1.715000	-0.038800
N	2.815900	1.323500	0.237600
N	1.033200	-0.644800	1.661900
N	2.384100	-0.753600	1.584900
N	1.437300	-0.642800	-1.344500
N	2.703600	-0.854800	-0.915300
C	3.645900	2.377300	0.120800
C	2.904300	3.487800	-0.238900
C	1.592800	3.017600	-0.333100
C	2.858900	-1.364600	2.683300
C	1.794400	-1.670700	3.513500
C	0.675300	-1.197000	2.830200

C	3.432900	-1.382500	-1.914600
C	2.620200	-1.531800	-3.026600
C	1.379200	-1.038800	-2.622400
B	3.170200	-0.173900	0.395200
H	4.348600	-0.322800	0.556900
H	4.706900	2.254800	0.299800
H	3.260400	4.493600	-0.411000
H	0.684600	3.546100	-0.598000
H	3.922600	-1.532900	2.796800
H	1.825100	-2.159600	4.476700
H	-0.365500	-1.229300	3.130600
H	4.483300	-1.600300	-1.766200
H	2.891700	-1.929100	-3.994300
H	0.449500	-0.955300	-3.175100
C	0.258400	-3.399600	-0.482700
H	-0.200000	-4.395500	-0.501500
H	0.822900	-3.248900	-1.407300
H	0.948100	-3.341300	0.368100
C	-2.119500	-2.371500	-1.751200
H	-1.545500	-2.142800	-2.656600
H	-2.486400	-3.403000	-1.809300
H	-2.971900	-1.683400	-1.702600
P	-1.056400	-2.142700	-0.286200
C	-2.011600	-2.897300	1.077900
H	-2.318300	-3.903900	0.769100
H	-1.373300	-2.985100	1.963600
H	-2.898800	-2.311400	1.325200

**Compound 29D Electronic Energy: -1708.109359 Hartree**

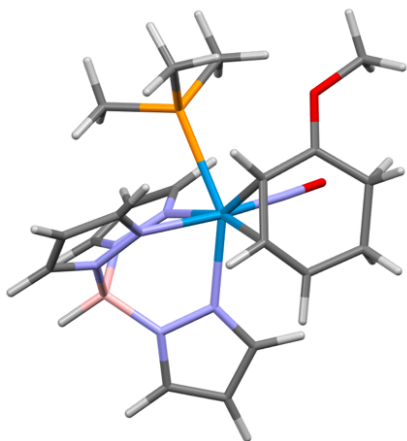


O	-0.919500	-1.457300	-2.772700
N	-0.608800	-1.076300	-1.693900
W	-0.097000	-0.400500	-0.120500
N	-1.074700	1.510400	-0.540000
N	-0.520800	2.692100	-0.158800
N	0.686400	0.652200	1.707000
N	1.087900	1.947400	1.624200
N	1.385500	0.781700	-1.203700
N	1.763300	2.018700	-0.791100
C	-1.266000	3.702000	-0.642100
C	-2.334800	3.176500	-1.347600
C	-2.160500	1.797000	-1.274500
C	1.548500	2.364000	2.813000
C	1.449700	1.318900	3.716000
C	0.903100	0.273600	2.979300
C	2.591600	2.553600	-1.702900
C	2.772400	1.646100	-2.734400
C	1.980500	0.556300	-2.386700
B	0.955500	2.738200	0.319700
H	1.327700	3.865900	0.458500
H	-0.970200	4.727600	-0.459700
H	-3.122300	3.715300	-1.854600
H	-2.765900	1.006400	-1.702900
H	1.910500	3.377600	2.930900
H	1.729300	1.316600	4.759600
H	0.658400	-0.725300	3.317200
H	2.982100	3.553400	-1.559900
H	3.380500	1.763500	-3.619600
H	1.817500	-0.372800	-2.919800
C	3.570300	-0.727300	0.314500
H	4.422200	-1.380800	0.536900
H	3.776000	-0.176800	-0.607400

H	3.440900	-0.018200	1.140500
C	2.403500	-2.908700	-1.224700
H	2.456800	-2.365700	-2.173300
H	3.351100	-3.434300	-1.058800
H	1.588400	-3.639500	-1.281000
P	2.085900	-1.771500	0.159800
C	2.246000	-2.844700	1.628300
H	3.228700	-3.327500	1.571500
H	2.205500	-2.250300	2.546300
H	1.483100	-3.628200	1.661400
C	-2.253800	-3.052500	-0.540200
C	-0.965400	-1.923800	1.320700
C	-1.885900	-0.799600	1.304300
C	-3.002700	-0.829800	0.461000
C	-3.286100	-1.923900	-0.506900
H	-0.307300	-2.095900	2.167600
H	-1.856900	-0.094700	2.130200
H	-4.281700	-2.307400	-0.248600
H	-1.971000	-3.296800	-1.571400
H	-3.408700	-1.469400	-1.499800
H	-2.689700	-3.985500	-0.149200
C	-1.050400	-2.857100	0.299100
H	-0.301000	-3.647300	0.242400
O	-3.905200	0.105700	0.442100
C	-3.881100	1.180300	1.408000
H	-4.710500	1.831000	1.133400
H	-4.035200	0.770500	2.410500
H	-2.936900	1.732200	1.355500



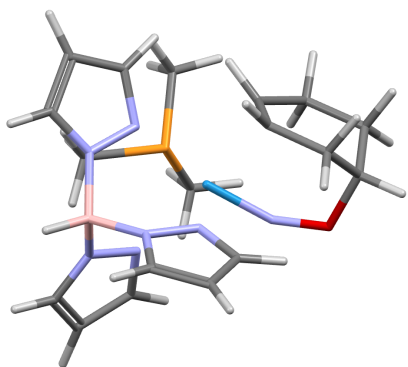
**Compound 29P Electronic Energy: -1708.107304 Hartree**



O	-1.642900	1.315900	-2.331000
N	-1.055600	0.929800	-1.370000
W	-0.150800	0.278900	0.022300
N	1.516900	1.712900	-0.034000
N	2.792800	1.308100	0.206800
N	1.075900	-0.725000	1.620900
N	2.421600	-0.833400	1.474600
N	1.288000	-0.567700	-1.377200
N	2.581000	-0.801300	-1.033400
C	3.630900	2.334700	-0.013500
C	2.894900	3.441400	-0.402800
C	1.576400	2.997500	-0.417000
C	2.943700	-1.517500	2.504000
C	1.917500	-1.874900	3.362000
C	0.771300	-1.355100	2.769300
C	3.260200	-1.203000	-2.119800
C	2.395200	-1.246700	-3.201800
C	1.173500	-0.820800	-2.691300
B	3.142100	-0.201000	0.281300
H	4.324400	-0.364700	0.355300
H	4.697600	2.198700	0.114400
H	3.262600	4.427600	-0.647000
H	0.672700	3.535100	-0.681300
H	4.010400	-1.696800	2.553300
H	1.990100	-2.426700	4.288000
H	-0.249500	-1.407800	3.127600
H	4.320000	-1.414100	-2.048000
H	2.621600	-1.532900	-4.218600
H	0.223500	-0.692600	-3.196200
C	0.380400	-3.353500	-0.533200
H	-0.056700	-4.357000	-0.593800

H	0.960500	-3.165600	-1.440400
H	1.041600	-3.306300	0.339800
C	-2.013200	-2.363600	-1.832100
H	-1.453300	-2.100900	-2.734800
H	-2.336800	-3.408400	-1.906700
H	-2.895700	-1.718000	-1.766100
P	-0.984600	-2.160100	-0.342900
C	-1.975800	-2.965000	0.960500
H	-2.146000	-4.001900	0.646800
H	-1.431300	-2.974100	1.909700
H	-2.943900	-2.475900	1.092300
C	-3.327500	1.983500	0.184300
C	-3.037000	0.607000	0.645800
C	-1.928900	0.269700	1.474100
C	-1.054900	1.349100	1.889200
C	-1.080100	2.544200	1.218300
C	-2.210000	3.008700	0.378200
H	-2.041500	-0.607500	2.105900
H	-0.348700	1.187700	2.700000
H	-0.307300	3.274000	1.450400
H	-2.605800	3.906600	0.872400
H	-3.646800	1.959200	-0.864900
H	-1.843500	3.365900	-0.592900
H	-4.231000	2.269700	0.749000
O	-3.851000	-0.359400	0.367800
C	-4.982900	-0.177100	-0.517400
H	-4.631500	0.121600	-1.509700
H	-5.463600	-1.153500	-0.563500
H	-5.671400	0.563400	-0.102600

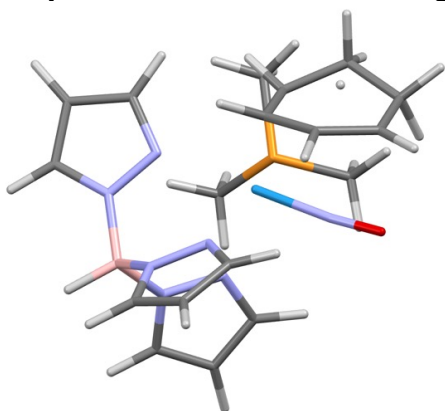
**Compound 32 Electronic Energy in Gas Phase: -1593.915966 Hartree**



W	-0.354700	0.149700	-0.133700
O	-2.477300	1.651200	-1.580100
N	-1.475800	0.882500	-1.256900
C	-2.133600	-0.036600	1.228500
H	-1.945100	-0.721200	2.054600
C	-1.558100	1.272700	1.348000
H	-0.958600	1.490300	2.233800
C	-4.186200	1.006300	0.066500
H	-4.881000	0.769000	-0.746600
H	-4.789900	1.444500	0.873300
C	-3.488600	-0.266700	0.563200
H	-3.396500	-0.959700	-0.285100
H	-4.156600	-0.768700	1.276600
C	-2.298000	2.462900	0.774400
H	-2.946800	2.895400	1.551100
H	-1.616300	3.269900	0.485900
C	-3.225100	2.089800	-0.364800
H	-3.757200	2.966000	-0.747800
P	-0.840100	-2.360100	-0.361100
C	0.695400	-3.360800	-0.315200
H	0.445400	-4.425000	-0.390500
H	1.362000	-3.090300	-1.139400
C	-1.859300	-3.251600	0.873900
H	-1.396500	-3.178300	1.863400
H	-2.874400	-2.849700	0.924200
C	-1.621200	-2.843000	-1.944900
H	-1.747200	-3.930700	-1.992500
H	-2.599700	-2.362200	-2.043600
H	-1.912100	-4.310400	0.596400
H	1.218700	-3.184700	0.631800
H	-0.997700	-2.523700	-2.785200
N	0.855100	-0.523100	1.655900
N	2.208400	-0.407600	1.610500

N	2.659700	-0.380100	-0.875400
N	1.396900	-0.451300	-1.356900
N	2.314200	1.747300	0.334000
N	1.007400	1.905100	-0.000300
C	0.568000	-1.129600	2.819700
H	-0.458000	-1.322200	3.105900
C	1.731000	-1.417700	3.525900
H	1.819600	-1.895000	4.490500
C	2.748400	-0.936500	2.719900
H	3.821500	-0.924100	2.860400
C	2.813300	-1.101600	-2.969400
H	3.205200	-1.442400	-3.916200
C	3.525100	-0.766700	-1.829000
H	4.589100	-0.766700	-1.630600
C	0.853800	3.184400	-0.359900
H	-0.102700	3.542300	-0.716800
C	2.059400	3.875600	-0.238500
H	2.247200	4.918400	-0.446600
C	2.958700	2.923200	0.197400
H	4.016300	2.989900	0.417300
B	2.927800	0.341200	0.471200
H	4.105200	0.397700	0.688100
C	1.481700	-0.878400	-2.624600
H	0.583900	-0.985600	-3.222400

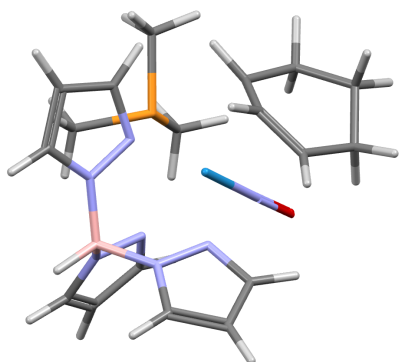
**Compound 33 Electronic Energy in Gas Phase: -1593.876621 Hartree**



W	-0.355800	0.184700	-0.075800
O	-1.998700	1.627600	-2.080400
N	-1.295600	0.936600	-1.368600
P	-1.030900	-2.256900	-0.397800
C	0.388100	-3.391200	-0.654600
H	0.033200	-4.426600	-0.707000
H	0.931800	-3.149800	-1.571900
C	-1.889800	-3.157800	0.949100
H	-1.240700	-3.200500	1.830000
H	-2.833200	-2.682200	1.227500
C	-2.112200	-2.562000	-1.842300
H	-2.323100	-3.631200	-1.957600
H	-3.055800	-2.020700	-1.714800
H	-2.095200	-4.183600	0.622600
H	1.078600	-3.292500	0.192000
H	-1.631400	-2.189600	-2.752200
N	0.897600	-0.620000	1.654200
N	2.250800	-0.563300	1.570200
N	2.592900	-0.536700	-0.930900
N	1.313300	-0.500200	-1.372100
N	2.423800	1.601800	0.306400
N	1.119200	1.844800	0.027000
C	0.622200	-1.248000	2.807900
H	-0.402300	-1.406500	3.120400
C	1.793300	-1.606300	3.470900
H	1.890800	-2.115800	4.418100
C	2.804600	-1.146900	2.646500
H	3.881200	-1.186500	2.750400
C	2.633000	-1.165800	-3.059700
H	2.971000	-1.488300	-4.033400
C	3.401100	-0.930000	-1.931800
H	4.469600	-0.999100	-1.773200
C	1.021000	3.146900	-0.260100
H	0.070200	3.564900	-0.567900

C	2.264900	3.767900	-0.150700
H	2.504800	4.807700	-0.316100
C	3.125900	2.746500	0.204100
H	4.192700	2.746800	0.386400
B	2.958600	0.154300	0.407800
H	4.146600	0.147400	0.572800
C	1.331200	-0.867100	-2.659600
H	0.408800	-0.891300	-3.228300
C	-2.086100	0.060500	1.308700
H	-1.889900	-0.602800	2.153400
C	-1.458100	1.364200	1.433400
H	-0.853000	1.607300	2.307200
C	-4.013400	1.043400	-0.096500
H	-3.858800	0.685000	-1.124600
H	-5.091500	1.239800	-0.026600
C	-3.561900	0.012800	0.939500
H	-3.860700	-0.981000	0.581200
H	-4.145000	0.172500	1.861500
C	-2.159100	2.497300	0.813700
H	-1.642800	3.457500	0.741800
C	-3.266000	2.319300	-0.054000
H	-3.640800	3.184800	-0.599100
H	-3.175800	2.788300	1.395800

**Compound 34 Electronic Energy in Gas Phase: -1593.937653 Hartree**

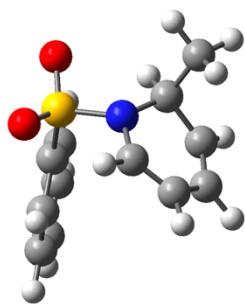


W	-0.366000	0.260900	-0.059700
O	-1.853200	0.942200	-2.534200
N	-1.242300	0.716400	-1.536600
P	-1.102000	-2.185100	-0.367000
C	0.303900	-3.358500	-0.310900
H	-0.071600	-4.383000	-0.411100
H	1.013400	-3.159200	-1.118600
C	-2.265600	-2.993800	0.794000
H	-1.859000	-2.995300	1.810400
H	-3.237500	-2.492700	0.794600
C	-1.897300	-2.518000	-1.979600
H	-2.174100	-3.575900	-2.049400
H	-2.795800	-1.902500	-2.090100
H	-2.407700	-4.033800	0.479000
H	0.824300	-3.261700	0.648900
H	-1.217700	-2.278400	-2.801500
N	0.792900	-0.596300	1.692500
N	2.146400	-0.631500	1.655000
N	2.515700	-0.696600	-0.835000
N	1.247900	-0.565000	-1.298200
N	2.489800	1.482600	0.321900
N	1.215100	1.821800	-0.013100
C	0.431800	-1.206000	2.832900
H	-0.613600	-1.290700	3.105400
C	1.552700	-1.643600	3.534300
H	1.582700	-2.158000	4.483300
C	2.622100	-1.253300	2.747000
H	3.689200	-1.366400	2.888700
C	2.546800	-1.295300	-2.974300
H	2.878300	-1.625900	-3.947500
C	3.309700	-1.129100	-1.830000
H	4.368600	-1.272100	-1.656400

C	1.249300	3.100900	-0.412700
H	0.347000	3.588300	-0.761100
C	2.542400	3.608600	-0.320500
H	2.880800	4.605600	-0.560500
C	3.295700	2.545300	0.141300
H	4.354400	2.463700	0.351500
B	2.917400	0.004200	0.490600
H	4.099600	-0.079800	0.668200
C	1.263800	-0.909700	-2.594700
H	0.359800	-0.840500	-3.188100
C	-2.250500	0.086400	1.237300
H	-2.237600	-0.719600	1.969900
C	-1.550700	1.271300	1.634700
H	-0.851700	1.271400	2.470000
C	-2.861500	2.651600	-0.009500
H	-2.680200	2.602200	-1.092300
H	-3.144500	3.695500	0.184000
C	-3.996200	1.718800	0.410100
H	-4.849400	1.832200	-0.266700
H	-4.337800	2.026300	1.408100
C	-3.569200	0.253600	0.479600
H	-3.513300	-0.158500	-0.537500
H	-4.352500	-0.317900	0.996100
C	-1.630900	2.375500	0.801400
H	-0.934800	3.193500	0.977700

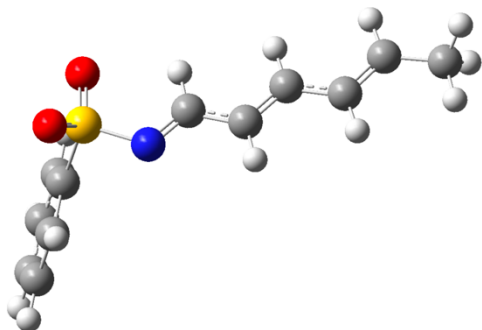


**Compound 35 Electronic Energy in MeCN: -1067.76279 Hartree**



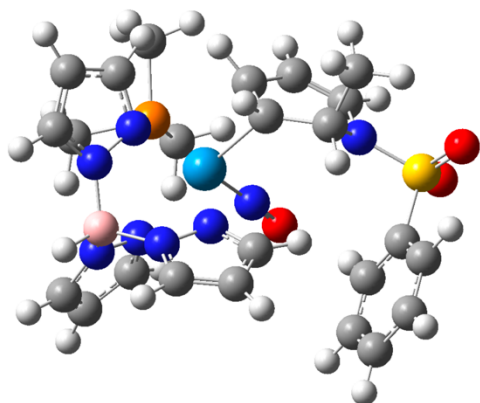
C	-1.546300	2.415700	0.182000
H	-1.399900	3.493300	0.204800
C	-1.533300	1.742900	-0.977300
H	-1.368400	2.241500	-1.930200
C	-1.561600	0.367900	1.471900
H	-1.572400	-0.218500	2.385800
N	-1.386800	-0.362400	0.279300
C	-1.703300	1.704400	1.437500
H	-1.891900	2.245400	2.359900
C	-1.812800	0.266800	-0.999600
H	-1.230600	-0.209500	-1.797500
C	-3.285200	-0.030800	-1.235800
H	-3.613400	0.417900	-2.180400
H	-3.452700	-1.113300	-1.282500
H	-3.896700	0.387800	-0.427600
S	-0.117300	-1.468100	0.242800
O	-0.317800	-2.292700	-0.941700
O	-0.070100	-2.073000	1.567700
C	1.346500	-0.490800	0.010700
C	1.899700	0.159800	1.112600
C	1.865200	-0.333100	-1.272400
C	2.999100	0.986800	0.916700
H	1.486000	0.010300	2.106900
C	2.967300	0.495000	-1.450600
H	1.418500	-0.860500	-2.111300
C	3.528800	1.154600	-0.360500
H	3.446200	1.497800	1.765300
H	3.389600	0.622400	-2.443900
H	4.389900	1.802000	-0.506400

**Compound 36 Electronic Energy in MeCN: -1067.760848 Hartree**



C	-4.658600	-0.501800	-0.358600
H	-4.694100	-0.866400	-1.387500
C	-5.765800	-0.534600	0.405900
C	-3.408500	0.004000	0.128700
H	-5.694700	-0.161100	1.430400
C	-7.085100	-1.041200	-0.035800
H	-7.061000	-1.393100	-1.072400
H	-7.420400	-1.865900	0.607000
H	-7.851300	-0.259400	0.051800
H	-3.388000	0.364500	1.160800
C	-2.267100	0.063800	-0.600100
H	-2.238700	-0.281300	-1.633600
C	-1.069300	0.587200	-0.026800
H	-1.120500	0.927100	1.018100
N	0.033700	0.657400	-0.705700
S	1.349700	1.328600	0.094800
O	1.051300	1.644500	1.494500
O	1.855500	2.394500	-0.768400
C	2.493700	-0.026200	0.053900
C	2.783800	-0.711000	1.228900
C	3.069400	-0.378100	-1.165200
C	3.678600	-1.774800	1.178900
H	2.319300	-0.408500	2.163700
C	3.957800	-1.444800	-1.201000
H	2.828200	0.178600	-2.067900
C	4.260800	-2.139700	-0.031400
H	3.921400	-2.318200	2.088300
H	4.417900	-1.733000	-2.142600
H	4.958700	-2.972900	-0.064900

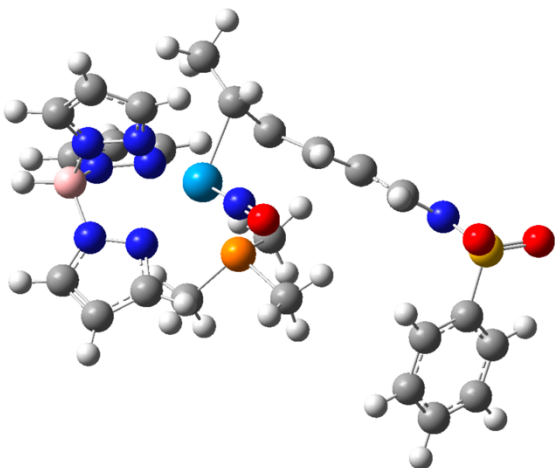
**Compound 37 Electronic Energy in MeCN: -2428.156693 Hartree**



W	0.754400	-0.294600	-0.052400
O	-0.911500	-0.771400	-2.476700
N	-0.309500	-0.547300	-1.441700
C	0.055900	-2.104100	1.071000
H	0.843800	-2.571900	1.666200
C	-0.577400	-0.897700	1.571000
H	-0.158000	-0.503900	2.504900
C	-2.072400	-2.750400	0.009100
H	-2.710900	-3.400300	-0.579900
N	-2.645600	-1.524400	0.423300
C	-0.804000	-3.041700	0.333500
H	-0.404900	-4.002400	0.009800
C	-2.094900	-0.888400	1.643000
H	-2.477200	0.143400	1.658400
C	-2.564700	-1.600800	2.908700
H	-2.138600	-1.109100	3.791200
H	-3.655800	-1.587000	2.996600
H	-2.226000	-2.644300	2.908600
S	-4.195600	-1.139900	-0.034900
O	-5.129900	-1.259000	1.086900
O	-4.473400	-1.898600	-1.252100
C	-4.083300	0.591200	-0.431200
C	-3.336100	0.971800	-1.544100
C	-4.770800	1.519200	0.345900
C	-3.285900	2.318600	-1.884600
H	-2.778400	0.227500	-2.112100
C	-4.705100	2.865600	-0.003400
H	-5.345600	1.187800	1.206900
C	-3.968900	3.261700	-1.117000
H	-2.708200	2.633900	-2.750300

H	-5.234300	3.603800	0.594100
H	-3.923700	4.314100	-1.388000
P	2.367500	-2.041700	-0.924700
C	4.072000	-1.416300	-1.189900
H	4.716900	-2.231600	-1.539200
H	4.083900	-0.609900	-1.930100
C	2.728500	-3.559600	0.032300
H	3.137400	-3.302000	1.015300
H	1.826200	-4.163400	0.168300
C	1.899300	-2.720100	-2.554400
H	2.645500	-3.446300	-2.898200
H	0.922600	-3.210000	-2.472100
H	3.472300	-4.153000	-0.513000
H	4.468300	-1.030400	-0.242100
H	1.816700	-1.910900	-3.287600
N	2.364000	0.011900	1.543200
N	3.044600	1.183800	1.606700
N	2.838200	2.003300	-0.770100
N	2.046600	1.043600	-1.301600
N	1.157300	2.693000	0.920400
N	0.193700	1.776600	0.639900
C	2.893100	-0.785700	2.479700
H	2.505900	-1.787400	2.628600
C	3.927600	-0.133900	3.153700
H	4.540300	-0.516300	3.957900
C	3.985800	1.117600	2.565500
H	4.624200	1.969800	2.763500
C	3.121900	2.094800	-2.966800
H	3.461000	2.377600	-3.953500
C	3.490300	2.651800	-1.753700
H	4.158400	3.471100	-1.518600
C	-0.980300	2.383200	0.834500
H	-1.904400	1.845300	0.657900
C	-0.789100	3.705300	1.244300
H	-1.546600	4.442200	1.473500
C	0.585100	3.856500	1.285900
H	1.202200	4.707300	1.547400
B	2.660000	2.382000	0.716700
H	3.330500	3.338600	0.993500
C	2.204800	1.095700	-2.628400
H	1.655100	0.412400	-3.266500

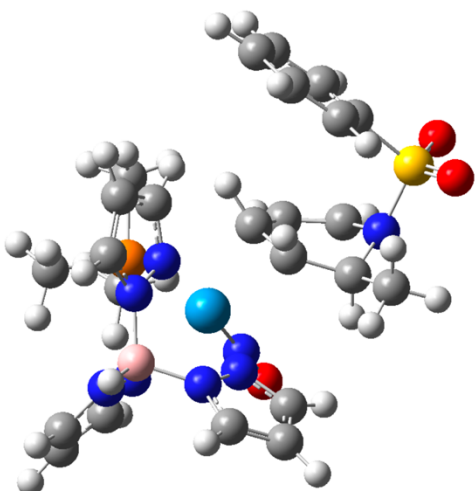
**Compound 38 Electronic Energy in MeCN: -2428.160046 Hartree**



W	-1.419000	-0.378600	-0.191500
O	0.240800	-0.556900	-2.660500
N	-0.429100	-0.514500	-1.651300
C	-0.259700	-1.988200	0.967400
H	-0.325900	-1.905900	2.056800
C	-1.405700	-2.518500	0.242000
C	1.047900	-2.051400	0.407800
H	-1.153600	-3.084100	-0.662500
C	-2.524300	-3.153000	1.032700
H	-2.696100	-2.638700	1.985200
H	-3.473300	-3.143500	0.479000
H	-2.296300	-4.203300	1.265800
H	1.095800	-2.231200	-0.671100
C	2.252800	-1.898600	1.050500
H	2.313800	-1.770500	2.131300
C	3.438400	-1.834900	0.291500
H	3.336200	-1.972100	-0.796700
N	4.612100	-1.596700	0.825600
S	5.875700	-1.427900	-0.236600
O	5.540600	-1.884100	-1.591700
O	7.062300	-1.988000	0.409200
C	6.050700	0.342500	-0.289300
C	5.223500	1.072400	-1.140700
C	6.965200	0.966600	0.552400
C	5.320100	2.459100	-1.145900
H	4.518800	0.560400	-1.793800
C	7.056700	2.355300	0.533900
H	7.598300	0.369200	1.203900
C	6.235100	3.097800	-0.310100
H	4.681000	3.041800	-1.805300

H	7.771300	2.857500	1.181400
H	6.308500	4.182900	-0.318600
P	0.161800	1.258000	0.979200
C	-0.600700	2.894600	1.301700
H	0.087000	3.502400	1.901900
H	-0.821200	3.421900	0.369000
C	0.823500	0.905500	2.649200
H	0.012300	0.974100	3.381700
H	1.276300	-0.086300	2.709700
C	1.657000	1.665900	0.009800
H	2.250700	2.431000	0.524700
H	2.261000	0.759100	-0.116200
H	1.579700	1.660300	2.896300
H	-1.536500	2.757700	1.858600
H	1.367100	2.035300	-0.980800
N	-2.745100	0.019200	1.617100
N	-3.961300	0.598600	1.454000
N	-3.561700	1.912900	-0.653400
N	-2.303900	1.515700	-0.957100
N	-4.510300	-0.370200	-0.803900
N	-3.349800	-0.998900	-1.116000
C	-2.567000	-0.124200	2.937100
H	-1.662300	-0.583700	3.318500
C	-3.669200	0.366200	3.638100
H	-3.820800	0.385100	4.708100
C	-4.531100	0.815900	2.652300
H	-5.511500	1.271600	2.715600
C	-2.721100	3.448700	-2.014400
H	-2.603200	4.329000	-2.630400
C	-3.834600	3.071000	-1.282300
H	-4.806900	3.535400	-1.172900
C	-3.651300	-1.970600	-1.981400
H	-2.870400	-2.619100	-2.362000
C	-5.025000	-1.981400	-2.238300
H	-5.571500	-2.646800	-2.891900
C	-5.529200	-0.946600	-1.470900
H	-6.538200	-0.571000	-1.353600
B	-4.514500	0.919300	0.052200
H	-5.622000	1.373500	0.132500
C	-1.791100	2.431800	-1.785900
H	-0.779700	2.318300	-2.161600

**Compound 39 Electronic Energy in MeCN: -2428.14982 Hartree**

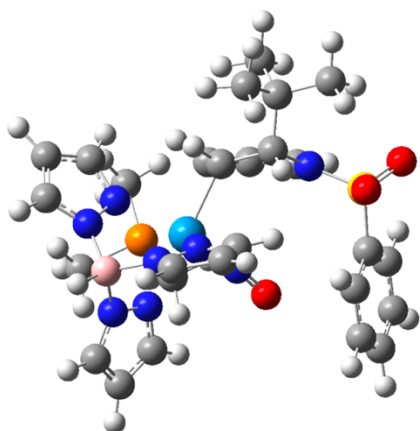


W	0.901800	0.071300	-0.512800
O	0.787300	0.942400	-3.363800
N	0.823400	0.581800	-2.204000
P	1.215500	-2.401100	-1.005900
C	2.677600	-3.133400	-0.173500
H	2.720200	-4.210600	-0.374100
H	3.602600	-2.667100	-0.527800
C	-0.070800	-3.616000	-0.528900
H	-0.248300	-3.573700	0.552000
H	-1.015000	-3.425200	-1.048900
C	1.485000	-2.798100	-2.769900
H	1.661700	-3.872200	-2.903400
H	0.602300	-2.501200	-3.347800
H	0.277800	-4.622600	-0.789600
H	2.597000	-2.973900	0.909200
H	2.348400	-2.241400	-3.149600
N	1.112500	-0.566000	1.669900
N	2.165300	-0.130200	2.405500
N	3.876900	0.238100	0.589100
N	3.148600	-0.010200	-0.525600
N	2.452800	2.129000	1.318200
N	1.542900	2.053000	0.313600
C	0.401900	-1.374600	2.466600
H	-0.504300	-1.847300	2.103800
C	0.996900	-1.471000	3.726000
H	0.658500	-2.044600	4.577400
C	2.115700	-0.660800	3.640700
H	2.879000	-0.418900	4.369800
C	5.327700	-0.207900	-1.027600

H	6.244400	-0.373500	-1.576100
C	5.189400	0.129300	0.308000
H	5.929400	0.313700	1.077000
C	1.305400	3.303400	-0.090700
H	0.614100	3.486900	-0.905700
C	2.053700	4.211600	0.665000
H	2.069500	5.289300	0.581000
C	2.771800	3.420000	1.542200
H	3.492800	3.677000	2.308300
B	3.188000	0.863400	1.827100
H	4.002700	1.154800	2.658900
C	4.016900	-0.272300	-1.508200
H	3.656200	-0.498400	-2.505900
C	-1.182800	-0.633800	-0.454800
H	-1.335600	-1.444000	0.264300
C	-1.132500	0.723500	0.053300
H	-1.210000	0.832800	1.141400
C	-2.843800	0.030800	-2.135700
H	-3.417300	-0.092700	-3.050800
N	-3.155000	1.195300	-1.350700
C	-1.906900	-0.833000	-1.719900
H	-1.685200	-1.698100	-2.348300
S	-4.594400	0.973400	-0.503300
O	-5.541500	0.439000	-1.479400
O	-4.926100	2.208000	0.199600
C	-4.303200	-0.297900	0.710300
C	-4.405100	-1.635300	0.330100
C	-3.891100	0.064900	1.990700
C	-4.059500	-2.624400	1.246000
H	-4.754200	-1.895200	-0.665600
C	-3.553800	-0.932100	2.899100
H	-3.837300	1.114700	2.270800
C	-3.626300	-2.272900	2.522700
H	-4.133000	-3.671600	0.962300
H	-3.232400	-0.662600	3.902400
H	-3.355100	-3.049400	3.234500
C	-1.911800	1.776800	-0.714300
H	-1.353600	2.080800	-1.612900
C	-2.175200	3.021000	0.108200
H	-2.762400	3.759800	-0.446500
H	-2.699300	2.799200	1.042800
H	-1.209200	3.466800	0.370500



**Compound 40 Electronic Energy in MeCN: -2545.920551 Hartree**

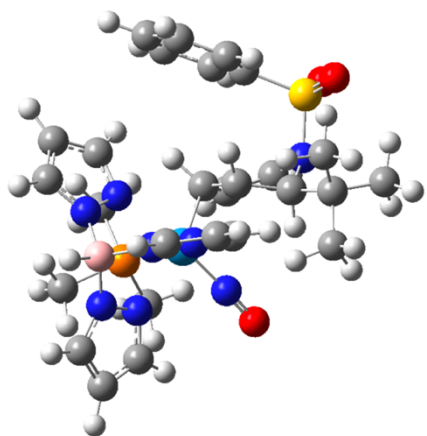


W	-0.857500	-0.117900	-0.236400
O	0.907400	-2.492900	-0.530700
N	0.280200	-1.469500	-0.360300
C	0.186700	1.186400	-1.725600
H	-0.501900	1.767300	-2.346200
C	0.446300	1.632000	-0.370900
H	-0.192200	2.457900	-0.043900
C	2.531400	0.458200	-1.886800
H	3.386200	0.040100	-2.413500
N	2.782200	0.891400	-0.563200
C	1.322900	0.605800	-2.450600
H	1.204700	0.303700	-3.491200
C	1.874600	1.863300	0.090900
H	1.966800	1.685600	1.169800
C	2.325600	3.350900	-0.112700
S	4.071900	0.215000	0.247000
O	4.055200	0.756400	1.604300
O	5.260800	0.385500	-0.589300
C	3.810600	-1.540000	0.383300
C	4.307600	-2.386600	-0.604200
C	3.193200	-2.037100	1.527700
C	4.175900	-3.760800	-0.439300
H	4.815800	-1.976400	-1.473300
C	3.074000	-3.412700	1.682800
H	2.837100	-1.356900	2.297900
C	3.563800	-4.271600	0.702500
H	4.568100	-4.434200	-1.197700
H	2.606400	-3.815200	2.578300
H	3.476400	-5.347900	0.833700
C	3.796300	3.534700	0.258600
H	3.994000	3.234500	1.294200
H	4.459000	2.953900	-0.395200

H	4.072500	4.592100	0.150700
C	2.133000	3.841500	-1.546000
H	1.086200	3.780100	-1.866900
H	2.442800	4.893000	-1.620700
H	2.742000	3.265900	-2.254700
C	1.501400	4.228200	0.835500
H	1.903600	5.249900	0.846500
H	0.447900	4.300400	0.539900
H	1.538400	3.845200	1.866000
P	-1.993100	-0.871500	-2.373700
C	-3.788000	-1.204300	-2.183300
H	-4.219800	-1.487100	-3.150900
H	-3.960400	-2.013300	-1.465900
C	-2.014300	0.198300	-3.859300
H	-2.498900	1.155200	-3.637200
H	-0.997700	0.388200	-4.217800
C	-1.344700	-2.436500	-3.058900
H	-1.904600	-2.717700	-3.958900
H	-0.286700	-2.308300	-3.313800
H	-2.580200	-0.306700	-4.651300
H	-4.290500	-0.299200	-1.819600
H	-1.425600	-3.238900	-2.318600
N	-2.573800	1.389200	-0.162100
N	-3.485200	1.340200	0.840400
N	-3.357300	-1.092500	1.478800
N	-2.364100	-1.515300	0.662700
N	-1.930800	0.561000	2.660400
N	-0.783500	0.360300	1.961400
C	-2.960300	2.376300	-0.979700
H	-2.375300	2.617600	-1.860200
C	-4.134700	2.970200	-0.512300
H	-4.685500	3.788900	-0.953600
C	-4.430000	2.279100	0.650000
H	-5.240100	2.390400	1.360200
C	-3.578400	-3.291100	1.301500
H	-3.935400	-4.305600	1.411700
C	-4.096900	-2.144400	1.878800
H	-4.929900	-2.000800	2.556000
C	0.223500	0.485400	2.830800
H	1.247200	0.352700	2.498300
C	-0.264400	0.775700	4.108200
H	0.303000	0.932800	5.014900
C	-1.637700	0.812400	3.951500
H	-2.432400	0.995200	4.664100
B	-3.324200	0.356000	2.014700
H	-4.192800	0.528000	2.825600

C	-2.484400	-2.842800	0.555900
H	-1.781600	-3.402800	-0.051100

**Compound 41 Electronic Energy in MeCN: -2545.898274 Hartree**

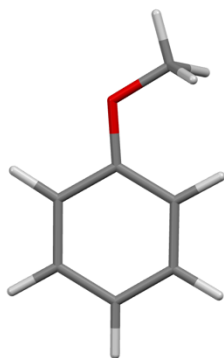


W	0.975100	0.250600	-0.447800
O	0.763800	1.884800	-2.929800
N	0.829100	1.251800	-1.894400
C	-0.987000	-0.712500	-0.637900
H	-0.990000	-1.626500	-0.037700
C	-1.172100	0.542700	0.085200
H	-1.355400	0.449300	1.161900
C	-2.914200	-0.275600	-2.087200
H	-3.567500	-0.441800	-2.940500
N	-3.336000	0.719800	-1.139200
C	-1.755900	-0.915200	-1.882900
H	-1.429600	-1.635800	-2.633500
S	-4.548400	0.094400	-0.152300
O	-5.554800	-0.433400	-1.072300
O	-4.943400	1.107300	0.822500
C	-3.902700	-1.294000	0.763700
C	-3.853700	-2.549200	0.160500
C	-3.430000	-1.088900	2.058200
C	-3.293600	-3.612500	0.862700
H	-4.254500	-2.692800	-0.839300
C	-2.882600	-2.160700	2.754000
H	-3.494300	-0.102200	2.511800
C	-2.806500	-3.416900	2.153300
H	-3.246500	-4.597000	0.403500
H	-2.513800	-2.016100	3.766700
H	-2.369700	-4.250500	2.699300
C	-2.112400	1.489500	-0.655000
H	-1.663400	1.687600	-1.638000

C	-2.388600	2.906400	-0.090700
C	-3.643400	3.526100	-0.709600
H	-4.562800	3.063600	-0.340700
H	-3.675500	4.596300	-0.461300
H	-3.627100	3.440100	-1.804400
C	-2.505500	2.959000	1.432700
H	-1.630900	2.531800	1.936200
H	-2.598300	4.003400	1.761500
H	-3.391700	2.417500	1.780000
C	-1.213800	3.775500	-0.573900
H	-1.331000	4.006200	-1.641300
H	-1.180200	4.727600	-0.027300
H	-0.244600	3.276400	-0.473000
P	1.532000	-1.823600	-1.792200
C	3.216100	-2.496100	-1.519800
H	3.333200	-3.419400	-2.099800
H	3.984900	-1.781600	-1.828800
C	0.579300	-3.371700	-1.541100
H	0.791400	-3.761100	-0.539000
H	-0.500900	-3.239000	-1.642100
C	1.486400	-1.568000	-3.600100
H	1.728500	-2.499500	-4.125700
H	0.495000	-1.220400	-3.909200
H	0.917400	-4.109600	-2.278500
H	3.348600	-2.726800	-0.455500
H	2.220500	-0.801700	-3.873200
N	1.370200	-1.231200	1.296500
N	2.542200	-1.154700	1.979700
N	4.046100	0.203000	0.444000
N	3.202700	0.455900	-0.581000
N	2.600800	1.331100	2.107100
N	1.540500	1.671900	1.320100
C	0.744100	-2.323800	1.754300
H	-0.227900	-2.610700	1.370900
C	1.507500	-2.962400	2.732700
H	1.261100	-3.859200	3.283900
C	2.641800	-2.179000	2.846000
H	3.509600	-2.267500	3.488000
C	5.308600	0.777600	-1.284200
H	6.158600	1.008000	-1.911100
C	5.317800	0.397100	0.047500
H	6.134900	0.263400	0.745700
C	1.069400	2.819100	1.824900
H	0.222500	3.311500	1.373600
C	1.812000	3.227600	2.933200
H	1.664700	4.110500	3.539200

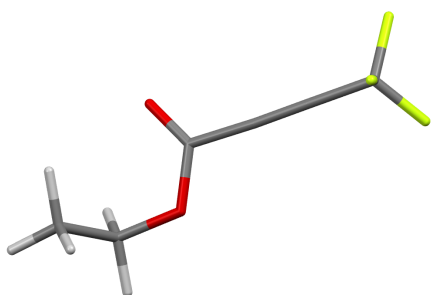
C	2.774900	2.248000	3.075600
H	3.576200	2.131600	3.794800
B	3.462400	0.074200	1.863200
H	4.345700	0.005100	2.673800
C	3.954900	0.807700	-1.629900
H	3.484900	1.057800	-2.574700

**Compound 42 Electronic Energy in Gas Phase: -346.520214 Hartree**



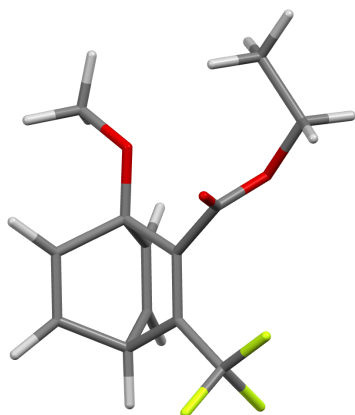
C	1.846700	0.994300	-0.000000
C	0.495700	1.302300	-0.000200
C	-0.455000	0.275700	0.000100
H	2.576100	1.798200	-0.000000
H	0.143200	2.327900	-0.000100
C	2.271200	-0.335900	-0.000300
H	3.329100	-0.574400	-0.000600
O	-1.754900	0.676800	0.000700
C	-2.744500	-0.327100	-0.000600
H	-3.703600	0.189900	-0.001600
H	-2.672400	-0.959600	-0.893700
H	-2.674600	-0.959900	0.892300
C	1.322600	-1.349400	-0.000000
C	-0.042300	-1.057000	0.000500
H	-0.762800	-1.865700	0.001100
H	1.637400	-2.388200	-0.000100

**Compound 43 Electronic Energy in Gas Phase: -681.236967 Hartree**



C	-1.433700	0.511200	-0.174200
O	-2.093900	-0.609500	-0.458400
C	-3.528800	-0.479100	-0.546800
H	-3.761800	0.430200	-1.105300
H	-3.839300	-1.351700	-1.121900
C	-4.156500	-0.458800	0.833300
H	-5.245200	-0.438100	0.741800
H	-3.872800	-1.351700	1.394600
H	-3.839700	0.428500	1.384000
O	-1.921400	1.597300	0.000900
C	0.006700	0.258000	-0.103100
C	1.196000	0.099700	-0.034100
C	2.652500	-0.103000	0.052700
F	2.974300	-0.711400	1.195700
F	3.086900	-0.859000	-0.957000
F	3.301500	1.060700	0.005800

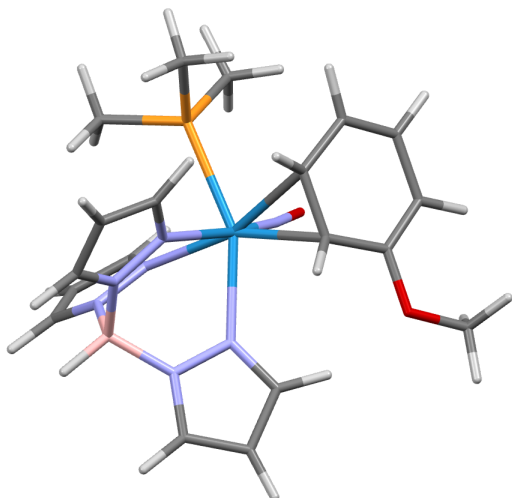
**Compound 44 Electronic Energy in Gas Phase: -1027.751524 Hartree**



C	-1.583600	2.180800	0.982500
H	-2.312600	2.639200	1.638300
C	-0.266700	2.242600	1.123400
H	0.269600	2.740600	1.921500
C	0.497400	1.459300	0.043800
C	-0.001800	1.979700	-1.314800
H	0.706500	2.312200	-2.063700
C	-1.319400	1.918400	-1.447600
H	-1.883500	2.214000	-2.323000
C	-2.021900	1.330800	-0.215700
H	-3.102900	1.256800	-0.326000
C	-1.362700	-0.038100	0.004900
C	-0.046800	0.019300	0.141200
C	-2.209200	-1.259700	0.005000
C	0.940200	-1.079100	0.375900
C	2.719000	-2.242500	-0.618500
H	2.897300	-2.618800	-1.626800
H	2.439600	-3.071200	0.035700
C	3.917500	-1.485700	-0.076700
H	3.703500	-1.114800	0.927500
H	4.149300	-0.636200	-0.722900
H	4.788900	-2.143900	-0.030200
C	2.529300	2.681200	0.170200
H	3.600300	2.484000	0.223400
H	2.241200	3.306500	1.023100
H	2.313000	3.230700	-0.753700
F	-3.109700	-1.226200	1.000500
F	-1.492000	-2.379500	0.135700
F	-2.909000	-1.352800	-1.140300
O	1.889600	1.423500	0.196100
O	1.144900	-1.594700	1.443500

O 1.595400 -1.355800 -0.755800

**Compound 45 Electronic Energy in Gas Phase: -1707.026587 Hartree**

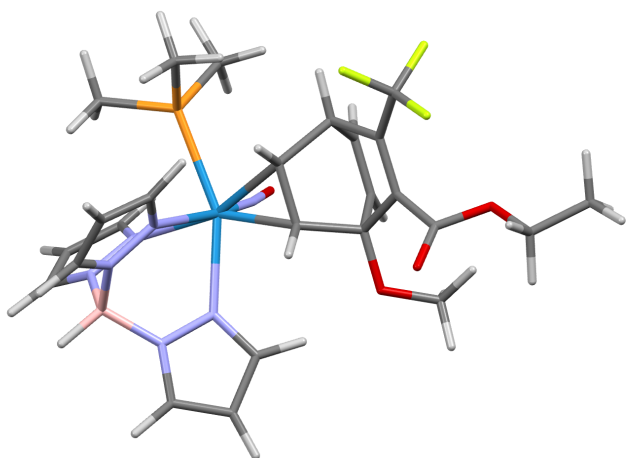


O	-1.814000	-0.608900	-2.523300
N	0.321200	2.091700	-0.027000
N	1.605400	2.490400	0.115700
N	1.359500	-0.073000	1.651100
N	2.515800	0.597400	1.481400
N	1.603100	0.015800	-1.390800
N	2.750500	0.618600	-1.037500
N	-1.203900	-0.359700	-1.518500
C	1.674300	3.834300	0.088700
C	0.397100	4.334300	-0.078600
C	-0.416200	3.195600	-0.143400
C	3.317700	0.420200	2.545000
C	2.668500	-0.400600	3.450800
C	1.442200	-0.678600	2.838900
C	3.614400	0.596400	-2.069600
C	3.008500	-0.051600	-3.133000
C	1.734800	-0.384800	-2.655400
B	2.765900	1.485300	0.241400
H	3.816100	2.054000	0.351000
H	2.628000	4.329800	0.192900
H	0.095500	5.367300	-0.140700
H	-1.487500	3.108500	-0.244600
H	4.285900	0.896600	2.580700
H	3.023100	-0.738000	4.411100
H	0.622800	-1.280300	3.203400
H	4.587100	1.055400	-1.975100
H	3.420500	-0.240900	-4.110900
H	0.902200	-0.870800	-3.148400



C	1.931200	-3.055600	-0.707900
H	2.087500	-4.132000	-0.594600
H	2.068500	-2.778200	-1.753600
H	2.673500	-2.513800	-0.113400
C	-0.859000	-3.470300	-1.277600
H	-0.806200	-2.983900	-2.255300
H	-0.592900	-4.527100	-1.361100
H	-1.886800	-3.359400	-0.924500
W	-0.211000	-0.140100	-0.090300
P	0.249100	-2.579200	-0.126900
C	0.192800	-3.595100	1.409700
H	0.258000	-4.657200	1.157500
H	1.048400	-3.331800	2.036800
H	-0.725000	-3.415200	1.970600
C	-1.740700	-0.884400	1.431600
C	-1.937800	0.529200	1.168100
C	-3.163500	0.909000	0.475100
H	-1.207400	-1.143600	2.344400
H	-1.571700	1.263300	1.885100
C	-2.789400	-1.815000	1.031700
H	-2.717600	-2.857000	1.334000
O	-3.330800	2.258700	0.376200
C	-4.504000	2.718000	-0.257900
H	-4.468000	3.806900	-0.220500
H	-4.544700	2.386200	-1.301800
H	-5.398100	2.361100	0.266400
C	-3.853900	-1.398700	0.309200
C	-4.052900	-0.006200	0.006900
H	-4.938300	0.291500	-0.538700
H	-4.611000	-2.109500	-0.007700

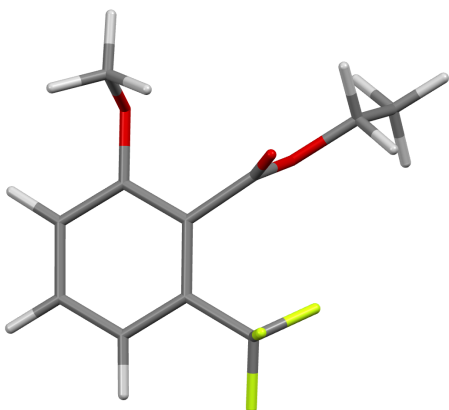
**Compound 46 Electronic Energy in Gas Phase: -2388.295626 Hartree**



B	3.669700	1.596500	1.308000
H	4.532100	2.190000	1.892300
C	1.337900	-0.620000	2.997500
H	0.452800	-1.236100	2.941400
C	2.118700	-0.300700	4.112300
H	1.980600	-0.619800	5.132400
C	3.100000	0.535000	3.608100
H	3.920600	1.043400	4.091400
C	4.131400	-0.254000	-1.740900
H	3.628300	-0.746600	-2.563900
C	5.471200	0.121600	-1.587300
H	6.287900	-0.038800	-2.272100
C	5.507100	0.768400	-0.362600
H	6.315700	1.253600	0.163400
C	0.905000	3.204500	-0.418900
H	-0.021800	3.074300	-0.960500
C	1.540700	4.370100	0.026900
H	1.228700	5.390900	-0.122100
C	2.651100	3.916800	0.714600
H	3.430700	4.446800	1.241000
C	-0.736800	-0.900300	0.287600
H	-0.744300	-1.272600	1.311900
C	-0.832400	0.529900	0.109600
H	-0.882400	1.161300	0.998600
C	-1.992000	0.883800	-0.869900
C	-1.780300	0.118800	-2.157400
H	-1.584600	0.640200	-3.087700
C	-1.691600	-1.197100	-1.999800
H	-1.435500	-1.885500	-2.797400
C	-1.823300	-1.643700	-0.564600
H	-1.790300	-2.729700	-0.443000
C	-3.120400	-1.058200	-0.017500

C	-3.227900	0.261800	-0.169100
C	-3.997400	-1.948100	0.789900
C	0.950200	-3.557100	1.092300
H	1.381300	-3.254800	2.049900
H	1.181900	-4.611400	0.918300
H	-0.133400	-3.429100	1.135300
C	3.439600	-3.022400	-0.107300
H	3.529500	-4.101000	0.047400
H	3.883900	-2.491200	0.739700
H	3.987600	-2.739700	-1.007000
C	1.118700	-3.404800	-1.765400
H	0.030000	-3.493000	-1.741600
H	1.559700	-4.402700	-1.833000
H	1.385900	-2.805100	-2.640200
C	-3.072700	2.714900	-1.932800
H	-3.215400	3.781200	-1.752300
H	-4.029000	2.197400	-1.781900
H	-2.762800	2.566100	-2.973700
F	-3.256100	-2.616200	1.701600
F	-4.955200	-1.298500	1.462300
F	-4.594300	-2.883100	0.033900
N	1.817400	-0.025900	1.901100
N	2.898700	0.680900	2.287500
N	3.428300	0.119700	-0.671400
N	4.270300	0.747900	0.165500
N	1.594700	2.131300	-0.033400
N	2.664400	2.572000	0.664600
N	1.042900	-0.230100	-2.088800
O	1.073600	-0.428500	-3.276300
O	-2.086200	2.276100	-1.021600
P	1.670900	-2.532800	-0.252000
W	1.202100	-0.075800	-0.352300
O	-4.018900	1.970500	1.286300
C	-4.261300	1.139000	0.448200
O	-5.482800	0.918800	-0.061800
C	-6.538700	1.669100	0.553600
H	-6.335700	2.737100	0.426600
H	-6.536700	1.457100	1.627200
C	-7.830200	1.245100	-0.109700
H	-8.672300	1.784300	0.330200
H	-7.801000	1.458500	-1.180500
H	-7.991800	0.173500	0.024900

**Compound 47 Electronic Energy in Gas Phase: -950.477002 Hartree**



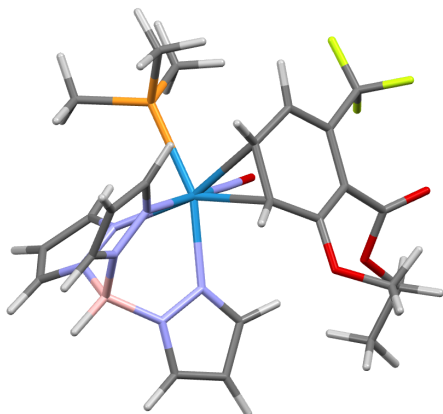
C	-2.726400	1.490400	-0.953800
C	-1.644300	2.346600	-0.785100
C	-0.433700	1.843800	-0.314900
H	-3.668100	1.876300	-1.328600
H	-1.711100	3.403100	-1.022800
C	-2.607400	0.138700	-0.641900
H	-3.445800	-0.535800	-0.768900
O	0.646900	2.669500	-0.156800
C	0.726400	3.236300	1.150900
H	1.622200	3.856900	1.163900
H	-0.153600	3.856600	1.356500
H	0.806500	2.449400	1.908000
C	-1.395200	-0.357100	-0.173500
C	-0.299200	0.490400	-0.010600
C	1.036300	0.015400	0.497100
O	1.322100	-0.063100	1.666200
O	1.856600	-0.285400	-0.506700
C	3.146500	-0.782500	-0.111600
H	2.998200	-1.672900	0.506600
H	3.640300	-0.025700	0.504700
C	-1.284100	-1.804700	0.226400
F	-2.251900	-2.546600	-0.328000
F	-0.106800	-2.333300	-0.145100
F	-1.376800	-1.953200	1.553300
C	3.914300	-1.083500	-1.378900
H	4.906100	-1.468300	-1.130800
H	3.388900	-1.832100	-1.975400
H	4.031000	-0.179500	-1.980200

**Compound 48 Electronic Energy in Gas Phase: -77.283153 Hartree**



C	-0.601200	-0.002300	-0.000100
C	0.601200	-0.002200	0.000100
H	-1.667600	0.013700	0.000100
H	1.667600	0.013600	-0.000100

**Compound 49 Electronic Energy in Gas Phase: -2310.987742 Hartree**

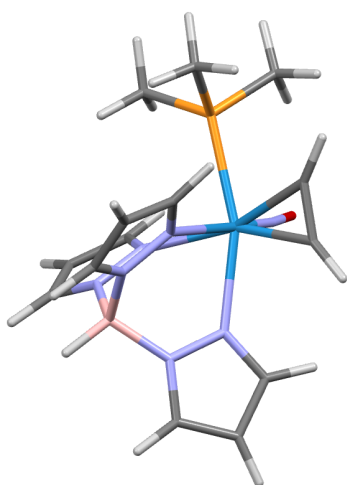


O	1.411000	-0.485600	1.960900
N	-0.923300	1.992100	-0.016900
N	-2.104300	2.631500	-0.155200
N	-2.523600	-0.081200	-1.508700
N	-3.468100	0.863200	-1.342200
N	-2.414200	0.225800	1.479600
N	-3.446900	1.034000	1.174600
N	0.505100	-0.363100	1.193400
C	-1.917600	3.959600	-0.019200
C	-0.574800	4.191600	0.210500
C	0.007500	2.916100	0.209300
C	-4.367100	0.800300	-2.339200
C	-4.000700	-0.223900	-3.195700
C	-2.834000	-0.743300	-2.626100
C	-4.216600	1.220200	2.262100

C	-3.671600	0.505000	3.315100
C	-2.529400	-0.091400	2.769600
B	-3.429300	1.843700	-0.149800
H	-4.369800	2.585400	-0.198200
H	-2.756700	4.635400	-0.091200
H	-0.085600	5.140700	0.358500
H	1.038800	2.620100	0.352500
H	-5.198000	1.489000	-2.366200
H	-4.498900	-0.542500	-4.096700
H	-2.203300	-1.548600	-2.974500
H	-5.086300	1.857700	2.209200
H	-4.036700	0.437200	4.326900
H	-1.781000	-0.718100	3.235700
C	-3.021800	-2.975900	1.192900
H	-3.196600	-4.051000	1.286300
H	-3.096400	-2.511700	2.176400
H	-3.792400	-2.535200	0.553300
C	-0.199700	-3.425300	1.605700
H	-0.220100	-2.868600	2.546200
H	-0.445400	-4.474300	1.790100
H	0.814600	-3.340200	1.205800
W	-0.786400	-0.252300	0.005500
P	-1.375900	-2.648000	0.436000
C	-1.447000	-3.865700	-0.942900
H	-1.704700	-4.854900	-0.555500
H	-2.214300	-3.557600	-1.658400
H	-0.487600	-3.926300	-1.458300
C	0.417000	-1.315300	-1.584600
C	0.547200	0.125100	-1.729400
C	1.824100	0.733100	-1.423200
H	-0.199100	-1.838800	-2.312600
H	-0.017800	0.628900	-2.510200
C	1.580900	-2.035500	-1.094000
H	1.556000	-3.119600	-1.057100
O	1.894900	2.007600	-1.873600
C	3.140100	2.596800	-2.210100
H	2.962900	3.203200	-3.100100
H	3.500900	3.234500	-1.400000
H	3.889100	1.829300	-2.430200
C	2.677500	-1.391300	-0.634400
C	2.821200	0.051800	-0.769100
C	3.938000	0.765400	-0.105600
O	5.100100	0.441800	-0.075700
O	3.479900	1.874400	0.526300
C	4.479200	2.652800	1.190300
H	5.250200	2.940900	0.466500

H	4.960800	2.034300	1.952500
C	3.762000	-2.207800	0.015200
F	3.361200	-3.487100	0.199800
F	4.879900	-2.267700	-0.717700
F	4.090800	-1.739700	1.224700
C	3.777000	3.853800	1.787000
H	4.491500	4.484300	2.321100
H	3.304900	4.453800	1.003400
H	3.002800	3.531500	2.487200

**Compound 50 Electronic Energy in Gas Phase: -1437.838229 Hartree**

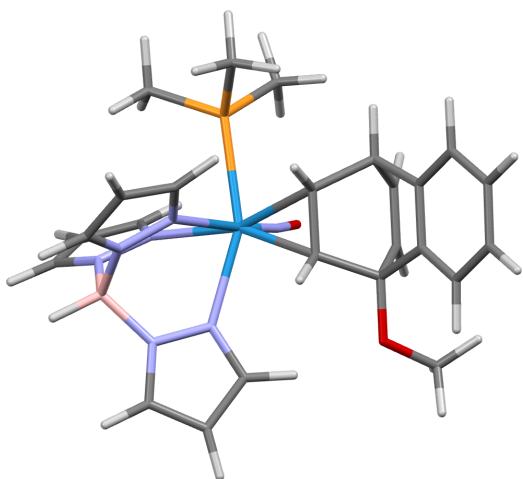


B	2.431100	0.619300	1.095200
H	3.433400	0.914400	1.683400
C	0.009800	-1.791400	2.223200
H	-0.838600	-2.396500	1.932200
C	0.860000	-1.891800	3.330800
H	0.798200	-2.585100	4.153700
C	1.815900	-0.913200	3.116900
H	2.689500	-0.634000	3.686900
C	0.163000	3.026100	-0.369800
H	-0.712100	3.181700	-0.984300
C	1.058000	3.954500	0.175500
H	1.030700	5.029200	0.097500
C	1.999000	3.175600	0.827000
H	2.886100	3.442800	1.381500
C	2.400400	-1.398500	-1.932800
H	1.802500	-1.887100	-2.688700
C	3.789700	-1.363900	-1.761200
H	4.545400	-1.833400	-2.369600
C	3.973000	-0.591900	-0.628100
H	4.870000	-0.289700	-0.108700

N	0.413300	-0.803600	1.424400
N	1.522800	-0.273300	1.970200
N	0.534100	1.784800	-0.057400
N	1.659600	1.883600	0.671600
N	1.799100	-0.699700	-0.972900
N	2.766000	-0.205300	-0.174200
P	-2.529800	0.339200	0.479900
W	-0.403400	-0.277500	-0.620600
C	-3.941600	-0.528600	-0.296200
H	-3.701700	-1.595700	-0.324100
H	-4.049900	-0.182700	-1.326100
H	-4.872400	-0.361100	0.252000
C	-3.047100	2.101400	0.480600
H	-3.072300	2.480600	-0.543200
H	-2.324600	2.690100	1.051400
H	-4.038400	2.210200	0.928700
C	-2.760500	-0.079200	2.256700
H	-3.718000	0.307300	2.616800
H	-1.946300	0.343900	2.849700
H	-2.749500	-1.163600	2.381800
C	-0.350400	0.309200	-2.647900
H	0.272400	0.244400	-3.528500
C	-1.461800	0.755600	-2.185800
H	-2.363900	1.278900	-2.474400
N	-1.076900	-1.897800	-0.756100
O	-1.582900	-2.993400	-0.711000



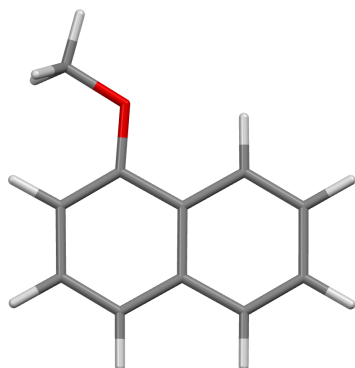
**Compound 51 Electronic Energy in Gas Phase: -1937.89255 Hartree**



B	3.156000	1.483200	1.102100
H	4.085800	2.058200	1.595000
C	0.865600	-0.548800	3.059900
H	-0.046200	-1.126000	3.097800
C	1.744600	-0.222300	4.097000
H	1.673800	-0.494100	5.137600
C	2.719000	0.545400	3.483100
H	3.597000	1.032900	3.879200
C	3.299700	-0.508800	-1.886600
H	2.712500	-1.008400	-2.647400
C	4.662900	-0.191400	-1.850800
H	5.416400	-0.418100	-2.587500
C	4.822200	0.501200	-0.661800
H	5.689800	0.967700	-0.219400
C	0.349300	3.151400	-0.494600
H	-0.620400	3.042900	-0.961100
C	1.073500	4.301900	-0.156300
H	0.803700	5.329600	-0.337200
C	2.208100	3.823600	0.472400
H	3.050900	4.335600	0.912400
C	-1.441300	-0.830800	0.525900
H	-1.370600	-1.139000	1.569200
C	-1.472500	0.592400	0.269700
H	-1.412300	1.269600	1.124100
C	-2.671300	0.963100	-0.646300
C	-2.600600	0.103300	-1.891000
H	-2.463600	0.543000	-2.872700
C	-2.577400	-1.205500	-1.656100
H	-2.441900	-1.949400	-2.434100
C	-2.617700	-1.569100	-0.189700
H	-2.615500	-2.649500	-0.011400

C	-3.853500	-0.903300	0.401400
C	-3.879400	0.479600	0.165700
C	0.213800	-3.536300	1.325700
H	0.744500	-3.217100	2.226100
H	0.376500	-4.607800	1.180400
H	-0.853400	-3.347800	1.456200
C	2.602300	-3.178500	-0.113500
H	2.654600	-4.252400	0.085100
H	3.148400	-2.633900	0.662600
H	3.078000	-2.965700	-1.071700
C	0.129700	-3.514700	-1.540000
H	-0.955200	-3.549600	-1.417800
H	0.520600	-4.533900	-1.599400
H	0.344500	-2.964700	-2.460800
C	-3.611600	2.776500	-1.873800
H	-3.814200	3.834300	-1.691600
H	-4.553200	2.217500	-1.819900
H	-3.195200	2.667800	-2.882200
N	1.282700	-0.022100	1.905300
N	2.420800	0.647600	2.176800
N	2.698600	-0.059600	-0.784800
N	3.629700	0.560600	-0.041700
N	1.011200	2.062800	-0.104100
N	2.150300	2.479100	0.491500
N	0.203600	-0.360500	-2.008400
O	0.144800	-0.611800	-3.185600
O	-2.696600	2.354700	-0.881700
P	0.852100	-2.604600	-0.123900
W	0.494000	-0.139200	-0.296500
C	-4.874500	1.268200	0.715000
C	-5.881900	0.664100	1.478300
C	-5.870700	-0.707500	1.695700
C	-4.843500	-1.497800	1.164300
H	-4.860000	2.343800	0.564600
H	-6.671900	1.273400	1.906200
H	-6.654100	-1.168800	2.288800
H	-4.820500	-2.568300	1.352800

**Compound 52 Electronic Energy in Gas Phase: -500.062368 Hartree**



C	1.078500	0.850200	-0.000100
C	0.234800	-0.291800	0.000100
C	-3.318100	-1.117800	-0.000600
H	-3.715400	-2.132100	-0.001400
H	-3.668100	-0.587000	-0.893800
H	-3.669600	-0.588100	0.892700
O	-1.913700	-1.243400	0.000500
C	0.808200	-1.587500	0.000100
C	2.172100	-1.741600	-0.000000
C	3.018800	-0.609100	-0.000100
C	2.483600	0.653800	-0.000100
H	0.148900	-2.447700	0.000100
H	2.605700	-2.736300	-0.000100
H	4.095800	-0.743300	-0.000100
H	3.129200	1.527700	-0.000200
C	0.501400	2.150100	-0.000200
C	-1.183600	-0.098300	0.000300
C	-0.857800	2.295100	0.000000
C	-1.718200	1.168300	0.000300
H	-2.789900	1.322500	0.000600
H	-1.300200	3.286200	0.000000
H	1.155500	3.016500	-0.000300